

**OPTIMAL LIGHTNING PERFORMANCE FOR 25 kV AC  
OVERHEAD CATENARY SYSTEM**



**Kelvin Melckzedeck Minja**

**A Thesis Submitted in Partial Fulfillment of the Requirements for the  
Degree of Master of Engineering in Electrical Engineering**

**Suranaree University of Technology**

**Academic Year 2017**

สมรรถนะไฟฟ้าที่เหมาะสม สำหรับระบบคาทอเดอไนรี  
แรงดันไฟฟ้ากระแสสลับเหนือศีรษะ 25 kV



นายเคลวิน เมล็กเซเดก มินจา

วิทยานิพนธ์นี้เป็นส่วนหนึ่งของการศึกษาตามหลักสูตรปริญญาวิศวกรรมศาสตรมหาบัณฑิต

สาขาวิชาวิศวกรรมไฟฟ้า

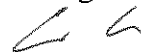
มหาวิทยาลัยเทคโนโลยีสุรนารี

ปีการศึกษา 2560

**OPTIMAL LIGHTNING PERFORMANCE INDEX FOR 25 kV AC  
OVERHEAD CATENARY SYSTEM**

Suranaree University of Technology has approved this thesis submitted in partial fulfillment of the requirements for a Master's Degree.

Thesis Examining Committee



---

(Assoc. Prof. Dr. Anant Oonsivilai)

Chairperson



---

(Asst. Prof. Dr. Boonruang Marungsri)

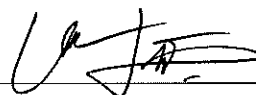
Member (Thesis Advisor)



---

(Assoc. Prof. Dr. Kaan Kerdchuen)

Member



---

(Dr. Uthen Leeton)

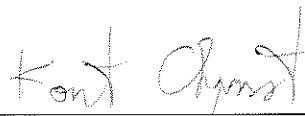
Member



---

(Prof. Dr. Santi Maensiri)

Vice Rector for Academic Affairs  
and Internationalization



---

(Assoc. Prof. Flt. Lt. Dr. Kontorn Chamniprasart)



Dean of Institute of Engineering

เคลวิน เมล็กเซเดก มินจา : สมรรถนะฟ้ําฟ้ําที่เหมาะสม สำหรับระบบคาเทอเนรี  
แรงดันไฟฟ้ากระแสสลับเหนือศรีษะ 25 kV (OPTIMAL LIGHTNING PERFORMANCE  
FOR 25 kV AC OVERHEAD CATENARY SYSTEM) อาจารย์ที่ปรึกษา :  
ผู้ช่วยศาสตราจารย์ ดร.บุญเรือง มะรังศรี, 254 หน้า

สมรรถนะฟ้ําฟ้ําของระบบคาเทอเนรีเหนือศรีษะที่ใช้อยู่ เป็นที่รู้จักกันอย่างดีเมื่อไม่กี่ปีที่ผ่านมา เนื่องจากจำนวนความถี่ของการผิดพลาดมีสาเหตุจากผลของสภาวะแรงดันเกิน จึงทำให้การป้องกันเพื่อต้านการรบกวนจากฟ้ําฟ้ําต่อระบบคาเทอเนรีเหนือศรีษะต้องนำตำแหน่งที่ถูกฟ้ําฟ้ํามาพิจารณาตามมาตรฐาน IEEE Std. 1313 เพื่อพยายามคงอัตราการผิดพลาดให้อยู่ในระดับต่ำ จึงทำให้มีการศึกษาเพื่อประมาณค่าสมรรถนะฟ้ําฟ้ํากันอย่างแพร่หลาย นอกจากนี้ด้วยการใช้การออกแบบเริ่มต้นเป็นฐาน ระบบที่มีอยู่ที่ประสบกับปัญหาค่าความเหมาะสมที่สุด ในขณะที่ของพารามิเตอร์ฟ้ําฟ้ําที่เหมาะสมสำหรับระบบคาเทอเนรีเหนือศรีษะ ถูกประมาณค่าจากอัตราการเกิดความผิดพลาดจากฟ้ําฟ้ํา โปรแกรม ATP-EMTP และวิธีเชิงพันธุกรรม (Genetic Algorithm) ของเทคนิคปัญญาประดิษฐ์ ในโปรแกรม MATLAB ถูกนำมาใช้ การปรับปรุงและและการหาค่าเหมาะสมที่สุด สำหรับสมรรถนะฟ้ําฟ้ําของระบบ ผลการศึกษาพบว่า ฟ้ําฟ้ําขั้วลบบแบบลำเดี่ยวและแบบขั้วหลายลำ ที่มีขนาดกระแสตั้งแต่ 34 kA ขึ้นไป สามารถทำให้เกิดวابلไฟ (Flashover) และวابلไฟแบบย้อนกลับ (Back flashover) เมื่อฟ้ําฟ้ําลงที่เสา (Pantograph) ฟ้ําฟ้ําลงที่ยอดของเสาไฟฟ้า (Mast) ฟ้ําฟ้ําสายดิน (Return หรือ Earth wire) และฟ้ําฟ้ําลงที่สายส่งจ่ายไฟฟ้าเหนือศรีษะ (Catenary wire) ที่ตำแหน่งบนเสาไฟฟ้าและระยะ ระหว่างเสาไฟฟ้าในทุกรูปแบบ นอกจากนี้ยังพบว่าผลของค่าความต้านทานของดินที่ทำให้การเกิดวابلไฟมีสูงขึ้นเด่นชัดเปรียบเทียบกับเกิดการเกิดวابلไฟแบบย้อนกลับเมื่อฟ้ําฟ้ําขั้วลบบแบบขั้วหลายลำครั้งฟ้ําฟ้ําลงบนเสาที่ขณะอยู่ระหว่างเสาไฟฟ้าจะมากกว่าจุดฟ้ําฟ้ําอื่น ๆ ยิ่งไปกว่านั้น ยังพบว่า การติดตั้งกับดักฟ้ําฟ้ําเป็นช่วง ๆ ตามสมรรถนะของกับดักฟ้ําฟ้ําเป็นวิธีการที่สะดวกในการสมรรถนะฟ้ําฟ้ําหรือบรรเทาการเกิดวابلไฟ สุดท้ายได้วิธีการเหมาะสมที่สุดถูกคำนวณ และนำเสนอ ระดับฉนวนของสายที่เหมาะสม ความต้านทานดิน ความสามารถในการดูดซับพลังงานของกับดักฟ้ําฟ้ํา ระยะห่างในการติดตั้ง และจำนวนในการติดตั้งกับดักฟ้ําฟ้ํา เพื่อกำจัดหรือลดความผิดพลาดที่เกิดจากฟ้ําฟ้ําให้น้อยที่สุด จากผลการศึกษานี้ได้ค่าพารามิเตอร์ใหม่ที่จะช่วยลดอัตราการเกิดความผิดพลาดจากฟ้ําฟ้ํานบนสายคาเทอเนรี ส่วนการตรวจสอบความถูกต้องของวิธีที่ได้นำเสนอ ในบางกรณีไม่สามารถทราบล่วงหน้าได้ เช่น ข้อกำหนดในการก่อสร้าง

ที่ต้องใช้ร่วมกันกับวิธีการที่ออกแบบไว้ ซึ่งวิธีการใหม่ที่เหมาะสมกับสมรรถนะฟ้าผ่าของระบบ  
เป็นงานที่ต้องทำต่อไปในอนาคต

สาขาวิชาวิศวกรรมไฟฟ้า  
ปีการศึกษา 2560

ลายมือชื่อนักศึกษา   
ลายมือชื่ออาจารย์ที่ปรึกษา 

KELVIN MELCKZEDECK MINJA : OPTIMAL LIGHTNING  
PERFORMANCE FOR 25 kV AC OVERHEAD CATENARY  
SYSTEM. THESIS ADVISOR : ASST. PROF. BOONRUANG  
MARUNGSRI, D.ENG, 254 PP.

LIGHTNING / PERFORMANCE INDEX / OPTIMIZATION/ OVERHEAD  
CATENARY SYSTEM

The lightning performance of Overhead Catenary System relying on the existed network has been well known in a recent year. Since Frequent Number of breakdown caused by overvoltage condition, the protection against lightning disturbances in Overhead Catenary System has been taken into consideration from striking points as per IEEE Std. 1313. In an effort to maintain failure rate at a low level, plenty of lightning performance estimation studies have been conducted. Also, based on their initial design, the existed system is faced as an optimization problem where optimum lightning parameters are examined for the overhead line, regards to the appropriateness of the lightning failure rate. ATP-EMTP software and Genetic Algorithm (GA) of Artificial Intelligence (AI) Techniques in MATLAB are utilized for improvement and optimization of the system lightning performance respectively. It was shown that the negative single and multiple lightning of magnitude - 34 kA and above leads backflashover and flashover when strikes on train's pantograph, top of Mast, Return wire (Earthing wire), and Catenary wire at the mast and between two masts in all configurations. Additionally, the grounding resistance was recognized to

have higher predominance in flashover compared to backflashover when negative multiple lightning strokes occur on pantograph than other striking points at the mid-span unlike along the mast. Moreover, it was seen that installation intervals with the performance of surge arresters are convenient to improve the lightning performance or mitigating the flashover. Lastly, the optimal methodology calculates and proposes the most suitable line insulation level, grounding resistance, the energy absorption capability of surge arresters, surge arresters' installation interval, and a number of installed surge arresters for the examined line, to eliminate or minimize the total failures caused by lightning at minimal. From these results, it is revealed that obtained results for the studied lines, i.e., the newly selected design parameters, significantly may reduce the failure rates caused by lightning, something fundamental in the case of catenary lines. In order to validate the potency of the proposed method, in some cases, the civil construction requirements are not known in advance, which required a new approach to be compatible with the lightning performance of the system in future work.

School of Electrical Engineering

Academic Year 2017

Student's Signature \_\_\_\_\_

Advisor's Signature \_\_\_\_\_



## ACKNOWLEDGMENT

Firstly, I would like to thank God for giving health and enabling me to do this work with the School of Electrical Engineering, Suranaree University of Technology here in Thailand.

Secondly, I would thank my Advisor, Assistant Professor Dr. Boornuang Marungsri for his guidance and support throughout my studies and to the accomplishment of this thesis. Also, special thanks should go to the committee members, Assistant Professor Dr. Anant Oonsivilai (Chairperson), Assistant Professor Dr. Boornuang Marungsri (Thesis Advisor), and Dr. Uthen Leeton (Member) for their advice.

Additionally, I would also like to thank all graduates and staffs from the school of Electrical Engineering and other schools in the University for supporting me as they were always willing to help me.

Finally, I must express my very profound gratitude to my parents and to my brothers for providing me with unfailing support and continuous spiritually encouragement throughout my years of study and through the process of researching and writing this thesis. This accomplishment would not have been possible without them. Thank you all.

Kelvin Melckzedeck Minja



# TABLE OF CONTENTS

	<b>Page</b>
ABSTRACT (THAI) .....	I
ABSTRACT (ENGLISH) .....	III
ACKNOWLEDGMENT .....	V
TABLE OF CONTENTS .....	VI
LIST OF TABLES .....	XIII
LIST OF FIGURES .....	XVII
<b>CHAPTER</b>	
<b>I INTRODUCTION .....</b>	<b>1</b>
1.1 General Introduction .....	1
1.2 Thai Railway Electrification System .....	4
1.3 Problem Statement .....	7
1.4 Case Study Overviews .....	10
1.5 Objective .....	11
1.6 Limitations of the Thesis .....	12
1.7 Thesis Structure .....	12
1.8 Chapter Summary .....	13
<b>II LITERATURE REVIEW .....</b>	<b>14</b>
2.1 Electric train .....	14
2.2 Railway electrification system .....	15
2.2.1 Overhead line system .....	16
2.2.1.1 Bow collector system. ....	17

## TABLE OF CONTENTS (Continued)

	<b>Page</b>
2.2.1.2 Trolley wire overhead line system .....	22
2.2.1.3 Catenary contact system.....	30
1 DC Catenary contact system .....	31
2 AC-DC Catenary contact system .....	33
3 AC-DC-AC Catenary contact system .....	34
2.2.2 Third railway system.....	36
2.2.3 Ground-level Power Supply System .....	40
2.3 Traction power supply .....	43
2.3.1 Traction power supply Networks.....	44
2.4 Railway Electric Traction .....	47
2.4.1 DC Traction Units.....	49
2.4.2 AC Traction Units .....	49
2.4.3 Multi-System Units .....	50
2.5 DC Motor Drive.....	50
2.6 AC Motor Drive.....	52
2.7 Lightning Vulnerability .....	58
2.7.1 Direct lightning strikes.....	60
2.7.2 Direct and Indirect lightning strikes to the overhead or cable .....	61
2.8 Lightning protection system .....	62

## TABLE OF CONTENTS (Continued)

	<b>Page</b>
2.8.1 Lightning protection level Classification .....	62
2.9 Lightning voltage surge .....	64
2.9.1 Lightning protection in Catenary Contact system.....	64
2.9.2 Application of surge arrester .....	66
2.10 Improvement and optimization techniques Review.....	73
2.11 Existed System .....	79
2.12 Preliminary Study .....	82
2.13 Analysis of Elevated Structure and Catenary Lightning Range of existed system.....	82
2.14 Proposed system.....	86
2.15 Chapter summary .....	89
<b>III METHODOLOGY .....</b>	<b>92</b>
3.1 Introduction.....	92
3.2 Catenary Contact System.....	92
3.3 Modeling of Lightning Source.....	94
3.4 Modeling of Mast.....	98
3.5 Modeling of Train.....	98
3.6 Modeling of Insulator .....	100
3.7 Modeling of Grounding Resistance .....	101
3.8 Modeling of Metal Oxide Surge Arrester. ....	102

## TABLE OF CONTENTS (Continued)

	<b>Page</b>
3.9 Optimization Method.....	106
3.10 Chapter summary.....	110
<b>IV SIMULATION RESULTS .....</b>	<b>112</b>
4.1 Introduction.....	112
4.2 Analysis of direct lightning strokes.....	112
4.3 Mitigation of Flashover from Multiple Lightning strokes in Overhead Catenary System.....	194
4.4 Lightning performance optimization for 25 kV AC, 50 Hz catenary contact system.....	197
4.4.1 Intelligence search method (Genetic Algorithm (GA)) ....	198
4.4.2 Test Function.....	199
4.5 Chapter summary.....	204
<b>V DISCUSSION .....</b>	<b>205</b>
5.1 Analysis of direct lightning strokes.....	205
5.1.1 The Effects of negative single lightning strokes on mast for case 1 .....	205
5.1.2 The Effects of negative single lightning strokes on mast for case 2 .....	206
5.1.3 The Effects of negative single lightning strokes on return line for case 1 .....	207

## TABLE OF CONTENTS (Continued)

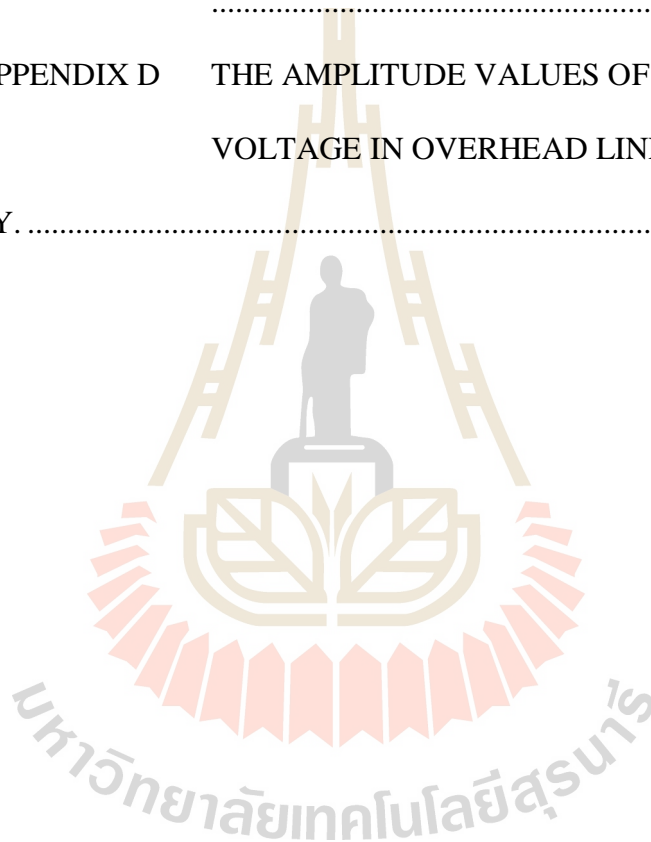
	<b>Page</b>
5.1.4 The Effects of negative single lightning strokes on return line for case 2 .....	208
5.1.5 The Effects of negative single lightning strokes on catenary line for case 1 .....	209
5.1.6 The Effects of negative single lightning strokes on catenary line for case 2 .....	210
5.1.7 The Effects of negative single lightning strokes on pantograph for case 1 .....	211
5.1.8 The Effects of negative single lightning strokes on pantograph for case 2 .....	212
5.1.9 The Effects of negative multiple lightning strokes on mast for case 1 .....	213
5.1.10 The Effects of negative multiple lightning strokes on mast for case 2 .....	214
5.1.11 The Effects of negative multiple lightning strokes on return line for case 1 .....	215
5.1.12 The Effects of negative multiple lightning strokes on return line for case 2 .....	217
5.1.13 The Effects of negative multiple lightning strokes on catenary line for case 1 .....	217

**TABLE OF CONTENTS (Continued)**

	<b>Page</b>
5.1.14 The Effects of negative multiple lightning strokes on catenary line for case 2.....	219
5.1.15 The Effects of negative multiple lightning strokes on pantograph for case 1 .....	219
5.1.16 The Effects of negative multiple lightning strokes on pantograph for case 2 .....	221
5.2 Mitigation of Flashover from Multiple Lightning strokes in Overhead Catenary System.....	222
5.2.1 The Mitigation of negative multiple lightning strokes on pantograph.....	222
5.3 Lightning performance optimization for 25 kV AC, 50 Hz catenary contact system.....	222
5.3.1 The optimal Lightning performance index for 25 kV AC overhead catenary system .....	223
5.4 Chapter summary .....	223
<b>VI CONCLUSION AND FUTURE WORK .....</b>	<b>224</b>
6.1 Conclusion .....	224
6.2 Future work .....	226
REFERENCES.....	228
RESEARCH PUBLICATION.....	244
<b>APPENDICES</b>	
APPENDIX A RESEARCH PUBLICATIONS.....	254

## TABLE OF CONTENTS (Continued)

	<b>Page</b>
APPENDIX B SOURCE EQUATIONS AND CODES FOR PERFORMANCE INDEX.....	287
APPENDIX C OUTCOME OF LIGHTNING STROKES EFFECTS .....	309
APPENDIX D THE AMPLITUDE VALUES OF INDUCED VOLTAGE IN OVERHEAD LINES .....	514
BIOGRAPHY.....	566



## LIST OF TABLES

Table	Page
1.1 Operation limit of Nominal Voltage for Railway Electrification System according to BS EN 50163 and IEC 60850 .....	3
1.2 Conductors in Double track Thai Railway Electrification System .....	7
2.1 Operation limit of Nominal Voltage for Railway Electrification System according to BS EN 50163 and IEC .....	44
2.2 Standards for lightning protection in Railway Facilities .....	66
2.3 Correlation of typical MO resistors to the line discharge classes according to IEC/EN 60099-4 .....	67
2.4 Operation limit of Nominal Voltage for Railway Electrification System according to BS EN 50163 and IEC 60850 .....	67
3.1 Details of 25 kV Overhead Catenary Transmission Line .....	93
3.2 Mast Configuration .....	94
3.3 Parameters of the single lightning source .....	95
3.4 Parameters of multiple lightning sources .....	95
3.5 Modeled Parameters of Mast .....	98
3.6 Details of 25 kV Overhead Catenary Transmission Line .....	101
3.7 V-I Characteristics for nonlinear resistor A0 and A1 of the Pinceti model...	105
4.1 Simulations setup for Configuration 2 for both Cases .....	114
4.2 Simulations setup for Configuration 3 for both Cases .....	114



## LIST OF TABLES (Continued)

<b>Table</b>		<b>Page</b>
4.3	Mast 4 induced voltages in Case 1 with multiple lightning strokes on the train's pantograph for configuration 1 .....	178
4.4	Mast 5 induced voltages in Case 1 with multiple lightning strokes on the train's pantograph for configuration 1 .....	178
4.5	Mast 7 induced voltages in Case 1 with multiple lightning strokes on the train's pantograph for configuration 1 .....	179
4.6	Mast 4 induced voltages in Case 2 with multiple lightning strokes on the train's pantograph for configuration 1 .....	179
4.7	Mast 5 induced voltages in Case 2 with multiple lightning strokes on the train's pantograph for configuration 1 .....	180
4.8	Mast 7 induced voltages in Case 2 with multiple lightning strokes on the train's pantograph for configuration 1 .....	180
4.9	Mast 4 induced voltages in Case 1 with multiple lightning strokes on the train's pantograph for configuration 1 .....	181
4.10	Mast 5 induced voltages in Case 1 with multiple lightning strokes on the train's pantograph for configuration 2 .....	181
4.11	Mast 7 induced voltages in Case 1 with multiple lightning strokes on the train's pantograph for configuration 2 .....	181

## LIST OF TABLES (Continued)

<b>Table</b>	<b>Page</b>
4.12 Mast 4 induced voltages in Case 1 with multiple lightning strokes on the train's pantograph for configuration 3 .....	182
4.13 Mast 5 induced voltages in Case 1 with multiple lightning strokes on the train's pantograph for configuration 3 .....	182
4.14 Mast 7 induced voltages in Case 1 with multiple lightning strokes on the train's pantograph for configuration 3 .....	182
4.15 Mast 4 induced voltages in Case 2 with multiple lightning strokes on the train's pantograph for configuration 2 .....	183
4.16 Mast 5 induced voltages in Case 2 with multiple lightning strokes on the train's pantograph for configuration 2 .....	183
4.17 Mast 7 induced voltages in Case 2 with multiple lightning strokes on the train's pantograph for configuration 2 .....	183
4.18 Mast 4 induced voltages in Case 2 with multiple lightning strokes on the train's pantograph for configuration 3 .....	184
4.19 Mast 5 induced voltages in Case 2 with multiple lightning strokes on the train's pantograph for configuration 3 .....	184
4.20 Mast 7 induced voltages in Case 2 with multiple lightning strokes on the train's pantograph for configuration 3 .....	184
4.21 Arrangement of the surge arrester's installation interval .....	195

## LIST OF TABLES (Continued)

<b>Table</b>		<b>Page</b>
4.22	Percentage of Mast Induced Voltage Against Lightning-Impulse Withstand Voltage of Insulators for -50 kA .....	196
4.23	Flashover across insulators for -50 kA .....	196
4.24	Parameters of the existed overhead catenary lines. ....	202
4.25	Optimum parameters of the examined overhead catenary lines .....	202
4.26	Optimum parameters of the examined overhead catenary lines .....	203

## LIST OF FIGURES

Figure	Page
1.1	Classification of Railway Electrification System in Europe..... 4
1.2	Double Track Railway Electrification system on elevated railway system and same cross-section view axis. .... 6
2.1	Current Collector. .... 17
2.2	An old tram with a bow collector. .... 19
2.3	Tram with a bow collector ..... 20
2.4	Rigid bow collectors at Snaefell Summit station..... 22
2.5	Circuit Configuration of Trolley Wire Overhead Line System ..... 23
2.6	Trolley Wheel on TCRT 1300 ..... 23
2.7	Machining trolley wheels..... 24
2.8	Modern trolley poles as installed on Vancouver's low floor electric trolley buses ..... 26
2.9	Locomotive with trolley poles ..... 29
2.10	Circuit Configuration of Substation receive power from three phase high voltage to electric train (a) near to substation (b) away from the substation... 32
2.11	Circuit Configuration of DC Catenary Contact System ..... 33
2.12	Circuit Configuration of AC-DC Catenary Contact System..... 34
2.13	Circuit Configuration of AC-DC-AC Catenary Contact System..... 35
2.14	Circuit Configuration of Transformerless AC-DC-AC Catenary Contact System ..... 36

## LIST OF FIGURES (Continued)

<b>Figure</b>	<b>Page</b>
2.15	Third rail at the West Falls Church Metro stop near Washington, D.C., electrified at 750 volts..... 37
2.16	A top-contact third railway in different design of shoes and shoe gear..... 38
2.17	A section of APS track ..... 42
2.18	The alternative of connection 50 Hz single phase tractions power substation to the three-phase network ..... 46
2.19	Basic design of 2×25 kV feeding system..... 47
2.20	Operation control in separately excited DC motor traction drive ..... 52
2.21	Torque-speed characteristic curve of the induction motor ..... 55
2.22	Traction duty cycle of mechanical and electrical variables ..... 57
2.23	The components of a Lightning Protection System (LPS): Air-Termination System, Down-conductors, Earth-termination System, equipotential Bonding in Railway Station ..... 63
2.24	Highest values of the voltage occurring in the systems depending on time duration ..... 69
2.25	The application of surge arresters in 15 kV A.C, 16.7 Hz railway current supply ..... 70
2.26	Installation of MO surge arrester on overhead line and the rails ..... 71
2.27	Installation of MO surge arrester on locomotives..... 71
2.28	Position of the surge arrester installation for lightning protection of train..... 72

## LIST OF FIGURES (Continued)

Figure	Page
2.29 Overall TPS & OCS Schematic Diagram .....	80
2.30 Overhead catenary system .....	81
2.31 Airport Rail link line in Thailand.....	81
2.32 Truck return circuit via running rails and return conductor.....	83
2.33 Substation infeed.....	83
2.34 The configuration of Overhead Catenary System.....	84
2.35 The range of triggered lightning of Catenary on the double-track elevated railway system .....	86
2.36 Lightning strike on train's pantograph (a) at the Mast and (b) at the mid-span of Masts in the 2D view .....	87
2.37 Lightning strike on train's pantograph (a) at the Mast in the 3D view.....	88
2.38 Lightning strike on train's pantograph (a) at the Mast and (b) at the mid-span of Masts in the 3D view.....	89
3.1 Transmission line data in ATP EMTP.....	93
3.2 Waveforms of the Single lightning of -34 kA (2.0/100 $\mu$ s) strokes modeled in ATP-EMTP .....	96
3.3 Waveforms of the Single lightning of -50 kA (2.0/100 $\mu$ s) strokes modeled in ATP- EMTP .....	96
3.4 Lightning current waveforms of the -34 kA first stroke-(1.0/100 $\mu$ s), subsequent stroke -(0.2/50 $\mu$ s) designed in ATP-EMTP .....	97

## LIST OF FIGURES (Continued)

Figure	Page
3.5	Lightning current waveforms of the -50 kA first stroke-(1.0/100 $\mu$ s), subsequent stroke -(0.2/50 $\mu$ s) designed in ATP-EMTP ..... 97
3.6	Mast with Train, Railway Transmission line, Pole, Ground, and Insulators at Mast in ATP-EMTP ..... 99
3.7	Train with Railway Transmission line at the mid-span of Masts in ATP-EMTP ..... 100
3.8	Pinceti model ..... 103
4.1	Arrangement of the masts with lightning source for case 1..... 113
4.2	Arrangement of the masts with lightning source for case 2..... 113
4.3	Auxiliary line induced voltages in Case 1 with -34 kA (2.0/100 $\mu$ s) for configuration 1 ..... 114
4.4	Auxiliary line induced voltages in Case 1 with -34 kA (2.0/100 $\mu$ s) for configuration 2 ..... 115
4.5	Auxiliary line induced voltages in Case 1 with -34 kA (2.0/100 $\mu$ s) for configuration 3 ..... 115
4.6	Auxiliary line induced voltages in Case 1 with -50 kA (2.0/100 $\mu$ s) for configuration 1 ..... 116
4.7	Auxiliary line induced voltages in Case 1 with -50 kA (2.0/100 $\mu$ s) for configuration 2 ..... 116

## LIST OF FIGURES (Continued)

<b>Figure</b>	<b>Page</b>
4.8    Auxiliary line induced voltages in Case 1 with -50 kA (2.0/100 $\mu$ s) for configuration 3 .....	117
4.9    Auxiliary line induced voltages in Case 2 with -34 kA (2.0/100 $\mu$ s) for configuration 1 .....	117
4.10    Auxiliary line induced voltages in Case 2 with -34 kA (2.0/100 $\mu$ s) for configuration 2 .....	118
4.11    Auxiliary line induced voltages in Case 2 with -34 kA (2.0/100 $\mu$ s) for configuration 3 .....	118
4.12    Auxiliary line induced voltages in Case 2 with -50 kA (2.0/100 $\mu$ s) for configuration 1 .....	119
4.13    Auxiliary line induced voltages in Case 2 with -50 kA (2.0/100 $\mu$ s) for configuration 2 .....	119
4.14    Auxiliary line induced voltages in Case 2 with -50 kA (2.0/100 $\mu$ s) for configuration 3 .....	120
4.15    Auxiliary line induced voltages in both Cases with -34 kA (2.0/100 $\mu$ s) for configuration 1 .....	120
4.16    Auxiliary line induced voltages in both Cases with -34 kA (2.0/100 $\mu$ s) for configuration 2 .....	121
4.17    Auxiliary line induced voltages in both Cases with -34 kA (2.0/100 $\mu$ s) for configuration 3 .....	121



## LIST OF FIGURES (Continued)

<b>Figure</b>	<b>Page</b>
4.18 Auxiliary line induced voltages in both Cases with -50 kA (2.0/100 $\mu$ s) for configuration 1 .....	122
4.19 Auxiliary line induced voltages in both Cases with -50 kA (2.0/100 $\mu$ s) for configuration 2 .....	122
4.20 Auxiliary line induced voltages in both Cases with -50 kA (2.0/100 $\mu$ s) for configuration 3 .....	123
4.21 Return line induced voltages in Case 1 with -34 kA (2.0/100 $\mu$ s) for configuration 1 .....	123
4.22 Return line induced voltages in Case 1 with -34 kA (2.0/100 $\mu$ s) for configuration 2 .....	124
4.23 Return line induced voltages in Case 1 with -34 kA (2.0/100 $\mu$ s) for configuration 3 .....	124
4.24 Return line induced voltages in Case 1 with -50 kA (2.0/100 $\mu$ s) for configuration 1 .....	125
4.25 Return line induced voltages in Case 1 with -50 kA (2.0/100 $\mu$ s) for configuration 2 .....	125
4.26 Return line induced voltages in Case 1 with -50 kA (2.0/100 $\mu$ s) for configuration 3 .....	126
4.27 Return line induced voltages in Case 2 with -34 kA (2.0/100 $\mu$ s) for configuration 1 .....	126

## LIST OF FIGURES (Continued)

<b>Figure</b>	<b>Page</b>
4.28 Return line induced voltages in Case 2 with -34 kA (2.0/100 $\mu$ s) for configuration 2 .....	127
4.29 Return line induced voltages in Case 2 with -34 kA (2.0/100 $\mu$ s) for configuration 3 .....	127
4.30 Return line induced voltages in Case 2 with -50 kA (2.0/100 $\mu$ s) for configuration 1 .....	128
4.31 Return line induced voltages in Case 2 with -50 kA (2.0/100 $\mu$ s) for configuration 2 .....	128
4.32 Return line induced voltages in Case 2 with -50 kA (2.0/100 $\mu$ s) for configuration 3 .....	129
4.33 Return line induced voltages in both Cases with -34 kA (2.0/100 $\mu$ s) for configuration 1 .....	129
4.34 Return line induced voltages in both Cases with -34 kA (2.0/100 $\mu$ s) for configuration 2 .....	130
4.35 Return line induced voltages in both Cases with -34 kA (2.0/100 $\mu$ s) for configuration 3 .....	130
4.36 Return line induced voltages in both Cases with -50 kA (2.0/100 $\mu$ s) for configuration 1 .....	131
4.37 Return line induced voltages in both Cases with -50 kA (2.0/100 $\mu$ s) for configuration 2 .....	131

## LIST OF FIGURES (Continued)

Figure	Page
4.38 Return line induced voltages in both Cases with -50 kA (2.0/100 $\mu$ s) for configuration 3 .....	132
4.39 Catenary line induced voltages in Case 1 with -34 kA (2.0/100 $\mu$ s) for configuration 1 .....	132
4.40 Catenary line induced voltages in Case 1 with -34 kA (2.0/100 $\mu$ s) for configuration 2 .....	133
4.41 Catenary line induced voltages in Case 1 with -34 kA (2.0/100 $\mu$ s) for configuration 3 .....	133
4.42 Catenary line induced voltages in Case 1 with -50 kA (2.0/100 $\mu$ s) for configuration 1 .....	134
4.43 Catenary line induced voltages in Case 1 with -50 kA (2.0/100 $\mu$ s) for configuration 2 .....	134
4.44 Catenary line induced voltages in Case 1 with -50 kA (2.0/100 $\mu$ s) for configuration 3 .....	135
4.45 Catenary line induced voltages in Case 2 with -34 kA (2.0/100 $\mu$ s) for configuration 1 .....	135
4.46 Catenary line induced voltages in Case 2 with -34 kA (2.0/100 $\mu$ s) for configuration 2 .....	136
4.47 Catenary line induced voltages in Case 2 with -34 kA (2.0/100 $\mu$ s) for configuration 3 .....	136

## LIST OF FIGURES (Continued)

Figure	Page
4.48 Catenary line induced voltages in Case 2 with -50 kA (2.0/100 $\mu$ s) for configuration 1 .....	137
4.49 Catenary line induced voltages in Case 2 with -50 kA (2.0/100 $\mu$ s) for configuration 2 .....	137
4.50 Catenary line induced voltages in Case 2 with -50 kA (2.0/100 $\mu$ s) for configuration 3 .....	138
4.51 Catenary line induced voltages in both Cases with -34 kA (2.0/100 $\mu$ s) for configuration 1 .....	138
4.52 Catenary line induced voltages in both Cases with -34 kA (2.0/100 $\mu$ s) for configuration 2 .....	139
4.53 Catenary line induced voltages in both Cases with -34 kA (2.0/100 $\mu$ s) for configuration 3 .....	139
4.54 Catenary line induced voltages in both Cases with -50 kA (2.0/100 $\mu$ s) for configuration 1 .....	140
4.55 Catenary line induced voltages in both Cases with -50 kA (2.0/100 $\mu$ s) for configuration 2 .....	140
4.56 Catenary line induced voltages in both Cases with -50 kA (2.0/100 $\mu$ s) for configuration 3 .....	141
4.57 Catenary line induced voltages in Case 1 with -34 kA (2.0/100 $\mu$ s) for configuration 1 .....	141

## LIST OF FIGURES (Continued)

Figure	Page
4.58 Catenary line induced voltages in Case 1 with -34 kA (2.0/100 $\mu$ s) for configuration 2 .....	142
4.59 Catenary line induced voltages in Case 1 with -34 kA (2.0/100 $\mu$ s) for configuration 3 .....	142
4.60 Catenary line induced voltages in Case 1 with -50 kA (2.0/100 $\mu$ s) for configuration 1 .....	143
4.61 Catenary line induced voltages in Case 1 with -50 kA (2.0/100 $\mu$ s) for configuration 2 .....	143
4.62 Catenary line induced voltages in Case 1 with -50 kA (2.0/100 $\mu$ s) for configuration 3 .....	144
4.63 Catenary line induced voltages in Case 2 with -34 kA (2.0/100 $\mu$ s) for configuration 1 .....	144
4.64 Catenary line induced voltages in Case 2 with -34 kA (2.0/100 $\mu$ s) for configuration 2 .....	145
4.65 Catenary line induced voltages in Case 2 with -34 kA (2.0/100 $\mu$ s) for configuration 3 .....	145
4.66 Catenary line induced voltages in Case 2 with -50 kA (2.0/100 $\mu$ s) for configuration 1 .....	146
4.67 Catenary line induced voltages in Case 2 with -50 kA (2.0/100 $\mu$ s) for configuration 2 .....	146

## LIST OF FIGURES (Continued)

Figure	Page
4.68 Catenary line induced voltages in Case 2 with -50 kA (2.0/100 $\mu$ s) for configuration 3 .....	147
4.69 Catenary line induced voltages in both Cases with -34 kA (2.0/100 $\mu$ s) for configuration 1 .....	147
4.70 Catenary line induced voltages in both Cases with -34 kA (2.0/100 $\mu$ s) for configuration 2 .....	148
4.71 Catenary line induced voltages in both Cases with -34 kA (2.0/100 $\mu$ s) for configuration 3 .....	148
4.72 Catenary line induced voltages in both Cases with -50 kA (2.0/100 $\mu$ s) for configuration 1 .....	149
4.73 Catenary line induced voltages in both Cases with -50 kA (2.0/100 $\mu$ s) for configuration 2 .....	149
4.74 Catenary line induced voltages in both Cases with -50 kA (2.0/100 $\mu$ s) for configuration 3 .....	150
4.75 Auxiliary line induced voltages in Case 1 with -34 kA, first stroke-(1.0/100 $\mu$ s), subsequent stroke-(0.2/50 $\mu$ s) for configuration 1 .....	150
4.76 Auxiliary line induced voltages in Case 1 with -34 kA, first stroke-(1.0/100 $\mu$ s), subsequent stroke-(0.2/50 $\mu$ s) for configuration 2 .....	151
4.77 Auxiliary line induced voltages in Case 1 with -34 kA, first stroke-(1.0/100 $\mu$ s), subsequent stroke-(0.2/50 $\mu$ s) for configuration 3 .....	151

## LIST OF FIGURES (Continued)

<b>Figure</b>	<b>Page</b>
4.78	Auxiliary line induced voltages in Case 1 with -50 kA, first stroke-(1.0/100 $\mu$ s), subsequent stroke-(0.2/50 $\mu$ s) for configuration 1..... 152
4.79	Auxiliary line induced voltages in Case 1 with -50 kA, first stroke-(1.0/100 $\mu$ s), subsequent stroke-(0.2/50 $\mu$ s) for configuration 2..... 152
4.80	Auxiliary line induced voltages in Case 1 with -50 kA, first stroke-(1.0/100 $\mu$ s), subsequent stroke-(0.2/50 $\mu$ s) for configuration 3..... 153
4.81	Auxiliary line induced voltages in Case 2 with -34 kA, first stroke-(1.0/100 $\mu$ s), subsequent stroke-(0.2/50 $\mu$ s) for configuration 1..... 153
4.82	Auxiliary line induced voltages in Case 2 with -34 kA, first stroke-(1.0/100 $\mu$ s), subsequent stroke-(0.2/50 $\mu$ s) for configuration 2..... 154
4.83	Auxiliary line induced voltages in Case 2 with -34 kA, first stroke-(1.0/100 $\mu$ s), subsequent stroke-(0.2/50 $\mu$ s) for configuration 3..... 154
4.84	Auxiliary line induced voltages in Case 2 with -50 kA, first stroke-(1.0/100 $\mu$ s), subsequent stroke-(0.2/50 $\mu$ s) for configuration 1..... 155
4.85	Auxiliary line induced voltages in Case 2 with -50 kA, first stroke-(1.0/100 $\mu$ s), subsequent stroke-(0.2/50 $\mu$ s) for configuration 2..... 155
4.86	Auxiliary line induced voltages in Case 2 with -50 kA, first stroke-(1.0/100 $\mu$ s), subsequent stroke-(0.2/50 $\mu$ s) for configuration 3..... 156
4.87	Auxiliary line induced voltages in both Cases with -34 kA, first stroke-(1.0/100 $\mu$ s), subsequent stroke-(0.2/50 $\mu$ s) for configuration 1 ..... 156

## LIST OF FIGURES (Continued)

Figure	Page
4.88	Auxiliary line induced voltages in both Cases with -34 kA, first stroke-(1.0/100 $\mu$ s), subsequent stroke-(0.2/50 $\mu$ s) for configuration 2 ..... 157
4.89	Auxiliary line induced voltages in both Cases with -34 kA, first stroke-(1.0/100 $\mu$ s), subsequent stroke-(0.2/50 $\mu$ s) for configuration 3 ..... 157
4.90	Auxiliary line induced voltages in both Cases with -50 kA, first stroke-(1.0/100 $\mu$ s), subsequent stroke-(0.2/50 $\mu$ s) for configuration 1 ..... 158
4.91	Auxiliary line induced voltages in both Cases with -50 kA, first stroke-(1.0/100 $\mu$ s), subsequent stroke-(0.2/50 $\mu$ s) for configuration 2 ..... 158
4.92	Auxiliary line induced voltages in both Cases with -50 kA, first stroke-(1.0/100 $\mu$ s), subsequent stroke-(0.2/50 $\mu$ s) for configuration 3 ..... 159
4.93	Return line induced voltages in Case 1 with -34 kA, first stroke-(1.0/100 $\mu$ s), subsequent stroke-(0.2/50 $\mu$ s) for configuration 1 ..... 159
4.94	Return line induced voltages in Case 1 with -34 kA, first stroke-(1.0/100 $\mu$ s), subsequent stroke-(0.2/50 $\mu$ s) for configuration 2 ..... 160
4.95	Return line induced voltages in Case 1 with -34 kA, first stroke-(1.0/100 $\mu$ s), subsequent stroke-(0.2/50 $\mu$ s) for configuration 3 ..... 160
4.96	Return line induced voltages in Case 1 with -50 kA, first stroke-(1.0/100 $\mu$ s), subsequent stroke-(0.2/50 $\mu$ s) for configuration 1 ..... 161
4.97	Return line induced voltages in Case 1 with -50 kA, first stroke-(1.0/100 $\mu$ s), subsequent stroke-(0.2/50 $\mu$ s) for configuration 2 ..... 161



## LIST OF FIGURES (Continued)

Figure	Page
4.98	Return line induced voltages in Case 1 with -50 kA, first stroke-(1.0/100 $\mu$ s), subsequent stroke-(0.2/50 $\mu$ s) for configuration 3..... 162
4.99	Return line induced voltages in Case 2 with -34 kA, first stroke-(1.0/100 $\mu$ s), subsequent stroke-(0.2/50 $\mu$ s) for configuration 1 ..... 162
4.100	Return line induced voltages in Case 2 with -34 kA, first stroke-(1.0/100 $\mu$ s), subsequent stroke-(0.2/50 $\mu$ s) for configuration 2..... 163
4.101	Return line induced voltages in Case 2 with -34 kA, first stroke-(1.0/100 $\mu$ s), subsequent stroke-(0.2/50 $\mu$ s) for configuration 3..... 163
4.102	Return line induced voltages in Case 2 with -50 kA, first stroke-(1.0/100 $\mu$ s), subsequent stroke-(0.2/50 $\mu$ s) for configuration 1..... 164
4.103	Return line induced voltages in Case 2 with -50 kA, first stroke-(1.0/100 $\mu$ s), subsequent stroke-(0.2/50 $\mu$ s) for configuration 2..... 164
4.104	Return line induced voltages in Case 2 with -50 kA, first stroke-(1.0/100 $\mu$ s), subsequent stroke-(0.2/50 $\mu$ s) for configuration 3..... 165
4.105	Return line induced voltages in both Cases with -34 kA, first stroke-(1.0/100 $\mu$ s), subsequent stroke-(0.2/50 $\mu$ s) for configuration 1..... 165
4.106	Return line induced voltages in both Cases with -34 kA, first stroke-(1.0/100 $\mu$ s), subsequent stroke-(0.2/50 $\mu$ s) for configuration 2..... 166
4.107	Return line induced voltages in both Cases with -34 kA, first stroke-(1.0/100 $\mu$ s), subsequent stroke-(0.2/50 $\mu$ s) for configuration 3..... 166

## LIST OF FIGURES (Continued)

Figure	Page
4.108 Return line induced voltages in both Cases with -50 kA, first stroke-(1.0/100 $\mu$ s), subsequent stroke-(0.2/50 $\mu$ s) for configuration 1.....	167
4.109 Return line induced voltages in both Cases with -50 kA, first stroke-(1.0/100 $\mu$ s), subsequent stroke-(0.2/50 $\mu$ s) for configuration 2.....	167
4.110 Return line induced voltages in both Cases with -50 kA, first stroke-(1.0/100 $\mu$ s), subsequent stroke-(0.2/50 $\mu$ s) for configuration 3.....	168
4.111 Catenary line induced voltages in Case 1 with -34 kA, first stroke-(1.0/100 $\mu$ s), subsequent stroke-(0.2/50 $\mu$ s) for configuration 1.....	168
4.112 Catenary line induced voltages in Case 1 with -34 kA, first stroke-(1.0/100 $\mu$ s), subsequent stroke-(0.2/50 $\mu$ s) for configuration 2.....	169
4.113 Catenary line induced voltages in Case 1 with -34 kA, first stroke-(1.0/100 $\mu$ s), subsequent stroke-(0.2/50 $\mu$ s) for configuration 3.....	169
4.114 Catenary line induced voltages in Case 1 with -50 kA, first stroke-(1.0/100 $\mu$ s), subsequent stroke-(0.2/50 $\mu$ s) for configuration 1.....	170
4.115 Catenary line induced voltages in Case 1 with -50 kA, first stroke-(1.0/100 $\mu$ s), subsequent stroke-(0.2/50 $\mu$ s) for configuration 2.....	170
4.116 Catenary line induced voltages in Case 1 with -50 kA, first stroke-(1.0/100 $\mu$ s), subsequent stroke-(0.2/50 $\mu$ s) for configuration 3.....	171
4.117 Catenary line induced voltages in Case 2 with -34 kA, first stroke-(1.0/100 $\mu$ s), subsequent stroke-(0.2/50 $\mu$ s) for configuration 1.....	171

## LIST OF FIGURES (Continued)

Figure	Page
4.118 Catenary line induced voltages in Case 2 with -34 kA, first stroke-(1.0/100 $\mu$ s), subsequent stroke-(0.2/50 $\mu$ s) for configuration 2.....	172
4.119 Catenary line induced voltages in Case 2 with -34 kA, first stroke-(1.0/100 $\mu$ s), subsequent stroke-(0.2/50 $\mu$ s) for configuration 3.....	172
4.120 Catenary line induced voltages in Case 2 with -50 kA, first stroke-(1.0/100 $\mu$ s), subsequent stroke-(0.2/50 $\mu$ s) for configuration 1.....	173
4.121 Catenary line induced voltages in Case 2 with -50 kA, first stroke-(1.0/100 $\mu$ s), subsequent stroke-(0.2/50 $\mu$ s) for configuration 2.....	173
4.122 Catenary line induced voltages in Case 2 with -50 kA, first stroke-(1.0/100 $\mu$ s), subsequent stroke-(0.2/50 $\mu$ s) for configuration 3.....	174
4.123 Catenary line induced voltages in both Cases with -34 kA, first stroke-(1.0/100 $\mu$ s), subsequent stroke-(0.2/50 $\mu$ s) for configuration 1.....	174
4.124 Catenary line induced voltages in both Cases with -34 kA, first stroke-(1.0/100 $\mu$ s), subsequent stroke-(0.2/50 $\mu$ s) for configuration 2.....	175
4.125 Catenary line induced voltages in both Cases with -34 kA, first stroke-(1.0/100 $\mu$ s), subsequent stroke-(0.2/50 $\mu$ s) for configuration 3.....	175
4.126 Catenary line induced voltages in both Cases with -50 kA, first stroke-(1.0/100 $\mu$ s), subsequent stroke-(0.2/50 $\mu$ s) for configuration 1.....	176
4.127 Catenary line induced voltages in both Cases with -50 kA, first stroke-(1.0/100 $\mu$ s), subsequent stroke-(0.2/50 $\mu$ s) for configuration 2.....	176

## LIST OF FIGURES (Continued)

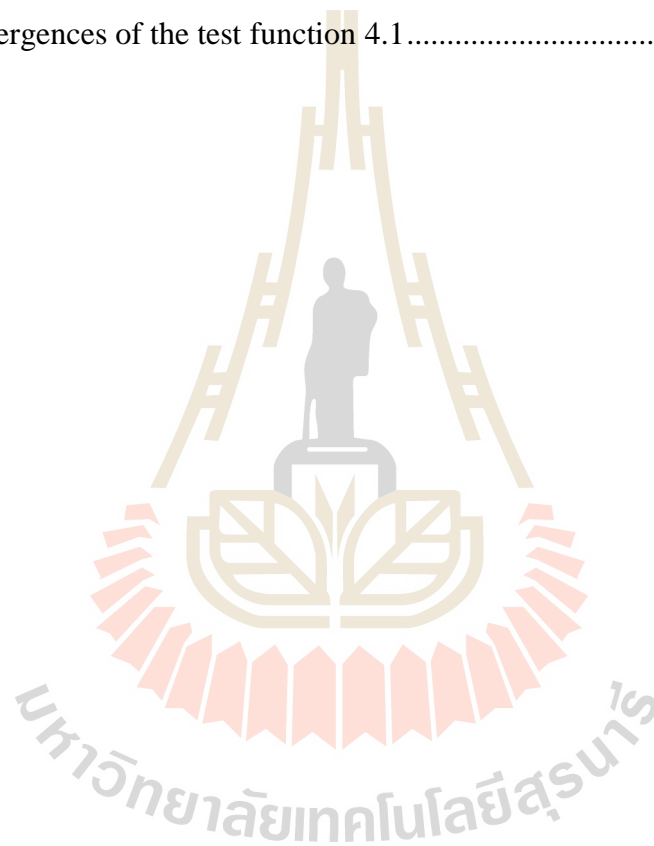
Figure	Page
4.128 Catenary line induced voltages in both Cases with -50 kA, first stroke-(1.0/100 $\mu$ s), subsequent stroke-(0.2/50 $\mu$ s) for configuration 3.....	177
4.129 Catenary line induced voltages in Case 1 with -34 kA, first stroke-(1.0/100 $\mu$ s), subsequent stroke-(0.2/50 $\mu$ s) for configuration 1.....	185
4.130 Catenary line induced voltages in Case 1 with -34 kA, first stroke-(1.0/100 $\mu$ s), subsequent stroke-(0.2/50 $\mu$ s) for configuration 2.....	185
4.131 Catenary line induced voltages in Case 1 with -34 kA, first stroke-(1.0/100 $\mu$ s), subsequent stroke-(0.2/50 $\mu$ s) for configuration 3.....	186
4.132 Catenary line induced voltages in Case 1 with -50 kA, first stroke-(1.0/100 $\mu$ s), subsequent stroke-(0.2/50 $\mu$ s) for configuration 1.....	186
4.133 Catenary line induced voltages in Case 1 with -50 kA, first stroke-(1.0/100 $\mu$ s), subsequent stroke-(0.2/50 $\mu$ s) for configuration 2.....	187
4.134 Catenary line induced voltages in Case 1 with -50 kA, first stroke-(1.0/100 $\mu$ s), subsequent stroke-(0.2/50 $\mu$ s) for configuration 3.....	187
4.135 Catenary line induced voltages in Case 2 with -34 kA, first stroke-(1.0/100 $\mu$ s), subsequent stroke-(0.2/50 $\mu$ s) for configuration 1.....	188
4.136 Catenary line induced voltages in Case 2 with -34 kA, first stroke-(1.0/100 $\mu$ s), subsequent stroke-(0.2/50 $\mu$ s) for configuration 2.....	188
4.137 Catenary line induced voltages in Case 2 with -34 kA, first stroke-(1.0/100 $\mu$ s), subsequent stroke-(0.2/50 $\mu$ s) for configuration 3.....	189

## LIST OF FIGURES (Continued)

Figure	Page
4.138 Catenary line induced voltages in Case 2 with -50 kA, first stroke-(1.0/100 $\mu$ s), subsequent stroke-(0.2/50 $\mu$ s) for configuration 1.....	189
4.139 Catenary line induced voltages in Case 2 with -50 kA, first stroke-(1.0/100 $\mu$ s), subsequent stroke-(0.2/50 $\mu$ s) for configuration 2.....	190
4.140 Catenary line induced voltages in Case 2 with -50 kA, first stroke-(1.0/100 $\mu$ s), subsequent stroke-(0.2/50 $\mu$ s) for configuration 3.....	190
4.141 Catenary line induced voltages in both Cases with -34 kA, first stroke-(1.0/100 $\mu$ s), subsequent stroke-(0.2/50 $\mu$ s) for configuration 1.....	191
4.142 Catenary line induced voltages in both Cases with -34 kA, first stroke-(1.0/100 $\mu$ s), subsequent stroke-(0.2/50 $\mu$ s) for configuration 2.....	191
4.143 Catenary line induced voltages in both Cases with -34 kA, first stroke-(1.0/100 $\mu$ s), subsequent stroke-(0.2/50 $\mu$ s) for configuration 3.....	192
4.144 Catenary line induced voltages in both Cases with -50 kA, first stroke-(1.0/100 $\mu$ s), subsequent stroke-(0.2/50 $\mu$ s) for configuration 1.....	192
4.145 Catenary line induced voltages in both Cases with -50 kA, first stroke-(1.0/100 $\mu$ s), subsequent stroke-(0.2/50 $\mu$ s) for configuration 2.....	193
4.146 Catenary line induced voltages in both Cases with -50 kA, first stroke-(1.0/100 $\mu$ s), subsequent stroke-(0.2/50 $\mu$ s) for configuration 3.....	193
4.147 Arrangement of the masts with lightning source for mitigation (case 1) .....	194
4.148 Arrangement of the masts with lightning source for mitigation (case 2) .....	195

**LIST OF FIGURES (Continued)**

<b>Figure</b>	<b>Page</b>
4.149 Airport Rail link line in Thailand.....	198
4.150 Flowchart of the GA procedure .....	199
4.151 Convergences of the test function 4.1.....	202



# CHAPTER 1

## INTRODUCTION

### 1.1 General Introduction

Since the second half of 19<sup>th</sup> Century, technology innovation has been improved and upgraded electrification of railway line due to the superiority of electric traction over diesel-electric traction and Hybrid traction. In the case of improvement, it has become a human demand from the benefit of increased speed, safety, efficiency, desired environment and reliability of economic enhancement depend on energy (Lu, 2011). As demonstrated in Utlu and Hepbasli 2006, Railway travel is the friendly mode of transport depend on energy efficiency and the environment. Little energy is dissipated through rolling resistance due to the very hard contact (Hibbeler, 2008). Due to the benefits of the convoy formation, Railway locomotive and multiple unit trains have good aerodynamic performance (Browand, McCallen, Ross, Orellano, and Sperling, 2009). Railway locomotive and multiple units can operate without having onboard prime mover by getting electric energy from Railway Electrification System. There are several different Railway Electrification systems in use throughout the world and classified them by Voltages, Current (D.C or A.C) and Contact System (Third rail or Catenary/Overhead line). It needs sufficiency capital expenditure to install Railway Electrification System, but it has many advantages.

Railway Electrification System has significant benefits of a higher power to weight ratio than another form of traction such as diesel, hybrid or steam that generate power on board. It enables faster acceleration and higher tractive effort on steep

gradients due to engine control technology, power electronics, and electric motor control. With the advent of modern electronic and electrical technology, it leads improvement in energy efficiency (Tan, Loh, and Holmes, 2005; Zhang et al. 2009; Park et al. 2008; Bae et al. 2005). On trains equipped with regenerative brakes, descending gradients require the minimal use of air brakes as the locomotive's traction motors; it becomes generators sending current back into the supply system and or onboard resistors. This conditions which convert the excess energy to heat and improve energy efficiency for Railway system (Oettich, Albrecht, and Scholz, 2004; Adinolfi et al. 1998; Adinolfi et al. 1997; Mellitt, Mouneimne, and Goodman, 1984).

It also includes the lack of exhaust fumes at the point of use, less noise and lower maintenance requirements of the traction units. Electric trains create fewer carbon emissions than diesel trains, especially in countries where electricity comes primarily from non-fossil sources in given sufficient traffic density.

Due to European and International standardization, there are six commonly used voltage which are 600 DC, 750 DC, 1,500 DC, 3 kV DC, 15 kV AC (16.7 Hz) and 25 kV AC (50 Hz). This voltage stated in standards BS EN 50163 and IEC 60850 while there are many other systems of voltage used for electrification systems of railway over the world, and the current systems list for electric rail traction covers both standard voltage and non-standard voltage systems.

DC Railway Electrification System was the early electrical system used low-voltage DC where traction supplier supplies directly to DC Electric motors which were controlled using a combination of resistors and relays that connected in parallel or series. During the mid-20<sup>th</sup> century, AC Railway Electrification System becomes useful due to rotary converters or mercury arc rectifiers which were used to convert



utility (mains) AC power to the required DC voltage at feeder stations. Nowadays, this is usually done by semiconductor rectifiers after stepping down the voltage from the utility supply. AC Railway Electrification System has many advantages over DC Railway Electrification System which is quite simple, but it requires thick cables and short distances between feeder stations because of the high currents required that led high losses (Frey, 2012).

**Table 1.1** Operation limit of Nominal Voltage for Railway Electrification System according to BS EN 50163 and IEC 60850 (Frey, 2012).

System Type	L.N.P Voltage	L.P Voltage	N. Voltage	H.P. Voltage	H.N.P Voltage
600 V DC	400 V	400 V	600 V	720 V	800 V
750 V DC	500 V	500 V	750 V	900 V	1 kV
1,500 V DC	1,000 V	1,000 V	1,500 V	1,800 V	1,950 V
3 kV DC	2 kV	2 kV	3 kV	3 kV	3 kV
15 kV AC, 16.7 Hz	11 kV	12 kV	15 kV	17.25 kV	18 kV
25 kV AC, 50 Hz	17.5 kV	19 kV	25 kV	27.5 kV	29 kV

L.N.P Voltage: Lowest Non-Permanent Voltage

L.P Voltage: Lowest Permanent Voltage

N. Voltage: Nominal Voltage

H.P. Voltage: Highest Permanent Voltage

H.N.P Voltage: Highest Non-Permanent Voltage

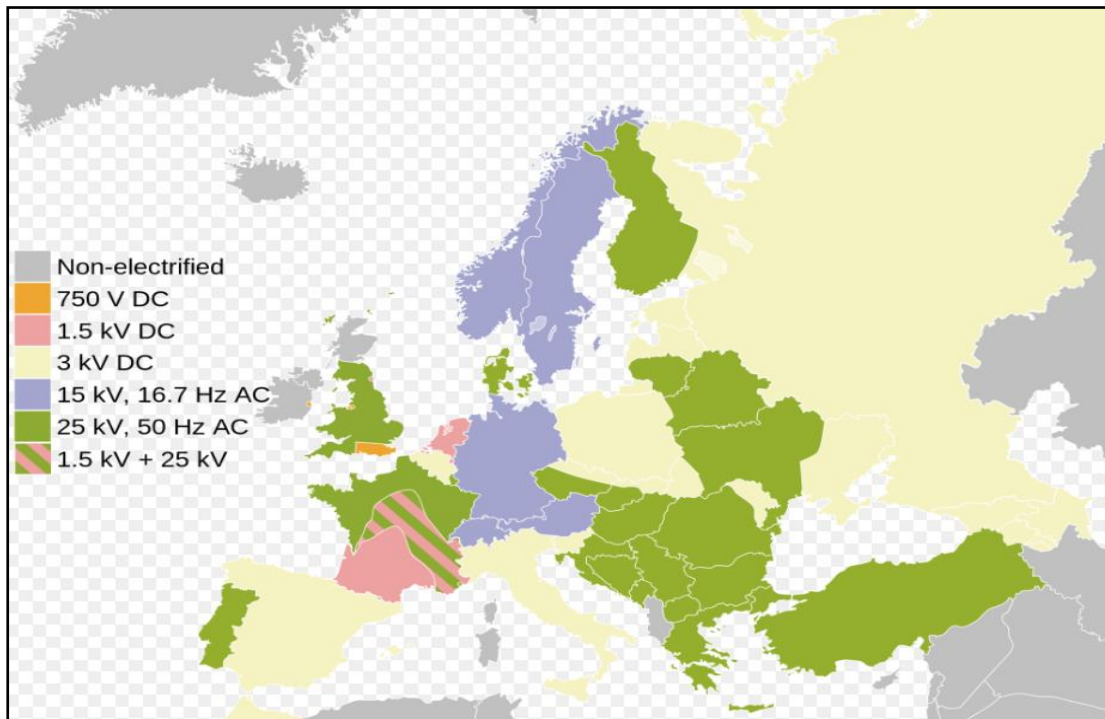


**Figure 1.1** Classification of Railway Electrification System in Europe (Frey, 2012).

## 1.2 Thai Railway Electrification System.

The main electrical traction power supply in Bangkok's Urban Transport consists of 750 V DC and 25 kV AC, 50 Hz system in different three railway systems. Bangkok Mass Transit System Company Limited (BTSC) operates 750 V DC Third Rail on the double-track elevated railway system. This company covers two lines which are Sukhumvit Line (connecting Mo Chit in the North with Bearing in the East of Bangkok) and Silom Line (connecting National Stadium in the Center with Bang Wa in the South-West of Bangkok) at 36.75 km track length. Bangkok Metro Public Company Ltd (BMCL) operates 750 V DC Third Rail which was first underground railway system since July 3, 2004, and it covers one single line (Blue line) from Hua Lamphong main railway station to the North of Bangkok (Bang Sue Station) at 20 km

track length. SRT Electrified Train (SRTET) operates 25 kV AC, 50 Hz Catenary Contact System on double-track elevated railway system since August 23, 2010, which connects Suvarnabhumi Airport to central Bangkok (Phayathai, Makkasan). This Airport Rail Link covers three lines which are Makkasan Express line, Phayathai Express line and City line at 28.6 km track length (UMIASEA, 2014).

The traction power supply can be subdivided into traction power generation, traction power transmission, traction power feeding, and traction power collection by mobile electric traction vehicle. In Thailand catenary railway, the traction power is supplied by AC 69 kV 50 Hz transmission lines as a part of the traction power supply grid. The traction power distribution is performed by the traction power substation and overhead contact lines. All traction power supply installations have to be designed, contracted and operated so that general requirement according to the standard user can be fulfilled. Therefore, contact lines are the networks which act as the traction power feeding system to an electric train.

The overhead line equipment of A 25 kV AC, 50 Hz Catenary Contact System on double-track elevated railway system consists of six conductors per single track on the elevated pole and ground as shown in Figure 1.2. Contact wire, and Catenary wire, both noted as wires which used for feeding power to the locomotive through the pantograph located on the locomotive roof with 25 kV AC, 50 Hz. The lines are interconnected at every 7-10 m as in cross-sectional view in Figure 1.2 and Messenger wire, provides support to Contact wire, in order to reduce Catenary system impedance. Earth wire, used for returning traction current to the feeding station and Feeder wire used to supply power to trackside equipment through Catenary and Contact wires.

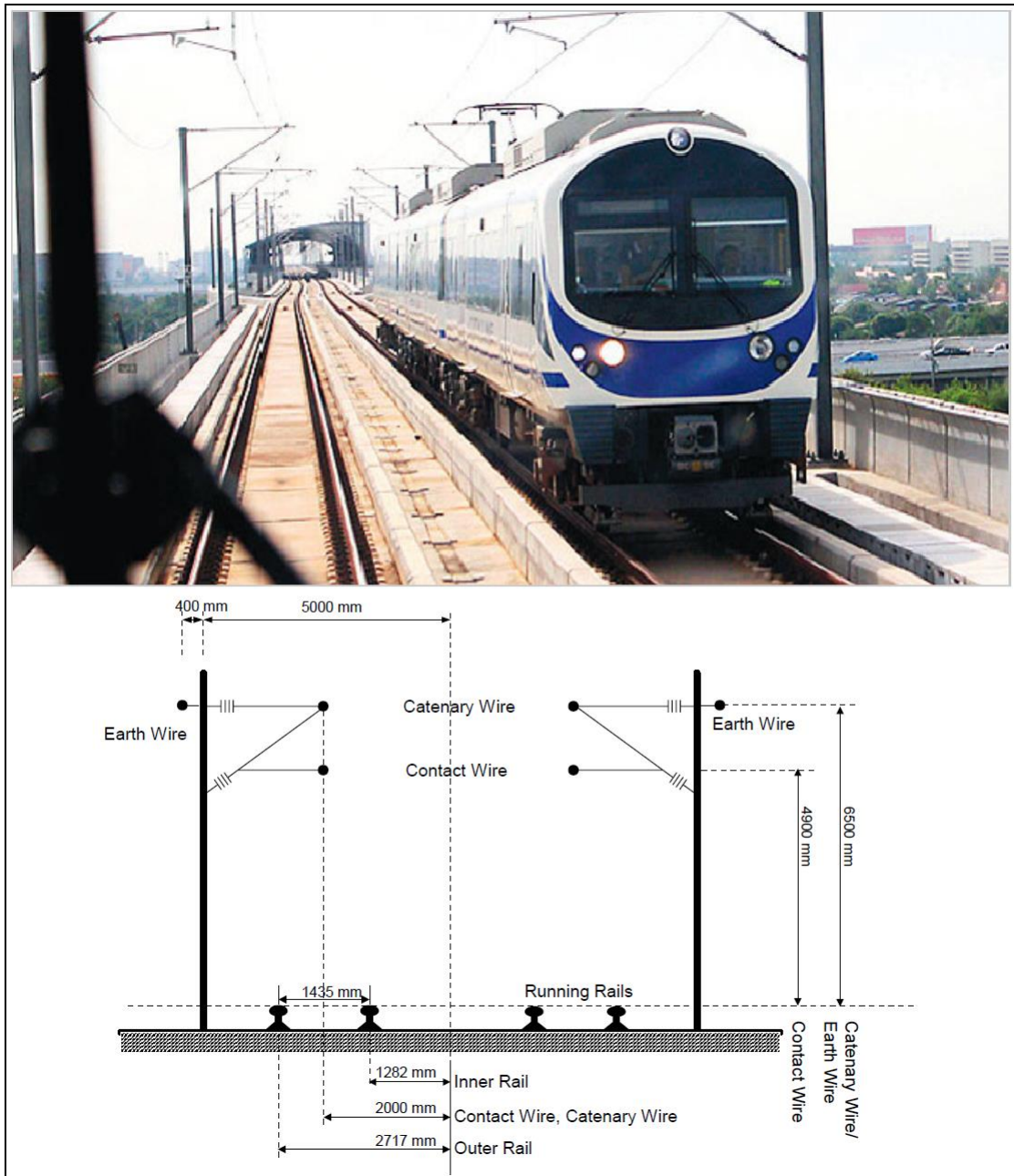


**Figure 1.2** Double Track Railway Electrification system on elevated railway system and same cross-section view axis (UMIASEA, 2014; Sandra, Martin, and Menter, 2007).

**Table 1.2** Conductors in Thai Railway Electrification System (Mazloom, 2010).

Conductor	Conductor Symbol	Conductivity (S/m)
I-Rail	R1	$4.4 \times 10^6$
S-Rail	R2	$4.4 \times 10^6$
Contact wire	R3	$5.8 \times 10^6$
Catenary wire	R4	$5.8 \times 10^6$
Earth Wire	R5	$3.5 \times 10^6$

### 1.3 Problem Statement

A 25 kV AC, 50 Hz Catenary Contact System on double-track elevated railway system is an among of railway electrification system which has an essential electrified railway transportation not only in peoples' daily life but also in the global economic growth of Thailand. Railroad transportation remains very relevant due to improvement on electrification of the rail line. Modern equipment that is applied to electric traction system, to increase speed, safety, efficiency, and reliability of economic enhancement, need for a careful and accurate coordination of protection system. This application concerns the overvoltage protection, which includes disturbances of atmospheric origin.

Security and reliability of power supply are very significant for electric energy utilities. Supply interruptions are mainly related to faults in its Overhead Catenary System, due to lightning strokes on them, producing dangerous overvoltages and damages on equipment. Actually, this disruption leads various electrical elements failure, power losses, and other unreliable condition on Overhead Catenary System. The necessity of adopting additional protection is worth to be verified under IEC standard (IEC 60913). Lightning overvoltage in power systems is caused by lightning strokes to phase conductor (shielding failure), shielding wire (back flashover), and ground in line proximity (Induced voltage) (IEEE Std. 1313). Lightning induces over-

voltages in the transmission line can cause flashover across insulators leading damage when it striking contact line installations and exceeds lightning withstand voltage level of insulators (Kiessling et al., 2009). Likewise, Lightning induces over-voltages in the mast can cause back flashover across insulators when it is striking on top of the mast and exceeds lightning withstand voltage level of insulators. Thailand is one among the Tropical countries having a lot of thunderstorm days and lightning discharge activities. It has been reported to have several incidences caused by the thunderstorm days and lightning events per year. The report about lightning statistics from Marungsri et al. (2008) showed that lightning often occurs in April-May but severely in June. The magnitude ranged 11-171 kA with a positive polarity which accounts for 5% and -10 to -139 kA with negative polarity is 95% of all lightning activities. In Omidiora and Lehtonen (2007); Martinez-Velasco and Aranda (2008); Rodriguez-Sanabria, Ramos-Robles, and Orama-Exclusa (2011) were stated that negative lightning could associate with multiple strokes per flash. Omidiora and Lehtonen (2007); Martinez-Velasco and Aranda (2008); Rodriguez-Sanabria, Ramos-Robles, and Orama-Exclusa (2011) showed the report for the multiple strokes averaging 3 to 4 strokes per flash with intervals of tens of milliseconds. Most of the researchers in Thailand have been based on single lightning strokes without considering the effects of multiple lightning strokes. Due to the frequent occurrence, enormous amounts of stroke currents have a high possibility of multiplicity due to its negative lightning strokes. For that reason, it made this study to be done in the overhead catenary system when both single stroke and multiple lightning strokes strike on train's pantograph, on top of Mast, Return wire (Earthing wire), and Catenary wire. Since slight differences in the design parameters values can affect their

lightning performance significantly, the correct and careful coordination of protection system should be considered as the most important issue of Overhead Catenary System for the rest of life due to lightning activities.

In an effort to maintain failure rates in low level to provide high power quality and avoiding damages and disturbances, plenty of lightning performances estimation studies have been proposed as in AIEE Committee Report (1950); Bewley, (1951); Fisher, Anderson, and Hagenguth (1960); Anderson (1961); Sargent, and Darveniza (1970); Darveniza, and Popolansky (1975); IEEE Working Group on Lightning Performance of Transmission Lines (1985); Bouquegneau, Dubois, and Trekat (1986); IEEE Working Group on Estimating the Lightning Performance of Transmission Lines, (1993); Chowdhuri, and Mehairjan (1997); He et al. (2005); Martinez, and Castro-Aranda (2003). Designing appears to be a most important issue in the lightning performance of transmission line, not only in design parameters values that affect the lightning performance but also in design parameters values that can optimize lightning performance to make improvements and modifications to an existing transmission line. Several Lightning Performance Optimization studies have been conducted in order to determine the minimum cost design of transmission lines. Consequently, it explores the sensitivity of the required present worth of revenue, to minimize the line total annual cost considering the relevant technical constraints. Both fixed and running cost items were taking into account the customer and utility costs of line outages as in Chang, and Zinn (1976); Grant, and Clayton (1987). Also, the economic aspects of the overhead distribution line lightning performance have been alternative design procedures for uncompensated overhead transmission lines based on the derivation of closed-form analytical expressions. For both line power and

current ratings, the geometrical data of the line tower is regarding its bundled conductors. The method of an optimal design for improving the lightning performance of overhead high-voltage transmission lines has been presented in Kennon, and Douglass (1990); Saied, Jaboori, and El-Nakid (1990); Katic, and Savic (1998); Saied (1999); Ekonomou et al. (2006).

The lightning performances estimation studies in 25 kV AC, 50 Hz Catenary Contact System based on simulation showed that the lightning performance of Overhead catenary system relying on their correct initial design of existing system needs to be optimized due to lightning activities in Thailand. This thesis proposes the developed methodology which is applied on operating Overhead Contact System with the help of Artificial Intelligence optimization algorithms, in order to validate desired results. The advanced method incorporates all the available protection, i.e., earthing wires and surges arresters, for the more effective lightning protection of transmission line which selects optimum values using optimization algorithm. Optimization algorithm calculates the optimum line insulation level, the grounding resistance, energy absorption capability of surge arresters, surge arresters' installation interval, and a number of installed surge arresters depend on the cost values to the lightning failure costs.

#### **1.4 Case Study Overviews**

The two interrelated studies considered in this thesis are;

- a) To the establishment of Typical values of modeled parameters for representing current situation based on the waveforms of Multiple lightning strokes, grounding resistances and Multi-grounding resistances of the existing system in ATPDraw.



- b) To analyze lightning performance of 25 kV AC, 50 Hz Catenary Contact System which divide into five studies;
- i. Characteristics and Behavior of Transient Current during single and Multiple Lightning strokes on Train's pantograph, on top of Mast, Return wire (Earthing wire), and Catenary wire,
  - ii. Analysis of Flashover affected by Grounding resistance in Transient Current characteristics during single and Multiple Lightning strokes on Train's pantograph, on top of Mast, Return wire (Earthing wire), and Catenary wire,
  - iii. Flashover Effect with Multi-Grounding resistance to nearby Masts in Transient Current behavior and characteristics during single and Multiple Lightning strokes on Train's pantograph, on top of Mast, Return wire (Earthing wire), and Catenary wire, and
  - iv. Mitigation of Flashover with Transient Current behavior and characteristics during Multiple Lightning strokes on Train's pantograph, on top of Mast, Return wire (Earthing wire), and Catenary wire.
  - v. The optimization of the lightning performance of 25 kV AC, 50 Hz Catenary Contact System with the help of MATLAB software.

## 1.5 Objective

The main objectives of the thesis are;

- a) To analyze and improve the lightning performance of Overhead Catenary System.

- b) To optimize insulation level, grounding resistance, surge arrester's energy absorption capability, the surge arrester installation interval, and number of surge arrester in Overhead Catenary System.

## 1.6 Limitations of the Thesis

In the intended improvement studies, analysis and mitigation of the lightning performance for the Catenary Contact System in transient current behavior during lightning strikes on Train's pantograph, on top of the mast, return wire (Earthing wire), and catenary wire due to overvoltage situations were performed. For analysis evaluation, the waveforms of lightning strokes, grounding resistances and Multi-grounding resistances effects were reviewed in transient current behavior and characteristics during single and multiple lightning strokes on the overhead line. In addition to mitigate overvoltage in the system, the transient current behavior during multiple lightning strikes on Train's pantograph as a critical overvoltage condition in A 2×25 kV, 50 Hz AC Catenary Contact System was desired. The estimation of optimum line insulation level, the grounding resistance, energy absorption capability of surge arresters, surge arresters' installation interval, and the number of installed surge arresters on overhead line equipment were determined under the proposed lightning performance index for stabilized the system against lightning disturbances.

## 1.7 Thesis Structure

The outlines of this thesis are as follows:

**Chapter 1** provides an introduction, Thai Railway Electrification System, Problem Statement, Case studies overview, objective, scope and Thesis Structure.

**Chapter 2** explains a review of Railway Electrification System, electric traction, DC motor drive, AC motor drive including the existed System, Preliminary Study, Analysis of Elevated Structure and Catenary Lightning Range, and proposed a system for overhead catenary system. This chapter gives the background of the electrical system behind railway electric vehicles.

**Chapter 3** illustrates the modeling of an essential element of an overhead catenary system including its setup and techniques for simulation purposes.

**Chapter 4** exhibits the outcomes for the simulating lightning consequences and mitigate the effects in ATP-EMTP. It also showed the optimum parameters with the help of AI optimization techniques in MATLAB software.

**Chapter 5** discusses the results obtained in Simulation and their usefulness in lightning protection for Railway electrification networks.

**Chapter 6** concludes the results of the overhead catenary system against lightning disturbances in line insulation and recommends actions to be carried out.

## 1.8 Chapter Summary

This chapter explained the general introduction about an electric train with their advantages at the different type and their various prime mover as electrical energy. Also, it described in short about Thai Railway Electrification System and its components Apart from that, in the problem statement, it showed how lightning strokes affect the overhead catenary system and what the action should take to protect the system. Lastly, it direct to the case study overview, objective, and scope of research including an outline of the thesis have been mentioned in this chapter.

## **CHAPTER 2**

### **LITERATURE REVIEW**

#### **2.1 Introduction**

This chapter reviewed electric train, including the significant potential for the application of electrification system in the railway, electrical supplies remain impressive as electric vehicle operates without having an on-board prime mover. An electric train is a series of a vehicle powered by electrical energy to run along a rail track which used to transport passengers or cargo. Electric locomotive, Electric Multiple Unit, A Battery Electric Multiple Unit, and Tram are the most of the electric trains used through the worlds. Since the second half of 19<sup>th</sup> century, technology innovation has been improved and upgraded electrification of railway line due to the advantage of electric traction over diesel-electric traction and Hybrid traction. In order to increase speed, safety, efficiency, desired environment and reliability of economic enhancement, a human being has demanded this service for energy dependent (Lu, 2011). As demonstrated in Utlu and Hepbasli 2006, Railway travel is the friendly mode of transport depend on energy efficiency and the environment. Little energy is dissipated through rolling resistance due to the full contact (Hibbeler, 2008). Due to the benefits of the convoy formation, Railway locomotive and multiple unit trains have good aerodynamic performance (Browand, McCallen, Ross, Orellano, and Sperling, 2009). Railway locomotive and multiple units can operate without having onboard prime mover by getting electric energy from Electricity.

## 2.2 Railway electrification system

A railway electrification system is a system which operates without having an on-board prime mover by supply electrical energy to railway trains and multiple unit locomotives. There are several different electrification systems in use throughout the world. Railway electrification requires a significant capital expenditure for installation although it has many advantages. A higher power-to-weight ratio is the main advantage of electric traction over diesel/steam-electric traction and Hybrid traction that create power on board. Electricity permits faster acceleration, and higher tractive effort on steep gradients to increase speed, safety, efficiency, desired environment and reliability of economic enhancement depend on electric energy as it becomes a human demand. On trains equipped with regenerative brakes, descending gradients require the little use of air brakes for the locomotive's traction motors as becoming generators sending current back into the supply system and onboard resistors, which transforms the excess energy to heat. The lack of exhaust fumes at the point of use, less noise and lower maintenance requirements of the electric traction units are the other advantages of a railway electrification system. Electric trains produce fewer carbon emissions than diesel trains especially for the countries where electricity comes primarily from non-fossil sources in a given sufficient traffic density.

Operations of electrified railway became more efficient because there is no need to switch between methods of electric traction unless it used more than one system (multi-system locomotives or other rolling stock) which still required a switch of traction method. Voltage, Currents, and Contact system are three parameters which used to classified Railway Electrification system. Overhead Line System, Third Rail

System, and Ground-Level Power Supply System are the railway electrification systems which discussed in this chapter as follow

### 2.2.1 Overhead line system

Overhead Line System is a railway electrification system which uses overhead lines or overhead wires to transmit electrical energy at a distance from the energy supply point to trams, trolleybuses, and trains. The voltages above 1 kV DC are usually limited to overhead wiring for safety reasons. The system of 600 V, 750 V, 1500 V, 3 kV for Direct Current (DC), 15 kV, and 25 kV for Alternative Current (AC) at 16.7 and 50 Hz are the most common voltages used by overhead line system (Frey, 2012).

The principle of one or more rails or overhead wires (particularly in tunnels) is designed by overhead line situated over rail tracks, raised to a high electrical potential by connection to feeder stations from a high-voltage electrical grid at regular intervals.

A pantograph, bow collector, or trolley pole are the devices used to collect their current from an overhead line system to the electric trains as shown in Figure 2.1. The device depresses against the underside of the lowest wire of an overhead catenary network and the catenary wire. The collectors of current are electrically conductive which allow current to flow through to the tram, trolleybuses, and train and back to the feeder station through the steel wheels on one or both running rails. Overhead line system is classified according to the devices used to collect current from an overhead line system to the electric trains. Bow Collector System, Trolley wire in overhead line system, and Catenary Overhead System are three overhead line systems presented in this chapter as follow

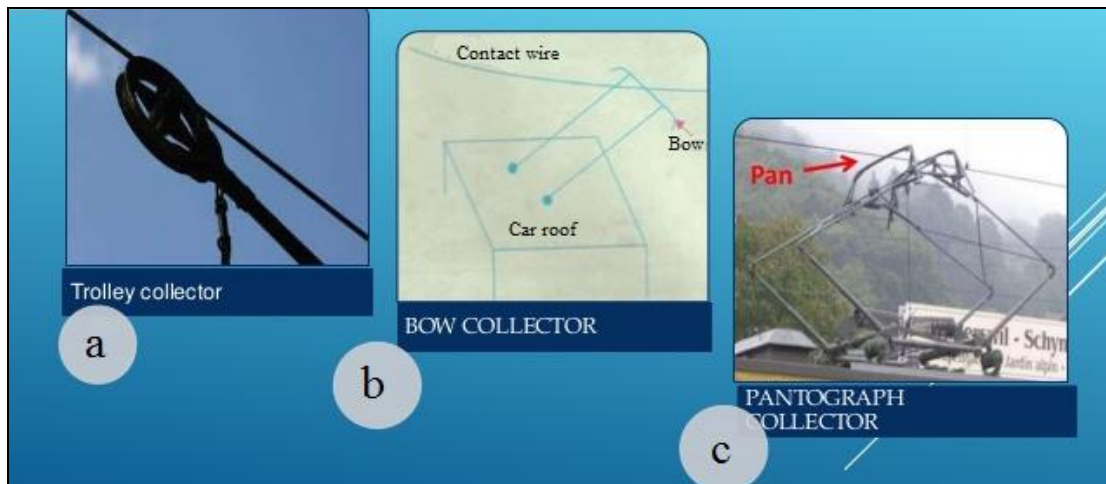


**Figure 2.1** Current Collector (Naupane and Rimal, 2016).

#### 2.2.1.1 Bow collector system.

Bow Collector System is an overhead line system which uses bow collector to collect current from an overhead line system to the electric tramcars. In either the late 1880s or early 1890s, the Siemens electric company was first used the bow collector by in its early electric tramcars conceived by German inventor Ernst Werner von Siemens. 600 V DC, 750 V DC were the most common voltages used by overhead line system (Frey, 2012).

The bow collector is one of the straightforward and most dependable methods of current collection used on tramways. The very earliest versions were simply a very heavy-gauge steel bars, or wire bent into a shape of rectangular and mounted long-side-down on the roof of tramcar. The collector height was on its top of the edge which would scrape across the wire above. The section of the top is made with a 1-inch broad or thereabouts steel rod, machined to have a bow-shaped cross section. This bow-shaped rod is referred to as the 'collector plate, and in later models may be up to several inches wide as shown in Figure 2.2.

For the simple framing methods mentioned above, it was gradually replaced by more sophisticated and complex methods, but the general operation mode remained the same (Kiessling et al., 2009). The design changes were most noticeable on systems where both single and double deck cars were used on the same network. Single deck trams usually have high and lightly constructed collectors with frames which complicated to support the huge collector of the cast-steel plate, while double deck cars usually have more massive collectors with less complex structures as shown in Figure 2.3. For maintaining good electrical contact, the bow collector must bring to bear enough intense pressure on above of the wire, and so that the complicated networks of weights or springs were put into use to ensure excellent electrical contact to maintain efficient operation (Kiessling et al., 2009).

Suitably, the top edge of the collector plate which would rise several inches above the wire collector should be mounted on the bow when the collector frame is standing straight up. Thus, when the time comes to move in the opposite direction, the collector must be swung over on it which usually leads opposite to the direction of travel. In the case of allowing this to happen, the wire of overhead must be lifted by several inches at places where the bows were swung over, in such ways the terminals were turn-outs. In the previous operation, it is usually achieved by pulleys and ropes. A horizontal position was folded down by the collector when the car was not in use. In early years, most of the cars had no means to swing over by the bows. It was thought that this could happen automatically when the tram car started traveling the other strategy, but collectors such as these were a nonfulfillment. Most Soviet trams of which some are still in use in ex-USSR had no means to swing the bowl over (Frey, 2012; Kiessling et al., 2009). These trams were



not invented to travel two ways. Another example is tramcar which had two bow collectors for the two directions of moving (Bow collector, 2017; Kiessling et al., 2009).



**Figure 2.2** An old tram with a bow collector (Bow collector, 2017).



**Figure 2.3** Tram with a bow collector (Bow collector, 2017).

The bow collector has fewer traveling parts than the trolley pole, but had high weight and sometimes more complex to construct. The overhead wires construction for bow collectors is simpler than trolley pole wiring. As bow collectors do not have revolving mountings, the collector could not jump off the fence to follow the wrong one in intersections as trolley poles sometimes do. Thus, the frogs of overhead and escorts for trolley poles were not obligatory with bow collectors. However, the collectors of the bow were much noisier than trolley poles. The overhead wires for bow collectors are stretched tighter than for trolley poles, and

straight sections are 'staggered', that is, the wire does not run completely straight down the track centerline, but rather zig-zags slightly across a small distance. The distributor was worn in the whole bow collector's collector plate and extends the collector's life.

On the Mountain Railway's implementation was unusual in that the overhead wire that slack and free to hang in a catenary. Bow collectors were used to avoiding problems with trolley poles in high winds on the hilly route (Hennessey, 2008). The hill line also was used a Fell rail for braking. Each car has two rigidly vertical bow collectors, with a slack wire above them making contact under its weight. At its suspension points, the collectors are not quite tall enough to make contact with the wire. As far enough apart, in relative to the spacing of pole, it was out of touch with the cable, while the other is mid span and making good contact. The collectors can only be lowered by unbolting them at roof level, while the power is off. This inability to isolate them easily hampered firefighting when car 5 caught fire.

Similarly, collectors were also utilized at first on the nearby and slightly earlier during Electric Railway invasion. With weak contact, and so the loose wire, the system was trouble initially developed. A tensioned cable usually gave a good connection when broke contact passed over the collector at the pole. The wire of slackening and deliberately lifting it up clear of the collector at the poles allowed its weight to give a reliable connection over the other collector, spaced to be at the midpoint between masts. In those years, a revised collector was in use within the short time. A small hinged bow frame was placed on top of the fixed uprights, giving a sprung contact as shown in Figure 2.4. Bow collectors systems were not last though and were replaced with trolley poles (Edwards, 1998).



**Figure 2.4** Rigid bow collectors at Snaefell Summit station (Hennessey, 2008).

#### **2.2.1.2 Trolley wire overhead line system.**

Trolley Wire Overhead Line System is an overhead line system which uses trolley pole to collect current from an overhead line system to the trolleybuses. It comprising a trolley wire, Span wire or bracket arms and Traction poles, and wall anchors (or rosettes). The name ‘trolley wire’ relates to the use of a trolley pole on the tram to collect current, although trolley wire systems may also be used for vehicles equipped with bow collectors or pantographs. 600 V DC, 750 V DC are the most common DC voltages used by Trolley Wire Overhead Line System

(Frey, 2012). Circuit Configuration of Trolley Wire Overhead Line System is the same as the Circuit Configuration of bow collector system as indicated in Figure 2.5 but different contact system as shown in Figure 2.6.

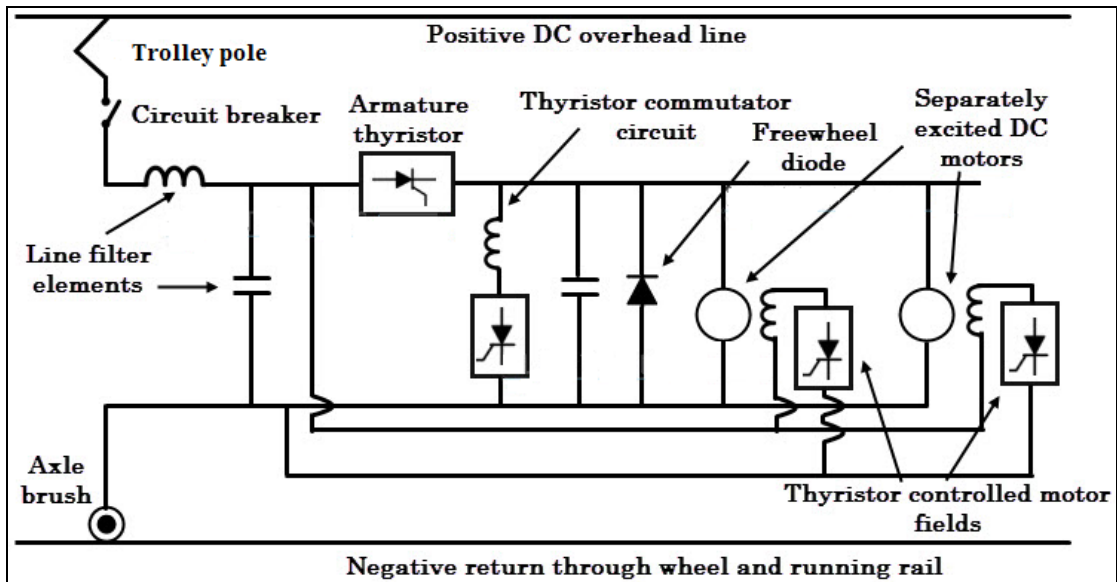


**Figure 2.5** Circuit Configuration of Trolley Wire Overhead Line System (Source: Naupane and Rimal, 2016).



**Figure 2.6** Trolley Wheel on TCRT 1300 (Frey, 2012).

A trolley pole was the device of a tapered cylindrical pole made up of wood or metal, utilized to transport electricity from a live overhead wire to the propulsion and control equipment of a trolley or tram bus. The use of overhead wire in a current collection network was reputed to be the electrical invention to ensure efficient power. Machining trolley wheels are shown in Figure 2.7.

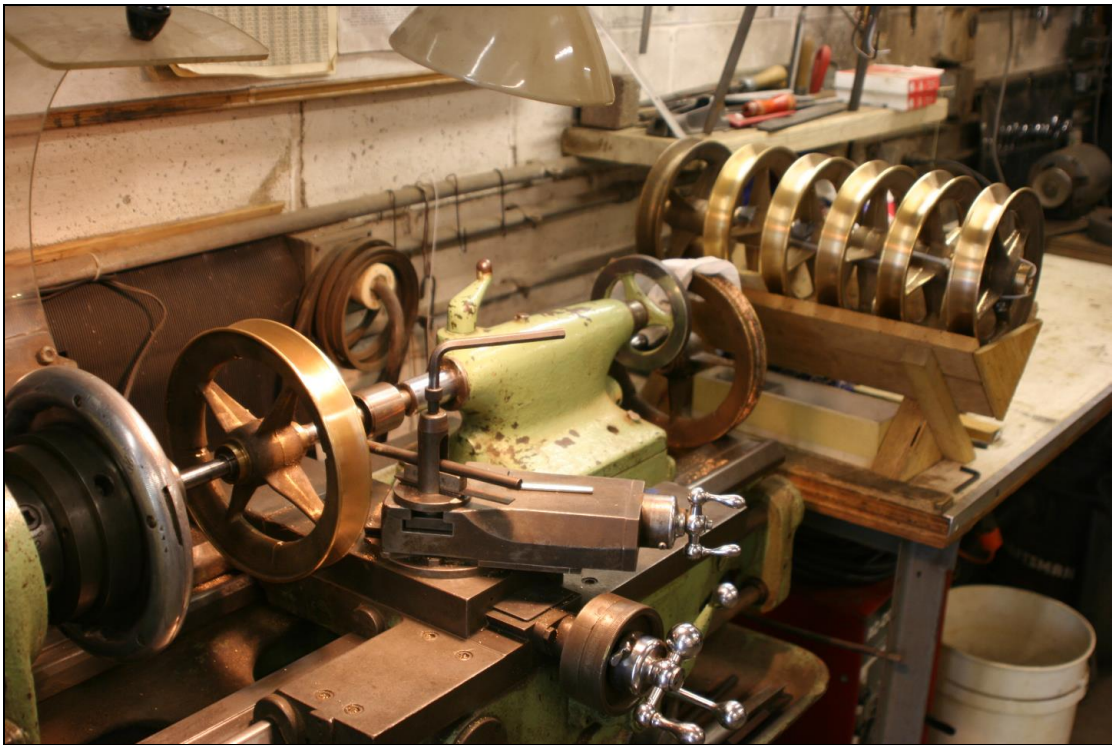


**Figure 2.7** Machining trolley wheels (Frey, 2012).

The invention of the trolley pole was predated by the term trolley. The earliest electric cars, the locomotives did not use a pole, but a system in which each engine dragged behind it, an overhead cable were connected to a small cart that rode on an overhead wires track. From the side of hauling lines, the car was made to seem like trolling as in fishing. Later, when a mast was added, a trolley pole

came to be known. The pole or the passenger car using the trolley pole was derived from the grooved conductive wheel stroller or cart which attached to the end of the pole in which the trolleys the overhead wire was also used by the term trolley for description.

An early development of an experimental tramway, Locomotive was built and having been developed by the brother of the Whitaker Wright in mining entrepreneur. At the Canadian National Exhibition (CNE), Wright has been assisted in the installation of electric railways and even have used a pole system, to evidence that its efficient system. Likewise, Wright was issued or never filed a patent. For the electric trolley pole invention, Official credit has gone to an American, for installed a working system in the railway system. As the Richmond Union Passenger Railway known, this 12-mile system was the first big-scale trolley line in the world, opening to great fanfare.

In through the 1940s and 1950s, The wheel of the grooved trolley was used on many large city systems; it was used on systems with old style around the cross-sectional wire of the overhead. The cart wheel was problematic at best that the grooved circumferential contact wheel compartments on the overhead underside wire provided minimal electrical contact and tended to arc spark excessively and maximized overhead wire wear. The newer sliding carbon trolley shoe was used with a unique grooved cross section of overhead trolley wire; the significant the sliding trolley shoe advantage was threefold which provided far better electrical contact with a considerable moderation in arcing sparking, it dramatically lower overhead wire wear as well. Many systems began changing to the sliding trolley shoe in the 1920s as it turned its extensive system in the late 1920s (Frey, 2012). Curiously, Philadelphia

did not turn its trolley wheels on its remaining streetcars until 1978. Although a vehicle with a cart wheel may evoke a look of old fashioned, the trolley shoe was far more practical and modern as well as economical in use as indicated in Figure 2.8.



**Figure 2.8** Modern trolley poles as installed on Vancouver's low floor electric trolley buses (Frey, 2012).

In Figure above, the overhead wire was not attached to a trolley pole. The pole sits atop a sprung base on the roof of the trolley vehicle, the springs maintaining the tension to keep the cart shoe or wheel in contact with the wire. In the case of the pole was made up of wood, a cable brought down the electrical current to the locomotive (Frey, 2012). For instance of a metal pole used as a wire, it required the base to be insulated from the vehicle body as itself may be electrically live.

On double-ended railway cars systems with running capability in both directions, the trolley pole was always be dragged behind the car and not pushed or rewiring as very likely as it could also destroy the overhead wires (Frey, 2012). At terminus ends, therefore, the conductor must revolve the pole of the trolley around to



face the correct heading, pulling it off the wire either with a pole or a rope and strolling it around to the other point. In many cases, two trolley poles were provided, one for each direction, so in this instance, it was just a raised one matter and reducing the other. Since the conductor reduced the other while the operator could high the pole at one end, this was much easier and save time for the engineer. Care must be taken to increase the downed pole first and eliminate the damage caused by arcing between the wire and pole. In the United States, the system of dual-pole was the most recurrent arranged on double-ended locomotives. However, thrusting of the pole called back-poling in the spear-poling was quite regular in which the trams were moved at slow speeds, such as at wye terminals also known as reversers while backing to the sheds.

Usually, Trolley poles were lowered and raised manually by a rope from the back of the locomotive (Frey, 2012). The cable feeds into a spring reel mechanism, called a trolley retriever or trolley catcher. The catcher of the trolley contains a detent, like that in an automotive shoulder for safety belt, which seizes the rope to prevent the trolley pole from flying upward at the pole that was desired. The similar looking in retriever added a mechanism of spring that yanks the mast downward when it should leave the wire, and pulled it away from all overhead wire fittings. Catchers are commonly used on trams operating at lower speeds, as in a city, while retrievers were used on suburban and interurban properties to limit destruction at high speed to the overhead.

On some older networks, the poles were raised and reduced using a long mast with a hook of the metal. As it's available, it may have been made of bamboo due to its natural straightness, length, and strength, combined with its

relatively light weight and the actuality that it is an insulator. Usually, Trolleybuses were carried one with the locomotive, for use in the event of retirement, but systems of tram normally had them placed along the route at locations where the pole of trolley could need inverting.

The poles used on trams were typically shorter than those used on trolleybuses, to allow the bus to take fuller significant of it's not being confined to a solid way in the rails of the street. By giving a lateral steerability degree that enables the trolleybus to load passengers at curbside, it was also done to all buses.

In a railway vehicle, at a trolley car or tram was used on, a single trolley pole regularly collects current from the wire of overhead, and the rails of the steel on the tracks react as the electrical return. On the other hand, Trolleybuses might use two trolley poles and dual overhead wires, wire, and one pole for the positive live current, the other for the negative or neutral return. Some of the tramway systems were also utilized the dual cable system, while others streetcar system were not. For aid in the spread-out reduction of electrolytic damage, underground pipes and metallic structures where most tram lines maneuvered with the wire positive concerning the rails.

All trolleybuses were used trolley poles, and thus trolley poles remained in use worldwide, wherever trolleybuses are in operation, currently in some 340 cities, and different manufacturers were continued to make them, including some cities apart from this towns. On most railway locomotive using overhead wire, however, the pole of trolley has provided the way to the bow collector, and later, the pantograph, a construction of folding metal that depresses a full contact pan against the wire of the overhead. While more complicated than the trolley pole, the

pantograph has the sign of being more stable, being almost free from wiring, at high speed, and being easier to increase and reduce automatically. Additionally, on double-ended trams, they remove the need to turn the trolley pole when changing direction manually. The use of bow collectors or pantographs exclusively also eliminates the need for frogs of wire by switches in the overhead wiring to make sure the pole goes in the correct direction at junctions as shown in Figure 2.9.



**Figure 2.9** Locomotive with trolley poles (Frey, 2012).

The very few tram/streetcar systems apart from heritage streetcar lines in worldwide continue to use trolley poles on vehicles used in standard service. Among the largest exceptions are the vehicle systems of the Subway-Surface lines and Tramways was one of the systems in small size using trolley poles for regular service.

These systems and a few others worldwide retain use of trolley poles, even on new streetcars, in order to resist the hardness and expense of restyling

stretches of existing overhead wires to accept pantographs. Light rail cars or Trams was equipped with pantographs normally cannot operate on lines with overhead wiring designed for trolley pole collection. It is possible to build overhead wiring that was able to accommodate both trolley poles and pantographs, but such models are more expensive to maintain and are seen only in cities where modern light rail cars or streetcars utilize same tracks with vehicles of preserved historic.

### **2.2.1.3 Catenary contact system**

Catenary Contact System is an overhead line system which uses a pantograph to collect current from an overhead line system to the trains. The pantograph of Catenary Contact System allowed an electric rail vehicle to travel at higher speeds without losing contact with the catenary which was an improvement over the simple trolley pole as prevailed up to that time of invented pantograph.

In a flat side, the pantograph was invented at the Railroad and in worldwide by Siemens & Halske. The simple diamond-shaped roller pantograph was invented by the Key System shops for their commuter trains which ran between Bay section of the some Area in some countries. In photographs of the first day of service, it also appeared in the modern locomotive. After that, for many decades, the same diamond shape was used by systems of electric rail around the world and still in use by some today (Frey, 2012).

During the mid-20th century, rotary converters or mercury arc rectifiers were used to convert utility (mains) AC power to the required DC voltage at feeder stations. Today, this is usually done by semiconductor rectifiers after stepping down the voltage from the utility supply.

In almost all overhead lines system as known variously as Overhead contact system (OCS) in Europe, except Spain and UK. Also, Overhead equipment (OHE) in the UK, India, Malaysia and Pakistan, Overhead line equipment (OHLE or OLE) in the UK, Overhead wiring (OHW) in Australia, and Catenary in United States, UK, India, Singapore in North East MRT Line, Spain and Canada (Frey, 2012). 1500 V DC, 3 kV DC, 15 kV AC, 16.7 Hz and 25 kV AC, 50 Hz are the most common voltages used by Catenary Contact system (Frey, 2012). Catenary Contact System is classified according to the driven actuating mechanism used to drive an electrical motor by received current from overhead line system. DC Catenary Contact system, AC-DC Catenary Contact system and AC-DC-AC Catenary Contact system are three Catenary Contact system which classified according to the driven actuating mechanism used to drive an electrical motor by received current from overhead line system.

### **1. DC Catenary contact system**

DC Catenary Contact system is a Catenary contact system which supplies DC power to the contact system (pantograph) and then applied to the DC motor. 750 V DC, 1500 V DC, and 3 kV DC are the most common voltages used by DC Catenary Contact system for DC motor drive.

Power supply voltages are fed from substations which are located 3-5 km for suburban services and 40 to 50 km for mainline services. These substations collect power (typically, 110/132 kV, 3 phase) from electric power grids. This three-phase high voltage is stepped down and converted into single phase low voltage using Scott-connected three phase transformers as shown in Figure 2.10.

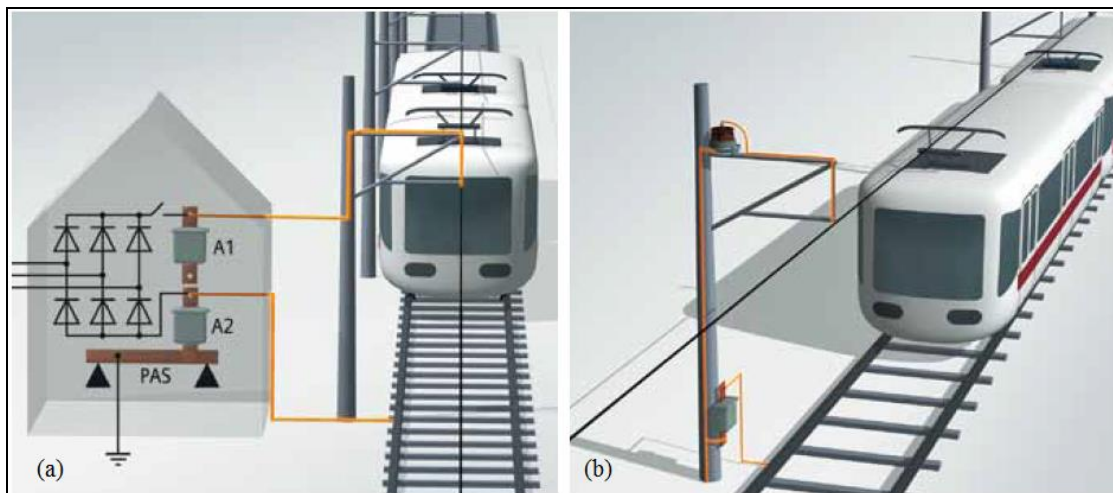


**Figure 2.10** Circuit Configuration of Substation receive power from three phase high voltage to electric train (a) near to substation (b) away from the substation (Source: Catalogue RAIL Surge Arresters, 2016)

The DC voltage using suitable converters or rectifier such as power electronic converter, rotary converters, mercury arc converters which were then converted from single phase low voltage and then supply to the contact system. In this system, electrical motors are operating on DC supply to produce necessary movement of the electric train. In this system, mostly DC series motors are used (Source: Naupane and Rimal, 2016). Circuit Configuration of DC Catenary Contact System is shown in Figure 2.11.

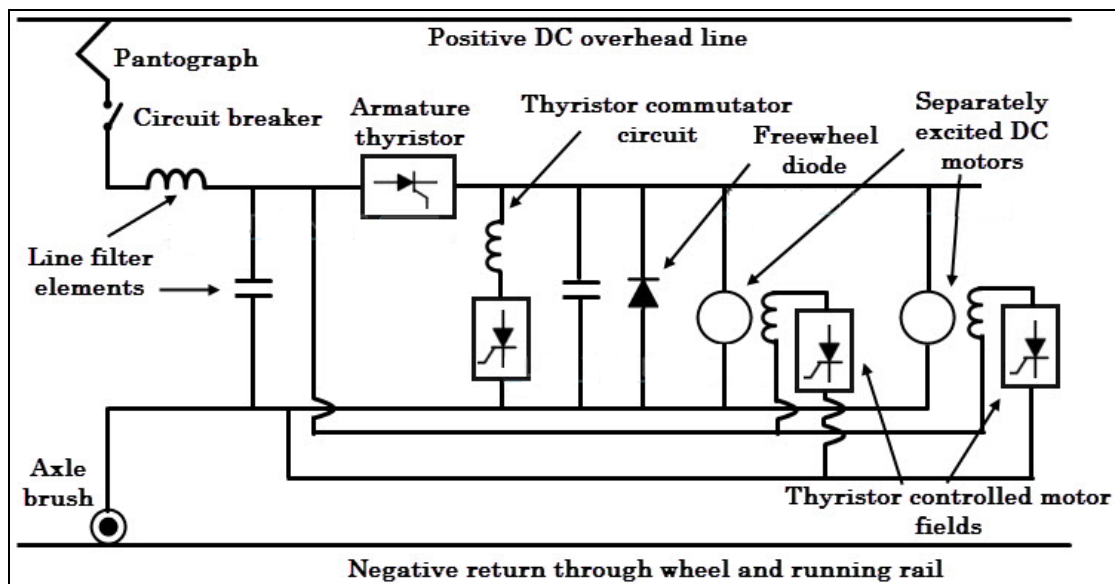


**Figure 2.11** Circuit Configuration of DC Catenary Contact System

(Source: Naupane and Rimal, 2016).

## 2. AC-DC Catenary contact system

AC-DC Catenary Contact System is a Catenary Contact System which used to supply AC single phase supply to the contact system (pantograph) and converted into DC using rectifier in the locomotive and then applied to DC series motor. This system is most popular and widely used system everywhere. It combines the single-phase high voltage AC distribution at the frequency of industrial with DC series motor traction. In this network, the overhead line carries single phase, 25 kV, 50/60 Hz supply which is then stepped down to the desired range using step-down transformer located in the locomotive unit itself (Wensheng, 2016). The significant of this system include less number of substations, higher starting efficiency, lower cost of fixed installations and simple substation design. (Source: Naupane and Rimal, 2016). Also, Single phase AC system has less distribution cost whereas DC system

has the excellent driving capability by DC series motors. Circuit Configuration of AC-DC Catenary Contact System is shown in Figure 2.12.

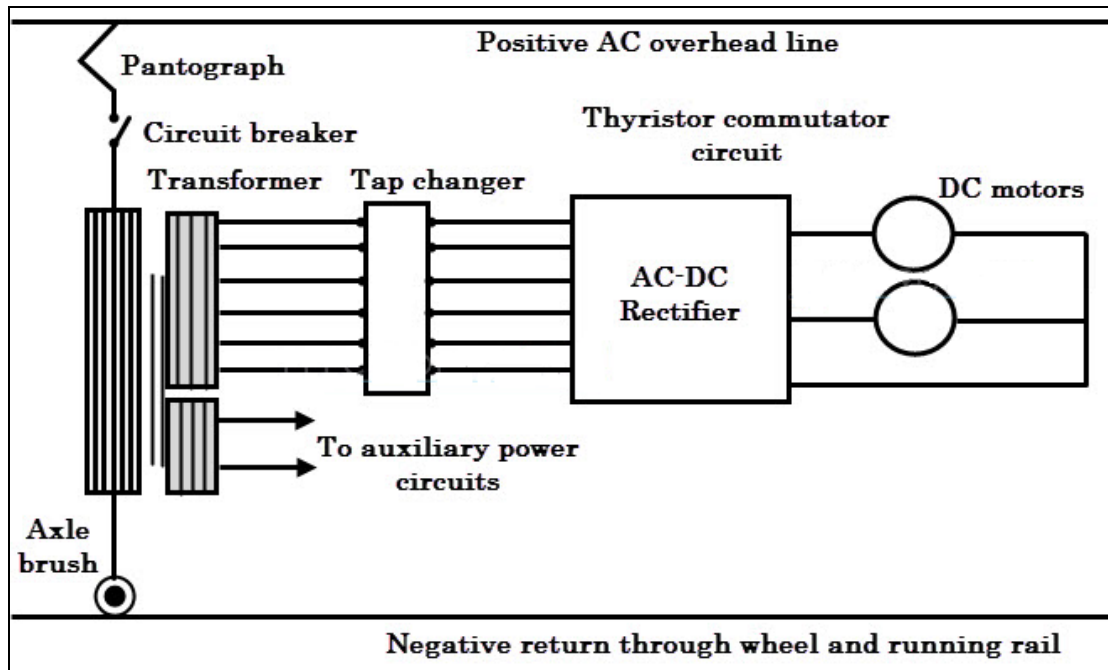


**Figure 2.12** Circuit Configuration of AC-DC Catenary Contact System

(Source: Naupane and Rimal, 2016).

### 3. AC-DC-AC Catenary contact system

AC-DC-AC Catenary Contact System is a Catenary Contact System which consists of single phase 15 kV, 16.7 Hz supply which is fed from the substation and is being carried through a single overhead conductor. The single-phase supply is then converted into three phase supply of the same frequency using phase converter equipment in the locomotive itself. The three-phase supply is then fed to induction motors to drive the vehicles. It is also possible to advance starting induction motors at high torque by diminishing the supply frequency at  $\frac{1}{2}$  to 9 Hz using



controlled inverter through silicon controlled rectifiers. The primary advantage of this system is that the two conductors of the overhead in the arrangement of three phase AC network are reduced to a single overhead wire and hence more economical (Source: Naupane and Rimal, 2016).

There is two type of AC-DC-AC Catenary Contact System which are AC-DC-AC Catenary Contact System with transformer and AC-DC-AC Catenary Contact System without a transformer (Transformerless AC-DC-AC Catenary Contact System). This type is due to usage of the transformer for stepped down voltage before applied to AC motor. Circuit Configuration of AC-DC-AC Catenary Contact System with transformer and Circuit Configuration of Transformerless AC-DC-AC Catenary Contact System with an electric multiple unit (EMU) is shown in Figure 2.13 and Figure 2.14 respectively.

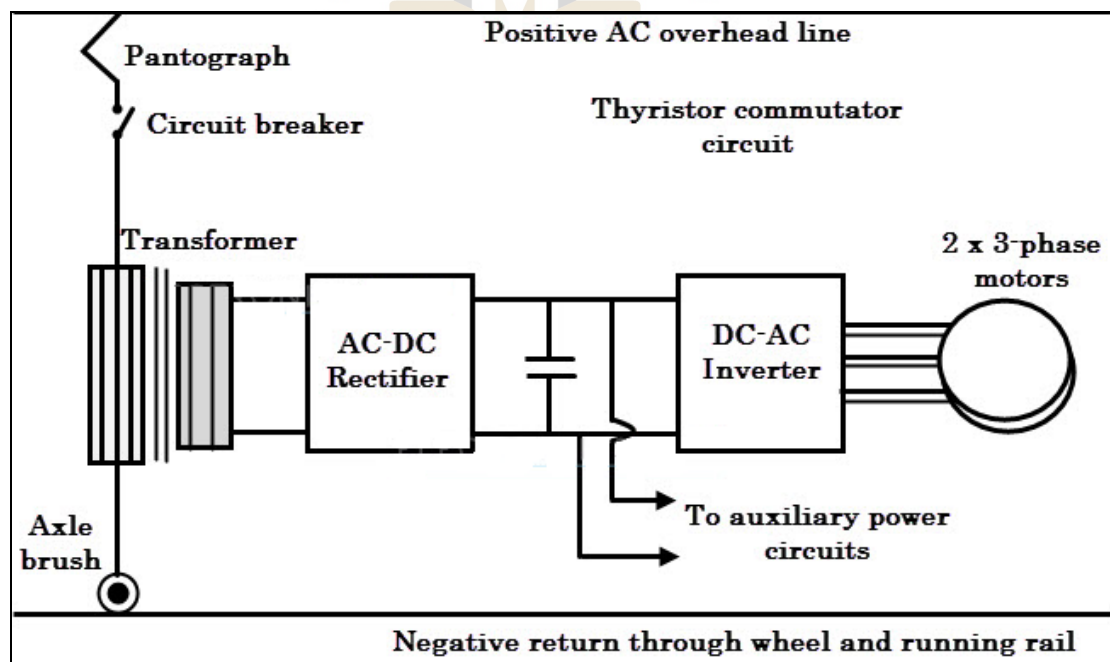


**Figure 2.13** Circuit Configuration of AC-DC-AC Catenary Contact System

(Source: Naupane and Rimal, 2016).

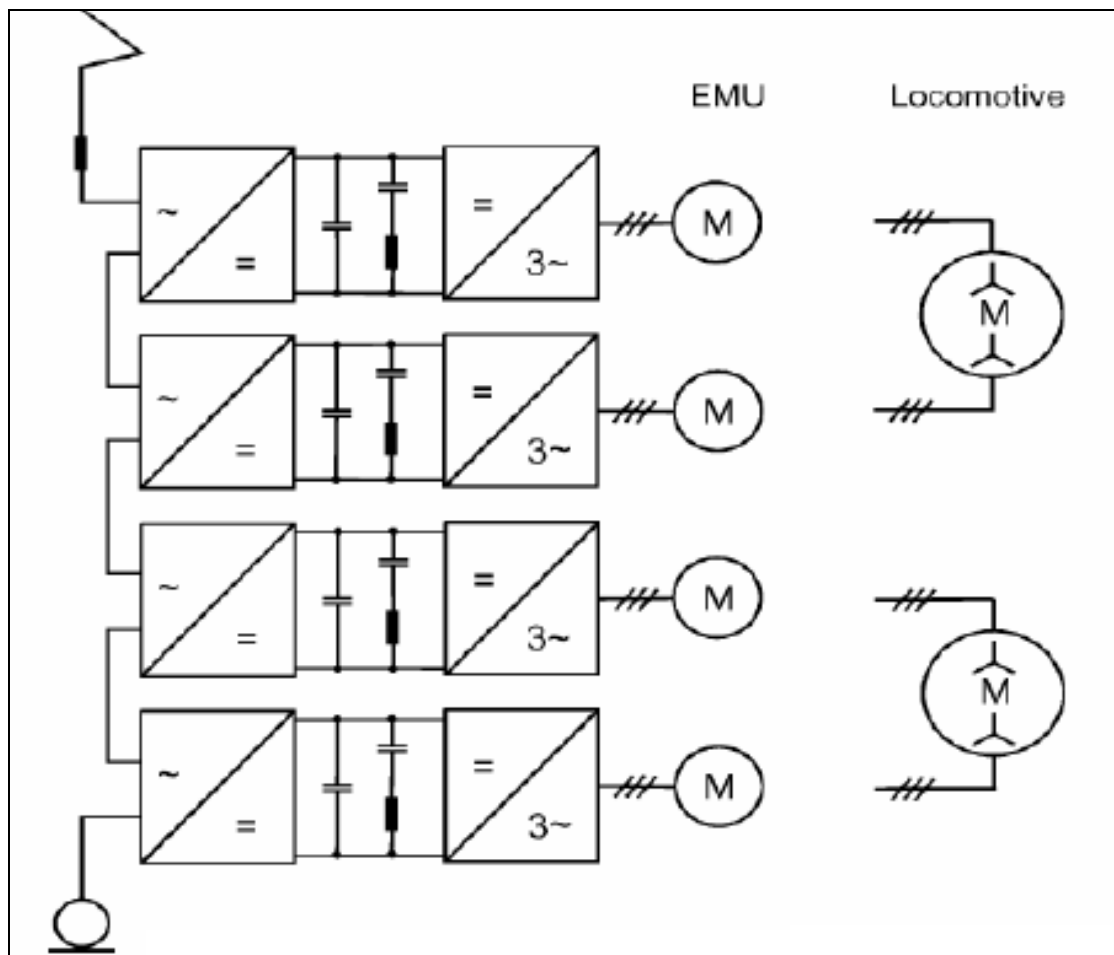


**Figure 2.14** Circuit Configuration of Transformerless AC-DC-AC Catenary Contact System (Wensheng, 2016).

### 2.2.2 Third railway system

A Third rail system is a system which used top contact (third rail) as a continuous rigid conductor placed alongside or between the running rails of a railway track to providing electric power to a railway train. 600 V DC, 750 V DC, and 1500 V DC are the most common voltages used by third rail system (Frey, 2012). It is used typically in a rapid transit or mass transit system, which has alignments in its corridors, almost entirely or fully separated from the outside environment. In most

instance, systems of third rail supply direct current (DC) electricity. The electrification of the third-rail system is unrelated to the third rail used in dual-gauge railways. The third rail is at the top contact, with a white canopy above it as shown in Figure 2.15.

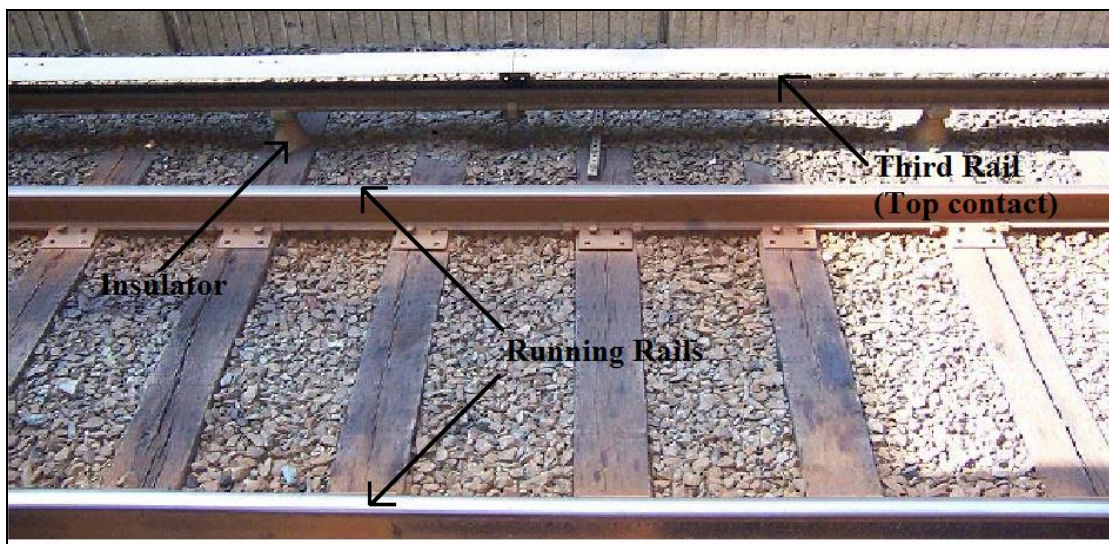


**Figure 2.15** Third rail at the West Falls Church Metro stop near Washington, D.C., electrified at 750 volts (Frey, 2012).

The current from the third rail returns to the power station through the two lower rails which are the conventional running rails. In Third rail systems, an electric traction power to railway trains was provided by using an additional track which called a conductor rail. On most systems, the rail of the conductor is replaced on the ends outside of the sleeper in the running rails, but in some cases, a central conductor rail is used. The conductor rail is supported on ceramic insulators or insulated brackets, typically at intervals of 10 feet (3 meters). The trains have blocks of the metal contact called shoes which make contact with the conductor rail as shown

in Figure 2.16. The generating station through the running rails is returned by the traction current. The conductor rail is usually made of the running rails and high conductivity steel which has to be electrically attached using wire devices or other bonds, to minimize resistance in the circuit of the electric. The conductor rails have to be obstructed at ramps and level crossings, and crossovers are provided at the ends of the sections to provide a smooth transition to the shoes of the train. The position of contact between the rail and the train was considerably by diversity in some of the earliest systems which used top contact, but developments used bottom or side contact, which permitted the conductor rail to be protected, covering track workers from accidental contact and protecting the conductor rail from leaf fall and snow.

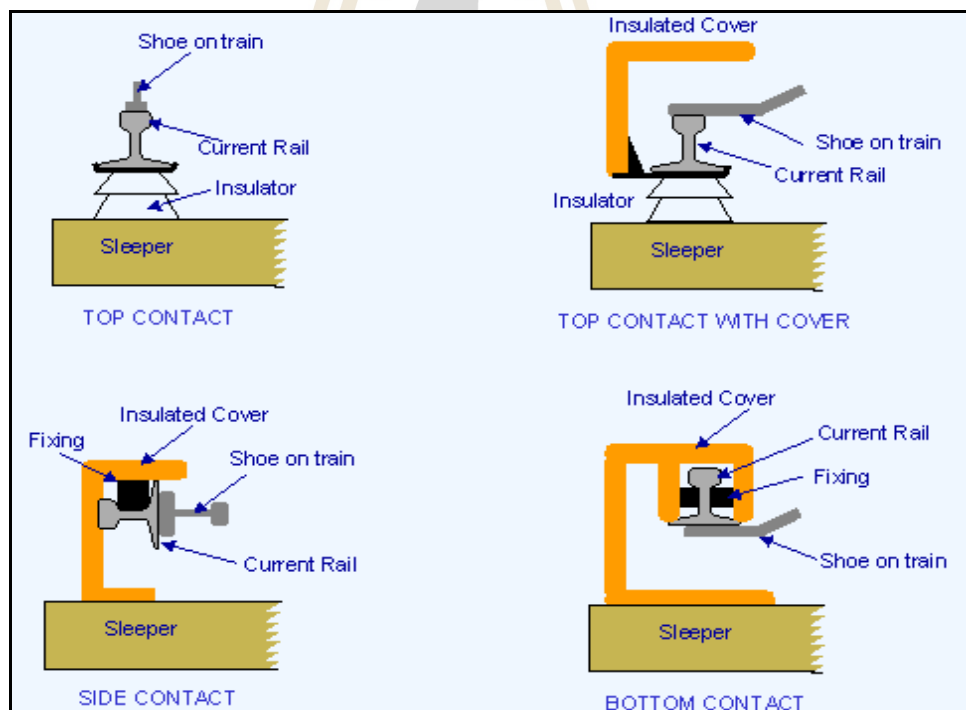


**Figure 2.16** A top-contact third railway in different design of shoes and shoe gear

(Source: Naupane and Rimal, 2016).

The systems of the electric traction where the power of electric is generated at a station of remote power and transmitted to the trains are substantially more cost-full than steam or diesel units, where the unit of power is carried on the train. This advantage is especially marked in urban and rapid transit systems with a high traffic density. So far as the first cost-effective is concerned, third-rail systems are comparatively cheap to install, relative to systems of overhead wire contact, as no structures for carrying the wires of overhead contact which are required, and then no need to reconstruct over bridges to give clearances. The visual intrusion on the environment was much less. However, third rail systems represent the hazard of higher system voltages, electric shock, (above 1500 V) which are not considered safe. Powerful currents were therefore used, resulting in considerable power loss in the system, and requiring relatively closely spaced feed points (sub-stations). In theory, a negative current is collected to the negative side of rectifier via the live rail, the third rail and so on EMU rail. When the track carries the actual current, the voltage will drop on the rail, and rail-to-ground resistance could not be completely insulated.

In safe reasons, it also extremely dangerous for a person to fall into the tracks due to the presence of an electrified rail. In this fact, however, can be prevented using doors of platform screen or the minimized risk by securing the conductor rail which is on the trackside away from the platform. Furthermore, third rail systems must either be fully grade-separated or, if they operate at grade, effective pedestrians should be stopped by implement some kind of mechanism from walking onto the tracks at grade crossings. The conductor rails end ramps where it changes sides or interrupted present a limitation of practical on speed due to the impact of mechanical on the shoe, and 160 km/h (100 mph) is considered the upper limit of possible

operation of the third-rail. However, no testing over 100 mph has been attempted. The worldwide speed record for a third rail train is almost 174 km/h (108 mph) that has attained on some electric cars by an EMU (Frey, 2012).

Third rail systems which used the top contact are prone to accumulations of ice and snow formed from refrozen snow, and this could interrupt operations. In some systems, the service was dedicated de-icing trains to deposit an oily fluid on the rail of the conductor to avoid the build-up. For a train, it is possible to stop in a location where all of its shoes are in gaps so that no power of traction is available because of the holes in the conductor rail at crossovers and level crossings. The train is said to be gapped. In these circumstances, the following vehicle is brought up behind the stranded train to push it onto the jumper cable or a conductor rail is supplied to use enough power to the locomotive to get one of its shoes of the contact back on the third rail. In some systems, this avoids the running of the very short vehicle which has fewer shoes.

### **2.2.3 Ground-level Power Supply System**

Ground-level power supply system is a railway electrification system which collects current from the ground surface. Alimentation par le Sol (APS) which mean feeding via the ground is a third-rail electrical pick-up modern method for street trams. It was innovated for the Bordeaux tramway, which was constructed from recent years and opened in nowadays (Frey, 2012). Currently, in this network, it is the only place that employed, but there were and are proposals to install it elsewhere (Frey, 2012).

As an alternative to overhead lines, the ground-level power supply is used as a primary for aesthetic reasons. The ground-level power supply is different from burying a third and fourth rail in an underground conduit (vault) between the running rails to collect current which was one of the first ways of supplying power to a tram system. In historical streetcar systems, current conduit collection was used in some cities around the world. It was fell into disuse because wires of overhead proved much less troublesome and expensive for railways of the street because in other cities all trams were replaced by buses for reasons unrelated to the power supply issue (Frey, 2012).

Unlike the track-side third rail and some mainline railways, APS does not pose a danger to animals or people and so can be used in city streets and pedestrian areas. APS uses a third rail placed between the running rails, divided electrically into eight-meter segments with three-meter neutral sections between as shown in Figure 2.17. In each tram, antennae next to which send radio signals to energize the power rail segments have skated by two power collection as the tram passes over them. At any one time, no more than two consecutive segments under the tram should be live.

In the modern Bordeaux tramway, the modern ground-level current collection was pioneered in some areas. The public had assumed that the new system would use a traditional conduit system, like that of the Bordeaux trams which ran and condemned when they well informed that it was not contemplated safe and that overhead wires were to be utilized instead. The planners developed APS as a modern way of replicating the conduit system.

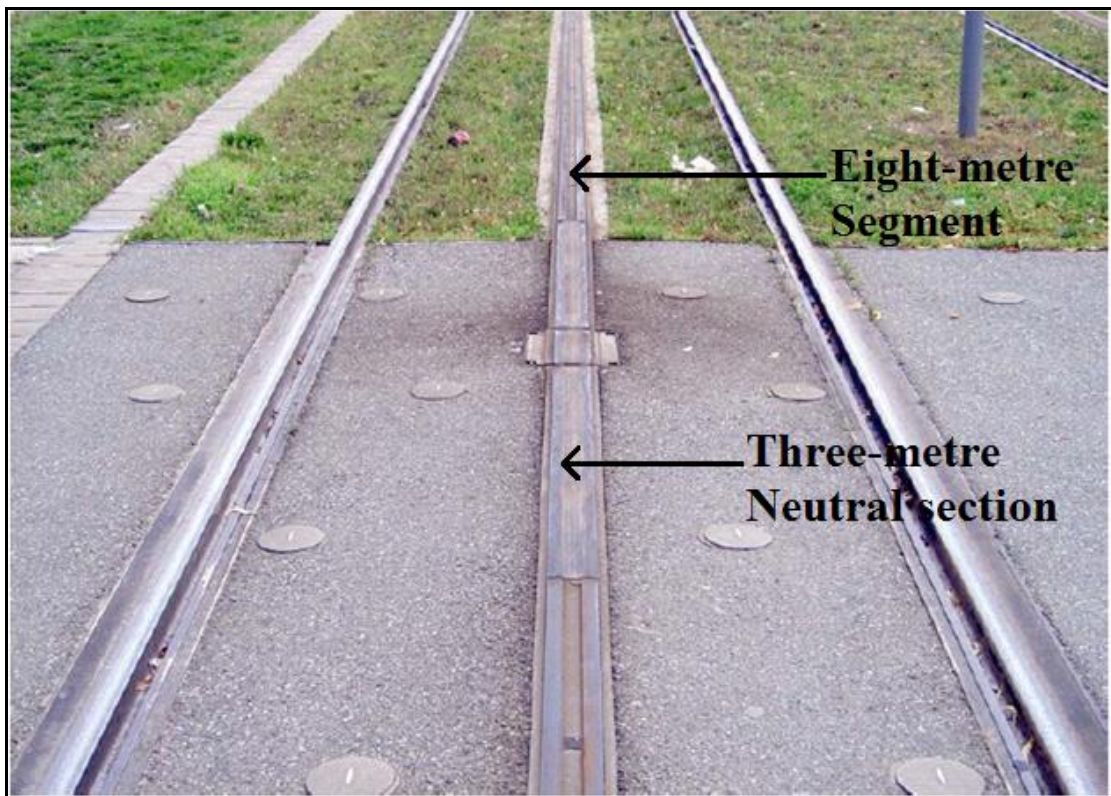


**Figure 2.17** A section of APS track (Frey, 2012).

APS was developed by Innorail, a subsidiary of Spie Enertrans but was sold to Alstom when Spie was acquired by Amec. There is 12 km of APS tramway in the three-line network of 43.3 km as of 2008. APS infrastructure is about 300% more expensive than overhead wires. Bordeaux Citadis trams use pantographs and electric overhead lines in outlying areas to compensate the cost of the trams due to APS implementation. Before use in Bordeaux, APS was proved and tested viable on a reserved track tramway in short section of it in the French city of Marseilles. Nevertheless, Bordeaux has experienced problems, with APS being so temperamental that if availability could not be managed, it would have to be replaced with overhead wires. APS was enhanced in nowadays. It was declared that 1 km of APS tramway is



to be transformed to overhead wires. The water-logging was problems which have included when the water does not drain quickly enough after torrential rains.

In recent year, Two new French tram systems were used APS over part of their networks. These were Tramway d'Angers and Tramway de Reims, with both systems which were opened. A couple of months later, another same network was added to the list, this being more developed, which used APS on a section of its second tram line. The planned Al Sufouh Tramway in Dubai was also used APS.

### **2.3 Traction power supply**

Traction power supply is an electric grid for supply electric to the electrified rail network. The objective of traction power supply is to ensure uninterrupted, reliable, and safe of the electric traction vehicle. The traction power supply is subdivided into traction power generation, traction power transmission, traction power feeding and traction power collection by mobile electric traction vehicle. Contact line system as traction power feeding system is subdivided into overhead contact line installation, third rail installation and overhead conductor rail facility (Kiessling et al., 2009). In order to comply with the requirement of reliable operation of electric traction, the following criteria are applicable, particular with regards to contact lines:

- The provision of uninterrupted traction power at the pantographs of the traction vehicles.
- The ability of the railway network to continuously absorb regenerated braking energy.

- Compliance with specified and standardized quality parameters for voltages available at pantographs of electric traction vehicles.

### 2.3.1 Traction power supply Networks.

Type of current is generally used to distinguish between the various type of Electric energy supply for electric traction. Operation limit of Nominal Voltage for Railway Electrification System according to BS EN 50163 and IEC 60850 is shown in Table 1.0 (Frey, 2012). There are DC traction network and AC traction network for traction power supply network., AC 16.7 Hz single phase traction power networks and 50 Hz single phase AC traction power system are standard power supply network in AC traction network.

**Table 2.1** Operation limit of Nominal Voltage for Railway Electrification System according to BS EN 50163 and IEC 60850 (Frey, 2012).

System Type	L.N.P Voltage	L.P Voltage	N. Voltage	H.P. Voltage	H.N.P Voltage	
	$V_n$	$V_{min2}$	$V_{min1}$	$V_{max1}$	$V_{max2}$	$V_{max3}$
600 V DC	400 V	400 V	600 V	720 V	800 V	-
750 V DC	500 V	500 V	750 V	900 V	1 kV	1270
1,500 V DC	1,000 V	1,000 V	1,500 V	1,800 V	1,950 V	2540
3 kV DC	2 kV	2 kV	3 kV	3 kV	3 kV	5075
15 kV AC,16.7 Hz	11 kV	12 kV	15 kV	17.25 kV	18 kV	24300
25 kV AC,50 Hz	17.5 kV	19 kV	25 kV	27.5 kV	29 kV	38750

L.N.P Voltage: Lowest Non-Permanent Voltage

L.P Voltage: Lowest Permanent Voltage

N. Voltage: Nominal Voltage

H.P. Voltage: Highest Permanent Voltage

H.N.P Voltage: Highest Non-Permanent Voltage

In 50 Hz single phase AC traction power network, power is supply with single phase and two phase AC 50 Hz in the universal AC traction supply which supplies electric energy for operation of 50 Hz single phase AC traction power network. Single Phase AC Power supply at 50 Hz loading power from the three-phase network of public energy supply. But this network causes current imbalance effect on the generators, which affect the consumer. The voltage imbalance is the ratio between the inverse voltage and direct voltage. This voltage occurred when power substation of three phase network powers traction was applicable. The voltage imbalance leads to a reduction in the life of three-phase asynchronous motors running on three phase currents. According to EN 60034-1, three phase motors may only be operated in power supply system where the voltage imbalance may not exceed 1% continuously or 1.5 % for only a few minutes. Figure 2.18 shows the alternative of connection 50 Hz single phase tractions power substation to the three-phase network without compensation for imbalance; indirect compensation of the imbalance; direct compensation of the imbalance ( $120^\circ$  connection) and direct compensation by  $120^\circ$  switching (Kiessling et al., 2009).

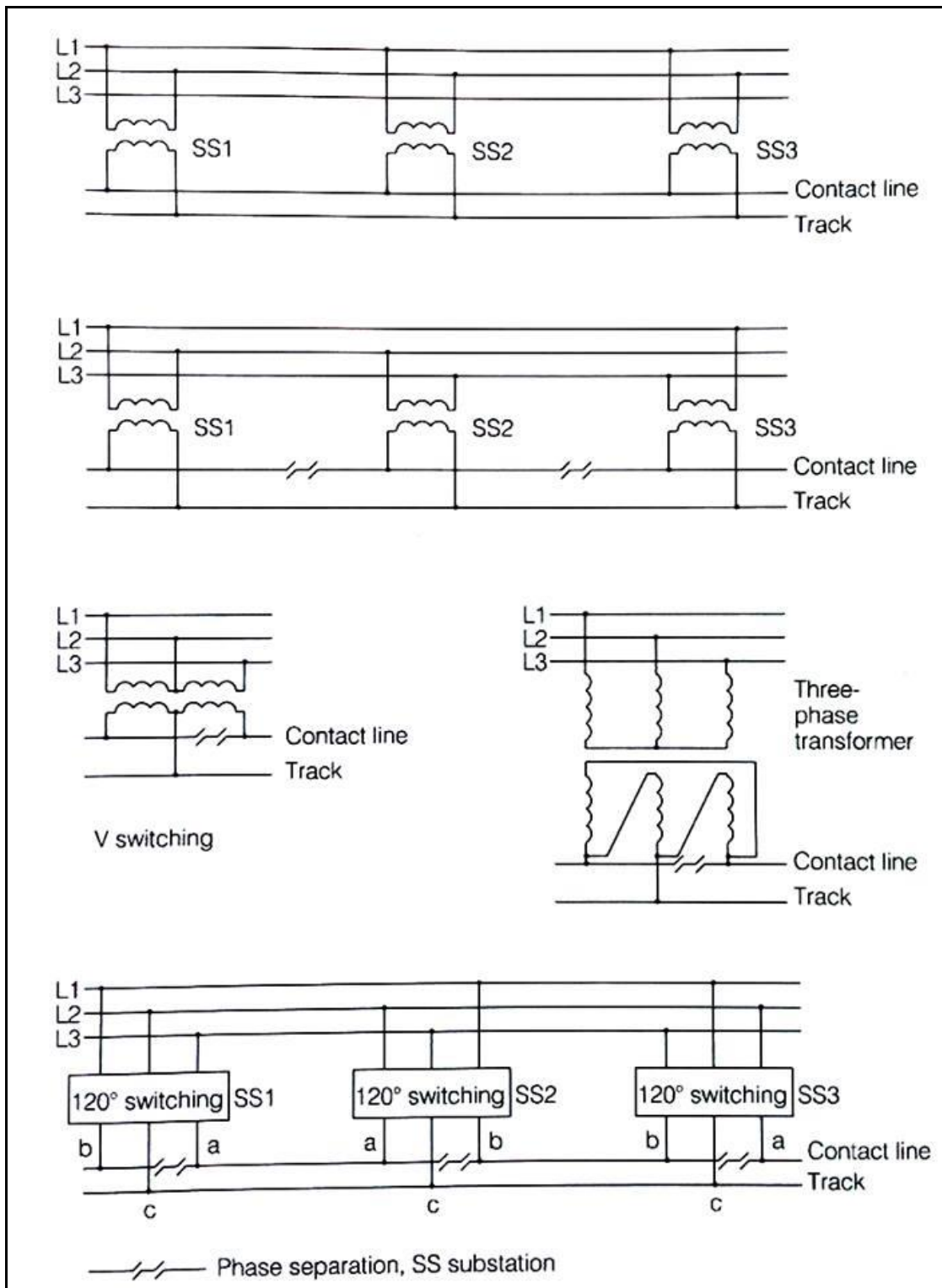


**Figure 2.18** The alternative of connection 50 Hz single phase traction power substation to the three-phase network (Kiessling et al., 2009).

Power supply with two-phase AC 50 Hz is used for high-performance traffic to improve transmission properties. This type of feeding is used additional autotransformers and return line at a potential of 25 kV. The return line acts as a negative feeder. Twin pole switchgear is required in the overhead line network. The basic design of this feeding system is seen in Figure 2.19.

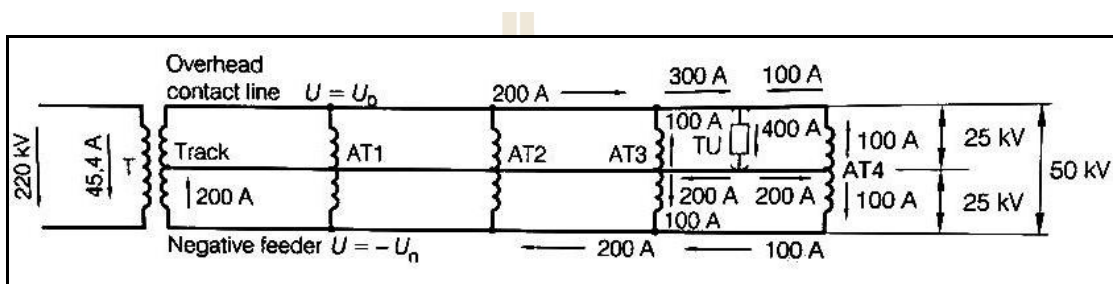


**Figure 2.19** Basic design of 2×25 kV feeding system (Kiessling et al., 2009).

## 2.4 Railway Electric Traction

Railway Electric Traction is the force used to generate motion between locomotives/multiple units and a railway, through the dry friction due to shear forces of the railway which commonly used on electrification system. Various type of locomotive and multiple units describes by Railway Electric traction. Most of the locomotive and Multiple Units due to a railway traction power system provides mechanical power from an electrical power that can be converted into kinetic and potential energy and can be used to overcome resistance to motion (Guzzella, and Sciarretta, 2007). Ability to start and haul for the specified route within maintaining timetable, long sufficiency lifetime without frequently services or nonavailability due to maintenance and standby, Fuel efficient, and environment-friendly are

requirements that should meet for Railway electric traction. These requirements should be considered in order for Railway electric traction to be running efficiently.

The earliest electric locomotives tended to be battery-powered. In 1834, Thomas Davenport, in Brandon, Vermont, erected a circular model railroad on which ran battery-powered locomotives or locomotives running on battery-powered rails. In 1839, an electric locomotive created by Robert Davidson, of Aberdeen, Scotland, and moved at 4 miles per hour on the Edinburgh-Glasgow railway. Thomas Edison built a small electrical track in 1880, using the rails and a dynamo as the motor as the current-carrying medium (Frey, 2012). The electric current flowed through the metal rim of otherwise wooden wheels, being picked up via contact brushes.

At the time of the ending 19<sup>th</sup> century, Rail electrification as a means of traction emerged, although in electric rail experiments have been detected back to the mid-nineteenth century. At this stage, due to the development of electric traction, DC motor, and low voltage DC traction line were the main electric traction power supply method due to simple torque control behavior. The inherence tractive characteristic of the induction motor and difficulty of supply electric from DC or single phase AC transmission line was the reason for the emergence of AC transmission line (Lu, 2011; Hill, 1994). The high voltage and industry frequency AC transmission became a reality in 1950's with the advancement of power electronics. Since 1950's, some of DC networks were replaced by 25 kV single-phase (16.7 and 50/60 Hz) AC transmission systems (Lu, 2011; Hill, 1994). Currently, low voltage DC transmission network and high voltage with frequency (16.7 and 50 Hz) AC transmission network became most two standard electric supply for electric traction. There are three types

of units according to power supply system based on Railway Electric Traction (Lu, 2011; Andrews, 1986; Hill, 1994; Frey, 2012).

#### **2.4.1 DC Traction Units**

DC Traction Units drawn direct current from either a conductor rail or an overhead line which is adjacent to the running rails. It was easy to control the vehicle-mounted traction equipment due to DC power supply system. It has a compact size and weight of monitoring devices regarded as power electronics technology (Lu, 2011). This network implies that DC Traction Units drawn higher current going through the supply circuits and caused higher electrical loss compare to AC Traction Units.

#### **2.4.2 AC Traction Units**

AC Traction Units drawn alternative current from an overhead line consists of a contact line carrying live current and catenaries, which is an insulated suspension system supporting the contact line adjacent to the running rails. Its overhead line is located at a certain height above the running rails. The Higher voltage level in an AC power supply system reduces the current and electrical loss. Also, fewer substations are required compared with the lower voltage in DC traction networks. Generally, it is economical to use such system for high-speed or heavy-haul railways (Frey, 2012).

### 2.4.3 Multi-System Units

AC Traction Units drawn either direct current or alternating current from either a conductor rail or an overhead line consists of a contact line carrying live current and catenaries, which is an insulated suspension system supporting the contact line adjacent to the running rails. Trains often have to pass from one system to another due to a variety of railway electrification systems which can vary within Multi-system units. This system is accomplished by turning trains at the stations for switching. In stations, it has overhead wires that can be interchanged from one voltage to another, and so the train appears with one locomotive and then departs with another. However, this is inconvenient and time-consuming. The switching stations have very expensive, and they were very sophisticated components (Frey, 2012). Multi-system locomotives that can operate at several different voltages and current types is another way to manage multi-system units. In the case of trains, it does not have to cease when passing through one system of the electrification to another, the changeover occurring where the train strands for a short time.

### 2.5 DC Motor Drive

Series and separately excited motors are the most common DC traction motors used in the railway electrification system (Lu, 2011). In the series motor, resulting in the fields are determined by the armature current due to the field winding which is connected in series with the armature. The series field allows current to flow in the motor after a corresponding field have been established. Without a relevant field having already been set, no current flows in the motor. When iron saturation occurs at a higher current, the field becomes non-linear., Wheel-slip correction can be



inherently realized with a high starting torque followed by a constant power operation regime with increasing speed for any series traction motor with a steady terminal voltage. For stable operation, this feature is desirable. By varying the terminal voltage at the starting stage and the field through the diverter resistor at a greater speed, Speed control for a series DC machine can be achieved. This process is usually referred to as a Field weakening operation. Although, wasteful of power and limited use occurred when a series resistor inserts into the motor circuit.

The overall characteristic as shown in Figure 2.20 obtained when the series resistance is varied in a camshaft controlled train. A constant torque generated at the beginning by maintained constant armature and field current. The output power is increased until the base speed with the growth of rotating speed. The output torque decreased by reduced field current. This operation called field weakening operation. The armature current begins to drop and further bring down the torque after the rotating speed is over the transition speed. Finally, the motor goes into a weak field operation.

The field excitation circuit is independent of the field circuit for the separately excited motor. By changing the field current or the armature voltage, the speed of the motor is controlled. This type of motor with its separately excited field can be used for regenerative braking. Three control operations have been identified with different characteristics regarding torque, current, speed, and power (Hill, 1994).

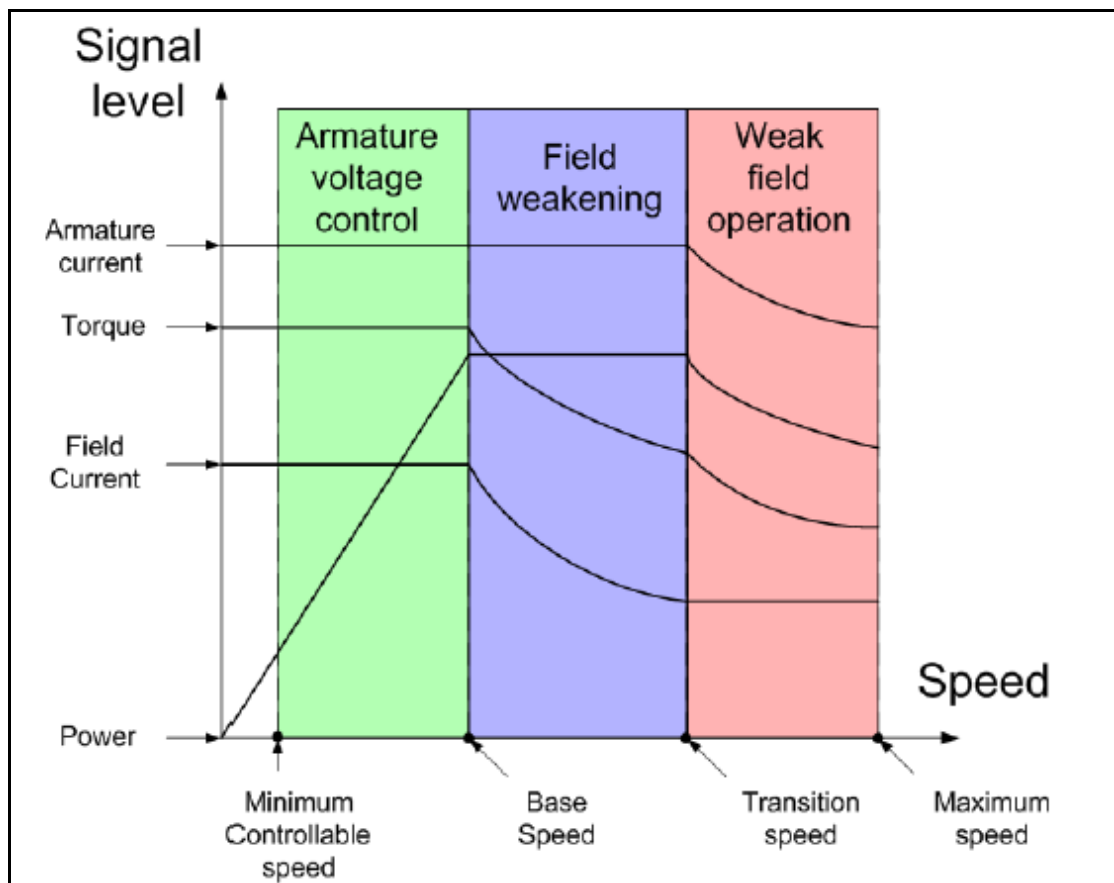


**Figure 2.20** Operation control in separately excited DC motor traction drive

(Lu, 2011).

## 2.6 AC Motor Drive

For regeneration and steep speed and torque characteristics, the induction machines have long been regarded as a suitable final drive for railway electric traction systems due to its inherent capability. After advancement of modern power electronics, the introduction of induction motors became more available. The two reasons for this are as follows:

- By changing the input frequency and voltage of the input power supply, speed control of the induction motor is achieved.

- Power electronics techniques solve the difficulties that obtained by the proper three-phase supply from a DC or single phase AC traction line.

In Hill (1994); Lu (2011) showed on the advancement of semiconductor devices, power electronics techniques became more developed. In the 1960s, trials of several experimental inverter-fed induction motor locomotive drives were raised due to the development of the power thyristor reduced current and voltage level which it could withstand and limits its application in high power fields. In the 1970s, deployment of the Current Source Inverter (CSI) in DC-fed metro traction drives was led by the development of a high-power force-commutated thyristor. Later, the Voltage Source Inverter (VSI) in railway were applicable in the large power Gate-Turn-O (GTO) thyristor. Until then, the GTO was replaced by the Insulated Gate Bipolar Transistor (IGBT) which has a lower operating current and higher switching speed. The pulse converter was developed, which is a four-quadrant AC-DC line converter that enables three-phase VSI-Induction Motor drives on single-phase AC supplied railways in the 1980s. Due to the advancement of technology in Induction motor drives, synchronous and asynchronous motors are the most common AC traction motor used in the railway electrification system (Lu, 2011).

In synchronous motors, the stator consists the armature winding, and the rotor comprises the field winding with induced the main voltage which producing the primary magnetic field. In normal practice, such roles of the winding are converse to it. A uniform rotating magnetic field is generated by the symmetric three-phase sinusoidal currents in an armature winding. The Direct Current (DC) through the field winding produces a steady-state magnetic field. The rotor field tries to line up with

the stator field which produces torque. The greater the torque on the rotor is obtained when there is the larger the angle between the two magnetic fields (Chapman, 2005). The synchronous motor was once used in electric railway traction and was replaced by the second type of AC motor until GTOs were introduced (Hill 1994; Lu, 2011).

The asynchronous motor is also referred to as an induction motor since the rotor voltage, and rotor magnetic field is induced rather than being connected physically by wires (Chapman, 2005; Lu, 2011). Asynchronous motor is not required Direct Current (DC) in the rotor winding. This current is the significant difference compare to synchronous motor. The three-phase current through stator induces a rotating flux in the air-gap. An opposite air-gap flux to this rotating flux vector set up in such a way the current is induced in the rotor conductor. The torque is produced due to the reaction between the rotor current and net air-gap flux. The following comments are made according to the individual induction motor torque-speed characteristic curve in Chapman (2005); Lu (2011) as shown in Figure 2.21 represented by the percentage of full-load torque which is the torque of point A.

1. The torque of the motor at synchronous speed in point B is zero.
2. Curve attain nearly linear the torque-speed characteristic between no load (Point B) and full load (Point A).
3. Breakdown torque or pull out torque is referred as a maximum torque
4. The motor can take up any amount that it can supply at full power due to the starting torque of the motor is slightly larger than its full-load torque.
5. The torque will switch its direction when the speed of motor goes higher than synchronous speed, implying that the machine switches to generator mode under regenerative conditions.

It is necessary to apply voltage and stator frequency for control the speed of the motor. It is practical to vary the speed of the motor to either above or below the base speed by using variable frequency control as shown in 2.21. In the case of avoiding magnetic saturation, the core of the induction motor and excessive magnetization currents were needed to flow through the machine as it is necessary to reduce the terminal voltage applied to the stator. This process is called derating (Hill, 1994). To control the torque and the speed needs to vary frequency induction motor drives. This method is referred as Vector control. The stator current vector is transformed into rotor flux linkage current in this control method, i.e., excitation current, vector and rotor torque current vector (Gabriel, Leonhard, and Nordby, 1980; Lu, 2011).

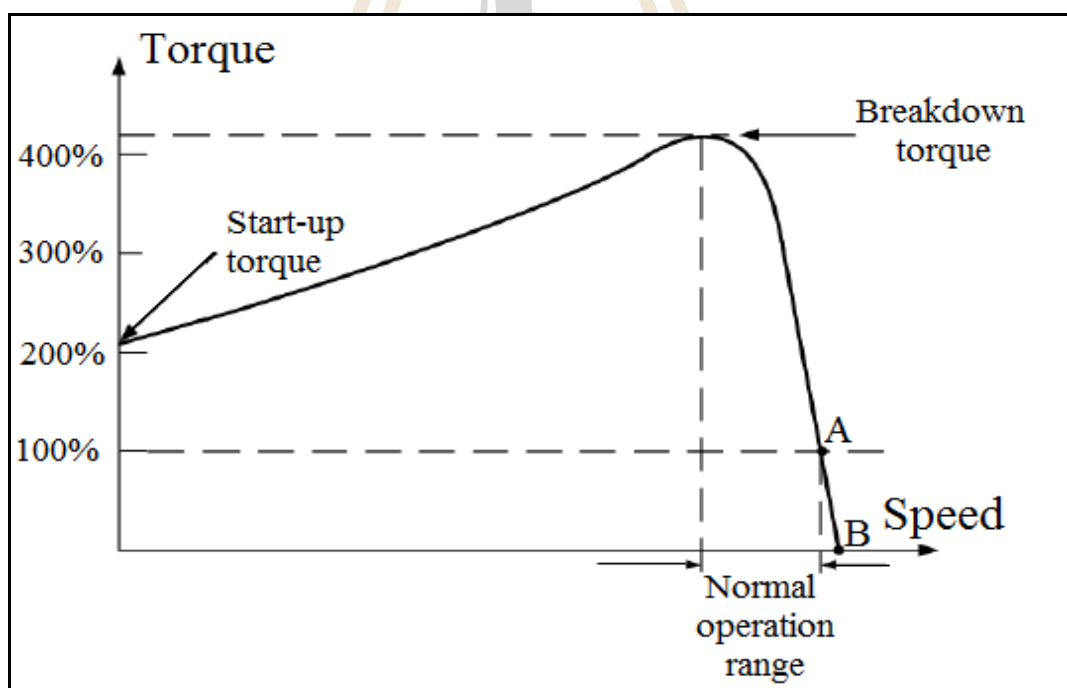


**Figure 2.21** Torque-speed characteristic curve of the induction motor

(Chapman, (2005); Lu, (2011)).

Different control of the operation in Torque-speed characteristic curve of the induction motor is shown in Figure 2.22. Firstly, it is necessary to introduce the relationship between flux and the voltage-to-frequency ratio  $V_a/\omega$  as in (2.1) and (2.2),

$$V_a(t) = E_a \sin(\omega t) = -N_p \frac{d(\phi)}{dt} \quad (2.1)$$

$$\phi(t) = \frac{E_a}{\omega N_p} \cos(\omega t) \quad (2.2)$$

where  $E_a$  is the air-gap Electromotive Force (EMF), which is approximately the same as terminal voltage  $V_a$  except at low speed when more voltage drop is introduced between  $E_a$  and  $V_a$ .  $\phi$  is the magnetic flux and  $N_p$  is a constant.

Flux is proportional to the voltage-to-frequency ratio as stated from (2.2). For the start-up stage, A constant flux should be maintained, and for a constant torque operation, constant flux region can be achieved by keeping voltage-to-frequency ratio constant.

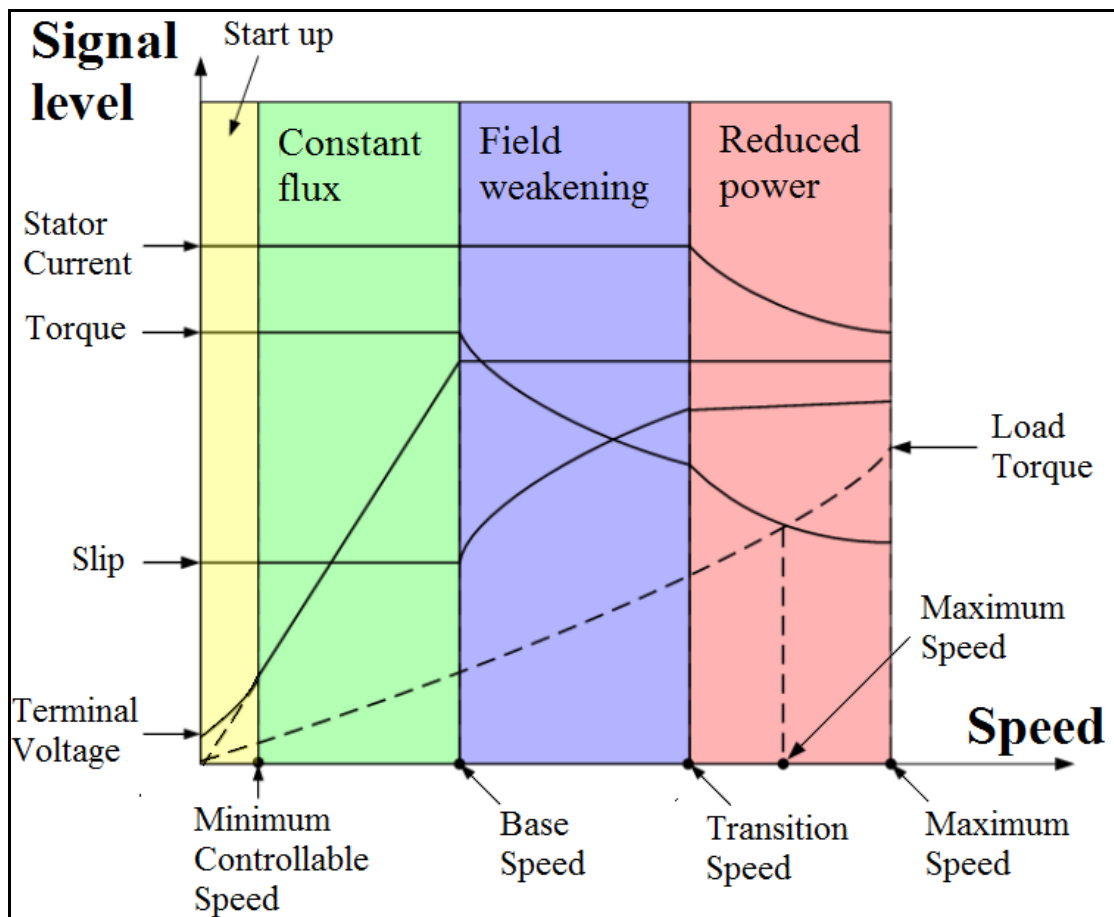


**Figure 2.22** Traction duty cycle of mechanical and electrical variables (Lu, 2011).

Various operation regions are identified throughout the whole traction duty cycle from low to higher speed.

- **Startup region:** At low speed, the stator resistance becomes comparable to the reactance as the impedance of stator which caused voltage drop increases.  $V_a / \omega$  must be increased to maintain a constant voltage-to-frequency ratio as a result of reducing the air-gap flux.
- **Constant flux region:** The torque in the machine is proportional to the air-gap flux density for a given current through the rotor. In constant torque operation, results in a constant flux density.

- **Field weakening region:** The frequency will increase further whereas the terminal voltage remains unchanged when the speed increases further above the base speed. Both the air-gap flux and available torque reduce during this period. This process is termed as field weakening. When machine slip increases, constant values of both the current and voltage are maintained. This stage will last until the working torque and breakdown torque became equal as shown from Figure 2.22.
- **Reduced power region:** Further speed increases are obtained by increasing the stator frequency while the line current decreases at this stage. If steady speed is achieved at which the maximum output torque equals to load torque, power consumption will reduce, and the slip will increase by a small amount.

## 2.7 Lightning Vulnerability

The result of the equivalent collection of the structure area or object and the density of flash for the region that the structure is located determine the probability that lightning will strike a structure or object. The average annual number of flashes to ground per square kilometer is predicted by Lightning Flash Density ( $N_g$ )/Ground Flash Density of that Area (CTBTO/IMS Earthing and Lightning Protection Minimum Standard, 2016). Some areas in the world have this value which is available from ground flash location networks of the map. Temperate regions  $N_g$  may be estimated in case of a map of  $N_g$  as in (2.3) is not available:

$$N_g \approx 0.1Td \quad (2.3)$$



where  $T_d$  is the average number of storm days per year (which can be obtained from isokeraunic maps from local meteorological services). Due to different weathering in some of the tropical countries in the world, they have different ground flash location networks of the map compare to the one above (De la Rosa et al. 2000). The ground lightning location systems of the map ( $N_g$ ) can be estimated based on thunderstorm hour records as in (2.4). But this  $N_g$  equal or higher than 4 is more suitable for lightning protection (IEEE Std. 1410).

$$N_g \approx 0.054T_h^{1.1} \quad (2.4)$$

where  $T_h$  is the average number of thunderstorm hours per annual.

The existence of large crowds, Necessity of service continuity, very high lightning flash frequency, Tall isolated structures, Buildings containing explosive or flammable materials and Buildings containing unique cultural heritage are the most cases which require lightning protection as per standard.

The necessity of service continuity, very high lightning flash frequency and Tall isolated structures are cases which need lightning protection in order to get the desired performance. Lightning Protection System (LPS) is the one which consists external and internal lightning protection of structures against physical damage. The external LPS protects the building against direct lightning flashes to the structure and also the flashes to the side of the structure in order to conduct the lightning current from the point of the strike to the ground. The flow of current to the earth through the external LPS avoids thermal or mechanical damage and dangerous sparking which may lead explosions or fire. An internal LPS precludes hazardous sparking within the area of the structure with the guide of either a separation distance or equipotential

bonding and hence insulation of electrical between the external LPS elements and other electrically conducting components internal to the structure. IEC Standard 62305 explains all necessary information for a proper lightning protection which is four parts such as Risk Management, General Principles, Physical damage to the structure and life hazards and Electrical, and electronic systems within structures (IEC 62305:1-4; DEHN + SÖHNE – Lightning Protection Guide, 2014).

### 2.7.1 Direct lightning strikes

Direct lightning strikes depend on the frequencies of lightning strikes which can be relevant for a stroked object. The following are the different frequencies of lightning strikes:

- Frequency of direct lightning strikes to the building or structure ( $N_d$ );
- Frequency in close lightning strikes with electromagnetic effects ( $N_M$ );
- Frequency of direct lightning strikes in utility lines entering the building or structure ( $N_L$ );
- The frequency of lightning strikes adjacent to utility lines entering the building or structure ( $N_I$ ).

Direct lightning strikes to a structure depend on the yearly lightning strike frequency to the building or structure ( $N_d$ ) as in (2.5) (IEC 62305-1).

$$N_d = N_g \times A_d \times C_d \times 10^{-6} \quad (2.5)$$

Where:  $N_d$  = the yearly lightning strike frequency to the site

$N_g$  = the annual average flash density in the region where the structure is located

$A_d$  = The structure collection area

$C_d$  = the factor of location.

### 2.7.2 Direct and Indirect lightning strikes to the overhead or cable

The frequency of lightning to or nearby a service line (power, a data line, telecommunication, etc.) entering a building or a station is determined Direct and Indirect lightning strikes to the overhead line, or cable (CTBTO/IMS Earthing and Lightning Protection Minimum Standard, 2016). This possibility can be predicted in (2.6), (2.7), (2.8) and (2.9) as follow:

$$N_L = N_g \times A_I \times C_e \times 10^{-6} \quad (\text{Direct lightning strikes}) \quad (2.6)$$

$$N_i = N_g \times A_i \times C_e \times 10^{-6} \quad (\text{Indirect lightning strikes}) \quad (2.7)$$

$$A_I = [L_C - 3 \times (H_a + H_b)] \times 6 \times H_C \quad (2.8)$$

$$A_i = 1000 \times L_C \quad (2.9)$$

Where:  $C_e$  is environmental factor

$A_I$  is the collection area of flashes hitting the service ( $m^2$ )

$A_i$  is the collection area of flashes to ground near the service ( $m^2$ )

$H_C$  is the service conductors height above ground (m)

$L_C$  is the service section length from the structure to the first node (m). A

maximum value  $L_c = 1\ 000$  m should be assumed.

$H_a$  is the height of the structure connected to service first point (m).

$H_b$  is the height of connected structure at last point of service (m) near to the structure.

$\rho$  is the resistivity of the earth ( $\Omega\text{m}$ ) in or on which the line is laid, up to a maximum value of  $\rho = 500 \Omega\text{m}$ .

## 2.8 Lightning protection system

The Lightning protection system is the system used to reduce physical damage due to the surge overvoltage in power system caused by lightning flashes (CTBTO/IMS Earthing and Lightning Protection Minimum Standard, 2016; DEHN + SÖHNE – Lightning Protection Guide, 2014). An external Lightning protection system (LPS) protect the structure against the direct lightning flashes and conduct it from the stroked point to the ground. Also, the lightning protection system should base on the regulation and type of classes of LPS to be used under the particular standard. If the rule does not meet the requirement class III of LPS should be utilized as a minimum (IEC 62305-3).

### 2.8.1 Lightning protection level classification

There is four lightning protection level (LPL) according to IEC 62305-1. For each LPL, a set of maximum and minimum parameters of lightning current is secured. In LPL I, Only 1% of lightning events are above the maximum values of lightning current parameters specified. For LPL II, the parameters are decreased to 75% compared to LPL I. For LPL III and IV; these values are 50 % of LPL I (CTBTO/IMS Earthing and Lightning Protection Minimum Standard, 2016). Lightning Protection classes such as classes I, II, III, and IV are represented with the

LPL I, II, III, and IV respectively. Air-Termination System, Down-conductors, Earth-termination System, Equipotential Bonding and Surge Protection based on Lightning Protection Zone (LPZ) are the components of a LPS. Air-Termination System decrease the probability of the lightning current to penetrate into the structure. Rods, Catenary wires, and meshed conductors are the components of Air-Termination System. Figure 2.23 shows the among of the elements in a Lightning Protection System (LPS): Air-Termination System, Down-conductors, Earth-termination System, Equipotential Bonding in Railway Station.

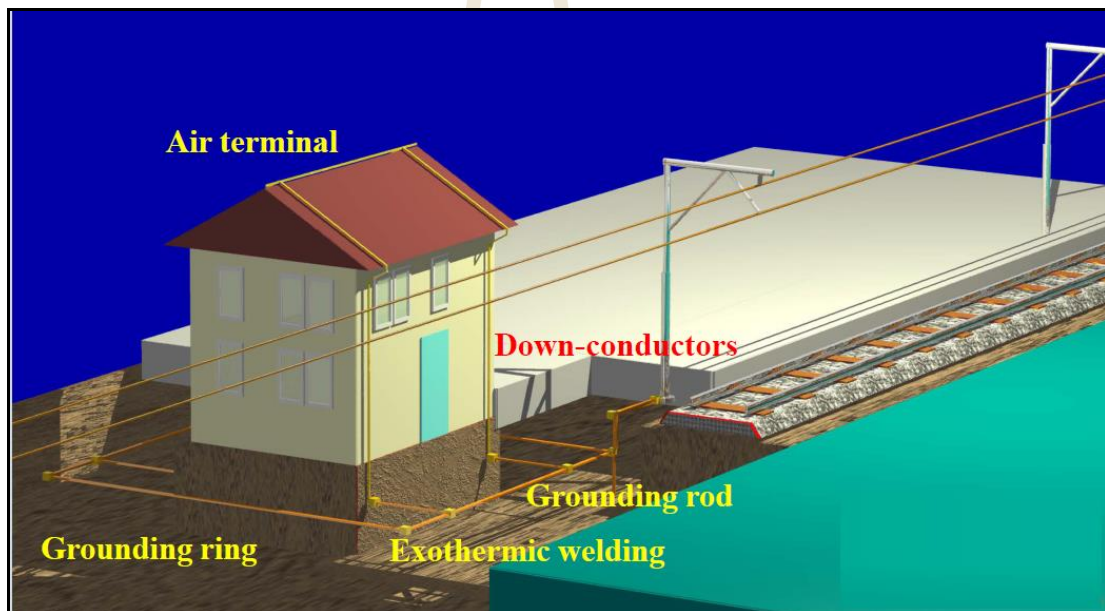


**Figure 2.23** The components of a Lightning Protection System (LPS): Air-Termination System, Down-conductors, Earth-termination System, equipotential Bonding in Railway Station (Pešič, and Grmovšek, 2007).

## 2.9 Lightning voltage surge

Surge Protection can protect lightning voltage surges based on Lightning Protection Zone (LPZ). A direct lightning strike on an overhead contact line will cause lightning voltage surges. The peak of lightning voltage surge is approximated by empirical equation (2.10) (Kiessling et al., 2009).

$$U_{B_{\max}} = 82 \cdot I_B \quad (2.10)$$

In overhead contact line installation, the impulse voltage limiting can be achieved by overvoltage protection devices. The most efficient overvoltage protection device is the valve-type arresters. They are used for an economic reason unless there is no an extremely of lightning existence since the limited protection is possible with overvoltage protection devices.

### 2.9.1 Lightning protection in Catenary Contact system

For A.C voltage railways, the overvoltage protection of the electrical energy supply installations of railroad facilities has an enlarging importance nowadays. The dimensioning and application of metal oxide (MO) surge arresters without spark gaps in alternating current networks with 16.7/50 Hz were used. Moreover, the modern MO surge arresters without spark gaps and with silicon insulation make it possible to develop solutions for specialized implementations. In the fact of developing new and more optimal overvoltage protection devices, the electrical railways were expanding very rapidly which shows the necessity to the people demands. In electrical supply networks, Overvoltages was resulted from the effects of lightning strokes and switching actions which cannot be prevented. For

endangering the electrical equipment, in all possible cases, the voltage withstand insulation capability cannot be created due to economic reasons. Therefore, reliable service and commercial calls for excellent protection of the electrical equipment against unacceptable overvoltages.

In fact, this overvoltage applies to all networks of the energy supply. There are different kinds of overvoltage and the possibility of reducing them. Generally, Surge Arrester may use according to the Dimensioning, testing and application of metal oxide surge arresters in medium voltage networks (Application Guidelines Overvoltage Protection, 2007). Lightning strokes are the most dangerous threat for rail networks. That is why it is obligatory to decrease the overvoltage to a safe value through proper protection. MO surge arresters without spark gaps give excellent protection in this situation. In this device, the technical outdated for protection appliances like spark gap and arcing horns arresters as well as surge arresters in porcelain housings, are not dealt with anymore. In applications, for instance on overland lines in regions with high risks of lightning on bridges or elevated poles, the total lightning current parts may emphasize the Metal Oxide (MO) surge arrester immediately due to nearby or direct lightning. Consequently, parameters of lightning current, resulting overvoltages, and energy stresses according to the standard need to be considered. Some of standards that were used for lightning protection in Railway Facilities are given in Table 2.2. All power supply, control and communication circuits and Railway Vehicle should be protected against lightning overvoltage.

**Table 2.2** Standards for lightning protection in Railway Facilities

No.	Standard	Description/ Title
1	EN 50163, IEC 60850	Railway applications – The Supply voltages of traction systems
2	EN 60099 -4, IEC 60099 –4, Ed2.1,2006-7,	Part 4: Metal-oxide (MO) arresters without gaps for a.c systems
3	EN 50124 – 1, IEC 62497 – 1, Ed1.0, 2010-02	Railway applications – Insulation coordination Part 1: Basic requirements – Clearances and creepage distances for all electrical and electronic equipment
4	EN 50124 – 2, IEC 62497 – 2, Ed1.0, 2010-02	Railway applications - Insulation coordination- Part 2: Overvoltages and related protection
5	IEEE Std. C62.22-2009	IEEE Guide for the application of metal oxide (MO) surge arresters for alternating- current systems.
6	IEC Std. 60099-5, edition 1.1, 2000	Surge arresters—Part 5: Selection and application recommendations
7	IEEE Std. C62.11-2005	IEEE Standard for Metal-Oxide (MO) Surge Arresters for Alternating Current Power Circuits (>1 kV)

### 2.9.2 Application of surge arrester

Up to last Century at the middle of the eighth decade, surge arrester was installed in Electrical Railway network. Spark gap arrester was used at that time as a protection against lightning overvoltage. It consists of series of SiC resistors and sparks gap. But due to its disadvantages over MO surge arrester, Spark gap arrester was replaced by MO surge arrester. MO surge arrester consists of series of Metal oxide resistors that replaced SiC resistor and Spark gap. Also, set of Metal oxide resistors of MO surge arrester is insulated with Silicon material. Hydrophobicity of the material, self-extinguishing Behaviour, no toxic elements, mechanical breakability



and small weight are the dominant properties of silicon for the insulation of Metal Oxide (MO) surge arresters. The diameter of the MO resistors correlates with the line discharge classes corresponding to IEC/EN 60099-4 are shown in Table 2.3. Also, definition and voltage values of A.C voltage railways, which are essential for surge arrester and the overvoltage protection are explained in European Standard EN 50163 and also in IEC 62497-2 (Ed.2.0, 2010-2). The Operation limit of Nominal Voltage for Railway Electrification System according to BS EN 50163 and IEC 60850 are given in Table 2.4 (Frey, 2012).

**Table 2.3** Correlation of typical MO resistors to the line discharge classes according to IEC/EN 60099-4

Line discharge class acc. IEC/EN 60099-4	1	2	2	3	4	5
Diameter of MO resistor in mm	38	42	47	62	75	108
Rectangular wave, 2 ms, in A	250	350	550	1000	1350	2000
Energy absorption in kJ/kVUc	3.6	3.5	5.5	9.0	13.3	19.8
Arrester Classification in kA	10	10	10	10	20	20
Surge Impedance of the line Z in $\Omega$	$4.9 U_r$	$2.4 U_r$	$4.9 U_r$	$1.3 U_r$	$0.8 U_r$	$0.5 U_r$

**Table 2.4:** Operation limit of Nominal Voltage for Railway Electrification System according to BS EN 50163 and IEC 60850 (Frey, 2012; ABB Application Guidelines Overvoltage Protection, 2011).

System Type	L.N.P Voltage	L.P Voltage	N. Voltage	H.P. Voltage	H.N.P Voltage	
			$V_n$	$V_{max1}$	$V_{max2}$	$V_{max3}$

**Table 2.4:** Operation limit of Nominal Voltage for Railway Electrification System

according to BS EN 50163 and IEC 60850 (Frey, 2012; ABB Application Guidelines Overvoltage Protection, 2011) (Continued).

15 kV AC,16.7 Hz	11 kV	12 kV	15 kV	17.25 kV	18 kV	24.311 kV
25 kV AC,50 Hz	17.5 kV	19 kV	25 kV	27.5 kV	29 kV	38.746 kV

L.N.P Voltage: Lowest Non-Permanent Voltage

L.P Voltage: Lowest Permanent Voltage

N. Voltage: Nominal Voltage

H.P. Voltage: Highest Permanent Voltage

H.N.P Voltage: Highest Non-Permanent Voltage

When designing the arresters for several system voltages, three behaviors are to be taken into attentiveness: the highest constant voltage that arises in the system, the arresters protection level, and the arrester energy absorption capability. The most important behavior taken into consideration by the model is that the arrester in the system should be stable no matter which stresses occur from the thermal point of view. The high voltage fluctuations in the line of supply due to the operating conditions caused it significant to set the constant voltage of the arrester  $U_c$  over the highest constant voltage of the system  $U_{max1}$  (see Figure 2.24 and Table 2.4). The largest non-permanent voltage  $U_{max2}$  can occur for maximum 5 min. Regarding the specification, but it is not known how often and in which time interval this voltage increase may seem. As the modern MO surge arresters have a very favorable protection level and a capability of high-energy absorption, it is possible to lay the

continuous operating voltage  $U_c$  of the arrester similar or higher  $U_{\max 2}$ , that is  $U_c \geq U_{\max 2}$  (ABB Application Guidelines Overvoltage Protection, 2011).

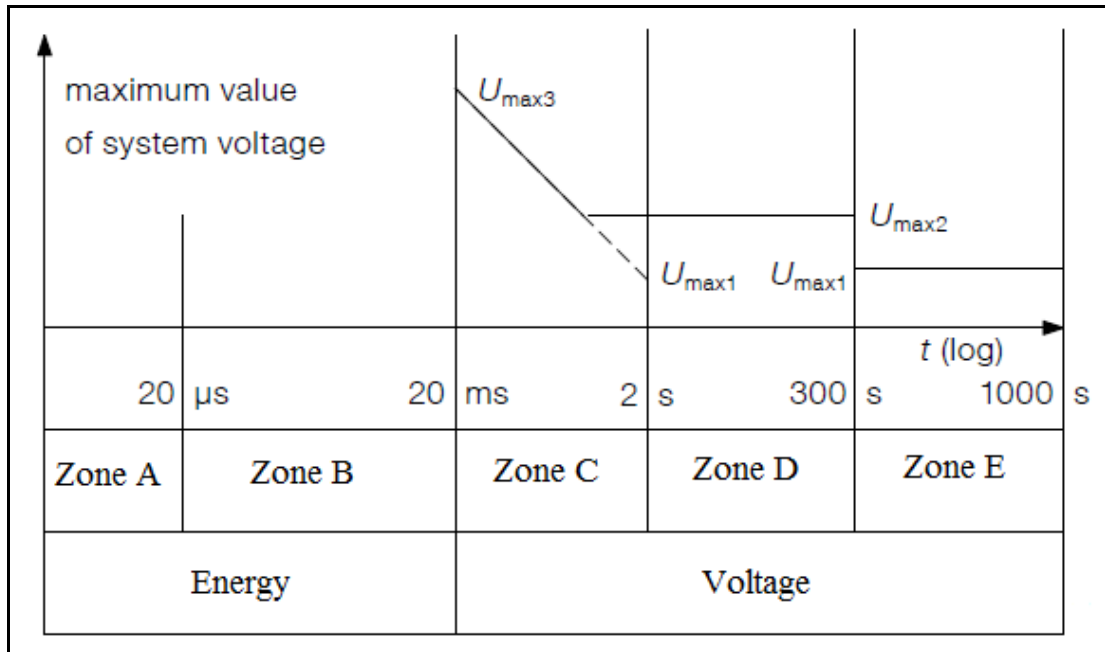


**Figure 2.24** Highest values of the voltage occurring in the systems depending on time duration (Pešič, and Grmovšek, 2007).

Key: Zone A: Lightning overvoltages.

Zone B: Switching Overvoltages, due to high impedance phenomena (currently turned off in inductive circuits).

Zone C: Temporary overvoltage, due to low impedance phenomena (voltage a variation on the primary network).

The term “temporary overvoltage” is identical to “Long-term overvoltage” in IEC 60850.

The variation of the ratio  $U/ U_{\max 2}$  versus duration is identified by  $U = U_{\max 2} \times t^{-k}$

where

$t$  is the time in ( $0.02 \leq t \leq 1$ )

$k$  is coefficient (0.0767 for 15 kV and 0.0741 for 25 kV)

Zone D: Highest Non-Permanent Voltage,  $U_{\max 2}$

Zone E: Highest Permanent Voltage,  $V_{\max 1}$

For the Lightning protection of AC Railway network, classes 3, 4, and 5 are used (Pešič, 2007). Arresters Class 3 as line arresters used to prevent flashover due to lightning overvoltage. Also, earthed shielding wires with the application of lightning protection structures, are essential for the protection concept. The arresters are intended to conduct the charge only when the overvoltage is higher than expected switching overvoltage in the system. This state leads automatically to unfavorable great protection ration  $U_p/U_c$ . Arresters Class 4 are used to protect substations, feeder, Overhead contact lines, running rails, locomotive and rolling stock against lightning overvoltage. Arresters Class 5 are used to protect contact lines and rolling stock against overvoltage in areas with high risk of direct lightning. Figure 2.25 shows a schematic representation of a 15 kV A.C, 16.7 Hz railway current supply and the surge arresters application while Figures 2.26 -2.27 show the installation of surge arrester on the overhead line & the rails and locomotive for the A.C system. The position of the surge arrester installation on the train is shown in Figure 2.28 where the first place is a current collector on the locomotive roof and the second position which may be optionally installed prior main circuit breaker to increase safe due to redundancy.

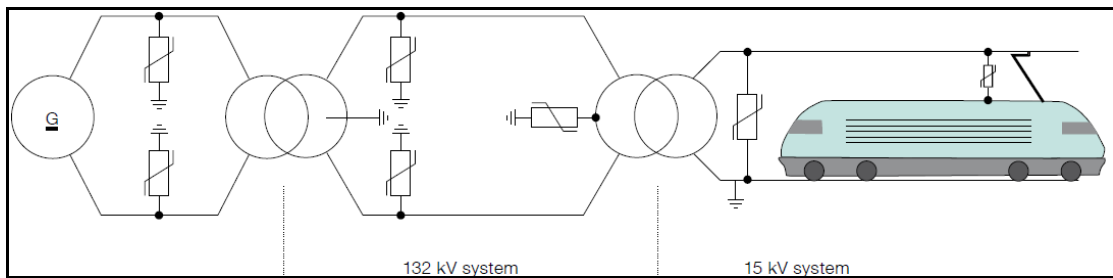


**Figure 2.25** The application of surge arresters in 15 kV A.C, 16.7 Hz railway current supply (Source: ABB Application Guidelines Overvoltage Protection, 2011).



**Figure 2.26** Installation of MO surge arrester on overhead line and the rails (Pešič, and Grmovšek, 2007).



**Figure 2.27** Installation of MO surge arrester on locomotives  
(Pešič, and Grmovšek, 2007).

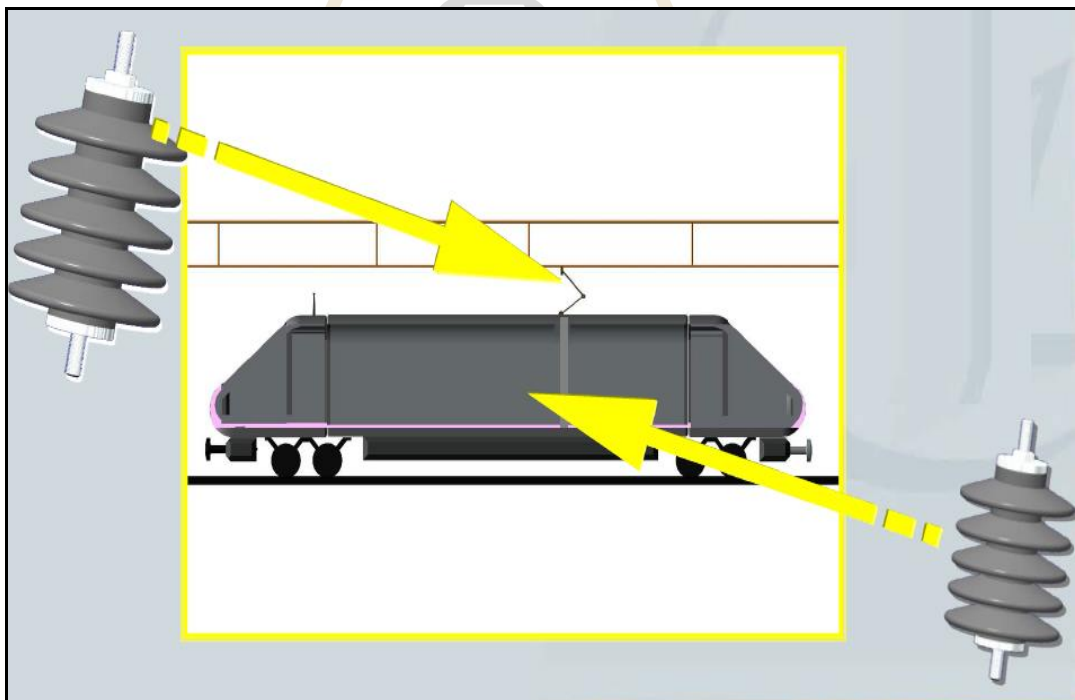


**Figure 2.28** Position of the surge arrester installation for lightning protection of train  
(Pešič, and Grmovšek, 2007).

## 2.10 Improvement and optimization techniques Review

Generally, Optimization refers to the procedure of selecting one feasible solution to minimize or maximize the objective function (Nocedal and Wright 2006; Jeter 1986). The purpose of this study is to optimize the lightning performance of 25 kV AC, 50 Hz Catenary Contact System in railway system of double-track elevated after surge arrester implementation. The application of surge arrester is used to improve the lightning performance by eliminating circuit tripping for Overhead Catenary line protection against Lightning. Also, the performance of the system is justified by sizing a surge arrester (SA) to install and analyzing different parameters of Overhead Catenary transmission line for surge arrester's application to determine the best location. The following are some of the studies presented estimation, improvement, and optimization of lightning performance in the power system.

Christodoulou, Gonos, and Stathopoulos (2008) presented a study of the Lightning performance of HV transmission lines protected by surge arresters: a simulation for the Hellenic transmission network. The analysis of transmission lines lightning failure shows that the simple solution to eliminate lightning flashovers completely is to install of surge arresters on every single tower although this solution needs massive capital investment. The arresters strategical installation from the electric companies at optimum locations were decided based on simulation studies, using Simulink and data collected from Hellenic Public Power Corporation S.A.

Christodoulou et al. (2009) described a numerical method for Optimization of Hellenic Overhead High-Voltage Transmission Lines Lightning Protection. The predominant objective of the study was to minimize the line total annual cost,

considering the significant technical constraints and both fixed and running cost items of overvoltage protection system to protect against lightning stroke to 150 kV Overhead high-voltage line based on the results of techno-economical optimization analysis of overvoltages in the power system. This study was done after studying Transmission line's lightning failures. Using a more sophisticated optimization algorithm, in contrast to this in Ekonomou et al. (2006), based on direct computation, optimum values of those four parameters which were calculated in order to minimize the defined performance indices. It must be mentioned that the optimization methodology incorporates all the available protection means, i.e., ground wires and surge arresters, something which is not a standard practice for all electric utilities' designs. New values for the studied transmission line parameters were proposed as a result of the adequate lightning protection of the lines. Comparison of the actual recorded and the computed lightning failure rates using the new optimum produced design parameter values and Percentage failure rate reduction between actually recorded lightning failures and lightning failures calculated using the new optimum provided design parameter values. Therefore, optimum values for the average insulation level, the tower footing resistance of each region of the transmission lines, the energy absorption capability of the surge arresters and the surge arresters' installation interval in each region were calculated. Due to the difficulties of the estimated interval, the usefulness of the proposed methodology can be easily noticed for cases of new transmission lines. If the examined transmission lines were constructed using the method obtained by calculating the parameter values, they would indeed present lower failure rates. Results show that installation interval of



surge arresters used in the sub-stations is 300–700m away from them (first and second tower of the transmission line).

Chmielewski and Dziadkowiec (2013) introduced Simulation of Fast transients in Typical 25 kV, A.C Railway Power Supply System. The simulation of the lightning phenomenon (Fast Transients) in a conventional railway catenary system conducted in PSCAD software. The phenomenon that was investigated lightning overvoltages caused in power system when lightning stroke to phase conductor (shielding failure) of the railway overhead catenary system. The voltages were measured in most vital points of the network which are a transformer, cable bushing or switchgear. The frequency dependent models of cables, overhead catenary lines, surge arresters, transformers, and rails were simulated in various system configuration and compared in determining possible overvoltages in railway system along with a proposal of rating and locations of additional surge arresters' installation.

Pastromas et al. (2016) demonstrated Investigation of grounding resistance effect on the MV grid of Hellenic electromotive railway during lightning strikes. The simulation of model time-domain solver was analyzed in ATP-EMTP. Lightning performance regarding current dissipation and voltage clearance were evaluated through the effect of earthing resistance in the ERMV during lightning strikes. Overhead contact medium voltage line (OHCL), Railway, Medium-voltage insulators and return wire were used for study as the main components. The outcomes include measured current in the poles and Measured voltage in the rails, catenary wire, the insulators and on the top of the poles due to a lightning strike on the top of the pole and the catenary wire. From the results, it was showed that the effects in poles are quite small than another one with maximum currents of 10 kA. It was noticed that

also that with an increase of lightning amplitude and earthing resistance most of the insulators led to the breakdown. It was acquired that the ideal earthing resistance is one of  $10 \Omega$  from the simulation. Insulation breakdown occurs on the pole that was hit by lightning strikes on the catenary wire while for a hit on the pole no failure has been noticed.

Yang and Zhang (2015) presented a Research on Lightning Protection Simulation of High-speed Railway Catenary Based on ATP-EMTP. The study used the improved electrical geometric model to analyzed the lightning strike station of the catenary. The established lightning strike catenary model was simulated under different factors affecting the change catenary voltage of the insulator and lightning withstand the level of change. Insulator terminal voltage waveform of positive feeder line and contact wire was measured during different waveforms of the lightning current hit pillars, positive feeder, and contact wire when power frequency voltage and protection wire was ignored respectively. Results showed that, when lightning hits the catenary pillar, lightning resisting level of positive feeder line and contact line decreases with the increase of the impulse grounding resistance, and the lightning resisting level of contact line is far greater than positive feeder line. Also, it showed that about 83% of the lightning current makes the positive feeder line insulator flashover; About 43% of the lightning current that causes the contact line insulator flashover. It has also been showed that when lightning strikes positive feeder and contact line, its insulation voltage has a same changing trend, but voltage peak of insulator contact line is far greater than the peak voltage of positive feeder line. The conclusions drawn from the analysis revealed that the positive feeder line and contact line is vulnerable to lightning strike. Also, protection wire is shield by the positive

feeder line, the probability of a lightning strike is extremely low. Moreover, when the lightning hits the catenary pillar, the shorter the front time of lightning current, the greater the damage to the catenary, and the smaller the pillar's impulse grounding resistance. Furthermore, the higher the lightning resisting level of catenary which is better for the lightning protection to the catenary. Lastly, the existence of the protection line can improve the enduring lightning level of the catenary. The power frequency voltage can make the lightning opposing level of positive feeder line insulator, and contact line insulator fluctuates, but for the whole catenary system, power frequency voltage reduces its lightning resisting level.

Achouri and Khamliche (2015) investigated a Protection of 25 kV Electrified Railway System. The investigation of the system was developed, and each element was represented by a model corresponding in EMTP Program. The ZnO arrester was installed on the roof of the vehicle parallel with a transformer which was the first element to meet in the traction vehicle. Analysis of the protective effect of the surge arrester used to protect primary of the locomotive transformer representing traction vehicle was discussed in the case of lightning strike a mast. Also, the analysis showed that arrester itself could support discharge current which it crosses through it during a lightning strike.

Wanjari (2014) presented an Effect of Lightning on the Electrified Transmission Railway System. The design of DC overhead system and an investigation was done in PSCAD/EMTDC software. The consequences of the transient overvoltages caused due to a lightning strike on AC and DC side of the substation and the effective method for eliminating such condition with the help of surge arrester was investigated and discussed. The high peak voltage was measured in

phase conductor. It was concluded that when the lightning strikes any of the phases in traction station on the AC side, the lightning overvoltage flows respecting the rectifier along with the induced overvoltages in the other phases which eventually affects the DC overhead line. Additionally, the phenomenon of lightning when strikes cause distortion into the supply voltage which creates further harmonics in the rectifier. It can also be said that the line which is a strike by lightning rises the flux around it which could produce a maximum force between two lines that can be hazardous. With the utilization of surge arresters in such system manifests the necessity and efficiency of decreasing the high voltage surges triggered due to lightning. Also, the location where the surge arresters should be placed is of great importance.

There are different Transient program softwares used for studying of estimation, improvement, and optimization of lightning performance in a power system. Among of this software are PSCAD/EMTDC, EMTP, ATP-EMTP, Simulink (MATLAB), ATPDraw, etc. These transient program softwares have different distinctive attributes, capacities, and capabilities. ATPDraw was chosen for estimating, improving and optimizing the lightning performance of Catenary Contact System.

The Alternative Transients Program (ATPDraw) is a powerful tool widely used in solving and analyzing electromagnetic and transient problems. It is also useful in performing insulation coordination in the power system. Built-in models and the use of TACS (Transient of Control Systems) and MODELS make it capable of simulating electromagnetic and electromechanical transients (Haginomori et al. 2016; Guardado, and Guardado 2016). It contains a large variety of detailed power equipment models or builds in setups that simplify the tedious work of creating a

system representation. Generally, this simulation software can be used in the design of an electrical system or in detecting or predicting an operating problem of a power system (Prikler, and Høidalen 2002). ATPDraw is used in this simulation process of observing the electrical response of the transmission system. In order to represent the electrical response of the transmission system, the electrical model of the transmission system apparatus has to be selected and validated to gain high accuracy result (Dugel 2007).

## 2.11 Existed System

A 25kV/50Hz Catenary contact system consists of traction power system (TPS) which supply power to Overhead contact system (OCS) as shown in Figure 2.29. The details of Overhead catenary system and Airport Rail link line in Thailand are indicated in Figures 2.30 – 2.31. The system has a function for safely transporting people or good without interruption, unreliable or unsafe operation of the electric traction vehicle under normal condition. To comply with requirements for reliable operation of electric traction, the following are applicable, particular about contact line:

- The provision of uninterrupted traction power at pantographs of traction vehicles
- The ability of the railway network to continuously absorb regenerative braking energy
- To have quality parameters for voltages available at pantographs of electric traction vehicles.

Compliance with IEC 62305-1, the system shows to have an interruption to the return circuit to the transformer because the rails as a part of the circuit need to be

protected against lightning overvoltages. In case if not protected, there will be an electromagnetic interference with electrical systems in the vicinity of the railway system.

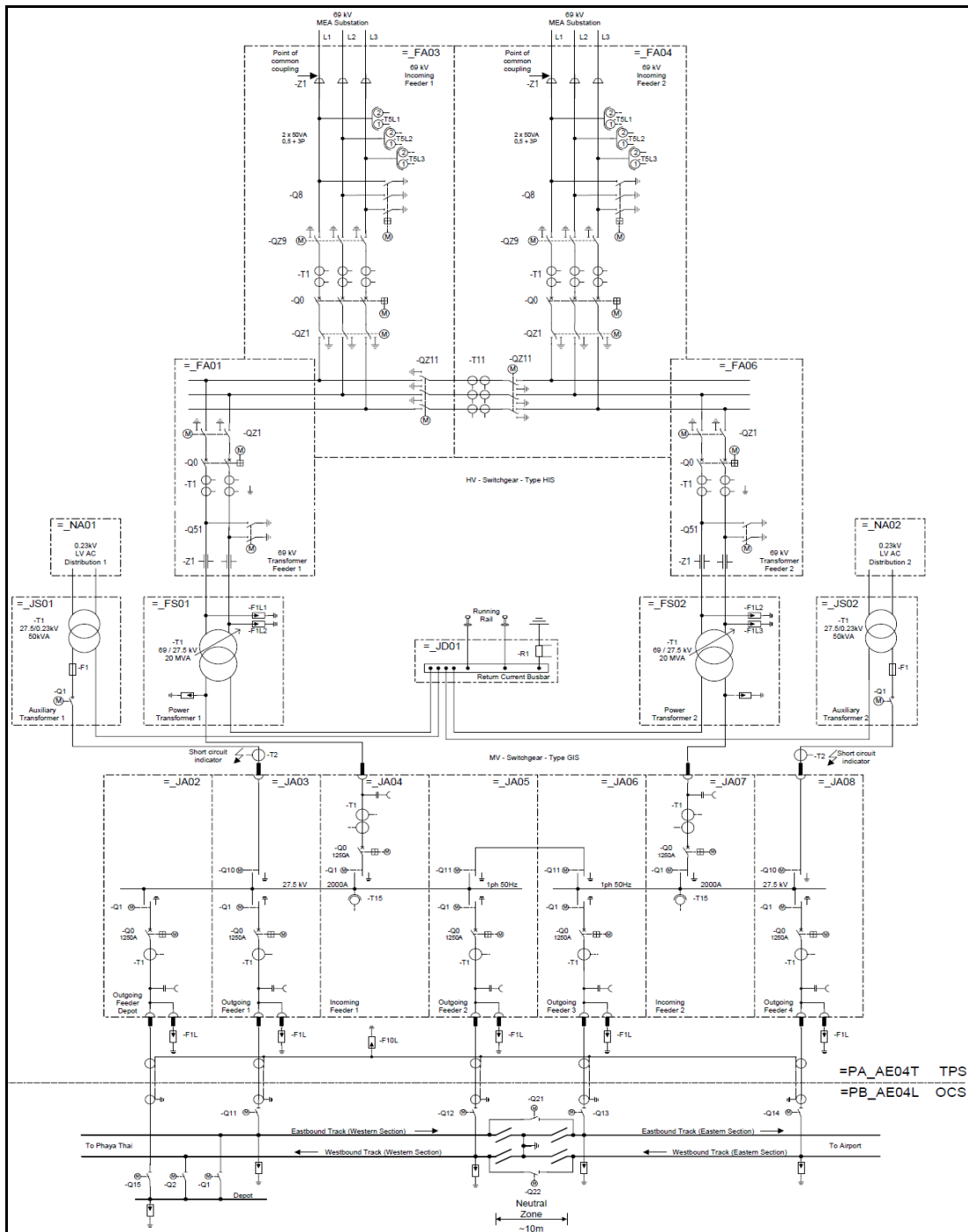


Figure 2.29 Overall TPS & OCS Schematic Diagram (Wilke, and Gabriel 2005).

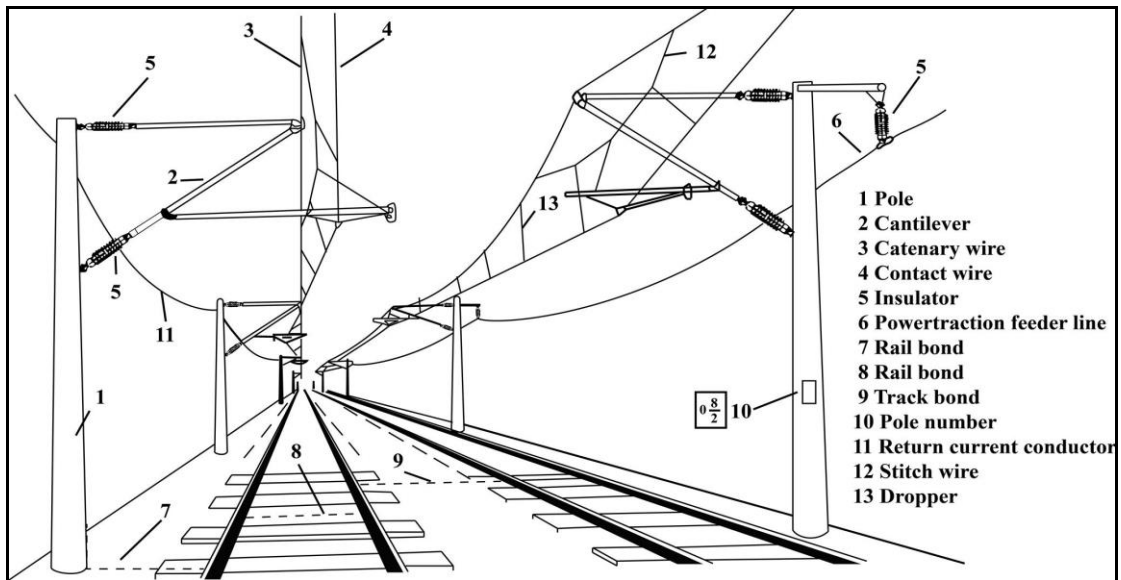


Figure 2.30 Overhead catenary system (Kiessling, et al., 2009).

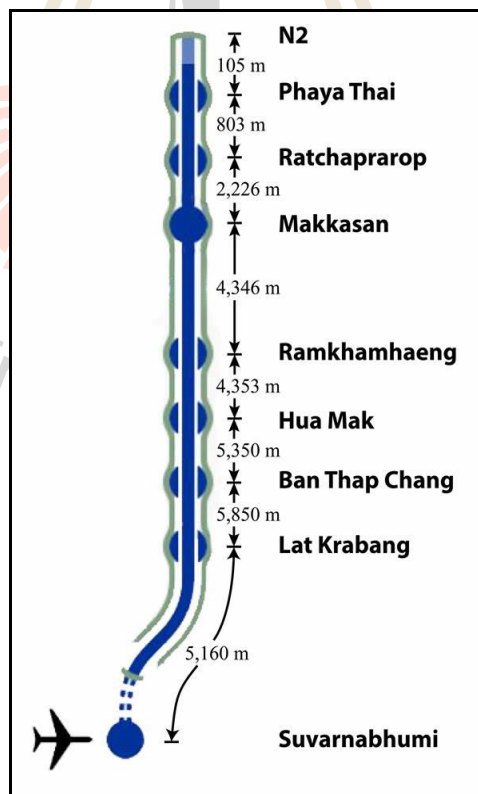


Figure 2.31 Airport Rail link line in Thailand (UMIASEA, 2014).

## 2.12 Preliminary Study

Preliminary investigation on Catenary Contact system shows that lightning performance of the overhead catenary system needs to be improved according to IEC 62305-1. Surge arrester has been recently used as an effective protection against lightning voltage surges (Nafar, Solookinejad, and Jabbari, 2014; Kiessling, et al., 2009; Saengsuwan, and Thipprasert, 2008; Mungkung, et al., 2007; Pešič, and Grmovšek, 2007; Imece, et al., 1996; Durbak, 1985). To date, Catenary Contact system has Surge arrester on its OCS. But, surge arrester need to be connected to the rails for more protection of the system include the rails against lightning stresses on elevated railway system (Pešič, and Grmovšek, 2007). The analysis of lightning Elevated Structure and Catenary Lightning Range of existed system explain in detail in the next part.

## 2.13 Analysis of Elevated Structure and Catenary Lightning Range of existed system.

Thai Overhead Catenary System consists of Substation, return conductor, Catenary line, and Running rails. There are also interconnections between the Overhead Catenary conductors on the double-track elevated railway system. In the double-track electrified railway system with Running rails (I-rail and S-rail), contact line and Return conductor (Earth wire) that are interconnected as a circuit shown in Figure 2.32. The substation infeed with two transformers is provided in Figure 2.33 and Configuration view in Figure 2.34 (Sandra, Martin, and Menter 2007; Kiessling, et al., 2009). The return conductors are also interconnected to the Substation systems,



and it's also connected to the S-rail at the midpoint. At every pole position, the S-rail (R2) is shorted to the elevated pole footing.

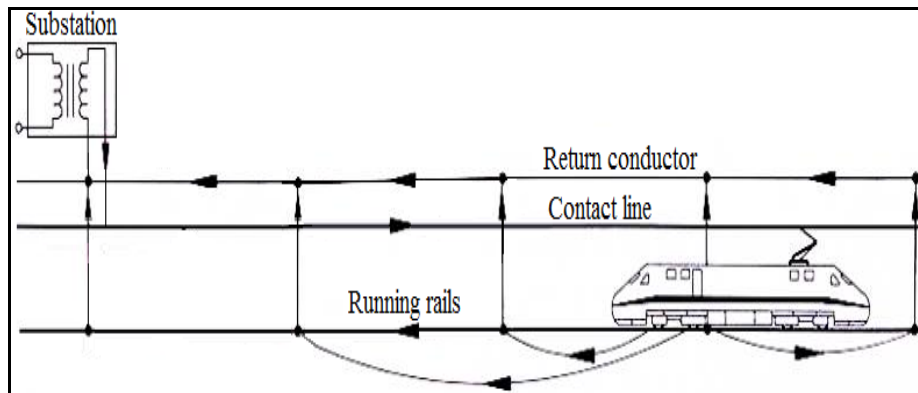


**Figure 2.32** Truck return circuit via running rails and return conductor (Kiessling, et al., 2009).

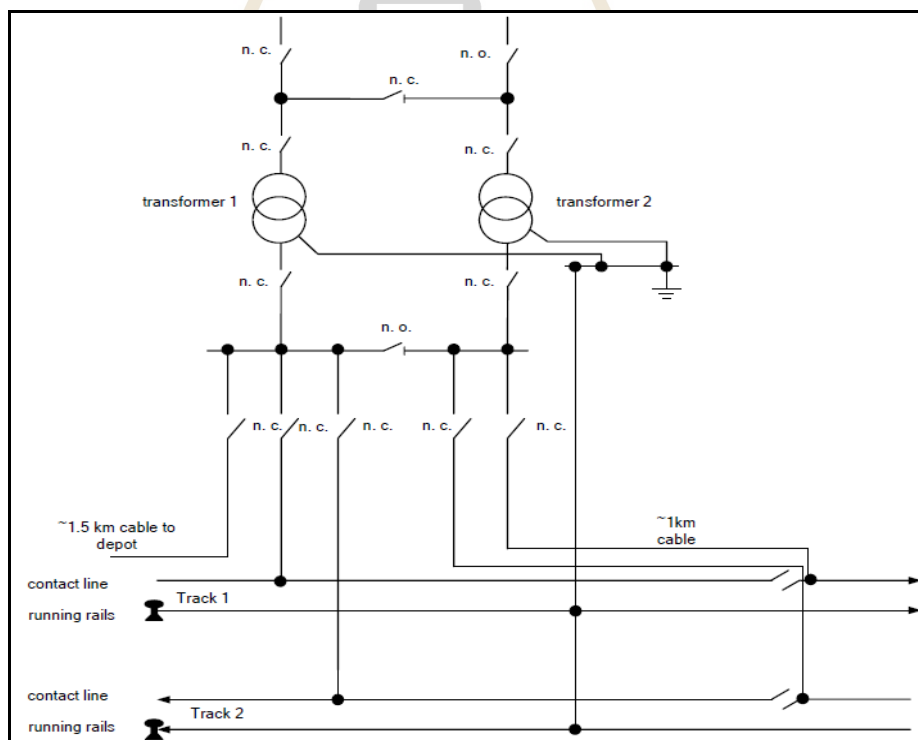


**Figure 2.33** Substation infeed (Sandra, Martin, and Menter 2007).

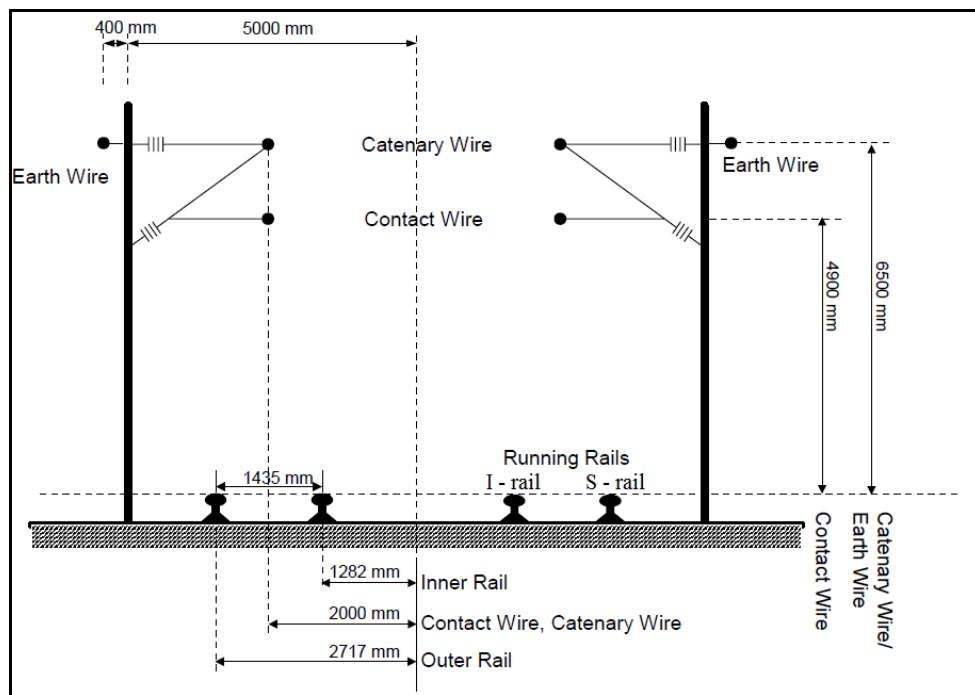


**Figure 2.34** The configuration of Overhead Catenary System  
(Sandra, Martin, and Menter 2007).

Due to the unpredictability of lightning strike point on multiple unit trains in pantograph which touches the catenary wire, it better to study the parts which are exposed to lightning according to the IEEE STD. 1234-1997, by using the formula (2.11) in (Yang and Zhang 2015).

$$\begin{cases} r_c = 1.34h^{0.6}I^{0.65} \\ r_c = r_g \end{cases} \quad (2.11)$$

where  $r_c$  is lightning strike distance of catenary which touches on pantograph of multiple unit trains, its UI is m;  $h$  is the average height of hanging wire, its UI is m;  $I$

is the lightning current amplitude, its IU is kA;  $r_g$  is lightning strike distance of earth on top of elevated pole, its UI is m.

The range of triggered lightning of catenary shown in Figure 2.35 as in (Yang and Zhang 2015) but in this study, was considered when it is on top of the elevated pole. AB arc line is triggered a lightning range of auxiliary line (feeder line) ( $r_{R6}$ ), CD arc is triggered a lightning range of catenary line (contact line and messenger line) (CA). The lightning current reaches first to the line which has a higher range of lightning strike distance compared to other wires. Auxiliary line (feeder line) ( $r_{R6}$ ) and return line ( $r_{R5}$ ) are on the same side on top of the mast. Whereas lightning strike distance of auxiliary line ( $r_{R6}$ ) is greater than return line ( $r_{R5}$ ) which lead  $r_{R6}$  to shield  $r_{R5}$  but there is no any shield for the catenary line that touch pantograph, and lead immense possibilities to be attacked by lightning strikes on it. In this study, we focus when multiple lightning strokes on Train's pantograph, on top of Mast, Return wire (Earthing wire), and Catenary wire because there is a possibility to strike on either of these lines. It is casual that catenary on high ground like on top of an elevated pole experience more lightning strike than that on low ground as in Liu, and Liu (2012).

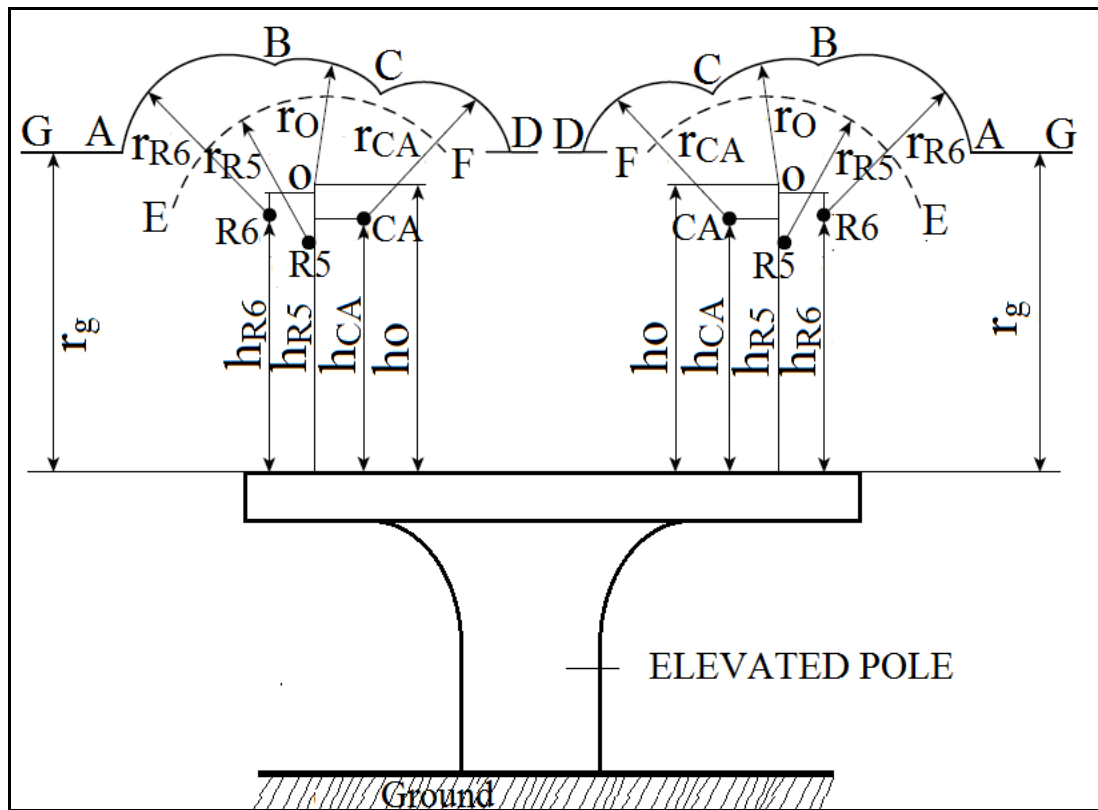


**Figure 2.35** The range of triggered lightning of Catenary on the double-track elevated railway system.

## 2.14 Proposed system.

This precise work model the existed system for estimating, improving and optimizing the lightning performance of Catenary Contact System due to frequency number of lightning overvoltage faults. In an effort to maintain failure rates at a low level, supplying high power quality and resisting damages and disturbances, plenty of lightning performance estimation studies have been conducted. According to the lightning performance, estimation studies of Overhead catenary lines are exclusively showed that the lightning performance of Overhead catenary system relying on their correct initial design of existing system needs to be improved and optimized. Analysis

Transient Program (ATPDraw) with the help of iterative optimization algorithm was used to estimate, improve and optimize the lightning performance due to overvoltage was caused by characteristic and behavior of transient current during multiple lightning strokes. The striking on Train's pantograph, on top of Mast, Return wire (Earthing wire), and Catenary wire of a 25 kV AC, 50 Hz Catenary Contact System on double-track elevated railway system at the Mast (7<sup>th</sup> Mast) for Case 1 as shown in Figure 2.36 (a) and Figure 2.37 include at the mid-span of Masts (sixth and seventh<sup>th</sup> Masts) for Case 2 as shown in Figure 2.36 (b) and Figure 2.38 were considered. The points 1-4 from the Figures 2.36-2.38 represent the lightning strokes strikes on Train's pantograph, on top of Mast, Return wire (Earthing wire), and Catenary wire respectively. By using this method, optimal values of the line insulation level, the tower footing resistance, energy absorption capability of surge arresters, surge arresters' installation interval and a number of installed surge arresters are calculated in order to minimize the defined objective function, aiming to reduce or even eliminate lightning failures. Optimization method was considered all the available protection means, i.e. Earth wires and surge arresters.

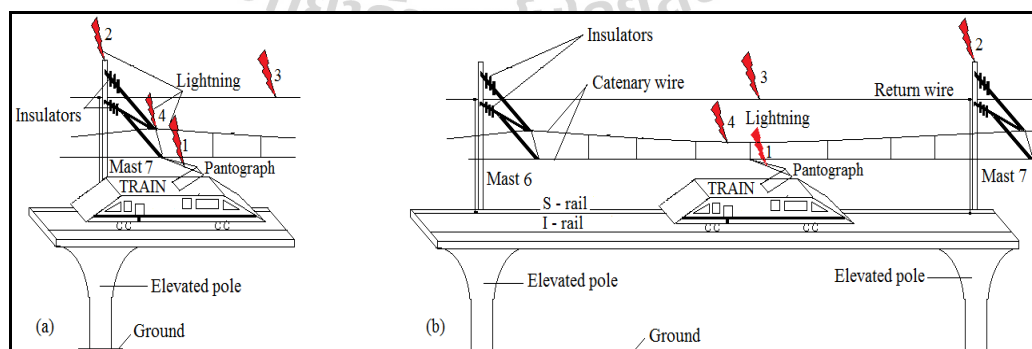


**Figure 2.36** Lightning strike on train's pantograph (a) at the Mast and (b) at the mid-span of Masts in the 2D view.

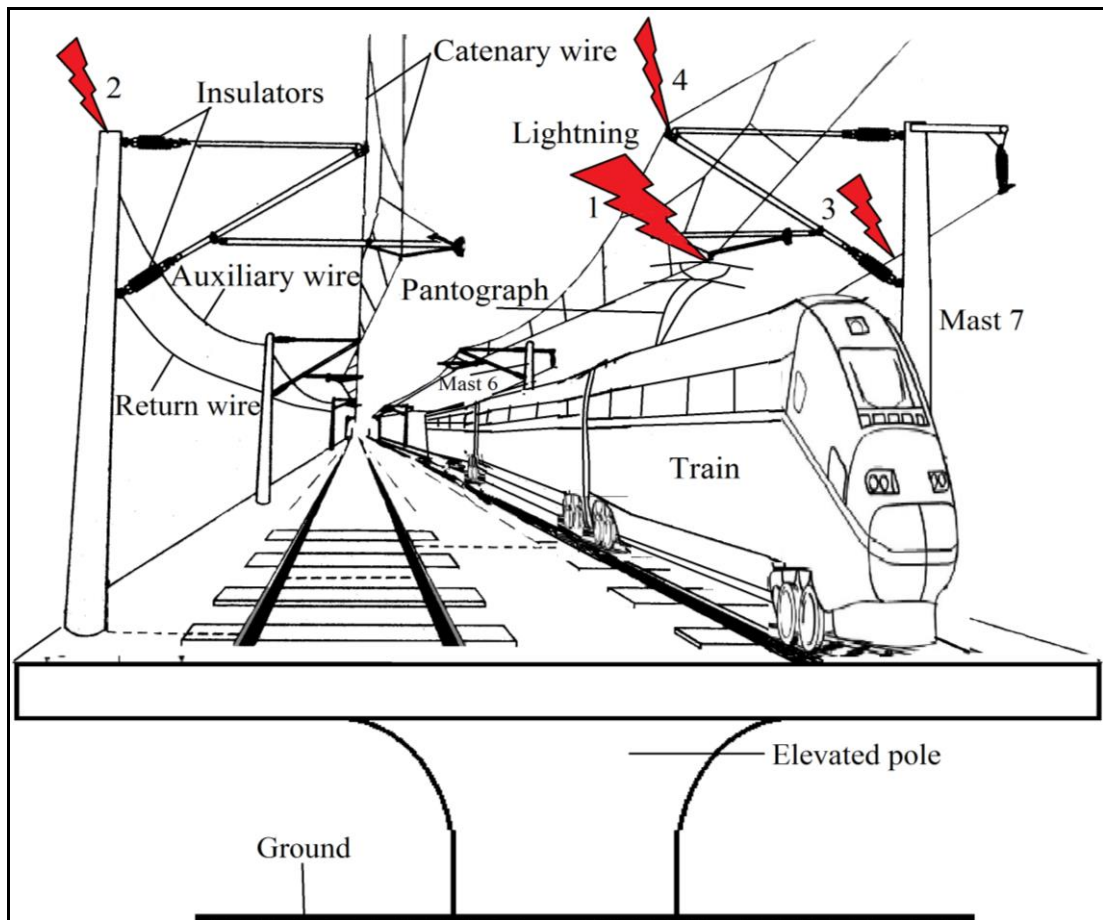


**Figure 2.37** Lightning strike on train's pantograph at the Mast in the 3D view.

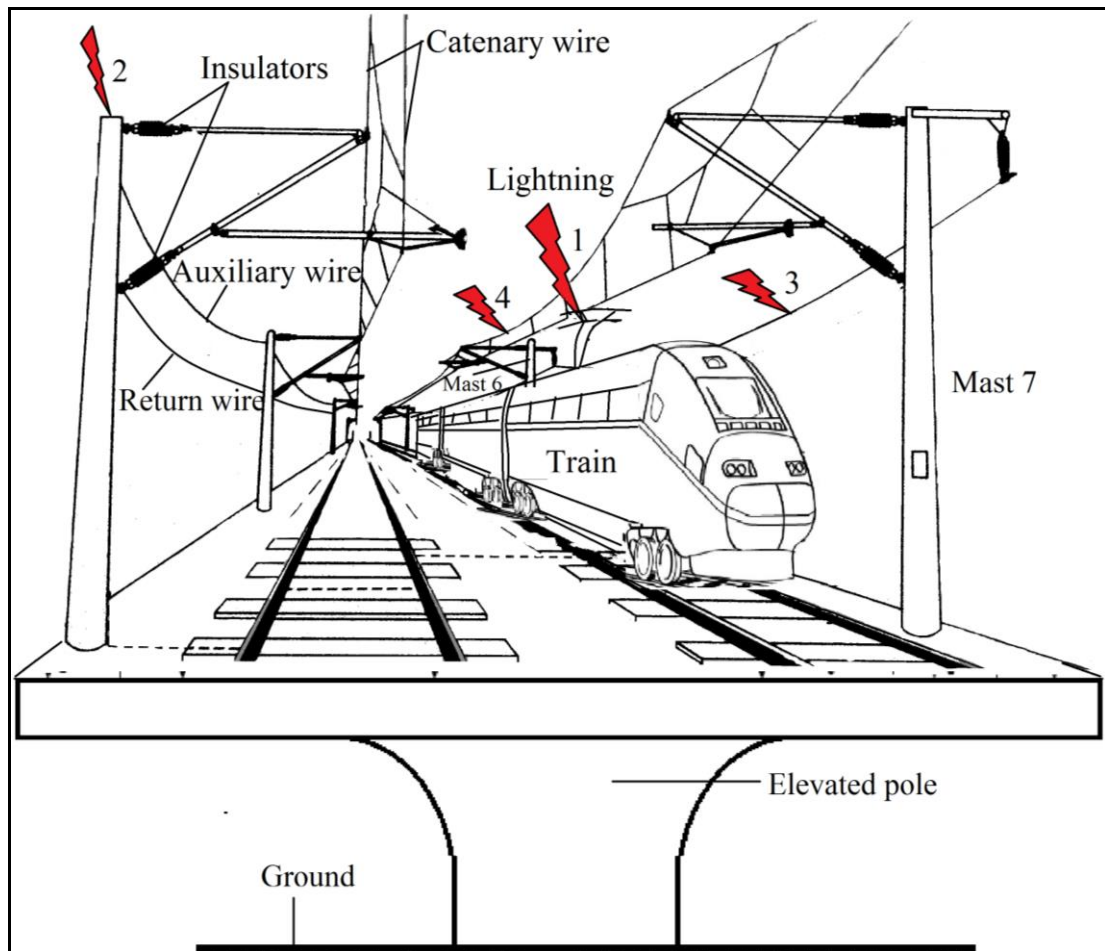


**Figure 2.38** Lightning strike on train's pantograph at the mid-span of Masts in the 3D view.

## 2.15 Chapter summary

This chapter has reviewed railway electrification systems, including electric railway traction and final DC and AC motor drives. Furthermore, with significant potential for the application of the railway electrification system, electric supplies remain impressive as electric vehicle operates without having an on-board prime mover. Three railway electrification systems were discussed. Overhead Line System, Third Rail System, and Ground-Level Power Supply System. DC Catenary Contact System, AC-DC Catenary Contact System, and AC-DC-AC Catenary Contact System

are the three most popular types of Overhead line system in the railway electrification system. Two Overhead line systems for the DC motor drive are discussed. There are two types of Overhead line systems for AC motor drive: AC-DC-AC Catenary Contact System and Transformerless AC-DC-AC Catenary Contact System. The AC motor type is also referred to as the induction motor, which is more popularly applied to railway electrification described by electric railway traction. The duty cycle of operation of induction motors is also discussed. Multi-system Units as used the multiple power systems, such as engines and motors, are commonly adopted on modern railway electric vehicles. The operations between these electrification systems are usually considered to be homogenous. However, the distinctive operation can be possible if the electrification systems can be decoupled and work independently. The power demand from the driver or the supervisory control unit is met by summed up power outputs from different sources.

Currently, AC-DC Catenary Contact System has been employed in Thailand due to inherent advantages in magnetic field protection and wheel slip correction in the DC motor drive. Usually, electricity in this electrified railway transmission system must be stably secured with effectively track system and control system. Electric Power is injected into the system which is in the form of overhead catenary transmission line without any disturbance. But the hardship of transmission line that injects power into a system along distance may likely cause the electrical breakdown when lightning strikes on multiple train's pantographs as a natural disturbance. Actually, this leads various electrical elements failure, power losses, and other unreliable condition on Catenary Contact System which gives rise to another problem: "how to optimize the lightning performance of the Catenary Contact system?". Such a



problem can only be answered with further study of optimization techniques for the power system.

In the improvement and optimization techniques review, it has been observed that most of the studies in Catenary Contact System made the focus on estimation and development of lightning performance without considering the optimization of lightning performance in Catenary Contact System. The best way is to estimate, improve and optimize. The best model is one that can obtain excellent method, which reduces the failure rates at low cost. This approach was compared to previous studies of the Lightning performance in high voltage transmission lines safeguard by surge arresters, a simulation for the Hellenic transmission network and Optimization of Hellenic Overhead High-Voltage Transmission Lines Lightning Protection by using Simulink and numerical techniques. These techniques are showing the usefulness of the method, which can prove to be a valuable tool for the studies of Catenary Contact System designers. Lastly, overhead catenary system in Airport Rail Link, Thailand has finally discussed. The preliminary Study, Analysis of Elevated Structure and Catenary Lightning Range were undertaken. The proposed system of an overhead catenary system based on two different cases has been shown. For designed the proposed system, the next chapter has been undertaken the significant elements in an overhead catenary system for representing the effectuated power network.

# **CHAPTER 3**

## **METHODOLOGY**

### **3.1 Introduction**

The proposed ATP-EMTP software which recognized as standard procedure in power system used to investigate transient current behavior during multiple lightning strokes on multiple unit train's pantographs. Modeling of multiple lightning sources, mast, multiple unit trains, overhead catenary transmission line, insulator, elevated pole, and the ground was guided to represent catenary contact system on the double-track elevated railway system for analyzing the problem.

As a version part of the electromagnetic transients' program, ATP-EMPT is the powerful tool for steady state and transient analysis of power systems (Lee and Goldsworthy 2011). It has been recognized as per international standard as IEEE and CIGRE in arithmetic circuits (Wu and Cao 2012). In this task, ATP-EMTP is utilized as time domain computation in overvoltage protection against lightning as indicating from Figures. 2.36-2.38.

### **3.2 Catenary Contact System**

Overhead Catenary Transmission line involved Catenary line, return line, Auxiliary line with running rails (S-rail, I-rail) and distributed-parameter line spans on both sides of the impact point. The details of Overhead Catenary Transmission line were given Table 3.1 as in Mazloom (2010); Achouri, Achouri, and Khamliche (2015); Yang and Zhang (2015) with Autotransformer and Booster transformer as

modeled by 1:1 ideal transformers in ATPDraw. Mast configuration parameters of 2×25 kV AC, 50 Hz Catenary Contact System are given in Table 3.2 (Andreotti, et al., 2014). Its cross-section view axis of double track Railway Electrification system on elevated railway system is shown in Figure 2.34. A Railway Transmission line was modeled by LCC\_8 with JMARTI model in ATPDraw as illustrated in Figure 3.1.

**Table 3.1** Details of 25 kV Overhead Catenary Transmission Line (Mazloom, 2010).

Overhead Catenary Transmission line					
Conductor	Catenary (R1)	Return (R2)	Auxiliary (R3)	S-rail	I-rail
Radius	5.06 cm	0.82 cm	0.56 cm	4.95 cm	4.95 cm
Ruling Span	Between the Masts				
	60				
Grounding System	Grounding Resistance ( $\Omega$ )			Pole Resistance ( $\Omega$ )	
	5-100			50	

#	Ph.no.	React [ohm/km AC]	Rout [cm]	Resis [ohm/km AC]	Horiz [m]	Vtower [m]	Vmid [m]
1	1	0	4.95	1.75E-6	-0.7175	0.96	0.96
2	2	0	0.82	6.04E-7	2.5775	5.5	5.5
3	3	0	5.06	1.39E-5	0	5.3	5.3
4	4	0	0.56	2.81E-7	3.62	8	8
5	5	0	4.95	1.75E-6	0.7175	0.96	0.96

**Figure 3.1** Transmission line data in ATP EMTP

**Table 3.2** Mast Configuration (Andreotti, et al., 2014).

Parameters (m)									
$h_1$	$h_2$	$h_3$	$h_4$	$h_5$	$r_1$	$r_2$	$r_3$	$r_4$	$r_5$
8	5.5	5.3	0.96	0.96	1.1625	0.12	2.4575	1.74	3.175

### 3.3 Modeling of Lightning Source

The report of lightning statistics in Thailand from Marungsri et al. 2008 shows that the Lightning often occurs in April-May but severely in June. The magnitude ranges 11-171 kA with positive polarity and -10 to -139 kA with negative polarity. Positive lightning strokes account for 5% while negative is 95% with the magnitude of -10 to -50 kA. Also, Negative lightning stroke association with multiple strokes per flash averaging 3 to 4 strokes per flash with intervals of tens of milliseconds were the most reported lightning incidences in Omidiora and Lehtonen 2007; Martinez-Velasco and Aranda 2008; Rodriguez-Sanabria, Ramos-Robles, and Orama-Exclusa 2011. Since negative lightning strokes may associate with subsequent strokes, only single stroke and multiple strokes in the first and second strokes are highly considered due to the effects of their current magnitudes in insulation (Martinez-Velasco and Aranda 2008). But the behavior of tower grounding electrode and surrounding soil at higher frequencies of up to 10 MHz is not yet explicitly represented (Pattanadech and Yutthagowith 2014). Therefore, the Heidler current function model in ATP-EMTP was used to represent the lightning current as shown in equation (3.1) (Das, 2010; Yang, and Zhang, 2015; Thanasaksiri, 2014).

$$i(t) = kI_m \left[ \frac{\left(\frac{t}{\tau_1}\right)^n}{1 + \left(\frac{t}{\tau_1}\right)^n} \right] e^{(-t/\tau_2)} \quad (3.1)$$

Where  $k$  is the correction coefficient for the peak current;

$\tau_1$  is the virtual front time;

$\tau_2$  is the virtual tail time;

$I_m$  is the lightning current peak; and

$n$  is the lightning current gradient factor

Parameters of lightning sources are given in Tables 3.3-3.4, and the waveforms of the single and multiple strokes as recommended by IEC 62305 are shown in Figures. 3.2-3.5 for -34 kA and 50 kA respectively.

**Table 3.3** Parameters of the single lightning source (Marungsri et al., 2008; IEC 62305:1-4; Thanasaksiri, 2014).

Parameter	First strokes
Type	Heidler 15
Amp. (kA)	-34
	-50
Front time ( $\mu$ s)	2
Tail time ( $\mu$ s)	100

**Table 3.4** Parameters of multiple lightning sources (Marungsri et al., 2008; IEC 62305:1-4).

Parameter	First strokes	Subsequent Strokes
Type	Heidler 15	Heidler 15
Amp. (kA)	-34	-34
	-50	-50
Front time ( $\mu$ s)	1	0.2
Tail time ( $\mu$ s)	100	50

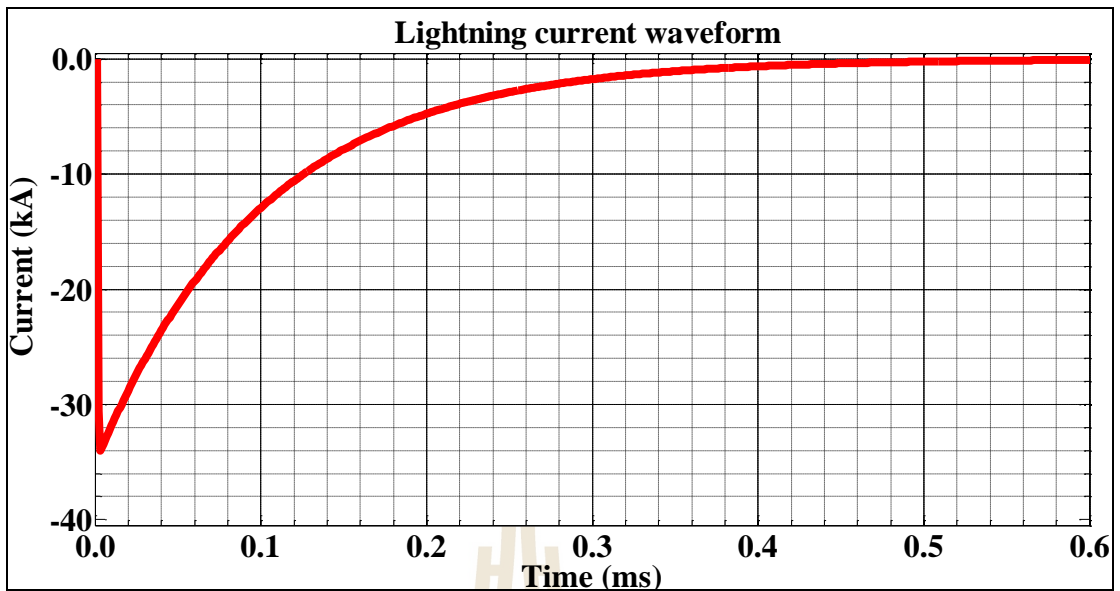


**Figure 3.2** Waveforms of the Single lightning of -34 kA (2.0/100  $\mu$ s) strokes modeled in ATP-EMTP.

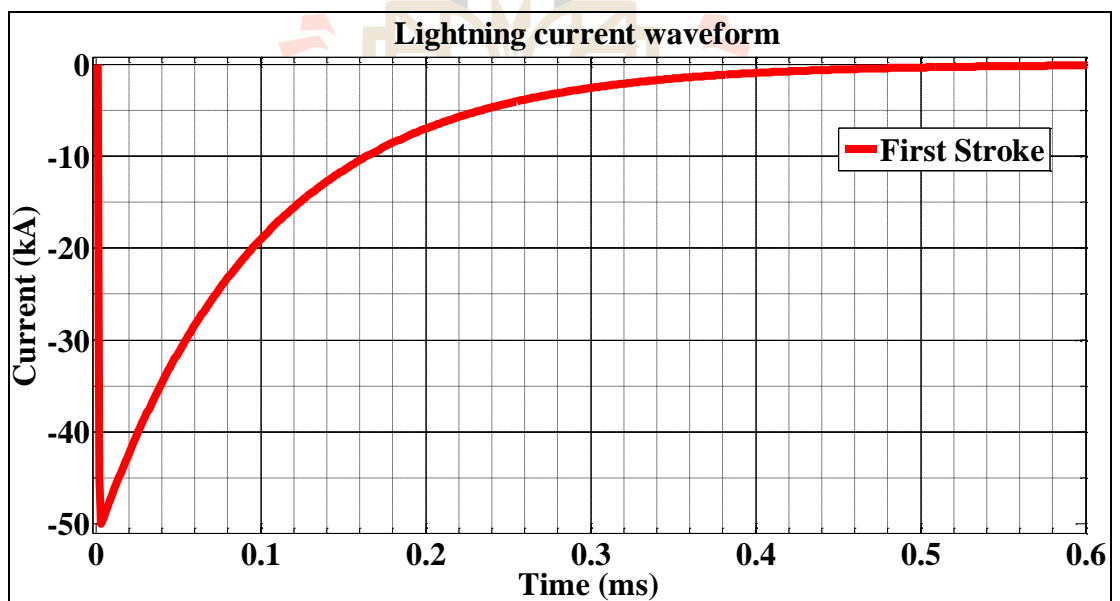


**Figure 3.3** Waveforms of the Single lightning of -50 kA (2.0/100  $\mu$ s) strokes modeled in ATP-EMTP.

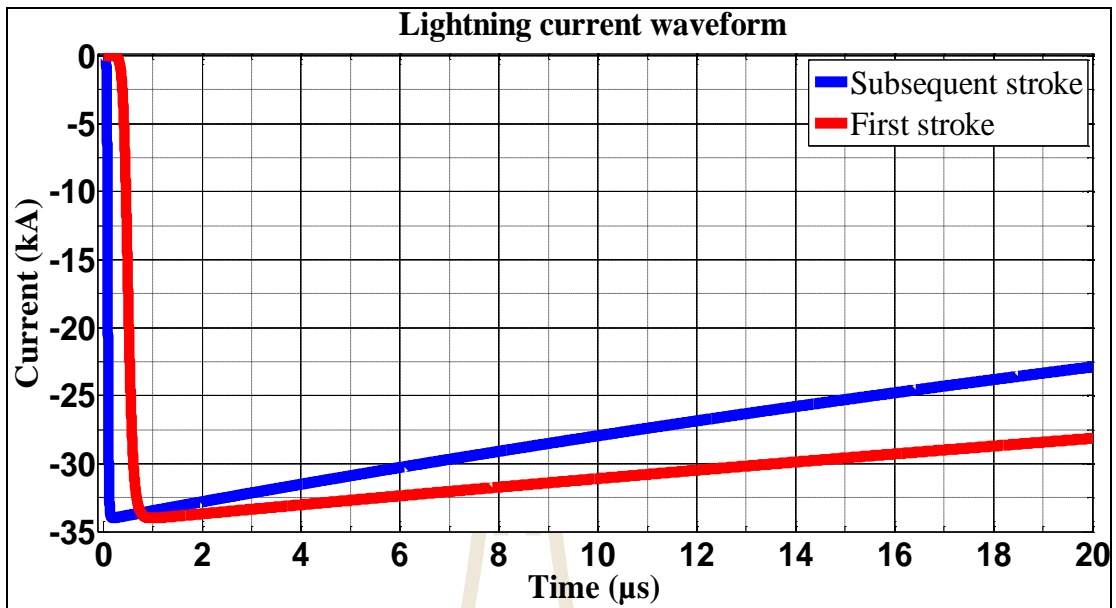


Figure 3.4 Lightning current waveforms of the -34 kA first stroke-(1.0/100 μs), subsequent stroke -(0.2/50 μs) designed in ATP-EMTP.

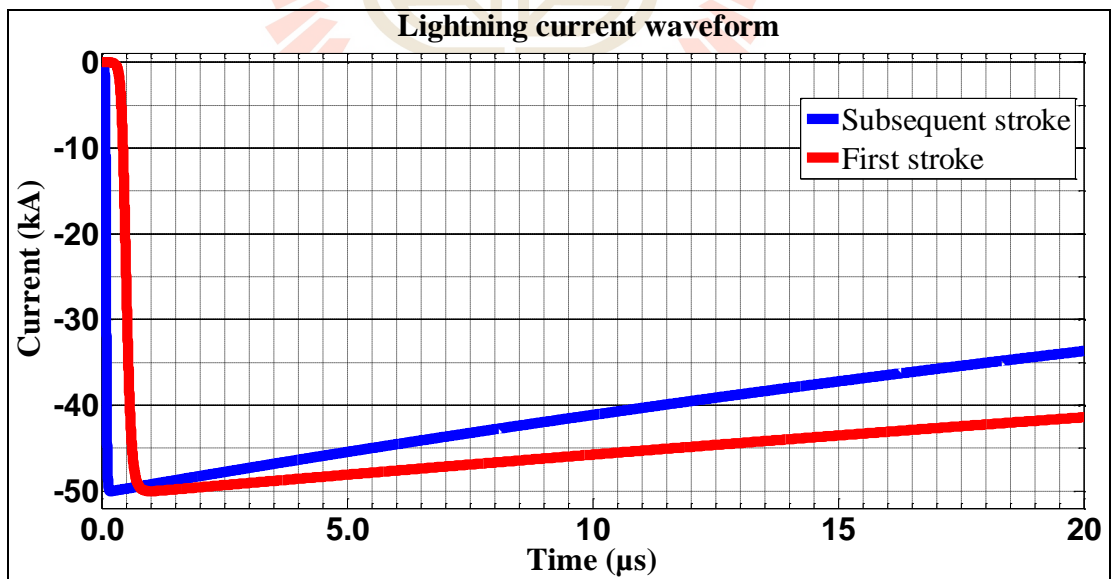


Figure 3.5 Lightning current waveforms of the -50 kA first stroke-(1.0/100 μs), subsequent stroke -(0.2/50 μs) designed in ATP-EMTP.

### 3.4 Modeling of Mast

The mast was modeled by cylindrical geometrical steel column in single wave impedance model as recommended by IEEE and CIGRE by expression (3.2) (Yang, and Zhang, 2015; Zhang, Sima, and Zhang, 2006). The modeled parameters of the mast are shown in Table 3.5.

$$Z = 60 \ln \cot \left[ 0.5 \arctan \left( \frac{R}{H} \right) \right] \quad (3.2)$$

where  $Z$  is the surge impedance, its IU is  $\Omega$ ;

$R$  is the equivalent radius of the mast; its IU is m;

$H$  is the height of the mast; its IU is m.

**Table 3.5** Modeled Parameters of Mast.

Location	Parameters
Auxiliary	$Z_{aux} = 157.64 \Omega$ , $L1 = 2.5$ m
Return	$Z_{return} = 293.57 \Omega$ , $L2 = 0.2$ m
Catenary	$Z_{catenary} = 113.77 \Omega$ , $L3 = 5.3$ m

### 3.5 Modeling of Train.

The train was modeled as electric locomotive which contains pantograph, locomotive transformer, diode rectifier bridge and DC motors as stated in (Zupan, Teklić, and Filipović-Grčić, 2013; Karagöz, 2014). Figure 3.6 shows the model of Train system at the Mast (7<sup>th</sup> Mast) for Case 1 with Mast, elevated pole, and grounding, Railway Transmission line, Ground, and Insulators modeled with a branch of capacitor and voltage controlled switch at Mast. Figure 3.7 shows the model of



train at the mid-span of Masts (6<sup>th</sup> and 7<sup>th</sup> Masts) for Case 2 with Railway transmission line

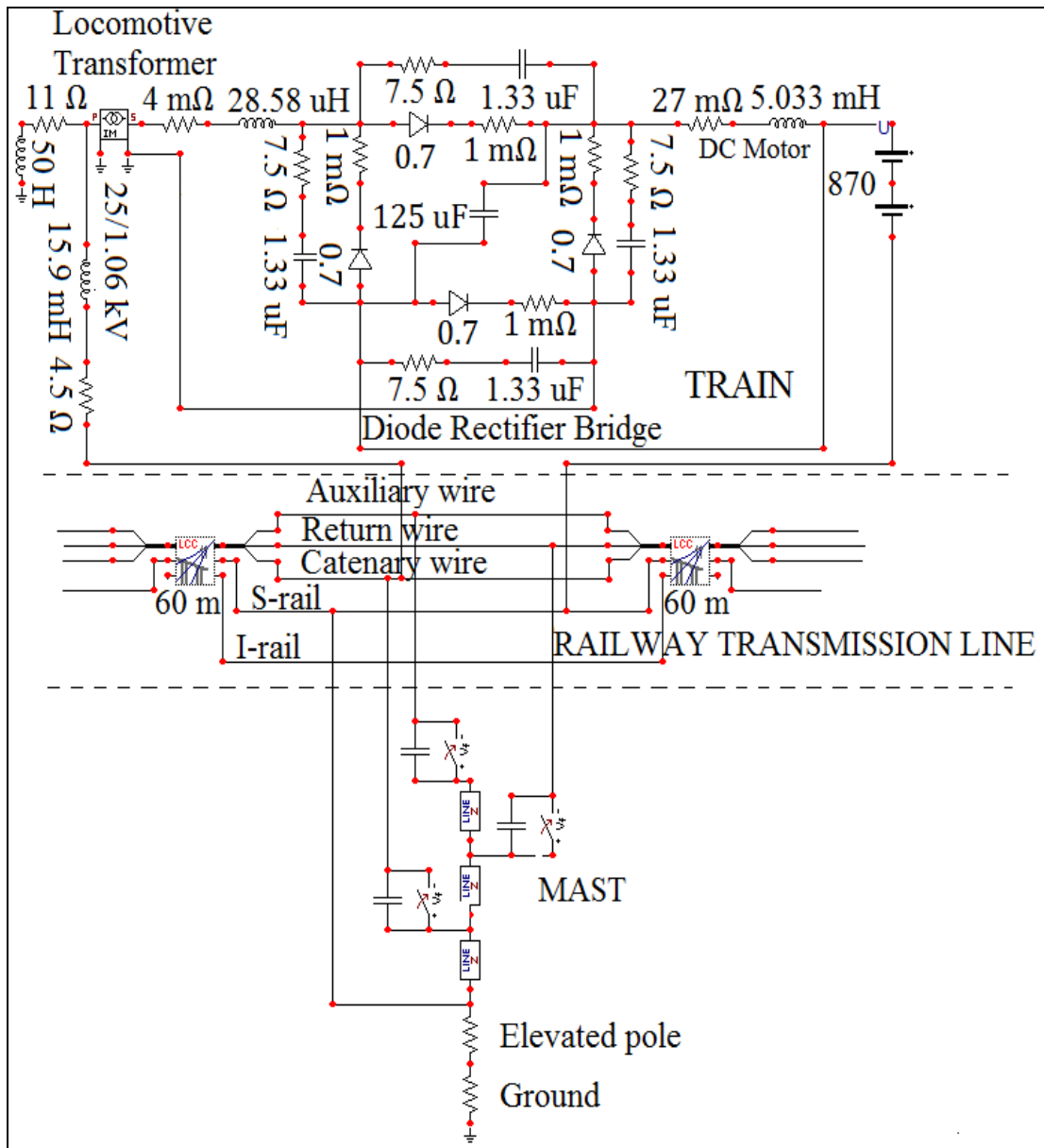


**Figure 3.6** Mast with Train, Railway Transmission line, Pole, Ground, and

Insulators at Mast in ATP-EMTP.

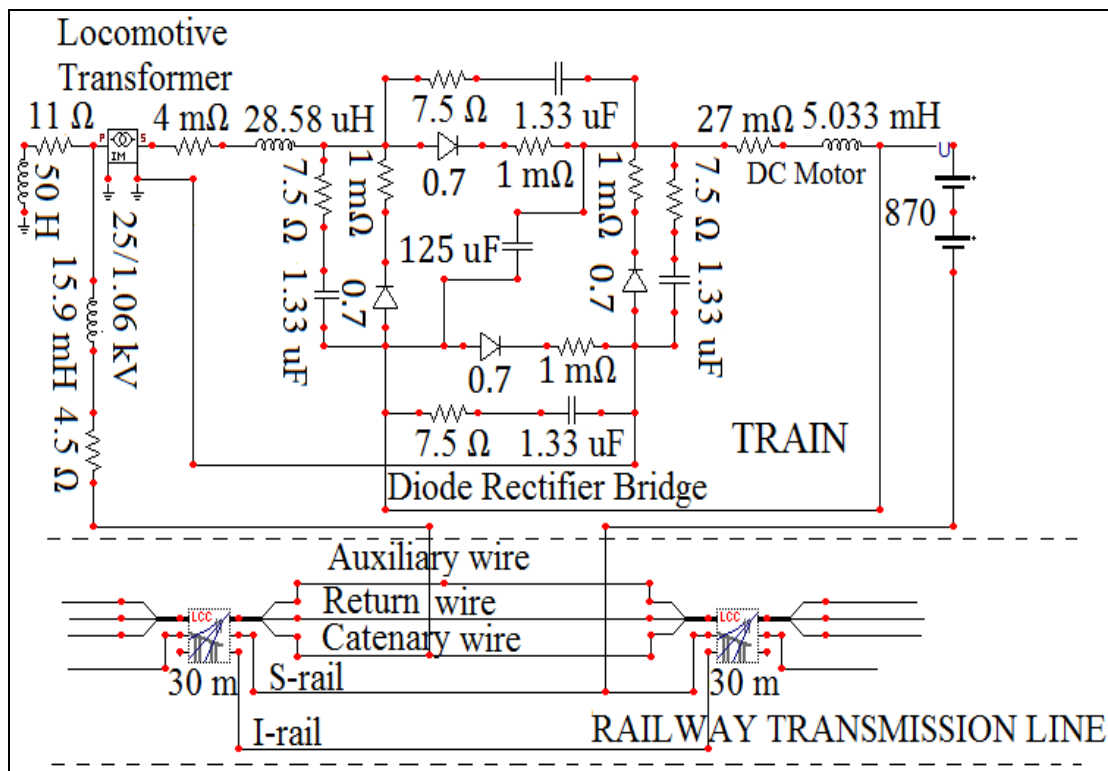


**Figure 3.7** Train with Railway Transmission line at the mid-span of Masts in ATP-EMTP.

### 3.6 Modeling of Insulator.

Generally, insulator resists the flow of current from phase conductor to the ground during normal operating condition. Since the capability of an insulator to withstand stress depends on its voltage withstand level, this behavior can be represented as a voltage controlled switch (Imece et al., 1996). Moreover, the effects of coupling conductors to mast structure can also be represented by the capacitor. If the voltage across insulator terminals is greater than control voltage of the switch, the switch closes which indicates flashover. Otherwise, if the voltage stress is less than control voltage, the switch remains open to show no flow of current across the insulator. In the simulation, the voltage controlled switch was designed by

Switchvc.sup model. The voltage withstand capabilities for the rod/composite, spool and pin as given in Table 3.6 were set as the control voltage of the switch (Mazloom, 2010). The values of capacitance for suspension insulators are 80 pF/unit while for pin insulators are around 100pF/unit (Imece et al., 1996).

**Table 3.6** Details of 25 kV Overhead Catenary Transmission Line (Mazloom, 2010).

Insulators (Impulse Withstand Voltage)		
Rod/Composite (R1)	Spool (R2)	Pin (R3)
225 kV	60 kV	140 kV

### 3.7 Modeling of Grounding Resistance.

Once the lightning current discharges to earth through the mast, the ionization process occurs around soil surrounding the grounding rod. This situation makes surrounding soil as non-linear and the frequency dependent. A non-linear frequency-dependent representation is required to obtain an accurate simulation (Martinez-Velasco and Aranda 2008; Pattanadech and Yutthagowith, 2014; Chisholm and Janischewskyj, 1989; Mousa, 1994). Due to difficulties of information to representing this behavior not always available, the reasonable model approximation of grounding resistance as recommended by IEC and IEEE standards is given in (3.3)-(3.4) (Yang, and Zhang, 2015; Imece et al. 1996; IEC 60071-2, 1996; IEEE Std. 1313.2, 1999; Martinez-Velasco and Aranda 2003).

$$R_f = \frac{R_g}{\sqrt{1 + \frac{I}{I_g}}} \quad (3.3)$$

Where  $R_f$  = tower grounding ( $\Omega$ )

$R_g$  = tower grounding resistance at low current and low frequency

$I$  = surge current into ground (kA)

$I_g$  = limiting current initiating soil ionization (kA) which is given in (Mousa, 1994)

$$I_g = \frac{1}{2\pi} \left( \frac{E_0 \rho_0}{R_g^2} \right) \quad (3.4)$$

Where  $\rho_0$  = soil resistivity ( $\Omega$ -m)

$E_0$  = soil ionization gradient (400kV/m) (Mousa, 1994)

### 3.8 Modeling of Metal Oxide Surge Arrester.

Metal Oxide Surge Arrester protect string insulator against lightning flashover in power system by maintaining voltage across insulator as in (Rodriguez-Sanabria, Ramos-Robles, and Orama-Exclusa 2011; Nafar, Solookinejad, and Jabbari 2014; Durbak 1985; Saengsuwan, and Thipprasert 2008; Mungkung et al. 2007). In order to attain the required performance, TLAs must be correctly matched with the existing line conditions. For Overhead line protection, TLA should not conduct or act as an open circuit at normal operation and conduct current during overvoltage without causing a fault (Nafar, Solookinejad, and Jabbari 2014; Ametaniand, and Kawamura 2005). This condition describes the behavior of TLA of having extremely high resistance during normal operation and a relatively small resistance during overvoltage. A good TLA should have a non-linear voltage versus current (V-I) characteristic. A Silicon Carbide (gapped arrester) has been in service for a long time, but its failure is mainly due to gap spark over caused by moisture ingress or

contamination (Mungkung et al. 2007). Despite its disadvantages over Silicon Carbide, Metal Oxide Surge Arrester (gapless) has been a substitute for a couple of years because of its high non-linear V-I characteristics. The model proposed by Durbak (1985) and adopted by the IEEE WG 3.4.11, (1992) including committee papers and standards (IEEE Std. C62.22-1997), and then modified by Pinceti (Rodriguez-Sanabria, Ramos-Robles, and Orama-Exclusa 2011; Durbak 1985, Mardira, and Saha 1996). Metal oxide surge arrester is modeled by using MOV Type 92 in ATPDraw represent a nonlinear resistor used in surge arrester as shown in Figure 3.8.

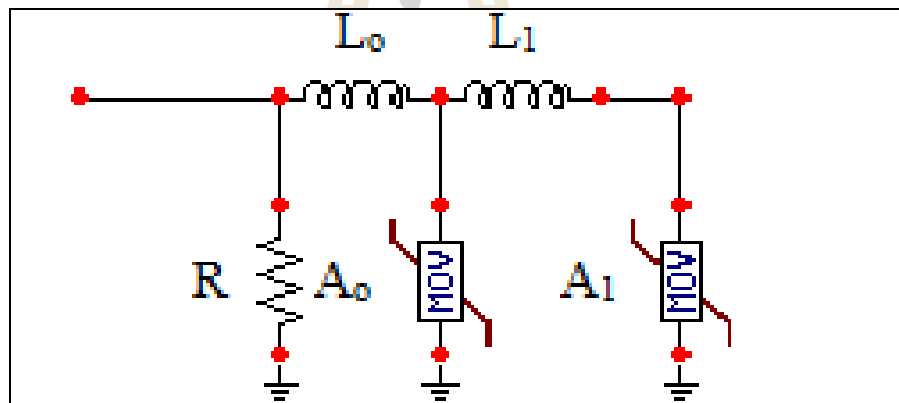


**Figure 3.8** Pinceti model

The model is composed of two sections of non-linear resistances  $A_0$  and  $A_1$  separated by inductances  $L_0$  and  $L_1$ . On IEEE WG 3.4.11, the non-linear characteristics of  $A_0$  and  $A_1$  are established in uniform designed curve. Additionally, these behaviors are referred to as peak values of residual voltages measured under a discharge test with a 10-kA multiple lightning current impulse in  $8/20 \mu\text{s}$  ( $V_{r8/20}$ ) (Nafar, Solookinejad, and Jabbari 2014; Durbak 1985; Mungkung et al. 2007; Mardira, and Saha 1996). The  $V_{10}$  is often taken as a 1 p.u value and the V-I curve can

be obtained by multiplying the per unit arrester voltages by  $V_{10}$  of that rating to get discharge voltages for nonlinear resistors  $A_0$  and  $A_1$  by using equation (3.5) and (3.6) respectively (IEEE WG 3.4.11, 1992). The data for arrester modeling was based on ABB MWK after Arrester selection under IEC and IEEE standards (ABB Surge arrester POLIM-S, 2016; IEC Std. 60099-5; IEEE Std. C62.22-1997) which proposed the procedures for selection of MO arresters. A one column arrester with 0.387 m length and the discharge voltage,  $V_{10}$ , for this arrester is 87 kV ( $U_r = 36.3$ ). The V-I curve is obtained from the power function equation (3.7) (Rodriguez-Sanabria, Ramos-Robles, and Orama-Exclusa 2011; Nafar, Solookinejad, and Jabbari 2014; Ametaniand, and Kawamura 2005; IEEE WG 3.4.11, 1992) as shown in Table 3.7.

$$\text{The Discharge Voltage in kV} = \left[ \text{Relative IR in p.u for } A_0(i) \times (V_{10} / 1.6) \right] \quad (3.5)$$

$$\text{The Discharge Voltage in kV} = \left[ \text{Relative IR in p.u for } A_1(i) \times (V_{10} / 1.6) \right] \quad (3.6)$$

$$i = p \left( \frac{V}{V_{ref}} \right)^q \quad (3.7)$$

where  $q$ =exponent,

$p$ =multiplier and

$V_{ref}$ =reference voltage.

Inductance  $L_1$  and  $L_0$  are calculated by means of equations (3.8), (3.9) and (3.10) in (Martinez-Velasco 2010).  $L_1$  (810 nH) acts as a filter affecting during surge voltages,  $L_0$  (270 nH) represents magnetic fields during arrester operation and  $R$  (1 M $\Omega$ ) with the aim of avoiding numerical troubles (Omidiora and Lehtonen 2007;

Mungkung et al. 2007; Abd-Allah, Ali, and Said, 2014). For normal operations, surge arrester current is less than 0.1 mA (Ametaniand, and Kawamura 2005). In order to suit the modeling, non-linear arrester characteristics should be modeled to at least 20 kA to 40 kA because high surge current to be discharged by arrester can occur above 10 kA during lightning (Mungkung et al. 2007). Parameters of the model are also shown in Table 3.7.

$$L_0 = \frac{1}{12}(K-1) \cdot V_n (\mu H) \quad (3.8)$$

$$L_1 = \frac{1}{4}(K-1) \cdot V_n (\mu H) \quad (3.9)$$

$$K = \frac{V_{1/T2}}{V_{10}} \quad (3.10)$$

Where  $V_n$  = the arrester rated voltage in kV

$V_{10}$  = the discharge voltage for a 10 kA, 8/20  $\mu$ s current in kV

$V_{1/T2}$  = the discharge voltage for a 10-kA steep current pulse in kV

The value  $V_{1/T2}$  is similar to the front of wave (FOW) discharge voltage defined in the IEEE standard (IEEE Std. C62.22-1997). The front of the wave (FOW) discharge voltage for selected arrester is 94.2 kV (Type POLIM-S Surge Arresters, 2008).

**Table 3.7** V-I Characteristics for nonlinear resistor  $A_0$  and  $A_1$  of the Pinceti model.

kA	$A_0$		$A_1$	
	V (p.u)	V(kV)	V (p.u)	V(kV)
0.01	1.40	76.125	-	-
0.1	1.54	83.7375	1.23	66.88125
1	1.68	91.35	1.36	73.95
2	1.74	94.6125	1.43	77.75625
4	1.80	97.875	1.48	80.475
6	1.82	98.9625	1.50	81.5625
8	1.87	101.68125	1.53	83.19375
10	1.90	103.3125	1.55	84.28125
12	1.93	104.94375	1.56	84.825
14	1.97	107.11875	1.58	85.9125
16	2.00	108.75	1.59	86.45625
18	2.05	111.46875	1.60	87
20	2.10	114.1875	1.61	87.54375
R=1 M $\Omega$ L <sub>0</sub> =270 nH    L <sub>1</sub> =810 nH				

### 3.9 Optimization Method.

The analysis of transmission lines lightning failure ( $N_T$ ) shows that the simple solution to eliminate lightning flashovers completely is to install of surge arresters on every single tower although this solution needs massive capital investment. Therefore, in order to reduce the lightning failure rates at a minimum cost, it could be worthwhile to investigate further on the most appropriate selection of these parameters (insulation level, grounding resistance, surge arrester's energy absorption capability, surge arresters' installation interval) (Christodoulou, et al., 2009). But this thesis would investigate more parameters include a number of surge arresters to be installed.

A performance index was defined from APPENDIX B for each region N of the examined transmission line in order to relate the total flashover failure rate annual cost to the total investment cost of the regional values. The insulation level, the grounding resistance, the energy absorption capability of surge arresters, the surge



arresters' installation interval, and a number of surge arresters to be installed are the regional values as in Equation (3.11) (Christodoulou, et al., 2009).

$$J_i = k_i(N_{Ti}) + g_{U_{ai}}(U_{ai}) + g_{R_i}(R_i) + g_{E_i}(E_i) + g_{I_i}(I_i) + g_{K_i}(K_i) \quad (3.11)$$

where  $i = 1, \dots, N$  region number;  $J_i$  is the performance cost index of the  $i^{\text{th}}$  region;  $k_i(\cdot)$  is the annual line failure cost;  $g_{ji}(\cdot)$  is the equivalent annual investment of the  $i^{\text{th}}$  region line design characteristic  $j$ ;  $N_{Ti}$  is the total flashover failure rate of region  $i$ ;  $U_{ai}$  is the insulation level of region  $i$ ;  $R_i$  is the grounding footing resistance of region  $i$ ;  $E_i$  is the energy absorption capability of the surge arresters of region  $i$ ;  $I_i$  is the surge arresters' installation interval of region  $i$  and  $K_i$  number of surge arresters to be installed. The annual line failure cost is given in equation (3.12):

$$k(\cdot) = C_{MEU} + C_{RE} + C_{FC} \quad (3.12)$$

where  $C_{MEU}$  is the mean annual cost of undelivered energy for the utility, equal to zero for non-open loop lines;  $C_{RE}$  is the mean cost of one permanent failure repair, and  $C_{FC}$  is the equivalent annual line failure consumer cost.

The full investment cost calculates the equivalent annual investment as in equation (3.13) (Christodoulou, et al., 2009).

$$g(\cdot) = \left( \frac{r(r+1)^t}{(r+1)^t - 1} + p \right) G(\cdot) \quad (3.13)$$

where  $G(\cdot)$  is the total cost of investment of the transmission line's design parameters;  $r$  is the annual interest rate;  $t$  is the estimated line exploitation period in years and  $p$  is an empirical coefficient which defines the ratio of the yearly maintenance cost to full investment cost.

The studied parameters, insulation level, grounding resistance of each region, energy absorption capability of the surge arresters, surge arresters' installation interval and a number of surge arresters to be installed in the form of a column vector  $x$  in equation (3.14).

$$\begin{cases} x = [x_1, x_2, \dots, x_{4N}]^T \\ x = [U_{a1}, U_{a2}, \dots, U_{aN}, R_1, R_2, \dots, R_N, E_1, E_2, \dots, E_N, I_1, I_2, \dots, I_N, K_1, K_2, \dots, K_N]^T \end{cases} \quad (3.14)$$

Optimal selection of  $x_i$ 's values minimize the set of the  $N$  performance indices defined in the equation (3.15) below:

$$\min_{U_{ai}, R_i, E_i, I_i} J_i = \min_{U_{ai}, R_i, E_i, I_i} [J_1 \ J_2 \ \dots \ J_N] \quad (3.15)$$

under the operating limits in equation (3.16):

$$\begin{cases} U_{ai_{\min}} \leq U_{ai} \leq U_{ai_{\max}} \\ R_{i_{\min}} \leq R_i \leq R_{i_{\max}} \\ E_{i_{\min}} \leq E_i \leq E_{i_{\max}} \\ I_{i_{\min}} \leq I_i \leq I_{i_{\max}} \\ K_{i_{\min}} \leq K_i \leq K_{i_{\max}} \end{cases} \quad (3.16)$$

where  $U_{ai_{\min}}, U_{ai_{\max}}, R_{i_{\min}}, R_{i_{\max}}, E_{i_{\min}}, E_{i_{\max}}, I_{i_{\min}}, I_{i_{\max}}, K_{i_{\min}}, K_{i_{\max}}$  are electrical utilities define limit values.

Application of an optimization algorithm determines the values of the optimum  $x_i$ , i.e. the insulation level, the tower footing resistance, the energy absorption capability of the surge arresters, the surge arresters' installation interval and a number of surge arresters to be installed. For the rest of the parameters the typical values of the horizontal spacing, between the ground wires  $b$ , the tower height  $h_t$ , the total inductance of the system  $L$ , the conductor line surge impedance  $Z_{surge}$ , which represent the standard equipment used by electrical utilities, were considered. All of the limit values and parameters result from safety, reliability, or economic considerations. They can be based on detailed engineering studies or little tradition. Optimization aims to minimize the objective vector function of several variables. The optimum solution vector  $x$  can be found for the  $J$  function presented in equation (3.14).

The minimization of (3.15) is carried out by intelligence search method called Genetic Algorithm (GA). The Genetic Algorithm was used to manipulate a set of initial random parameters in order to reduce programming complication. The toolbox that was employed in MATLAB to solve this algorithm is called GADS TOOLBOX (Genetic Algorithm and Direct Search Toolbox, 2004; El-Abiad, and Jaimes, 1969; Leeton, and Kulworawanichpong, 2011). The best result was observed in the generation process. The following steps as developed on Genetic Algorithm has been achieved.

**Step 1** Randomly initializes values for insulation level  $U_a$ , grounding resistance  $R$ , energy absorption capability of the surge arresters  $E$ , surge arresters' installation interval  $I$  and a number of surge arresters to be installed  $K$ .

**Step 2** Determine  $J_i$ 's function in reference to the overhead catenary system data, from (21).

**Step 3** Repeat

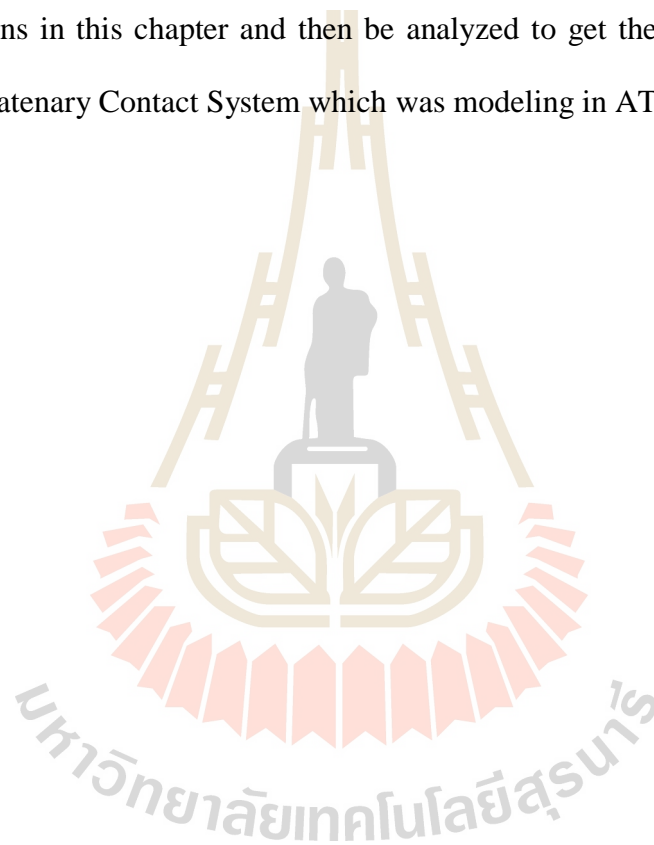
1. Select  $N_{Ti}$  from insulation level  $U_a$ , grounding resistance  $R$ , energy absorption capability of the surge arresters  $E$ , surge arresters' installation interval  $I$  and a number of surge arresters to be installed  $K$ .
2. Perform crossover on  $N_{Ti}$  from insulation level  $U_a$ , grounding resistance  $R$ , energy absorption capability of the surge arresters  $E$ , surge arresters' installation interval  $I$  and a number of surge arresters to be installed  $K$ .
3. Perform mutation of insulation level  $U_a$ , grounding resistance  $R$ , energy absorption capability of the surge arresters  $E$ , surge arresters' installation interval  $I$  and a number of surge arresters to be installed  $K$ .
4. Determine  $J_i$ 's of insulation level  $U_a$ , grounding resistance  $R$ , energy absorption capability of the surge arresters  $E$ , surge arresters' installation interval  $I$  and a number of surge arresters to be installed  $K$ .

Step 4: Until the best individual is good enough.

### 3.10 Chapter summary.

Implementation of the relevant model parameters in ATPDraw has been finished in this chapter. Typical values of modeled parameters are described and

provided for each component. Models are a circuit or mathematical or electrical representation of physical equipment so that its characteristic using output when applied to the particular input. In ATP-EMTP simulation, the input and output that are usually observed like current, voltage, power and energy. A complete set of representations of an Overhead Catenary Line system is a combination of every model of the transmission line equipment itself. The following chapter contains the results of the simulations in this chapter and then be analyzed to get the conclusion in 25 kV AC, 50 Hz Catenary Contact System which was modeling in ATP-EMTP.



# CHAPTER 4

## SIMULATION RESULTS

### 4.1 Introduction

This chapter demonstrates the results of the simulations carried out by the ATP-EMTP simulation for analysis of direct lightning strokes with mitigation of the flashover from single and multiple lightning strokes on overhead catenary system and the MATLAB simulation for the lightning performance optimization for 25 kV AC, 50 Hz catenary contact system.

### 4.2 Analysis of Direct Lightning strokes

For analysis purpose, the direct lightning strokes were effectuated by ATP-EMPT. Since direct lightning strikes likely to cause the charges to flow in the form of two same current waves in both directions, it strikes starting from the point of hitting. One side from the stroke point was considered and inspected by arranging the masts with its ground resistances into three configurations with two cases each. The first configuration was based on studying the effect of flashover from the affected mast to nearby masts when their grounding resistances ( $R_f$ ) are similar (same soil profile) when lightning strikes on train's pantograph based on two cases (see Fig. 4.1-4.2). The second configuration was done when their grounding resistances ( $R_f$ ) are different but in increasing order (different soil profile). Lastly, the third configuration was done when their grounding resistances are also different but in decreasing order (different soil profile). Table 4.1 and 4.2 show the arrangement of configuration 2 and

3 respectively. Since the lightning source was set at various points such as Mast, Return line, Catenary line and Train's pantograph at respective positions near to mast 4 (M4), the concern was to check the effect of flashover and back flashover into affected mast (M4), the nearby mast (mast 5 or M5) and far end mast (mast 7 or M7) under same and different soil profiles. The simulation results of the mast induced voltages across the insulators in the overhead catenary system are shown in APPENDIX C. The amplitude values of Mast induced voltages in the catenary, auxiliary and return lines for case one and two are recapitulated in Tables from APPENDIX D and analyzed in Figures. 4.3-4.146 for both cases.

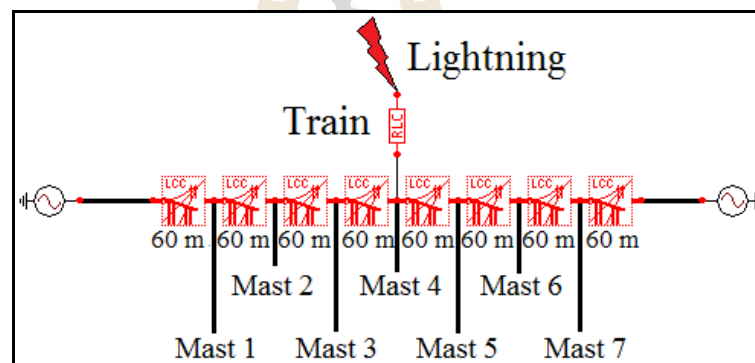


**Figure 4.1** Arrangement of the masts with lightning source for case 1

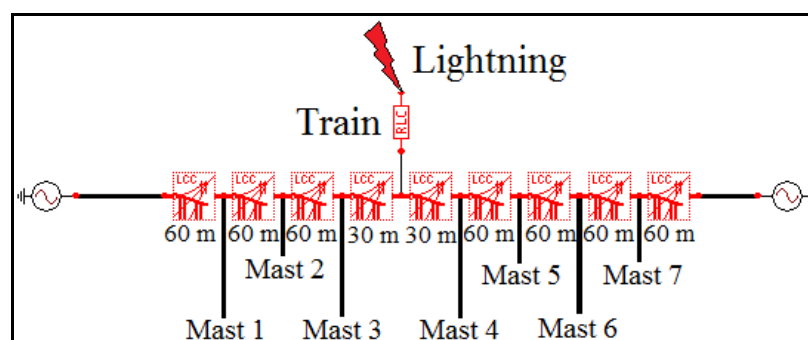


**Figure 4.2** Arrangement of the masts with lightning source for case 2

**Table 4.1** Simulations setup for Configuration 2 for both Cases

Simulation	First			Second			Third		
Mast	M4	M5	M7	M4	M5	M7	M4	M5	M7
Rf( $\Omega$ )	5	10	20	5	20	50	5	50	100

**Table 4.2** Simulations setup for Configuration 3 for both Cases

Simulation	First			Second			Third		
Mast	M4	M5	M7	M4	M5	M7	M4	M5	M7
Rf( $\Omega$ )	100	50	20	100	20	10	100	10	5

Figures. 4.3-4.20 contain the outcome of analyzed mast induced voltage across stressed insulators of the auxiliary line when single lightning strokes on the mast for both cases with all configurations.

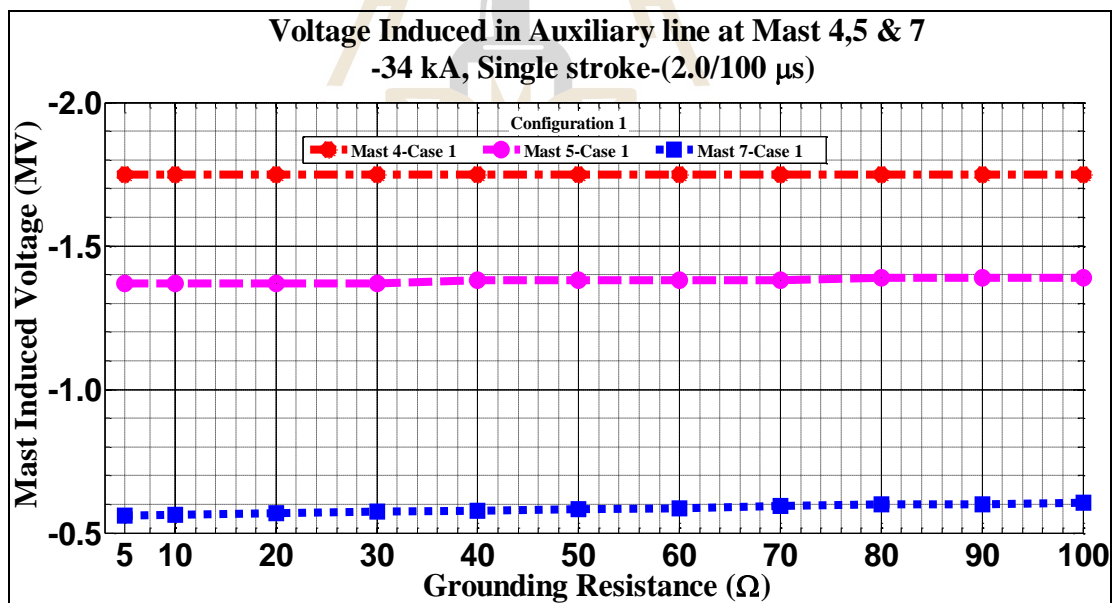


**Figure 4.3** Auxiliary line induced voltages in Case 1 with -34 kA (2.0/100  $\mu$ s) for configuration 1



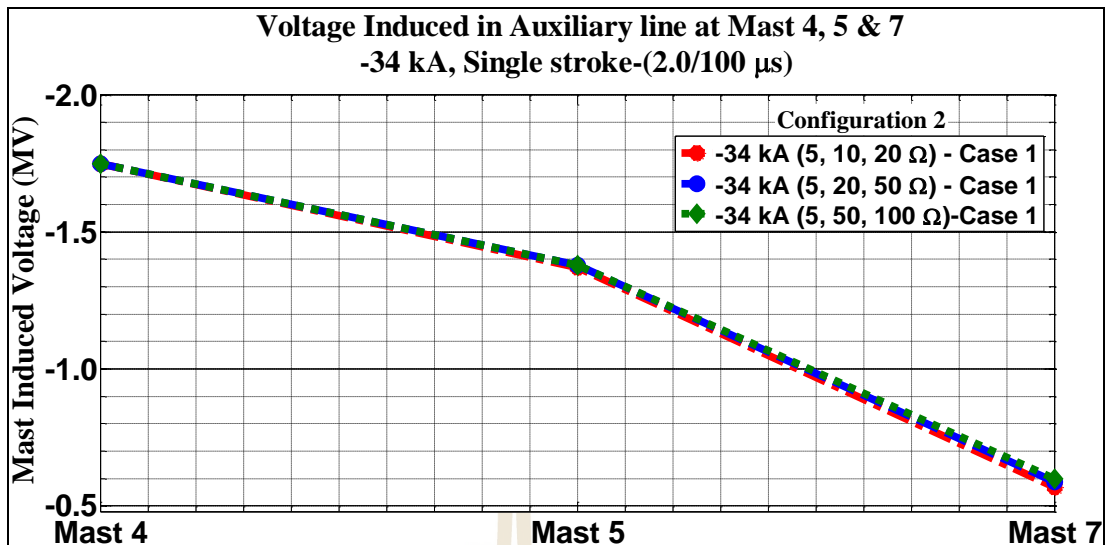


**Figure 4.4** Auxiliary line induced voltages in Case 1 with -34 kA (2.0/100  $\mu$ s) for configuration 2

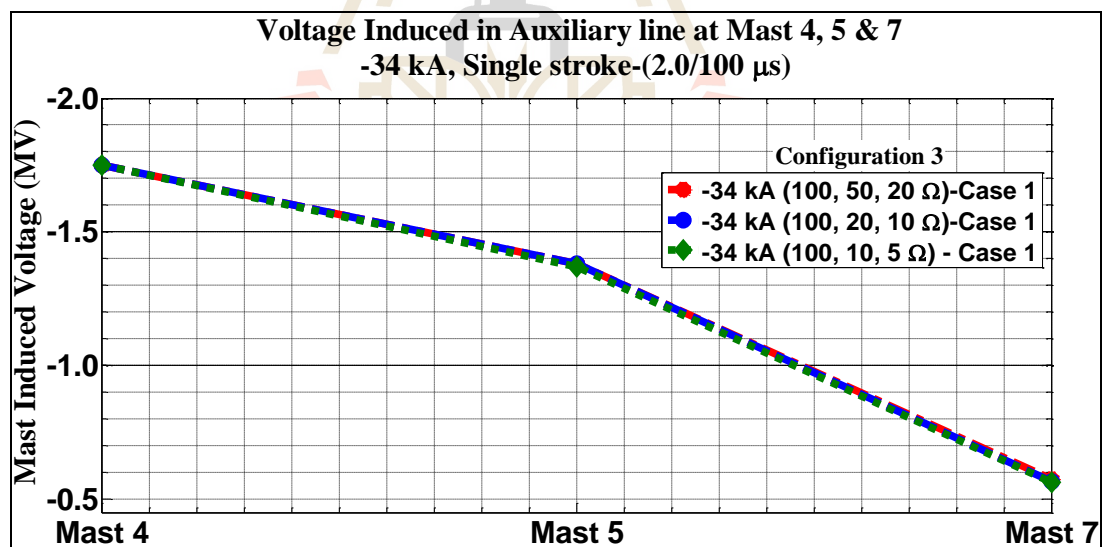


**Figure 4.5** Auxiliary line induced voltages in Case 1 with -34 kA (2.0/100  $\mu$ s) for configuration 3

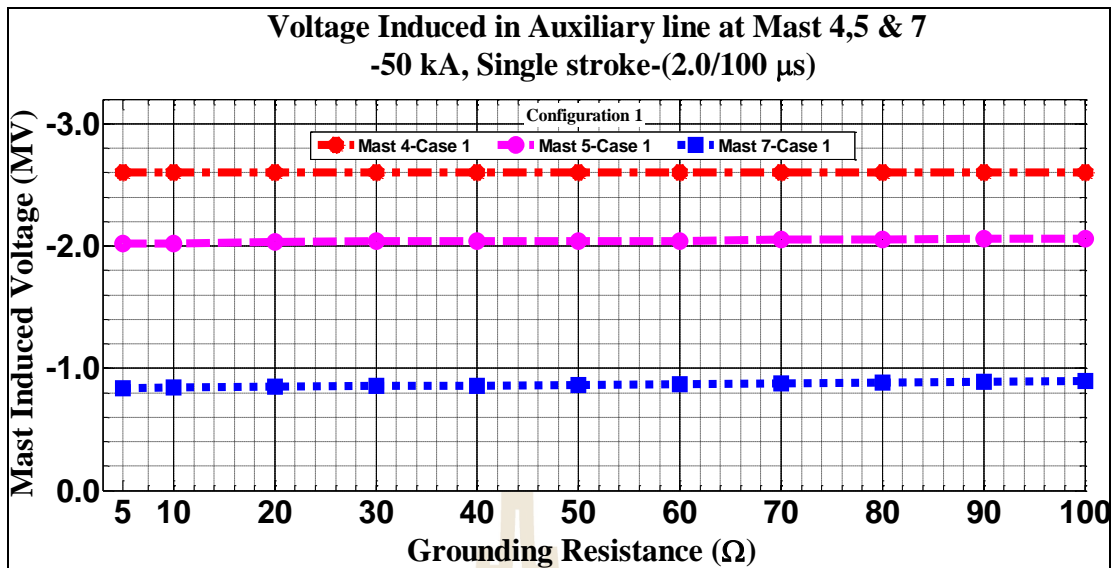


**Figure 4.6** Auxiliary line induced voltages in Case 1 with -50 kA (2.0/100  $\mu$ s) for configuration 1

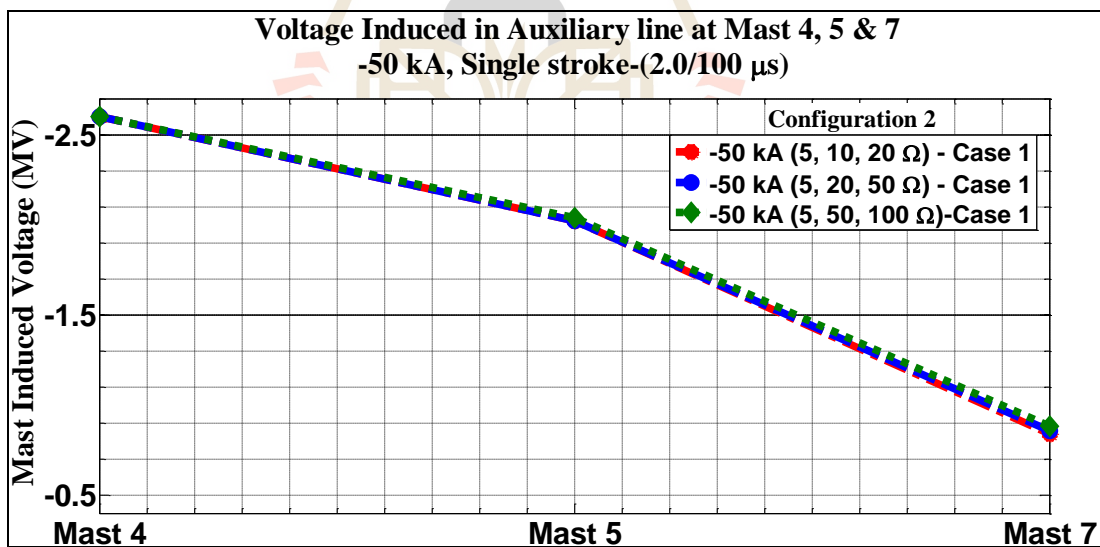


**Figure 4.7** Auxiliary line induced voltages in Case 1 with -50 kA (2.0/100  $\mu$ s) for configuration 2

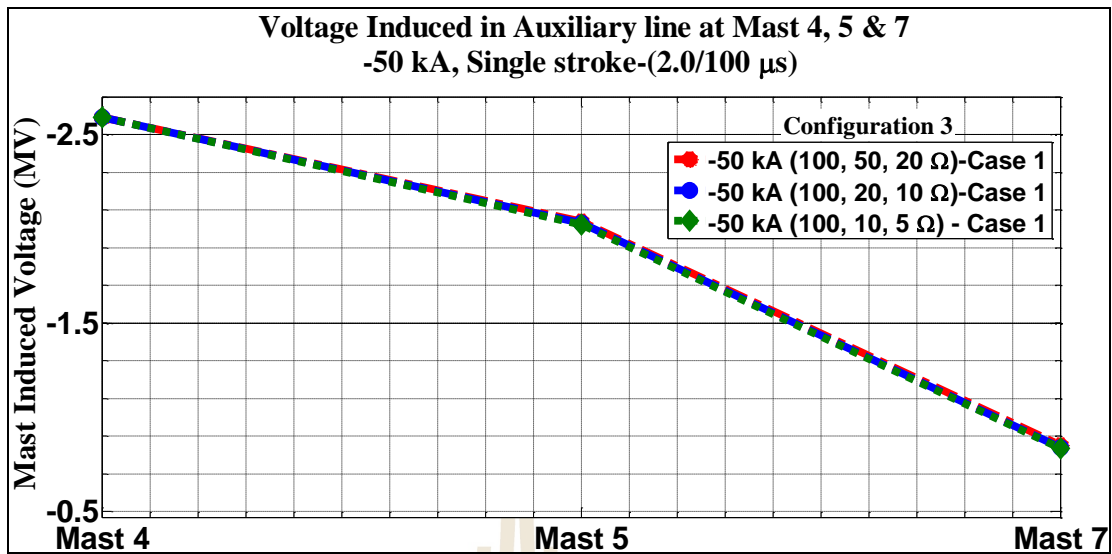


**Figure 4.8** Auxiliary line induced voltages in Case 1 with -50 kA (2.0/100  $\mu$ s) for configuration 3

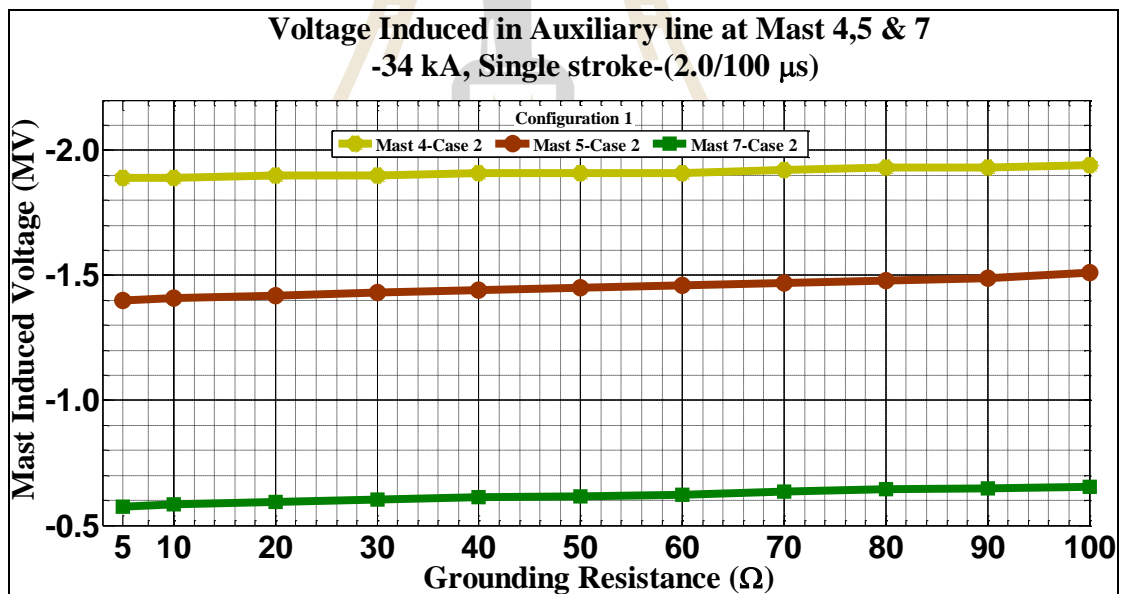


**Figure 4.9** Auxiliary line induced voltages in Case 2 with -34 kA (2.0/100  $\mu$ s) for configuration 1

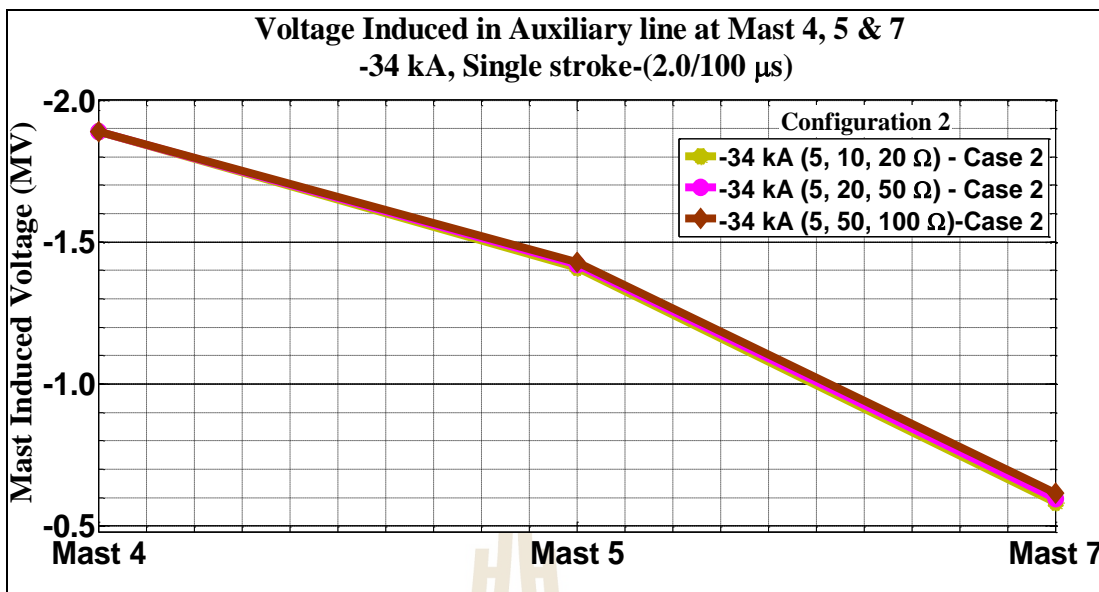


Figure 4.10 Auxiliary line induced voltages in Case 2 with -34 kA (2.0/100 μs) for configuration 2

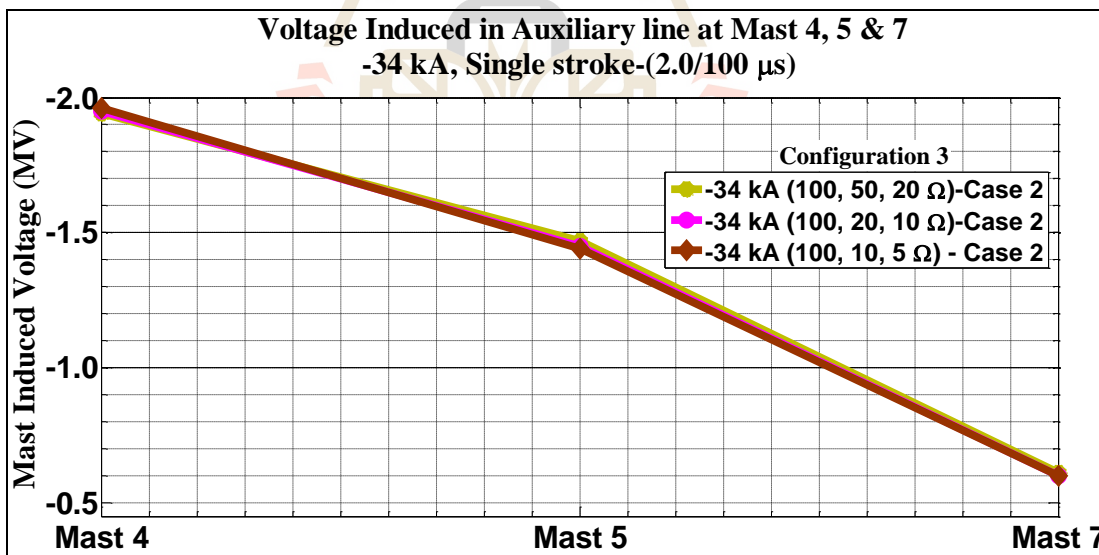


Figure 4.11 Auxiliary line induced voltages in Case 2 with -34 kA (2.0/100 μs) for configuration 3

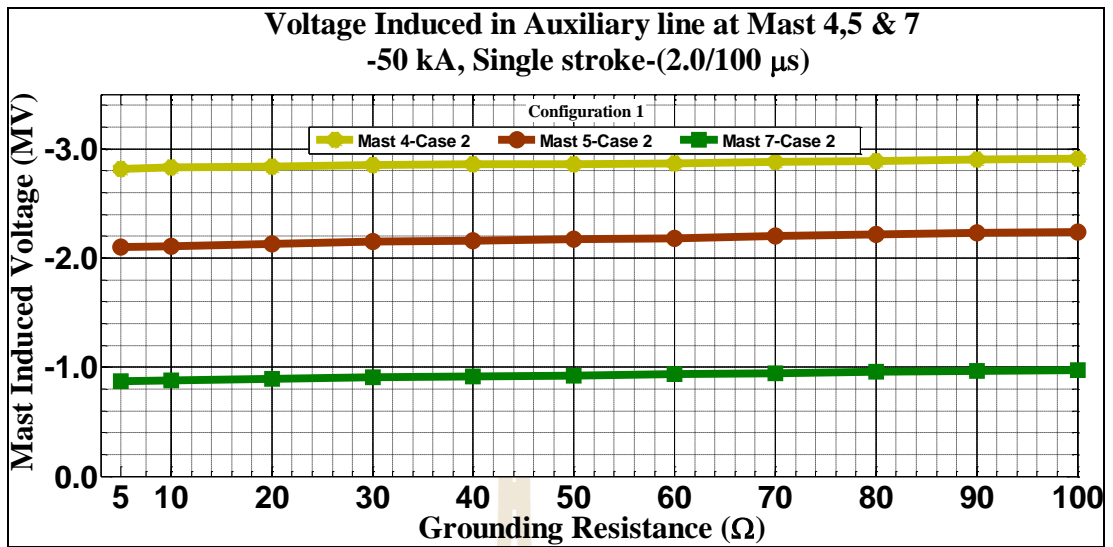


Figure 4.12 Auxiliary line induced voltages in Case 2 with -50 kA (2.0/100  $\mu$ s) for configuration 1

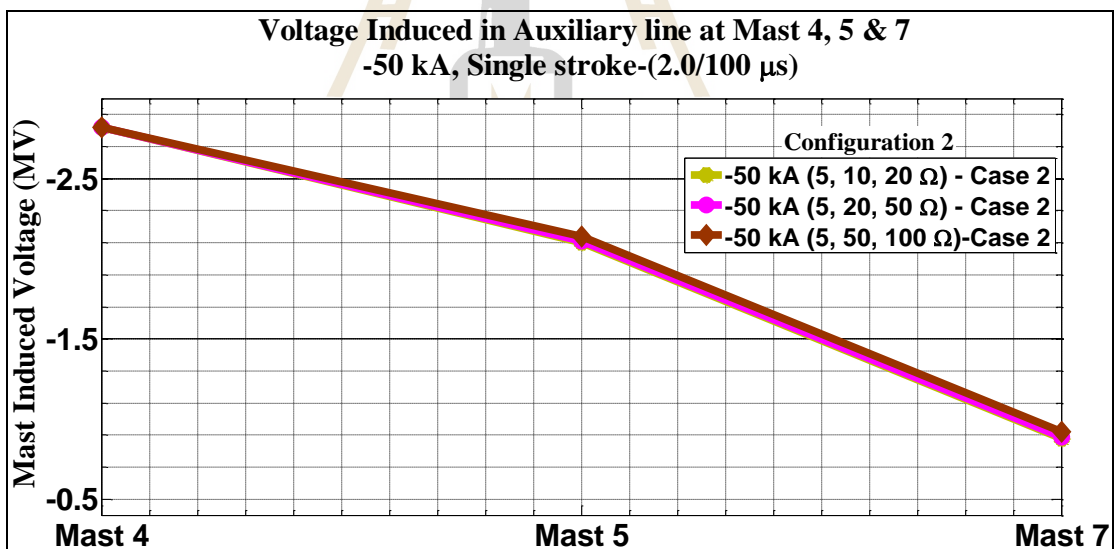
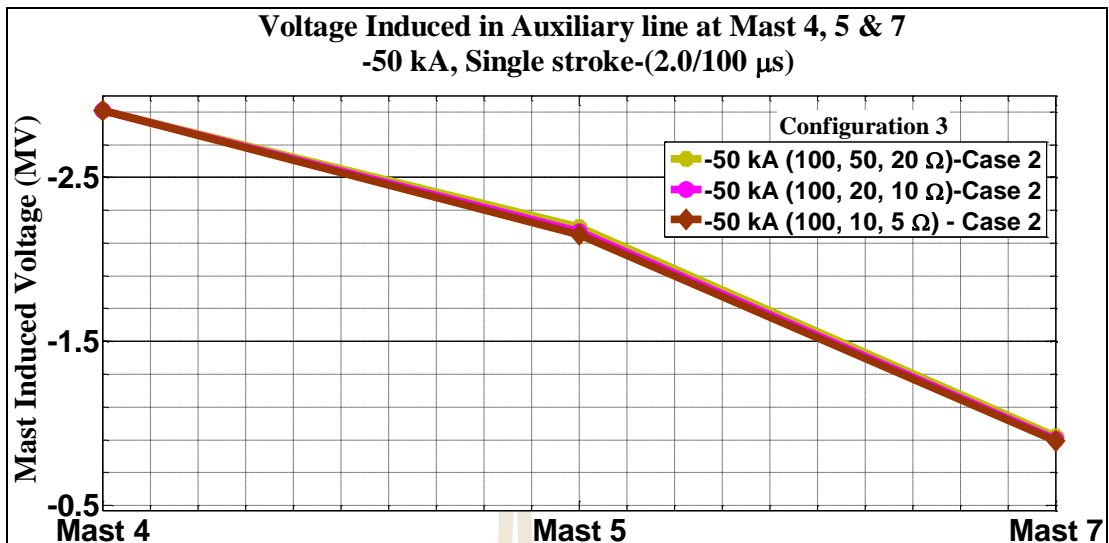
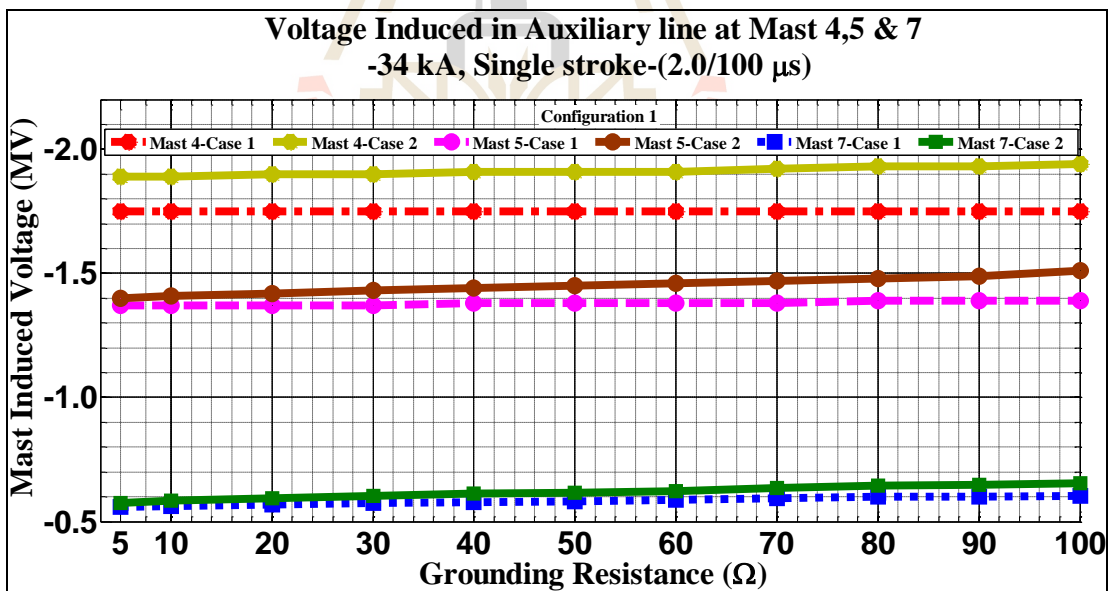


Figure 4.13 Auxiliary line induced voltages in Case 2 with -50 kA (2.0/100  $\mu$ s) for configuration 2



**Figure 4.14** Auxiliary line induced voltages in Case 2 with -50 kA (2.0/100  $\mu$ s) for configuration 3



**Figure 4.15** Auxiliary line induced voltages in both Cases with -34 kA (2.0/100  $\mu$ s) for configuration 1

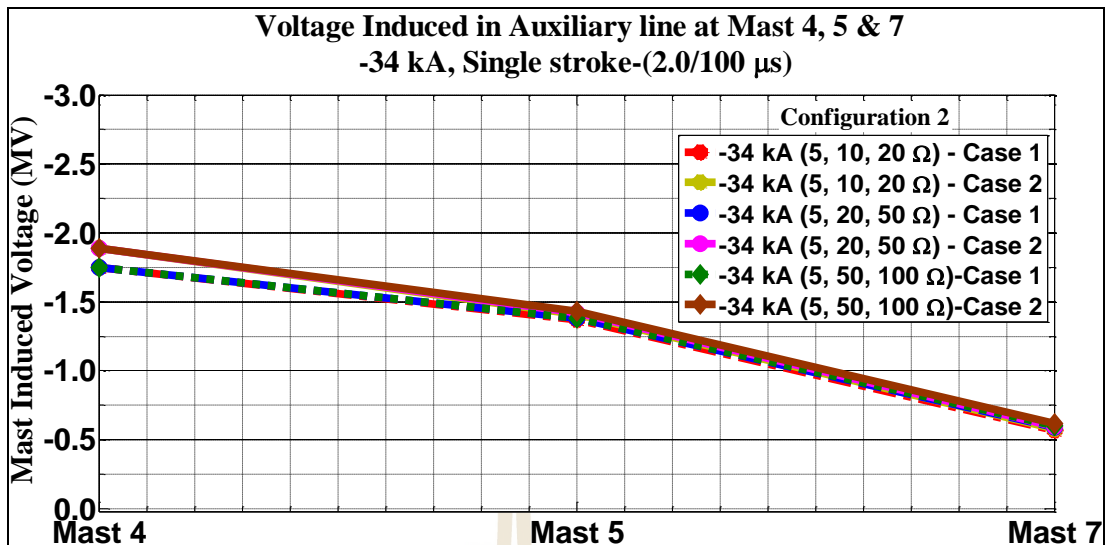


**Figure 4.16** Auxiliary line induced voltages in both Cases with -34 kA (2.0/100  $\mu$ s) for configuration 2

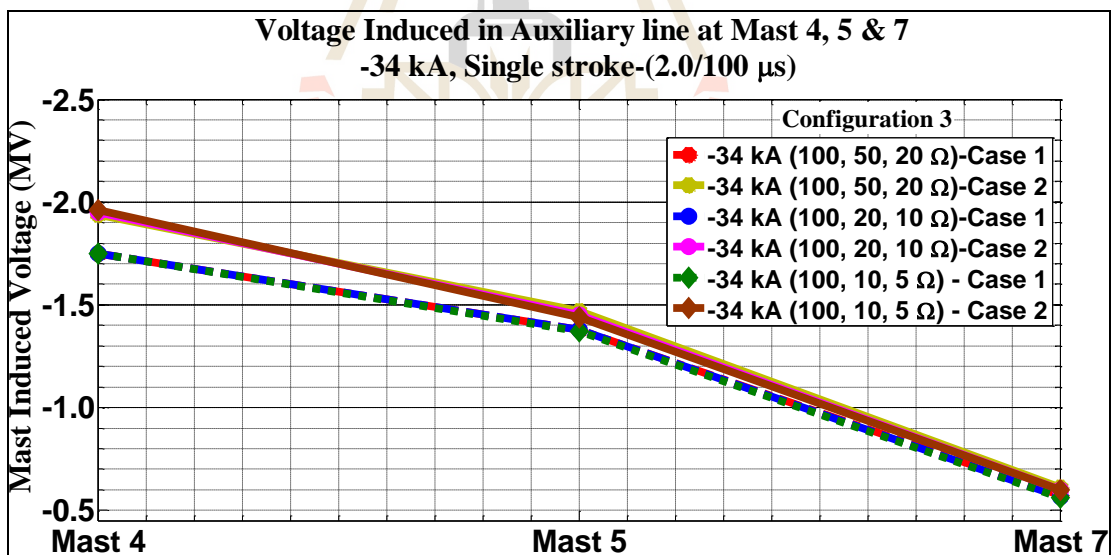


**Figure 4.17** Auxiliary line induced voltages in both Cases with -34 kA (2.0/100  $\mu$ s) for configuration 3

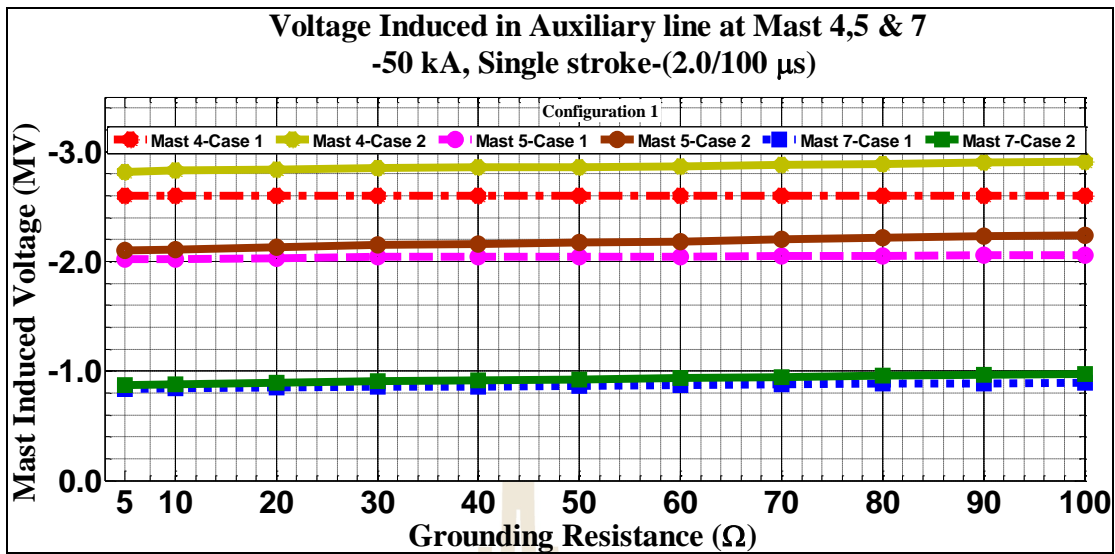


Figure 4.18 Auxiliary line induced voltages in both Cases with -50 kA (2.0/100 μs) for configuration 1

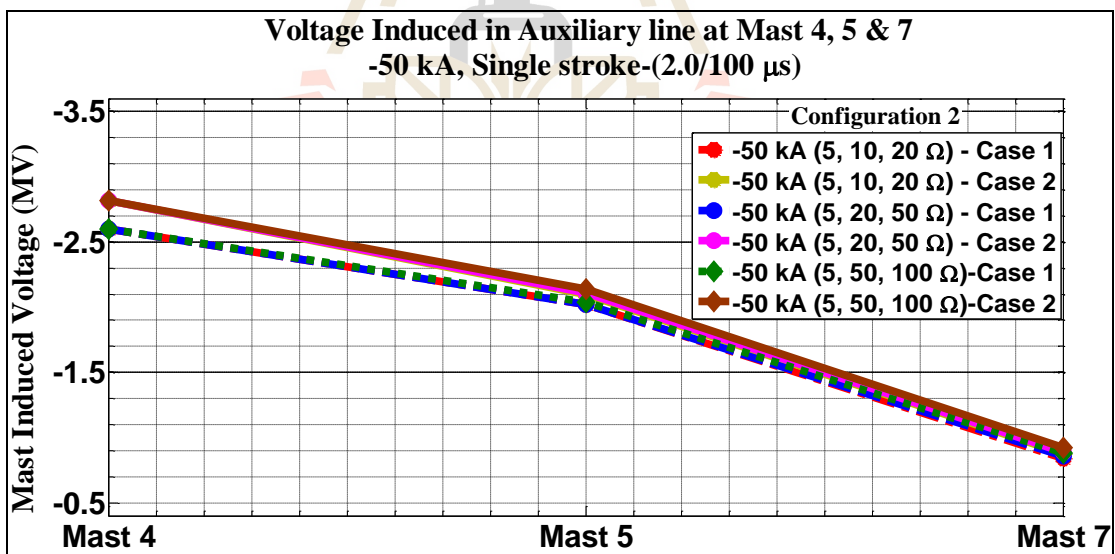


Figure 4.19 Auxiliary line induced voltages in both Cases with -50 kA (2.0/100 μs) for configuration 2



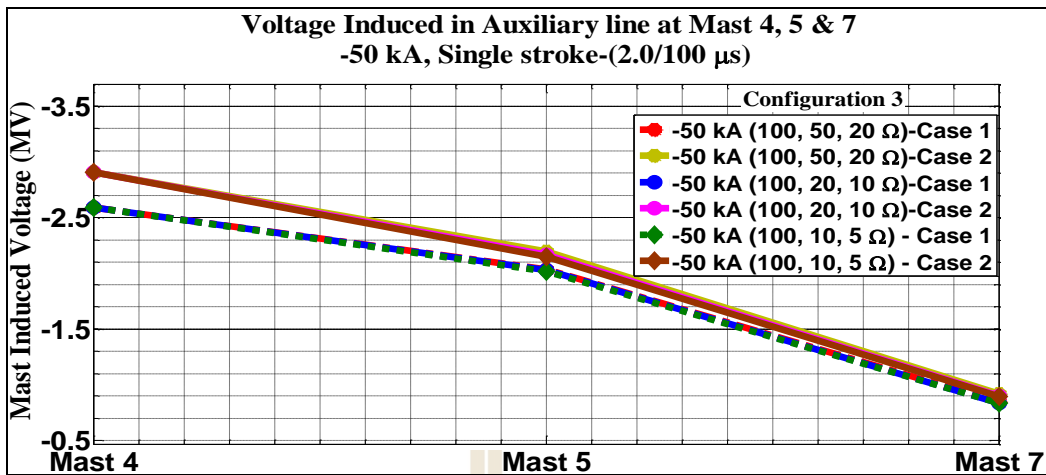


Figure 4.20 Auxiliary line induced voltages in both Cases with -50 kA (2.0/100 μs) for configuration 3

For both cases with all configurations, Figures 4.21-4.38 carry out the analyzed results of mast induced voltage across stressed insulators of the return line when single lightning strokes on return line.

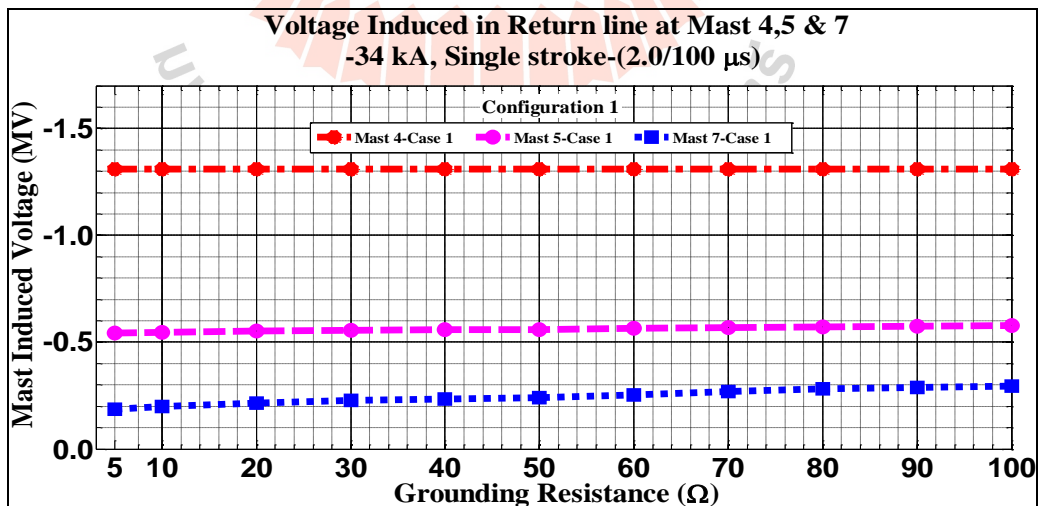


Figure 4.21 Return line induced voltages in Case 1 with -34 kA (2.0/100 μs) for configuration 1

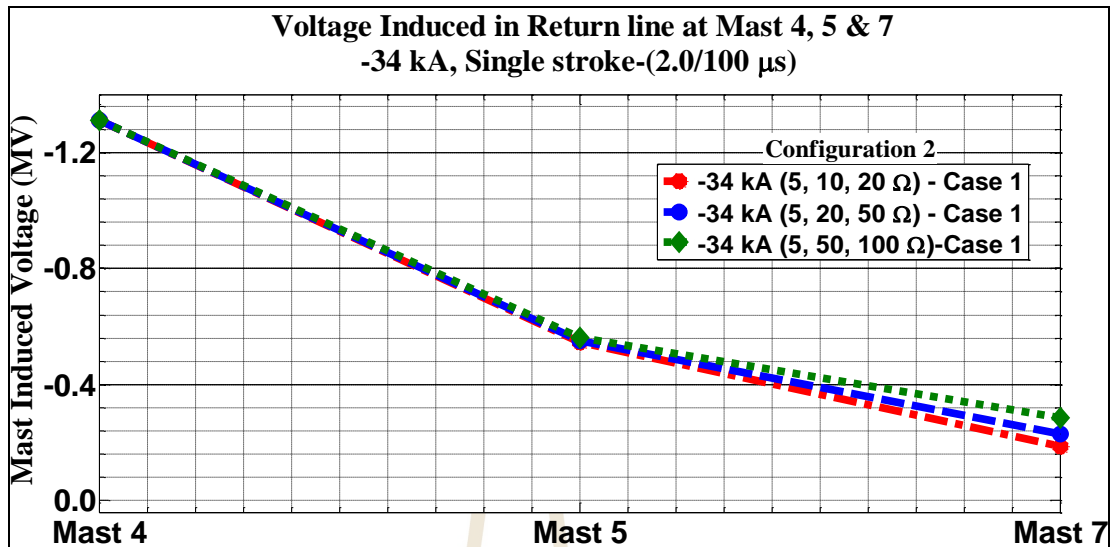


Figure 4.22 Return line induced voltages in Case 1 with -34 kA (2.0/100  $\mu$ s) for configuration 2

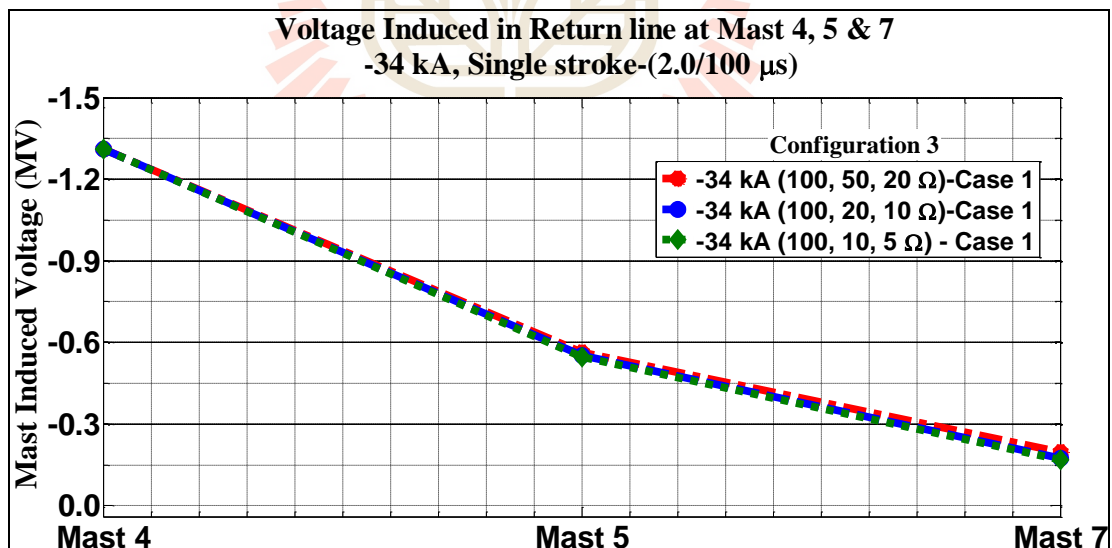


Figure 4.23 Return line induced voltages in Case 1 with -34 kA (2.0/100  $\mu$ s) for configuration 3

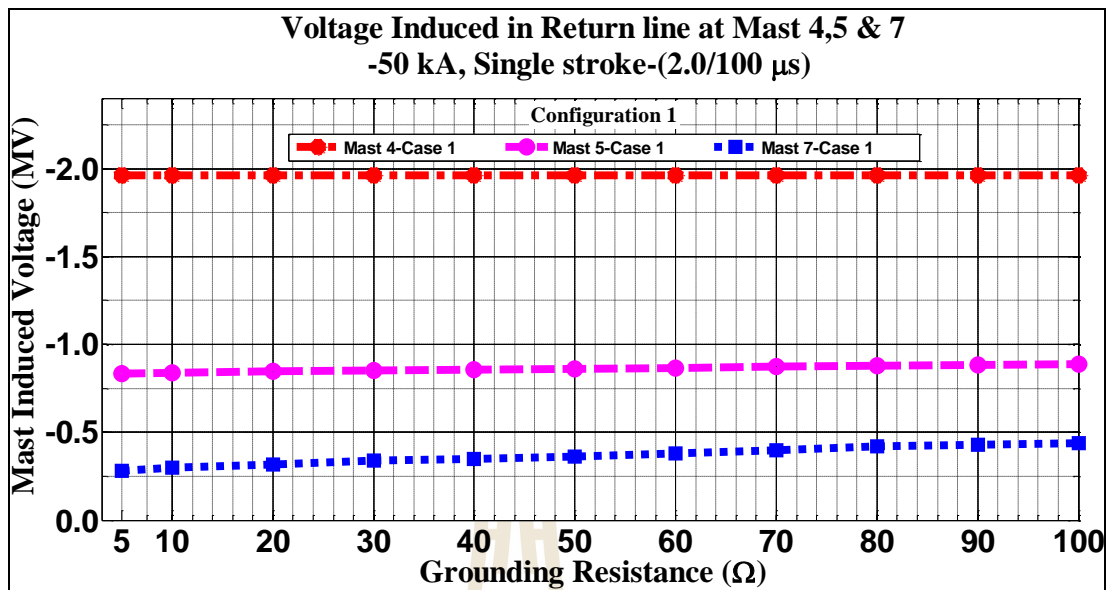


Figure 4.24 Return line induced voltages in Case 1 with -50 kA (2.0/100  $\mu$ s) for configuration 1

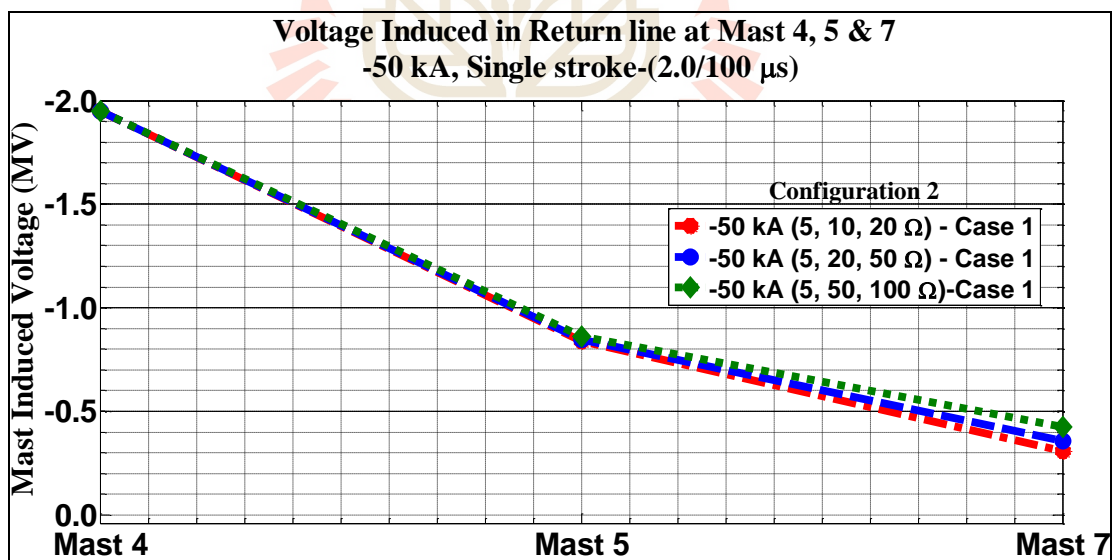


Figure 4.25 Return line induced voltages in Case 1 with -50 kA (2.0/100  $\mu$ s) for configuration 2

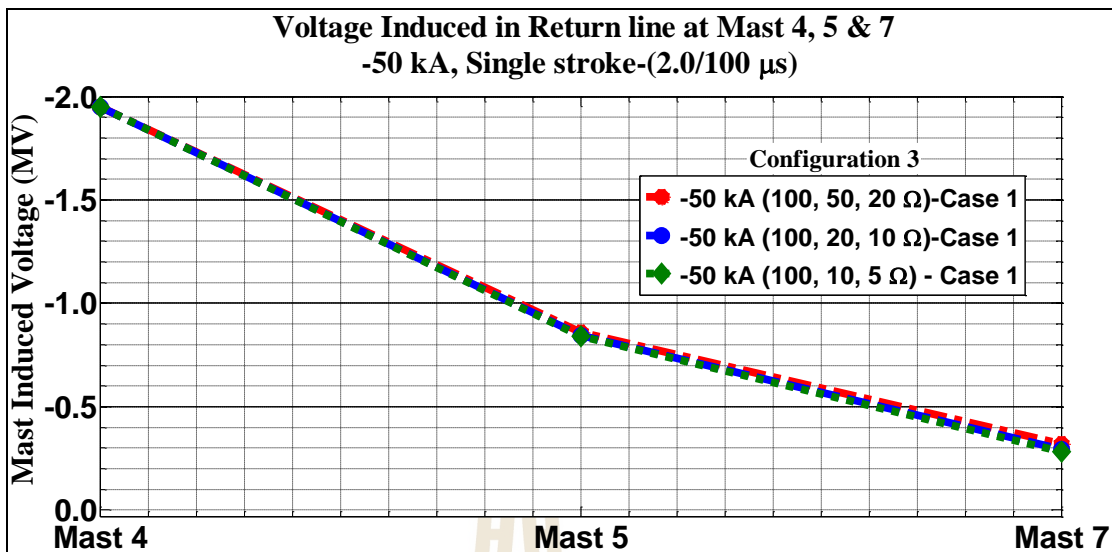


Figure 4.26 Return line induced voltages in Case 1 with -50 kA (2.0/100  $\mu$ s) for configuration 3

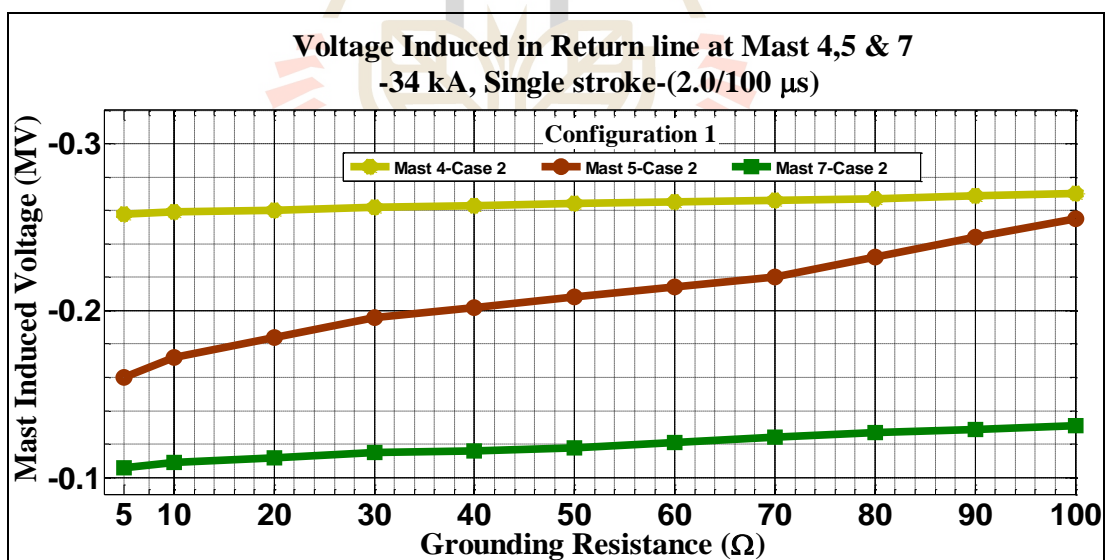
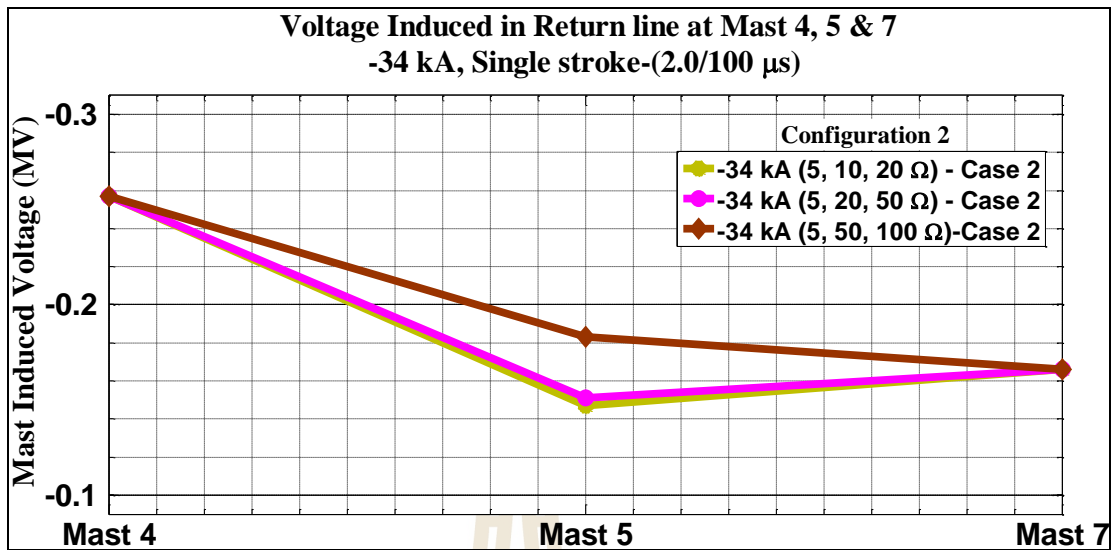
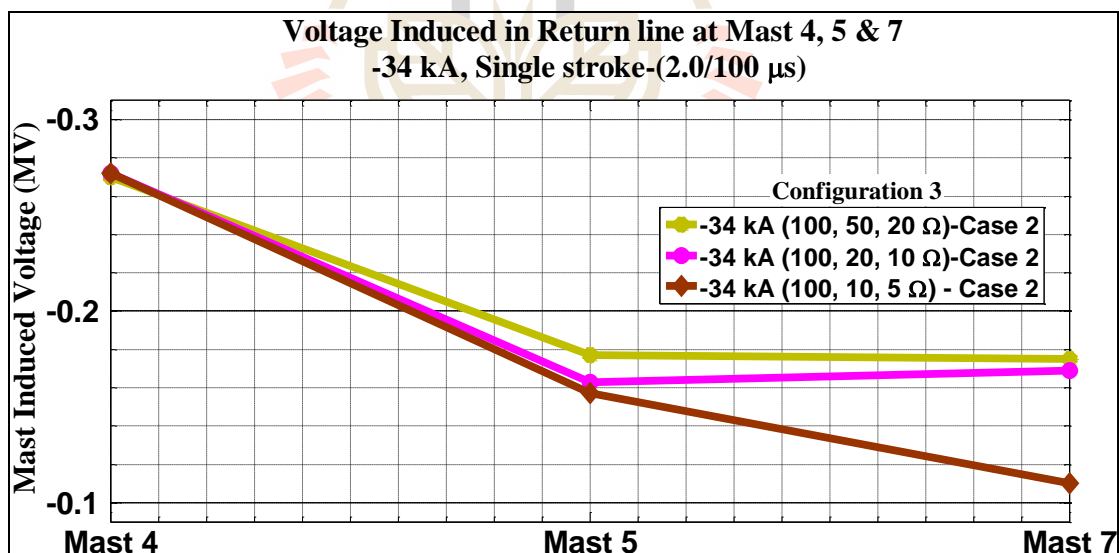


Figure 4.27 Return line induced voltages in Case 2 with -34 kA (2.0/100  $\mu$ s) for configuration 1



**Figure 4.28** Return line induced voltages in Case 2 with -34 kA (2.0/100  $\mu$ s) for configuration 2



**Figure 4.29** Return line induced voltages in Case 2 with -34 kA (2.0/100  $\mu$ s) for configuration 3

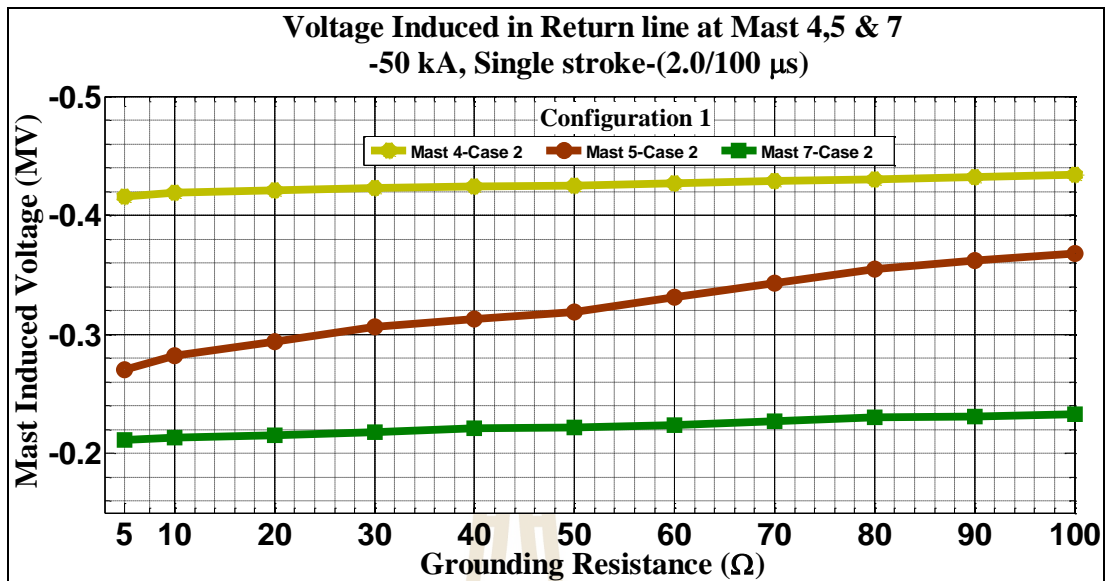


Figure 4.30 Return line induced voltages in Case 2 with -50 kA (2.0/100  $\mu$ s) for configuration 1

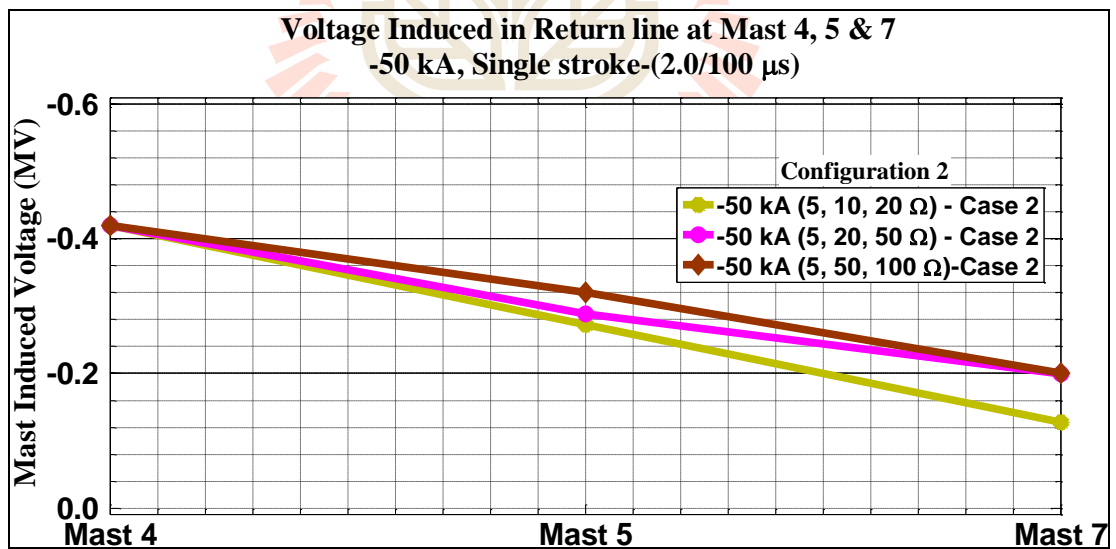


Figure 4.31 Return line induced voltages in Case 2 with -50 kA (2.0/100  $\mu$ s) for configuration 2

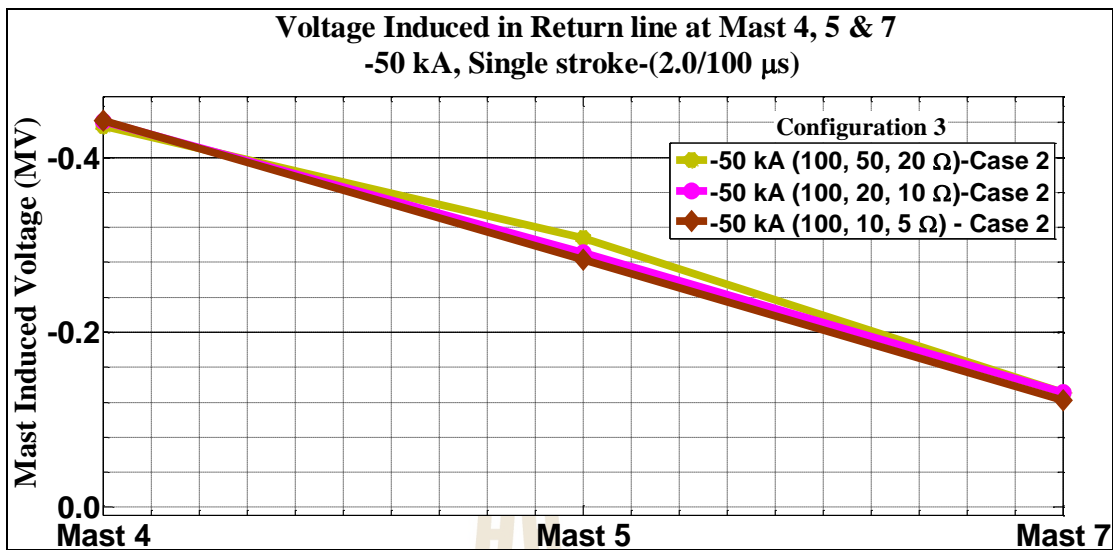


Figure 4.32 Return line induced voltages in Case 2 with -50 kA (2.0/100  $\mu$ s) for configuration 3

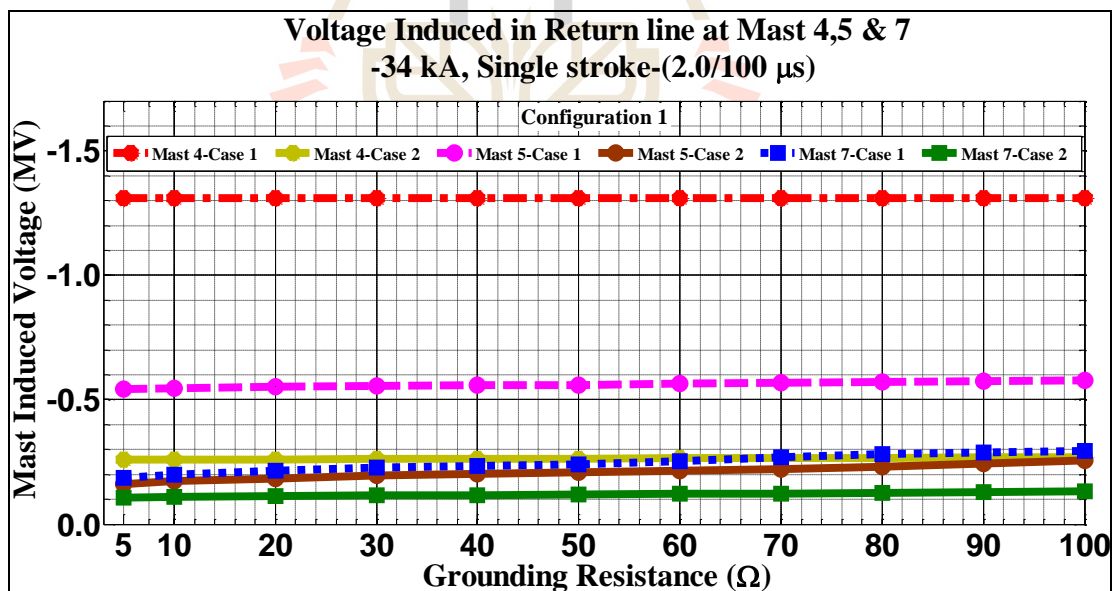
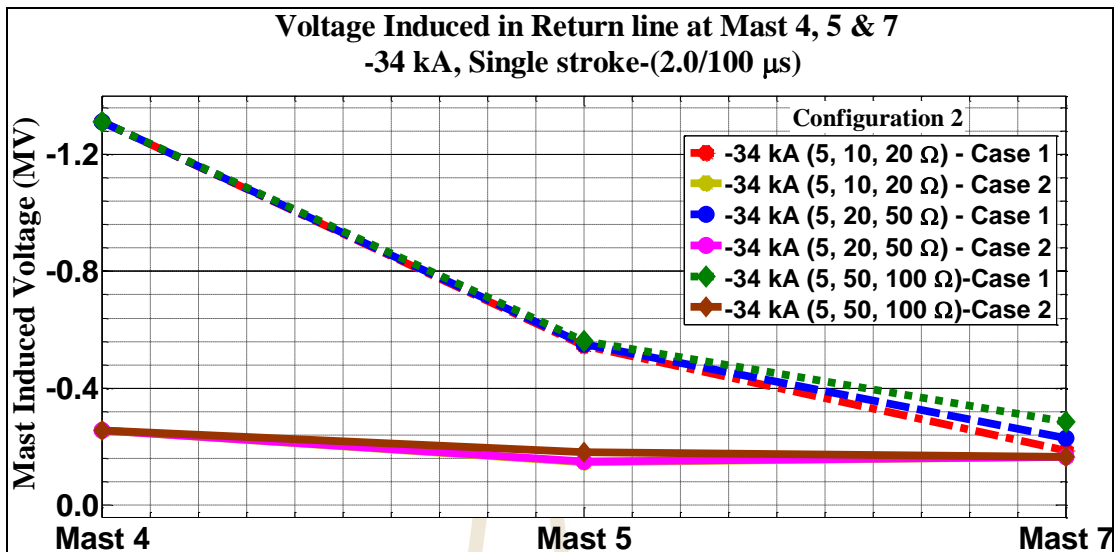
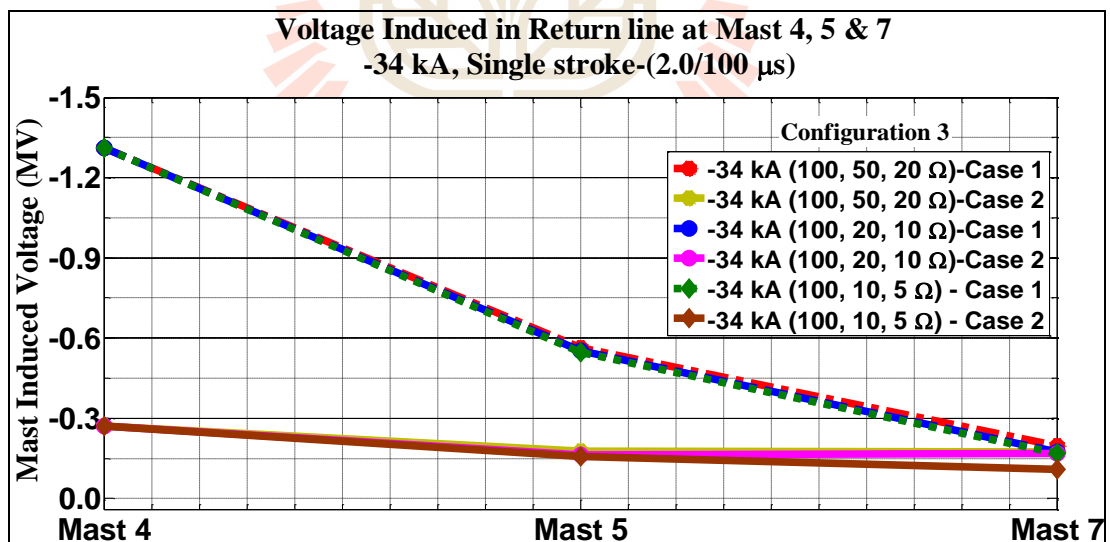


Figure 4.33 Return line induced voltages in both Cases with -34 kA (2.0/100  $\mu$ s) for configuration 1



**Figure 4.34** Return line induced voltages in both Cases with -34 kA (2.0/100  $\mu$ s) for configuration 2



**Figure 4.35** Return line induced voltages in both Cases with -34 kA (2.0/100  $\mu$ s) for configuration 3



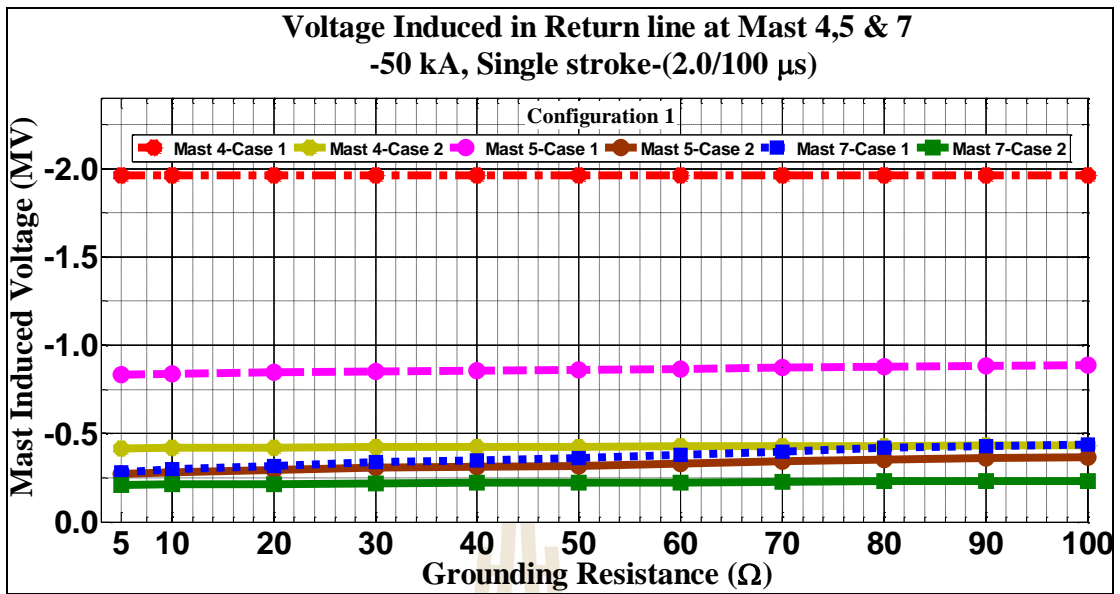


Figure 4.36 Return line induced voltages in both Cases with -50 kA (2.0/100 μs) for configuration 1

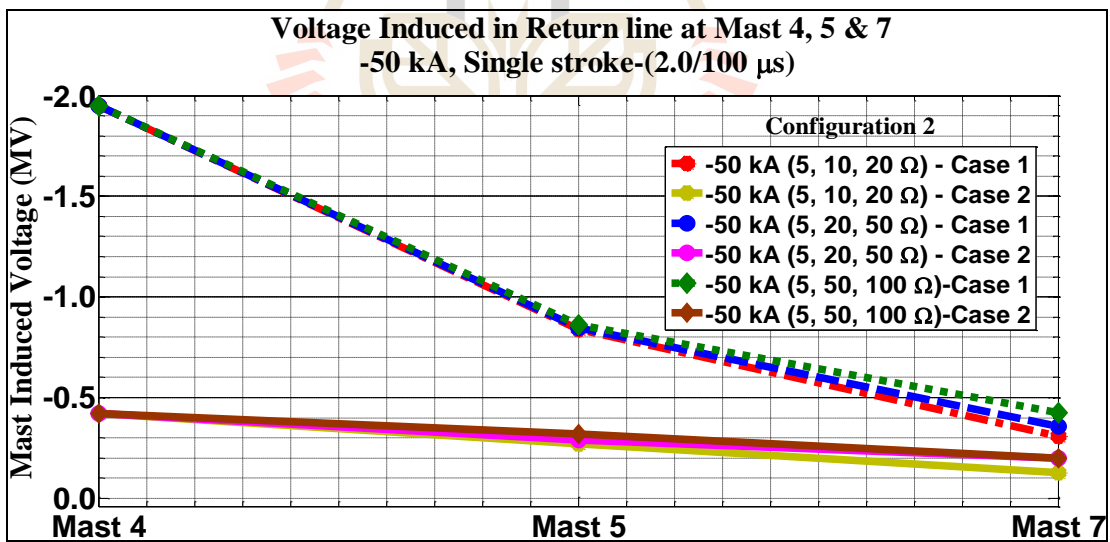
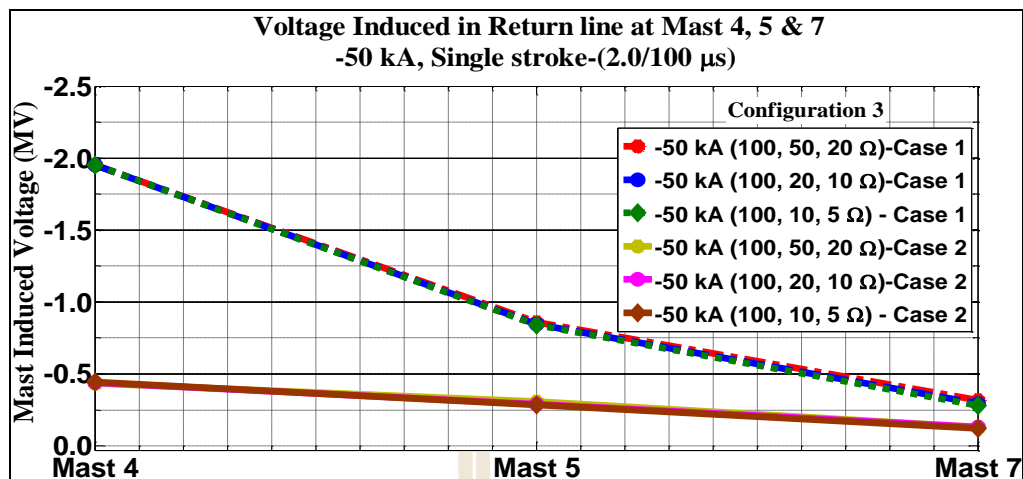
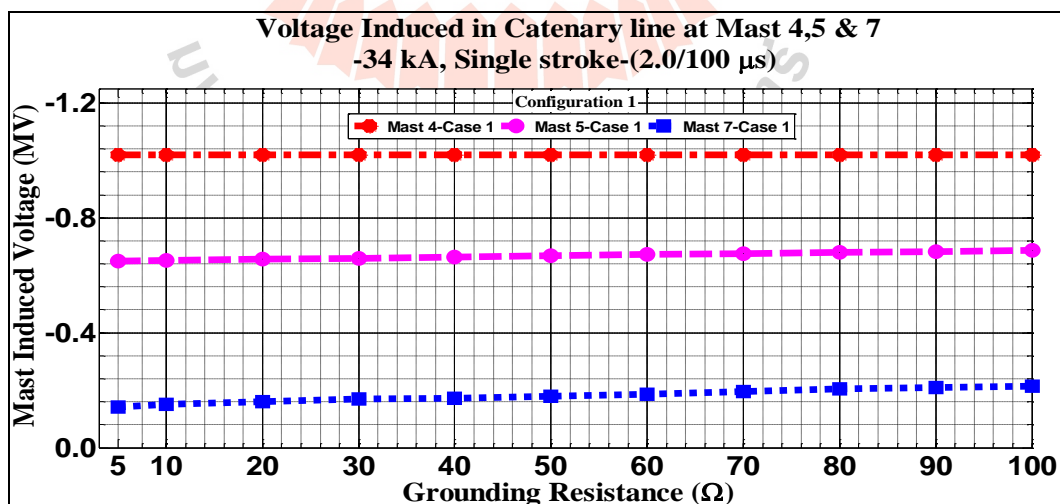


Figure 4.37 Return line induced voltages in both Cases with -50 kA (2.0/100 μs) for configuration 2



**Figure 4.38** Return line induced voltages in both Cases with -50 kA (2.0/100  $\mu$ s) for configuration 3

The outcome of analyzed mast induced voltage across stressed insulators of the catenary line when single lightning strokes on catenary line for both cases with all configurations are shown in Figures. 4.39-4.56.



**Figure 4.39** Catenary line induced voltages in Case 1 with -34 kA (2.0/100  $\mu$ s) for configuration 1

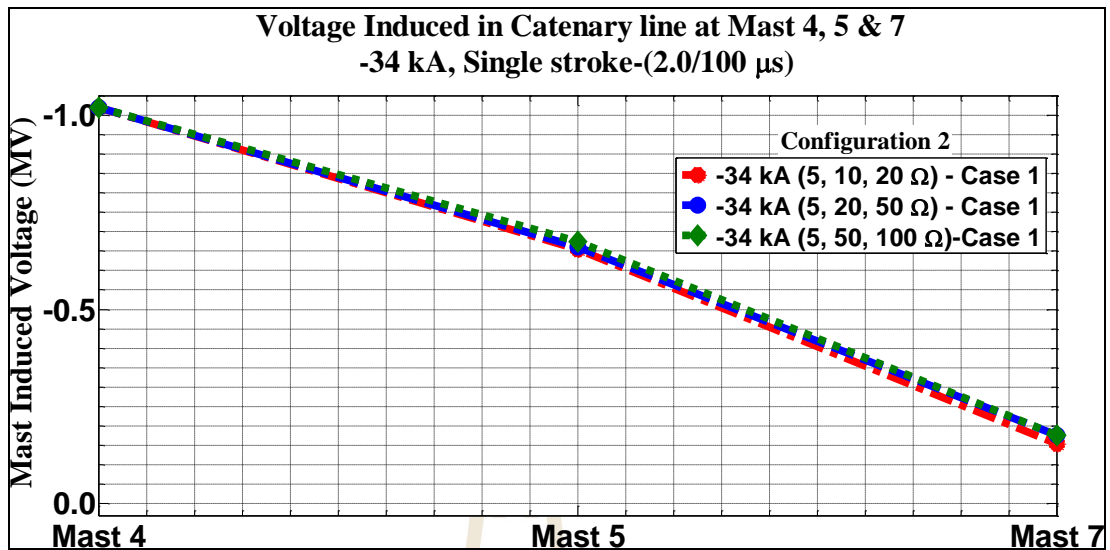


**Figure 4.40** Catenary line induced voltages in Case 1 with -34 kA (2.0/100  $\mu$ s) for configuration 2

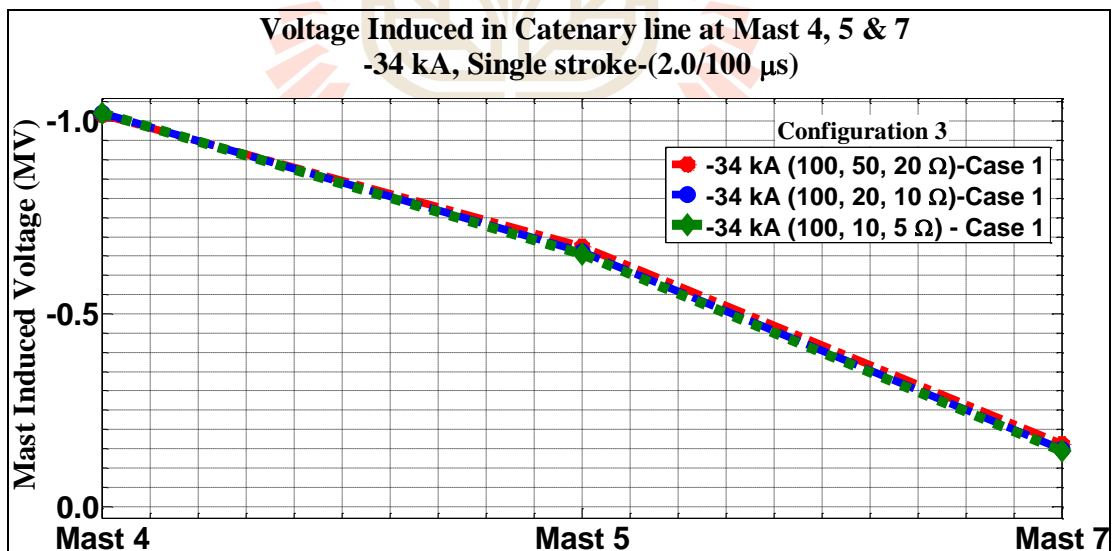


**Figure 4.41** Catenary line induced voltages in Case 1 with -34 kA (2.0/100  $\mu$ s) for configuration 3

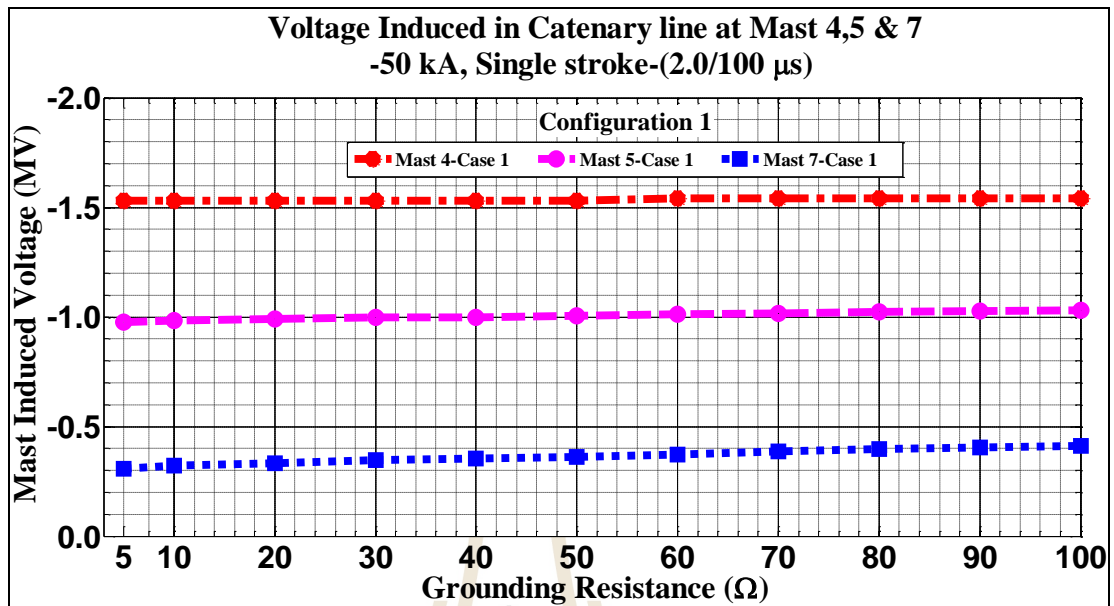


Figure 4.42 Catenary line induced voltages in Case 1 with -50 kA (2.0/100  $\mu$ s) for configuration 1

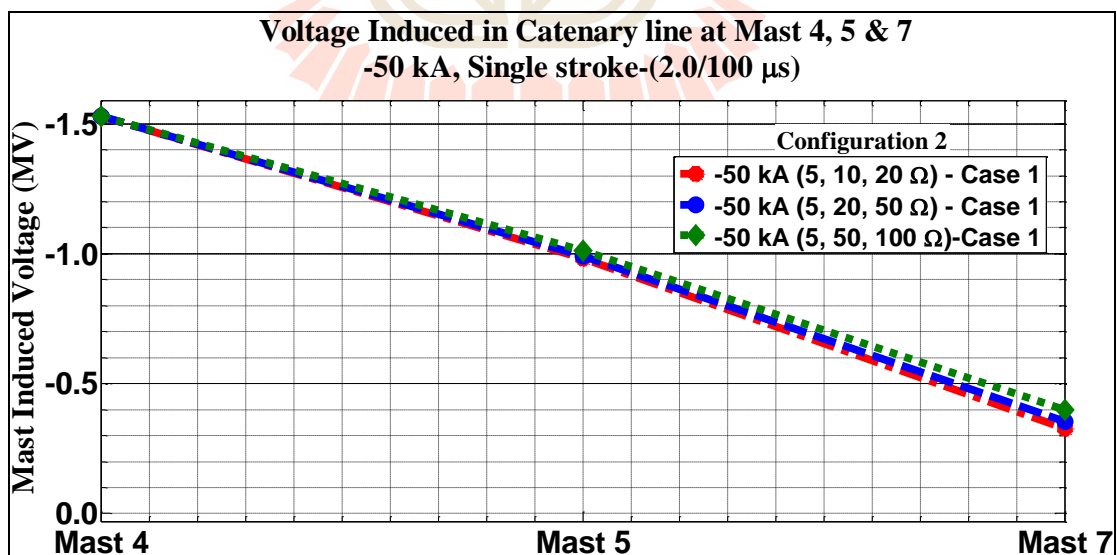


Figure 4.43 Catenary line induced voltages in Case 1 with -50 kA (2.0/100  $\mu$ s) for configuration 2

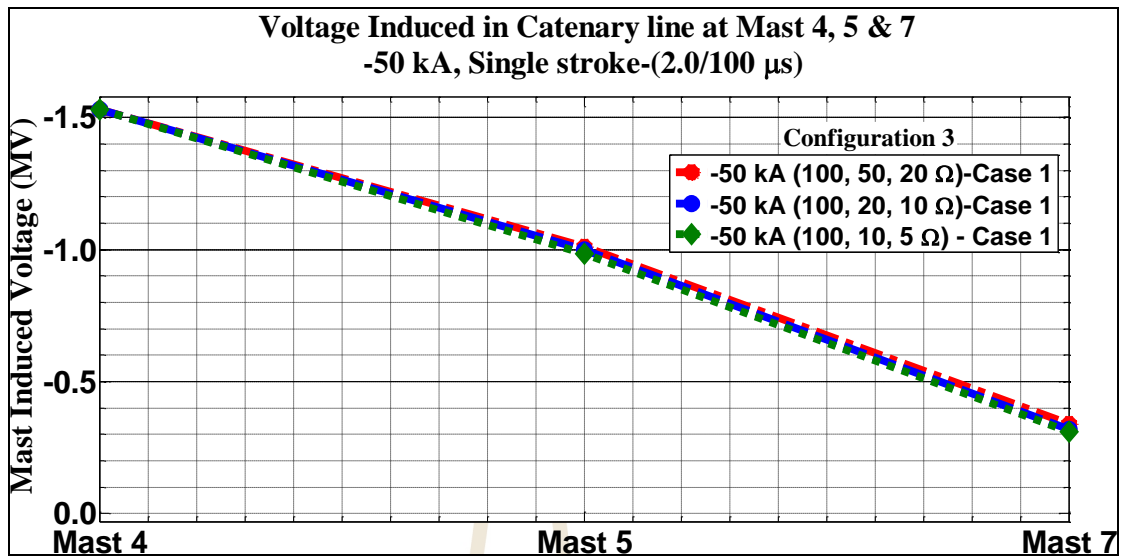


Figure 4.44 Catenary line induced voltages in Case 1 with -50 kA (2.0/100  $\mu$ s) for configuration 3

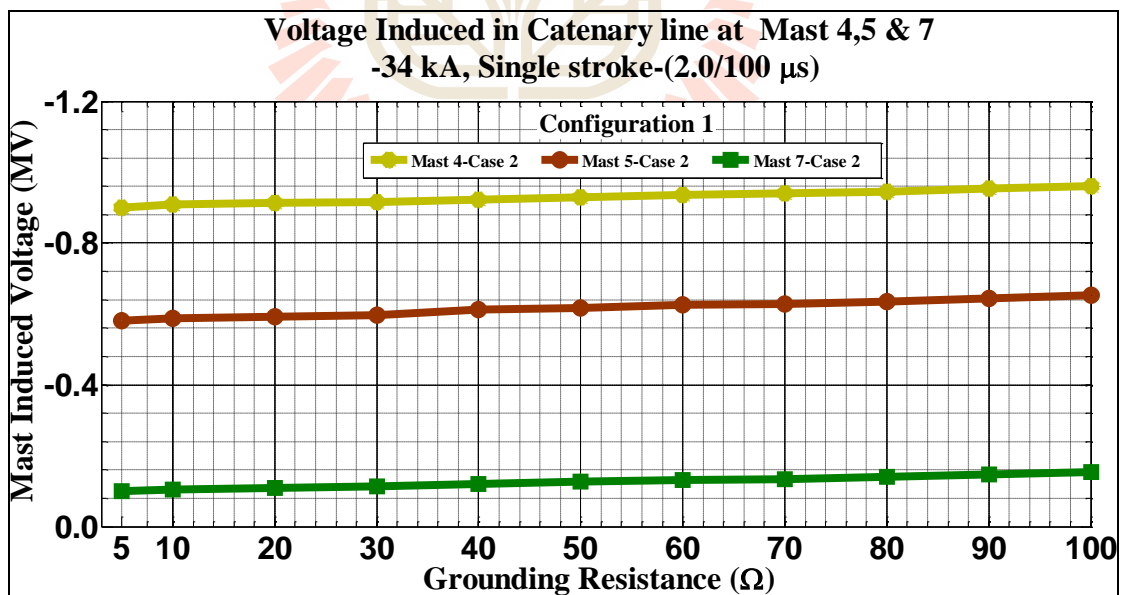
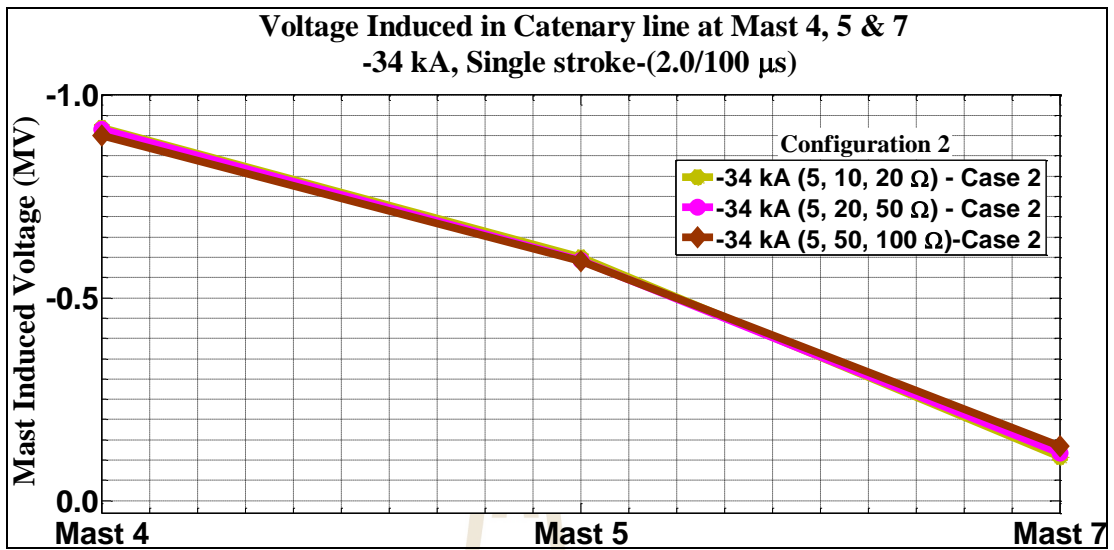
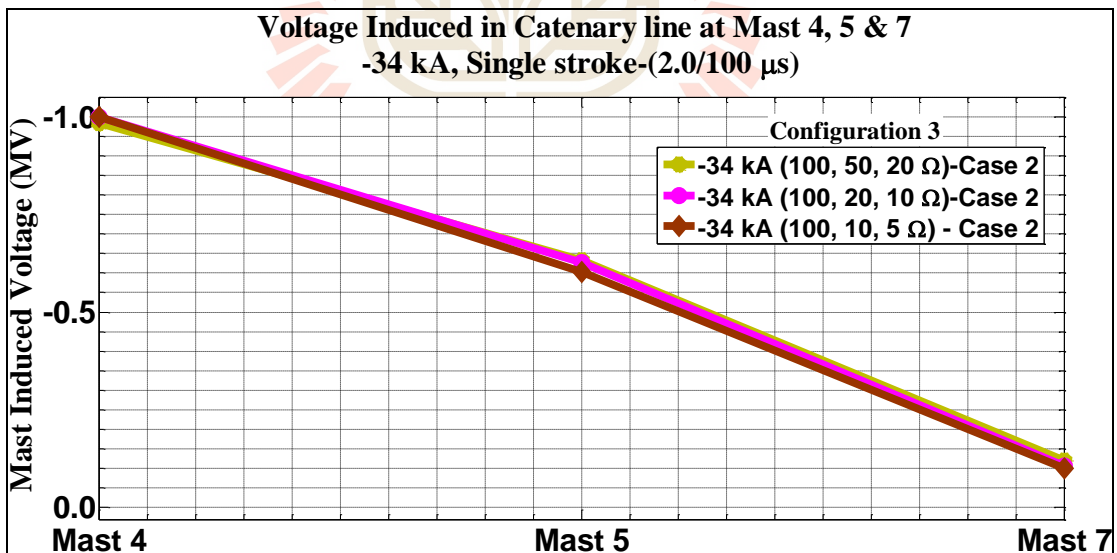


Figure 4.45 Catenary line induced voltages in Case 2 with -34 kA (2.0/100  $\mu$ s) for configuration 1



**Figure 4.46** Catenary line induced voltages in Case 2 with -34 kA (2.0/100  $\mu$ s) for configuration 2



**Figure 4.47** Catenary line induced voltages in Case 2 with -34 kA (2.0/100  $\mu$ s) for configuration 3

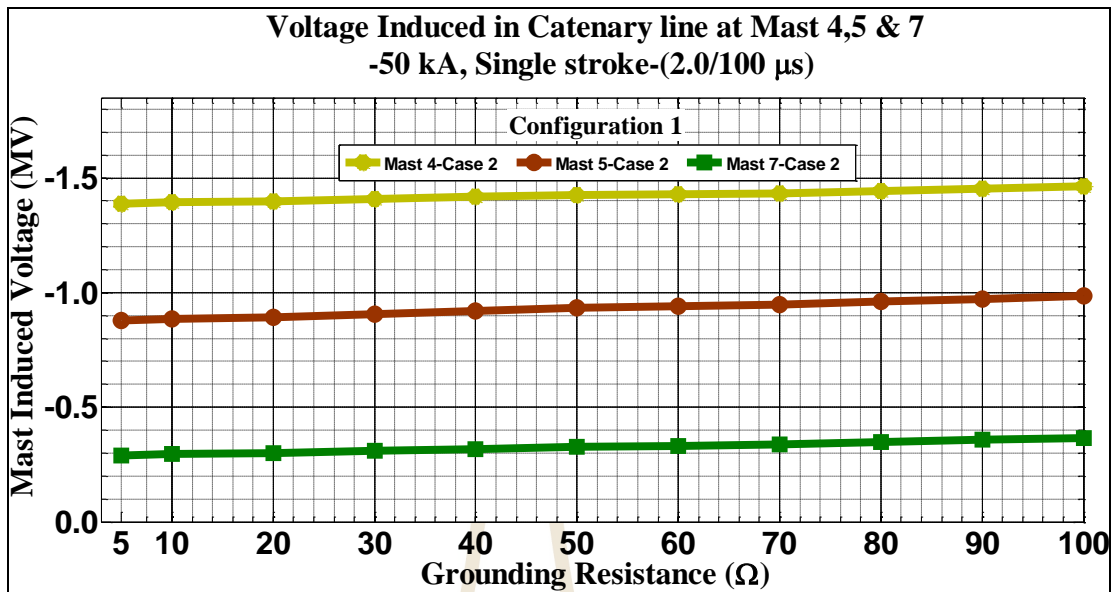


Figure 4.48 Catenary line induced voltages in Case 2 with -50 kA (2.0/100  $\mu$ s) for configuration 1

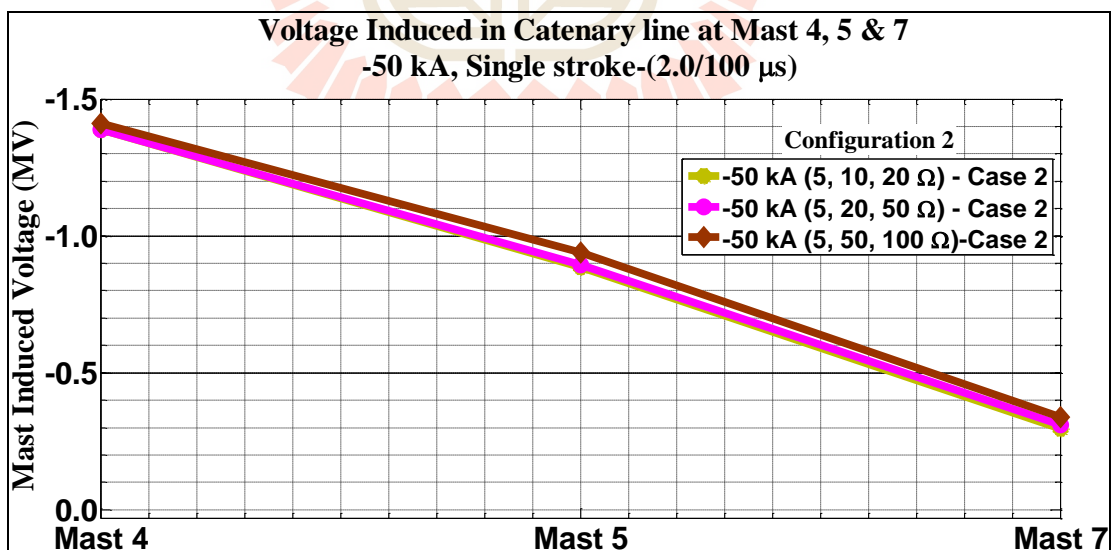


Figure 4.49 Catenary line induced voltages in Case 2 with -50 kA (2.0/100  $\mu$ s) for configuration 2

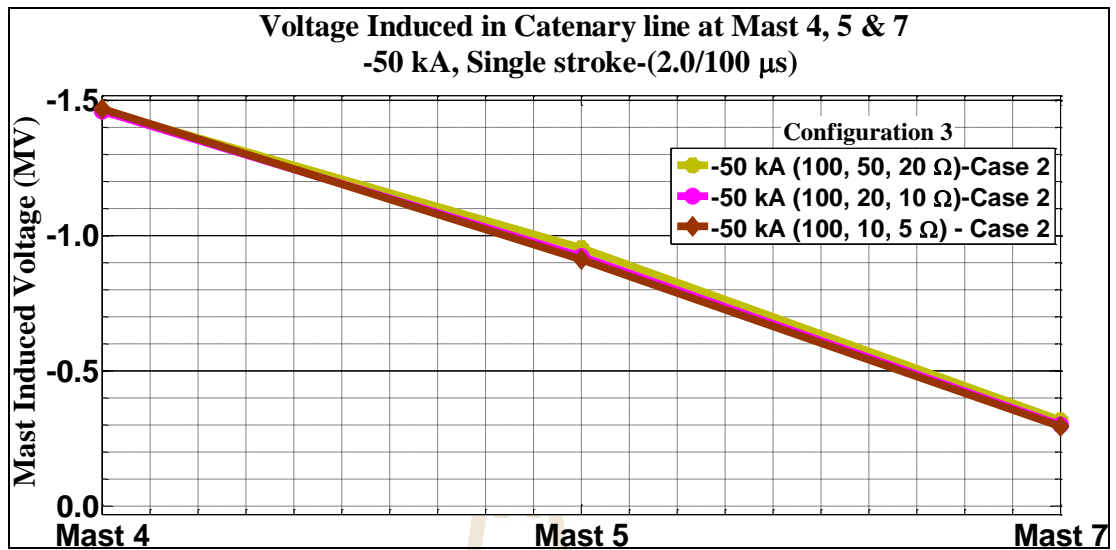


Figure 4.50 Catenary line induced voltages in Case 2 with -50 kA (2.0/100  $\mu$ s) for configuration 3

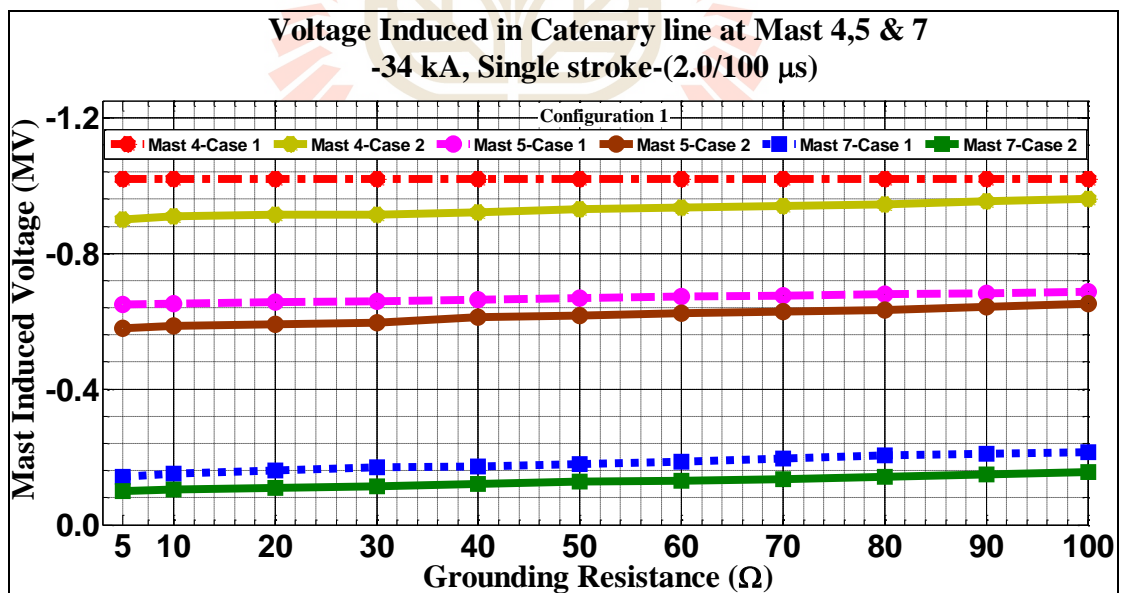


Figure 4.51 Catenary line induced voltages in both Cases with -34 kA (2.0/100  $\mu$ s) for configuration 1





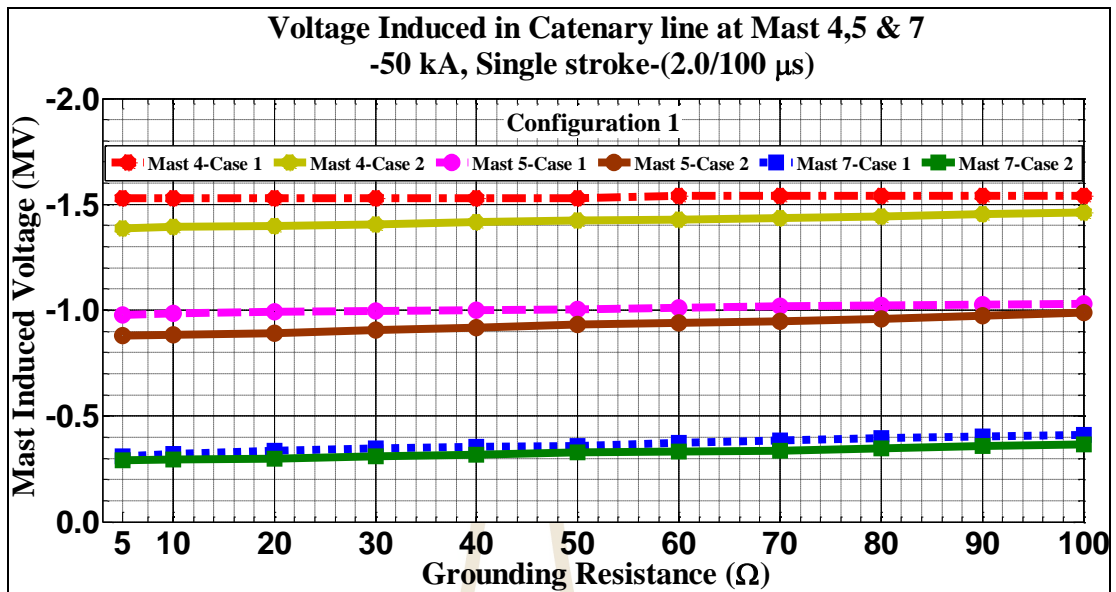


Figure 4.54 Catenary line induced voltages in both Cases with -50 kA (2.0/100  $\mu$ s) for configuration 1

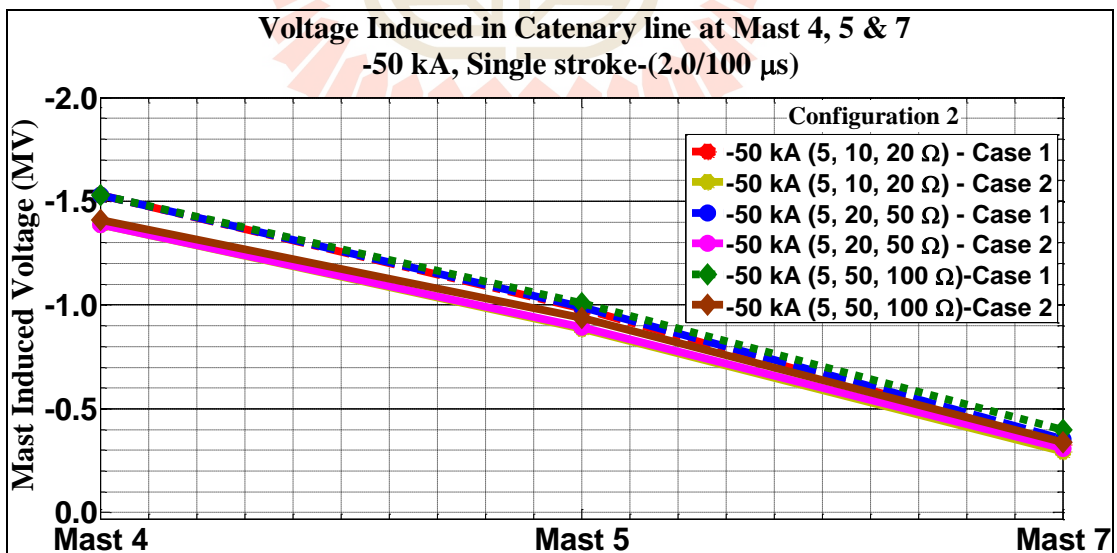
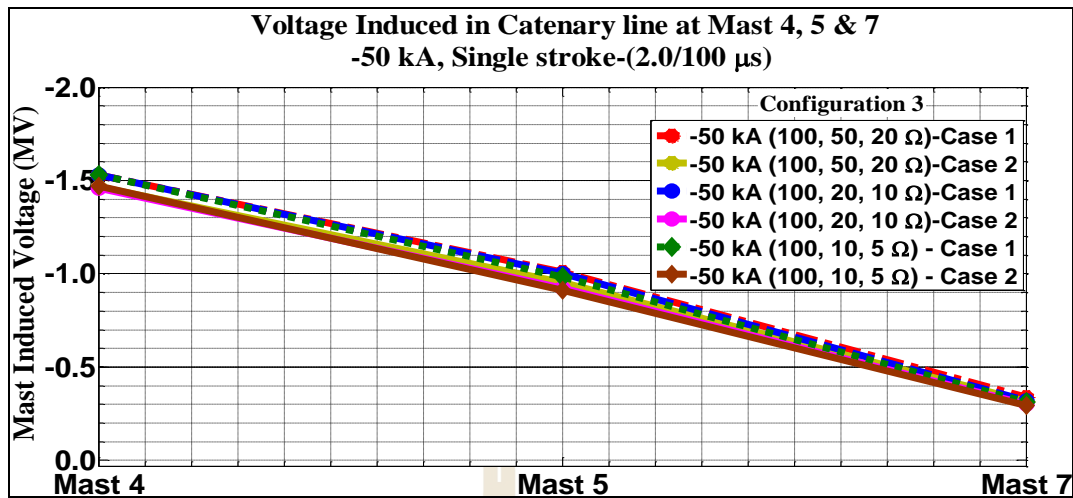
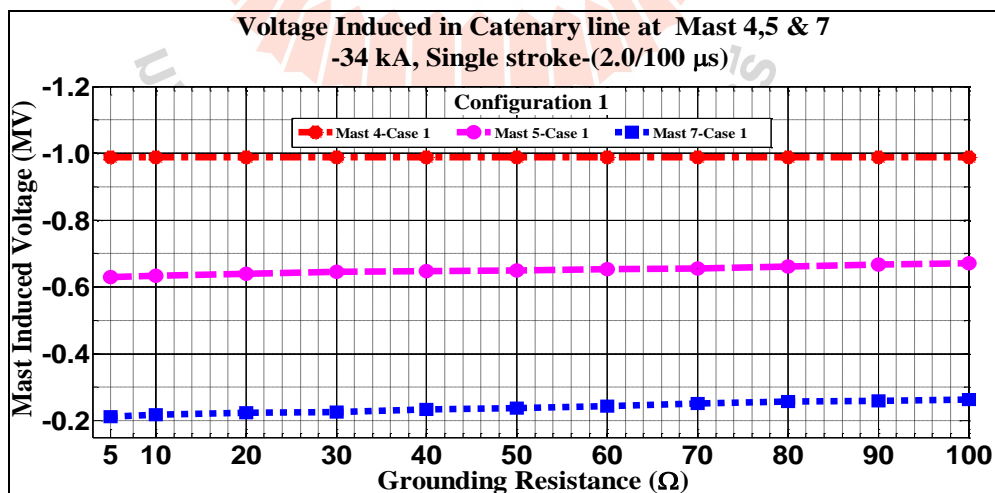


Figure 4.55 Catenary line induced voltages in both Cases with -50 kA (2.0/100  $\mu$ s) for configuration 2



**Figure 4.56** Catenary line induced voltages in both Cases with -50 kA (2.0/100 μs) for configuration 3

In Figures. 4.57-4.74, the outcome of analyzed mast induced voltage across stressed insulators of the catenary line when single lightning strokes on pantograph for both cases with all configurations are shown.



**Figure 4.57** Catenary line induced voltages in Case 1 with -34 kA (2.0/100 μs) for configuration 1

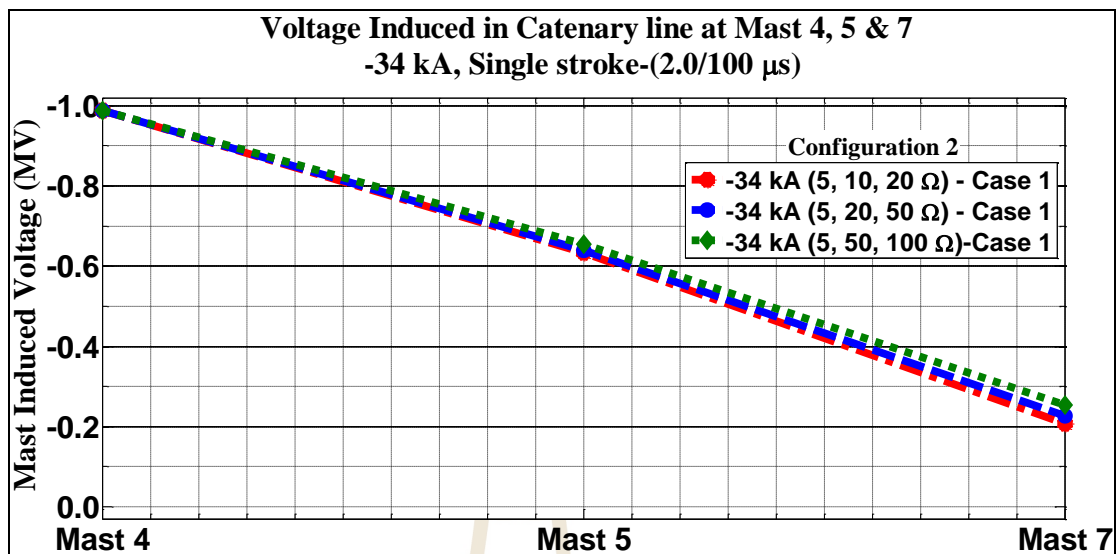


Figure 4.58 Catenary line induced voltages in Case 1 with -34 kA (2.0/100  $\mu$ s) for configuration 2

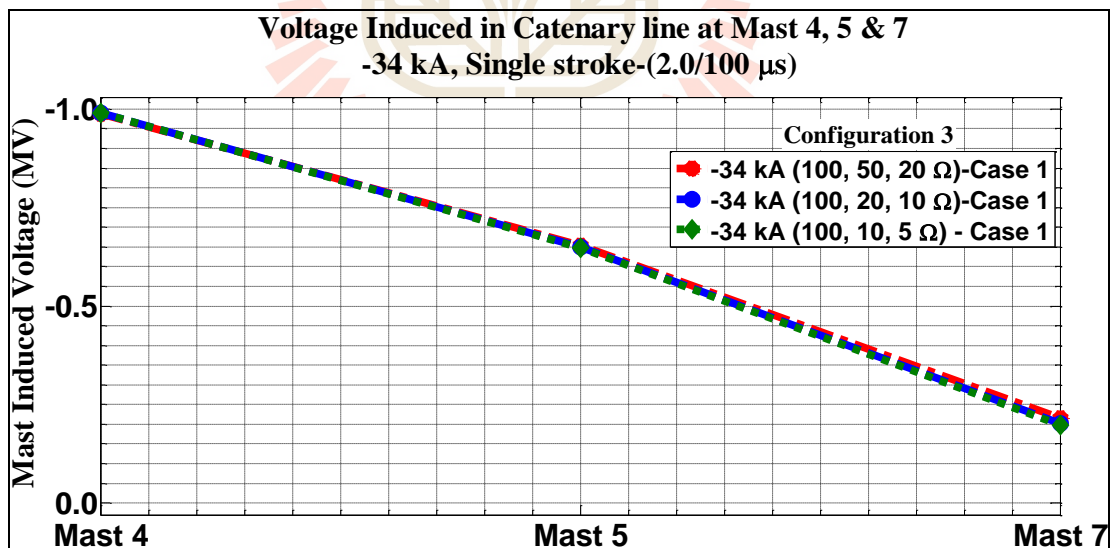


Figure 4.59 Catenary line induced voltages in Case 1 with -34 kA (2.0/100  $\mu$ s) for configuration 3

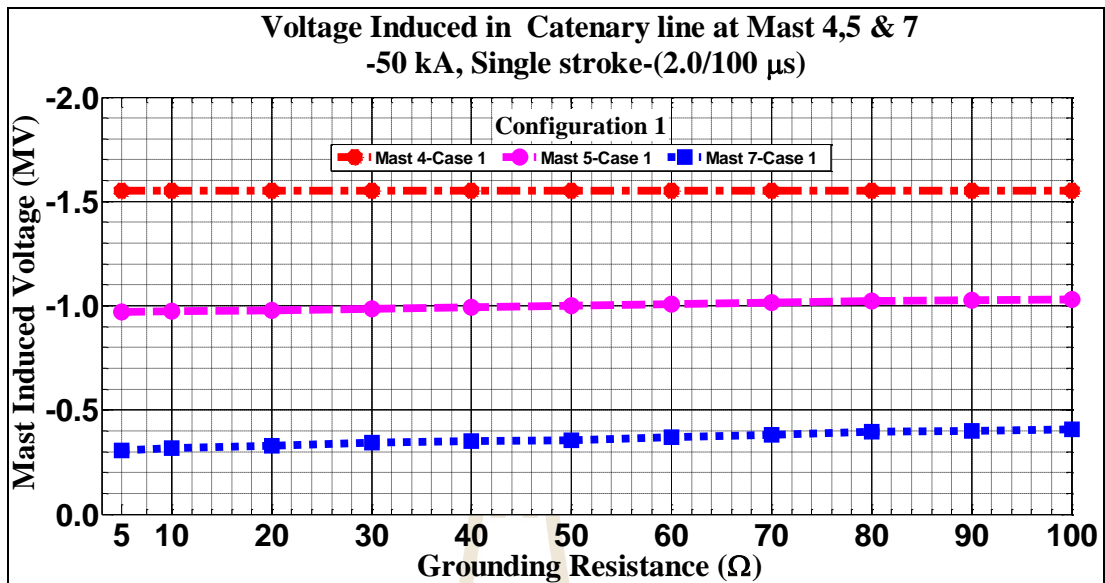


Figure 4.60 Catenary line induced voltages in Case 1 with -50 kA (2.0/100  $\mu$ s) for configuration 1

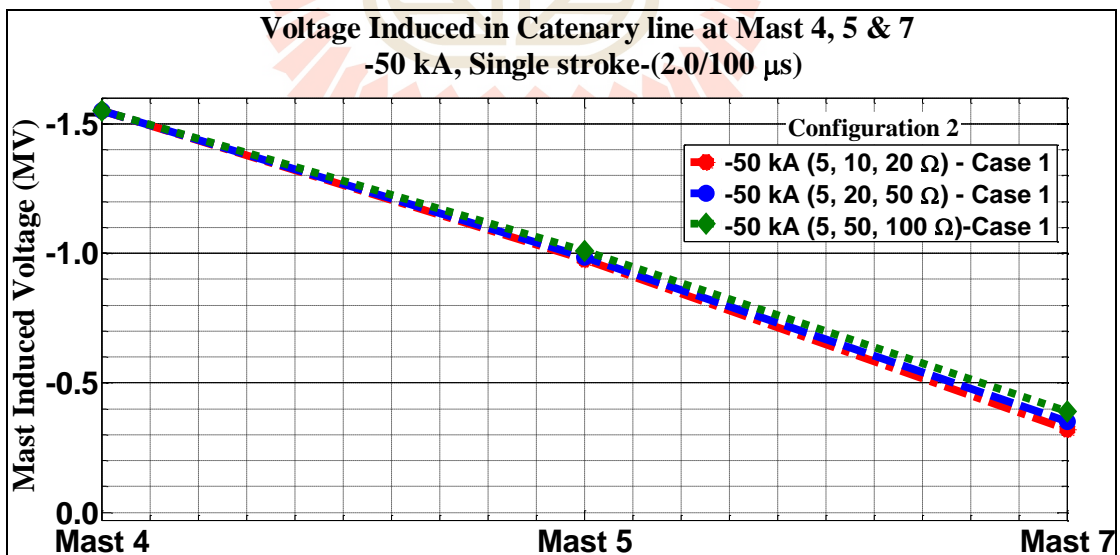


Figure 4.61 Catenary line induced voltages in Case 1 with -50 kA (2.0/100  $\mu$ s) for configuration 2

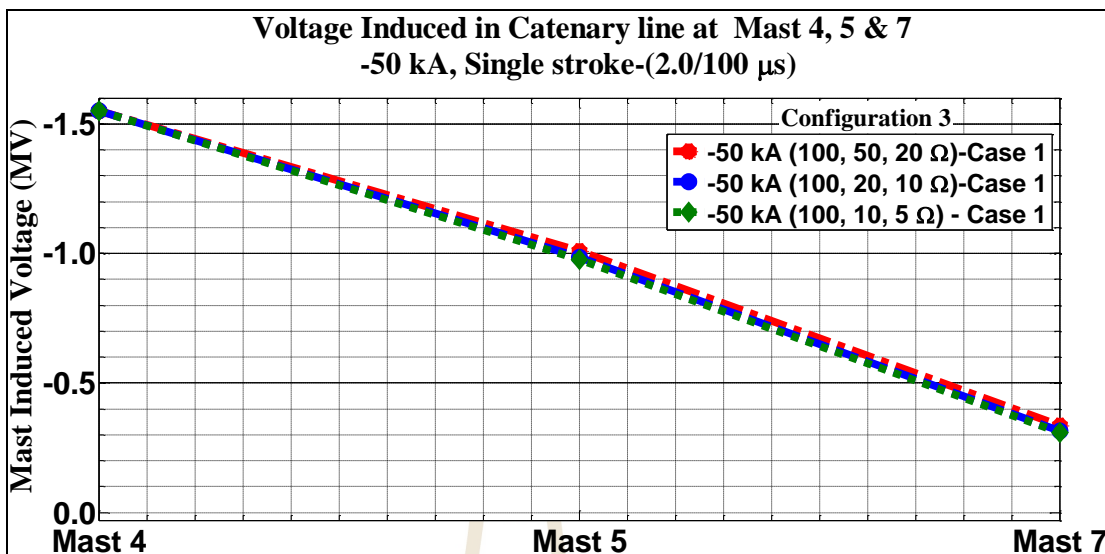


Figure 4.62 Catenary line induced voltages in Case 1 with -50 kA (2.0/100  $\mu$ s) for configuration 3

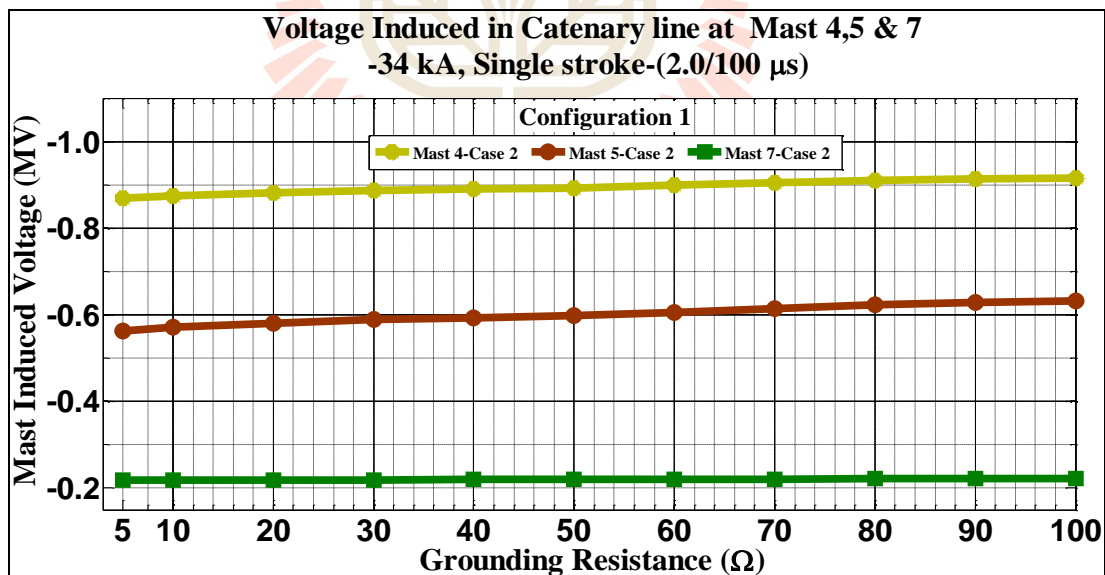


Figure 4.63 Catenary line induced voltages in Case 2 with -34 kA (2.0/100  $\mu$ s) for configuration 1

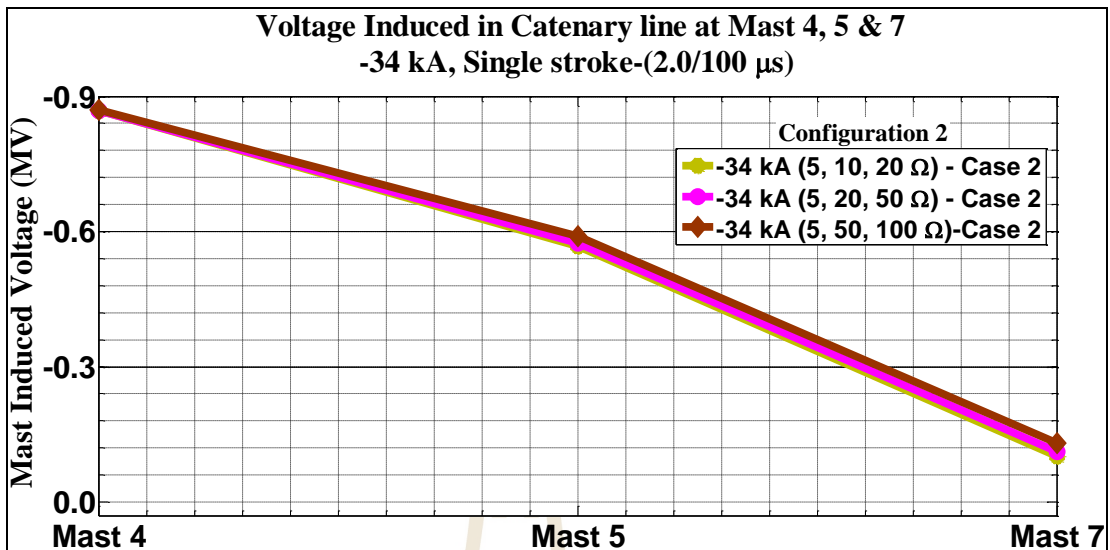


Figure 4.64 Catenary line induced voltages in Case 2 with -34 kA (2.0/100  $\mu$ s) for configuration 2

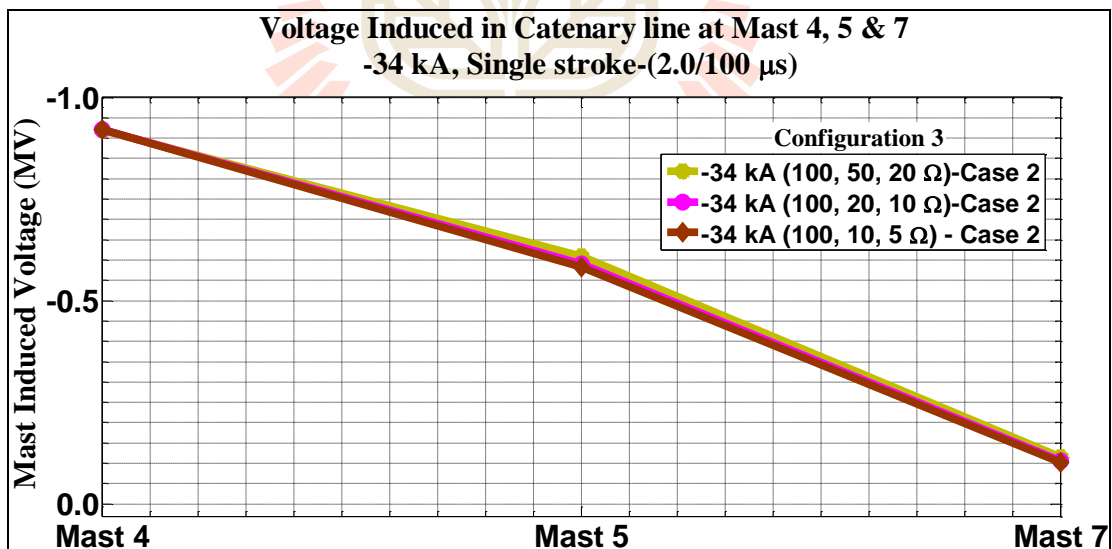


Figure 4.65 Catenary line induced voltages in Case 2 with -34 kA (2.0/100  $\mu$ s) for configuration 3

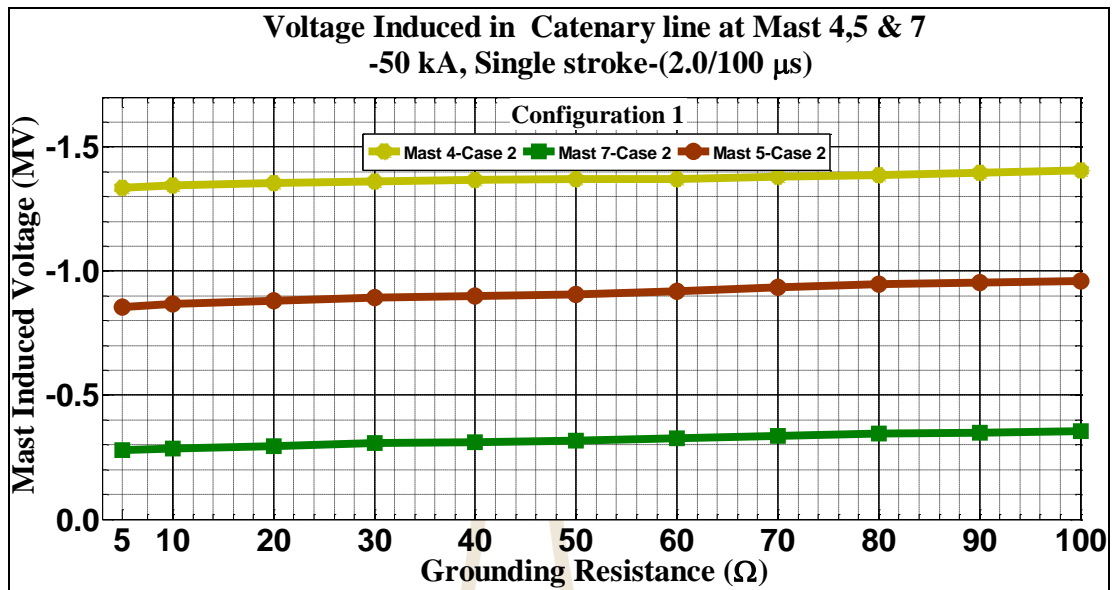


Figure 4.66 Catenary line induced voltages in Case 2 with -50 kA (2.0/100  $\mu$ s) for configuration 1

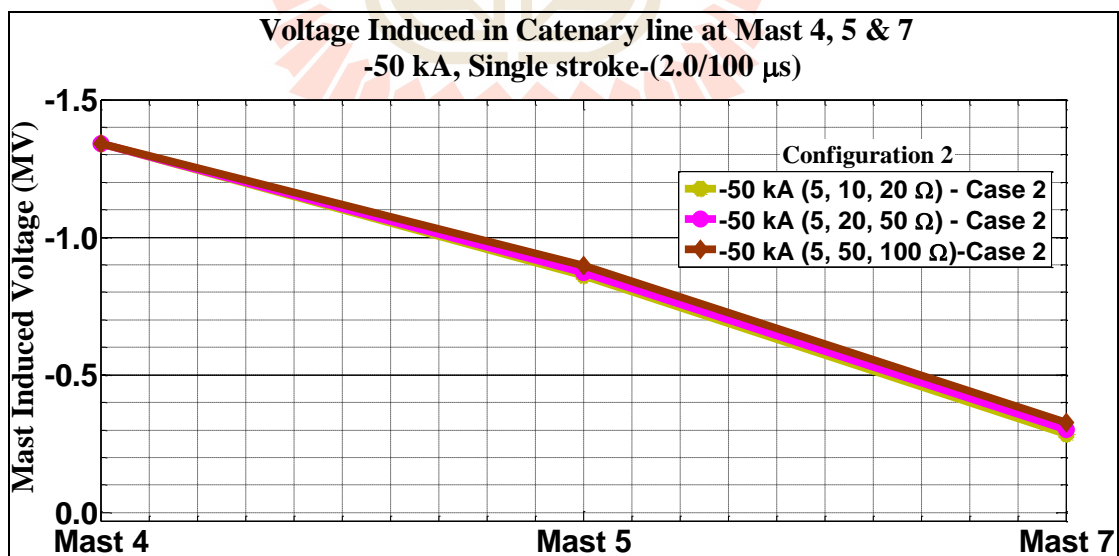


Figure 4.67 Catenary line induced voltages in Case 2 with -50 kA (2.0/100  $\mu$ s) for configuration 2



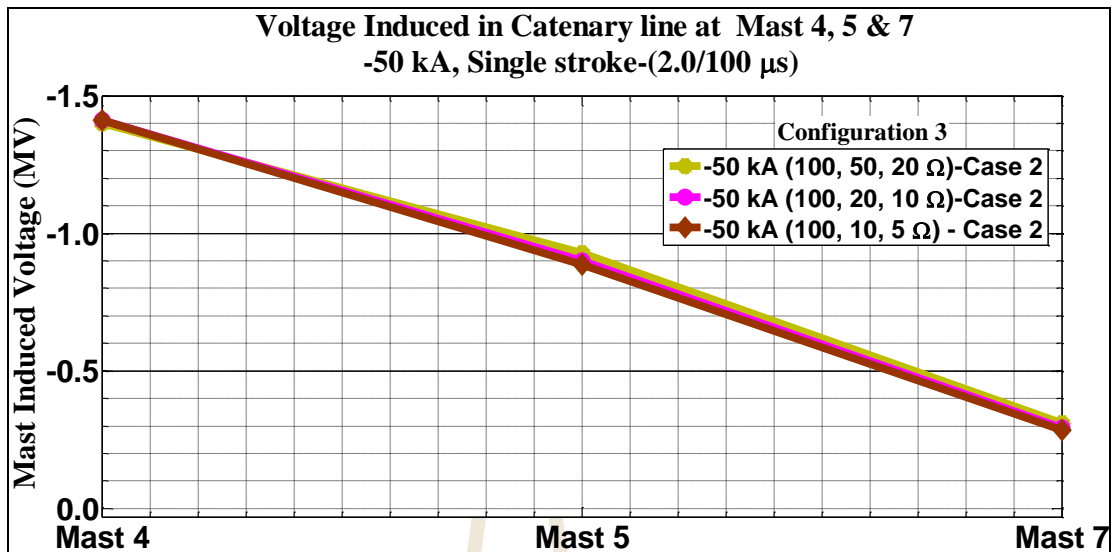


Figure 4.68 Catenary line induced voltages in Case 2 with -50 kA (2.0/100  $\mu$ s) for configuration 3

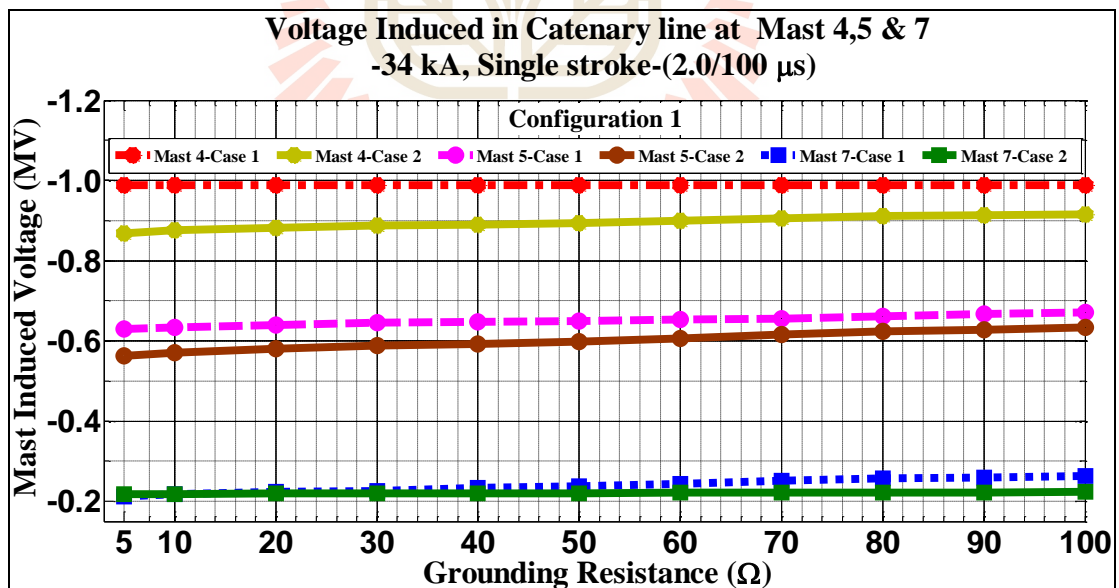
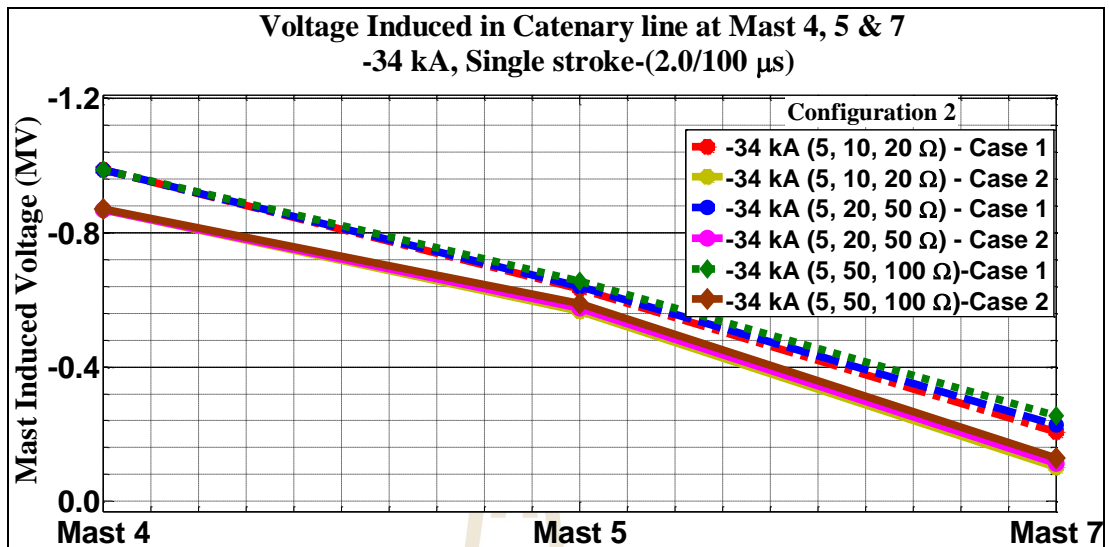
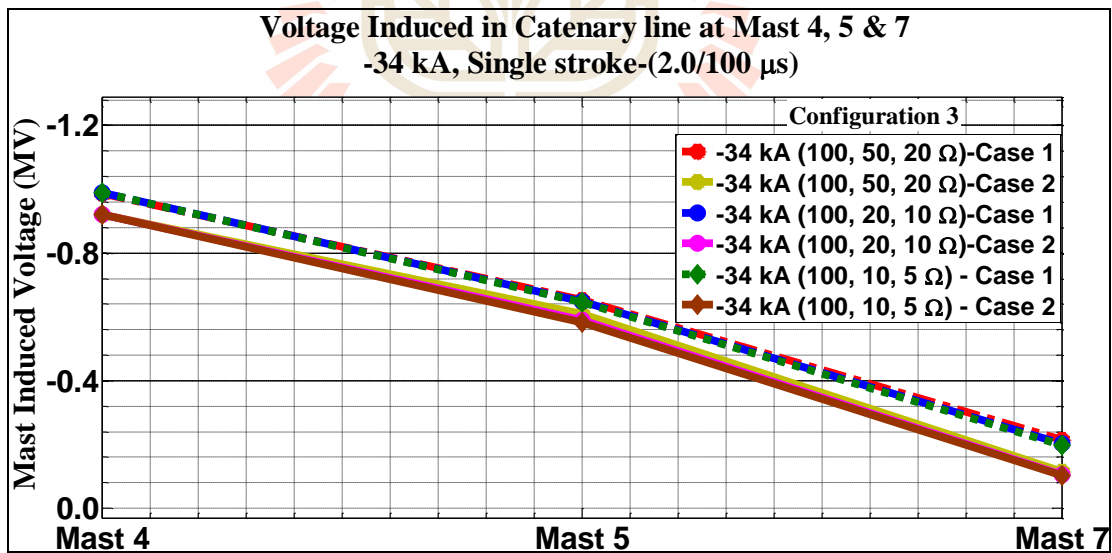


Figure 4.69 Catenary line induced voltages in both Cases with -34 kA (2.0/100  $\mu$ s) for configuration 1



**Figure 4.70** Catenary line induced voltages in both Cases with -34 kA (2.0/100  $\mu$ s) for configuration 2



**Figure 4.71** Catenary line induced voltages in both Cases with -34 kA (2.0/100  $\mu$ s) for configuration 3

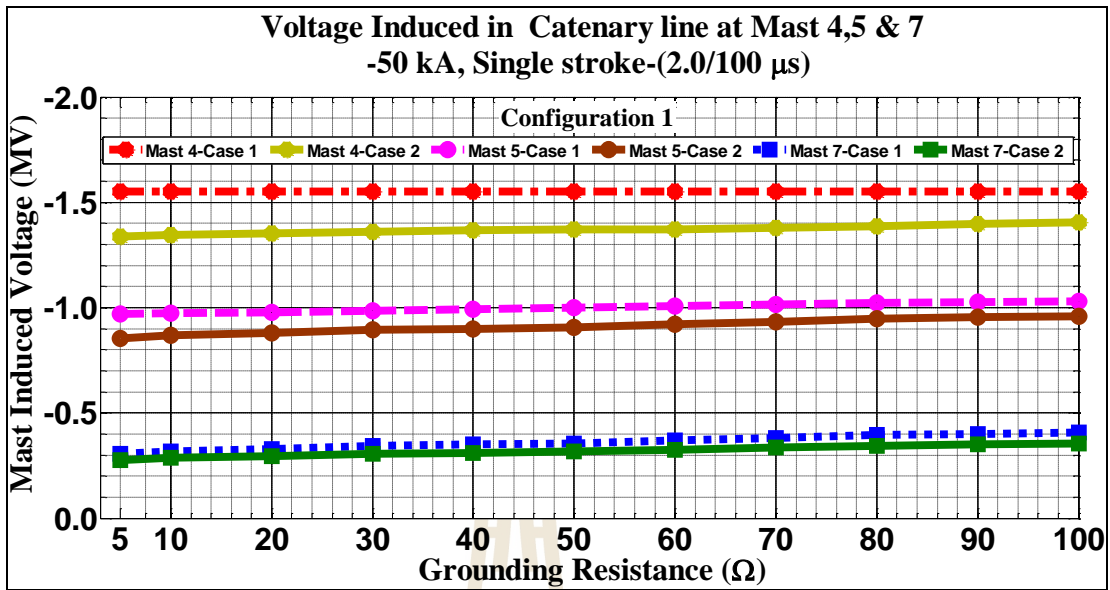


Figure 4.72 Catenary line induced voltages in both Cases with -50 kA (2.0/100 μs) for configuration 1

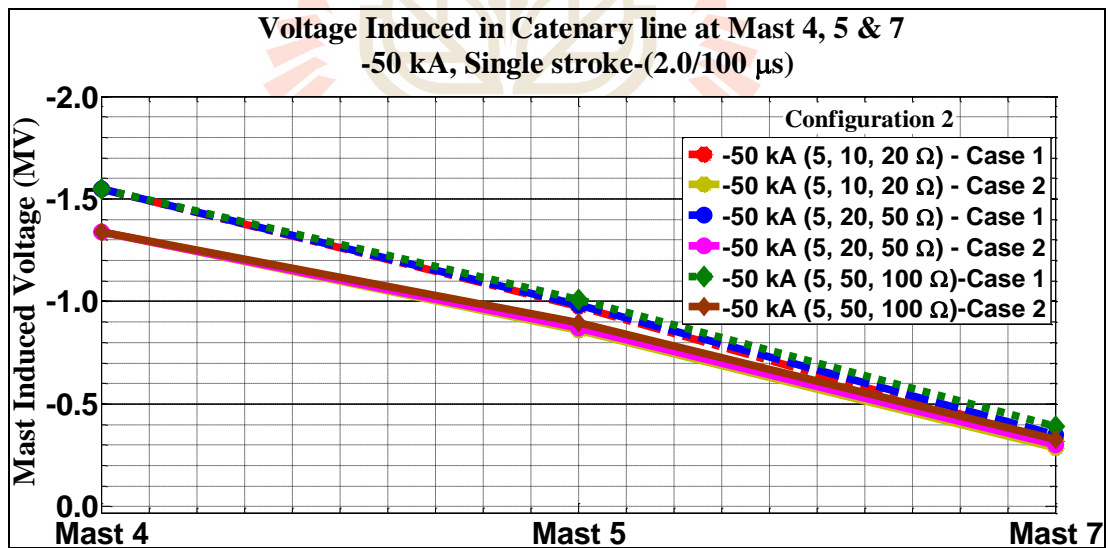
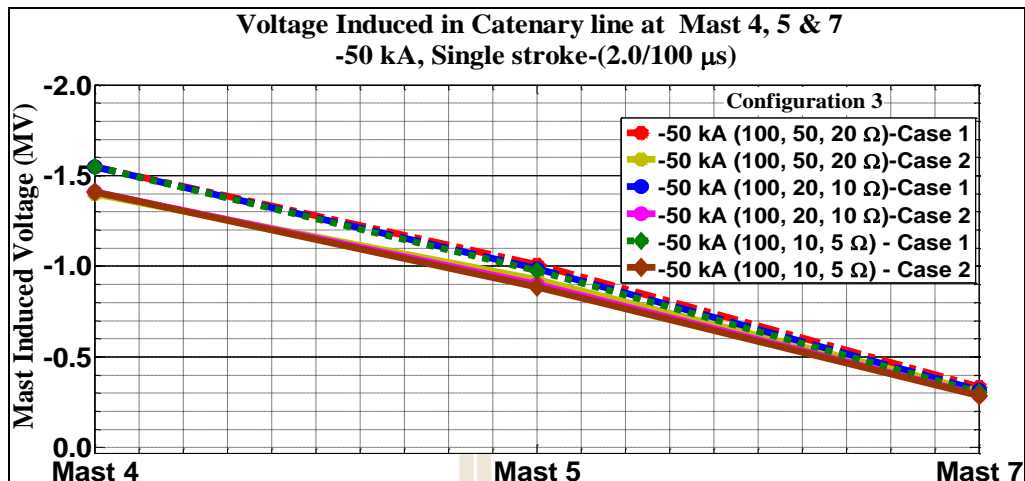
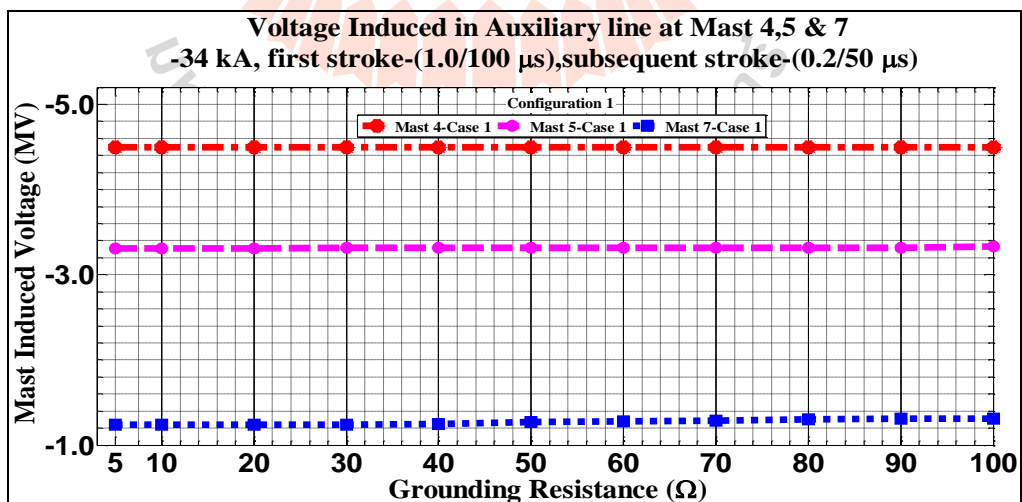


Figure 4.73 Catenary line induced voltages in both Cases with -50 kA (2.0/100 μs) for configuration 2



**Figure 4.74** Catenary line induced voltages in both Cases with -50 kA (2.0/100  $\mu$ s) for configuration 3

Figures. 4.75-4.92 contain the outcome of analyzed mast induced voltage across stressed insulators of the auxiliary line when multiple lightning strokes on the mast for both cases with all configurations.



**Figure 4.75** Auxiliary line induced voltages in Case 1 with -34 kA, first stroke-(1.0/100  $\mu$ s), subsequent stroke-(0.2/50  $\mu$ s) for configuration 1

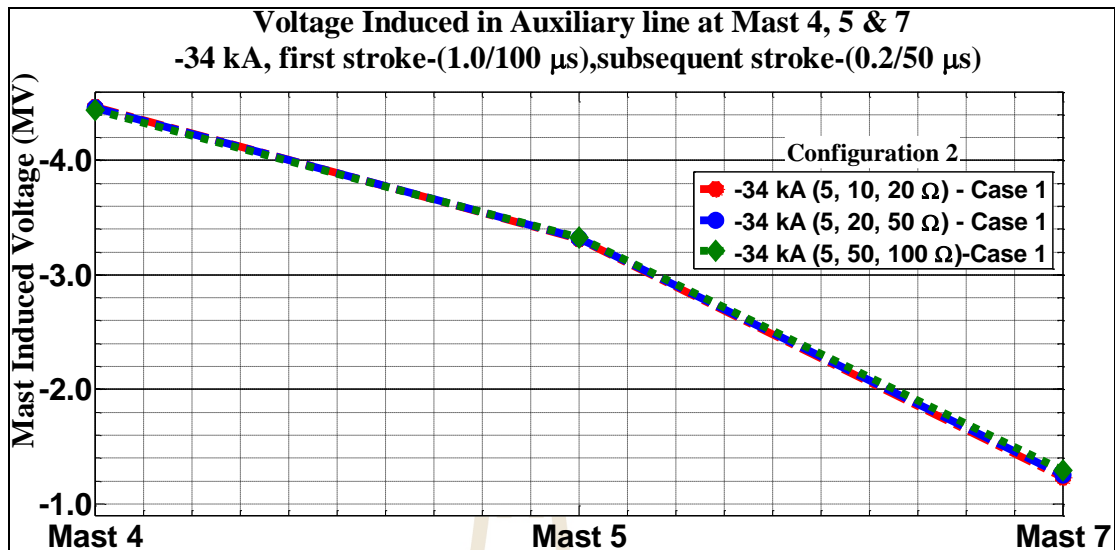


**Figure 4.76** Auxiliary line induced voltages in Case 1 with -34 kA, first stroke-(1.0/100  $\mu$ s), subsequent stroke-(0.2/50  $\mu$ s) for configuration 2

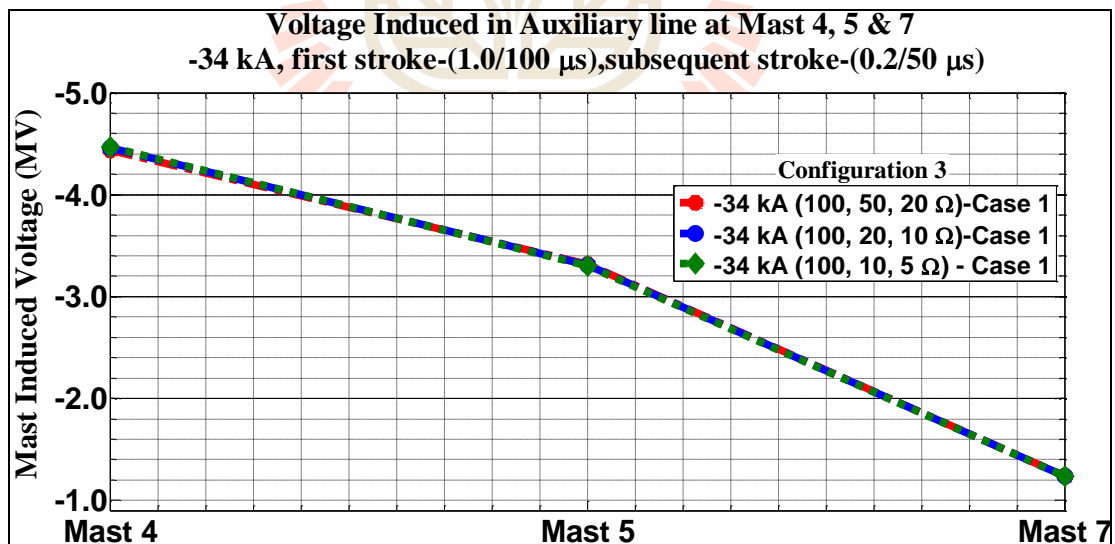


**Figure 4.77** Auxiliary line induced voltages in Case 1 with -34 kA, first stroke-(1.0/100  $\mu$ s), subsequent stroke-(0.2/50  $\mu$ s) for configuration 3

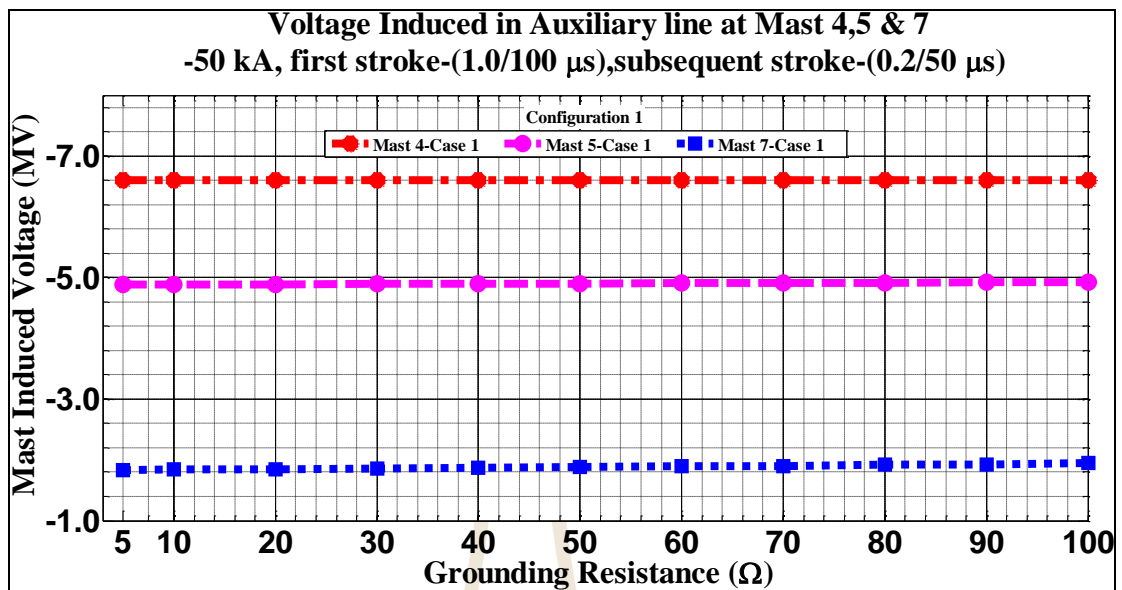


**Figure 4.78** Auxiliary line induced voltages in Case 1 with -50 kA, first stroke-(1.0/100  $\mu$ s), subsequent stroke-(0.2/50  $\mu$ s) for configuration 1

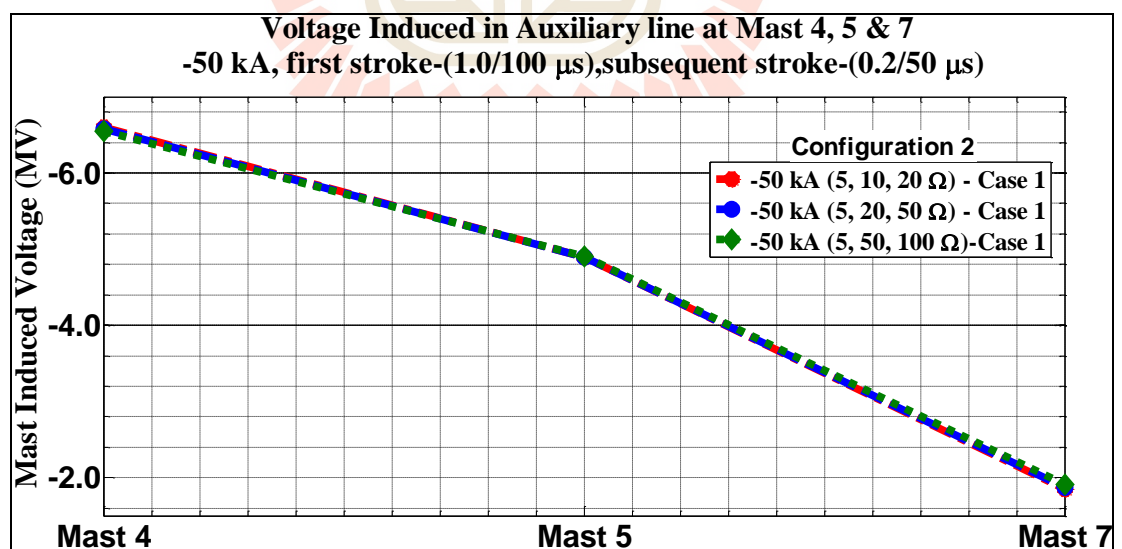


**Figure 4.79** Auxiliary line induced voltages in Case 1 with -50 kA, first stroke-(1.0/100  $\mu$ s), subsequent stroke-(0.2/50  $\mu$ s) for configuration 2

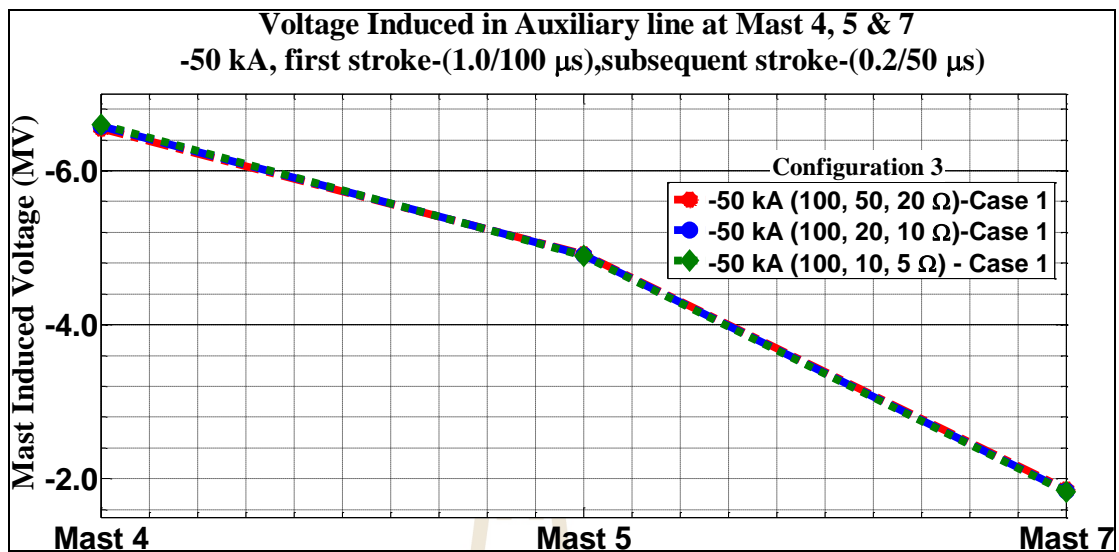


**Figure 4.80** Auxiliary line induced voltages in Case 1 with -50 kA, first stroke-(1.0/100  $\mu$ s), subsequent stroke-(0.2/50  $\mu$ s) for configuration 3

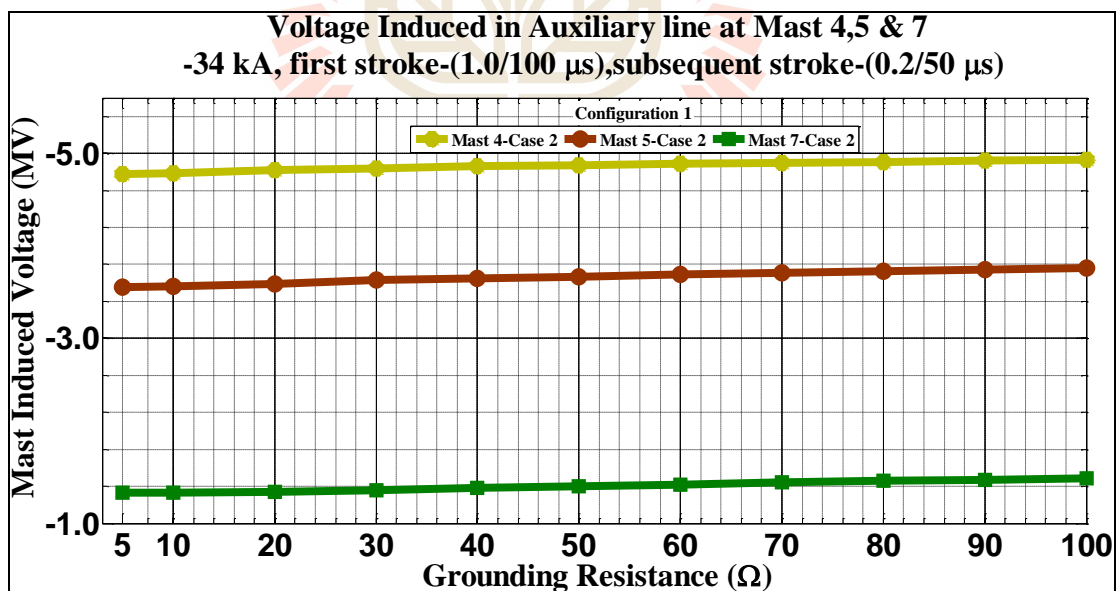


**Figure 4.81** Auxiliary line induced voltages in Case 2 with -34 kA, first stroke-(1.0/100  $\mu$ s), subsequent stroke-(0.2/50  $\mu$ s) for configuration 1

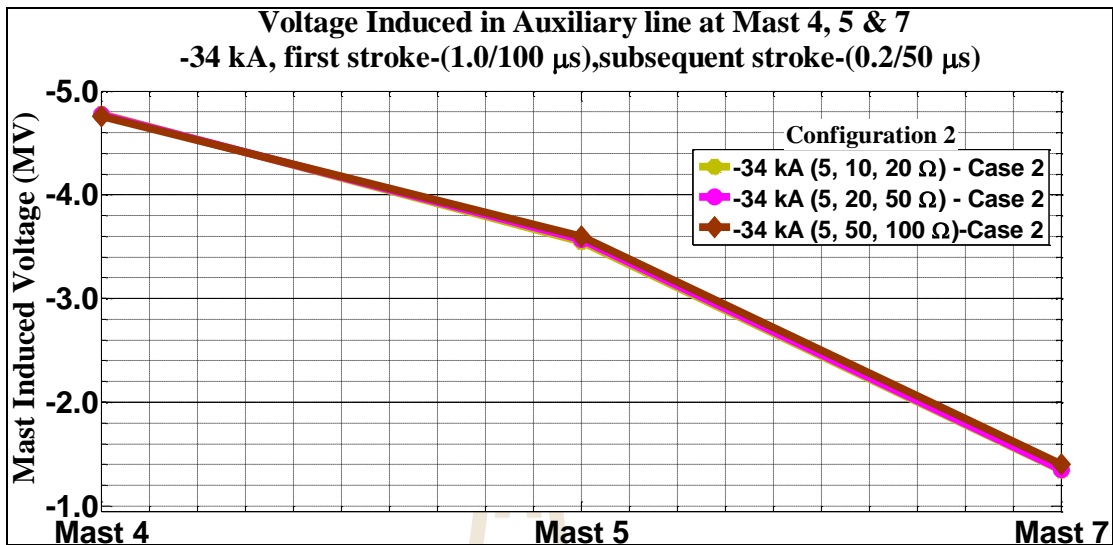


**Figure 4.82** Auxiliary line induced voltages in Case 2 with -34 kA, first stroke-(1.0/100  $\mu$ s), subsequent stroke-(0.2/50  $\mu$ s) for configuration 2

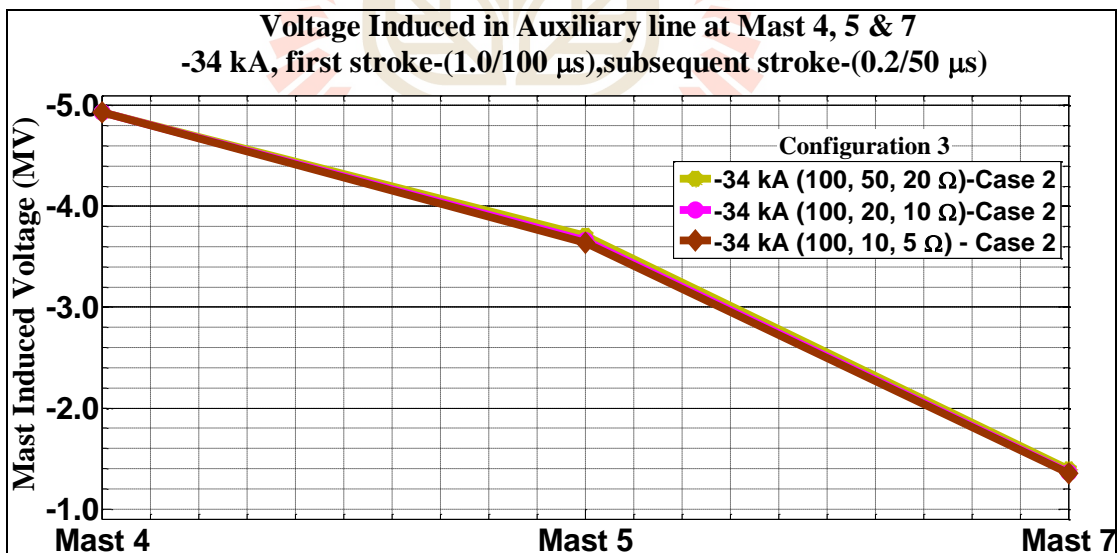


**Figure 4.83** Auxiliary line induced voltages in Case 2 with -34 kA, first stroke-(1.0/100  $\mu$ s), subsequent stroke-(0.2/50  $\mu$ s) for configuration 3



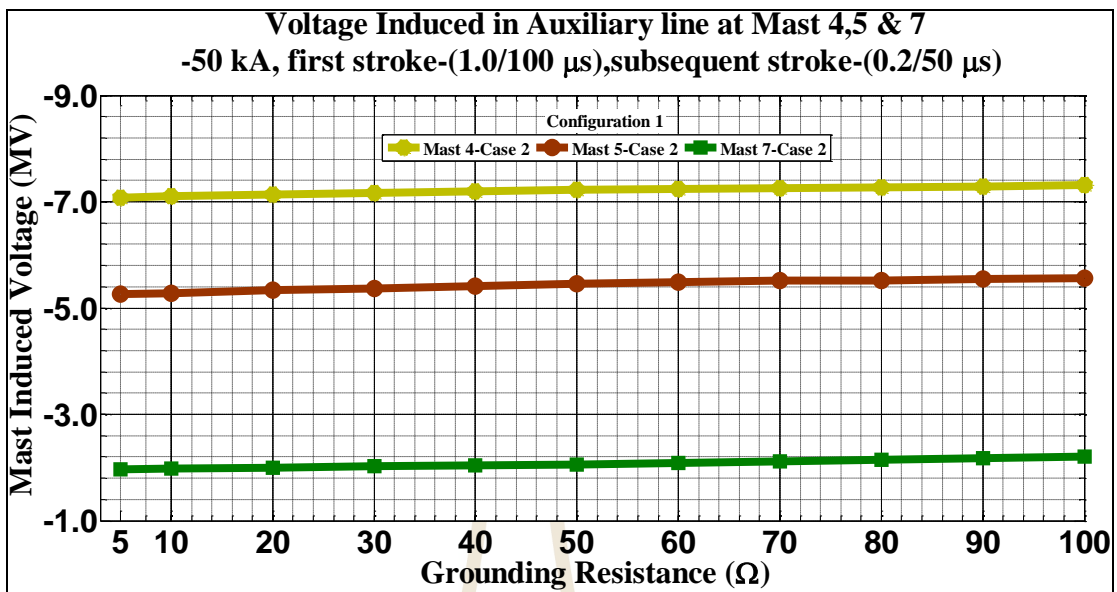


**Figure 4.84** Auxiliary line induced voltages in Case 2 with -50 kA, first stroke-(1.0/100  $\mu$ s), subsequent stroke-(0.2/50  $\mu$ s) for configuration 1

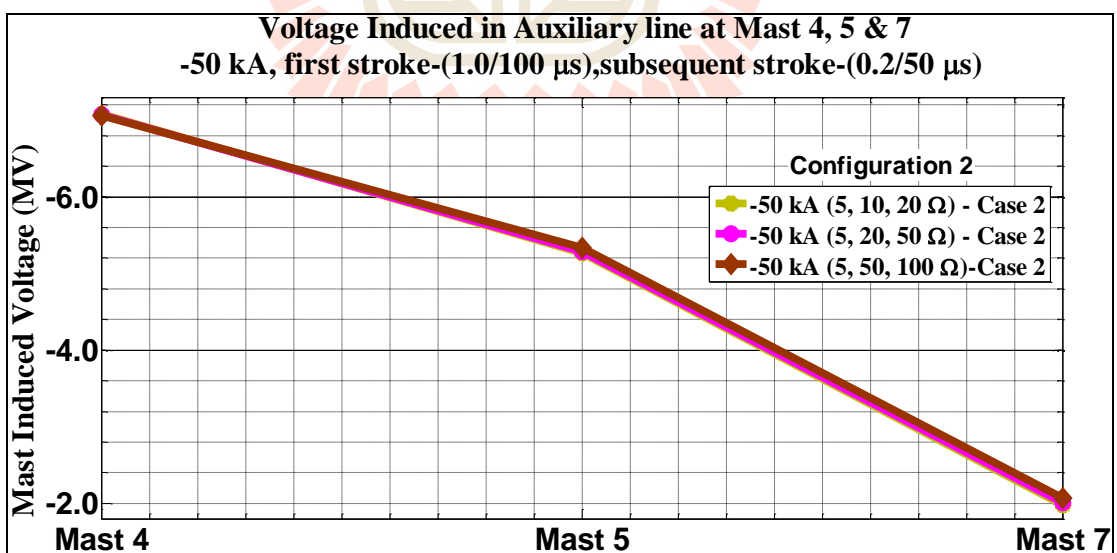


**Figure 4.85** Auxiliary line induced voltages in Case 2 with -50 kA, first stroke-(1.0/100  $\mu$ s), subsequent stroke-(0.2/50  $\mu$ s) for configuration 2

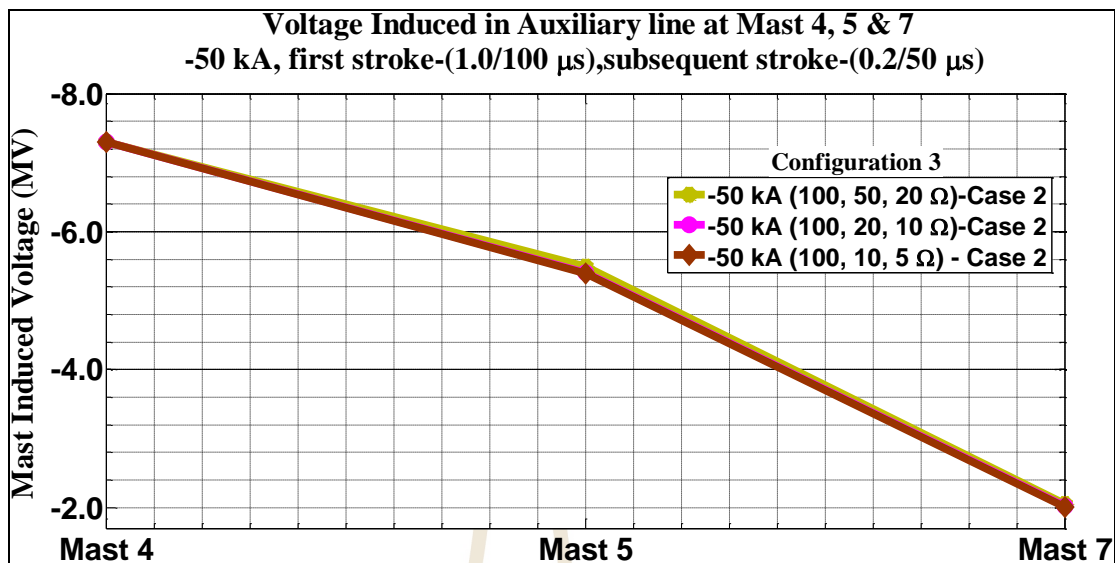


**Figure 4.86** Auxiliary line induced voltages in Case 2 with -50 kA, first stroke-(1.0/100  $\mu$ s), subsequent stroke-(0.2/50  $\mu$ s) for configuration 3

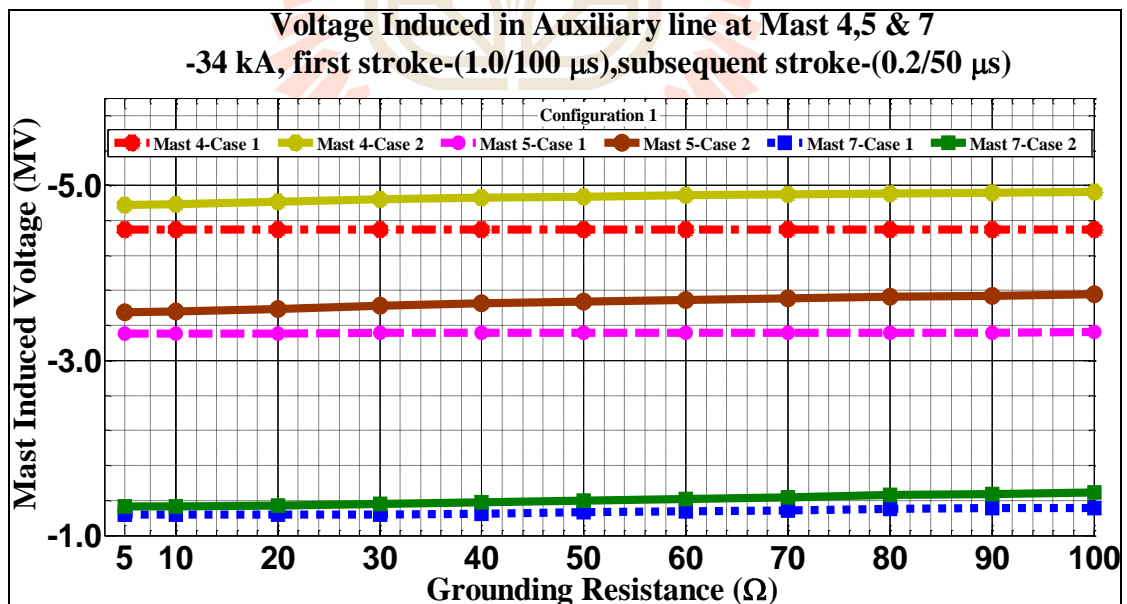


**Figure 4.87** Auxiliary line induced voltages in both Cases with -34 kA, first stroke-(1.0/100  $\mu$ s), subsequent stroke-(0.2/50  $\mu$ s) for configuration 1

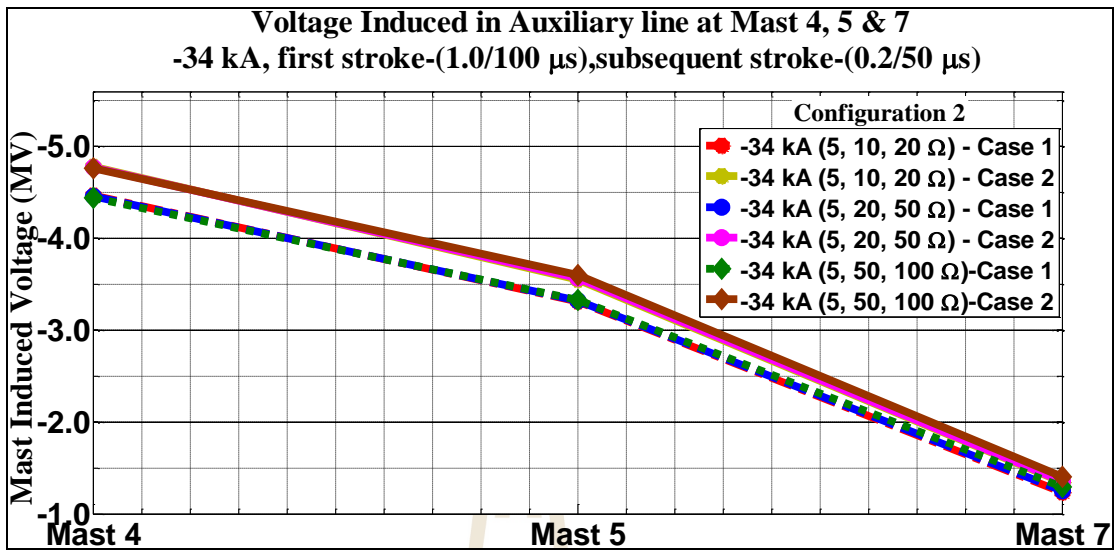


**Figure 4.88** Auxiliary line induced voltages in both Cases with -34 kA, first stroke-(1.0/100  $\mu$ s), subsequent stroke-(0.2/50  $\mu$ s) for configuration 2

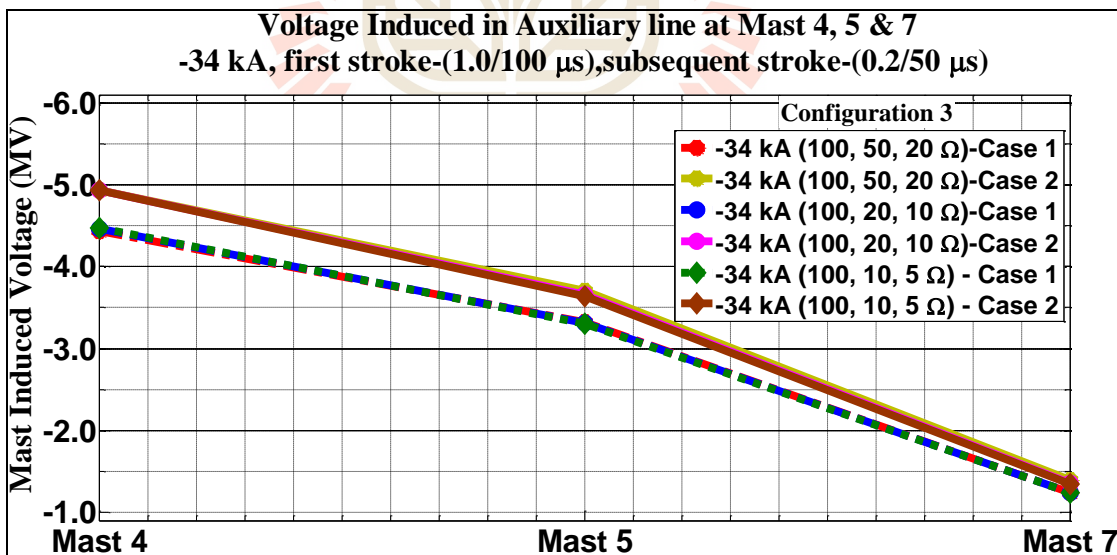


**Figure 4.89** Auxiliary line induced voltages in both Cases with -34 kA, first stroke-(1.0/100  $\mu$ s), subsequent stroke-(0.2/50  $\mu$ s) for configuration 3

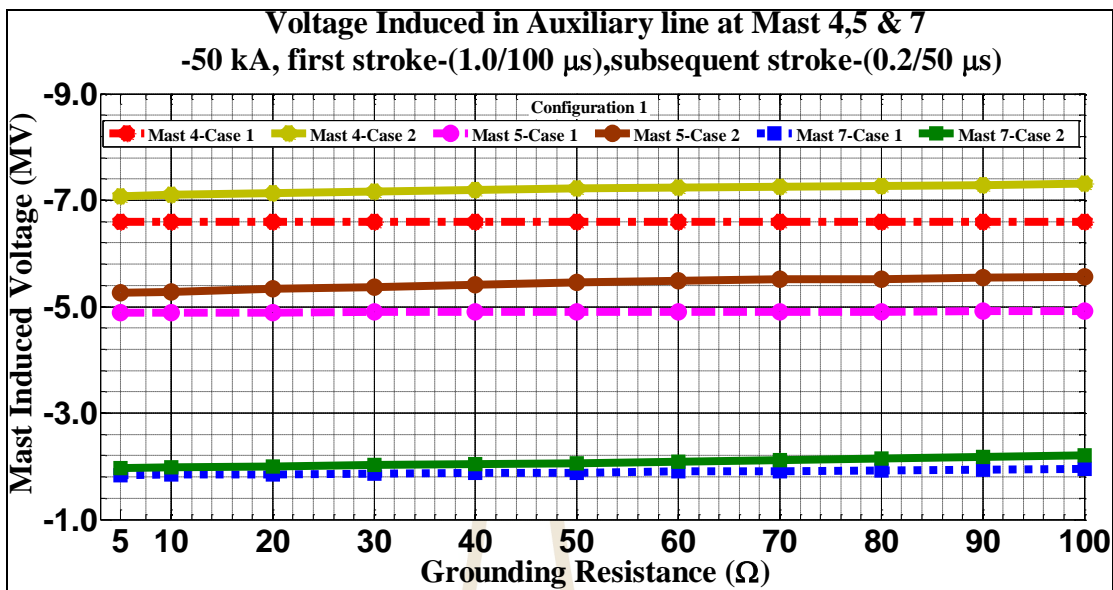


Figure 4.90 Auxiliary line induced voltages in both Cases with -50 kA, first stroke-(1.0/100 μs), subsequent stroke-(0.2/50 μs) for configuration 1

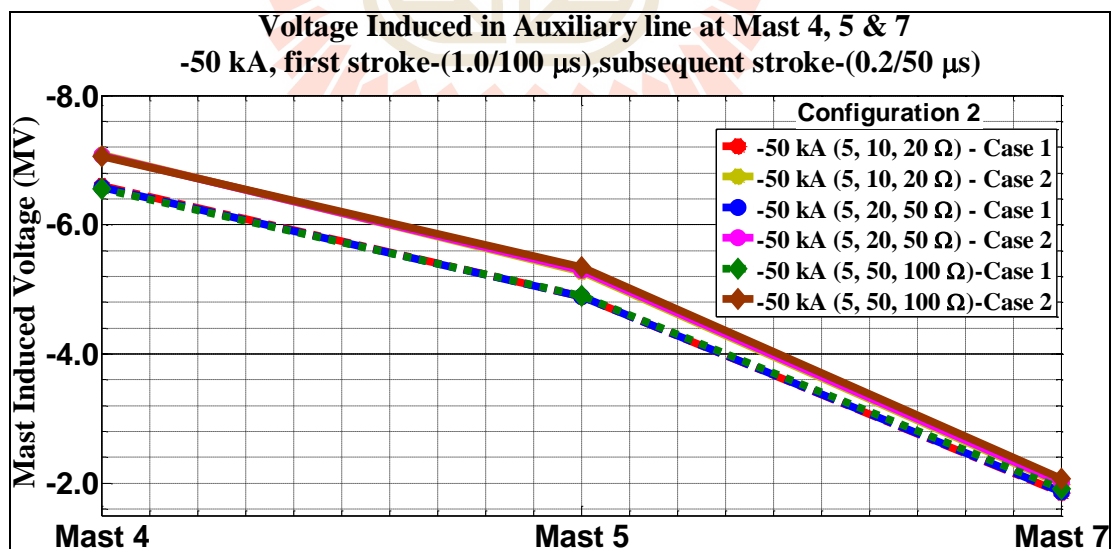
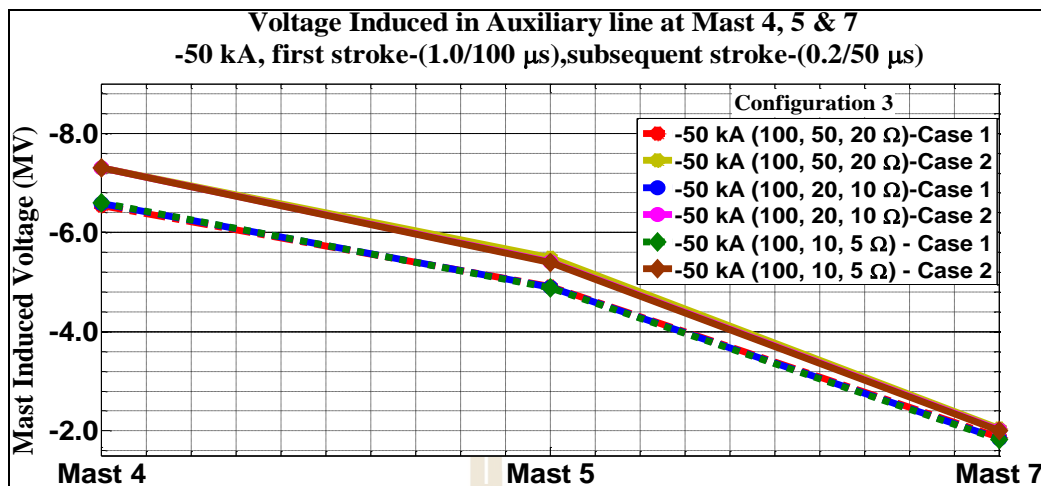
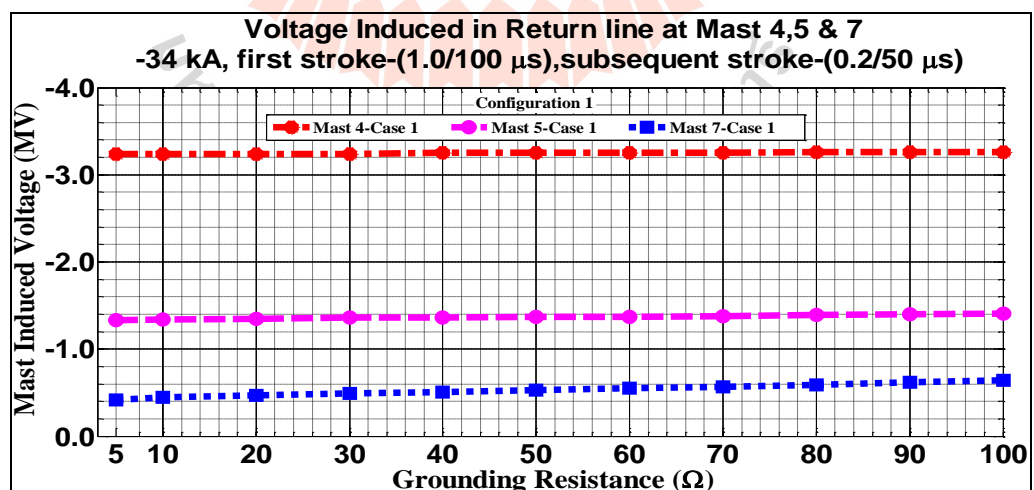


Figure 4.91 Auxiliary line induced voltages in both Cases with -50 kA, first stroke-(1.0/100 μs), subsequent stroke-(0.2/50 μs) for configuration 2



**Figure 4.92** Auxiliary line induced voltages in both Cases with -50 kA, first stroke-(1.0/100  $\mu$ s), subsequent stroke-(0.2/50  $\mu$ s) for configuration 3

For both cases with all configurations, Figures 4.93-4.110 carry out the analyzed results of mast induced voltage across stressed insulators of the return line when multiple lightning strokes on return line.



**Figure 4.93** Return line induced voltages in Case 1 with -34 kA, first stroke-(1.0/100  $\mu$ s), subsequent stroke-(0.2/50  $\mu$ s) for configuration 1

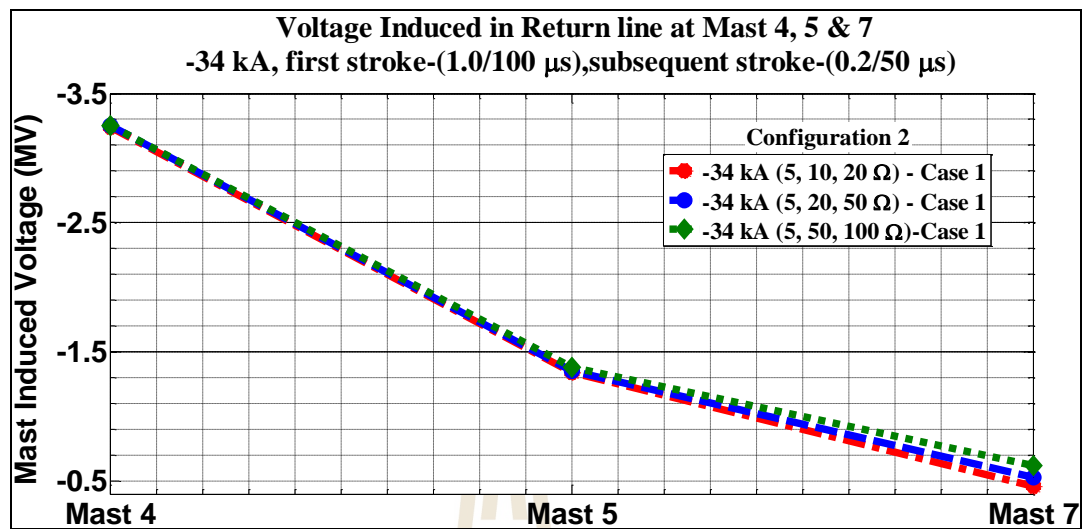


**Figure 4.94** Return line induced voltages in Case 1 with -34 kA, first stroke-(1.0/100  $\mu$ s), subsequent stroke-(0.2/50  $\mu$ s) for configuration 2

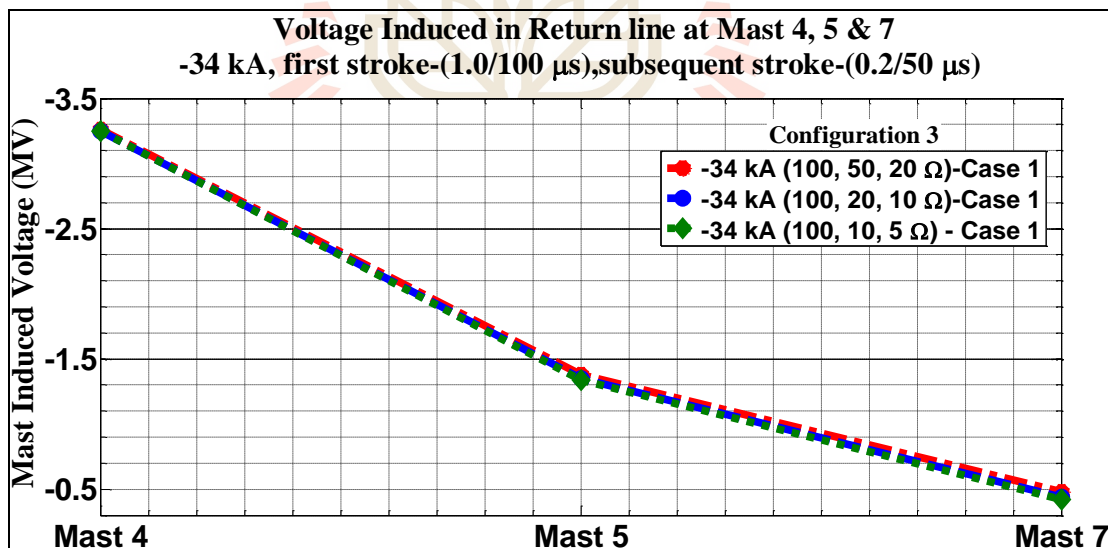


**Figure 4.95** Return line induced voltages in Case 1 with -34 kA, first stroke-(1.0/100  $\mu$ s), subsequent stroke-(0.2/50  $\mu$ s) for configuration 3

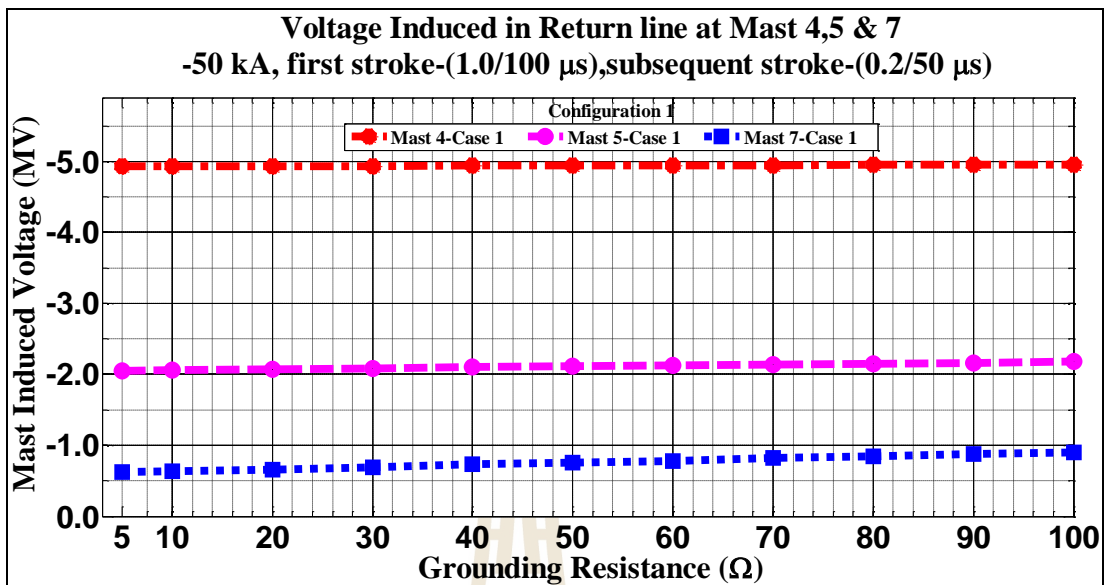


Figure 4.96 Return line induced voltages in Case 1 with -50 kA, first stroke-(1.0/100 μs), subsequent stroke-(0.2/50 μs) for configuration 1

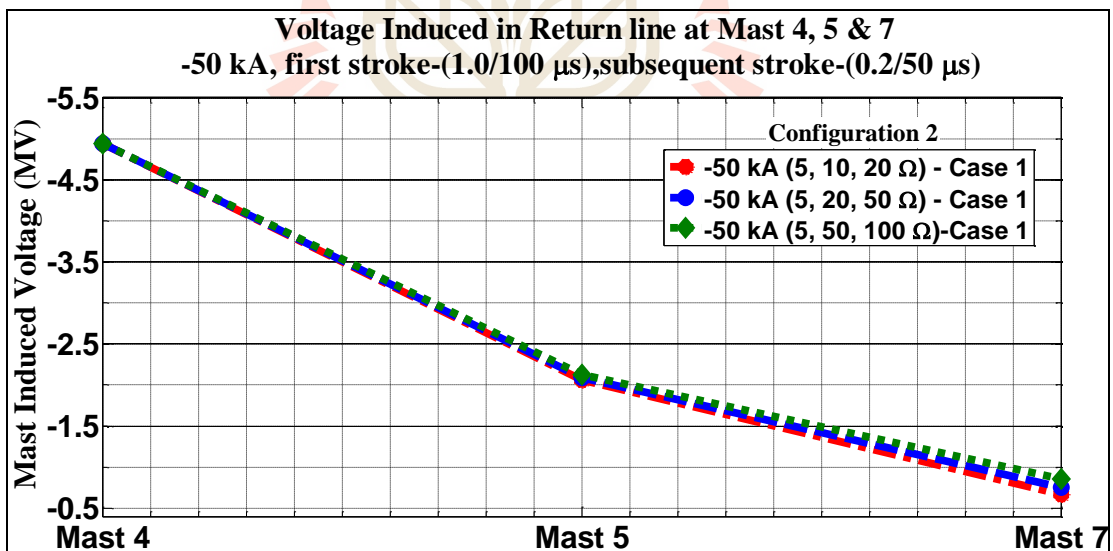


Figure 4.97 Return line induced voltages in Case 1 with -50 kA, first stroke-(1.0/100 μs), subsequent stroke-(0.2/50 μs) for configuration 2

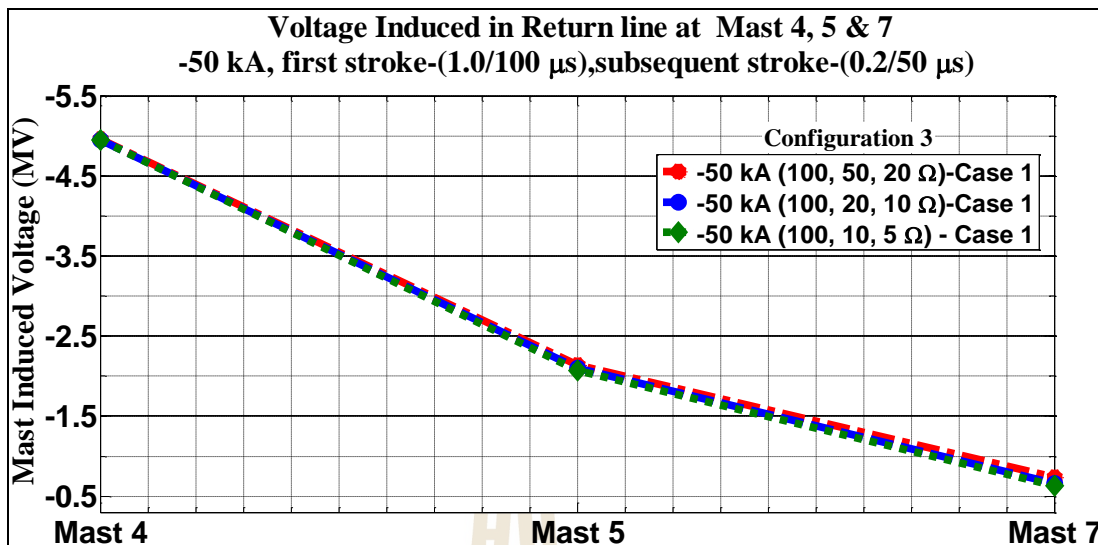


Figure 4.98 Return line induced voltages in Case 1 with -50 kA, first stroke-(1.0/100  $\mu$ s), subsequent stroke-(0.2/50  $\mu$ s) for configuration 3

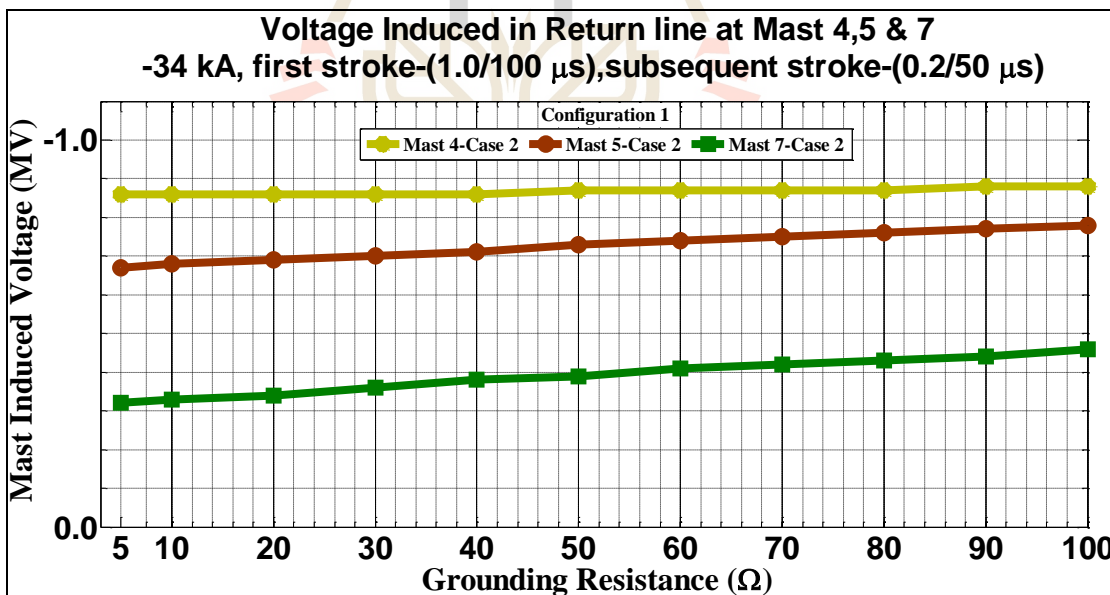


Figure 4.99 Return line induced voltages in Case 2 with -34 kA, first stroke-(1.0/100  $\mu$ s), subsequent stroke-(0.2/50  $\mu$ s) for configuration 1



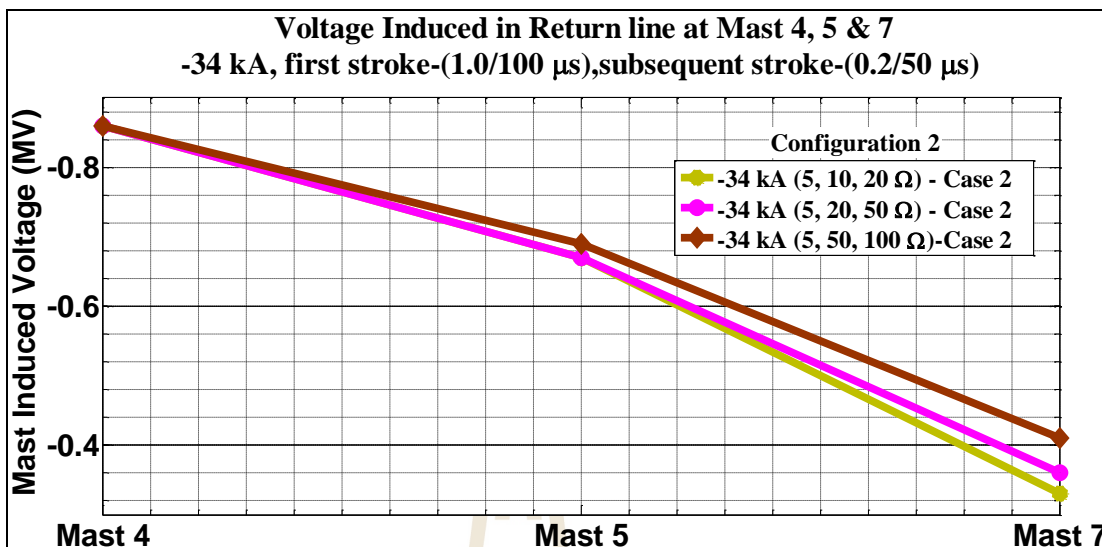


Figure 4.100 Return line induced voltages in Case 2 with -34 kA, first stroke-(1.0/100  $\mu$ s), subsequent stroke-(0.2/50  $\mu$ s) for configuration 2

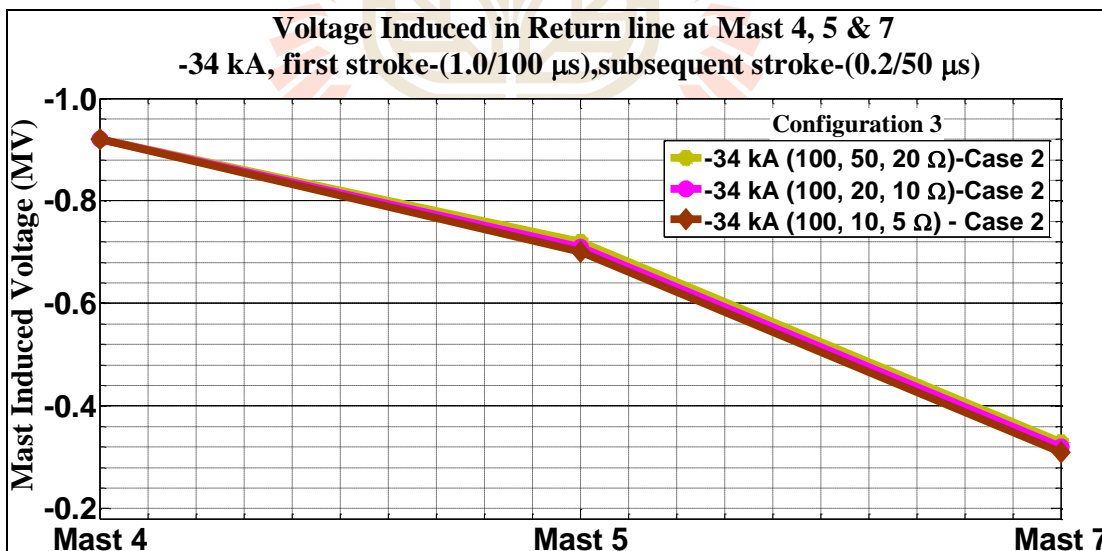


Figure 4.101 Return line induced voltages in Case 2 with -34 kA, first stroke-(1.0/100  $\mu$ s), subsequent stroke-(0.2/50  $\mu$ s) for configuration 3

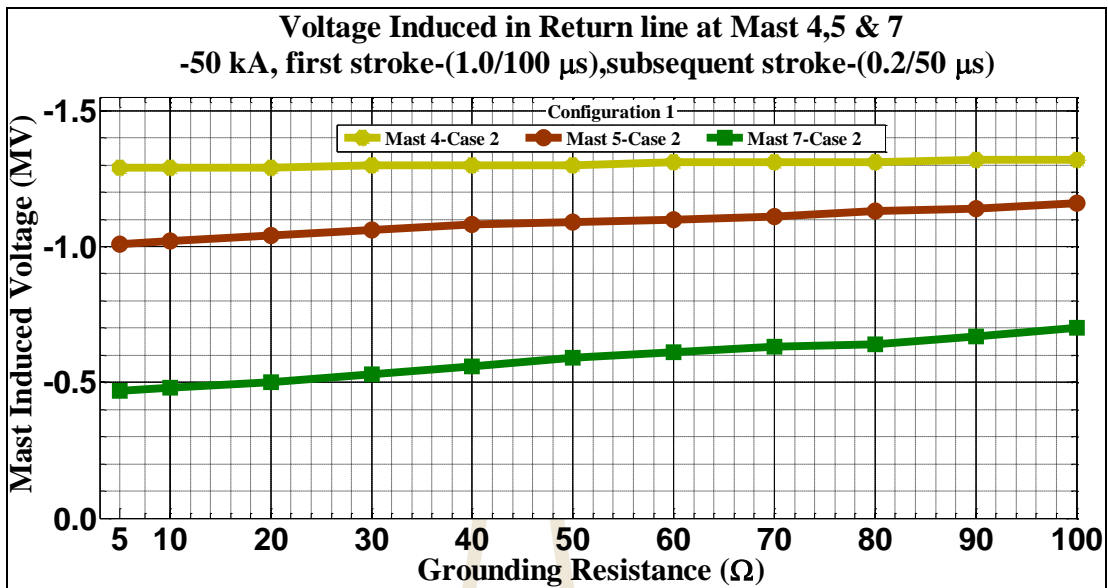


Figure 4.102 Return line induced voltages in Case 2 with -50 kA, first stroke-(1.0/100 μs), subsequent stroke-(0.2/50 μs) for configuration 1

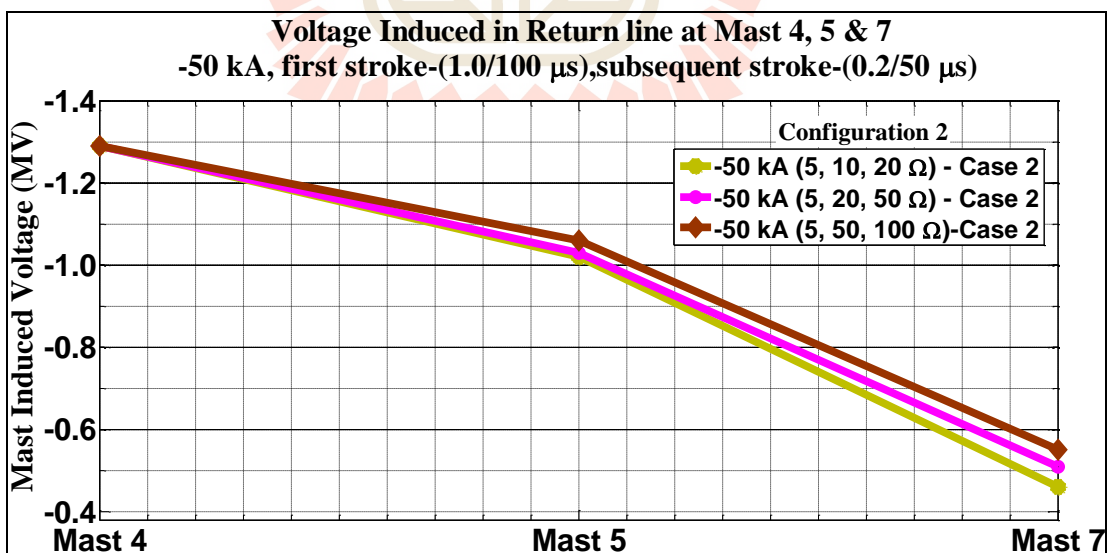
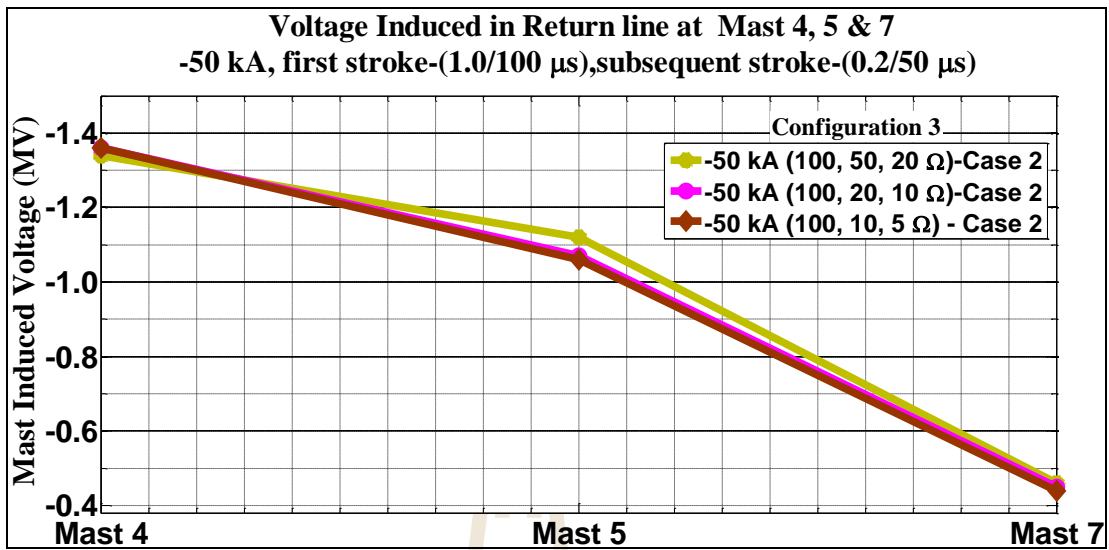
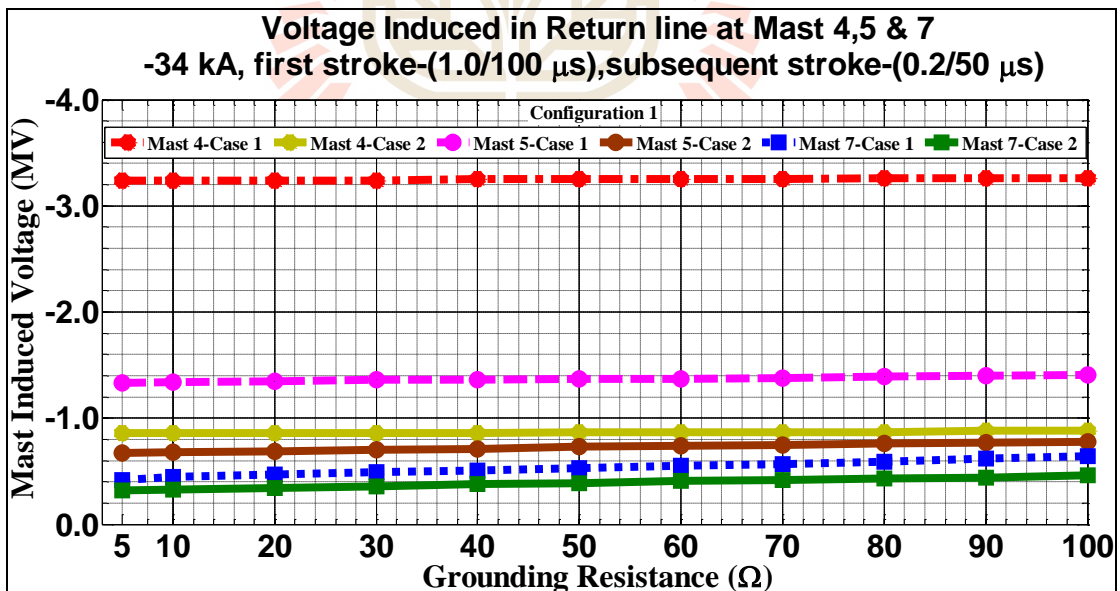


Figure 4.103 Return line induced voltages in Case 2 with -50 kA, first stroke-(1.0/100 μs), subsequent stroke-(0.2/50 μs) for configuration 2



**Figure 4.104** Return line induced voltages in Case 2 with -50 kA, first stroke-(1.0/100  $\mu$ s), subsequent stroke-(0.2/50  $\mu$ s) for configuration 3



**Figure 4.105** Return line induced voltages in both Cases with -34 kA, first stroke-(1.0/100  $\mu$ s), subsequent stroke-(0.2/50  $\mu$ s) for configuration 1

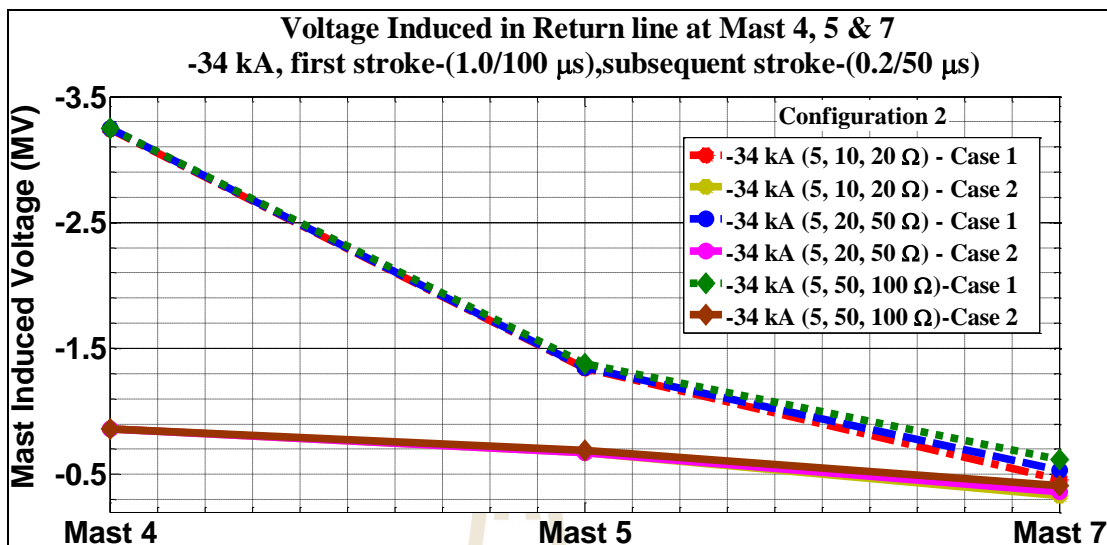


Figure 4.106 Return line induced voltages in both Cases with -34 kA, first stroke-(1.0/100  $\mu$ s), subsequent stroke-(0.2/50  $\mu$ s) for configuration 2

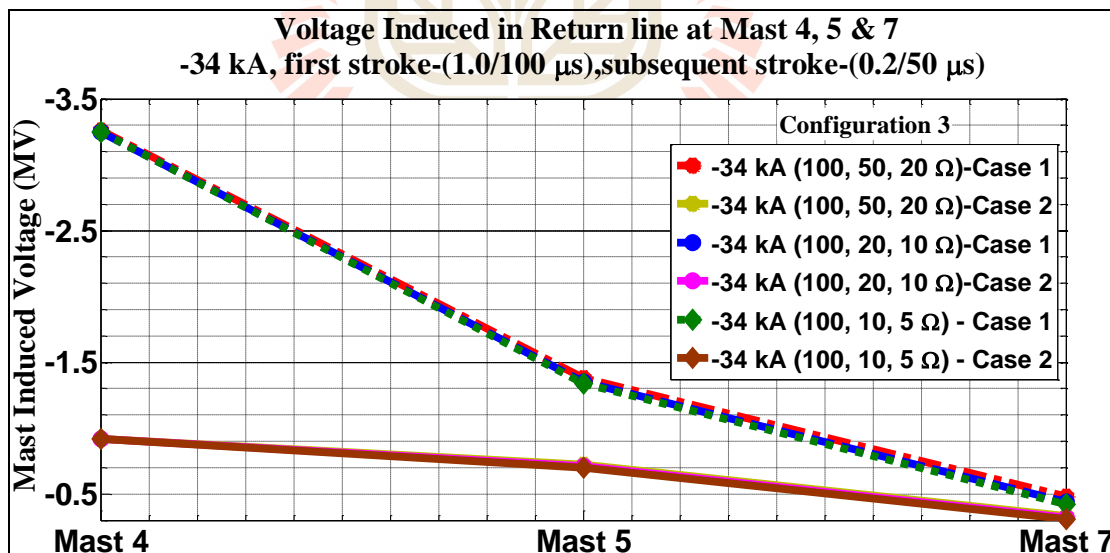


Figure 4.107 Return line induced voltages in both Cases with -34 kA, first stroke-(1.0/100  $\mu$ s), subsequent stroke-(0.2/50  $\mu$ s) for configuration 3

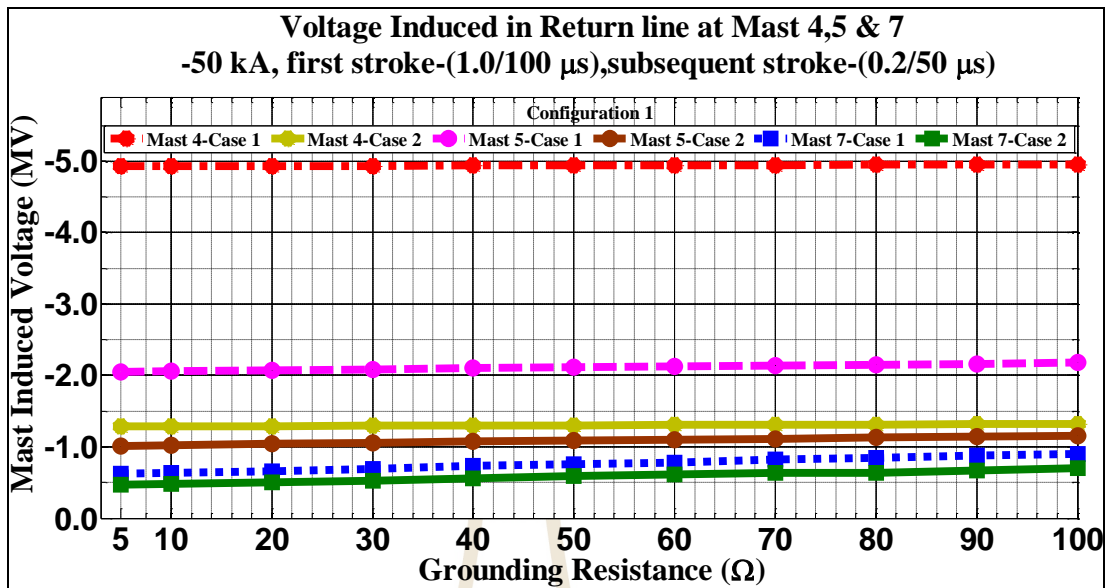


Figure 4.108 Return line induced voltages in both Cases with -50 kA, first stroke-(1.0/100  $\mu$ s), subsequent stroke-(0.2/50  $\mu$ s) for configuration 1

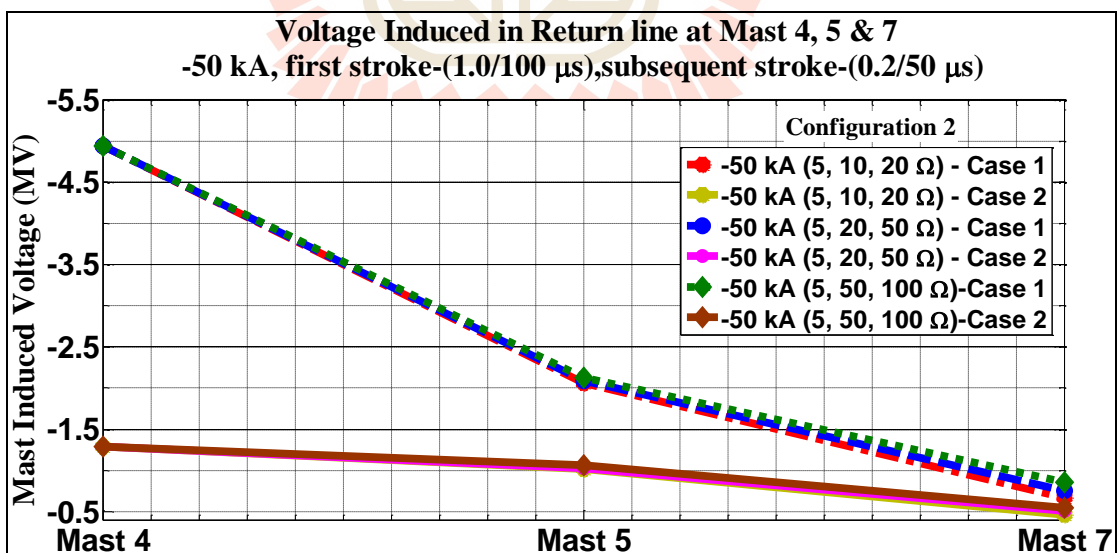
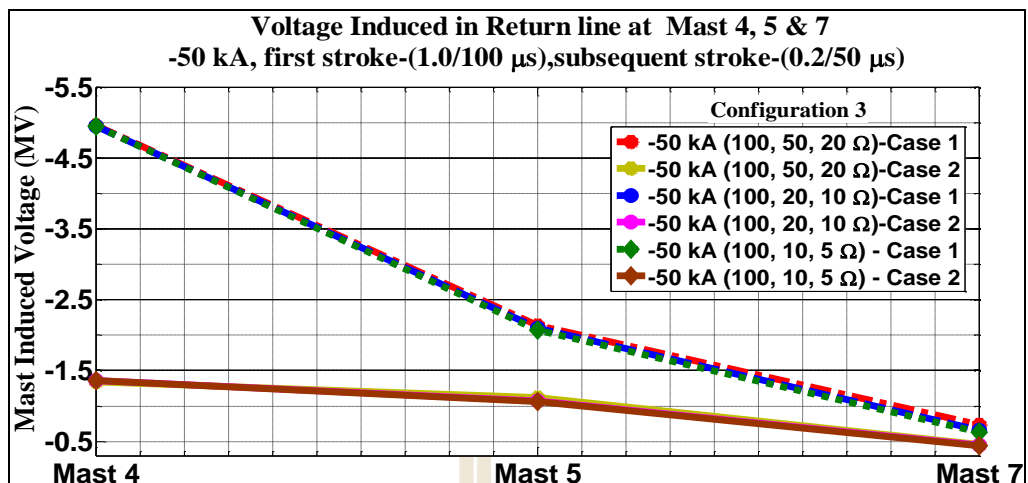
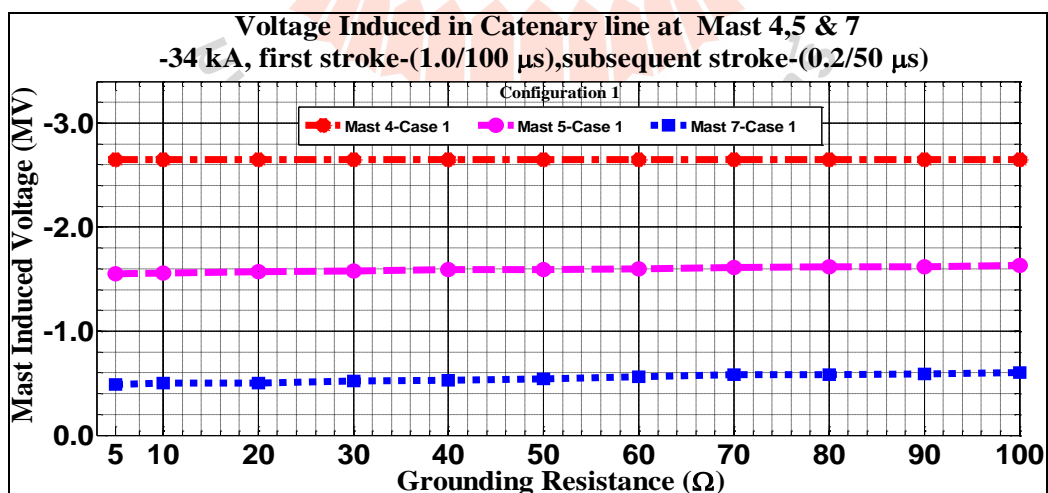


Figure 4.109 Return line induced voltages in both Cases with -50 kA, first stroke-(1.0/100  $\mu$ s), subsequent stroke-(0.2/50  $\mu$ s) for configuration 2



**Figure 4.110** Return line induced voltages in both Cases with -50 kA, first stroke- (1.0/100  $\mu$ s), subsequent stroke-(0.2/50  $\mu$ s) for configuration 3

The outcome of analyzed mast induced voltage across stressed insulators of the catenary line when multiple lightning strokes on catenary line for both cases with all configurations are shown in Figures. 4.111-4.128.



**Figure 4.111** Catenary line induced voltages in Case 1 with -34 kA, first stroke- (1.0/100  $\mu$ s), subsequent stroke-(0.2/50  $\mu$ s) for configuration 1

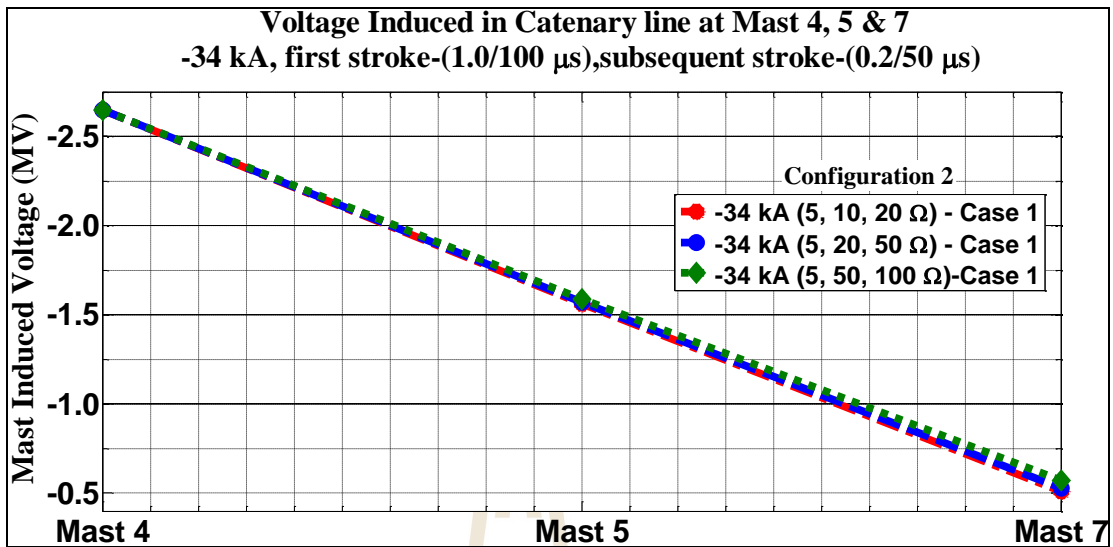


Figure 4.112 Catenary line induced voltages in Case 1 with -34 kA, first stroke-(1.0/100  $\mu$ s), subsequent stroke-(0.2/50  $\mu$ s) for configuration 2

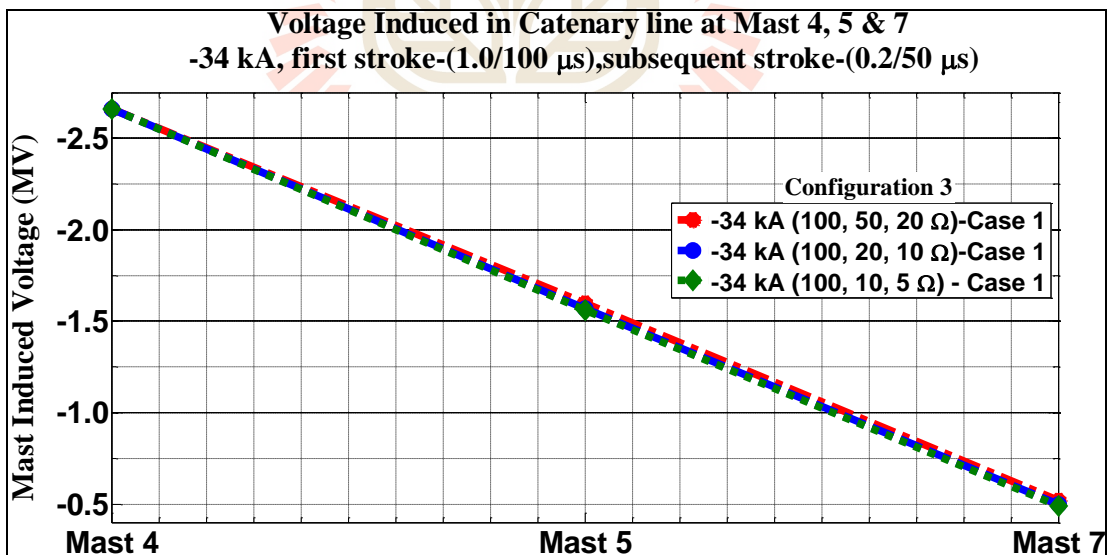
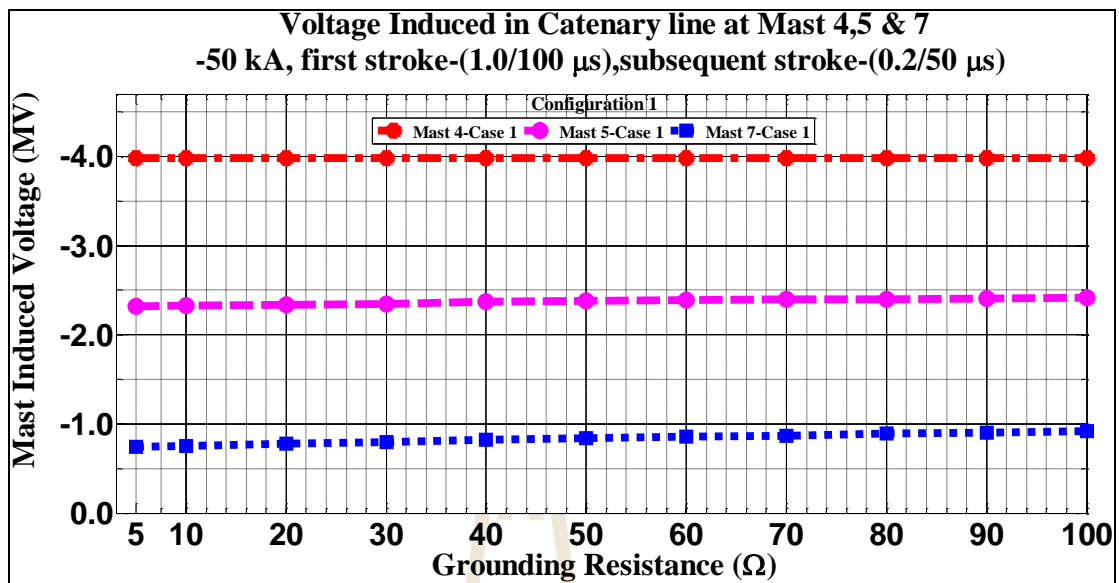
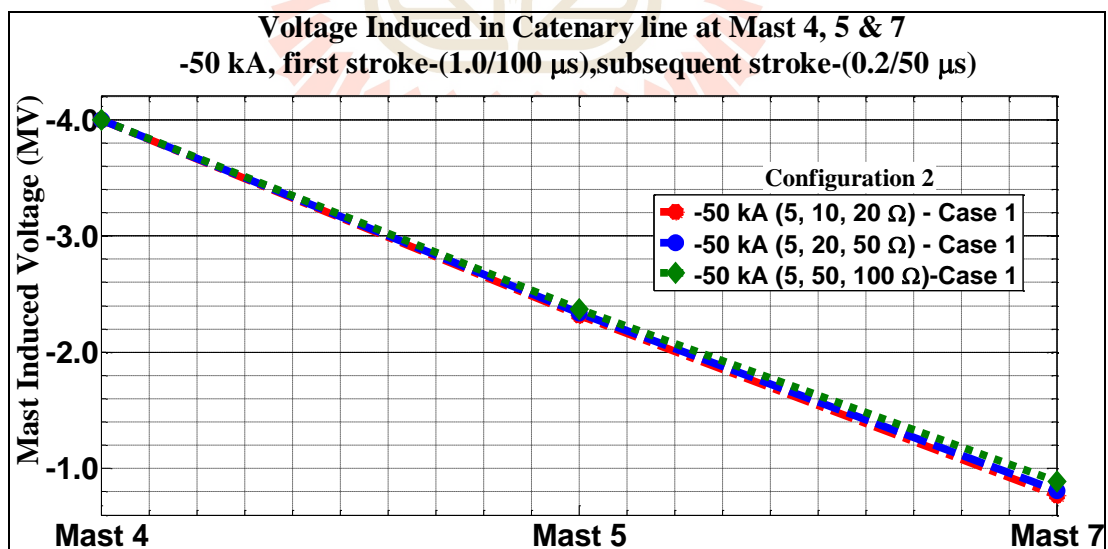


Figure 4.113 Catenary line induced voltages in Case 1 with -34 kA, first stroke-(1.0/100  $\mu$ s), subsequent stroke-(0.2/50  $\mu$ s) for configuration 3



**Figure 4.114** Catenary line induced voltages in Case 1 with -50 kA, first stroke-(1.0/100  $\mu$ s), subsequent stroke-(0.2/50  $\mu$ s) for configuration 1



**Figure 4.115** Catenary line induced voltages in Case 1 with -50 kA, first stroke-(1.0/100  $\mu$ s), subsequent stroke-(0.2/50  $\mu$ s) for configuration 2



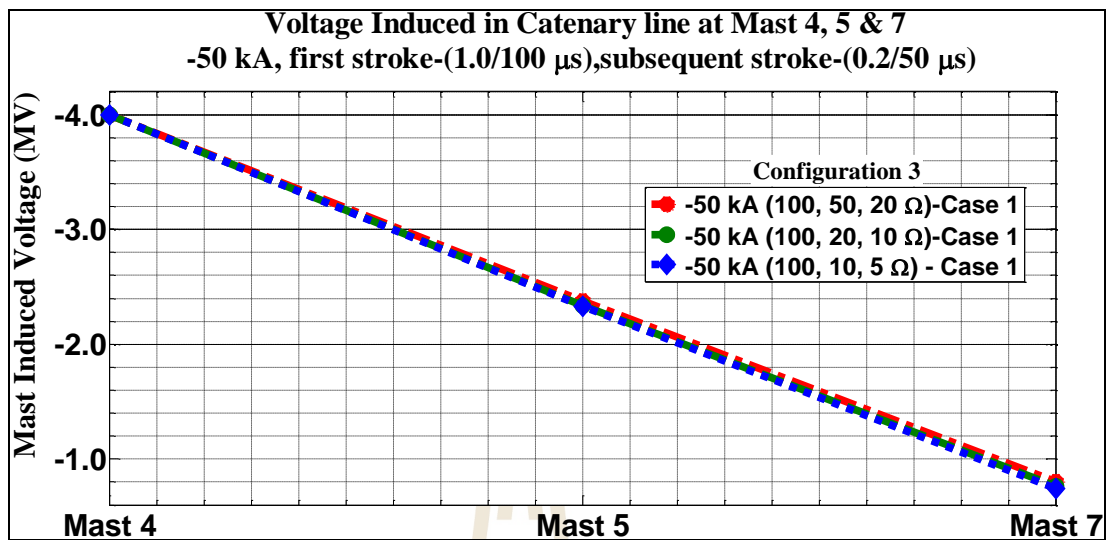


**Figure 4.116** Catenary line induced voltages in Case 1 with -50 kA, first stroke-(1.0/100  $\mu$ s), subsequent stroke-(0.2/50  $\mu$ s) for configuration 3

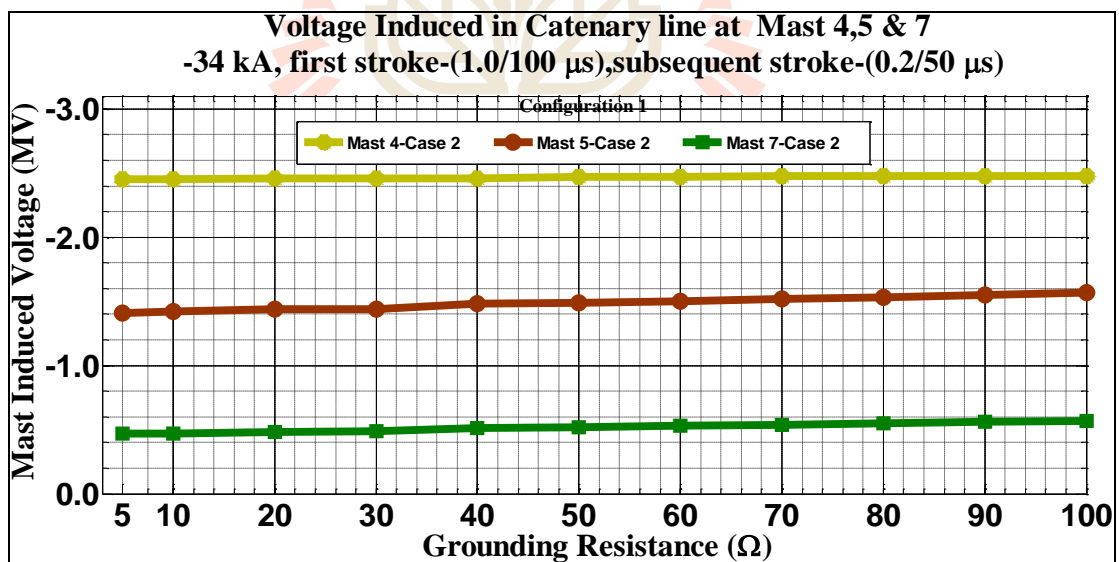


**Figure 4.117** Catenary line induced voltages in Case 2 with -34 kA, first stroke-(1.0/100  $\mu$ s), subsequent stroke-(0.2/50  $\mu$ s) for configuration 1

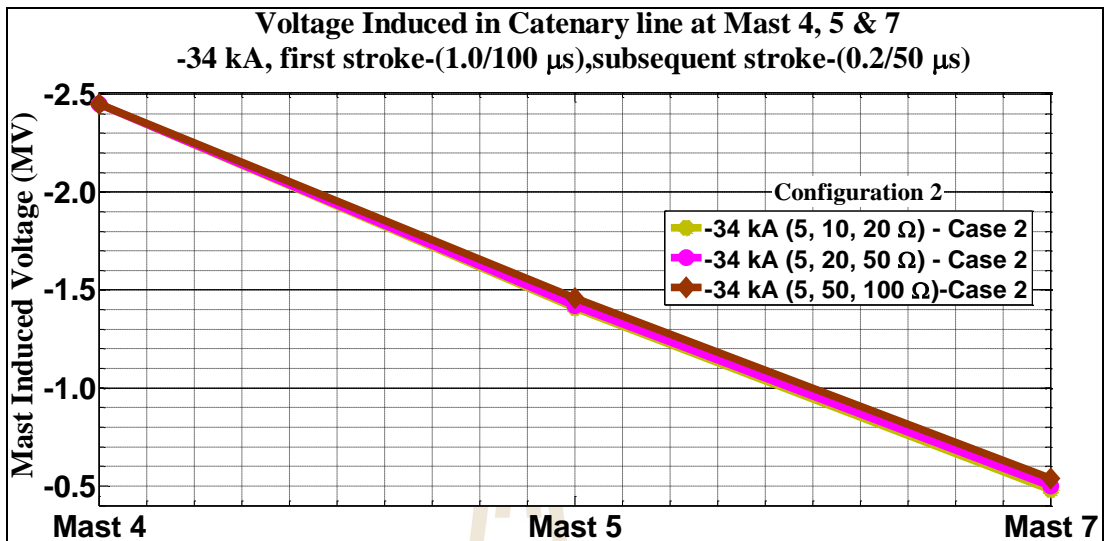


**Figure 4.118** Catenary line induced voltages in Case 2 with -34 kA, first stroke-(1.0/100  $\mu$ s), subsequent stroke-(0.2/50  $\mu$ s) for configuration 2

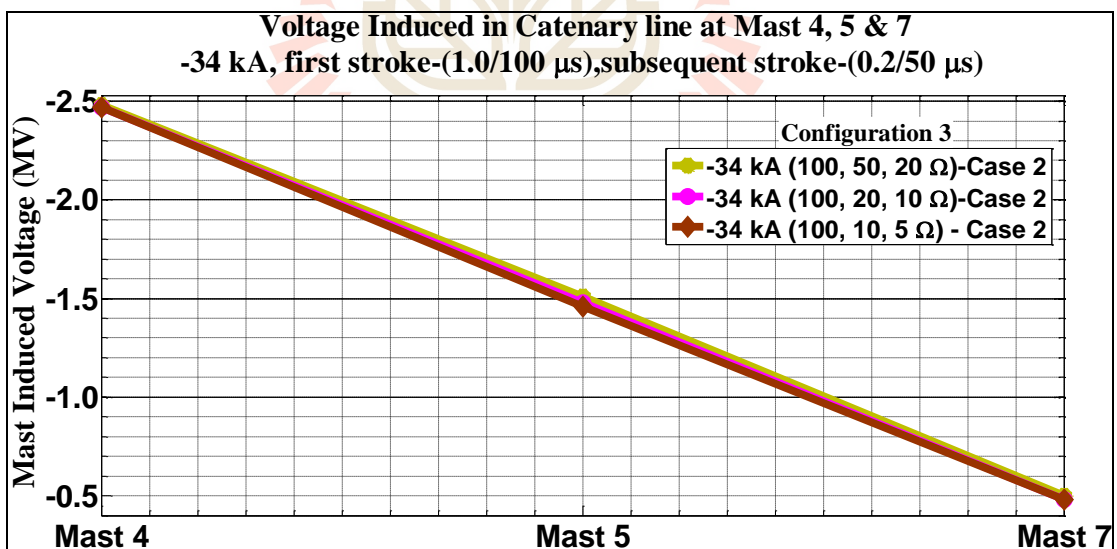


**Figure 4.119** Catenary line induced voltages in Case 2 with -34 kA, first stroke-(1.0/100  $\mu$ s), subsequent stroke-(0.2/50  $\mu$ s) for configuration 3

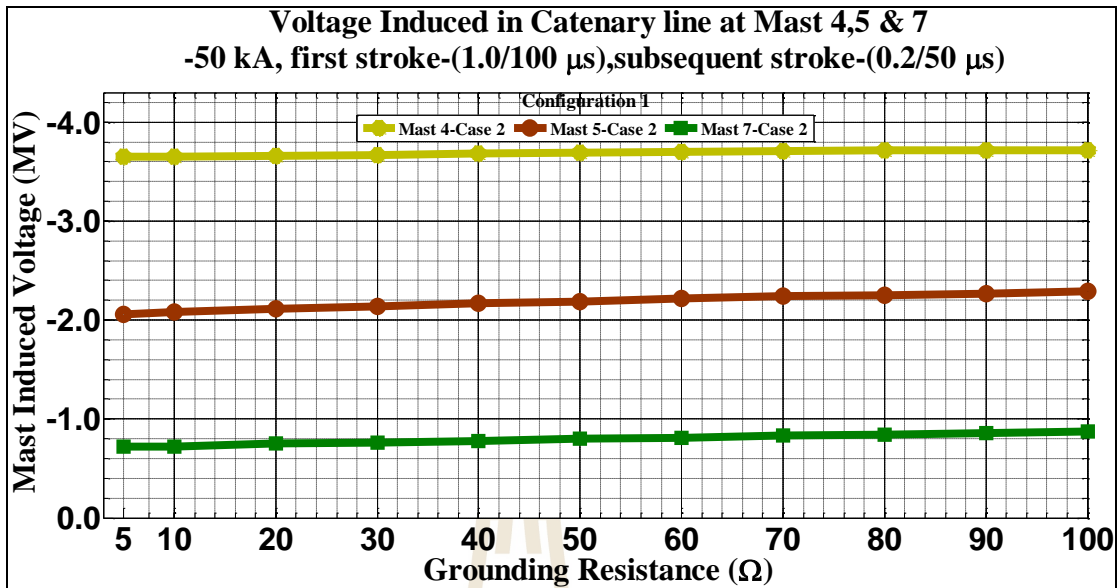


Figure 4.120 Catenary line induced voltages in Case 2 with -50 kA, first stroke- (1.0/100  $\mu$ s), subsequent stroke-(0.2/50  $\mu$ s) for configuration 1

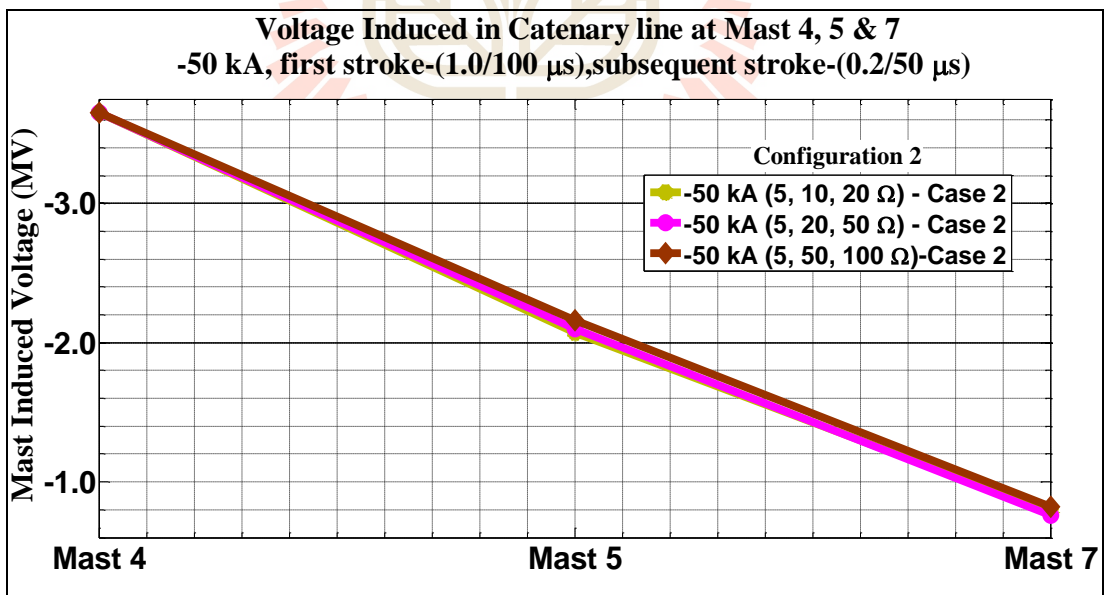


Figure 4.121 Catenary line induced voltages in Case 2 with -50 kA, first stroke- (1.0/100  $\mu$ s), subsequent stroke-(0.2/50  $\mu$ s) for configuration 2

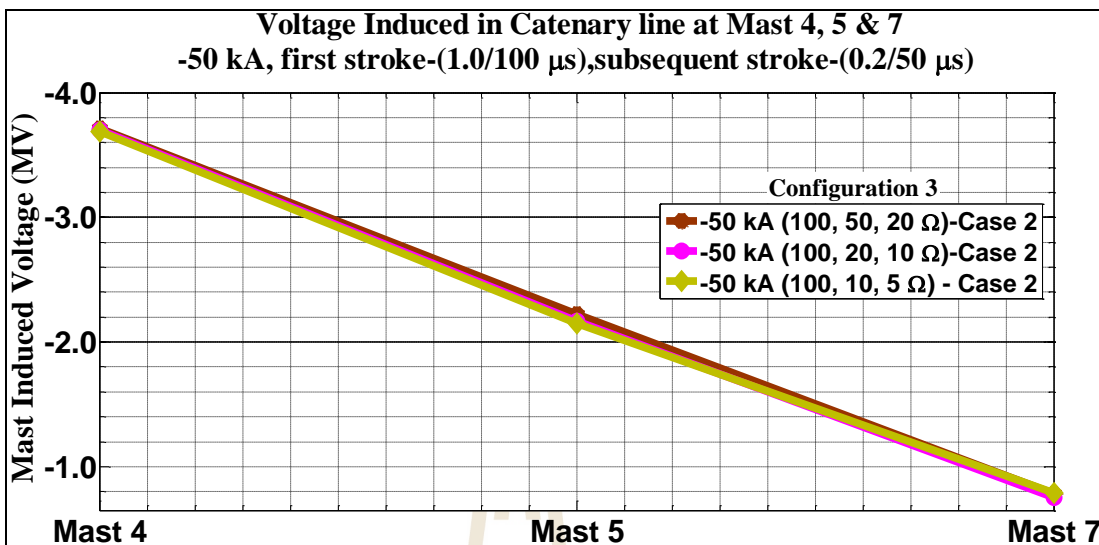


Figure 4.122 Catenary line induced voltages in Case 2 with -50 kA, first stroke-(1.0/100  $\mu$ s), subsequent stroke-(0.2/50  $\mu$ s) for configuration 3

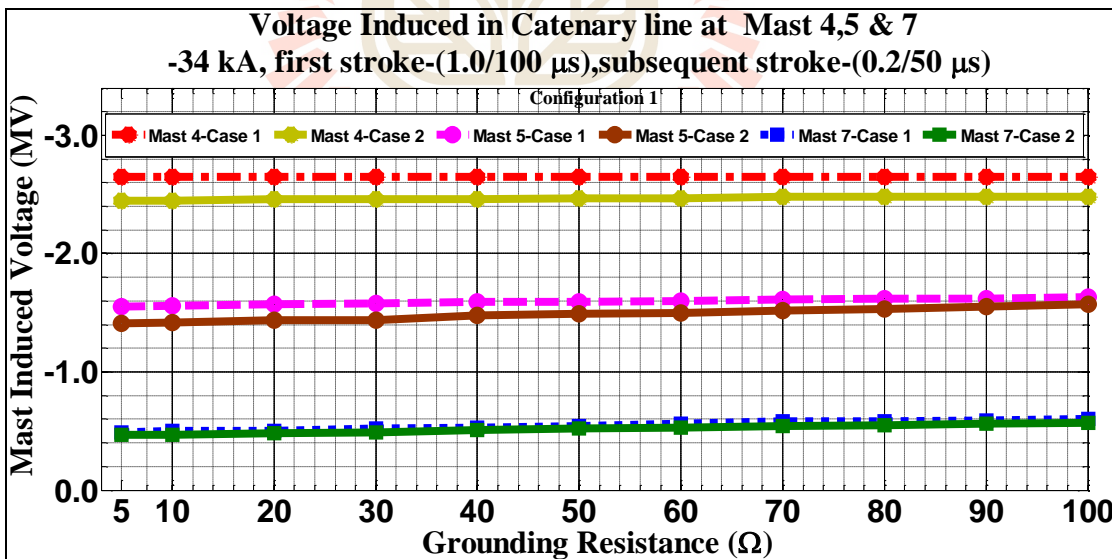
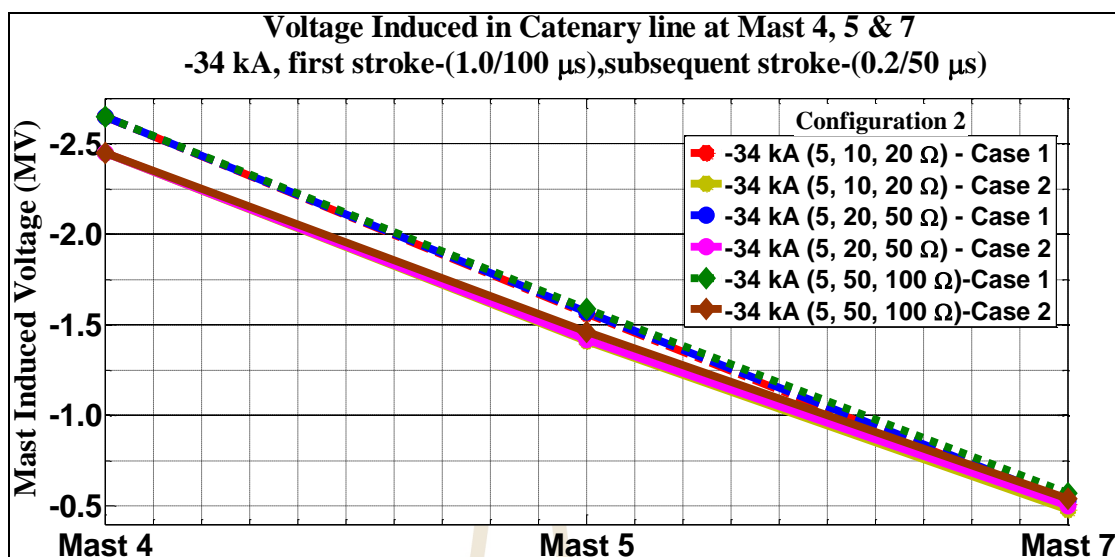
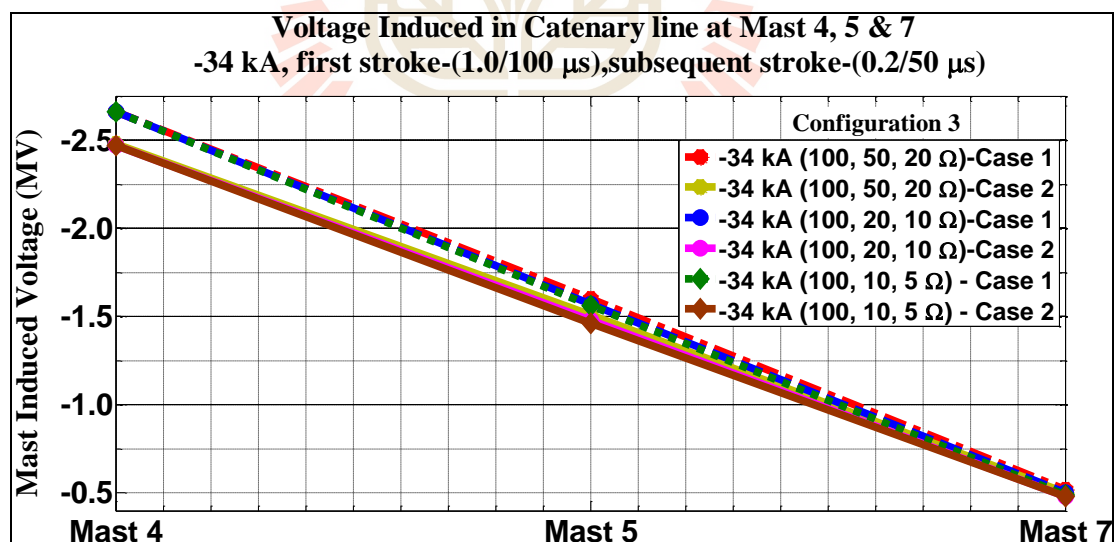


Figure 4.123 Catenary line induced voltages in both Cases with -34 kA, first stroke-(1.0/100  $\mu$ s), subsequent stroke-(0.2/50  $\mu$ s) for configuration 1



**Figure 4.124** Catenary line induced voltages in both Cases with -34 kA, first stroke-(1.0/100  $\mu$ s), subsequent stroke-(0.2/50  $\mu$ s) for configuration 2



**Figure 4.125** Catenary line induced voltages in both Cases with -34 kA, first stroke-(1.0/100  $\mu$ s), subsequent stroke-(0.2/50  $\mu$ s) for configuration 3

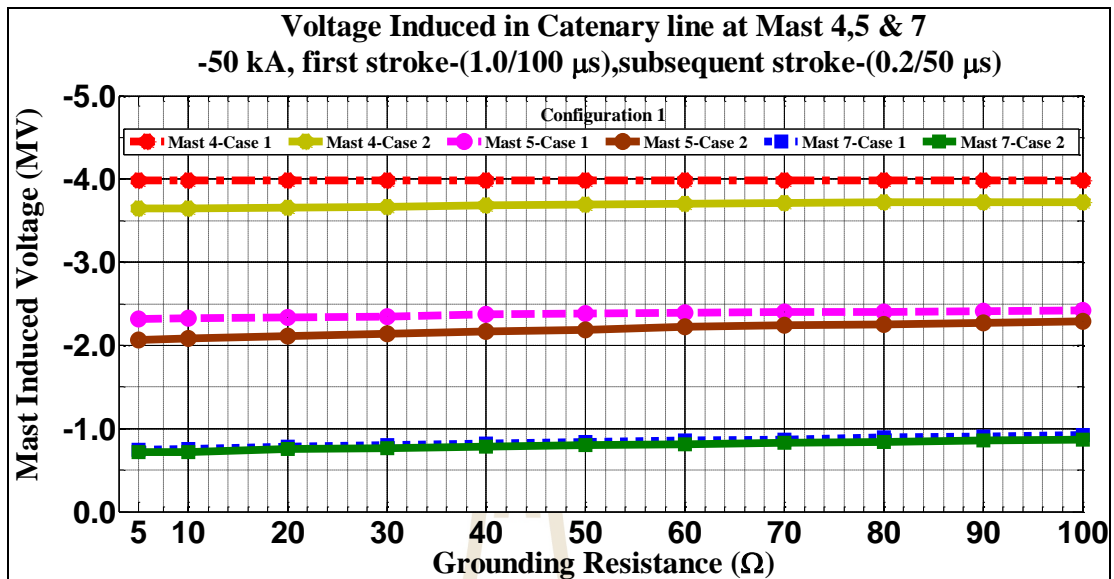


Figure 4.126 Catenary line induced voltages in both Cases with -50 kA, first stroke- (1.0/100 μs), subsequent stroke-(0.2/50 μs) for configuration 1

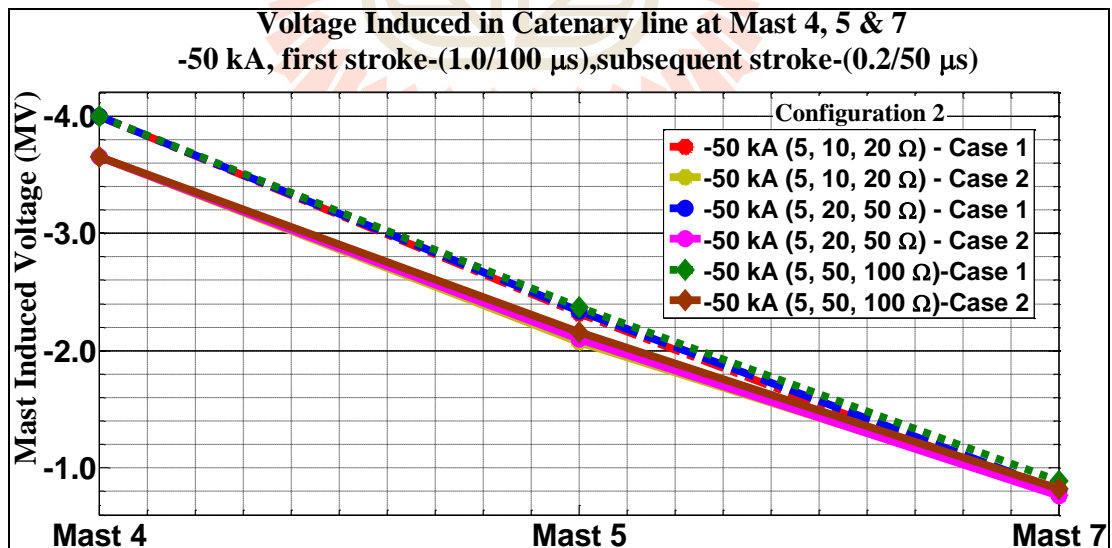
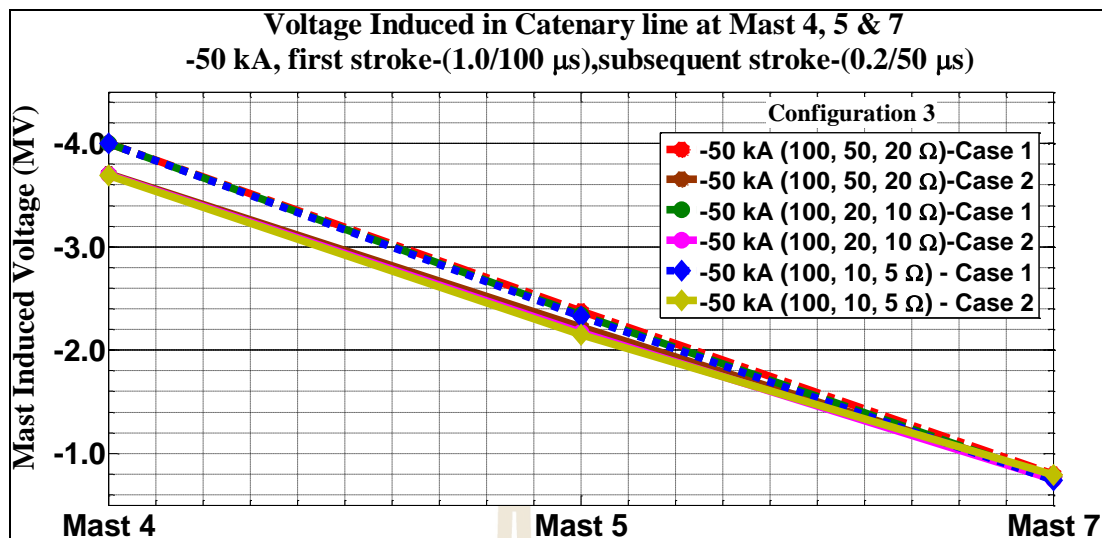


Figure 4.127 Catenary line induced voltages in both Cases with -50 kA, first stroke- (1.0/100 μs), subsequent stroke-(0.2/50 μs) for configuration 2



**Figure 4.128** Catenary line induced voltages in both Cases with -50 kA, first stroke-(1.0/100  $\mu$ s), subsequent stroke-(0.2/50  $\mu$ s) for configuration 3

Due to attentive outcome during multiple lightning strokes on pantograph, the values in Tables 4.3-4.20 were obtained after being analyzed the data from the Figures in APPENDIX C. The 1<sup>st</sup> row details configuration, the cases and stroked points. The 2<sup>nd</sup> row shows the position of the affected mast. 3<sup>rd</sup> row illustrate the type of waveforms. The 4<sup>th</sup> row starts from the 2<sup>nd</sup> column gives the magnitude of lightning strokes that have been used. The 1<sup>st</sup> column starts from the 5<sup>th</sup> row shows the ground resistances that have been exploited. The 2<sup>nd</sup> to the 4<sup>th</sup> column and the 5<sup>th</sup> to the 7<sup>th</sup> column start from the 6<sup>th</sup> row indicate the magnitude of mast induced voltages in different lines of an overhead catenary system for 34 kA and 50 kA respectively. For configuration 2 and 3, respective rows for each table at a time represent the arrangement of grounding resistance as shown in simulation setup in Tables 4.1-4.2.

**Table 4.3** Mast 4 induced voltages in Case 1 with multiple lightning strokes on the train's pantograph for configuration 1

Configuration 1 - Case 1 (Pantograph)						
Mast 4						
First stroke-(1.0/100 $\mu$ s), Subsequent stroke-(0.2/50 $\mu$ s)						
Rf	- 34 kA			- 50 kA		
( $\Omega$ )	Auxiliary	Return	Catenary	Auxiliary	Return	Catenary
5	1.53	2.30	2.70	2.30	3.44	4.05
10	1.53	2.30	2.70	2.30	3.44	4.06
20	1.53	2.30	2.70	2.30	3.44	4.06
30	1.53	2.30	2.70	2.30	3.44	4.06
40	1.53	2.30	2.70	2.30	3.44	4.06
50	1.53	2.30	2.70	2.30	3.44	4.06
60	1.53	2.30	2.70	2.30	3.44	4.06
70	1.53	2.30	2.70	2.30	3.44	4.06
80	1.53	2.30	2.70	2.30	3.44	4.06
90	1.53	2.30	2.70	2.30	3.44	4.06
100	1.53	2.30	2.70	2.30	3.44	4.06

**Table 4.4** Mast 5 induced voltages in Case 1 with multiple lightning strokes on the train's pantograph for configuration 1

Configuration 1 - Case 1 (Pantograph)						
Mast 5						
First stroke-(1.0/100 $\mu$ s), Subsequent stroke-(0.2/50 $\mu$ s)						
Rf	- 34 kA			- 50 kA		
( $\Omega$ )	Auxiliary	Return	Catenary	Auxiliary	Return	Catenary
5	1.25	1.52	1.56	1.88	2.27	2.35
10	1.25	1.52	1.57	1.89	2.28	2.36
20	1.27	1.53	1.58	1.91	2.30	2.38
30	1.27	1.54	1.60	1.92	2.32	2.39
40	1.28	1.55	1.60	1.93	2.33	2.41
50	1.29	1.56	1.61	1.94	2.34	2.42
60	1.30	1.57	1.62	1.95	2.35	2.43
70	1.30	1.58	1.63	1.96	2.36	2.44
80	1.31	1.59	1.63	1.97	2.37	2.46
90	1.31	1.59	1.64	1.98	2.38	2.48
100	1.32	1.60	1.65	1.98	2.39	2.50



**Table 4.5** Mast 7 induced voltages in Case 1 with multiple lightning strokes on the train's pantograph for configuration 1

Configuration 1 - Case 1 (Pantograph)						
Mast 7						
First stroke-(1.0/100 $\mu$ s), Subsequent stroke-(0.2/50 $\mu$ s)						
Rf	- 34 kA			- 50 kA		
( $\Omega$ )	Auxiliary	Return	Catenary	Auxiliary	Return	Catenary
5	0.42	0.49	0.49	0.73	0.74	0.75
10	0.50	0.50	0.50	0.74	0.75	0.76
20	0.53	0.50	0.51	0.76	0.78	0.79
30	0.54	0.52	0.52	0.79	0.80	0.81
40	0.56	0.53	0.54	0.81	0.82	0.83
50	0.57	0.55	0.55	0.83	0.84	0.85
60	0.58	0.56	0.56	0.85	0.86	0.87
70	0.59	0.57	0.57	0.86	0.88	0.89
80	0.60	0.58	0.58	0.88	0.90	0.91
90	0.61	0.59	0.59	0.89	0.92	0.93
100	0.62	0.60	0.60	0.91	0.94	0.94

**Table 4.6** Mast 4 induced voltages in Case 2 with multiple lightning strokes on the train's pantograph for configuration 1

Configuration 1 - Case 2 (Pantograph)						
Mast 4						
First stroke-(1.0/100 $\mu$ s), Subsequent stroke-(0.2/50 $\mu$ s)						
Rf	- 34 kA			- 50 kA		
( $\Omega$ )	Auxiliary	Return	Catenary	Auxiliary	Return	Catenary
5	1.55	2.26	2.41	2.33	3.40	3.62
10	1.56	2.26	2.41	2.34	3.41	3.62
20	1.57	2.27	2.42	2.36	3.42	3.64
30	1.58	2.28	2.43	2.37	3.43	3.65
40	1.59	2.28	2.43	2.37	3.44	3.66
50	1.59	2.29	2.44	2.40	3.45	3.67
60	1.60	2.30	2.44	2.40	3.45	3.67
70	1.61	2.30	2.45	2.42	3.46	3.68
80	1.61	2.30	2.46	2.44	2.46	3.68
90	1.62	2.30	2.46	2.44	2.48	3.69
100	1.63	2.31	2.50	2.44	3.47	3.70

**Table 4.7** Mast 5 induced voltages in Case 2 with multiple lightning strokes on the train's pantograph for configuration 1

Configuration 1 - Case 2 (Pantograph)						
Mast 5						
First stroke-(1.0/100 $\mu$ s), Subsequent stroke-(0.2/50 $\mu$ s)						
Rf	- 34 kA			- 50 kA		
( $\Omega$ )	Auxiliary	Return	Catenary	Auxiliary	Return	Catenary
5	1.19	1.34	1.36	1.80	2.00	2.03
10	1.20	1.35	1.37	1.81	2.02	2.05
20	1.21	1.37	1.39	1.83	2.05	2.08
30	1.22	1.38	1.41	1.85	2.08	2.11
40	1.24	1.40	1.43	1.87	2.10	2.14
50	1.25	1.42	1.45	1.88	2.13	2.16
60	1.26	1.43	1.46	1.90	2.15	2.19
70	1.27	1.45	1.47	1.91	2.17	2.21
80	1.28	1.46	1.50	1.93	2.20	2.24
90	1.30	1.48	1.51	1.94	2.21	2.25
100	1.30	1.49	1.52	1.95	2.22	2.26

**Table 4.8** Mast 7 induced voltages in Case 2 with multiple lightning strokes on the train's pantograph for configuration 1

Configuration 1 - Case 2 (Pantograph)						
Mast 7						
First stroke-(1.0/100 $\mu$ s), Subsequent stroke-(0.2/50 $\mu$ s)						
Rf	- 34 kA			- 50 kA		
( $\Omega$ )	Auxiliary	Return	Catenary	Auxiliary	Return	Catenary
5	0.51	0.46	0.45	0.76	0.71	0.71
10	0.51	0.46	0.46	0.77	0.72	0.72
20	0.52	0.48	0.47	0.78	0.73	0.73
30	0.53	0.48	0.49	0.80	0.75	0.75
40	0.54	0.50	0.49	0.81	0.77	0.77
50	0.55	0.51	0.50	0.82	0.79	0.79
60	0.56	0.52	0.51	0.83	0.80	0.80
70	0.56	0.53	0.52	0.85	0.82	0.82
80	0.57	0.54	0.53	0.86	0.84	0.84
90	0.58	0.54	0.55	0.87	0.85	0.85
100	0.59	0.56	0.55	0.88	0.86	0.86

**Table 4.9** Mast 4 induced voltages in Case 1 with multiple lightning strokes on the train's pantograph for configuration 1

Configuration 2 - Case 1 (Pantograph)						
Mast 4						
First stroke-(1.0/100 $\mu$ s), Subsequent stroke-(0.2/50 $\mu$ s)						
Rf	- 34 kA			- 50 kA		
( $\Omega$ )	Auxiliary	Return	Catenary	Auxiliary	Return	Catenary
5	1.53	2.30	2.7	2.33	3.53	4.16
5	1.53	2.29	2.71	2.33	3.53	4.2
5	1.53	2.30	2.72	2.30	3.42	4.21

**Table 4.10** Mast 5 induced voltages in Case 1 with multiple lightning strokes on the train's pantograph for configuration 2

Configuration 2 - Case 1 (Pantograph)						
Mast 5						
First stroke-(1.0/100 $\mu$ s), Subsequent stroke-(0.2/50 $\mu$ s)						
Rf	- 34 kA			- 50 kA		
( $\Omega$ )	Auxiliary	Return	Catenary	Auxiliary	Return	Catenary
10	1.25	1.52	1.60	1.97	2.38	2.46
20	1.26	1.53	1.61	1.98	2.4	2.5
50	1.29	1.56	1.62	1.95	2.33	2.51

**Table 4.11** Mast 7 induced voltages in Case 1 with multiple lightning strokes on the train's pantograph for configuration 2

Configuration 2 - Case 1 (Pantograph)						
Mast 7						
First stroke-(1.0/100 $\mu$ s), Subsequent stroke-(0.2/50 $\mu$ s)						
Rf	- 34 kA			- 50 kA		
( $\Omega$ )	Auxiliary	Return	Catenary	Auxiliary	Return	Catenary
20	0.52	0.50	0.50	0.78	0.79	0.8
50	0.55	0.53	0.53	0.83	0.84	0.85
100	0.60	0.58	0.58	0.88	0.90	0.91

**Table 4.12** Mast 4 induced voltages in Case 1 with multiple lightning strokes on the train's pantograph for configuration 3

Configuration 3 - Case 1 (Pantograph)						
Mast 4						
First stroke-(1.0/100 $\mu$ s), Subsequent stroke-(0.2/50 $\mu$ s)						
Rf	- 34 kA			- 50 kA		
( $\Omega$ )	Auxiliary	Return	Catenary	Auxiliary	Return	Catenary
100	1.53	2.30	2.70	2.30	3.44	4.06
100	1.53	2.3	2.71	2.30	3.45	4.07
100	1.53	2.30	2.71	2.30	3.46	4.07

**Table 4.13** Mast 5 induced voltages in Case 1 with multiple lightning strokes on the train's pantograph for configuration 3

Configuration 3 - Case 1 (Pantograph)						
Mast 5						
First stroke-(1.0/100 $\mu$ s), Subsequent stroke-(0.2/50 $\mu$ s)						
Rf	- 34 kA			- 50 kA		
( $\Omega$ )	Auxiliary	Return	Catenary	Auxiliary	Return	Catenary
50	1.29	1.56	1.61	1.95	2.34	2.42
20	1.27	1.54	1.6	1.91	2.30	2.38
10	1.26	1.52	1.58	1.90	2.29	2.36

**Table 4.14** Mast 7 induced voltages in Case 1 with multiple lightning strokes on the train's pantograph for configuration 3

Configuration 3 - Case 1 (Pantograph)						
Mast 7						
First stroke-(1.0/100 $\mu$ s), Subsequent stroke-(0.2/50 $\mu$ s)						
Rf	- 34 kA			- 50 kA		
( $\Omega$ )	Auxiliary	Return	Catenary	Auxiliary	Return	Catenary
20	0.54	0.52	0.52	0.79	0.80	0.81
10	0.52	0.49	0.49	0.75	0.76	0.77
5	0.50	0.49	0.49	0.73	0.74	0.75

**Table 4.15** Mast 4 induced voltages in Case 2 with multiple lightning strokes on the train's pantograph for configuration 2

Configuration 2 - Case 2 (Pantograph)						
Mast 4						
First stroke-(1.0/100 $\mu$ s), Subsequent stroke-(0.2/50 $\mu$ s)						
Rf	- 34 kA			- 50 kA		
( $\Omega$ )	Auxiliary	Return	Catenary	Auxiliary	Return	Catenary
5	1.55	2.26	2.41	2.33	3.40	3.62
5	1.55	2.26	2.42	2.33	3.40	3.63
5	1.56	2.26	2.43	2.34	3.41	3.64

**Table 4.16** Mast 5 induced voltages in Case 2 with multiple lightning strokes on the train's pantograph for configuration 2

Configuration 2 - Case 2 (Pantograph)						
Mast 5						
First stroke-(1.0/100 $\mu$ s), Subsequent stroke-(0.2/50 $\mu$ s)						
Rf	- 34 kA			- 50 kA		
( $\Omega$ )	Auxiliary	Return	Catenary	Auxiliary	Return	Catenary
10	1.19	1.34	1.36	1.80	2.01	2.04
20	1.20	1.35	1.38	1.82	2.03	2.07
50	1.22	1.39	1.42	1.84	2.08	2.12

**Table 4.17** Mast 7 induced voltages in Case 2 with multiple lightning strokes on the train's pantograph for configuration 2

Configuration 2 - Case 2 (Pantograph)						
Mast 7						
First stroke-(1.0/100 $\mu$ s), Subsequent stroke-(0.2/50 $\mu$ s)						
Rf	- 34 kA			- 50 kA		
( $\Omega$ )	Auxiliary	Return	Catenary	Auxiliary	Return	Catenary
20	0.51	0.48	0.46	0.77	0.72	0.72
50	0.53	0.49	0.48	0.80	0.75	0.75
100	0.55	0.52	0.52	0.83	0.81	0.81

**Table 4.18** Mast 4 induced voltages in Case 2 with multiple lightning strokes on the train's pantograph for configuration 3

Configuration 3 - Case 2 (Pantograph)						
Mast 4						
First stroke-(1.0/100 $\mu$ s), Subsequent stroke-(0.2/50 $\mu$ s)						
Rf	- 34 kA			- 50 kA		
( $\Omega$ )	Auxiliary	Return	Catenary	Auxiliary	Return	Catenary
100	1.63	2.30	2.45	2.43	3.46	3.68
100	1.62	2.30	2.44	2.43	3.45	3.67
100	1.61	2.3	2.43	2.42	3.44	3.66

**Table 4.19** Mast 5 induced voltages in Case 2 with multiple lightning strokes on the train's pantograph for configuration 3

Configuration 3 - Case 2 (Pantograph)						
Mast 5						
First stroke-(1.0/100 $\mu$ s), Subsequent stroke-(0.2/50 $\mu$ s)						
Rf	- 34 kA			- 50 kA		
( $\Omega$ )	Auxiliary	Return	Catenary	Auxiliary	Return	Catenary
50	1.27	1.44	1.47	1.91	2.16	2.20
20	1.24	1.41	1.43	1.88	2.11	2.15
10	1.24	1.39	1.41	1.86	2.09	2.12

**Table 4.20** Mast 7 induced voltages in Case 2 with multiple lightning strokes on the train's pantograph for configuration 3

Configuration 3 - Case 2 (Pantograph)						
Mast 7						
First stroke-(1.0/100 $\mu$ s), Subsequent stroke-(0.2/50 $\mu$ s)						
Rf	- 34 kA			- 50 kA		
( $\Omega$ )	Auxiliary	Return	Catenary	Auxiliary	Return	Catenary
20	0.55	0.50	0.49	0.82	0.77	0.77
10	0.53	0.48	0.47	0.79	0.74	0.74
5	0.52	0.46	0.46	0.78	0.72	0.72

In Figures. 4.129-4.146, the outcome of analyzed mast induced voltage across stressed insulators of the catenary line when multiple lightning strokes on pantograph for both cases with all configurations are shown.

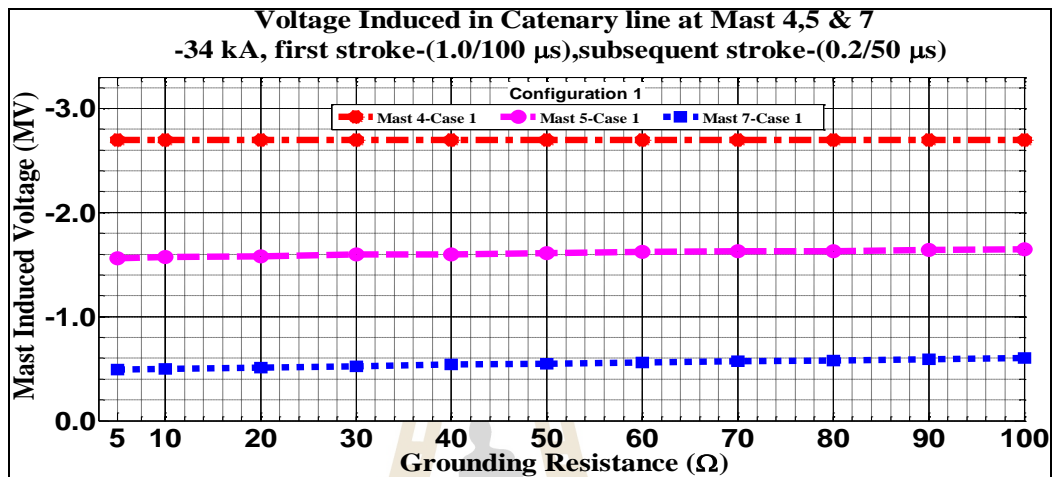


Figure 4.129 Catenary line induced voltages in Case 1 with -34 kA, first stroke-(1.0/100  $\mu$ s), subsequent stroke-(0.2/50  $\mu$ s) for configuration 1

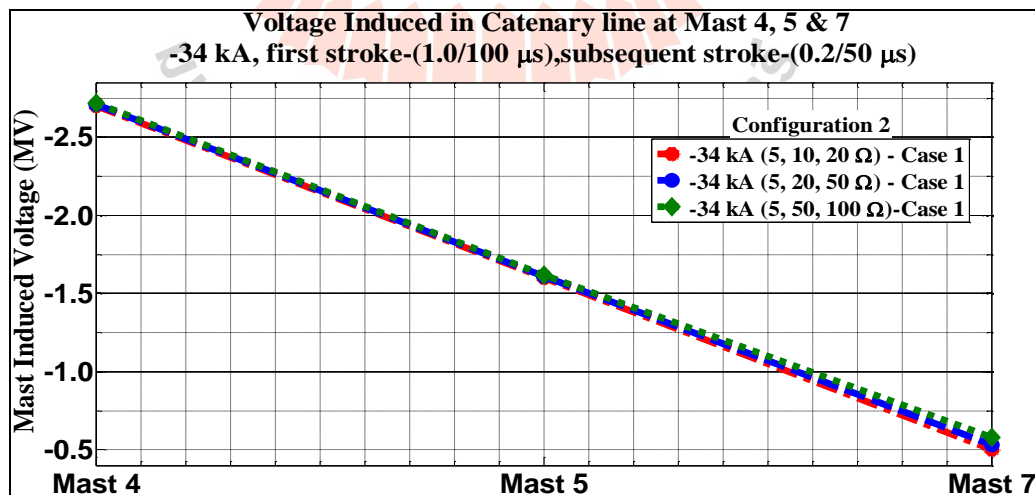
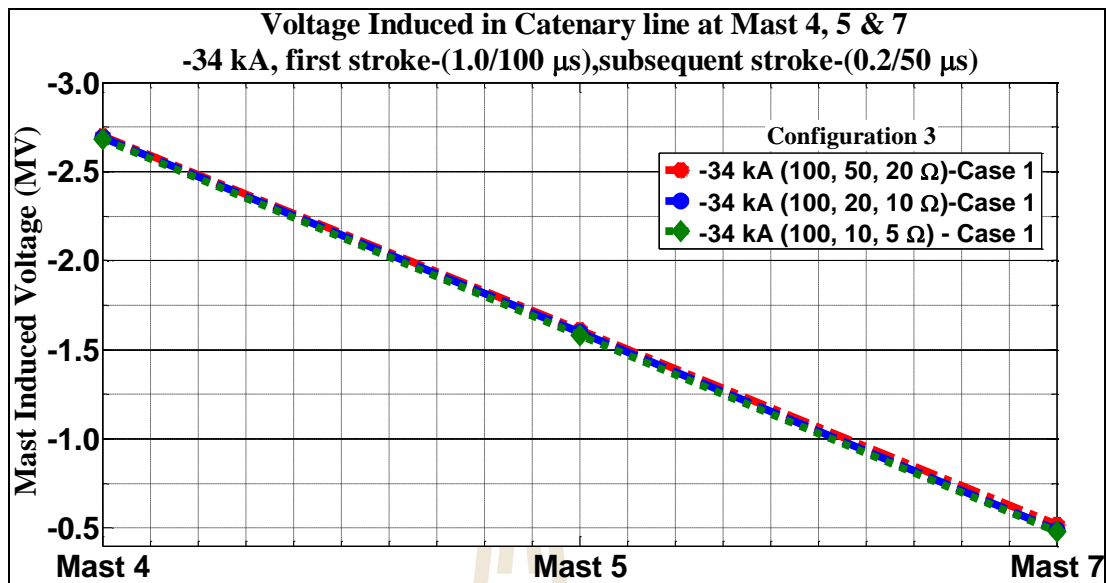
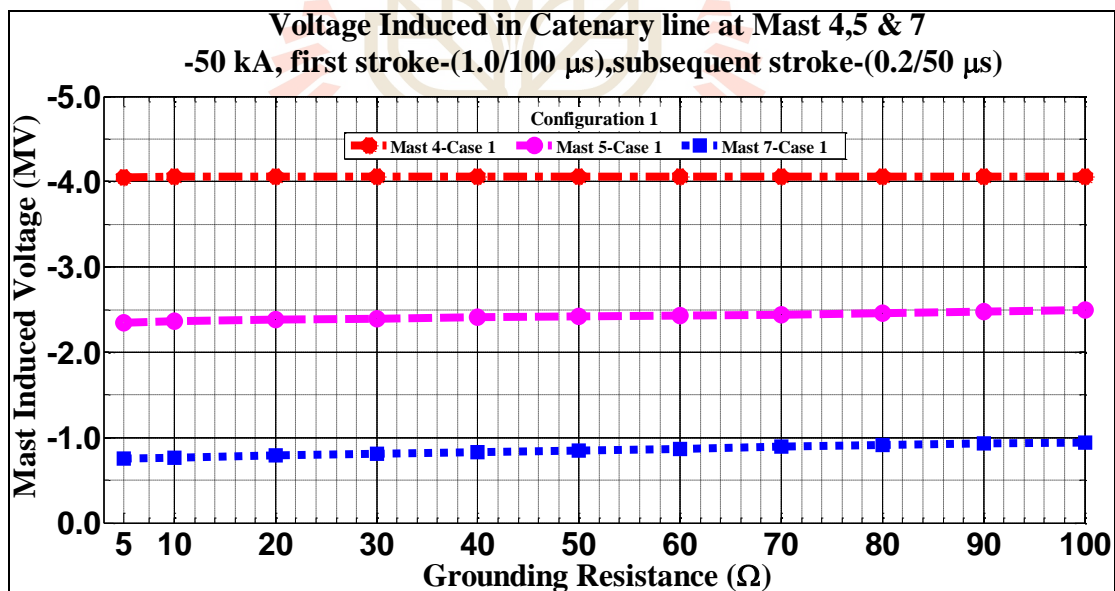


Figure 4.130 Catenary line induced voltages in Case 1 with -34 kA, first stroke-(1.0/100  $\mu$ s), subsequent stroke-(0.2/50  $\mu$ s) for configuration 2



**Figure 4.131** Catenary line induced voltages in Case 1 with -34 kA, first stroke-(1.0/100  $\mu$ s), subsequent stroke-(0.2/50  $\mu$ s) for configuration 3



**Figure 4.132** Catenary line induced voltages in Case 1 with -50 kA, first stroke-(1.0/100  $\mu$ s), subsequent stroke-(0.2/50  $\mu$ s) for configuration 1



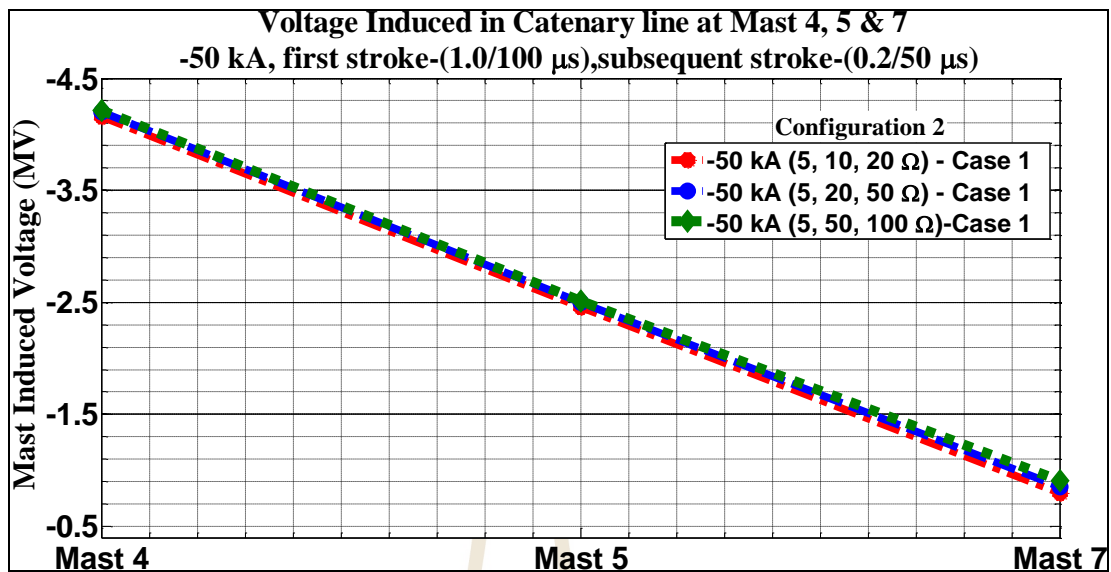


**Figure 4.133** Catenary line induced voltages in Case 1 with -50 kA, first stroke-(1.0/100  $\mu$ s), subsequent stroke-(0.2/50  $\mu$ s) for configuration 2

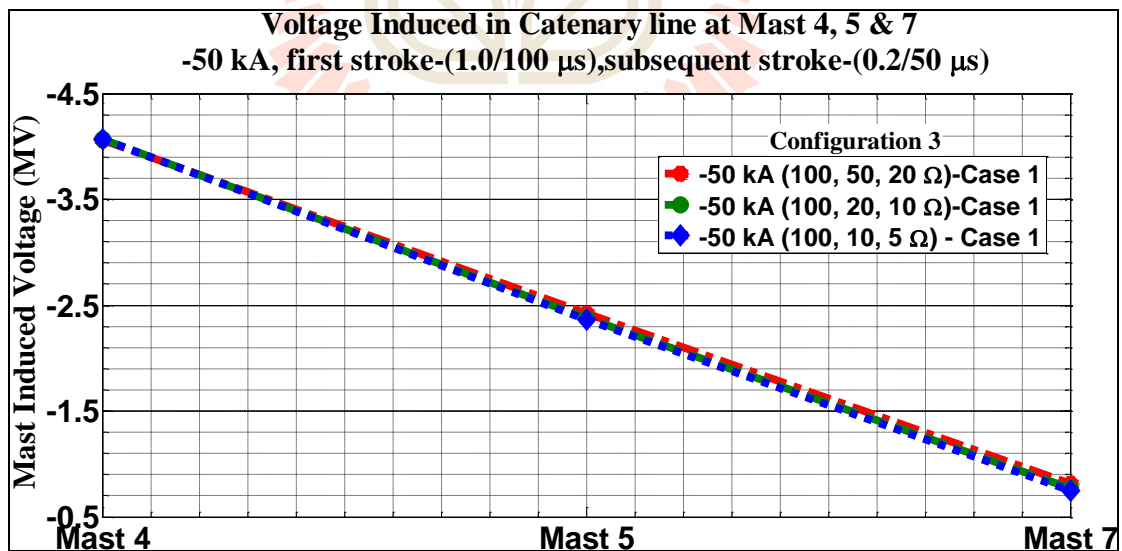


**Figure 4.134** Catenary line induced voltages in Case 1 with -50 kA, first stroke-(1.0/100  $\mu$ s), subsequent stroke-(0.2/50  $\mu$ s) for configuration 3

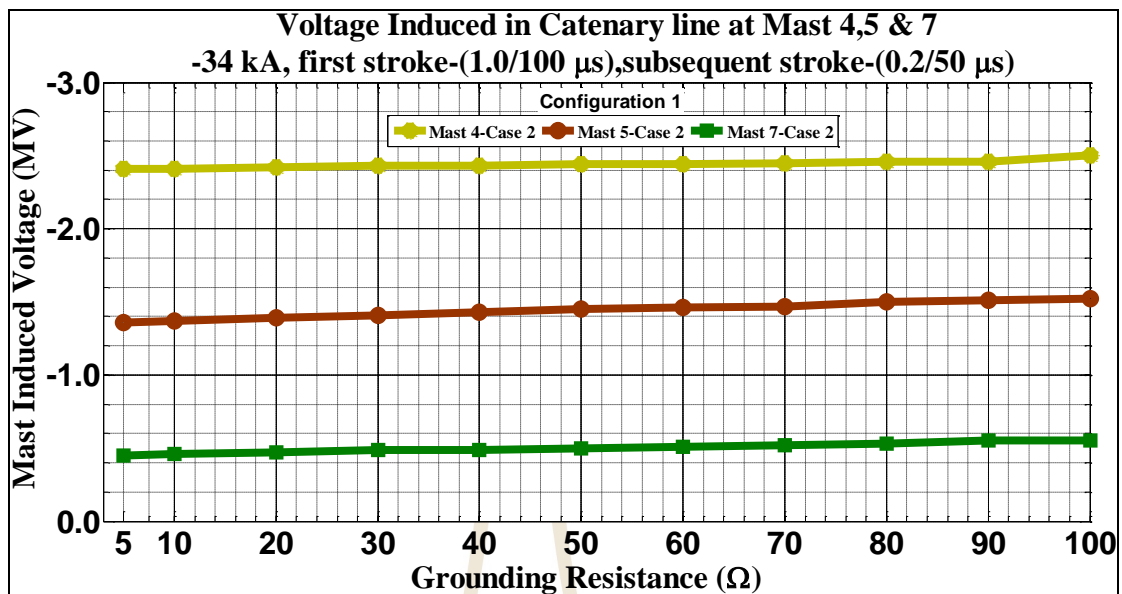


Figure 4.135 Catenary line induced voltages in Case 2 with -34 kA, first stroke-(1.0/100  $\mu$ s), subsequent stroke-(0.2/50  $\mu$ s) for configuration 1

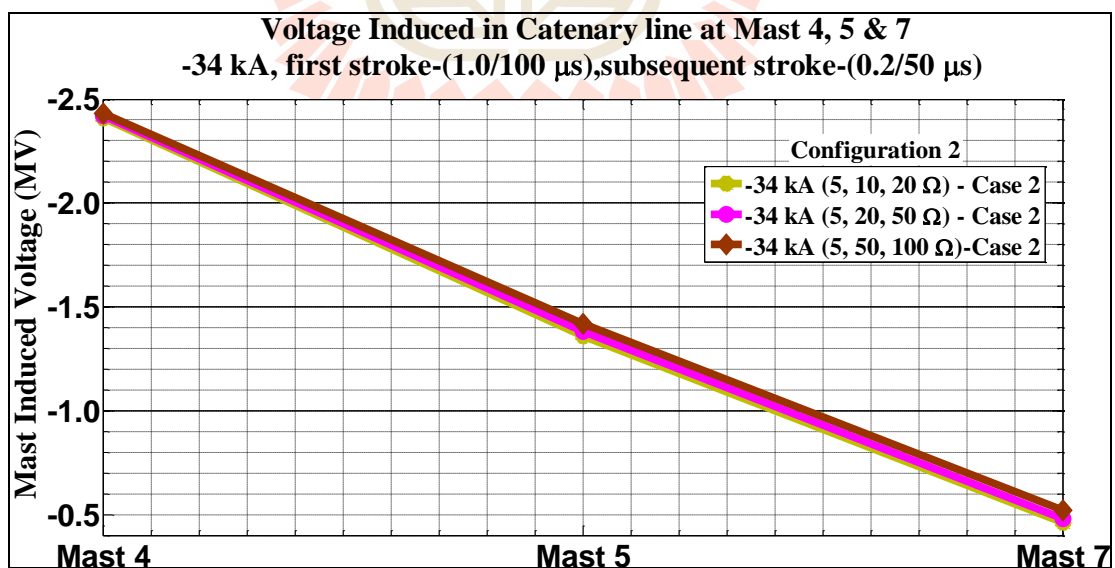


Figure 4.136 Catenary line induced voltages in Case 2 with -34 kA, first stroke-(1.0/100  $\mu$ s), subsequent stroke-(0.2/50  $\mu$ s) for configuration 2

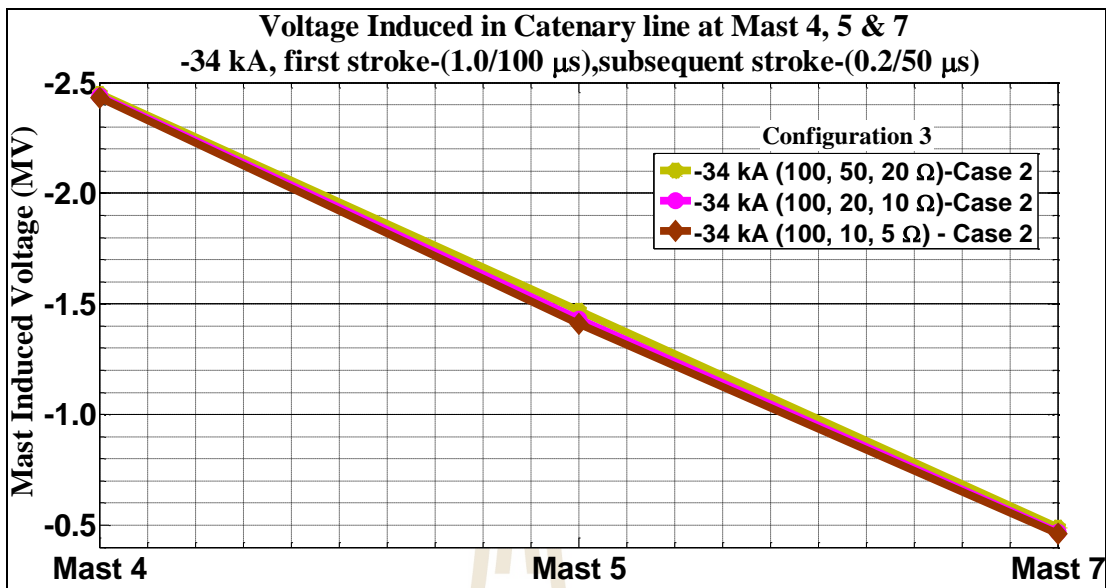


Figure 4.137 Catenary line induced voltages in Case 2 with -34 kA, first stroke-(1.0/100  $\mu$ s), subsequent stroke-(0.2/50  $\mu$ s) for configuration 3

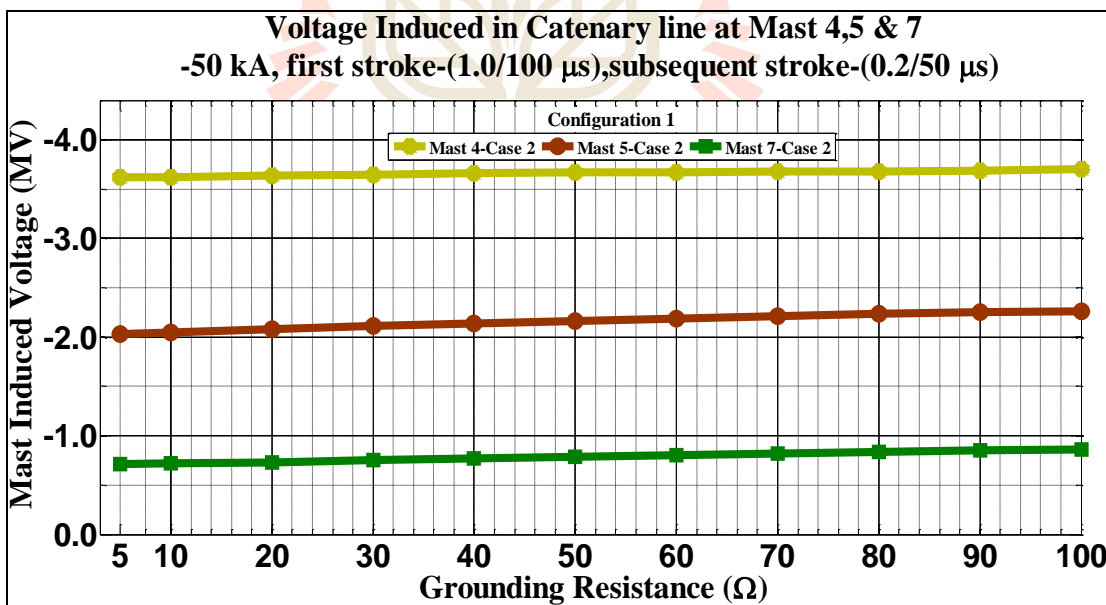
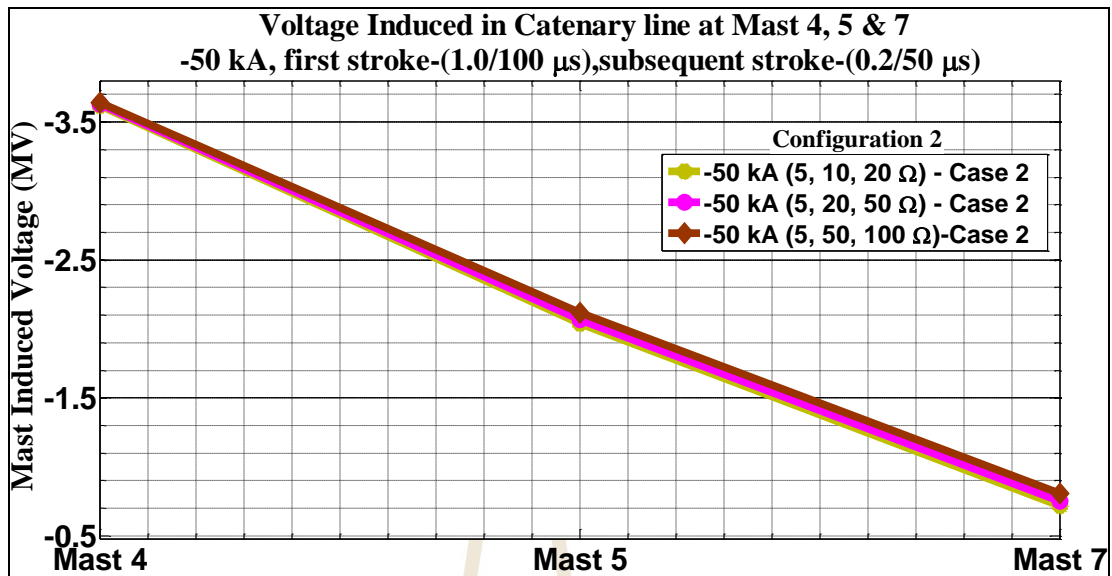
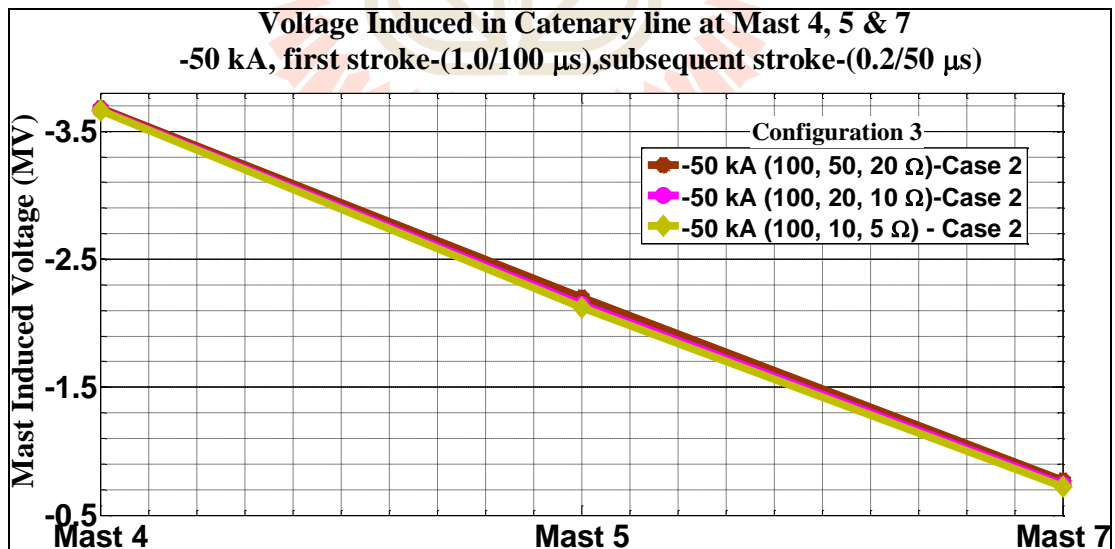


Figure 4.138 Catenary line induced voltages in Case 2 with -50 kA, first stroke-(1.0/100  $\mu$ s), subsequent stroke-(0.2/50  $\mu$ s) for configuration 1



**Figure 4.139** Catenary line induced voltages in Case 2 with -50 kA, first stroke-(1.0/100  $\mu$ s), subsequent stroke-(0.2/50  $\mu$ s) for configuration 2



**Figure 4.140** Catenary line induced voltages in Case 2 with -50 kA, first stroke-(1.0/100  $\mu$ s), subsequent stroke-(0.2/50  $\mu$ s) for configuration 3

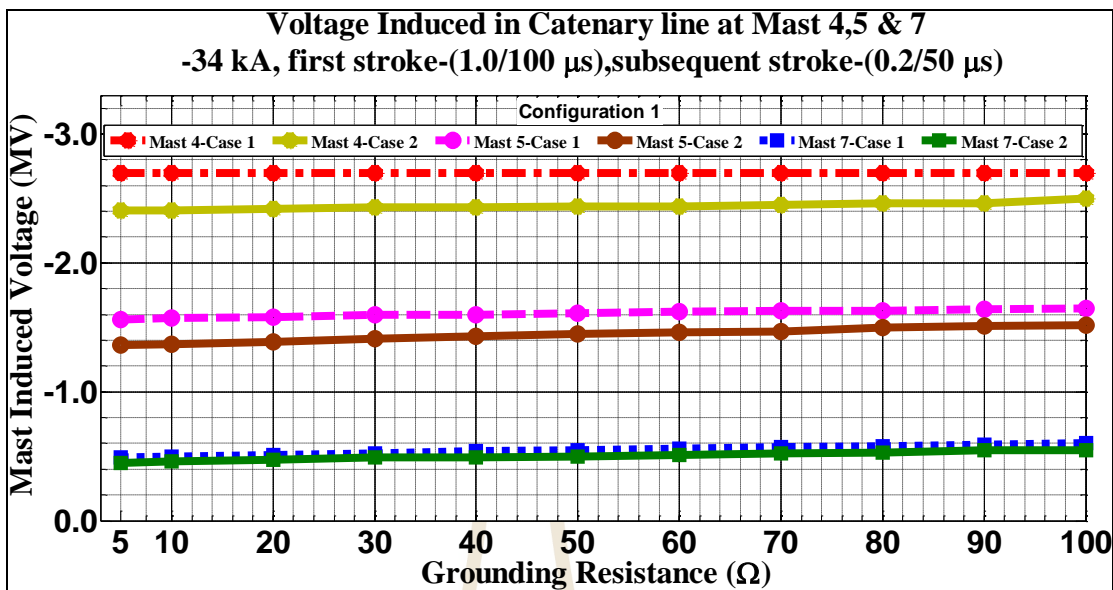


Figure 4.141 Catenary line induced voltages in both Cases with -34 kA, first stroke-(1.0/100 μs), subsequent stroke-(0.2/50 μs) for configuration 1

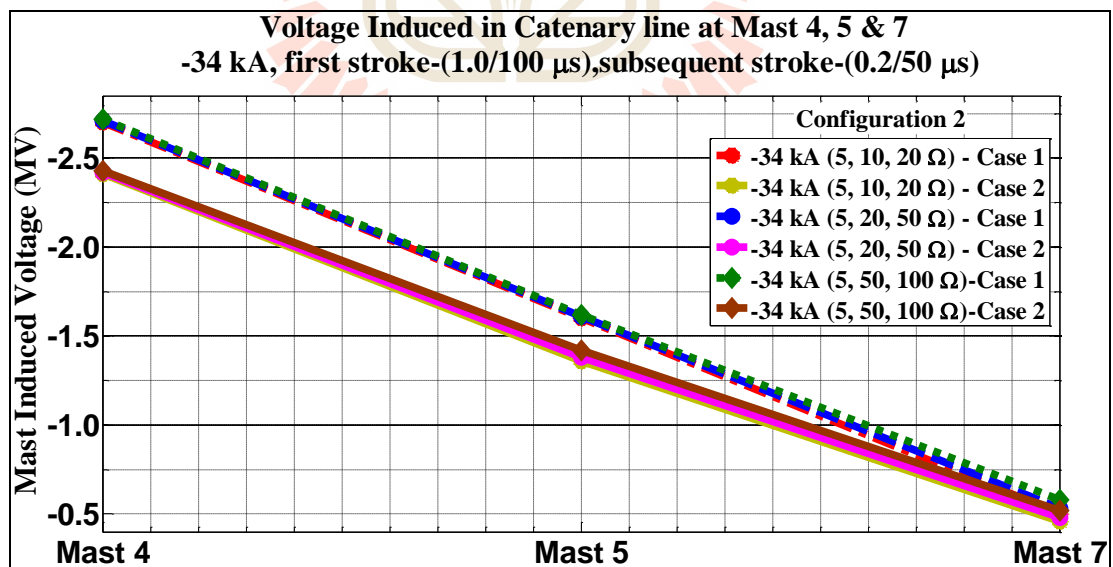
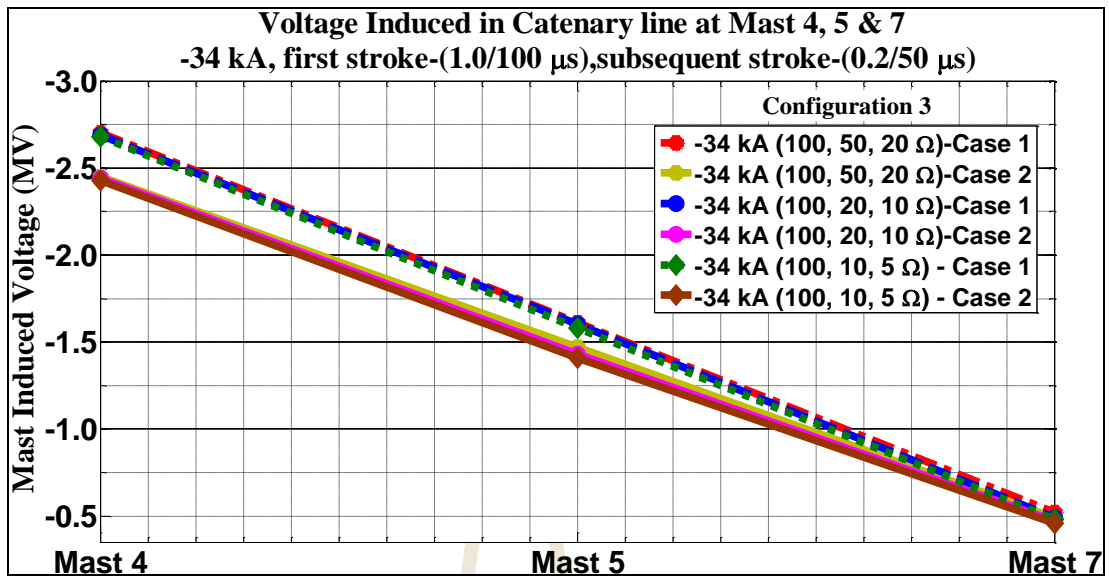
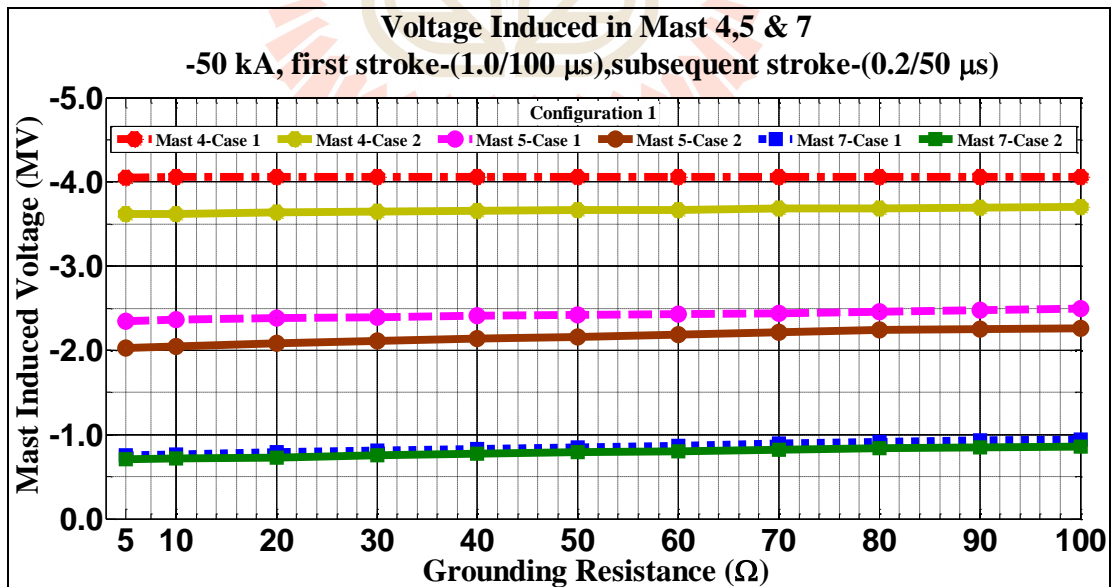


Figure 4.142 Catenary line induced voltages in both Cases with -34 kA, first stroke-(1.0/100 μs), subsequent stroke-(0.2/50 μs) for configuration 2



**Figure 4.143** Catenary line induced voltages in both Cases with -34 kA, first stroke-(1.0/100  $\mu$ s), subsequent stroke-(0.2/50  $\mu$ s) for configuration 3



**Figure 4.144** Catenary line induced voltages in both Cases with -50 kA, first stroke-(1.0/100  $\mu$ s), subsequent stroke-(0.2/50  $\mu$ s) for configuration 1

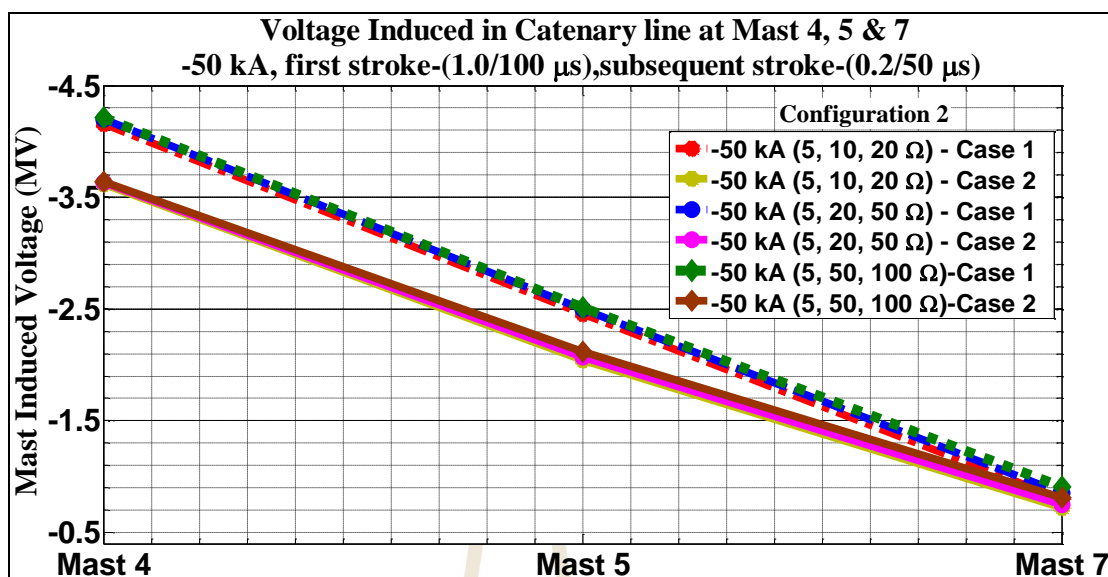


**Figure 4.145** Catenary line induced voltages in both Cases with -50 kA, first stroke-(1.0/100  $\mu$ s), subsequent stroke-(0.2/50  $\mu$ s) for configuration 2

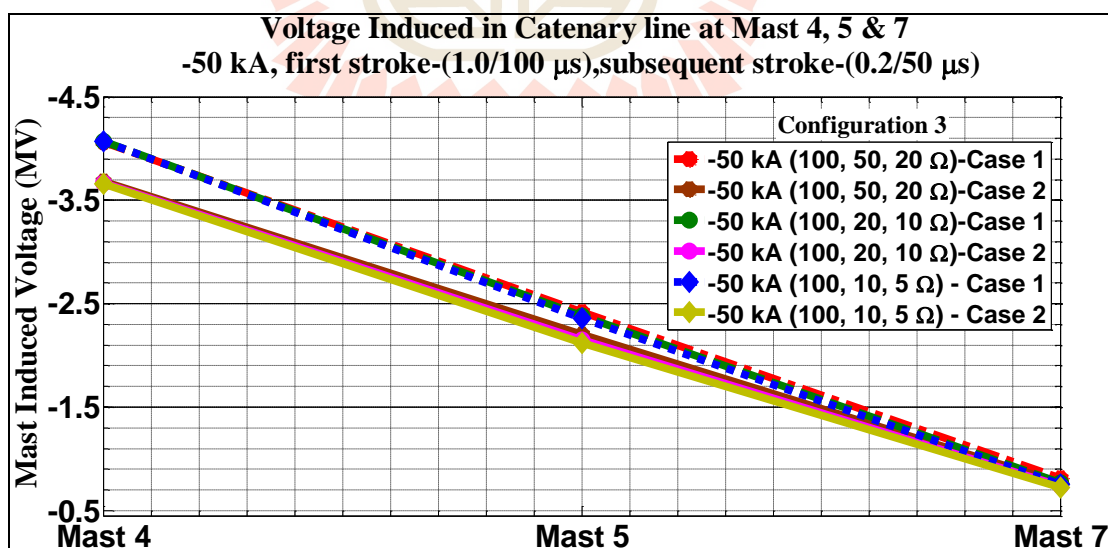


**Figure 4.146** Catenary line induced voltages in both Cases with -50 kA, first stroke-(1.0/100  $\mu$ s), subsequent stroke-(0.2/50  $\mu$ s) for configuration 3

### 4.3 Mitigation of flashover from multiple lightning strokes in overhead catenary system

In mitigating overvoltage in AC Railway System, the effective protection against lightning must be used. Surge arrester has been recently used as an effective protection against lightning voltage surges (Kiessling, et al., 2009; Nafar, Solookinejad, and Jabbari 2014; Durbak 1985; Saengsuwan, and Thipprasert, 2008; Mungkung, et al., 2007; Imece, et al., 1996; Pešič, and Grmovšek, 2007). Regardless of its importance in reducing lightning overvoltage, installed surge arrester in all masts seem to have better performance although this solution is costly (Shariatinasab, Vahidi, and Hosseinian 2009). Therefore, installation of Surge arrester at intervals in every mast needs to study in order to improve economic conditions of the power network. The negative multiple lightning strokes was considered to be a strike on a pantograph at the Mast (seventh Mast) for Case 1 as shown in Figure 4.147 and at the mid-span of Masts (sixth and seventh Masts) for Case 2 as shown in Figure 4.148 after being investigated in analysis of direct lightning strokes and seen to be more critical than other conditions. The six surge arrester's installation intervals are shown in Table 4.21.

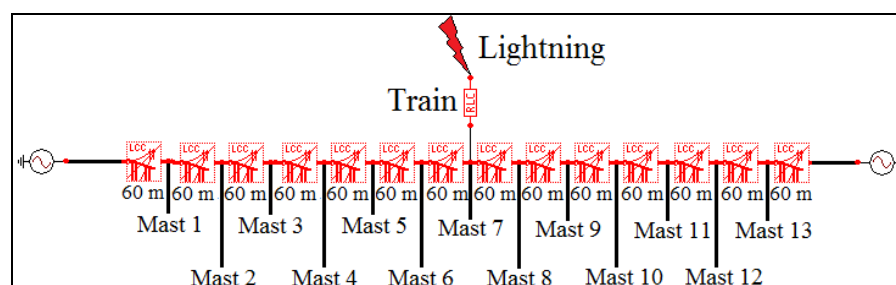


**Figure 4.147** Arrangement of the masts with lightning source for mitigation (case 1)



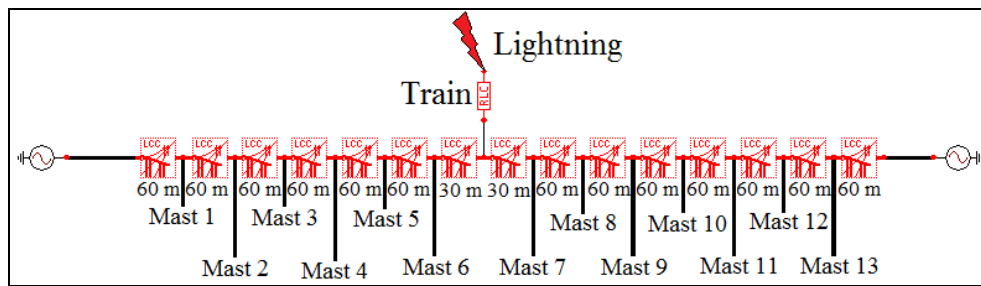


**Figure 4.148** Arrangement of the masts with lightning source for mitigation (case 2)

**Table 4.21** Arrangement of the surge arrester’s installation interval

Interval	Mast												
	1	2	3	4	5	6	7	8	9	10	11	12	13
1	<input type="checkbox"/>	<input type="checkbox"/>	<input type="checkbox"/>	<input type="checkbox"/>	<input type="checkbox"/>	<input type="checkbox"/>	<input type="checkbox"/>	<input type="checkbox"/>	<input type="checkbox"/>	<input type="checkbox"/>	<input type="checkbox"/>	<input type="checkbox"/>	<input type="checkbox"/>
2	<input checked="" type="checkbox"/>	<input checked="" type="checkbox"/>	<input checked="" type="checkbox"/>	<input checked="" type="checkbox"/>	<input checked="" type="checkbox"/>	<input checked="" type="checkbox"/>	<input checked="" type="checkbox"/>	<input checked="" type="checkbox"/>	<input checked="" type="checkbox"/>	<input checked="" type="checkbox"/>	<input checked="" type="checkbox"/>	<input checked="" type="checkbox"/>	<input checked="" type="checkbox"/>
3	<input checked="" type="checkbox"/>	<input type="checkbox"/>	<input checked="" type="checkbox"/>	<input type="checkbox"/>	<input checked="" type="checkbox"/>	<input checked="" type="checkbox"/>	<input checked="" type="checkbox"/>	<input type="checkbox"/>	<input checked="" type="checkbox"/>	<input type="checkbox"/>	<input checked="" type="checkbox"/>	<input type="checkbox"/>	<input checked="" type="checkbox"/>
4	<input type="checkbox"/>	<input checked="" type="checkbox"/>	<input type="checkbox"/>	<input checked="" type="checkbox"/>	<input type="checkbox"/>	<input checked="" type="checkbox"/>	<input type="checkbox"/>	<input checked="" type="checkbox"/>	<input type="checkbox"/>	<input checked="" type="checkbox"/>	<input type="checkbox"/>	<input checked="" type="checkbox"/>	<input type="checkbox"/>
5	<input checked="" type="checkbox"/>	<input type="checkbox"/>	<input type="checkbox"/>	<input checked="" type="checkbox"/>	<input type="checkbox"/>	<input type="checkbox"/>	<input checked="" type="checkbox"/>	<input type="checkbox"/>	<input type="checkbox"/>	<input checked="" type="checkbox"/>	<input checked="" type="checkbox"/>	<input type="checkbox"/>	<input type="checkbox"/>
6	<input type="checkbox"/>	<input type="checkbox"/>	<input checked="" type="checkbox"/>	<input type="checkbox"/>	<input type="checkbox"/>	<input checked="" type="checkbox"/>	<input type="checkbox"/>	<input type="checkbox"/>	<input checked="" type="checkbox"/>	<input type="checkbox"/>	<input type="checkbox"/>	<input checked="" type="checkbox"/>	<input type="checkbox"/>

**Key:**

– No Surge Arrester

– Surge Arrester

A 25 kV overhead catenary system with 13 masts for both Cases were simulated in ATP-EMTP with multiple lightning sources on the train’s pantograph where elevated poles of 50 Ω and ground resistances of 5,10,50 and 100 Ω were accounted for presenting different soil profiles respectively at different Surge Arrester’s installation intervals. The magnitude was set to -50 kA in waveforms of the first stroke-(1.0/100 μs), and subsequent stroke-(0.2/50 μs) for Surge Arrester’s installation intervals and results are tabulated in Table 4.22. The obtained values are percentages of mast induced

voltages against lightning impulse withstand voltage of insulators in Mast 7 under 25 kV Overhead Catenary system.

**Table 4.22** Percentage of Mast Induced Voltage Against Lightning-Impulse Withstand Voltage of Insulators for -50 kA

-50 kA, First stroke-(1.0/100 $\mu$ s), Subsequent stroke-(0.2/50 $\mu$ s) (%)						
Case 1						
Rf	Surge Arrester's installation interval ( <i>I</i> )					
	1	2	3	4	5	6
5	920	47.11	47.56	920	46.67	924
10	924	48.44	48.44	924	47.56	924
50	942	53.33	54.22	924	52	924
100	951	62.22	56.44	929	56.88	929
Case 2						
5	778	62.22	62.22	769	62.22	769
10	804	62.22	62.22	769	62.22	769
50	813	62.22	62.22	773	62.22	773
100	818	62.22	62.22	778	62.22	778

The occurrence of flashover across insulators of Mast 7 is indicated in Table 4.23.

**Table 4.23** Flashover across insulators for -50 kA

-50 kA, First stroke-(1.0/100 $\mu$ s), Subsequent stroke-(0.2/50 $\mu$ s)						
Case 1						
Rf	Surge Arrester's installation interval ( <i>I</i> )					
	1	2	3	4	5	6
5	O	X	X	O	X	O
10	O	X	X	O	X	O
50	O	X	X	O	X	O
100	O	X	X	O	X	O
Case 2						
5	O	X	X	O	X	O
10	O	X	X	O	X	O
50	O	X	X	O	X	O
100	O	X	X	O	X	O

**Key:**

Rf – grounding resistances

O – Flashover

X – No Flashover

#### **4.4 Lightning performance optimization for 25 kV AC, 50 Hz catenary contact system**

The analysis presented in Section 4.3 concerning the mitigation of catenary lines' lightning overvoltage, shows clearly the optimum surge arrester installation interval ( $I$ ) which determined the number of surge arrester ( $K$ ) to be installed on the line based on simulation studies as in Minja, Chombo, Promvichai and Marungsri 2017; Christodoulou, Gonos and Stathopoulos 2008. In the case of influence the shielding failure, the Backflashover failure and the arrester failure rates, significant variation of the catenary line insulation level, the grounding resistance and the energy absorption capability of surge arresters must be examined to ensure full protection in the networks. Additionally, in order to reduce the lightning failure rates at a minimum cost, it could be worthwhile to investigate further the most appropriate selection of these parameters (insulation level ( $U_a$ ), grounding resistance ( $R$ ), and surge arrester's energy absorption capability ( $E$ )). Therefore, these remain parameters were optimized by using AI technique which is Genetics Algorithms codes under MATLAB software. Figure 4.149 shows the examined overhead catenary lines of 28.193 km in which optimum parameters has been obtained.

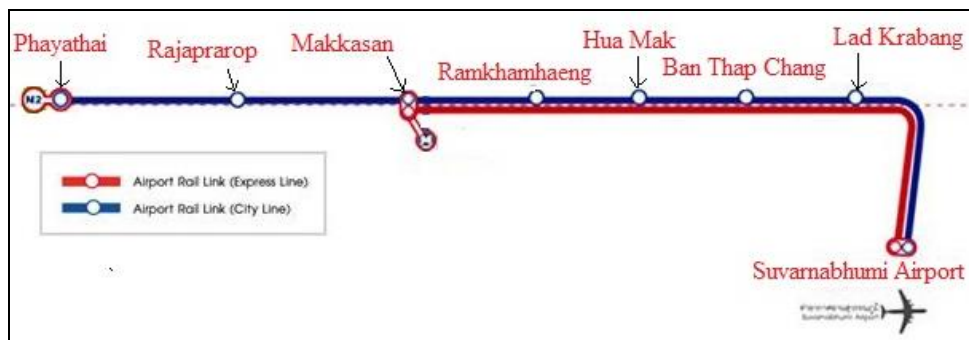


**Figure 4.149** Airport Rail link line in Thailand (UMIASEA, 2014).

#### 4.4.1 Intelligence search method (Genetic Algorithm (GA))

There are many existing different approaches to adjust the control parameters. The GA is well-known as in Somsai, Oonsivilai, Srikaew, and Kulworawanichpong 2007 as among of subsisted tool that has been used in a hundred of works employing the GA technique to optimize the system objective in various forms. The GA is a search method of the stochastic that leads a set of the population in solution space evolved using the fundamental of genetic evolution and natural selection, called genetic operators, e.g., crossover, mutation, etc. With continuous modernizing new generation, a set of updated solutions gradually converges to the real solution. Because the GA is very widely and popular used in most research areas where an intelligent search technique is implemented, it can briefly summarized as shown in the flowchart in Figure 4.150 (El-Abiad and Jaimes, 1969).

In this thesis, the GA is selected to build up an algorithm to solve optimal lightning performance index (all generation from obtainable generating units). For reduce programming complication, the Genetic Algorithm (GADS TOOLBOX in MATLAB) is employed to produce a set of initial random parameters (Genetic

Algorithm and Direct Search Toolbox, 2004). With the process of searching, the parameters are modified to give the best result.

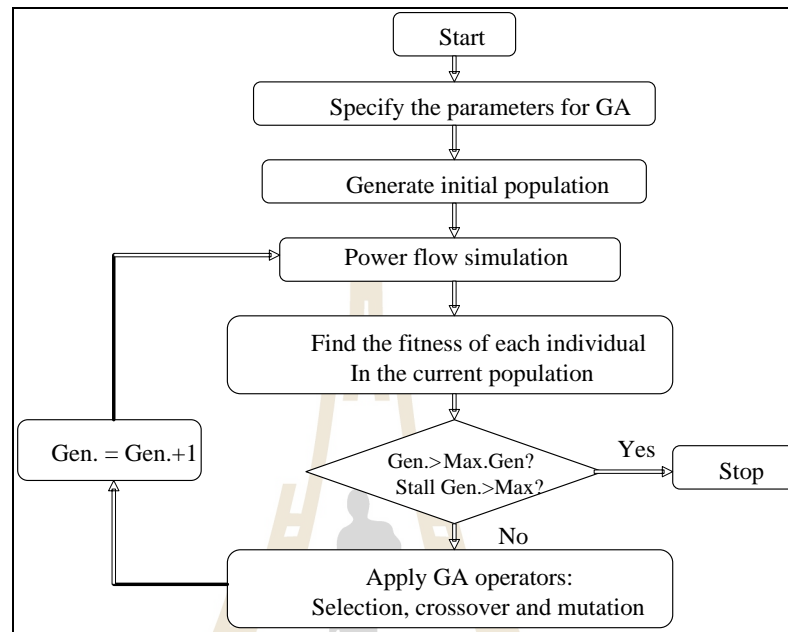


**Figure 4.150** Flowchart of the GA procedure (El-Abiad and Jaimes, 1969).

#### 4.4.2 Test Function

The test of this function is carried out by applying the same parameter setting to all the key cutting algorithms and genetic algorithms as follows.

- Population size is 1000
- Maximum iteration is 100
- No stalled generation is involved
- 16-bit resolution is utilized for each variable

$$f(x_1, x_2, x_3) = f_1(x_1, x_2) + f_2(x_1) + f_3(x_3) \quad (4.1)$$

$$f_1(x_1, x_2) = N_L \left( \frac{1}{\left( X_2/2 + L \right)} \right) \left( \left( \frac{1289842 \left( X_2 I_{peak}/2 - 0.85 X_1 + L di/dt \right)^{1/5}}{171 \left( X_2 I_{peak}/2 - 0.85 X_1 + L di/dt \right)^{17/5} + 1289842} \right) \right) \left( \frac{di/dt}{(di/dt)_{min}} \right)^{\left( \frac{I_{peak}}{I_{peak}_{min}} \right)} \quad (4.2)$$

$$f_2(x_1) = \frac{2N_g I}{10} \frac{Dc}{\sqrt{2\pi} 0.61} \left( \frac{61 \sqrt{\pi} \operatorname{erf} \left( \frac{25 \cdot 2^{3/2} \sqrt{\operatorname{abs} \left( \log \left( I/33.3 \right) \right)}}{61} \right)}{25 \cdot 2^{5/2} \sqrt{\log e^1}} \right)^{I_{max}} \quad (4.3)$$

2X<sub>1</sub>/Z<sub>surge</sub>

$$f_3(x_3) = P_A + P_B \quad (4.4)$$

$$P_A = \left\{ \left( \frac{1.89}{24^{1.89}} \cdot \frac{3.41 \times 10^{11} \log \left( \frac{1.28 \times 10^6 I_A(t)^{189/100} - 31 \sqrt{7698601 + 520397837}}{1.28 \times 10^6 I_A(t)^{189/100} + 31 \sqrt{7698601 + 520397837}} \right)}{189 \sqrt{7698601}} \right) \left( 1 - \frac{X_c}{X_r} \right) \right\}_{I_A(t)} \quad (4.5)$$

$$\times \frac{1.82}{30^{1.82}} \cdot \frac{3.25 \times 10^{12} \arctan \left( \frac{1909284 T_r^{(91/50)} + 931603729}{\sqrt{256887407}} \right)}{13 \sqrt{256887407}} \Bigg|_{T_r}^{\infty}$$

$$P_B = \left\{ \left( \frac{1.89}{24^{1.89}} \cdot \frac{3.41 \times 10^{11} \log \left( \frac{1.28 \times 10^6 I_B(t)^{189/100} - 31\sqrt{7698601} + 520397837}{1.28 \times 10^6 I_B(t)^{189/100} + 31\sqrt{7698601} + 520397837} \right)}{189\sqrt{7698601}} \right) \left( \frac{X_c}{X_r} \right) \right\}_{I_B(T_r)}^{\infty} \quad (4.6)$$

$$\times \frac{1.82}{30^{1.82}} \cdot \frac{3.25 \times 10^{12} \arctan \left( \frac{1909284 T_r^{(9/50)} + 931603729}{\sqrt{256887407}} \right)}{13\sqrt{256887407}} \Bigg|_{T_r}^{\infty}$$

$$T_r = \frac{2 \times X_3}{\sum_{j=1}^{n-1} [(V_j I_j + V_{j+1} I_{j+1})]} \quad (4.7)$$

For the test function shown as equations (4.1)-(4.7) from APPENDIX B has infinitely local minima as in Biskas, et al., 2006. The point (0,0,0) is said to be the global minimum. After 30 trials of solutions, the selected convergence from each method is shown in Figure 4.151. Table 4.25 shows parameters of the existed overhead catenary lines. Table 4.26 - 4.27 contain optimum parameters of the examined overhead catenary lines.

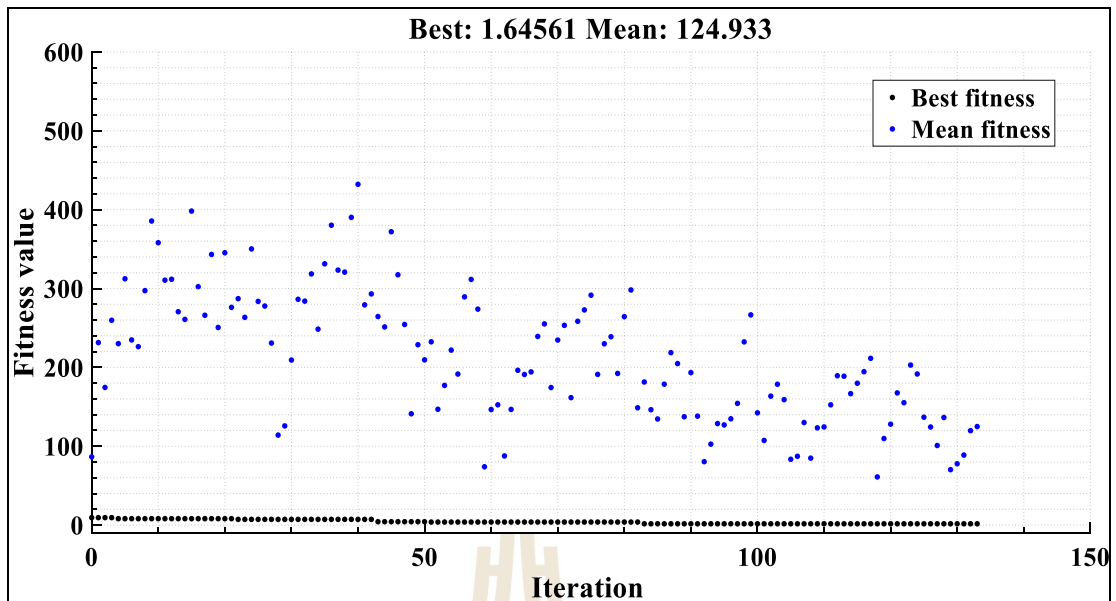


**Figure 4.151** Convergences of the test function 4.1.

**Table 4.24** Parameters of the existed overhead catenary lines.

Masts	$N_T$	$U_a$ (kV)	$R$ ( $\Omega$ )	$E$ (kJ/kV)	$I$	$K$
470	0.0473	27.5	90	9	-	2

**Table 4.25** Optimum parameters of the examined overhead catenary lines.

S/N	$N_T$	$U_a$ (kV)	$R$ ( $\Omega$ )	$E$ (kJ/kV)	$I$	$K$
1	0.115	20.1232	85.5331	10.0084	5	234
2	0.0475	18.9919	77.2244	8.5084	5	234
3	-3.7738	20.2446	81.4699	10.0048	5	234
4	1.0481	19.0008	99.8624	4.9901	5	234
5	-12.1645	23.2593	99.1070	5.8757	5	234
6	-4.8932	23.1282	98.3646	4.9955	5	234
7	-5.9329	19.9138	79.4948	4.9988	5	234
8	0.5895	22.0129	92.4554	4.9931	5	234
9	-11.0377	19.3929	76.4419	4.9990	5	234
10	0.1445	21.1129	87.8110	4.9926	5	234
11	-16.3649	22.8600	96.7690	6.1781	5	234
12	0.0878	18.9919	77.5596	7.3442	5	234
13	-0.0278	20.3248	90.1515	4.9911	5	234
14	-0.0096	19.8515	80.0338	10.0071	5	234
15	0.0279	21.1468	86.9343	4.9938	5	234
16	-0.0607	19.2267	75.8701	10.0066	5	234



**Table 4.25** Optimum parameters of the examined overhead catenary lines

(Continued).

S/N	$N_T$	$U_a$ (kV)	$R$ ( $\Omega$ )	$E$ (kJ/kV)	$I$	$K$
17	0.4297	20.4715	82.7757	4.9953	5	234
18	-24.5733	23.2840	99.2754	9.5247	5	234
19	0.3632	18.9931	74.6968	6.7742	5	234
20	-1.0260	18.9928	75.2252	8.9662	5	234
21	0.0674	22.0909	100.0088	10.0007	5	234
22	-0.1296	18.9911	82.6223	7.0493	5	234
23	0.8399	21.3599	88.1736	4.9938	5	234
24	-0.1359	19.7954	78.8818	10.0056	5	234
25	-11.3622	20.8345	84.8923	8.7285	5	234
26	-0.0544	18.9911	82.4745	9.0536	5	234
27	-24.3956	21.1729	86.8991	8.0774	5	234
28	0.0396	18.9905	90.8708	6.5421	5	234
29	-0.0031	20.4484	91.8501	10.0090	5	234
30	-5.1708	21.8283	90.7182	4.9976	5	234
Average	-3.91053	20.52755	86.48158	7.25351	5	234

Keys: Amax = [27.5 100 10];

Amin = [19 5 5];

**Table 4.26** Optimum parameters of the examined overhead catenary lines.

S/N	$N_T$	$U_a$ (kV)	$R$ ( $\Omega$ )	$E$ (kJ/kV)	$I$	$K$
1	0.4791	18.9942	74.2120	8.4183	5	234
2	-20.2574	19.0378	74.3691	5.6651	5	234
3	-21.8451	19.0420	74.3975	9.0954	5	234
4	-13.8391	19.1109	74.7903	10.0012	5	234
5	-10.1914	19.1117	74.7962	4.9975	5	234
6	-19.3527	19.0221	74.3000	10.0026	5	234
7	-16.9429	19.1043	74.7666	4.9976	5	234
8	0.0469	19.0827	74.9678	4.9935	5	234
9	-11.6704	19.1019	74.7481	10.0032	5	234
10	-4.4066	19.0356	74.3803	4.9953	5	234
11	-0.1672	19.1021	74.8620	4.9942	5	234
12	-11.5282	19.0460	74.4287	4.9965	5	234
13	-8.3035	19.0380	74.4517	10.0049	5	234
14	-0.0696	19.0467	74.9225	10.0067	5	234
15	-20.2986	19.1364	74.9517	4.9987	5	234
16	-6.7409	19.1287	74.8955	10.0031	5	234

**Table 4.26** Optimum parameters of the examined overhead catenary lines

(Continued).

S/N	$N_T$	$U_a$ (kV)	$R$ ( $\Omega$ )	$E$ (kJ/kV)	$I$	$K$
17	-18.6207	19.0965	74.7095	7.1605	5	234
18	-1.5248	19.1029	74.9805	10.0061	5	234
19	0.9256	18.9928	74.9810	5.9683	5	234
20	-7.5848	19.0865	74.6743	10.0042	5	234
21	0.8973	19.0312	74.5008	4.9939	5	234
22	-7.5491	19.0760	74.6494	10.0047	5	234
23	-15.0660	18.9949	74.4100	5.9987	5	234
24	-13.5096	18.9949	74.3820	8.5426	5	234
25	-1.5140	18.9955	74.1298	10.0010	5	234
26	-13.1822	19.0685	74.5405	8.7459	5	234
27	0.1577	18.9958	74.3725	10.0047	5	234
28	-8.1725	19.1113	74.7915	4.9978	5	234
29	-5.5796	19.1059	75.0046	10.0035	5	234
30	-5.3639	18.9939	74.4879	8.0520	5	234
Average	-8.69247	19.05959	74.62848	7.755257	5	234

Keys:  $A_{max} = [27.5 \ 75 \ 10]$ ;  
 $A_{min} = [19 \ 0 \ 5]$ ;

#### 4.5 Chapter summary

This chapter has exhibited the results of the direct lightning effectiveness and its mitigation on the overhead catenary system by using ATP-EMTP simulation software. The optimum parameters of lightning performance have also been enforced by using AI optimizations techniques in MATLAB software. For discussion purpose, the next chapter has been discussed and innovated the final concept to be concluded for the overhead catenary network.

# CHAPTER 5

## DISCUSSION

### 5.1 Analysis of direct lightning strokes

In this section, two different cases are discussed according to the behavior and characteristics of direct lightning strokes as following sections.

#### 5.1.1 The Effects of negative single lightning strokes on mast for case 1

Results of mast induced voltages in Case 1 for different configurations with -34 kA and -50 kA are shown in Tables D.3-D.5, and Tables D.9-D.14. The obtained values were analyzed in Figures. 4.3-4.8 for the auxiliary line as stressed line. It can be noted that the mast induced voltages were above withstand capabilities of line insulators for both catenary, auxiliary, and return lines (see Tables D.3-D.5, and Tables 4.12-4.16). But, the auxiliary line was showed to be more affected followed by catenary line and then return line. Marungsri et al. 2008 studied about back flashover affected by tower grounding resistance and concluded that the higher the lightning magnitude, the higher is the tower induced voltages. As seen in Figures. 4.3-4.8, It can also be found that an increase in lightning magnitude from -34 kA to -50 kA resulted into increase in mast induced voltage. However, back flashover was early observed with -34 kA which meant a back flashover occurred from -34 kA and above with negative single lightning strokes. Furthermore, grounding resistance showed less significance in the performance of single lightning. Therefore, when the mast is stroke by negative single lightning stroke for case 1, back flashover was

seemed to occur from -34 kA and above, in all magnitude and all grounding resistance. Apart from the occurrence of back flashover, the auxiliary line was appeared to have the highest level of mast induced voltage compared to other lines as shown in Tables D.3-D.5, and Tables D.9-D.14. Additionally, single negative lightning discharges affected by grounding resistance was observed in limited extent for case 2 in all configurations. This behavior was noticed especially from 5  $\Omega$  to 100  $\Omega$  for configuration 1 in case 2. Also, the ground resistances effect was observed at mast 5 and mast 7 for configurations 2 and 3. In case 1, this effect was in low performances. In all configurations, grounding resistance of nearby and far end mast showed the effect into lightning withstands the level of insulators below induced voltage in Mast 4, 5 and 7 as in Tables D.3-D.5, and Tables D.9-D.14. However, grounding resistances attains high potential effects by a large lightning magnitude for Mast 4. Moreover, negative single lightning strokes from -34 kA and above may lead critical induced voltage due to untimely mast induced voltage to be held with -34 kA above insulators withstands level. Moreover, case 1 induced low overvoltage compared to case 2 (see Figure 4.15-4.20). Therefore, the grounding resistances effect of the nearby mast and far end mast with the stroke on the mast by negative single lightning may cause back flashover to nearby and far end masts for case 1.

### **5.1.2 The Effects of negative single lightning strokes on mast for case 2**

Results of mast induced voltages in Case 2 for different configurations with -34 kA and -50 kA are given from Tables D.6-D.8, and Tables D.15-D.20. Figures 4.9-4.14 illustrates the summary of induced voltages in the auxiliary lines. As depicted in Tables D.6-D.8, and Tables D.15-D.20, It can be observed that the mast induced voltages are above withstand capabilities of line insulators for both catenary,

auxiliary, and return lines. Although the effects of lightning magnitude and lightning magnitude were also seen as in Case 1 but grounding resistance showed the significant contribution to the back flashovers in Case 2. In general, back flashover was seemed to occur from -34 kA and above, in all grounding resistance when the mast is stroke by negative single lightning in case 2. Again, the auxiliary line was seemed to have the highest mast induced voltage amongst the lines (see Tables D.6-D.8, and Tables D.15-D.20).

### **5.1.3 The Effects of negative single lightning strokes on return line for case 1**

Results of mast induced voltages in Case 1 for different configurations with -34 kA and -50 kA are shown in Tables D.21-D.23, and Tables D.27-D.32. The obtained values were analyzed in Figures. 4.21-4.26 for return line as stressed line. It can be noted that the mast induced voltages were above withstand capabilities of line insulators for both catenary, auxiliary, and return lines as seen in Tables D.21-D.23, and Tables D.27-D.32. Nevertheless, the return line was shown to be more affected followed by catenary line and then auxiliary line. Marungsri et al. 2008 studied about back flashover affected by tower grounding resistance and concluded that the higher the lightning magnitude, the higher is the tower induced voltages. As seen in Figures. 4.21-4.26, It can also be found that an increase in lightning magnitude from -34 kA to -50 kA resulted into increase in mast induced voltage. However, flashover was early observed with -34 kA which meant a flashover occurred from -34 kA and above with negative single lightning strokes. Furthermore, grounding resistance showed less significance in the performance of single lightning. Therefore, when the return line is stroke by single multiple lightning for case 1, flashover was seemed to occur from -34

kA and above, in all magnitude and all grounding resistance. Apart from the occurrence of flashover, the return line was appeared to have the highest level of mast induced voltage compared to other lines as shown in Tables D.21-D.23, and Tables D.27-D.32. Additionally, single negative lightning discharges affected by grounding resistance was observed in limited extent for case 2 in all configurations. This behavior was noticed especially from 5  $\Omega$  to 100  $\Omega$  for configuration 1 in case 2. Also, the ground resistances effect was observed at mast 5 and mast 7 for configurations 2 and 3. In case 1, this effect was affected by low performances. In all configurations, grounding resistance of nearby and far end mast showed the influence into lightning withstands the level of insulators below induced voltage in Mast 4, 5 and 7 as in Tables D.21-D.23, and Tables D.27-D.32. However, grounding resistances attains high potential effects with high lightning magnitude for Mast 4. Moreover, negative single lightning strokes from -34 kA and above may lead critical induced voltage due to untimely mast induced voltage to be held with -34 kA above insulators withstand level. Moreover, case 1 produced high overvoltage compared to case 2 (see Figure 4.33-4.38). Therefore, the grounding resistances effect of the nearby mast and far end mast with the stroke on the mast by negative single lightning may cause a flashover to nearby and far end masts for case 1.

#### **5.1.4 The Effects of negative single lightning strokes on return line for case 2**

Results of mast induced voltages in Case 2 for different configurations with -34 kA and -50 kA are given from Tables D.24-D.26, and Tables D.33-D.38. Figures 4.27-4.32 illustrates the summary of induced voltages in the return line. As depicted in Tables D.24-D.26, and Tables D.33-D.38, It can be observed that the mast

induced voltages are above withstand capabilities of line insulators for both catenary, auxiliary, and return lines. Although the effects of lightning magnitude were also seen as in Case 1 but grounding resistance showed the significant contribution to the flashovers in Case 2. In general, flashover was seemed to occur from -34 kA and above, in all grounding resistance when the return line is stroke by negative single lightning in case 2. Again, the return line was seemed to have the highest mast induced voltage amongst the lines (see Tables D.24-D.26, and Tables D.33-D.38).

#### **5.1.5 The Effects of negative single lightning strokes on catenary line for case 1**

Results of mast induced voltages in Case 1 for different configurations with -34 kA and -50 kA are shown in Tables D.39-D.41 and Tables D.45-D.50. The obtained values were analyzed in Figures. 4.39-4.44 for the catenary line as stressed line. It can be noted that the mast induced voltages were above withstand capabilities of line insulators for both catenary, auxiliary, and return lines (see Tables D.39-D.41, and Tables D.45-D.50). Nonetheless, the catenary line was shown to be more affected followed by return line and then auxiliary line. Marungsri et al. 2008 studied about back flashover affected by tower grounding resistance and concluded that the higher the lightning magnitude, the higher is the tower induced voltages. As seen in Tables D.39-D.41 and Tables D.45-D.50, It can also be found in Figures. 4.39-4.44 that an increase in lightning magnitude from -34 kA to -50 kA resulted into increase in mast induced voltage. However, flashover was early observed with -34 kA which meant a flashover occurred from -34 kA and above with negative single lightning strokes. Furthermore, grounding resistance showed less significance in the performance of single lightning. Therefore, when the catenary line is stroke by negative single

lightning for case 1, flashover was seemed to occur from -34 kA and above, in all magnitude and all grounding resistance. Apart from the occurrence of flashover, the catenary line was appeared to have the highest level of mast induced voltage compared to other lines as shown in Tables D.39-D.41, and Tables D.45-D.50. Additionally, negative single lightning discharges affected by grounding resistance was observed in limited extent for case 2 in all configurations. This behavior was noticed especially from 5  $\Omega$  to 100  $\Omega$  for configuration 1. Also, the ground resistances effect was observed at mast 5 and mast 7 for configurations 2 and 3. In case 1, this effect was affected in low performances. In all configurations, grounding resistance of nearby and far end mast showed the influence into lightning withstands the level of insulators below induced voltage in Mast 4, 5 and 7 as in Tables D.39-D.41, and Tables D.45-D.50. However, grounding resistances attains high potential effects with high lightning magnitude for Mast 4. Moreover, negative single lightning strokes from -34 kA and above may lead critical induced voltage due to untimely mast induced voltage to be held with -34 kA above insulators withstand level. Besides, case 1 caused high overvoltage compared to case 2 (see Figure 4.51-4.56). Therefore, the grounding resistances effect of the nearby mast and far end mast with the stroke on catenary by negative single lightning may cause back flashover to nearby and far end masts for case 1.

#### **5.1.6 The Effects of negative single lightning strokes on catenary line for case 2**

Results of mast induced voltages in Case 2 for different configurations with -34 kA and -50 kA are given from Tables D.42-D.44, and Tables D.51-D.56. Figures 4.45-4.50 illustrates the summary of induced voltages in the catenary line. As



depicted in Tables D.42-D.44, and Tables D.51-D.56, It can be observed that the most induced voltages are above withstand capabilities of line insulators for both catenary, auxiliary, and return lines. Although the effects of lightning magnitude were also seen as in Case 1 but grounding resistance showed the significant contribution to the flashovers in Case 2. In general, flashover was seemed to occur from -34 kA and above, in all grounding resistance when the catenary line is stroke by negative single lightning in case 2. Again, the catenary line was seemed to have the highest most induced voltage amongst the lines (see Tables D.42-D.44, and Tables D.51-D.56).

#### **5.1.7 The Effects of negative single lightning strokes on pantograph for case 1**

Results of most induced voltages in Case 1 for different configurations with -34 kA and -50 kA are shown in Tables D.57-D.59, and Tables D.63-D.68. The obtained values were analyzed in Figures. 4.57-4.62 for the catenary line as stressed line. It can be noted that the most induced voltages were above withstand capabilities of line insulators for both catenary, auxiliary, and return lines. Although, the catenary line was shown to be more affected followed by return line and then auxiliary line. Marungsri et al. 2008 studied about back flashover affected by tower grounding resistance and concluded that the higher the lightning magnitude, the higher is the tower induced voltages. As seen in Tables D.57-D.59, and Tables D.63-D.68, It can also be found in Figures. 4.57-4.62 that an increase in lightning magnitude from -34 kA to -50 kA resulted into increase in most induced voltage. However, flashover was early observed with -34 kA which meant a flashover occurred from -34 kA and above with negative single lightning strokes. Furthermore, grounding resistance showed less significance in the performance of single lightning. Therefore, when the pantograph is

stroke by negative single lightning for case 1, flashover was seemed to occur from -34 kA and above, in all magnitude and all grounding resistance. Apart from the occurrence of flashover, the catenary line was appeared to have the highest level of mast induced voltage compared to other lines as shown in Tables D.57-D.59, and Tables D.63-D.68. Additionally, single negative lightning discharges affected by grounding resistance was observed in limited extent for case 2 in all configurations. This behavior was noticed especially from 5  $\Omega$  to 100  $\Omega$  for configuration 1. Also, the ground resistances effect was observed at mast 5 and mast 7 for configurations 2 and 3. In case 1, this effect was affected in low performances. In all configurations, grounding resistance of nearby and far end mast showed the effect into lightning withstands the level of insulators below induced voltage in Mast 4, 5 and 7 as in Tables D.57-D.59, and Tables D.63-D.68. However, grounding resistances attains high potential effects with high lightning magnitude for Mast 4. Moreover, negative single lightning strokes from -34 kA and above may lead critical induced voltage due to untimely mast induced voltage to be held with -34 kA above insulators withstand level. Besides, case 1 induced high overvoltage compared to case 2 (see Figure 4.69-4.74). Therefore, the grounding resistances effect of the nearby mast and far end mast with the stroke on pantograph by negative single lightning may cause back flashover to nearby and far end masts for case 1.

#### **5.1.8 The Effects of negative single lightning strokes on pantograph for case 2**

Results of mast induced voltages in Case 2 for different configurations with -34 kA and -50 kA are given from Tables D.60-D.62, and Tables D.69-D.74. Figures 4.63-4.68 illustrates the summary of induced voltages in the catenary line. As

depicted in Tables D.60-D.62, and Tables D.69-D.74, It can be observed in Figures 4.63-4.68 that the mast induced voltages are above withstand capabilities of line insulators for both catenary, auxiliary, and return lines. Although the effects of lightning magnitude were also seen as in Case 1 but grounding resistance showed the significant contribution to the flashovers in Case 2. In general, flashover was seemed to occur from -34 kA and above, in all grounding resistance when the pantograph is stroke by negative single lightning in case 2. Again, the catenary line was seemed to have the highest mast induced voltage amongst the lines (see Tables D.60-D.62, and Tables D.69-D.74).

#### **5.1.9 The Effects of negative multiple lightning strokes on mast for case 1**

Results of mast induced voltages in Case 1 for different configurations with -34 kA and -50 kA are shown in Tables D.75-D.77, and Tables D.81-D.86. The obtained values were analyzed in Figures. 4.75-4.80 for the auxiliary line as stressed line. It can be noted that the mast induced voltages were above withstand capabilities of line insulators for both catenary, auxiliary, and return lines. Though, the auxiliary line was showed to be more affected followed by catenary line and then return line. Marungsri et al. 2008 studied about back flashover affected by tower grounding resistance and concluded that the higher the lightning magnitude, the higher is the tower induced voltages. As seen in Figures. 4.75-4.80, It can also be found that an increase in lightning magnitude from -34 kA to -50 kA resulted into increase in mast induced voltage. However, back flashover was early observed with -34 kA which meant a back flashover occurred from -34 kA and above with negative multiple lightning strokes. Furthermore, grounding resistance showed less significance in the performance of multiple lightning. Therefore, when the mast is stroke by negative

multiple lightning for case 1, back flashover was seemed to occur from -34 kA and above, in all magnitude and all grounding resistance. Apart from the occurrence of flashover, the auxiliary line was appeared to have the highest level of mast induced voltage compared to other lines as shown in Tables D.75-D.77, and Tables D.81-D.86. Additionally, negative multiple lightning discharges affected by grounding resistance was observed in limited extent for case 2 in all configurations. This behavior was noticed especially from 5  $\Omega$  to 100  $\Omega$  for configuration 1. Also, the ground resistances effect was observed at mast 5 and mast 7 for configurations 2 and 3. In case 1, this effect was affected in low performances. In all configurations, grounding resistance of nearby and far end mast showed the influence into lightning withstands the level of insulators below induced voltage in Mast 4, 5 and 7 as in Figures. 4.75-4.80. However, grounding resistances attains high potential effects with high lightning magnitude for Mast 4. Moreover, negative multiple lightning strokes from -34 kA and above may lead critical induced voltage due to untimely mast induced voltage to be held with -34 kA above insulators withstand level. Besides, case 1 caused low overvoltage compared to case 2 (see Figures. 4.75-4.80). Although, case 1 with multiple lightning strokes consumed more overvoltage than with single lightning strokes. Therefore, the grounding resistances effect of the nearby mast and far end mast with the stroke on the mast by negative multiple lightning may cause back flashover to nearby and far end masts for case 1.

#### **5.1.10 The Effects of negative multiple lightning strokes on mast for case 2**

Results of mast induced voltages in Case 2 for different configurations with -34 kA and -50 kA are given from Tables D.78-D.80, and Tables D.87-D.92. Figures 4.81-4.86 illustrates the summary of induced voltages in the auxiliary lines.

As depicted in Tables D.78-D.80, and Tables D.87-D.92, It can also be observed in Figures 4.81-4.86 that the mast induced voltages are above withstand capabilities of line insulators for both catenary, auxiliary, and return lines. Although the effects of lightning magnitude were also seen as in Case 1 but grounding resistance showed the significant contribution to the back flashovers in Case 2. Also, case 2 with multiple lightning strokes attained more overvoltages compare to case 2 with single lightning strokes. In general, back flashover was seemed to occur from -34 kA and above, in all grounding resistance when the mast is stroke by negative multiple lightning in case 2. Again, the auxiliary line was seemed to have the highest mast induced voltage amongst the lines (see Tables D.78-D.80, and Tables D.87-D.92).

#### **5.1.11 The Effects of negative multiple lightning strokes on return line for case 1**

Results of mast induced voltages in Case 1 for different configurations with -34 kA and -50 kA are shown in Tables D.93-D.95, and Tables D.99-D.104. The obtained values were analyzed in Figures. 4.93-4.98 for return line as stressed line. It can be noted that the mast induced voltages were above withstand capabilities of line insulators for both catenary, auxiliary, and return lines (see Tables D.93-D.95, and Tables D.99-D.104). However, the return line was showed to be more affected followed by catenary line and then return line. Marungsri et al. 2008 studied about back flashover affected by tower grounding resistance and concluded that the higher the lightning magnitude, the higher is the tower induced voltages. As seen in Tables D.93-D.95, and Tables D.99-D.104, It can also be found in Figures. 4.93-4.98 that an increase in lightning magnitude from -34 kA to -50 kA resulted into increase in mast induced voltage. However, flashover was early observed with -34 kA which meant a

flashover occurred from -34 kA and above with negative multiple lightning strokes. Furthermore, grounding resistance showed less significance in the performance of multiple lightning. Therefore, when the return line is stroke by negative multiple lightning for case 1, flashover was seemed to occur from -34 kA and above, in all magnitude and all grounding resistance. Apart from the occurrence of flashover, the return line was appeared to have the highest level of mast induced voltage compared to other lines as shown in Tables D.93-D.95, and Tables D.99-D.104. Additionally, negative multiple lightning discharges affected by grounding resistance was observed in limited extent for case 2 in all configurations. This behavior was noticed especially from 5  $\Omega$  to 100  $\Omega$  for configuration 1. Also, the ground resistances effect was observed at mast 5 and mast 7 for configurations 2 and 3. In case 1, this effect was affected in low performances. In all configurations, grounding resistance of nearby and far end mast showed the influence into lightning withstands the level of insulators below induced voltage in Mast 4, 5 and 7 as in Figures. 4.93-4.98. However, grounding resistances attains high potential effects with high lightning magnitude for Mast 4. Moreover, negative multiple lightning strokes from -34 kA and above may lead critical induced voltage due to untimely mast induced voltage beheld with -34 kA above insulators withstand level. Moreover, case 1 produced high overvoltage compared to case 2 (see Figure 4.105-4.110). Although, case 1 with multiple lightning strokes caused more overvoltages than case 1 with single lightning strokes. Therefore, the grounding resistances effect of the nearby mast and far end mast with the stroke on return line by negative single lightning may cause a flashover to nearby and far end masts for case 1.

### **5.1.12 The Effects of negative multiple lightning strokes on return line for case 2**

Results of mast induced voltages in Case 2 for different configurations with -34 kA and -50 kA are given from Tables D.96-D.98, and Tables D.105-D.110. Figures 4.99-4.104 illustrates the summary of induced voltages in the return lines. As depicted in Tables D.96-D.98, and Tables D.105-D.110., It can be observed that the mast induced voltages are above withstand capabilities of line insulators for both catenary, auxiliary, and return lines. Although the effects of lightning magnitude were also seen as in Case 1 but grounding resistance showed the significant contribution to the flashovers in Case 2. In general, flashover was seemed to occur from -34 kA and above, in all grounding resistance when the return line is stroke by negative multiple lightning in case 2. Again, the return line was seemed to have the highest mast induced voltage amongst the lines (see Tables D.96-D.98, and Tables D.105-D.110).

### **5.1.13 The Effects of negative multiple lightning strokes on catenary line for case 1**

Results of mast induced voltages in Case 1 for different configurations with -34 kA and -50 kA are shown in Tables D.111-D.113, and Tables D.117-D.122. The obtained values were analyzed in Figures. 4.111-4.116 for the catenary line as stressed line. It can be noted that the mast induced voltages were above withstand capabilities of line insulators for both catenary, auxiliary, and return lines. Regardless of lines, the catenary line was shown to be more affected followed by return line and then auxiliary line. Marungsri et al. 2008 studied about back flashover affected by tower grounding resistance and concluded that the higher the lightning magnitude, the higher is the tower induced voltages. As seen in Tables D.111-D.113, and Tables

D.117-D.122, It can also be found in Figures. 4.111-4.116 that an increase in lightning magnitude from -34 kA to -50 kA resulted into increase in mast induced voltage. However, flashover was early observed with -34 kA which meant a flashover occurred from -34 kA and above with negative multiple lightning strokes. Furthermore, grounding resistance showed less significance in the performance of multiple lightning. Therefore, when the catenary line is stroke by negative multiple lightning for case 1, flashover was seemed to occur from -34 kA and above, in all magnitude and all grounding resistance. Apart from the occurrence of flashover, the catenary line was appeared to have the highest level of mast induced voltage compared to other lines as shown in Tables D.111-D.113, and Tables D.117-D.122. Additionally, negative multiple lightning discharges affected by grounding resistance was observed in limited extent for case 2 in all configurations. This behavior was noticed especially from 5  $\Omega$  to 100  $\Omega$  for configuration 1. Also, the ground resistances effect was observed at mast 5 and mast 7 for configurations 2 and 3. In case 1, this effect was affected in low performances. In all configurations, grounding resistance of nearby and far end mast showed the influence into lightning withstands the level of insulators below induced voltage in Mast 4, 5 and 7 as in Figures. 4.111-4.116. However, grounding resistances attains high potential effects with high lightning magnitude for Mast 4. Moreover, negative multiple lightning strokes from -34 kA and above may lead critical induced voltage due to untimely mast induced voltage beheld with -34 kA above insulators withstand level. Moreover, case 1 caused high overvoltage compared to case 2 (see Figure 4.123-4.128). Besides, case 1 with multiple lightning strokes led more overvoltage than case 1 with single lightning strokes. Therefore, the grounding resistances effect of the nearby mast and far end



mast with the stroke on catenary line by negative multiple lightning may cause a flashover to nearby and far end masts for case 1.

#### **5.1.14 The Effects of negative multiple lightning strokes on catenary line for case 2**

Results of mast induced voltages in Case 2 for different configurations with -34 kA and -50 kA are given from Tables D.114-5.116, and Tables D.123-D.128. Figures 4.117-4.122 illustrates the summary of induced voltages in the catenary line. As depicted in Tables D.114-D.116, and Tables D.123-D.128, It can be observed that the mast induced voltages are above withstand capabilities of line insulators for both catenary, auxiliary, and return lines. Although the effects of lightning magnitude and lightning magnitude were also seen as in Case 1 but grounding resistance showed the significant contribution to the flashovers in Case 2. In general, flashover was seemed to occur from -34 kA and above, in all grounding resistance when the catenary line is stroke by negative multiple lightning in case 2. Again, the catenary line was seemed to have the highest mast induced voltage amongst the lines (see Tables D.114-D.116, and Tables D.123-D.128).

#### **5.1.15 The Effects of negative multiple lightning strokes on pantograph for case 1**

Results of mast induced voltages in Case 1 for different configurations with -34 kA and -50 kA are shown in Tables 4.3-4.5 and Tables 4.9-4.14. The obtained values were analyzed in Figures. 4.129-4.134 for the catenary line as stressed line. It can be noted that the mast induced voltages were above withstand capabilities of line insulators for both catenary, auxiliary, and return lines. In

whatever way, the catenary line was shown to be more affected followed by return line and then auxiliary line. Marungsri et al. 2008 studied about back flashover affected by tower grounding resistance and concluded that the higher the lightning magnitude, the higher is the tower induced voltages. As seen in Tables 4.3-4.5, and Tables 4.9-4.14, It can also be found in Figures. 4.129-4.134 that an increase in lightning magnitude from -34 kA to -50 kA resulted into increase in mast induced voltage. However, flashover was early observed with -34 kA which meant a flashover occurred from -34 kA and above with negative multiple lightning strokes. Furthermore, grounding resistance showed less significance in the performance of multiple lightning. Therefore, when the pantograph is stroke by negative multiple lightning for case 1, flashover was seemed to occur from -34 kA and above, in all magnitude and all grounding resistance. Apart from the occurrence of flashover, the catenary line was appeared to have the highest level of mast induced voltage compared to other lines as shown in Tables 4.3-4.5, and Tables 4.9-4.14. Additionally, negative multiple lightning discharges affected by grounding resistance was observed in limited extent for case 2 in all configurations. This behavior was noticed especially from 5  $\Omega$  to 100  $\Omega$  for configuration 1. Also, the ground resistances effect was observed at mast 5 and mast 7 for configurations 2 and 3. In case 1, this effect was affected in low performances. In all configurations, grounding resistance of nearby and far end mast showed the influence into lightning withstands the level of insulators below induced voltage in Mast 4, 5 and 7 as in Figures. 4.129-4.134. However, grounding resistances attains high potential effects with high lightning magnitude for Mast 4. Moreover, negative multiple lightning strokes from -34 kA and above may lead critical induced voltage due to untimely mast induced voltage be held

with -34 kA above insulators withstand level. Moreover, case 1 caused high overvoltage compared to case 2 (see Figure 4.141-4.146). Besides, case 1 with multiple lightning has more overvoltage compared case 1 with single lightning. Therefore, the grounding resistances effect of the nearby mast and far end mast with the stroke on pantograph by negative multiple lightning may cause flashover to nearby and far end masts for case 1.

#### **5.1.16 The Effects of negative multiple lightning strokes on pantograph for case 2**

Results of mast induced voltages in Case 2 for different configurations with -34 kA and -50 kA are given from Tables 4.6-4.8, and Tables 4.15-4.20. Figures 4.135-4.140 illustrates the summary of induced voltages in the catenary lines. As depicted in Tables 4.6-4.8, and Tables 4.15-4.20, It can be observed that the mast induced voltages are above withstand capabilities of line insulators for both catenary, auxiliary, and return lines. Although the effects of lightning magnitude and lightning magnitude were also seen as in Case 1 but grounding resistance showed the significant contribution to the flashovers in Case 2. In general, flashover was seemed to occur from -34 kA and above, in all grounding resistance when the pantograph is stroke by negative multiple lightning in case 2. Again, the catenary line was seemed to have the highest mast induced voltage amongst the lines (see Tables 4.6-4.8, and Tables 4.15-4.20).

## **5.2 Mitigation of Flashover from Multiple Lightning strokes in Overhead Catenary System**

In Section 5.1, the review bestowed concerning the characteristics and behavior of lightning overvoltage and relieved the critical lightning stroke which needed to be more examined to ensure total protection against its disturbances as discussed as follows.

### **5.2.1 The Mitigation of negative multiple lightning strokes on pantograph**

From Tables 4.23 shows that flashover may occur if the lightning magnitude of -50 kA strikes on pantograph at the mast without surge arrester for all waveforms and ground resistances in case 1 and 2. It was seen that the Surge Arrester's installation intervals 2, 3 and 5 had no flashover in the magnitude of -50 kA for all waveforms and ground resistances. However, installation intervals 1, 4 and 6 showed flashovers in the magnitude of -50 kA for all ground resistances.

## **5.3 Lightning performance optimization for 25 kV AC, 50 Hz catenary contact system**

In Section 5.2, the evaluation conferred concerning the mitigation of lightning overvoltage and found the reasonable installation of surge arrester which helps to determined number of arrester to be installed. But, in order to ensure minimum cost for reducing lightning disturbance, more assessment could be taken as discussed in following sub section.

### 5.3.1 The optimal Lightning performance index for 25 kV AC overhead catenary system

From Tables 4.25-4.26 shows optimum parameters in the examined overhead catenary lines of the proposed optimum design method to Airport Rail Link. The values of optimum for the average insulation level, the grounding resistance of the overhead catenary line, the surge arrester's energy absorption capability, the interval of surge arresters' installation and a number of installed surge arresters in overhead line are calculated. In the examined catenary lines, it is evident that the proposed combined values of these parameters to decrease the total lightning failures. But, any improvements or modifications to the insulation level and the tower footing resistance of this operating line is practically impossible, and the installation of the proposed surge arresters at the calculated interval is recently complicated, the proposed methodology usefulness can be easily noticed for cases of new catenary lines. In using the method obtained by calculating the parameter values, failure rates would certainly in low for the examined catenary line which was presently constructed.

In reality, the method drawback can be considered as the proposal of optimum values for the design parameters, which are difficult to be applied. It is challenging for the construction engineers to construct for instance an insulation level value exactly equal to 19.05959 kV or grounding resistance values exactly equal to 74.62848 Ohm in average.

## 5.4 Chapter summary

This chapter has discussed the reviewed results from the previous chapter. The lightning failure rate was seemed to be reasonable with optimization method. For conclude interpreted results, the next chapter has been finalized for general predictions.

## CHAPTER 6

### CONCLUSION AND FUTURE WORK

#### 6.1 Conclusion

In this research, analysis of the lightning performance of 25 kV AC, 50 Hz Catenary Contact System based on five studies as explained in case study overview has been examined. The effect to flashover and Backflashover with multi-grounding resistances of nearby and far end masts when negative single and multiple lightning strokes on train's pantograph, on top of Mast, return wire (earthing wire) and Catenary wire of the overhead catenary system were prosperous evaluated using ATP-EMTP. Also, the mitigation of transient current negative multiple lightning strokes was included. Finally, the optimization of the lightning performance of 25 kV AC, 50 Hz Catenary Contact System with the help of MATLAB software were evaluated. Various connotations after being examined results have been enunciated and expressed as follows.

It is noticed that negative single and multiple lightning of magnitude -34 kA and above may cause flashover when strikes on train's pantograph, top of Mast, Return wire (Earthing wire), and Catenary wire for both cases in all configurations. The grounding resistance is observed to have a higher influence in mast induced voltages when a lightning strike occurs in case 2 compared with case 1. In the case of all lightning magnitudes, waveforms, and grounding resistances, affected line exhibited higher mast induced voltages in case 1 compared to case 2 except when it strikes on the mast. Although as lightning induced overvoltage in the catenary line

leads more distortion on the system as per standard, highly, consideration should have been focused on this line. Consequences, the catenary line, was seen to be more affected when negative multiple lightning strokes on the pantograph. The greatest one occurred when lightning strokes the pantograph in case 1. Flashovers have been noticed with multiple strokes from -34 kA and above in all waveforms and grounding resistances compared to single strokes in literature and this study, this needs considerable attention. As the effective protection against multiple lightning strokes cannot be self-assured by enhancement of designing insulation only. Therefore, assisted protective methods should be included. In mitigation method, the application of Surge Arrester to reduce flashover in a 25 kV Overhead Catenary system on the elevated railway system have also been investigated. Performances of surge arrester and installation intervals in different soil profiles under the lightning magnitude of -50 kA for case 1 and 2 were studied. It was found that the performance of surge arrester depends much on the installation intervals. It was seen that Surge Arrester's installation interval 5 is the cheapest installation interval to be implemented while installation interval 2 is the most cost full one. In order to ensure costly protection against lightning overvoltages, more parameters should be examined and be compactable with previous parameters which were based on simulation. Consequently, in optimization method, three investigated additional parameters in AI optimization techniques and obtained optimum values were effectuated and concluded.

Finally, the methodology calculates and proposes the most suitable line insulation level, grounding resistance, the energy absorption capability of surge arresters, surge arresters' installation interval, and a number of installed surge

arresters for the examined line, to eliminate or minimize the total failures caused by lightning at a low cost. The developed optimization design methodology can be applied to Airport Rail Link lines of 25 kV. The obtained results for the examined lines, i.e. the newly selected design parameters, significantly reduce the failure rates caused by lightning, something fundamental in the case of catenary lines. But, in reality, any improvements or modifications to the existing design parameters of this line is practically impossible, this method can be valuable to electric power utilities, developing new catenary lines and reducing significantly any future failures caused by lightning.

## 6.2 Future work

The primary considerations for the future works should include the following,

- (a) Verification of the proposed study context remains to be the confirmed work for all the studies covered in this thesis which were based on theoretical simulation. For the further improvement of lightning performance in the catenary railway system, it's hoped that these ideas can provide aspirations.
- (b) Further research should also consider some other constraints. As the future plan in Airport Rail Link, more number of engines or electric motors can be installed to support increasing the people demands. Additionally, the application of such strategies should not be limited only to this field but can be expanded into any area with multiple Unit Trains demands. In some cases, the civil construction requirements are not known in advance, and



this will require a new method to be compatible with the lightning performance of the system.



## REFERENCES

- Andrews, H. I., (1986), **Railway traction: the principles of mechanical and electrical railway traction**, Studies in mechanical engineering 5, Amsterdam, Oxford: Elsevier Science.
- AIEE Committee Report (1950), A method of estimating the lightning performance of transmission lines, **AIEE Trans. 69**, (pp. 1187–1196).
- Anderson, J.G., (1961), Monte Carlo computer calculation of transmission line lightning performance, **AIEE Trans. 80**, (pp. 414–420).
- Adinolfi, A., Lamedica, R., Modesto, C., Prudenzi, A., and Vimercati, S., (Oct. 1998), Experimental assessment of energy saving due to trains regenerative braking in an electrified subway line, **IEEE Transactions on Power Delivery**, 13: 1536–1542.
- Adinolfi, A., Lamedica, R., Modesto C., Prudenzi, A., and Vimercati, S., (1997), Experimental assessment of energy saving due to trains regenerative braking in an electrified subway line, **IEEE Industrial and Commercial Power Systems Technical Conference**, (pp. 211–216).
- Application Guidelines Overvoltage Protection, (2007), **Dimensioning, testing, and application of metal oxide surge arresters in medium voltage networks**, 4th revised edition 2007, ABB Switzerland Ltd., Wetztingen/Switzerland.
- ABB Application Guidelines Overvoltage Protection, (3ed), (2011), Metal-oxide surge arresters in railway facilities. Retrieved from [https://library.e.abb.com/public/3231c0994ad34a13c12578d200341040/986\\_abb\\_awr\\_bahnen\\_E\\_low.pdf](https://library.e.abb.com/public/3231c0994ad34a13c12578d200341040/986_abb_awr_bahnen_E_low.pdf).

- Achouri, F., Achouri, I., and Khamliche, M., (2015), Protection of 25 kV Electrified Railway System, **4th International Conference on Electrical Engineering(ICEE)**, (pp. 1-6).
- Andreotti, A., Martinis, U.D., Pierno, A., and Rakov, V.A., (2014), A New Tool for Lightning Induced Voltage Calculations: CiLIV, **General Assembly and Scientific Symposium (URSI GASS), 2014 XXXIth URSI**, (pp. 1-4).
- Ali, F.M., Geri, A., Lauria, S., and Maccioni, M., (26 February 2016), Monte Carlo Evaluation of the Impact of Subsequent Strokes on Back Flashover Rate, **Environment and Electrical Engineering (EEEIC), 2015 IEEE 15th International Conference**, (pp.1210 – 1215).
- Ametaniand, A., and Kawamura, T., (April 2005), A Method of a Lightning Surge Analysis Recommended in Japan Using EMTP, 20(2): 867-875.
- ABB Surge arrester POLIM-S, (2016). Data sheet 1HC0075857 E01 AB. Retrieved from [https://library.e.abb.com/public/1ea09f10ad44056185257bcc00547e5b/POLIM-S%20to%20245kV\\_2GNM110077\\_7-11.pdf](https://library.e.abb.com/public/1ea09f10ad44056185257bcc00547e5b/POLIM-S%20to%20245kV_2GNM110077_7-11.pdf).
- Abd-Allah, M.A., Ali, M.N., and Said, A., (2014), Toward an Accurate Modeling of Frequency Dependent Wind Farm Components under Transient Conditions, **WSEAS Transactions on Power Systems**, 9: 395-407.
- Bae, C.H., Han, M.S., Kim, Y.K., Choi, C.Y., and Jang, S.J., (2005), Simulation study of the regenerative inverter for DC traction substation, **in Proceedings of the Eighth International Conference on Electrical Machines and Systems**, 2: 1452–1456.

- Bouquegneau, C., Dubois, M., and Trekat, J., (1986), Probabilistic analysis of the lightning performance of high-voltage transmission lines, *Electr. Power Syst. Res.* **102**, (pp.1–2).
- Browand, F., McCallen, R., Ross, Orellano, J. A., and Sperling, S., (2009), The Aerodynamics of Heavy Vehicles II: Trucks, Buses, and Trains, **vol. 41 of Lecture Notes in Applied and Computational Mechanics, ch. Aerodynamic Improvements and Associated Energy Demand Reduction of Trains**, Springer Berlin / Heidelberg, (pp. 219–231).
- Bewley, L.V. (2ed), (1951), **Traveling Waves on Transmission Systems**, John Wiley & Sons Inc., NY.
- BS EN 60034-1:2010, **Rotating electrical machines. Rating and performance**, British standards.
- Bow collector, (2017), Electrification in railway facilities. Retrieved from [https://en.wikipedia.org/wiki/Bow\\_collector](https://en.wikipedia.org/wiki/Bow_collector)
- Biskas, P.N., Ziogos, N.P., Tellidou, A., Zoumas, C.E., Bakirtzis, A.G., and Petridis, V., (2006), Comparison of two metaheuristics with mathematical programming methods for the solution of OPF Generation, Transmission and Distribution, 153: 16 – 24.
- CIGRE Working Group 33.1, (1991), Guide to procedure for estimating the lightning performance of transmission lines, **IEEE Tech. Bul. 63**.
- Chapman, S. J. (4ed), (2005), **Electric Machinery Fundamentals. Australia**, The McGraw-Hill Companies, Electric Motors.
- Christodoulou, CA., Gonos, IF., and Stathopoulos, IA., (2008), Lightning performance of high voltage transmission lines protected by surge arresters: a simulation

for the Hellenic transmission network, **In Proceedings of the 29th International Conference on Lightning Protection, Uppsala, Sweden**, (pp. 6b-7-1–6b-7-8).

Christodoulou, C.A., Ekonomou, L., Fotis G.P., Harkioulakis N., and Stathopoulos I.A., (2009), Optimization of Hellenic overhead high-voltage transmission lines lightning protection, **Energy**, 34: 502–509.

Chmielewski, T., and Dziadkowiec, A., (2013), Simulation of Fast transients in Typical 25 kV, A.C Railway Power Supply System, **Zeszyty Naukowe Wydziału Elektrotechniki i Automatyki Politechniki Gdańskiej**, 23(36): 43-46.

Chowdhuri, P., and Mehairjan, S., (1997), Alternative to Monte Carlo method for the estimation of lightning incidence to overhead lines, **IEE Proc. Gen. Transmission Distribution**, 144(2): 129–131.

Chisholm, W.A., and Janischewskyj, W., (1989), Lightning surge response of ground electrodes, **IEEE Trans. on Power Delivery**, 14(2): 1329-1337.

Chang, W.S., and Zinn, C.D., (1976), Minimization of the cost of an electrical transmission line system,” **IEEE Trans.**, 95(4): 1091–1098.

CTBTO/IMS Earthing and Lightning Protection Minimum Standard, (2016). Retrieved from [http://eng.ctbto.org/download/attachments/4849747/CTBTO+Earthing+and+Lightning+Protection+Guid+V1\\_1\\_01\\_2010.pdf?version=1&modificationDate=1302605430000](http://eng.ctbto.org/download/attachments/4849747/CTBTO+Earthing+and+Lightning+Protection+Guid+V1_1_01_2010.pdf?version=1&modificationDate=1302605430000).

Catalogue\_RAIL\_Surge\_Arresters\_en, (2016). Retrieved from [https://w3.siemens.com/mcms/industrial-controls/de/railway/Documents/Catalogue\\_RAIL\\_Surge\\_Arresters\\_en.Pdf](https://w3.siemens.com/mcms/industrial-controls/de/railway/Documents/Catalogue_RAIL_Surge_Arresters_en.Pdf).

- Dai, Y, and Ni, Q., (2003), Testing different conjugate gradient methods for large-scale unconstrained optimization, **Computation Math**, 21(3): 311–320.
- Das, J.C. (2ed), (2010), **Transients in Electrical Systems, Analysis, Recognition and mitigation**, John Wiley and Sons, Inc.
- Dugel, S. R. B., (May 2007), Insulation Coordination of Quadruple Circuit High Voltage Transmission Lines Using ATP- EMTP, **Master Degree Thesis, Universiti Teknologi Malaysia**, (pp. 51-99).
- Durbak, D.W., (January 1985), Zinc-oxide arrester model for fast surges, **EMTP Newsletter**, 5(1): 1-9.
- De la Rosa, F., Cummins, K., Deller, L., Diendorfer, G., Galván, A., Husse, J., Larsen, V., Nucci, C.A., Rachidi, F., Rakov, V., Torres, H., and Uman, M.A., (December 2000), Characterization of lightning for applications in Electric Power Systems, **Technical Brochure, No.172, CIGRE WG. 33.01.02**.
- DEHN + SÖHNE – Lightning Protection Guide. (2015), Surge Protection Lightning Protection/Earthing Safety Equipment DEHN protects. Retrieved from [https://www.dehn-international.com/sites/default/files/uploads/dehn/pdf/blitzplaner/bpl2015/lpg\\_2015\\_e\\_complete.pdf](https://www.dehn-international.com/sites/default/files/uploads/dehn/pdf/blitzplaner/bpl2015/lpg_2015_e_complete.pdf)
- Edwards, B., (1998), The Manx Electric Railway, **B & C Publications**, (pp. 6–7).
- Ekonomou, L., Iracleous, DP., Gonos, IF., and Stathopoulos, IA., (2006), An optimal design method for improving the lightning performance of overhead high voltage transmission lines, **Electr Power Syst Res**, 76: 493–499.
- El-Abiad A.H., and Jaimes, F.J., (1969), A method for optimum scheduling of power and voltage magnitude, **IEEE Transactions. Power Apparatus and System**, 88: 413 – 422.

- Fletcher, R. (2ed), (1987), **Practical methods of optimization**, New York: Wiley-Interscience.
- Frey, S., (1ed), (2012), **Railway Electrification System & Engineering**, Ansari Road, Darya Ganj, Delhi.
- Fisher, F.A., Anderson, J.G., and Hagenguth, J.H., (1960), Determination of lightning response of transmission lines by means of geometrical models, **AIEE Trans.** 78: 1725–1736.
- Gabriel, R., Leonhard, W., and Nordby, C. J., (March 1980), Field-oriented control of a standard AC motor using microprocessors, **IEEE Transactions on Industry Applications**, IA-16: 186–192.
- Grant, I.S., and Clayton, R.E., (1987), Transmission line optimization, **IEEE Trans. Power Delivery**, 2(2): 520–526.
- Genetic Algorithm and Direct Search Toolbox for use with MATLAB, User's Guide. Retrieved from <http://www.upch.edu.pe/facien/fc/dbmbqf/zimic/ubioinfo/bks/Bioinformatics/Bioinformatics%20%20Genetic%20Algorithm%20And%20Direct%20Search%20Toolbox%20-%20Matlab.pdf>
- Guzzella, L., and Sciarretta, A., (2ed), (2007), **Vehicle Propulsion Systems, Introduction to Modeling and Optimization**, Springer Berlin Heidelberg.
- Guardado, R. A., and Guardado, J. L., (August 2016), A PMU Model for Wide-Area Protection in ATP/EMTP," **IEEE Trans. Power Del.**, 31(4).
- Haginomori, E., Koshiduka, T., Arai, J., and Ikeda, H., (1ed), (2016), **Power System Transient Analysis: Theory and Practice using Simulation Programs (ATP-EMTP)**, UK: John Wiley & Sons.

- Hennessey, R.A.S., (July 2008), Sparks: the electrical consultants, **Backtrack.**, 22(7): 390–396.
- Hibbeler, R. C., (7ed), (2008), **Mechanics of Materials**, Singapore; London: Prentice Hall.
- Electric Traction Systems and Their Advantages (2015). Retrieved from [http://www.electronicshub.org/electric-traction-system/#Single\\_Phase\\_AC\\_Traction\\_System](http://www.electronicshub.org/electric-traction-system/#Single_Phase_AC_Traction_System).
- Hill, R. J., (June 1994), Electric railway traction: Part 2 traction drives with three-phase induction motors, **Power Engineering Journal**, 8: 143–15.
- Hill, R. J., (Feb. 1994), Electric railway traction: Part 1 electric traction and DC traction motor drives, **Power Engineering Journal**, 8: 47–56.
- Hill, R., (Dec. 1994), Electric railway traction. Part 3. traction power supplies,” **Power Engineering Journal**, 8: 275 –286.
- Hilemann, A.R., (1989), **Insulation Coordination for Power Systems**, New York, USA: Marcel Dekker.
- He, J., Tu, Y., Zeng, R., Lee, L.B., Chang, S.H., and Guan, Z., (2005), Numerical analysis for shielding failure of the transmission line under lightning stroke, **IEEE Trans. Power Delivery**, 20(2): 815–822.
- Holt, R., and Nguyen, T.T., (1999), Monte Carlo estimation of the rates of lightning strikes on power lines,” **Electr. Power Syst.**, 49: 201–210.
- IEC Std. 60099-4, **Surge arresters—Part 4: Metal-oxide surge arresters without gaps for a.c. systems.**
- Imece, A. F., Durbak, D.W., Elahi, H., Kolluri, S., Lux, A., Mader, D., McDemott, T. E., Morched, A., Mousa, A. M., Natarajan, R., Rugeles, L., and Tarasiewicz,



- E., (1996), Modeling Guidelines for Fast Front Transients, **IEEE Transactions on Power Delivery**, 11(1): 493-506.
- IEEE Working Group on Surge Arrester Modeling, (January 1992), Modeling of metal oxide surge arresters, **IEEE Transactions on Power Delivery**, 7(1): 302–309.
- IEEE Working Group on Lightning Performance of Transmission Lines, (1985), A simplified method for estimating the lightning performance of transmission lines, **IEEE Trans.**, 104: 919–927.
- IEEE Working Group on Estimating the Lightning Performance of Transmission Lines, (1993), Estimating lightning performance of transmission lines II—Updates to analytical models, **IEEE Trans.**, 8: 1254–1267.
- IEEE Std. C62.22-2009, (3 July 2009), **IEEE Guide for the Application of Metal-Oxide Surge Arresters for Alternating-Current Systems**, IEEE Power & Energy Society.
- IEEE Std. C62.11-2005, (22 March 2006), **IEEE Standard for Metal-Oxide Surge Arresters for Alternating Current Power Circuits (>1 kV)**, IEEE Power & Energy Society.
- IEC 60071-2, (1996), **Insulation Coordination, Part 2: Application Guide**, IEC Standards.
- IEC Std. 60099-5, (2000), **Surge arresters—Part 5: Selection and application recommendations**, edition 1.1.
- IEC 62305-1:2006-01, **Protection against lightning - Part 1: General principles**, IEC Standards.

- IEC 62305-2:2006-01, **Protection against lightning - Part 2: Risk management**, IEC Standards.
- IEC 62305-3:2006-01, **Protection against lightning - Part 3: Physical damage to structures and life hazard**, IEC Standards.
- IEC 62305-4:2006-01, **Protection against lightning - Part 4: Electrical and electronic systems within structures**, IEC Standards.
- IEEE Std. 1313.2-1999, **IEEE Guide for the Application of Insulation Coordination**, IEEE Standards.
- IEC Std. 60913, (2013), **Railway applications – Fixed installations – Electric traction overhead contact lines**, IEC Standards.
- IEEE Std. 1410-2004, **IEEE Guide for Improving the Lightning Performance of Electric Power Overhead Distribution Lines**, IEEE Standards.
- Jeter, M.W., (1986), **Mathematical Programming: An Introduction to Optimization**, Monographs and textbooks in pure and applied mathematics, New York: M. Dekker, Inc.
- Karagöz, M., (2014), Analysis of the Pantograph Arcing and Its Effect of the Railway Vehicle,” **Master Degree Thesis, Middle East Technical University**.
- Kiessling, Puschmann, Schmieder, and Schneider, (2ed), (2009), **Contact Lines for Electric Railways**, Planning, Design, Implementation, Maintenance.
- Kennon, RE, and Douglass, DA., (1990), EHV transmission line design opportunities for cost reduction, **IEEE Trans Power Delivery**, 5(2): 1145–1152.
- Katic, NA, and Savic, MS., (1998), Technical and economical optimization of overhead power distribution line lightning protection, **IEE Proc—Gen Tran Distribution**, 145(3): 239–244.

- Lu, S., (October 2011), Optimising Power Management Strategies for Railway Traction Systems, **Doctor Degree Thesis, The University of Birmingham, UK.**, (pp. 1-20).
- Lee, G., and Goldsworthy, C., (2011), Introduction to the Alternative Transients Program (ATP), **IEEE SPDC Spring Meeting in Bonneville Power Administration (BPA)**, (pp. 1-110).
- Leeton, U., and Kulworawanichpong, T., (2011), Application of Key Cutting Algorithms for Optimal Power Flow Problems, **The 8th Electrical Engineering/ Electronics, Computer, Telecommunications and Information Technology (ECTI) Association of Thailand - Conference 2011**, (pp. 897 – 900).
- Liu, J., and Liu, M.G., (2012), Improved electro-geometric model for estimating lightning outage rate of catenary, **IET Electrical Systems in Transportation**, 2: 1-8.
- Lira, G.R.S., Fernandes, D., and Costa, E.G., (2007), Computation of Energy Absorption and Residual Voltage in Metal Oxide Surge Arrester from Digital Models and Lab Test: A Comparative Study, **International Conference On Power System Transients (IPST'07) In Lyon, France**, (pp. 1-6).
- Minja, K.M., Chombo, P.V., Promvichai, N., and Marungsri, B., (7-8 March 2017), Mitigation of Flashover from Multiple Lightning strokes in Overhead Catenary System by using ATPDraw, **2017 IEEJ PE&S – IEEE PES Thailand Symposium on Advanced Technology in Power System, Bangkok, Thailand**, (pp 119-123)

- Martinez, J.A., and Castro-Aranda, F., (2003), Lightning performance analysis of transmission lines using the EMTP, **Power Eng. Soc. Gen. Meet. 1**, (pp. 295–300).
- Mungkung, N., Wongcharoen, S., Tanitteerapan, T., Saejao, C., and Arunyasot, D., (2007), Analysis of Lightning Surge Condition Effect on Surge Arrester in Electrical Power System by using ATP/EMTP Program, **International Journal of Electrical, Energetic, Electronic and Communication Engineering**, 1(4): 32-34.
- Mardira, P., and Saha, T.K., (January 1996), A Simplified Lightning Model for Metal Oxide Surge Arrester, **IEEE Transactions on Power Delivery**, 11(1): 493-506.
- Martinez-Velasco, J. A., and Aranda F. C., (2008), EMTP Implementation of a Monte Carlo Method for Lightning Performance Analysis of Transmission Lines, **Ingeniare. Revista chilena de ingeniería**, 16(1): 169-180.
- Martinez-Velasco, J. A., and Aranda F. C., (2003), Parametric Analysis of the Lightning Performance of Overhead Transmission Lines Using an Electromagnetic Transients Program, **International Conference on Power Systems Transients-IPST 2003 in New Orleans, USA**, (pp. 1-6).
- Marungsri, B., Boonpoke, S., Rawangpai, A., Oonsivilai, A., and Kritayakornupong, C., (2008), Study of Tower Grounding Resistance Effected Back Flashover to 500kV Transmission Line in Thailand by using ATP/EMTP, **International Journal of Electrical, Computer, Energetic, Electronic and Communication Engineering**, 2(6): 1061-1068.

- Martinez-Velasco, J.A., (2010), **Power System Transients: Parameter Determination**, CRC Press: The US.
- Mellitt, B.Z., Mouneimne, S., and Goodman, C.J., (1984), Simulation study of DC transit systems with inverting substations, **Electric Power Applications, IEE Proceedings B**, 131(2): 38–50.
- Mazloom, Z., (2010), Multi-conductor transmission line model for electrified railways: A method for responses of lumped devices, **Doctoral Thesis, KTH Electrical Engineering University, Stockholm, Sweden**, (pp. 59-72).
- Mousa, A.M., (1994), The soil ionization gradient associated with discharge of high currents into concentrated electrodes, **IEEE Trans. on Power Delivery**, 9(3): 1669-1677.
- Nafar, M., Solookinejad, G., and Jabbari, M., (May 2014), Comparison of IEEE and Pinceti Models of Surge Arresters, **Research Journal of Engineering Sciences**, 3(5): 32-34.
- Nocedal, J., and Wright, S. J. (2ed) (2006), **Numerical Optimization. Springer Series in Operations Research and Financial Engineering**, Springer New York.
- Naupane, A., and Rimal, B., Electric Traction System, Engineering, 2016. Retrieved from <http://www.slideshare.net/BishalRimal2/electric-traction-system-final-upload>
- Oettich, S., Albrecht, T., and Scholz, S., (2004), Improvements of energy efficiency of urban rapid rail systems, **Urban Transport X**, 16: 573–582.
- Omidiora, M.A., and Lehtonen, M., (September 15-17, 2007), Performance of Surge Arrester to Multiple Lightning Strokes on Nearby Distribution Transformer,

**Proceedings of the 7th WSEAS International Conference on Power Systems, Beijing, China, (pp. 59-65).**

Omidiora, M.A., and Lehtonen, M., (October 24-26, 2007), Simulation of Combined Shield Wire and MOV Protection on Distribution Lines in Severe Lightning Areas, **Proceedings of the World Congress on Engineering and Computer Science.**

Overhead line, (2009). Retrieved from [https://en.wikipedia.org/wiki/Overhead\\_line](https://en.wikipedia.org/wiki/Overhead_line).

Park, C.B., Lee, B.S., Lee, H.W., Kwon, S.Y., and Park, H.J., (2008), Air-gap control system of a linear induction motor for a railway transit, in **International Conference on Electrical Machines**, 1- 4: 2000–2003.

Pešič, R., and Grmovšek, B., (September 2007), Application of lightning protection and surge arresters in railway facilities, **Iskra Zaščite**, (pp. 1-49).

Pastromas, S., Papamikou, A., Peppas, G., and Pyrgioti, E., (September 2016), Investigation of grounding resistance effect on the MV grid of Hellenic electromotive railway during lightning strikes, **33<sup>rd</sup> International Conference on Lightning Protection.**

Pattanadech, N., and Yutthagowith, P., (2014), A Transmission Model of Vertical Grounding Electrodes, **AORCTechnical meeting 2014**, (pp. 1-7).

Prikler, L., and Høidalen, H. K., (October 2002), **ATPDRAW version 3.5 for Windows 9x/NT/2000/XP**, Users' Manual, SINTEF Energy Research, Preliminary Release No. 1.1.

Rodriguez-Sanabria, D., Ramos-Robles, C., and Orama-Exclusa, L., Lightning and Lightning Arrester Simulation in Electrical Power Distribution Systems, (pp. 1-9).

- Somsai, K., Oonsivilai, A., Srikaew, A., and Kulworawanichpong, T., (September 2007), Optimal PI controller design and simulation of a static var compensator using MATLAB's SIMULINK, **The 7<sup>th</sup> WSEAS International Conference on POWER SYSTEMS, Beijing, China**, (pp. 30 – 35).
- Shariatinasab, R., Vahidi, B., and Hosseinian, S.H., (2009), Statistical evaluation of lightning-related failures for the optimal location of surge arresters on the power networks, **IET Generation Transmission & Distribution**, 3:129–144.
- Shi, Z.J., and Shen, J., (2005), A new descent algorithm with curve search rule, **Apply Math Computation**, 161: 753–68.
- Sandra, W., Martin, A., and Menter, F., (6 April 2007), Traction Power Study and Simulation, **Airport Rail Link Consortium, Railway Electrification (REL) Traction Power Supply (TPS) - Suvarnabhumi Airport Rail Link and City Air Terminal**, (pp. 43).
- Saengsuwan, T., and Thipprasert, W., (2008), The Lightning Arrester Modeling Using ATP-EMTP, **Kasetsart J (Nat. Sci.)**, 42: 156-164.
- Sargent, M.A., and Darveniza, M., (1970), Lightning performance of double-circuit transmission lines, **IEEE Trans.**, 89: 913–925.
- Saied, M.M., Jaboori, M., and El-Nakid, D., (1990), On the optimal design of high voltage overhead transmission lines, **J Electr Mach Power System**, 18(3): 293–312.
- Saied, M.M., (1999), An alternative procedure for the design of high voltage overhead transmission lines, **In IEEE/PES Transmission and Distribution Conference and Exposition, New Orleans, Louisiana**, (pp. 708–714).

- Tan, P.C., Loh, P.C., and Holmes, D.G., (Apr. 2005), Optimal impedance termination of 25-kv electrified railway systems for improved power quality, **IEEE Transactions on Power Delivery**, 20: 1703 – 1710.
- Thanasaksiri, T., (2014), Improving the Lightning Performance of Overhead Distribution and Sub-Transmission Lines Applying Additional Underbuilt Shield Wire, **ECTI Transactions on Electrical Eng., Electronics, and Communications**, 12(2): 1-8.
- Type POLIM-S Surge Arresters. (2008), Maximum System Voltage 2.52 to 245 kV. Retrieved from [https://library.e.abb.com/public/1ea09f10ad44056185257bcc00547e5b/POLIM-S%20to%20245kV\\_2GNM110077\\_7-11.pdf](https://library.e.abb.com/public/1ea09f10ad44056185257bcc00547e5b/POLIM-S%20to%20245kV_2GNM110077_7-11.pdf).
- Utlu, Z., and Hepbasli, A., (Sep. 2006), Assessment of the energy utilization efficiency in the Turkish transportation sector between 2000 and 2020 using energy and energy analysis method, **Energy Policy**, 34: 1611–1618.
- UMIASEA (2014), **Thailand's Railway Industry-Overview and Opportunities for Foreigners Businesses**, UMI Asia (Thailand) Ltd.
- Wensheng, S., (2016), **Introduction to Electric Traction AC Drive System**, Train Control & Traction Drive Lab, Southwest Jiaotong University.
- Wu, W., and Cao, X., (2012), Power System Electromagnetic Transient Calculation with EMTP Application, **Beijing: China Water & Power Press**, (pp. 232-249).
- Wanjari, A.V., (July 2014), Effect of Lightning on the Electrified Transmission Railway System, **International Journal of Advanced Research in Electrical, Electronics and Instrumentation Engineering**, 3(7): 10663-10671.



- Wilke, and Gabriel, (August 2005), **Overall TPS Schematic Diagram**, Suvarnabhumi Airport Rail Link and City Air Terminal.
- Yang, Y., and Zhang, Y., (March 1, 2015), Research on Lightning Protection Simulation of High-speed Railway Catenary Based on ATP-EMTP, **Journal of information & Computation Science**, 12(4): 1511-1521.
- Zhang, Z.W., Wu, B., Kang, J.S., and Luo, L.F., (Apr. 2009), A multi-purpose balanced transformer for railway traction applications, **IEEE Transactions on Power Delivery**, 24: 711–718.
- Zupan, A., Teklić, A.T., and Filipović-Grčić, B., (July 1-4, 2013), Modeling of 25 kV Electric Railway System for Power Quality Studies, **EuroCon 2013.Zagreb, Croatia**, (pp. 844-849).
- Zhang, Y., Sima, W., and Zhang, Z., (2006), Summary of the study of tower models for lightning protection analysis, **High Voltage Engineering**, (pp. 93-97).

# Transient Current Behaviour during Multiple Lightning strokes on Multiple Unit Trains

Kelvin Melckzedek Minja, Pius Victor Chombo,  
Narupon Promvichai, and Boonruang Marungsri, Non-members

## ABSTRACT

This paper studies transient current behavior during multiple lightning strokes on multiple unit trains of catenary contact system in airport rail link (Bangkok). Since lightning flashover across insulators is a source of power network failure, the protection against overvoltage disturbances in the overhead catenary system has been recently taken into consideration as its parameters. In this study, the impact in lightning strokes current magnitude with IEC 62305 waveforms of the first and subsequent stroke were evaluated. Moreover, in invariant elevated pole and grounding resistance, lightning strikes on multi-car trains' pantographs at the mast and mid-range of the masts were the interested locations for investigation. The modeled elements of the necessary system have been effectuated in ATP-EMTP software. The flashover was shown to occur for lightning current from -34 kA and above at targeted positions. Also, the mast induced voltage was recognized to increase with lightning magnitude. The striking on three-car trains resulted in high consequences compared to the four-car trains. However, the overcritical mast induced voltage often occurred in the catenary line once it strikes on three-car trains' pantograph across the mast unlike at mid-range. Therefore, protection against lightning multiplicity into multi-car trains and striking points should be highly considered.

**Keywords:** Electrified Multiple Unit Trains, Catenary, Multiple Lightning Strokes, Transient Current, Mast Induced Voltage, ATP-EMTP.

## 1. INTRODUCTION

Improvement on electrification of railway line due to the advantage of electric traction over diesel-electric traction and hybrid traction has become more important for everyday life. Also, for energy dependent, a human, desired environment, and economic growth have been demanded electric train services since the second half of 19<sup>th</sup> century, due to technology innovation improvement to increase speed, safety,

efficiency, and reliability of economic enhancement [1-2]. Typically, electricity in electrified railway transmission system must be stably secured with effectively track system and control system. Power is injected into the system which is in the form of overhead catenary transmission line without disturbance. Although the hardship of transmission line that injects power into a system along distance when lightning strikes on multiple unit trains as a natural disturbance, may likely cause the electrical breakdown. Actually, this disruption leads various electrical elements failure, power losses, and other unreliable condition on catenary contact system.

Induced over-voltages in a mast is a most exist issue which causes flashover across insulators due to lightning strikes on multiple unit trains of catenary contact system. Lightning strokes disturbances have influenced the overhead lines on double-track elevated railway system in an existing environment without any prevention. Flashover occurs when the induced voltage in a mast exceeds lightning withstand voltage level of insulators. This incidence makes the study of lightning to be more important in reliability, protection, and durable insulation design to prevent power losses in 2×25 kV AC, 50 Hz electrified railway power system. The significances of this system over 1×25 kV AC, 50 Hz electrified railway system have been stated in [3].

The experience of thunderstorm days and lightning activities per year in Thailand has led to the study of transient current behavior during multiple lightning strokes on multiple unit train's pantographs of the overhead catenary system on the elevated railway system. It uses catenary for the most traction power supply system to deliver power to electric locomotive by pantograph which is exposed to the lightning activities. The report of lightning statistics in Thailand from [4] showed that the Lightning often occurs in April-May but severely in June. The magnitude ranges 11-171 kA with positive polarity and -10 to -139 kA with negative polarity. Positive lightning strokes account for 5% while negative is 95% with the magnitude of -10 to -50 kA. In [5-8] showed that negative polarity lightning stroke could associate with multiple strokes per flash and [5,7-8] reported that the multiple strokes are averaging 3 to 4 strokes per flash with intervals of tens of milliseconds. The negative polarity of multiple lightning strokes was taken as much concern in the study, especially for 2×25 kV

Manuscript received on July 24, 2017 ; revised on July 31, 2014.

The authors are with Electrical Engineering, Institute of Engineering, Suranaree University of Technology, 111 University Avenue, Nakhon Ratchasima 30000, Thailand, E-mail : bmsivee@sut.ac.th

AC, 50 Hz catenary contact system on the double-track elevated railway system. The overhead catenary system connects Phayathai BTS station in the center and Suvarnabhumi airport in the East of Bangkok in Thailand. In addition, airport rail link covers three lines which are city line, Makkasan express line and Phayathai express line at 28.6 km track length. Currently, city line has 5 three-car trains, and express lines have 4 four-car trains (1 for baggage) [9]. For the purpose of the study, seven masts on elevated poles at the line of 480 m length with 60 m spacing in case 1 and six masts on elevated poles at the line of 420 m length with 60 m spacing in case 2 were considered. Case 1 was preferred when multiple unit trains' pantographs are at 4<sup>th</sup> Mast and case 2 between 3<sup>rd</sup> and 4<sup>th</sup> Masts. The negative multiple lightning strokes on three-car and four-car trains' pantograph were analyzed for city and express line respectively.

## 2. THE ANALYSIS OF ELEVATED STRUCTURE AND CATENARY LIGHTNING RANGE

Thai catenary contact system consists of auto-transformer (AT), booster transformer (BT) and tracks circuit which includes relay and rectifier units. There are also interconnections between the overhead catenary conductors on the double-track elevated railway system. In the double-track electrified railway system with I-rail (R1), S-rail (R2), catenary line (contact line (R3) and messenger line (R4)), return line (R5) and auxiliary line (R6) that are interconnected as a circuit shown in Fig. 1 and cross-sectional view in Fig. 2 [9]. The return conductors are also interconnected to the booster transformer (BT) systems, and it's also connected to the S-rail at the midpoint between two consecutive transformers at every 5 km. At every pole position, the S-rail (R2) is shorted to the elevated pole footing.

Due to the unpredictability of lightning strike point on multiple unit train's pantographs which touches the catenary wire, it better to study the parts which are exposed to lightning according to the IEEE STD. 1234-1997, by using the formula (1) in [10].

$$\begin{cases} r_c = 1.34h^{0.6}I^{0.65} \\ r_c = r_g \end{cases} \quad (1)$$

where  $r_c$  is lightning strike distance of catenary which touches on pantograph of multiple unit trains, its UI is m;  $h$  is the average height of hanging wire, its UI is m;  $I$  is the lightning current amplitude, its UI is kA;  $r_g$  is lightning strike distance of earth on top of elevated pole, its UI is m.

The range of triggered lightning of catenary shown in Fig. 3 as in [10] but in this study, was considered when it is on top of the elevated pole. AB arc line is triggered a lightning range of auxiliary line (R6), CD arc is triggered a lightning range of catenary line (contact line and messenger line) (CA). The lightning

current reaches first to the line which has a higher range of lightning strike distance compared to other wires. Auxiliary line (R6) and return line (R5) are on the same side on top of the mast. Lightning strike distance of auxiliary line (R6) is greater than return line (R5) which lead R6 to shield R5, but there is no any shield for the catenary line that touch pantograph, and lead great possibilities to be attacked by lightning strikes on it. In this study, we focus when multiple lightning strokes on multiple unit train's pantographs because pantograph touches catenary line. It is casual that catenary on high ground like on top of an elevated pole experience more lightning strike than that on low ground as in [11].

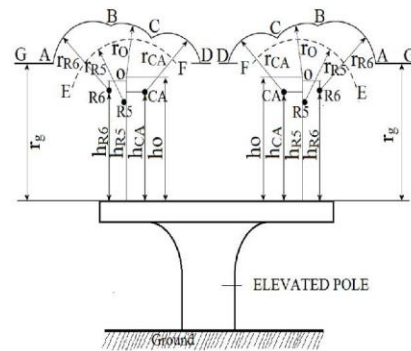


Fig.3: The range of triggered lightning of Catenary on the double-track elevated railway system.

## 3. MODELLING

The proposed ATP-EMTP software which recognized as standard procedure in power system used to investigate transient current behavior during multiple lightning strokes on multiple unit train's pantographs. Modeling of multiple lightning sources, mast, multiple unit trains, overhead catenary transmission line, insulator, elevated pole, and the ground was guided to represent catenary contact system on the double-track elevated railway system for analyzing the problem.

### 3.1 Multiple Lightning Source Model

Since negative lightning strokes may associate with subsequent strokes, only the first and second strokes are highly considered due to the effects of their current magnitudes in insulation [6]. But the behavior of tower grounding electrode and surrounding soil at higher frequencies of up to 10 MHz is not yet explicitly represented [12]. Frequently, both triangular and

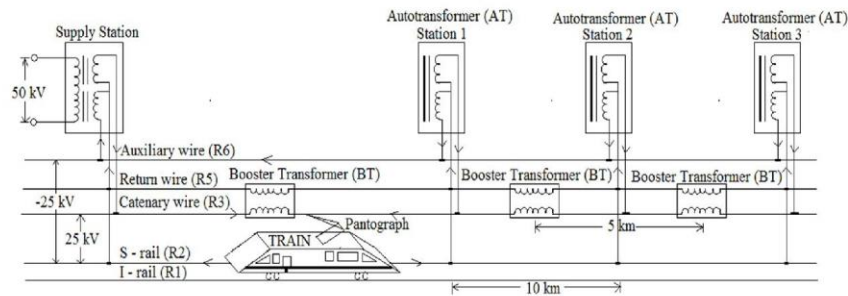


Fig.1: Power Supply Circuit of 2x25 kV AC, 50 Hz Catenary Contact System.

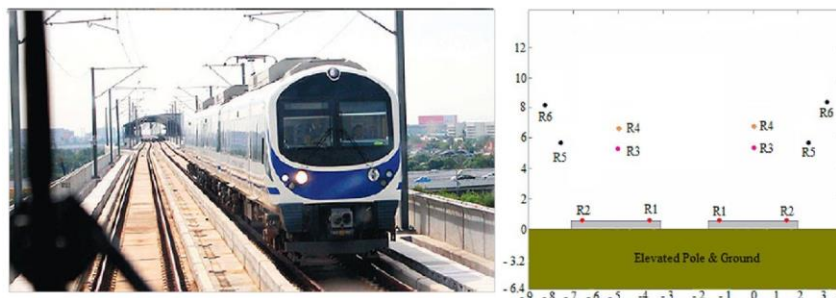


Fig.2: Double track Railway Electrification system on elevated railway system and same cross-section view axis [9].

exponential waveforms have been utilized to represent return strokes currents of lightning. Presently, it is deduced that a concave waveform can be better representation since it could not show a discontinuity at the initial stage. Several expressions have been suggested for such waveforms [13-15]. Therefore, the Heidler current function model in ATP-EMTP was used to represent the lightning current as one of the most widely used as shown in (2) [16-17].

$$i(t) = \frac{I_P}{k} \cdot \frac{\left(\frac{t}{\tau_1}\right)^n}{1 + \left(\frac{t}{\tau_1}\right)^n} \cdot \exp\left(-\frac{t}{\tau_2}\right) \quad (2)$$

where  $I_P$  is the peak value of the lightning stroke;  $k$  is the adjustment constant;  $n$  is a factor influencing the rate of rise;  $t$  is the time instant of the maximum rate of rise;  $\tau_1$  and  $\tau_2$  are the coefficients of the decay time and front time respectively.

The calculation of variables  $\tau_1, \tau_2$  and  $n$  are explained in [18]. The correction factor of Amplitude, which regularly appears in the mathematic expression

of Heidler function [14], is automatically modified and does not materialize in ATP-EMTP. Heidler-type is suitable throughout the concave lightning current front of the wave, regarding the natural lightning, is modeled.

Parameters of lightning sources are given in Table 1. Fig. 4 depicts the lightning waveforms of -34 kA normalized the first stroke with 1.0/100  $\mu$ s and subsequent stroke with 0.2/50  $\mu$ s as recommended by IEC 62305 [19]. The allocation of the lightning sources in selected railway transmission line for the city and express line in case 1 and 2 are shown in Figs. 5-8.

### 3.2 Mast Model

The mast is modeled by cylindrical geometrical steel column in single wave impedance model as recommended by IEEE and CIGRE by expression from surge impedance equation (3) in [10,20] and modeled

**Table 1:** Multiple lightning sources Parameters [4,19]

Parameter	First strokes	Subsequent Strokes
Type	Heidler 15	Heidler 15
Amp. (kA)	-34	-34
	-50	-50
	-100	-100
Front time ( $\mu s$ )	1	0.2
Tail time ( $\mu s$ )	100	50

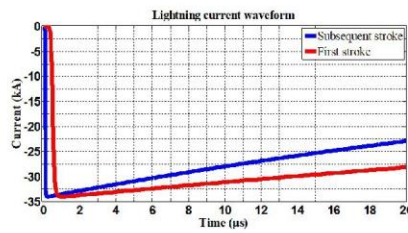


**Fig.4:** Lightning current waveforms of the -34 kA first stroke-(1.0/100  $\mu s$ ), subsequent stroke -(0.2/50  $\mu s$ ) designed in ATP-EMTP.

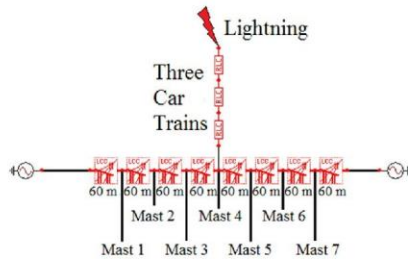


**Fig.5:** City line with lightning source (Case 1).

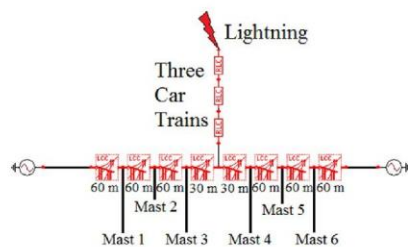


**Fig.6:** City line with lightning source (Case 2).

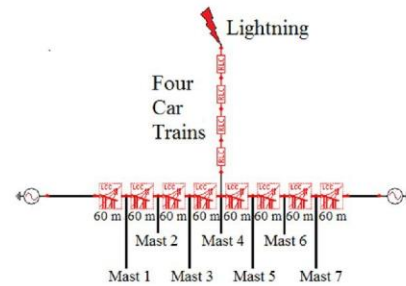


**Fig.7:** Express line with lightning source (Case 1).

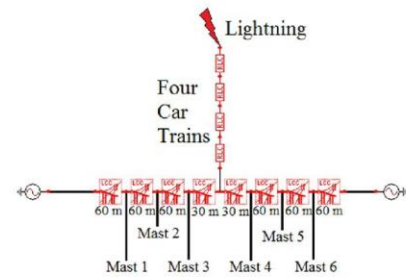


**Fig.8:** Express line with lightning source (Case 2).

parameters are shown in Table 2.

$$Z = 60In \cot \left[ 0.5 \arctan \left( \frac{R}{H} \right) \right] \quad (3)$$

where  $Z$  is the surge impedance, its IU is  $\Omega$ ;  $R$  is the equivalent radius of the mast, its IU is m;  $H$  is the height of the mast, its IU is m.

**Table 2:** Modelled Parameters of Mast Model

Location	Parameters
Auxiliary	$Z_{aux}= 176.35 \Omega, L_1= 3.3 \text{ m}$
Return	$Z_{return}=275.1 \Omega, L_2= 0.2 \text{ m}$
Catenary	$Z_{catenary}= 126.88 \Omega, L_3= 6.3 \text{ m}$

**3.3 Insulator Model**

Generally, insulator resists the flow of current from phase conductor to the ground during normal operating condition. Since the capability of an insulator to withstand stress depends on its voltage withstand level, this behavior can be represented as a voltage controlled switch [21]. Moreover, the effects of coupling conductors to mast structure can

also be represented by the capacitor. If the voltage across insulator terminals is greater than control voltage of the switch, the switch closes which indicates flashover. Otherwise, if the voltage stress is less than control voltage, the switch remains open to show no flow of current across the insulator. In the simulation, the voltage controlled switch was designed by Switchvc.sup model. The voltage withstand capabilities for the rod/composite, spool and pin as given in Table 3 [22] were set as the control voltage of the switch. The values of capacitance for suspension insulators are 80 pF/unit while for pin insulators are around 100pF/unit [21].

**Table 3: Impulse withstand level of Insulators [22]**

Insulators	Impulse Withstand level
Rod/Composite (R3/R4)	225 kV
Spool (R5)	60 kV
Pin (R6)	140 kV

### 3.4 Grounding Resistance Model

Once the lightning current discharges to earth through the mast, the ionization process occurs around soil surrounding the grounding rod. This situation makes surrounding soil as non-linear and the frequency dependent. A non-linear frequency-dependent representation is required to obtain an accurate simulation [6,12,23-24]. Due to difficulties of information to representing this behavior not always available, the reasonable model approximation of grounding resistance as recommended by IEC and IEEE standards is given in (4) [10,21,25-27].

$$R_g = \frac{R_0}{\sqrt{1 + \frac{2\pi R_0^2 I}{E_0 \rho}}} \quad (4)$$

From expression,  $R_g$  is grounding resistance, its IU is  $\Omega$ ;  $R_0$  is the striking impedance value in low-frequency power flow, its IU is  $\Omega$ ;  $I$  is the striking lightning current passing through the grounding system, its IU is kA;  $\rho$  is the soil resistivity, its IU is  $\Omega \cdot m$ ;  $E_0$  is the soil ionization intensity, usually take a value of 400 kV/m [24].

### 3.5 Multiple Unit Trains Model

The electric train was modeled as electric locomotive which contains pantograph, locomotive transformer, diode rectifier bridge and DC motors as stated in [28-29]. The rectifier bridge is represented by the parallel RC elements and the series resistance of the diodes. A series reactor is connected between the motor and the rectifier bridge in order to smooth the direct current [28]. Three-car trains in city line consisted 6 DC motors while four-car trains in express line carried 8 DC motors. The network of an

electric vehicle with elements listed above and one DC motor are indicated in Figs. 9-10. In the case of positions, Fig. 9 and 10 show when the pantograph is at the mast and mid-span of the masts respectively. Railway transmission line with 60 m spacing, elevated pole resistance and grounding resistance, and Insulators are shown in Fig. 9.

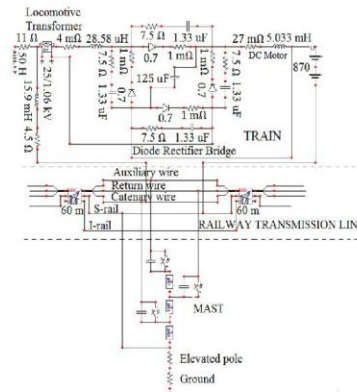


**Fig.9: Mast with Train, Railway Transmission line, Pole, Ground, and Insulators at elevated pole in ATP EMTP.**

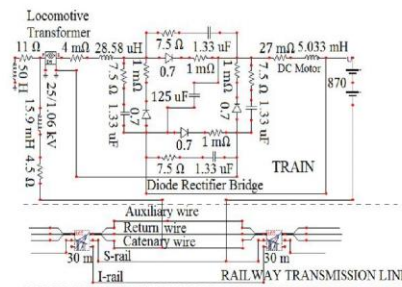


**Fig.10: Train with Railway Transmission line between elevated poles in ATP EMTP.**

### 3.6 Overhead Catenary Transmission Line Model

The overhead catenary transmission line was modeled by LCC 8 with JMARTI model in ATP EMTP as shown in Fig. 11 and it consists of a catenary line, return line, auxiliary line, S-rail and I-rail on elevated poles at every 60 m along overhead cate-

nary system as in [22,30] with autotransformer and booster transformer. Autotransformer and booster transformer were modeled as 1:1 ideal transformers in ATP EMTP as shown in [10]. This type of transformer used to force the traction current to return through designated return conductors to traction supply in order to reduce stray current which may cause electromagnetic interference with electrical systems in the vicinity of the railway system and to ensure the return of transmission energy to the substation from the train. Mast cross section view of 25 kV electrified railway line have been shown in Fig. 3.

Phase	React	Rtot	Rstr	Htot	Vmax	Vmid
1	0	4.95	1.75E-6	-0.7175	0.95	0.95
2	0	0.82	6.04E-7	-2.5795	5.5	5.5
3	0	5.95	1.35E-6	0	5.3	5.3
4	0	0.95	2.81E-7	3.62	8	8
5	0	4.95	1.75E-6	0.7175	0.95	0.95

Fig.11: Railway Transmission line data in ATP EMTP.

4. SIMULATION ANALYSIS

As a version part of the electromagnetic transients program, ATP-EMTP is the powerful tool for steady state and transient analysis of power systems [31]. It has been recognized as per international standard as IEEE and CIGRE in arithmetic circuits [32]. In this task, ATP-EMTP is utilized as time domain computation in overvoltage protection against lightning as indicating from Figs. 9-10.

The traction voltage of the system is 25 kV AC, 50 Hz as stated by IEC standard [33]. A nominal voltage was inserted to both sides of the termination of the line. A 25 kV railway transmission line with arrangements of masts as in Figs. 5-8 were simulated in ATP-EMTP. Multiple lightning sources were inserted on train's pantograph. The elevated poles and grounding resistance were set to 50  $\Omega$  and 5  $\Omega$  unchanged respectively. The magnitude, front time and tail time of negative multiple lightning strokes were studied as factors that cause a transient current which leads flashover across insulators. As the impulse voltage withstand capability of insulation depends on the front time of lightning stroke current, the different multiple lightning stroke currents were initiated. The present magnitude of -34 kA was started to be simulated and followed by -50 kA and -100 kA as specified

in Table 1. First strokes-(1.0/100  $\mu$ s) and subsequent stroke-(0.2/50  $\mu$ s) waveforms were used in the simulation for both city line and express line.

4.1 Simulation Results

Figs. 12-17 and Figs. 18-23 contain the outcome of mast induced voltage waveforms stressed insulators of the auxiliary, return and catenary line for city line and express line respectively. For instance, Figs. 12-14 and Figs. 18-20 are represented case 1 while Figs. 15-17 and Figs. 21-23 are evinced case 2. Figs. 12-23 differ in the magnitude of mast induced voltages across insulators. Table 4 and 6 show the

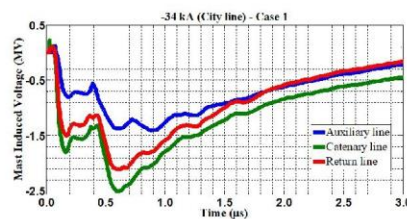


Fig.12: Mast induced voltage waveform of the -34 kA first stroke-(1.0/100  $\mu$ s), subsequent stroke-(0.2/50  $\mu$ s).

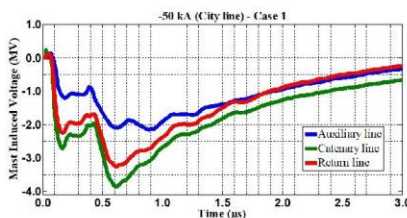


Fig.13: Mast induced voltage waveform of the -50 kA first stroke-(1.0/100  $\mu$ s), subsequent stroke-(0.2/50  $\mu$ s).

magnitude of mast induced voltages and Table 5 and 7 show flashovers across insulators.

Table 4: Magnitude of mast induced voltages (MV)

City line								
Case 1								
-34kA			-50kA			-100kA		
Aux	Ret	Cat	Aux	Ret	Cat	Aux	Ret	Cat
1.41	2.11	2.51	2.15	3.25	3.85	4.41	6.72	8.0
Case 2								
-34kA			-50kA			-100kA		
Aux	Ret	Cat	Aux	Ret	Cat	Aux	Ret	Cat
1.62	2.18	2.32	2.26	3.30	3.51	4.62	6.72	7.15

Key:

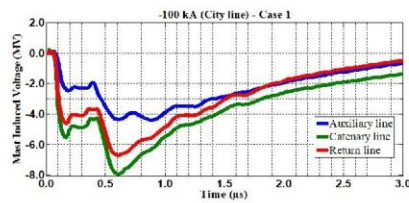


**Fig.14:** Mast induced voltage waveform of the -100 kA first stroke-(1.0/100  $\mu$ s), subsequent stroke-(0.2/50  $\mu$ s).

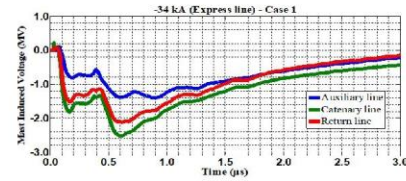


**Fig.18:** Mast induced voltage waveforms of the -34 kA first stroke-(1.0/100  $\mu$ s), subsequent stroke-(0.2/50  $\mu$ s).

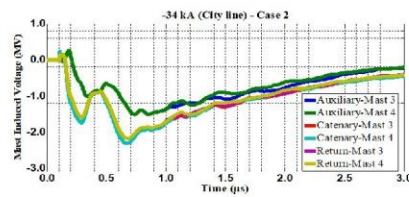


**Fig.15:** Mast induced voltage waveform of the -34 kA first stroke-(1.0/100  $\mu$ s), subsequent stroke-(0.2/50  $\mu$ s).

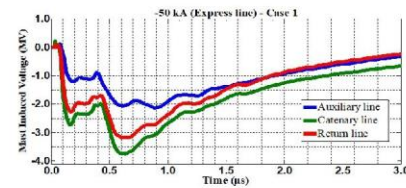


**Fig.19:** Mast induced voltage waveforms of the -50 kA first stroke-(1.0/100  $\mu$ s), subsequent stroke-(0.2/50  $\mu$ s).

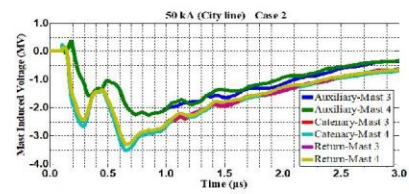


**Fig.16:** Mast induced voltage waveform of the -50 kA first stroke-(1.0/100  $\mu$ s), subsequent stroke-(0.2/50  $\mu$ s).

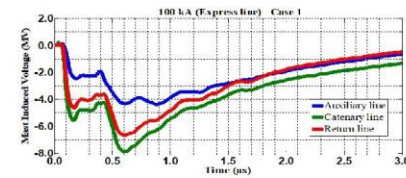


**Fig.20:** Mast induced voltage waveform of the -100 kA first stroke-(1.0/100  $\mu$ s), subsequent stroke-(0.2/50  $\mu$ s).

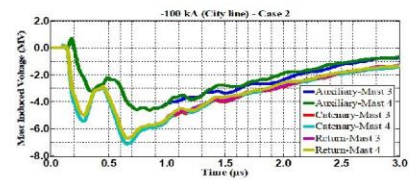


**Fig.17:** Mast induced voltage waveform of the -100 kA first stroke-(1.0/100  $\mu$ s), subsequent stroke-(0.2/50  $\mu$ s).

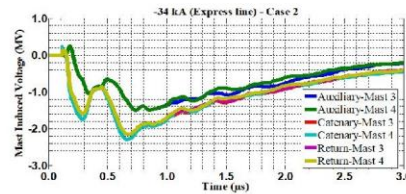


**Fig.21:** Mast induced voltage waveform of the -34 kA first stroke-(1.0/100  $\mu$ s), subsequent stroke-(0.2/50  $\mu$ s).



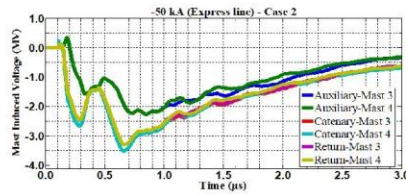


Fig.22: Mast induced voltage waveform of the -50 kA first stroke-(1.0/100 μs), subsequent stroke-(0.2/50 μs).

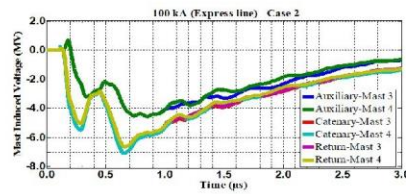


Fig.23: Mast induced voltage waveform of the -100 kA first stroke-(1.0/100 μs), subsequent stroke-(0.2/50 μs).

Table 5: Flashover across insulators

City line								
-34kA			-50kA			-100kA		
Aux	Ret	Cat	Aux	Ret	Cat	Aux	Ret	Cat
S	S	S	S	S	S	S	S	S
-34kA			-50kA			-100kA		
S	S	S	S	S	S	S	S	S

Table 6: Magnitude of mast induced voltages (MV)

Express line								
-34kA			-50kA			-100kA		
Aux	Ret	Cat	Aux	Ret	Cat	Aux	Ret	Cat
1.40	2.12	2.52	2.12	3.18	3.75	4.37	6.66	7.88
-34kA			-50kA			-100kA		
1.81	2.15	2.30	2.27	3.30	3.61	4.86	6.66	7.98

Table 7: Flashover across insulators

Express line								
-34kA			-50kA			-100kA		
Aux	Ret	Cat	Aux	Ret	Cat	Aux	Ret	Cat
S	S	S	S	S	S	S	S	S
-34kA			-50kA			-100kA		
S	S	S	S	S	S	S	S	S

S-Flashover, Aux-Auxiliary line, Ret-Return line, Cat- Catenary line

5. DISCUSSION

According to the simulation results, two different sections are discussed. The first and second parts are described when three-car and four-car train's pantograph struck by multiple lightning strokes with negative polarity respectively.

5.1 Effect of Negative Multiple Lightning Strokes on Three-Car Train's Pantograph

As shown in Figs. 12-17, the mast induced voltages in the auxiliary, return, and catenary lines are above the lightning withstand levels of their respective insulators. The amounts of mast induced voltages are shown in Table 4. However, the flashover was observed to occur from -34 kA and above in both case 1 and case 2 (see Table 5). Also, the mast induced voltages were seen to increase with lightning magnitudes from -34 kA to -100 kA. The catenary line in case 1 and case 2 was seemed to be the most affected line from -34 kA to -100 kA. The worst case for the catenary line was occurred in -100 kA for case 1.

5.2 Effect of Negative Multiple Lightning Strokes on Four-Car Train's Pantograph

From the illustrations of Figs. 18-23, the lightning withstands levels of the auxiliary, return, and catenary lines are below the mast induced voltages across their respective insulators. The quantities of mast induced voltages are exhibited in Table 6. Moreover, in both case 1 and case 2, lightning magnitude from -34 kA and above caused the flashover (see Table 7). Additionally, the mast induced voltages were noticed to increase with lightning magnitudes from -34 kA to -100 kA. The catenary line in case 1 and case 2 was discerned to be the most pretentious line from -34 kA to -100 kA. The worst case for the catenary line was appeared in -100 kA for case 1.

6. CONCLUSION

In this paper, the transient current behavior when multiple lightning strokes on three-car and four-car trains' pantographs have been studied. The investigation of flashover voltage across auxiliary, return, and catenary lines insulators on the elevated railway system were analyzed. The occurrence of flashover was observed for any the lightning magnitude from -34 kA to -100 kA for case 1 and case 2 of both three-car and four-car train. Moreover, the mast induced voltage was seen to increase with the magnitude of lightning strokes current. The effect of lightning current was observed more in three-car train compared to the four-car train. The catenary line of the three-car train was the most stressed line in contrast to auxiliary and return line. The maximum value of the mast induced

voltage in the catenary line of the three-car train was seen to occur when the pantograph was across the mast. Since the mast induced voltage across insulator of the catenary line was seemed to decrease from three-car train (8.0 MV) to four-car train (7.88 MV), it was suggested to study the behavior of lightning current for other multi-car trains.

#### 7. ACKNOWLEDGEMENT

Authors would like to express their gratitude to the support of High Voltage Insulation Technology Laboratory of Suranaree University of Technology, Thailand.

#### References

- [1] S. Lu, *Optimising Power Management Strategies for Railway Traction*, D. Eng. Thesis, The University of Birmingham, UK, pp. 8-20, 2011.
- [2] A. V. Wanjari, "Effect of Lightning on the Electrified Transmission Railway System," *International Journal of Advanced Research in Electrical, Electronics and Instrumentation Engineering*, Vol. 3, Issues .7, pp. 10663- 10671, 2014.
- [3] C. Courtois, "Why the 2×25 kV Alternative [Autotransformer Traction Supply]," *The French Experience, IEE Colloquium*, pp. 1/1-1/4, 1993.
- [4] B. Marungsri, S. Boonpoke, A. Rawangpai, A. Oonsivilai, and C. Kritayakornpong, "Study of Tower Grounding Resistance Effected Back Flashover to 500kV Transmission Line in Thailand by using ATP/EMTP," *International Journal of Electrical, Computer, Energetic, Electronic and Communication Engineering*, Vol. 2, No. 6, pp. 1061-1068, 2008.
- [5] M.A. Omidiora, and M. Lehtonen, "Performance of Surge Arrester to Multiple Lightning Strokes on Nearby Distribution Transformer," *Proceedings of the 7th WSEAS International Conference on Power Systems, Beijing, China*, pp. 59-65, 2007.
- [6] J. A. Martinez-Velasco, and F. C. Aranda, "EMTP Implementation of a Monte Carlo Method for Lightning Performance Analysis of Transmission Lines," *Ingeniare. Revista chilena de ingenieria*, Vol. 16, No. 1, pp. 169-180, 2008.
- [7] M.A. Omidiora, and M. Lehtonen, "Simulation of Combined Shield Wire and MOV Protection on Distribution Lines in Severe Lightning Areas," *Proceedings of the World Congress on Engineering and Computer Science*, 2007.
- [8] D. Rodriguez-Sanabria, C. Ramos-Robles, and L. Orama-Exclusa, "Lightning and Lightning Arrester Simulation in Electrical Power Distribution Systems," pp. 1-9.
- [9] UMIASEA, *Thailand's Railway Industry- Overview and Opportunities for Foreigners Businesses*, UMI Asia (Thailand) Ltd, 2014.
- [10] Y. Yang, and Y. Zhang, "Research on Lightning Protection Simulation of High-speed Railway Catenary Based on ATP-EMTP," *Journal of Information & Computation Science* 12:4, pp. 1511-1521, 2015.
- [11] J. Liu, and M.G. Liu, "Improved electrogeometric model for estimating lightning outage rate of catenary," *IET Electrical Systems in Transportation*, Vol. 2, pp. 1-8, 2012.
- [12] N. Pattanadech and P. Yutthagowith, "A Transmission Model of Vertical Grounding Electrodes," *AORCTechnical meeting 2014*, pp. 1-7, 2014.
- [13] IEC 60071-4, "Insulation Coordination, Part 4: Application Guide," 2004-06.
- [14] F. Heidler, "Analytische Blitzstromfunktion zur LEMP-Berechnung," *18th International Conference on Lightning Protection (ICLP)*, pp. 63 - 66, 1985.
- [15] CIGRE Technical Brochure No. 63, "Guide to procedures for estimating the lightning performance of transmission lines," 1991.
- [16] F. M. Gatta, A. Geri, S. Lauria, and M. Maccioni, "Monte Carlo Evaluation of the Impact of Subsequent Strokes on Backflashover Rate," *2015 IEEE 15th International Conference on Environment and Electrical Engineering (EEEIC)*, pp. 1210 - 1215, 2015.
- [17] T. Thanasaksiri, "Improving the Lightning Performance of Overhead Distribution and Sub-Transmission Lines Applying Additional Underbuilt Shield Wire," *ECTI Transactions on Electrical Eng., Electronics, and Communications*, Vol 12, No 2, pp. 1-8, 2014.
- [18] D. Lovric, S. Vujevic and T. Modric, "On the estimation of Heidler function parameters for reproduction of various standardized and recorded lightning current waveshapes," *International transactions on Electrical Energy Systems 2013*, Vol 23, No 2, pp. 290-300, 2013.
- [19] IEC 62305:2010, "Protection against lightning," 2010.
- [20] Y. Zhang, W. Sima, and Z. Zhang, "Summary of the study of tower models for lightning protection analysis," *High Voltage Engineering*, pp. 93-97, 2006.
- [21] A. F. Imece, D. W. Durbak, H. Elahi, S. Kolhuri, A. Lux, D. Mader, T. E. McDermott, A. Morched, A. M. Mousa, R. Natarajan, L. Rugeles, and E. Tarasiewicz, "Modeling Guidelines for Fast Front Transients," *IEEE Transactions on Power Delivery*, Vol. 11, No. 1, pp. 493-506, 1996.
- [22] Ziya Mazloom, *Multi-conductor transmission line model for electrified railways: A method for responses of lumped devices*, Doctoral Thesis, KTH Electrical Engineering University, Stockholm, Sweden, pp. 59-72, 2010.

- [23] W.A. Chisholm and W. Janischewskyj, "Lightning surge response of ground electrodes," *IEEE Trans. on Power Delivery*, vol. 14, No. 2, pp. 1329-1337, 1989.
- [24] A.M. Mousa, "The soil ionization gradient associated with discharge of high currents into concentrated electrodes," *IEEE Trans. on Power Delivery*, Vol. 9, No. 3, pp. 1669-1677, 1994.
- [25] IEC 60071-2, "Insulation Coordination, Part 2: Application Guide," 1996.
- [26] IEEE Std. 1313.2 - 1999, "IEEE guide for the application of insulation coordination," Technical Council of the IEEE Power Engineering Society, 1999.
- [27] J. A. Martinez-Velasco, and F. C. Aranda, "Parametric Analysis of the Lightning Performance of Overhead Transmission Lines Using an Electromagnetic Transients Program," *International Conference on Power Systems Transients-IPST 2003 in New Orleans, USA*, pp. 1-6, 2003.
- [28] A. Zupan, A. T. Teklic, and B. Filipovic-Grcic, "Modeling of 25 kV Electric Railway System for Power Quality Studies," *EuroCon 2013.Zagreb, Croatia*, pp. 844-849, 2013.
- [29] M. Karagoz, *Analysis of the Pantograph Arcing and Its Effect of the Railway Vehicle*, M. Degree Thesis, Middle East Technical University. pp. 59-72, 2014.
- [30] F. Achouri, I. Achouri, and M. Khamliche, "Protection of 25 kV Electrified Railway System," *4th International Conference on Electrical Engineering (ICEE)*, pp. 1-6, 2015.
- [31] G. Lee, and C. Goldsworthy, "Introduction to the Alternative Transients Program (ATP)," *IEEE SPDC Spring Meeting in Bonneville Power Administration (BPA)*, pp. 1-110, 2011.
- [32] W. Wu, X. Cao, "Power System Electromagnetic Transient Calculation with EMTP Application," *Beijing: China Water & Power Press*, pp. 232-249, 2012.
- [33] IEC 60850:2014, "Railway Applications-Supply Voltages of Traction Systems," *International Electrotechnical Commission standard*, 2014.



**Kelvin Melckzedek Minja** was born in Tanga, Tanzania in 1989. He completed his B.Eng. in Electrical Engineering in 2015 from Dar es Salaam Institute of Technology. He is currently a Master's Degree student at the School of Electrical Engineering, Institute of Engineering at the Suranaree University of Technology in Thailand.



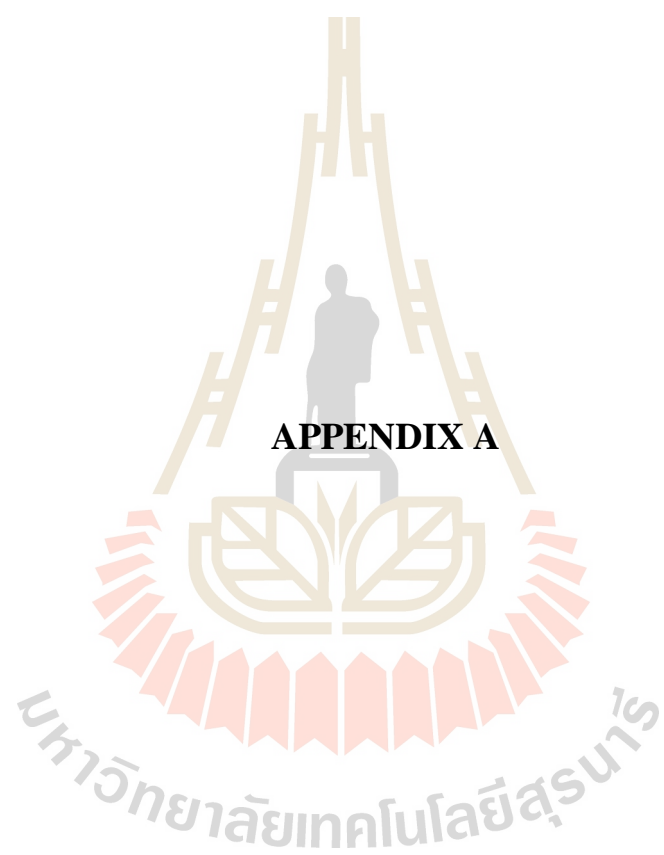
**Pius Victor Chombo** has obtained his B.Eng. Degree in Electrical Engineering from Dar es Salaam Institute of Technology, Tanzania in 2013. He is now a Master's Degree student in the School of Electrical Engineering, the Suranaree University of Technology in Thailand. His interest research topics include High Voltage Systems Design and Monitoring, Laboratory and System Programming.



**Narupon Promvichai** has obtained his B.Eng. Degree in the School of Electrical Engineering, the Suranaree University of Technology in Thailand, 2015. He is now a Master's Degree student in the School of Electrical Engineering, the Suranaree University of Technology in Thailand.



**Boonruang Marungsri** was born on 1973 in Nakhon Ratchasima Province, Thailand. He received his B. Eng. in 1996 and M. Eng. in 1999 from Chulalongkorn University, Thailand and D. Eng. in 2006 from Chubu University, Kasugai, Aichi, Japan, all in electrical engineering, respectively. Dr. Marungsri is currently a lecturer in School of Electrical Engineering, Suranaree University of Technology, Thailand. His areas of interest are electrical power system and high voltage insulation technologies.



**APPENDIX A**

## List of Publications

### ARTICLES IN JOURNALS

Minja, K.M., Chombo, P.V., Promvichai, N., and Marungsri, B. (2017). **Analysis of Flashover Induced by Transient Current During Multiple Lightning Strokes on a Train**, Accepted to be published by International Review on Modelling and Simulations (IREMOS), Vol. 10, No. 3, pp. 160-168.

Minja, K.M., Chombo, P.V., Promvichai, N., and Marungsri, B. (2017). **Transient Current Behaviour during Multiple Lightning strokes on Multiple Unit Trains**, Accepted to be published by ECTI Transactions on Electrical Eng., Electronics, and Communications, Vol 15, No 2, pp. 47-56.

### ARTICLES IN CONFERENCES

Minja, K.M., Chombo, P.V., Promvichai, N., Leeton, U., and Marungsri, B. (2017). **Characteristics and Behavior of Transient Current during Multiple Lightning strokes on a Train in Thailand by using ATPDraw**, Accepted to be published by Proceedings of the 5<sup>th</sup> IIAE International Conference on Industrial Application Engineering 2017, pp. 199-205.

Minja, K.M., Chombo, P.V., Promvichai, N., Leeton, U., and Marungsri, B. (2017). **Mitigation of Flashover from Multiple Lightning strokes in Overhead Catenary System by using ATPDraw**, Accepted to be published by 2017 IEEJ PE&S – IEEE PES Thailand Symposium on Advanced Technology in Power System, Bangkok, Thailand, pp. 119-123.

## Characteristics and Behavior of Transient Current during Multiple Lightning strokes on a Train in Thailand by using ATPDraw

Kelvin Melckzedek Minja, Pius Victor Chombo, Narupon Promvichai, Uthen Leeton, Boonruang Marungsri\*

School of Electrical Engineering, Suranaree University of Technology  
111 University Avenue, Muang District, Nakhon Ratchasima 30000, Thailand.

\*Corresponding Author: bmshvee@sut.ac.th

### Abstract

This study describes characteristics and behavior of transient current during Multiple lightning strokes on train's pantograph of 2x25 kV AC, 50 Hz Catenary Contact System. 25 kV AC, 50 Hz Catenary Contact System on double-track elevated railway system which connects Suvarnabhumi Airport to central Bangkok (Phayathai, Makkasan) was used in the study. The characteristics of transient current in term of its magnitude, front times and tail times affected by Multiple lightning strokes were studied. The assumption of studies based on the return Multiple lightning strokes current ranging 1–200 kA, front time of multiple lightning strokes between 1–3  $\mu$ s, elevated pole resistance of 50  $\Omega$  and grounding resistance of 5  $\Omega$ . The Behaviour of transient current when the pantograph is at the Mast (4<sup>th</sup> Mast) for Case 1 and at the mid-span of Masts (3<sup>rd</sup> and 4<sup>th</sup> Masts) for Case 2 were also studied. The Catenary Contact System on elevated railway system with a train and multiple lightning strokes were modeled in ATPDraw software. Transient current of negative multiple lightning strokes showed flashovers across insulators in any magnitude and waveform for Case 1 and Case 2. The improved protection for Catenary Contact System should consider the effects of negative multiple lightning strokes.

**Keywords:** Catenary, Elevated pole, Multiple lightning strokes, Flashover, ATPDraw.

### 1. Introduction

Until recently, Catenary Contact System has been the most traction power supply system to deliver power to electric train<sup>(1-2)</sup>. However, most of the overhead catenary transmission lines suffer from the lightning problems<sup>(2-3)</sup>.

Lightning strokes are the major source of transient current with random characteristics and behavior which may lead to power system failure<sup>(3-5)</sup>. The overvoltage due to transient current during lightning strokes was shown to be mostly likely caused by a stroke to phase conductor, shielding wire, and ground in line proximity<sup>(3,6)</sup>. But the stability of power system can be more affected when lightning strikes on conductors<sup>(6-7)</sup>. Flashover occurs when the induced overvoltage exceeds lightning withstand voltage level of insulators<sup>(2)</sup>. Current research studies have explained lightning effects when strikes in the Overhead Catenary Transmission line<sup>(1,3,8-13)</sup>.

Thailand is among of tropical countries which experience thunderstorm days and lightning activities per year. The report of lightning statistics in Thailand from Marungsri et al.<sup>(14)</sup> showed that lightning often occurs in April-May but severely in June. The magnitude of 11-171 kA with positive polarity and -10 to -139 kA with negative polarity were reported. Positive lightning strokes were accounted for 5% while negative were 95% with the magnitude of -10 to -50 kA. Negative lightning was showed to have a higher possibility of a multiplicity of strokes per flash<sup>(15-18)</sup>. Most of the studies in the overhead catenary system have been examined the effects of lightning strikes on the mast, conductors, and traction substation by using several transient programs for simulation<sup>(1,3,8-12)</sup>. These studies have been done on single lightning strokes without considering the effects of multiple lightning strokes. Despite the fact that the lightning protection was studied, but it is important to understand the variation of transient current behavior during multiple lightning strokes in different waveforms while doing lightning protection analysis.

In this paper, characteristic of transient current in a 25

kV Overhead Catenary transmission line is presented by using ATPDraw software. The behaviors of peak current, when negative multiple lightning strokes strike on pantograph are investigated.

**2. Background**

The examined system uses overhead catenary transmission line on elevated railway system which is designed with catenary wire, return wire and auxiliary wire as indicated in Fig. 1. The supply voltage of the system is 25 kV AC-50 Hz as per IEC 60850:2014<sup>(19)</sup>. An overhead catenary transmission line of 480 m length supported by 7 masts with 60 m spacing was selected for simulation. The supply voltage was applied on both end points of the line. Since lightning behavior is unpredictable, the strike on pantograph as part of the conductor was mostly considered. Case 1 was considered the strike on pantograph at the 4<sup>th</sup> Mast (see Fig. 1(a)) and Case 2 between the 3<sup>rd</sup> and 4<sup>th</sup> Masts (see Fig. 1(b)). The magnitudes of -34 kA, -50 kA, and -100 kA with 1/30.2  $\mu$ s, 1.2/50  $\mu$ s, 2/77.5  $\mu$ s and 3/75  $\mu$ s waveforms were used as lightning sources<sup>(14)</sup>. The elevated poles and grounding resistances were assumed to be 50  $\Omega$  and 5  $\Omega$  respectively.

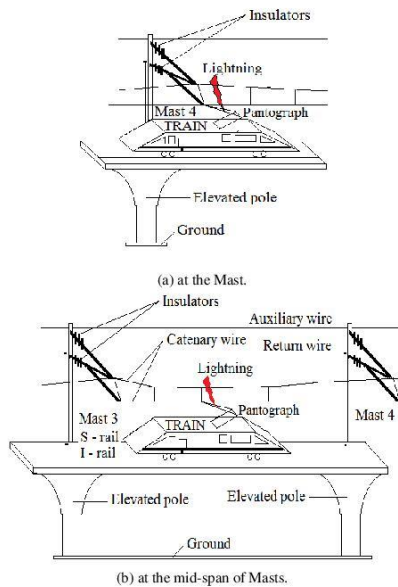


Fig. 1. Lightning strike on train's pantograph.

**3. Modeling of Catenary Contact System**

**3.1 Overhead Catenary Transmission line**

The details of Overhead Catenary Transmission line involved Catenary line (R1), return line (R2), Auxiliary line (R3) with running rails (S-rail, I-rail) and distributed-parameter line spans on both sides of the impact point were given Table 1<sup>(12)</sup>. A Railway Transmission line was modeled by LCC\_8 with JMARTI model in ATPDraw as shown in Fig. 2. Catenary line, return line, Auxiliary line includes S-rail and I-rail were considered in this study as in Mazloom<sup>(12)</sup>; Achouri, Achouri, and Khamliche<sup>(8)</sup> with Autotransformer and Booster transformer as modeled by 1:1 ideal transformers in ATPDraw. Yang and Zhang<sup>(9)</sup> showed that Autotransformer and Booster transformer force the traction current to return through designated return conductors to traction supply. Also, it reduces stray current which may cause electromagnetic interference with electrical systems in the vicinity of the railway system. Mast configuration parameters of 2x25 kV AC, 50 Hz Catenary Contact System are given in Table 2<sup>(13)</sup>.

Table 1. Details of 25 kV Overhead Catenary Transmission Line<sup>(12)</sup>.

Overhead Catenary Transmission line					
Conductors	Catenary	Return	Auxiliary	S-rail	I-rail
Radius (cm)	5.06	0.82	0.56	4.95	4.95
Ruling Span	Between Masts (m)				
	60				
Earthing Resistance	Grounding ( $\Omega$ )		Elevated Pole ( $\Omega$ )		
	5		50		
Insulators (Impulse Withstand Voltage)					
	Rod/Composite (R1)	Spool (R2)	Pin (R3)		
	225 kV	60 kV	140 kV		

Table 2. Mast Configuration<sup>(13)</sup>.

Parameters					
$h_1$ (m)	$h_2$ (m)	$h_3$ (m)	$h_4$ (m)	$h_5$ (m)	$h_6$ (m)
8	6.55	5.5	5.3	0.96	0.96
$r_1$ (m)	$r_2$ (m)	$r_3$ (m)	$r_4$ (m)	$r_5$ (m)	$r_6$ (m)
1.12	2.5	0.12	2.5	1.74	3.26

#	PI (m)	Posut (ohm/ln AC)	Rout (ohm)	Resis (ohm/ln AC)	Alice (m)	Wlowe (m)	Wind (m)
1	1	0	4.95	1.75E-6	0.70	0.33	0.90
2	2	0	0.82	3.04E-7	2.62	5.5	5.5
3	3	0	0.06	1.39E-5	0	5.3	5.3
7	A	U	1.86	2.57E-7	3.82	0	0
8	E	U	4.95	1.75E-6	0.70	0.33	0.90

Fig. 2. Transmission line data in ATPDraw.

**3.2 Multiple Lightning Source Model**

Negative lightning stroke with magnitudes of -10 to -50 kA, its association with multiple strokes per flash averaging 3 to 4 strokes per flash with intervals of tens of milliseconds were the most reported lightning incidences in Marungsri et al.<sup>(14)</sup>, Omidiora and Lehtonen<sup>(15,17)</sup>, Martinez-Velasco and Aranda<sup>(16)</sup>, Rodriguez-Sanabria, Ramos-Robles, and Orama-Exclusa<sup>(18)</sup>. Three strokes per flash were used with intervals of 1 ms. The 1<sup>st</sup> stroke was modeled with Heidler ideal source, the 2<sup>nd</sup> and 3<sup>rd</sup> strokes were modeled with two slope Ramp Type 13 in ATPDraw based on the characteristic of the lightning strokes. Parameters of lightning sources are given in Table 3, and the waveform of the multiple strokes is shown in Fig. 3.

Table 3. Parameters of multiple lightning sources<sup>(14-18)</sup>.

Parameters	Source 1	Source 2	Source 3
Type	Heidler 15	Ramp 13	Ramp 13
Multiple lightning sources. (kA)	-34	-26	-23
	-50	-42	-39
	-100	-92	-89
To	0	0	0
A1	0	0	0
T1(sec)	0	0.0003	0.0003
TSta (sec)	0	0.0016	0.0029
TSto (sec)	0.0006	0.0019	0.0032

Three ideal sources were used for the multiple lightning stroke current, with time duration of 0.6 ms for 1<sup>st</sup> stroke and 0.3 ms for 2<sup>nd</sup> and 3<sup>rd</sup> strokes each.

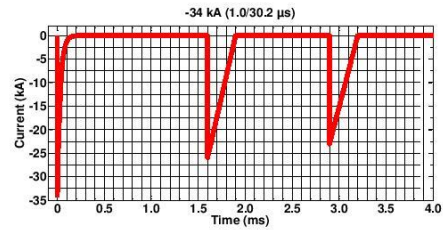


Fig. 3. Waveforms of the 1<sup>st</sup>, 2<sup>nd</sup> and 3<sup>rd</sup> lightning of -34 kA (1.0/30.2 μs) strokes modeled in ATP EMTP.

**3.3 Mast Model**

The mast was modeled by cylindrical geometrical steel column in single wave impedance model as recommended by IEEE and CIGRE in expression (1)<sup>(9,20)</sup>. The modeled parameters of the mast are shown in Table 4.

$$Z = 60 \ln \cot \left[ 0.5 \arctan \left( \frac{R}{H} \right) \right] \quad (1)$$

Table 4. Modeled Parameters of Mast.

Location	Parameters
Auxiliary	Zaux= 157.64 Ω, L1= 2.5 m
Return	Zreturn=293.57 Ω, L2= 0.2 m
Catenary	Zcatenary= 113.77 Ω, L3= 5.3 m

**3.4 Train Model**

The three-car train was modeled as electric locomotive which contains Pantograph, Locomotive transformer, Diode rectifier bridge and two DC motors as in Zupan, Teklić, and Filipović-Grčić<sup>(21)</sup>; Karagöz<sup>(22)</sup>. Figs. 4 shows the model of Train contains Pantograph, Locomotive transformer, Diode rectifier bridge and one DC motor with Railway Transmission line, Mast, Elevated pole, Ground and Insulators at the Mast and at the mid-span of Masts. Insulators of Mast were modeled with a branch of capacitor and voltage controlled switch as shown in Fig. 4(a). To model this insulator, Switchvc.sup model was used in ATPDraw with voltage withstand capability as calculated values given in Table 1<sup>(23)</sup>.



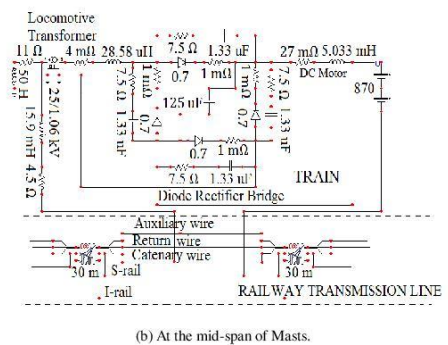
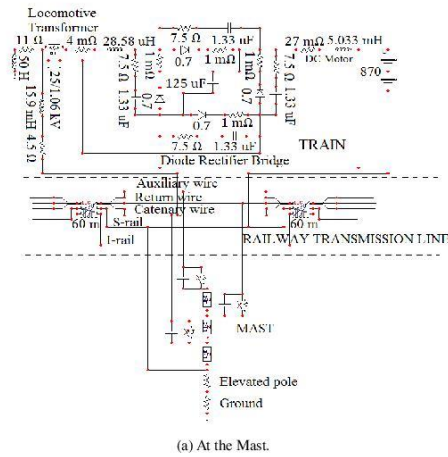


Fig. 4. Train modeled in ATPDraw.

### 4. Simulation Results

A 25 kV Railway Transmission line with 7 masts in Case 1 and Case 2 were simulated in ATPDraw with multiple lightning sources on the pantograph where elevated poles and grounding resistance were set to 50 Ω and 5 Ω unchanged respectively. The magnitude, front time and tail time of negative multiple lightning strokes were studied as factors that cause a transient current which leads flashover across insulators.

As the impulse voltage withstand capability of insulator depends on the front time of lightning stroke current, the multiple lightning stroke current of -34 kA with 1/30.2 μs, 1.2/50 μs, 2/77.5 μs and 3/75 μs was first used in

the simulation. The lightning induced voltages across the insulators of the Mast 4 in Auxiliary, Return, and Catenary lines are shown in Fig. 5, 6, 7, and 8. Results of lightning induced voltages across the insulators with the magnitude of -50 and -100 kA in Auxiliary, Return and Catenary lines at 1/30.2 μs, 1.2/50 μs, 2/77.5 μs and 3/75 μs waveforms are shown in Fig. 9, 10, 11, 12, 13, 14, 15 and 16.

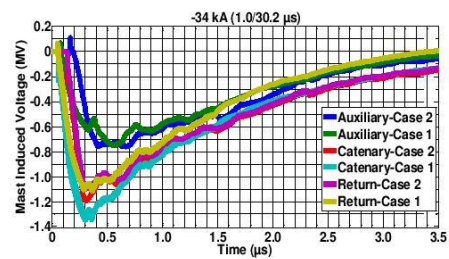


Fig. 5. Mast Induced Voltage Waveform of the 1<sup>st</sup>, 2<sup>nd</sup> and 3<sup>rd</sup> lightning current of -34 kA (1.0/30.2 μs) strokes.

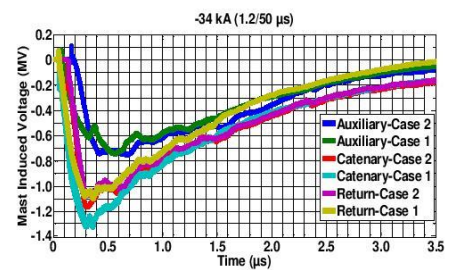


Fig. 6. Mast Induced Voltage Waveform of the 1<sup>st</sup>, 2<sup>nd</sup> and 3<sup>rd</sup> lightning current of -34 kA (1.2/50 μs) strokes.

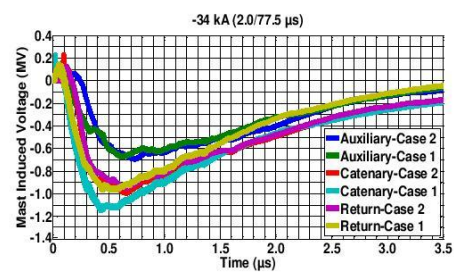


Fig. 7. Mast Induced Voltage Waveform of the 1<sup>st</sup>, 2<sup>nd</sup> and 3<sup>rd</sup> lightning current of -34 kA (2/77.5 μs) strokes.

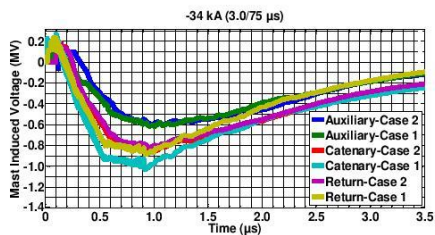


Fig. 8. Mast Induced Voltage Waveform of the 1<sup>st</sup>, 2<sup>nd</sup> and 3<sup>rd</sup> lightning current of -34 kA (3/75 μs) strokes.

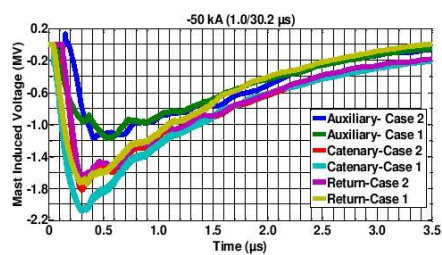


Fig. 9. Mast Induced Voltage Waveform of the 1<sup>st</sup>, 2<sup>nd</sup> and 3<sup>rd</sup> lightning current of -50 kA (1.0/30.2 μs) strokes.

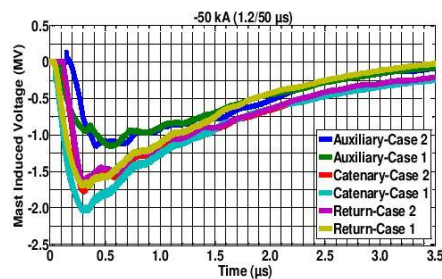


Fig. 10. Mast Induced Voltage Waveform of the 1<sup>st</sup>, 2<sup>nd</sup> and 3<sup>rd</sup> lightning current of -50 kA (1.2/50 μs) strokes.

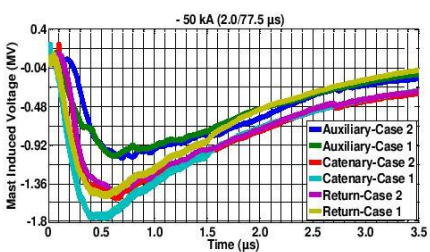


Fig. 11. Mast Induced Voltage Waveform of the 1<sup>st</sup>, 2<sup>nd</sup> and 3<sup>rd</sup> lightning current of -50 kA (2.0/77.5 μs) strokes.

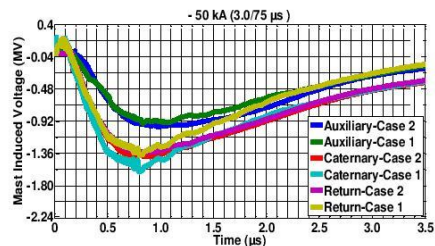


Fig. 12. Mast Induced Voltage Waveform of the 1<sup>st</sup>, 2<sup>nd</sup> and 3<sup>rd</sup> lightning current of -50 kA (3.0/75 μs) strokes.

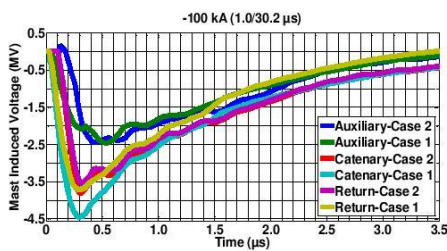


Fig. 13. Mast Induced Voltage Waveform of the 1<sup>st</sup>, 2<sup>nd</sup> and 3<sup>rd</sup> lightning current of -100 kA (1.0/30.2 μs) strokes.

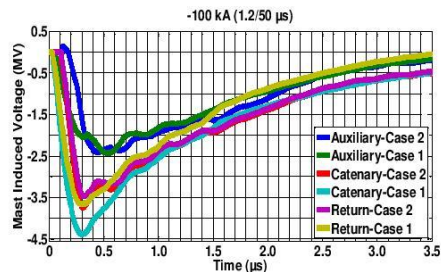


Fig. 14. Mast Induced Voltage Waveform of the 1<sup>st</sup>, 2<sup>nd</sup> and 3<sup>rd</sup> lightning current of -100 kA (1.2/50 μs) strokes.

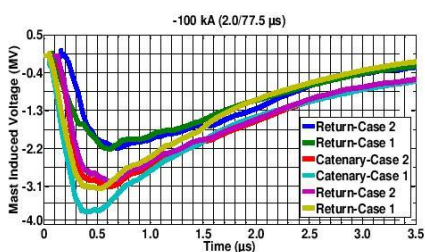


Fig. 15. Mast Induced Voltage Waveform of the 1<sup>st</sup>, 2<sup>nd</sup> and 3<sup>rd</sup> lightning current of -100 kA (2.0/77.5 μs) strokes.

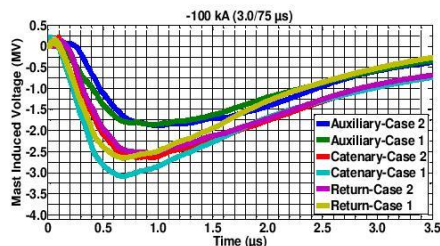


Fig. 16. Mast Induced Voltage Waveform of the 1<sup>st</sup>, 2<sup>nd</sup> and 3<sup>rd</sup> lightning current of -100 kA (3.0/75 μs) strokes.

The magnitudes of mast induced voltages and flashover across insulators with multiple lightning strokes current for Case 1 and Case 2 are shown in Table 5 and Table 6 respectively.

Table 5. Magnitudes of Mast induced voltages (MV).

Case 1									
Lightning	-34 kA			-50 kA			-100 kA		
Waveforms	Ax	Rt	Ct	Ax	Rt	Ct	Ax	Rt	Ct
1.0/30.2 μs	0.8	1.1	1.3	1.2	1.7	2.1	2.5	3.7	4.5
1.2/50 μs	0.7	1.1	1.3	1.2	1.7	2.0	2.4	3.7	4.4
2.0/77.5 μs	0.7	1.0	1.2	1.1	1.5	1.8	2.2	3.2	3.7
3.0/75 μs	0.6	0.9	1.0	0.9	1.4	1.6	1.9	2.7	3.1
Case 2									
Lightning	-34 kA			-50 kA			-100 kA		
Waveforms	Ax	Rt	Ct	Ax	Rt	Ct	Ax	Rt	Ct
1.0/30.2 μs	0.8	1.1	1.2	1.2	1.7	1.8	2.5	3.5	3.8
1.2/50 μs	0.8	1.1	1.2	1.2	1.6	1.8	2.4	3.5	3.8
2.0/77.5 μs	0.7	1.0	1.0	1.1	1.5	1.5	2.2	3.0	3.1
3.0/75 μs	0.6	0.8	0.9	1.0	1.3	1.4	1.9	2.5	2.6

Table 6. Flashover across insulators.

Case 1									
Lightning	-34 kA			-50 kA			-100 kA		
Waveforms	Ax	Rt	Ct	Ax	Rt	Ct	Ax	Rt	Ct
1.0/30.2 μs	s	s	s	s	s	s	s	s	s
1.2/50 μs	s	s	s	s	s	s	s	s	s
2.0/77.5 μs	s	s	s	s	s	s	s	s	s
3.0/75 μs	s	s	s	s	s	s	s	s	s
Case 2									
Lightning	-34 kA			-50 kA			-100 kA		
Waveforms	Ax	Rt	Ct	Ax	Rt	Ct	Ax	Rt	Ct
1.0/30.2 μs	s	s	s	s	s	s	s	s	s
1.2/50 μs	s	s	s	s	s	s	s	s	s
2.0/77.5 μs	s	s	s	s	s	s	s	s	s
3.0/75 μs	s	s	s	s	s	s	s	s	s

Key: S - flashover, Ax - Auxiliary line, Rt - Return line and Ct - Catenary line

### 5. Conclusion

This paper has studied the characteristics of transient current in term of its magnitude, front times and tail times of negative Multiple lightning strokes and its behavior when the pantograph is at the Mast (4<sup>th</sup> Mast) and at the mid-span of Masts (3<sup>rd</sup> and 4<sup>th</sup> Masts). The analysis was made for the flashover voltage across insulators of a 2x25 kV,50 Hz AC Catenary Contact system used in Thailand. It was seen that shorter front time, resulted into higher mast induced voltage. Similarly, a higher magnitude of Multiple lightning strokes, induced higher voltages across mast insulators for case 1 and case 2. The Flashover occurred for all waveforms and current magnitude from -34 kA to -100 kA when pantograph was at the Mast and at the mid-span of Masts. Critical flashover voltage was found in case 1 compared to case 2. Therefore, short front time and high magnitude of negative multiple lightning strokes are key parameters which may be considered in lightning protection.

### Acknowledgment

This work was supported by Laboratory of High Voltage Insulation Technologies of Suranaree University of Technology, Thailand.

### References

- (1) Sokratis Pastromas, Alkistis Papamikou, Georgios Peppas, and Eleftheria Pyrgioti : "Investigation of grounding resistance effect on the MV grid of Hellenic electromotive railway during lightning strikes", 33<sup>rd</sup> International Conference on Lightning Protection, pp. 1-7, 2016.
- (2) Friedrich Kiessling, Rainer Puschmann, Axel Schmieder, and Egid Schneider : "Contact Lines for Electrical Railways: Planning - Design - Implementation - Maintenance", 2<sup>nd</sup> edition, Siemens Aktiengesellschaft, Berlin and Murnich, pp. 123-876, 2009.
- (3) Tomasz Chmielewski, and Andrzej Dziadkowiec : "Simulations of Fast Transients in typical 25 kV a.c. railway power supply system", Seminarium ZASTOSOWANIE KOMPUTERÓW W NAUCE I

- TECHNICE 2013, Gdańsk, Polska, Vol. 23, No. 36, pp. 43-46, 2013.
- (4) R. Bhattarai, R. Rashedin, S. Venkatesan, A. Haddad, H. Griffiths, and N. Harid : "Lightning performance of 275 kV Transmission lines", 43<sup>rd</sup> International Universities Power Engineering Conference, pp. 1-5, 2008.
- (5) IEEE Std 1100 : "IEEE Recommended Practice for Powering and Grounding Electronic Equipment", IEEE Standards, 1999.
- (6) IEEE Std 1313.2 : "IEEE Guide for the Application of Insulation Coordination", IEEE Standards, 1999.
- (7) Pantelis N. Mikropoulos and Thomas E. Tsovilis : "Estimation of the shielding performance of overhead transmission lines: the effects of lightning attachment model and lightning crest current distribution", IEEE Transactions on Dielectrics and Electrical Insulation, Vol. 19, No. 6, pp. 2155-2164, 2012.
- (8) Farid Achouri, Imed Achouri, and Mabrouk Khamliche : "Protection of 25 kV Electrified Railway System", 4th International Conference on Electrical Engineering(ICEE), pp. 1-6, 2015.
- (9) Yuxin Yang, and Youpeng Zhang : "Research on Lightning Protection Simulation of High-speed Railway Catenary Based on ATP-EMTP", Journal of information & Computation Science, Vol 12, No. 4, pp. 1511-1521, 2015.
- (10) Liu, J., and Liu, M.G. "Improved electro-geometric model for estimating lightning outage rate of catenary," IET Electrical Systems in Transportation, Vol. 2, pp. 1-8, 2012.
- (11) Avishkar Vijay Wanjari : "Effect of Lightning on the Electrified Transmission Railway System", International Journal of Advance Research in Electrical, Electronics and Instrumentation Engineering, Vol. 3, Issue. 7, pp. 10663-10671, 2014.
- (12) Ziya Mazloom : "Multi-conductor transmission line model for electrified railways: A method for responses of lumped devices", Doctoral Thesis, KTH Electrical Engineering University, Stockholm, Sweden, pp. 59-72, 2010.
- (13) Amedeo Andreotti, Umberto De Martinis, Antonio Pierno1, and Vladimir A. Rakov : "A New Tool for Lightning Induced Voltage Calculations: CiLIV", General Assembly and Scientific Symposium (URSI GASS), 2014 XXXIth URSL, pp. 1-4, 2014.
- (14) Boonruang Marungsri, Suphachai Boonpoke, Anucha Rawangpai, Anant Oonsivilai, and Chanin Kritayakornupong : "Study of Tower Grounding Resistance Effected Back Flashover to 500kV Transmission Line in Thailand by using ATP/EMTP", International Journal of Electrical, Computer, Energetic, Electronic and Communication, Vol. 2, No. 6, pp. 1061-1068, 2008.
- (15) Michael A. Omidiora, and Matti Lehtonen : "Performance of Surge Arrester to Multiple Lightning Strokes on Nearby Distribution Transformer", Proceedings of the 7th WSEAS International Conference on Power Systems, Beijing, China, pp. 59-65, 2007.
- (16) Juan A. Martínez-Velasco, and Ferley Castro-Aranda : "EMTP Implementation of a Monte Carlo Method for Lightning Performance Analysis of Transmission Lines", Ingeniare. Revista chilena de ingeniería, Vol. 16, No. 2, pp. 169-180, 2008.
- (17) Michael A. Omidiora, and Matti Lehtonen : "Simulation of Combined Shield Wire and MOV Protection on Distribution Lines in Severe Lightning Areas", Proceedings of the World Congress on Engineering and Computer Science, 2007.
- (18) Doeg Rodríguez-Sanabria, Carlos Ramos-Robles, and Lionel R. Orama-Exclusa : "Lightning and Lightning Arrester Simulation in Electrical Power Distribution Systems", pp. 1-9, 2011.
- (19) IEC 60850 : "Railway Applications – Supply Voltages of Traction Systems", International Electrotechnical Commission standard, 2014.
- (20) Zhang Yongji, Sima Wenxia, and Zhang Zhijin : "Summary of the study of tower models for lightning protection analysis", High Voltage Engineering, pp. 93-97, 2006.
- (21) Alan Župan, Ana Tomasović Teklić, and Božidar Filipović-Grčić : "Modeling of 25 kV Electric Railway System for Power Quality Studies", EuroCon 2013, Zagreb, Croatia, pp. 844-849, 2013.
- (22) Mustafa Karagöz : "Analysis of the Pantograph Arcing and Its Effect of the Railway Vehicle", Master Degree Thesis, Middle East Technical University, pp. 59-72, 2014.
- (23) Ali F. Imece, Daniel W. Durbak, Hamid Elahi, Sharma Kolluri, Andre Lux, Doug Mader, Thomas E. McDemott, Atef Morched, Abdul M. Mousa, Ramasamy Natarajan, Luis Rugeles, and Eva Tarasiewicz : "Modeling Guidelines for Fast Front Transients", IEEE Transactions on Power Delivery, Vol. 11, No. 1, pp. 493-506, 1996.

# Mitigation of Flashover from Multiple Lightning strokes in Overhead Catenary System by using ATPDraw.

Kelvin Melckzedek Minja, Pius Victor Chombo, Narupon Promvichai and Boonruang Marungsri \*

School of Electrical Engineering, Institute of Engineering, Suranaree University of Technology  
111 University Avenue, Nakhon Ratchasima 30000, Thailand.

\* Corresponding Author Email: bmshee@sut.ac.th

**Abstract**—This paper studies significance of mitigating flashover across insulators used in Overhead Catenary System. The improvement of lightning performance with surge arrester's installation intervals between Phayathai to Rajaprarop was analyzed by using ATPDraw software. The multiple lightning strokes with a front time of 1–3  $\mu$ s, elevated pole resistance of 50  $\Omega$  and soil resistance ranging 5-100  $\Omega$  were used in the simulation. It was seen that the flashover might occur when lightning strikes on the pantograph in installation interval 1, 4 and 6. However, the flashover was not observed to happen when it hits on the pantograph in installation interval 2, 3 and 5. From these results, it is evinced that installation intervals are convenient to improve the lightning performance or mitigating the flashover.

**Keywords**—catenary; flashover; multiple lightning strokes; surge arrester; installation interval.

## I. INTRODUCTION

Catenary contact system is among of Electric Railway transportation line which continues to be admired by many people due to its improvement on electrification of the overhead catenary system in recent years [1-3]. It consists of two parts which are traction power supply and overhead catenary system. However, lightning has become the primary disturbance of overhead catenary system which sometimes can lead to failure in the system [1-2]. The overvoltages due to lightning strokes were shown to either occur in stroke to phase conductor, shield wire or ground in line proximity [1, 4]. Flashover across insulators caused by the lightning induced voltage in the overhead contact line has been presented in [2, 5]. Current studies have demonstrated the effects of lightning when strikes in the overhead catenary system [1, 3, 5-11].

Thailand is one among the countries which use Overhead Contact system in its Railway public transportation. Reports have shown the presence of lightning magnitude with negative polarity ranges -10 to -139 kA which accounts for 95% [12]. The current magnitude of -50 kA was the most occurring and minimum amount of all lightning incidences [12]. However, it has been presented that the association of Negative lightning with multiple strokes averaging 3 to 4 strokes per flash in intervals of tens of milliseconds [13-16]. In Catenary contact system, the mostly like area to be stroke by lightning are a mast, conductors, and traction substation [1, 3, 5-7, 9-11]. But

the Lightning lead to the most severe overvoltage when it strikes on conductors [4, 17]. Mitigating overvoltage in AC Railway System, effective protection against lightning must be used. Surge arrester has been recently used as an effective protection against lightning voltage surges [2,18-23]. Regardless of its importance in reduce lightning overvoltage, installed surge arrester in all masts seem to have better performance although this solution is very expensive [24]. Therefore, installation of Surge arrester at intervals in every mast needs to study in order to improve economic conditions of power network [25].

In the overhead catenary system, ATPDraw software is utilized to simulate the effects of transient current with surge arrester application on the elevated railway system. The performance of surge arrester connected to the catenary wire and rails when negative multiple lightning stroke strike on pantograph are examined at different installation intervals.

## II. BACKGROUND

The overhead catenary system electrifies Thai Railway public transportation with a nominal voltage of 25 kV AC-50 Hz as per IEC 60850:2014 [26]. Overhead Catenary system on elevated railway system consists of catenary wire, return wire and auxiliary wire as shown in Fig. 1. Due to the vulnerability of lightning occurrences, the strokes on train's pantograph as a part of the conductor were highly presented. For simulation, 13 masts with 60 m spacing in the overhead catenary system of 840 m were selected between Phayathai to Rajaprarop as shown in Fig. 2. The nominal voltage was applied on both endpoints of the line. The configuration of installed surge arresters connected to catenary wire and rails is indicated in Fig. 1 as in [23, 27]. The surge arrester at six installation intervals was investigated. The six surge arrester's installation intervals are shown in Table I. The negative multiple lightning strokes was considered to be a strike on a pantograph at the Mast (7<sup>th</sup> Mast) for Case 1 as shown in Fig. 1(a) and at the mid-span of Masts (6<sup>th</sup> and 7<sup>th</sup> Masts) for Case 2 as shown in Fig. 1(b). The magnitudes of -50 kA with 1/30.2  $\mu$ s, 1.2/50  $\mu$ s, 2/77.5  $\mu$ s and 3/75  $\mu$ s waveforms was used as a lightning source [12]. The consequence of an action in the grounding resistances of 5, 10, 50, and 100  $\Omega$  was assumed to present different soil profiles. The induced voltage was measured across insulators as the most stressed parts in the system.

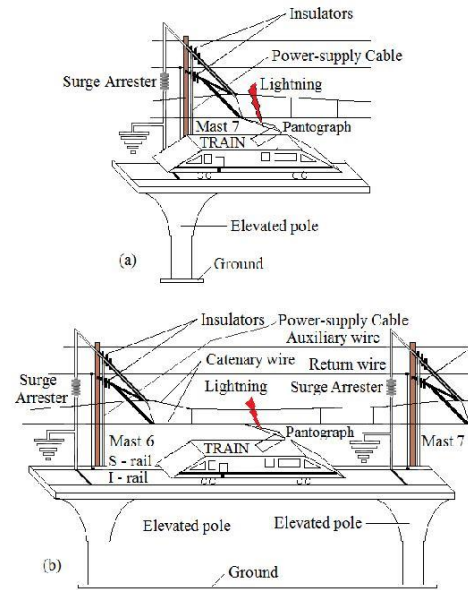


Fig. 1. Lightning stroke on train's pantograph (a) at the Mast and (b) at the mid-span of Masts, with Installed Surge Arrester.

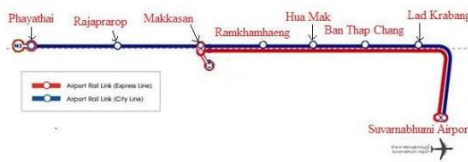


Fig. 2. Airport Rail link line in Thailand [28].

TABLE I. ARRANGEMENT OF THE SURGE ARRESTER'S INSTALLATION INTERVAL

Interval	Mast												
	1	2	3	4	5	6	7	8	9	10	11	12	13
1	☐	☐	☐	☐	☐	☐	☐	☐	☐	☐	☐	☐	☐
2	☐	☐	☐	☐	☐	☐	☐	☐	☐	☐	☐	☐	☐
3	☐	☐	☐	☐	☐	☐	☐	☐	☐	☐	☐	☐	☐
4	☐	☐	☐	☐	☐	☐	☐	☐	☐	☐	☐	☐	☐
5	☐	☐	☐	☐	☐	☐	☐	☐	☐	☐	☐	☐	☐
6	☐	☐	☐	☐	☐	☐	☐	☐	☐	☐	☐	☐	☐

☐ - No Surge Arrester  
☒ - Surge Arrester

III. MODELING OF CATENARY CONTACT SYSTEM

A. Overhead Catenary System

Overhead Catenary System was modeled by LCC\_8 with JMARTI model in ATPDraw as shown in Fig. 3 [6]. It consists of Catenary line (R1), return line (R2), Auxiliary line (R3), S-rail and I-rail with a radius of 5.06 cm, 0.82 cm, 0.56 cm, 4.95 cm and 4.95 cm respectively. Also, it has the span of 60 m between Masts along Overhead Catenary system with Autotransformer [6-7]. The autotransformer was modeled as 1:1 ideal transformers in ATPDraw to force the traction current to return through designated return conductors to traction supply in order to reduce stray current which may cause electromagnetic interference with electrical systems in the vicinity of the railway system [6]. Mast cross section view of 25 kV Overhead Catenary system has been shown in Andreotti et al. [8].

Line no.	Phase	Rout	Rloss	R-ortz	Vvower	Vvrid
	[ohm/km/AC]	[ohm]	[ohm/km/AC]	[m]	[kV]	[kV]
1	U	4.95	1.75E-5	0.46	0.56	0.56
2	0	0.82	3.04E-7	2.62	5.5	5.5
3	0	0.56	1.05E-7	0	5.3	5.3
4	0	0.56	2.61E-7	3.62	8	8
5	0	4.95	1.75E-5	0.76	0.90	0.90

Fig. 3. Railway Transmission line data in ATP EMTP

B. Multiple Lightning Source Model

A -50 kA was considered as a lightning magnitude. The 1st stroke was modeled with Heidler ideal source while 2nd and 3rd strokes were modeled with slope Ramp Type 13 in ATPDraw. The waveforms of 1.0/30.2 μs, 1.2/50 μs, 2.0/77.5 μs and 3.0/75 μs were set in the Heidler ideal source. Lightning source parameters are given in Table II, and the first waveform is shown in Fig. 4.

TABLE II. LIGHTNING SOURCE PARAMETERS [12-16].

Parameters	Source 1	Source 2	Source 3
Type	Heidler 15	Ramp 13	Ramp 13
Lightning (kA)	- 50	- 42	- 39
To	0	0	0
A1	0	0	0
T1(sec)	0	0.0003	0.0003
TSta (sec)	0	0.0016	0.0029
TSto (sec)	0.0006	0.0019	0.0032

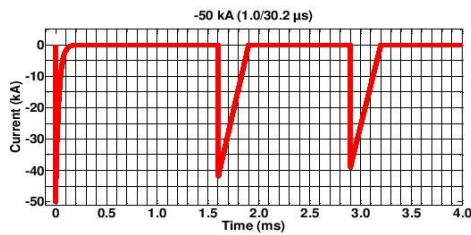


Fig. 4. Waveforms of the 1<sup>st</sup>, 2<sup>nd</sup> and 3<sup>rd</sup> lightning of -50 kA (1.0/30.2 μs) strokes modeled in ATPDraw.

The ideal sources were used for the multiple lightning stroke current, with time duration of 0.6 ms for 1<sup>st</sup> stroke and 0.3 ms for 2<sup>nd</sup> and 3<sup>rd</sup> strokes each.

C. Mast Model

The mast is modeled by cylindrical geometrical steel column in single wave impedance model as recommended by IEEE and CIGRE by expression from surge impedance as in (1) [9,29].

$$Z = 60 \ln \cot (0.5 \arctan (R/H)) \quad (1)$$

D. Train Model

The three-car train was modeled in ATPDraw as electric locomotive which contains Pantograph, Locomotive transformer, Diode rectifier bridge and two DC motors [30-31].

E. Insulator of the Mast.

A branch of capacitor and voltage controlled switch was used to model insulators of Mast. The conventional capacitor's value for suspension insulators are 80 pF/unit while for pin insulators are around 100pF/unit [22]. Switchvc.sup and capacitor in ATPDraw were used to model Rod/Composite (R1), Spool (R2), and Pin (R3) insulators with voltage withstand capability of 225 kV, 60 kV, and 140 kV respectively [6].

F. Metal Oxide Surge Arrester.

Metal Oxide Surge Arrester that used in the simulation have a rated of 36.3 kV with the nominal discharge current of 10 kA, discharge energy class 3 and withstand energy capability of 9 kJ/kV [32]. The MO surge arrester was selected under IEC Std. 60099-5 and IEEE Std. C62.22-2009 [33-34]. In ATPDraw software, it was modeled by using MOV Type 92 present two non-linear resistances A0 and A1 with V-I curve characteristics as shown in Fig. 5 and separated by two inductances with resistance R (1 MΩ) placed between model terminal as shown in Fig. 6. The V-I curve characteristics, Inductances L0 (270 nH) and L1 (810 nH) were calculated using equations (2) - (7). Durbak has proposed this model and adopted by the IEEE WG 3.4.11, including committee papers

and standards (IEEE Std. C62.22-2009), and then modified by Pinceti [19,16,35-37].

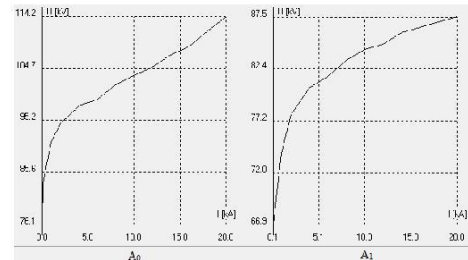


Fig. 5. Non-linear resistances V-I curve of A0 and A1 in ATPDraw.

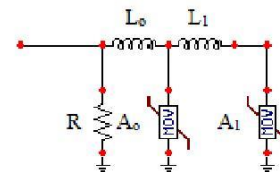


Fig. 6. Pinceti model in ATPDraw.

$$V \text{ in kV} = [\text{Relative IR in p.u. for } A_0(i) \times V_{10}/1.6] \quad (2)$$

$$V \text{ in kV} = [\text{Relative IR in p.u. for } A_1(i) \times V_{10}/1.6] \quad (3)$$

$$i = p(V/V_{ref})^q \quad (4)$$

$$L_0 = 1/12 \times (K-1) \times V_n \text{ (}\mu\text{H)} \quad (5)$$

$$L_1 = 1/4 \times (K-1) \times V_n \text{ (}\mu\text{H)} \quad (6)$$

$$K = V_{1/T2}/V_{10} \quad (7)$$

Where

V = the discharge voltage in kV, V<sub>ref</sub> = reference voltage in kV, q = exponent, p = multiplier, V<sub>n</sub> = the arrester rated voltage in kV, V<sub>10</sub> = the discharge voltage for a 10 kA, 8/20 μs current in kV, and V<sub>1/T2</sub> = the discharge voltage for a 10-kA steep current pulse in kV

The value is similar to the front of wave (FOW) discharge voltage defined in the IEEE standard [36]. The front of the

wave (FOW), discharge voltage for selected arrester, is 94.2 kV [38].

IV. RESULTS AND DISCUSSION.

A 25 kV Overhead Catenary system with 13 masts for both Cases were simulated in ATPDraw with multiple lightning sources on the train's pantograph where elevated poles of 50 Ω and grounding resistances (Rf) of 5,10,50 and 100 Ω were accounted for presenting different soil profiles respectively at different Surge Arrester's installation intervals. The magnitude was set to -50 kA in waveforms of 1.0/30.2 μs, 1.2/50 μs, 2.0/77.5 μs and 3.0/75 μs for Surge Arrester's installation interval. The occurrence of flashover across insulators of Mast 7 is indicated in Tables III-VI.

TABLE III. FLASHOVER ACROSS INSULATORS (1.0/30.2 μs).

50 kA, 1.0/30.2 μs						
Case 1						
Rf	Surge Arrester's installation interval					
	1	2	3	4	5	6
5	O	X	X	O	X	O
10	O	X	X	O	X	O
50	O	X	X	O	X	O
100	O	X	X	O	X	O
Case 2						
5	O	X	X	O	X	O
10	O	X	X	O	X	O
50	O	X	X	O	X	O
100	O	X	X	O	X	O

TABLE IV. FLASHOVER ACROSS INSULATORS (1.2/50 μs).

50 kA, 1.2/50 μs						
Case 1						
Rf	Surge Arrester's installation interval					
	1	2	3	4	5	6
5	O	X	X	O	X	O
10	O	X	X	O	X	O
50	O	X	X	O	X	O
100	O	X	X	O	X	O
Case 2						
5	O	X	X	O	X	O
10	O	X	X	O	X	O
50	O	X	X	O	X	O
100	O	X	X	O	X	O

TABLE V. FLASHOVER ACROSS INSULATORS (2.0/77.5 μs).

50 kA, 2.0/77.5 μs						
Case 1						
Rf	Surge Arrester's installation interval					
	1	2	3	4	5	6
5	O	X	X	O	X	O
10	O	X	X	O	X	O
50	O	X	X	O	X	O
100	O	X	X	O	X	O
Case 2						
5	O	X	X	O	X	O
10	O	X	X	O	X	O
50	O	X	X	O	X	O
100	O	X	X	O	X	O

Rf – grounding resistances

O – Flashover

X – No Flashover

TABLE VI. FLASHOVER ACROSS INSULATORS (3.0/75 μs).

50 kA, 3.0/75 μs						
Case 1						
Rf	Surge Arrester's installation interval					
	1	2	3	4	5	6
5	O	X	X	O	X	O
10	O	X	X	O	X	O
50	O	X	X	O	X	O
100	O	X	X	O	X	O
Case 2						
5	O	X	X	O	X	O
10	O	X	X	O	X	O
50	O	X	X	O	X	O
100	O	X	X	O	X	O

Rf – grounding resistances

O – Flashover

X – No Flashover.

From Tables III-VI show that flashover may occur if the lightning magnitude of -50 kA strikes on pantograph at the mast without surge arrester for all waveforms and ground resistances in case 1 and 2. It was seen that the Surge Arrester's installation intervals 2, 3 and 5 had no flashover in the magnitude of -50 kA for all waveforms and ground resistances. However, installation intervals 1, 4 and 6 showed flashovers in the magnitude of -50 kA for all waveforms and ground resistances.

V. CONCLUSION.

This paper has studied the application of Surge Arrester to mitigate flashover in a 25 kV Overhead Catenary system on the elevated railway system. Performances of surge arrester and installation intervals in different soil profiles under the lightning magnitude of -50 kA and waveforms of 1.0/30.2 μs, 1.2/50 μs, 2.0/77.5 μs and 3.0/75 μs for case 1 and 2 were studied. It was found that the performance of surge arrester depends much on the installation intervals. It was seen that Surge Arrester's installation interval 5 is the cheapest installation interval to be implemented while installation interval 2 is the most cost full one.

ACKNOWLEDGMENT

The supports with Laboratory of High Voltage Insulation Technologies of Suranaree University of Technology, Thailand are greatly appreciated.

REFERENCES

- [1] T. Chmielewski, and A. Dziadkowiec, "Simulations of Fast Transients in typical 25 kV a.c. railway power supply system," Seminarium ZASTOSOWANIE KOMPUTERÓW W NAUCE I TECHNICIE 2013, Gdańsk, Polska, vol. 23, no. 36, pp. 43-46, 2013.
- [2] F. Kiessling, R. Puschmann, A. Schmieder, and E. Schneider, Contact Lines for Electrical Railways: Planning - Design - Implementation - Maintenance, 2nd ed, Siemens Aktiengesellschaft, Berlin and Munich, 2009, pp.820-876.
- [3] S. Pastromas, A. Papamikou, G. Peppas, and E. Pyrgioti, "Investigation of grounding resistance effect on the MV grid of Hellenic electromotive railway during lightning strikes," 33rd International Conference on Lightning Protection, pp. 1-7, 2016.
- [4] IEEE Std. 1313.2-1999, "IEEE Guide for the Application of Insulation Coordination," IEEE Standards, 1999.



2017 IEEE PE&S – IEEE PES Thailand Symposium on Advanced Technology in Power System, Bangkok, Thailand, 7-8 March 2017

- [5] H. Lingohr, U. Stahlberg, B. Richter, and V. Hinrichsen, "Overvoltage protection design for DC railways," *Elektrische Bahnen*, vol. 101, no. 7, pp. 315-320, 2003.
- [6] Z. Mazloom, "Multi-conductor transmission line model for electrified railways: A method for responses of lumped devices," Doctoral Thesis, KTH Electrical Engineering University, Stockholm, Sweden, pp. 59-72, 2010.
- [7] F. Achouri, I. Achouri, and M. Khamliche, "Protection of 25 kV Electrified Railway System," 4th International Conference on Electrical Engineering (ICEE), pp. 1-6, 2015.
- [8] A. Andreotti, U. D. Martinis, A. Piemol, and V. A. Rakov, "A New Tool for Lightning Induced Voltage Calculations: CiLIV," General Assembly and Scientific Symposium (URSI GASS), 2014 XXXIth URSI, pp. 1-4, 2014.
- [9] Y. Yang, and Y. Zhang, "Research on Lightning Protection Simulation of High-speed Railway Catenary Based on ATP-EMTP," *Journal of Information & Computation Science*, Vol. 12, No. 4, pp. 1511-1521, 2015.
- [10] A.V. Wanjari, "Effect of Lightning on the Electrified Transmission Railway System," *International Journal of Advance Research in Electrical, Electronics and Instrumentation Engineering*, vol. 3, issue. 7, pp. 10663-10671, 2014.
- [11] J. Liu, and M.G. Liu, "Improved electro-geometric model for estimating lightning outage rate of catenary," *IET Electrical Systems in Transportation*, Vol. 2, pp. 1-8, 2012.
- [12] B. Marungsri, S. Boonpoke, A. Rawangpai, A. Oonsivilai, and C. Kritayakornpong, "Study of Tower Grounding Resistance Effected Back Flashover to 500kV Transmission Line in Thailand by using ATP/EMTP," *International Journal of Electrical, Computer, Energetic, Electronic, and Communication Engineering*, vol. 2, no. 6, pp. 1061-1068, 2008.
- [13] M.A. Omidiora, and M. Lehtonen, "Performance of Surge Arrester to Multiple Lightning Strokes on Nearby Distribution Transformer," *Proceedings of the 7th WSEAS International Conference on Power Systems*, Beijing, China, pp. 59-65, 2007.
- [14] J. A. Martinez-Velasco, and F. C. Aranda, "EMTP Implementation of a Monte Carlo Method for Lightning Performance Analysis of Transmission Lines," *Ingeniare. Revista chilena de ingenieria*, Vol. 16, No. 1, pp. 169-180, 2008.
- [15] M. A. Omidiora, and M. Lehtonen, "Simulation of Combined Shield Wire and MOV Protection on Distribution Lines in Severe Lightning Areas," *Proceedings of the World Congress on Engineering and Computer Science*, 2007.
- [16] D. Rodriguez-Sanabria, C. Ramos-Robles, and L. Orama-Exclusa, "Lightning and Lightning Arrester Simulation in Electrical Power Distribution Systems," pp. 1-9, 2011.
- [17] P.N. Mikropoulos and T.E. Tsovilis, "Estimation of the shielding performance of overhead transmission lines: the effects of lightning attachment model and lightning crest current distribution," *IEEE Transactions on Dielectrics and Electrical Insulation*, vol. 19, no. 6, pp. 2155-2164, 2012.
- [18] M. Nafar, G. Solookinejad, and M. Jabbari, "Comparison of IEEE and Pinceti Models of Surge Arresters," *Research Journal of Engineering Sciences*, Vol. 3, No. 5, pp. 32-34, 2014.
- [19] D.W. Durbak, "Zinc-oxide arrester model for fast surges," *EMTP Newsletter*, vol. 5, no. 1, pp. 1-9, 1985.
- [20] T. Saengsuwan, and W. Thipprasert, "The Lightning Arrester Modeling Using ATP-EMTP," *TENCON 2004. 2004 IEEE Region 10 Conference*, vol. 3, pp. 377-380, 2004.
- [21] N. Mungkung, S. Wongcharoen, T. Tanitceerapan, C. Saejao, and D. Arunyasot, "Analysis of Lightning Surge Condition Effect on Surge Arrester in Electrical Power System by using ATP/EMTP Program," *International Journal of Electrical, Energetic, Electronic and Communication Engineering*, vol. 1, no. 4, pp. 32-34, 2007.
- [22] A.F. Imece, D.W. Durbak, H. Elahi, S. Kolluri, A. Lux, D. Mader, T.E. McDemott, A. Morched, A.M. Mousa, R. Natarajan, L. Rugeles, and E. Tarasiewicz, "Modeling Guidelines for Fast Front Transients," *IEEE Transactions on Power Delivery*, vol. 11, no. 1, pp. 493-506, 1996.
- [23] R. Pešić, and B. Gmrovšek, "Application of lightning protection and surge arresters in railway facilities," *Iskra Zašćite*, pp. 1-49, 2007.
- [24] R. Shariatinasab, B. Valiidi, and S.H. Hosseini, "Statistical evaluation of lightning-related failures for the optimal location of surge arresters on the power networks," *IET Generation Transmission & Distribution*, Vol. 3, pp. 129 – 144, 2009.
- [25] C.A. Christodoulou, I. F. Gonos and I. A. Stathopoulos, "Lightning performance of high voltage transmission lines protected by surge arresters: a simulation for the Hellenic transmission network," 29th International Conference on Lightning Protection, pp. 6b-7-1 - 6b-7-8, 2008.
- [26] IEC 60850, "Railway Applications – Supply Voltages of Traction Systems," *International Electrotechnical Commission standard*, 2014.
- [27] ABB Application Guidelines Overvoltage Protection, Metal-oxide surge arresters in railway facilities, 3<sup>rd</sup> ed, 2011 [On-line]. Available: [https://library.e.abb.com/public/3231c0994ad34a13c12578d200341040/986\\_abb\\_awr\\_bahnen\\_E\\_low.pdf](https://library.e.abb.com/public/3231c0994ad34a13c12578d200341040/986_abb_awr_bahnen_E_low.pdf).
- [28] UMIASEA, Thailand's Railway Industry-Overview and Opportunities for Foreigners Businesses. : UMI Asia (Thailand) Ltd, 2014.
- [29] Z. Yongji, S. Wenxia, and Z. Zhijin, "Summary of the study of tower models for lightning protection analysis," *High Voltage Engineering*, pp. 93-97, 2006.
- [30] A. Župan, A. T. Teklić, and B. Filipović-Grčić, "Modeling of 25 kV Electric Railway System for Power Quality Studies," *EuroCon 2013.Zagreb, Croatia*, pp. 844-849, 2013.
- [31] M. Karagöz, "Analysis of the Pantograph Arcing and Its Effect of the Railway Vehicle," *Master Degree Thesis, Middle East Technical University*, pp. 59-72, 2014.
- [32] ABB Surge arrester POLIM-S, (2016), "Data sheet 1HC0075857 E01 AB," [On-line]. Available: [https://library.e.abb.com/public/1ea09f10ad44056185257bcc00547e5b/POLIM-S%20to%20245kV\\_2GNM110077\\_7-11.pdf](https://library.e.abb.com/public/1ea09f10ad44056185257bcc00547e5b/POLIM-S%20to%20245kV_2GNM110077_7-11.pdf).
- [33] IEC Std. 60099-5, "Surge arresters—Part 5: Selection and application recommendations," edition 1.1, 2000.
- [34] IEEE Std. C62.22-2009, "IEEE Guide for the Application of Metal-Oxide Surge Arresters for Alternating-Current Systems," *IEEE Power & Energy Society*, 3 July 2009.
- [35] IEEE Working Group on Surge Arrester Modeling, "Modeling of metal oxide surge arresters," *IEEE Transactions on Power Delivery*, vol. 7, no. 1, pp. 302–309, 1992.
- [36] IEEE Std. C62.22-2009, "IEEE Guide for the Application of Metal-Oxide Surge Arresters for Alternating-Current Systems," *IEEE Power & Energy Society*, 2009.
- [37] P. Pinceti and M. Giannettoni, "A simplified model for zinc oxide surge arresters," *IEEE Transactions on Power Delivery*, vol. 14, no. 2, pp. 393–398, 1999.
- [38] Type POLIM-S Surge Arresters. (2008), "Maximum System Voltage 2.52 to 245 kV," [On-line]. Available: [https://library.e.abb.com/public/1ea09f10ad44056185257bcc00547e5b/POLIM-S%20to%20245\\_kV\\_2GNM110077\\_7-11.pdf](https://library.e.abb.com/public/1ea09f10ad44056185257bcc00547e5b/POLIM-S%20to%20245_kV_2GNM110077_7-11.pdf).

## Analysis of Flashover Induced by Transient Current During Multiple Lightning Strokes on a Train

Kelvin M. Minja, Pius V. Chombo, Narupon Promvichai, Boonruang Marungsri

**Abstract** – Power system outage due to the occurrence of flashover (across insulators) when lightning induced voltages exceed insulators' voltage withstand capabilities have been a major investigation in recent studies. Since the Overhead catenary system uses overhead power lines which are exposed to lightning incidences, the concerns have been made in protection against lightning strikes. The knowledge of lightning and its most influential parameters are of great importance in the safe and reliable operation of the Overhead catenary system. In this work, analysis of flashover when lightning strikes on train's pantograph at the mast and between two masts were studied. Furthermore, the effects of the magnitude, waveforms, polarity, multiplicity and grounding resistance were investigated. In this task, the impact of lightning parameters has been achieved with computer simulation tool (ATPDraw). It was shown that the negative multiple lightning of magnitude - 34 kA and above leads flashover when strikes on pantograph at the mast and between two masts. However, the grounding resistance was recognized to have higher predominance in mast induced voltages when a lightning strike occurs at the mid-span unlike along the mast. Hence, the lightning protection design should consider the multiplicity of negative lightning strokes outcome from the point of hitting. **Copyright © 2017 Praise Worthy Prize S.r.l. - All rights reserved.**

**Keywords:** Catenary, Multiple Lightning Strokes, Flashover, Grounding Resistance, ATP Draw

### Nomenclature

$A_x$	Auxiliary line
$R_t$	Return line
$C_t$	Catenary line
$X_1$	S-Rail
$X_2$	I-Rail
$X_3$	Catenary line with composite insulator
$X_4$	Return line with spool insulator
$X_5$	Auxiliary line with pin insulator
$R_1$	Radius between mast and auxiliary line
$R_2$	Radius between mast and return line
$R_3$	Radius between mast and catenary line
$H$	Height of the mast
$L_1$	Vertical distance between auxiliary and return line
$L_2$	Vertical distance between return and catenary line
$L_3$	Distance between catenary line and ground
$Z_{aux}$	Impedance of the auxiliary line
$Z_{return}$	Impedance of the return line
$Z_{catenary}$	Impedance of the catenary line
$R_f$	Mast grounding resistance
IU	International unit

### I. Introduction

Until now, catenary contact system has become more useful for feeding traction power to electric vehicle [1]-

[6]. In spite of modernization in the electrified railway system, lightning has been a crucial problem in the overhead catenary system [1]-[2]. Statistically, most of the power system outage caused by transient current characteristics are due to lightning strokes [1], [7]-[9]. A power system failure of the overhead catenary system is triggered by direct lightning strokes to phase conductor, shielding wire and ground in line proximity [1], [10]. However, lightning strokes on phase conductor influence dynamic overvoltages, which can disturb the stability of system to a great extent [9]-[11]. It has been reported that when induced overvoltage overreach insulation withstands capability, lightning flashover across insulators occurs [2]. Many works have been performed to estimate the lightning strokes consequences in the overhead catenary system [1], [3]-[4], [12]-[17].

Catenary contact system is among of elevated railway system that has been affected by lightning incidences in Bangkok, Thailand. It has been reported in [18] lightning magnitude ranges 11-171 kA with a positive polarity which accounts for 5% and -10 to -139 kA with negative polarity is 95% of all flash activities. In addition, [19]-[22] described that negative lightning could associate with multiple strokes per flash. Ref. [19], [21]-[22] showed the reported multiple strokes averaging 3 to 4 strokes per flash with intervals of tens of milliseconds. In recent studies, lightning end results were analyzed when it strikes on the mast, conductors, and traction substation of the overhead catenary system by using different

Kelvin M. Minja, Pius V. Chombo, Narupon Promvichai, Boonruang Marungsri

simulation software [1], [3]-[4], [13]-[14], [16]-[17]. But the analyses from these studies were done in single lightning strokes without regard to the enforcement of multiple lightning strokes. Consequently, it is important to analyze characteristics of transient current during multiple lightning strokes in different waveforms and grounding resistance before establishing lightning protection design.

In this study, the effects of grounding resistance in transient current waveforms of multiple lightning strokes are investigated. The transient conditions are simulated using ATPDraw due to it is the capability for solving the electromagnetic transient problem [3]-[4], [9], [14], [18]-[23]. The characteristics depend on the amplitude of transient current during negative multiple lightning strokes on pantograph are examined.

## II. Background

A nominal voltage of 25 kV AC-50 Hz is normally used in the railway traction power system [24]. The conductor arrangement in the double-track overhead catenary system on Thai elevated railway system is shown in Figs. 1-2.

The line of 480 m was accompanied by seven masts with 60 m spacing in the simulation. This line was selected between Phayathai and Rajaprarop (see Fig. 3). The supply voltage was injected at both end points of the line. The negative multiple lightning strokes on train's pantograph were taken as much concern as it strikes on phase conductor.

The pantograph was considered when it is at the Mast (seventh Mast) for Case 1 as shown in Fig. 1 and at the mid-span of Masts (sixth and seventh Masts) for Case 2 as shown in Fig. 2. The lightning sources were presented by the magnitudes of -34 kA, and -50 kA with 1/30.2  $\mu$ s, 1.2/50  $\mu$ s, 2/77.5  $\mu$ s and 3/75  $\mu$ s waveforms as in [18]. The elevated poles resistance of 50  $\Omega$  and grounding resistances of 5, 10, 20, 30, 40, 50, 70, 80, 90 and 100  $\Omega$  were used.

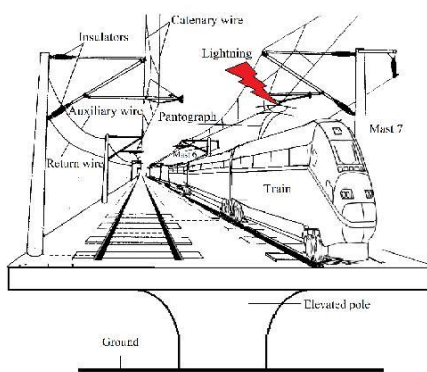


Fig. 1. Lightning strike on train's pantograph at the Mast

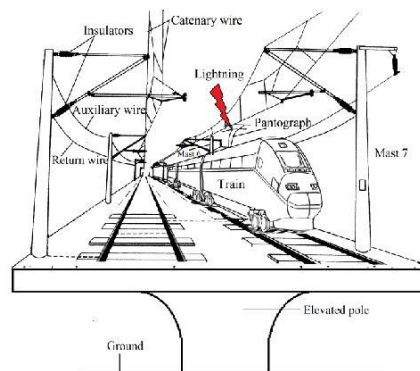


Fig. 2. Lightning strike on train's pantograph at the mid-span of Masts



Fig. 3. Airport Rail link line in Thailand [25]

## III. Catenary Contact System

### III.1. Railway Transmission Line

The railway transmission line is made up on the double-track elevated railway system whereas masts on the elevated poles have a span of 60 meters (see Figs. 1-2). It comprises of the catenary line, return line, and auxiliary line. A double track consists of rails (S-rail and I-rail) with distributed-parameters along both sides of the impact point. Table I presents details of the railway transmission line on elevated poles [13]. An LCC\_8 with JMARTI model as shown in Fig. 4 was used to represent a transmission line in ATPDraw. As reported in [26],[29], it was seen that stray current in the railway transmission line might result in electromagnetic interference and large unbalanced traction load with electricity in the vicinity of the railway system. However, the report in [4] showed that an autotransformer and booster transformer could force the traction current to return through designated return conductors of traction supply in order to reduce stray current. Hence, an autotransformer and booster transformer can ensure restitution of transmission energy to the substation from the train. Therefore, a 1:1 ideal transformer was used to model an autotransformer in ATPDraw. Its modeling details are given in [13]-[14]. In Fig. 5, the cross-section

view of the electrified railway system of a double-track elevated rail system and mast configuration parameters of 2x25 kV AC, 50 Hz from [15] are presented.

TABLE I  
DETAILS OF 25 KV TRANSMISSION LINE  
FOR ELECTRIFIED RAILWAY [2], [13]

Conductors		Radius
Catenary ( $X_1$ )		5.06 cm
Return ( $X_4$ )		0.82 cm
Auxiliary ( $X_5$ )		0.56 cm
Ruling span between Masts		60 m
Railway		Radius
S-rail ( $X_1$ )		4.95 cm
I-rail ( $X_2$ )		4.95 cm
Insulators		Impulse Withstand Voltage (MV)
Composite ( $X_3$ )		0.225
Spool ( $X_4$ )		0.060
Pin ( $X_5$ )		0.140
Ground System		
Grounding resistance		5 - 100 $\Omega$
Elevated Pole Resistance		50 $\Omega$

Fig. 4. Railway Transmission lines data in ATPDraw

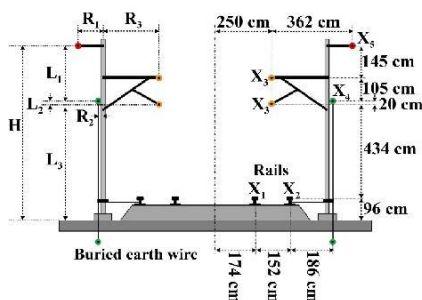


Fig. 5. Cross-section view axis of Railway Electrification system on Double Track elevated railway system [15]

III.2. Multiple Lightning Source

Since the disastrous potency of multiple lightning was aimed in the study, some parameters were set in the

ATPDraw models to characterize its behavior. Following the most occurring tendency of negative lightning strokes in Thailand [18], the magnitude of lightning current was considered with a negative polarity.

Although the report of [18] showed the lightning magnitude to range from -10 kA to -139 kA, but only -34 kA and -50 kA were used in this study.

Furthermore, three strokes per flash with intervals of 1ms were used to represent multiplicity as considered in [19], [21]-[22].

The first stroke was modeled with Heidler ideal source at time duration of 0.6 ms; the second and third strokes were designed with two slope Ramp Type 13 at time duration of 0.3 ms for each in ATPDraw. Other parameters of multiple lightning sources are given in Table II.

Fig. 6 illustrates the waveform of the first, second and third strokes of the lightning current with the magnitude of -50 kA.

TABLE II  
PARAMETERS OF MULTIPLE LIGHTNING SOURCES [18]-[22]

Parameter	Source 1	Source 2	Source 3
Type	Heidler 15	Ramp 13	Ramp 13
Amp. (kA)	-34/-50	-26/-42	-23/-39
$T_0$	0	0	0
$A1$	0	0	0
$T1(s)$	0	0.0003	0.0003
$TSta(s)$	0	0.0016	0.0029
$TSto(s)$	0.0006	0.0019	0.0032

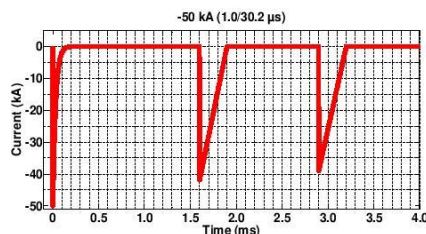


Fig. 6. Waveform of the 1<sup>st</sup>, 2<sup>nd</sup> and 3<sup>rd</sup> strokes of the lightning current with the magnitude of -50 kA and waveform of 1.0/30.2  $\mu$ s in ATPDraw

III.3. Mast and Insulator

The cylindrical geometric model in single wave impedance was used to represent the mast model. In the literature of [4] and [27], this model was mostly explained to be recommended by IEEE and CIGRE. Hence, this model as given in [4] was taken to represent the mast.

However, the impedances in the catenary, auxiliary, and return lines have an important virtue in the modeling of the mast; therefore, their impedances were estimated from (1) and tabulated in Table III. As seen from (1),  $R$  and  $H$  are the radii of lines and height of the mast respectively.

Moreover, Fig. 5 depicts the values of  $R$  for catenary, auxiliary and return lines. The results of computed impedances from (1) have been summarized in Table III.

In ATPDraw, the mast was designed by using Linezt\_1.sup model. With this type, line impedances and their corresponding heights from the ground were assigned to represent the mast.

Three types of insulators used for supporting three lines in the mast are given in Table I. Since in ATPDraw an insulator is represented by a capacitor in parallel with voltage controlled switch [28], the values of withstanding capability to be assigned to the switch for each insulation was taken from Table I.

From [2], composite, pin and spool insulators were shown to have ten, five and one units per insulator respectively. As discussed in [14], the capacitance of 8.8 pF was given for eleven units of a silicone insulator. Then a Switchvc.sup model was used to incorporate the values of voltage withstands capability and capacitances when simulating in ATPDraw:

$$Z = 60 \ln \cot \left[ 0.5 \arctan \left( \frac{R}{H} \right) \right] \quad (1)$$

where:

- $Z$  is the surge impedance; its IU is  $\Omega$ ;
- $R$  is the equivalent radius of the mast; its IU is m;
- $H$  is the height of the mast; its IU is m.

TABLE III  
MAST MODELED PARAMETERS

Location	Parameters
Auxiliary	$Z_{aux} = 159.85 \Omega$ , $L_1 = 2.5$ m, $R_1 = 1.12$ m, $H = 8$ m
Return	$Z_{return} = 293.57 \Omega$ , $L_2 = 0.2$ m, $R_2 = 0.12$ m, $H = 8$ m
Catenary	$Z_{catenary} = 112.79 \Omega$ , $L_3 = 5.3$ m, $R_3 = 2.5$ m, $H = 8$ m

### III.4. Train Model

A three-car train which consists of the pantograph, locomotive transformer, diode bridge rectifier and two DC motors was used to represent the design of an electric locomotive train. The rectifier bridge is represented by the parallel RC elements and the series resistance of the diodes.

A series reactor is connected between the motor and the rectifier bridge in order to smooth the direct current [29].

The system of the electric locomotive train with components mentioned above is shown in Figs.8-9 as presented in [29]-[30]. Since the study is performed when the pantograph of a powertrain is at the mast and the mid-span of masts, Figs. 7-8 show an electric locomotive train positioned across the mast and mid-span respectively.

As shown in Fig. 8, a railway transmission line has a span of 60 meters and  $50 \Omega$  resistance of elevated pole. Furthermore, grounding resistances of 5, 10, 20, 30, 40, 50, 70, 80, 90 and 100  $\Omega$  were taken to represent different soil profiles.

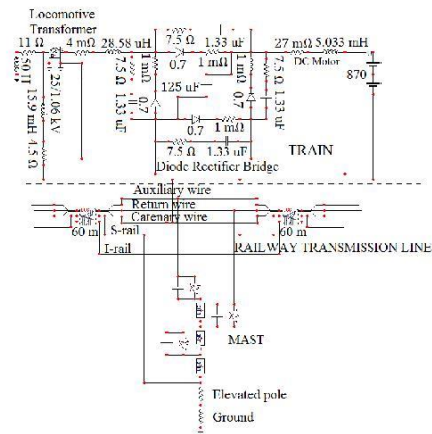


Fig. 7. An electric locomotive train across the mast

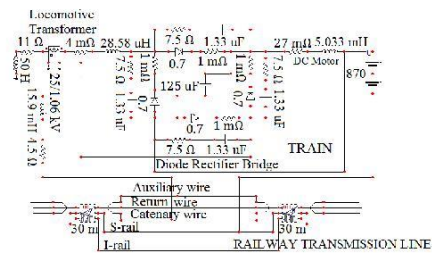


Fig. 8. An electric locomotive train at the mid-span of Masts

## IV. Results and Discussion

The simulation results of peak mast induced voltages across the insulators in the auxiliary, return, and catenary lines are shown in Figs. 9-16 for case 1 and Figs. 17-24 for case 2.

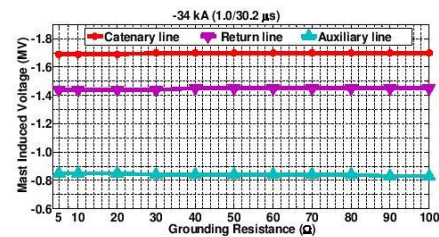


Fig. 9. Mast induced voltages in Case 1 with -34 kA (1.0/30.2  $\mu$ s)

Kelvin M. Minja, Pius V. Chombo, Narupon Promvichai, Boonruang Marungsri

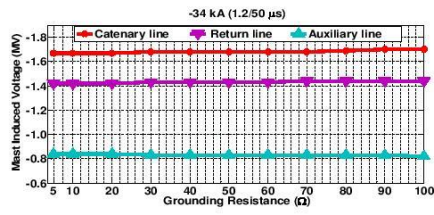


Fig. 10. Mast induced voltages in Case 1 with -34 kA (1.2/50  $\mu$ s)

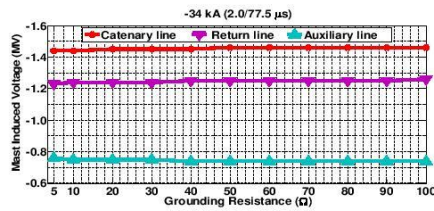


Fig. 11. Mast induced voltages in Case 1 with -34 kA (2/77.5  $\mu$ s)

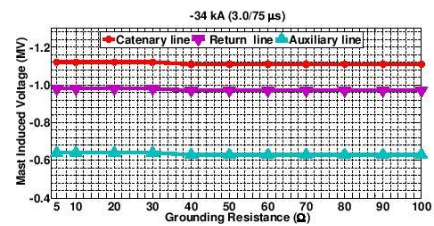


Fig. 12. Mast induced voltages in Case 1 with -34 kA (3/75  $\mu$ s)

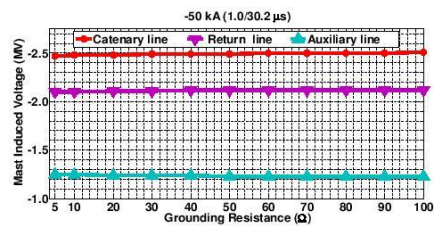


Fig. 13. Mast induced voltages in Case 1 with -50 kA (1.0/30.2  $\mu$ s)

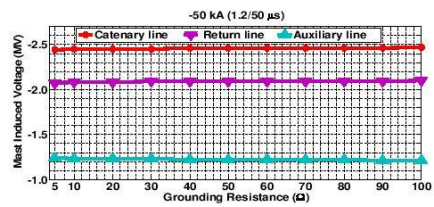


Fig. 14. Mast induced voltages in Case 1 with -50 kA (1.2/50  $\mu$ s)

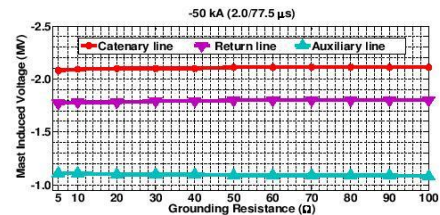


Fig. 15. Mast induced voltages in Case 1 with -50 kA (2/77.5  $\mu$ s)

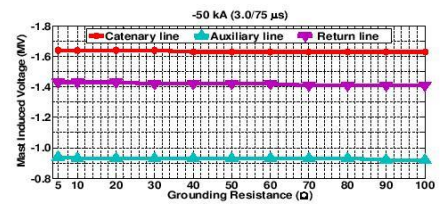


Fig. 16. Mast induced voltages in Case 1 with -50 kA (3/75  $\mu$ s)

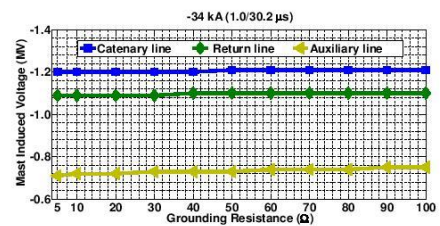


Fig. 17. Mast induced voltages in Case 2 with -34 kA (1.0/30.2  $\mu$ s)

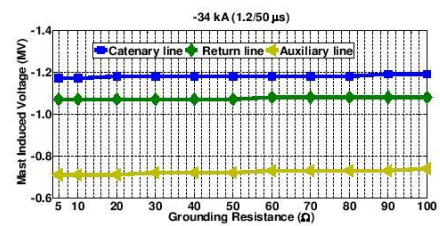


Fig. 18. Mast induced voltages in Case 2 with -34 kA (1.2/50  $\mu$ s)

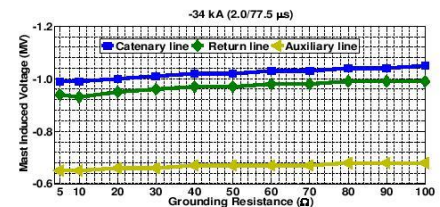


Fig. 19. Mast induced voltages in Case 2 with -34 kA (2/77.5  $\mu$ s)

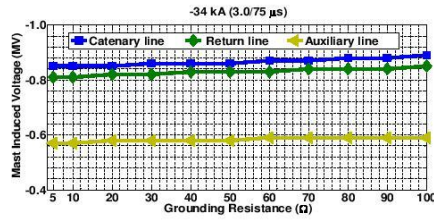


Fig. 20. Mast induced voltages in Case 2 with -34 kA (3/75 μs)

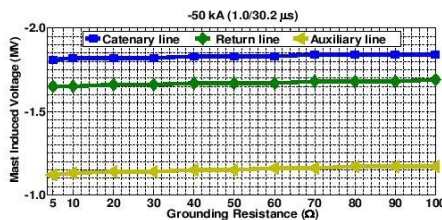


Fig. 21. Mast induced voltages in Case 2 with -50 kA (1.0/30.2 μs)

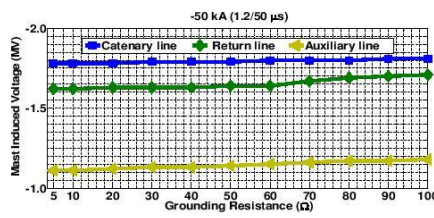


Fig. 22. Mast induced voltages in Case 2 with -50 kA (1.2/50 μs)

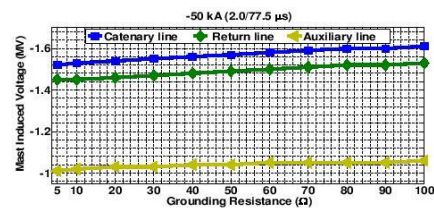


Fig. 23. Mast induced voltages in Case 2 with -50 kA (2/77.5 μs)

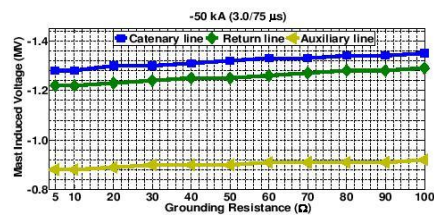


Fig. 24. Mast induced voltages in Case 2 with -50 kA (3/75 μs)

The amplitude values of Mast induced voltages in catenary (Ct), auxiliary (Ax) and return (Rt) lines for Case one and two are recapitulated in Tables IV-V. The values in Tables IV-V were obtained after being analyzed the data from the Figs. 9-24. The 1<sup>st</sup> row details the cases as explained from Figs. 1-2 and Figs. 7-8. The 2<sup>nd</sup>, 16<sup>th</sup>, 28<sup>th</sup>, and 40<sup>th</sup> rows start from the 2<sup>nd</sup> column illustrate the type of waveforms. The 3<sup>rd</sup> row starts from the 2<sup>nd</sup> column gives the magnitude of multiple lightning strokes that have been used. The 1<sup>st</sup> column starts from the 2<sup>nd</sup> row shows the ground resistances that have been exploited. The 2<sup>nd</sup> to the 4<sup>th</sup> column and the 5<sup>th</sup> to the 7<sup>th</sup> column start from the 4<sup>th</sup> row indicate the magnitude of mast induced voltages in different lines of an overhead catenary system for 34 kA and 50 kA respectively.

TABLE IV  
MAGNITUDE OF MAST INDUCED VOLTAGES (MV) FOR CASE 1

Case 1						
Waveform 1.0/30.2 μs						
Rf	-34 kA			-50 kA		
(Ω)	Ax	Rt	Ct	Ax	Rt	Ct
5	0.85	1.44	1.69	1.25	2.1	2.47
10	0.85	1.44	1.69	1.25	2.1	2.48
20	0.85	1.44	1.69	1.25	2.11	2.48
30	0.85	1.44	1.7	1.25	2.11	2.49
40	0.85	1.45	1.7	1.25	2.12	2.49
50	0.85	1.45	1.7	1.25	2.12	2.49
60	0.85	1.45	1.7	1.25	2.12	2.5
70	0.86	1.45	1.7	1.26	2.12	2.5
80	0.86	1.45	1.7	1.26	2.12	2.5
90	0.86	1.45	1.7	1.26	2.12	2.5
100	0.75	1.1	1.21	1.17	1.69	1.84
Rf	Waveform 1.2/50 μs					
5	0.84	1.42	1.67	1.24	2.07	2.44
10	0.84	1.42	1.67	1.24	2.08	2.45
20	0.84	1.42	1.67	1.24	2.08	2.45
30	0.84	1.43	1.68	1.24	2.09	2.45
40	0.84	1.43	1.68	1.24	2.09	2.46
50	0.84	1.43	1.68	1.24	2.09	2.46
60	0.84	1.43	1.68	1.24	2.09	2.46
70	0.85	1.44	1.68	1.24	2.09	2.46
80	0.85	1.44	1.69	1.24	2.09	2.46
90	0.85	1.44	1.7	1.25	2.09	2.46
100	0.85	1.44	1.7	1.25	2.1	2.47
Rf	Waveform 2.0/77.5 μs					
5	0.75	1.23	1.44	1.11	1.77	2.08
10	0.75	1.24	1.44	1.11	1.78	2.09
20	0.75	1.24	1.45	1.11	1.78	2.10
30	0.75	1.24	1.45	1.11	1.79	2.1
40	0.76	1.25	1.45	1.11	1.79	2.1
50	0.76	1.25	1.46	1.12	1.8	2.11
60	0.76	1.25	1.46	1.12	1.8	2.11
70	0.76	1.25	1.46	1.12	1.8	2.11
80	0.76	1.25	1.46	1.12	1.8	2.11
90	0.76	1.25	1.46	1.12	1.8	2.11
100	0.76	1.26	1.46	1.12	1.8	2.11
Rf	Waveform 3.0/75 μs					
5	0.64	0.98	1.12	0.94	1.43	1.64
10	0.64	0.98	1.12	0.95	1.43	1.64
20	0.64	0.98	1.12	0.95	1.43	1.64
30	0.64	0.98	1.12	0.95	1.42	1.64
40	0.64	0.97	1.11	0.95	1.42	1.63
50	0.64	0.97	1.11	0.95	1.42	1.63
60	0.65	0.97	1.11	0.95	1.42	1.63
70	0.65	0.97	1.11	0.95	1.41	1.63
80	0.65	0.97	1.11	0.95	1.41	1.63
90	0.65	0.97	1.11	0.96	1.41	1.63
100	0.65	0.97	1.11	0.96	1.41	1.63

TABLE V  
MAGNITUDE OF MAST INDUCED VOLTAGES (MV) FOR CASE 2

Case 2							
Rf	Waveform 1.0/30.2 μs						
	-34 kA			-50 kA			
(Q)	Ax	Rt	Ct	Ax	Rt	Ct	
5	0.71	1.09	1.2	1.12	1.65	1.81	
10	0.72	1.09	1.2	1.13	1.65	1.82	
20	0.72	1.09	1.2	1.14	1.66	1.82	
30	0.73	1.09	1.2	1.14	1.66	1.82	
40	0.73	1.1	1.2	1.15	1.67	1.83	
50	0.73	1.1	1.21	1.15	1.67	1.83	
60	0.74	1.1	1.21	1.16	1.67	1.83	
70	0.74	1.1	1.21	1.16	1.68	1.84	
80	0.74	1.1	1.21	1.17	1.68	1.84	
90	0.75	1.1	1.21	1.17	1.68	1.84	
100	0.75	1.1	1.21	1.17	1.69	1.84	
Rf	Waveform 1.2/50 μs						
5	0.71	1.07	1.17	1.11	1.62	1.78	
10	0.71	1.07	1.17	1.11	1.62	1.78	
20	0.71	1.07	1.18	1.12	1.63	1.78	
30	0.72	1.07	1.18	1.13	1.63	1.79	
40	0.72	1.07	1.18	1.13	1.63	1.79	
50	0.72	1.07	1.18	1.14	1.64	1.79	
60	0.73	1.08	1.18	1.15	1.64	1.80	
70	0.73	1.08	1.18	1.16	1.67	1.80	
80	0.73	1.08	1.18	1.17	1.69	1.80	
90	0.73	1.08	1.19	1.17	1.7	1.81	
100	0.74	1.08	1.19	1.18	1.71	1.81	
Rf	Waveform 2.0/77.5 μs						
5	0.65	0.94	0.99	1.01	1.45	1.52	
10	0.65	0.93	0.99	1.02	1.45	1.53	
20	0.66	0.95	1	1.03	1.46	1.54	
30	0.66	0.96	1.01	1.03	1.47	1.55	
40	0.67	0.97	1.02	1.04	1.48	1.56	
50	0.67	0.97	1.02	1.04	1.49	1.57	
60	0.67	0.98	1.03	1.05	1.5	1.58	
70	0.67	0.98	1.03	1.05	1.51	1.59	
80	0.68	0.99	1.04	1.05	1.52	1.6	
90	0.68	0.99	1.04	1.05	1.52	1.6	
100	0.68	0.99	1.05	1.06	1.53	1.61	
Rf	Waveform 3.0/75 μs						
5	0.85	1.44	1.69	1.25	2.1	2.47	
10	0.85	1.44	1.69	1.25	2.1	2.48	
20	0.85	1.44	1.69	1.25	2.11	2.48	
30	0.85	1.44	1.7	1.25	2.11	2.49	
40	0.85	1.45	1.7	1.25	2.12	2.49	
50	0.85	1.45	1.7	1.25	2.12	2.49	
60	0.85	1.45	1.7	1.25	2.12	2.5	
70	0.86	1.45	1.7	1.26	2.12	2.5	
80	0.86	1.45	1.7	1.26	2.12	2.5	
90	0.86	1.45	1.7	1.26	2.12	2.5	
100	0.75	1.1	1.21	1.17	1.69	1.84	

In the following sections, two different cases are discussed.

IV.1. *The Effects of Negative Multiple Lightning Strokes on Train's Pantograph at the Mast.*

Results of mast induced voltages in Case 1 for -34 kA and -50 kA are shown in Figs. 9-16, and summarized in Table IV. It can be noted that the mast induced voltages were above withstand capabilities of line insulators for both catenary, auxiliary, and return lines. Marungsri et al. [18] studied about back flashover affected by tower grounding resistance and concluded that the shorter the waveform, the higher is the tower induced voltages. As seen in Figs. 9-12, it can be clearly observed that the

shortest waveform has the highest mast induced voltages in Catenary, Auxiliary, and Return line as well.

It can also be found that an increase in lightning magnitude from -34 kA to -50 kA resulted into increase in mast induced voltage (see Figs. 9-16). However, flashover was early observed with -34 kA which meant a flashover occurred from -34 kA and above with negative multiple lightning strokes. Furthermore, grounding resistance showed less significance in the performance of multiple lightning. Therefore, when the pantograph is stroke by negative multiple lightning along the mast, flashover was seemed to occur from -34 kA and above, in all waveforms and all grounding resistance. Apart from the occurrence of flashover, the catenary line was appeared to have the highest level of mast induced voltage compared to other lines as shown in Tables IV-V.

IV.2. *The Effects of Negative Multiple Lightning Strokes on Train's Pantograph at the Mid-Span of Masts*

Results of mast induced voltages in Case 2 for -34 kA and -50 kA are given from Figs. 17-24. Table V illustrates the summary of induced voltages in the catenary, auxiliary, and return lines. As depicted in Figs. 17-20, It can be observed that the mast induced voltages are above withstand capabilities of line insulators for both catenary, auxiliary, and return lines. The same results were seen in Figs. 21-24 for -50 kA. Although the effects of lightning magnitude and shorter waveform were also seen as in Case 1 but grounding resistance showed the significant contribution to the flashovers in Case 2. In general, flashover was seemed to occur from -34 kA and above, in all waveforms and all grounding resistance when the pantograph is stroke by negative multiple lightning at the mid-span. Again, the catenary line was seemed to have the highest mast induced voltage amongst the lines (see Table V).

V. **Conclusion**

The following have been summarized for the conclusion:

- It is noticed that negative multiple lightning of magnitude -34 kA and above may cause flashover when strikes the pantograph along the mast or at the mid-span.
- The grounding resistance is observed to have a higher influence in mast induced voltages when a lightning stroke occurs at the mid-span compared with along the mast.
- All waveforms resulted into flashovers although shorter waveforms displayed more top mast induced voltages. Therefore, negative multiple lightning of any waveform can lead into flashover.
- In the case of all lightning magnitudes, waveforms, and grounding resistances, catenary line exhibited higher mast induced voltages. The greatest one



Kelvin M. Minja, Pius V. Chombo, Narupon Promvichai, Boonruang Marungsri

occurred when lightning strokes the pantograph along the mast.

Flashovers have been noticed with multiple strokes from -34kA and above in all waveforms and grounding resistances compared to single strokes in literature, this needs considerable attention in designing insulation and protection systems.

### Acknowledgements

The authors gratefully appreciate the support of High Voltage Insulation Technology Laboratory of Suranaree University of Technology, Thailand.

### References

- [1] T. Chmielewski, A. Dziadkowiec, Simulations of Fast Transients in typical 25 kV a.c. railway power supply system, *Seminarium ZASTOSOWANIE KOMPUTERÓW W NAUCE I TECHNICE 2013, Gdańsk, Polska, Vol. 23*(No. 36):43-46, 2013.
- [2] F. Kiessling, R. Puschmann, A. Schmieder, E. Schneider, 2Ed, *Contact Lines for Electrical Railways: Planning - Design - Implementation - Maintenance* (Siemens Aktiengesellschaft, Berlin and Munich, 2009).
- [3] S. Pastromas, A. Papamikou, G. Peppas, E. Pyrgioti, Investigation of grounding resistance effect on the MV grid of Hellenic electromotive railway during lightning strikes, *33rd International Conference on Lightning Protection*, pp. 1-7, 2016.
- [4] Y. Yang, and Y. Zhang, Research on Lightning Protection Simulation of High-speed Railway Catenary Based on ATP-EMTP, *Journal of information & Computation Science*, Vol. 12(Issue 4):1511-1521, 2015.
- [5] Ined, M., Mourad, F., Habib, R., Study and design of a hybrid linear actuator for a railway system, (2010) *International Review on Modelling and Simulations (IREMOS)*, 3 (5), pp. 791-795.
- [6] Barro, R., Hegazy, O., Lataire, P., Coosemans, T., Van Mierlo, J., An accurate multi-train simulation tool for energy recovery evaluation in DC rail networks, (2011) *International Review on Modelling and Simulations (IREMOS)*, 4 (6), pp. 2985-3003.
- [7] R. Bhattarai, R. Rashedin, S. Venkatesan, A. Haddad, H. Griffiths, N. Harid, Lightning performance of 275 kV Transmission Lines, *43rd International Universities Power Engineering Conference*, pp. 1-5, 2008.
- [8] IEEE Std. 1100, IEEE Recommended Practice for Powering and Grounding Electronic Equipment, *IEEE Standards*, 1999.
- [9] P. Lertwanitrot, P. Kettranan, P. Itthisathienkul, A. Ngaopitakkul, Characteristics and Behaviour of Transient Current during Lightning Strikes on Transmission Tower, *Proceedings of the International MultiConference of Engineers and Computer Scientists 2015 (IMECS 2015)*, Vol 2, pp. 708-713, Hong Kong, March 2015.
- [10] IEEE Std. 1313.2, IEEE Guide for the Application of Insulation Coordination, *IEEE Standards*, 1999.
- [11] P.N. Mikropoulos and T.E. Tsovilis, Estimation of the shielding performance of overhead transmission lines: the effects of lightning attachment model and lightning crest current distribution, *IEEE Transactions on Dielectrics and Electrical Insulation*, Vol. 19(No. 6):2155-2164, 2012.
- [12] H. Lingohr, U. Stahlberg, B. Richter, and V. Hinrichsen, Overvoltage protection design for DC railways, *Elektrische Bahnen*, Vol. 101(No. 7):315-320, 2003.
- [13] Ziya Mazloom, *Multi-conductor transmission line model for electrified railways: A method for responses of lumped devices*, Ph.D. dissertation, KTH Electrical Engineering University, Stockholm, Sweden, 2010.
- [14] F. Achouri, I. Achouri, M. Khamliche, Protection of 25 kV Electrified Railway System, *4th International Conference on Electrical Engineering (ICEE)*, pp. 1-6, 2015.
- [15] A. Andreotti, U. D. Martinis, A. Pierno, V. A. Rakov, A New Tool for Lightning Induced Voltage Calculations: CiLIV, *General Assembly and Scientific Symposium (URSI GASS), 2014 XXXIth URSI*, pp. 1-4, August 2014.
- [16] J. Liu, and M.G. Liu, Improved electro-geometric model for estimating lightning outage rate of catenary, *IET Electrical Systems in Transportation*, Vol. 2(Issue 1):1-8, 2012.
- [17] A.V. Wanjari, Effect of Lightning on the Electrified Transmission Railway System, *International Journal of Advance Research in Electrical, Electronics and Instrumentation Engineering*, Vol. 3(Issue. 7):10663-10671, 2014.
- [18] B. Marungsri, S. Boonpoke, A. Rawangpai, A. Oonsivilai, and C. Kritayakompong, Study of Tower Grounding Resistance Effected Back Flashover to 500kV Transmission Line in Thailand by using ATP/EMTP, *International Journal of Electrical, Computer, Energetic, Electronic and Communication Engineering*, Vol. 2(No. 6):1061-1068, 2008.
- [19] M.A. Omidiora, M. Lehtonen, Performance of Surge Arrester to Multiple Lightning Strokes on Nearby Distribution Transformer, *Proceedings of the 7th WSEAS International Conference on Power Systems*, pp. 59-65, Beijing, China, September 2007.
- [20] J.A. Martinez-Velasco, and F.C. Aranda, EMTP Implementation of a Monte Carlo Method for Lightning Performance Analysis of Transmission Lines, *Ingeniare. Revista chilena de ingeniería*, Vol. 16(No. 1):169-180, 2008.
- [21] M.A. Omidiora, M. Lehtonen, Simulation of Combined Shield Wire and MOV Protection on Distribution Lines in Severe Lightning Areas, *Proceedings of the World Congress on Engineering and Computer Science, San Francisco, USA, October 2007*.
- [22] J. C. Das, Analysis and control of large-shunt-capacitor-bank switching transients, in *IEEE Transactions on Industry Applications*, vol. 41, no. 6, pp. 1444-1451, Nov.-Dec. 2005.
- [23] Sarajcev, P., Wind farm surge arresters energy capability and risk of failure analysis, (2010) *International Review on Modelling and Simulations (IREMOS)*, 3 (5), pp. 926-937.
- [24] IEC 60850, Railway Applications – Supply Voltages of Traction Systems, *International Electrotechnical Commission standard*, 2014.
- [25] UMIASEA, Thailand's Railway Industry-Overview and Opportunities for Foreigners Businesses, (Thailand: UMI Asia Ltd, 2014, pp. 126-142).
- [26] Kalantari, M., Sadeghi, M.J., Farshad, S., Fazel, S.S., Modeling and comparison of traction transformers based on the utilization factor definitions, (2011) *International Review on Modelling and Simulations (IREMOS)*, 4 (1), pp. 342-351.
- [27] Y Zhang, W. Sima, and Z. Zhang, Summary of the study of tower models for lightning protection analysis, *High Voltage Engineering*, Vol. 32(No. 7):93-97, 2006.
- [28] A. F. Imece, D. W. Durbak, H. Elahi, S. Kolluri, A. Lux, D. Mader, T. E. McDermott, A. Morched, A. M. Mousa, R. Natarajan, L. Rugeles, and E. Tarasiewicz, Modeling Guidelines for Fast Front Transients, *IEEE Transactions on Power Delivery*, Vol. 11(No. 1):493-506, January 1996.
- [29] A. Zupan, A.T. Teklić, B. Filipović-Grčić, Modeling of 25 kV Electric Railway System for Power Quality Studies, *EuroCon 2013, Zagreb, Croatia*, pp. 844-849, July 2013.
- [30] Mustafa Karagöz, *Analysis of the Pantograph Arcing and Its Effect of the Railway Vehicle*, Master Degree dissertation, Middle East Technical University, January 2014.

### Authors' information

School of Electrical Engineering, Suranaree University of Technology  
111 University Avenue, Nakhon Ratchasima 30000, Thailand.



**Kelvin Melckzedek Minja** was born in Tanga, Tanzania in 1989. He completed his B.Eng. Degree in Electrical Engineering in 2015 from Dar es Salaam Institute of Technology. He is currently a master's degree student in the School of Electrical Engineering, Institute of Engineering at the Suranaree University of Technology, Thailand.

*Kelvin M. Minja, Pius V. Chombo, Narupon Promvichai, Boonruang Marungsri*



System Programming.

**Pius Victor Chombo** has obtained his B.Eng. Degree in Electrical Engineering from Dar es Salaam Institute of Technology, Tanzania in 2013. He is now a master's degree student in the School of Electrical Engineering, the Suranaree University of Technology in Thailand. His interest research topics include High Voltage Systems Design and Monitoring, Laboratory and



**Narupon Promvichai** has obtained his B.Eng. Degree in the School of Electrical Engineering, the Suranaree University of Technology in Thailand, 2015. He is now a master's degree student in the School of Electrical Engineering, the Suranaree University of Technology in Thailand.



Dr. Marungsri is

**Boonruang Marungsri** was born on 1973 in Nakhon Ratchasima Province, Thailand. He received his B. Eng. in 1996 and M. Eng. in 1999 from Chulalongkorn University, Thailand and D. Eng. in 2006 from Chubu University, Kasugai, Aichi, Japan, all in electrical engineering, respectively. Dr. Marungsri is currently a lecturer in School of Electrical Engineering, Suranaree University of Technology, Thailand. His areas of interest are electrical power system and high voltage insulation technologies.

# Transient Current Behaviour during Multiple Lightning strokes on Multiple Unit Trains

Kelvin Melckzedek Minja, Pius Victor Chombo,  
Narupon Promvichai, and Boonruang Marungsri, Non-members

## ABSTRACT

This paper studies transient current behavior during multiple lightning strokes on multiple unit trains of catenary contact system in airport rail link (Bangkok). Since lightning flashover across insulators is a source of power network failure, the protection against overvoltage disturbances in the overhead catenary system has been recently taken into consideration as its parameters. In this study, the impact in lightning strokes current magnitude with IEC 62305 waveforms of the first and subsequent stroke were evaluated. Moreover, in invariant elevated pole and grounding resistance, lightning strikes on multi-car trains' pantographs at the mast and mid-range of the masts were the interested locations for investigation. The modeled elements of the necessary system have been effectuated in ATP-EMTP software. The flashover was shown to occur for lightning current from -34 kA and above at targeted positions. Also, the mast induced voltage was recognized to increase with lightning magnitude. The striking on three-car trains resulted in high consequences compared to the four-car trains. However, the overcritical mast induced voltage often occurred in the catenary line once it strikes on three-car trains' pantograph across the mast unlike at mid-range. Therefore, protection against lightning multiplicity into multi-car trains and striking points should be highly considered.

**Keywords:** Electrified Multiple Unit Trains, Catenary, Multiple Lightning Strokes, Transient Current, Mast Induced Voltage, ATP-EMTP.

## 1. INTRODUCTION

Improvement on electrification of railway line due to the advantage of electric traction over diesel-electric traction and hybrid traction has become more important for everyday life. Also, for energy dependent, a human, desired environment, and economic growth have been demanded electric train services since the second half of 19<sup>th</sup> century, due to technology innovation improvement to increase speed, safety,

efficiency, and reliability of economic enhancement [1-2]. Typically, electricity in electrified railway transmission system must be stably secured with effectively track system and control system. Power is injected into the system which is in the form of overhead catenary transmission line without disturbance. Although the hardship of transmission line that injects power into a system along distance when lightning strikes on multiple unit trains as a natural disturbance, may likely cause the electrical breakdown. Actually, this disruption leads various electrical elements failure, power losses, and other unreliable condition on catenary contact system.

Induced over-voltages in a mast is a most exist issue which causes flashover across insulators due to lightning strikes on multiple unit trains of catenary contact system. Lightning strokes disturbances have influenced the overhead lines on double-track elevated railway system in an existing environment without any prevention. Flashover occurs when the induced voltage in a mast exceeds lightning withstand voltage level of insulators. This incidence makes the study of lightning to be more important in reliability, protection, and durable insulation design to prevent power losses in 2×25 kV AC, 50 Hz electrified railway power system. The significances of this system over 1×25 kV AC, 50 Hz electrified railway system have been stated in [3].

The experience of thunderstorm days and lightning activities per year in Thailand has led to the study of transient current behavior during multiple lightning strokes on multiple unit train's pantographs of the overhead catenary system on the elevated railway system. It uses catenary for the most traction power supply system to deliver power to electric locomotive by pantograph which is exposed to the lightning activities. The report of lightning statistics in Thailand from [4] showed that the Lightning often occurs in April-May but severely in June. The magnitude ranges 11-171 kA with positive polarity and -10 to -139 kA with negative polarity. Positive lightning strokes account for 5% while negative is 95% with the magnitude of -10 to -50 kA. In [5-8] showed that negative polarity lightning stroke could associate with multiple strokes per flash and [5,7-8] reported that the multiple strokes are averaging 3 to 4 strokes per flash with intervals of tens of milliseconds. The negative polarity of multiple lightning strokes was taken as much concern in the study, especially for 2×25 kV

Manuscript received on July 24, 2017 ; revised on July 31, 2014.

The authors are with Electrical Engineering, Institute of Engineering, Suranaree University of Technology, 111 University Avenue, Nakhon Ratchasima 30000, Thailand, E-mail : bmshivee@sut.ac.th

AC, 50 Hz catenary contact system on the double-track elevated railway system. The overhead catenary system connects Phayathai BTS station in the center and Suvarnabhumi airport in the East of Bangkok in Thailand. In addition, airport rail link covers three lines which are city line, Makkasan express line and Phayathai express line at 28.6 km track length. Currently, city line has 5 three-car trains, and express lines have 4 four-car trains (1 for baggage) [9]. For the purpose of the study, seven masts on elevated poles at the line of 480 m length with 60 m spacing in case 1 and six masts on elevated poles at the line of 420 m length with 60 m spacing in case 2 were considered. Case 1 was preferred when multiple unit trains' pantographs are at 4<sup>th</sup> Mast and case 2 between 3<sup>rd</sup> and 4<sup>th</sup> Masts. The negative multiple lightning strokes on three-car and four-car trains' pantograph were analyzed for city and express line respectively.

## 2. THE ANALYSIS OF ELEVATED STRUCTURE AND CATENARY LIGHTNING RANGE

Thai catenary contact system consists of auto-transformer (AT), booster transformer (BT) and tracks circuit which includes relay and rectifier units. There are also interconnections between the overhead catenary conductors on the double-track elevated railway system. In the double-track electrified railway system with I-rail (R1), S-rail (R2), catenary line (contact line (R3) and messenger line (R4)), return line (R5) and auxiliary line (R6) that are interconnected as a circuit shown in Fig. 1 and cross-sectional view in Fig. 2 [9]. The return conductors are also interconnected to the booster transformer (BT) systems, and it's also connected to the S-rail at the midpoint between two consecutive transformers at every 5 km. At every pole position, the S-rail (R2) is shorted to the elevated pole footing.

Due to the unpredictability of lightning strike point on multiple unit train's pantographs which touches the catenary wire, it better to study the parts which are exposed to lightning according to the IEEE STD. 1234-1997, by using the formula (1) in [10].

$$\begin{cases} r_c = 1.34h^{0.6}I^{0.65} \\ r_c = r_g \end{cases} \quad (1)$$

where  $r_c$  is lightning strike distance of catenary which touches on pantograph of multiple unit trains, its UI is m;  $h$  is the average height of hanging wire, its UI is m;  $I$  is the lightning current amplitude, its UI is kA;  $r_g$  is lightning strike distance of earth on top of elevated pole, its UI is m.

The range of triggered lightning of catenary shown in Fig. 3 as in [10] but in this study, was considered when it is on top of the elevated pole. AB arc line is triggered a lightning range of auxiliary line (R6), CD arc is triggered a lightning range of catenary line (contact line and messenger line) (CA). The lightning

current reaches first to the line which has a higher range of lightning strike distance compared to other wires. Auxiliary line (R6) and return line (R5) are on the same side on top of the mast. Lightning strike distance of auxiliary line (R6) is greater than return line (R5) which lead R6 to shield R5, but there is no any shield for the catenary line that touch pantograph, and lead great possibilities to be attacked by lightning strikes on it. In this study, we focus when multiple lightning strokes on multiple unit train's pantographs because pantograph touches catenary line. It is casual that catenary on high ground like on top of an elevated pole experience more lightning strike than that on low ground as in [11].

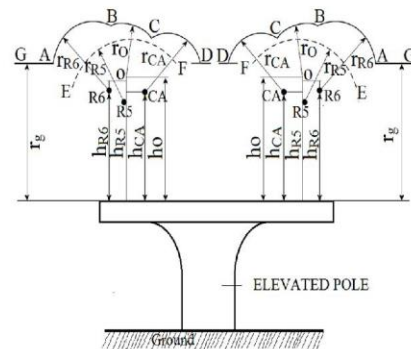


Fig. 3: The range of triggered lightning of Catenary on the double-track elevated railway system.

## 3. MODELLING

The proposed ATP-EMTP software which recognized as standard procedure in power system used to investigate transient current behavior during multiple lightning strokes on multiple unit train's pantographs. Modeling of multiple lightning sources, mast, multiple unit trains, overhead catenary transmission line, insulator, elevated pole, and the ground was guided to represent catenary contact system on the double-track elevated railway system for analyzing the problem.

### 3.1 Multiple Lightning Source Model

Since negative lightning strokes may associate with subsequent strokes, only the first and second strokes are highly considered due to the effects of their current magnitudes in insulation [6]. But the behavior of tower grounding electrode and surrounding soil at higher frequencies of up to 10 MHz is not yet explicitly represented [12]. Frequently, both triangular and

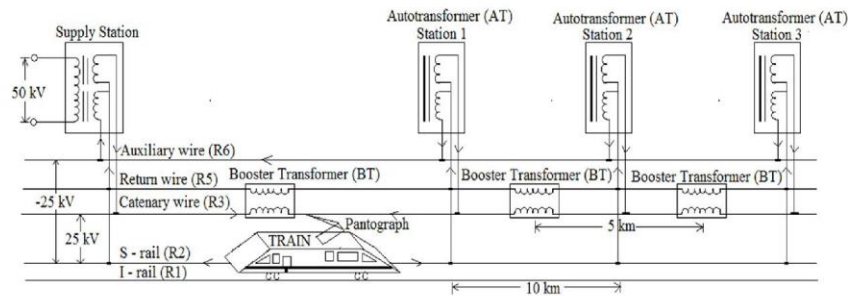


Fig.1: Power Supply Circuit of 2x25 kV AC, 50 Hz Catenary Contact System.

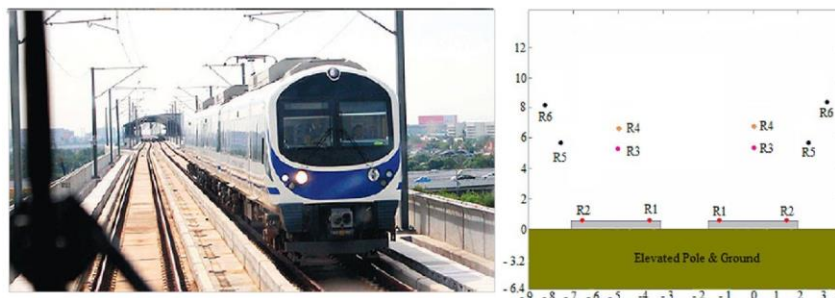


Fig.2: Double track Railway Electrification system on elevated railway system and same cross-section view axis [9].

exponential waveforms have been utilized to represent return strokes currents of lightning. Presently, it is deduced that a concave waveform can be better representation since it could not show a discontinuity at the initial stage. Several expressions have been suggested for such waveforms [13-15]. Therefore, the Heidler current function model in ATP-EMTP was used to represent the lightning current as one of the most widely used as shown in (2) [16-17].

$$i(t) = \frac{I_P}{k} \cdot \frac{\left(\frac{t}{\tau_1}\right)^n}{1 + \left(\frac{t}{\tau_1}\right)^n} \cdot \exp\left(-\frac{t}{\tau_2}\right) \quad (2)$$

where  $I_P$  is the peak value of the lightning stroke;  $k$  is the adjustment constant;  $n$  is a factor influencing the rate of rise;  $t$  is the time instant of the maximum rate of rise;  $\tau_1$  and  $\tau_2$  are the coefficients of the decay time and front time respectively.

The calculation of variables  $\tau_1, \tau_2$  and  $n$  are explained in [18]. The correction factor of Amplitude, which regularly appears in the mathematic expression

of Heidler function [14], is automatically modified and does not materialize in ATP-EMTP. Heidler-type is suitable throughout the concave lightning current front of the wave, regarding the natural lightning, is modeled.

Parameters of lightning sources are given in Table 1. Fig. 4 depicts the lightning waveforms of -34 kA normalized the first stroke with 1.0/100  $\mu$ s and subsequent stroke with 0.2/50  $\mu$ s as recommended by IEC 62305 [19]. The allocation of the lightning sources in selected railway transmission line for the city and express line in case 1 and 2 are shown in Figs. 5-8.

### 3.2 Mast Model

The mast is modeled by cylindrical geometrical steel column in single wave impedance model as recommended by IEEE and CIGRE by expression from surge impedance equation (3) in [10,20] and modeled

**Table 1:** Multiple lightning sources Parameters [4,19]

Parameter	First strokes	Subsequent Strokes
Type	Heidler 15	Heidler 15
Amp. (kA)	-34	-34
	-50	-50
	-100	-100
Front time ( $\mu s$ )	1	0.2
Tail time ( $\mu s$ )	100	50

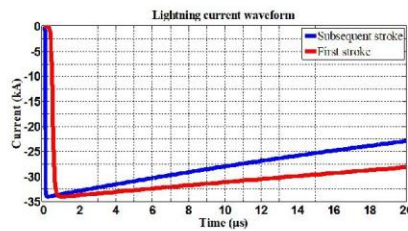


**Fig.4:** Lightning current waveforms of the -34 kA first stroke-(1.0/100  $\mu s$ ), subsequent stroke -(0.2/50  $\mu s$ ) designed in ATP-EMTP.

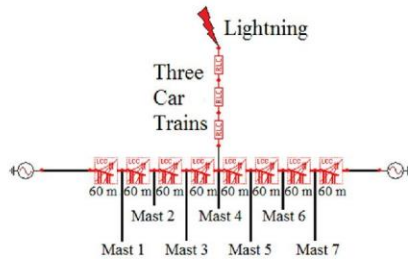


**Fig.5:** City line with lightning source (Case 1).

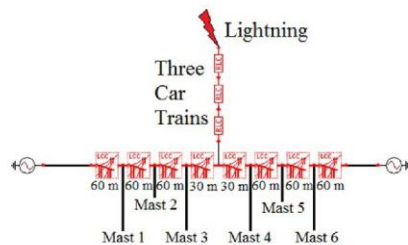


**Fig.6:** City line with lightning source (Case 2).

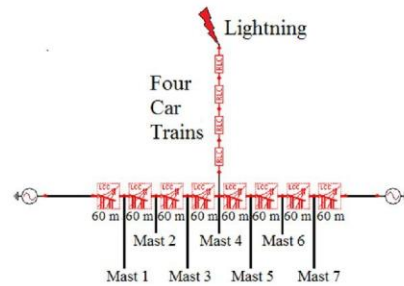


**Fig.7:** Express line with lightning source (Case 1).

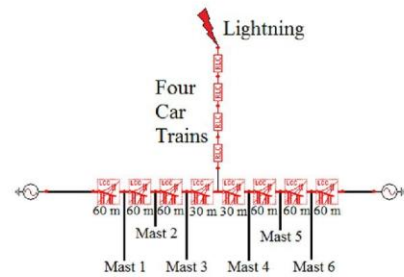


**Fig.8:** Express line with lightning source (Case 2).

parameters are shown in Table 2.

$$Z = 60In \cot \left[ 0.5 \arctan \left( \frac{R}{H} \right) \right] \quad (3)$$

where  $Z$  is the surge impedance, its IU is  $\Omega$ ;  $R$  is the equivalent radius of the mast, its IU is m;  $H$  is the height of the mast, its IU is m.

**Table 2:** Modelled Parameters of Mast Model

Location	Parameters
Auxiliary	$Z_{aux}= 176.35 \Omega, L_1= 3.3 \text{ m}$
Return	$Z_{return}=275.1 \Omega, L_2= 0.2 \text{ m}$
Catenary	$Z_{catenary}= 126.88 \Omega, L_3= 6.3 \text{ m}$

**3.3 Insulator Model**

Generally, insulator resists the flow of current from phase conductor to the ground during normal operating condition. Since the capability of an insulator to withstand stress depends on its voltage withstand level, this behavior can be represented as a voltage controlled switch [21]. Moreover, the effects of coupling conductors to mast structure can

also be represented by the capacitor. If the voltage across insulator terminals is greater than control voltage of the switch, the switch closes which indicates flashover. Otherwise, if the voltage stress is less than control voltage, the switch remains open to show no flow of current across the insulator. In the simulation, the voltage controlled switch was designed by Switchvc.sup model. The voltage withstand capabilities for the rod/composite, spool and pin as given in Table 3 [22] were set as the control voltage of the switch. The values of capacitance for suspension insulators are 80 pF/unit while for pin insulators are around 100pF/unit [21].

**Table 3: Impulse withstand level of Insulators [22]**

Insulators	Impulse Withstand level
Rod/Composite (R3/R4)	225 kV
Spool (R5)	60 kV
Pin (R6)	140 kV

### 3.4 Grounding Resistance Model

Once the lightning current discharges to earth through the mast, the ionization process occurs around soil surrounding the grounding rod. This situation makes surrounding soil as non-linear and the frequency dependent. A non-linear frequency-dependent representation is required to obtain an accurate simulation [6,12,23-24]. Due to difficulties of information to representing this behavior not always available, the reasonable model approximation of grounding resistance as recommended by IEC and IEEE standards is given in (4) [10,21,25-27].

$$R_g = \frac{R_0}{\sqrt{1 + \frac{2\pi R_0^2 I}{E_0 \rho}}} \quad (4)$$

From expression,  $R_g$  is grounding resistance, its IU is  $\Omega$ ;  $R_0$  is the striking impedance value in low-frequency power flow, its IU is  $\Omega$ ;  $I$  is the striking lightning current passing through the grounding system, its IU is kA;  $\rho$  is the soil resistivity, its IU is  $\Omega \cdot m$ ;  $E_0$  is the soil ionization intensity, usually take a value of 400 kV/m [24].

### 3.5 Multiple Unit Trains Model

The electric train was modeled as electric locomotive which contains pantograph, locomotive transformer, diode rectifier bridge and DC motors as stated in [28-29]. The rectifier bridge is represented by the parallel RC elements and the series resistance of the diodes. A series reactor is connected between the motor and the rectifier bridge in order to smooth the direct current [28]. Three-car trains in city line consisted 6 DC motors while four-car trains in express line carried 8 DC motors. The network of an

electric vehicle with elements listed above and one DC motor are indicated in Figs. 9-10. In the case of positions, Fig. 9 and 10 show when the pantograph is at the mast and mid-span of the masts respectively. Railway transmission line with 60 m spacing, elevated pole resistance and grounding resistance, and Insulators are shown in Fig. 9.

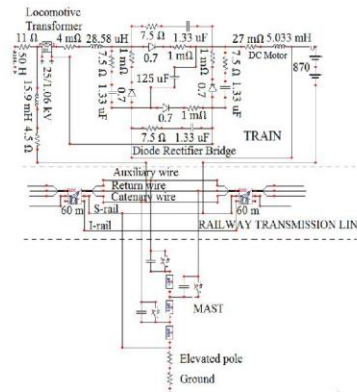


**Fig.9: Mast with Train, Railway Transmission line, Pole, Ground, and Insulators at elevated pole in ATP EMTP.**

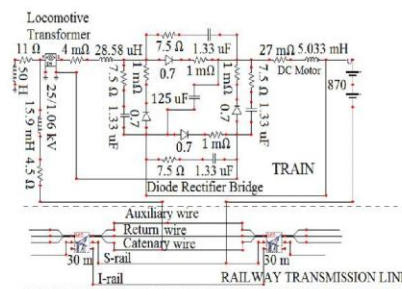


**Fig.10: Train with Railway Transmission line between elevated poles in ATP EMTP.**

### 3.6 Overhead Catenary Transmission Line Model

The overhead catenary transmission line was modeled by LCC 8 with JMARTI model in ATP EMTP as shown in Fig. 11 and it consists of a catenary line, return line, auxiliary line, S-rail and I-rail on elevated poles at every 60 m along overhead cate-

nary system as in [22,30] with autotransformer and booster transformer. Autotransformer and booster transformer were modeled as 1:1 ideal transformers in ATP EMTP as shown in [10]. This type of transformer used to force the traction current to return through designated return conductors to traction supply in order to reduce stray current which may cause electromagnetic interference with electrical systems in the vicinity of the railway system and to ensure the return of transmission energy to the substation from the train. Mast cross section view of 25 kV electrified railway line have been shown in Fig. 3.

Phase	React	Rtot	Rstr	Htot	Vmax	Vmid
1	0	4.95	1.75E-6	-0.7175	0.95	0.95
2	0	0.82	6.04E-7	-2.5795	5.5	5.5
3	0	5.95	1.35E-6	0	5.3	5.3
4	0	0.95	2.81E-7	3.62	8	8
5	0	4.95	1.75E-6	0.7175	0.95	0.95

Fig.11: Railway Transmission line data in ATP EMTP.

4. SIMULATION ANALYSIS

As a version part of the electromagnetic transients program, ATP-EMTP is the powerful tool for steady state and transient analysis of power systems [31]. It has been recognized as per international standard as IEEE and CIGRE in arithmetic circuits [32]. In this task, ATP-EMTP is utilized as time domain computation in overvoltage protection against lightning as indicating from Figs. 9-10.

The traction voltage of the system is 25 kV AC, 50 Hz as stated by IEC standard [33]. A nominal voltage was inserted to both sides of the termination of the line. A 25 kV railway transmission line with arrangements of masts as in Figs. 5-8 were simulated in ATP-EMTP. Multiple lightning sources were inserted on train's pantograph. The elevated poles and grounding resistance were set to 50  $\Omega$  and 5  $\Omega$  unchanged respectively. The magnitude, front time and tail time of negative multiple lightning strokes were studied as factors that cause a transient current which leads flashover across insulators. As the impulse voltage withstand capability of insulation depends on the front time of lightning stroke current, the different multiple lightning stroke currents were initiated. The present magnitude of -34 kA was started to be simulated and followed by -50 kA and -100 kA as specified

in Table 1. First strokes-(1.0/100  $\mu$ s) and subsequent stroke-(0.2/50  $\mu$ s) waveforms were used in the simulation for both city line and express line.

4.1 Simulation Results

Figs. 12-17 and Figs. 18-23 contain the outcome of mast induced voltage waveforms stressed insulators of the auxiliary, return and catenary line for city line and express line respectively. For instance, Figs. 12-14 and Figs. 18-20 are represented case 1 while Figs. 15-17 and Figs. 21-23 are evinced case 2. Figs. 12-23 differ in the magnitude of mast induced voltages across insulators. Table 4 and 6 show the

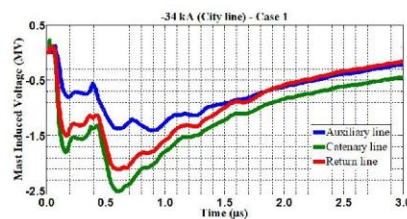


Fig.12: Mast induced voltage waveform of the -34 kA first stroke-(1.0/100  $\mu$ s), subsequent stroke-(0.2/50  $\mu$ s).

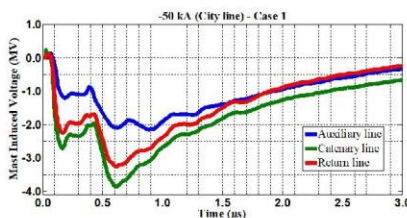


Fig.13: Mast induced voltage waveform of the -50 kA first stroke-(1.0/100  $\mu$ s), subsequent stroke-(0.2/50  $\mu$ s).

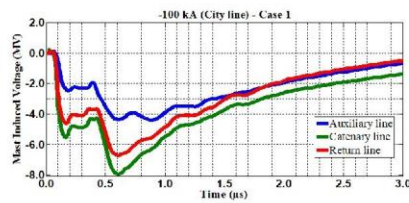
magnitude of mast induced voltages and Table 5 and 7 show flashovers across insulators.

Table 4: Magnitude of mast induced voltages (MV)

City line								
Case 1								
-34kA			-50kA			-100kA		
Aux	Ret	Cat	Aux	Ret	Cat	Aux	Ret	Cat
1.41	2.11	2.51	2.15	3.25	3.85	4.41	6.72	8.0
Case 2								
-34kA			-50kA			-100kA		
Aux	Ret	Cat	Aux	Ret	Cat	Aux	Ret	Cat
1.52	2.18	2.32	2.26	3.30	3.51	4.62	6.72	7.15

Key:





**Fig.14:** Mast induced voltage waveform of the -100 kA first stroke-(1.0/100  $\mu$ s), subsequent stroke-(0.2/50  $\mu$ s).

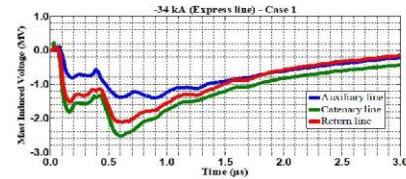


**Fig.18:** Mast induced voltage waveforms of the -34 kA first stroke-(1.0/100  $\mu$ s), subsequent stroke-(0.2/50  $\mu$ s).

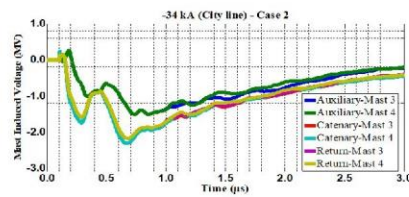


**Fig.15:** Mast induced voltage waveform of the -34 kA first stroke-(1.0/100  $\mu$ s), subsequent stroke-(0.2/50  $\mu$ s).

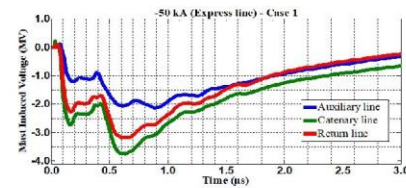


**Fig.19:** Mast induced voltage waveforms of the -50 kA first stroke-(1.0/100  $\mu$ s), subsequent stroke-(0.2/50  $\mu$ s).

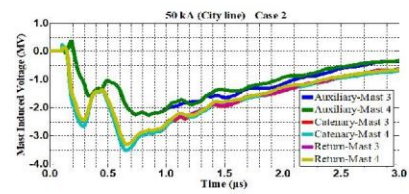


**Fig.16:** Mast induced voltage waveform of the -50 kA first stroke-(1.0/100  $\mu$ s), subsequent stroke-(0.2/50  $\mu$ s).

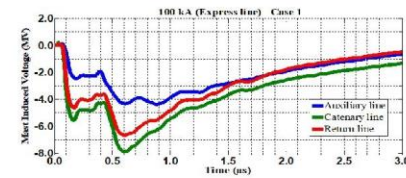


**Fig.20:** Mast induced voltage waveform of the -100 kA first stroke-(1.0/100  $\mu$ s), subsequent stroke-(0.2/50  $\mu$ s).

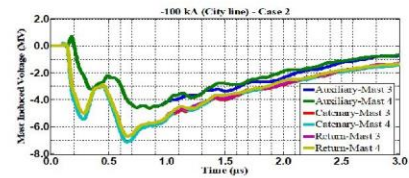


**Fig.17:** Mast induced voltage waveform of the -100 kA first stroke-(1.0/100  $\mu$ s), subsequent stroke-(0.2/50  $\mu$ s).

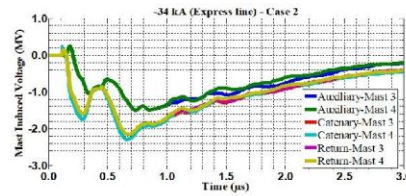


**Fig.21:** Mast induced voltage waveform of the -34 kA first stroke-(1.0/100  $\mu$ s), subsequent stroke-(0.2/50  $\mu$ s).

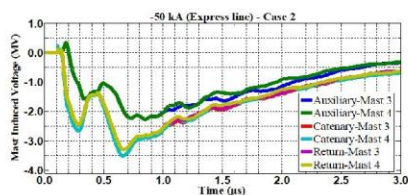


Fig.22: Mast induced voltage waveform of the -50 kA first stroke-(1.0/100 μs), subsequent stroke-(0.2/50 μs).

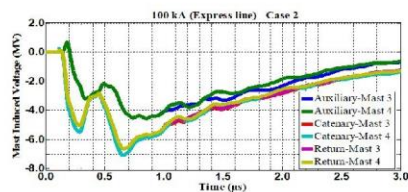


Fig.23: Mast induced voltage waveform of the -100 kA first stroke-(1.0/100 μs), subsequent stroke-(0.2/50 μs).

Table 5: Flashover across insulators

City line								
-34kA			-50kA			-100kA		
Aux	Ret	Cat	Aux	Ret	Cat	Aux	Ret	Cat
S	S	S	S	S	S	S	S	S
Case 2								
-34kA			-50kA			-100kA		
S	S	S	S	S	S	S	S	S

Table 6: Magnitude of mast induced voltages (MV)

Express line								
-34kA			-50kA			-100kA		
Aux	Ret	Cat	Aux	Ret	Cat	Aux	Ret	Cat
1.40	2.12	2.52	2.12	3.18	3.75	4.37	6.66	7.88
Case 2								
-34kA			-50kA			-100kA		
1.81	2.15	2.30	2.27	3.30	3.61	4.86	6.66	7.98

Table 7: Flashover across insulators

Express line								
-34kA			-50kA			-100kA		
Aux	Ret	Cat	Aux	Ret	Cat	Aux	Ret	Cat
S	S	S	S	S	S	S	S	S
Case 2								
-34kA			-50kA			-100kA		
S	S	S	S	S	S	S	S	S

S-Flashover, Aux-Auxiliary line, Ret-Return line, Cat- Catenary line

5. DISCUSSION

According to the simulation results, two different sections are discussed. The first and second parts are described when three-car and four-car train's pantograph struck by multiple lightning strokes with negative polarity respectively.

5.1 Effect of Negative Multiple Lightning Strokes on Three-Car Train's Pantograph

As shown in Figs. 12-17, the mast induced voltages in the auxiliary, return, and catenary lines are above the lightning withstand levels of their respective insulators. The amounts of mast induced voltages are shown in Table 4. However, the flashover was observed to occur from -34 kA and above in both case 1 and case 2 (see Table 5). Also, the mast induced voltages were seen to increase with lightning magnitudes from -34 kA to -100 kA. The catenary line in case 1 and case 2 was seemed to be the most affected line from -34 kA to -100 kA. The worst case for the catenary line was occurred in -100 kA for case 1.

5.2 Effect of Negative Multiple Lightning Strokes on Four-Car Train's Pantograph

From the illustrations of Figs. 18-23, the lightning withstands levels of the auxiliary, return, and catenary lines are below the mast induced voltages across their respective insulators. The quantities of mast induced voltages are exhibited in Table 6. Moreover, in both case 1 and case 2, lightning magnitude from -34 kA and above caused the flashover (see Table 7). Additionally, the mast induced voltages were noticed to increase with lightning magnitudes from -34 kA to -100 kA. The catenary line in case 1 and case 2 was discerned to be the most pretentious line from -34 kA to -100 kA. The worst case for the catenary line was appeared in -100 kA for case 1.

6. CONCLUSION

In this paper, the transient current behavior when multiple lightning strokes on three-car and four-car trains' pantographs have been studied. The investigation of flashover voltage across auxiliary, return, and catenary lines insulators on the elevated railway system were analyzed. The occurrence of flashover was observed for any the lightning magnitude from -34 kA to -100 kA for case 1 and case 2 of both three-car and four-car train. Moreover, the mast induced voltage was seen to increase with the magnitude of lightning strokes current. The effect of lightning current was observed more in three-car train compared to the four-car train. The catenary line of the three-car train was the most stressed line in contrast to auxiliary and return line. The maximum value of the mast induced

voltage in the catenary line of the three-car train was seen to occur when the pantograph was across the mast. Since the mast induced voltage across insulator of the catenary line was seemed to decrease from three-car train (8.0 MV) to four-car train (7.88 MV), it was suggested to study the behavior of lightning current for other multi-car trains.

#### 7. ACKNOWLEDGEMENT

Authors would like to express their gratitude to the support of High Voltage Insulation Technology Laboratory of Suranaree University of Technology, Thailand.

#### References

- [1] S. Lu, *Optimising Power Management Strategies for Railway Traction*, D. Eng. Thesis, The University of Birmingham, UK, pp. 8-20, 2011.
- [2] A. V. Wanjari, "Effect of Lightning on the Electrified Transmission Railway System," *International Journal of Advanced Research in Electrical, Electronics and Instrumentation Engineering*, Vol. 3, Issues .7, pp. 10663- 10671, 2014.
- [3] C. Courtois, "Why the 2x25 kV Alternative [Autotransformer Traction Supply]," *The French Experience, IEE Colloquium*, pp. 1/1-1/4, 1993.
- [4] B. Marungsri, S. Boonpoke, A. Rawangpai, A. Oonsivilai, and C. Kritayakornpong, "Study of Tower Grounding Resistance Effected Back Flashover to 500kV Transmission Line in Thailand by using ATP/EMTP," *International Journal of Electrical, Computer, Energetic, Electronic and Communication Engineering*, Vol. 2, No. 6, pp. 1061-1068, 2008.
- [5] M.A. Omidiora, and M. Lehtonen, "Performance of Surge Arrester to Multiple Lightning Strokes on Nearby Distribution Transformer," *Proceedings of the 7th WSEAS International Conference on Power Systems, Beijing, China*, pp. 59-65, 2007.
- [6] J. A. Martinez-Velasco, and F. C. Aranda, "EMTP Implementation of a Monte Carlo Method for Lightning Performance Analysis of Transmission Lines," *Ingeniare. Revista chilena de ingenieria*, Vol. 16, No. 1, pp. 169-180, 2008.
- [7] M.A. Omidiora, and M. Lehtonen, "Simulation of Combined Shield Wire and MOV Protection on Distribution Lines in Severe Lightning Areas," *Proceedings of the World Congress on Engineering and Computer Science*, 2007.
- [8] D. Rodriguez-Sanabria, C. Ramos-Robles, and L. Orama-Exclusa, "Lightning and Lightning Arrester Simulation in Electrical Power Distribution Systems," pp. 1-9.
- [9] UMIASEA, *Thailand's Railway Industry- Overview and Opportunities for Foreigners Businesses*, UMI Asia (Thailand) Ltd, 2014.
- [10] Y. Yang, and Y. Zhang, "Research on Lightning Protection Simulation of High-speed Railway Catenary Based on ATP-EMTP," *Journal of Information & Computation Science* 12:4, pp. 1511-1521, 2015.
- [11] J. Liu, and M.G. Liu, "Improved electrogeometric model for estimating lightning outage rate of catenary," *IET Electrical Systems in Transportation*, Vol. 2, pp. 1-8, 2012.
- [12] N. Pattanadach and P. Yutthagowith, "A Transmission Model of Vertical Grounding Electrodes," *AORCTechnical meeting 2014*, pp. 1-7, 2014.
- [13] IEC 60071-4, "Insulation Coordination, Part 4: Application Guide," 2004-06.
- [14] F. Heidler, "Analytische Blitzstromfunktion zur LEMP-Berechnung," *18th International Conference on Lightning Protection (ICLP)*, pp. 63 - 66, 1985.
- [15] CIGRE Technical Brochure No. 63, "Guide to procedures for estimating the lightning performance of transmission lines," 1991.
- [16] F. M. Gatta, A. Geri, S. Lauria, and M. Maccioni, "Monte Carlo Evaluation of the Impact of Subsequent Strokes on Backflashover Rate," *2015 IEEE 15th International Conference on Environment and Electrical Engineering (EEEIC)*, pp. 1210 - 1215, 2015.
- [17] T. Thanasaksiri, "Improving the Lightning Performance of Overhead Distribution and Sub-Transmission Lines Applying Additional Underbuilt Shield Wire," *ECTI Transactions on Electrical Eng., Electronics, and Communications*, Vol 12, No 2, pp. 1-8, 2014.
- [18] D. Lovric, S. Vujevic and T. Modric, "On the estimation of Heidler function parameters for reproduction of various standardized and recorded lightning current waveshapes," *International transactions on Electrical Energy Systems 2013*, Vol 23, No 2, pp. 290-300, 2013.
- [19] IEC 62305:2010, "Protection against lightning," 2010.
- [20] Y. Zhang, W. Sima, and Z. Zhang, "Summary of the study of tower models for lightning protection analysis," *High Voltage Engineering*, pp. 93-97, 2006.
- [21] A. F. Imece, D. W. Durbak, H. Elahi, S. Kolhuri, A. Lux, D. Mader, T. E. McDermott, A. Morched, A. M. Mousa, R. Natarajan, L. Rugeles, and E. Tarasiewicz, "Modeling Guidelines for Fast Front Transients," *IEEE Transactions on Power Delivery*, Vol. 11, No. 1, pp. 493-506, 1996.
- [22] Ziya Mazloom, *Multi-conductor transmission line model for electrified railways: A method for responses of lumped devices*, Doctoral Thesis, KTH Electrical Engineering University, Stockholm, Sweden, pp. 59-72, 2010.

- [23] W.A. Chisholm and W. Janischewskyj, "Lightning surge response of ground electrodes," *IEEE Trans. on Power Delivery*, vol. 14, No. 2, pp. 1329-1337, 1989.
- [24] A.M. Mousa, "The soil ionization gradient associated with discharge of high currents into concentrated electrodes," *IEEE Trans. on Power Delivery*, Vol. 9, No. 3, pp. 1669-1677, 1994.
- [25] IEC 60071-2, "Insulation Coordination, Part 2: Application Guide," 1996.
- [26] IEEE Std. 1313.2 - 1999, "IEEE guide for the application of insulation coordination," Technical Council of the IEEE Power Engineering Society, 1999.
- [27] J. A. Martinez-Velasco, and F. C. Aranda, "Parametric Analysis of the Lightning Performance of Overhead Transmission Lines Using an Electromagnetic Transients Program," *International Conference on Power Systems Transients-IPST 2003 in New Orleans, USA*, pp. 1-6, 2003.
- [28] A. Zupan, A. T. Teklic, and B. Filipovic-Grcic, "Modeling of 25 kV Electric Railway System for Power Quality Studies," *EuroCon 2013.Zagreb, Croatia*, pp. 844-849, 2013.
- [29] M. Karagoz, *Analysis of the Pantograph Arcing and Its Effect of the Railway Vehicle*, M. Degree Thesis, Middle East Technical University. pp. 59-72, 2014.
- [30] F. Achouri, I. Achouri, and M. Khamliche, "Protection of 25 kV Electrified Railway System," *4th International Conference on Electrical Engineering (ICEE)*, pp. 1-6, 2015.
- [31] G. Lee, and C. Goldsworthy, "Introduction to the Alternative Transients Program (ATP)," *IEEE SPDC Spring Meeting in Bonneville Power Administration (BPA)*, pp. 1-110, 2011.
- [32] W. Wu, X. Cao, "Power System Electromagnetic Transient Calculation with EMTP Application," *Beijing: China Water & Power Press*, pp. 232-249, 2012.
- [33] IEC 60850:2014, "Railway Applications-Supply Voltages of Traction Systems," *International Electrotechnical Commission standard*, 2014.



**Kelvin Melckzedek Minja** was born in Tanga, Tanzania in 1989. He completed his B.Eng. in Electrical Engineering in 2015 from Dar es Salaam Institute of Technology. He is currently a Master's Degree student at the School of Electrical Engineering, Institute of Engineering at the Suranaree University of Technology in Thailand.



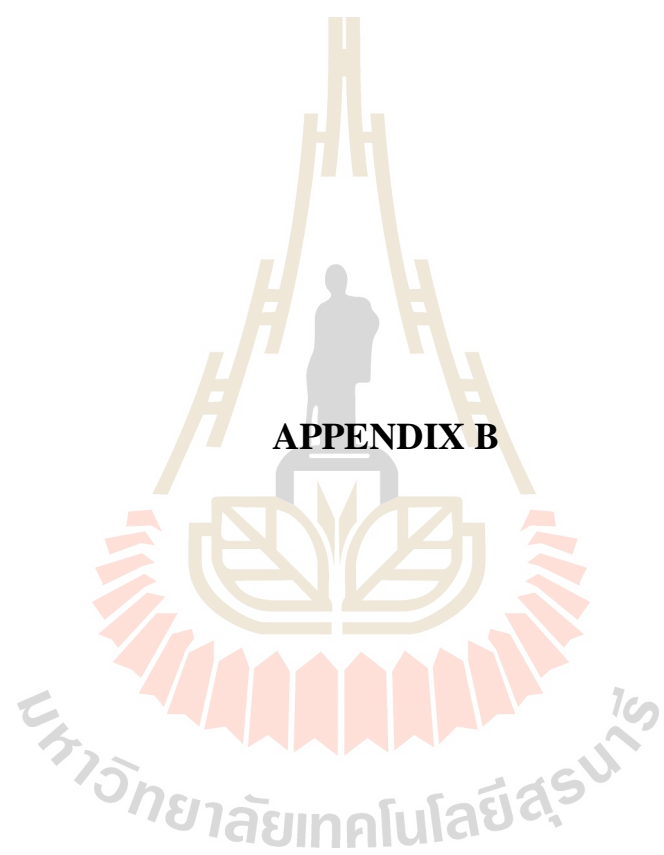
**Pius Victor Chombo** has obtained his B.Eng. Degree in Electrical Engineering from Dar es Salaam Institute of Technology, Tanzania in 2013. He is now a Master's Degree student in the School of Electrical Engineering, the Suranaree University of Technology in Thailand. His interest research topics include High Voltage Systems Design and Monitoring, Laboratory and System Programming.



**Narupon Promvichai** has obtained his B.Eng. Degree in the School of Electrical Engineering, the Suranaree University of Technology in Thailand, 2015. He is now a Master's Degree student in the School of Electrical Engineering, the Suranaree University of Technology in Thailand.



**Boonruang Marungsri** was born on 1973 in Nakhon Ratchasima Province, Thailand. He received his B. Eng. in 1996 and M. Eng. in 1999 from Chulalongkorn University, Thailand and D. Eng. in 2006 from Chubu University, Kasugai, Aichi, Japan, all in electrical engineering, respectively. Dr. Marungsri is currently a lecturer in School of Electrical Engineering, Suranaree University of Technology, Thailand. His areas of interest are electrical power system and high voltage insulation technologies.



**APPENDIX B**

## SOURCE EQUATIONS FOR PERFORMANCE INDEX

The below are the equations of origin used in the Lightning performance optimization for 25 kV AC, 50 Hz catenary contact system presented in this research and manipulated in MATLAB software.

- **Equations for Backflashover failure rate.**

This section shows the source equations used to estimate backflashover failure rate as shown in bellows equations (B.1)-(B.13).

$$N_{BF} = N_L \int_{(I_{peak})_{min}}^{(I_{peak})_{max}} \int_{(di/dt)_{min}}^{(di/dt)_{max}} P(\delta) \partial I_{peak} \partial (di/dt) \quad (B.1)$$

$$\delta(I_{peak}, di/dt) = \frac{RI_{peak}}{2} - 0.85U_a + L di/dt \quad (B.2)$$

$$\partial(\delta) = \partial \left( \frac{RI_{peak}}{2} - 0.85U_a + L di/dt \right) \quad (B.3)$$

$$\partial(\delta) = \left( \frac{R}{2} + L \right) \partial I_{peak} \partial (di/dt) \quad (B.4)$$

$$\partial I_{peak} \partial (di/dt) = \frac{\partial(\delta)}{\frac{R}{2} + L} \quad (B.5)$$

$$N_{BF} = N_L \left( \frac{1}{\frac{R}{2} + L} \right) \int_{(I_{peak})_{min}}^{(I_{peak})_{max}} \int_{(di/dt)_{min}}^{(di/dt)_{max}} P(\delta) \partial(\delta) \quad (B.6)$$

But

$$P(\delta) = \frac{1}{1 + \left(\frac{\delta}{31}\right)^{2.6}} \quad (\text{B.7})$$

$$N_{BF} = N_L \left( \frac{1}{\left(\frac{R}{2} + L\right)} \right) \int_{(I_{peak})_{\min}}^{(I_{peak})_{\max}} \int_{(di/dt)_{\min}}^{(di/dt)_{\max}} \left( \frac{1}{1 + \left(\frac{\delta}{31}\right)^{2.6}} \right) \partial(\delta) \quad (\text{B.8})$$

Due to the complexity of equation (B.8) integral calculator which found in the android phone from play store as shown in Figure. B.1 was used to manipulate the variables.

**Function f(x)**

$f: [a,b] \subset \mathbb{R} \rightarrow \mathbb{R}$   
 $x \rightarrow y=f(x)$

f(x):

Interval:

a:  b:

**Plot f(x)**

**Clear Graphic**

**Indefinite integral**

$$\int f(x)dx = \frac{1289842 x^{\frac{1}{5}}}{171 x^{\frac{17}{5}} + 1289842}$$

**calculate**

### B.1 Integral function for Backflashover failure rate



$$N_{BF} = N_L \left( \frac{1}{R/2 + L} \right) \left| \left( \frac{1289842(\delta)^{1/5}}{171(\delta)^{17/5} + 1289842} \right) \right|_{(di/dt)_{\min}}^{(di/dt)_{\max}} \left| \right|_{(I_{peak})_{\min}}^{(I_{peak})_{\max}} \quad (\text{B.9})$$

Since

$$\delta(I_{peak}, di/dt) = RI_{peak}/2 - 0.85U_a + L di/dt \quad (\text{B.10})$$

$$N_{BF} = N_L \left( \frac{1}{R/2 + L} \right) \left| \left( \frac{1289842 \left( RI_{peak}/2 - 0.85U_a + L di/dt \right)^{1/5}}{171 \left( RI_{peak}/2 - 0.85U_a + L di/dt \right)^{17/5} + 1289842} \right) \right|_{(di/dt)_{\min}}^{(di/dt)_{\max}} \left| \right|_{(I_{peak})_{\min}}^{(I_{peak})_{\max}} \quad (\text{B.11})$$

$$N_L = \left[ \left( \frac{N_g}{10} \right) (28h_t^{0.6} + g) \right] \quad (\text{B.12})$$

$$N_g = 0.04 T^{1.25} \quad (\text{B.13})$$

Requirements for Backflashover rate from different regions in the system

$L = 5.4 \mu\text{H}$  (The total inductance of equivalent inductance of the system (Mast and grounding system inductance) in  $\mu\text{H}$  (IEEE Working Group, 1993)).

$N_g = 6.68 \text{ strikes}/\text{km}^2/\text{yr}$  (the ground flash density in flashes per  $\text{km}^2$  (CIGRE Working Group 33.1, (1991),)).

$T = 60$  the yearly keraunic level in Thailand (IEEE Working Group, 1985)

$h_t = 8 \text{ m}$  (the mast height in m).

$g = 10.8$  m (The horizontal spacing in m, between ground wires)

$$N_L = 72.35$$

$$(I_{peak})_{max} = 139 \text{ kA peak lightning current at maximum in kA}$$

$$(I_{peak})_{min} = 0.29 \text{ kA peak lightning current at minimum in kA}$$

$$(di/dt)_{max} = \text{lightning steepness at maximum in kA}/\mu\text{s}$$

$$(di/dt)_{min} = \text{lightning steepness at minimum in kA}/\mu\text{s}$$

$$U_{ai_{max}} = 27.5 \text{ kV Insulation level at maximum}$$

$$U_{ai_{min}} = 19 \text{ kV Insulation level at maximum}$$

$$R_{i_{max}} = 100 \ \Omega \text{ Ground resistance at maximum}$$

$$R_{i_{min}} = 5 \ \Omega \text{ Ground resistance at minimum}$$

- **Equations for shielding failure rate.**

This section shows the source equations used to estimate shielding failure rate as shown in bellows equations (B.14)- (B.31).

$$N_{SF} = \frac{2N_g l}{10} \int_{I_{min}}^{I_{max}} Dc f(I) \partial I \quad (\text{B.14})$$

But

$$f(I) = \frac{1}{\sqrt{2\pi} \delta_{in} I} \exp \left[ \frac{-(\ln I - \ln \bar{I})^2}{2\delta_{in}^2} \right] \quad (\text{B.15})$$

The value  $\bar{I} = 33.3$  kA and  $\delta_{in} = 0.61$  for  $I \geq 20$  kA

$$f(I) = \frac{1}{\sqrt{2\pi} 0.61 I} \exp \left[ \frac{-(\ln I - \ln 33.3)^2}{0.7442} \right] \quad (\text{B.16})$$

$$N_{SF} = \frac{2N_g l}{10} \frac{Dc}{\sqrt{2\pi} 0.61} \int_{I_{\min}}^{I_{\max}} \frac{1}{I} \exp \left[ \frac{-(\ln I - \ln 33.3)^2}{0.7442} \right] \partial I \quad (\text{B.17})$$

Let

$$U = \ln I - \ln 33.3 \quad (\text{B.18})$$

then

$$U = \ln I - 3.506 \quad (\text{B.19})$$

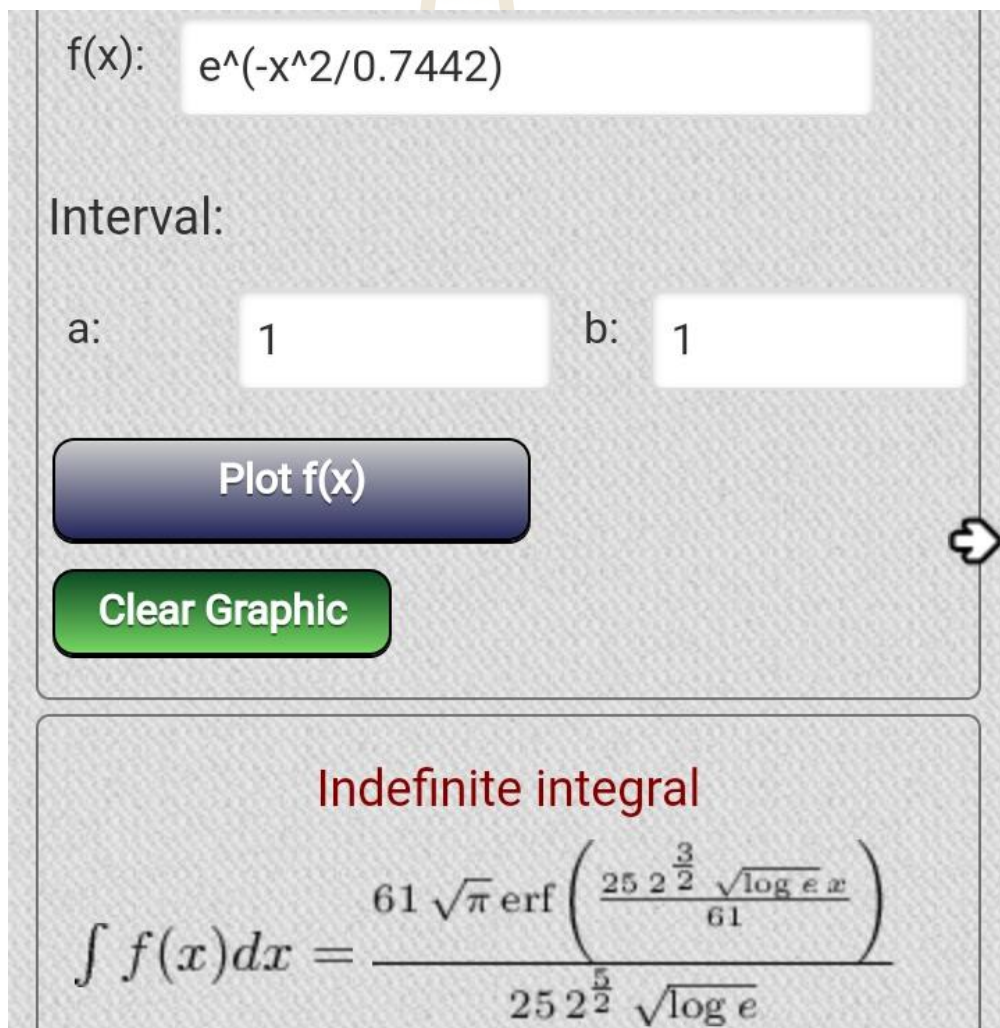
$$\ln I = U + 3.506 \quad (\text{B.20})$$

$$\partial U = \frac{1}{I} \partial I \quad (\text{B.21})$$

$$\partial I = I \partial U \quad (\text{B.22})$$

$$N_{SF} = \frac{2N_g l}{10} \frac{Dc}{\sqrt{2\pi} \cdot 0.61} \int_{I_{\min}}^{I_{\max}} \exp\left[\frac{-U^2}{0.7442}\right] \partial U \quad (\text{B.23})$$

Due to the difficulty of equation (B.23) integral calculator which found in the android phone from play store as shown in Figure. B.2 was used to calculate the variables.



f(x):  $e^{-x^2/0.7442}$

Interval:

a:  b:

**Plot f(x)**

**Clear Graphic**

**Indefinite integral**

$$\int f(x) dx = \frac{61 \sqrt{\pi} \operatorname{erf}\left(\frac{25 \cdot 2^{\frac{3}{2}} \sqrt{\log e} x}{61}\right)}{25 \cdot 2^{\frac{5}{2}} \sqrt{\log e}}$$

### B.2 Integral function for shielding failure rate

$$N_{SF} = \frac{2N_g l}{10} \frac{Dc}{\sqrt{2\pi} 0.61} \left| \frac{61\sqrt{\pi} \operatorname{erf} \left( \frac{25 \cdot 2^{3/2} \sqrt{\log e^u}}{61} \right)}{25 \cdot 2^{5/2} \sqrt{\log e^1}} \right|_{I_{\min}}^{I_{\max}} \quad (\text{B.24})$$

But

$$U = \ln I - 3.506 \quad (\text{B.25})$$

$$N_{SF} = \frac{2N_g l}{10} \frac{Dc}{\sqrt{2\pi} 0.61} \left| \frac{61\sqrt{\pi} \operatorname{erf} \left( \frac{25 \cdot 2^{3/2} \sqrt{\log e^{\ln I - 3.506}}}{61} \right)}{25 \cdot 2^{5/2} \sqrt{\log e^1}} \right|_{I_{\min}}^{I_{\max}} \quad (\text{B.26})$$

Then

$$N_{SF} = \frac{2N_g l}{10} \frac{Dc}{\sqrt{2\pi} 0.61} \left| \frac{61\sqrt{\pi} \operatorname{erf} \left( \frac{25 \cdot 2^{3/2} \sqrt{\operatorname{abs}(\log(I/33.3))}}{61} \right)}{25 \cdot 2^{5/2} \sqrt{\log e^1}} \right|_{I_{\min}}^{I_{\max}} \quad (\text{B.27})$$

Since

$$I_{\min} = \frac{2U_a}{Z_{surge}} \quad (B.28)$$

$$N_{SF} = \frac{2N_g l}{10} \frac{Dc}{\sqrt{2\pi} 0.61} \left| \frac{61\sqrt{\pi} \operatorname{erf} \left( \frac{25 \cdot 2^{3/2} \sqrt{\operatorname{abs}(\log(I/33.3))}}{61} \right)}{25 \cdot 2^{3/2} \sqrt{\log e^I}} \right|^{I_{\max}} \quad (B.29)$$

$$Z_{surge} = 60 \sqrt{\ln\left(\frac{4h_c}{d}\right) \ln\left(\frac{4h_c}{D}\right)} \quad (B.30)$$

$$N_g = 0.04 T^{1.25} \quad (B.31)$$

Requirements for Shield failure rate from different regions in the system

$l = 28.193$  km The line length in km

$Dc = 1.8$  m (the shield failure width in m)

$N_g = 6.68$  strikes/km<sup>2</sup>/yr (the ground flash density in flashes per km<sup>2</sup> (CIGRE Working Group 33.1, (1991),)).

$T = 60$  the yearly keraunic level in Thailand (IEEE Working Group,1985)

$I_{\max} = 25$  kA maximum lightning current in kA

$I_{\min} = 0.29$  kA maximum lightning current in kA

$Z_{surge} = 174.97 \Omega$  (The conductor line surge impedance)

$h_c = 4.9$  m (conductor height at the mast in m (Sandra, Martin, and Menter 2007))

$D = 1.112$  m (the equivalent conductor diameter with corona (Kiessling, et al., 2009))

$d = 1.012$  m (the equivalent conductor diameter without corona)

$U_{ai_{\max}} = 27.5$  kV (Insulation level at maximum)

$U_{ai_{\min}} = 19$  kV (Insulation level at maximum)

- **Equations for arrester failure rate.**

This section shows the source equations used to estimate arrester failure rate as shown in bellows equations (B.32)-(B.47).

$$A_T = N_L P_T \quad (\text{B.32})$$

$$P_T = P_A + P_B \quad (\text{B.33})$$

Where

$P_A$  = the probability that an arrester fails due to lightning strokes on the phase conductor

$P_B$  = the probability that an arrester fails due to lightning strokes on the overhead ground wire.

$$P_A = \int_{T_r}^{\infty} \left\{ \int_{I_A(t)}^{\infty} f(I_P) h_A(I_P) dI_P \right\} g(T_t) dT_t \quad (\text{B.34})$$

$$P_B = \int_{T_r}^{\infty} \left\{ \int_{I_B(t)}^{\infty} f(I_P) h_B(I_P) dI_P \right\} g(T_t) dT_t \quad (\text{B.35})$$

$$P_T = \int_{T_r}^{\infty} \left\{ \int_{I_A(t)}^{\infty} f(I_P) h_A(I_P) dI_P \right\} g(T_t) dT_t + \int_{T_r}^{\infty} \left\{ \int_{I_B(t)}^{\infty} f(I_P) h_B(I_P) dI_P \right\} g(T_t) dT_t \quad (\text{B.36})$$

But

$$f(I_P) = \frac{n_c}{I_{50}^{n_t}} \cdot \frac{I_P^{n_c-1}}{\left[ 1 + \left( \frac{I_P}{I_{50}} \right)^{n_c} \right]^2} \quad (\text{B.37})$$

$$g(T_t) = \frac{n_t}{T_{50}^{n_t}} \cdot \frac{T_t^{n_t-1}}{\left[ 1 + \left( \frac{T_t}{T_{50}} \right)^{n_t} \right]^2} \quad (\text{B.38})$$

$$h_A(I_P) = 1 - \frac{X_c}{X_r} \quad (\text{B.39})$$

$$h_B(I_P) = \frac{X_c}{X_r} \quad (\text{B.40})$$

Since  $n_c = 1.89$ ,  $n_t = 1.82$ ,  $I_{50} = 24$ , and  $T_{50} = 30$



Then

$$f(I_P) = \frac{1.89}{24^{1.89}} \cdot \frac{I_P^{0.89}}{\left[1 + \left(\frac{I_P}{24}\right)^{1.89}\right]^2} \quad (\text{B.41})$$

$$g(T_t) = \frac{1.82}{30^{1.82}} \cdot \frac{T_t^{0.82}}{\left[1 + \left(\frac{T_t}{30}\right)^{1.82}\right]^2} \quad (\text{B.42})$$

$$P_T = \int_{T_r}^{\infty} \left\{ \int_{I_A(t)}^{\infty} \left( \frac{1.89}{24^{1.89}} \cdot \frac{I_P^{0.89}}{\left[1 + \left(\frac{I_P}{24}\right)^{1.89}\right]^2} \right) \left(1 - \frac{X_c}{X_r}\right) dI_P \right\} \left( \frac{1.82}{30^{1.82}} \cdot \frac{T_t^{0.82}}{\left[1 + \left(\frac{T_t}{30}\right)^{1.82}\right]^2} \right) dT_t \quad (\text{B.43})$$

$$+ \int_{T_r}^{\infty} \left\{ \int_{I_B(t)}^{\infty} \left( \frac{1.89}{24^{1.89}} \cdot \frac{I_P^{0.89}}{\left[1 + \left(\frac{I_P}{24}\right)^{1.89}\right]^2} \right) \left(\frac{X_c}{X_r}\right) dI_P \right\} \left( \frac{1.82}{30^{1.82}} \cdot \frac{T_t^{0.82}}{\left[1 + \left(\frac{T_t}{30}\right)^{1.82}\right]^2} \right) dT_t$$

Due to the difficulty of equation (B.43) integral calculator which found in the android phone from play store as shown in Figures. B.3-B.6 was used to calculate the variables.

**Function  $f(x)$**


$f: [a,b] \subset \mathbb{R} \rightarrow \mathbb{R}$   
 $x \rightarrow y=f(x)$

f(x):

Interval:

a:  b:

**Plot  $f(x)$**

**Clear Graphic** 

---

**Indefinite integral**

$$\int f(x)dx = \frac{340834094200 \log\left(\frac{1281552 x^{\frac{18}{10}}}{1281552 x^{\frac{18}{10}}}\right)}{189 \sqrt{769}}$$

**calculate**

### B.3 Integral function for arrester failure rate

**Function f(x)**


$f: [a,b] \subset \mathbb{R} \rightarrow \mathbb{R}$   
 $x \rightarrow y=f(x)$

f(x):

Interval:

a:  b:

**Plot f(x)**

**Clear Graphic** 

---

**Indefinite integral**

$$\int f(x)dx = \frac{\left( \frac{x \frac{189}{100} - 31 \sqrt{7698601 + 520397837}}{x \frac{189}{100} + 31 \sqrt{7698601 + 520397837}} \right)}{\sqrt{7698601}}$$

**calculate**

**B.4** Integral function for arrester failure rate (Continued)

**Function f(x)**


$f: [a,b] \subset \mathbb{R} \rightarrow \mathbb{R}$   
 $x \rightarrow y=f(x)$

f(x):

Interval:

a:  b:

**Plot f(x)**

**Clear Graphic** 

---

**Indefinite integral**

$$\int f(x)dx = \frac{3246862279800 \arctan\left(\frac{190928}{13\sqrt{25688740}}\right)}{13\sqrt{25688740}}$$

**calculate**

**B.5** Integral function for arrester failure rate (Continued)

**Function f(x)**


$f: [a,b] \subset \mathbb{R} \rightarrow \mathbb{R}$   
 $x \rightarrow y=f(x)$

f(x):

Interval:

a:       b:

**Plot f(x)**

**Clear Graphic** 

---

**Indefinite integral**

$$\int f(x)dx = \frac{\arctan\left(\frac{1909284x^{\frac{91}{50}} + 931603729}{\sqrt{256887407}}\right)}{3\sqrt{256887407}}$$

**calculate**

**B.6** Integral function for arrester failure rate (Continued)

$$P_A = \left\{ \left( \frac{1.89}{24^{1.89}} \cdot \frac{3.41 \times 10^{11} \log \left( \frac{1.28 \times 10^6 I_A(t)^{189/100} - 31\sqrt{7698601} + 520397837}{1.28 \times 10^6 I_A(t)^{189/100} + 31\sqrt{7698601} + 520397837} \right)}{189\sqrt{7698601}} \right) \left( 1 - \frac{X_c}{X_r} \right) \right\}_{I_A(T_r)}^{\infty} \quad (\text{B.44})$$

$$\times \frac{1.82}{30^{1.82}} \cdot \frac{3.25 \times 10^{12} \arctan \left( \frac{1909284T_r^{(9/50)} + 931603729}{\sqrt{256887407}} \right)}{13\sqrt{256887407}} \Big|_{T_r}^{\infty}$$

$$P_B = \left\{ \left( \frac{1.89}{24^{1.89}} \cdot \frac{3.41 \times 10^{11} \log \left( \frac{1.28 \times 10^6 I_B(t)^{189/100} - 31\sqrt{7698601} + 520397837}{1.28 \times 10^6 I_B(t)^{189/100} + 31\sqrt{7698601} + 520397837} \right)}{189\sqrt{7698601}} \right) \left( \frac{X_c}{X_r} \right) \right\}_{I_B(T_r)}^{\infty} \quad (\text{B.45})$$

$$\times \frac{1.82}{30^{1.82}} \cdot \frac{3.25 \times 10^{12} \arctan \left( \frac{1909284T_r^{(9/50)} + 931603729}{\sqrt{256887407}} \right)}{13\sqrt{256887407}} \Big|_{T_r}^{\infty}$$

Requirements for Arrester failure rate from different regions in the system

$$X_c = 2.7 \text{ m}$$

$$X_r = 4.5 \text{ m}$$

$I_A(T_r)$  = The minimum stroke peak current in kA required to damage the arrester, when lightning hits on a phase conductor, depending on each time-to-half value.

$I_B(T_r)$  = The minimum stroke peak current in kA expected to destroy the arrester, once lightning hits on the overhead ground wire, depending on each time-to-half value.

$T_r$  = The rise time of the incident waveform

$$E = \int_0^t V(t)i(t)dt \cong \sum_{j=1}^{n-1} \left[ 0.5T_r (V_j I_j + V_{j+1} I_{j+1}) \right] \quad (\text{B.46}) \quad (\text{Lira, Fernandes, and}$$

Costa 2007)

$$T_r = \frac{2 \times E}{\sum_{j=1}^{n-1} \left[ (V_j I_j + V_{j+1} I_{j+1}) \right]} \quad (\text{B.47})$$

## SOURCE CODES FOR PERFORMANCE INDEX

The below are the source codes utilized in the MATLAB software for optimal lightning performance index of 25 kV AC, 50 Hz catenary contact system examined in this research and manipulated by AI Optimization techniques.

- **Codes for representing Existed System.**

This section shows the source codes used to estimate Total failure rate of existed system as shown in bellows.

### 1. Codes for the Main run

```

clc;
clear all;
close all;

tic
global rho Amax Amin
rho=1e6;
Amax = [27.5 100];
Amin = [19 5];
rand('state',sum(100*clock))
numberOfVariables=length(Amax);
    fobj001 = @ obj_function_total;
    optionsGA = gaoptimset('PopulationType','doubleVector',...
        'PopInitRange',[Amin;Amax],...
        'PopulationSize',1000,...
        'CrossoverFraction', 0.8000,...
        'Generations',100000);
    [xopt,fval,EXITFLAG,OUTPUT] =
ga(fobj001,numberOfVariables,[],[],[],[],[],[],[],optionsGA);
    fval
    xopt

```

toc

## 2. Codes for Objective Function

```

function [f]=obj_function_total(x)

global rho Amax Amin

Amax = [27.5 100];
Amin = [19 5];

L=5.4;
b1=139;
b2=0.29;
c1=2;
c2=1;
Ng=6.68;
ht=8;
g=10.8;
NL=((Ng/10*(28*ht^(0.6))+g));
a1=((x(2)*b1)/2)-(0.85*x(1))+(L*c1);
a2=((x(2)*b2)/2)-(0.85*x(1))+(L*c2);

Ng=6.68;
l=28.193;
Dc=1.8;
Zsurge=174.97 ;
d1=25;
d2=(2*x(1))/Zsurge;
objective_function=(NL*((1/((x(2)/2)+L))*((1289842*(a1^(1/5)))/((171*
a1^(17/5))+1289842))-
((1289842*(a2^(1/5)))/((171*a2^(17/5))+1289842)))+(2*Ng*l*Dc)/(10*sq
rt(2*pi)*0.61))*((61*sqrt(pi)*erf(25*2^(3/2)*sqrt(abs(log10 (d1/exp
(3.506)))))/61)/25*2^(5/2)*(sqrt(log10 (exp (1)))))-
(61*sqrt(pi)*erf(25*2^(3/2)*sqrt(abs(log10 (d2/exp
(3.506)))))/61)/25*2^(5/2)*(sqrt(log10 (exp (1))))));

%=====make Penalty Function=====
Var = [x];
PT = 0; %panelty Term
for k=1:length(Var)
    up(k)=0;
    down(k)=0;
    if Var(k)>Amax(k)
        up(k)=rho*(Var(k)-Amax(k))^2;
    elseif Amin(k)>Var(k)
        down(k)=rho*(Amin(k)-Var(k))^2;
    end
    PT=PT+up(k)+down(k);
end
f=objective_function+PT;
return

```



- **Codes for representing Proposed System.**

This section shows the source equations used to estimate backflashover failure rate as shown in bellows equations.

### 1. Codes for the Main run

```

clc;
clear all;
close all;

tic
global rho Amax Amin
rho=1e6;
Amax = [27.5 100 10];
Amin = [19 5 5];
rand('state',sum(100*clock))
numberOfVariables=length(Amax);
fobj001 = @obj_function_total_3;
optionsGA = gaoptimset('PopulationType','doubleVector',...
    'PopInitRange',[Amin;Amax],...
    'PopulationSize',1000,...
    'CrossoverFraction',0.8000,...
    'Generations',100000);
[xopt,fval,EXITFLAG,OUTPUT] =
ga(fobj001,numberOfVariables,[],[],[],[],[],[],[],optionsGA);
fval
xopt
toc

```

### 2. Codes for Objective Function

```

function [f]=obj_function_total_3(x)
global rho Amax Amin

Amax = [27.5 100 10];
Amin = [19 5 5];
L=5.4;
b1=139;
b2=0.29;
c1=2;
c2=1;

a1=((x(2)*b1)/2)-(0.85*x(1))+(L*c1);
a2=((x(2)*b2)/2)-(0.85*x(1))+(L*c2);

l=28.193;

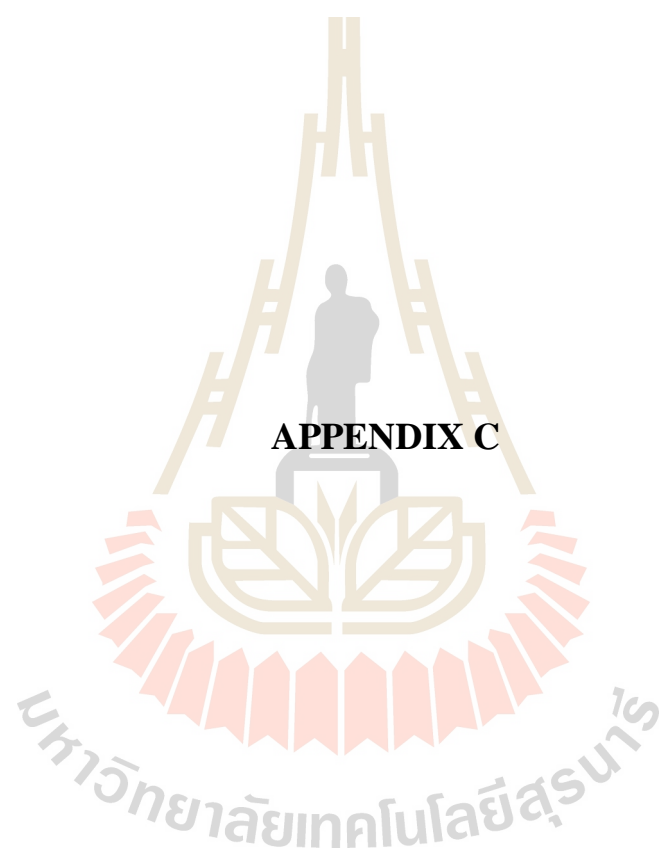
```

```

Dc=1.8;
Zsurge=174.97 ;
d1=25;
d2=(2*x(1))/Zsurge;
Isl=29;
Isg=10;
Xc=2.7;
Xr=4.5;
Tr=(2*x(3))/((76.125*0.01)+(83.7375*0.1)+(91.35*1)+(94.6125*2)+(97.87
5*4)+(98.9625*6)+(101.68125*8)+(103.3125*10)+(104.94375*12)+(107.1187
5*14)+(108.75*16)+(111.46875*18)+(114.1875*20));
Ng=6.68;
ht=8;
g=10.8;
NL=((Ng/10*(28*ht^(0.6))+g));

objective_function=(NL*((1/((x(2)/2)+L))*((1289842*(a1^(1/5)))/((171*
a1^(17/5))+1289842))-
((1289842*(a2^(1/5)))/((171*a2^(17/5))+1289842)))+(2*Ng*1*Dc)/(10*sq
rt(2*pi)*0.61))*((61*sqrt(pi)*erf(25*2^(3/2)*sqrt(abs(log10 (d1/exp
(3.506)))))/61)/25*2^(5/2)*(sqrt(log10 (exp (1)))))-
(61*sqrt(pi)*erf(25*2^(3/2)*sqrt(abs(log10 (d2/exp
(3.506)))))/61)/25*2^(5/2)*(sqrt(log10 (exp (1)))))+(((214.3-((1-
(Xc/Xr))*4.65e-3)*(((340834094200)*log10
(abs((1281552*((Isl)^(189/100)))-
((31*sqrt(7698601))+520397837)))/((1281552*((Isl)^(189/100)))+(31*sqrt
(7698601))+520397837))))/(189*sqrt(7698601)))))* (267.53-(3.73e-
3*((3246862279800*(atan
(((1909284*(Tr^(91/50)))+931603729)/(sqrt(256887407)))))))/(13*sqrt(256
887407)))))+((214.3-((Xc/Xr))*4.65e-3)*(((340834094200)*log10
(abs((1281552*((Isg)^(189/100)))-
((31*sqrt(7698601))+520397837)))/((1281552*((Isg)^(189/100)))+(31*sqrt
(7698601))+520397837))))/(189*sqrt(7698601)))))* (267.53-(3.73e-
3*((3246862279800*(atan
(((1909284*(Tr^(91/50)))+931603729)/(sqrt(256887407)))))))/(13*sqrt(256
887407))))));
%=====make Penalty Function=====
Var = [x];
PT = 0; %panelty Term
for k=1:length(Var)
    up(k)=0;
    down(k)=0;
    if Var(k)>Amax(k)
        up(k)=rho*(Var(k)-Amax(k))^2;
    elseif Amin(k)>Var(k)
        down(k)=rho*(Amin(k)-Var(k))^2;
    end
    PT=PT+up(k)+down(k);
end
f=objective_function+PT;
return

```



**APPENDIX C**

## **OUTCOME OF MULTIPLE LIGHTNING STROKES EFFECTS**

This section shows the simulation results of peak Mast induced voltages across the insulators in the auxiliary, return and Catenary lines as stressed lines when multiple lightning stroke strike on mast, catenary line, pantograph and auxiliary line of overhead catenary system in Airport Rail Link, Bangkok, Thailand

### **C.1 Simulation Analysis**

Direct lightning strikes likely to cause the charges to flow in the form of two equal current waves in both directions, starting from the point of hitting. One side from the stroke point was considered and inspected by arranging the masts with its ground resistances into three configurations with two cases each. The first configuration was based on studying the effect of flashover from the affected mast to nearby masts when their grounding resistances ( $R_f$ ) are similar (same soil profile) when lightning strikes on train's pantograph based on two cases (see Figures 3.8-3.10). The second configuration was done when their grounding resistances ( $R_f$ ) are different but in increasing order (different soil profile). Lastly, the third configuration was done when their grounding resistances are also different but in decreasing order (different soil profile). Table C.1 and C.2 show the arrangement of configuration 2 and 3 respectively. Since the lightning source was set in Train's pantograph at respective positions near to mast 4 (M4), the concern was to check the effect of flashover into the nearby mast (mast 5 or M5) and far end mast (mast 7 or M7) under same and different soil profiles.

**Table C.1** Simulations setup for Configuration 2 for both Cases

Simulation	First			Second			Third		
Mast	M4	M5	M7	M4	M5	M7	M4	M5	M7
Rf ( $\Omega$ )	5	10	20	5	20	50	5	50	100

**Table C.2** Simulations setup for Configuration 3 for both Cases

Simulation	First			Second			Third		
Mast	M4	M5	M7	M4	M5	M7	M4	M5	M7
Rf ( $\Omega$ )	100	50	20	100	20	10	100	10	5

## C.2 The consequences when the mast struck by negative multiple lightning strokes for Configuration 1 in Case 1 and 2.

In this part, the effects of negative multiple lightning strokes to nearby mast and far mast when it strikes on mast 4 are showed.

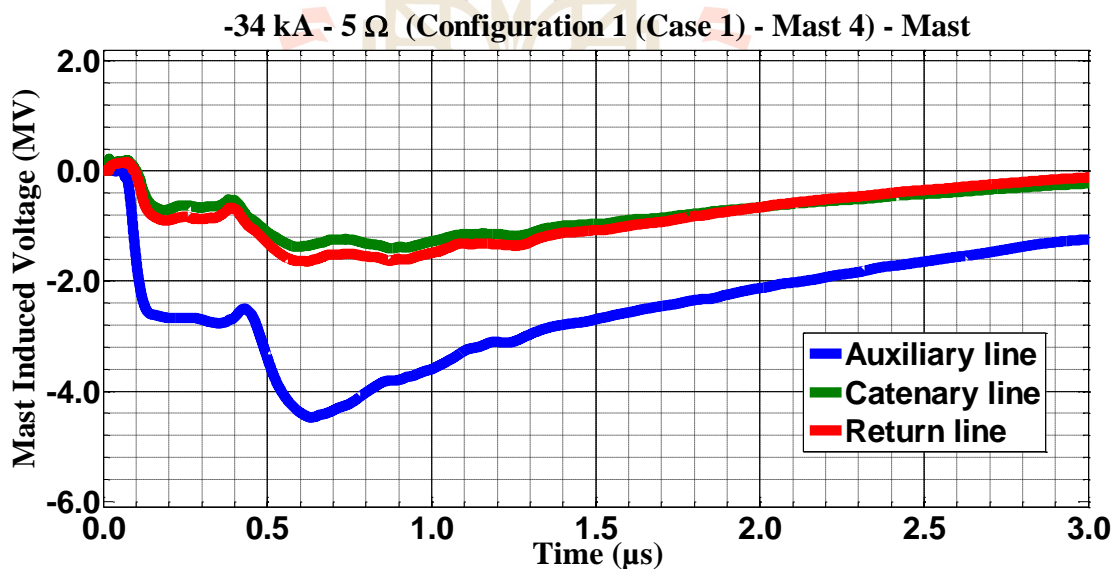


**Figure C.1** Mast 4, 5, and 7 induced voltage waveform of the -34 kA first stroke-(1.0/100  $\mu$ s), subsequent stroke-(0.2/50  $\mu$ s) strikes on Mast 4 with 5  $\Omega$  for Case 1

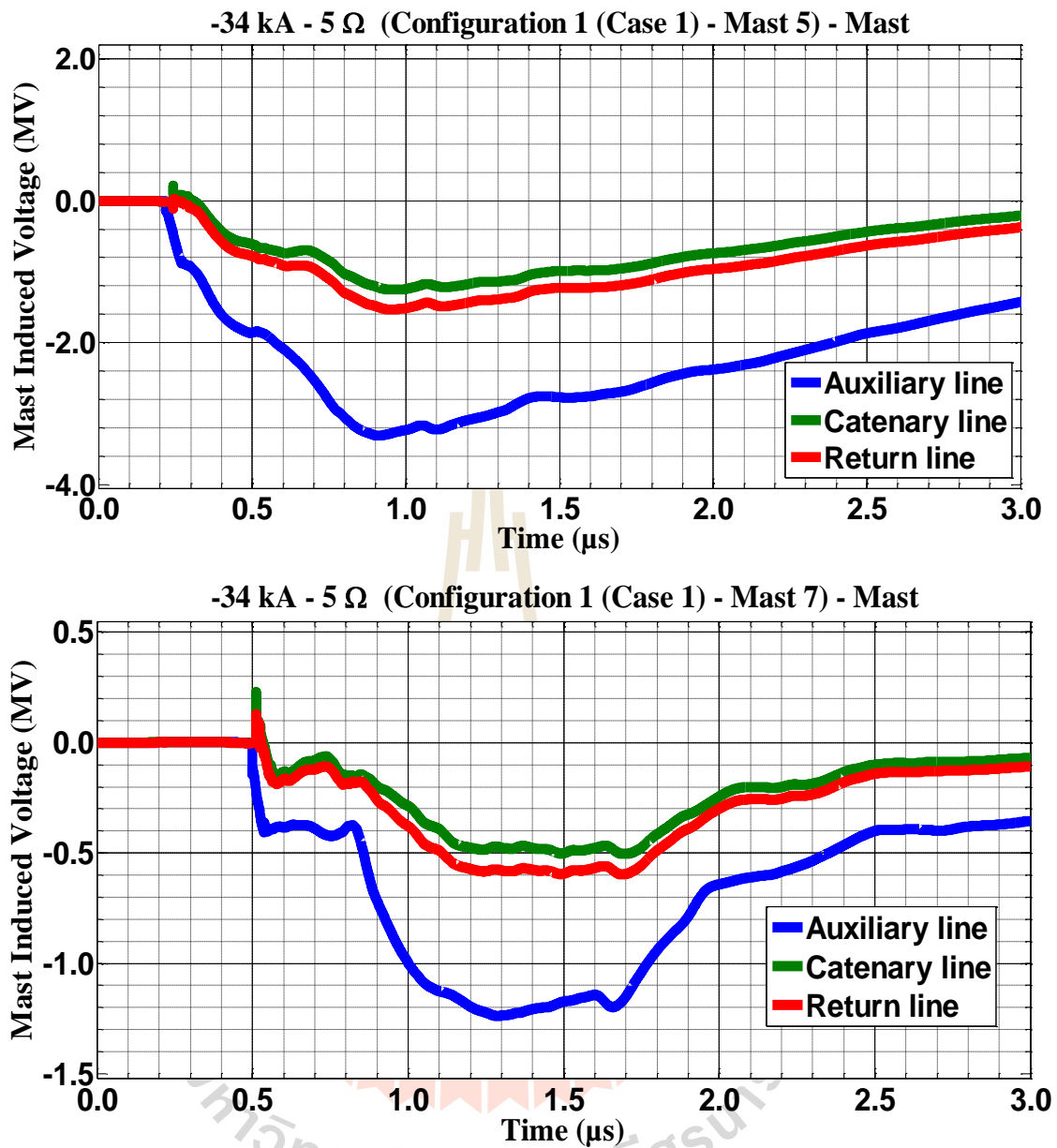


**Figure C.1** Mast 4, 5, and 7 induced voltage waveform of the -34 kA first stroke-(1.0/100  $\mu$ s), subsequent stroke-(0.2/50  $\mu$ s) strikes on Mast 4 with 5  $\Omega$  for Case 1

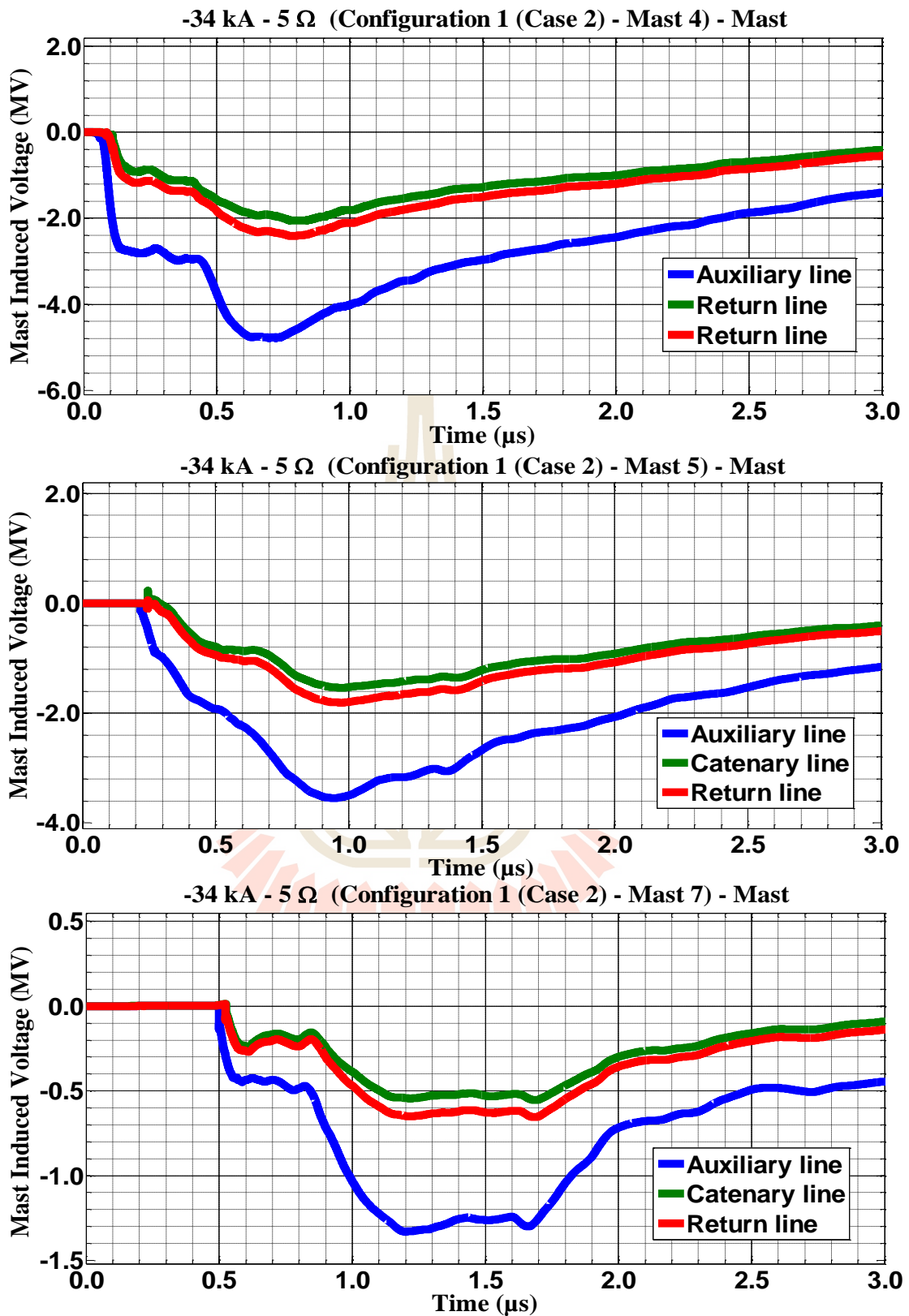


**Figure C.2** Mast 4, 5, and 7 induced voltage waveform of the -34 kA first stroke-(1.0/100  $\mu$ s), subsequent stroke-(0.2/50  $\mu$ s) strikes on Mast 4 with 5  $\Omega$  for Case 2

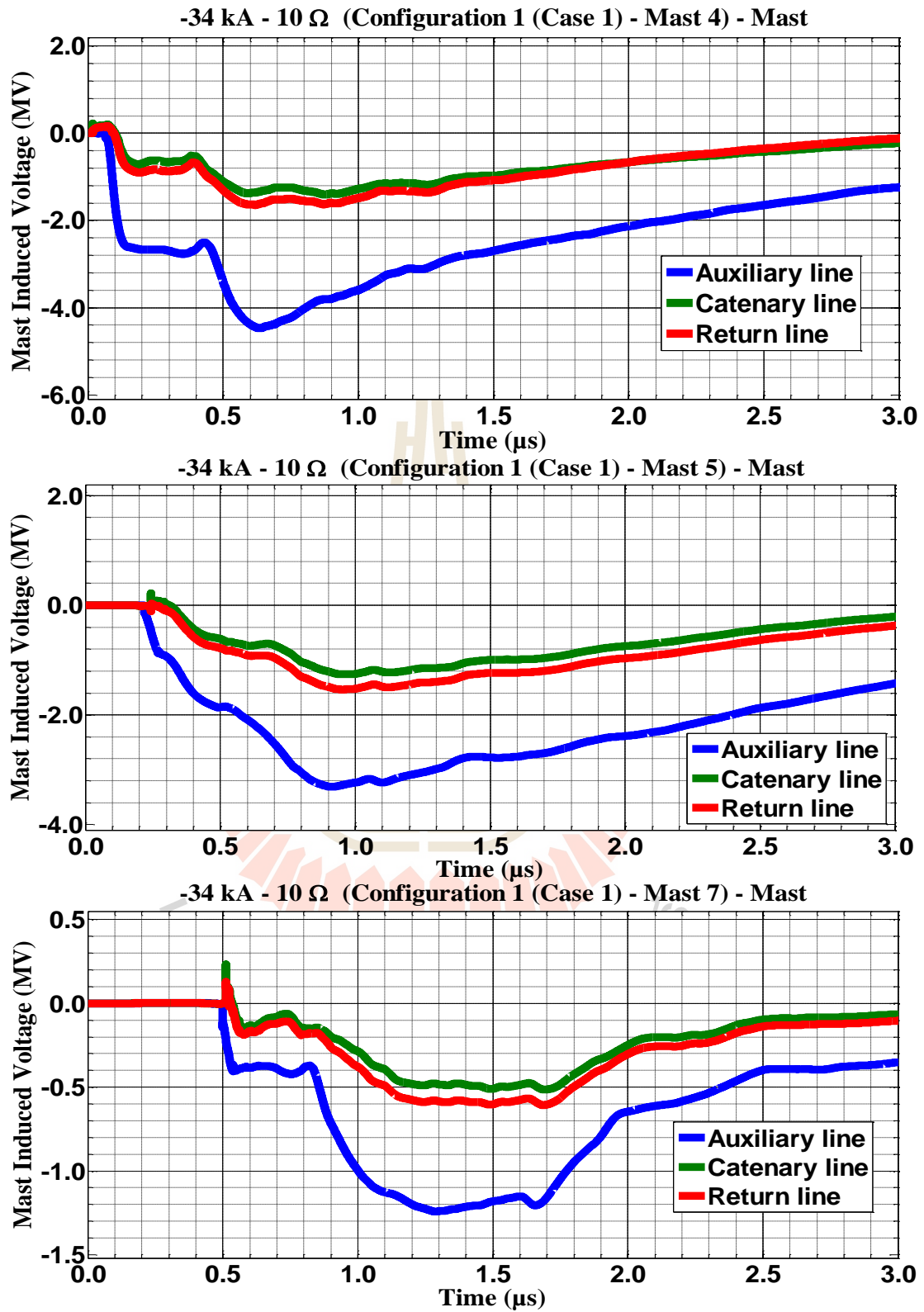


**Figure C.3** Mast 4, 5, and 7 induced voltage waveform of the -34 kA first stroke-(1.0/100 μs), subsequent stroke-(0.2/50 μs) strikes on Mast 4 with 10 Ω for Case 1



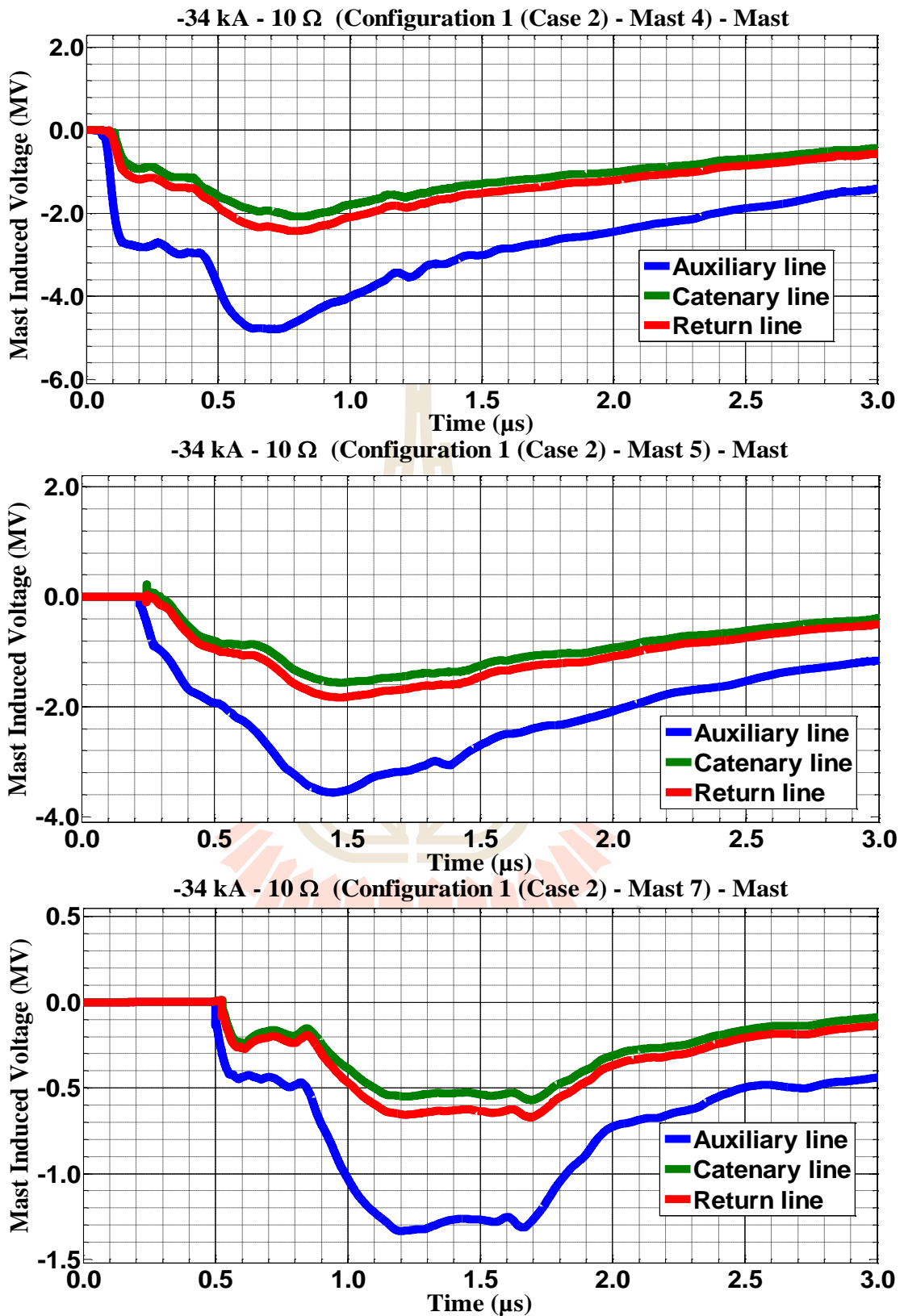


**Figure C.4** Mast 4, 5, and 7 induced voltage waveform of the -34 kA first stroke-(1.0/100 μs), subsequent stroke-(0.2/50 μs) strikes on Mast 4 with 10 Ω for Case 2

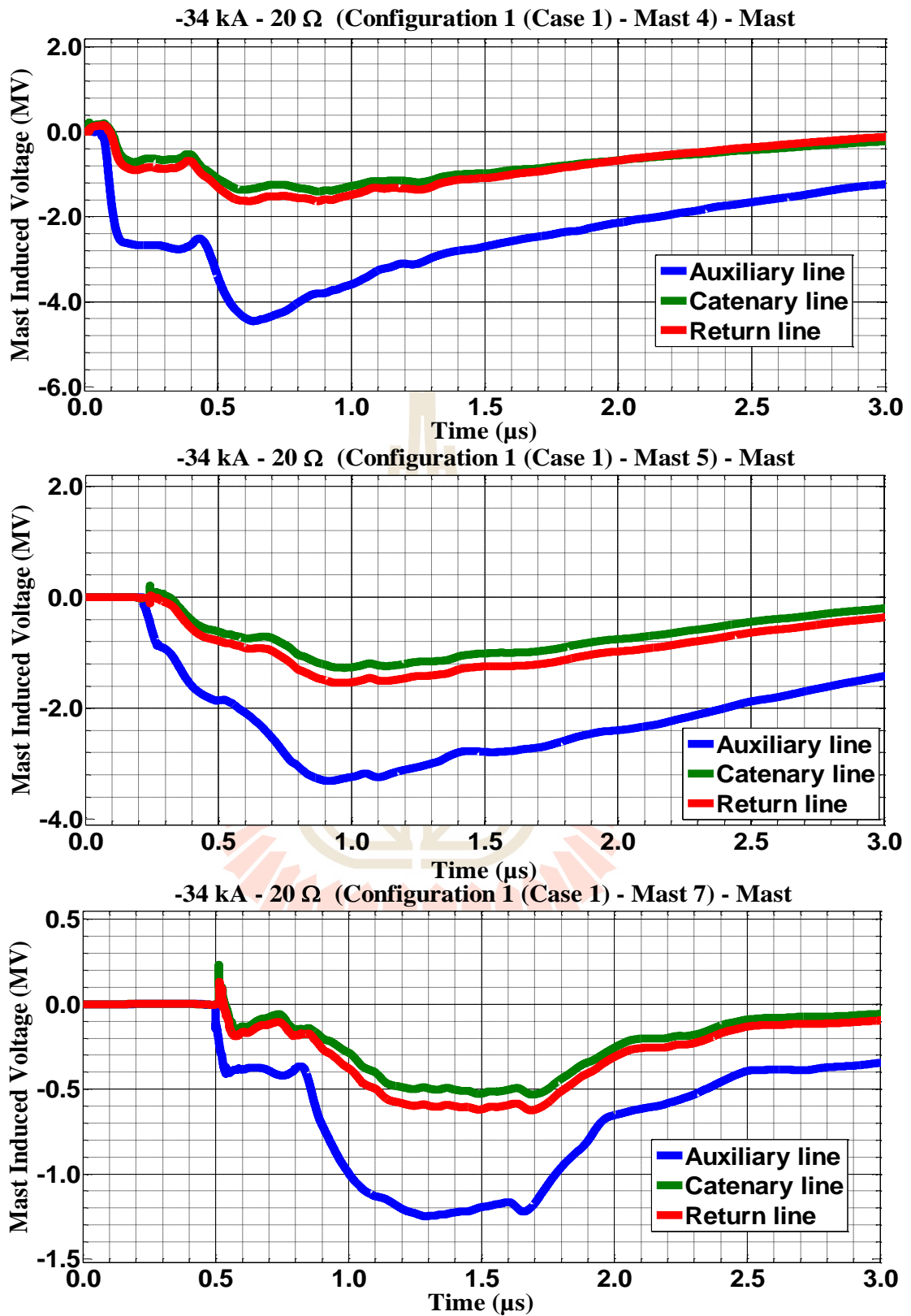


**Figure C.5** Mast 4, 5, and 7 induced voltage waveform of the -34 kA first stroke-(1.0/100 μs), subsequent stroke-(0.2/50 μs) strikes on Mast 4 with 20 Ω for Case 1

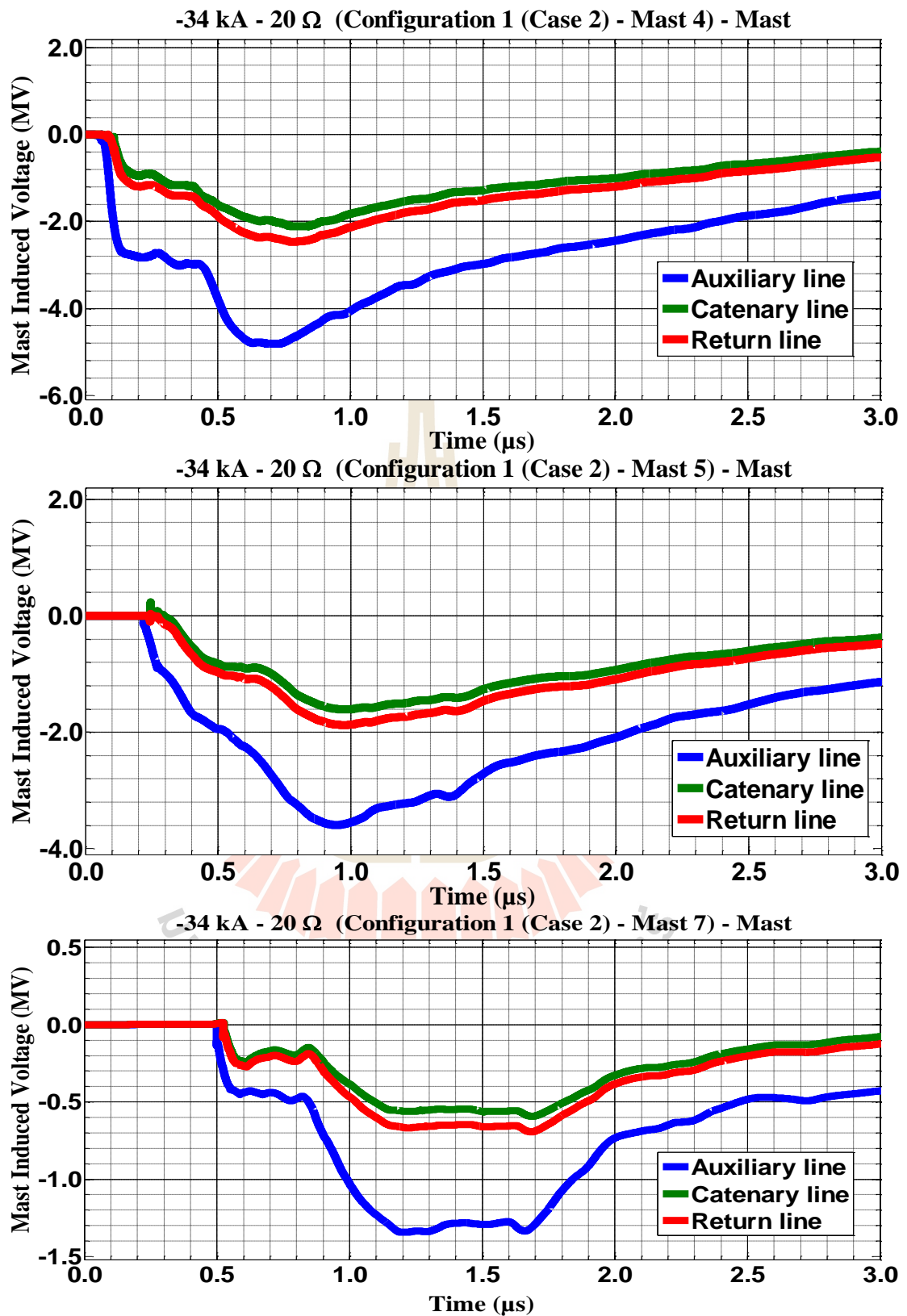


**Figure C.6** Mast 4, 5, and 7 induced voltage waveform of the  $-34 \text{ kA}$  first stroke-(1.0/100  $\mu\text{s}$ ), subsequent stroke-(0.2/50  $\mu\text{s}$ ) strikes on Mast 4 with  $20 \Omega$  for Case 2

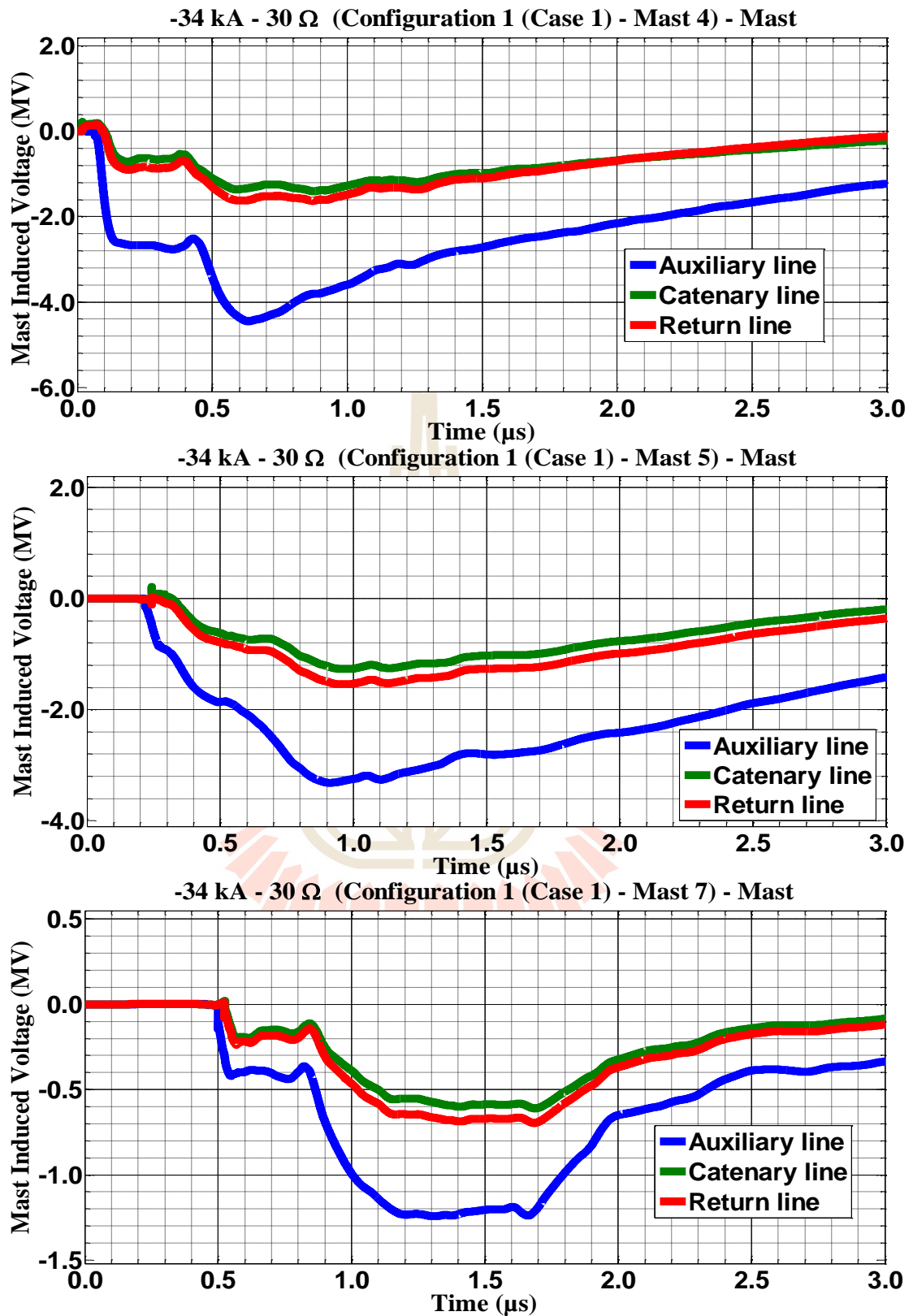


**Figure C.7** Mast 4, 5, and 7 induced voltage waveform of the -34 kA first stroke-(1.0/100  $\mu\text{s}$ ), subsequent stroke-(0.2/50  $\mu\text{s}$ ) strikes on Mast 4 with 30  $\Omega$  for Case 1

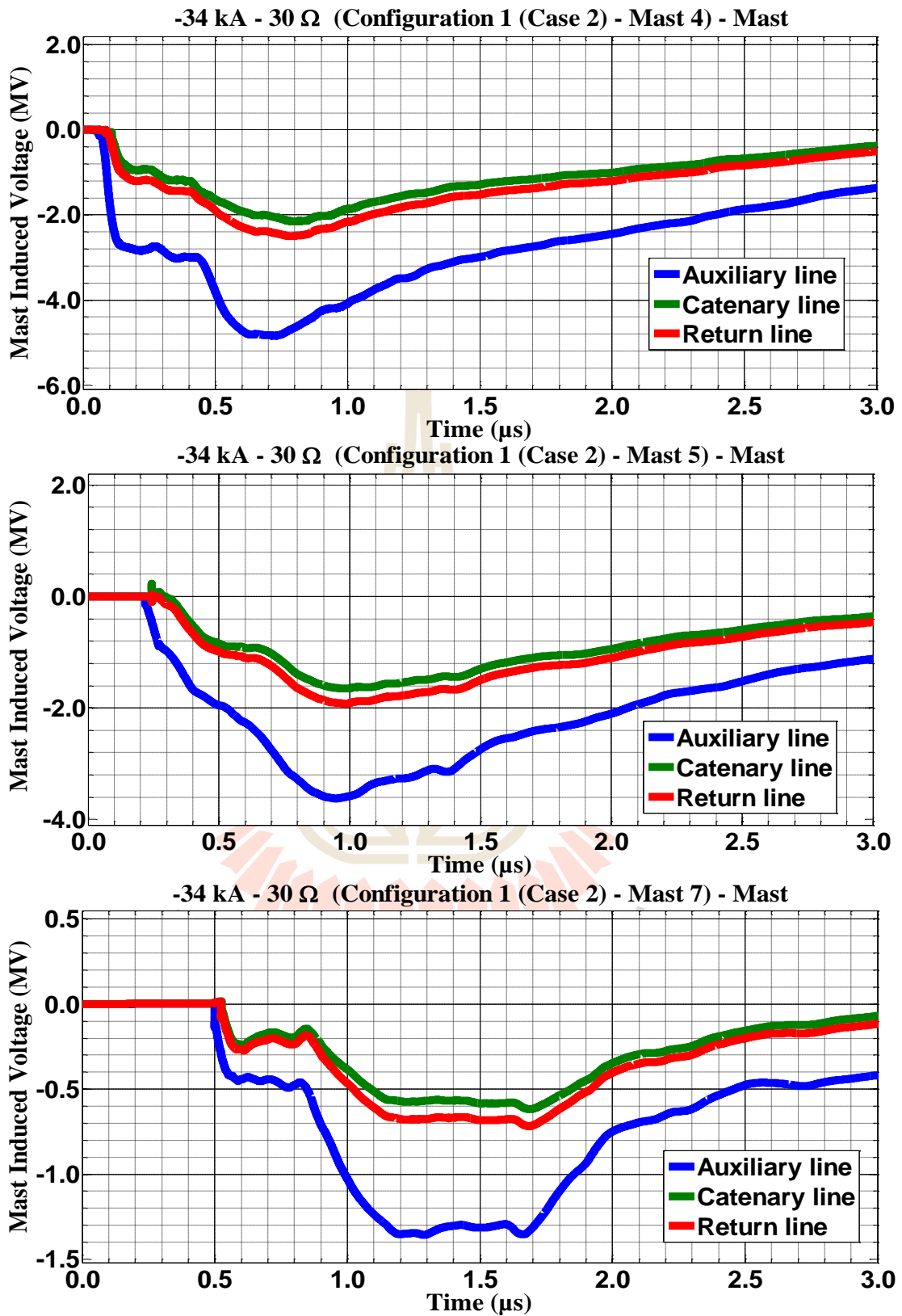


**Figure C.8** Mast 4, 5, and 7 induced voltage waveform of the -34 kA first stroke-(1.0/100 μs), subsequent stroke-(0.2/50 μs) strikes on Mast 4 with 30 Ω for Case 2

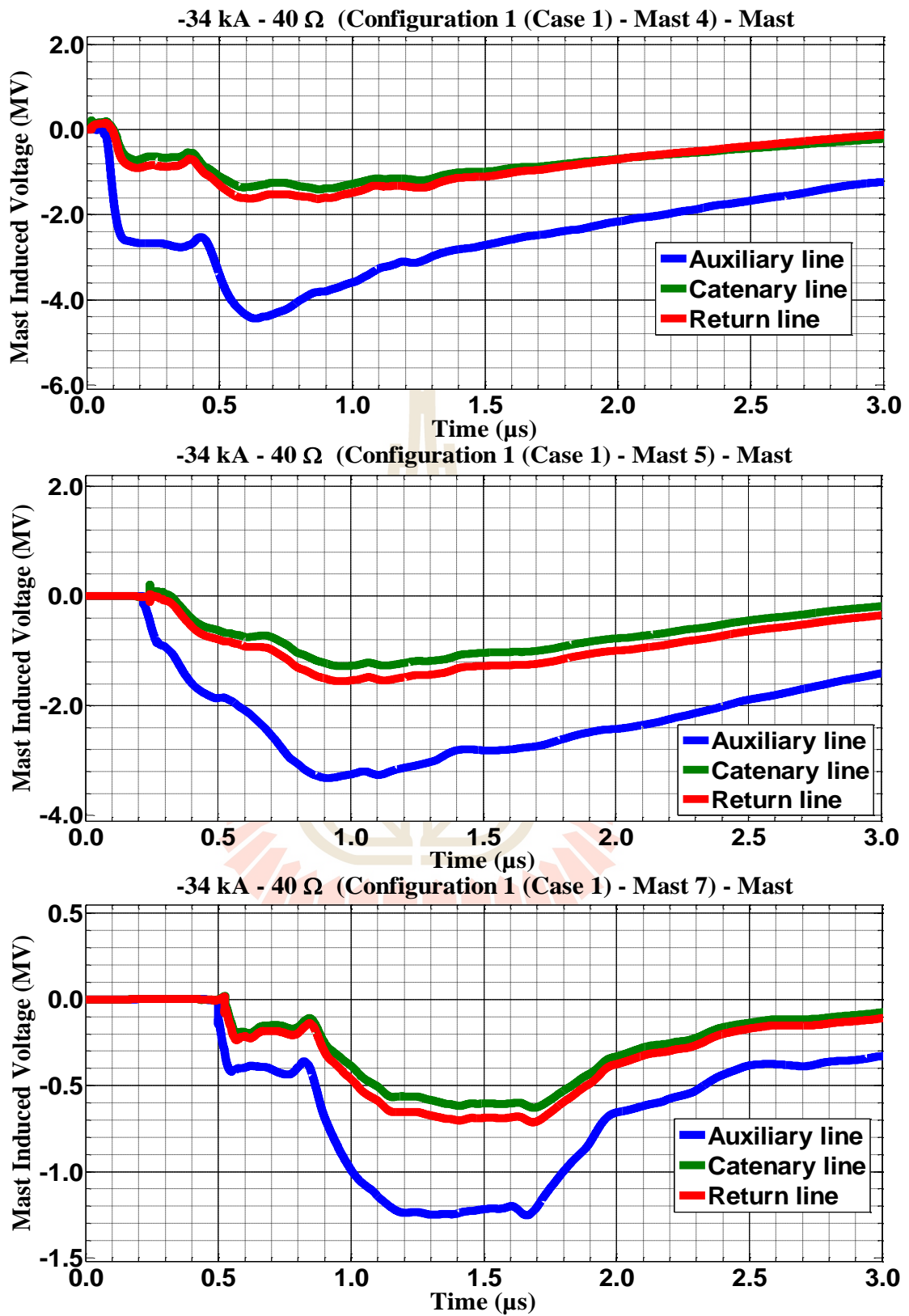


**Figure C.9** Mast 4, 5, and 7 induced voltage waveform of the -34 kA first stroke-(1.0/100 μs), subsequent stroke-(0.2/50 μs) strikes on Mast 4 with 40 Ω for Case 1

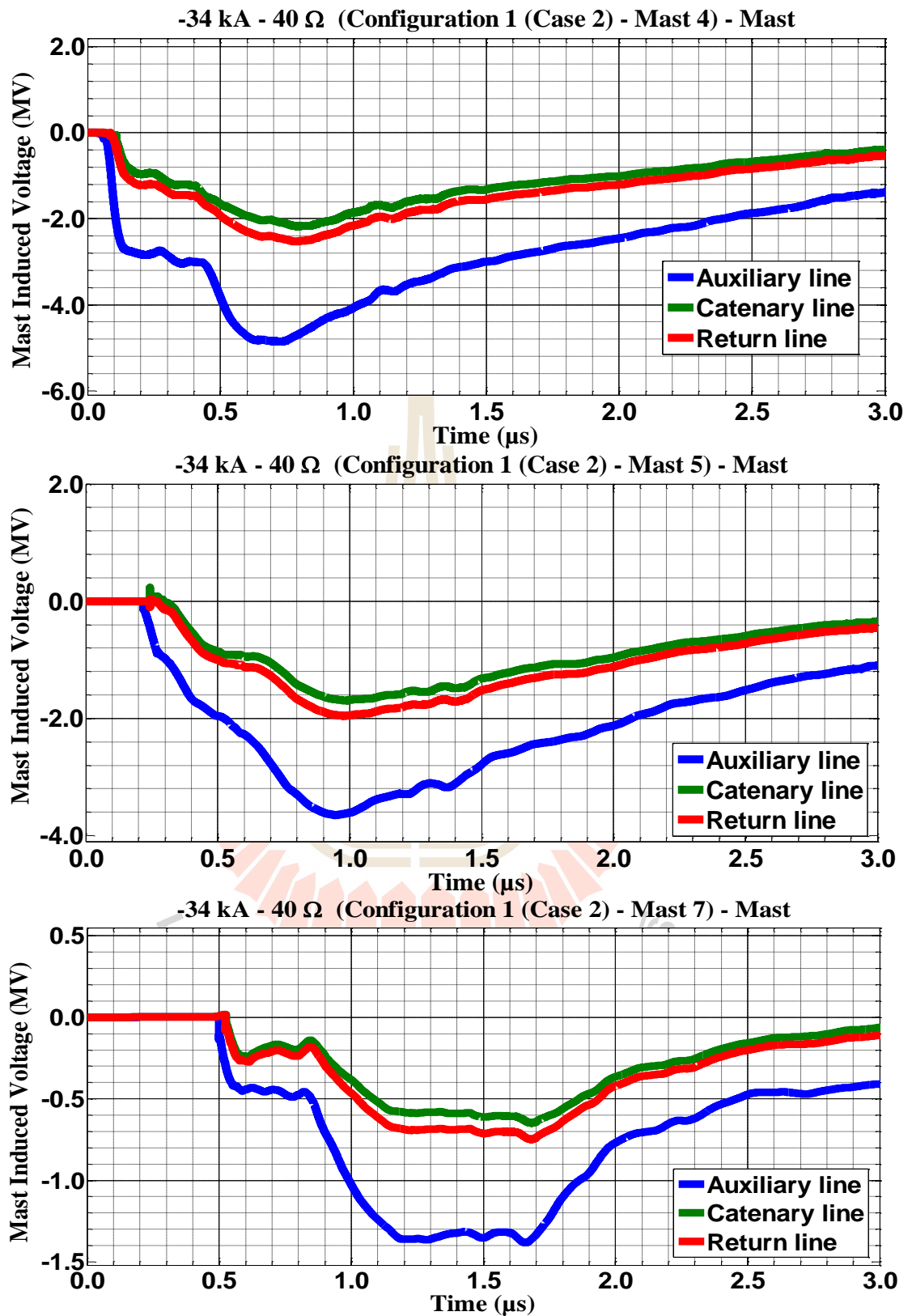


**Figure C.10** Mast 4, 5, and 7 induced voltage waveform of the -34 kA first stroke-(1.0/100  $\mu\text{s}$ ), subsequent stroke-(0.2/50  $\mu\text{s}$ ) strikes on Mast 4 with 40  $\Omega$  for Case 2

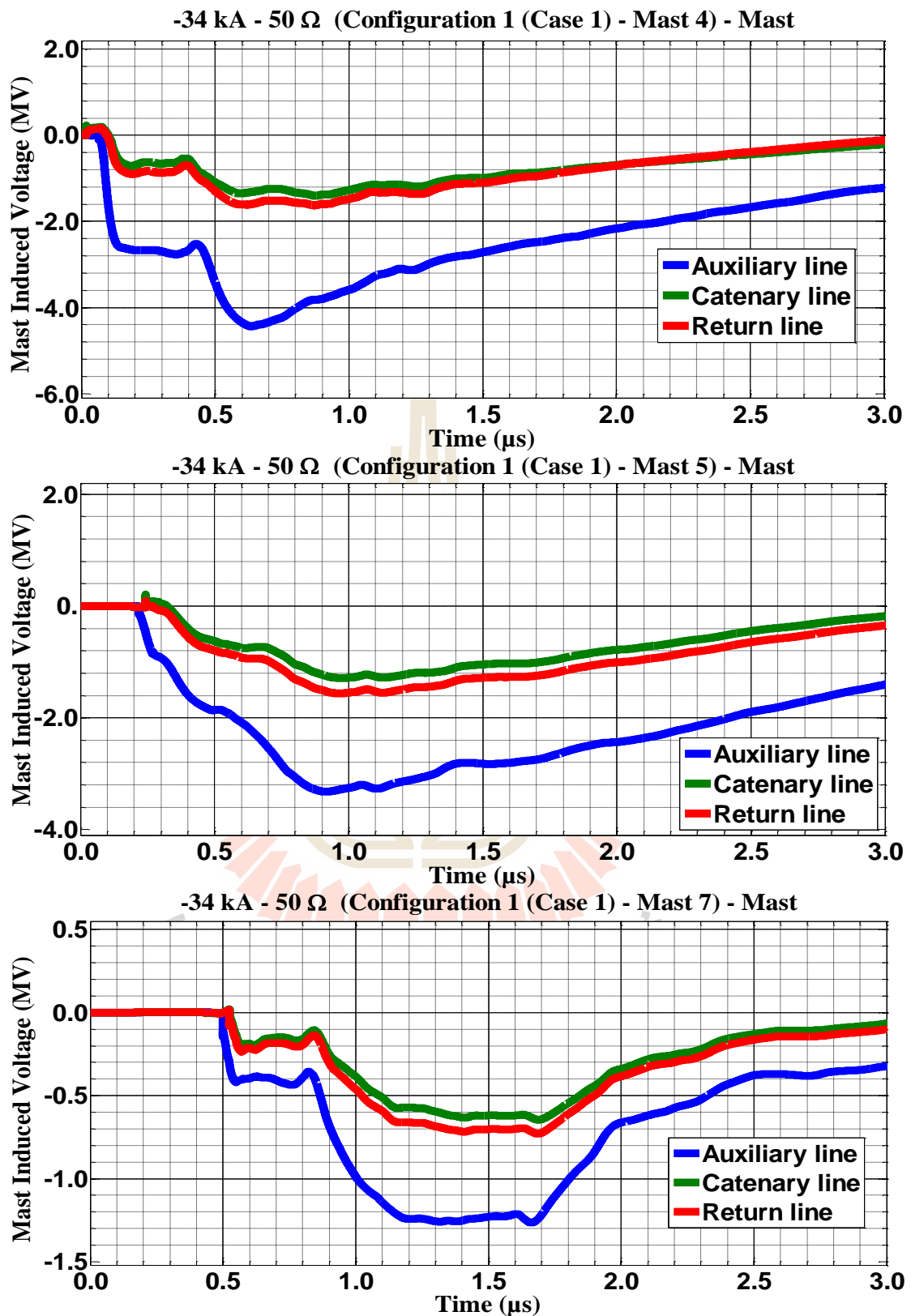


**Figure C.11** Mast 4, 5, and 7 induced voltage waveform of the -34 kA first stroke-(1.0/100 μs), subsequent stroke-(0.2/50 μs) strikes on Mast 4 with 50 Ω for Case 1



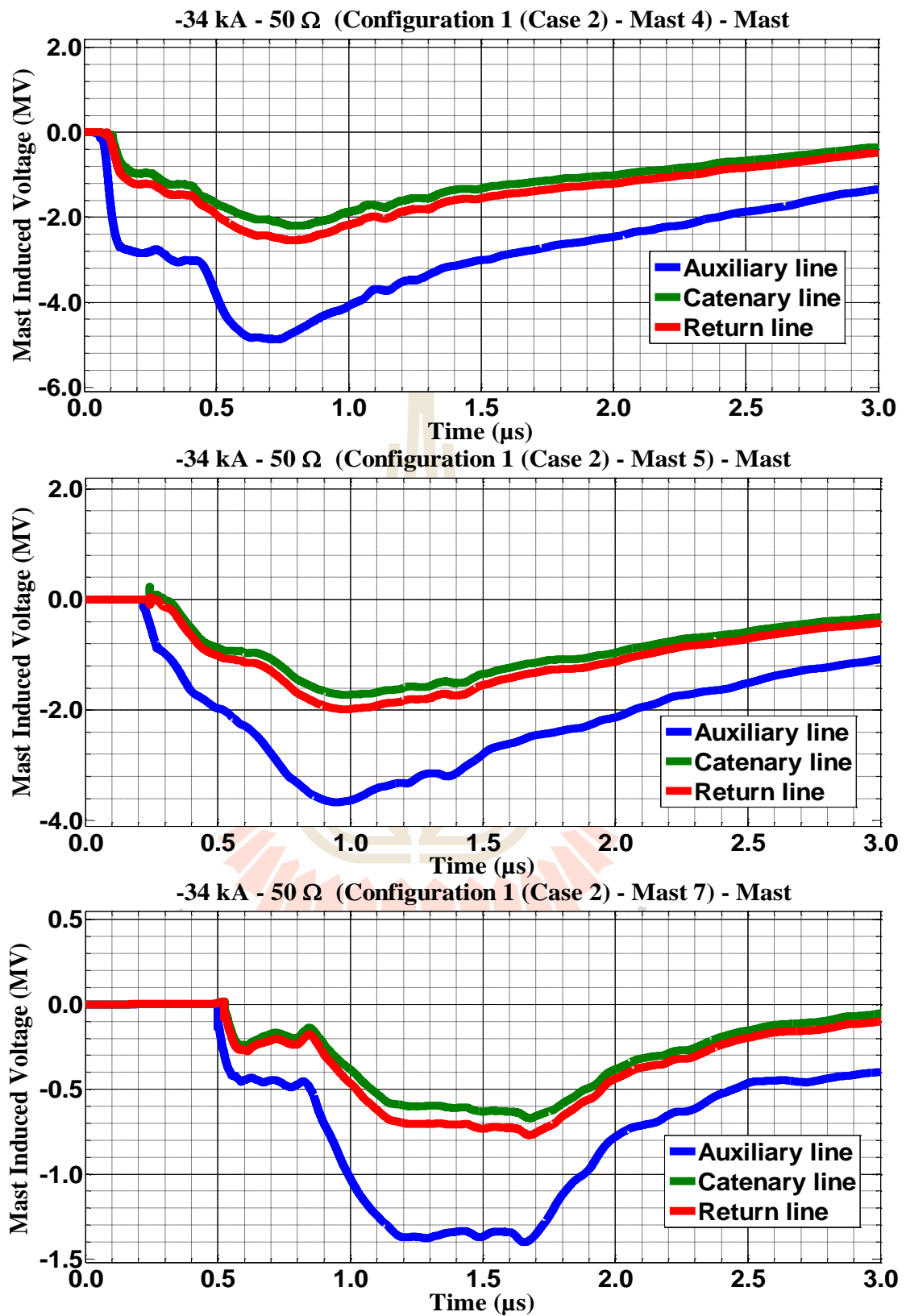


Figure C.12 Mast 4, 5, and 7 induced voltage waveform of the -34 kA first stroke-(1.0/100  $\mu\text{s}$ ), subsequent stroke-(0.2/50  $\mu\text{s}$ ) strikes on Mast 4 with 50  $\Omega$  for Case 2

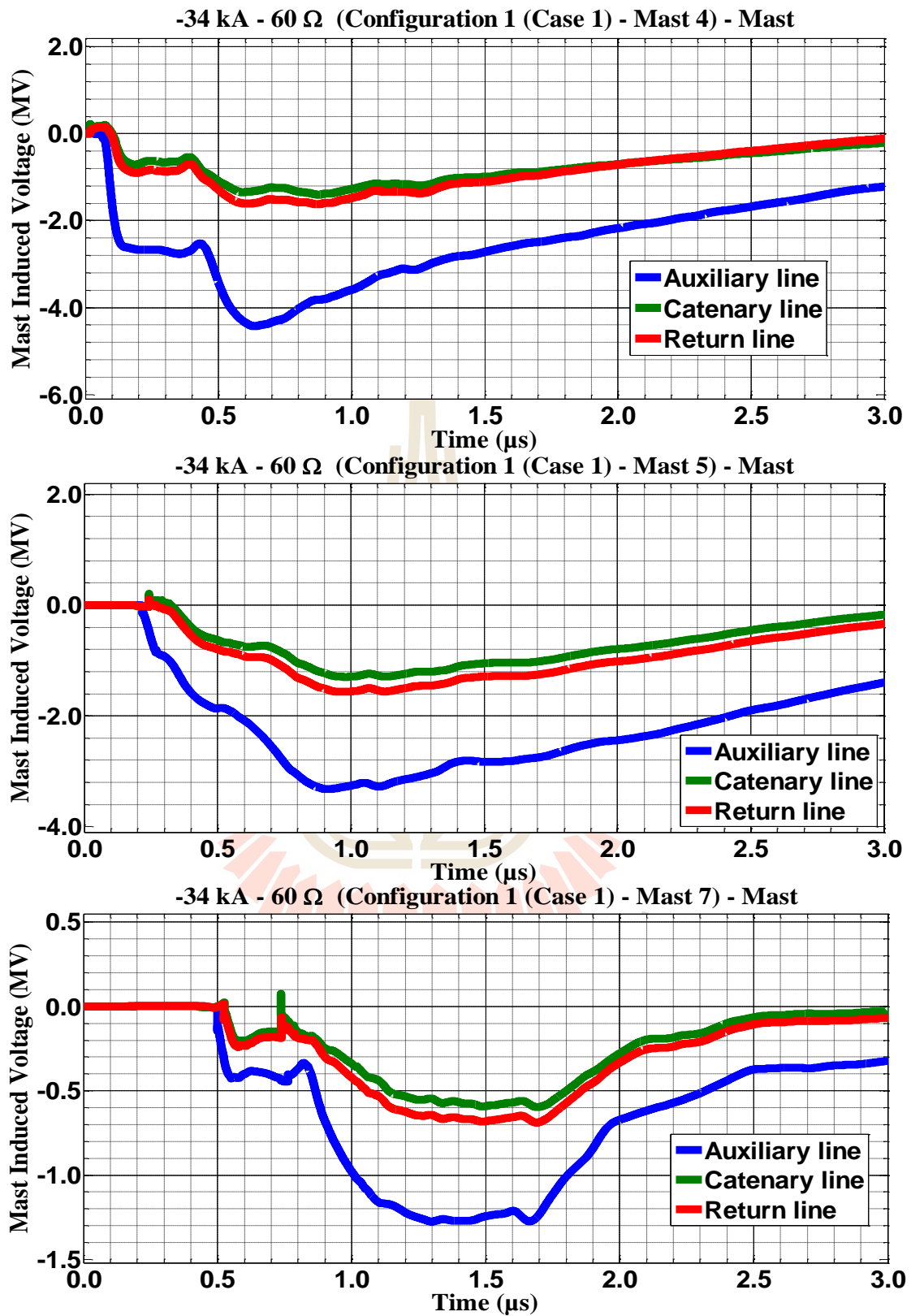


Figure C.13 Mast 4, 5, and 7 induced voltage waveform of the -34 kA first stroke-(1.0/100  $\mu\text{s}$ ), subsequent stroke-(0.2/50  $\mu\text{s}$ ) strikes on Mast 4 with 60  $\Omega$  for Case 1

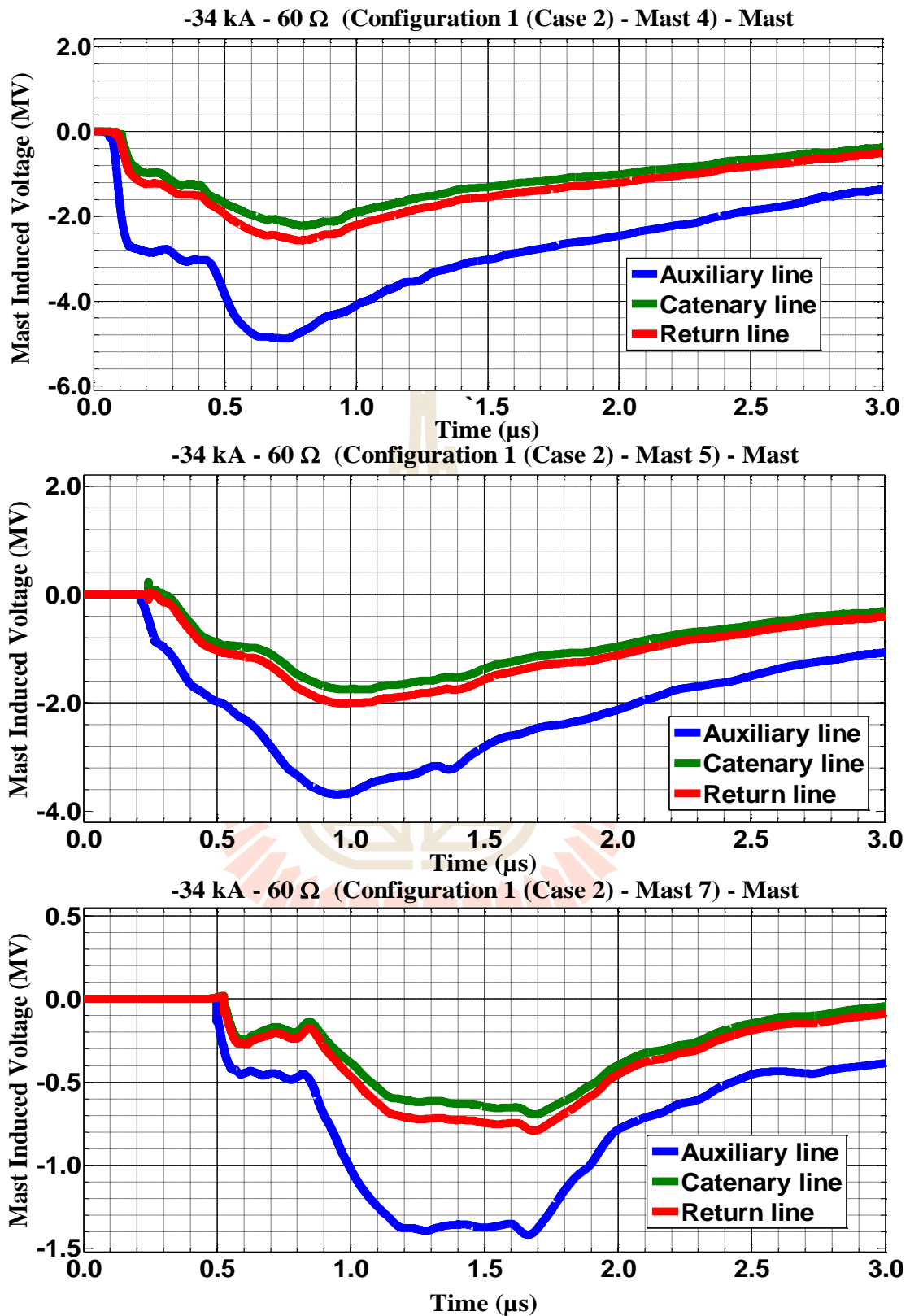
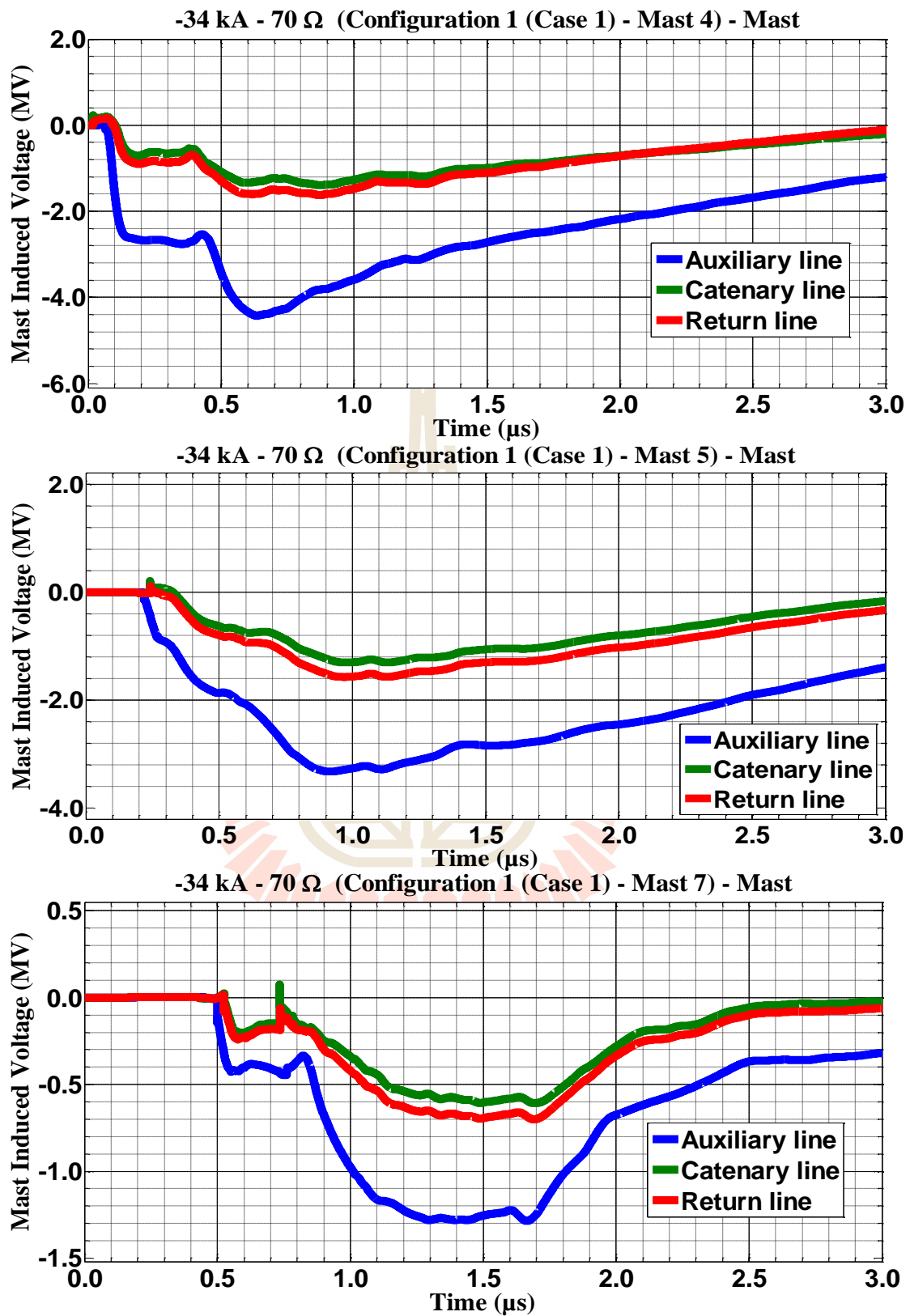
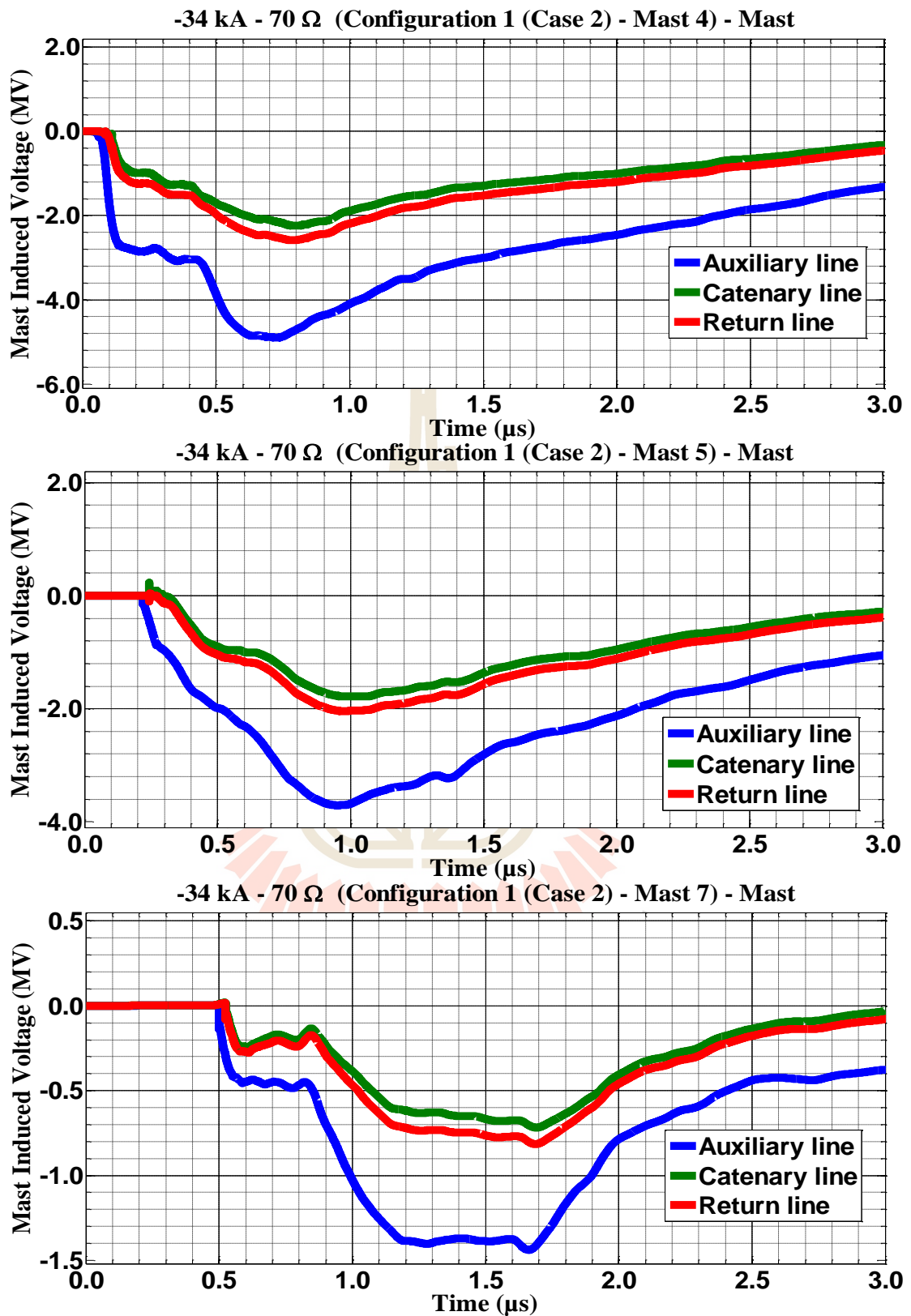


Figure C.14 Mast 4, 5, and 7 induced voltage waveform of the -34 kA first stroke-(1.0/100  $\mu\text{s}$ ), subsequent stroke-(0.2/50  $\mu\text{s}$ ) strikes on Mast 4 with 60  $\Omega$  for Case 2



**Figure C.15** Mast 4, 5, and 7 induced voltage waveform of the -34 kA first stroke-(1.0/100 μs), subsequent stroke-(0.2/50 μs) strikes on Mast 4 with 70 Ω for Case 1



**Figure C.16** Mast 4, 5, and 7 induced voltage waveform of the -34 kA first stroke-(1.0/100  $\mu\text{s}$ ), subsequent stroke-(0.2/50  $\mu\text{s}$ ) strikes on Mast 4 with 70  $\Omega$  for Case 2

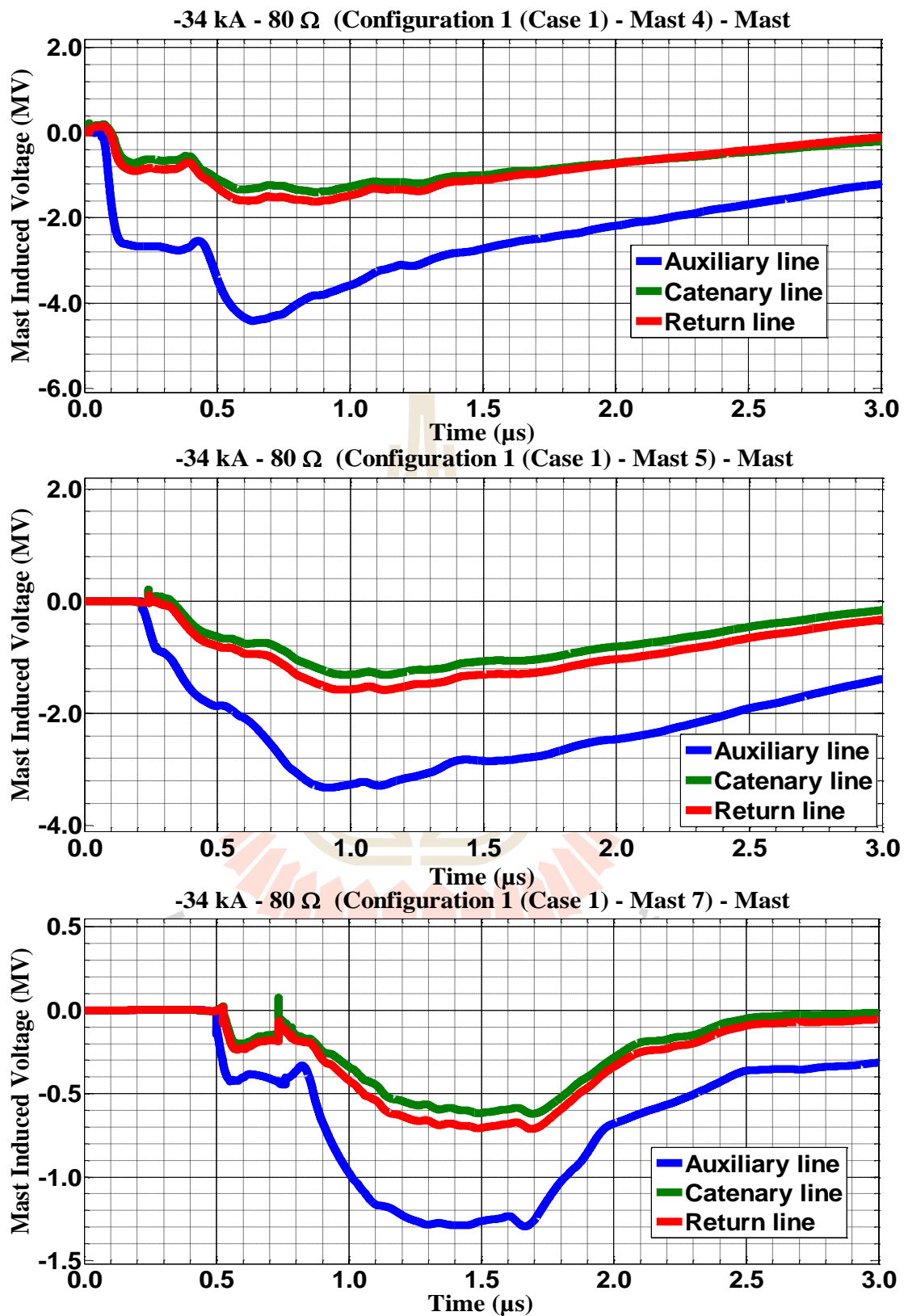


**Figure C.17** Mast 4, 5, and 7 induced voltage waveform of the -34 kA first stroke-(1.0/100 μs), subsequent stroke-(0.2/50 μs) strikes on Mast 4 with 80 Ω for Case 1

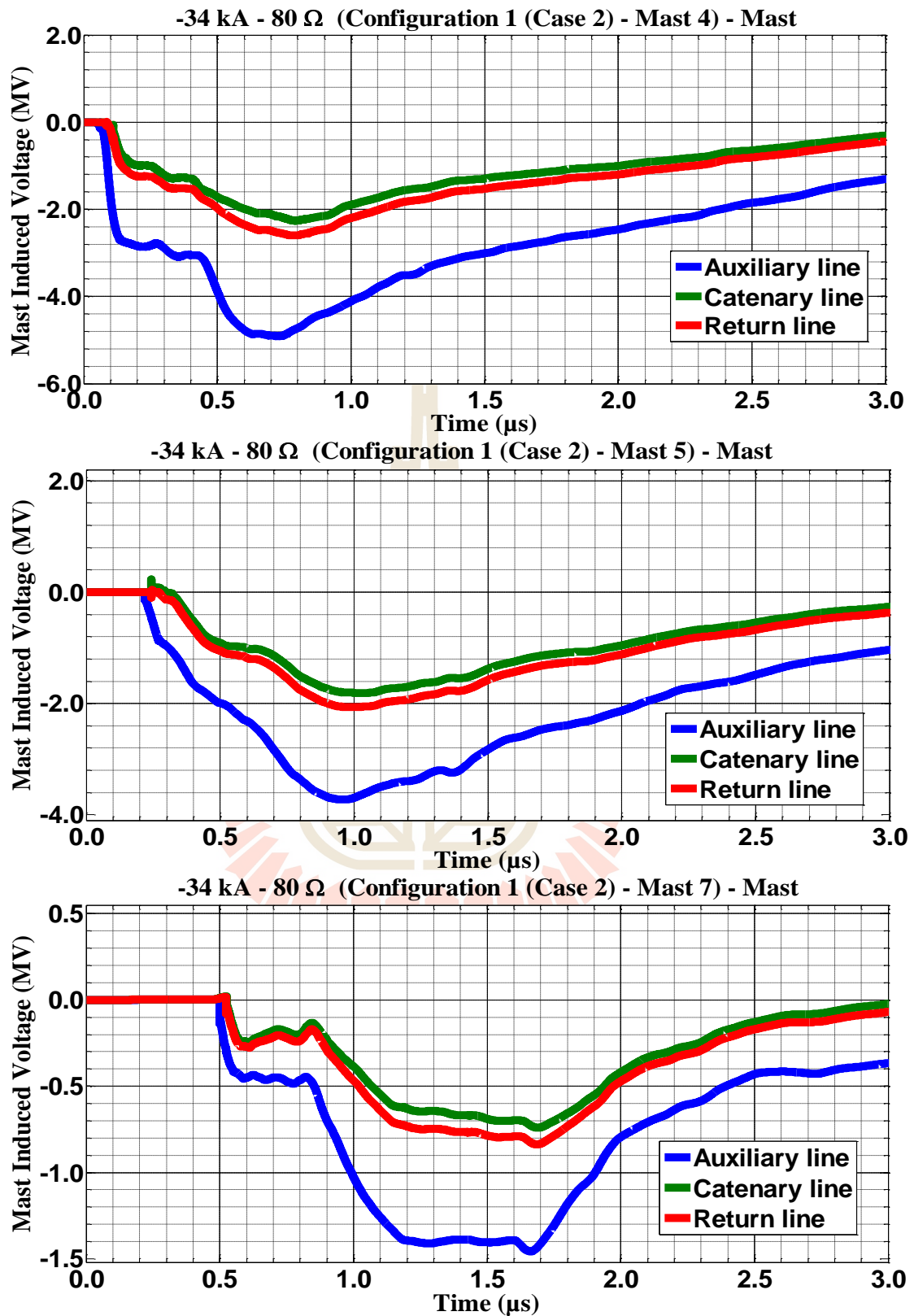
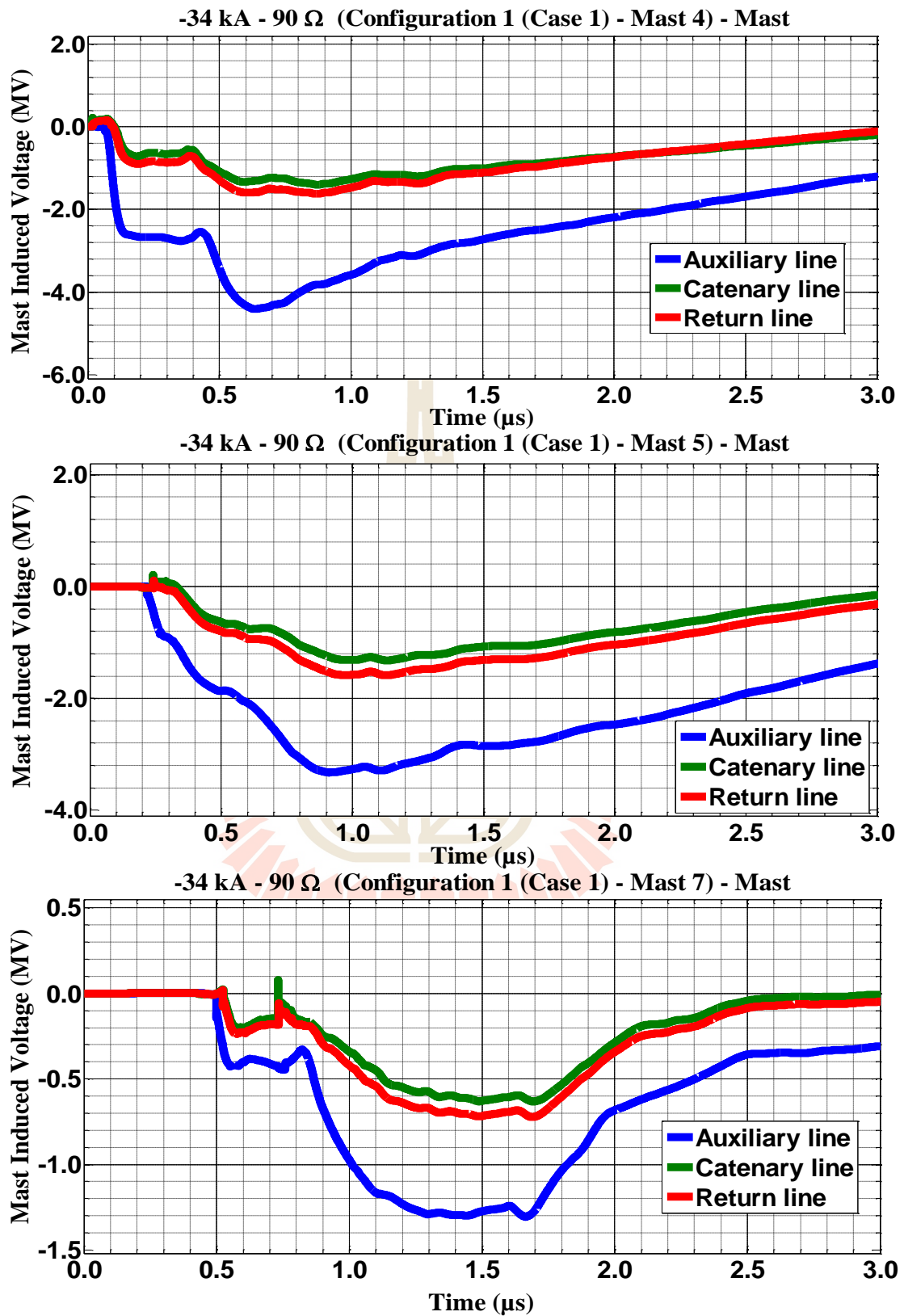
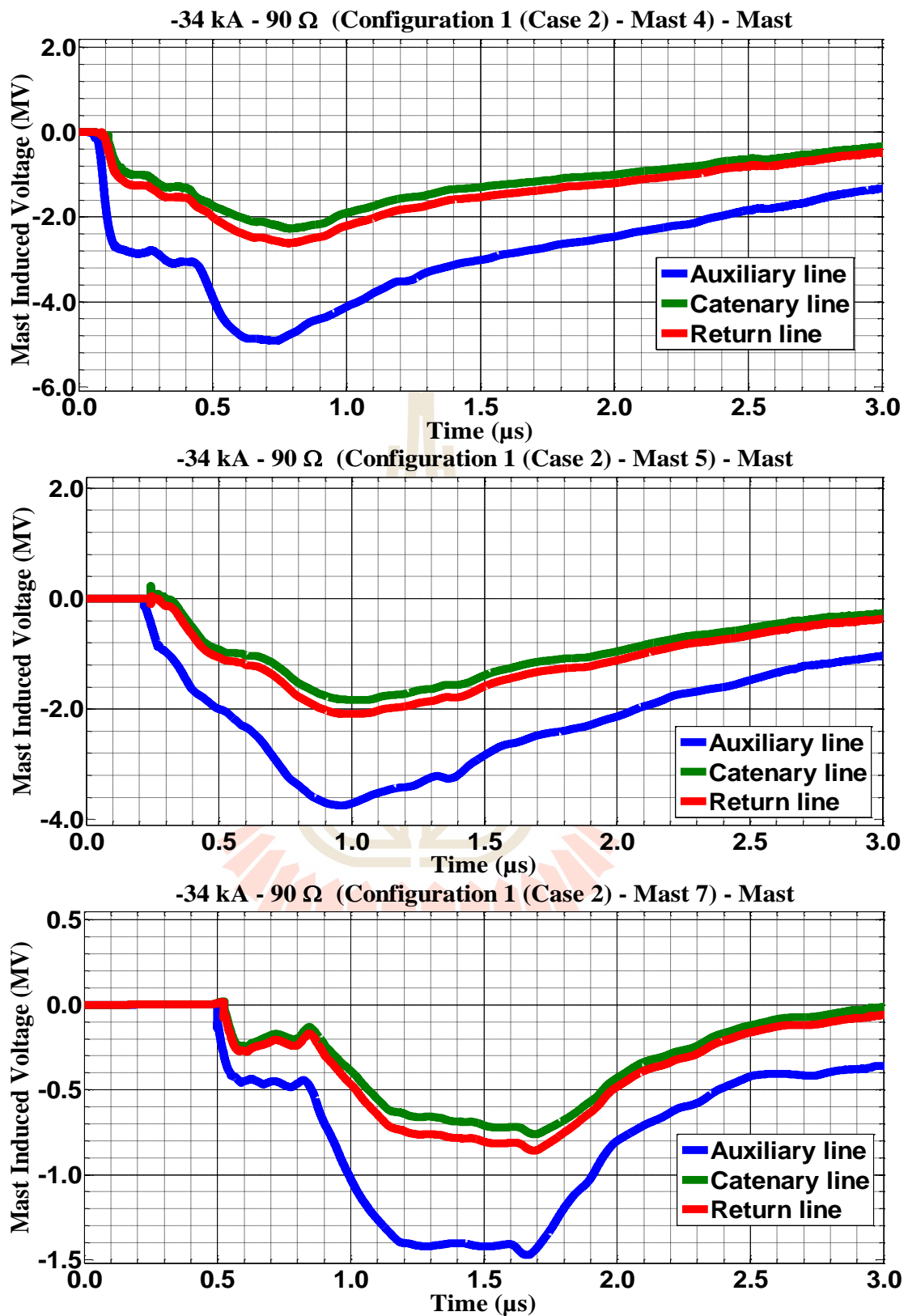


Figure C.18 Mast 4, 5, and 7 induced voltage waveform of the -34 kA first stroke-(1.0/100  $\mu\text{s}$ ), subsequent stroke-(0.2/50  $\mu\text{s}$ ) strikes on Mast 4 with 80  $\Omega$  for Case 2



**Figure C.19** Mast 4, 5, and 7 induced voltage waveform of the -34 kA first stroke-(1.0/100  $\mu\text{s}$ ), subsequent stroke-(0.2/50  $\mu\text{s}$ ) strikes on Mast 4 with 90  $\Omega$  for Case 1





**Figure C.20** Mast 4, 5, and 7 induced voltage waveform of the -34 kA first stroke-(1.0/100  $\mu\text{s}$ ), subsequent stroke-(0.2/50  $\mu\text{s}$ ) strikes on Mast 4 with 90  $\Omega$  for Case 2

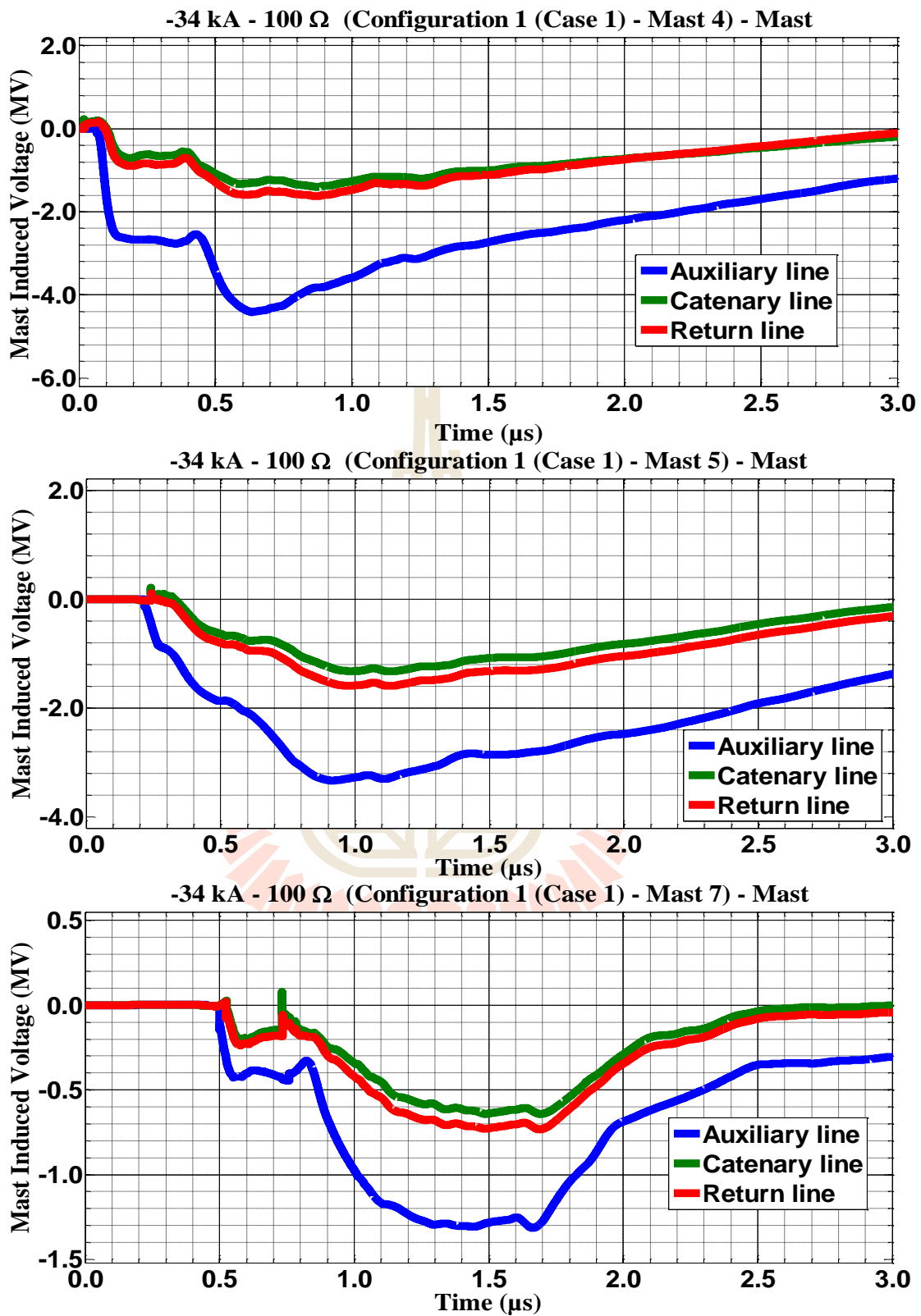


**Figure C.21** Mast 4, 5, and 7 induced voltage waveform of the -34 kA first stroke-(1.0/100 μs), subsequent stroke-(0.2/50 μs) strikes on Mast 4 with 100 Ω for Case 1

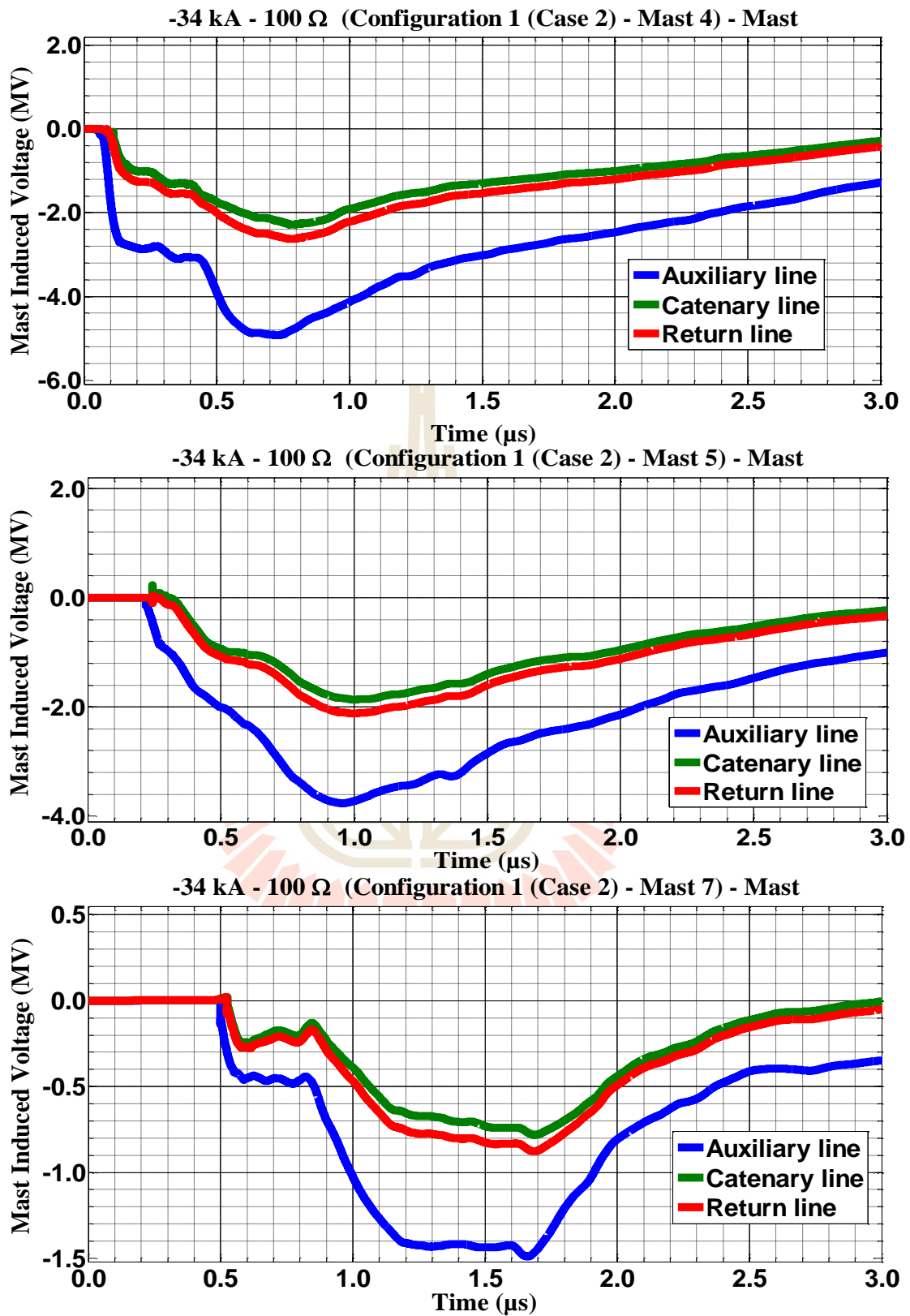


Figure C.22 Mast 4, 5, and 7 induced voltage waveform of the -34 kA first stroke-(1.0/100 μs), subsequent stroke-(0.2/50 μs) strikes on Mast 4 with 100 Ω for Case 2

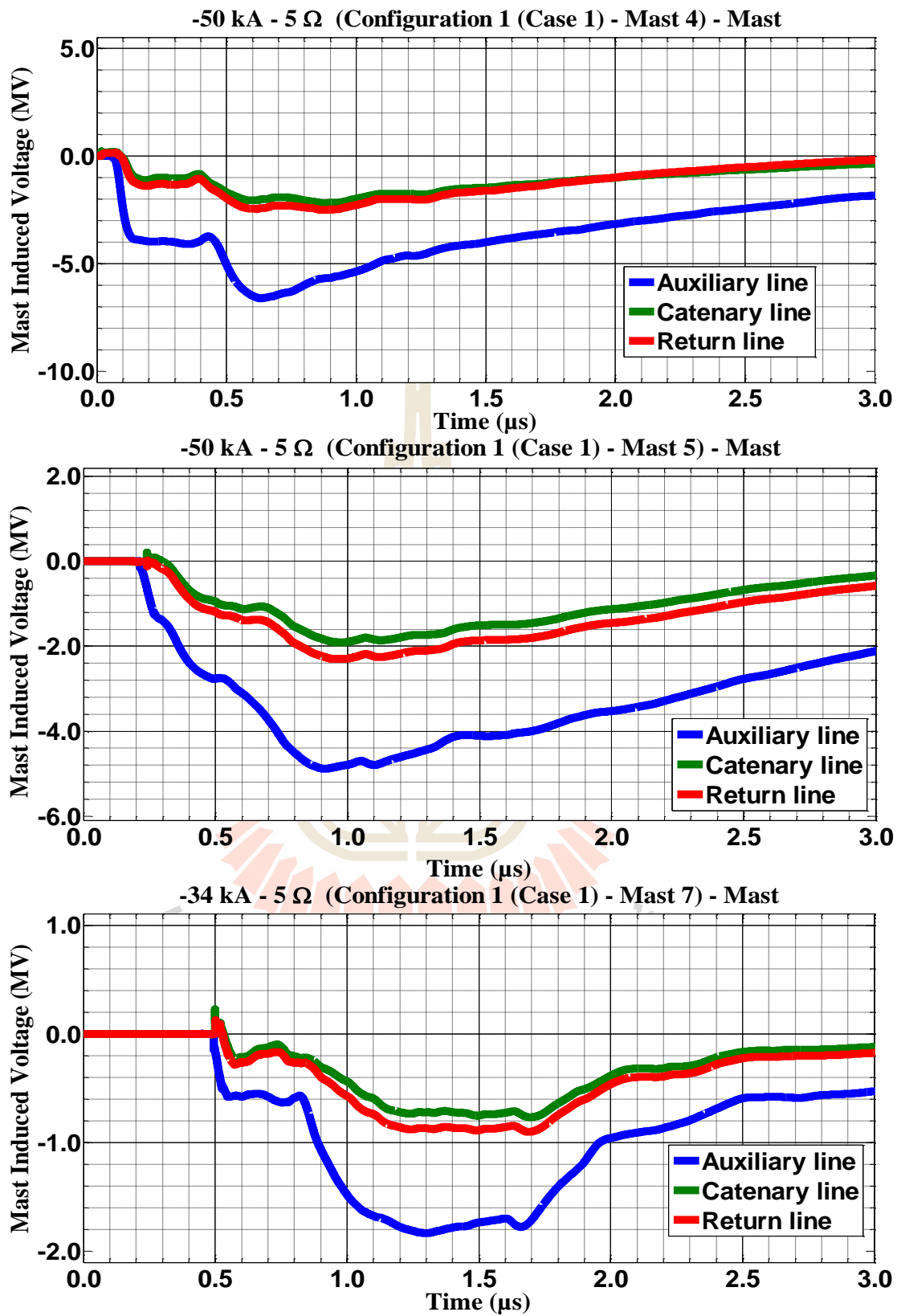
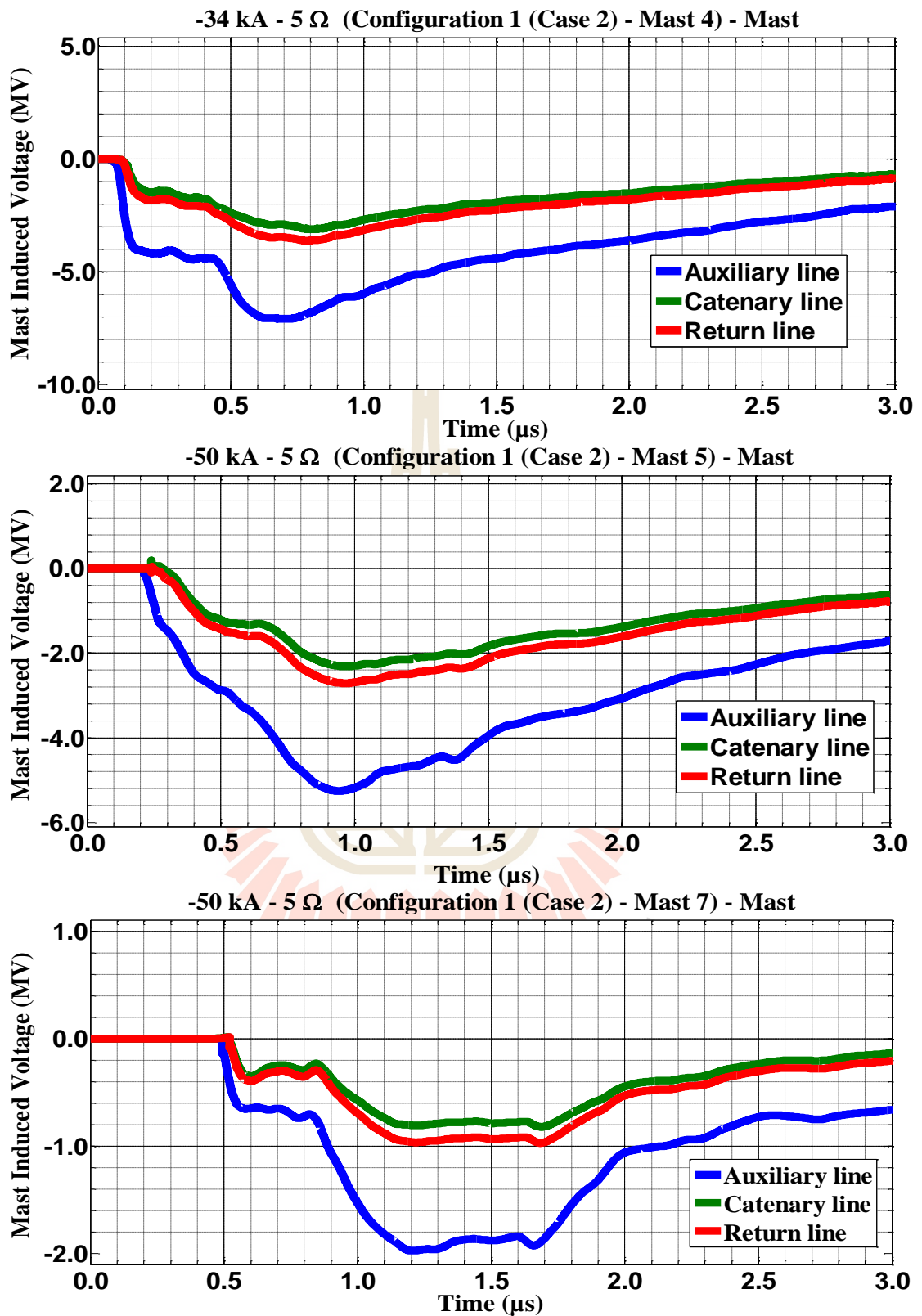


Figure C.23 Mast 4, 5, and 7 induced voltage waveform of the -50 kA first stroke-(1.0/100 μs), subsequent stroke-(0.2/50 μs) strikes on Mast 4 with 5 Ω for Case 1



**Figure C.24** Mast 4, 5, and 7 induced voltage waveform of the -50 kA first stroke-(1.0/100  $\mu\text{s}$ ), subsequent stroke-(0.2/50  $\mu\text{s}$ ) strikes on Mast 4 with 5  $\Omega$  for Case 2

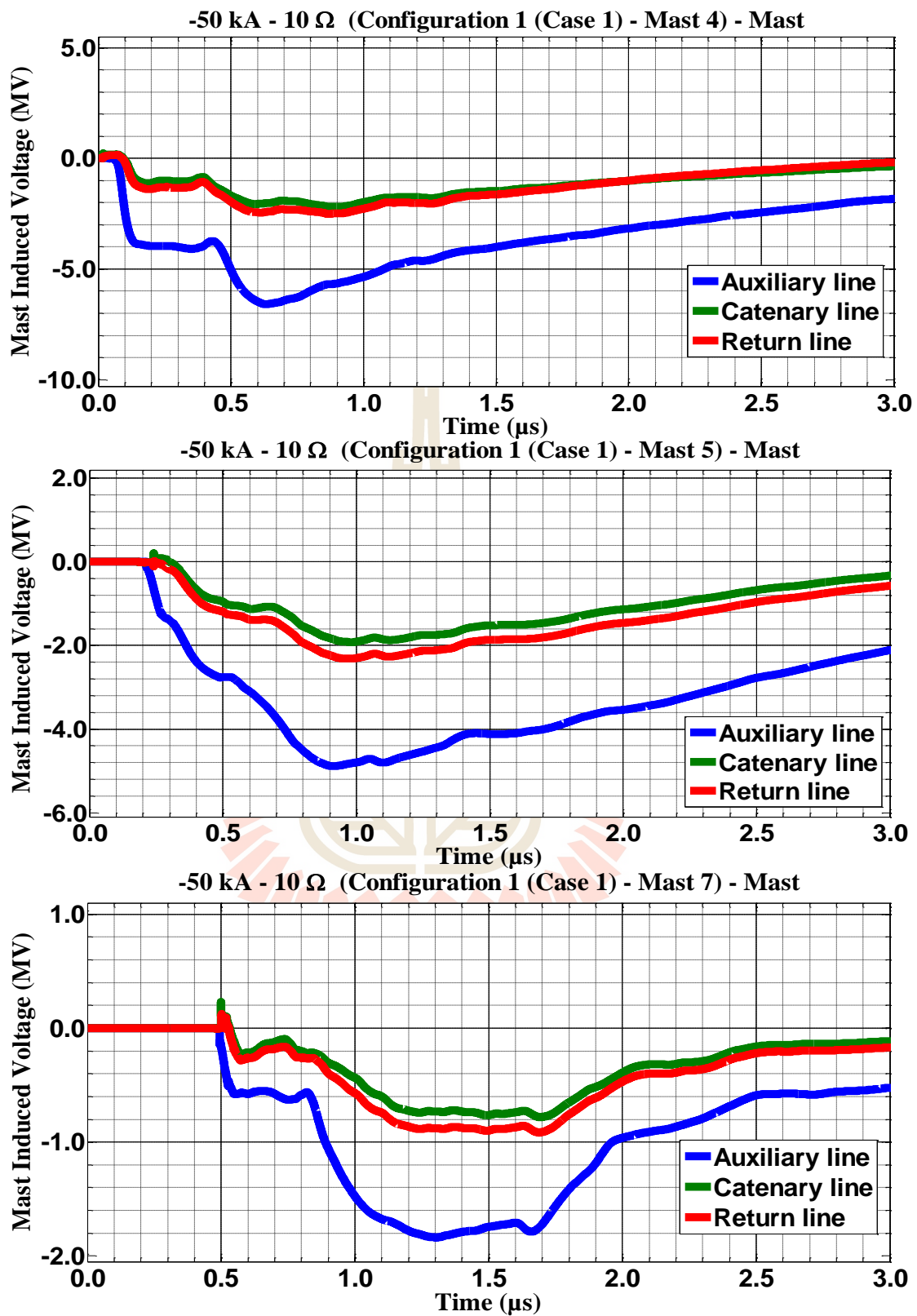


Figure C.25 Mast 4, 5, and 7 induced voltage waveform of the -50 kA first stroke-(1.0/100 μs), subsequent stroke-(0.2/50 μs) strikes on Mast 4 with 10 Ω for Case 1

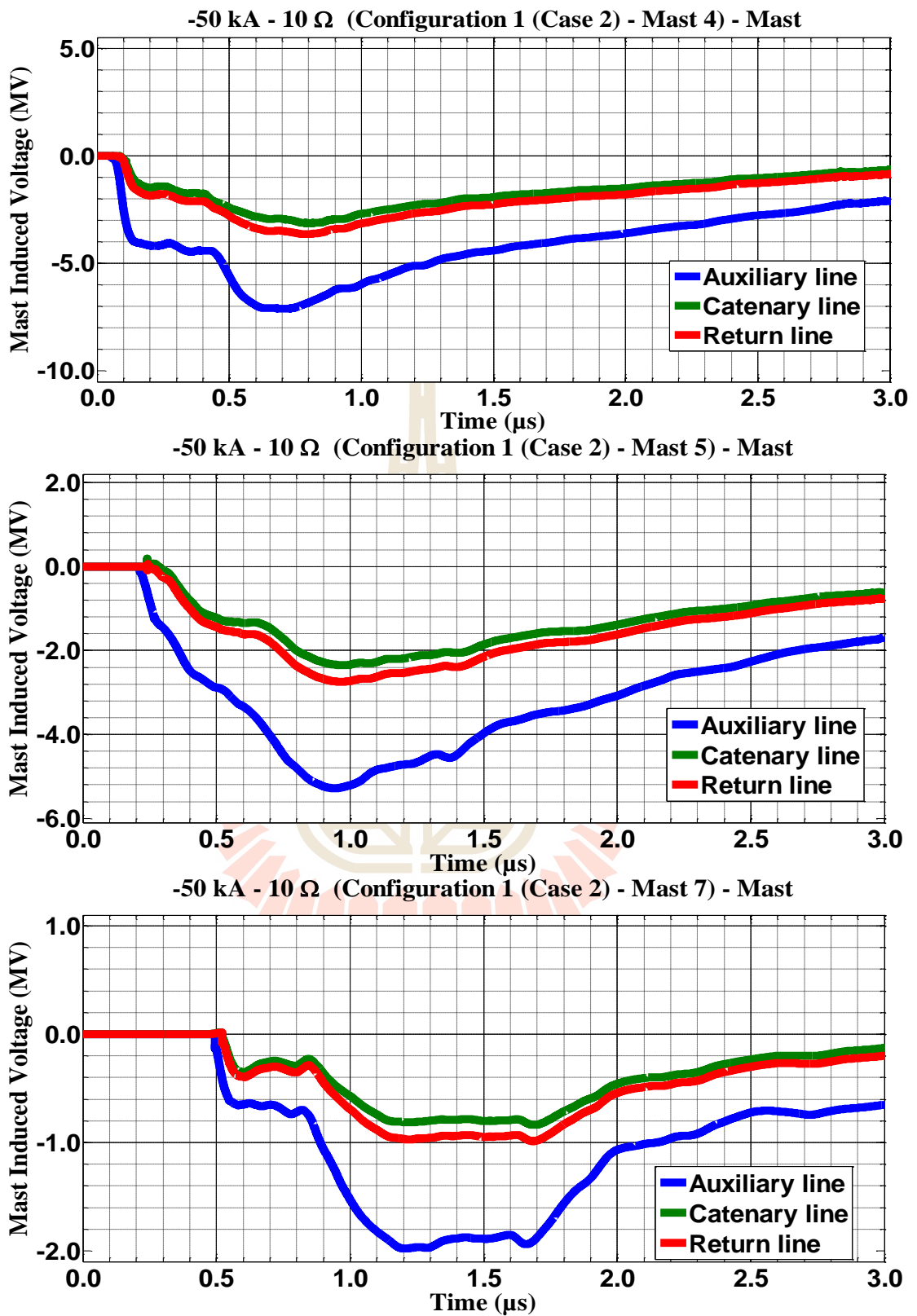


Figure C.26 Mast 4, 5, and 7 induced voltage waveform of the -50 kA first stroke-(1.0/100 μs), subsequent stroke-(0.2/50 μs) strikes on Mast 4 with 10 Ω for Case 2

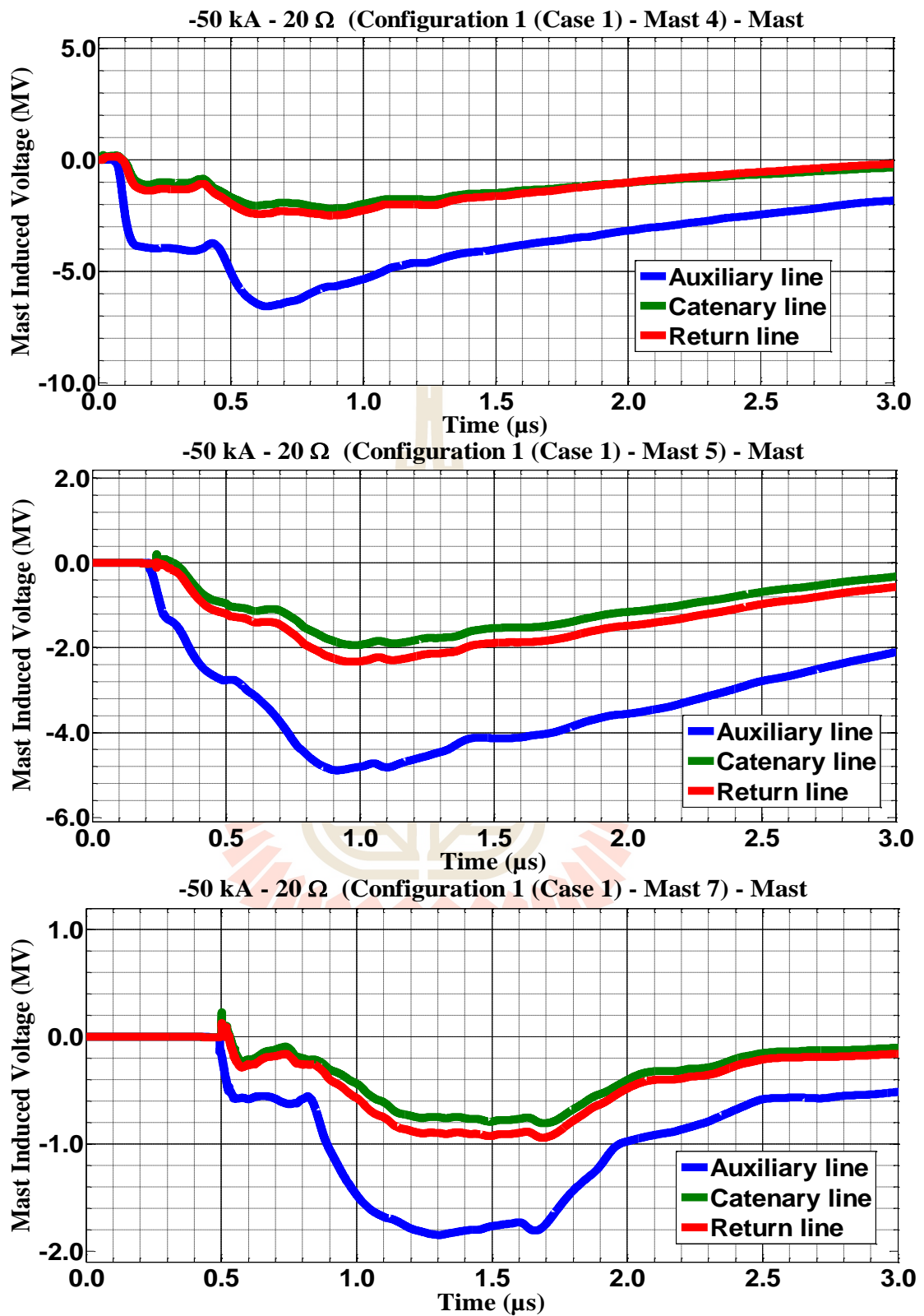


Figure C.27 Mast 4, 5, and 7 induced voltage waveform of the -50 kA first stroke-(1.0/100  $\mu\text{s}$ ), subsequent stroke-(0.2/50  $\mu\text{s}$ ) strikes on Mast 4 with 20  $\Omega$  for Case 1



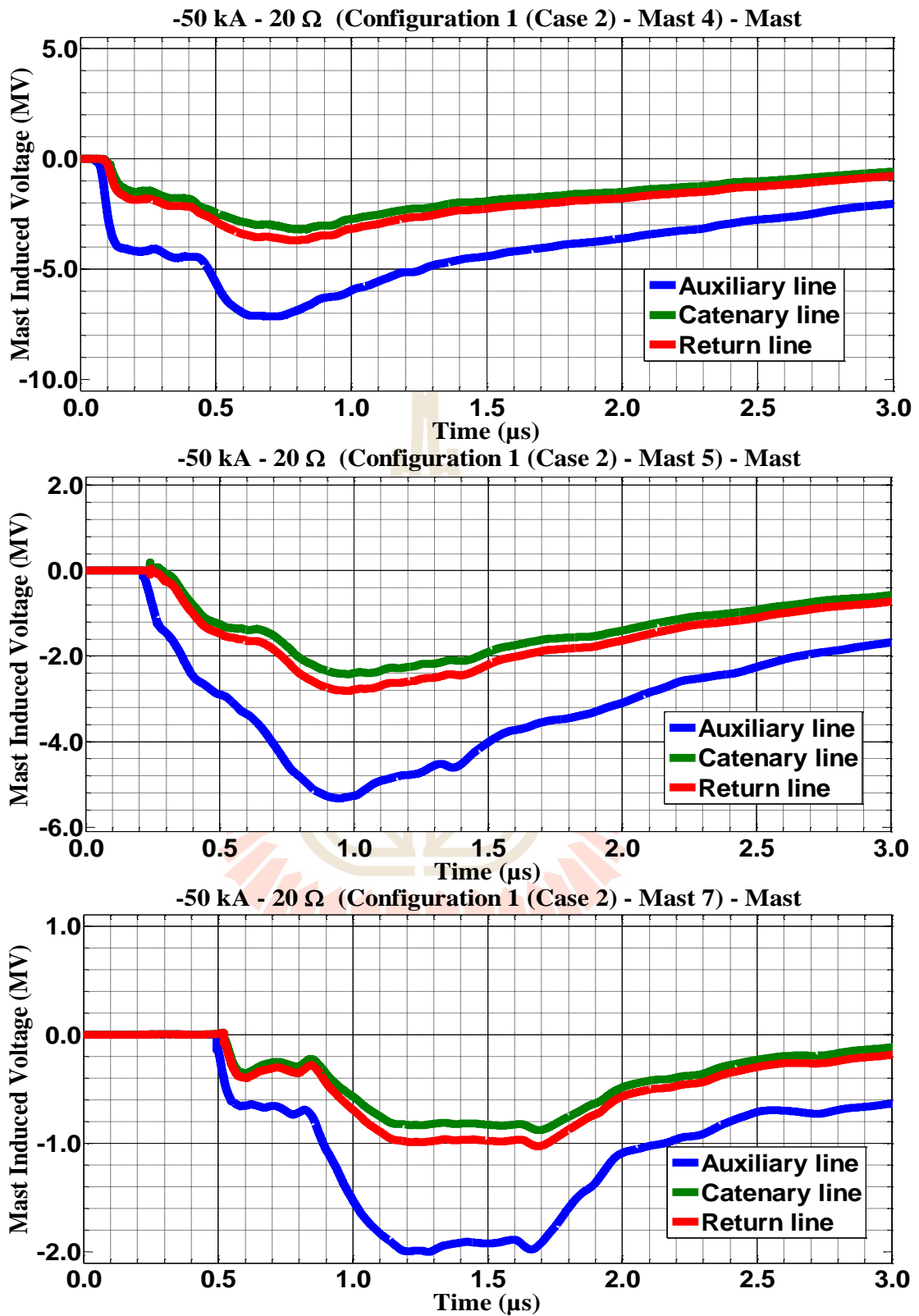


Figure C.28 Mast 4, 5, and 7 induced voltage waveform of the -50 kA first stroke-(1.0/100  $\mu\text{s}$ ), subsequent stroke-(0.2/50  $\mu\text{s}$ ) strikes on Mast 4 with 20  $\Omega$  for Case 2

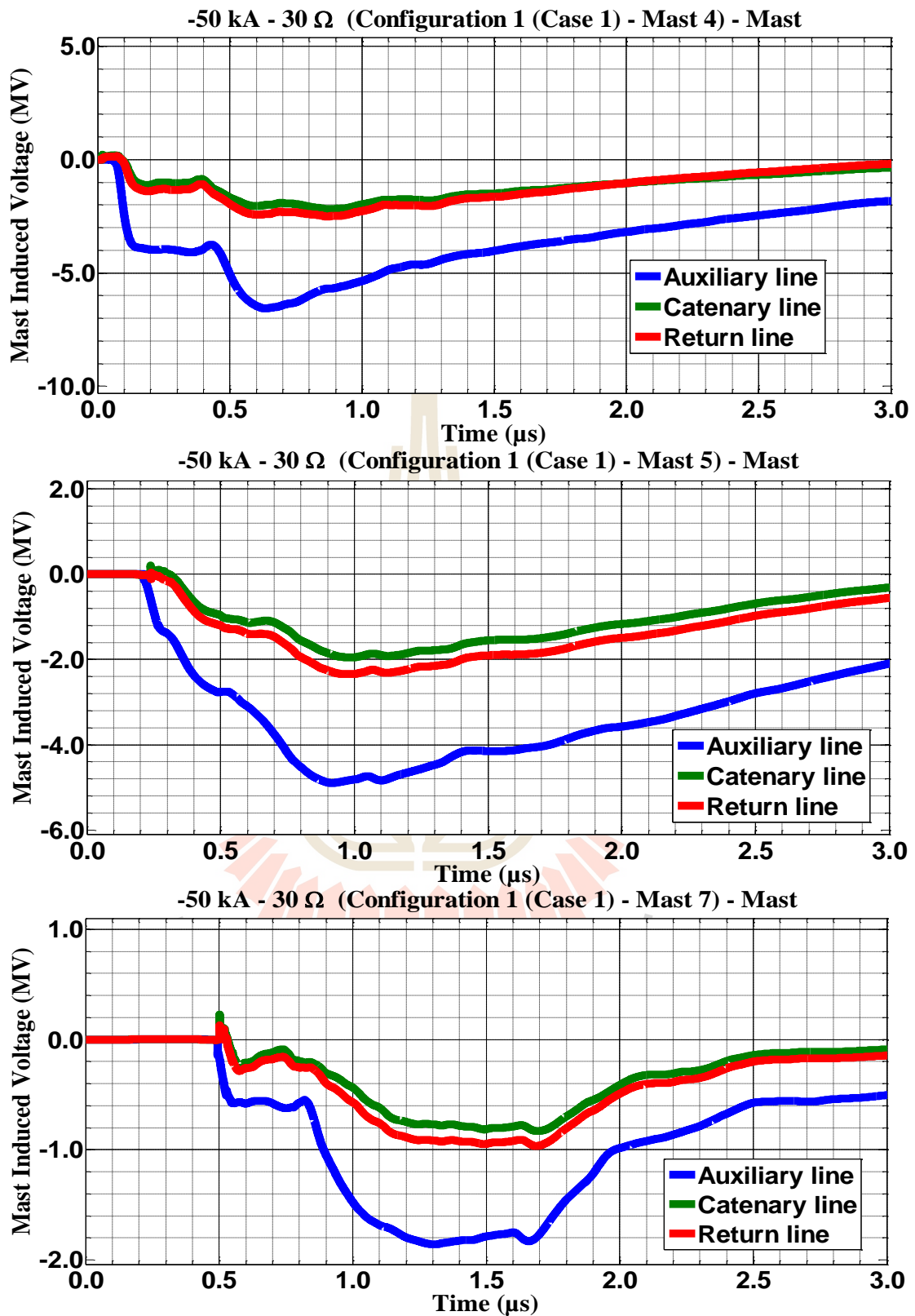


Figure C.29 Mast 4, 5, and 7 induced voltage waveform of the -50 kA first stroke-(1.0/100 μs), subsequent stroke-(0.2/50 μs) strikes on Mast 4 with 30 Ω for Case 1

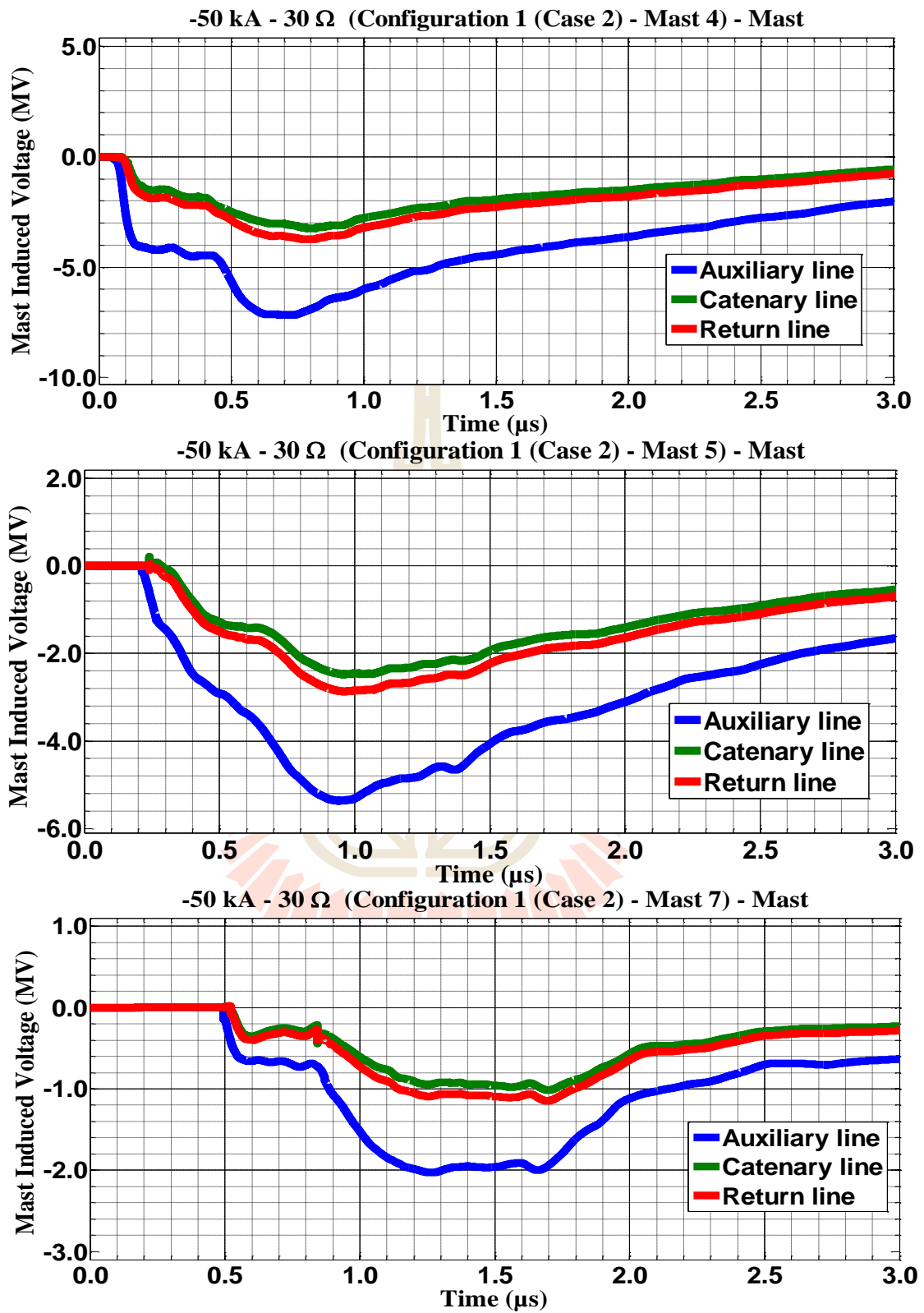
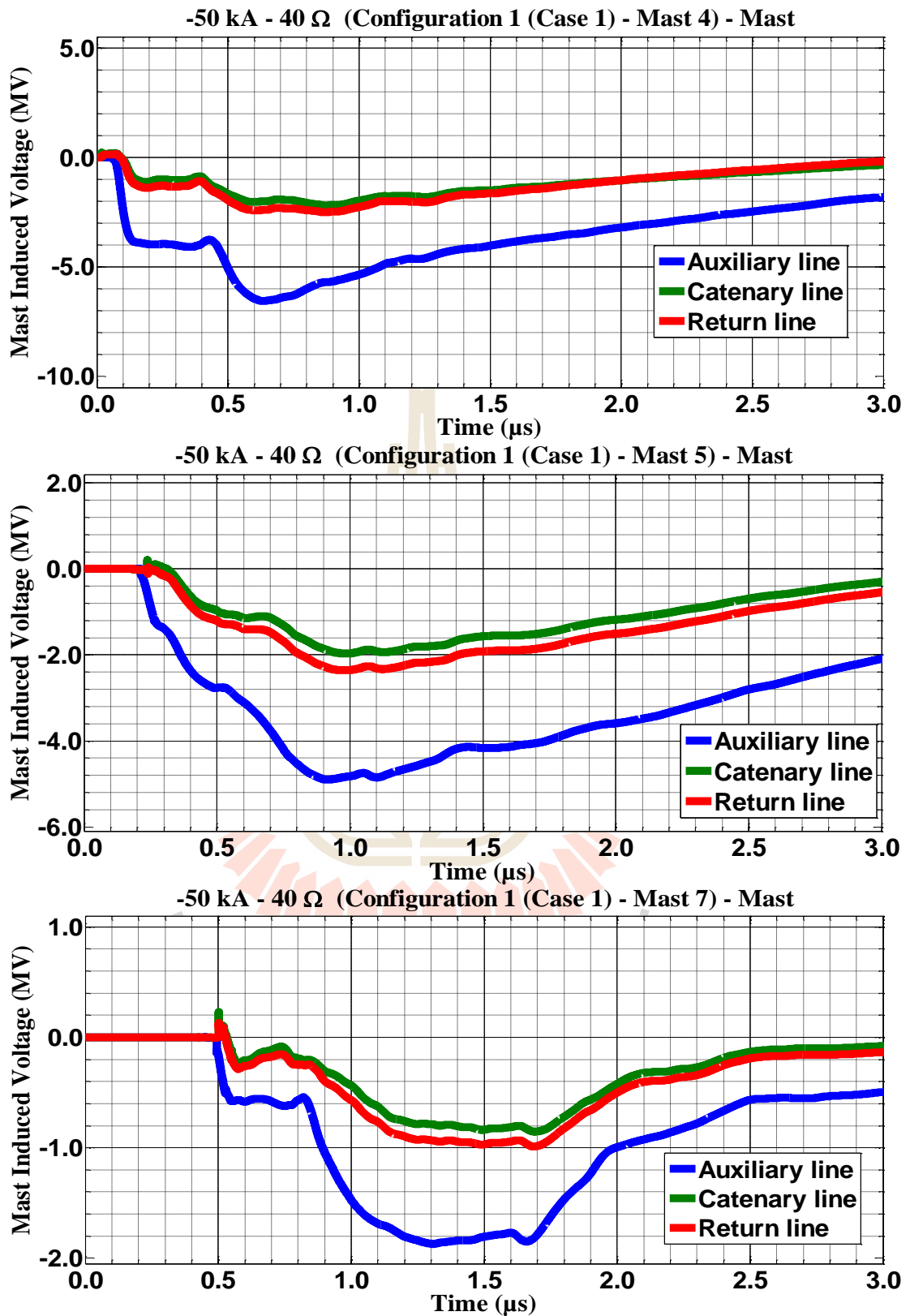


Figure C.30 Mast 4, 5, and 7 induced voltage waveform of the -50 kA first stroke-(1.0/100  $\mu\text{s}$ ), subsequent stroke-(0.2/50  $\mu\text{s}$ ) strikes on Mast 4 with 30  $\Omega$  for Case 2



**Figure C.31** Mast 4, 5, and 7 induced voltage waveform of the -50 kA first stroke-(1.0/100 μs), subsequent stroke-(0.2/50 μs) strikes on Mast 4 with 40 Ω for Case 1

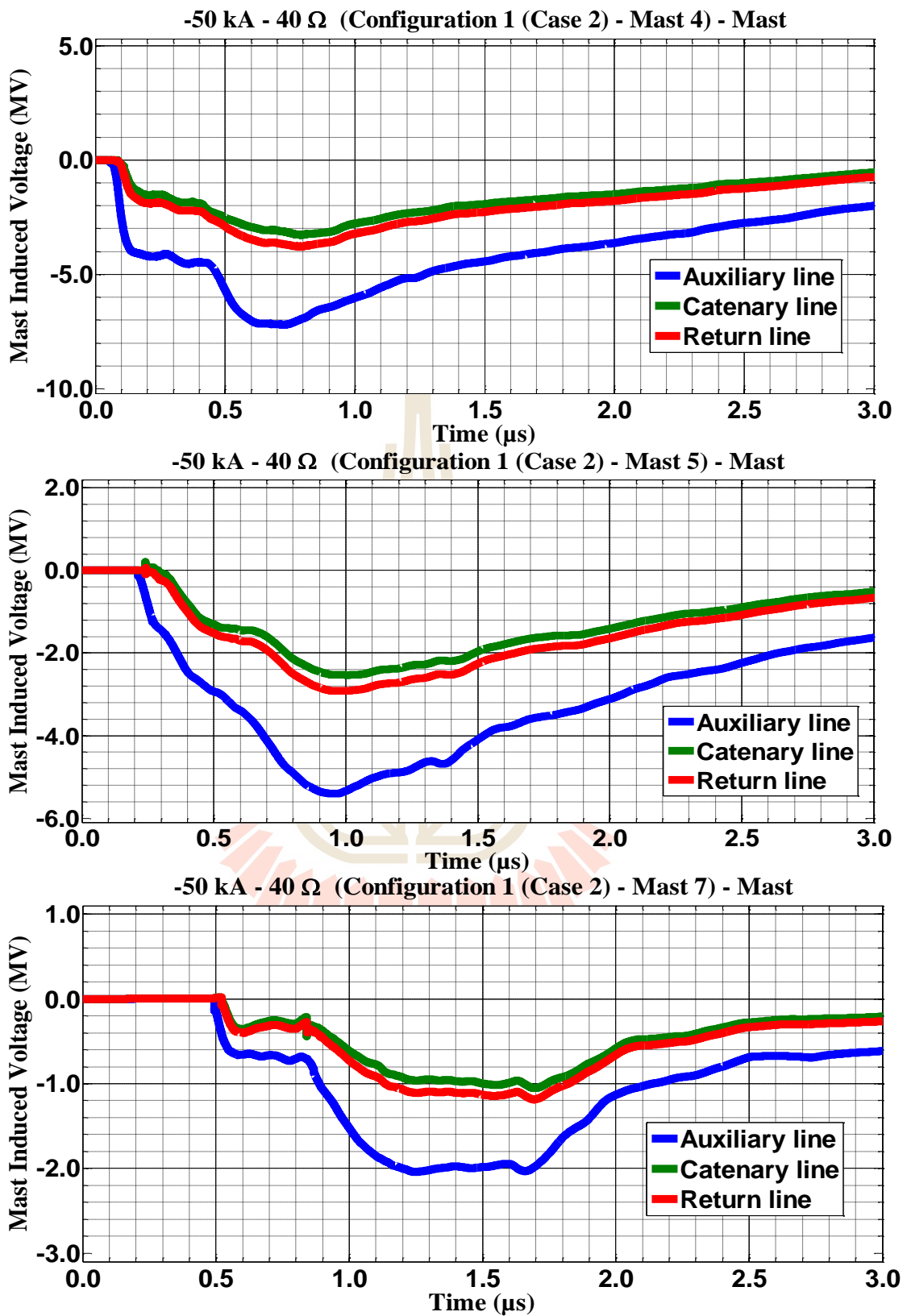


Figure C.32 Mast 4, 5, and 7 induced voltage waveform of the -50 kA first stroke-(1.0/100  $\mu\text{s}$ ), subsequent stroke-(0.2/50  $\mu\text{s}$ ) strikes on Mast 4 with 40  $\Omega$  for Case 2

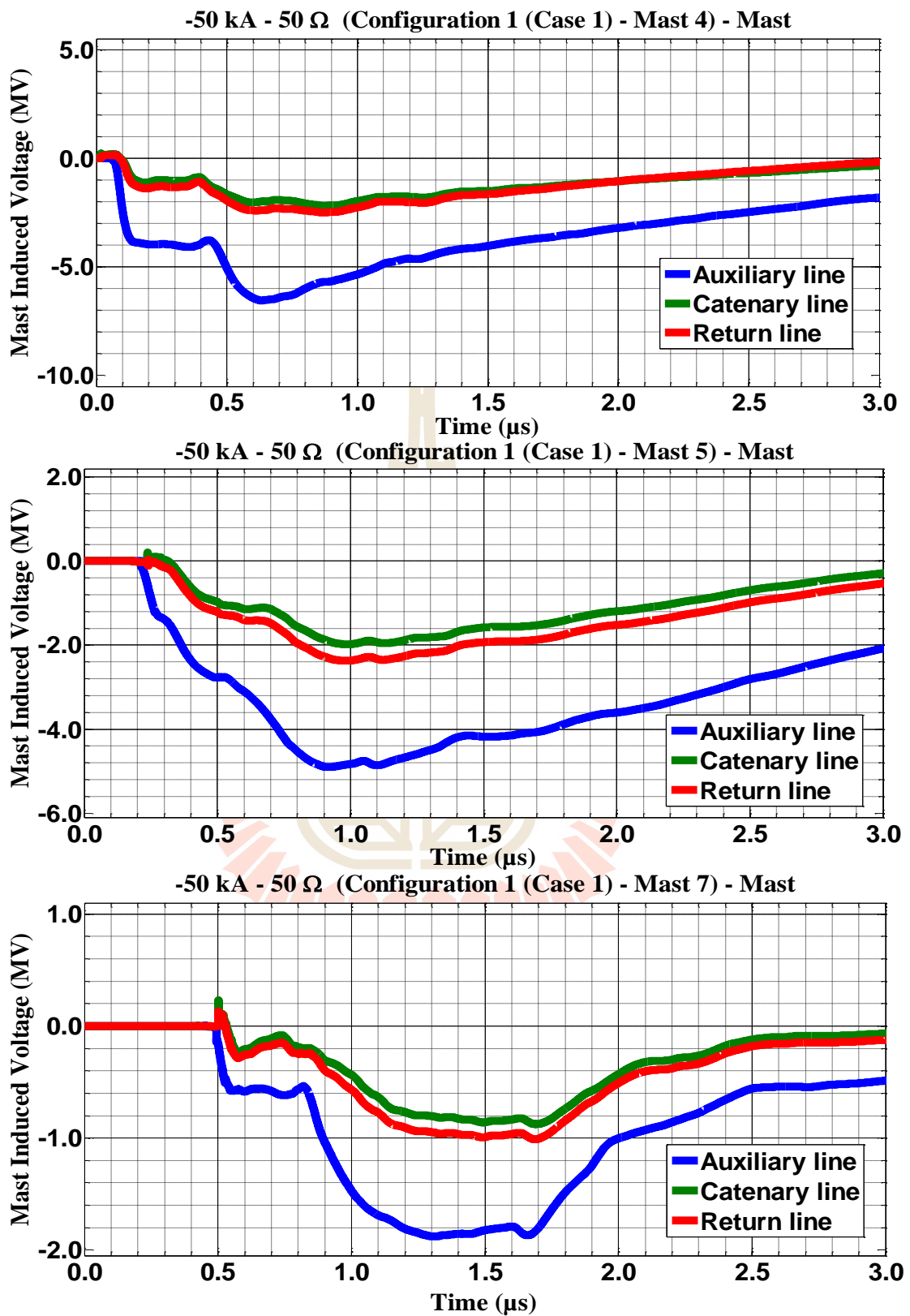


Figure C.33 Mast 4, 5, and 7 induced voltage waveform of the -50 kA first stroke-(1.0/100 μs), subsequent stroke-(0.2/50 μs) strikes on Mast 4 with 50 Ω for Case 1

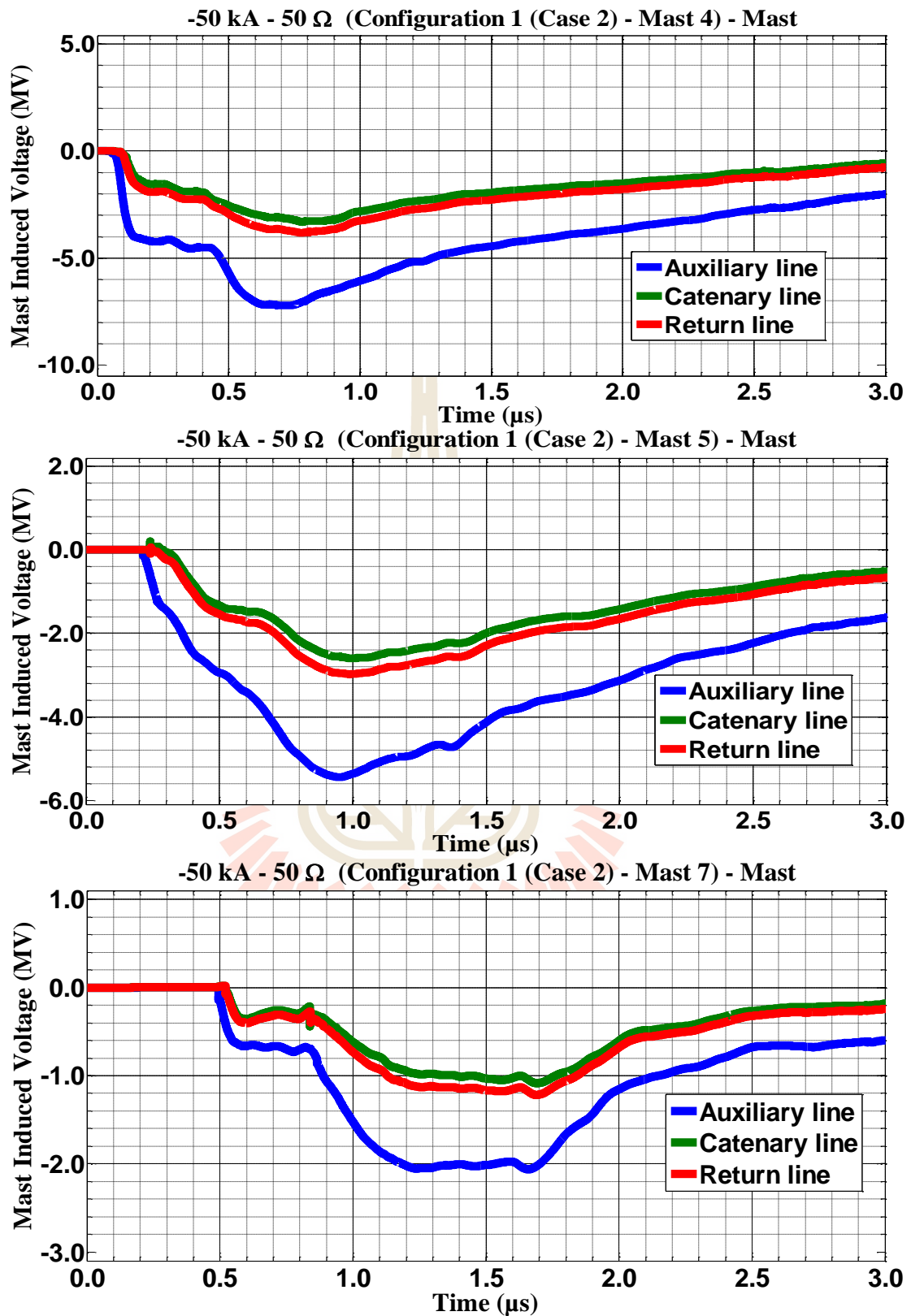


Figure C.34 Mast 4, 5, and 7 induced voltage waveform of the -50 kA first stroke-(1.0/100 μs), subsequent stroke-(0.2/50 μs) strikes on Mast 4 with 50 Ω for Case 2

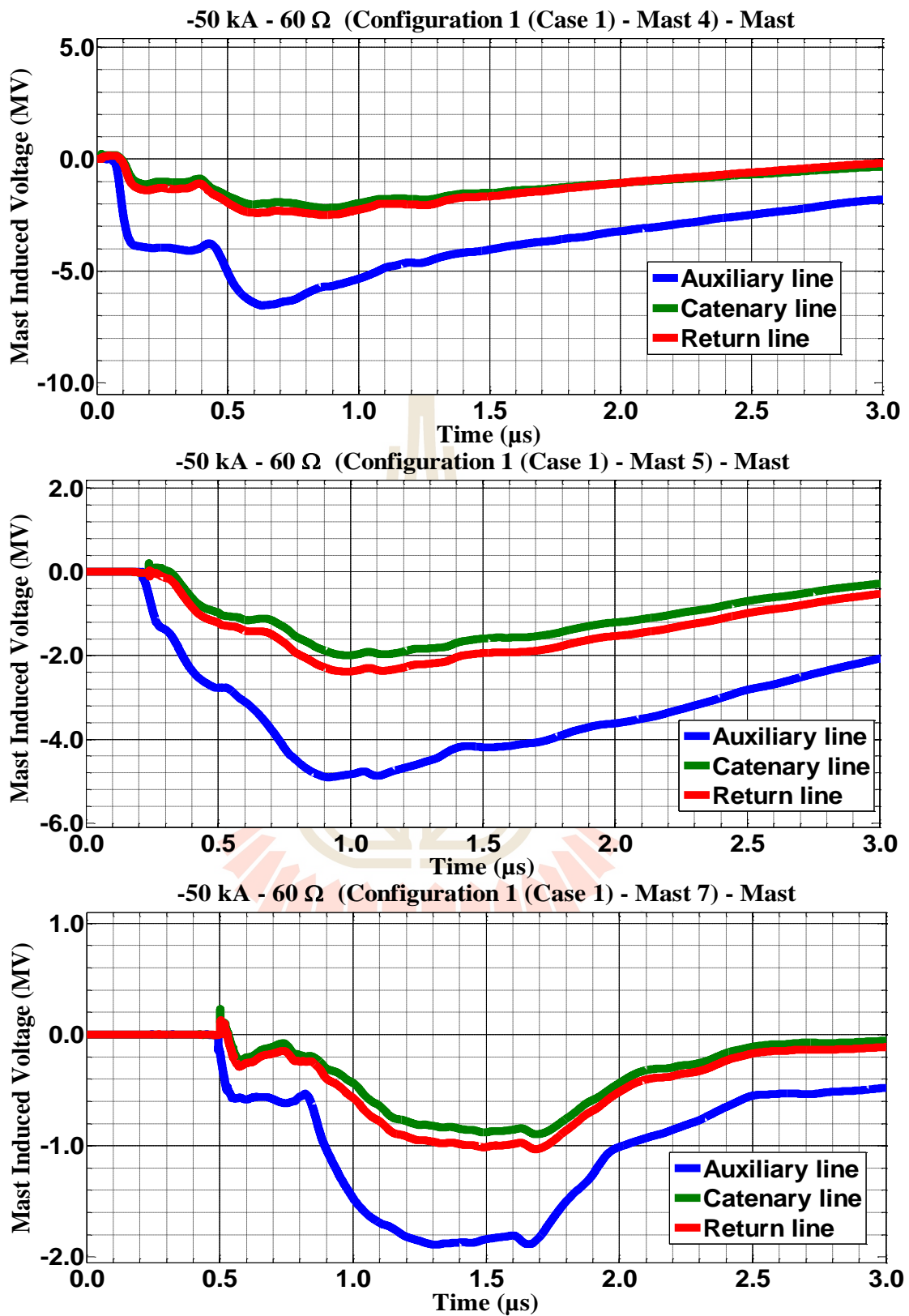


Figure C.35 Mast 4, 5, and 7 induced voltage waveform of the -50 kA first stroke-(1.0/100  $\mu\text{s}$ ), subsequent stroke-(0.2/50  $\mu\text{s}$ ) strikes on Mast 4 with 60  $\Omega$  for Case 1



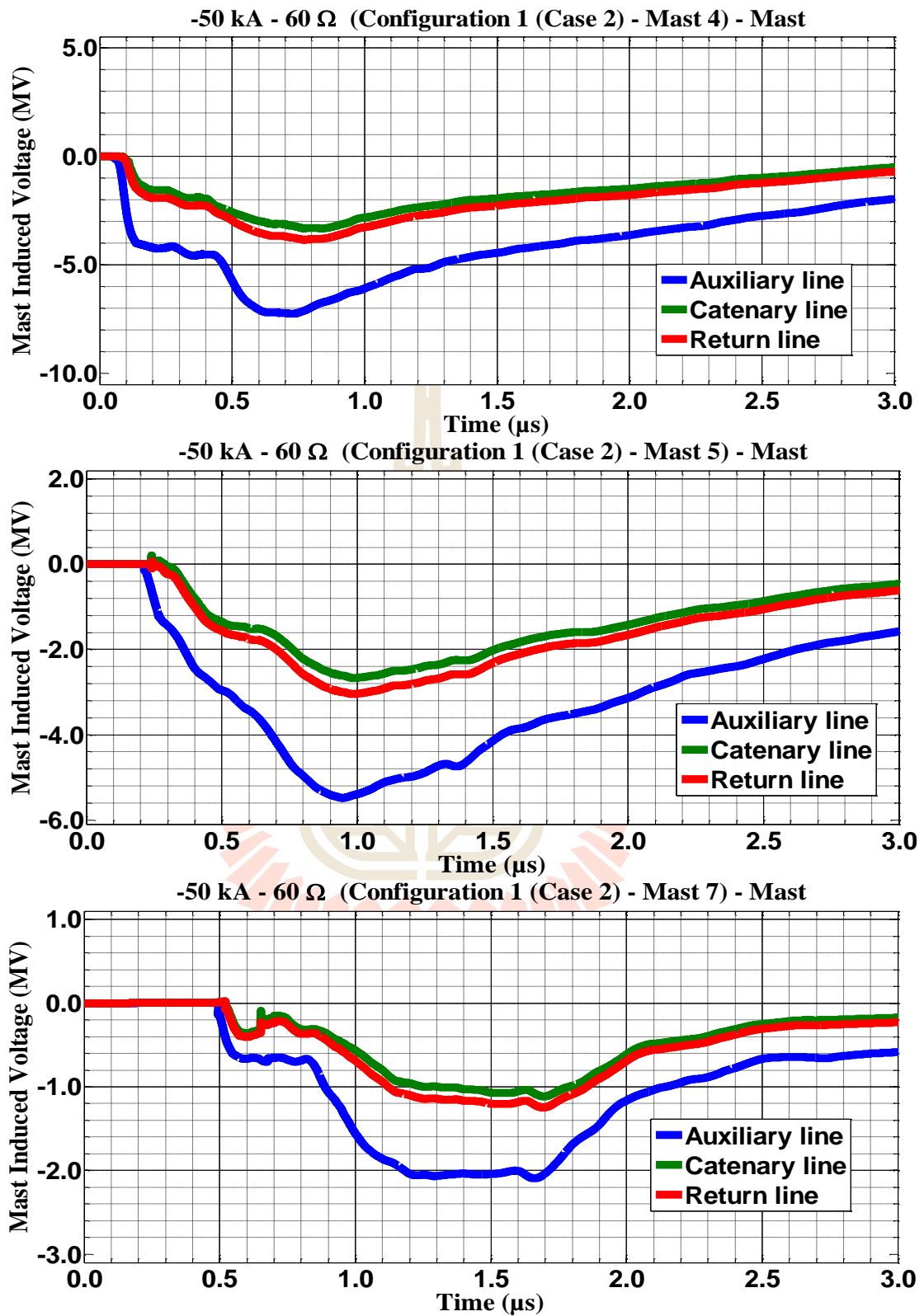
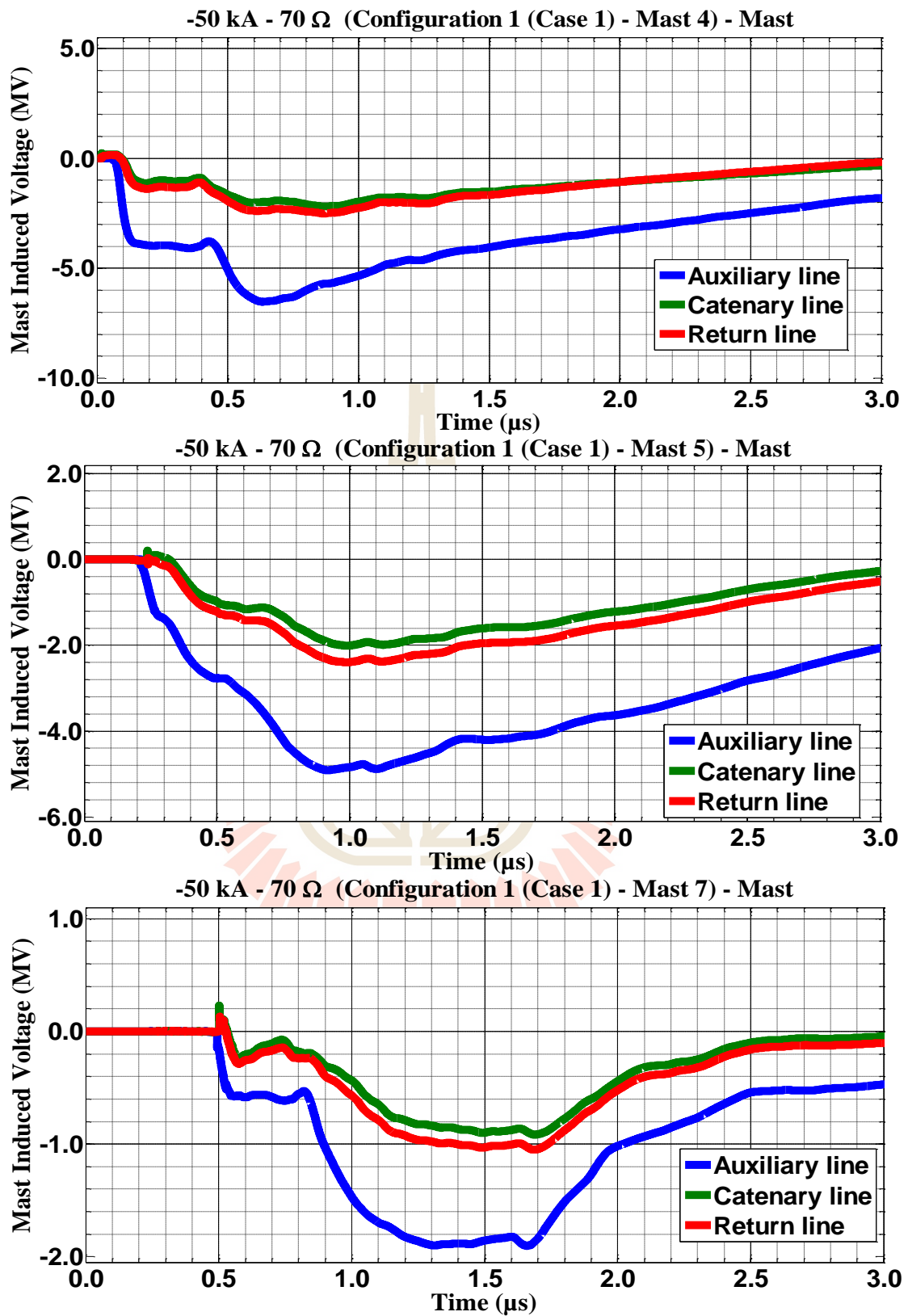
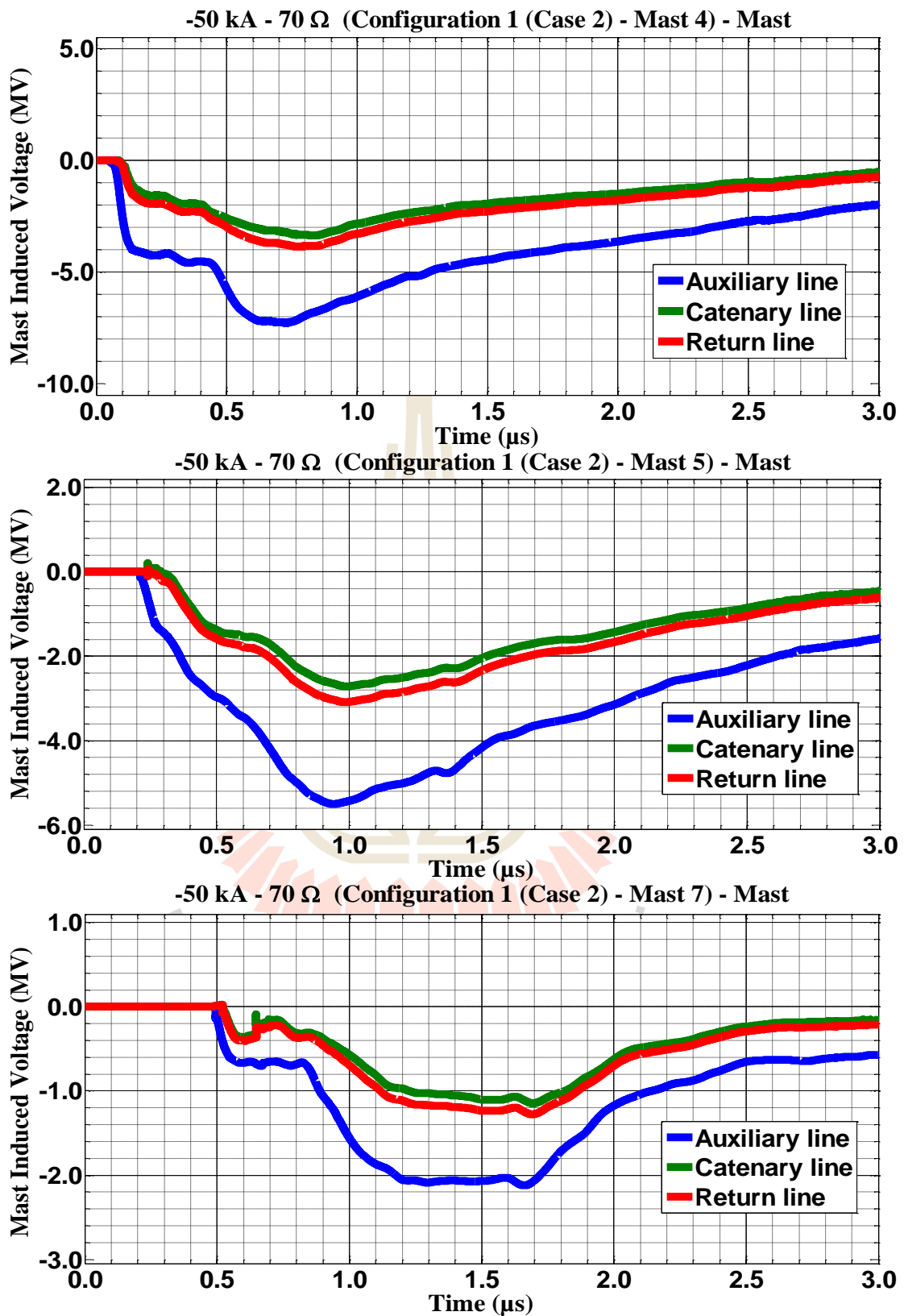


Figure C.36 Mast 4, 5, and 7 induced voltage waveform of the -50 kA first stroke-(1.0/100  $\mu\text{s}$ ), subsequent stroke-(0.2/50  $\mu\text{s}$ ) strikes on Mast 4 with 60  $\Omega$  for Case 2



**Figure C.37** Mast 4, 5, and 7 induced voltage waveform of the -50 kA first stroke-(1.0/100 μs), subsequent stroke-(0.2/50 μs) strikes on Mast 4 with 70 Ω for Case 1



**Figure C.38** Mast 4, 5, and 7 induced voltage waveform of the -50 kA first stroke-(1.0/100 μs), subsequent stroke-(0.2/50 μs) strikes on Mast 4 with 70 Ω for Case 2

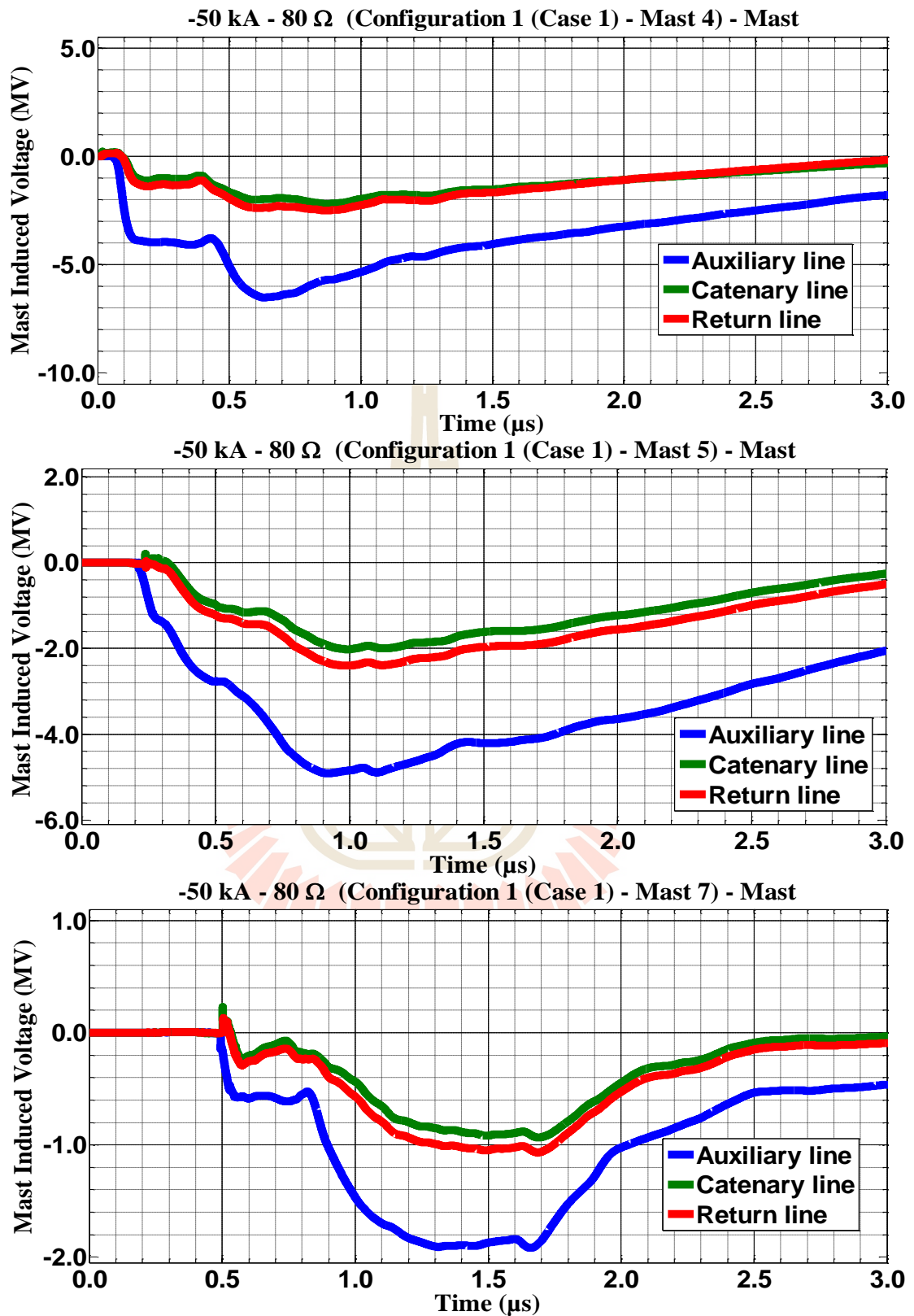


Figure C.39 Mast 4, 5, and 7 induced voltage waveform of the -50 kA first stroke-(1.0/100  $\mu\text{s}$ ), subsequent stroke-(0.2/50  $\mu\text{s}$ ) strikes on Mast 4 with 80  $\Omega$  for Case 1

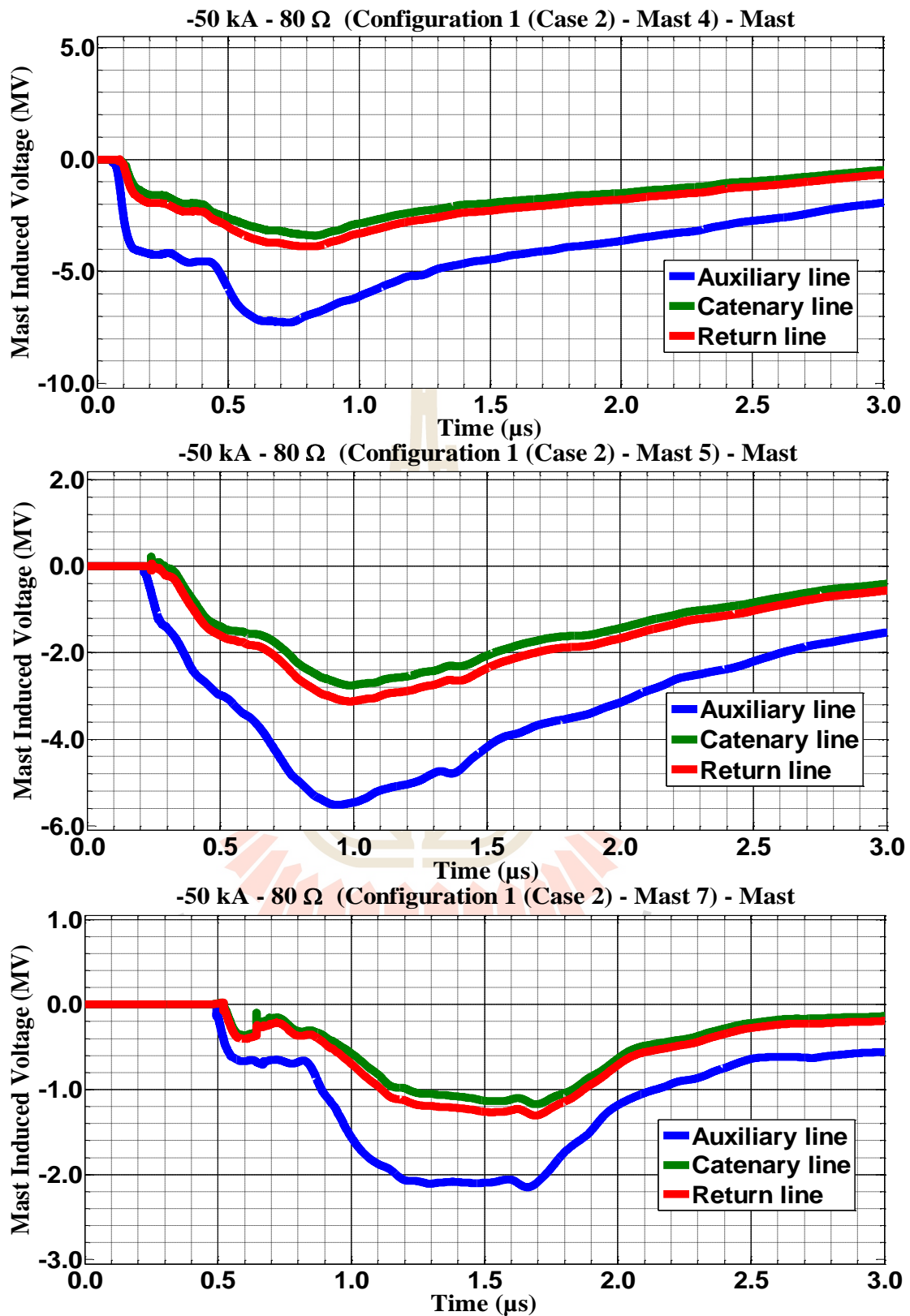


Figure C.40 Mast 4, 5, and 7 induced voltage waveform of the -50 kA first stroke-(1.0/100  $\mu\text{s}$ ), subsequent stroke-(0.2/50  $\mu\text{s}$ ) strikes on Mast 4 with 80  $\Omega$  for Case 2

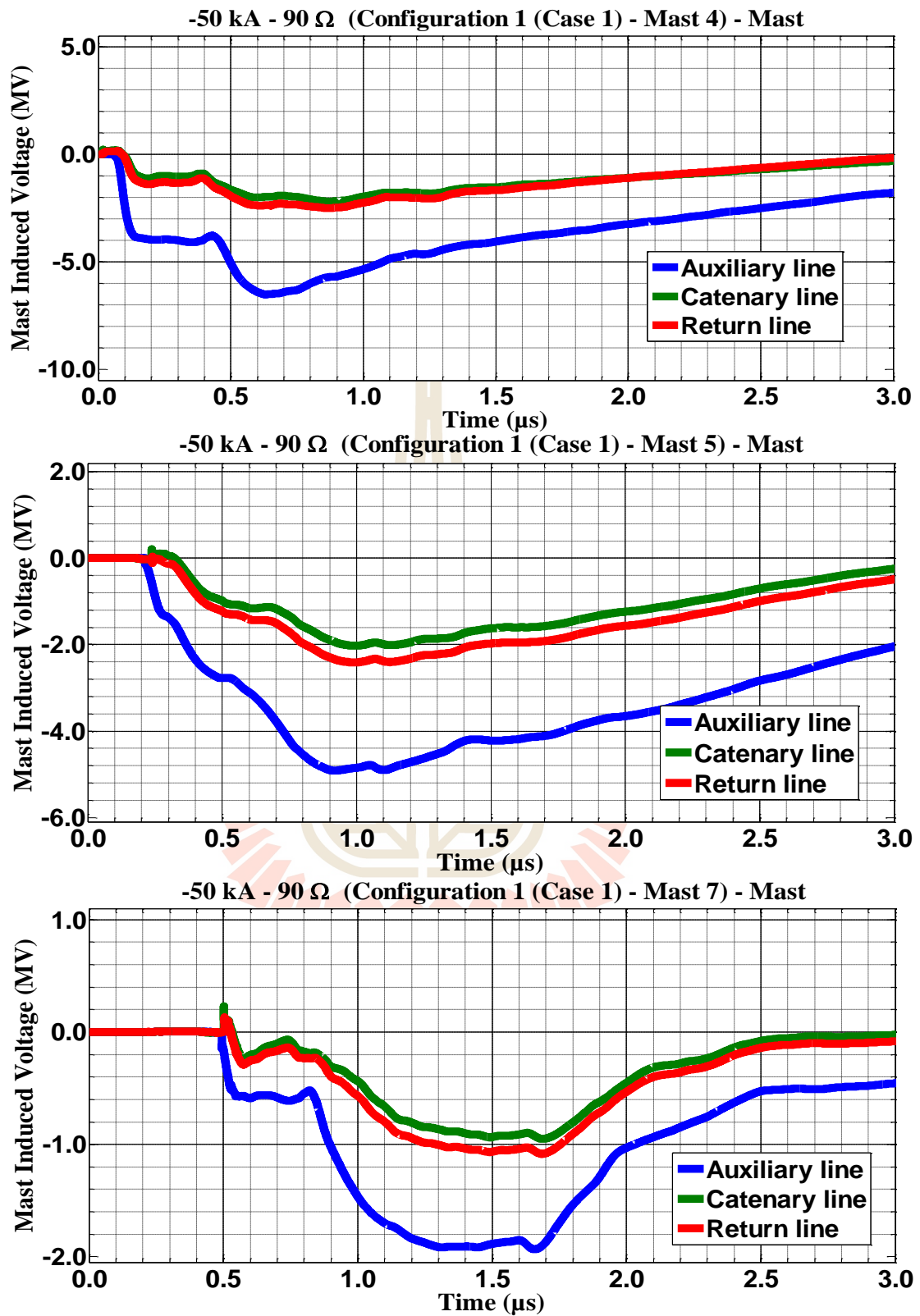
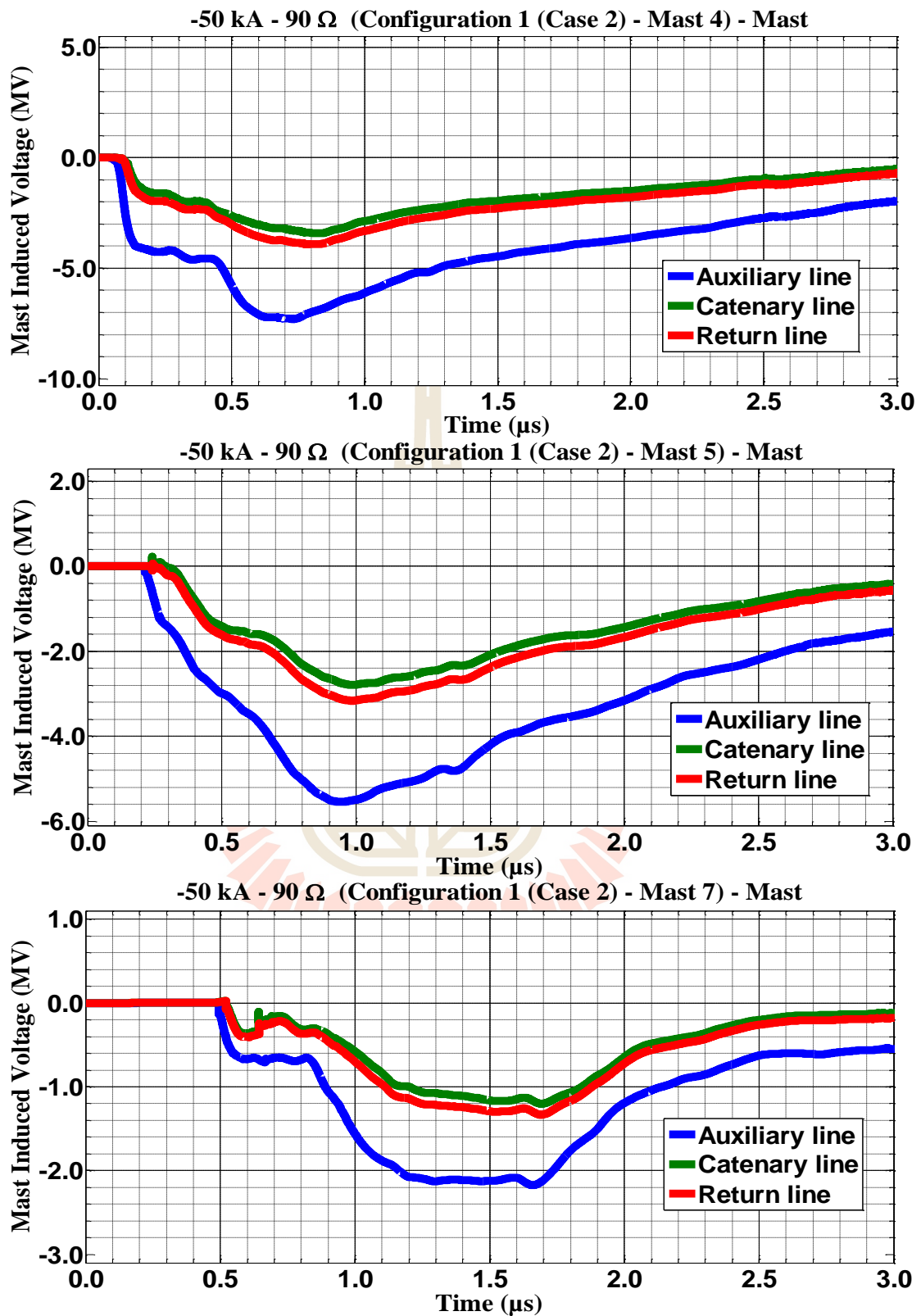
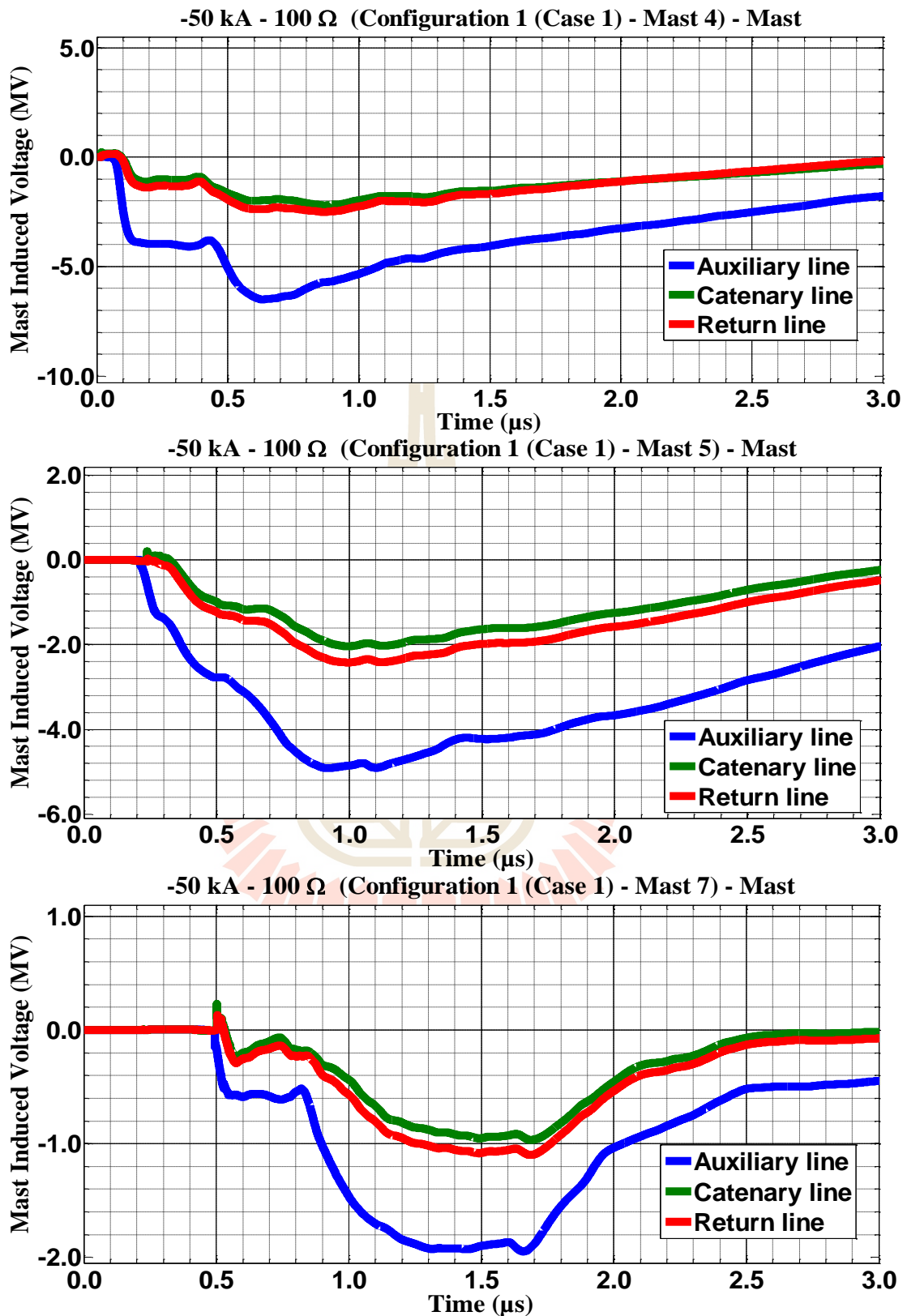


Figure C.41 Mast 4, 5, and 7 induced voltage waveform of the -50 kA first stroke-(1.0/100 μs), subsequent stroke-(0.2/50 μs) strikes on Mast 4 with 90 Ω for Case 1



**Figure C.42** Mast 4, 5, and 7 induced voltage waveform of the -50 kA first stroke-(1.0/100  $\mu\text{s}$ ), subsequent stroke-(0.2/50  $\mu\text{s}$ ) strikes on Mast 4 with 90  $\Omega$  for Case 2



**Figure C.43** Mast 4, 5, and 7 induced voltage waveform of the -50 kA first stroke-(1.0/100  $\mu\text{s}$ ), subsequent stroke-(0.2/50  $\mu\text{s}$ ) strikes on Mast 4 with 100  $\Omega$  for Case 1



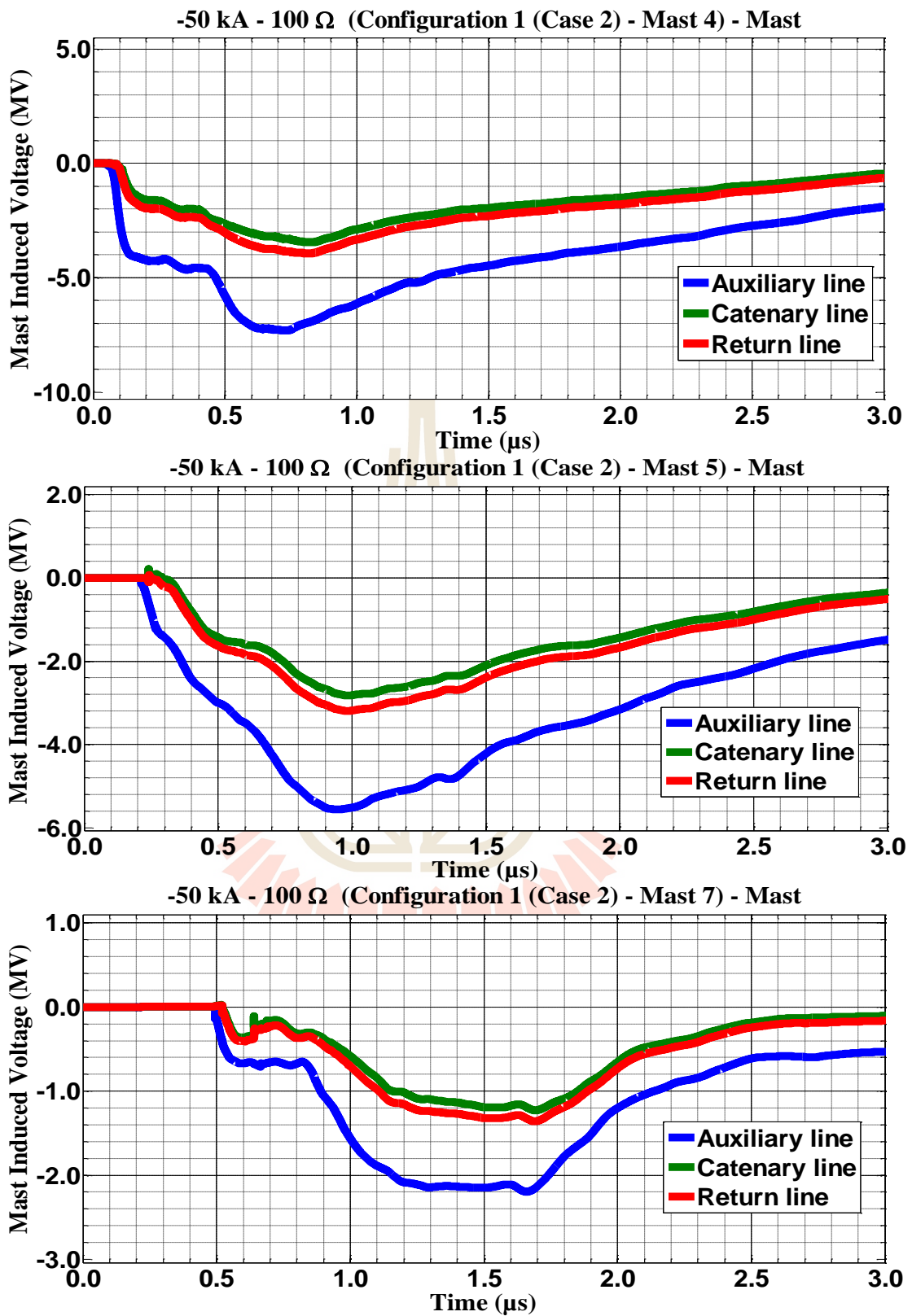


**Figure C.44** Mast 4, 5, and 7 induced voltage waveform of the -50 kA first stroke-(1.0/100 μs), subsequent stroke-(0.2/50 μs) strikes on Mast 4 with 100 Ω for Case 2

### C.3 The consequences when the mast struck by negative multiple lightning strokes for Configuration 2 in Case 1 and 2.

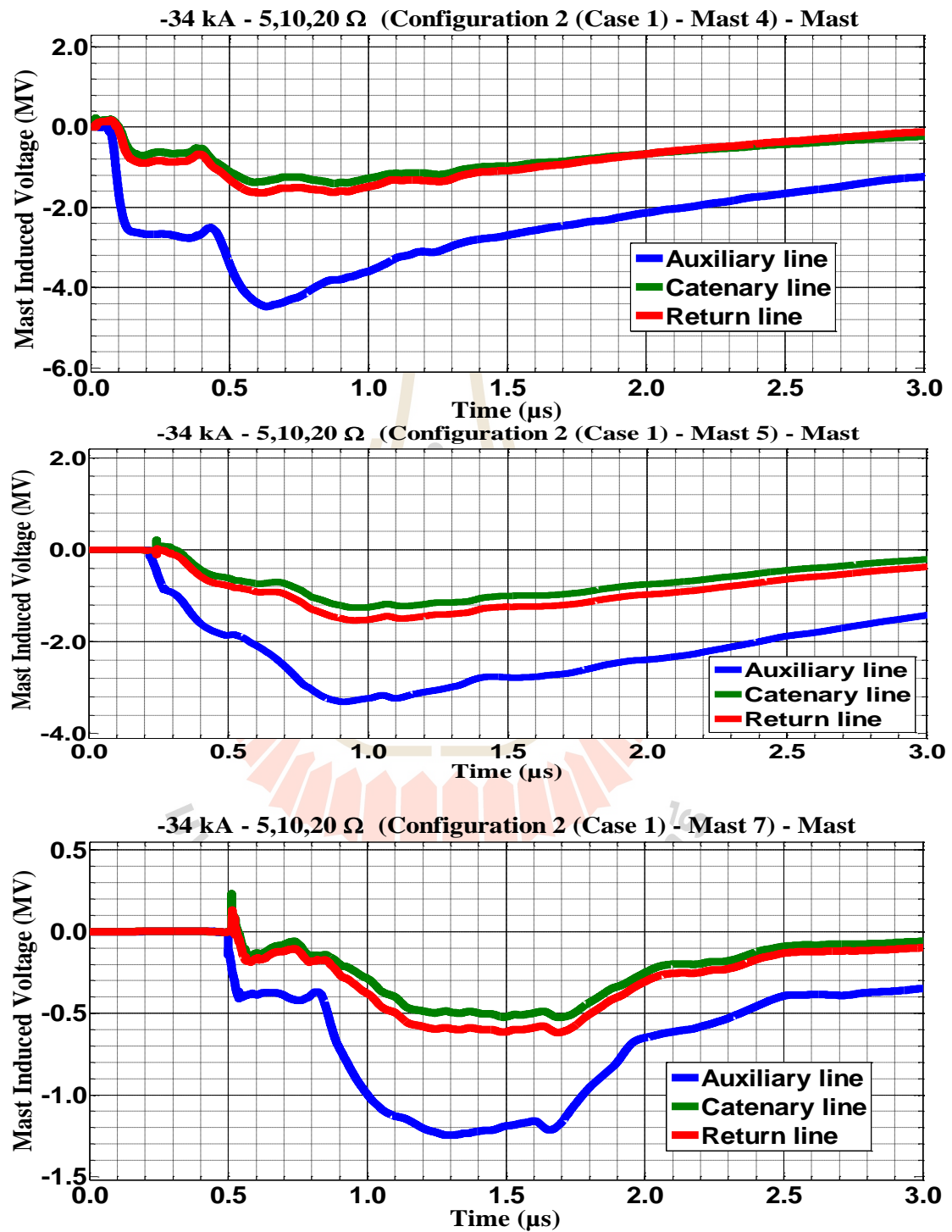


**Figure C.45** Mast 4, 5, and 7 with 5,10,20 Ω induced voltage waveform of the -34 kA first stroke-(1.0/100 μs), subsequent stroke-(0.2/50 μs) strikes on Mast 4 for Case 1

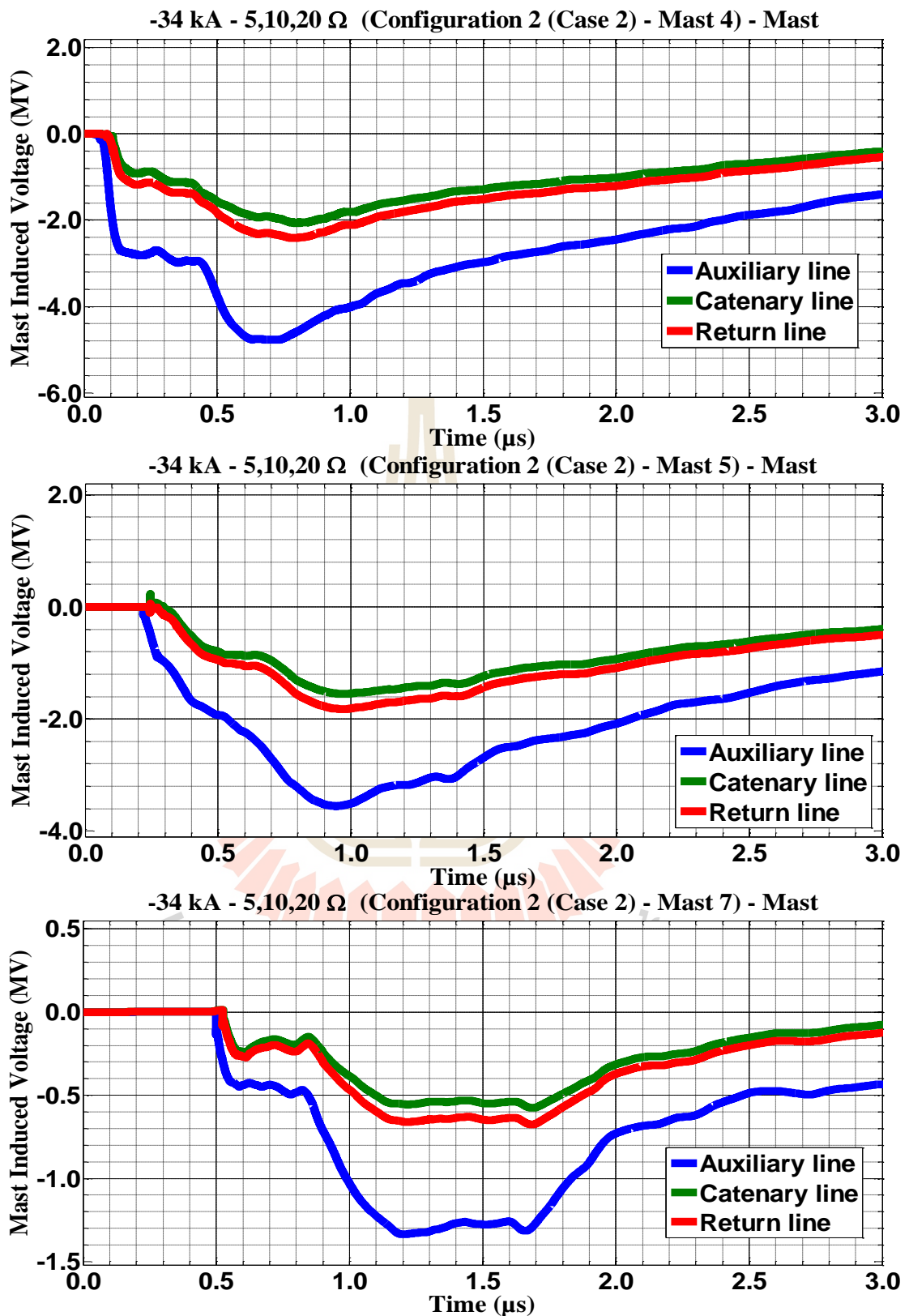


**Figure C.46** Mast 4, 5, and 7 with 5,10,20 Ω induced voltage waveform of the -34 kA first stroke-(1.0/100 μs), subsequent stroke-(0.2/50 μs) strikes on Mast 4 for Case 2

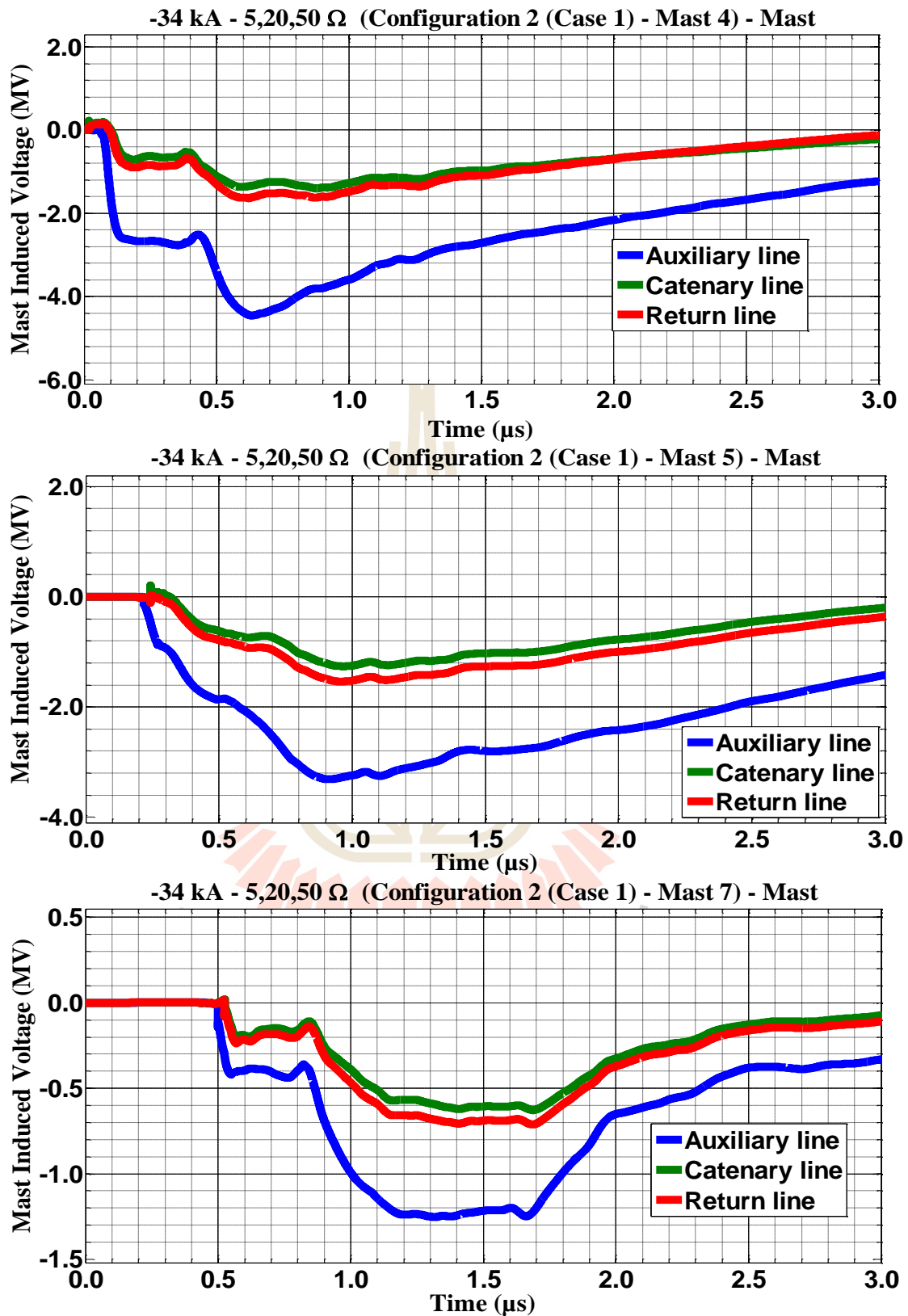
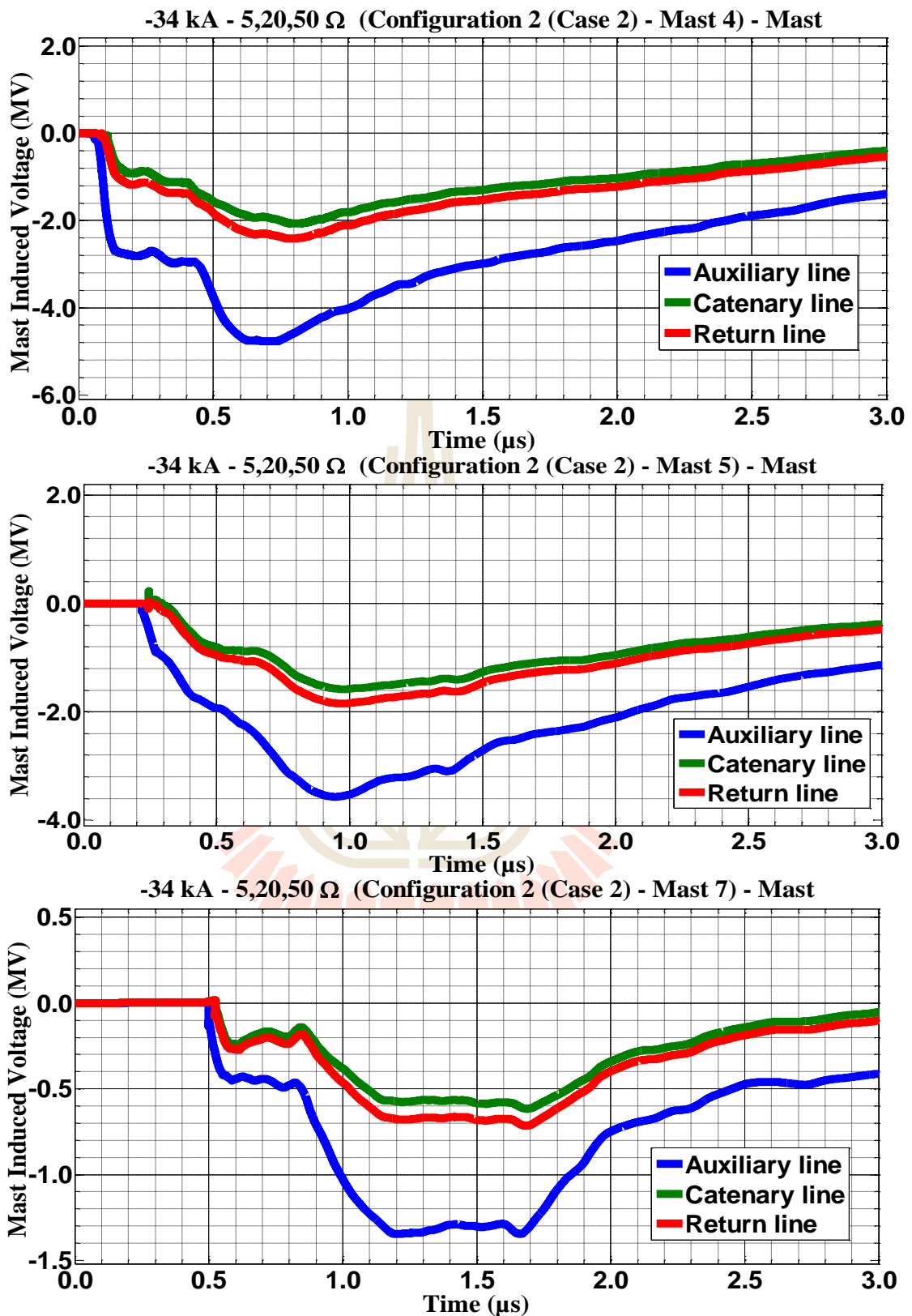
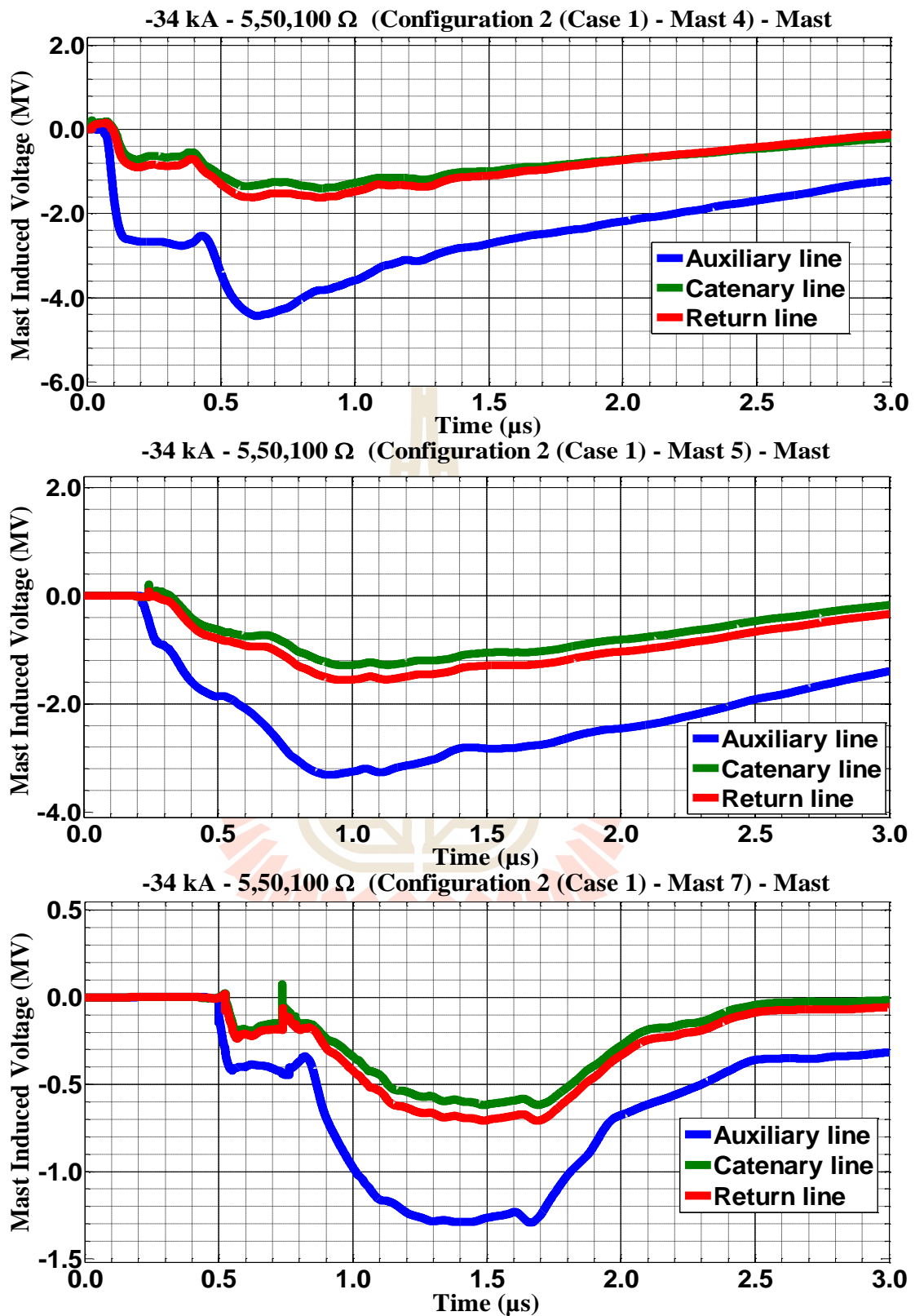


Figure C.47 Mast 4, 5, and 7 with 5,20,50 Ω induced voltage waveform of the -34 kA first stroke-(1.0/100 μs), subsequent stroke-(0.2/50 μs) strikes on Mast 4 for Case 1



**Figure C.48** Mast 4, 5, and 7 with 5,20,50 Ω induced voltage waveform of the -34 kA first stroke-(1.0/100 μs), subsequent stroke-(0.2/50 μs) strikes on Mast 4 for Case 2



**Figure C.49** Mast 4, 5, and 7 with 5,50,100  $\Omega$  induced voltage waveform of -34 kA first stroke-(1.0/100  $\mu\text{s}$ ), subsequent stroke-(0.2/50  $\mu\text{s}$ ) strikes on Mast 4 for Case 1

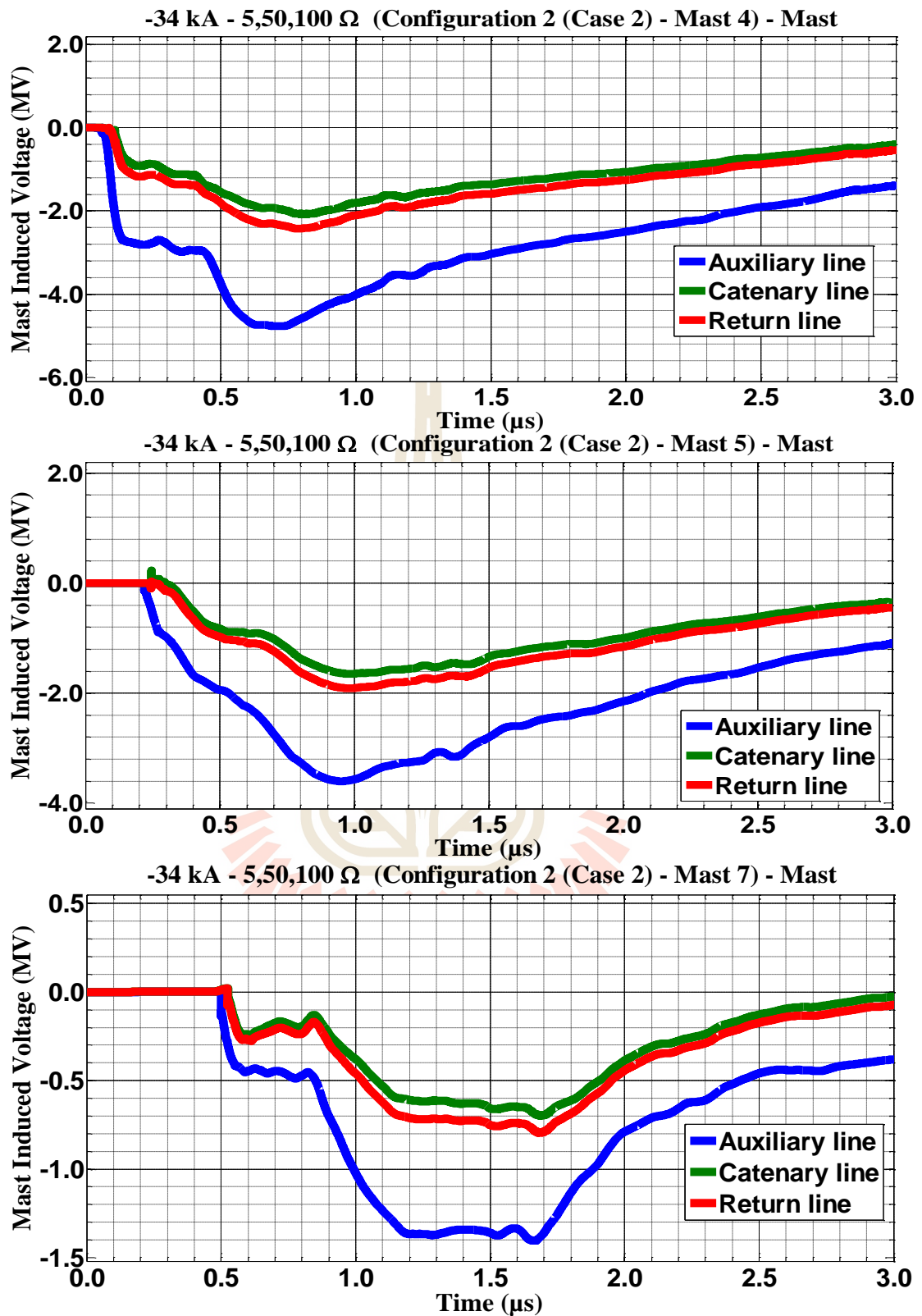


**Figure C.50** Mast 4, 5, and 7 with 5,50,100 Ω induced voltage waveform of -34 kA first stroke-(1.0/100 μs), subsequent stroke-(0.2/50 μs) strikes on Mast 4 for Case 2

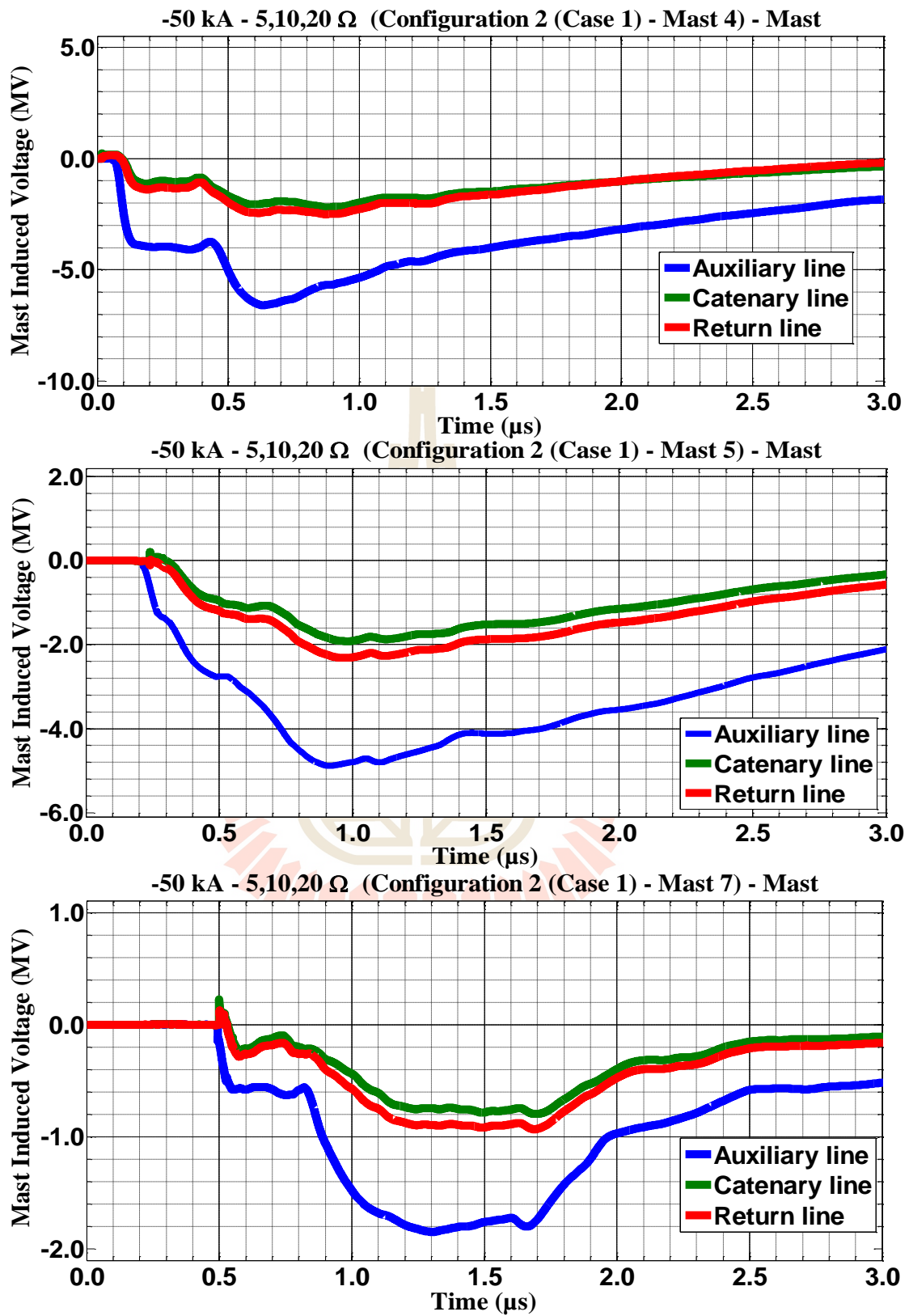


**Figure C.51** Mast 4, 5, and 7 with 5,10,20 Ω induced voltage waveform of the -50 kA first stroke-(1.0/100 μs), subsequent stroke-(0.2/50 μs) strikes on Mast 4 for Case 1



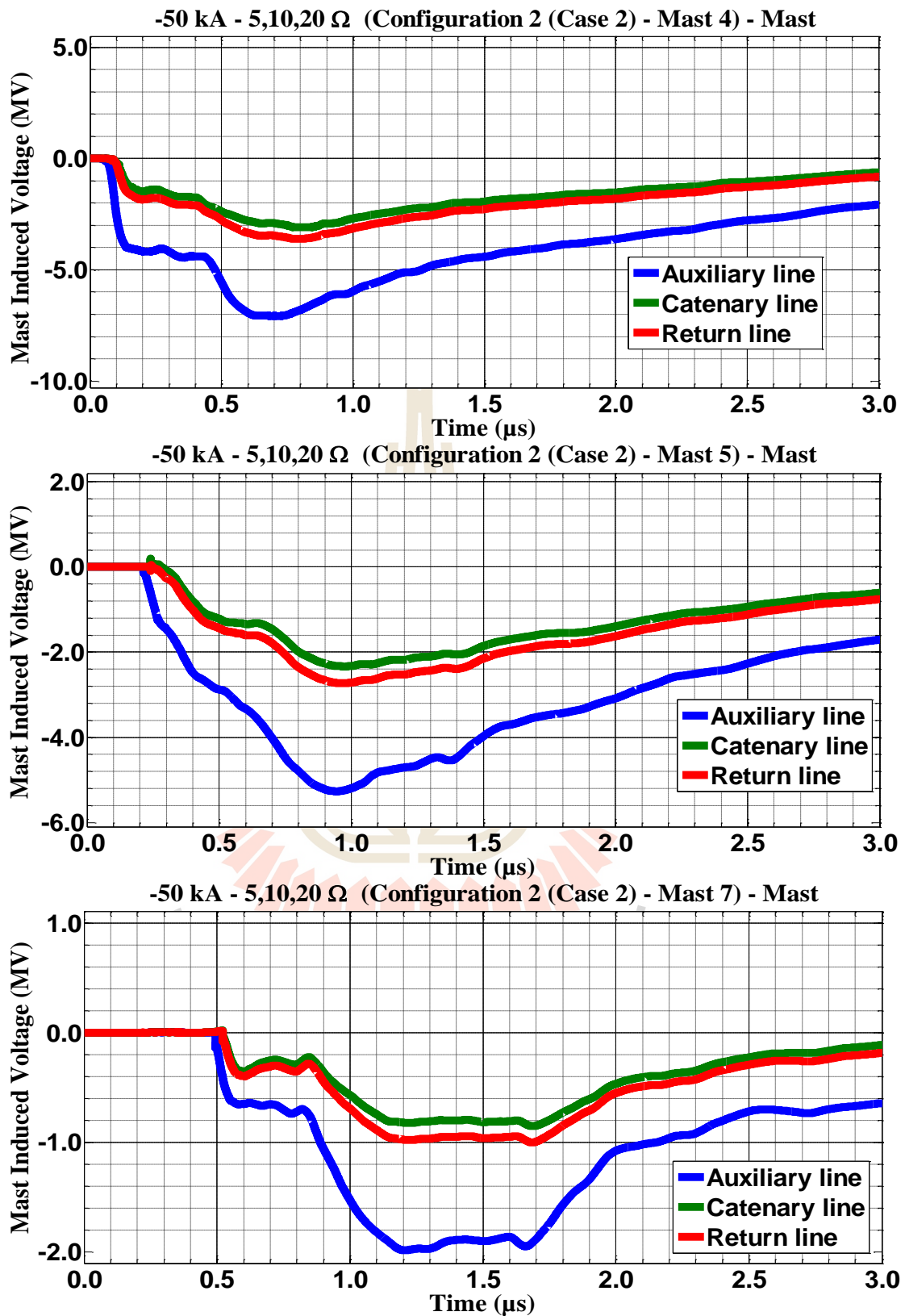
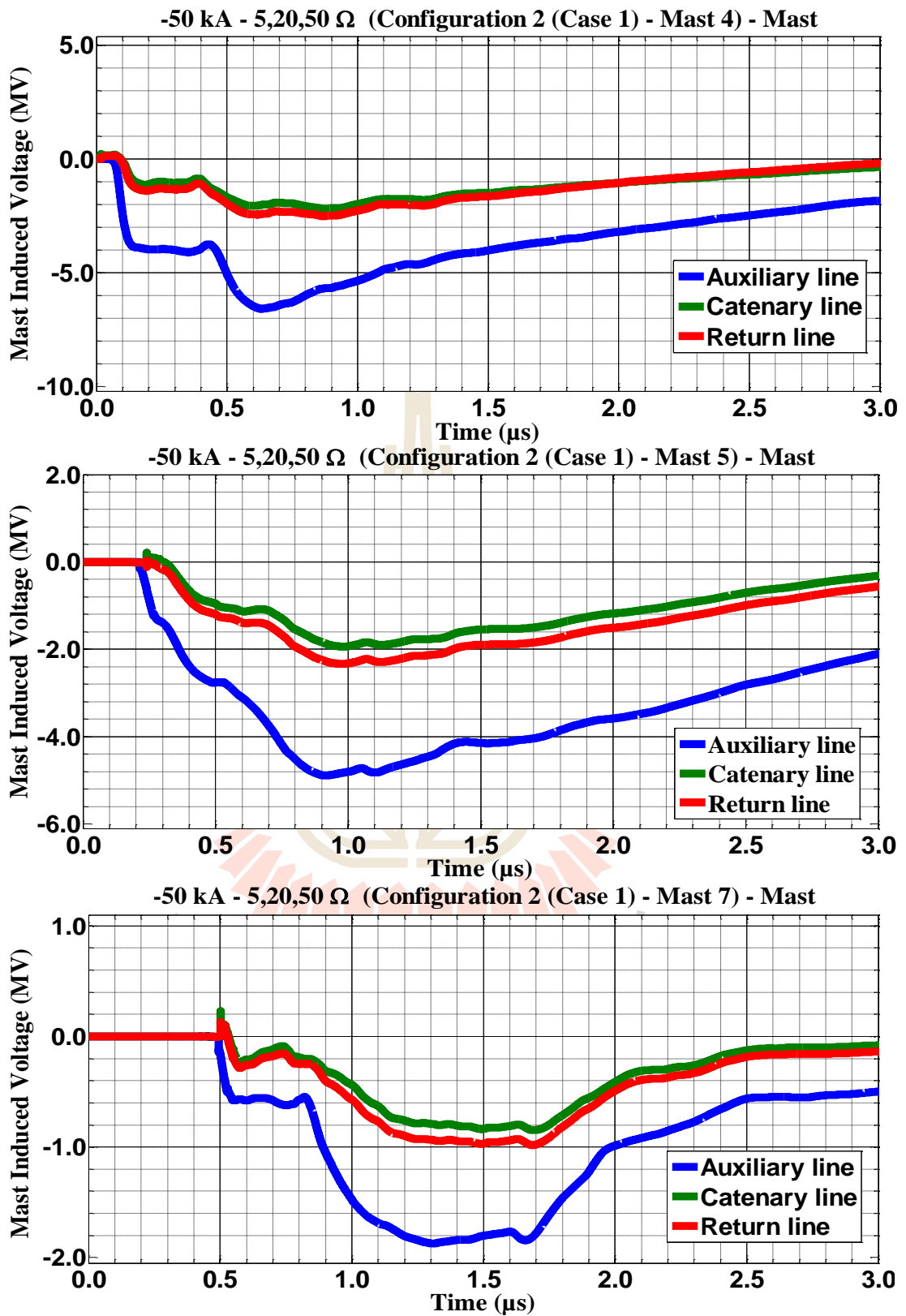
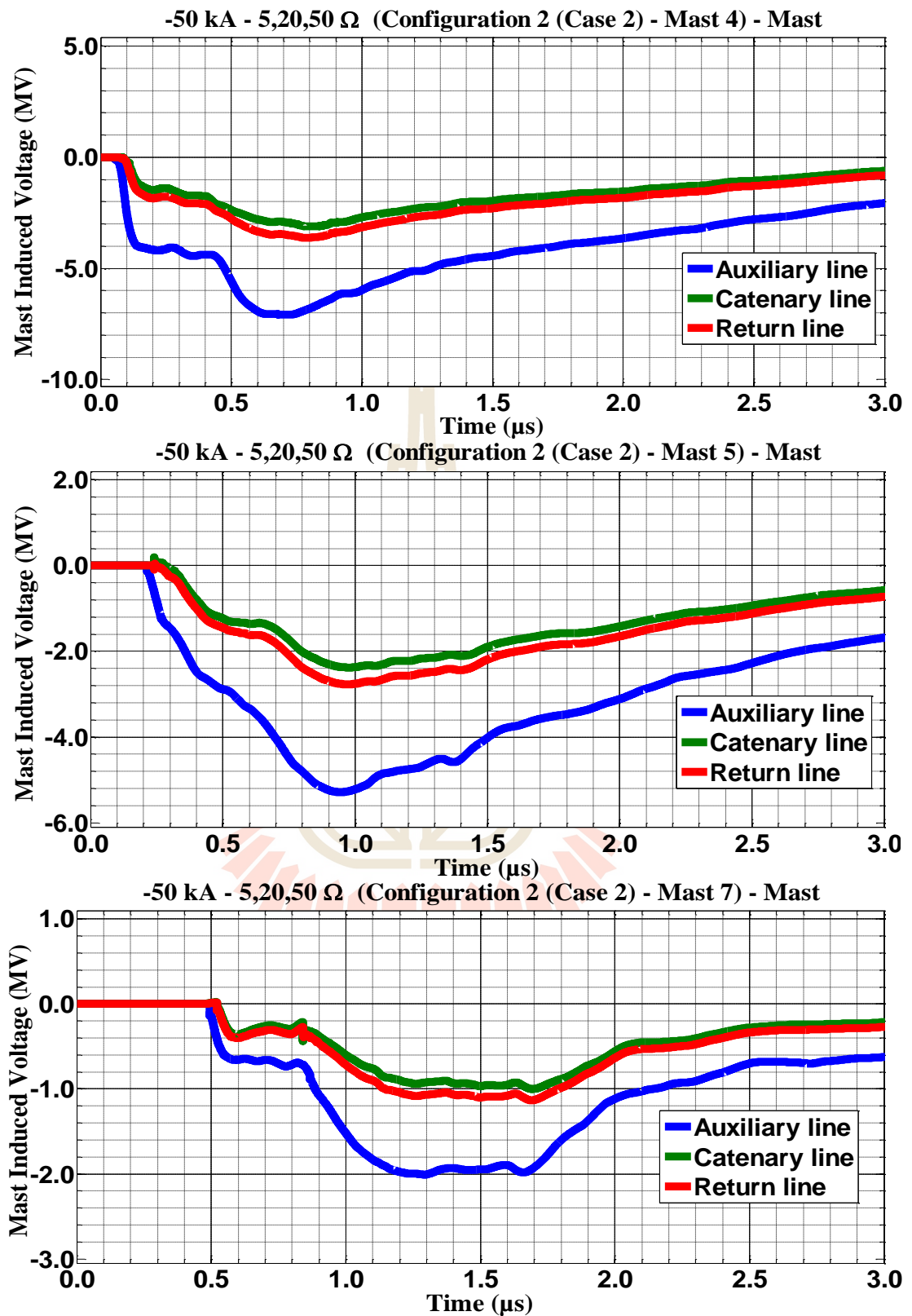


Figure C.52 Mast 4, 5, and 7 with 5,10,20 Ω induced voltage waveform of the -50 kA first stroke-(1.0/100 μs), subsequent stroke-(0.2/50 μs) strikes on Mast 4 for Case 2



**Figure C.53** Mast 4, 5, and 7 with 5,20,50  $\Omega$  induced voltage waveform of the -50 kA first stroke-(1.0/100  $\mu$ s), subsequent stroke-(0.2/50  $\mu$ s) strikes on Mast 4 for Case 1



**Figure C.54** Mast 4, 5, and 7 with 5,20,50  $\Omega$  induced voltage waveform of the -50 kA first stroke-(1.0/100  $\mu\text{s}$ ), subsequent stroke-(0.2/50  $\mu\text{s}$ ) strikes on Mast 4 for Case 2

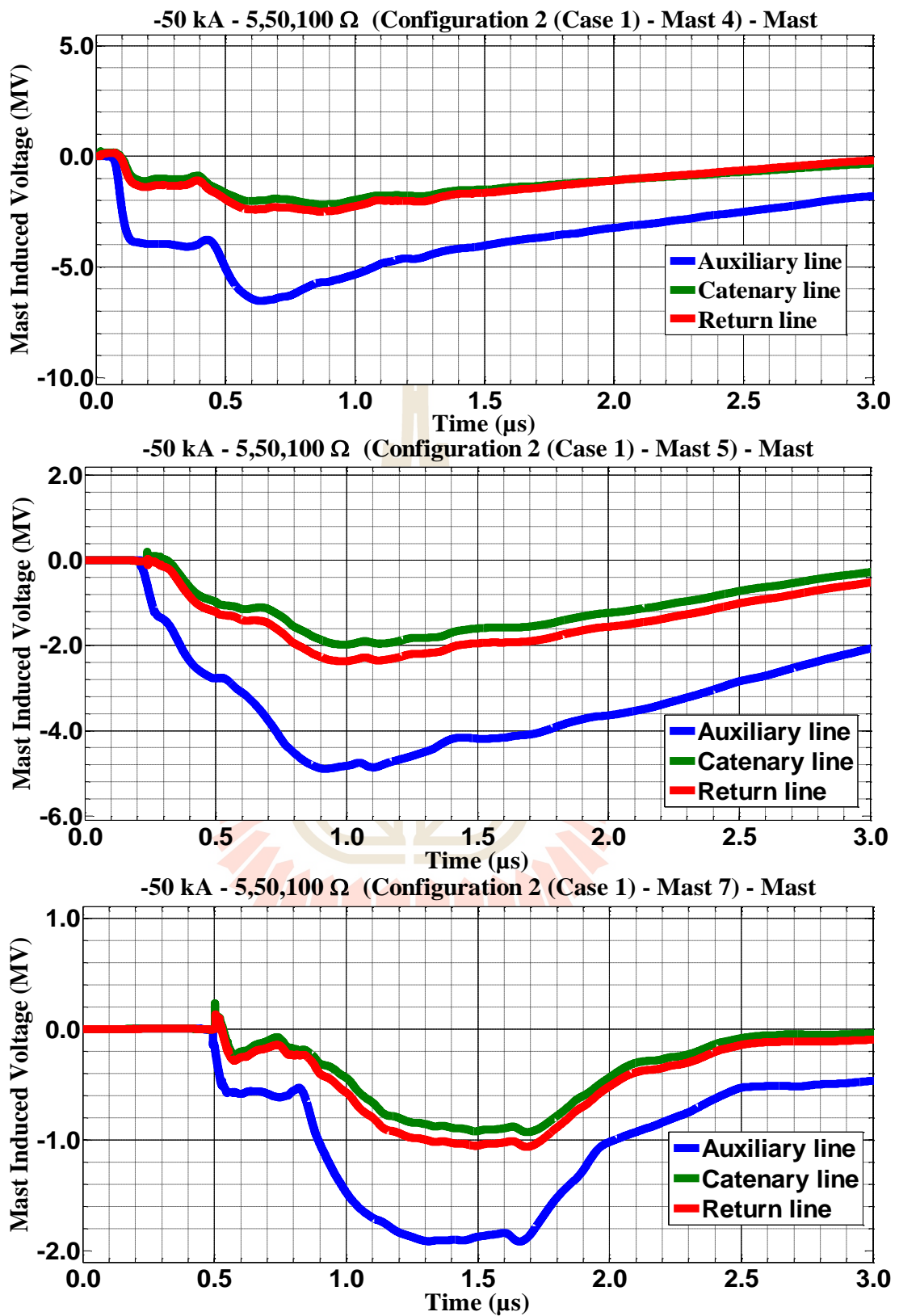


**Figure C.55** Mast 4, 5, and 7 with 5,50,100  $\Omega$  induced voltage waveform of -50 kA first stroke-(1.0/100  $\mu\text{s}$ ), subsequent stroke-(0.2/50  $\mu\text{s}$ ) strikes on Mast 4 for Case 1

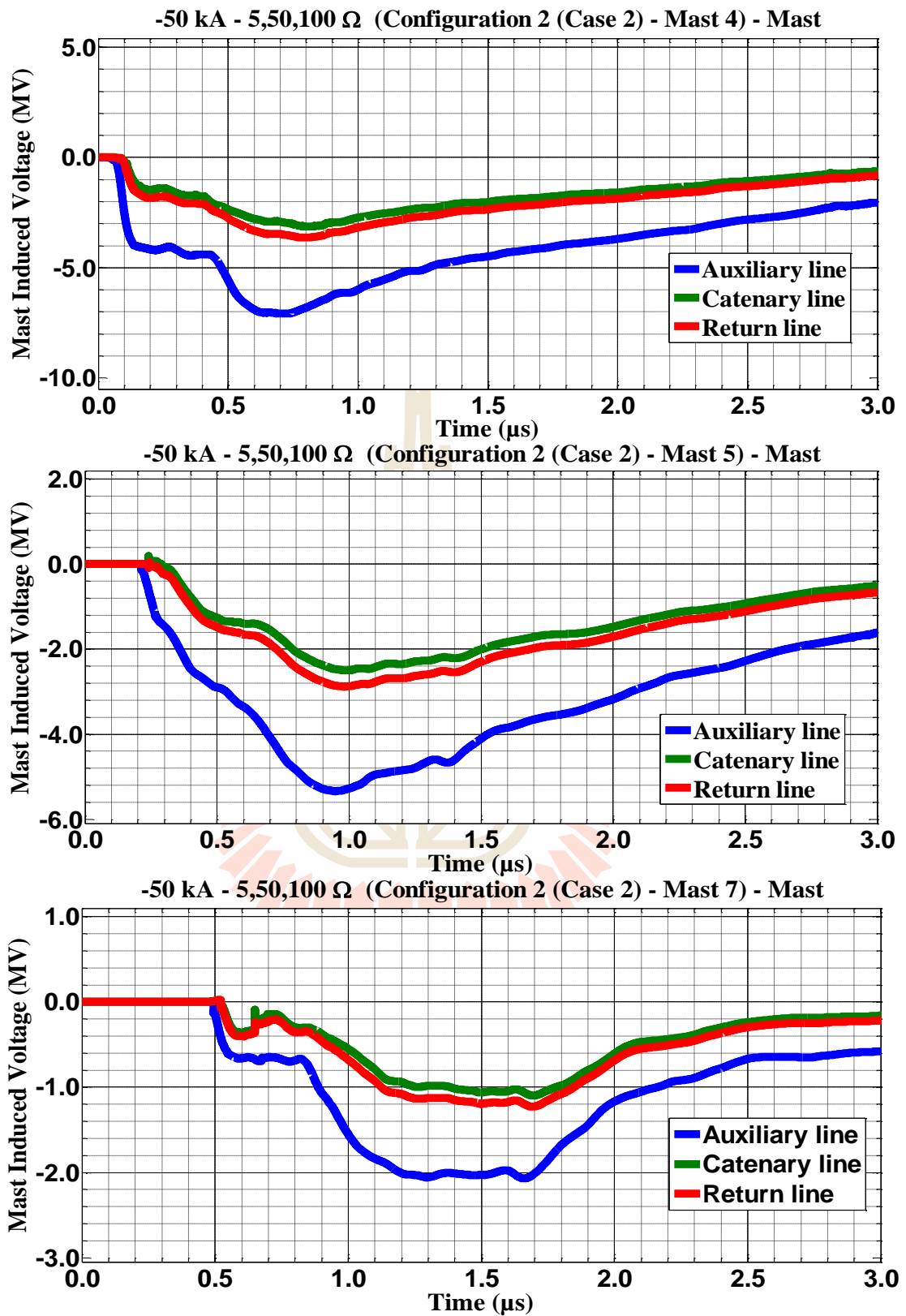


**Figure C.56** Mast 4, 5, and 7 with 5,50,100 Ω induced voltage waveform of -50 kA first stroke-(1.0/100 μs), subsequent stroke-(0.2/50 μs) strikes on Mast 4 for Case 2

#### C.4 The consequences when the mast struck by negative multiple lightning strokes for Configuration 3 in Case 1 and 2.

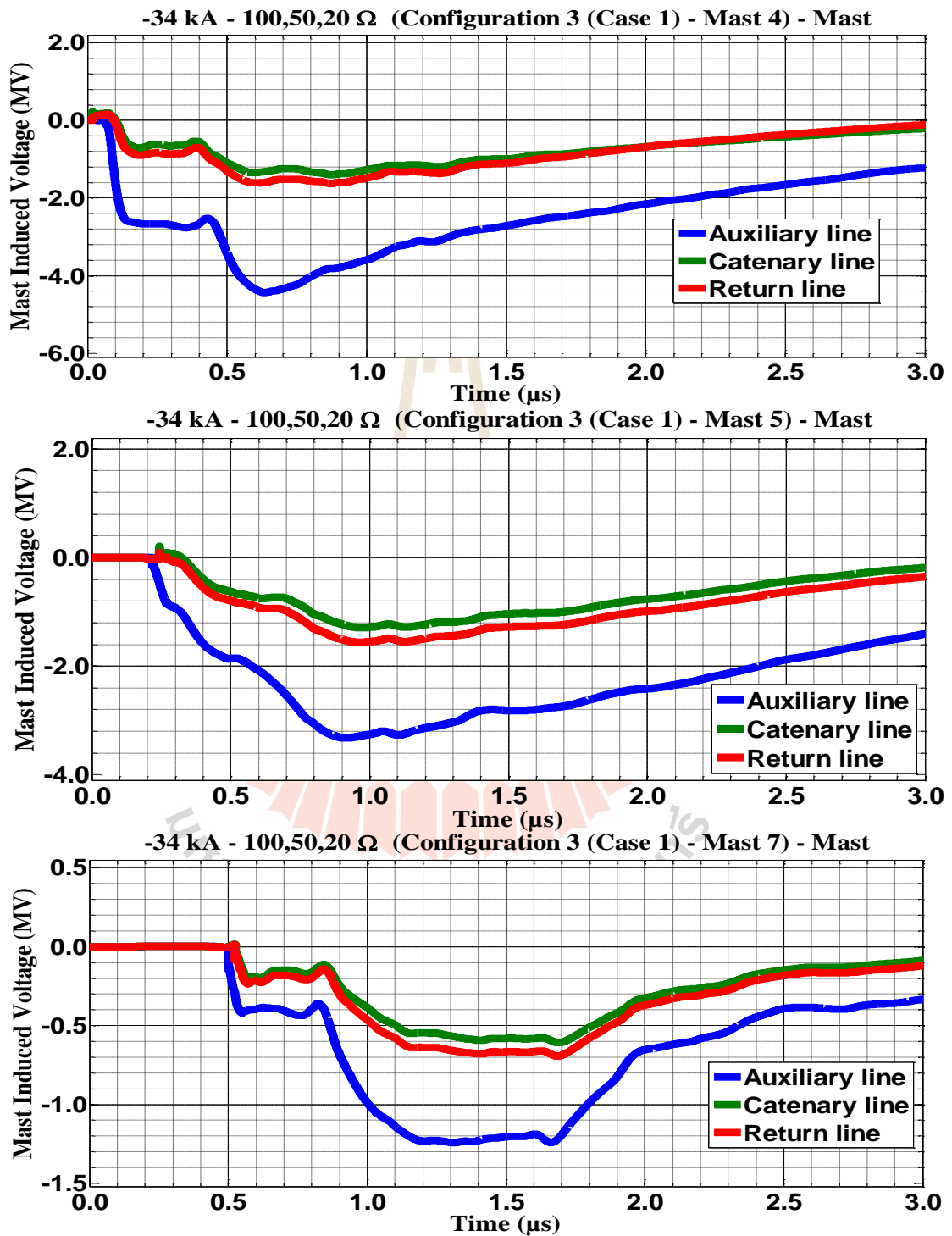
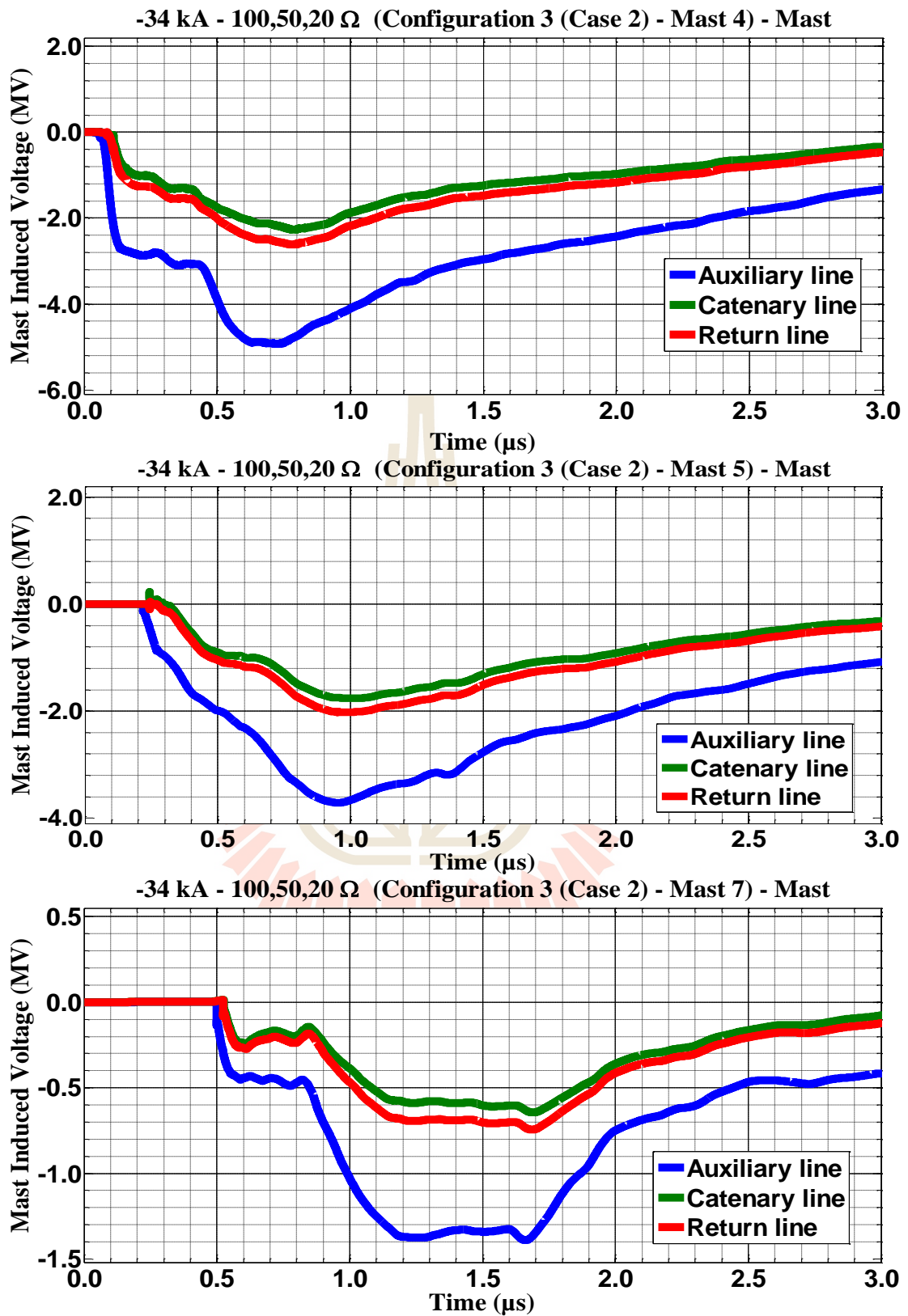


Figure C.57 Mast 4, 5, and 7 with 100,50,20  $\Omega$  induced voltage waveform of -34 kA first stroke-(1.0/100  $\mu\text{s}$ ), subsequent stroke-(0.2/50  $\mu\text{s}$ ) strikes on Mast 4 for Case 1



**Figure C.58** Mast 4, 5, and 7 with 100,50,20  $\Omega$  induced voltage waveform of -34 kA first stroke-(1.0/100  $\mu$ s), subsequent stroke-(0.2/50  $\mu$ s) strikes on Mast 4 for Case 2

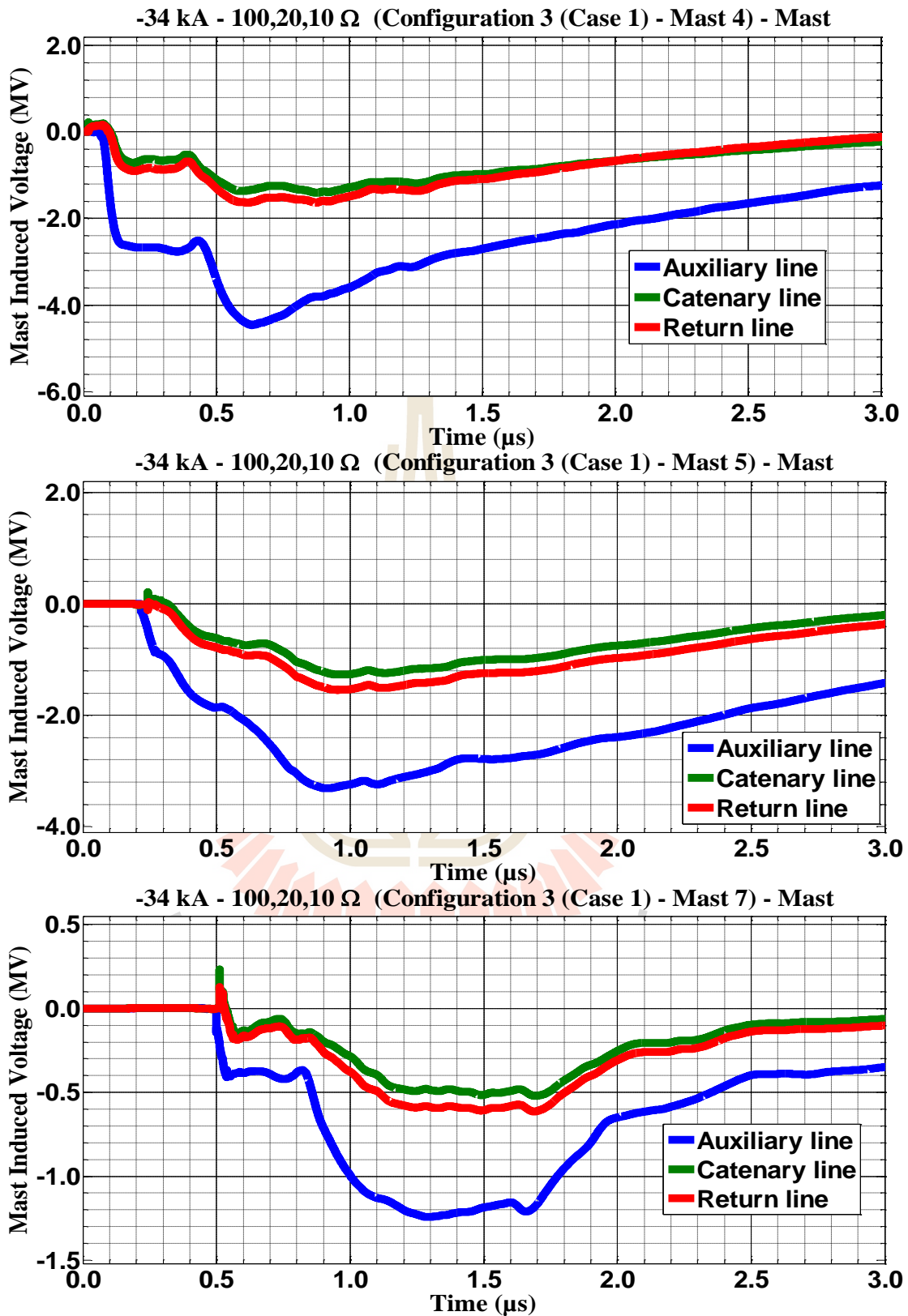
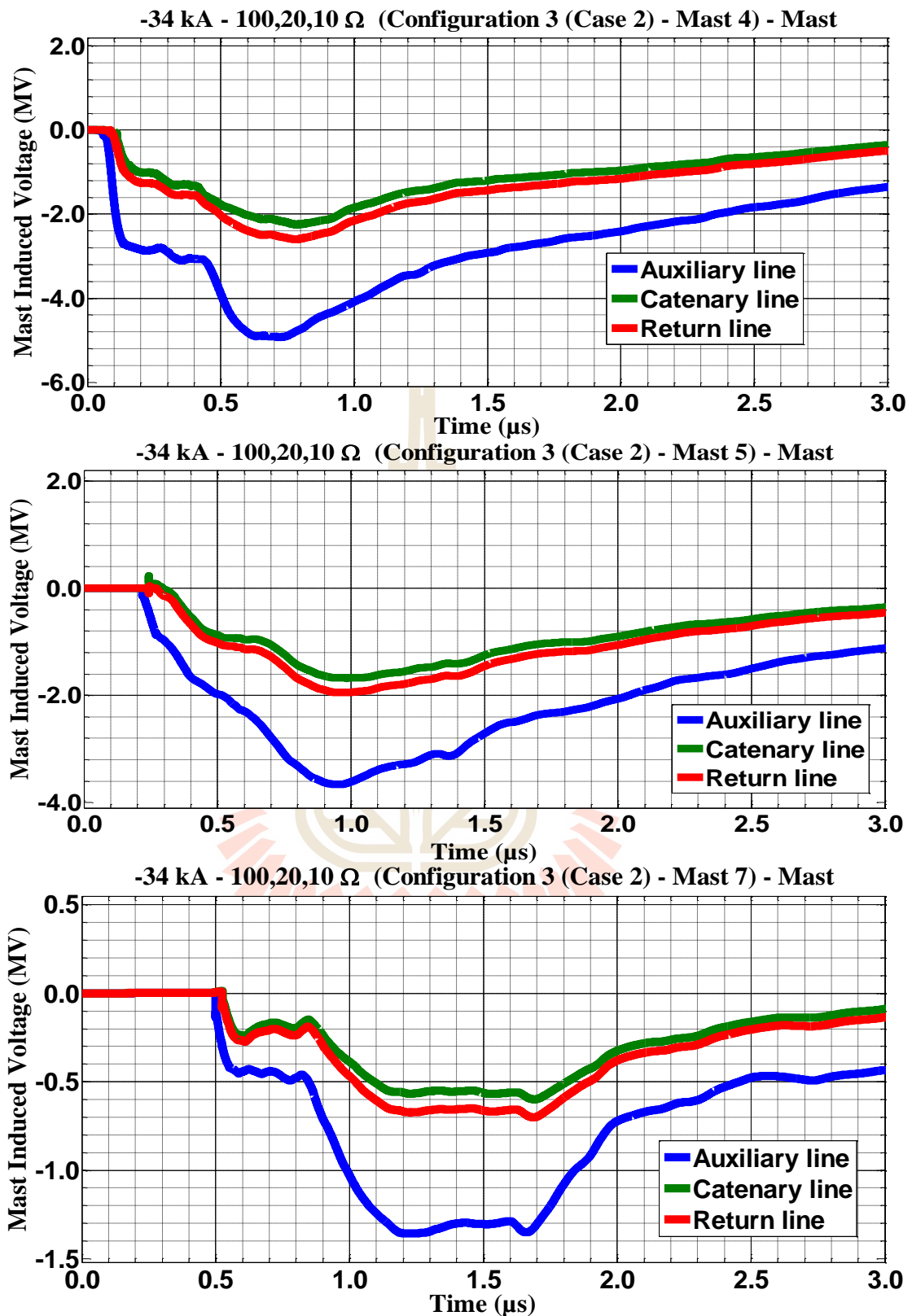
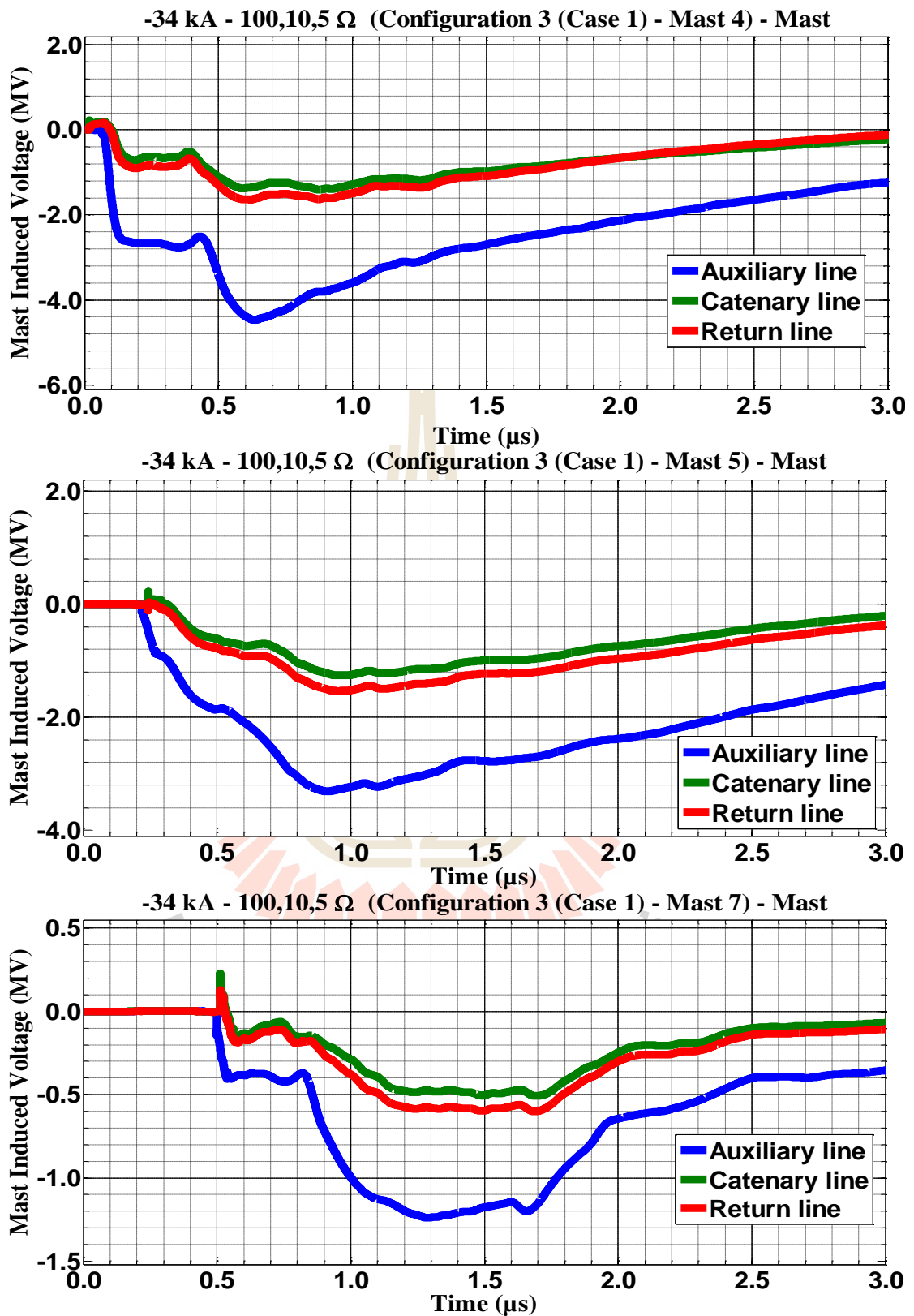


Figure C.59 Mast 4, 5, and 7 with 100,20,10  $\Omega$  induced voltage waveform of -34 kA first stroke-(1.0/100  $\mu\text{s}$ ), subsequent stroke-(0.2/50  $\mu\text{s}$ ) strikes on Mast 4 for Case 1





**Figure C.60** Mast 4, 5, and 7 with 100,20,10  $\Omega$  induced voltage waveform of -34 kA first stroke-(1.0/100  $\mu\text{s}$ ), subsequent stroke-(0.2/50  $\mu\text{s}$ ) strikes on Mast 4 for Case 2



**Figure C.61** Mast 4, 5, and 7 with 100,10,5  $\Omega$  induced voltage waveform of -34 kA first stroke-(1.0/100  $\mu\text{s}$ ), subsequent stroke-(0.2/50  $\mu\text{s}$ ) strikes on Mast 4 for Case 1

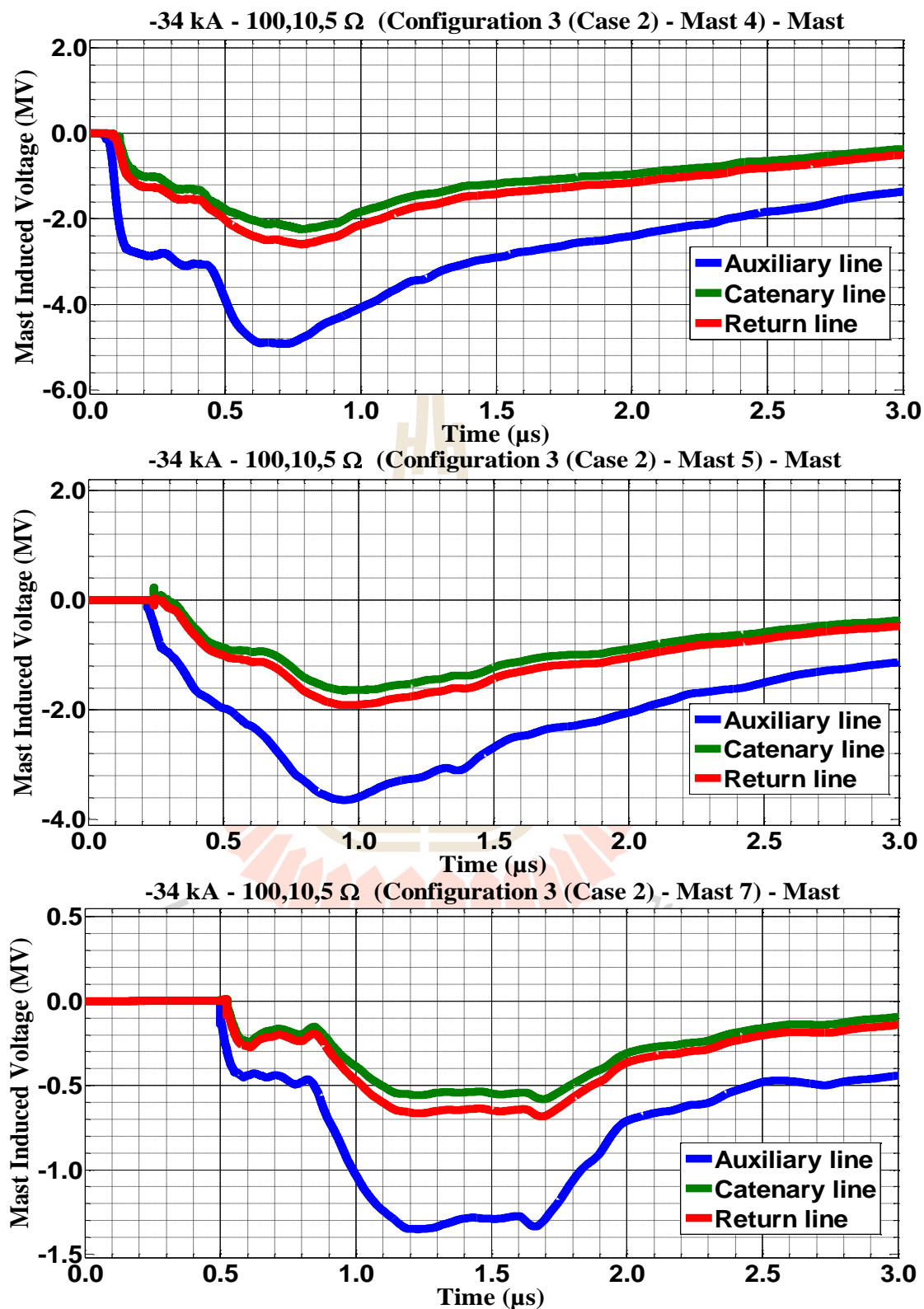


**Figure C.62** Mast 4, 5, and 7 with 100,10,5 Ω induced voltage waveform of -34 kA first stroke-(1.0/100 μs), subsequent stroke-(0.2/50 μs) strikes on Mast 4 for Case 2

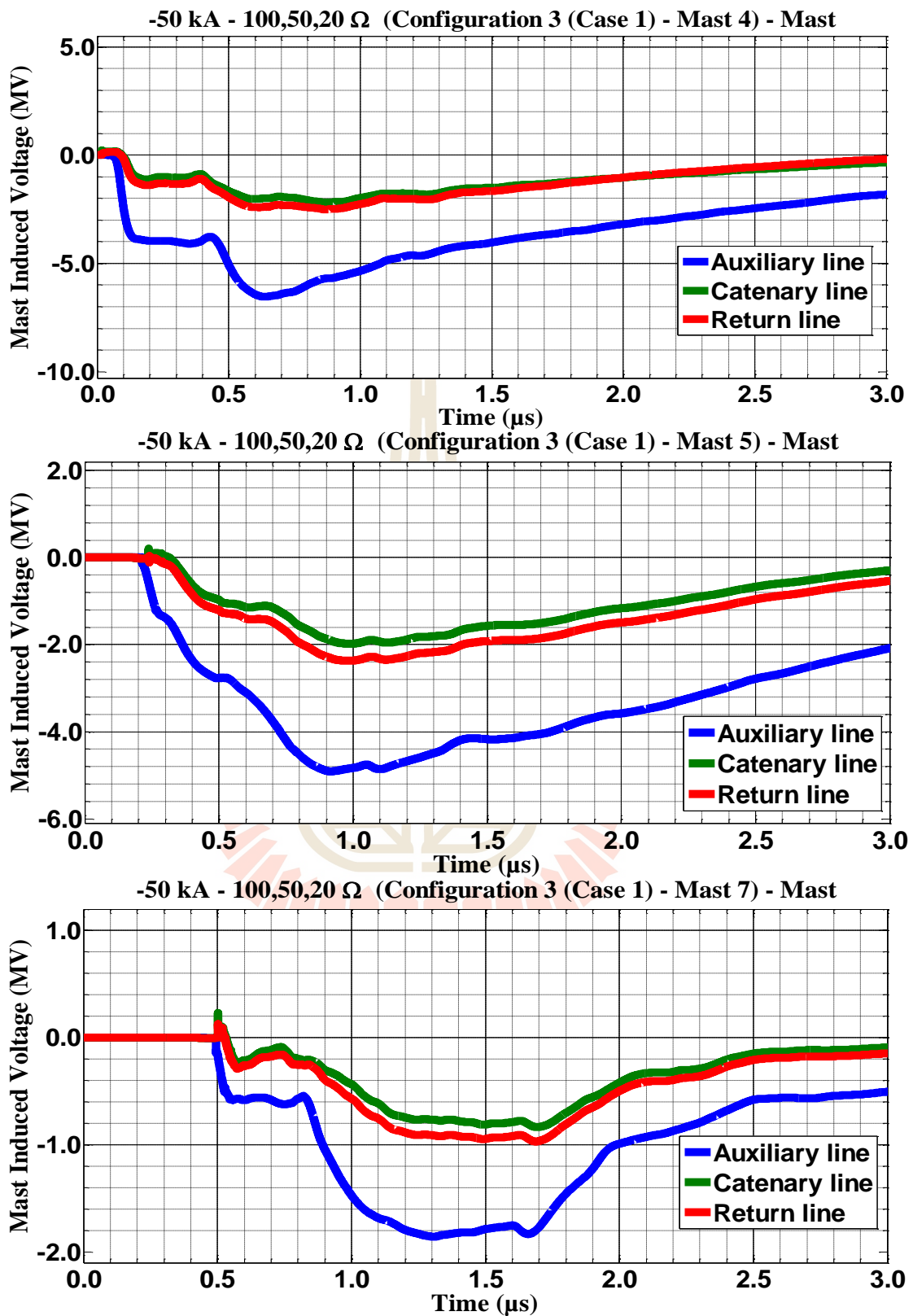
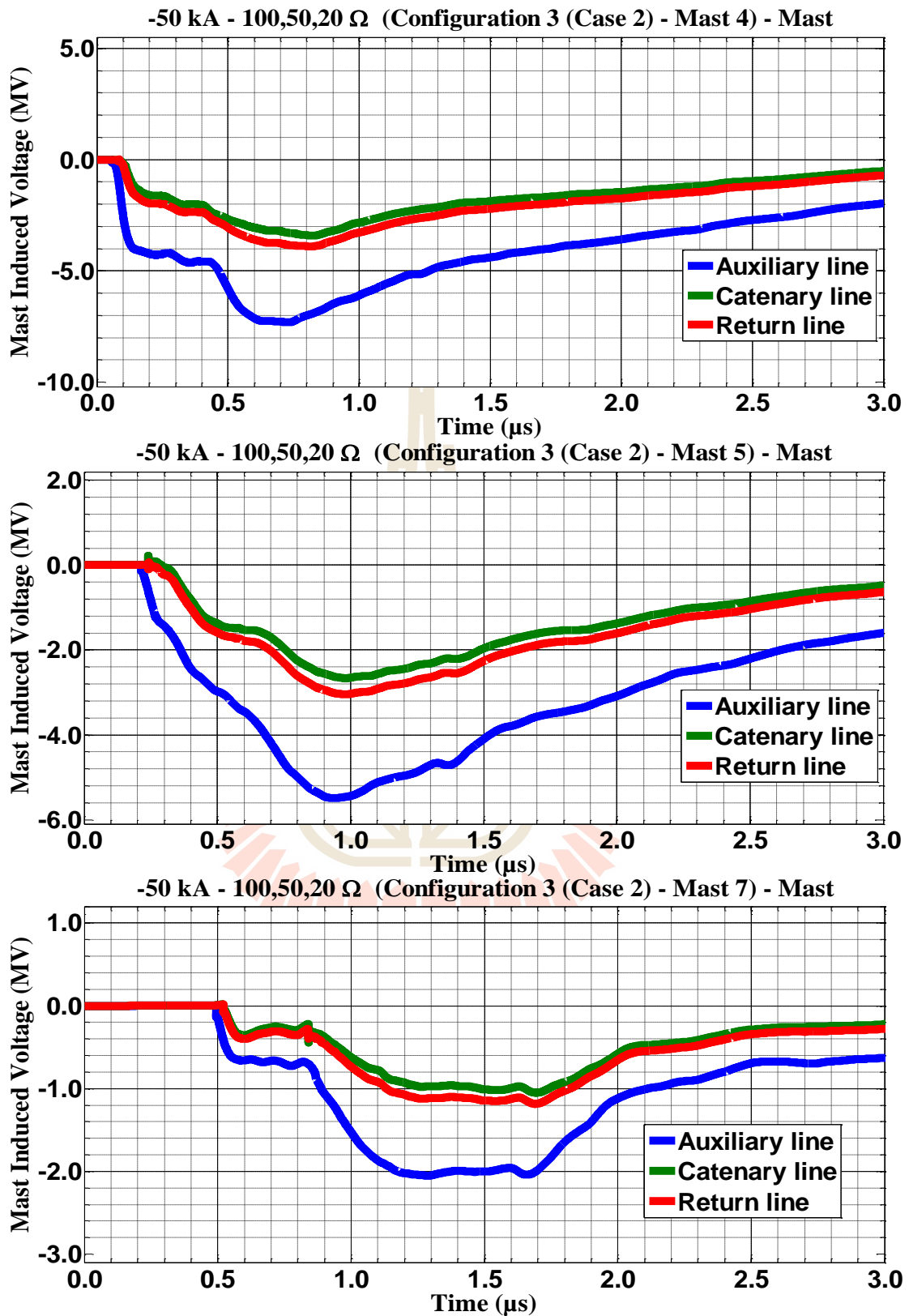


Figure C.63 Mast 4, 5, and 7 with 100,50,20 Ω induced voltage waveform of -50 kA first stroke-(1.0/100 μs), subsequent stroke-(0.2/50 μs) strikes on Mast 4 for Case 1



**Figure C.64** Mast 4, 5, and 7 with 100,50,20 Ω induced voltage waveform of -50 kA first stroke-(1.0/100 μs), subsequent stroke-(0.2/50 μs) strikes on Mast 4 for Case 2

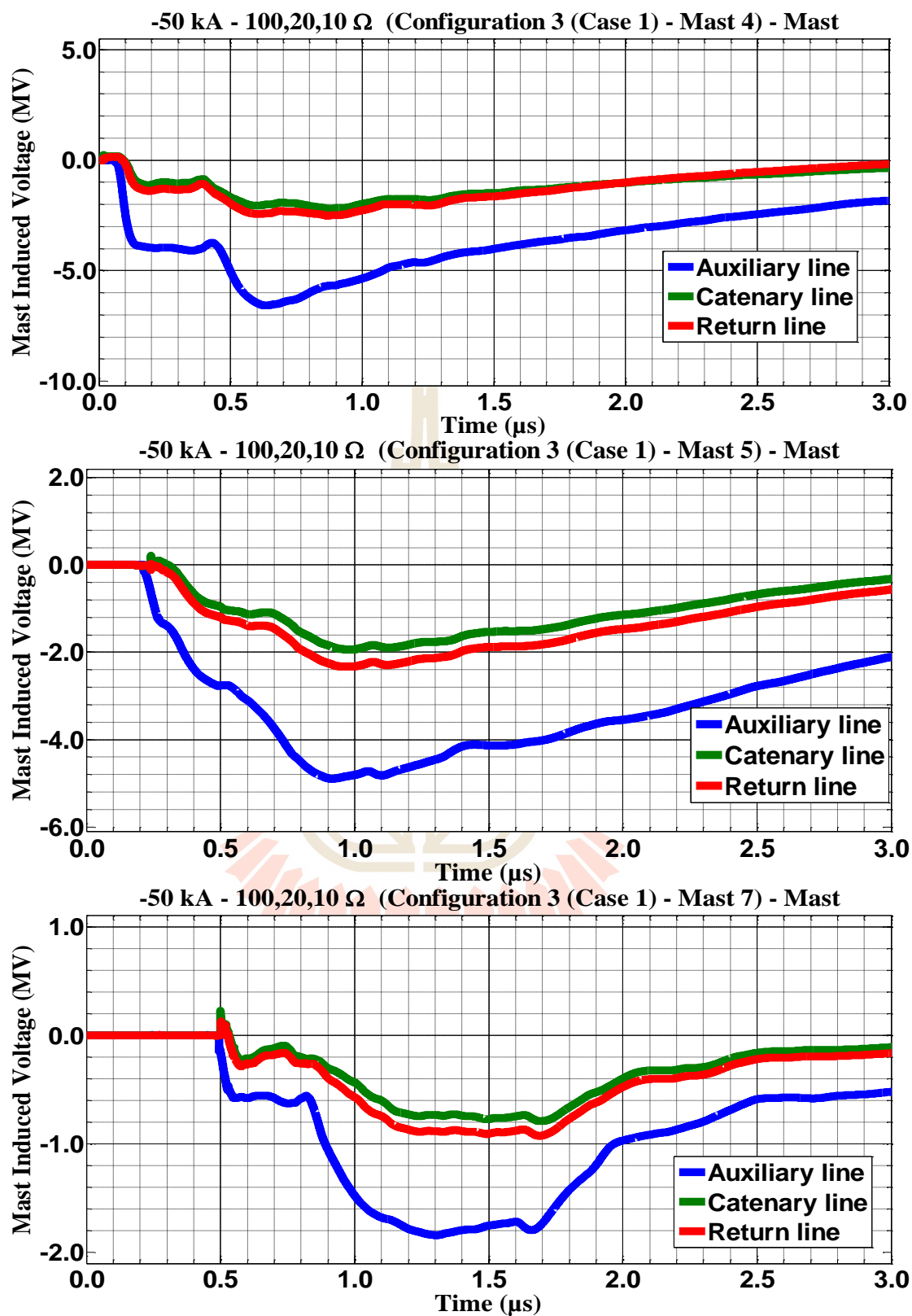


Figure C.65 Mast 4, 5, and 7 with 100,20,10 Ω induced voltage waveform of -50 kA first stroke-(1.0/100 μs), subsequent stroke-(0.2/50 μs) strikes on Mast 4 for Case 1

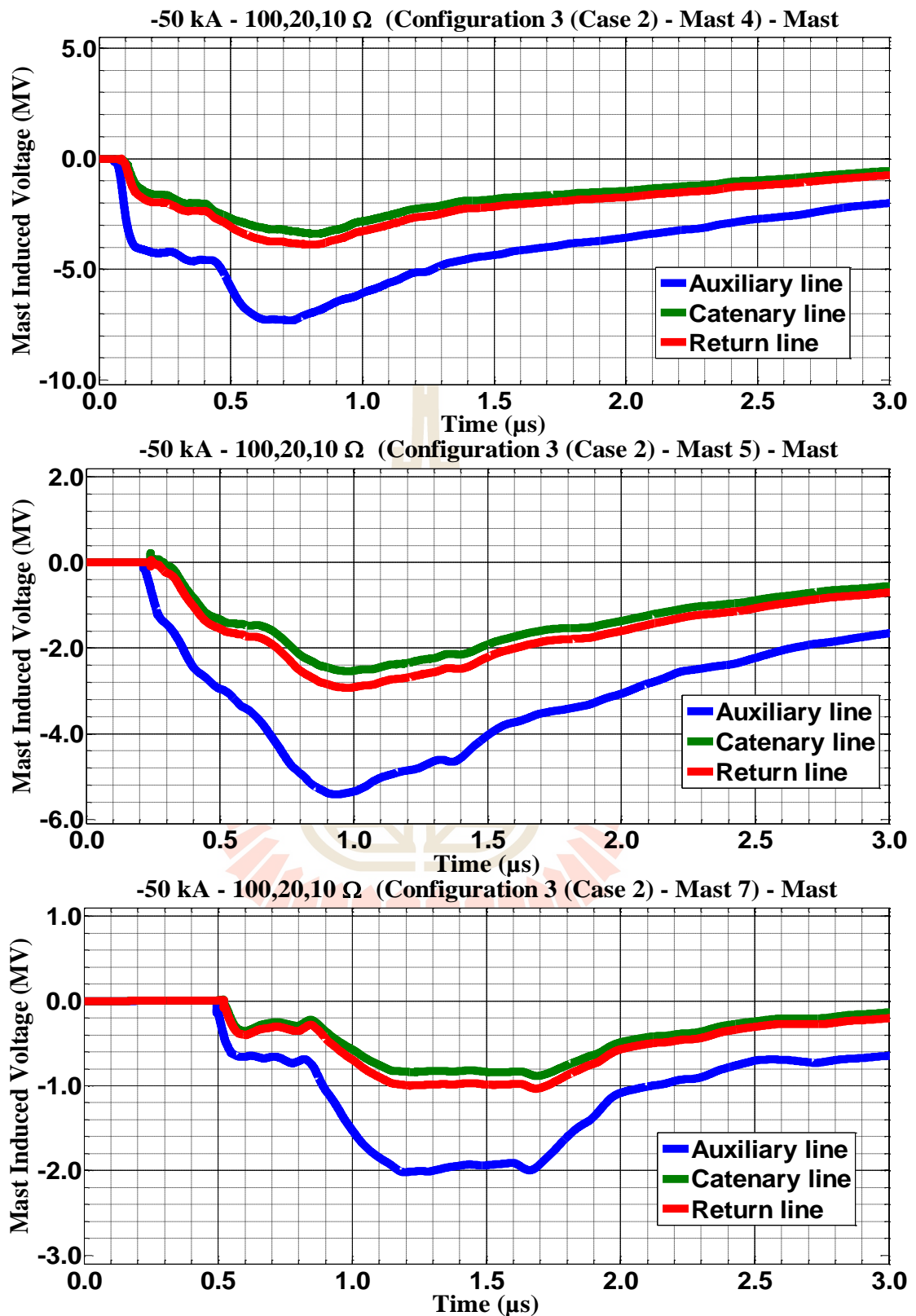
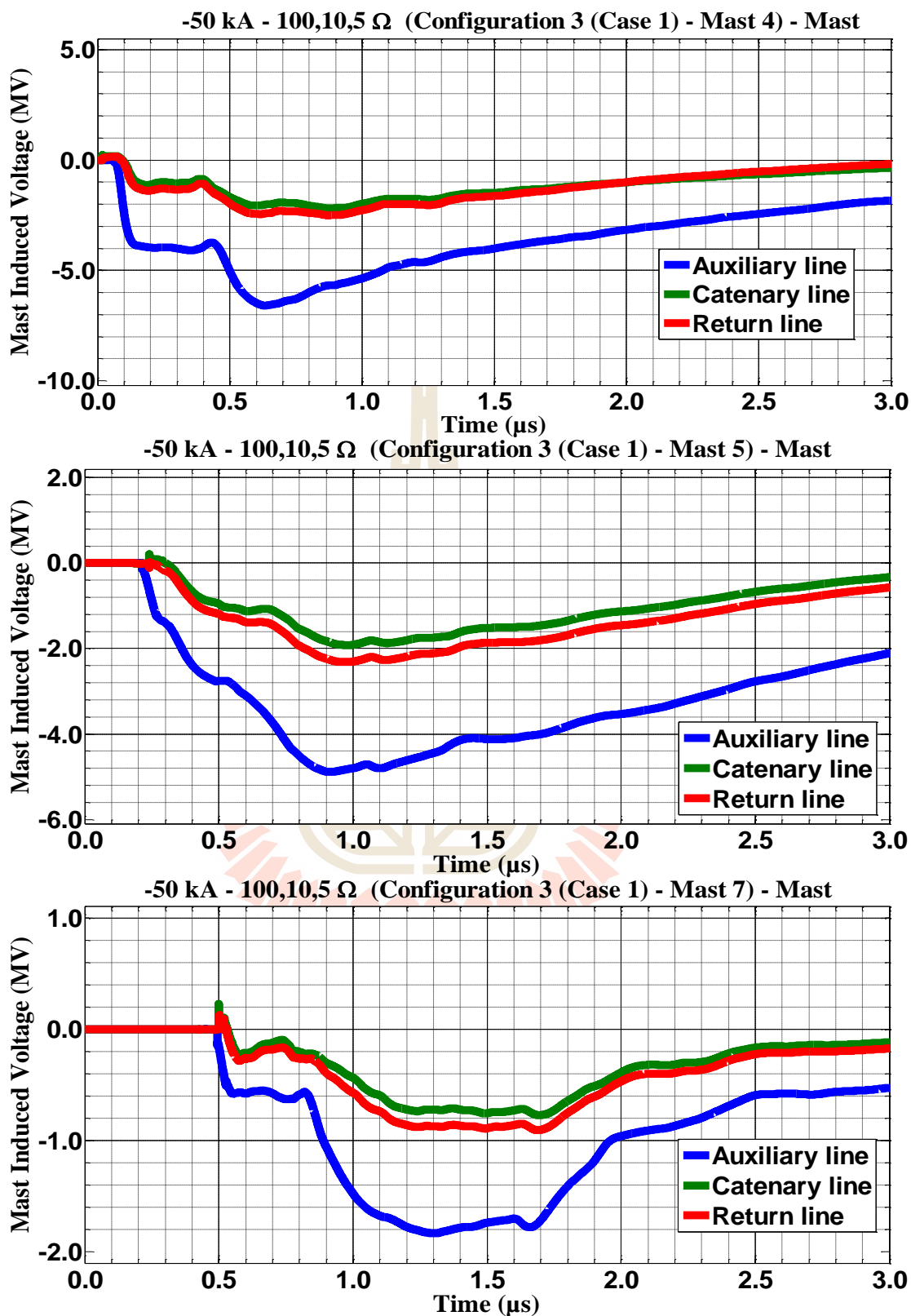


Figure C.66 Mast 4, 5, and 7 with 100,20,10  $\Omega$  induced voltage waveform of -50 kA first stroke-(1.0/100  $\mu$ s), subsequent stroke-(0.2/50  $\mu$ s) strikes on Mast 4 for Case 2



**Figure C.67** Mast 4, 5, and 7 with 100,10,5 Ω induced voltage waveform of -50 kA first stroke-(1.0/100 μs), subsequent stroke-(0.2/50 μs) strikes on Mast 4 for Case 1



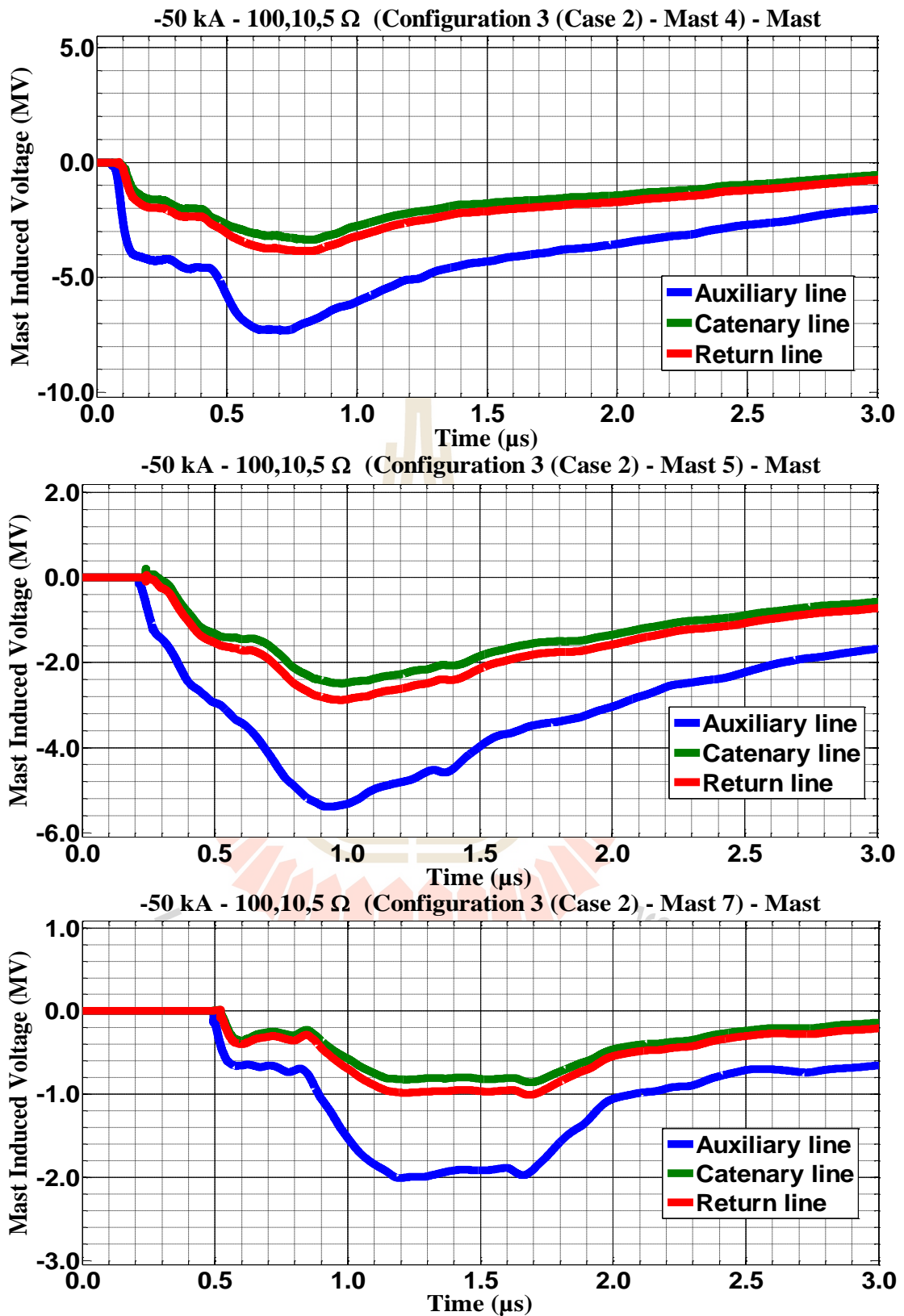
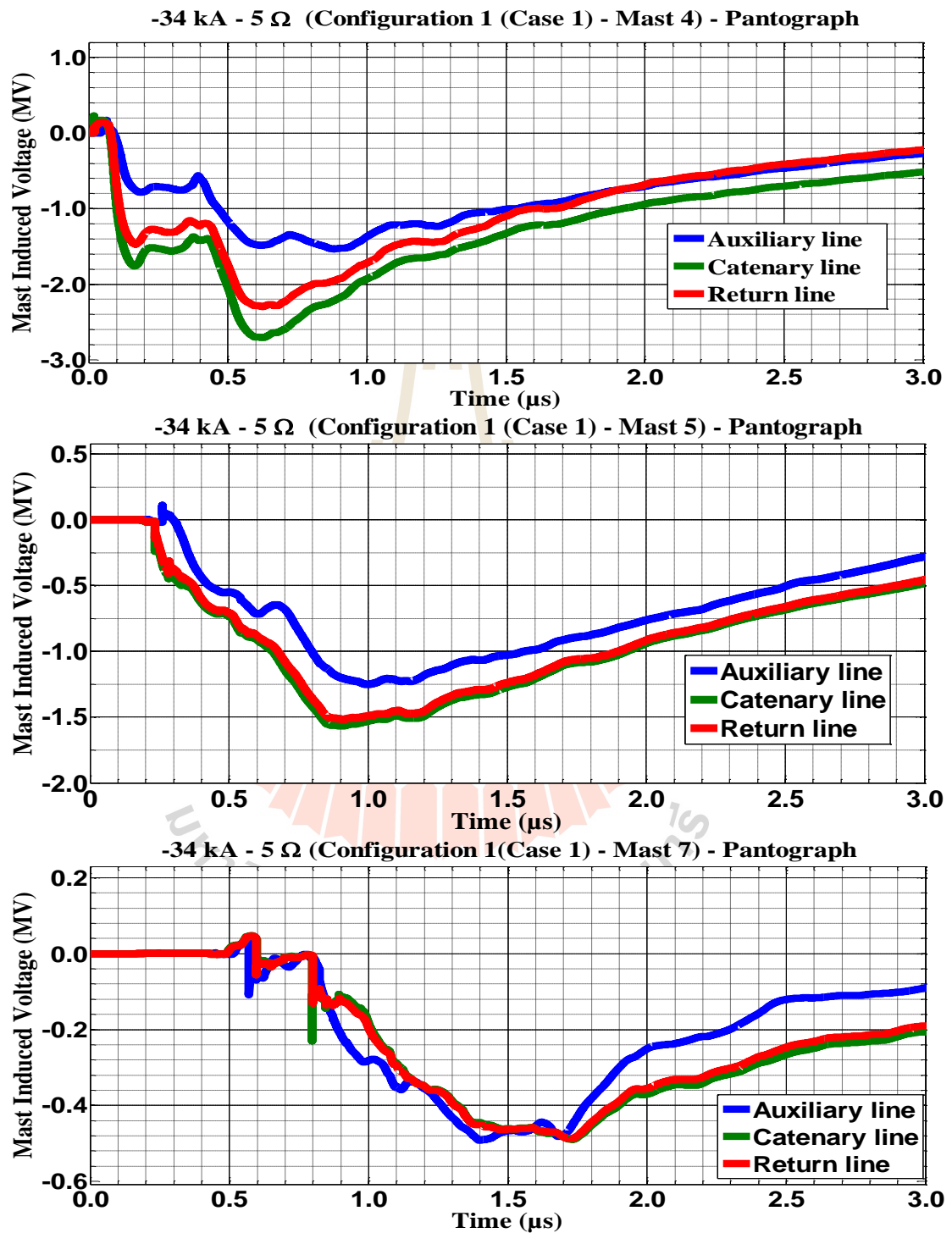
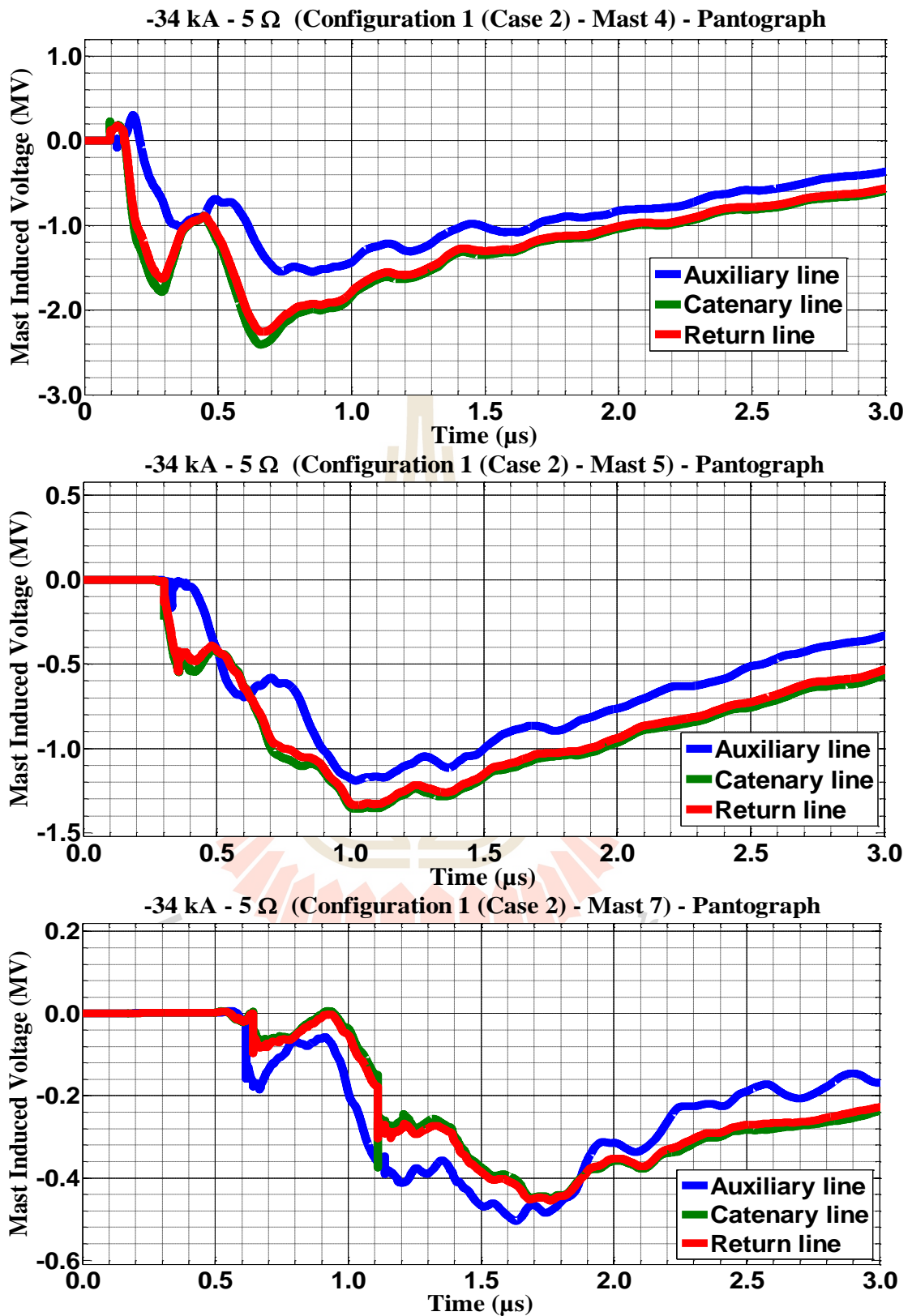


Figure C.68 Mast 4, 5, and 7 with 100,10,5 Ω induced voltage waveform of -50 kA first stroke-(1.0/100 μs), subsequent stroke-(0.2/50 μs) strikes on Mast 4 for Case 2

**C.5 The consequences when the pantograph struck by negative multiple lightning strokes for Configuration 1 in Case 1 and 2.**



**Figure C.69** Mast 4, 5, and 7 with 5 Ω induced voltage waveform of the -34 kA first stroke-(1.0/100 μs), subsequent stroke-(0.2/50 μs) strikes on pantograph for Case 1



**Figure C.70** Mast 4, 5, and 7 with 5  $\Omega$  induced voltage waveform of the -34 kA first stroke-(1.0/100  $\mu\text{s}$ ), subsequent stroke-(0.2/50  $\mu\text{s}$ ) strikes on pantograph for Case 2

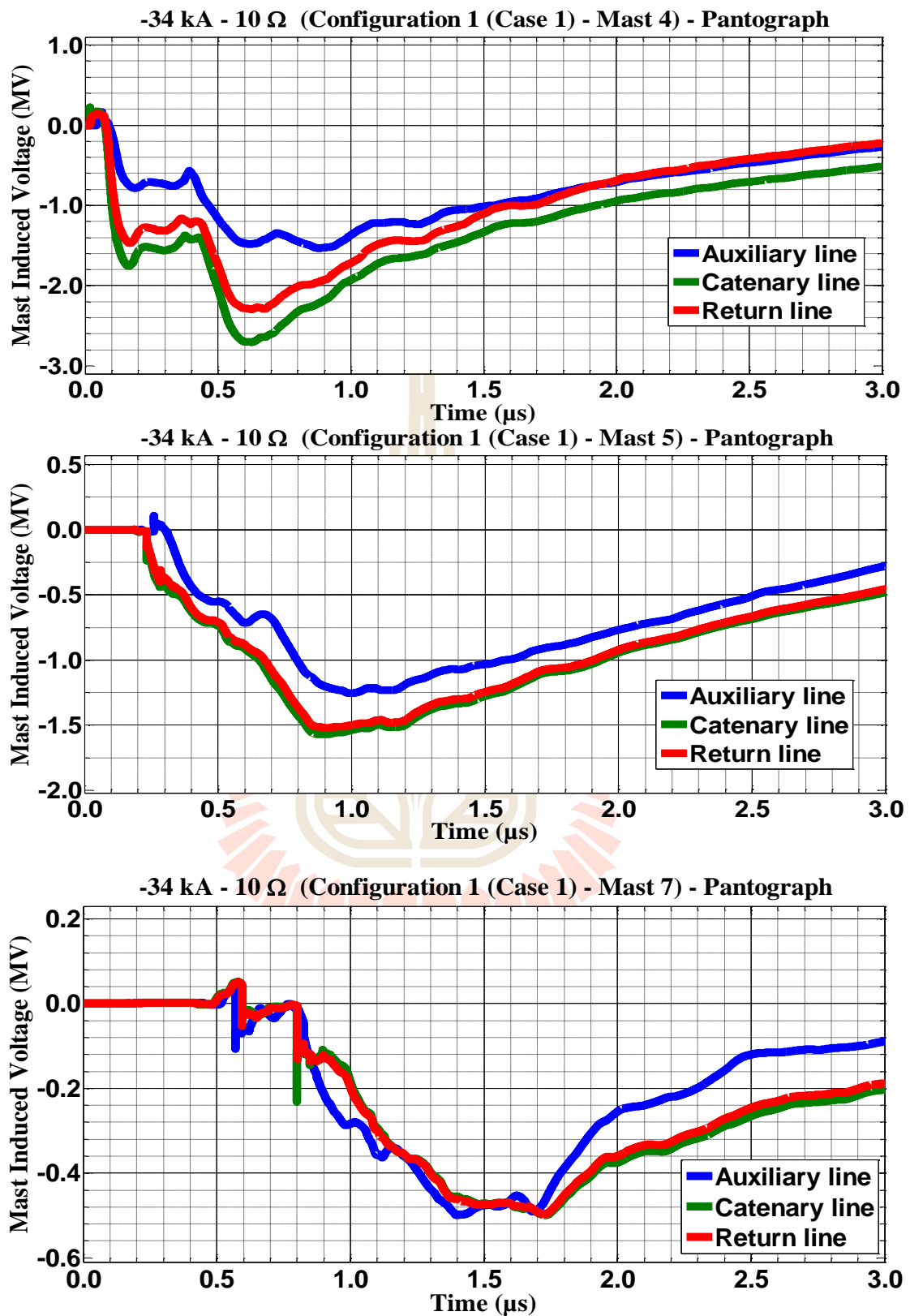


**Figure C.71** Mast 4, 5, and 7 with 10  $\Omega$  induced voltage waveform of the -34 kA first stroke-(1.0/100  $\mu\text{s}$ ), subsequent stroke-(0.2/50  $\mu\text{s}$ ) strikes on pantograph for Case 1

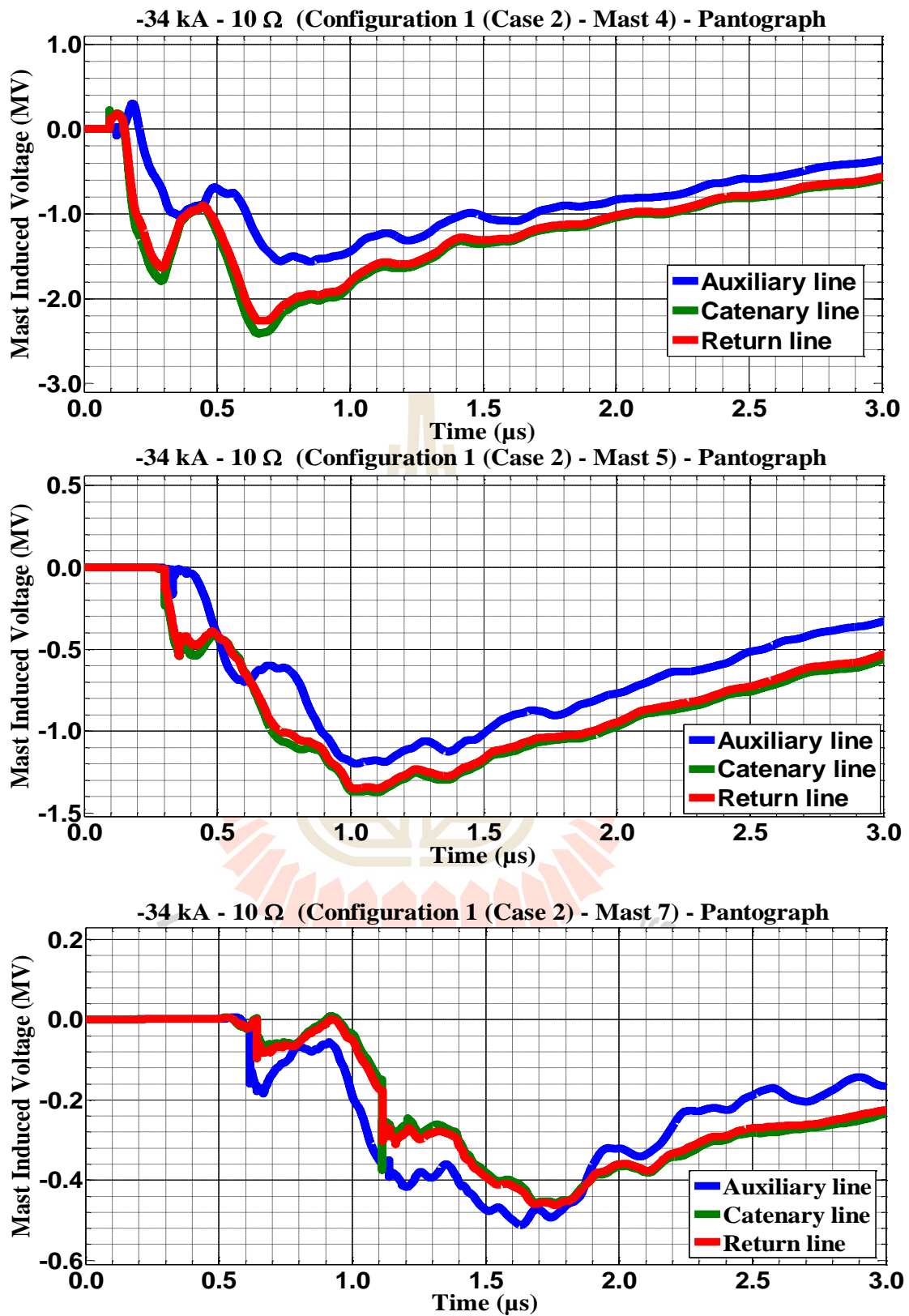
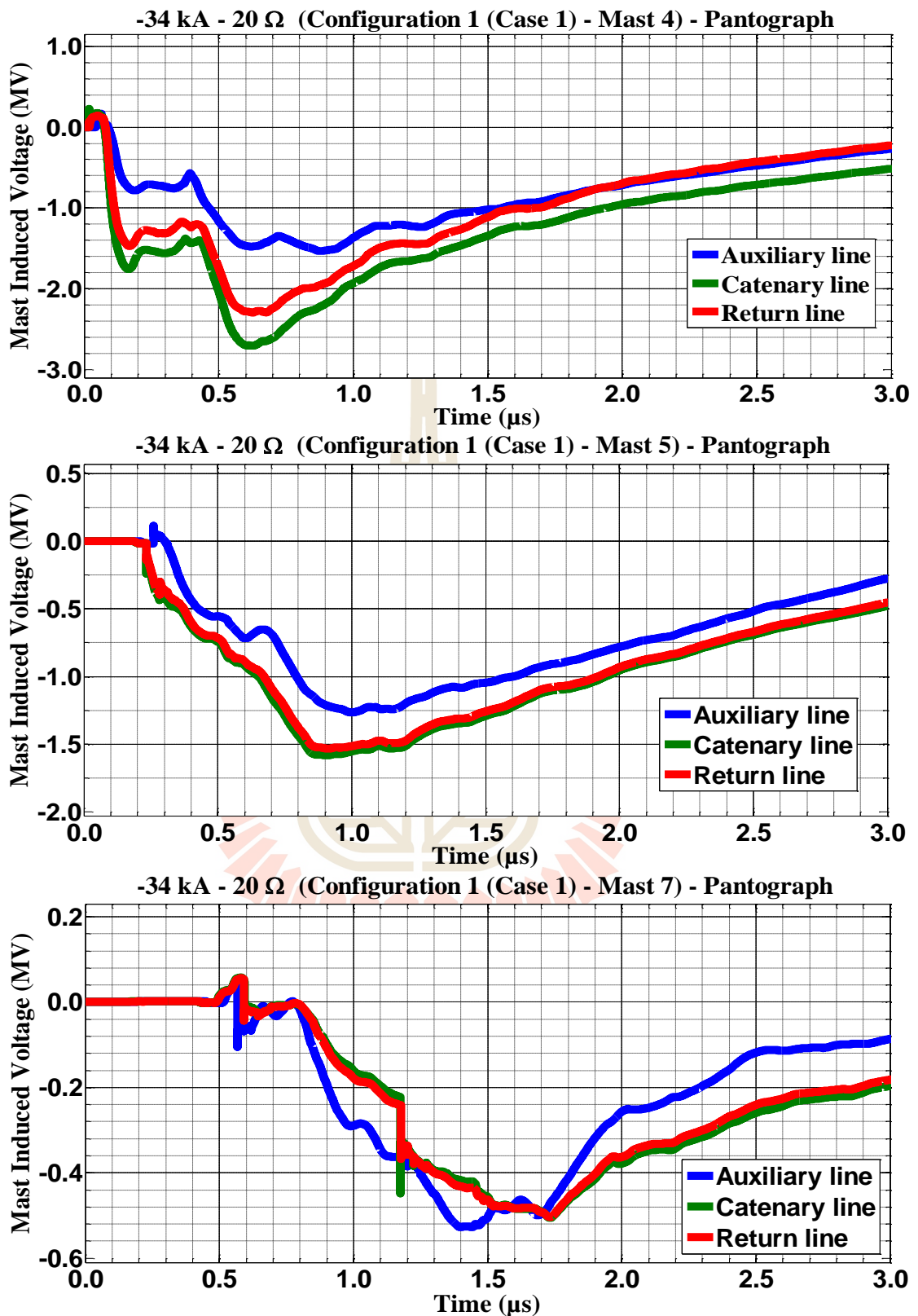


Figure C.72 Mast 4, 5, and 7 with 10  $\Omega$  induced voltage waveform of the -34 kA first stroke-(1.0/100  $\mu\text{s}$ ), subsequent stroke-(0.2/50  $\mu\text{s}$ ) strikes on pantograph for Case 2



**Figure C.73** Mast 4, 5, and 7 with 20 Ω induced voltage waveform of the -34 kA first stroke-(1.0/100 μs), subsequent stroke-(0.2/50 μs) strikes on pantograph for Case 1

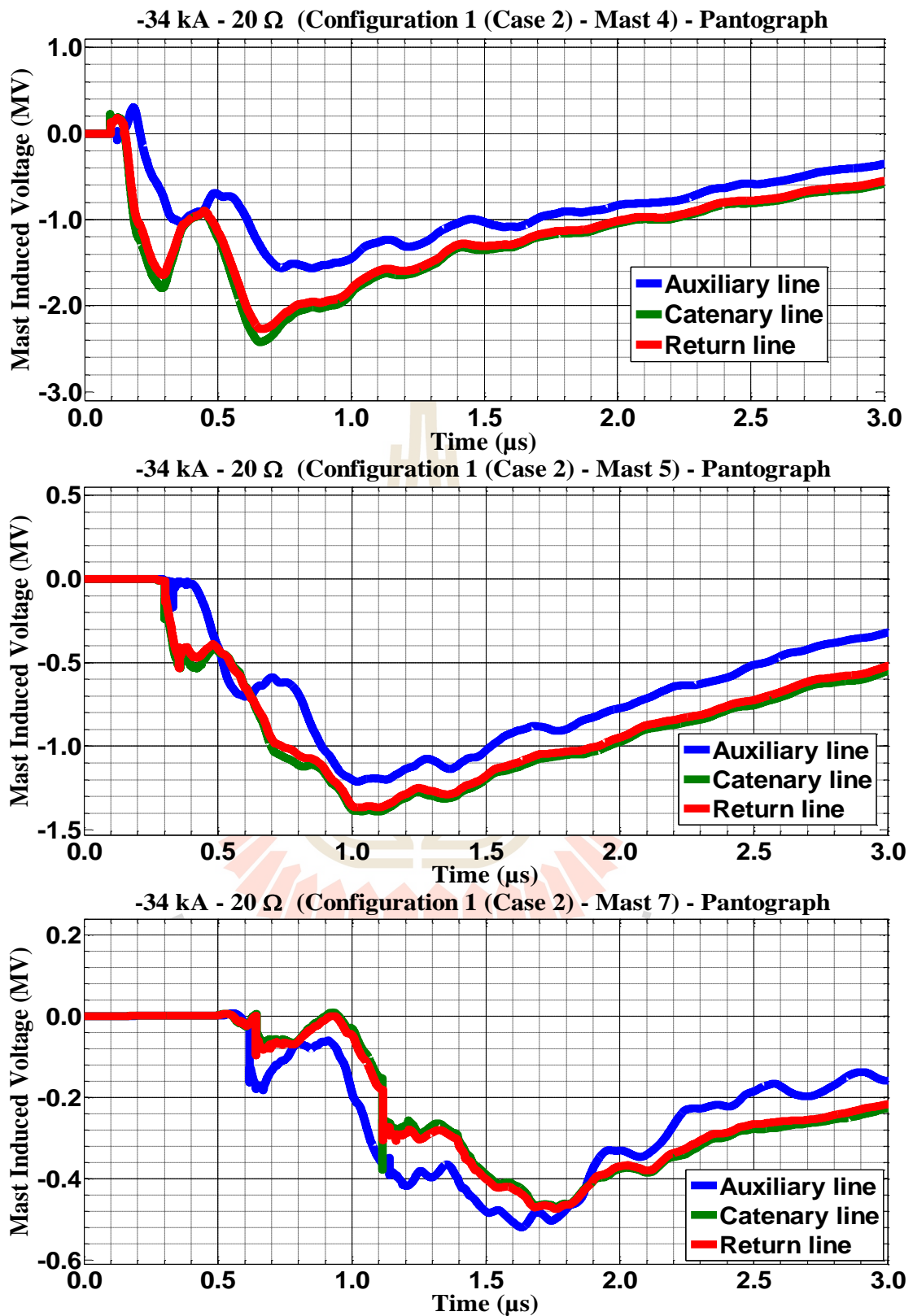


Figure C.74 Mast 4, 5, and 7 with 20  $\Omega$  induced voltage waveform of the -34 kA first stroke-(1.0/100  $\mu\text{s}$ ), subsequent stroke-(0.2/50  $\mu\text{s}$ ) strikes on pantograph for Case 2

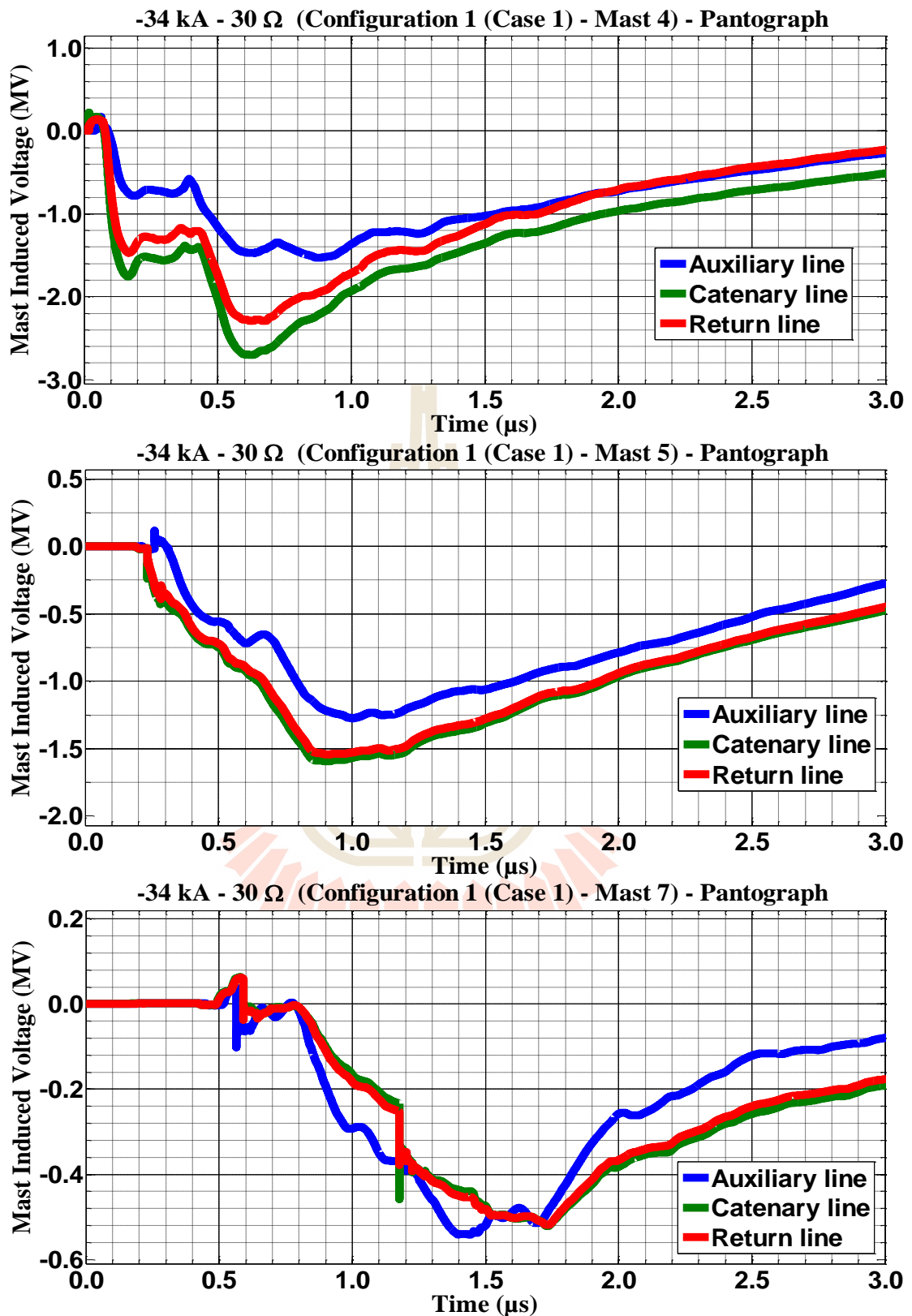
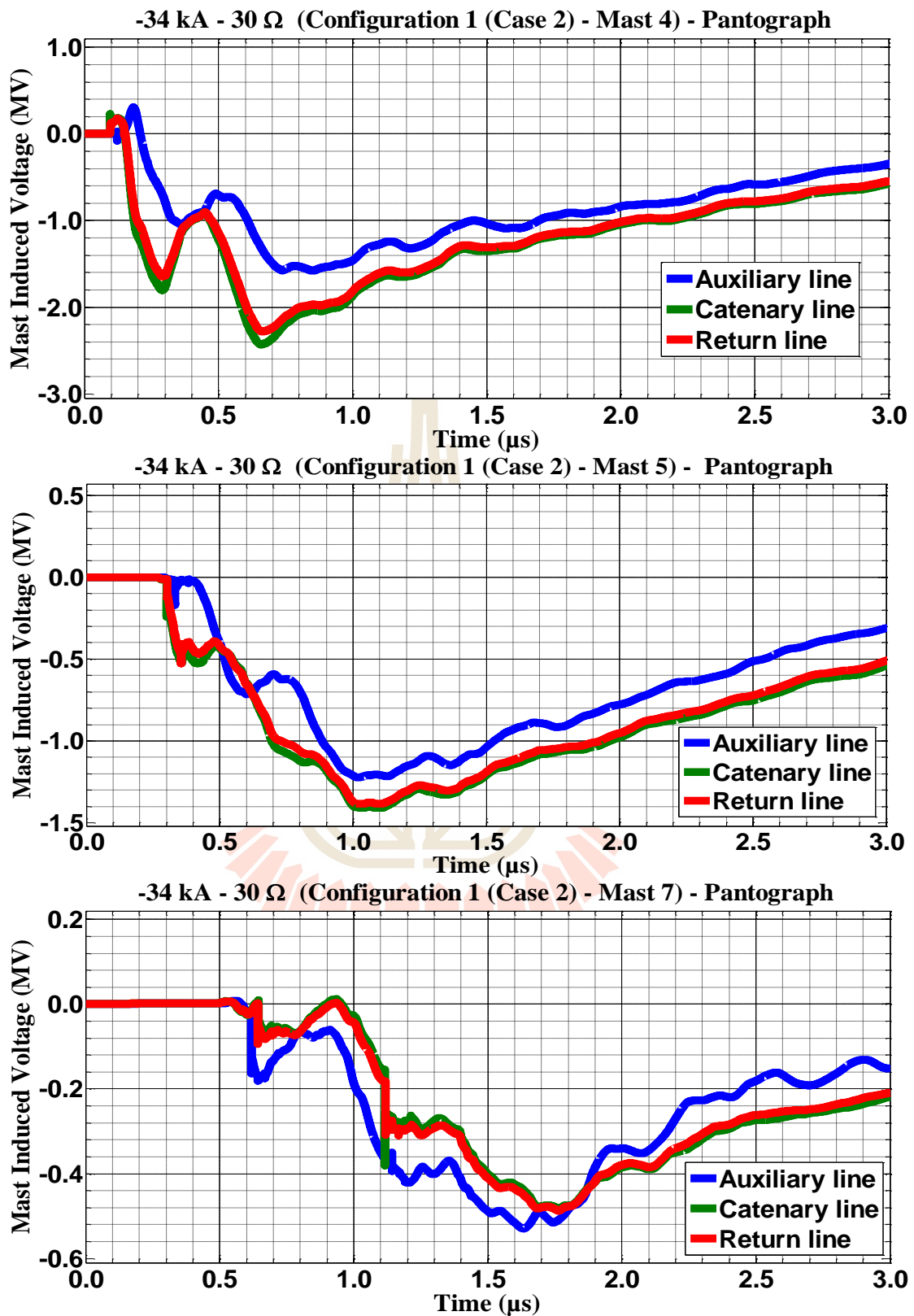
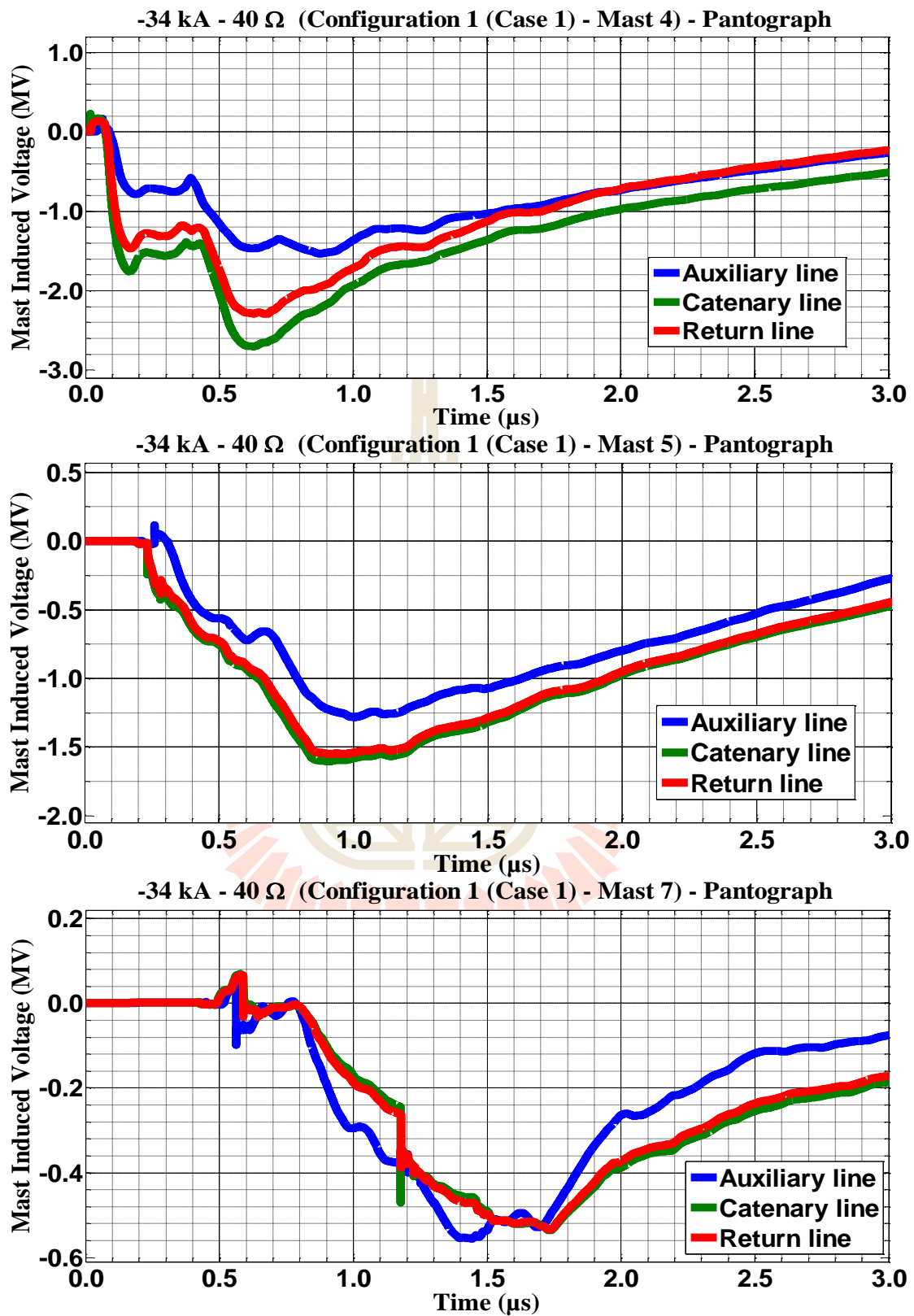


Figure C.75 Mast 4, 5, and 7 with 30 Ω induced voltage waveform of the -34 kA first stroke-(1.0/100 μs), subsequent stroke-(0.2/50 μs) strikes on pantograph for Case 2





**Figure C.76** Mast 4, 5, and 7 with 30  $\Omega$  induced voltage waveform of the -34 kA first stroke-(1.0/100  $\mu\text{s}$ ), subsequent stroke-(0.2/50  $\mu\text{s}$ ) strikes on pantograph for Case 2



**Figure C.77** Mast 4, 5, and 7 with 40  $\Omega$  induced voltage waveform of the -34 kA first stroke-(1.0/100  $\mu\text{s}$ ), subsequent stroke-(0.2/50  $\mu\text{s}$ ) strikes on pantograph for Case 1

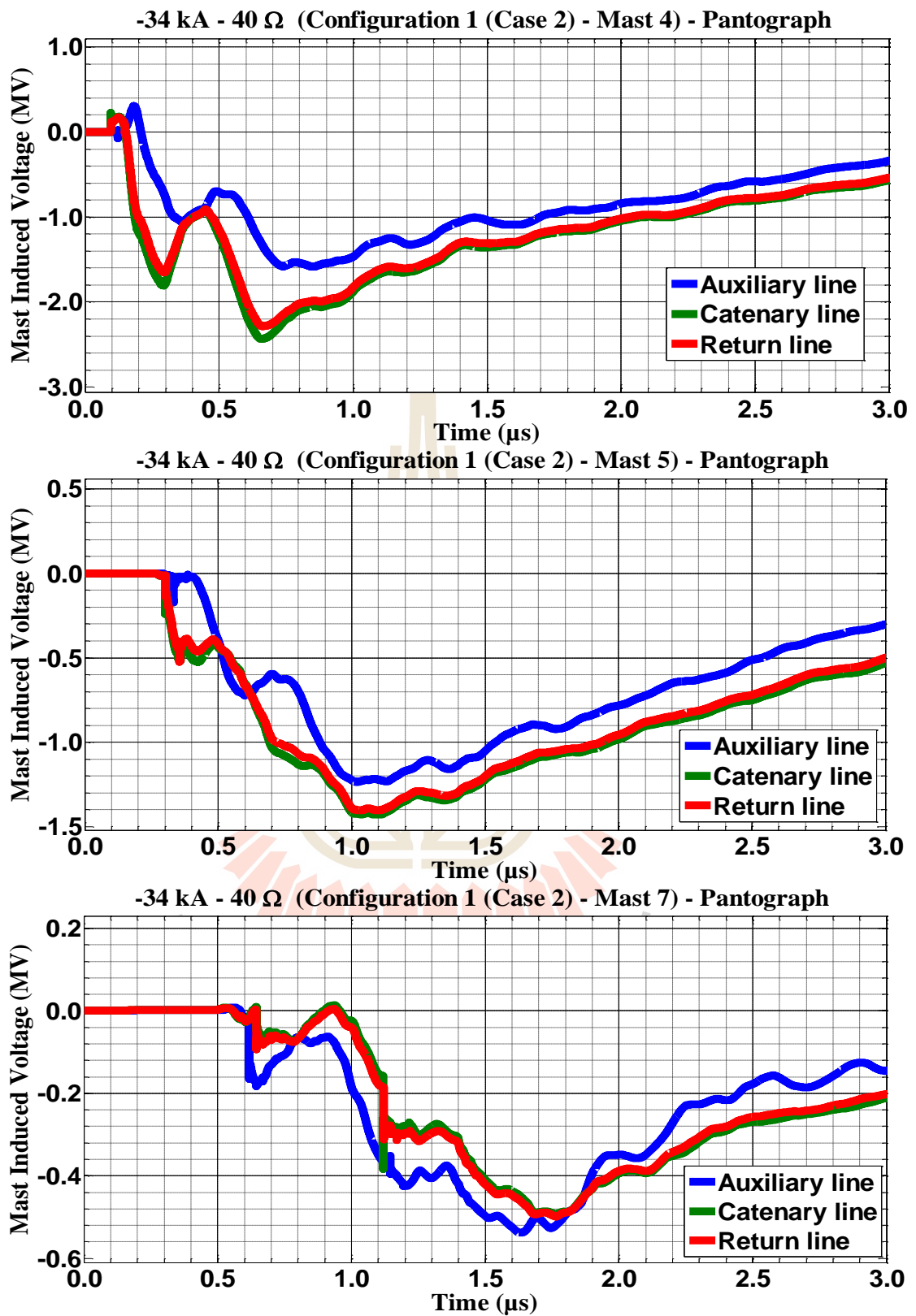


**Figure C.78** Mast 4, 5, and 7 with 40  $\Omega$  induced voltage waveform of the -34 kA first stroke-(1.0/100  $\mu$ s), subsequent stroke-(0.2/50  $\mu$ s) strikes on pantograph for Case 2

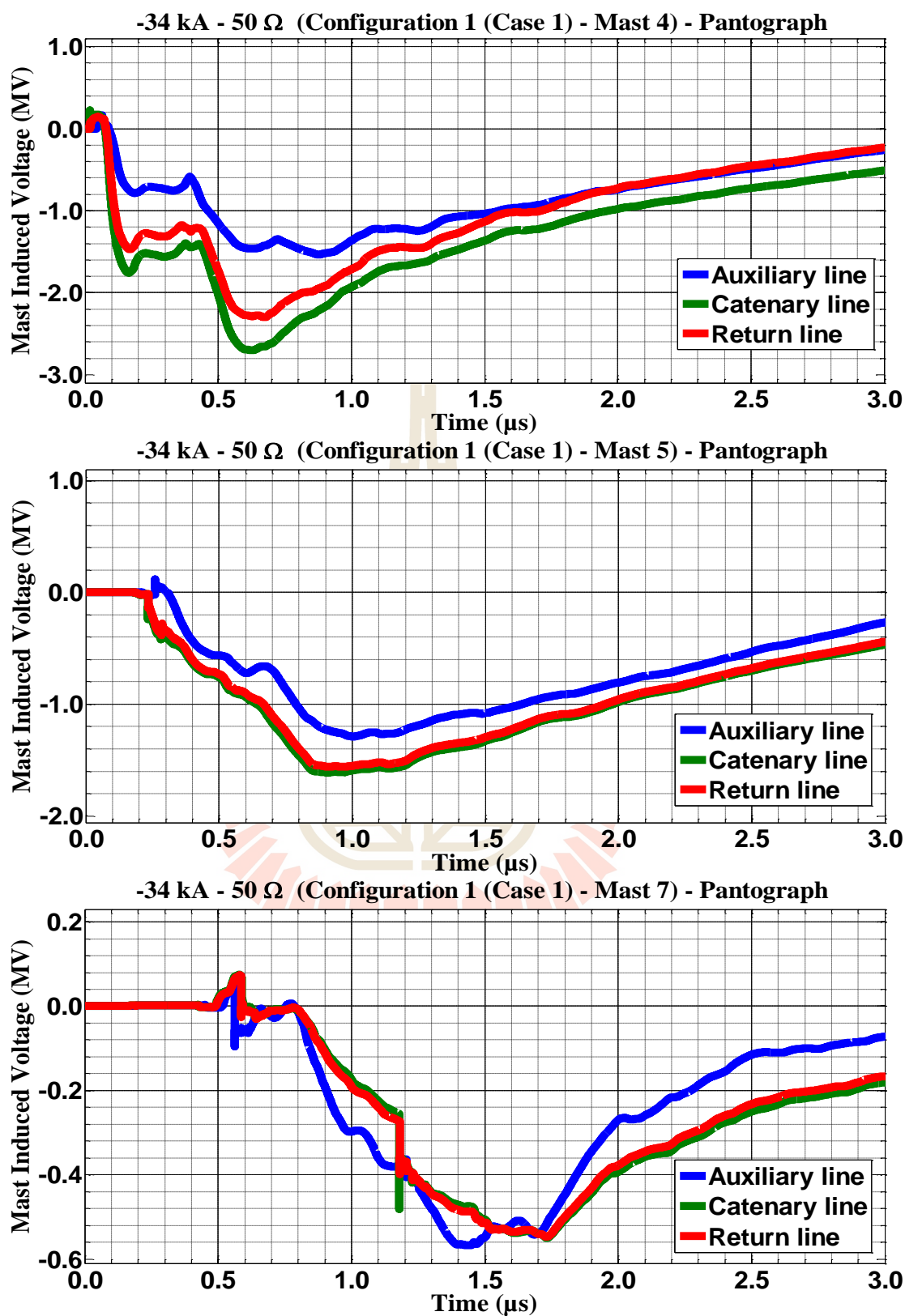


**Figure C.79** Mast 4, 5, and 7 with 50  $\Omega$  induced voltage waveform of the -34 kA first stroke-(1.0/100  $\mu$ s), subsequent stroke-(0.2/50  $\mu$ s) strikes on pantograph for Case 1

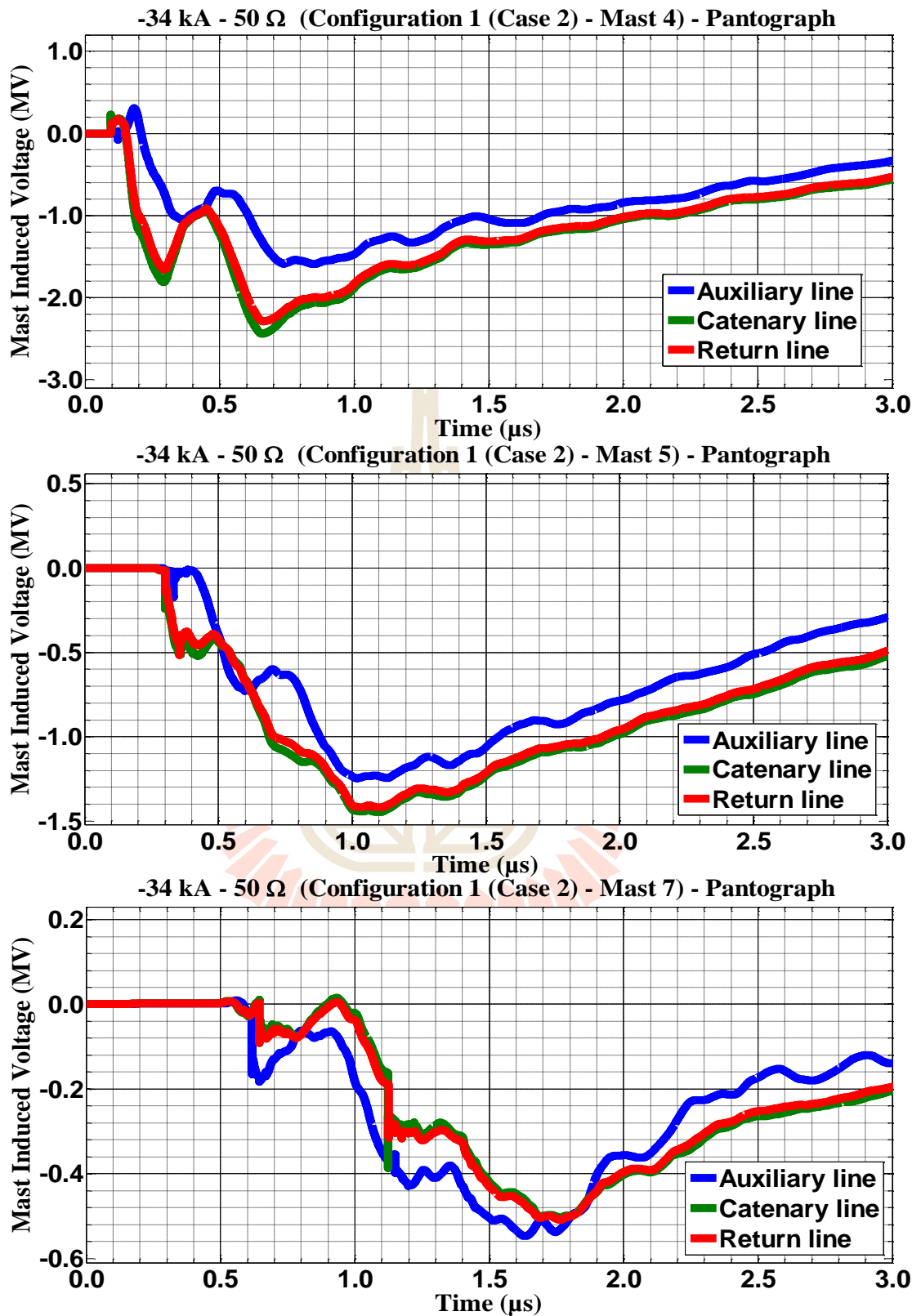


**Figure C.80** Mast 4, 5, and 7 with 50  $\Omega$  induced voltage waveform of the -34 kA first stroke-(1.0/100  $\mu$ s), subsequent stroke-(0.2/50  $\mu$ s) strikes on pantograph for Case 2

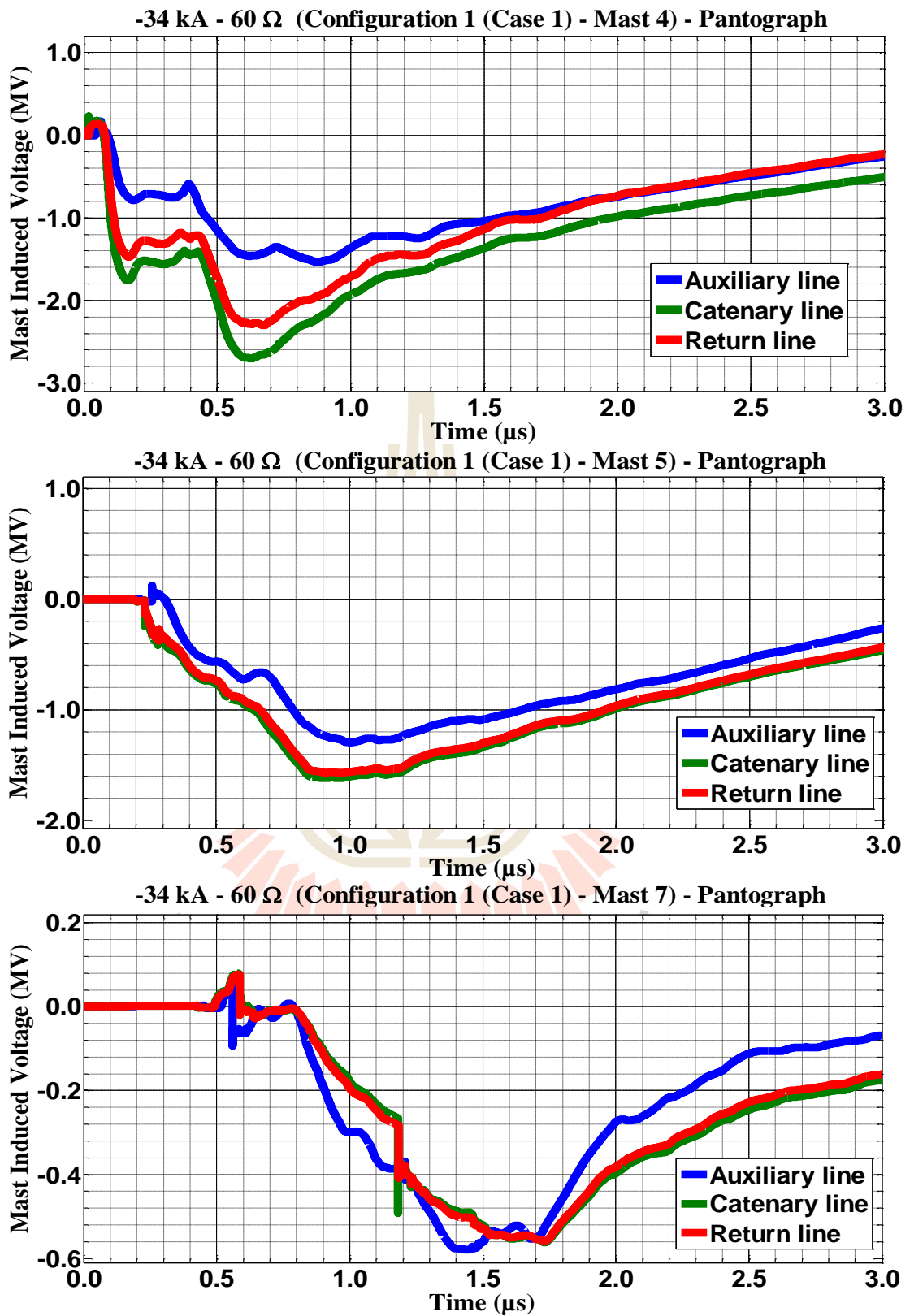


**Figure C.81** Mast 4, 5, and 7 with 60  $\Omega$  induced voltage waveform of the -34 kA first stroke-(1.0/100  $\mu$ s), subsequent stroke-(0.2/50  $\mu$ s) strikes on pantograph for Case 1

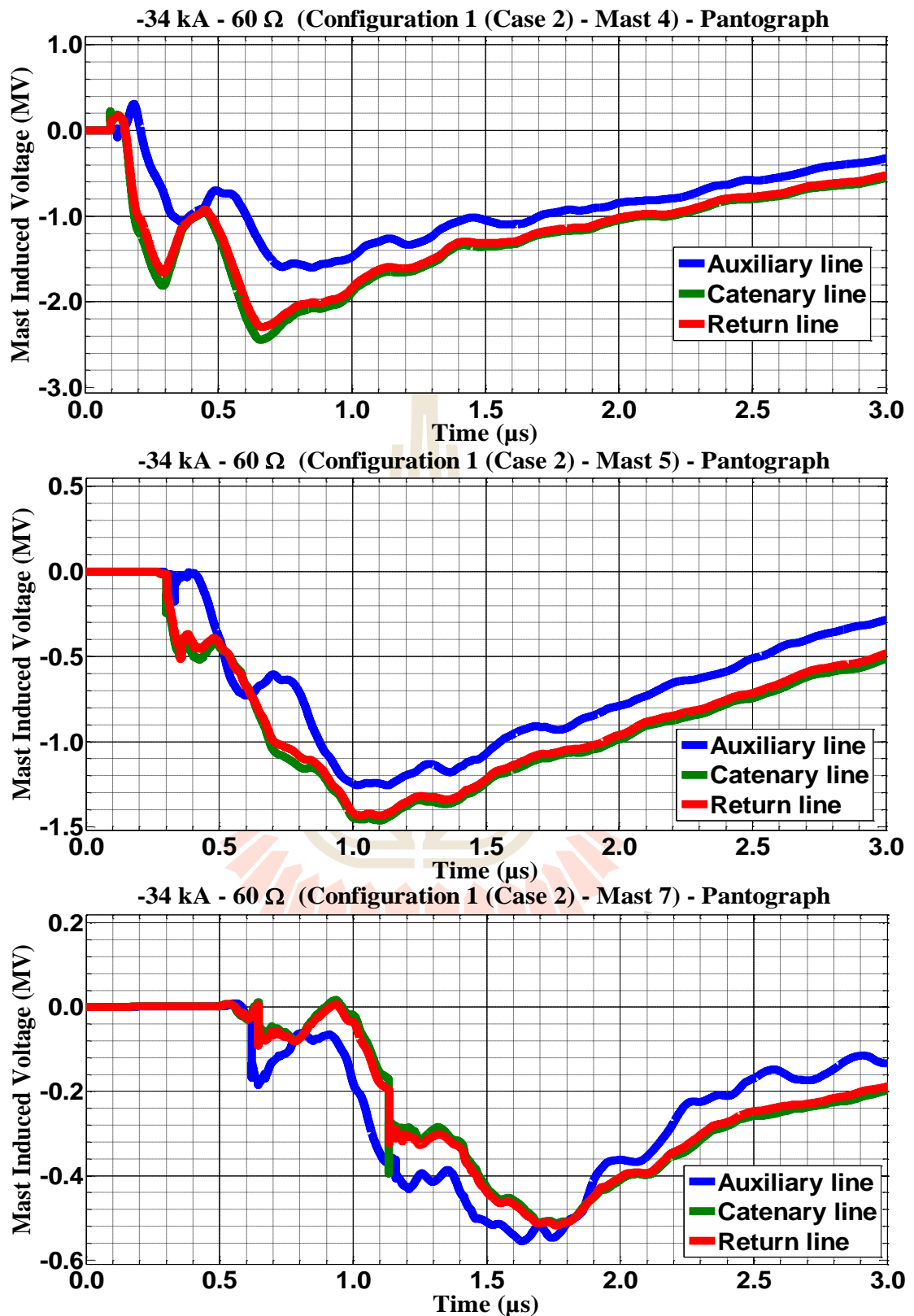


**Figure C.82** Mast 4, 5, and 7 with 60  $\Omega$  induced voltage waveform of the -34 kA first stroke-(1.0/100  $\mu\text{s}$ ), subsequent stroke-(0.2/50  $\mu\text{s}$ ) strikes on pantograph for Case 2

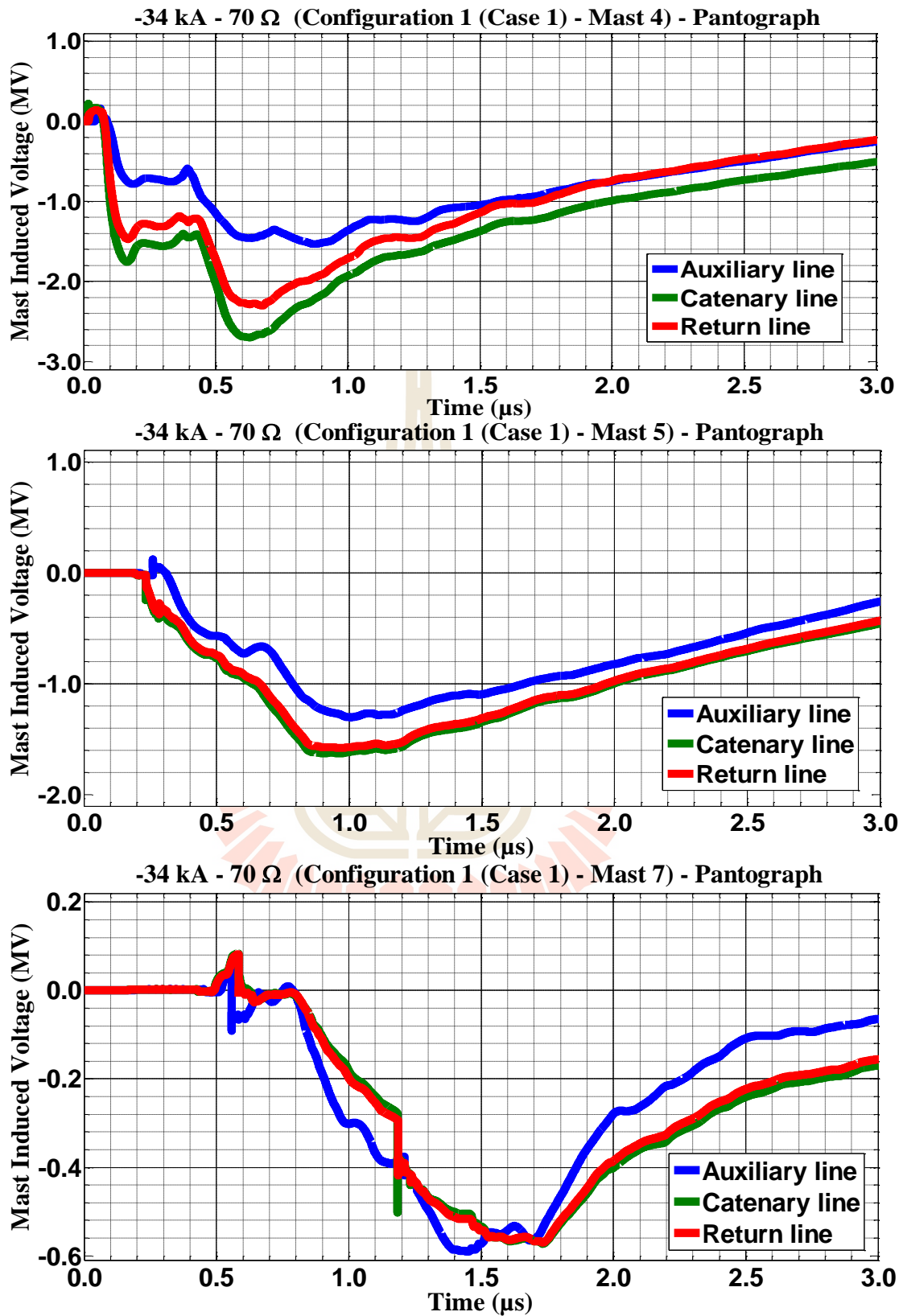


**Figure C.83** Mast 4, 5, and 7 with 70  $\Omega$  induced voltage waveform of the -34 kA first stroke-(1.0/100  $\mu$ s), subsequent stroke-(0.2/50  $\mu$ s) strikes on pantograph for Case 1



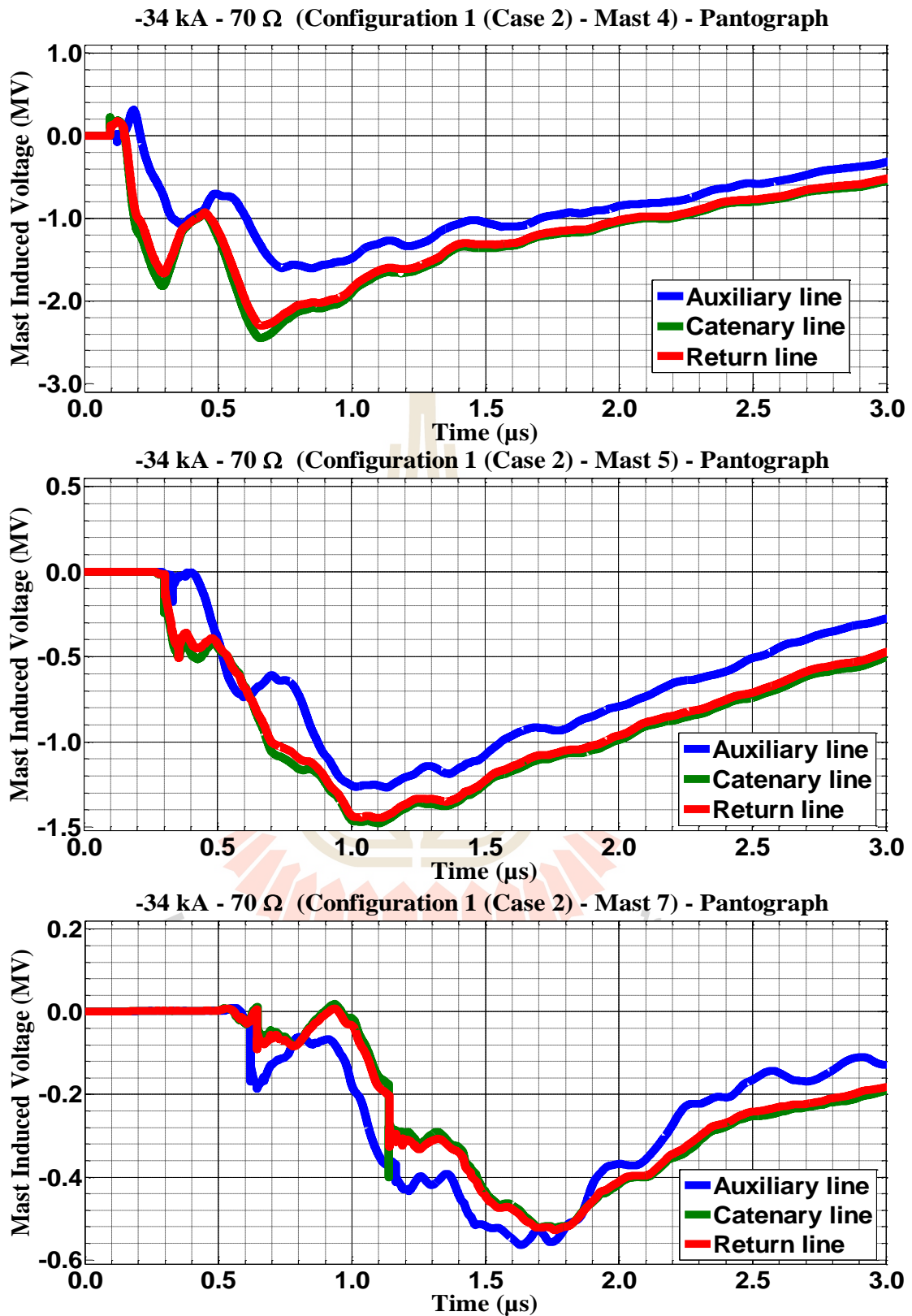


**Figure C.84** Mast 4, 5, and 7 with 70  $\Omega$  induced voltage waveform of the -34 kA first stroke-(1.0/100  $\mu$ s), subsequent stroke-(0.2/50  $\mu$ s) strikes on pantograph for Case 2

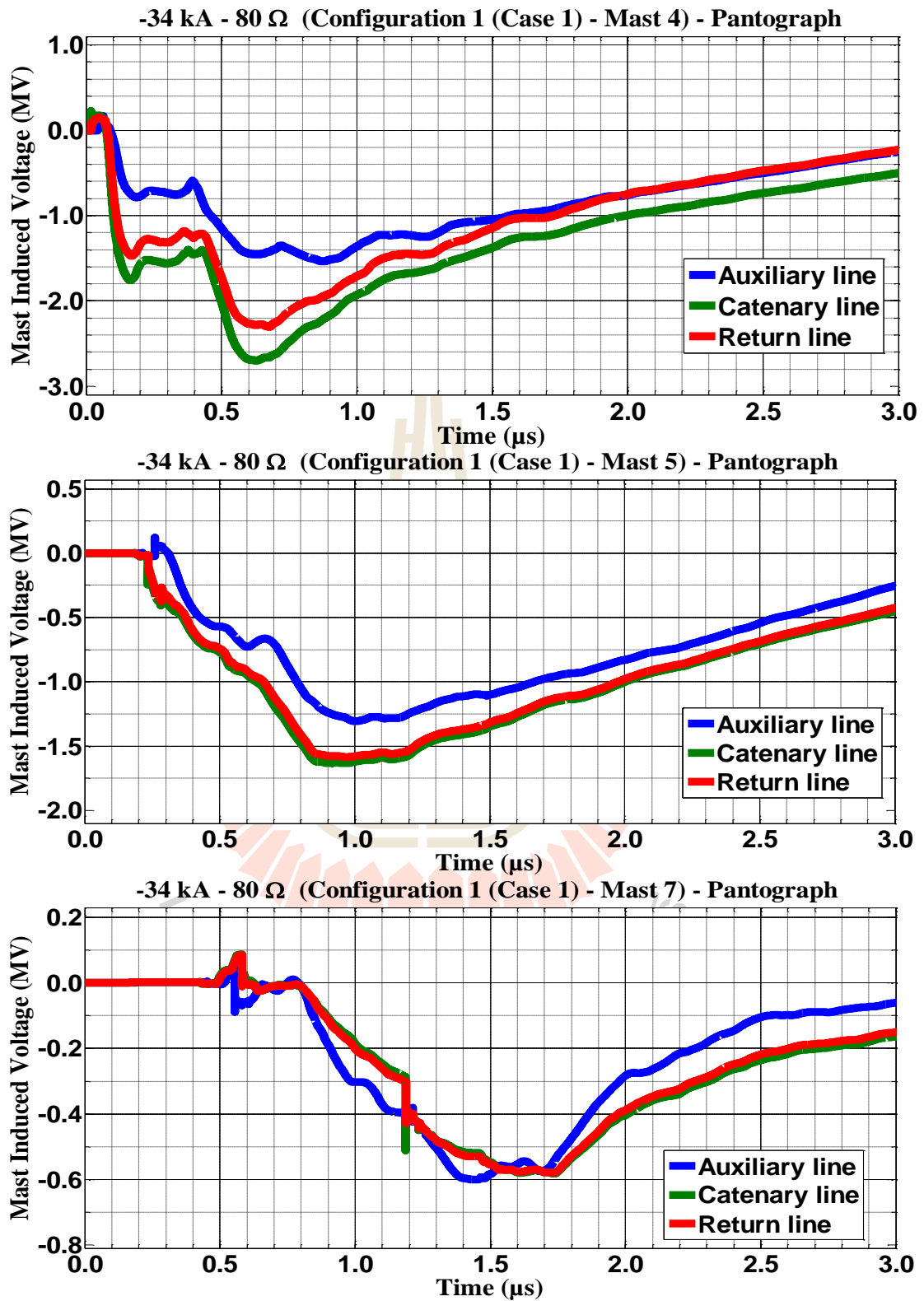
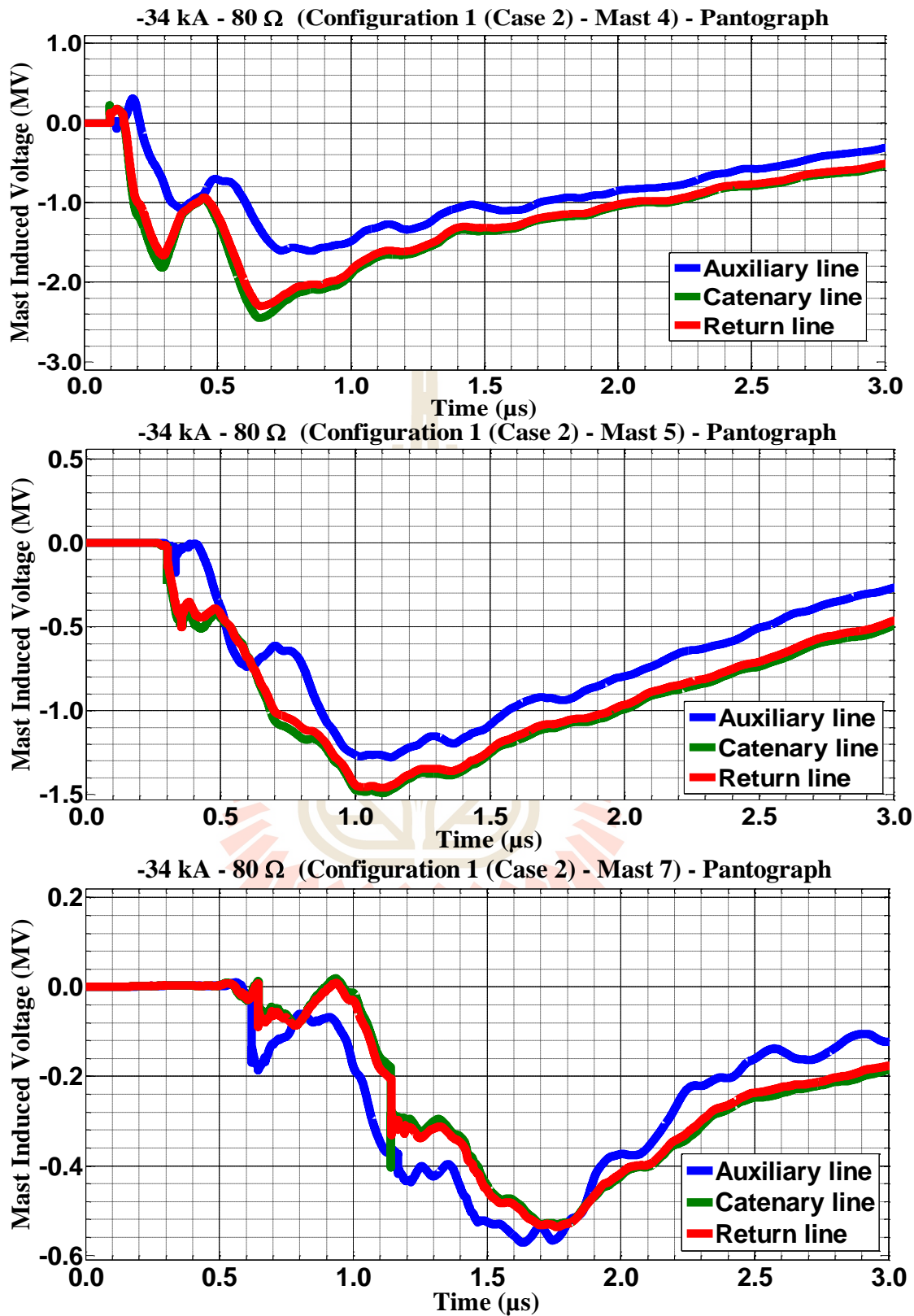
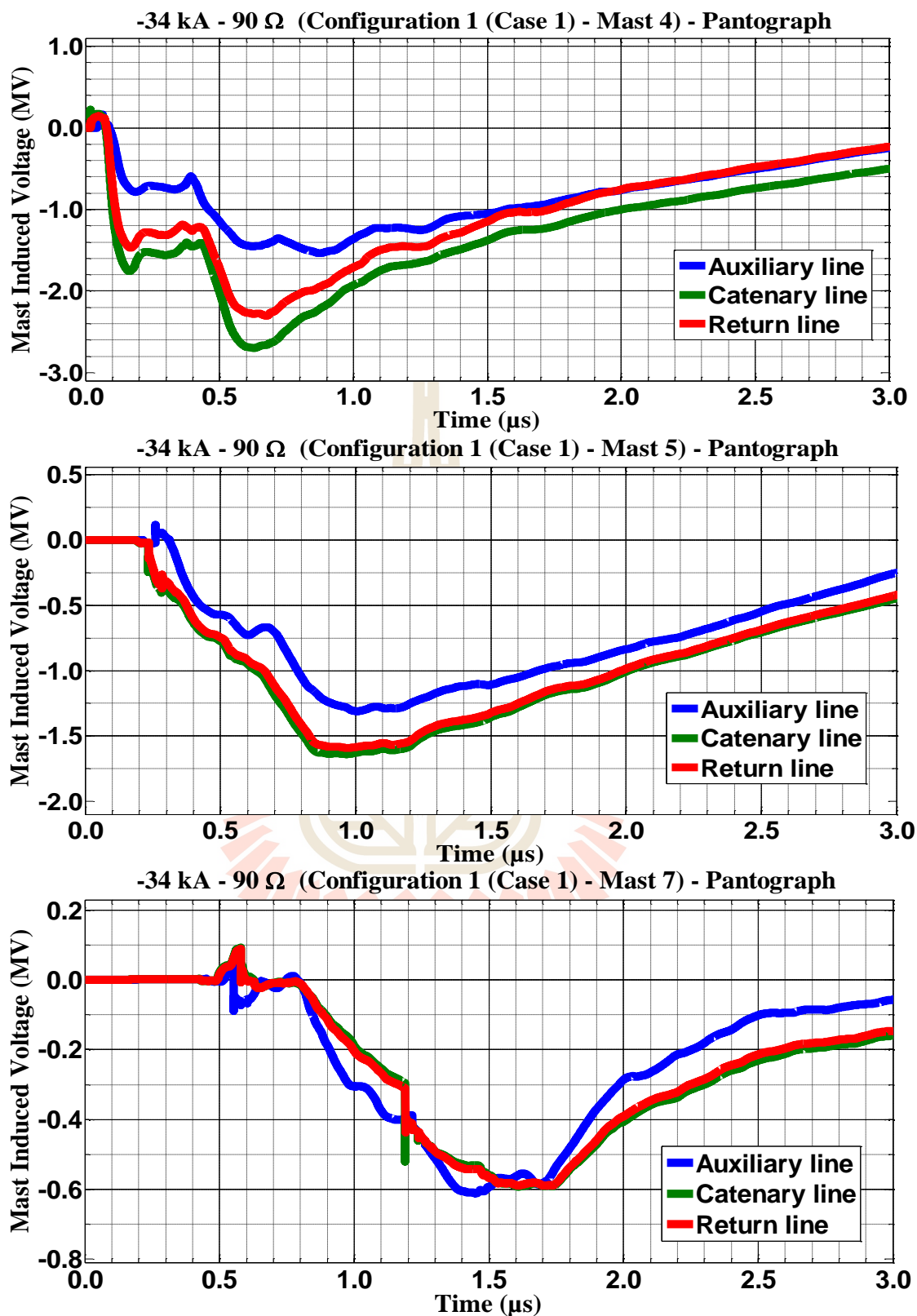


Figure C.85 Mast 4, 5, and 7 with 80  $\Omega$  induced voltage waveform of the -34 kA first stroke-(1.0/100  $\mu\text{s}$ ), subsequent stroke-(0.2/50  $\mu\text{s}$ ) strikes on pantograph for Case 1



**Figure C.86** Mast 4, 5, and 7 with 80  $\Omega$  induced voltage waveform of the -34 kA first stroke-(1.0/100  $\mu$ s), subsequent stroke-(0.2/50  $\mu$ s) strikes on pantograph for Case 2



**Figure C.87** Mast 4, 5, and 7 with 90  $\Omega$  induced voltage waveform of the -34 kA first stroke-(1.0/100  $\mu$ s), subsequent stroke-(0.2/50  $\mu$ s) strikes on pantograph for Case 1

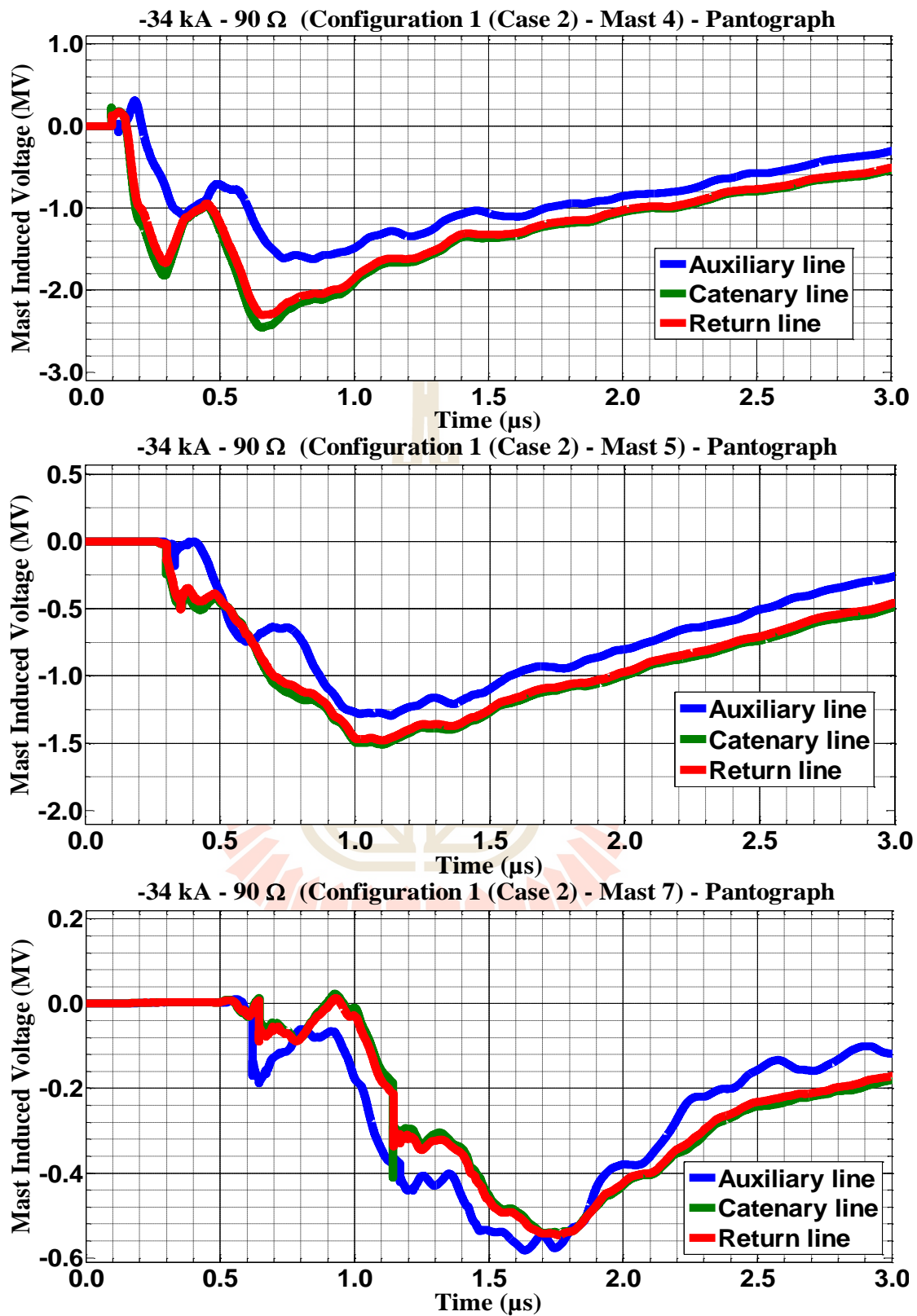


**Figure C.88** Mast 4, 5, and 7 with 90  $\Omega$  induced voltage waveform of the -34 kA first stroke-(1.0/100  $\mu$ s), subsequent stroke-(0.2/50  $\mu$ s) strikes on pantograph for Case 2

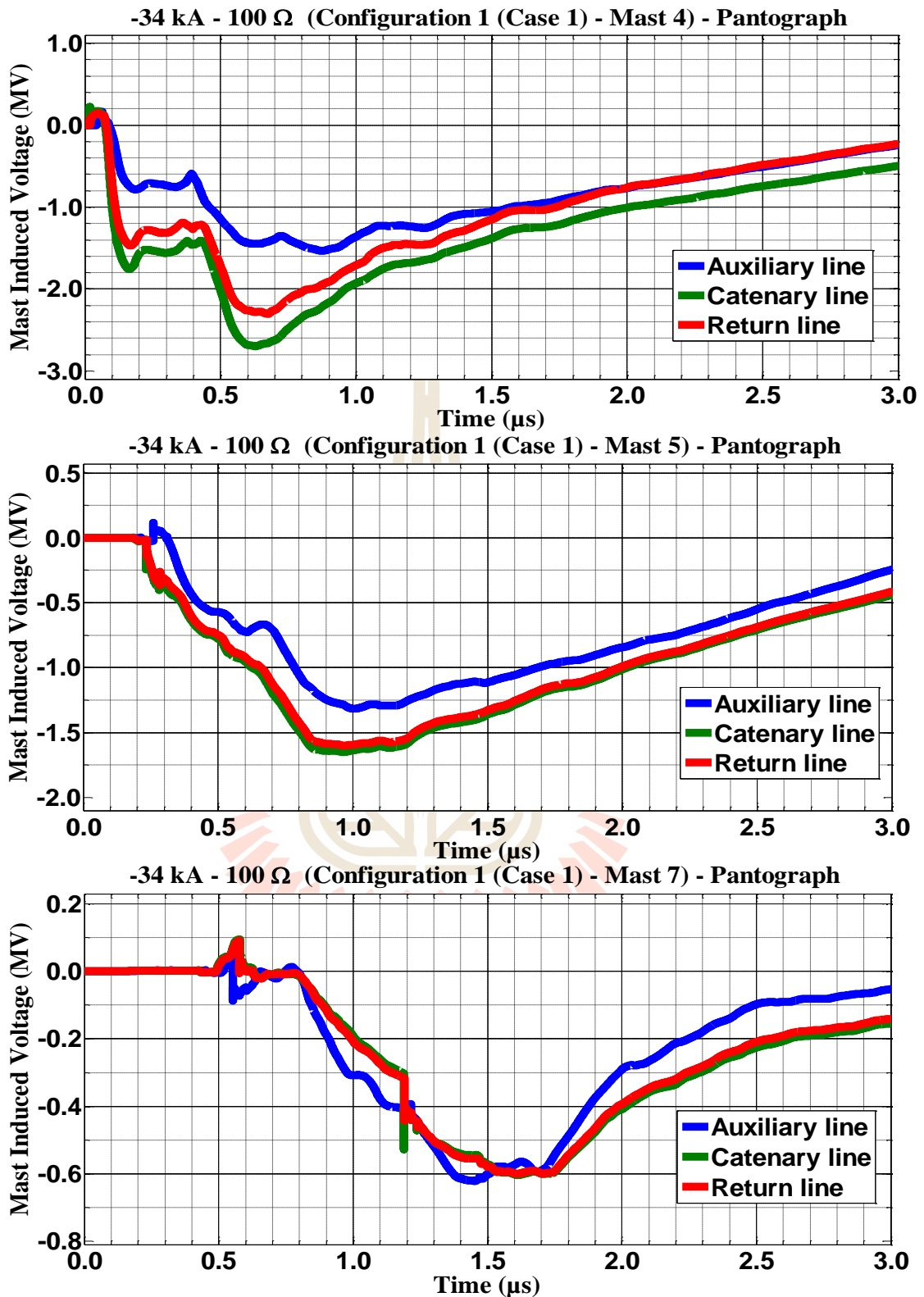


**Figure C.89** Mast 4, 5, and 7 with 100  $\Omega$  induced voltage waveform of the -34 kA first stroke-(1.0/100  $\mu\text{s}$ ), subsequent stroke-(0.2/50  $\mu\text{s}$ ) strikes on pantograph for Case 1

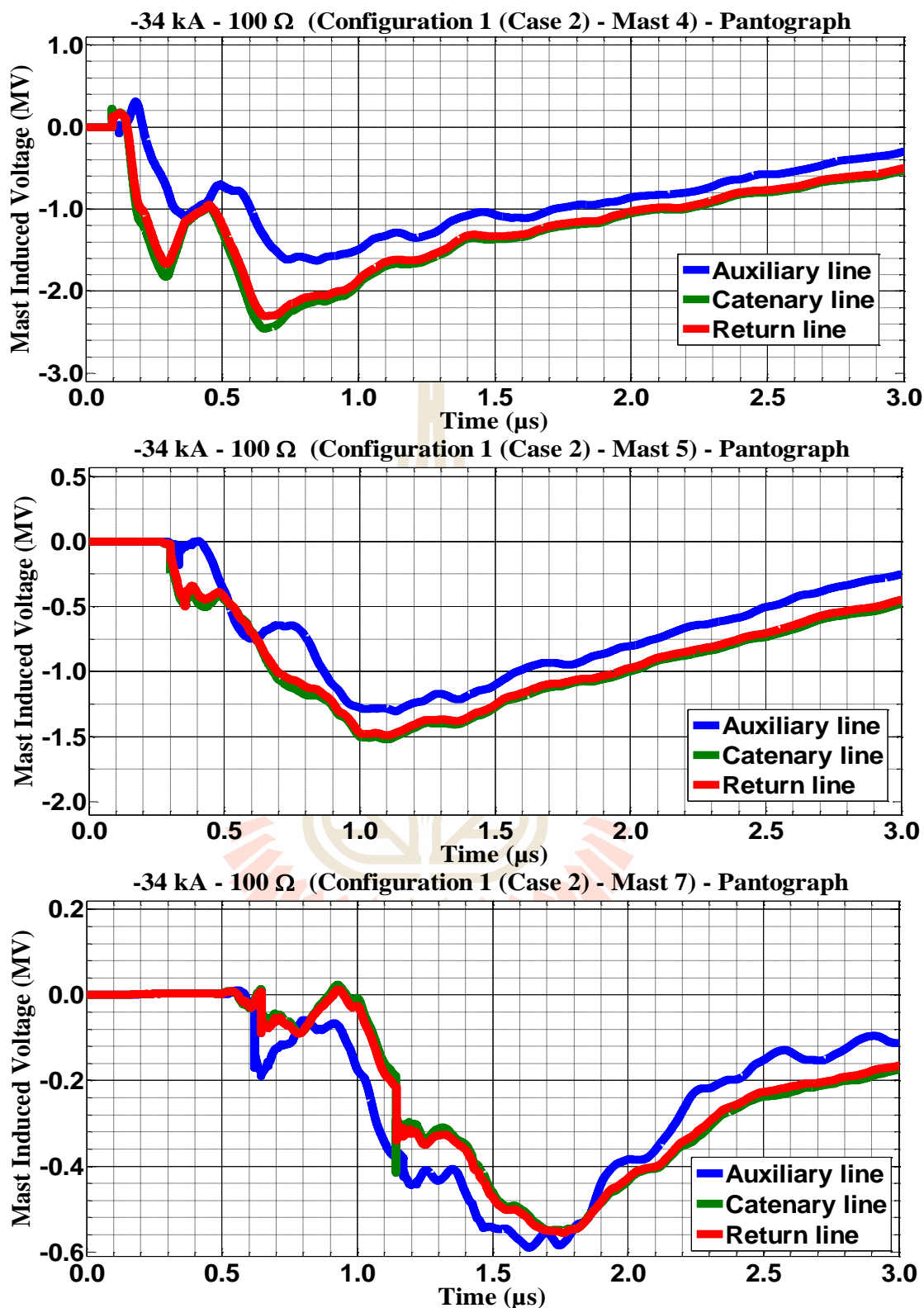
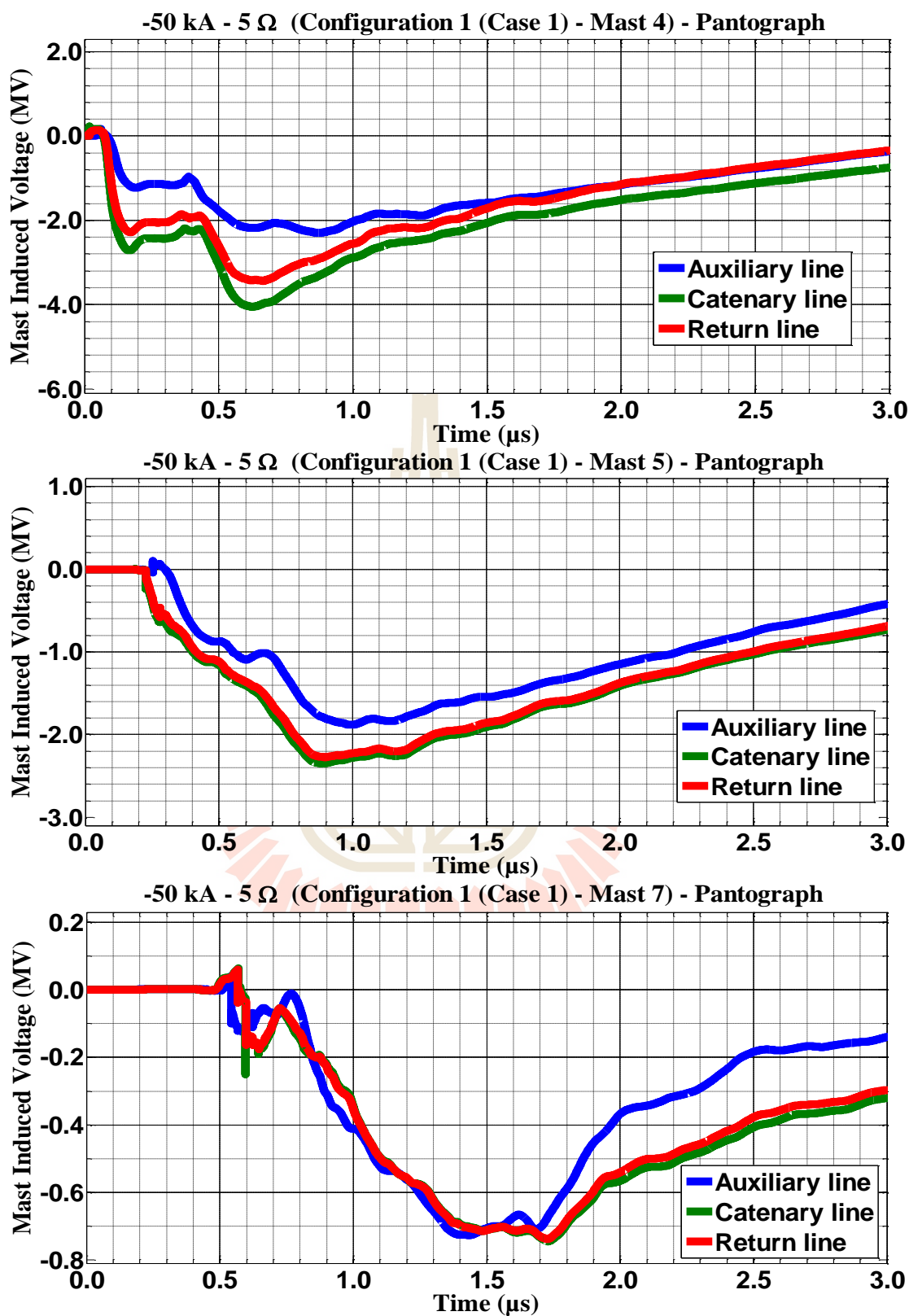


Figure C.90 Mast 4, 5, and 7 with 100  $\Omega$  induced voltage waveform of the -34 kA first stroke-(1.0/100  $\mu\text{s}$ ), subsequent stroke-(0.2/50  $\mu\text{s}$ ) strikes on pantograph for Case 2



**Figure C.91** Mast 4, 5, and 7 with 5  $\Omega$  induced voltage waveform of the -50 kA first stroke-(1.0/100  $\mu\text{s}$ ), subsequent stroke-(0.2/50  $\mu\text{s}$ ) strikes on pantograph for Case 1



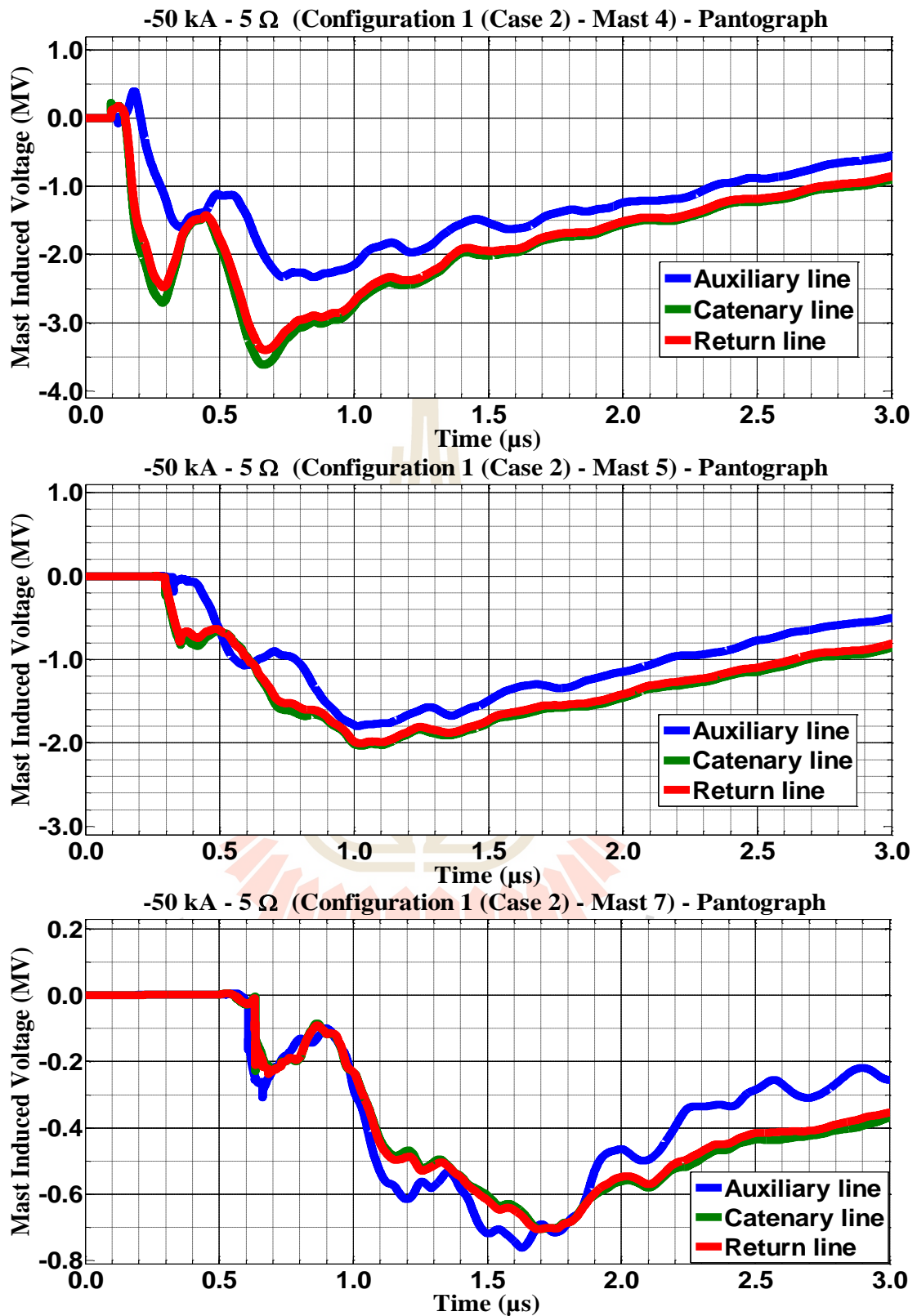


Figure C.92 Mast 4, 5, and 7 with 5  $\Omega$  induced voltage waveform of the -50 kA first stroke-(1.0/100  $\mu\text{s}$ ), subsequent stroke-(0.2/50  $\mu\text{s}$ ) strikes on pantograph for Case 2

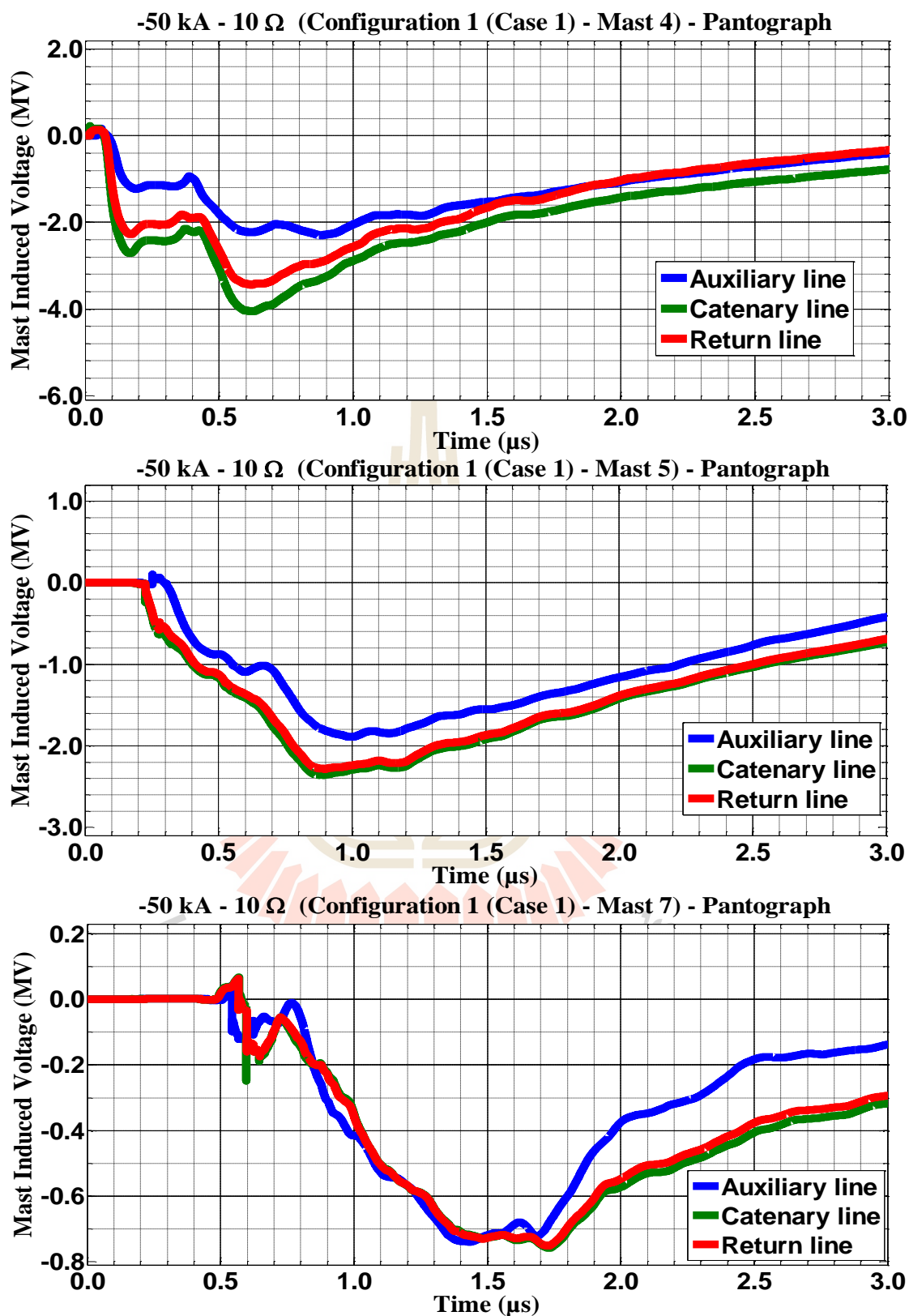


Figure C.93 Mast 4, 5, and 7 with 10 Ω induced voltage waveform of the -50 kA first stroke-(1.0/100 μs), subsequent stroke-(0.2/50 μs) strikes on pantograph for Case 1

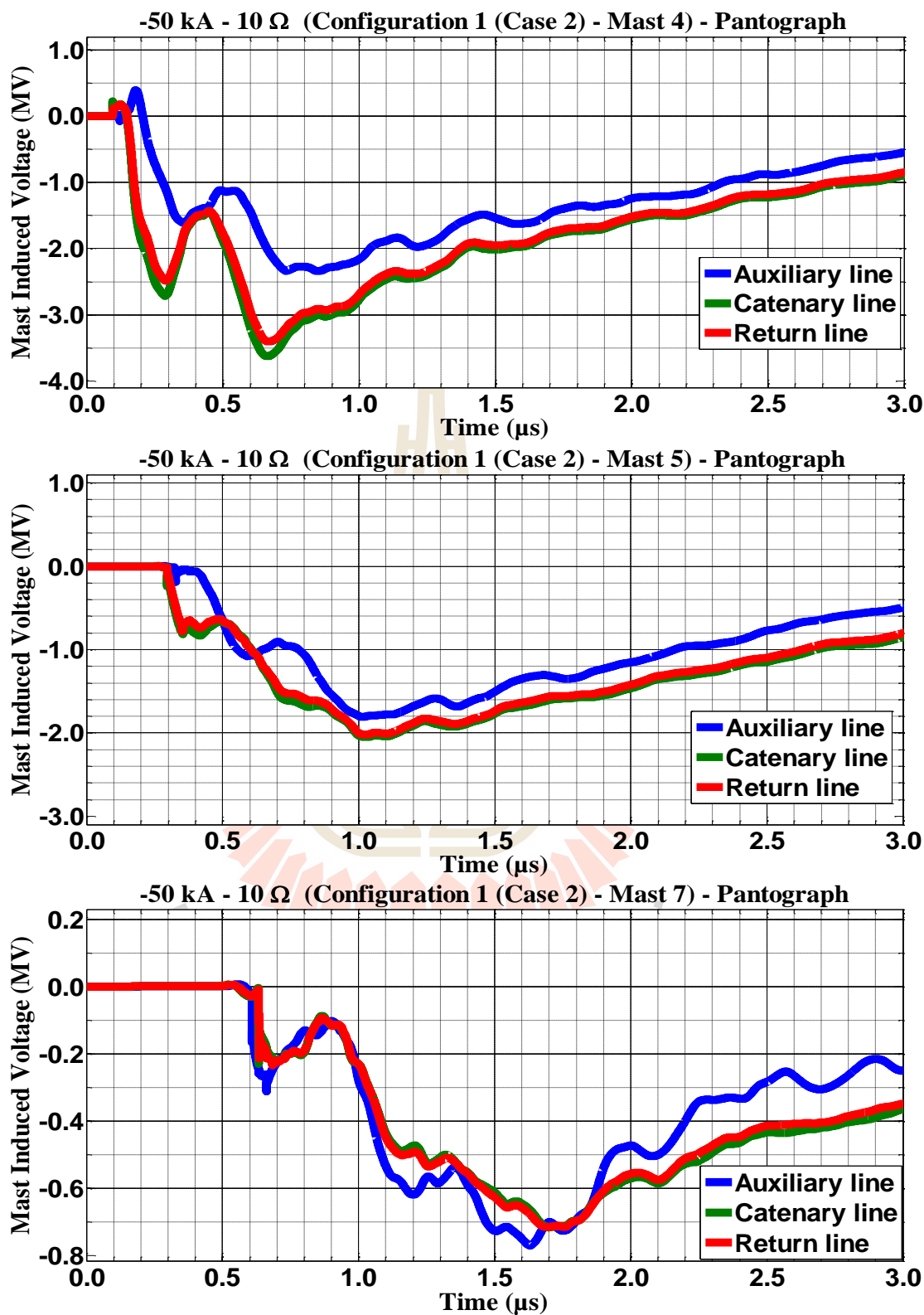


Figure C.94 Mast 4, 5, and 7 with 10  $\Omega$  induced voltage waveform of the -50 kA first stroke-(1.0/100  $\mu\text{s}$ ), subsequent stroke-(0.2/50  $\mu\text{s}$ ) strikes on pantograph for Case 2

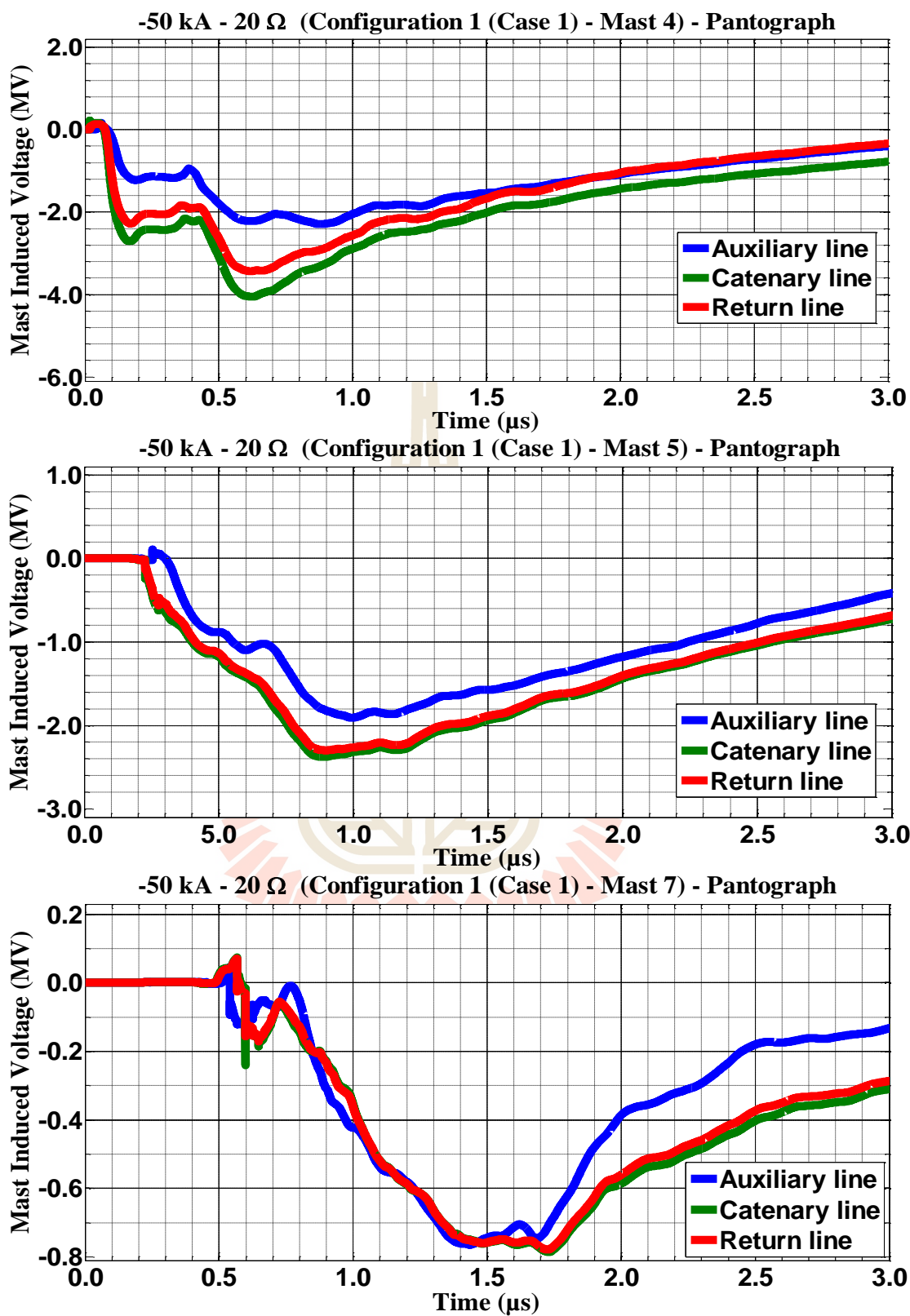
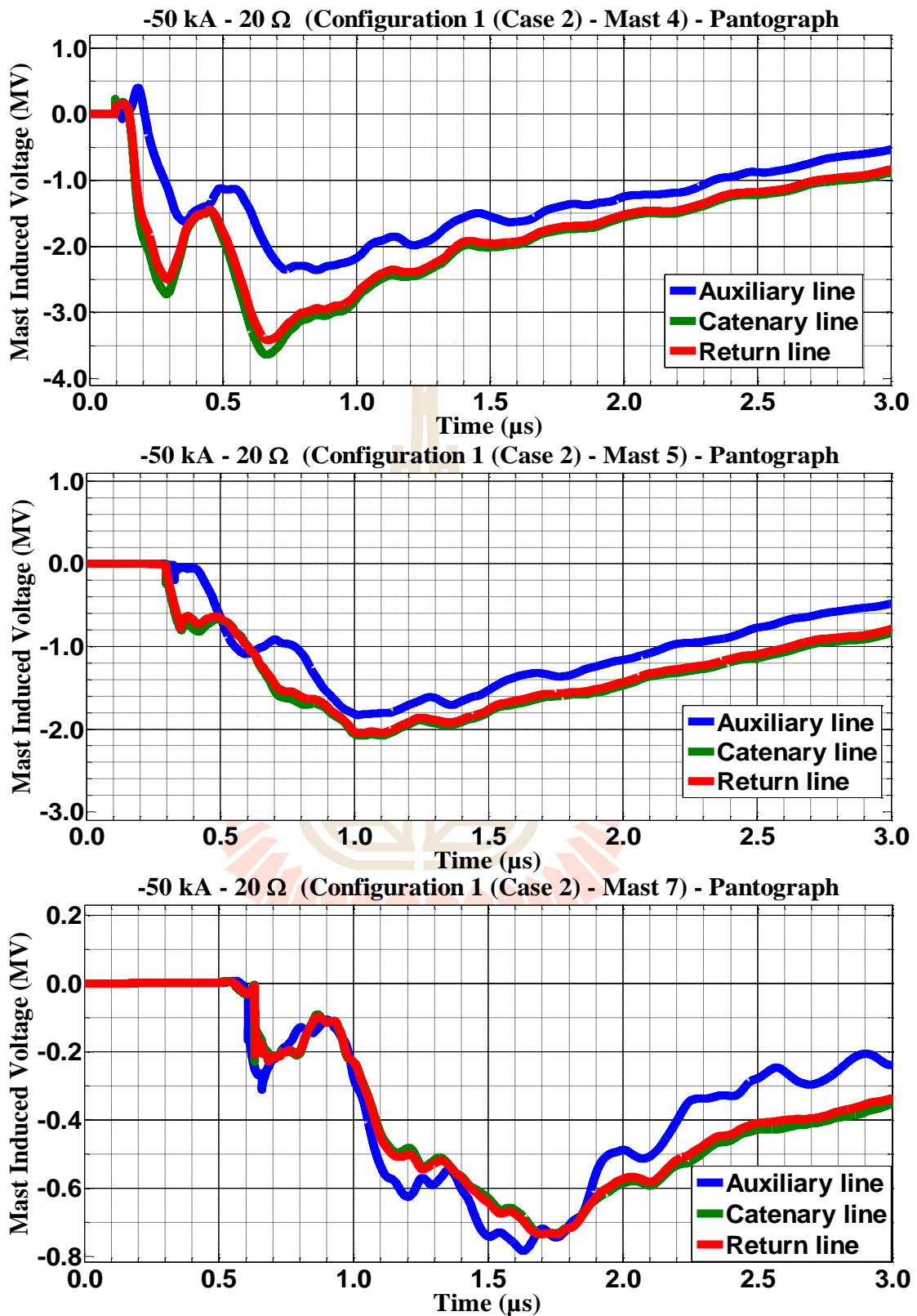
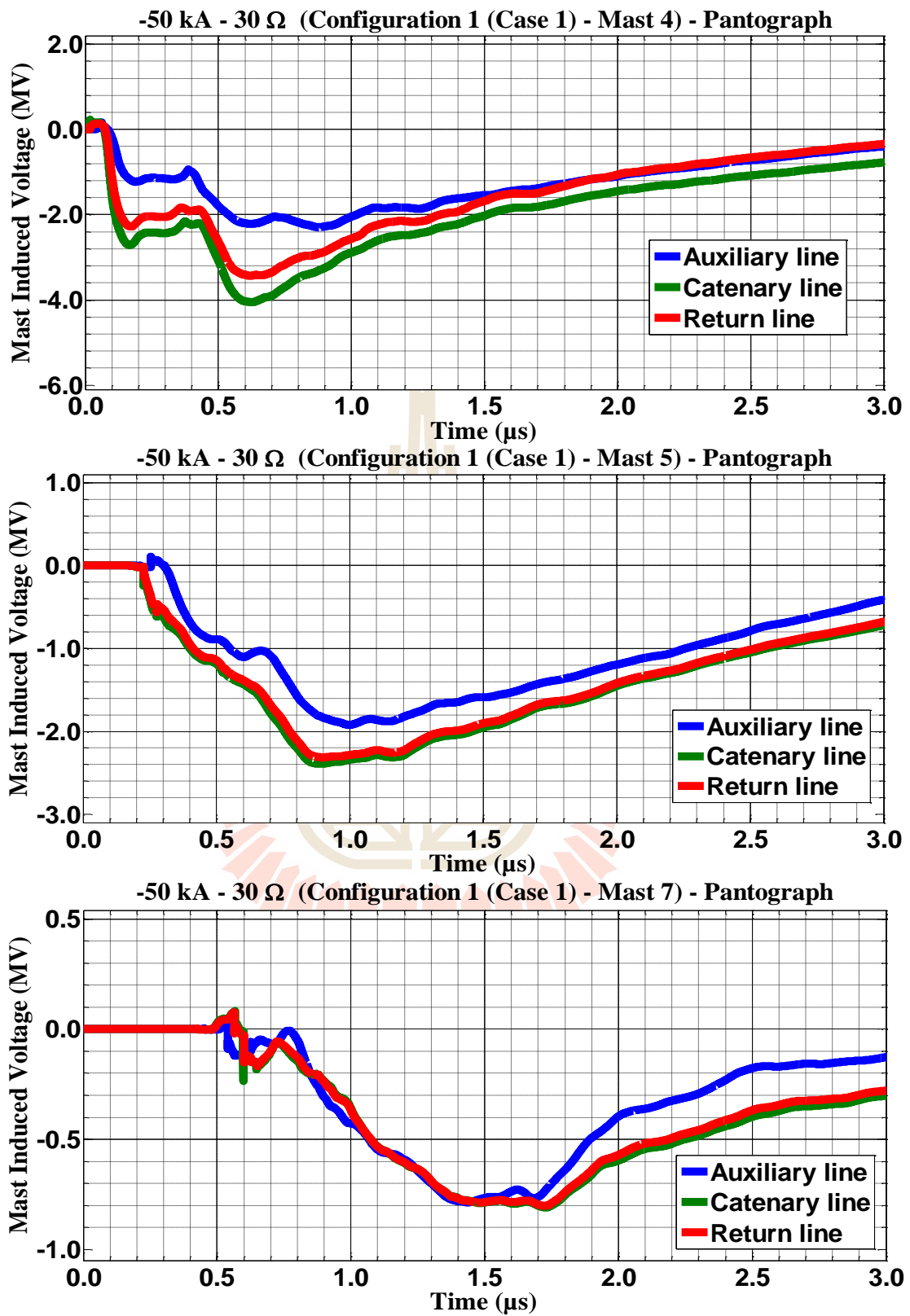


Figure C.95 Mast 4, 5, and 7 with 20  $\Omega$  induced voltage waveform of the -50 kA first stroke-(1.0/100  $\mu\text{s}$ ), subsequent stroke-(0.2/50  $\mu\text{s}$ ) strikes on pantograph for Case 1



**Figure C.96** Mast 4, 5, and 7 with 20 Ω induced voltage waveform of the -50 kA first stroke-(1.0/100 μs), subsequent stroke-(0.2/50 μs) strikes on pantograph for Case 2



**Figure C.96** Mast 4, 5, and 7 with 30 Ω induced voltage waveform of the -50 kA first stroke-(1.0/100 μs), subsequent stroke-(0.2/50 μs) strikes on pantograph for Case 1

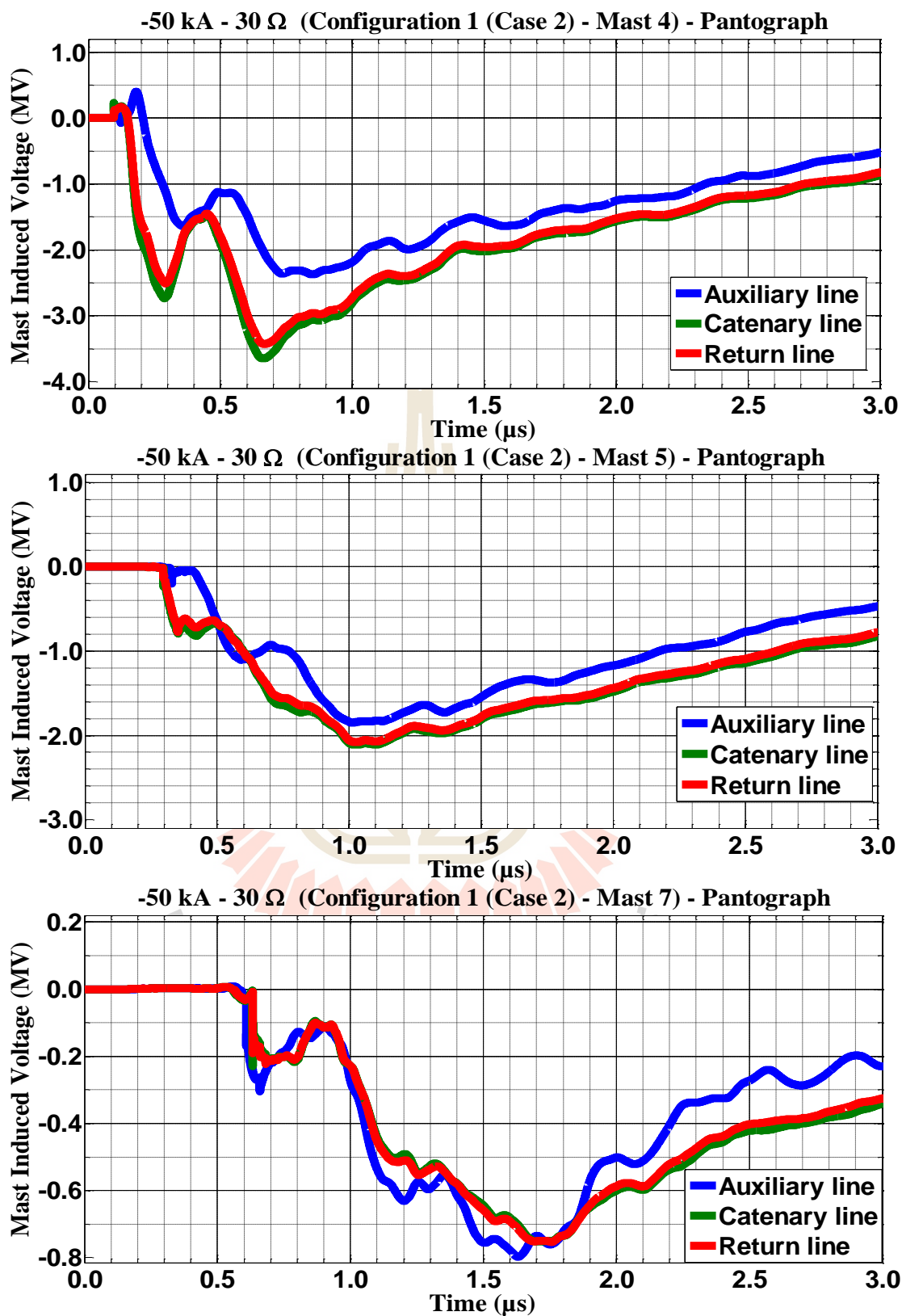


**Figure C.97** Mast 4, 5, and 7 with 30  $\Omega$  induced voltage waveform of the -50 kA first stroke-(1.0/100  $\mu\text{s}$ ), subsequent stroke-(0.2/50  $\mu\text{s}$ ) strikes on pantograph for Case 2

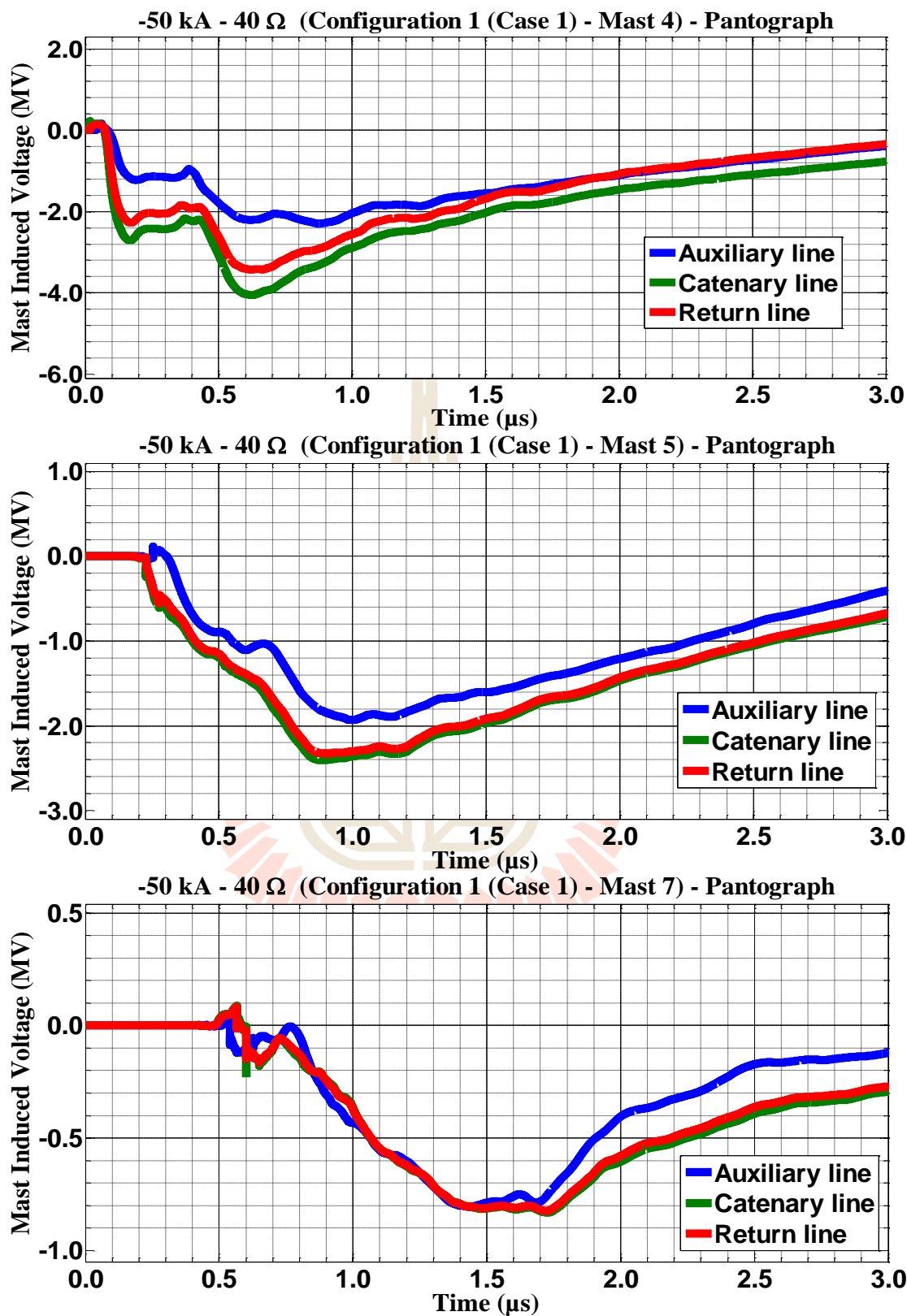


**Figure C.98** Mast 4, 5, and 7 with 40  $\Omega$  induced voltage waveform of the -50 kA first stroke-(1.0/100  $\mu$ s), subsequent stroke-(0.2/50  $\mu$ s) strikes on pantograph for Case 1



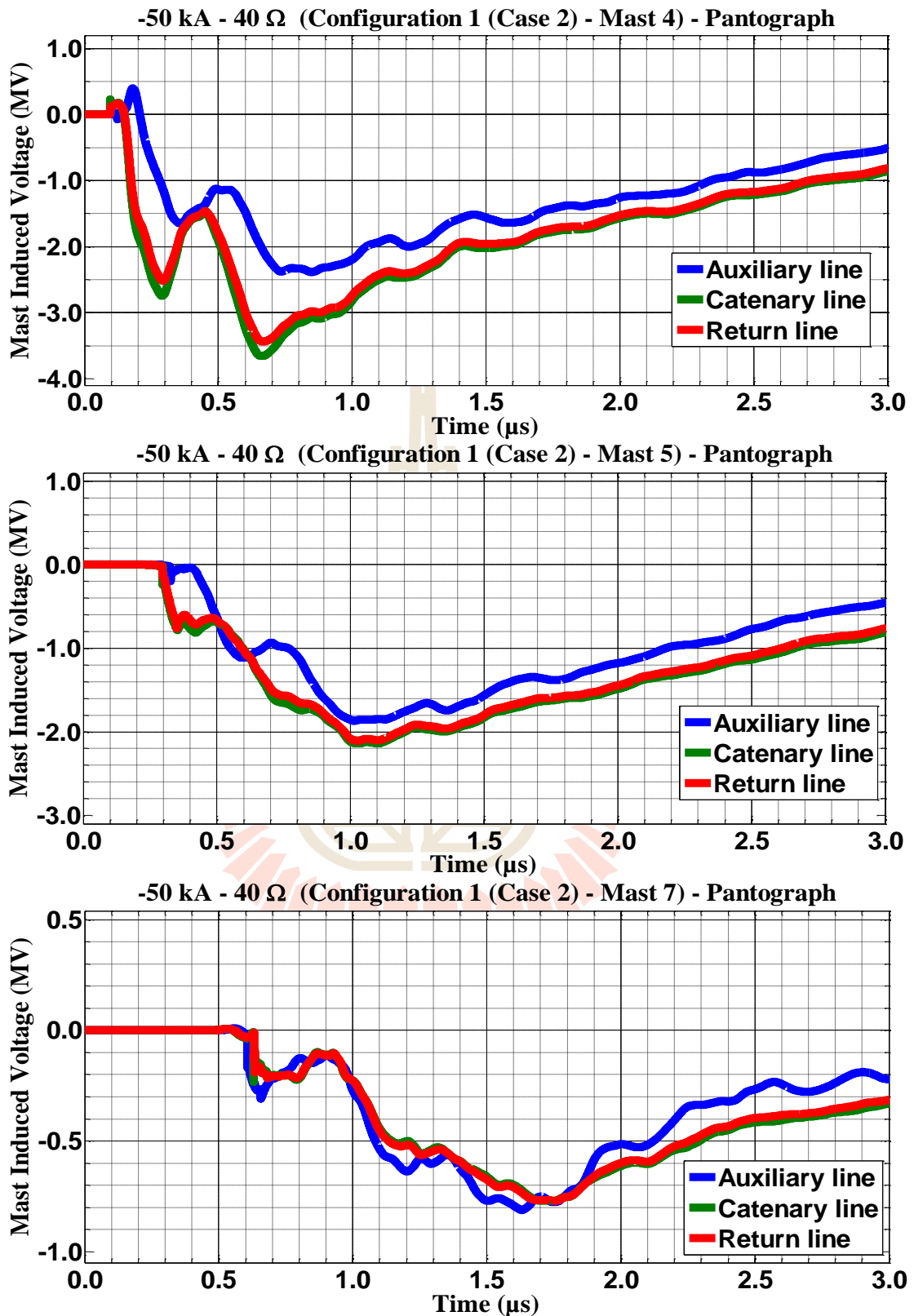


**Figure C.99** Mast 4, 5, and 7 with 40  $\Omega$  induced voltage waveform of the -50 kA first stroke-(1.0/100  $\mu\text{s}$ ), subsequent stroke-(0.2/50  $\mu\text{s}$ ) strikes on pantograph for Case 2

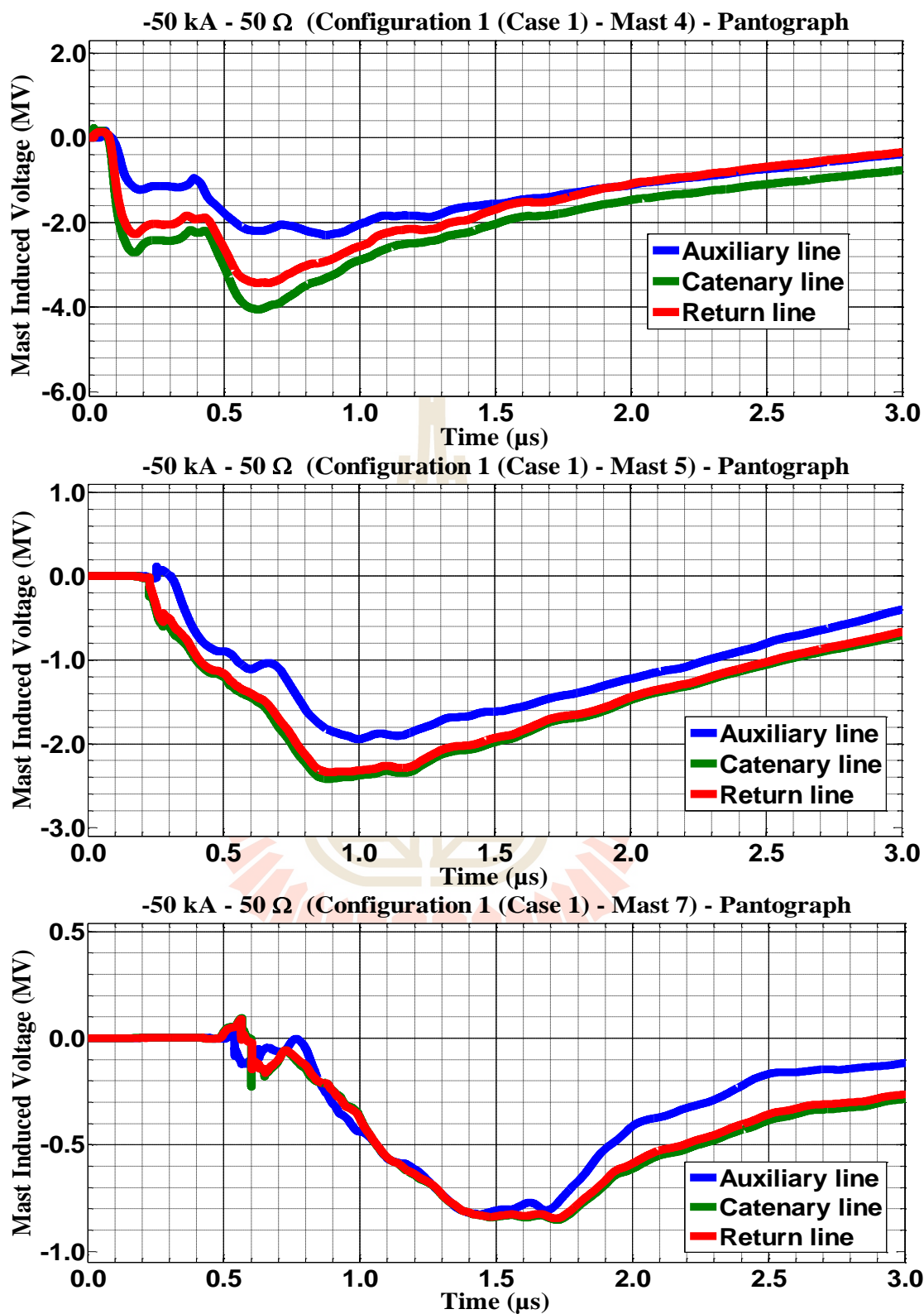


Figure C.100 Mast 4, 5, and 7 with 50 Ω induced voltage waveform of the -50 kA first stroke-(1.0/100 μs), subsequent stroke-(0.2/50 μs) strikes on pantograph for Case 1

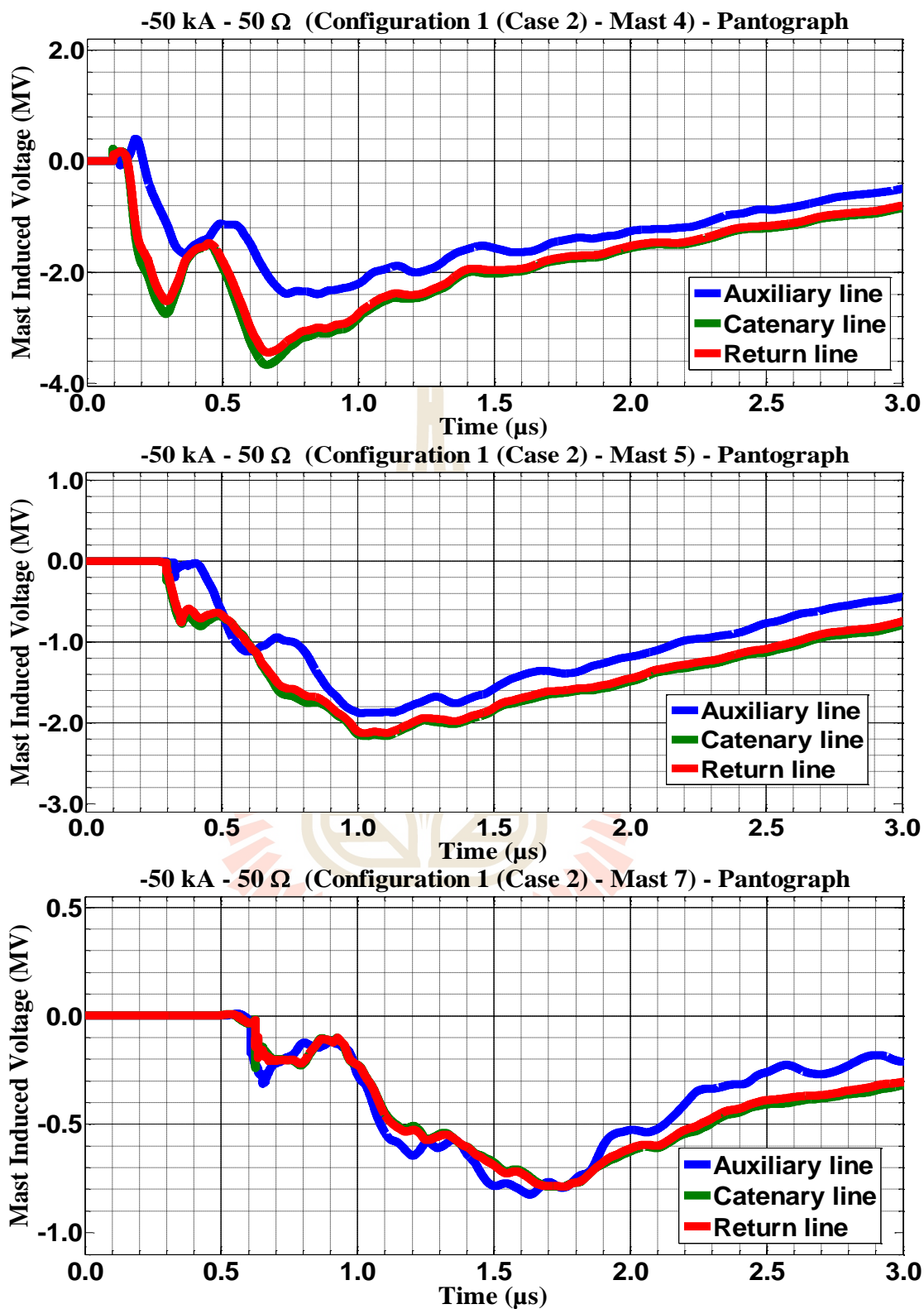


Figure C.101 Mast 4, 5, and 7 with 50 Ω induced voltage waveform of the -50 kA first stroke-(1.0/100 μs), subsequent stroke-(0.2/50 μs) strikes on pantograph for Case

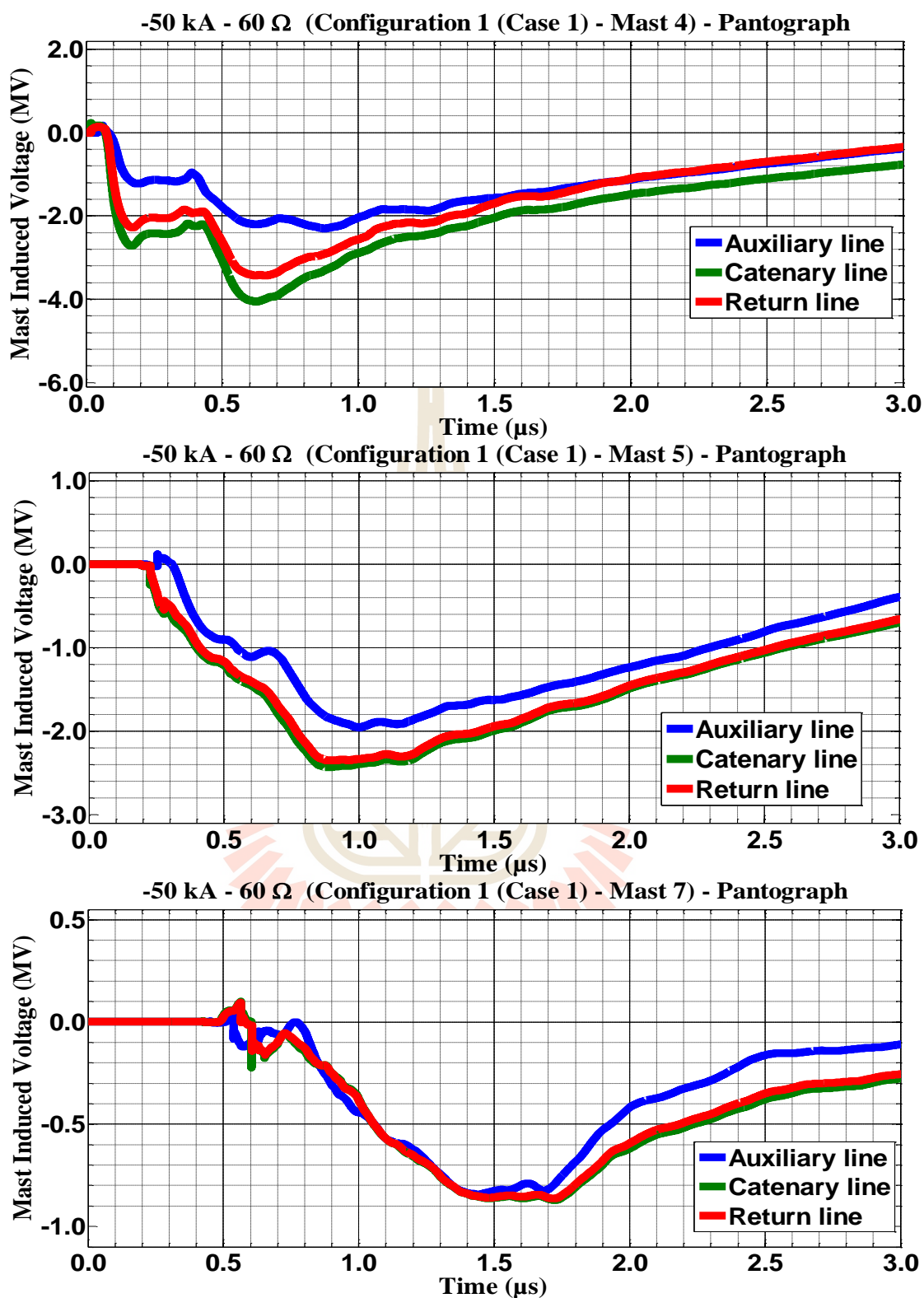


Figure C.102 Mast 4, 5, and 7 with 60  $\Omega$  induced voltage waveform of the -50 kA first stroke-(1.0/100  $\mu\text{s}$ ), subsequent stroke-(0.2/50  $\mu\text{s}$ ) strikes on pantograph for Case

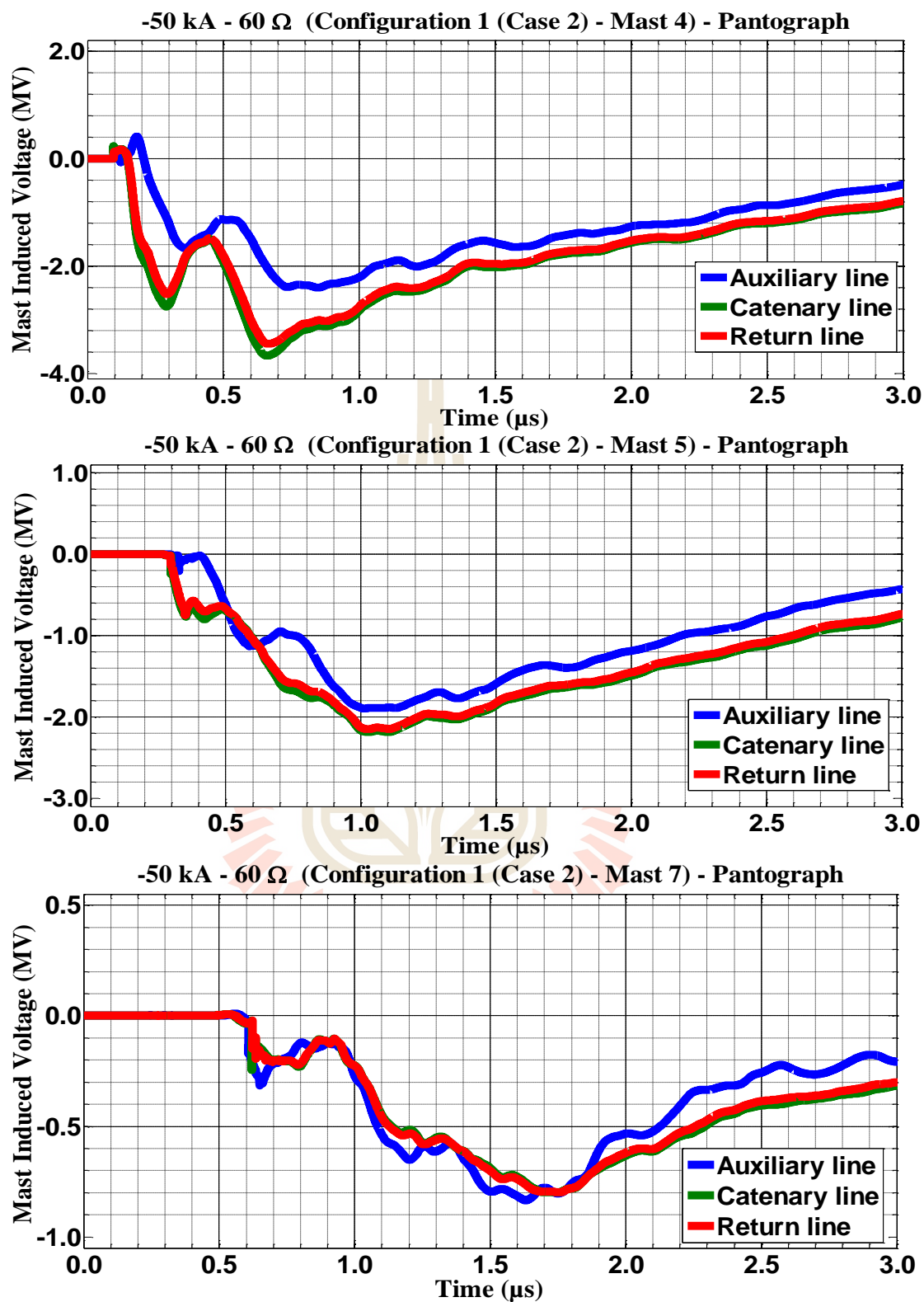


Figure C.103 Mast 4, 5, and 7 with 60 Ω induced voltage waveform of the -50 kA first stroke-(1.0/100 μs), subsequent stroke-(0.2/50 μs) strikes on pantograph for Case

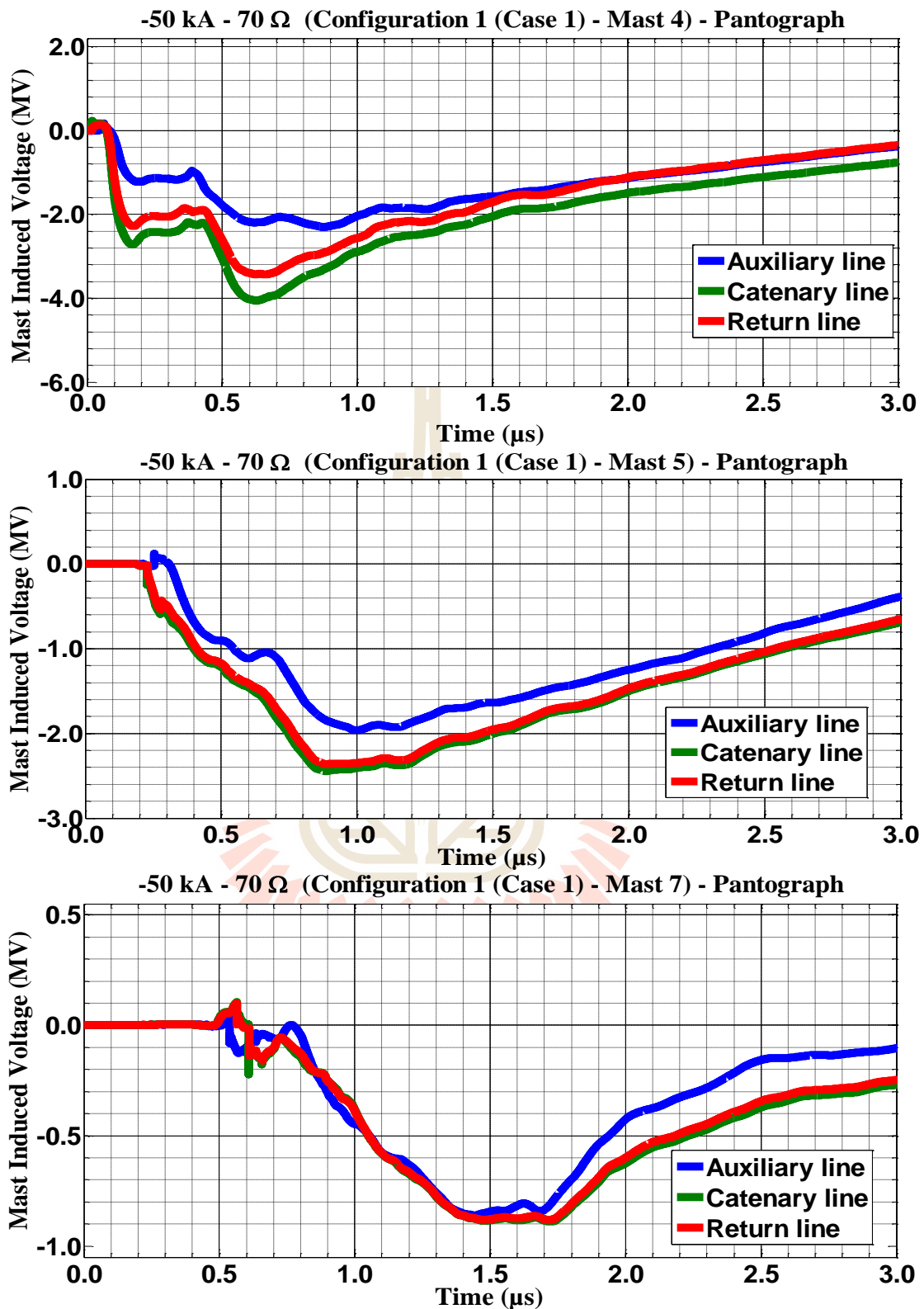


Figure C.104 Mast 4, 5, and 7 with 70 Ω induced voltage waveform of the -50 kA first stroke-(1.0/100 μs), subsequent stroke-(0.2/50 μs) strikes on pantograph for Case 1

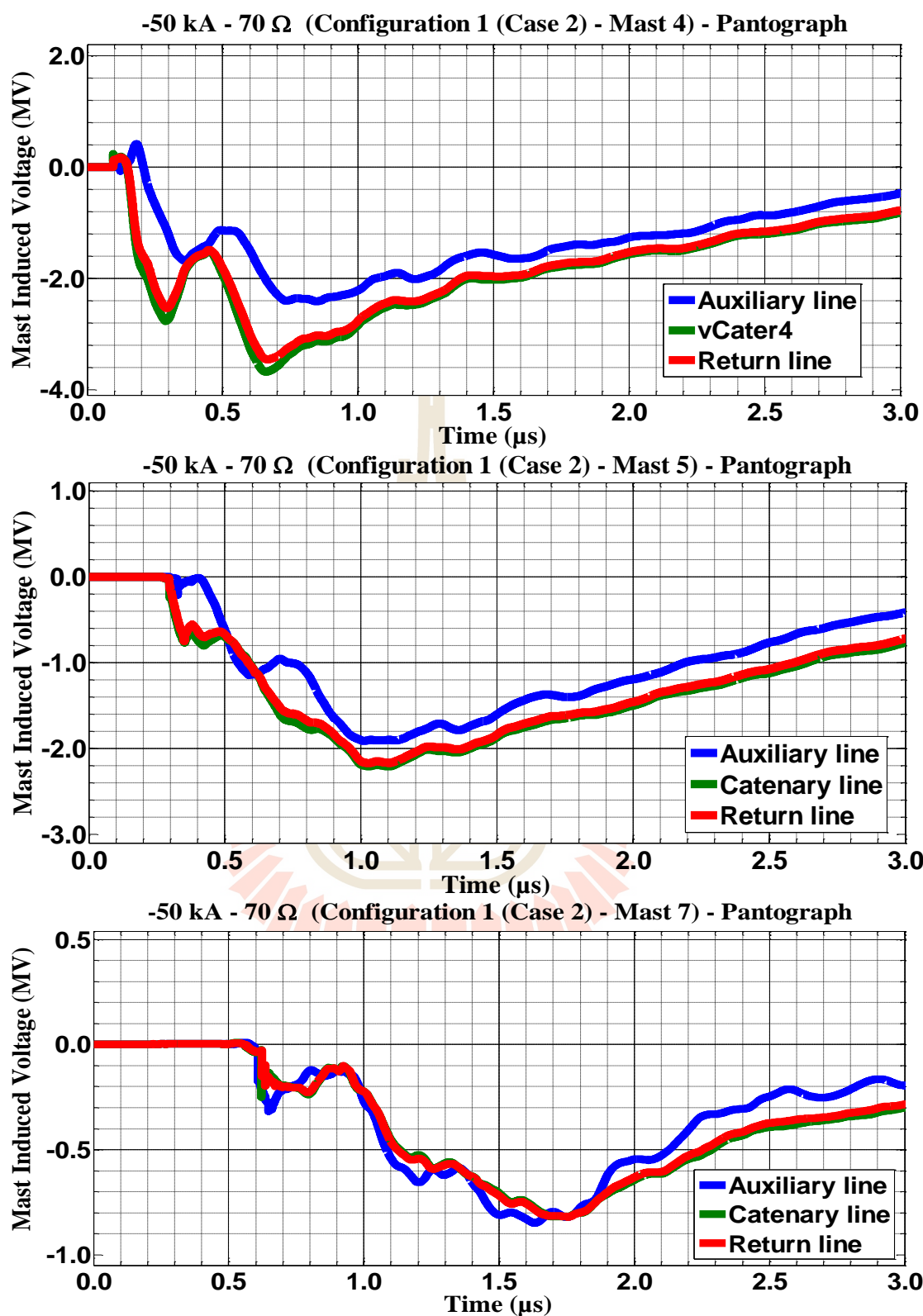


Figure C.105 Mast 4, 5, and 7 with 70 Ω induced voltage waveform of the -50 kA first stroke-(1.0/100 μs), subsequent stroke-(0.2/50 μs) strikes on pantograph for Case

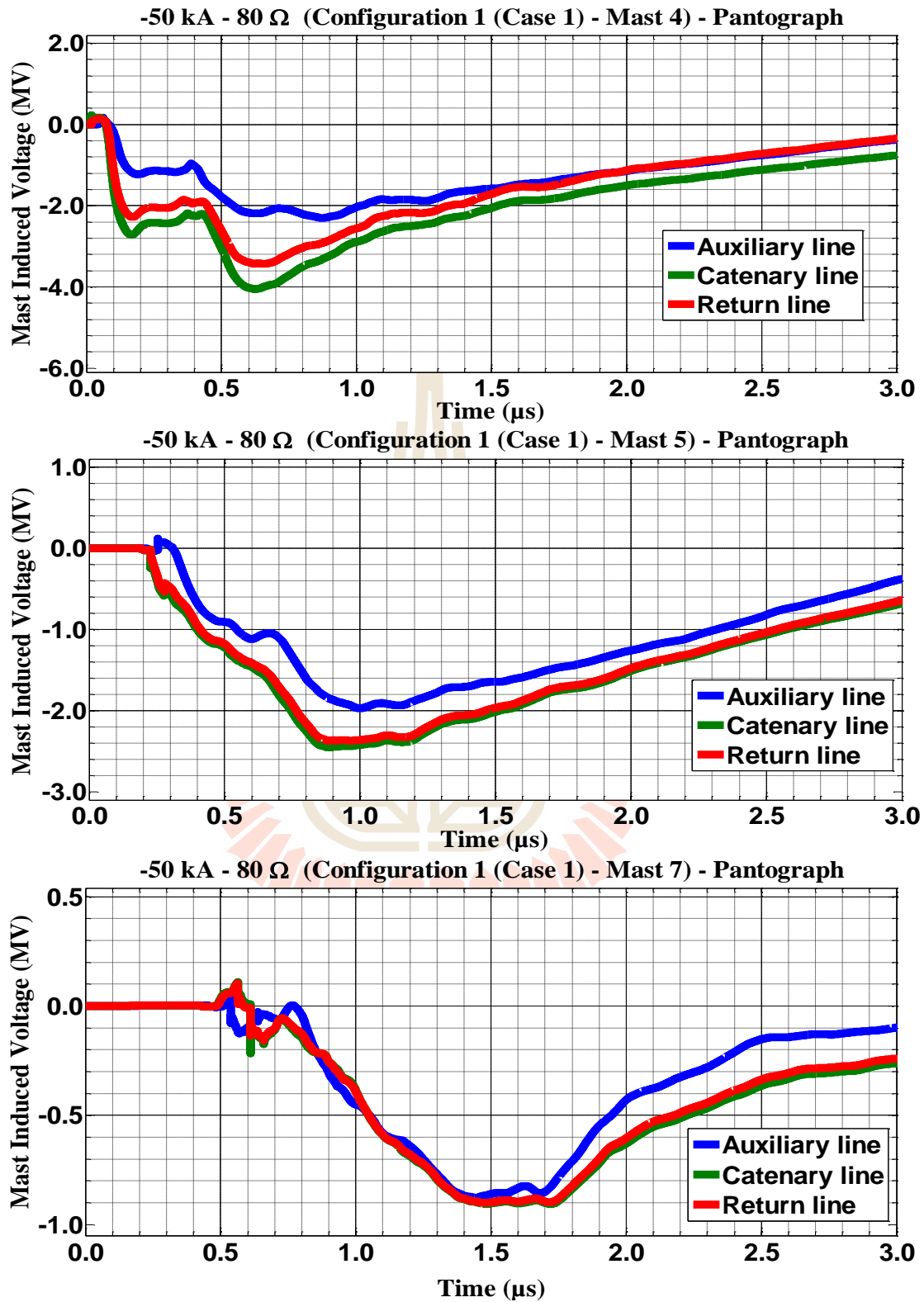
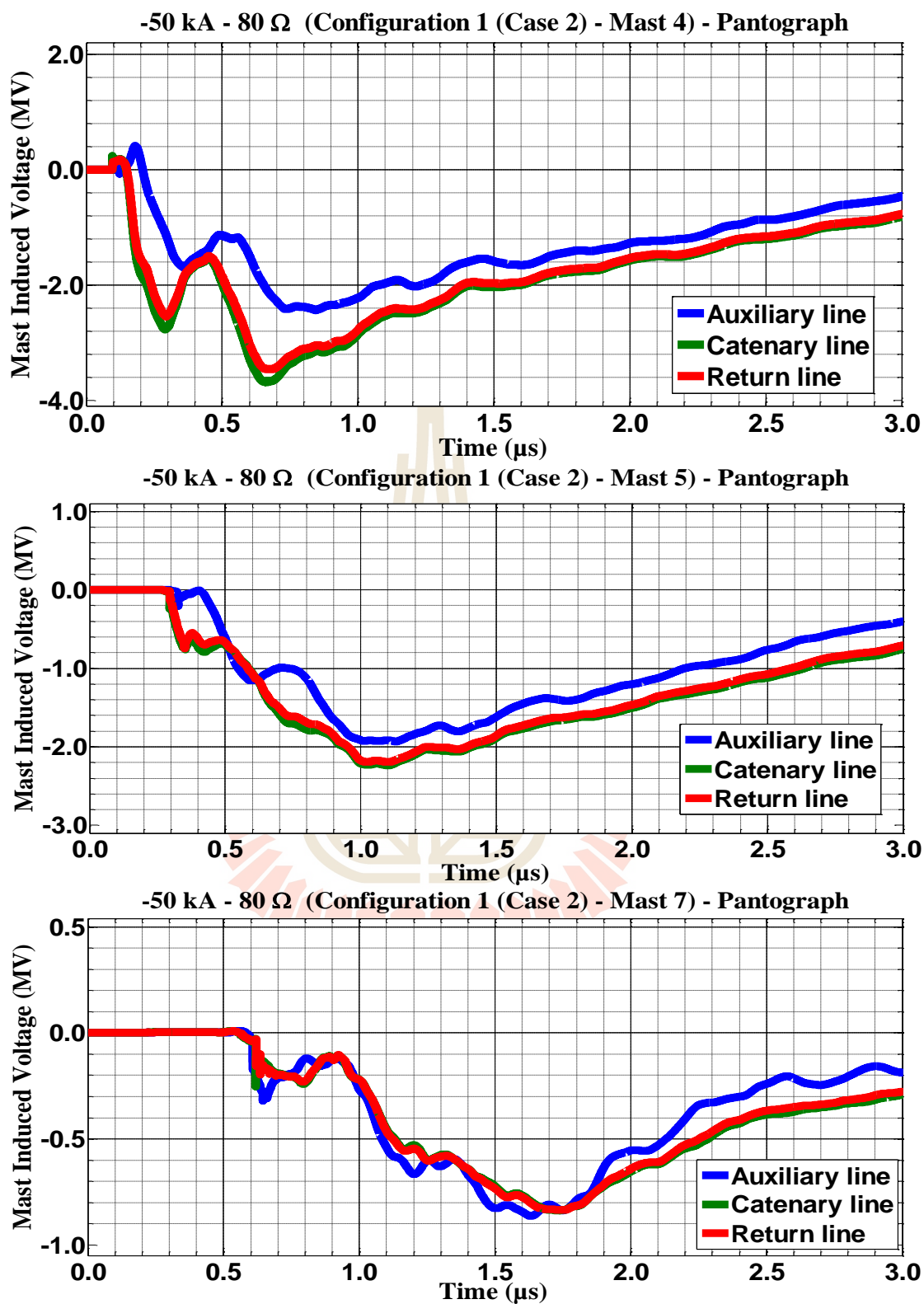


Figure C.106 Mast 4, 5, and 7 with 80 Ω induced voltage waveform of the -50 kA first stroke-(1.0/100 μs), subsequent stroke-(0.2/50 μs) strikes on pantograph for Case 1





**Figure C.107** Mast 4, 5, and 7 with 80  $\Omega$  induced voltage waveform of the -50 kA first stroke-(1.0/100  $\mu$ s), subsequent stroke-(0.2/50  $\mu$ s) strikes on pantograph for Case 2

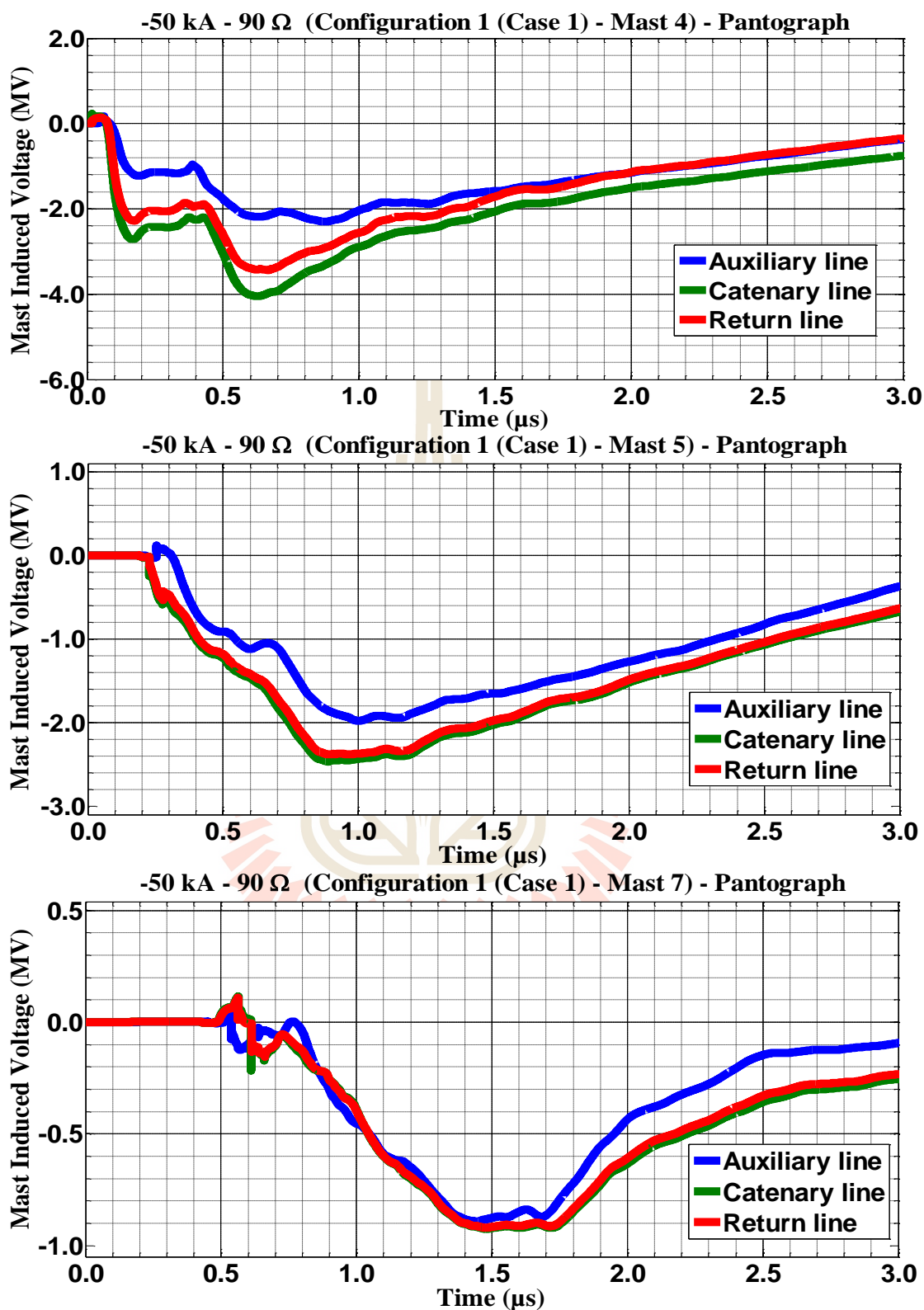


Figure C.108 Mast 4, 5, and 7 with 90  $\Omega$  induced voltage waveform of the -50 kA first stroke-(1.0/100  $\mu\text{s}$ ), subsequent stroke-(0.2/50  $\mu\text{s}$ ) strikes on pantograph for Case 1

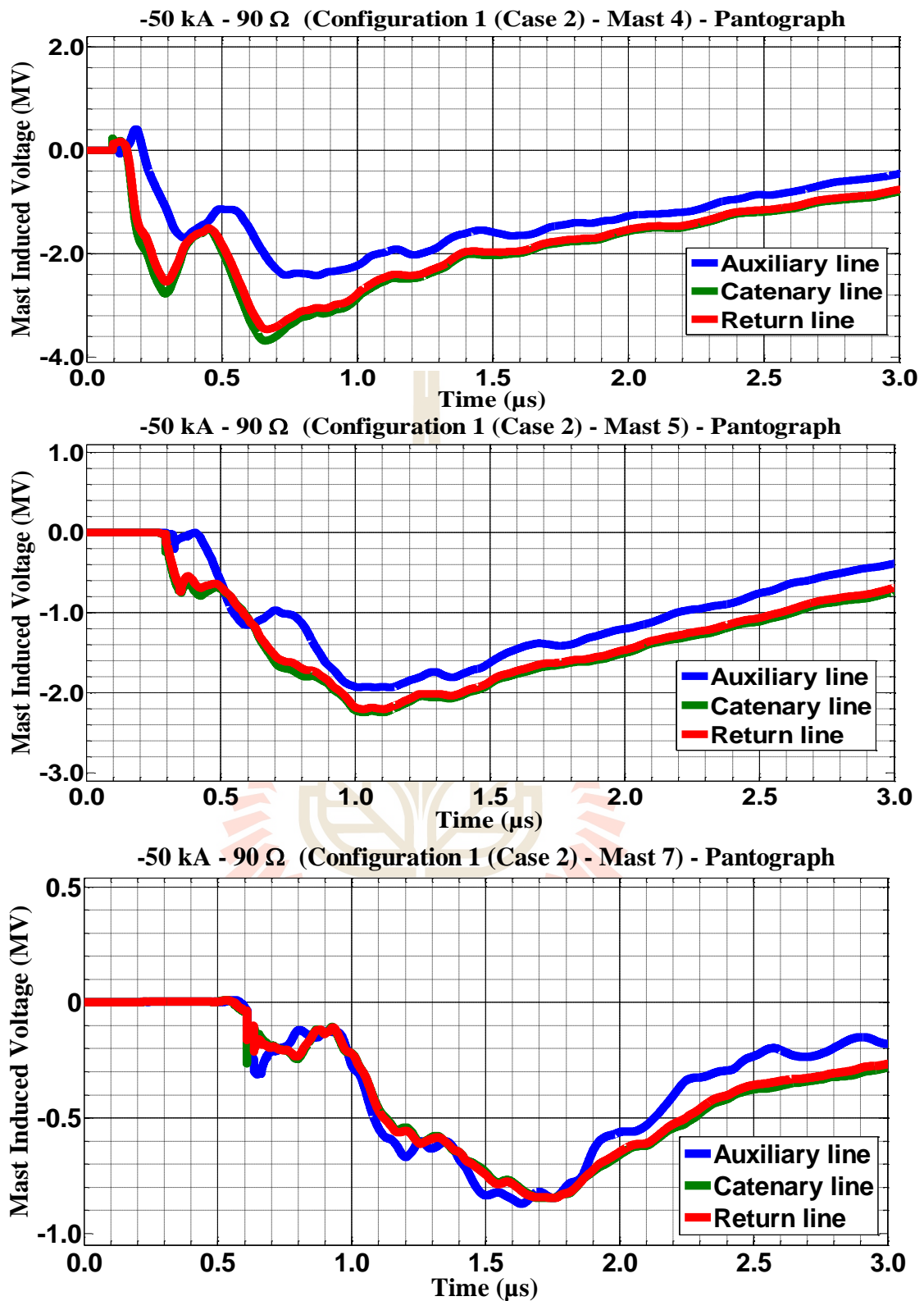


Figure C.109 Mast 4, 5, and 7 with 90  $\Omega$  induced voltage waveform of the -50 kA first stroke-(1.0/100  $\mu\text{s}$ ), subsequent stroke-(0.2/50  $\mu\text{s}$ ) strikes on pantograph for Case 2

### C.6 The consequences when the pantograph struck by negative multiple lightning strokes for Configuration 2 in Case 1 and 2.

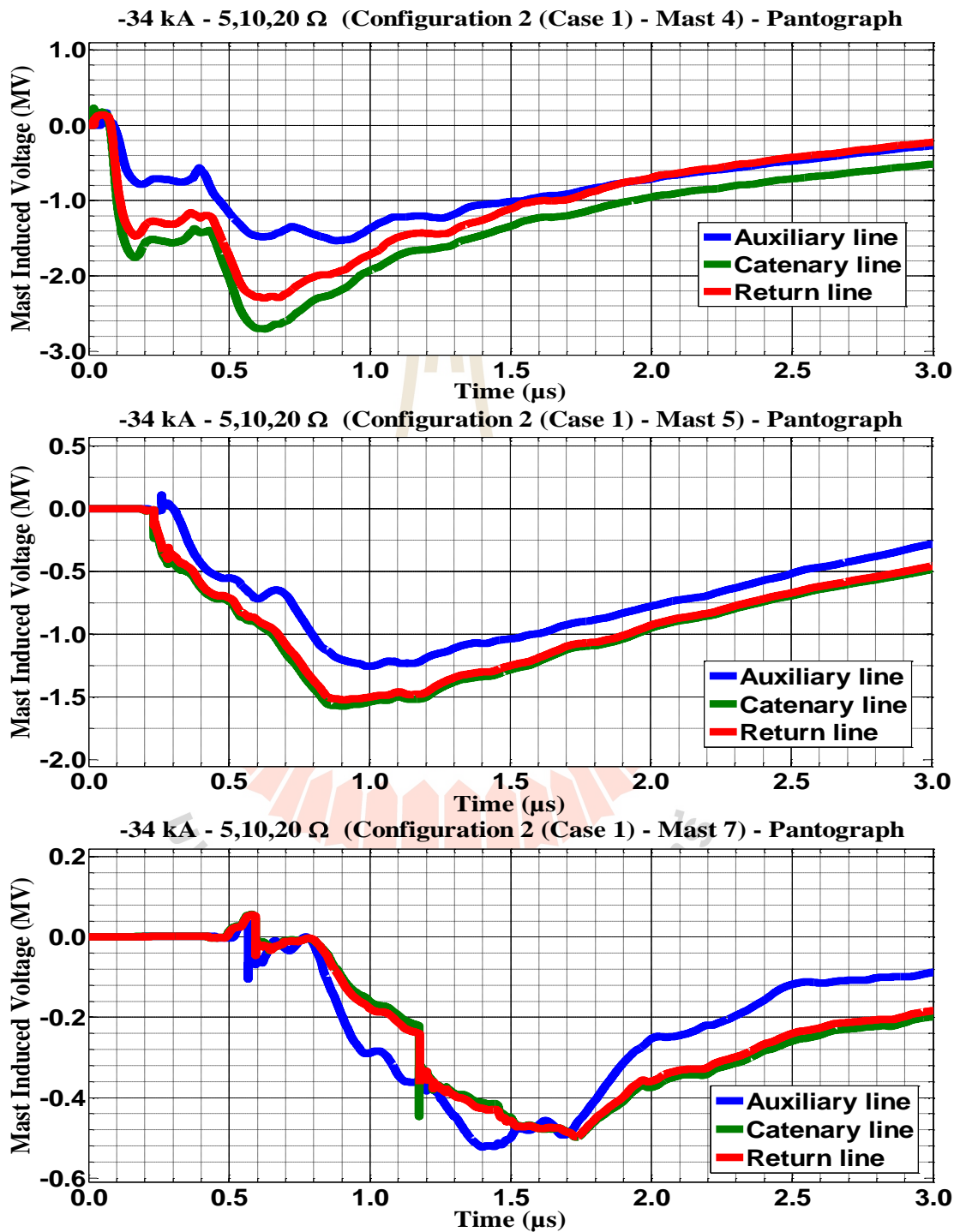
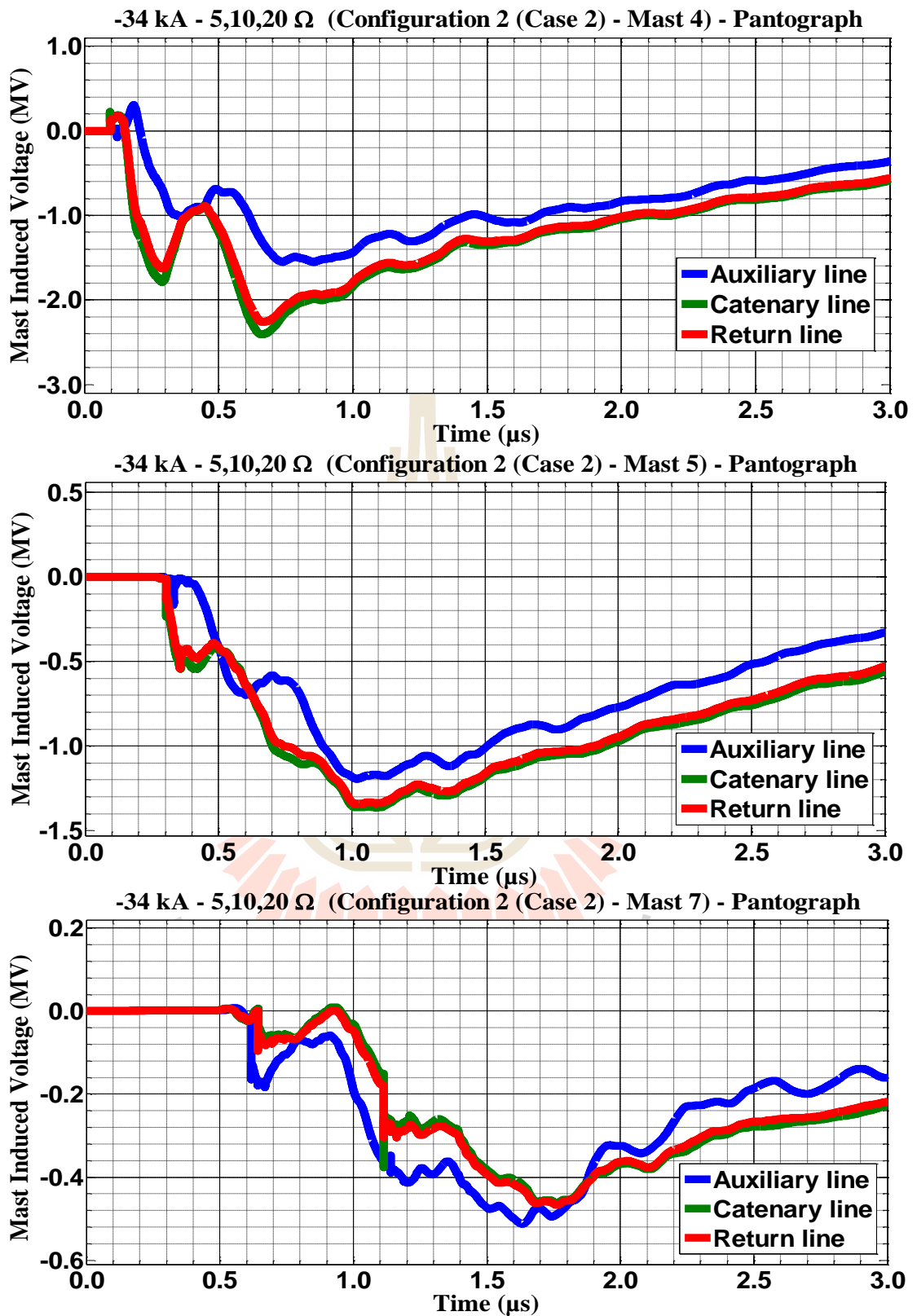
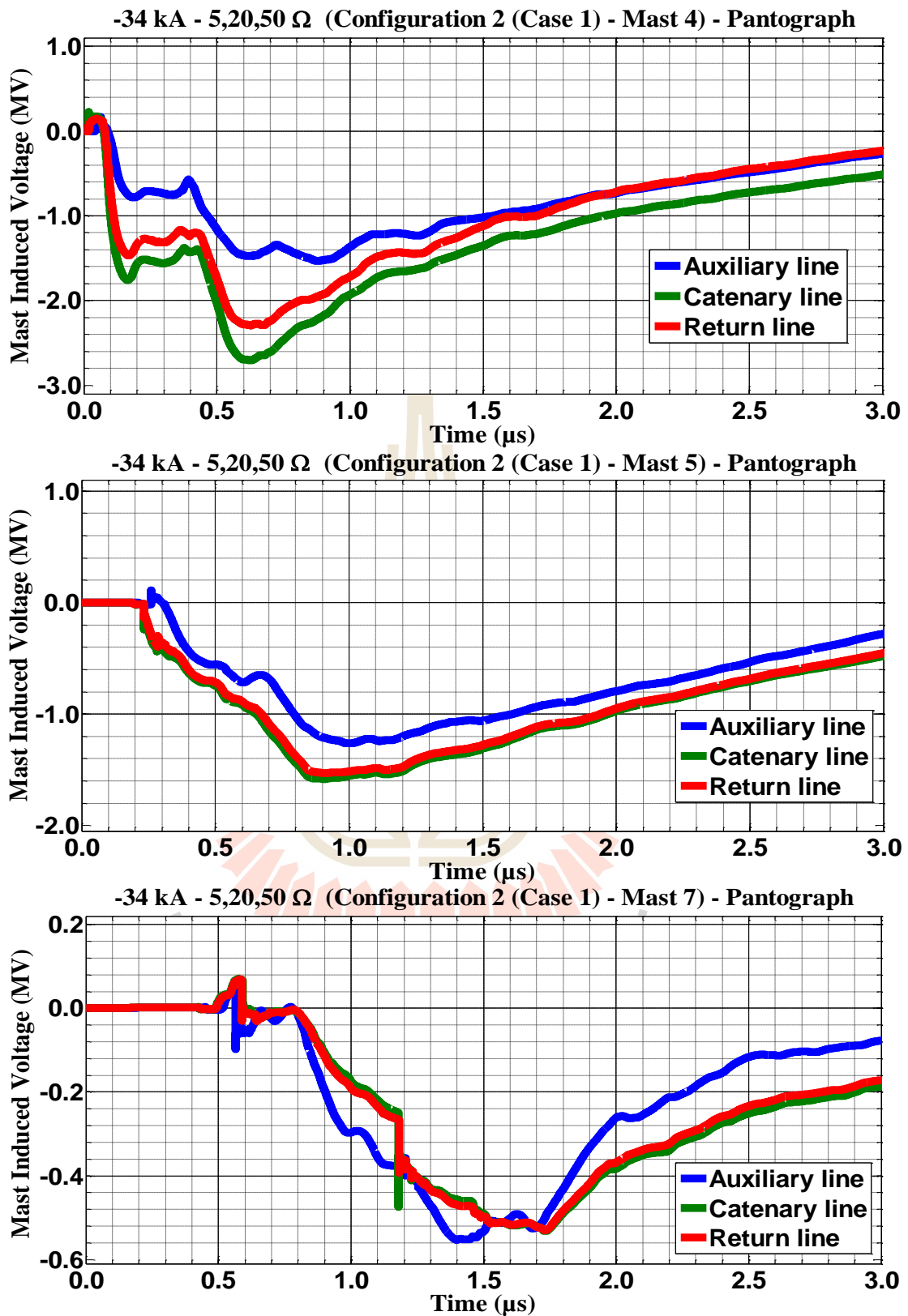


Figure C.110 Mast 4, 5, and 7 with 5,10,20 Ω induced voltage waveform of -34 kA first stroke-(1.0/100 μs), subsequent stroke-(0.2/50 μs) strikes on Mast 4 for Case 1



**Figure C.111** Mast 4, 5, and 7 with 5,10,20 Ω induced voltage waveform of -34 kA first stroke-(1.0/100 μs), subsequent stroke-(0.2/50 μs) strikes on Mast 4 for Case 2



**Figure C.112** Mast 4, 5, and 7 with 5,20,50  $\Omega$  induced voltage waveform of -34 kA first stroke-(1.0/100  $\mu$ s), subsequent stroke-(0.2/50  $\mu$ s) strikes on Mast 4 for Case 1

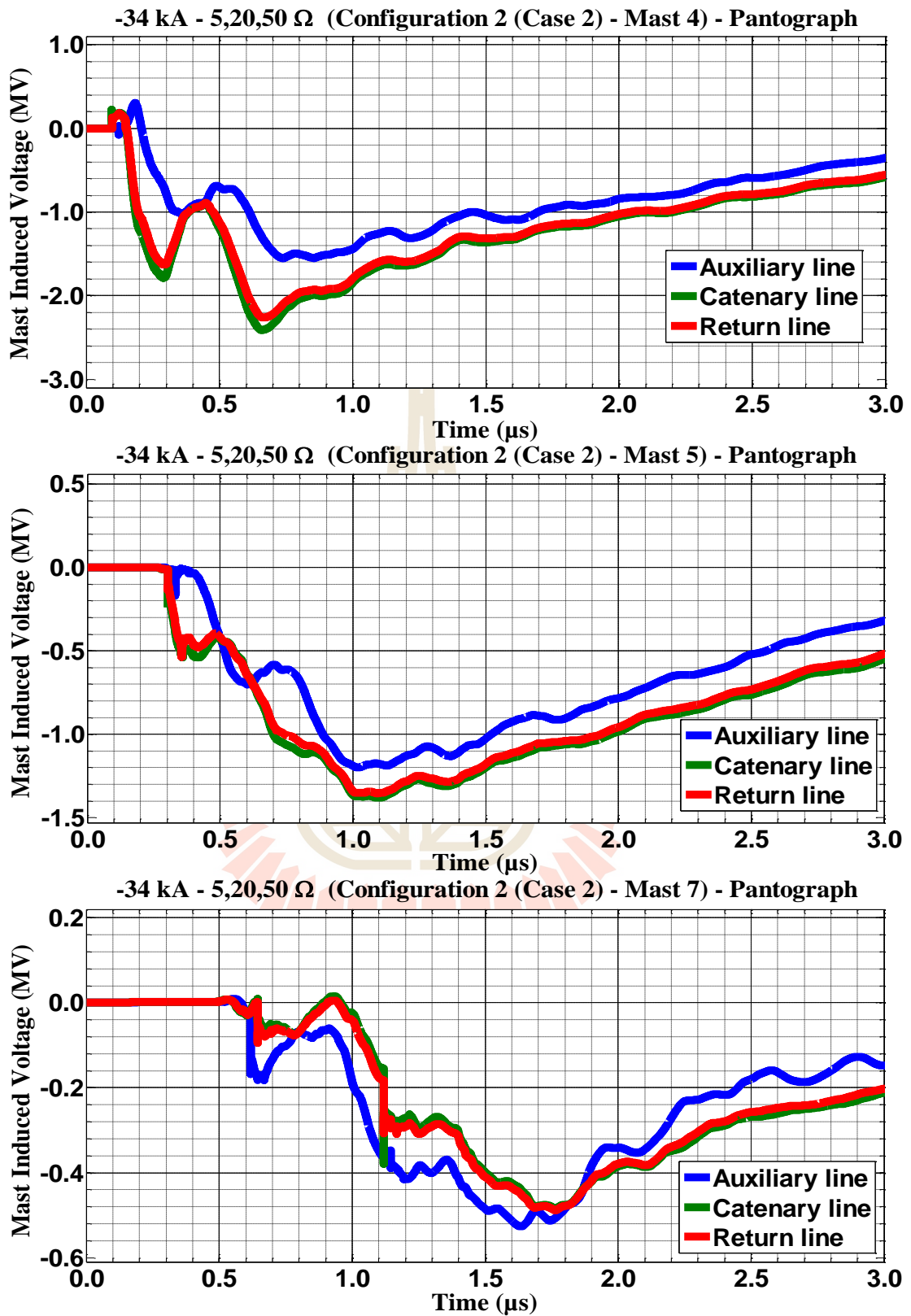


**Figure C.113** Mast 4, 5, and 7 with 5,20,50 Ω induced voltage waveform of -34 kA first stroke-(1.0/100 μs), subsequent stroke-(0.2/50 μs) strikes on Mast 4 for Case 2

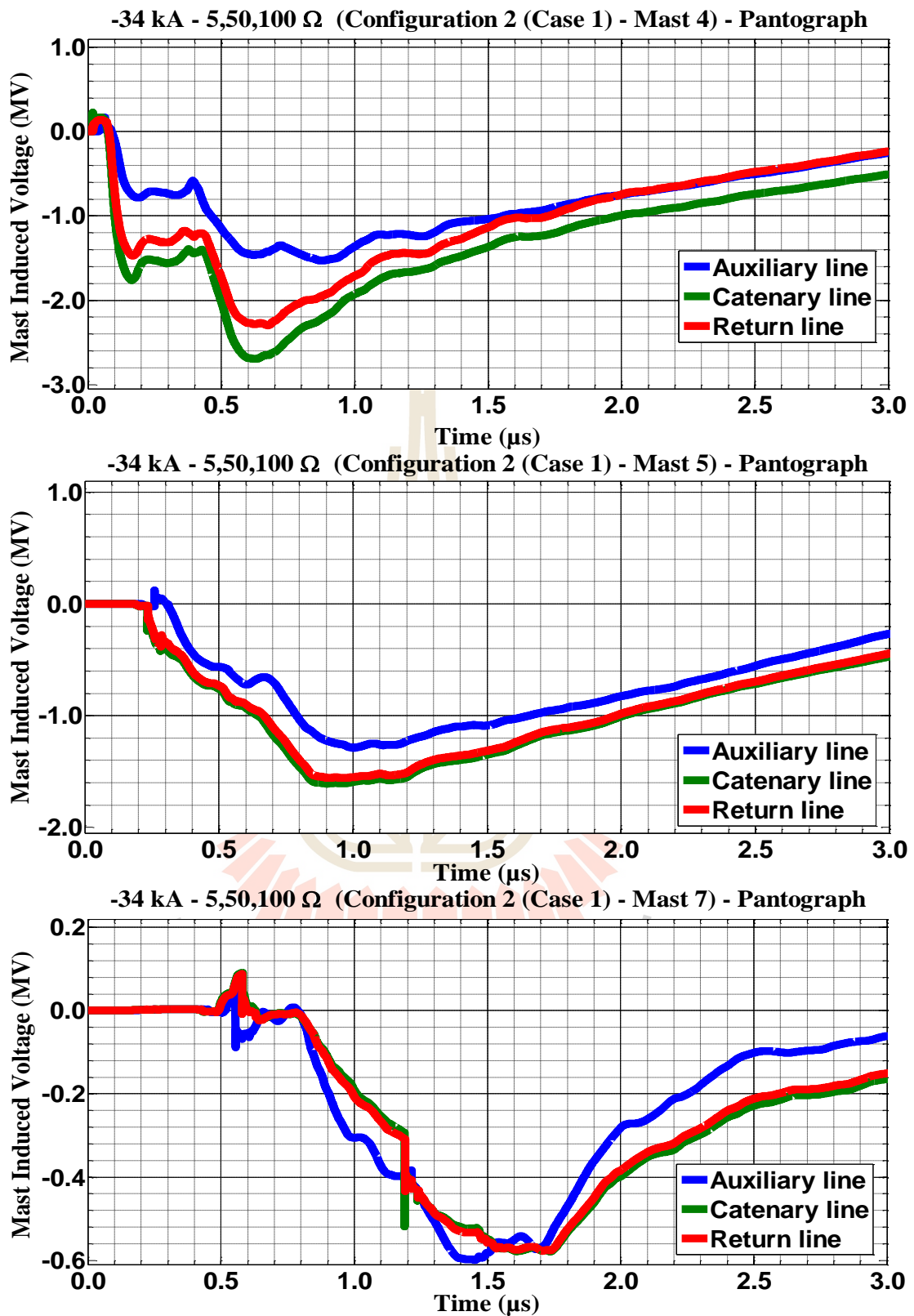


**Figure C.114** Mast 4, 5, and 7 with 5,50,100  $\Omega$  induced voltage waveform of -34 kA first stroke-(1.0/100  $\mu$ s), subsequent stroke-(0.2/50  $\mu$ s) strikes on Mast 4 for Case 1



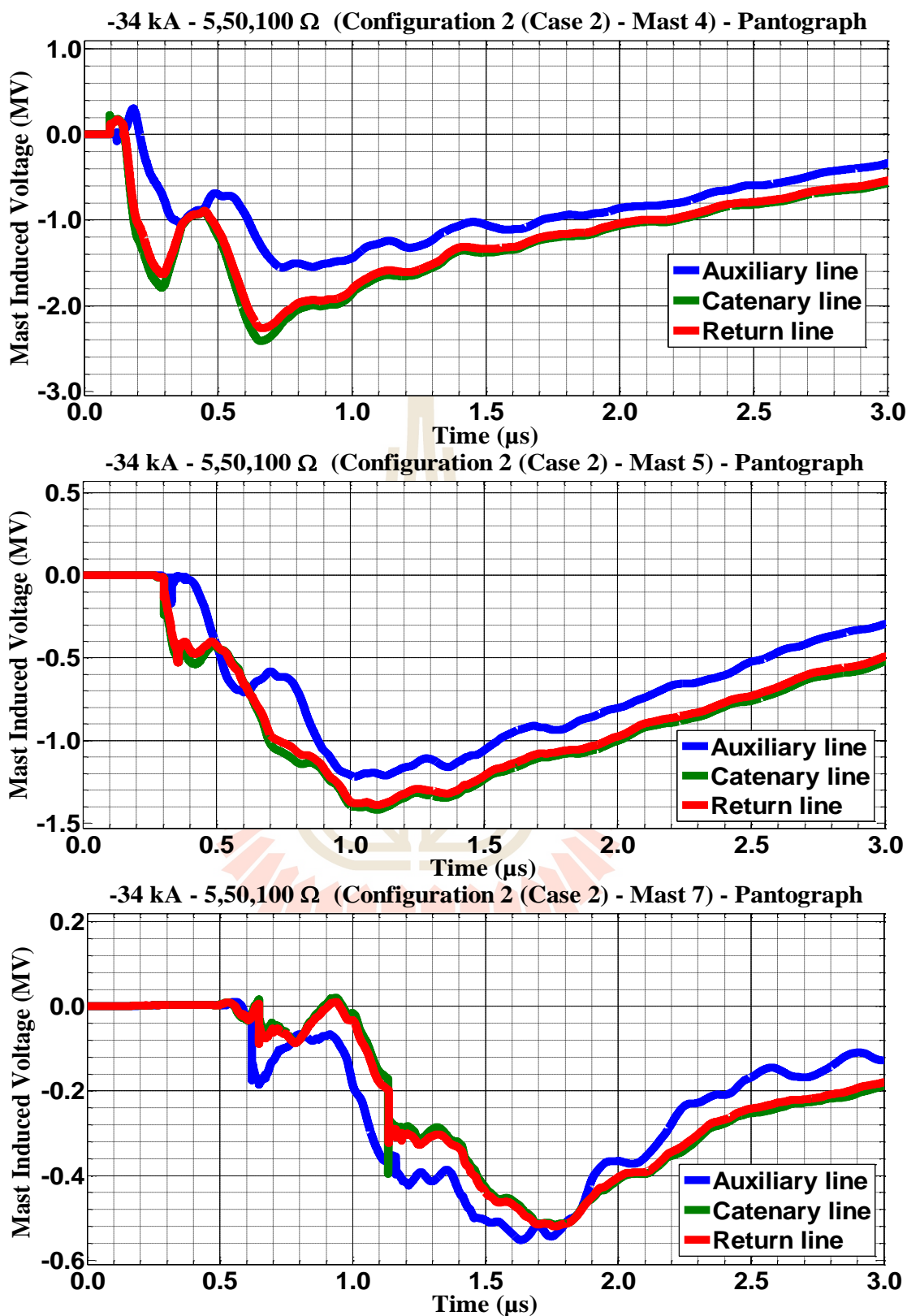


**Figure C.115** Mast 4, 5, and 7 with 5,50,100 Ω induced voltage waveform of -34 kA first stroke-(1.0/100 μs), subsequent stroke-(0.2/50 μs) strikes on Mast 4 for Case 2

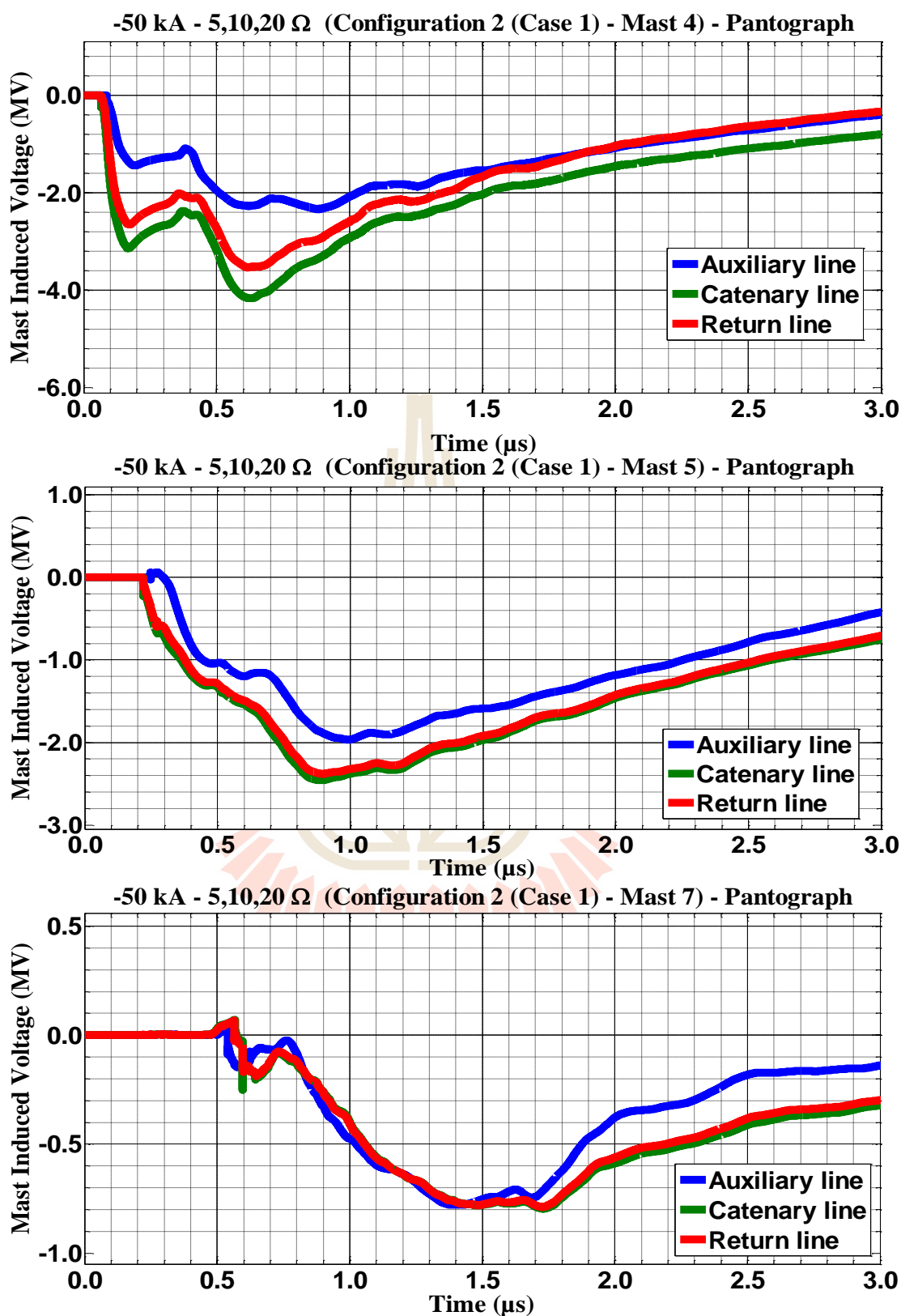


**Figure C.116** Mast 4, 5, and 7 with 5,10,20  $\Omega$  induced voltage waveform of -50 kA first stroke-(1.0/100  $\mu$ s), subsequent stroke-(0.2/50  $\mu$ s) strikes on Mast 4 for Case 1

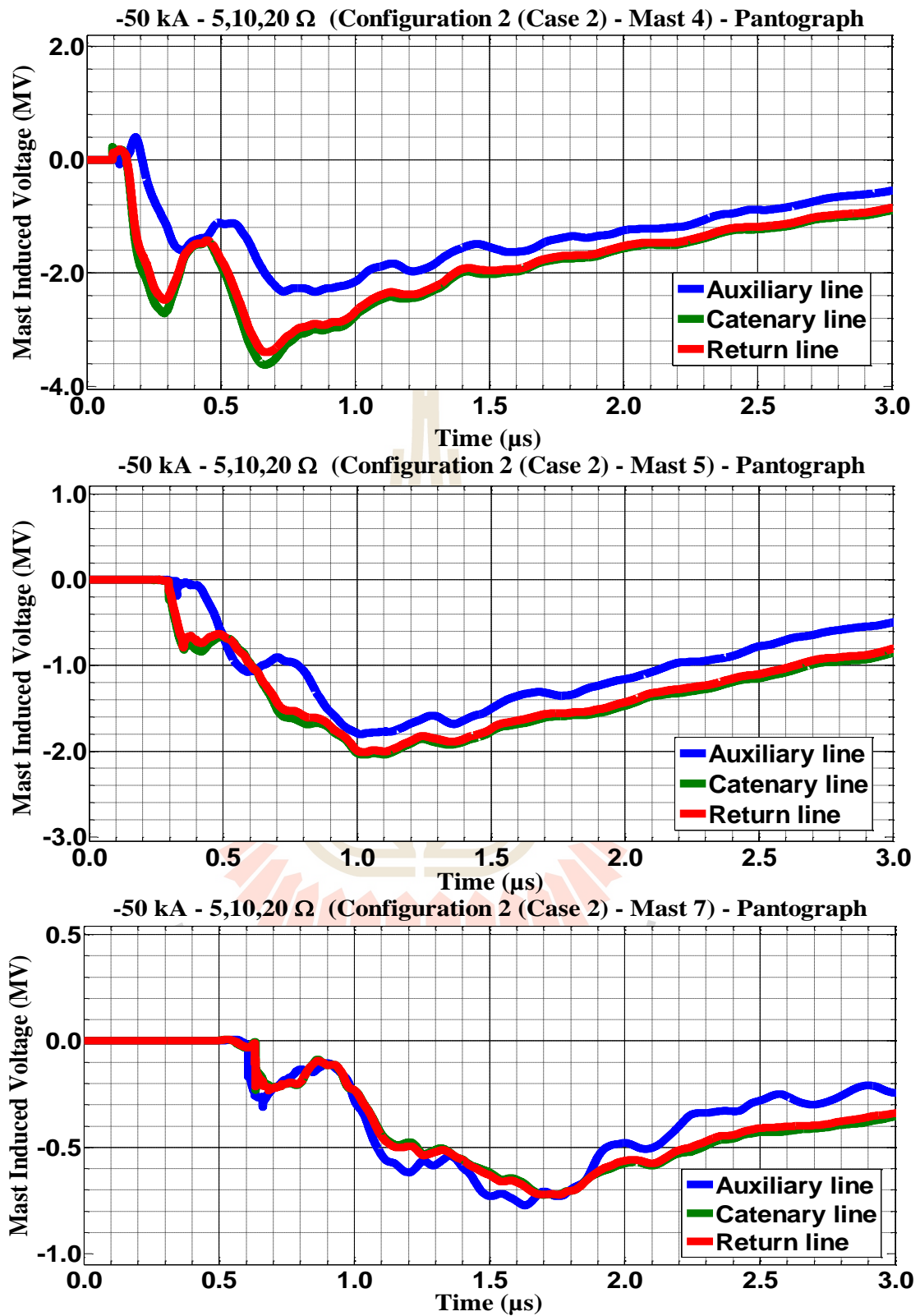


**Figure C.117** Mast 4, 5, and 7 with 5,10,20  $\Omega$  induced voltage waveform of -50 kA first stroke-(1.0/100  $\mu$ s), subsequent stroke-(0.2/50  $\mu$ s) strikes on Mast 4 for Case 2

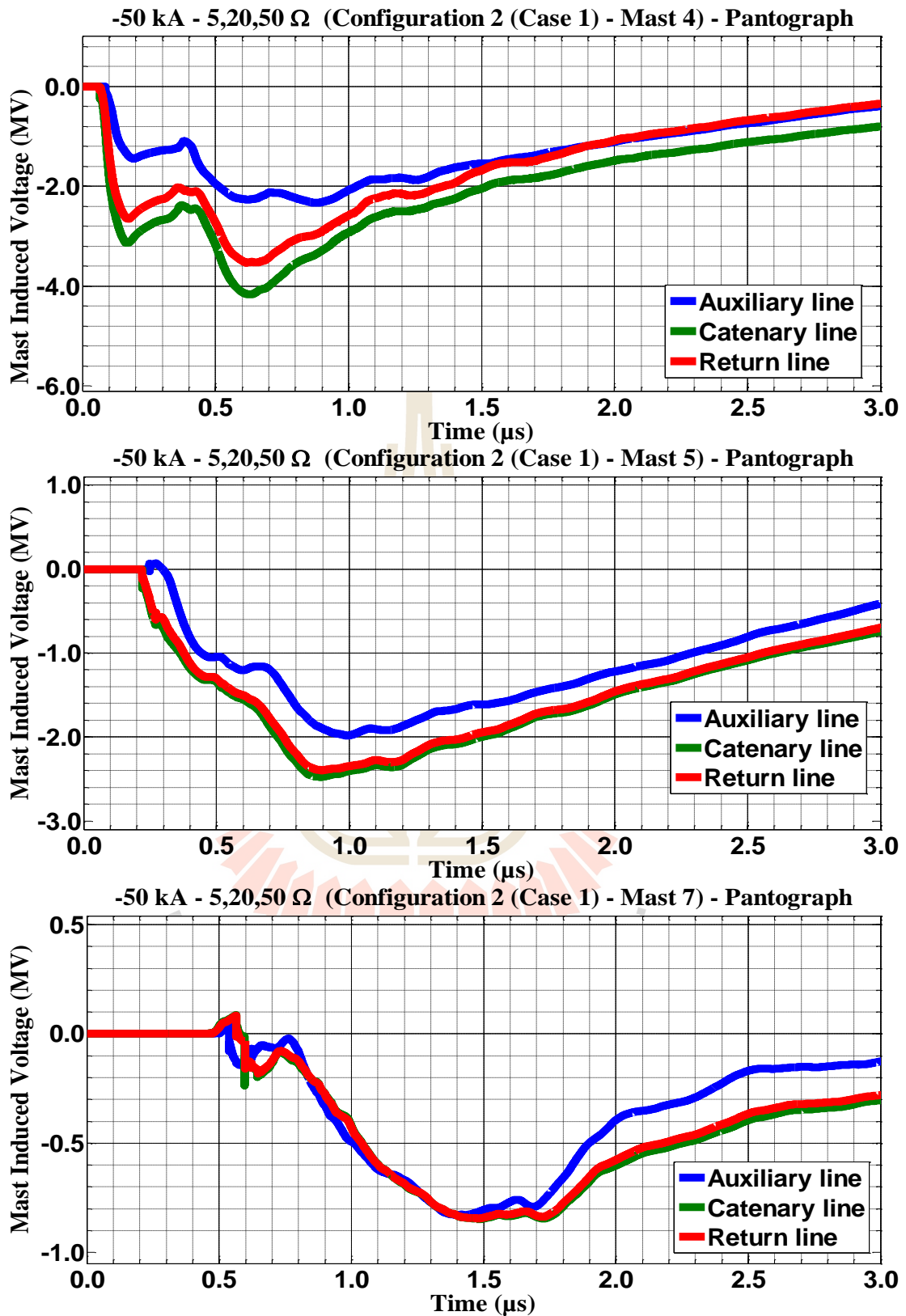


**Figure C.118** Mast 4, 5, and 7 with 5,20,50 Ω induced voltage waveform of -50 kA first stroke-(1.0/100 μs), subsequent stroke-(0.2/50 μs) strikes on Mast 4 for Case 1

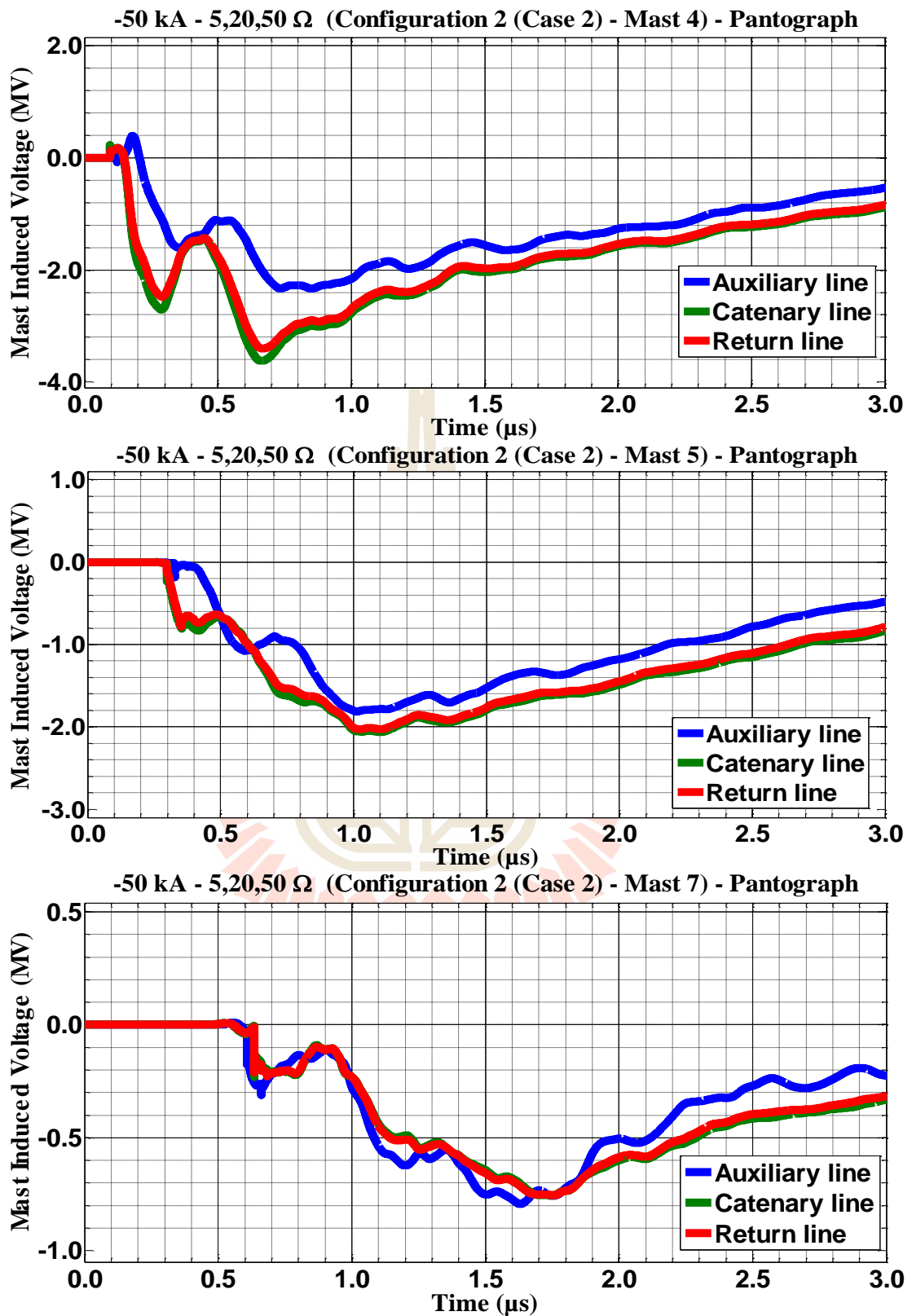


**Figure C.119** Mast 4, 5, and 7 with 5,20,50  $\Omega$  induced voltage waveform of -50 kA first stroke-(1.0/100  $\mu$ s), subsequent stroke-(0.2/50  $\mu$ s) strikes on Mast 4 for Case 2

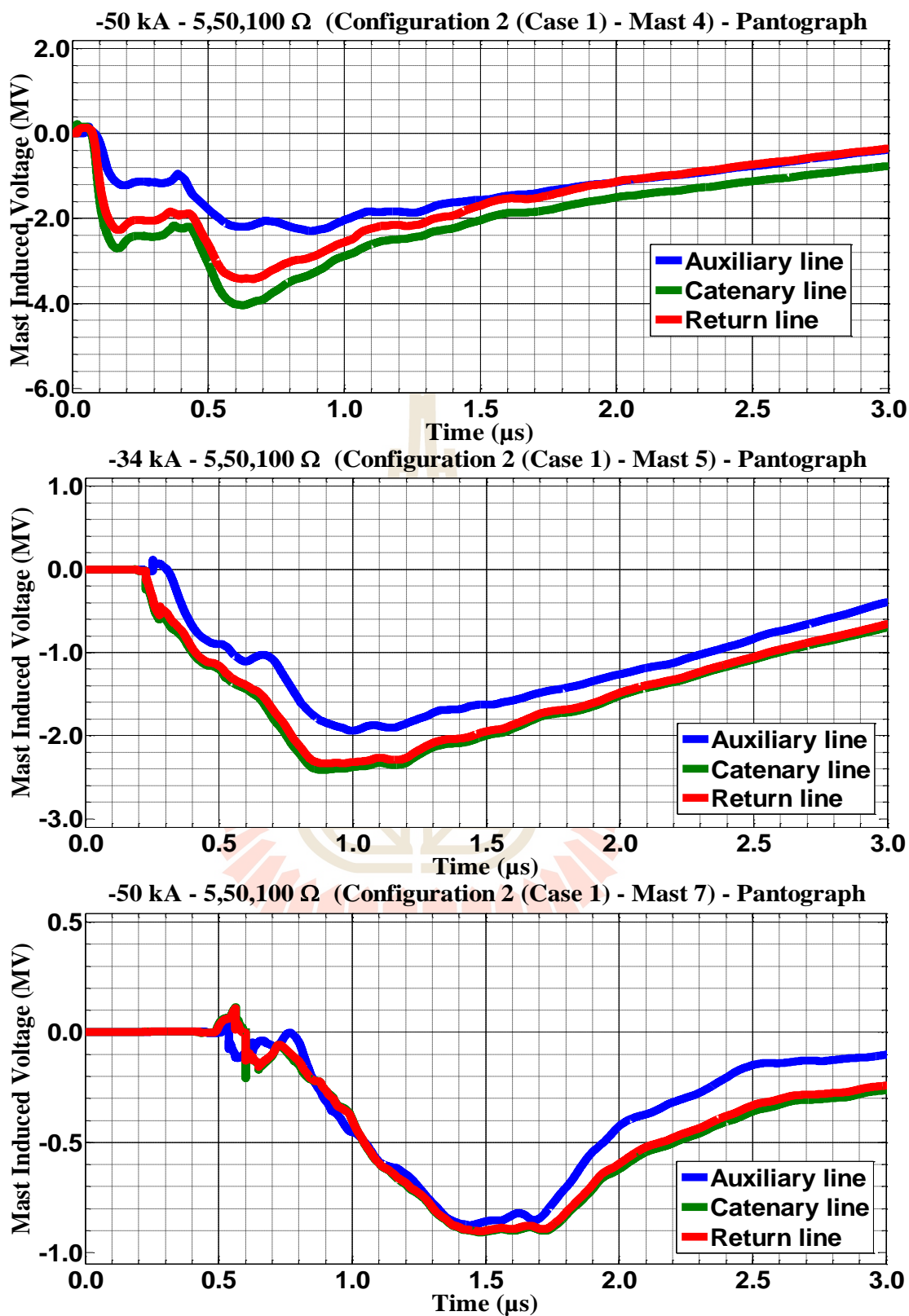
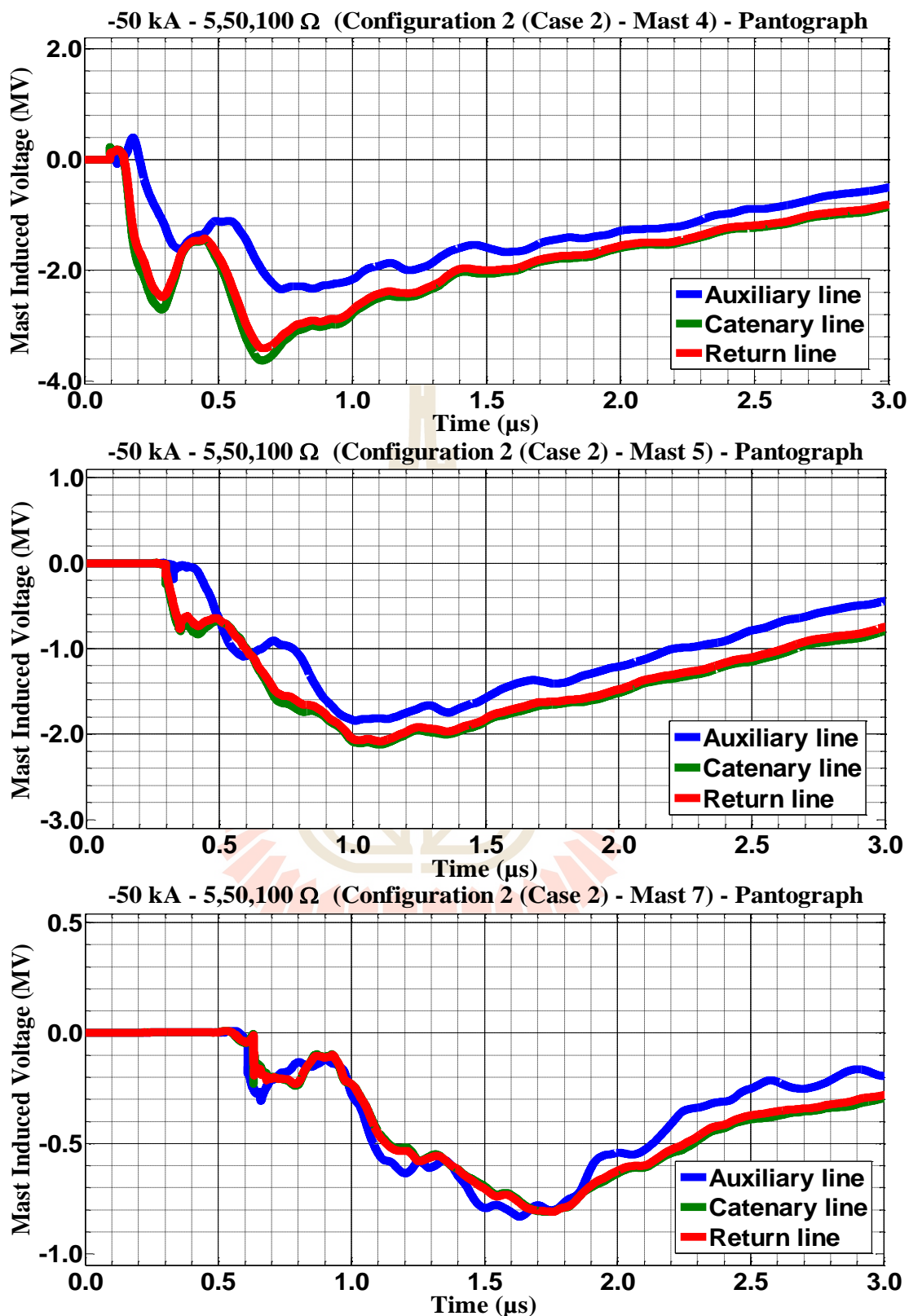


Figure C.120 Mast 4, 5, and 7 with 5,50,100  $\Omega$  induced voltage waveform of -50 kA first stroke-(1.0/100  $\mu\text{s}$ ), subsequent stroke-(0.2/50  $\mu\text{s}$ ) strikes on Mast 4 for Case 1



**Figure C.121** Mast 4, 5, and 7 with 5,50,100  $\Omega$  induced voltage waveform of -50 kA first stroke-(1.0/100  $\mu$ s), subsequent stroke-(0.2/50  $\mu$ s) strikes on Mast 4 for Case 2

### C.7 The consequences when the pantograph struck by negative multiple lightning strokes for Configuration 3 in Case 1 and 2.

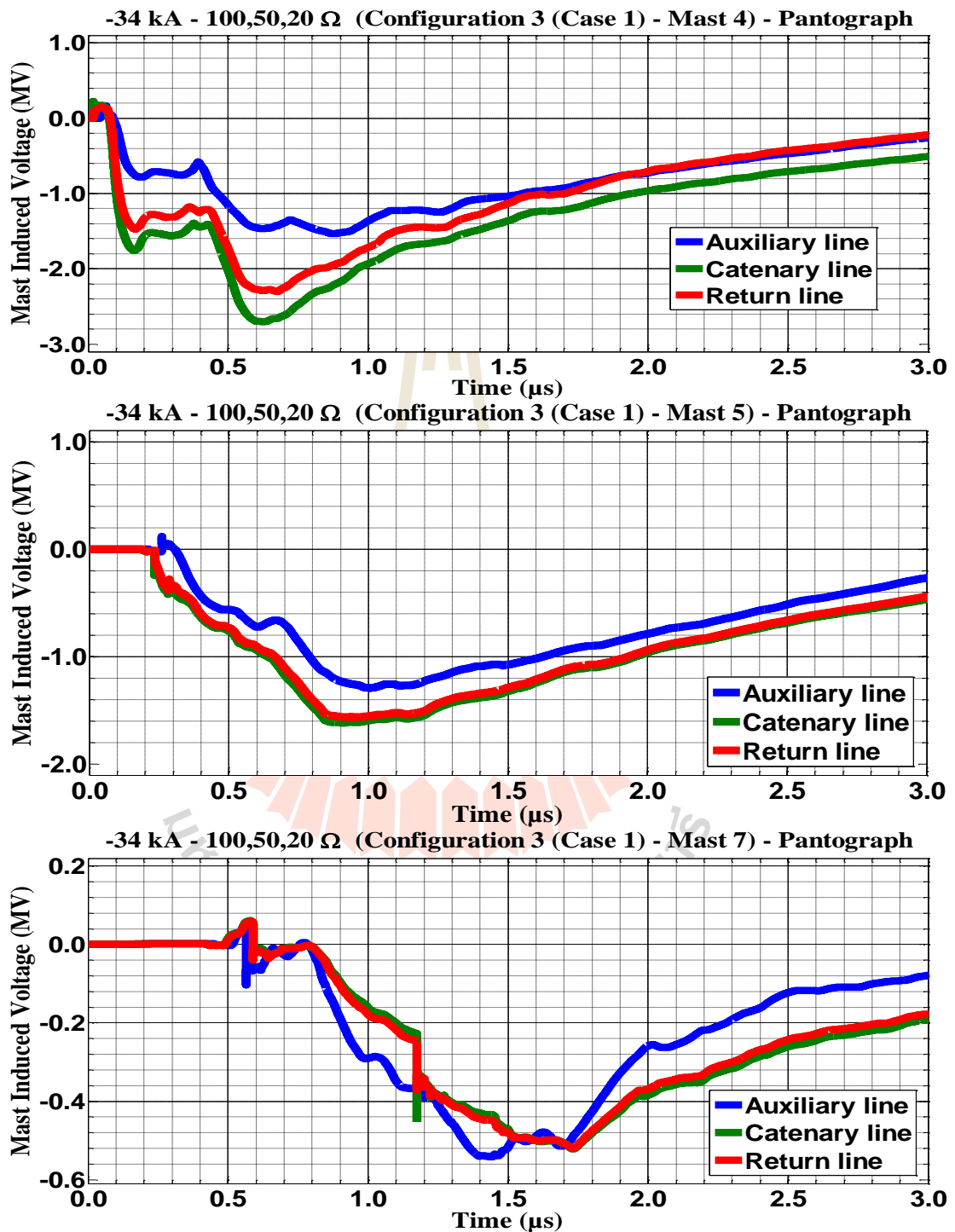
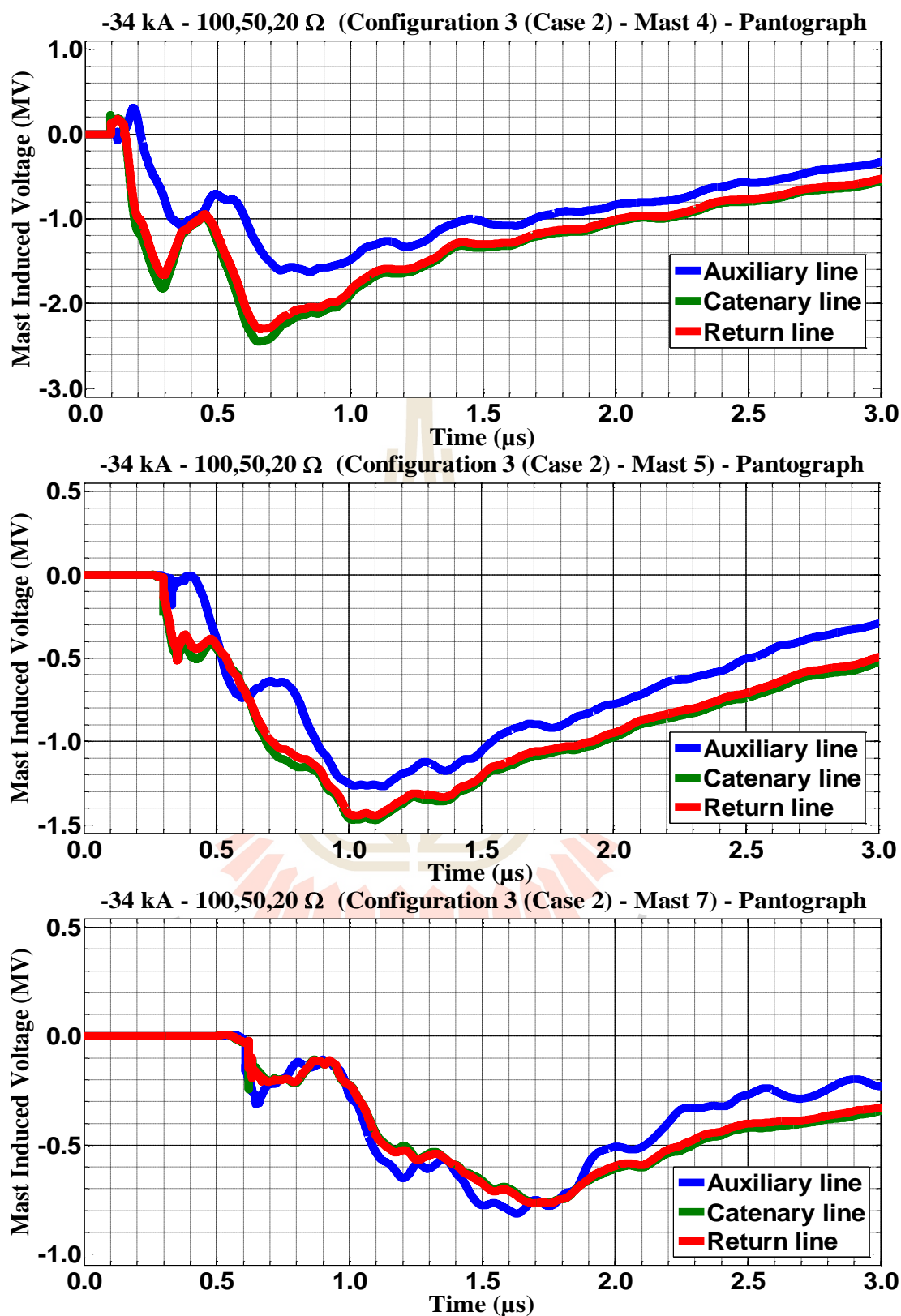
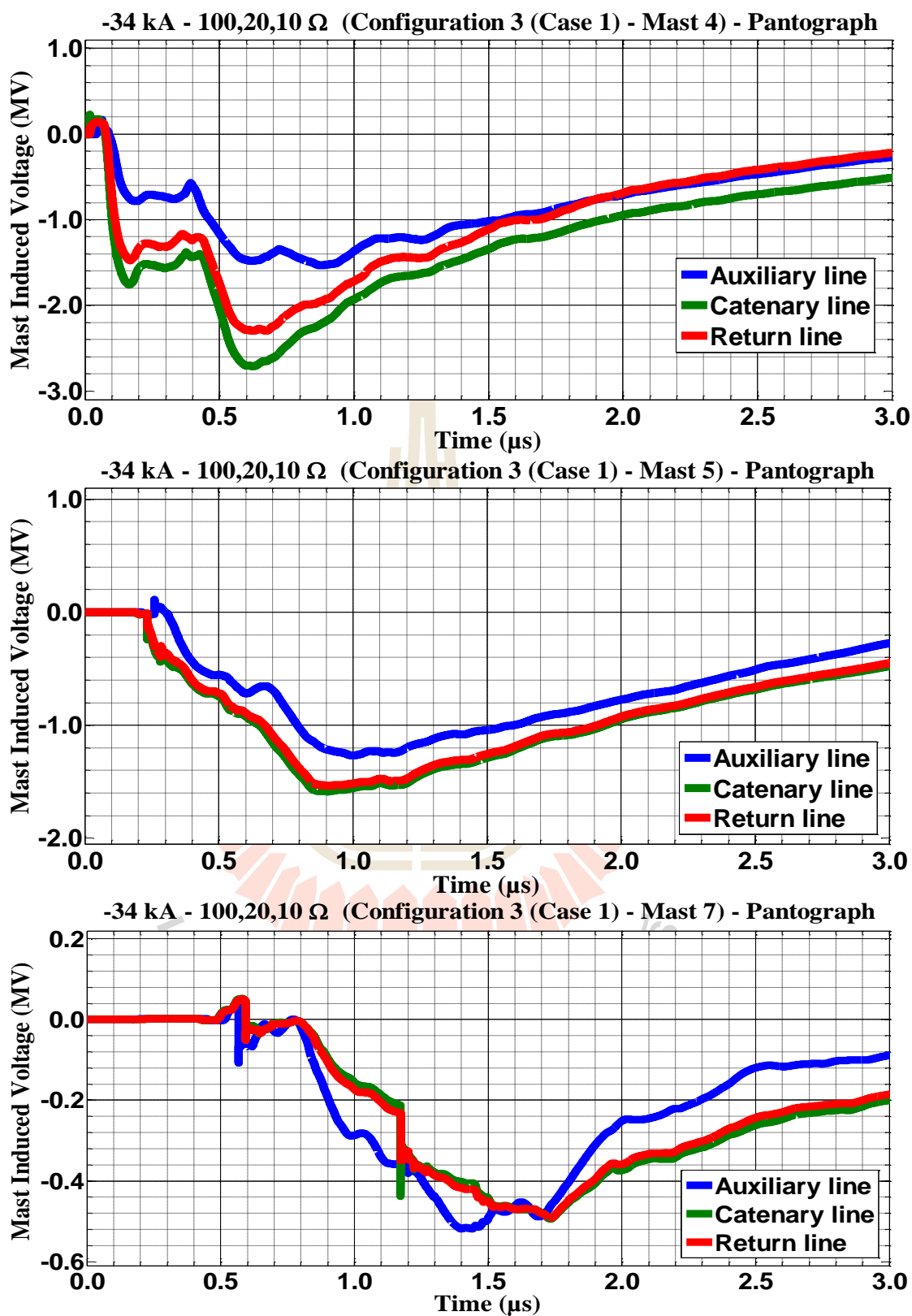


Figure C.122 Mast 4, 5, and 7 with 100,50,20 Ω induced voltage waveform of -34 kA first stroke-(1.0/100 μs), subsequent stroke-(0.2/50 μs) strikes on Mast 4 for Case 1





**Figure C.123** Mast 4, 5, and 7 with 100,50,20 Ω induced voltage waveform of -34 kA first stroke-(1.0/100 μs), subsequent stroke-(0.2/50 μs) strikes on Mast 4 for Case 2



**Figure C.124** Mast 4, 5, and 7 with 100,20,10  $\Omega$  induced voltage waveform of -34 kA first stroke-(1.0/100  $\mu$ s), subsequent stroke-(0.2/50  $\mu$ s) strikes on Mast 4 for Case 1

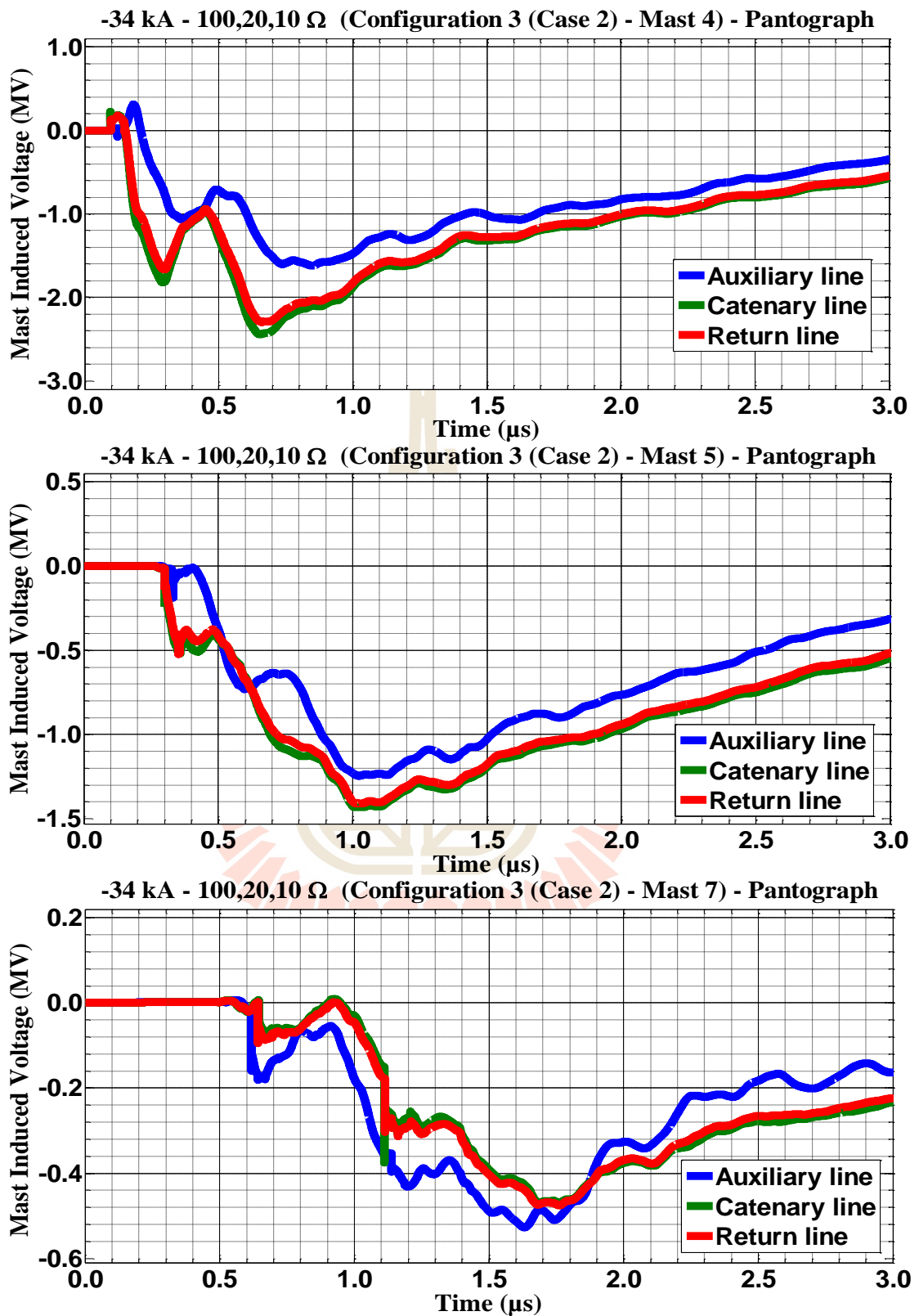


**Figure C.125** Mast 4, 5, and 7 with 100,20,10  $\Omega$  induced voltage waveform of -34 kA first stroke-(1.0/100  $\mu$ s), subsequent stroke-(0.2/50  $\mu$ s) strikes on Mast 4 for Case 2

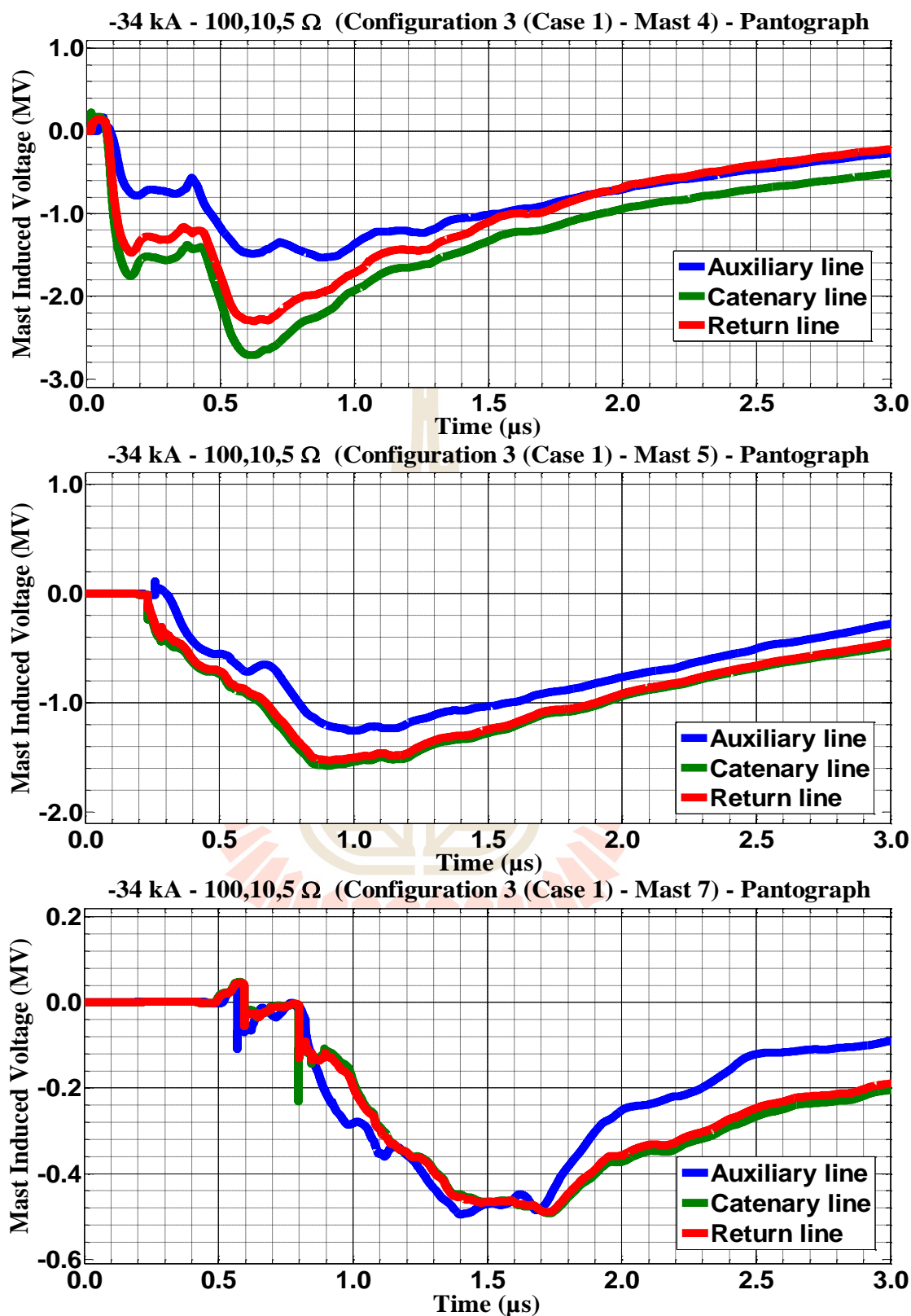
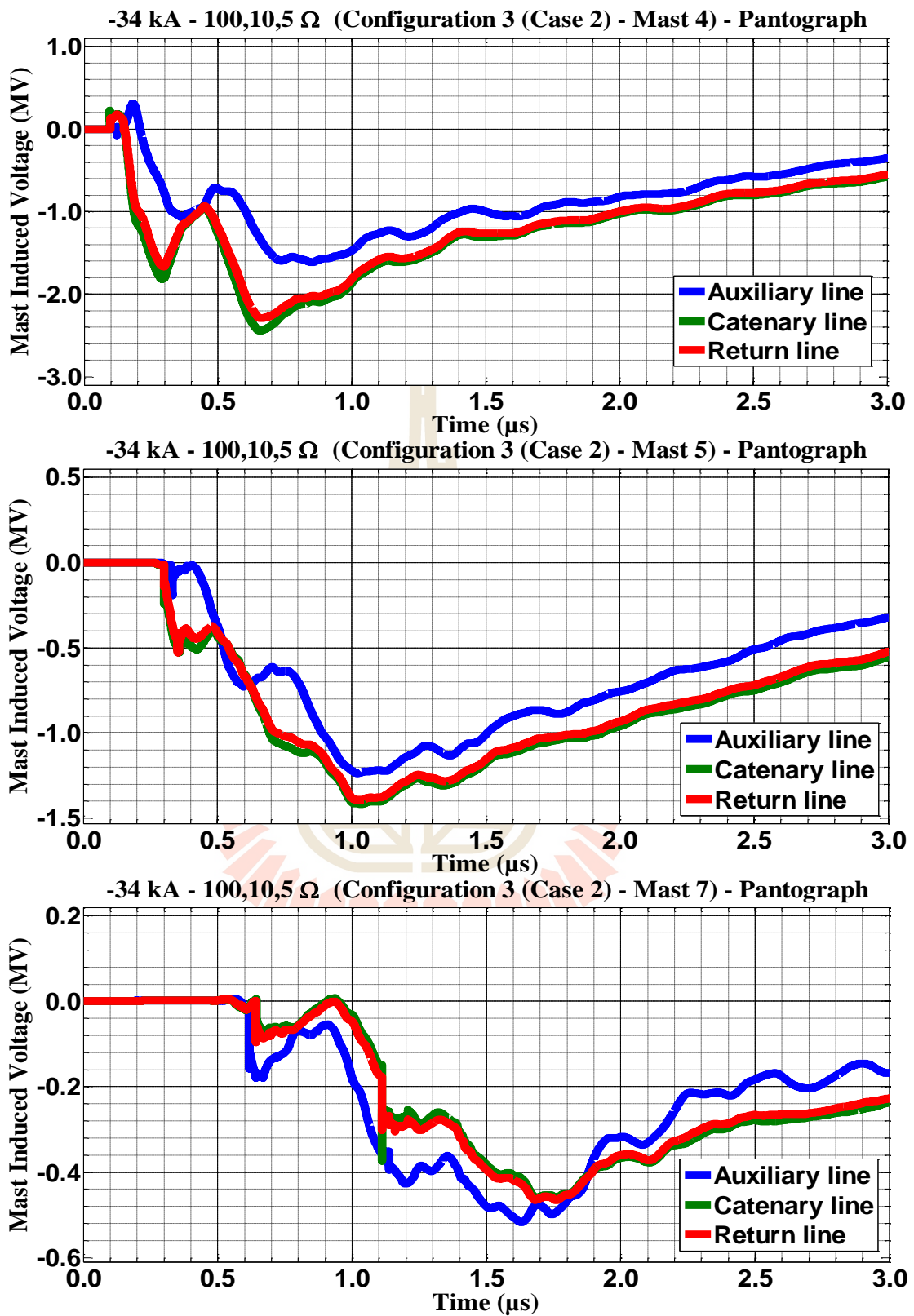
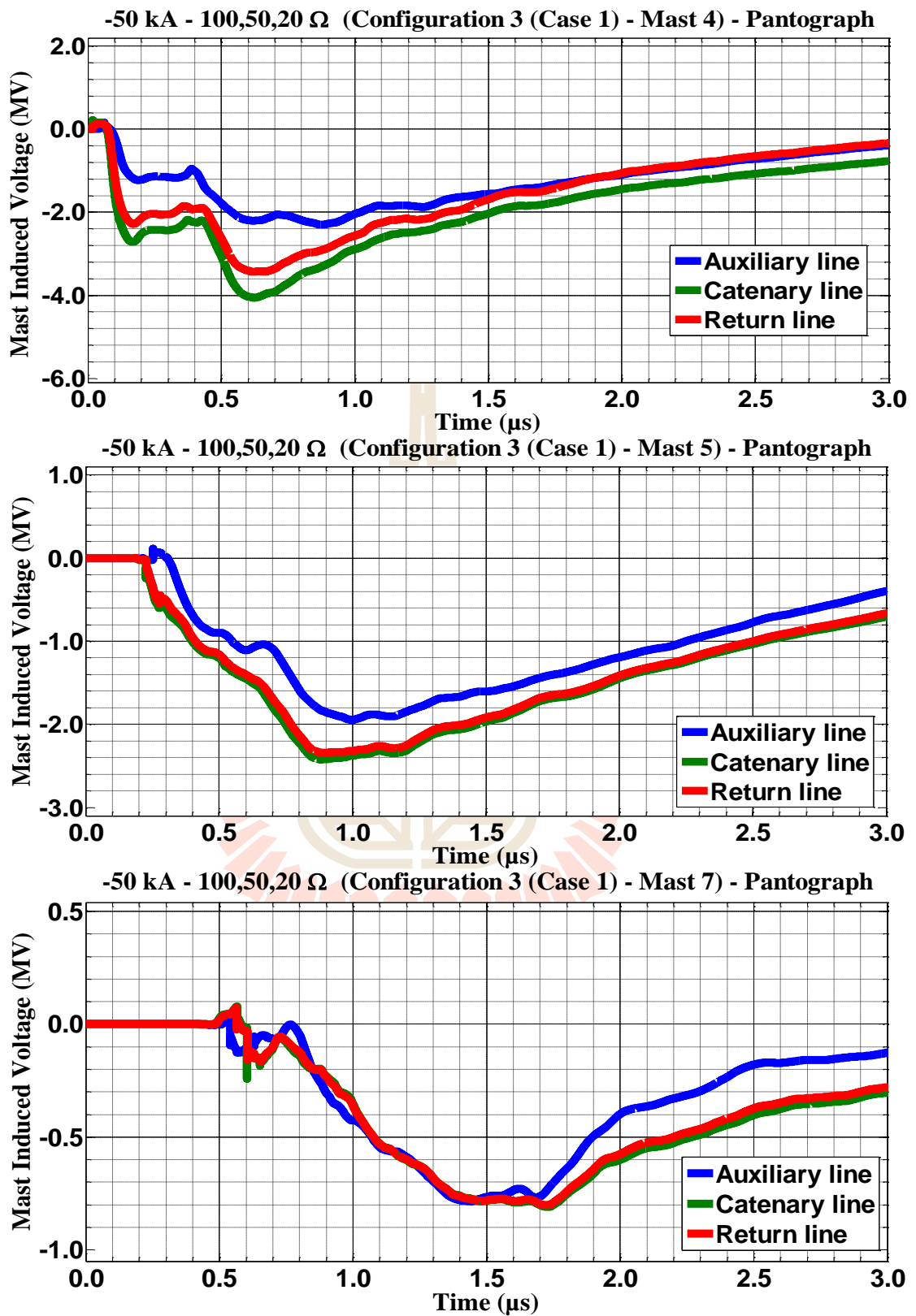


Figure C.126 Mast 4, 5, and 7 with 100,10,5  $\Omega$  induced voltage waveform of -34 kA first stroke-(1.0/100  $\mu$ s), subsequent stroke-(0.2/50  $\mu$ s) strikes on Mast 4 for Case 1



**Figure C.127** Mast 4, 5, and 7 with 100,10,5  $\Omega$  induced voltage waveform of -34 kA first stroke-(1.0/100  $\mu$ s), subsequent stroke-(0.2/50  $\mu$ s) strikes on Mast 4 for Case 2



**Figure C.128** Mast 4, 5, and 7 with 100,50,20  $\Omega$  induced voltage waveform of -50 kA first stroke-(1.0/100  $\mu$ s), subsequent stroke-(0.2/50  $\mu$ s) strikes on Mast 4 for Case 1

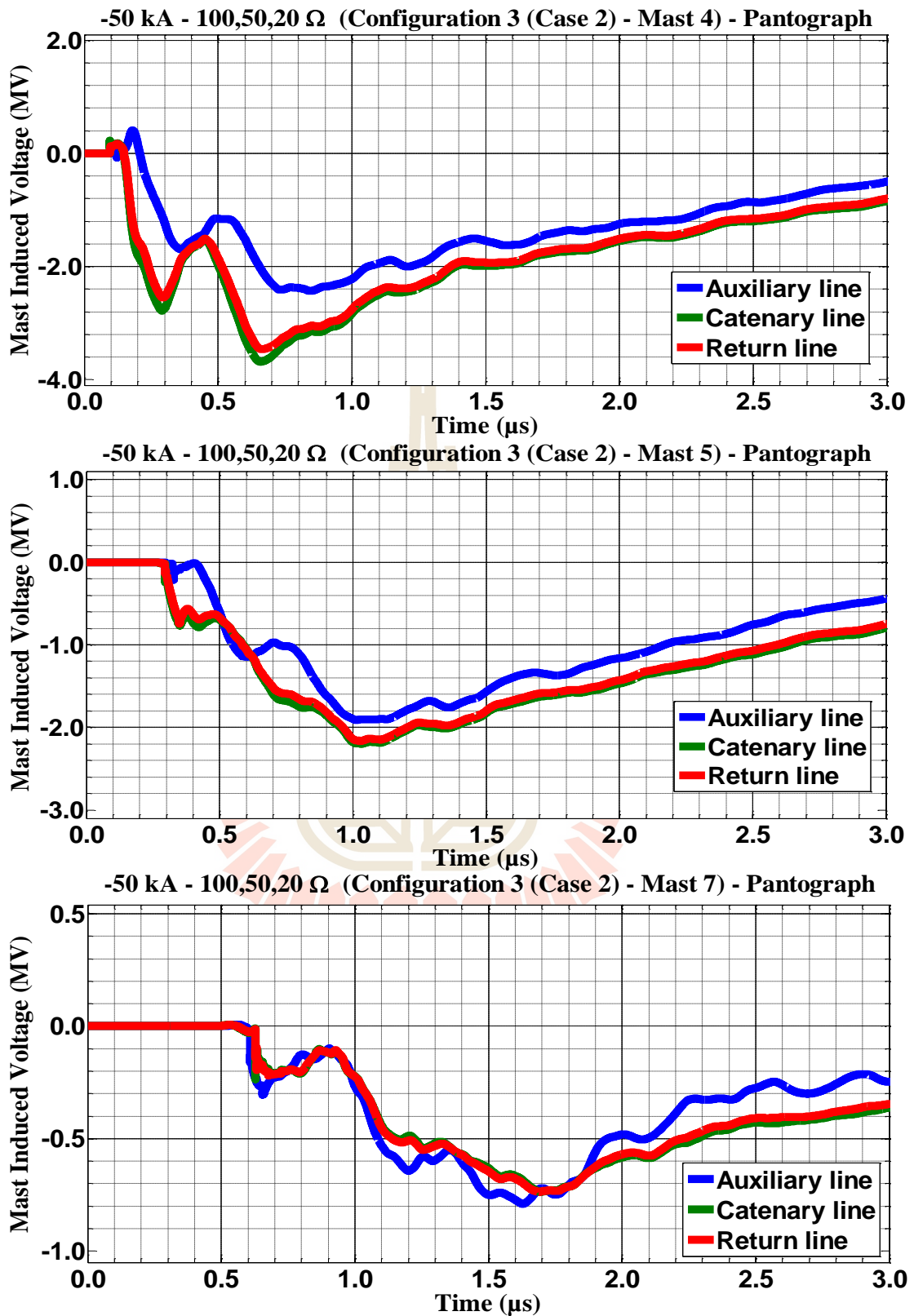


**Figure C.129** Mast 4, 5, and 7 with 100,50,20  $\Omega$  induced voltage waveform of -50 kA first stroke-(1.0/100  $\mu$ s), subsequent stroke-(0.2/50  $\mu$ s) strikes on Mast 4 for Case 2

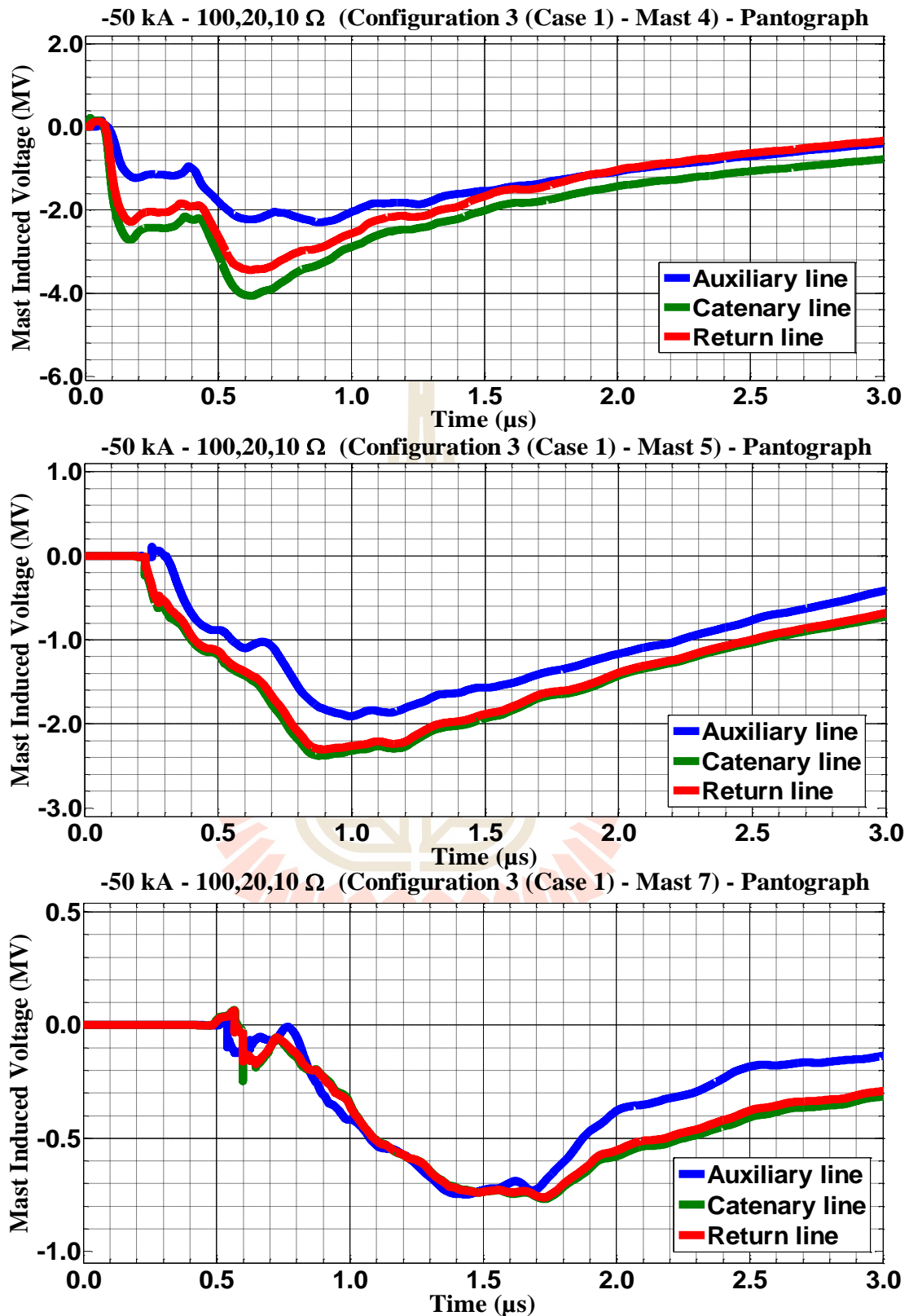


**Figure C.130** Mast 4, 5, and 7 with 100,20,10  $\Omega$  induced voltage waveform of -50 kA first stroke-(1.0/100  $\mu$ s), subsequent stroke-(0.2/50  $\mu$ s) strikes on Mast 4 for Case 1



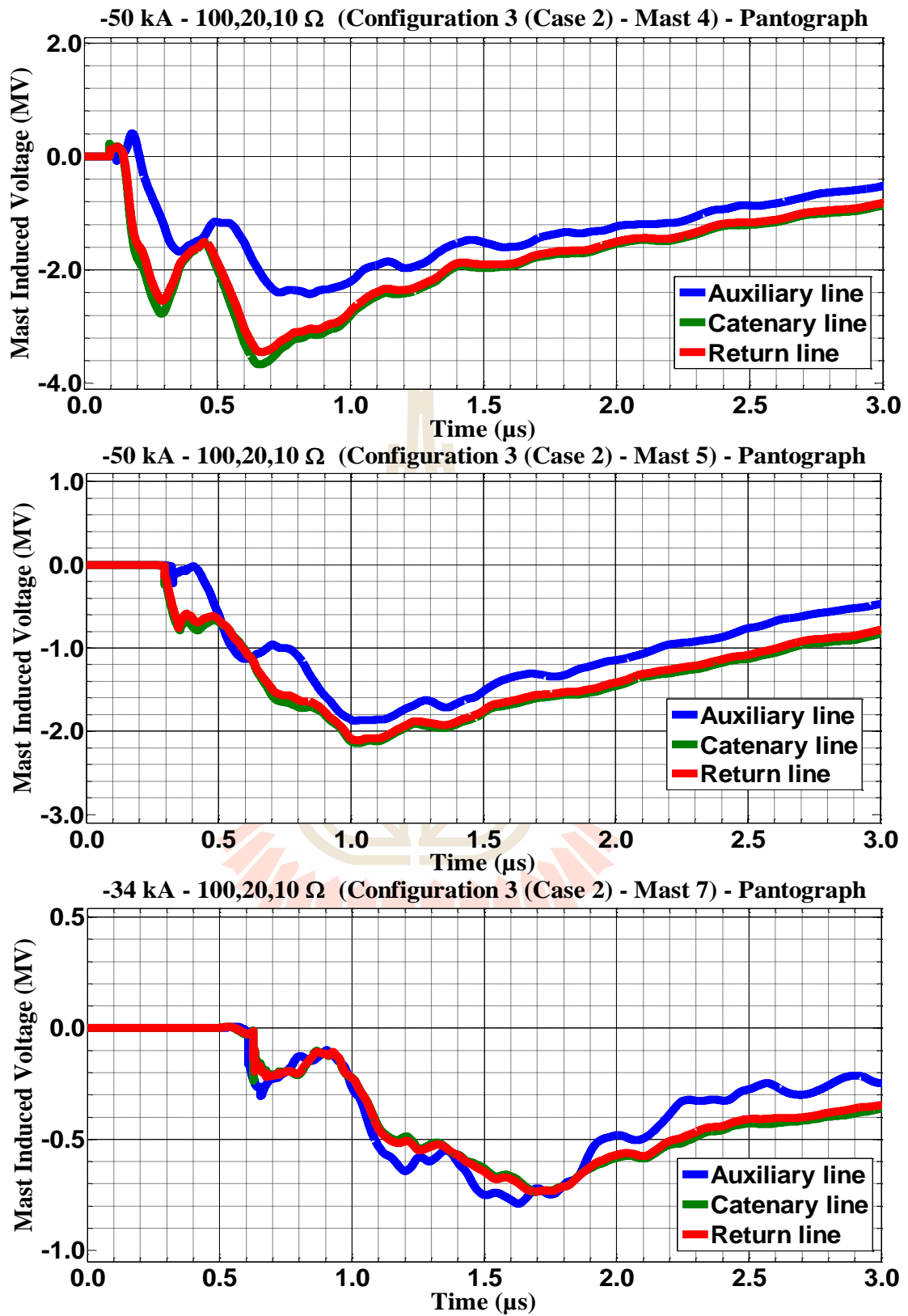


**Figure C.131** Mast 4, 5, and 7 with 100,20,10 Ω induced voltage waveform of -50 kA first stroke-(1.0/100 μs), subsequent stroke-(0.2/50 μs) strikes on Mast 4 for Case 2

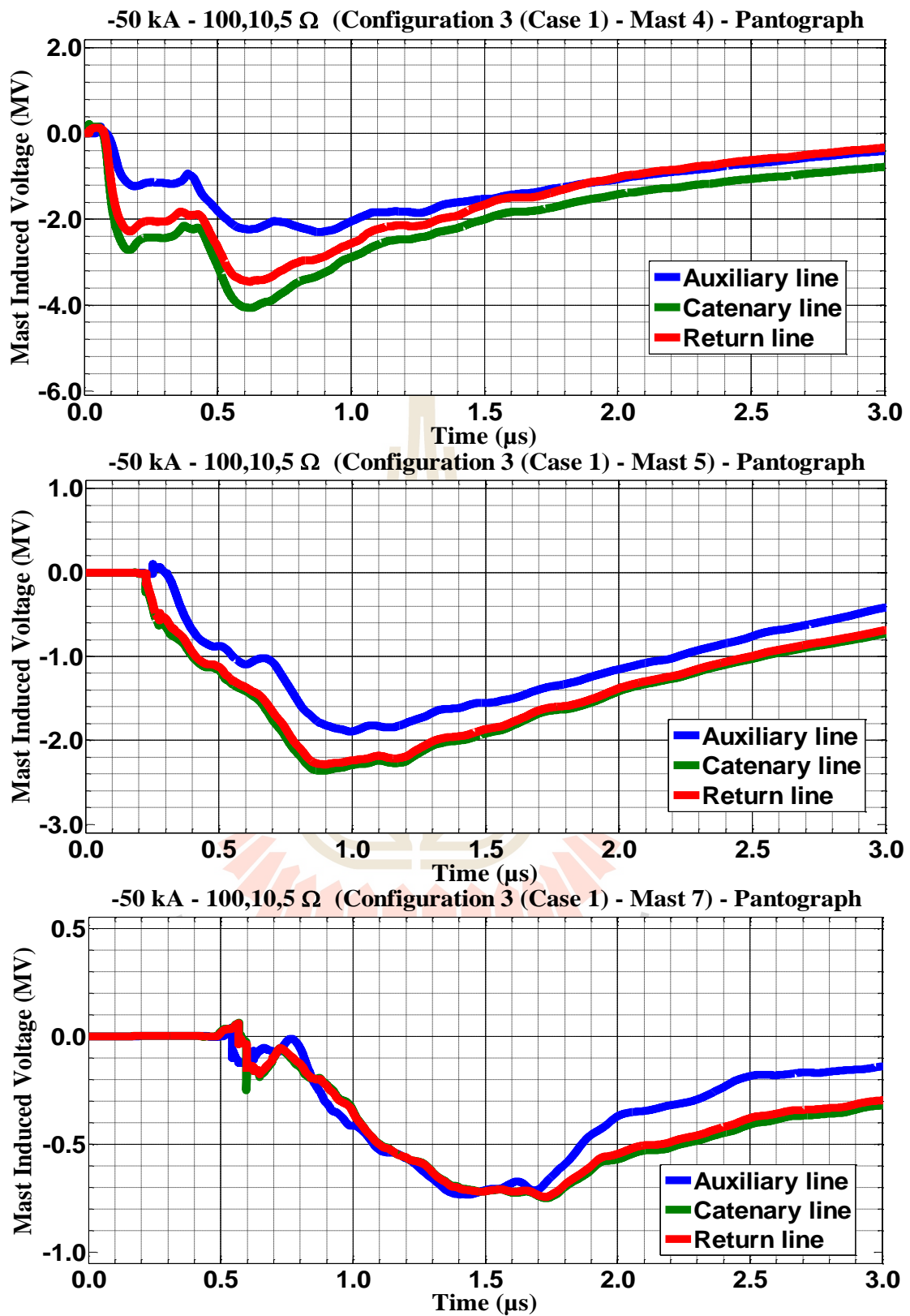


**Figure C.132** Mast 4, 5, and 7 with 100,10,5  $\Omega$  induced voltage waveform of -50 kA first stroke-(1.0/100  $\mu\text{s}$ ), subsequent stroke-(0.2/50  $\mu\text{s}$ ) strikes on Mast 4 for Case 1

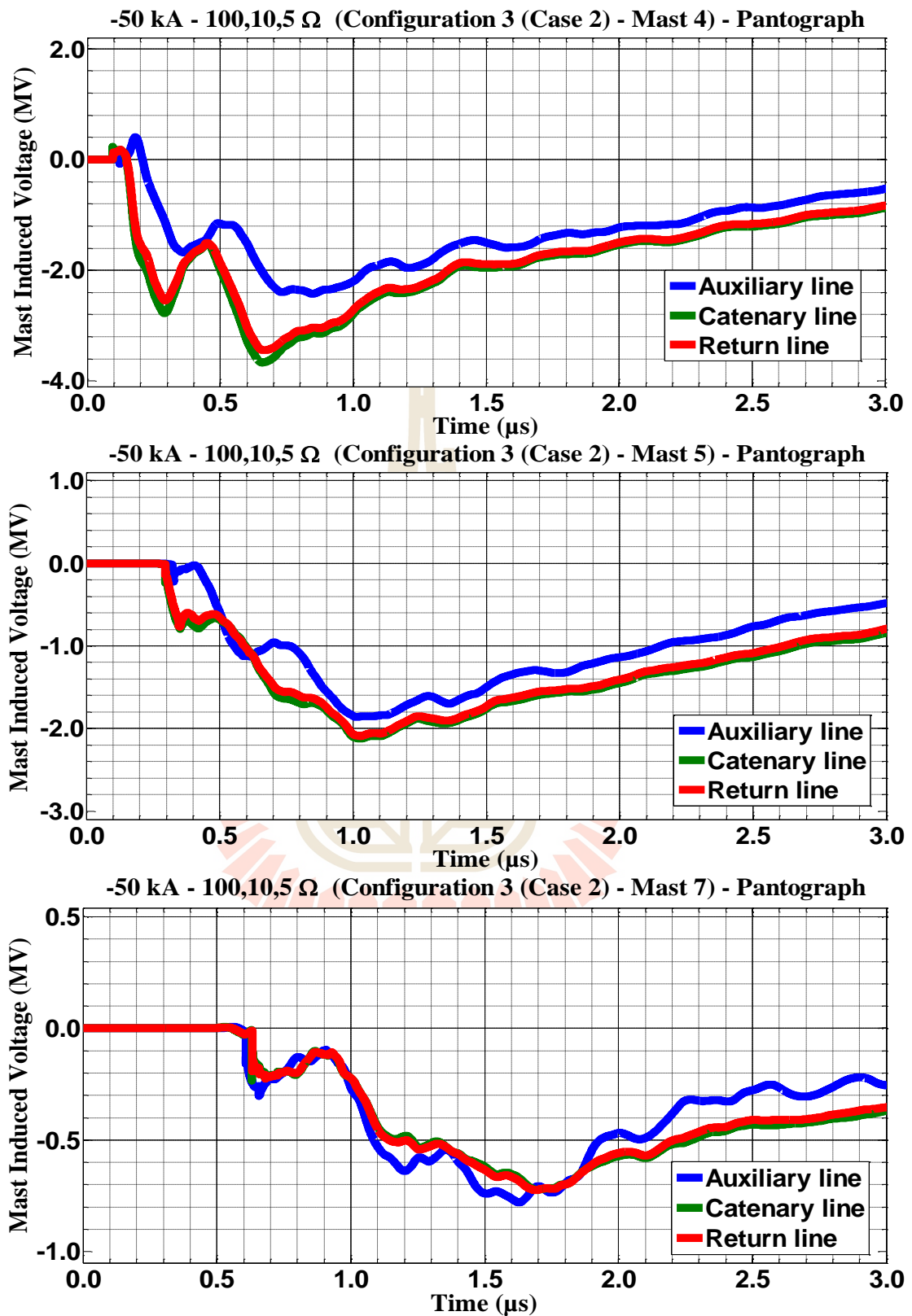


**Figure C.133** Mast 4, 5, and 7 with 100,10,5  $\Omega$  induced voltage waveform of -50 kA first stroke-(1.0/100  $\mu$ s), subsequent stroke-(0.2/50  $\mu$ s) strikes on Mast 4 for Case 2

**C.8 The consequences when the catenary struck by negative multiple lightning strokes for Configuration 1 in Case 1 and 2.**

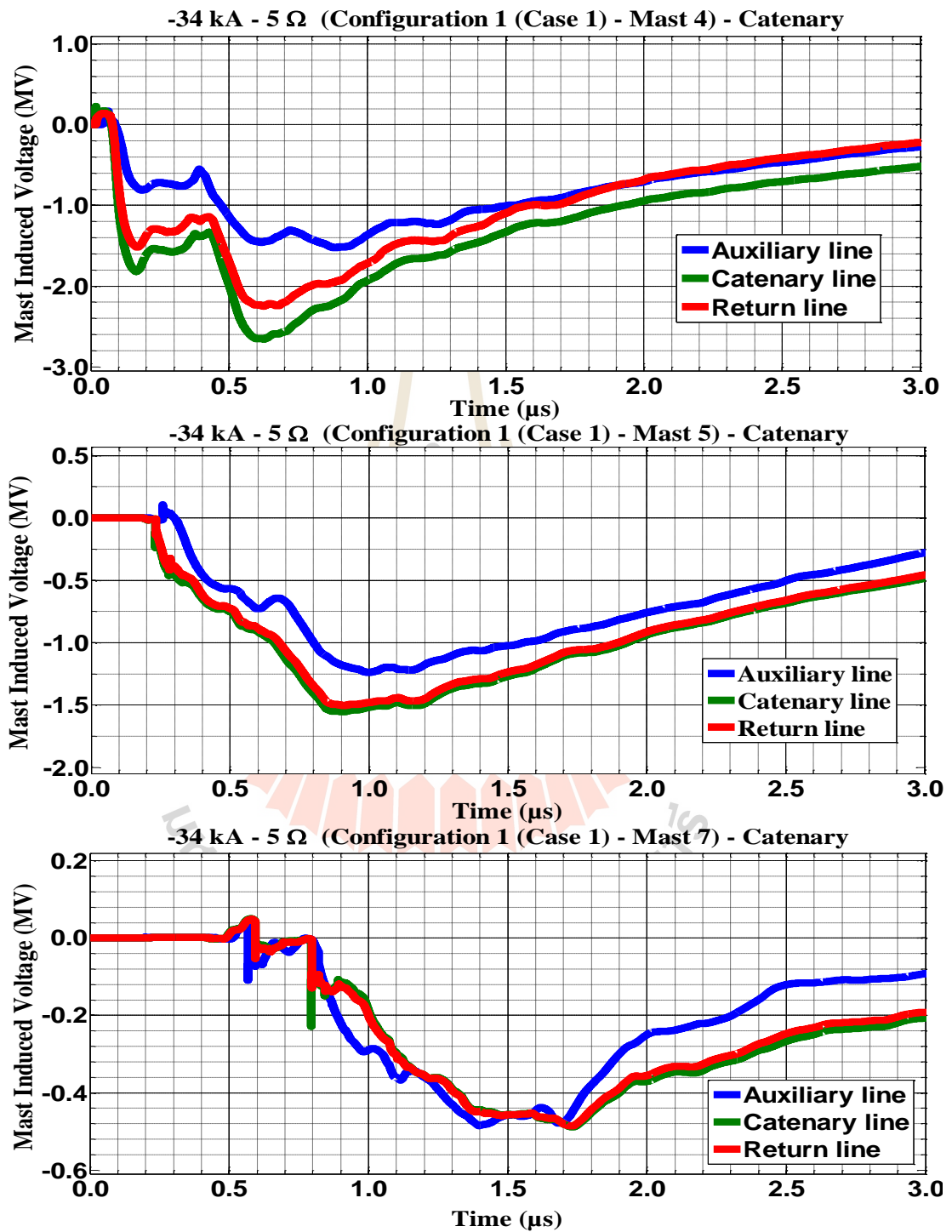


**Figure C.134** Mast 4, 5, and 7 induced voltage waveform of the -34 kA first stroke-(1.0/100  $\mu\text{s}$ ), subsequent stroke-(0.2/50  $\mu\text{s}$ ) strikes on Mast 4 with 5  $\Omega$  for Case 1

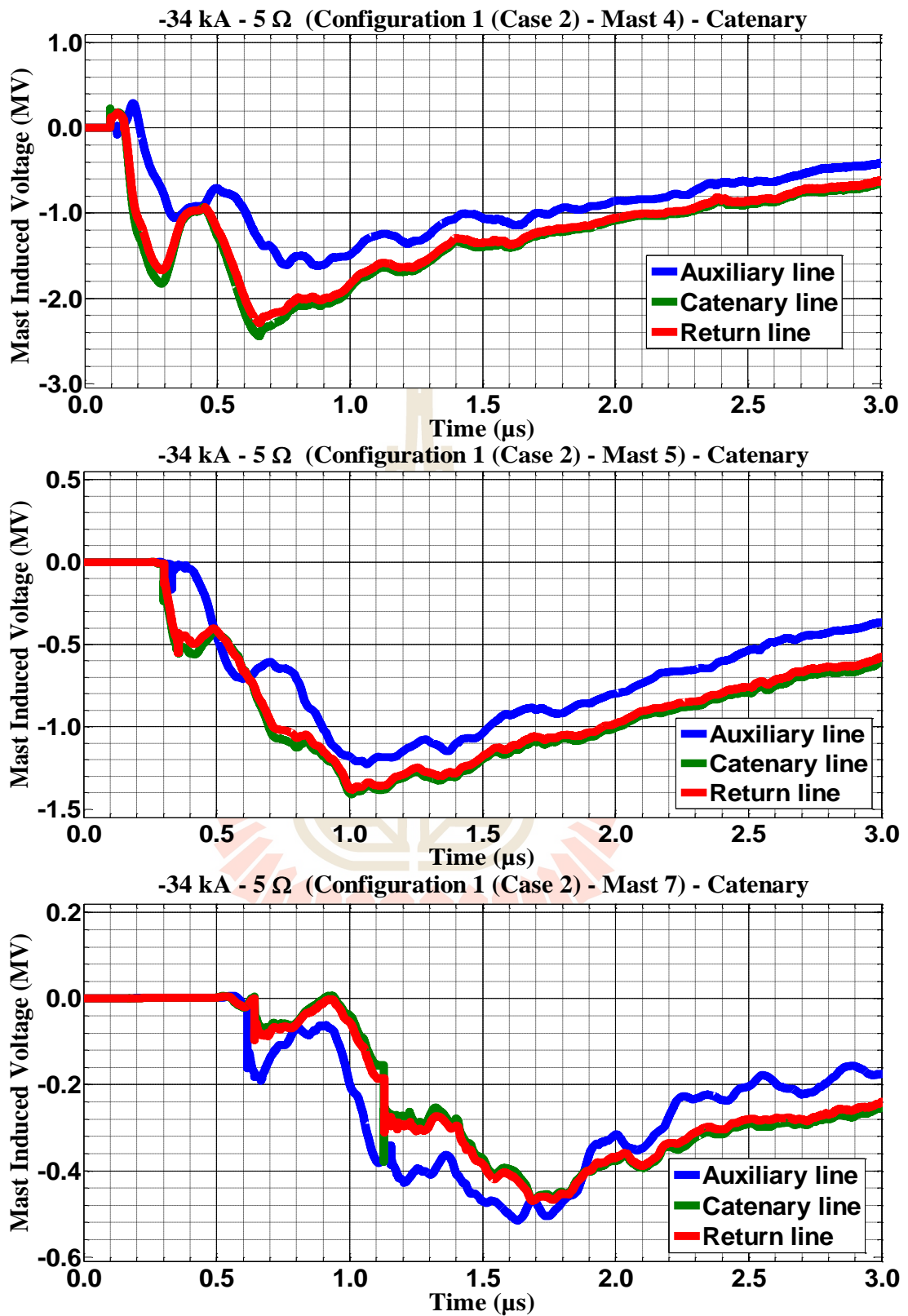


**Figure C.135** Mast 4, 5, and 7 induced voltage waveform of the -34 kA first stroke-(1.0/100  $\mu\text{s}$ ), subsequent stroke-(0.2/50  $\mu\text{s}$ ) strikes on Mast 4 with 5  $\Omega$  for Case 2

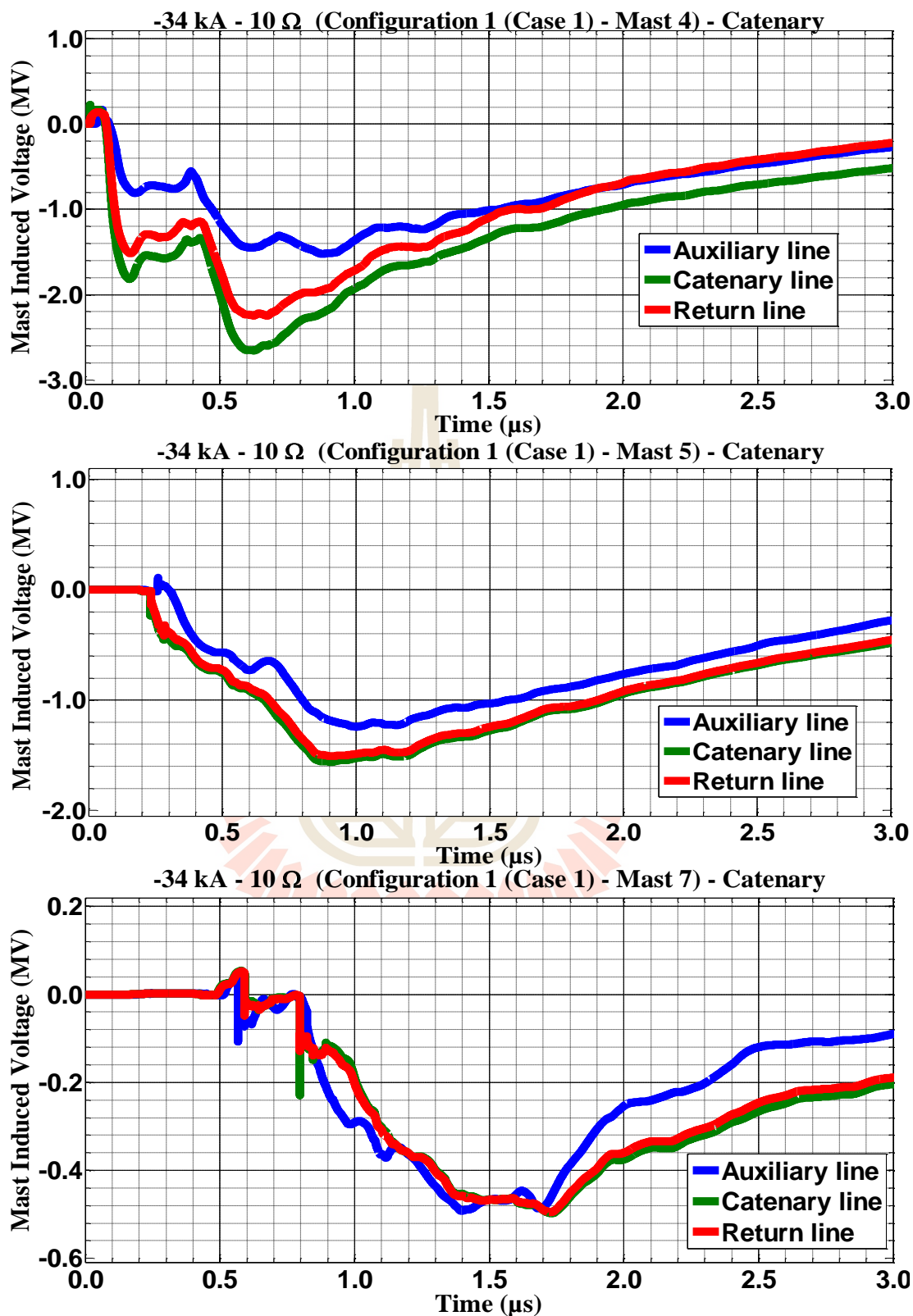


**Figure C.136** Mast 4, 5, and 7 induced voltage waveform of the -34 kA first stroke-(1.0/100  $\mu\text{s}$ ), subsequent stroke-(0.2/50  $\mu\text{s}$ ) strikes on Mast 4 with 10  $\Omega$  for Case 1

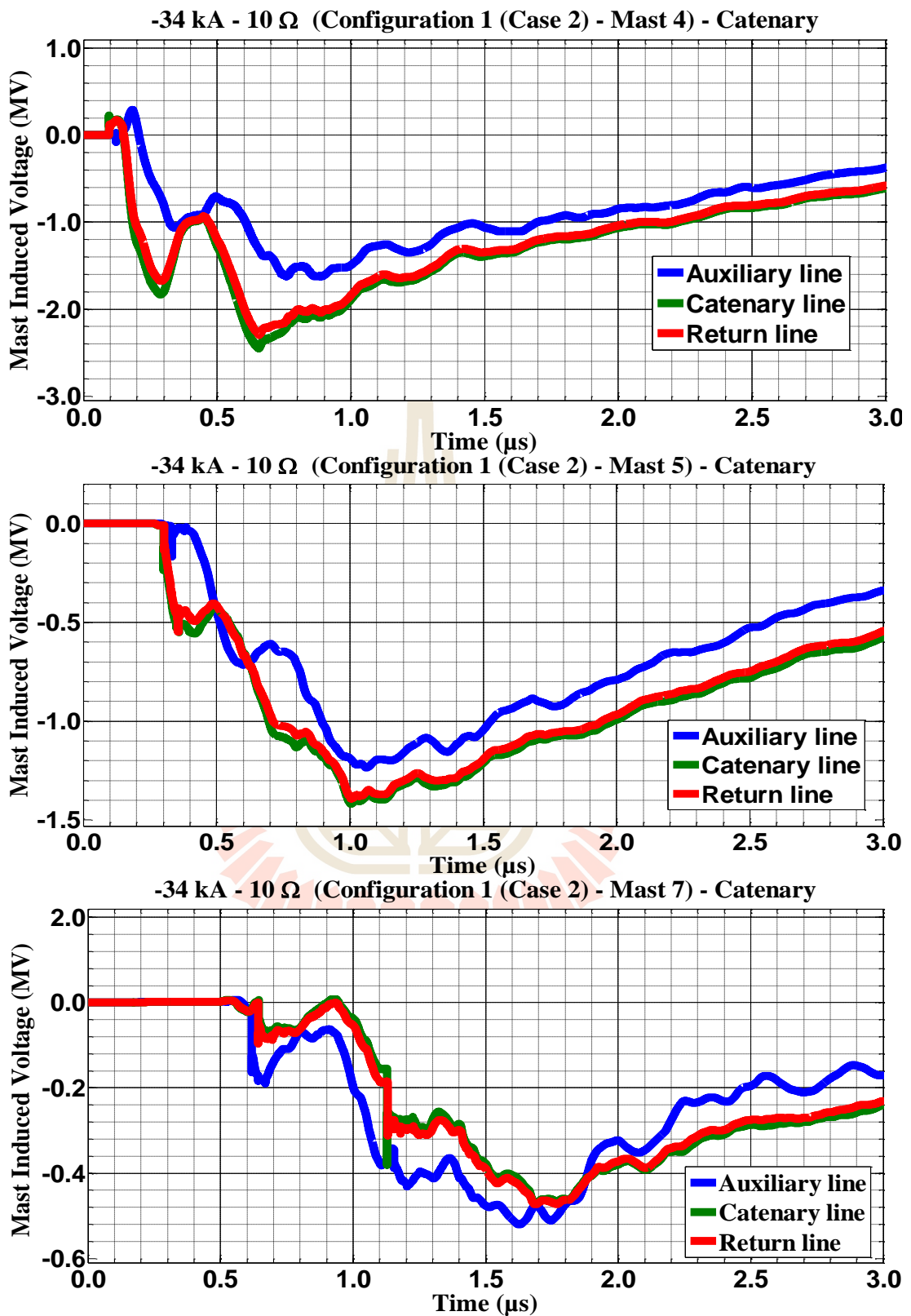


**Figure C.137** Mast 4, 5, and 7 induced voltage waveform of the  $-34 \text{ kA}$  first stroke-(1.0/100  $\mu\text{s}$ ), subsequent stroke-(0.2/50  $\mu\text{s}$ ) strikes on Mast 4 with  $10 \Omega$  for Case 2

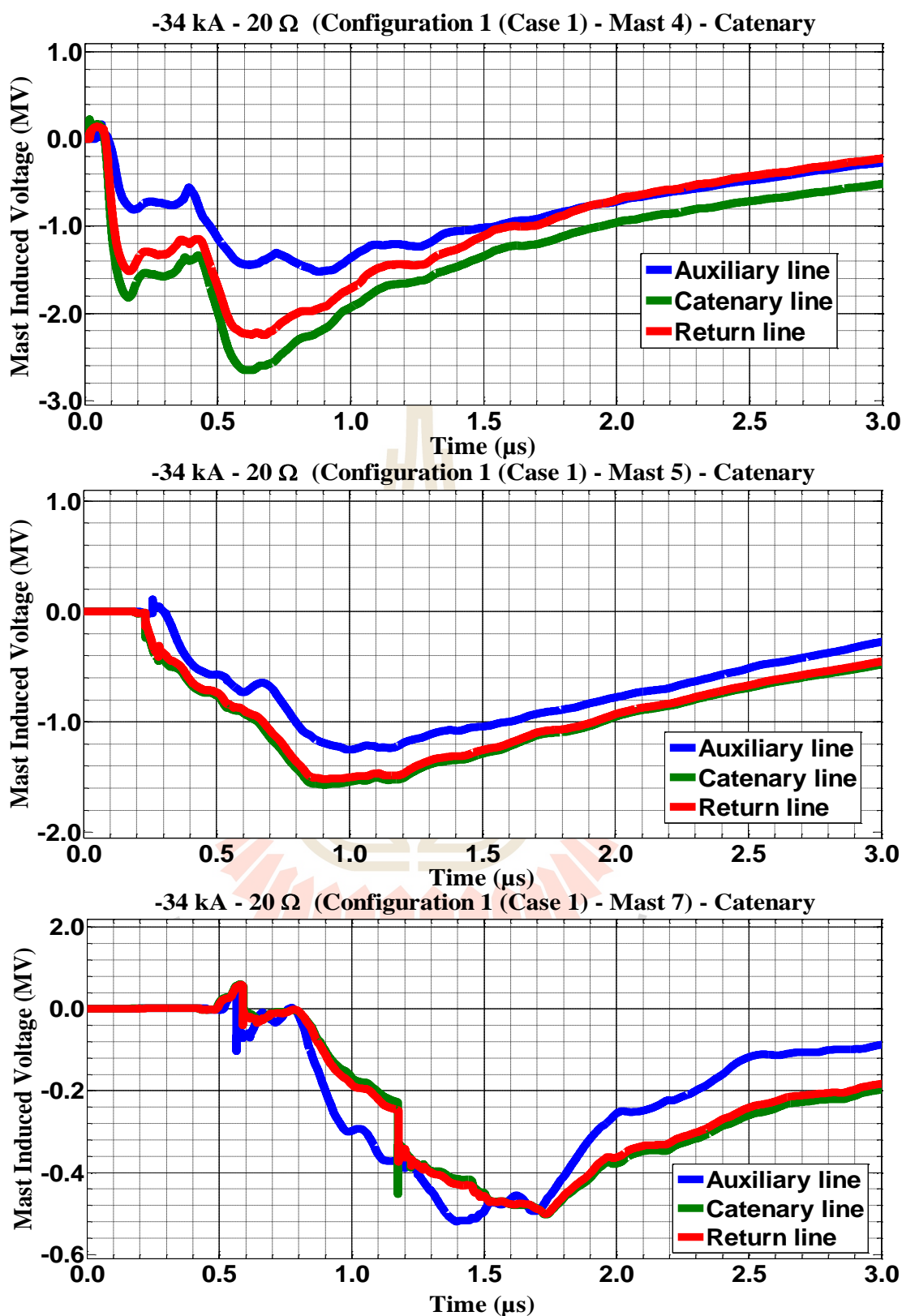


**Figure C.138** Mast 4, 5, and 7 induced voltage waveform of the -34 kA first stroke-(1.0/100  $\mu\text{s}$ ), subsequent stroke-(0.2/50  $\mu\text{s}$ ) strikes on Mast 4 with 20  $\Omega$  for Case 1



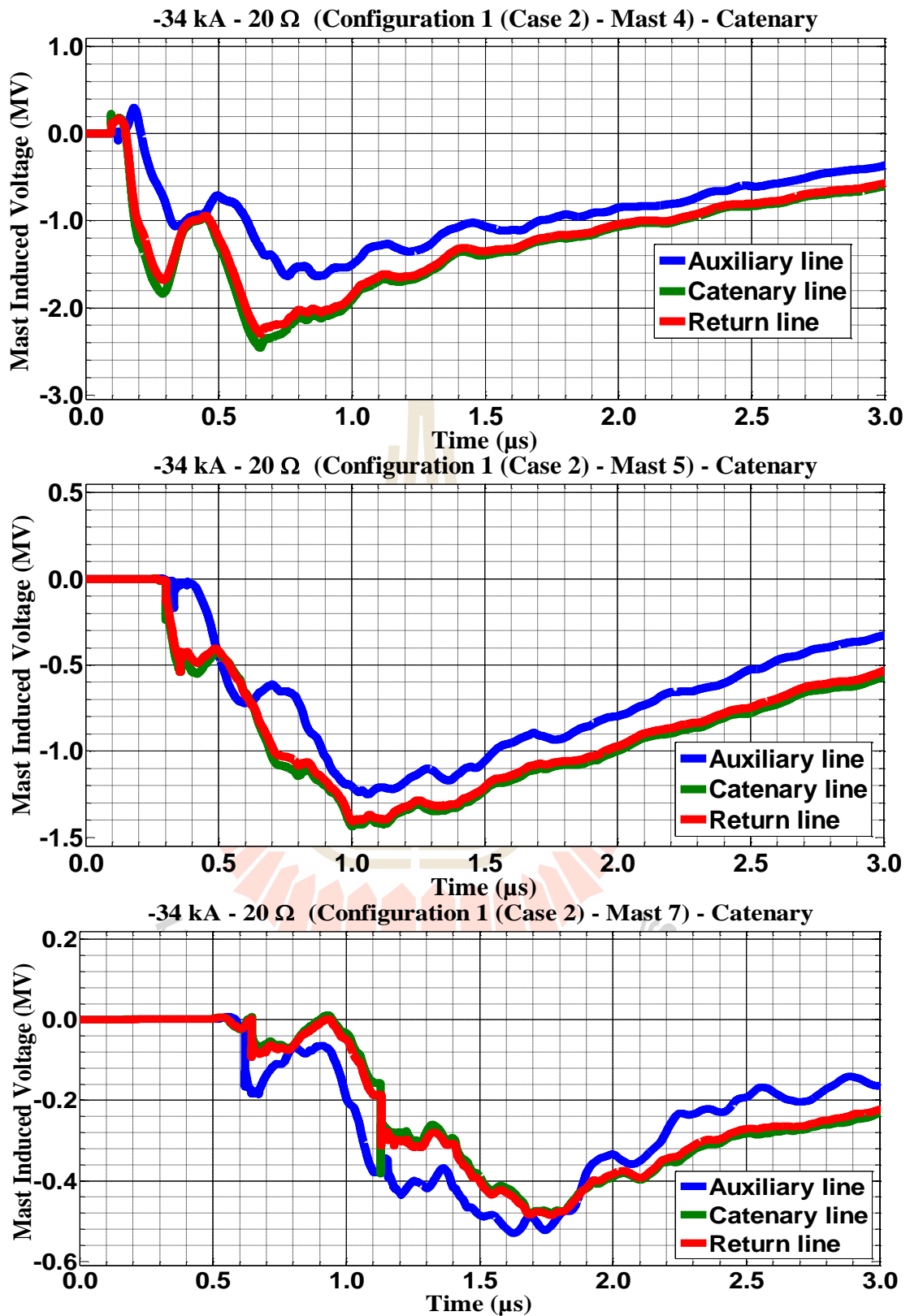


**Figure C.139** Mast 4, 5, and 7 induced voltage waveform of the -34 kA first stroke-(1.0/100  $\mu\text{s}$ ), subsequent stroke-(0.2/50  $\mu\text{s}$ ) strikes on Mast 4 with 20  $\Omega$  for Case 2

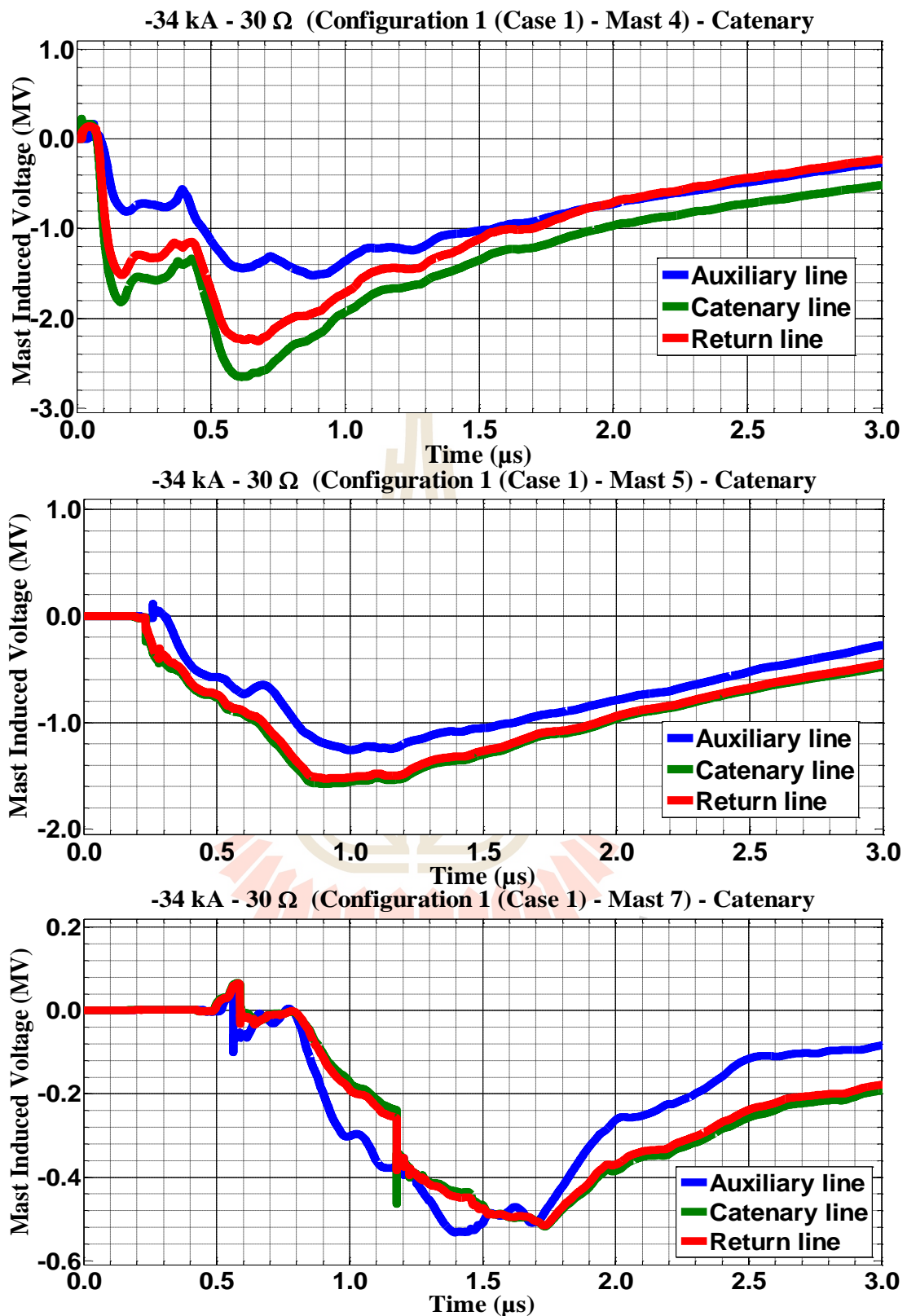


**Figure C.140** Mast 4, 5, and 7 induced voltage waveform of the -34 kA first stroke-(1.0/100  $\mu\text{s}$ ), subsequent stroke-(0.2/50  $\mu\text{s}$ ) strikes on Mast 4 with 30  $\Omega$  for Case 1

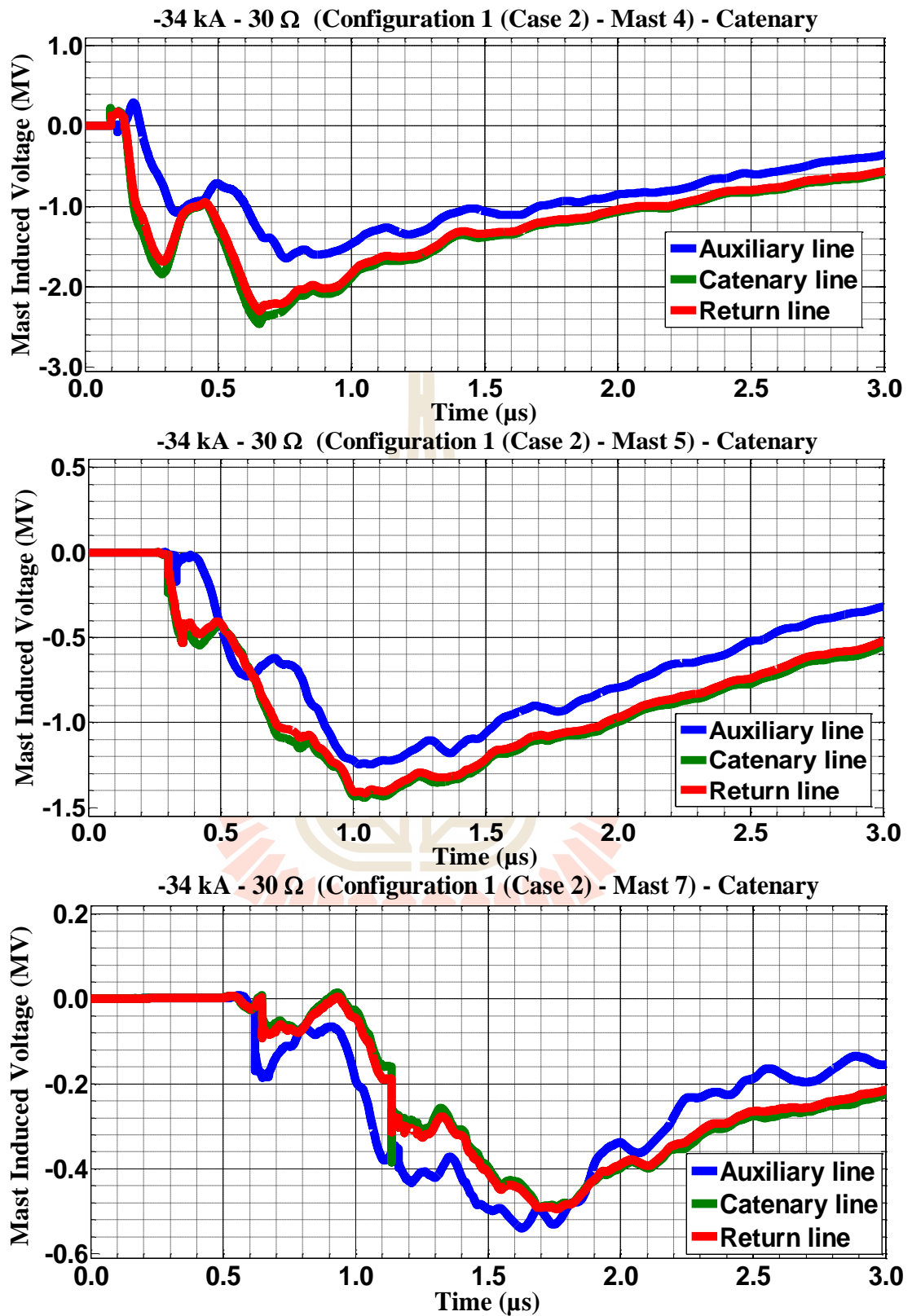


**Figure C.141** Mast 4, 5, and 7 induced voltage waveform of the -34 kA first stroke-(1.0/100  $\mu\text{s}$ ), subsequent stroke-(0.2/50  $\mu\text{s}$ ) strikes on Mast 4 with 30  $\Omega$  for Case 2

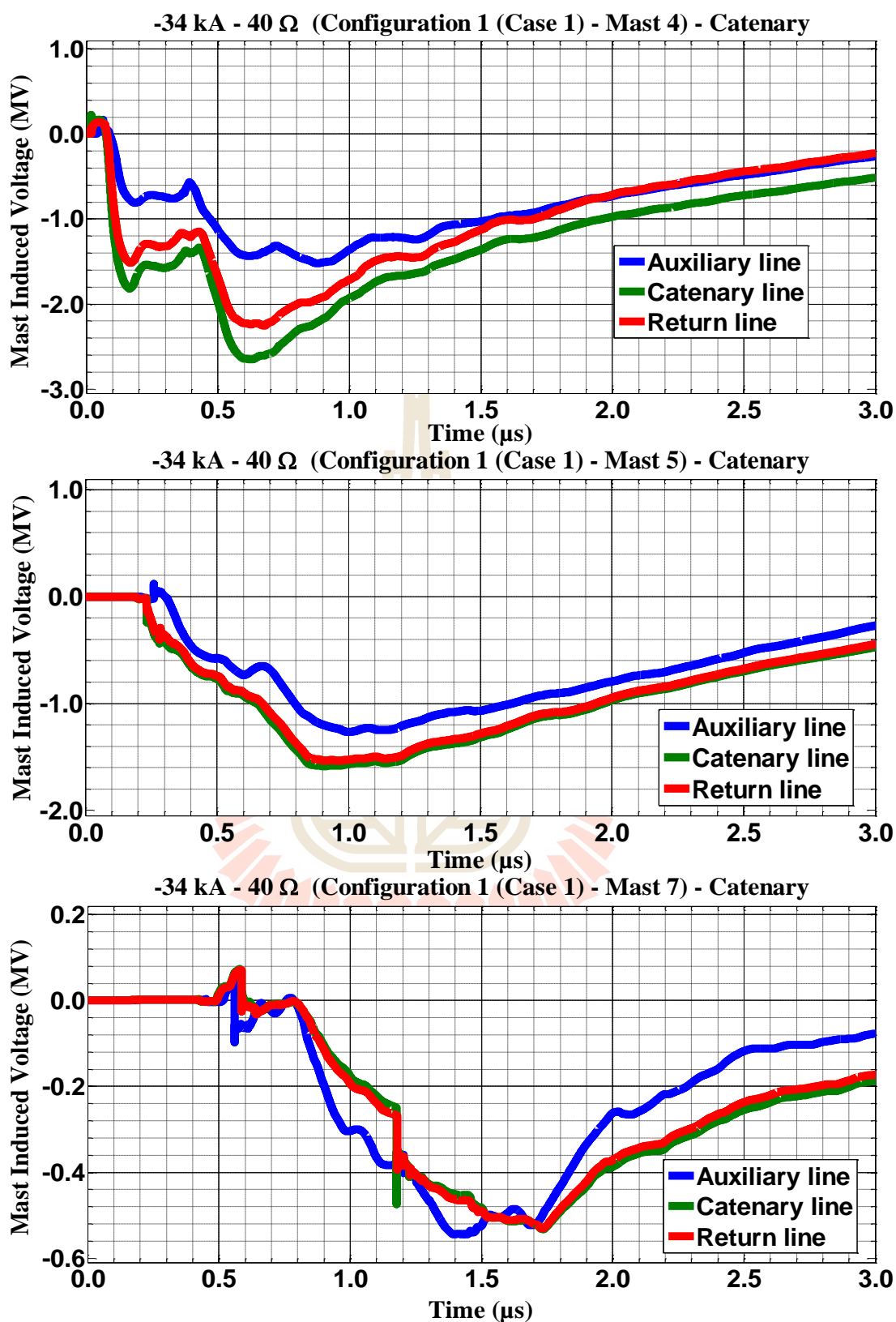


**Figure C.142** Mast 4, 5, and 7 induced voltage waveform of the -34 kA first stroke-(1.0/100  $\mu\text{s}$ ), subsequent stroke-(0.2/50  $\mu\text{s}$ ) strikes on Mast 4 with 40  $\Omega$  for Case 1

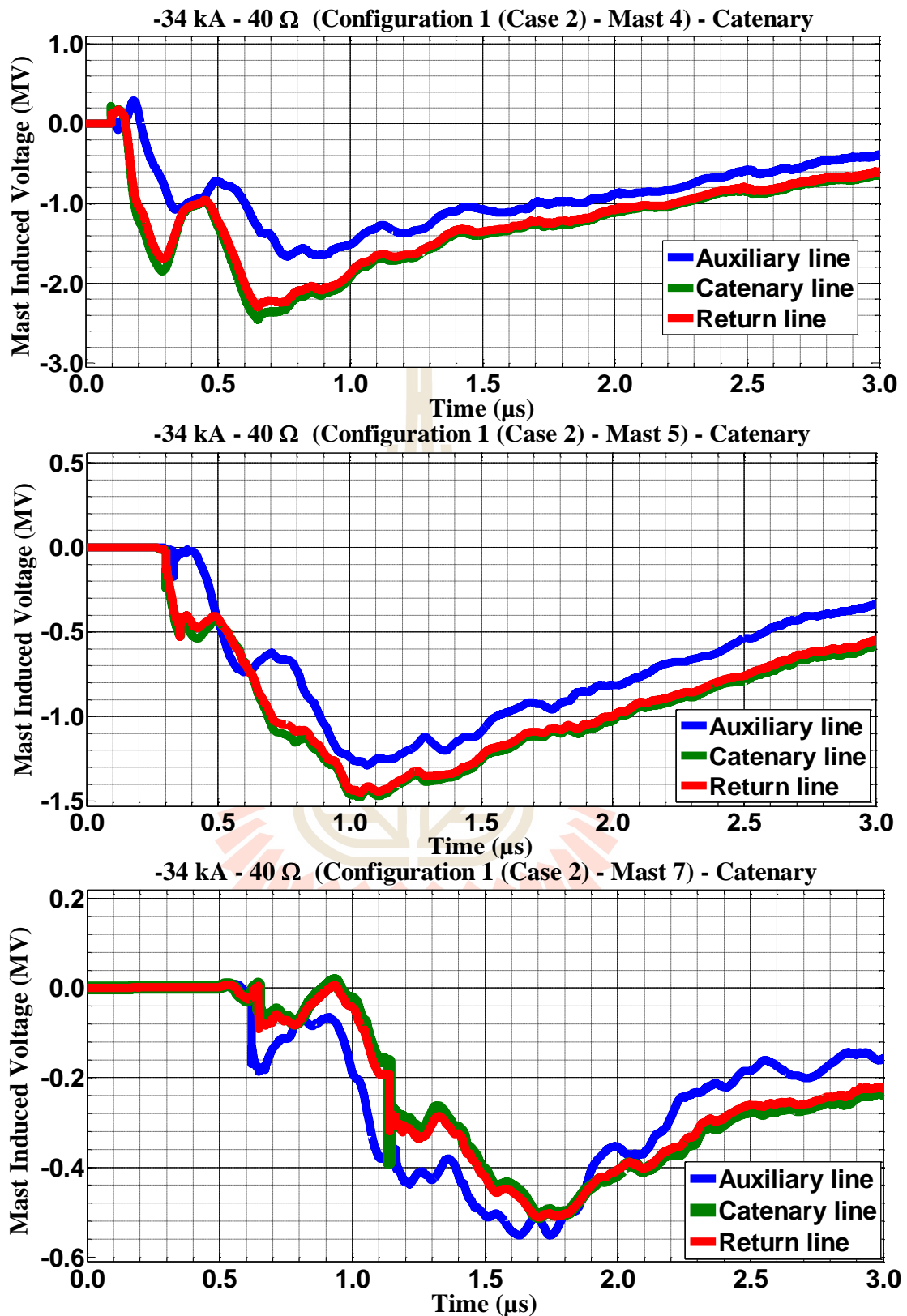


**Figure C.143** Mast 4, 5, and 7 induced voltage waveform of the -34 kA first stroke-(1.0/100 μs), subsequent stroke-(0.2/50 μs) strikes on Mast 4 with 40 Ω for Case 2

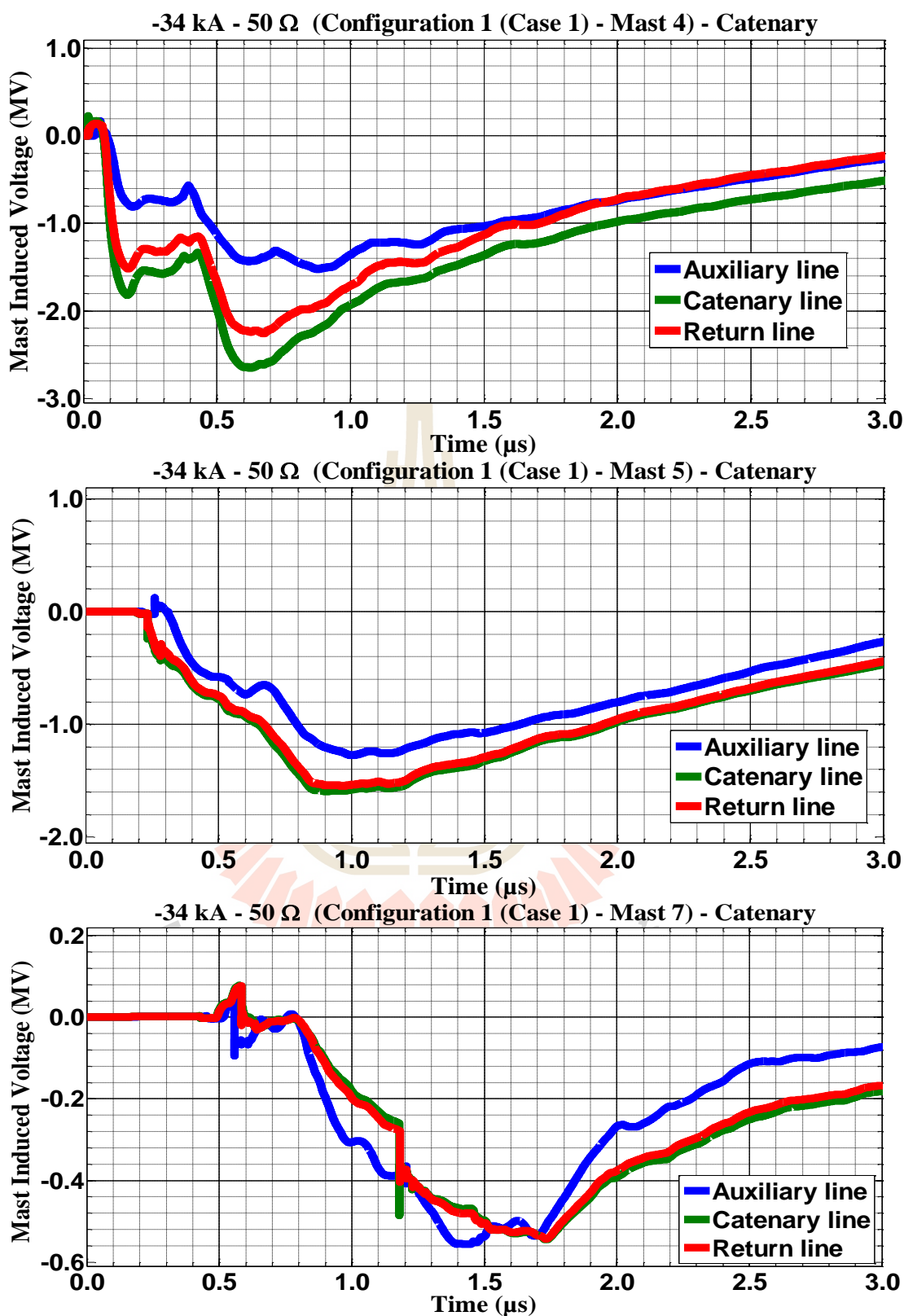


**Figure C.144** Mast 4, 5, and 7 induced voltage waveform of the -34 kA first stroke-(1.0/100  $\mu\text{s}$ ), subsequent stroke-(0.2/50  $\mu\text{s}$ ) strikes on Mast 4 with 50  $\Omega$  for Case 1

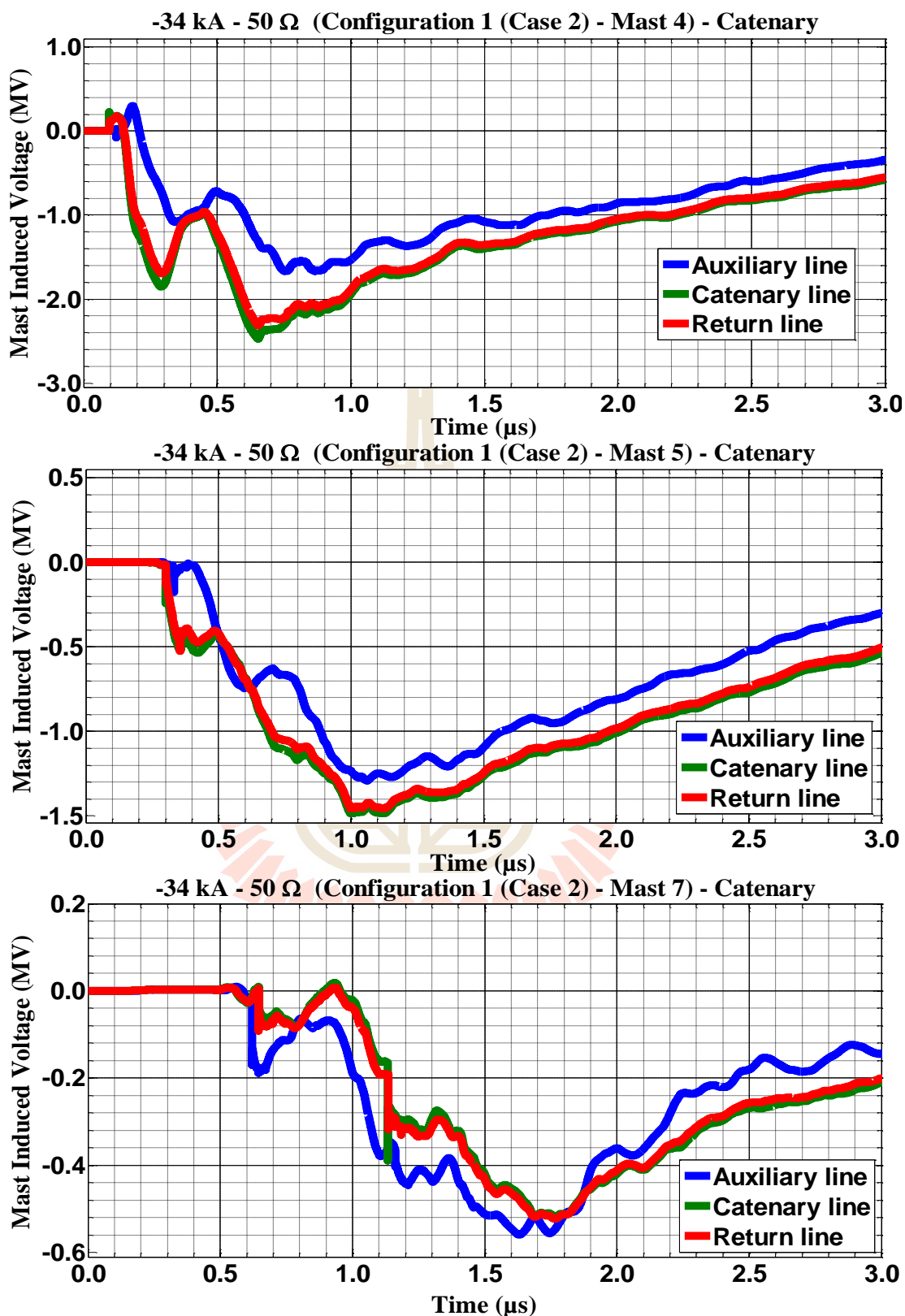


**Figure C.145** Mast 4, 5, and 7 induced voltage waveform of the -34 kA first stroke-(1.0/100  $\mu\text{s}$ ), subsequent stroke-(0.2/50  $\mu\text{s}$ ) strikes on Mast 4 with 50  $\Omega$  for Case 2

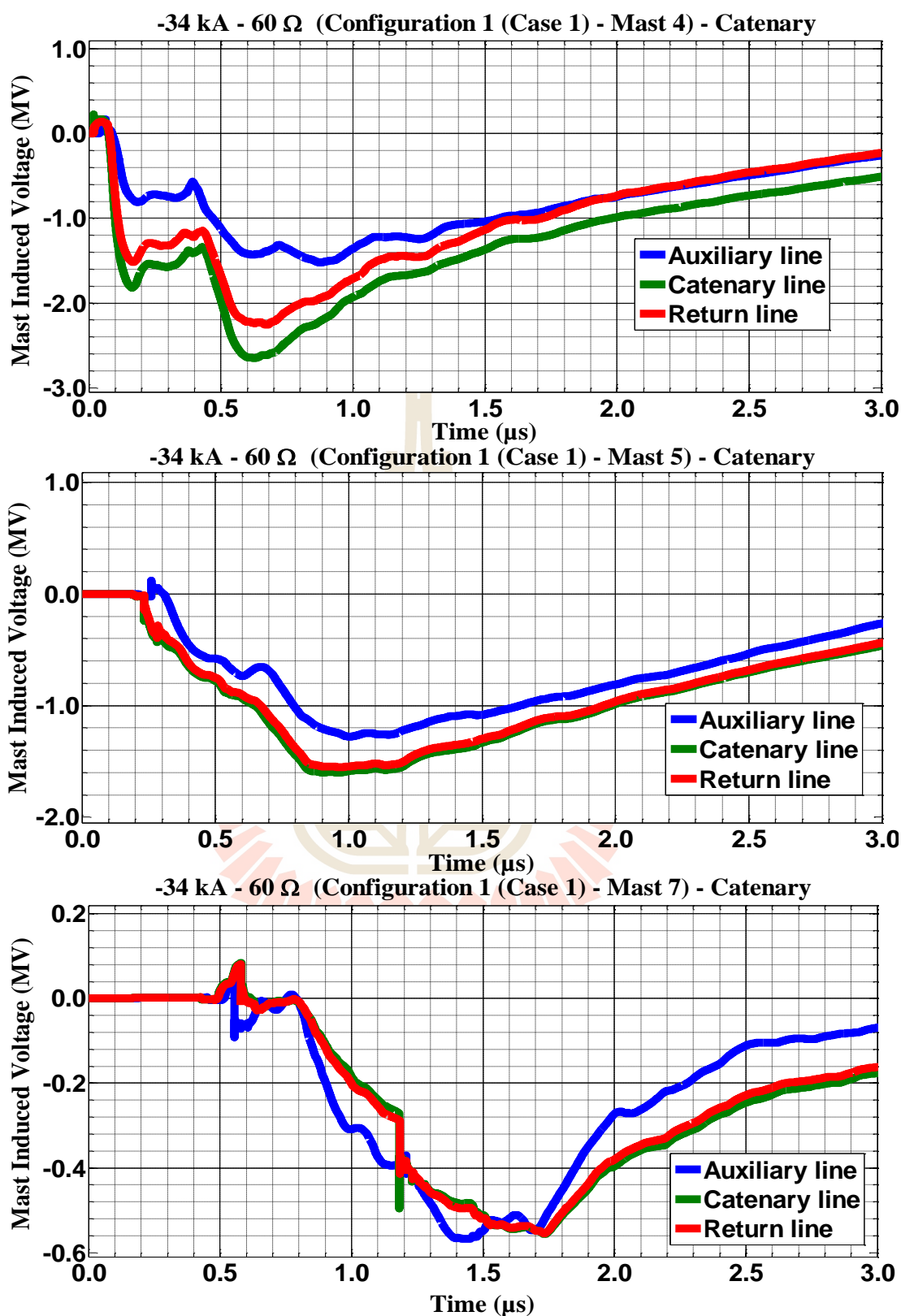


**Figure C.146** Mast 4, 5, and 7 induced voltage waveform of the -34 kA first stroke-(1.0/100  $\mu$ s), subsequent stroke-(0.2/50  $\mu$ s) strikes on Mast 4 with 60  $\Omega$  for Case 1



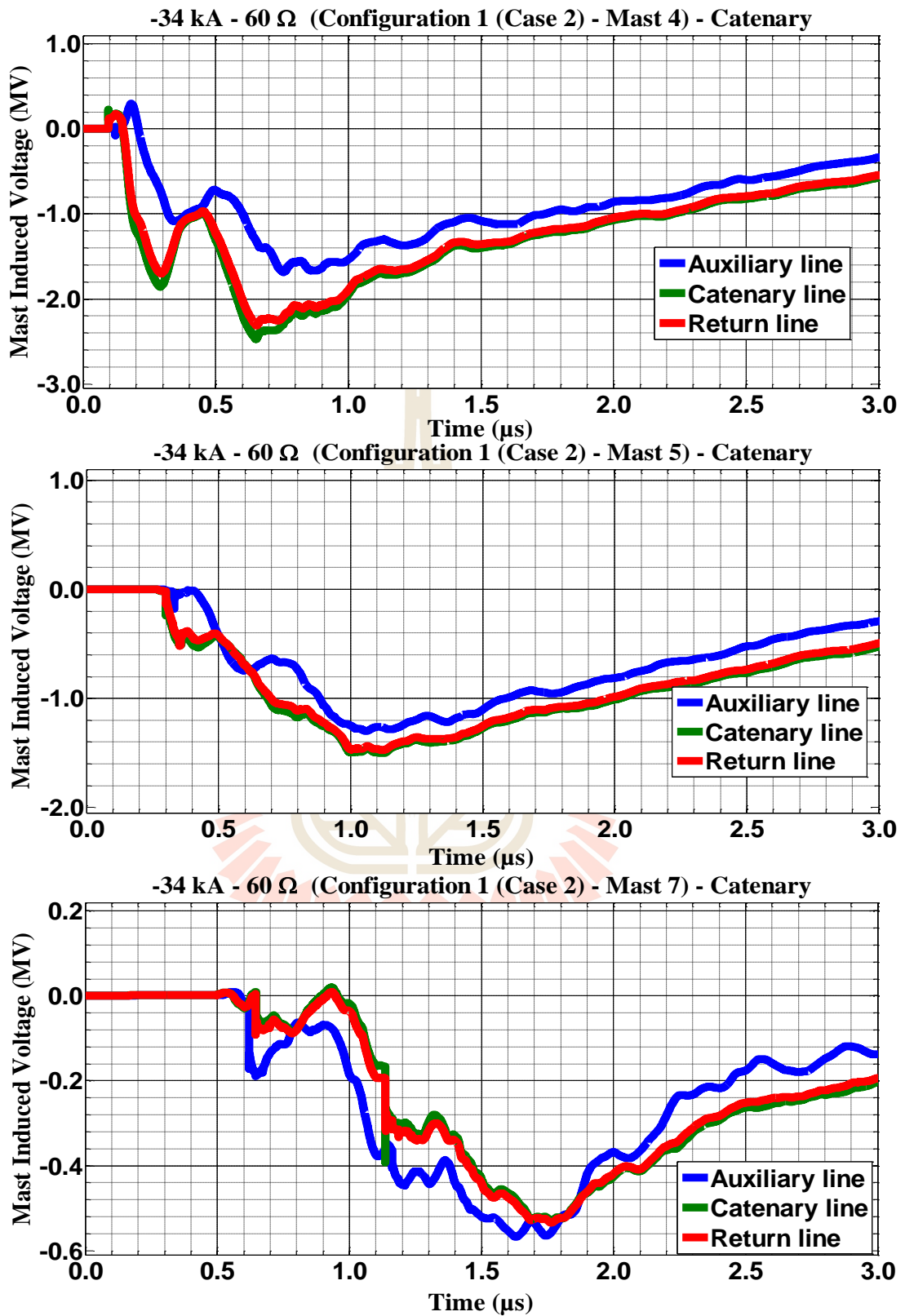


**Figure C.147** Mast 4, 5, and 7 induced voltage waveform of the -34 kA first stroke-(1.0/100  $\mu\text{s}$ ), subsequent stroke-(0.2/50  $\mu\text{s}$ ) strikes on Mast 4 with 60  $\Omega$  for Case 2

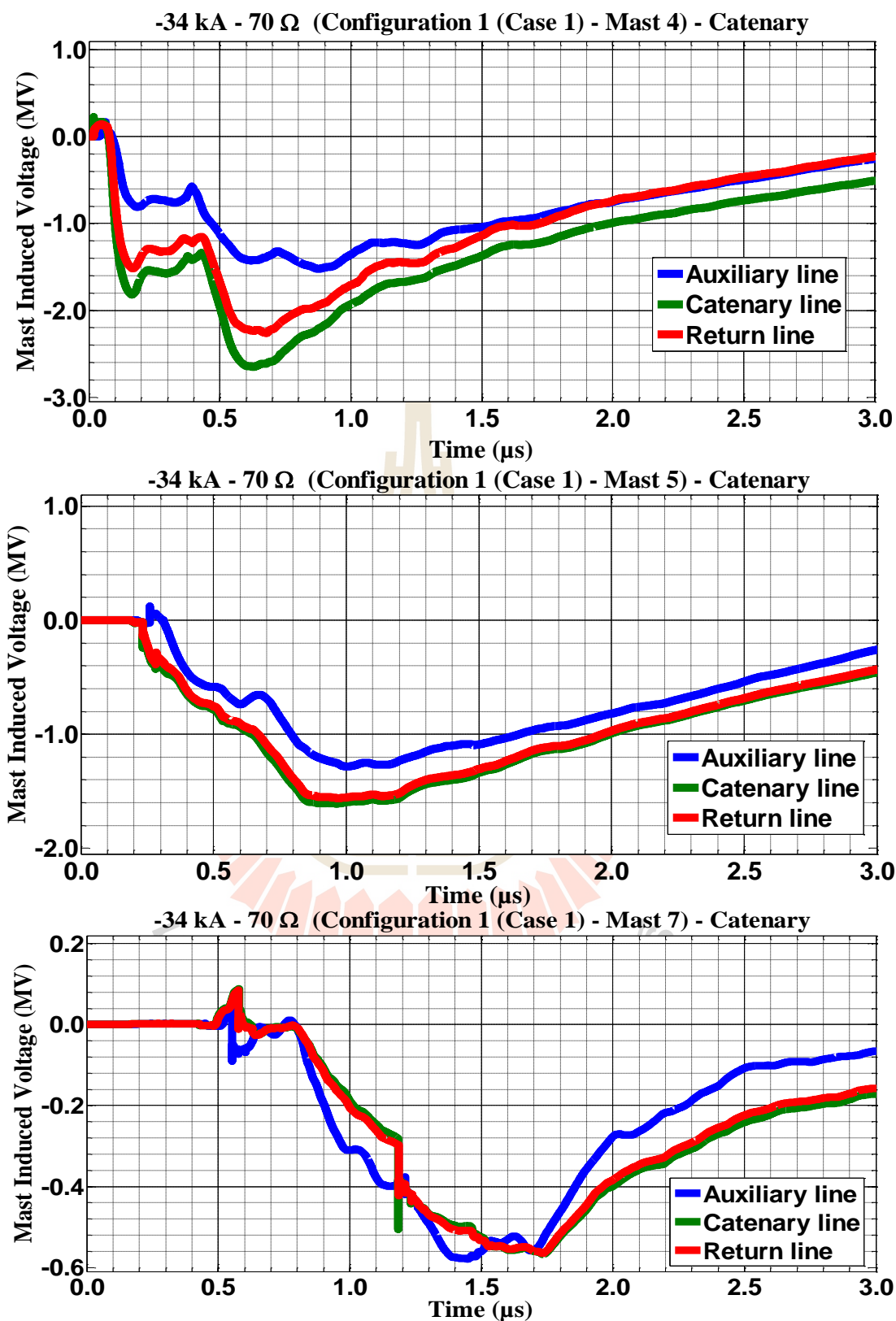


**Figure C.148** Mast 4, 5, and 7 induced voltage waveform of the -34 kA first stroke-(1.0/100 μs), subsequent stroke-(0.2/50 μs) strikes on Mast 4 with 70 Ω for Case 1

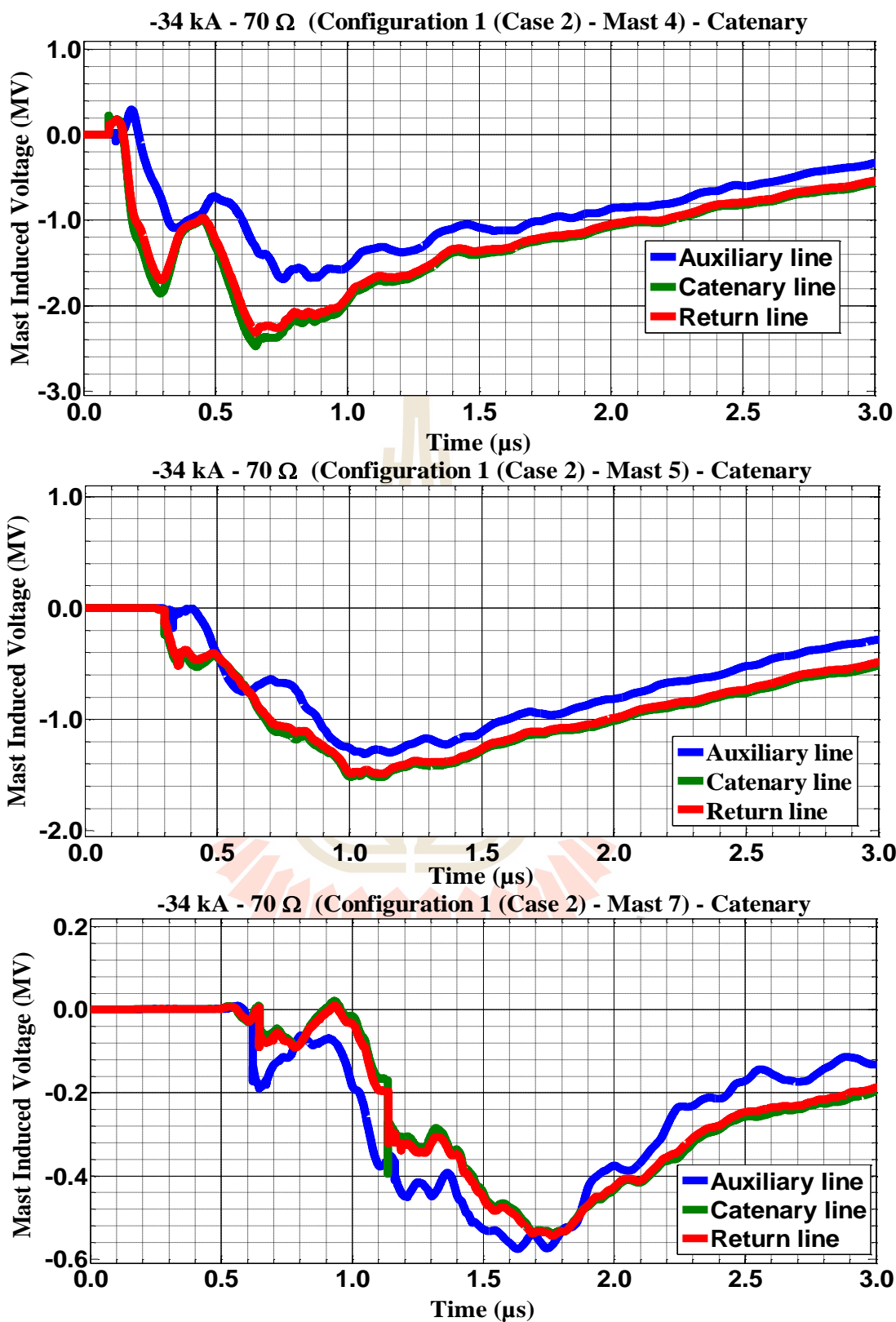


**Figure C.149** Mast 4, 5, and 7 induced voltage waveform of the -34 kA first stroke-(1.0/100 μs), subsequent stroke-(0.2/50 μs) strikes on Mast 4 with 70 Ω for Case 2

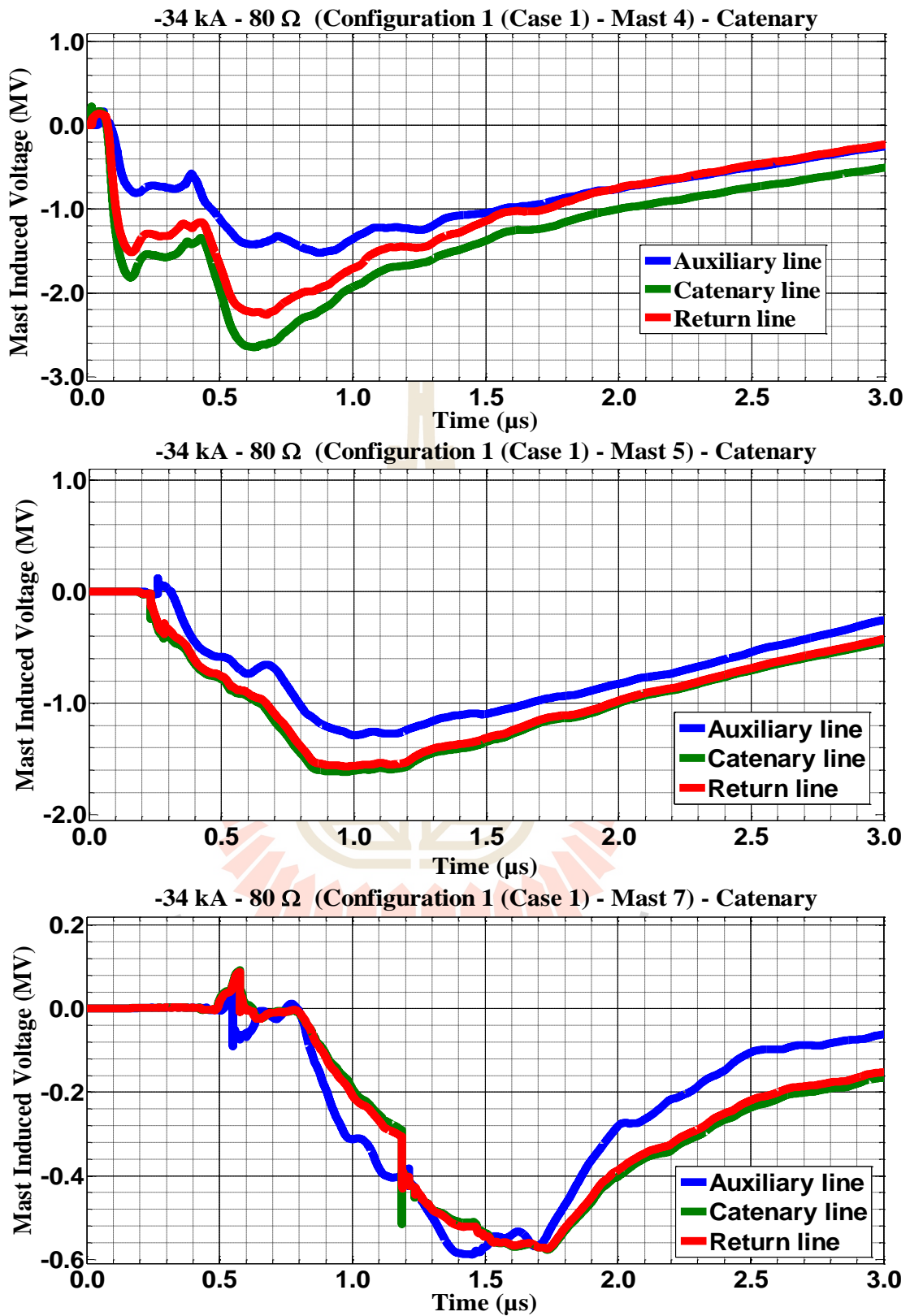


**Figure C.150** Mast 4, 5, and 7 induced voltage waveform of the -34 kA first stroke-(1.0/100  $\mu\text{s}$ ), subsequent stroke-(0.2/50  $\mu\text{s}$ ) strikes on Mast 4 with 80  $\Omega$  for Case 1

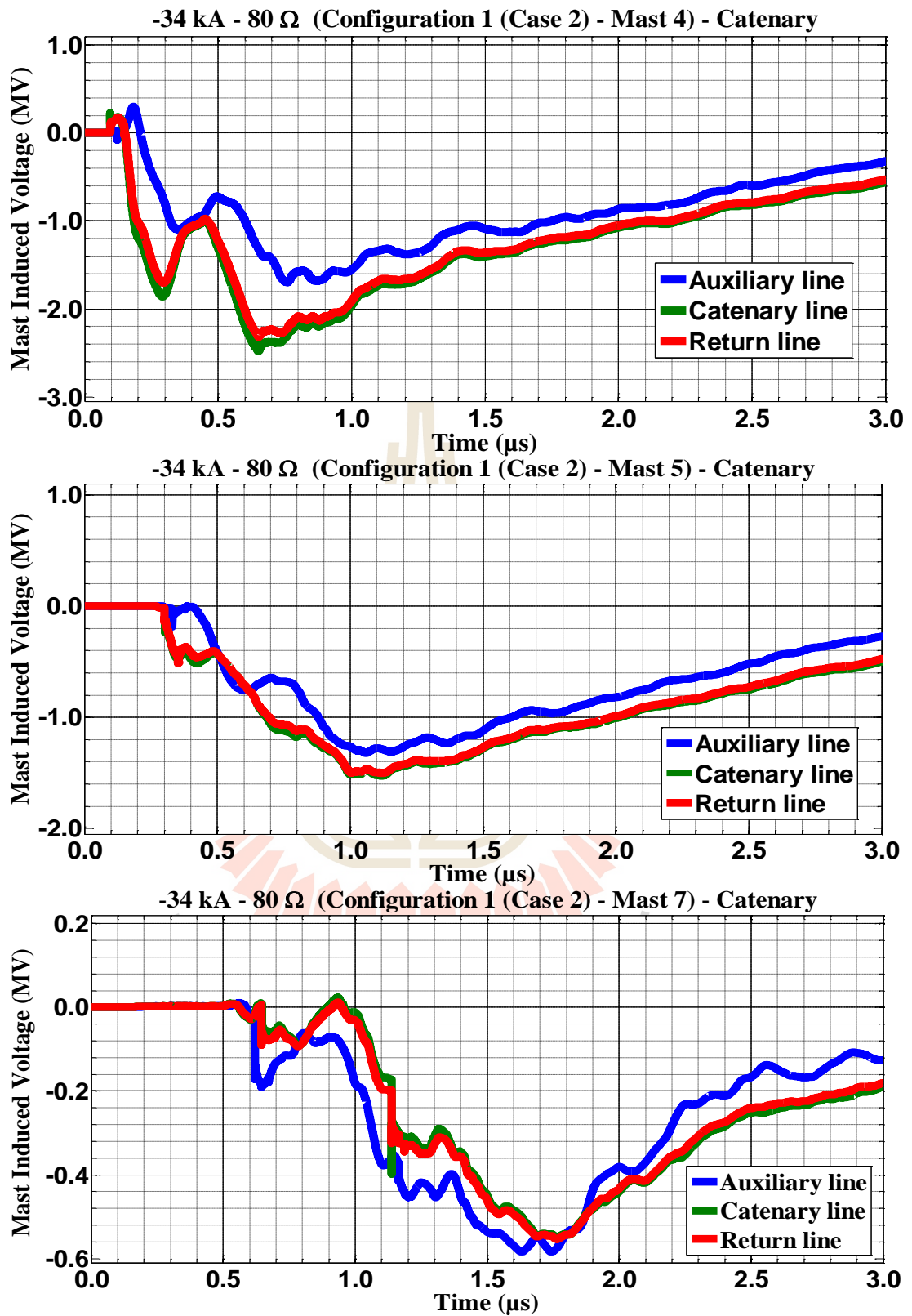


**Figure C.151** Mast 4, 5, and 7 induced voltage waveform of the -34 kA first stroke-(1.0/100  $\mu\text{s}$ ), subsequent stroke-(0.2/50  $\mu\text{s}$ ) strikes on Mast 4 with 80  $\Omega$  for Case 2

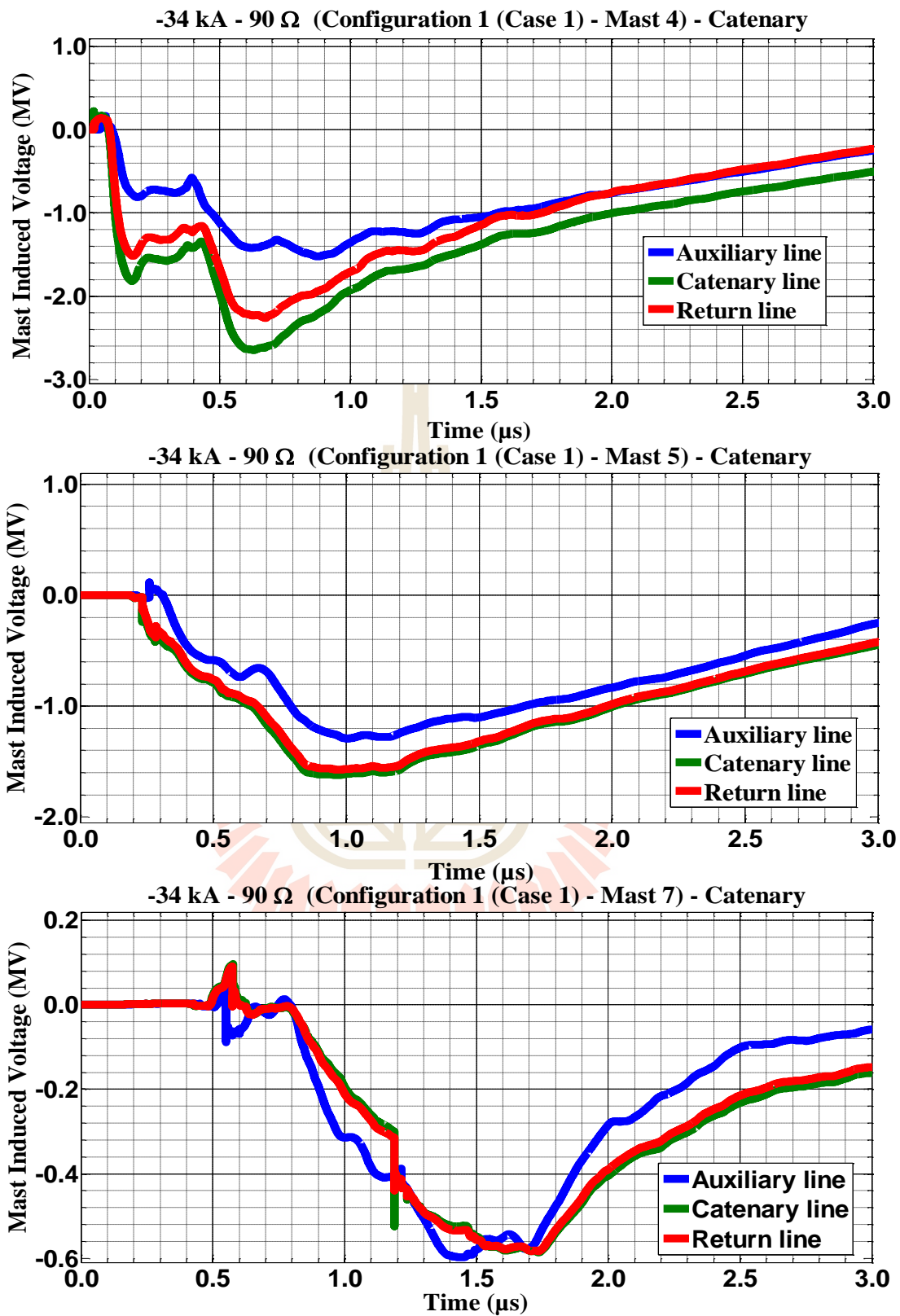


**Figure C.152** Mast 4, 5, and 7 induced voltage waveform of the -34 kA first stroke-(1.0/100  $\mu\text{s}$ ), subsequent stroke-(0.2/50  $\mu\text{s}$ ) strikes on Mast 4 with 90  $\Omega$  for Case 1

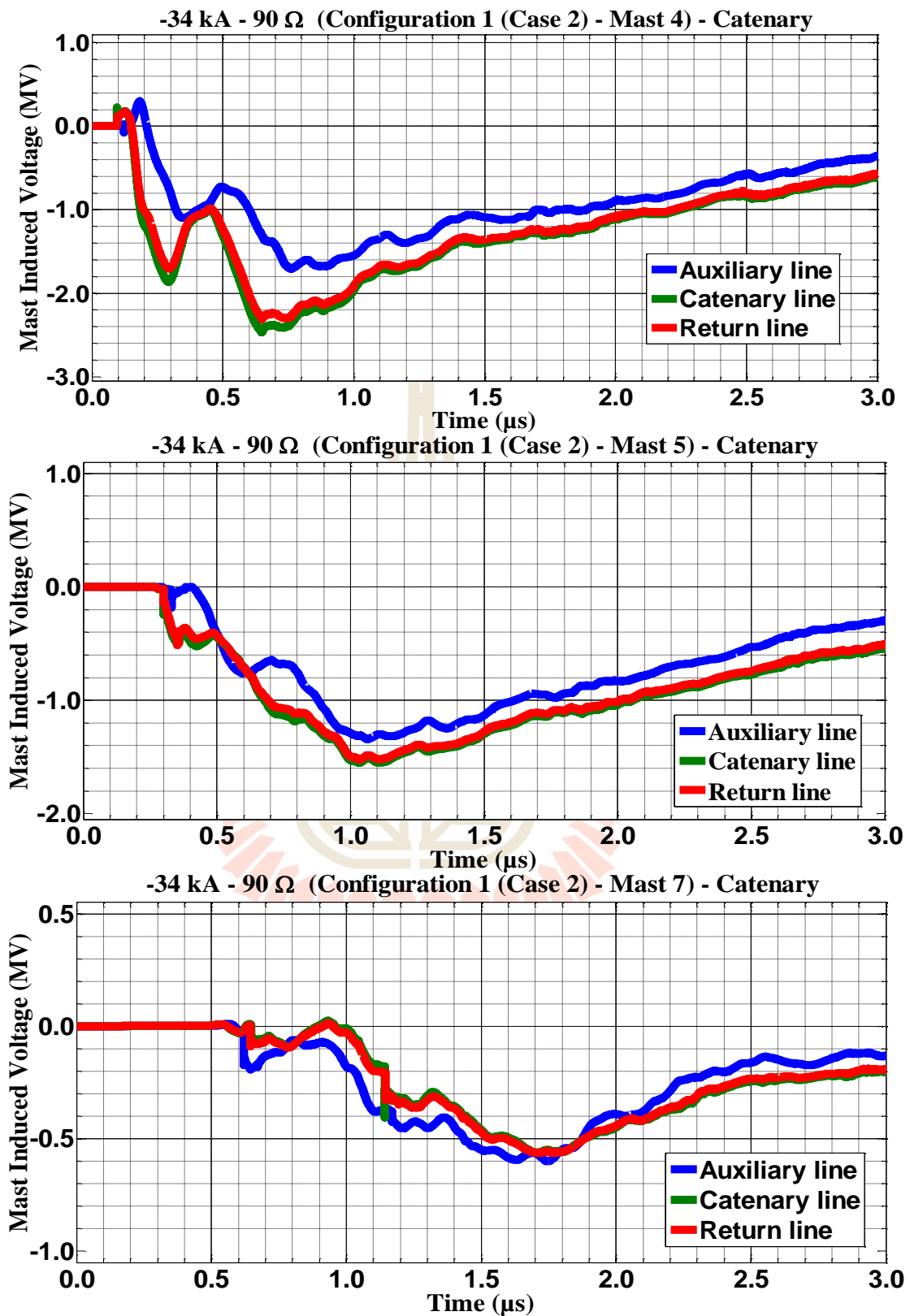


**Figure C.153** Mast 4, 5, and 7 induced voltage waveform of the -34 kA first stroke-(1.0/100  $\mu\text{s}$ ), subsequent stroke-(0.2/50  $\mu\text{s}$ ) strikes on Mast 4 with 90  $\Omega$  for Case 2

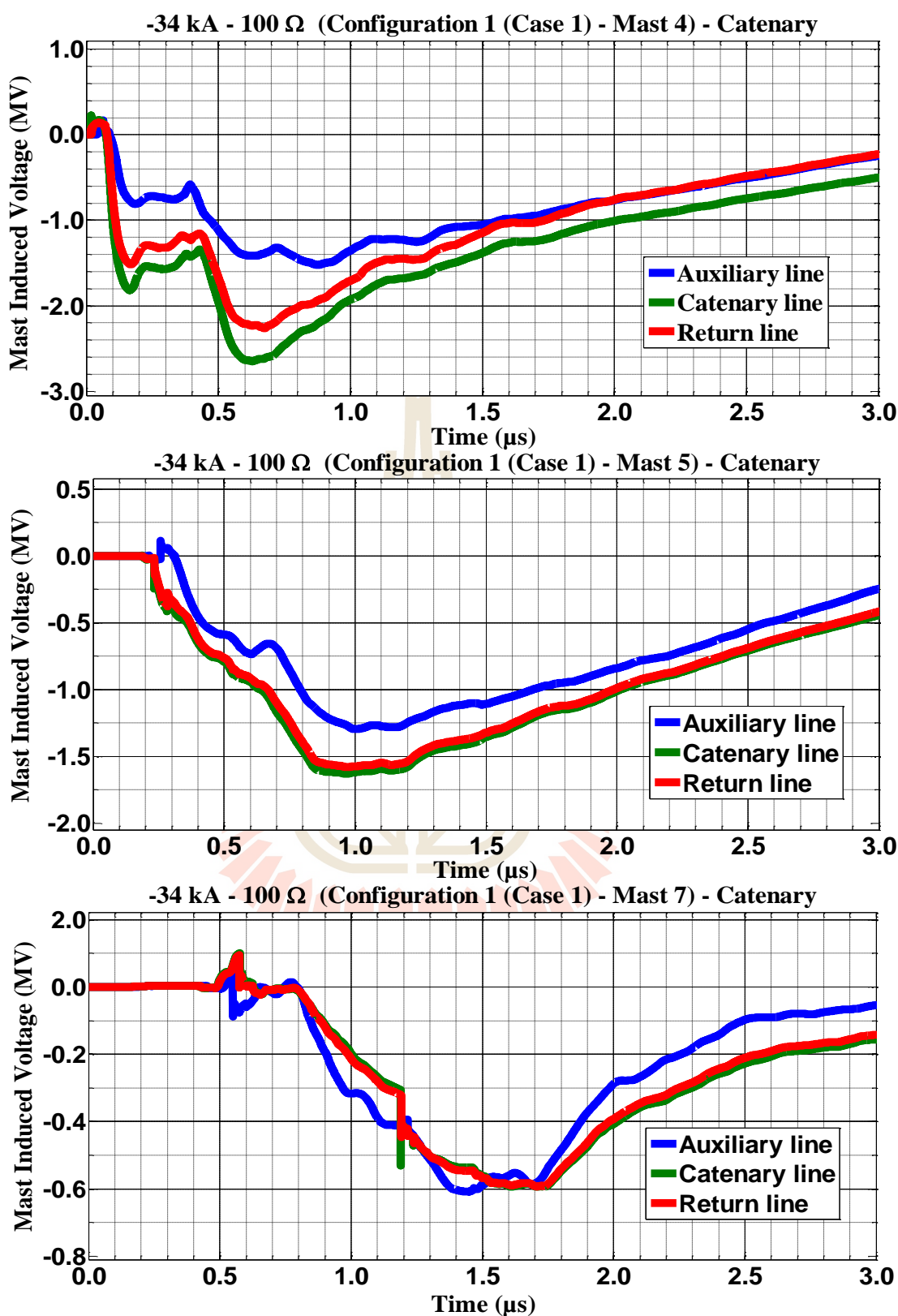


**Figure C.154** Mast 4, 5, and 7 induced voltage waveform of the -34 kA first stroke-(1.0/100  $\mu\text{s}$ ), subsequent stroke-(0.2/50  $\mu\text{s}$ ) strikes on Mast 4 with 100  $\Omega$  for Case 1



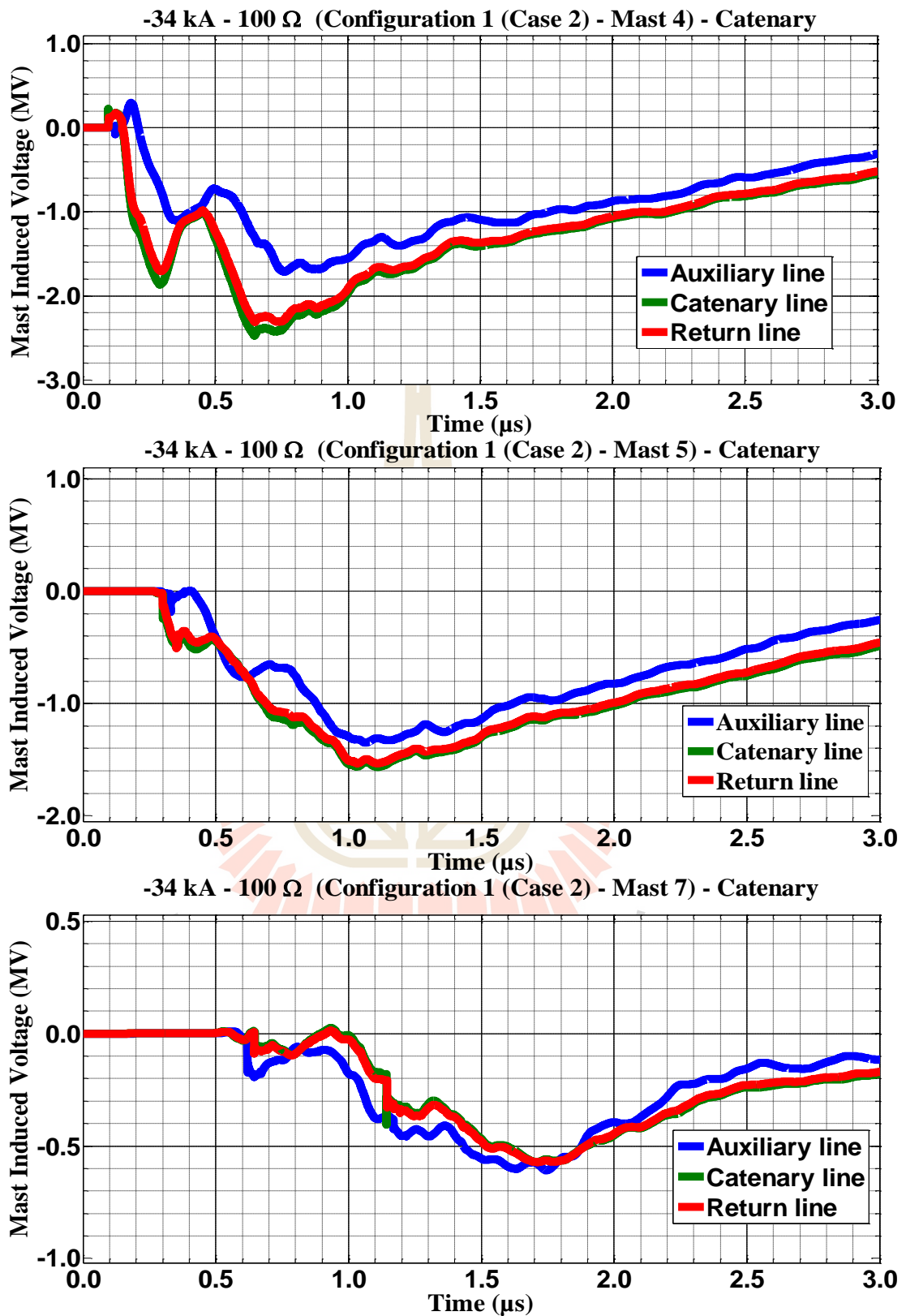


**Figure C.155** Mast 4, 5, and 7 induced voltage waveform of the -34 kA first stroke-(1.0/100  $\mu\text{s}$ ), subsequent stroke-(0.2/50  $\mu\text{s}$ ) strikes on Mast 4 with 100  $\Omega$  for Case 2

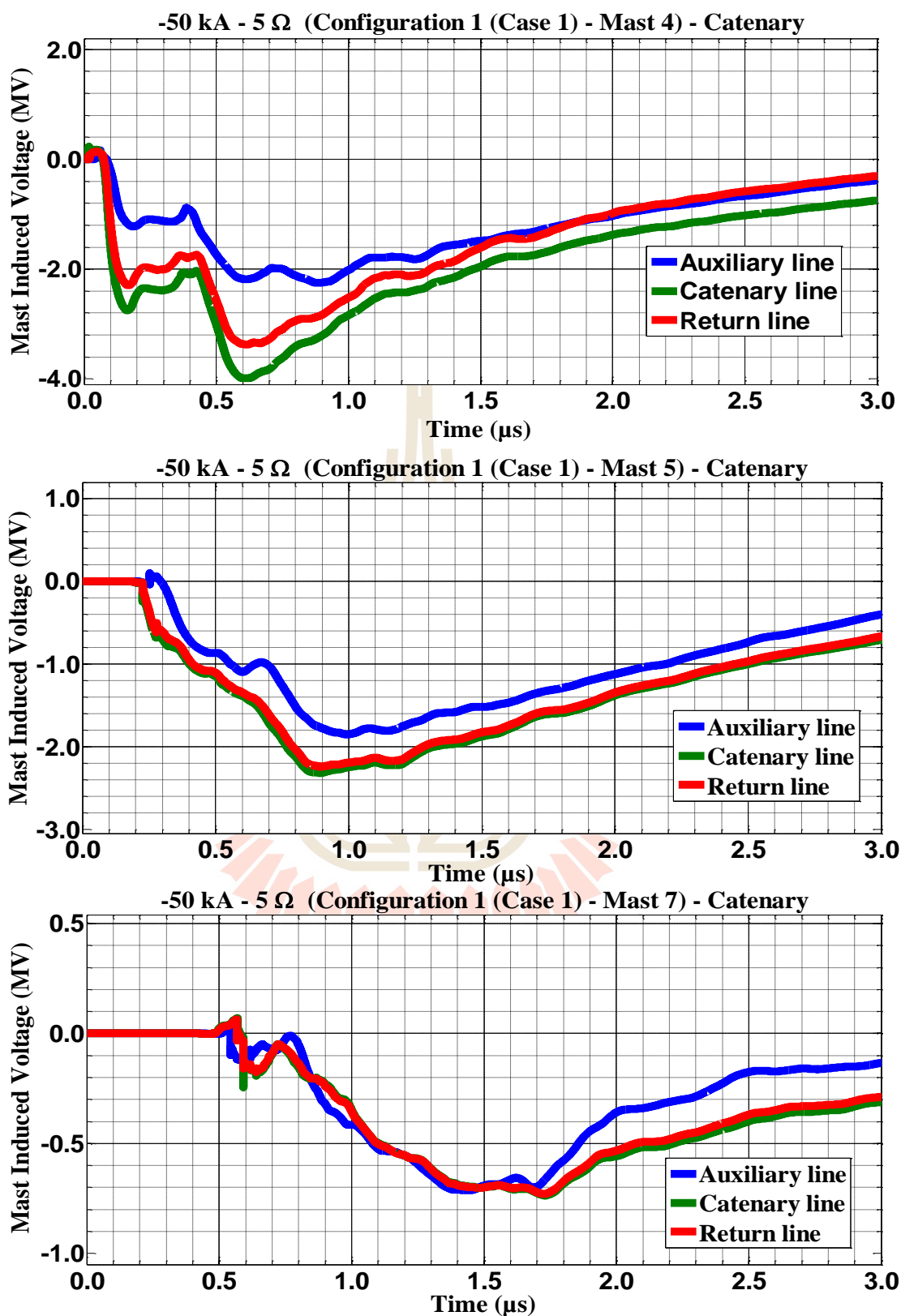


**Figure C.156** Mast 4, 5, and 7 induced voltage waveform of the -50 kA first stroke-(1.0/100  $\mu\text{s}$ ), subsequent stroke-(0.2/50  $\mu\text{s}$ ) strikes on Mast 4 with 5  $\Omega$  for Case 1

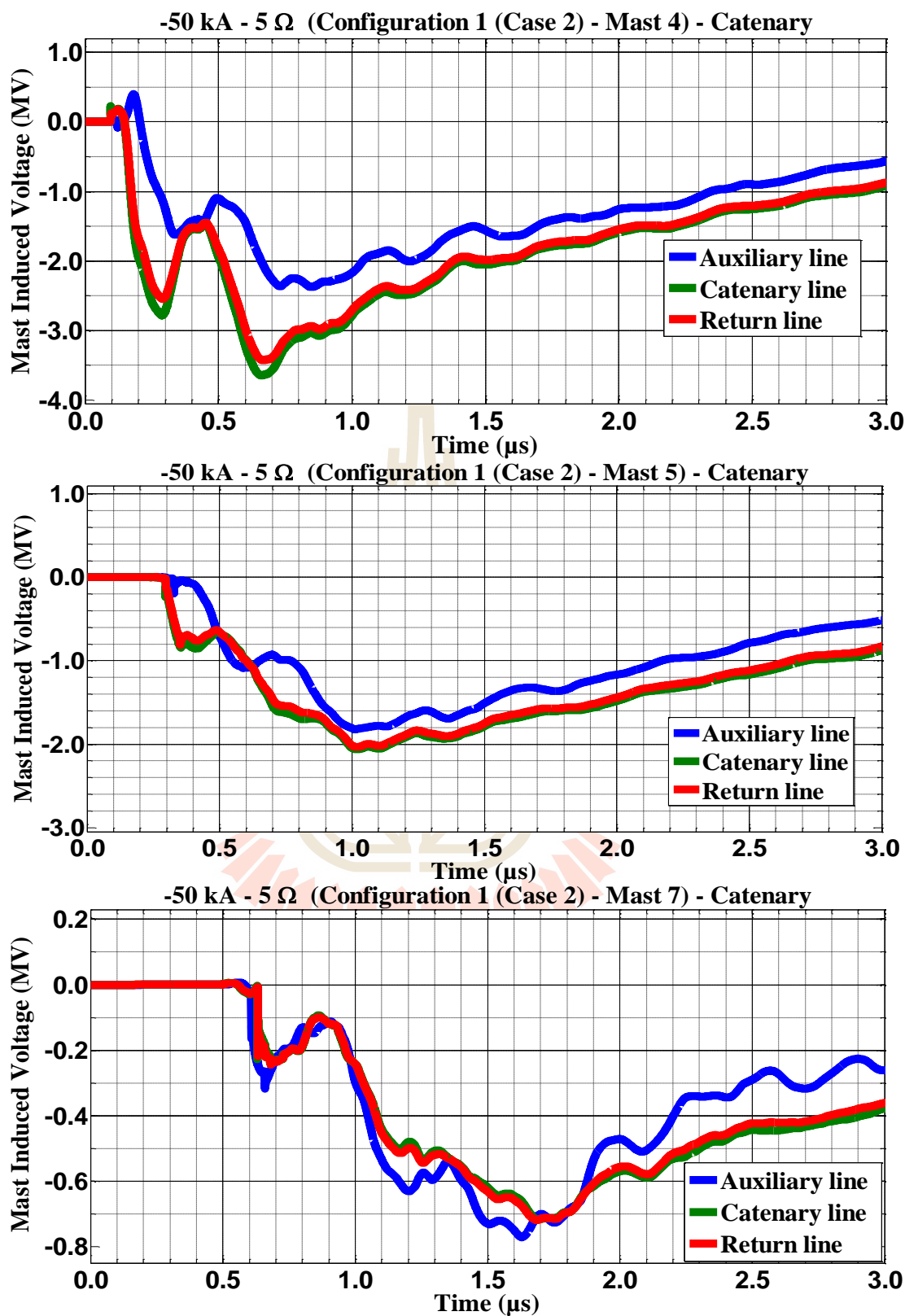


**Figure C.157** Mast 4, 5, and 7 induced voltage waveform of the -50 kA first stroke-(1.0/100 μs), subsequent stroke-(0.2/50 μs) strikes on Mast 4 with 5 Ω for Case 2

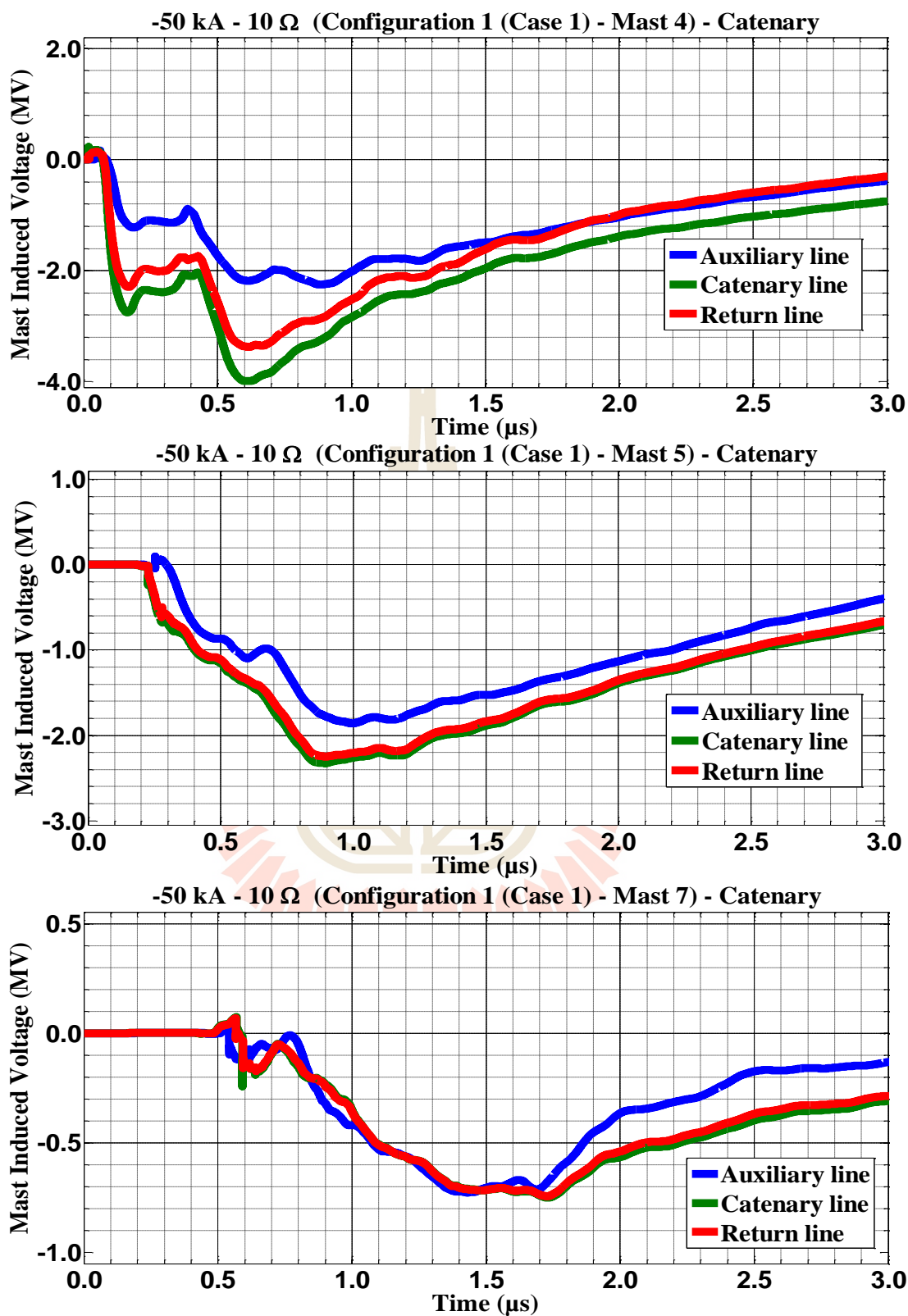


**Figure C.158** Mast 4, 5, and 7 induced voltage waveform of the -50 kA first stroke-(1.0/100  $\mu\text{s}$ ), subsequent stroke-(0.2/50  $\mu\text{s}$ ) strikes on Mast 4 with 10  $\Omega$  for Case 1

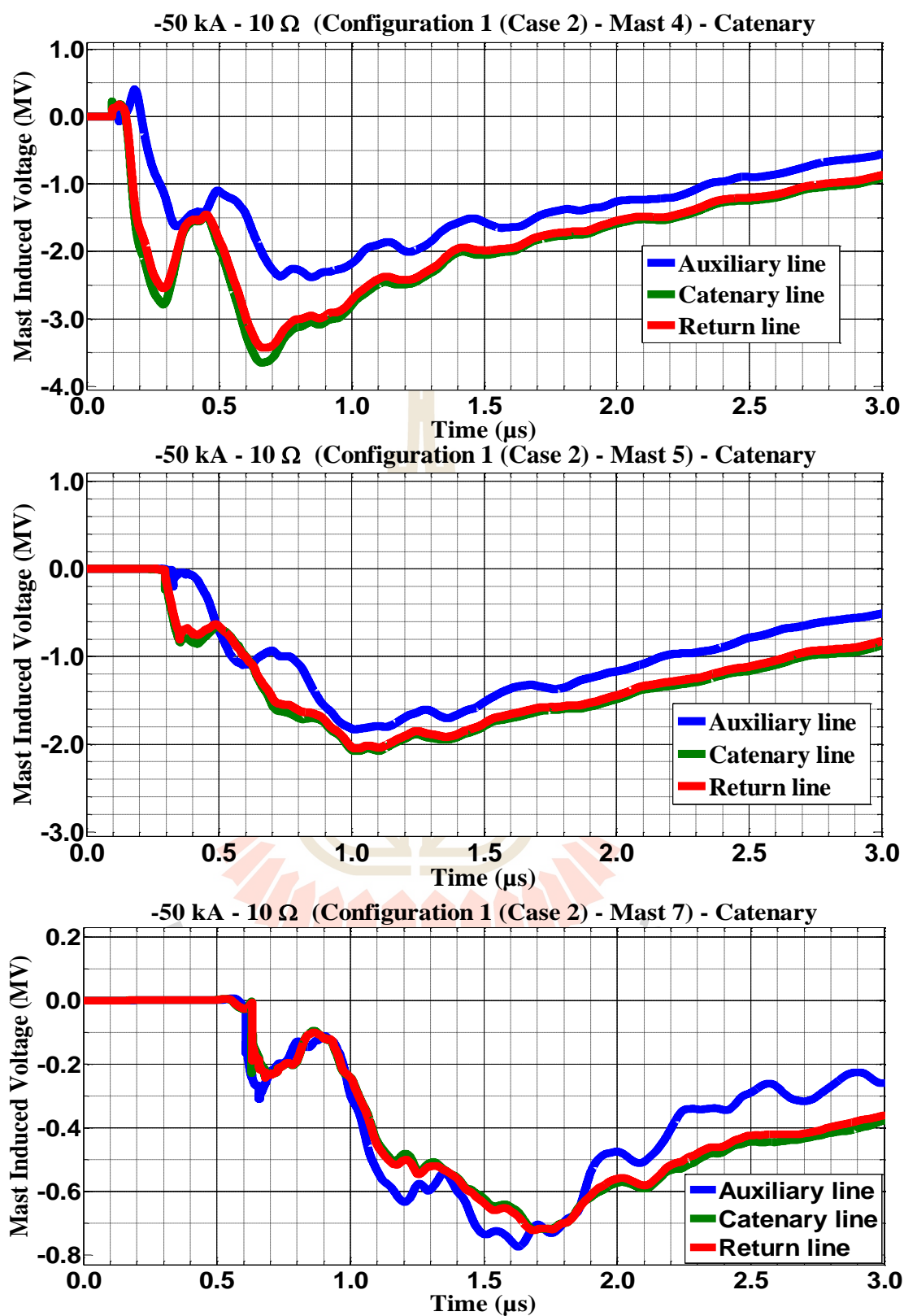


**Figure C.159** Mast 4, 5, and 7 induced voltage waveform of the -50 kA first stroke-(1.0/100  $\mu\text{s}$ ), subsequent stroke-(0.2/50  $\mu\text{s}$ ) strikes on Mast 4 with 10  $\Omega$  for Case 2

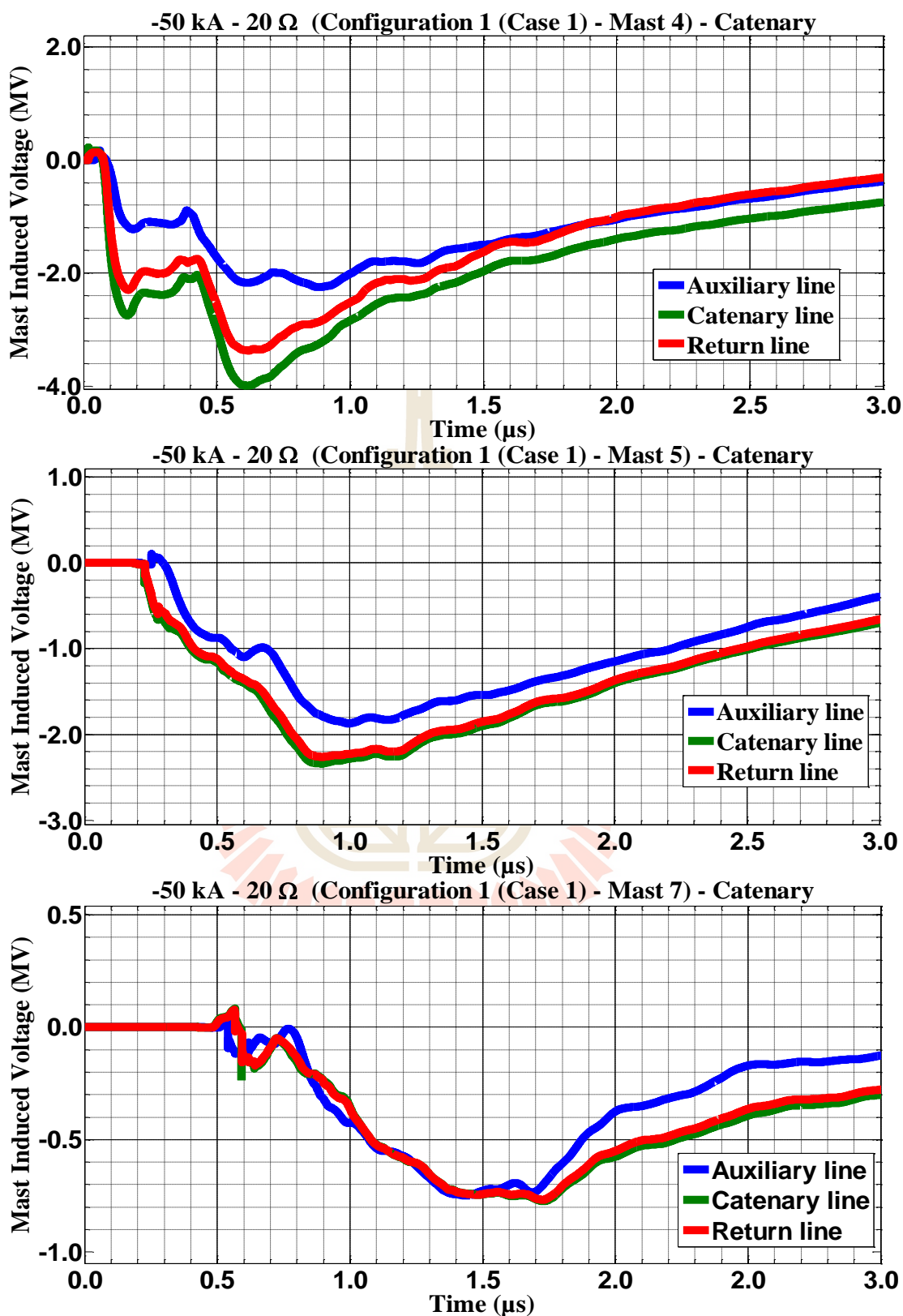


**Figure C.160** Mast 4, 5, and 7 induced voltage waveform of the -50 kA first stroke-(1.0/100  $\mu\text{s}$ ), subsequent stroke-(0.2/50  $\mu\text{s}$ ) strikes on Mast 4 with 20  $\Omega$  for Case 1

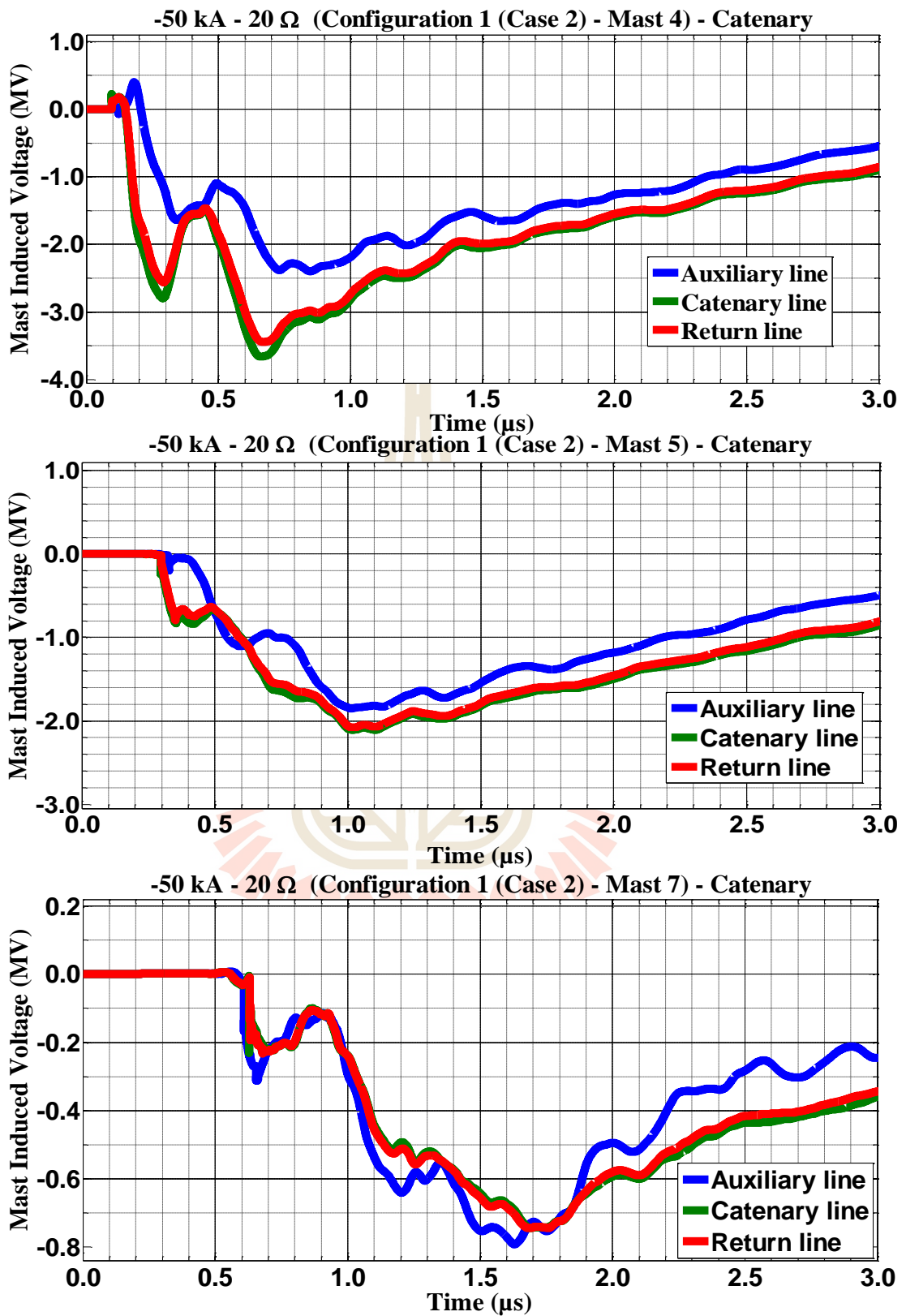


**Figure C.161** Mast 4, 5, and 7 induced voltage waveform of the  $-50 \text{ kA}$  first stroke- $(1.0/100 \mu\text{s})$ , subsequent stroke- $(0.2/50 \mu\text{s})$  strikes on Mast 4 with  $20 \Omega$  for Case 2

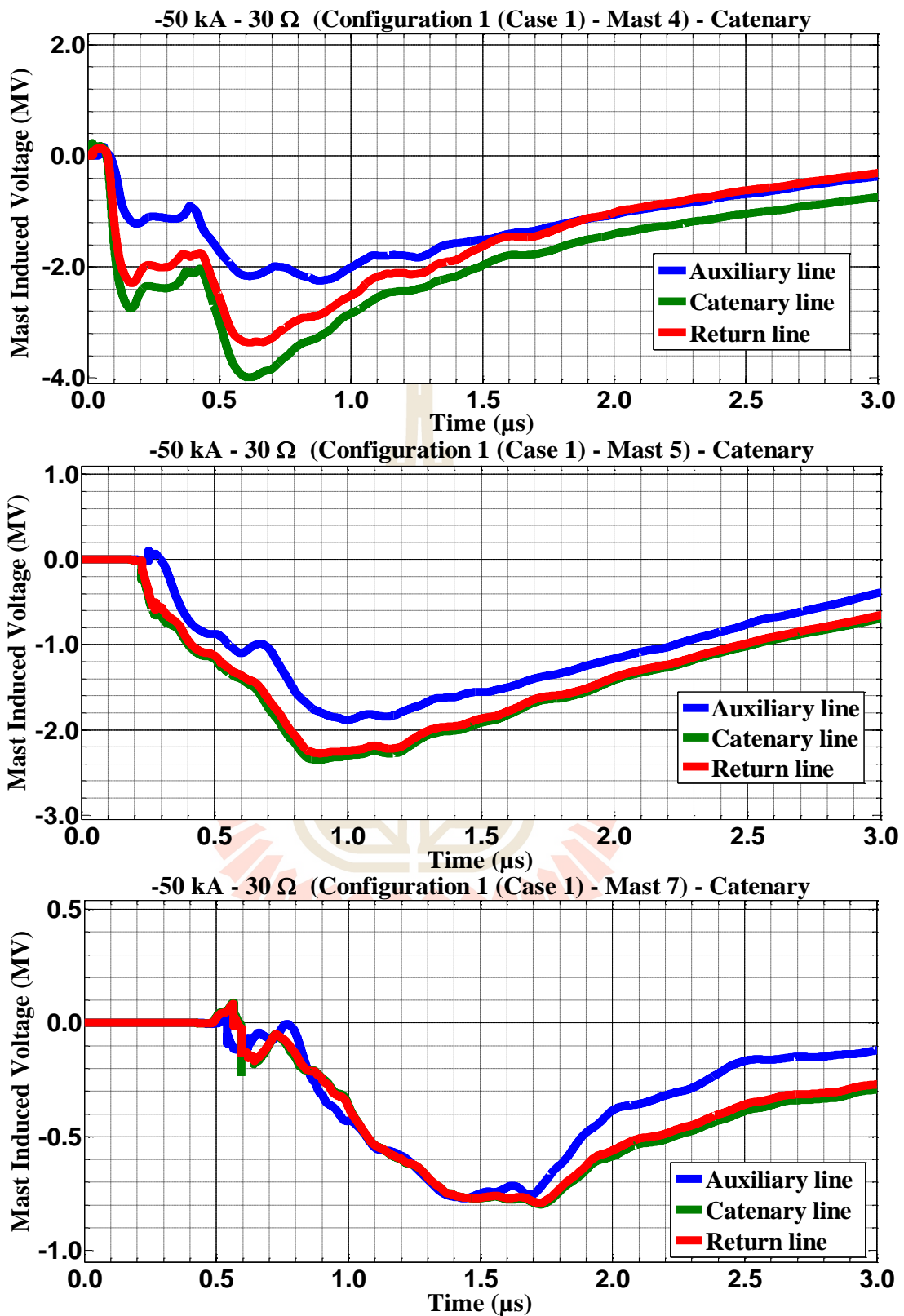


**Figure C.162** Mast 4, 5, and 7 induced voltage waveform of the -50 kA first stroke-(1.0/100  $\mu\text{s}$ ), subsequent stroke-(0.2/50  $\mu\text{s}$ ) strikes on Mast 4 with 30  $\Omega$  for Case 1



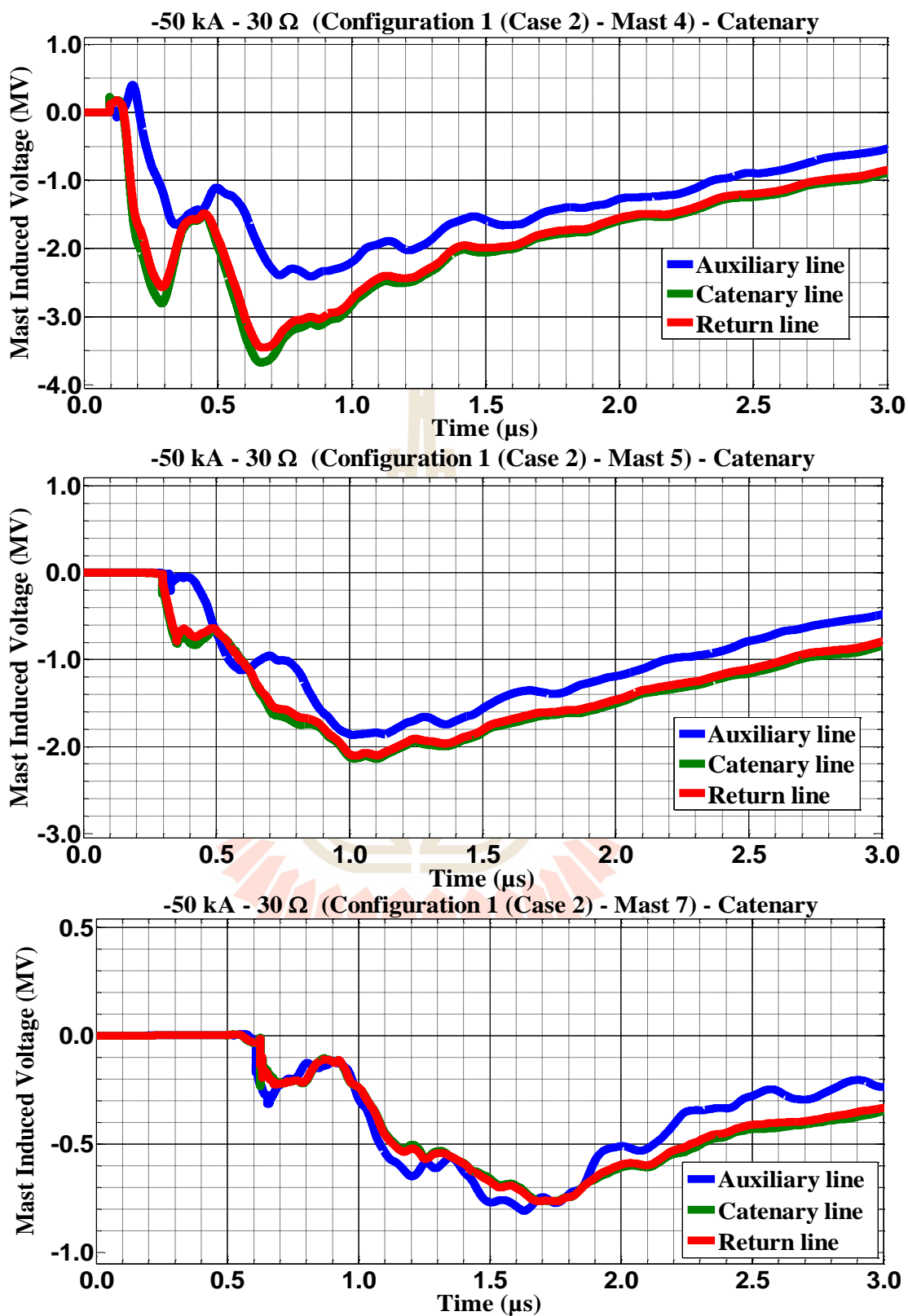


**Figure C.163** Mast 4, 5, and 7 induced voltage waveform of the -50 kA first stroke-(1.0/100 μs), subsequent stroke-(0.2/50 μs) strikes on Mast 4 with 30 Ω for Case 2

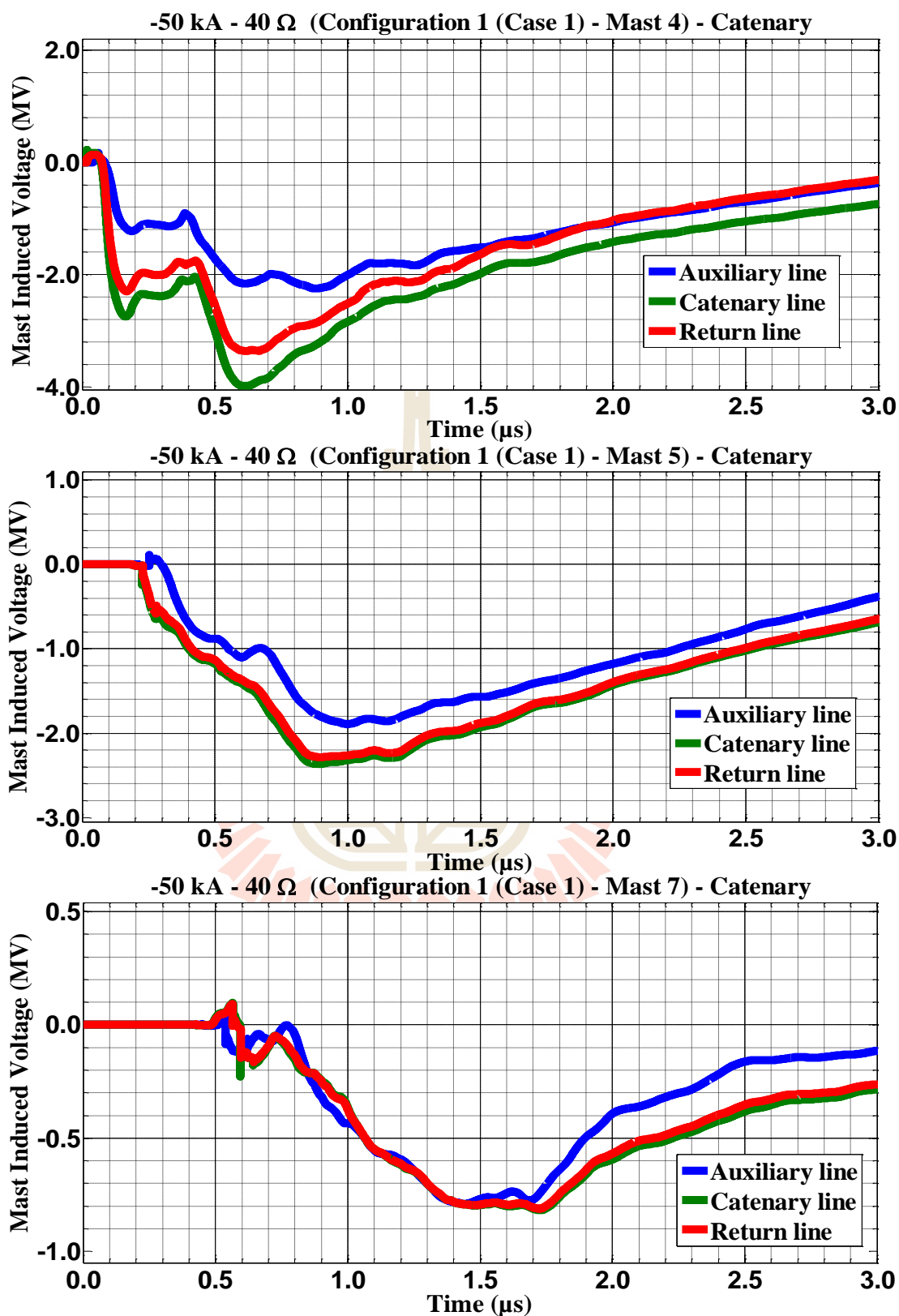


**Figure C.164** Mast 4, 5, and 7 induced voltage waveform of the -50 kA first stroke-(1.0/100  $\mu\text{s}$ ), subsequent stroke-(0.2/50  $\mu\text{s}$ ) strikes on Mast 4 with 40  $\Omega$  for Case 1

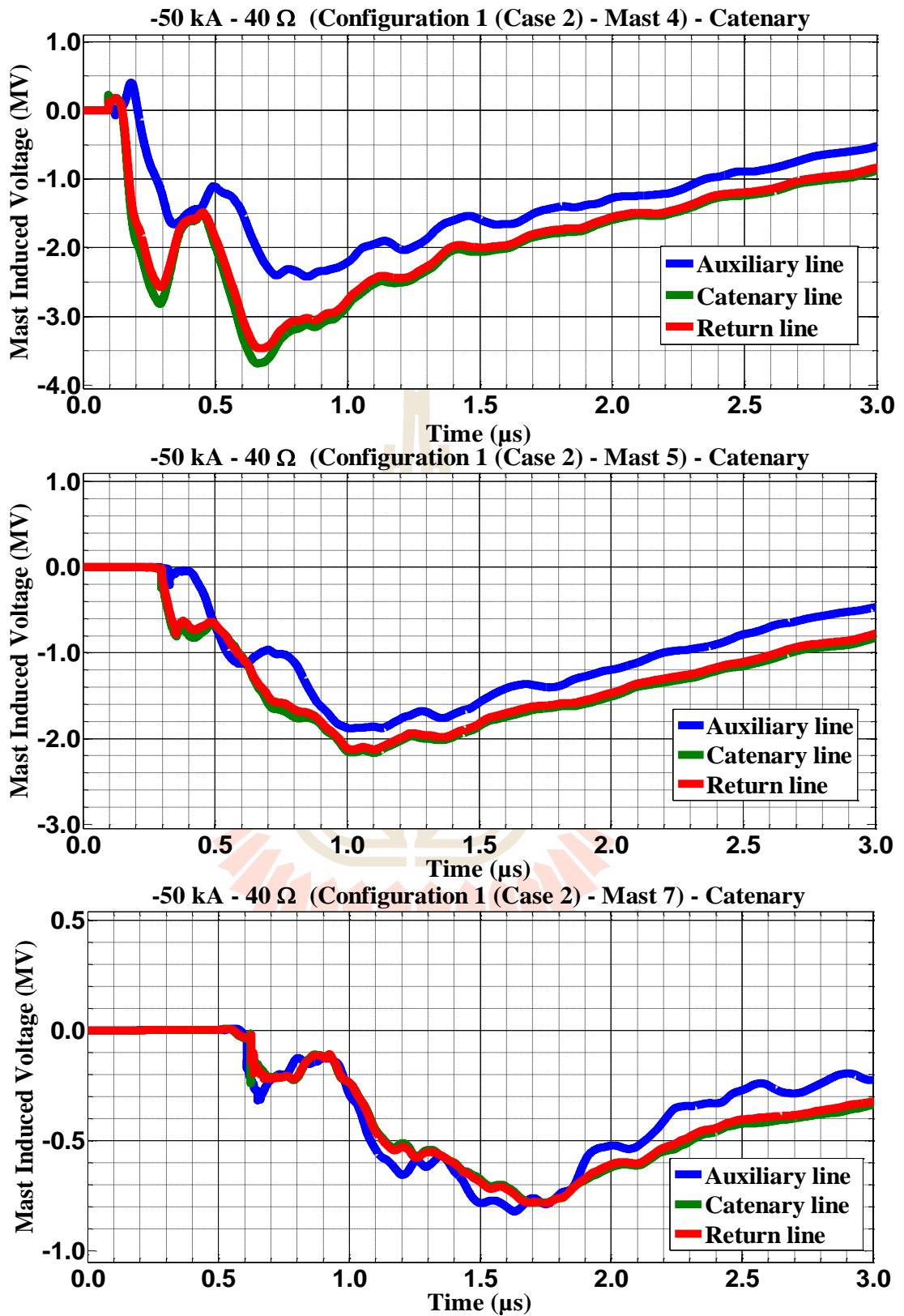


**Figure C.165** Mast 4, 5, and 7 induced voltage waveform of the -50 kA first stroke-(1.0/100 μs), subsequent stroke-(0.2/50 μs) strikes on Mast 4 with 40 Ω for Case 2

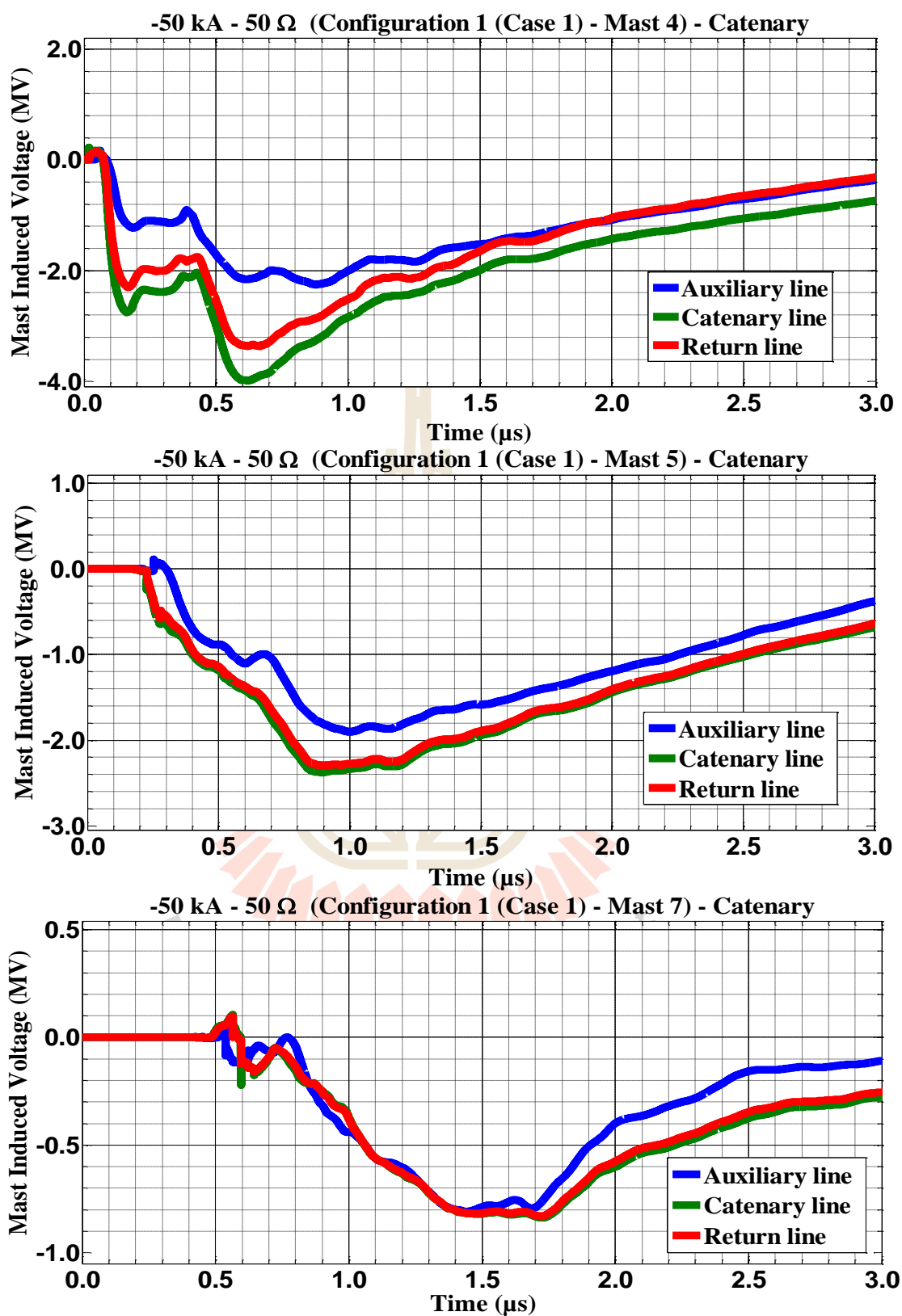


**Figure C.166** Mast 4, 5, and 7 induced voltage waveform of the -50 kA first stroke-(1.0/100  $\mu\text{s}$ ), subsequent stroke-(0.2/50  $\mu\text{s}$ ) strikes on Mast 4 with 50  $\Omega$  for Case 1

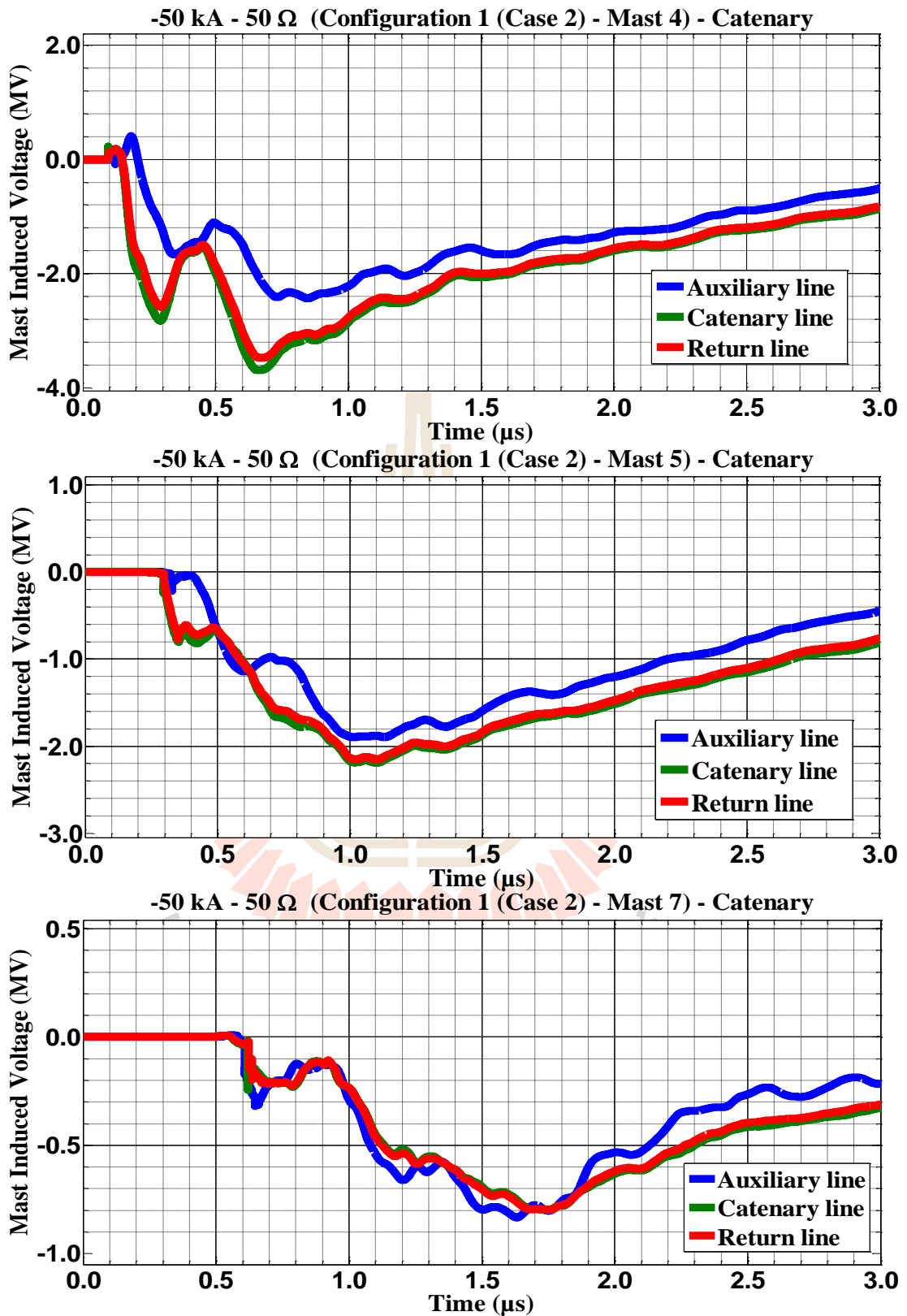


**Figure C.167** Mast 4, 5, and 7 induced voltage waveform of the -50 kA first stroke-(1.0/100 μs), subsequent stroke-(0.2/50 μs) strikes on Mast 4 with 50 Ω for Case 2



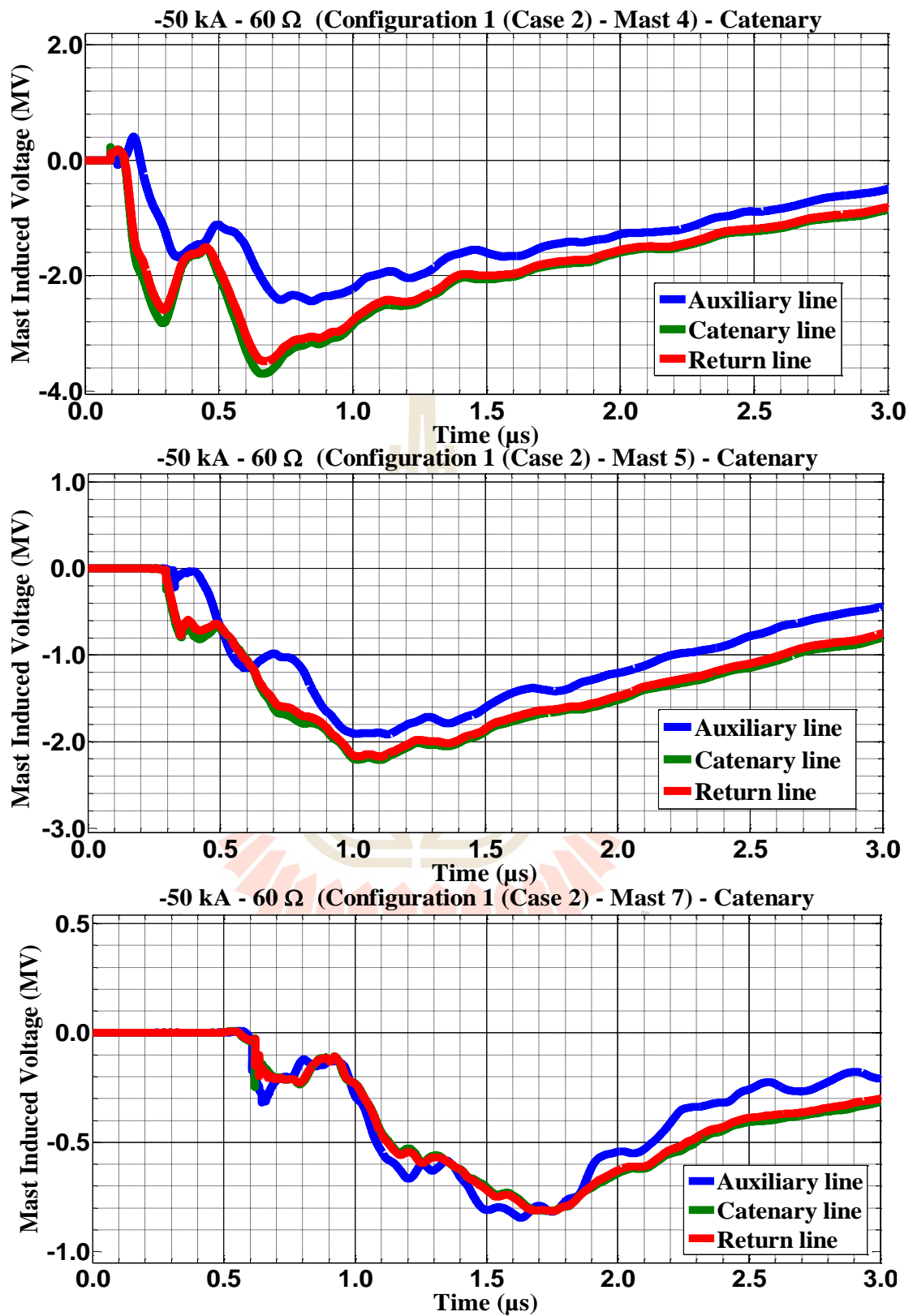


**Figure C.169** Mast 4, 5, and 7 induced voltage waveform of the  $-50 \text{ kA}$  first stroke-( $1.0/100 \mu\text{s}$ ), subsequent stroke-( $0.2/50 \mu\text{s}$ ) strikes on Mast 4 with  $60 \Omega$  for Case 2

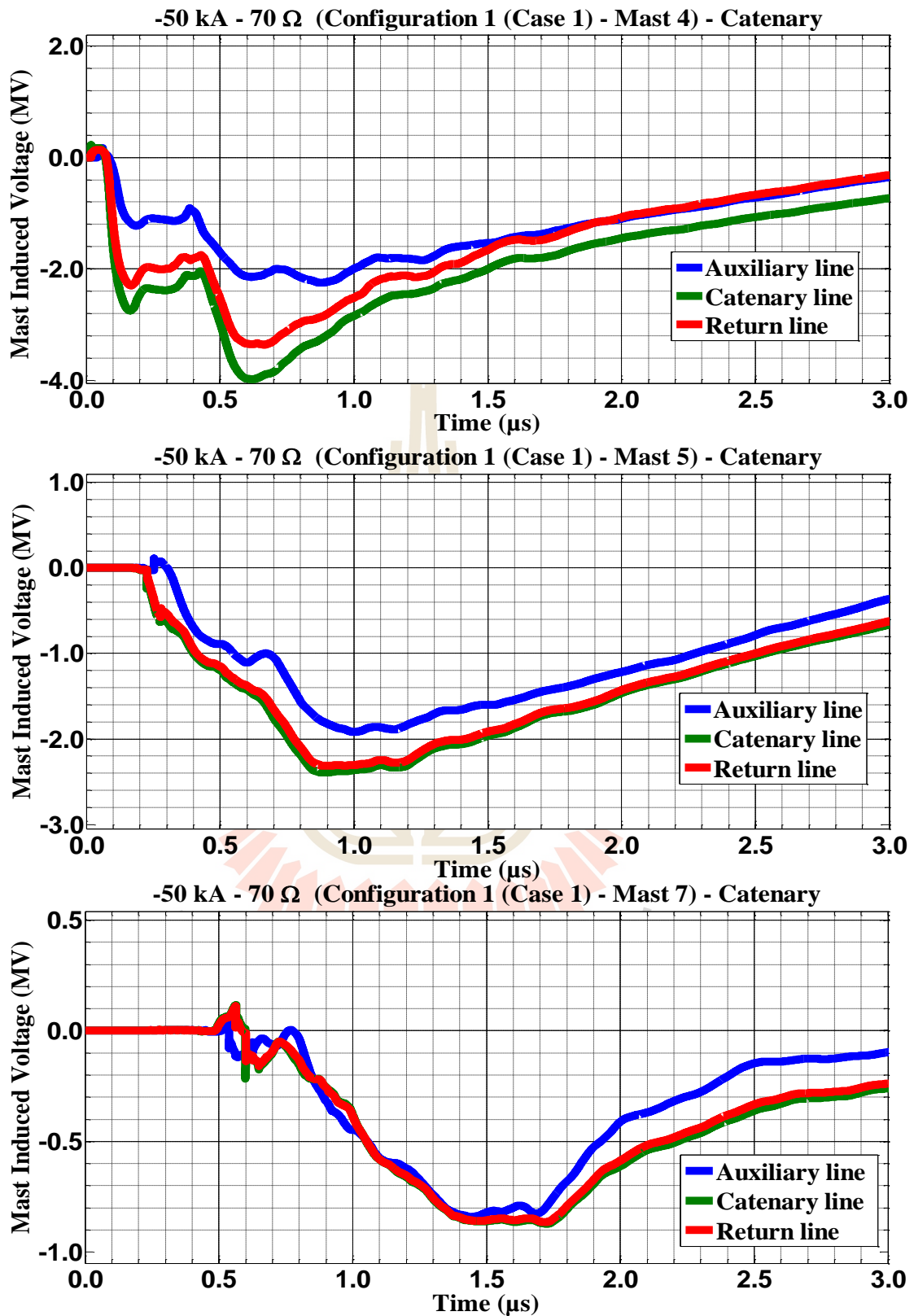


**Figure C.170** Mast 4, 5, and 7 induced voltage waveform of the -50 kA first stroke-(1.0/100  $\mu\text{s}$ ), subsequent stroke-(0.2/50  $\mu\text{s}$ ) strikes on Mast 4 with 70  $\Omega$  for Case 1



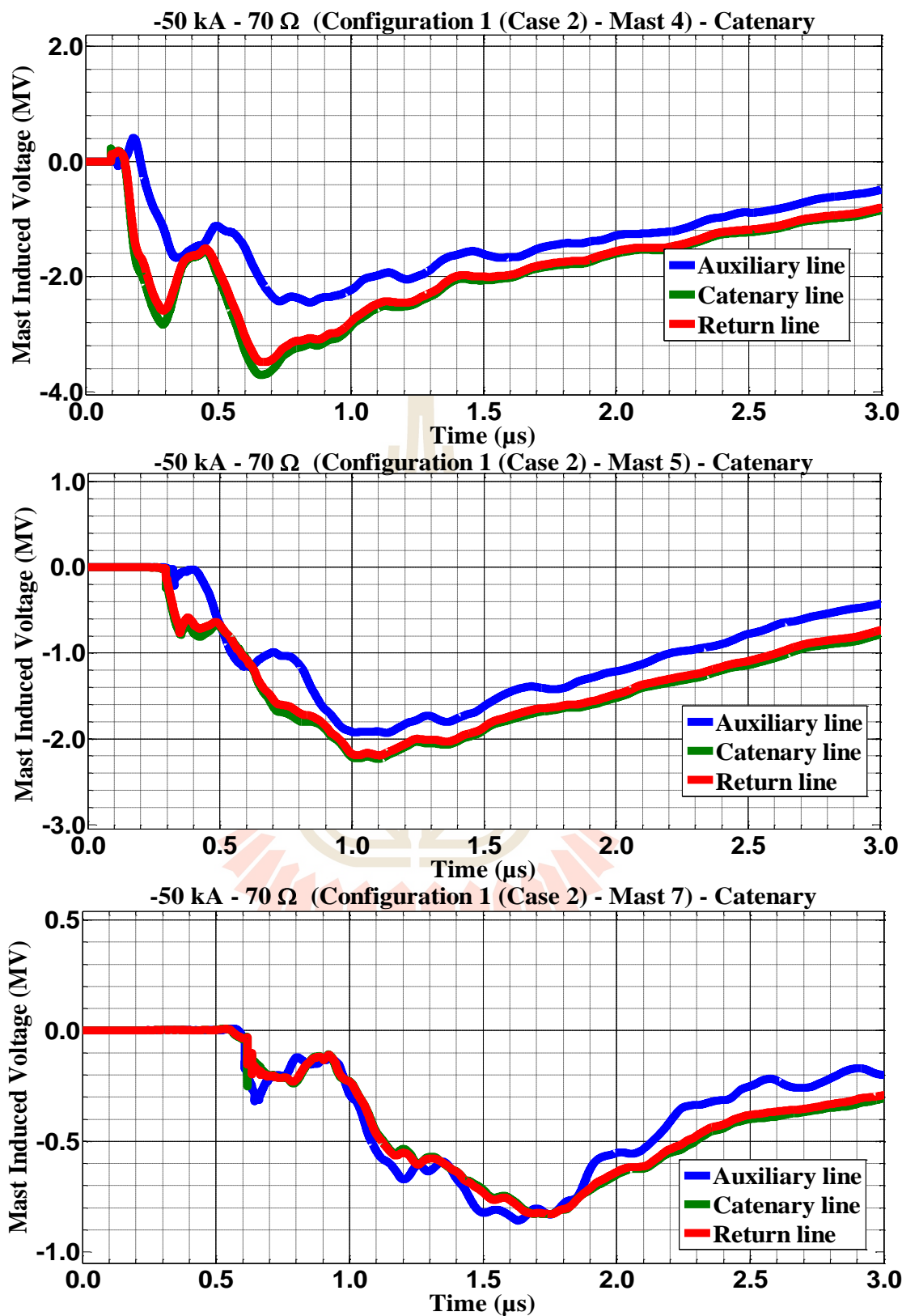
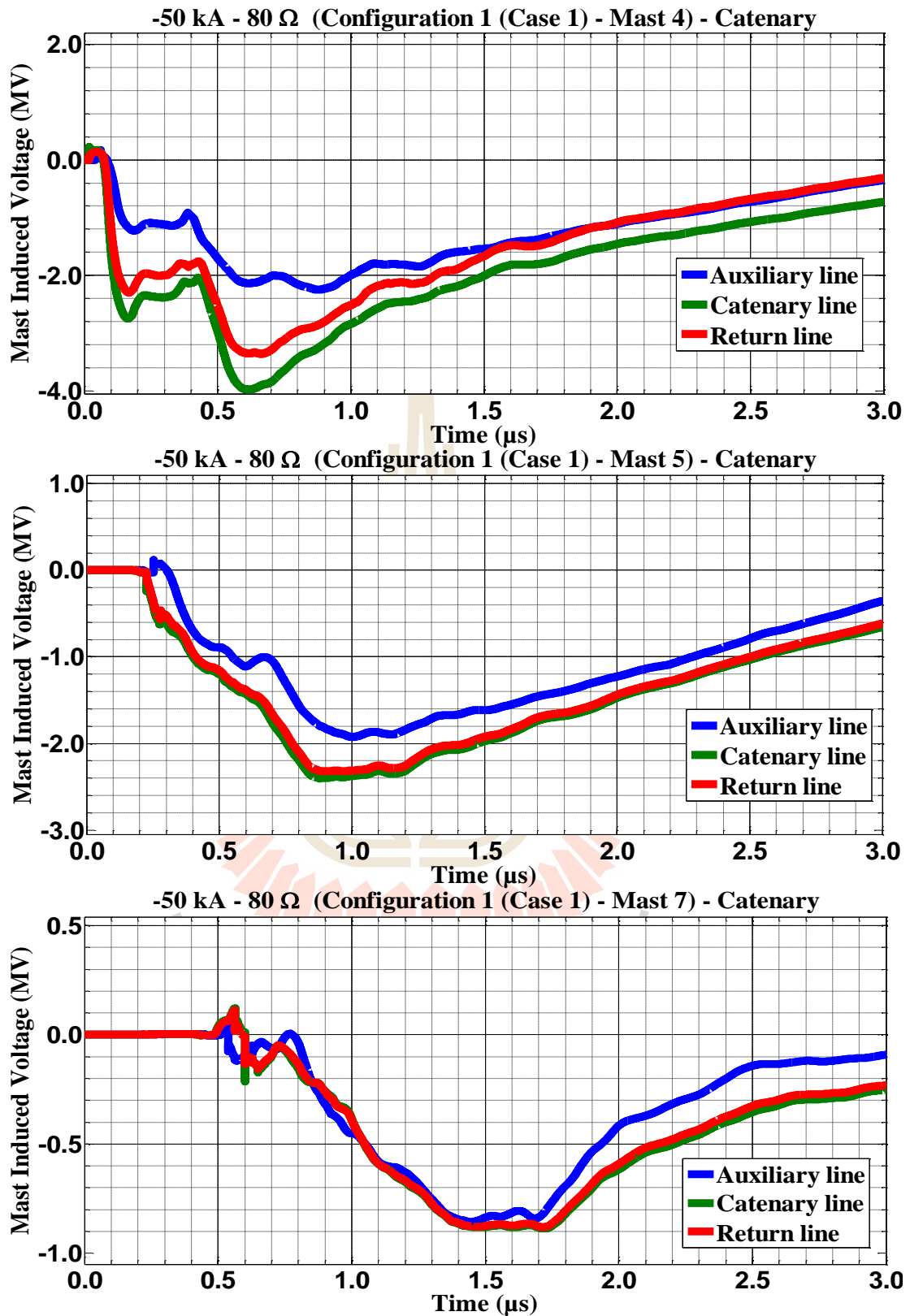
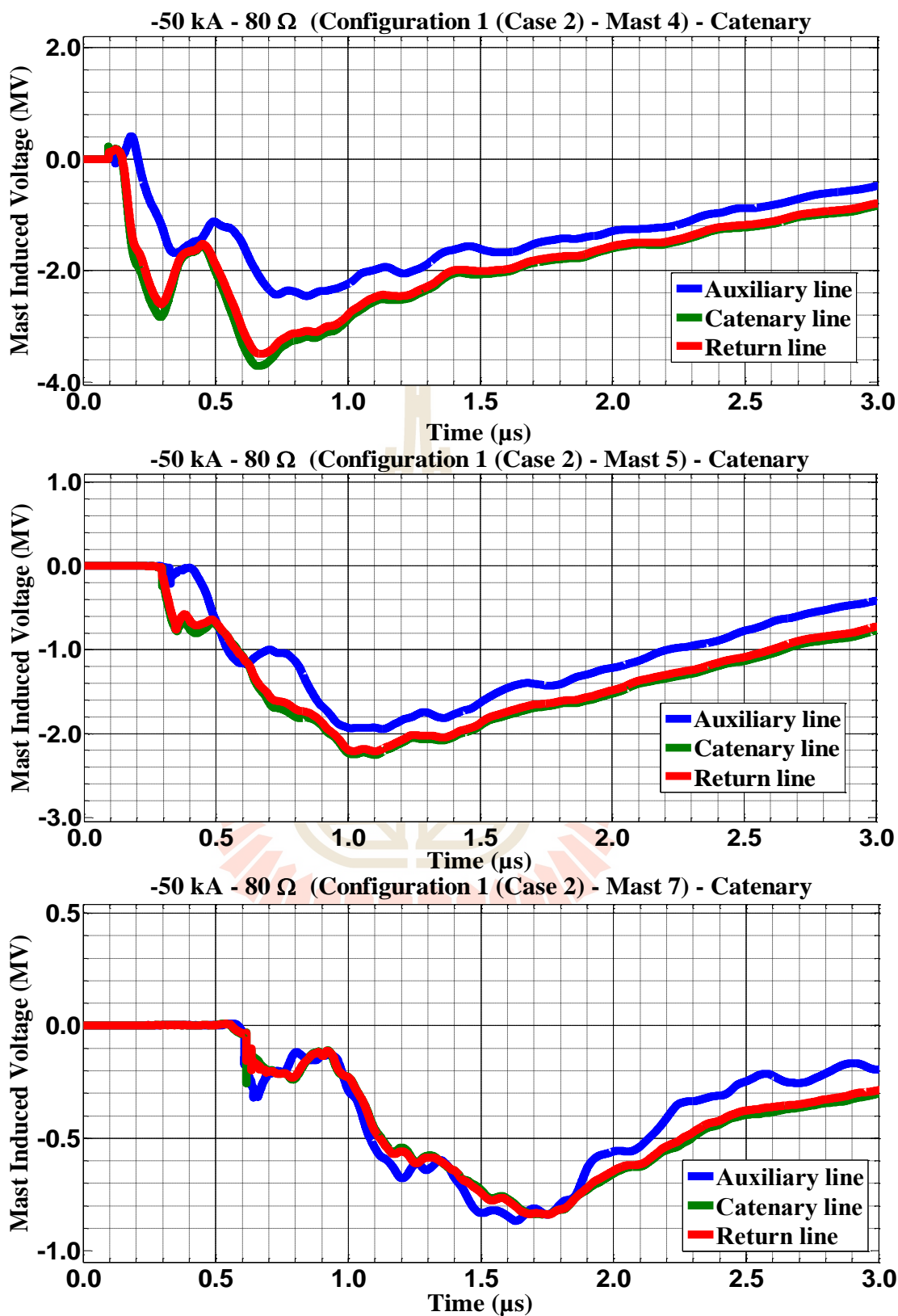


Figure C.171 Mast 4, 5, and 7 induced voltage waveform of the -50 kA first stroke-(1.0/100  $\mu\text{s}$ ), subsequent stroke-(0.2/50  $\mu\text{s}$ ) strikes on Mast 4 with 70  $\Omega$  for Case 2



**Figure C.172** Mast 4, 5, and 7 induced voltage waveform of the -50 kA first stroke-(1.0/100 μs), subsequent stroke-(0.2/50 μs) strikes on Mast 4 with 80 Ω for Case 1



**Figure C.173** Mast 4, 5, and 7 induced voltage waveform of the -50 kA first stroke-(1.0/100  $\mu\text{s}$ ), subsequent stroke-(0.2/50  $\mu\text{s}$ ) strikes on Mast 4 with 80  $\Omega$  for Case 2

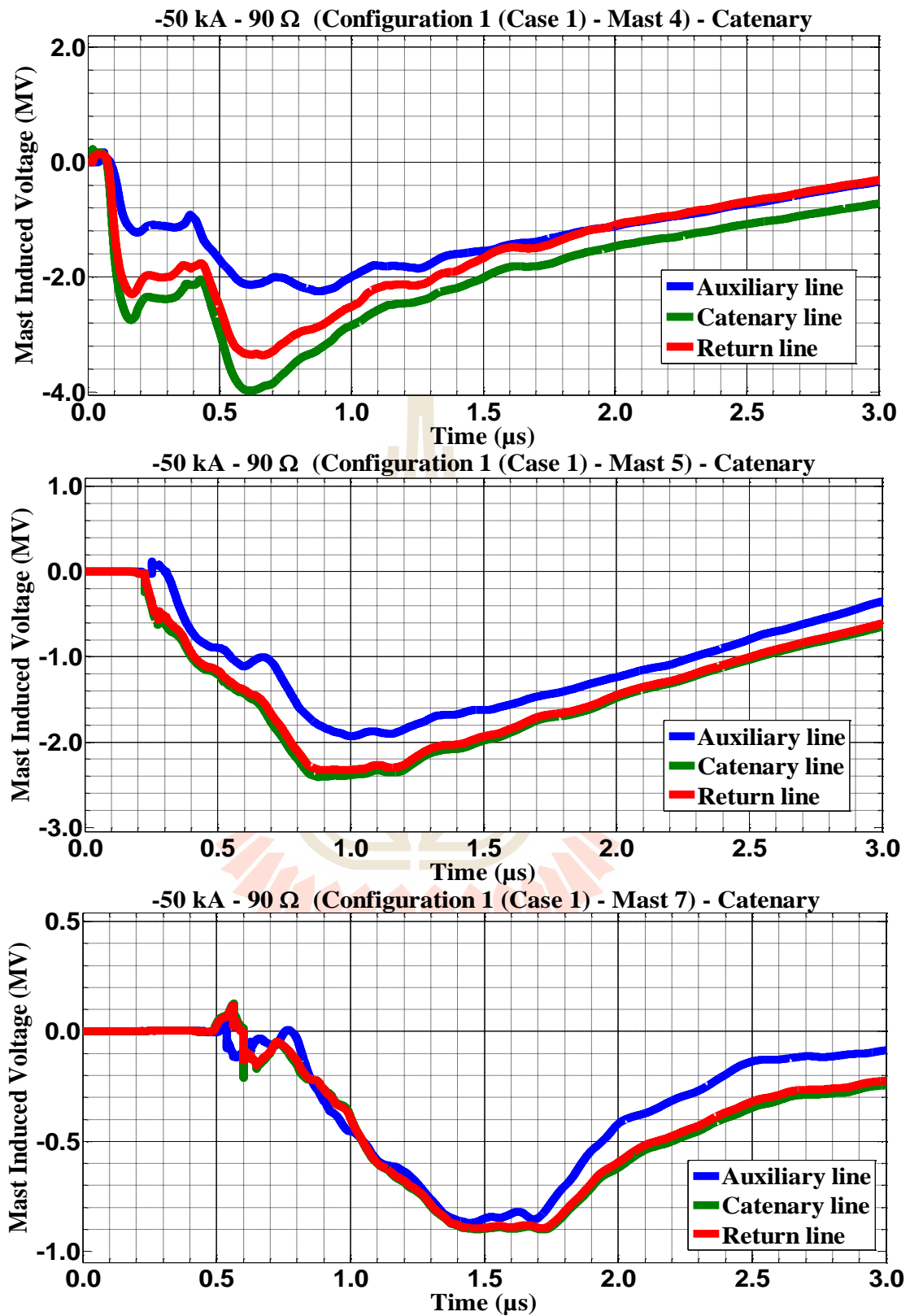


**Figure C.174** Mast 4, 5, and 7 induced voltage waveform of the -50 kA first stroke-(1.0/100  $\mu\text{s}$ ), subsequent stroke-(0.2/50  $\mu\text{s}$ ) strikes on Mast 4 with 90  $\Omega$  for Case 1

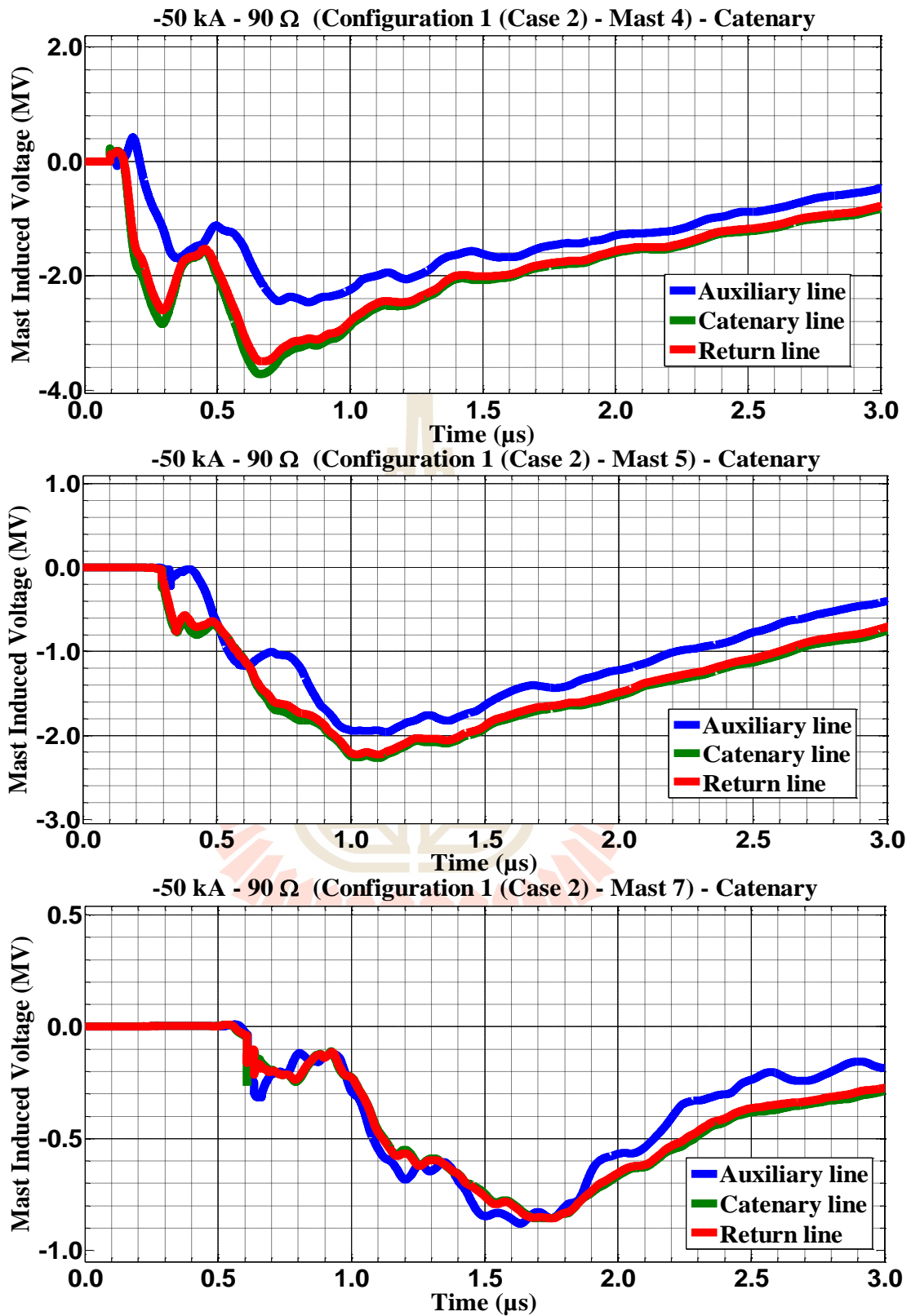


**Figure C.175** Mast 4, 5, and 7 induced voltage waveform of the -50 kA first stroke-(1.0/100  $\mu\text{s}$ ), subsequent stroke-(0.2/50  $\mu\text{s}$ ) strikes on Mast 4 with 90  $\Omega$  for Case 2

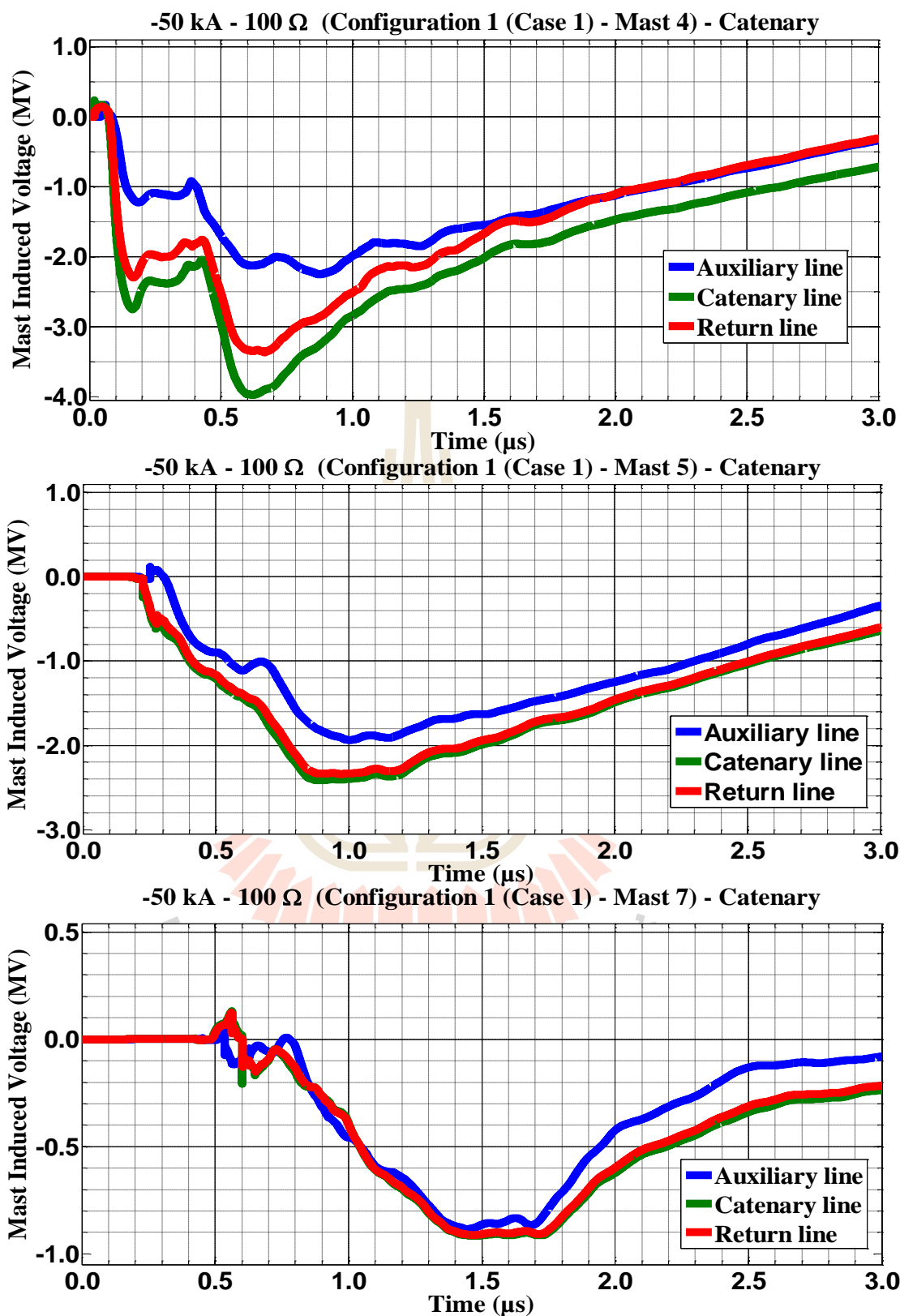


**Figure C.176** Mast 4, 5, and 7 induced voltage waveform of the -50 kA first stroke-(1.0/100 μs), subsequent stroke-(0.2/50 μs) strikes on Mast 4 with 100 Ω for Case 1

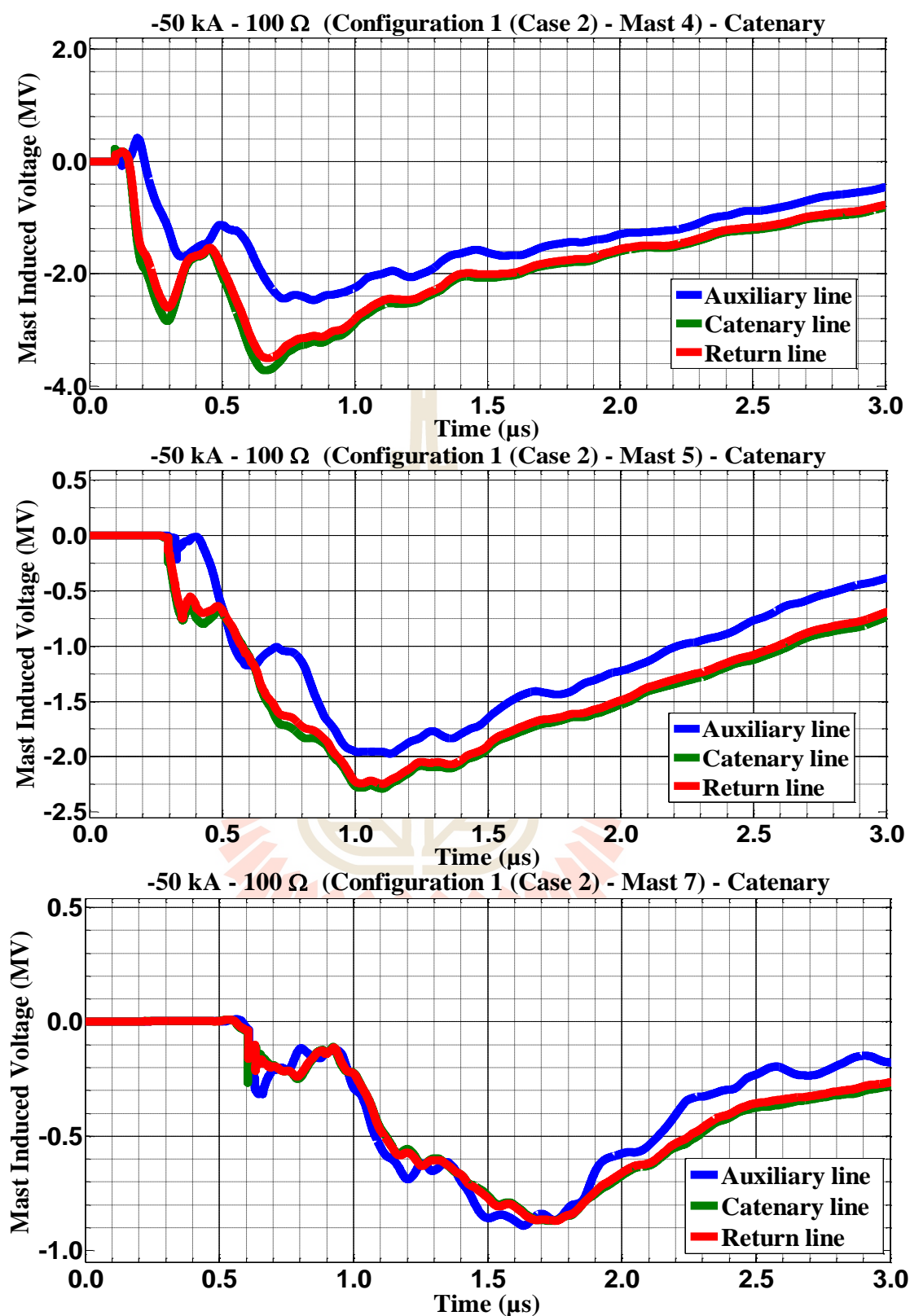


**Figure C.177** Mast 4, 5, and 7 induced voltage waveform of the -50 kA first stroke-(1.0/100  $\mu\text{s}$ ), subsequent stroke-(0.2/50  $\mu\text{s}$ ) strikes on Mast 4 with 100  $\Omega$  for Case 2

**C.9 The consequences when the catenary struck by negative multiple lightning strokes for Configuration 2 in Case 1 and 2.**

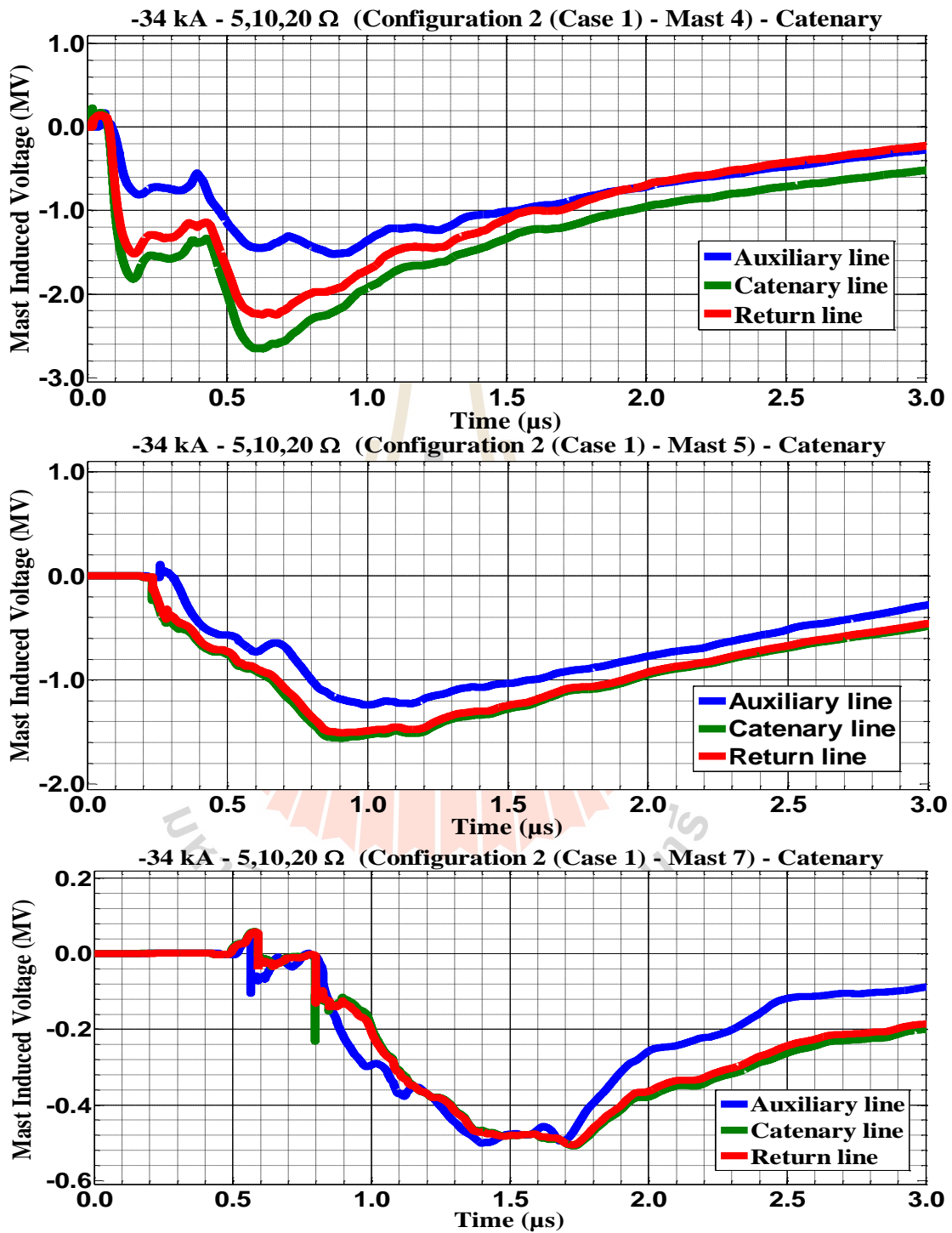


**Figure C.178** Mast 4, 5, and 7 with 5,10,20 Ω induced voltage waveform of -34 kA first stroke-(1.0/100 μs), subsequent stroke-(0.2/50 μs) strikes on Mast 4 for Case 1



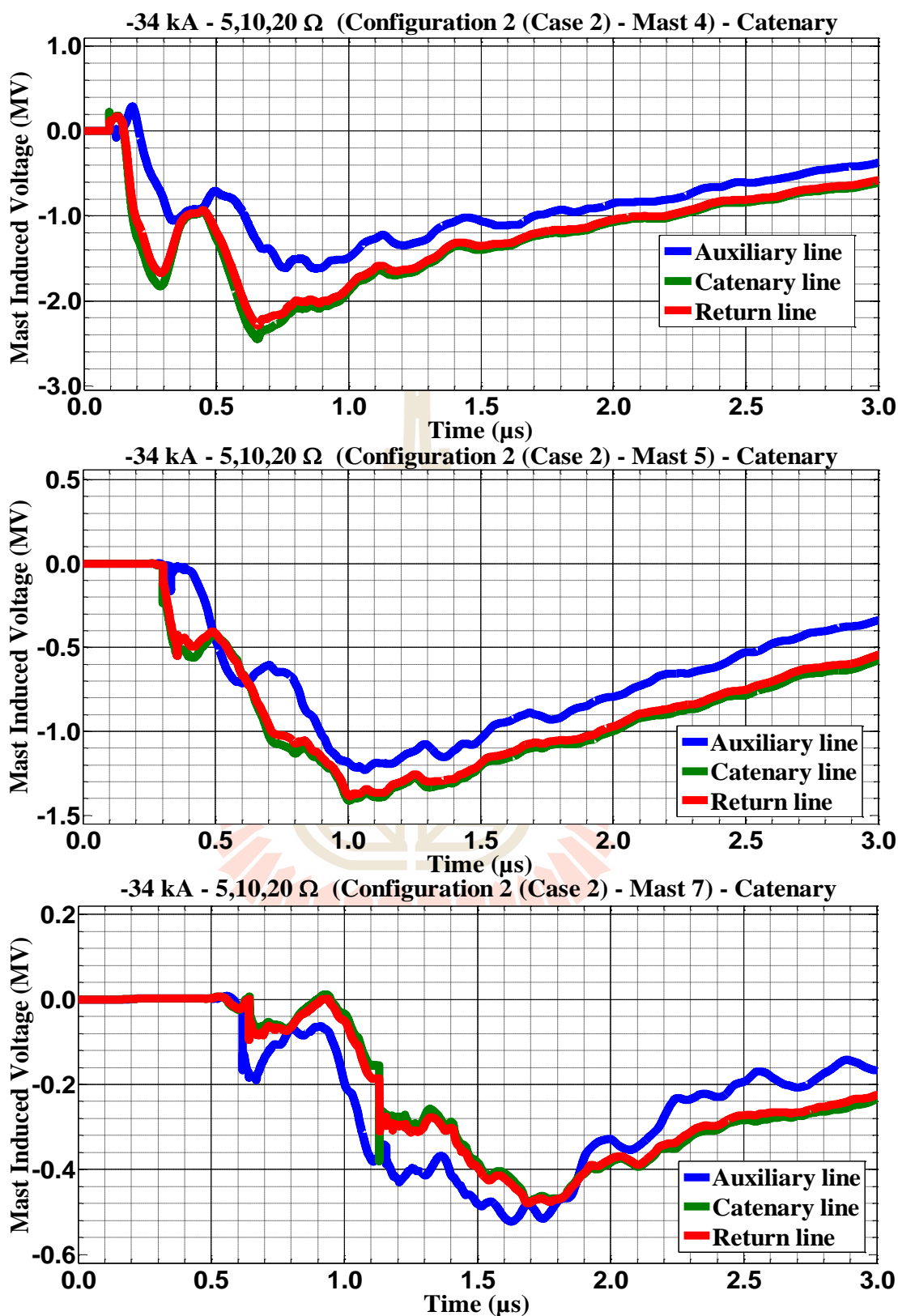


**Figure C.179** Mast 4, 5, and 7 with 5,10,20 Ω induced voltage waveform of -34 kA first stroke-(1.0/100 μs), subsequent stroke-(0.2/50 μs) strikes on Mast 4 for Case 2

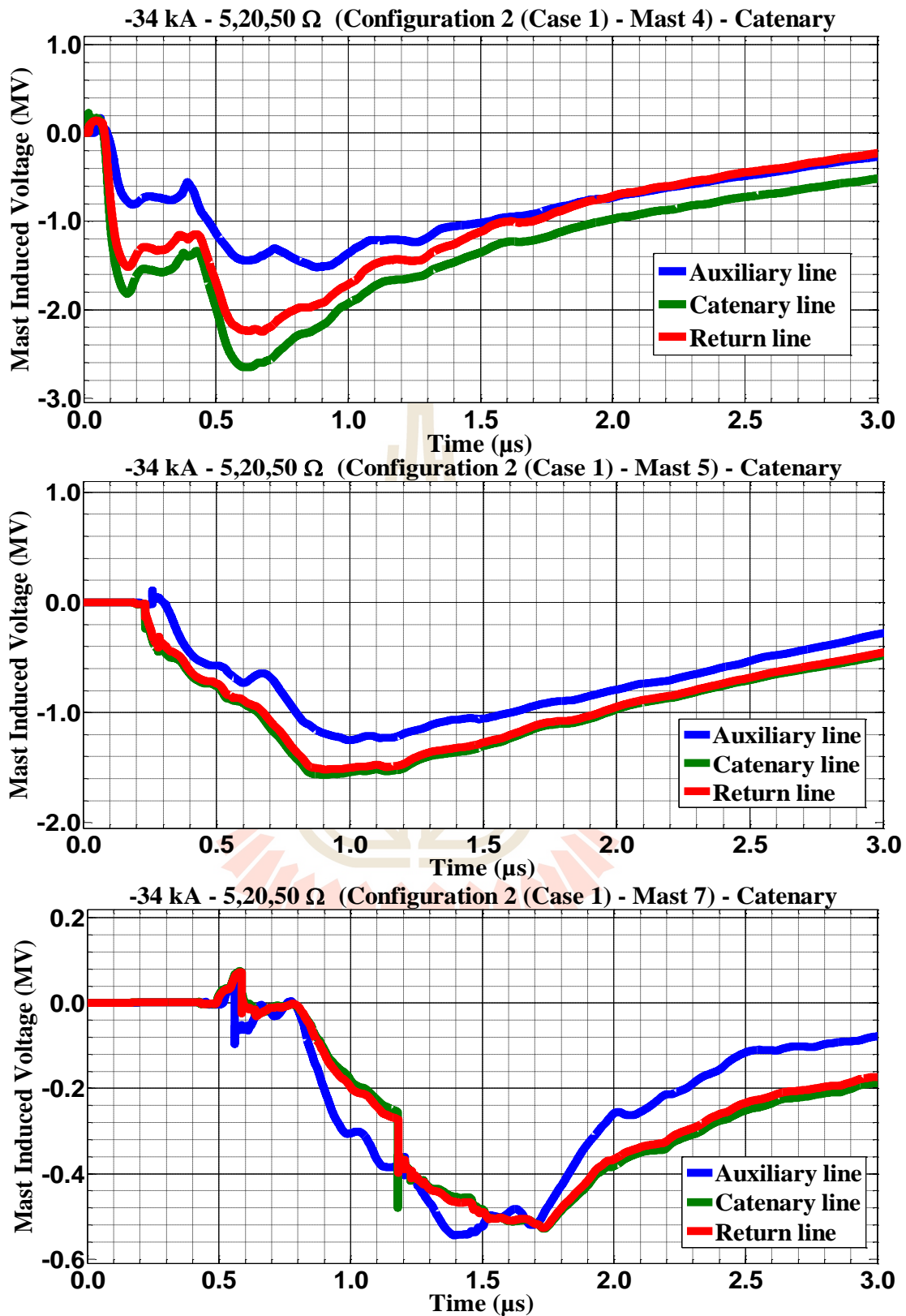


**Figure C.180** Mast 4, 5, and 7 with 5,20,50 Ω induced voltage waveform of -34 kA first stroke-(1.0/100 μs), subsequent stroke-(0.2/50 μs) strikes on Mast 4 for Case 1

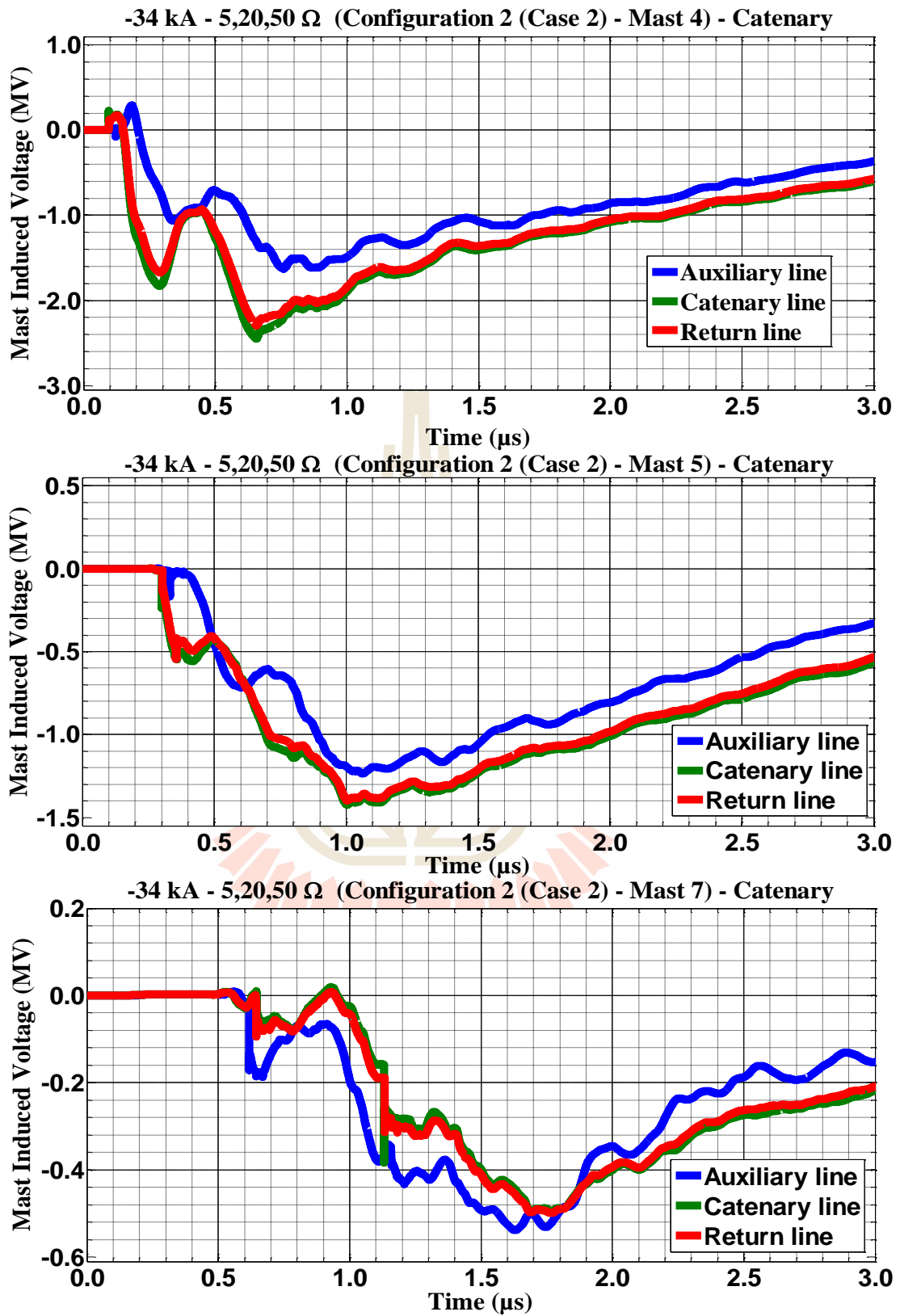


**Figure C.181** Mast 4, 5, and 7 with 5,20,50 Ω induced voltage waveform of -34 kA first stroke-(1.0/100 μs), subsequent stroke-(0.2/50 μs) strikes on Mast 4 for Case 2

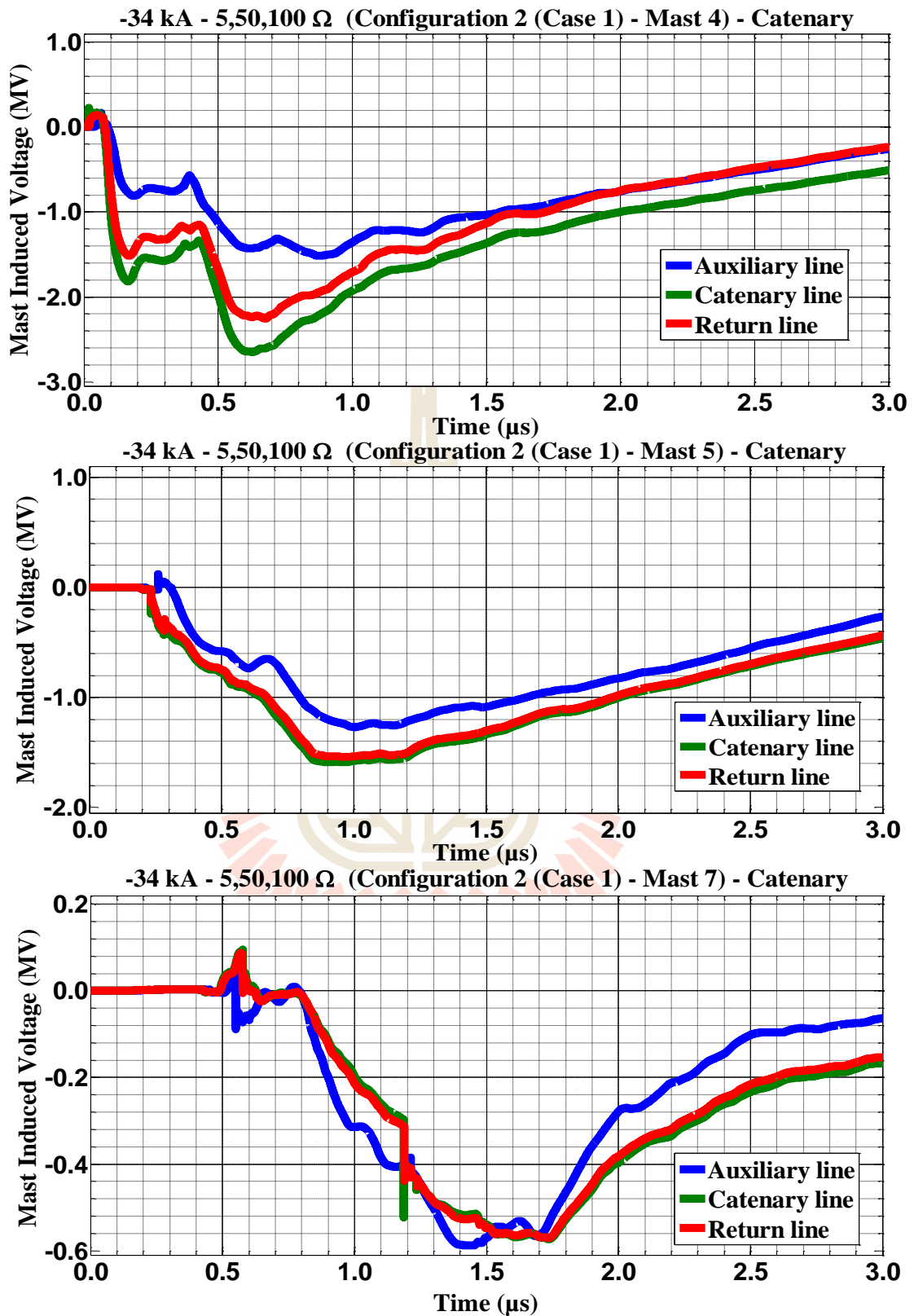


**Figure C.182** Mast 4, 5, and 7 with 5,50,100 Ω induced voltage waveform of -34 kA first stroke-(1.0/100 μs), subsequent stroke-(0.2/50 μs) strikes on Mast 4 for Case 1

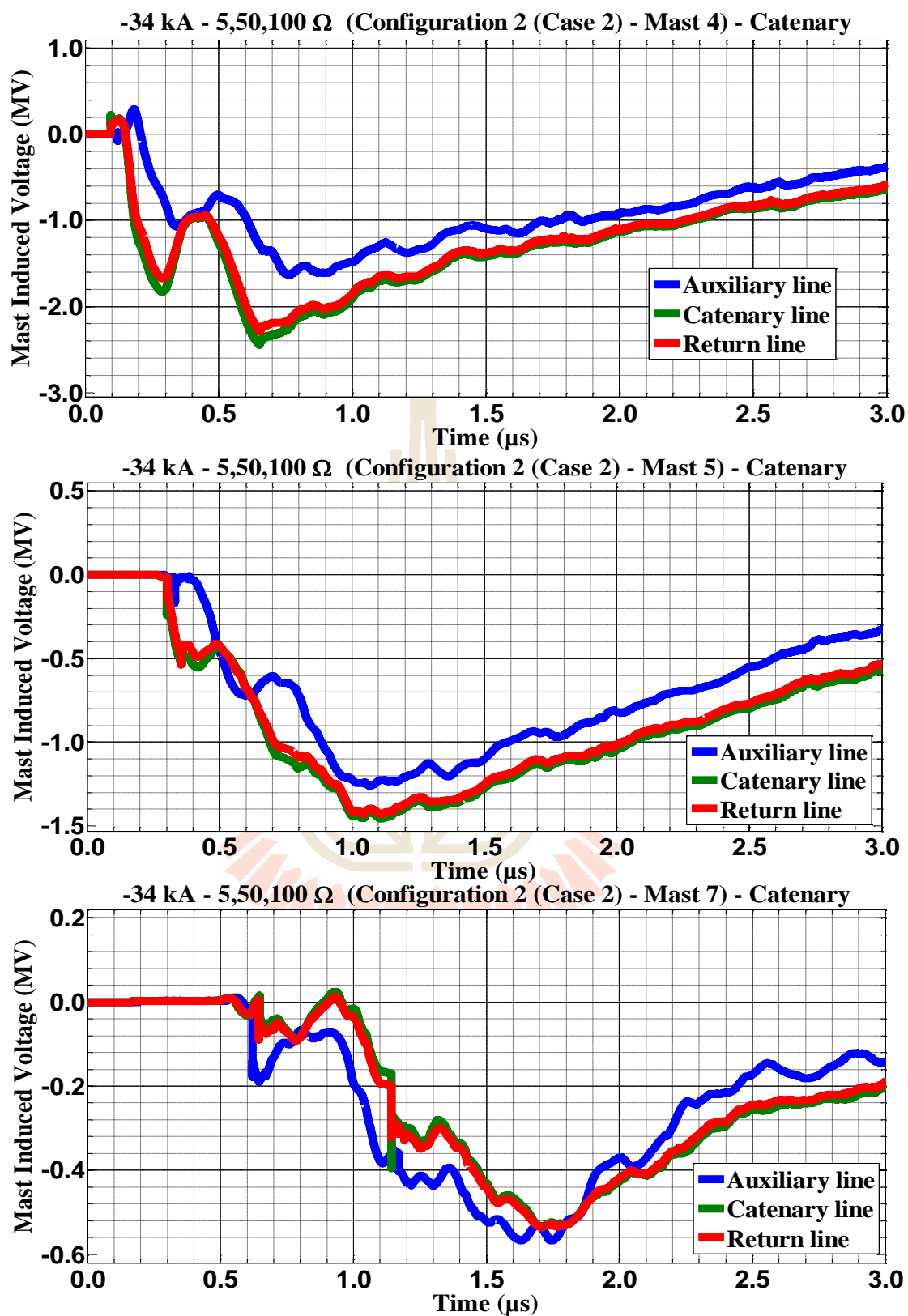


**Figure C.183** Mast 4, 5, and 7 with 5,50,100 Ω induced voltage waveform of -34 kA first stroke-(1.0/100 μs), subsequent stroke-(0.2/50 μs) strikes on Mast 4 for Case 2

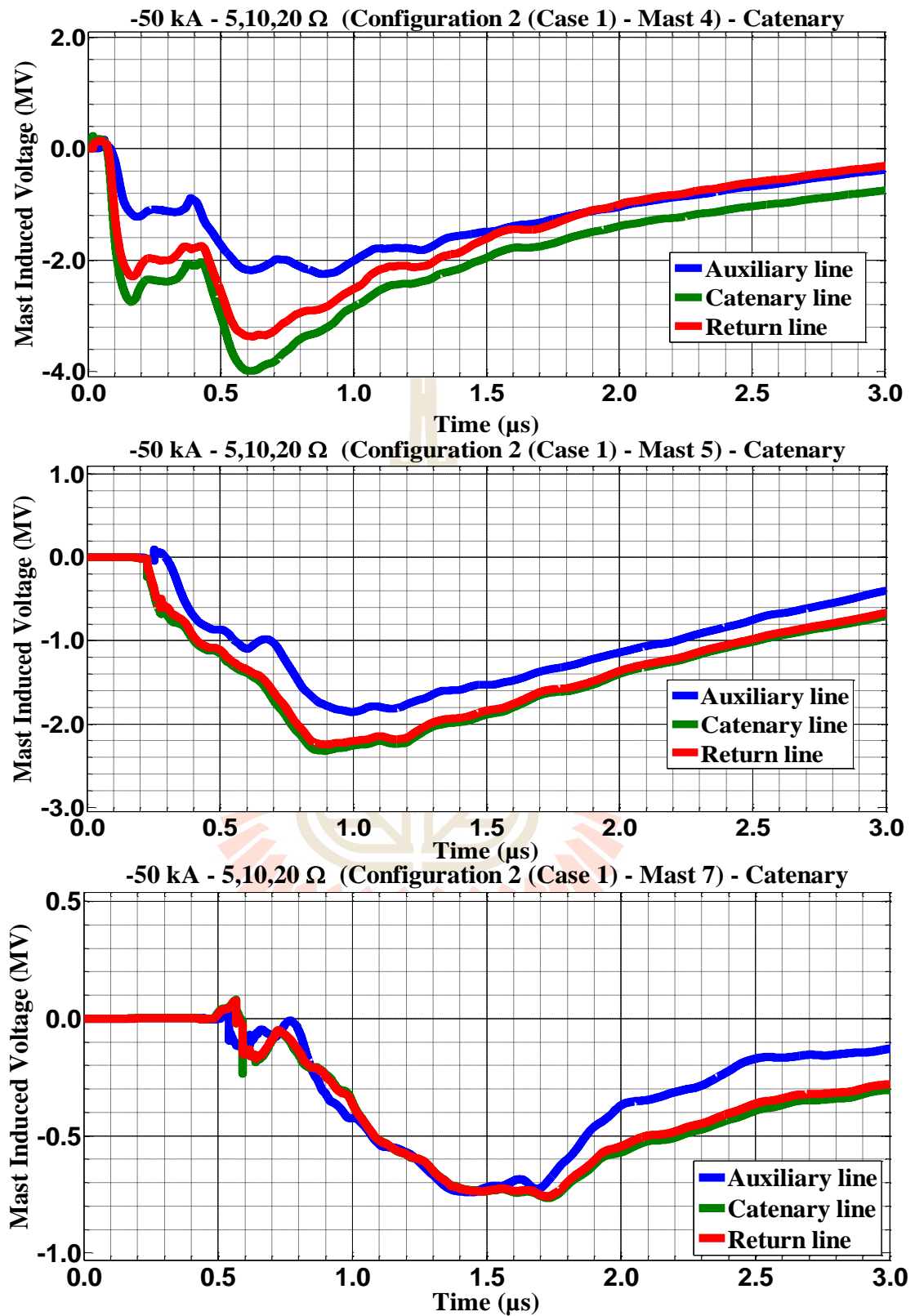
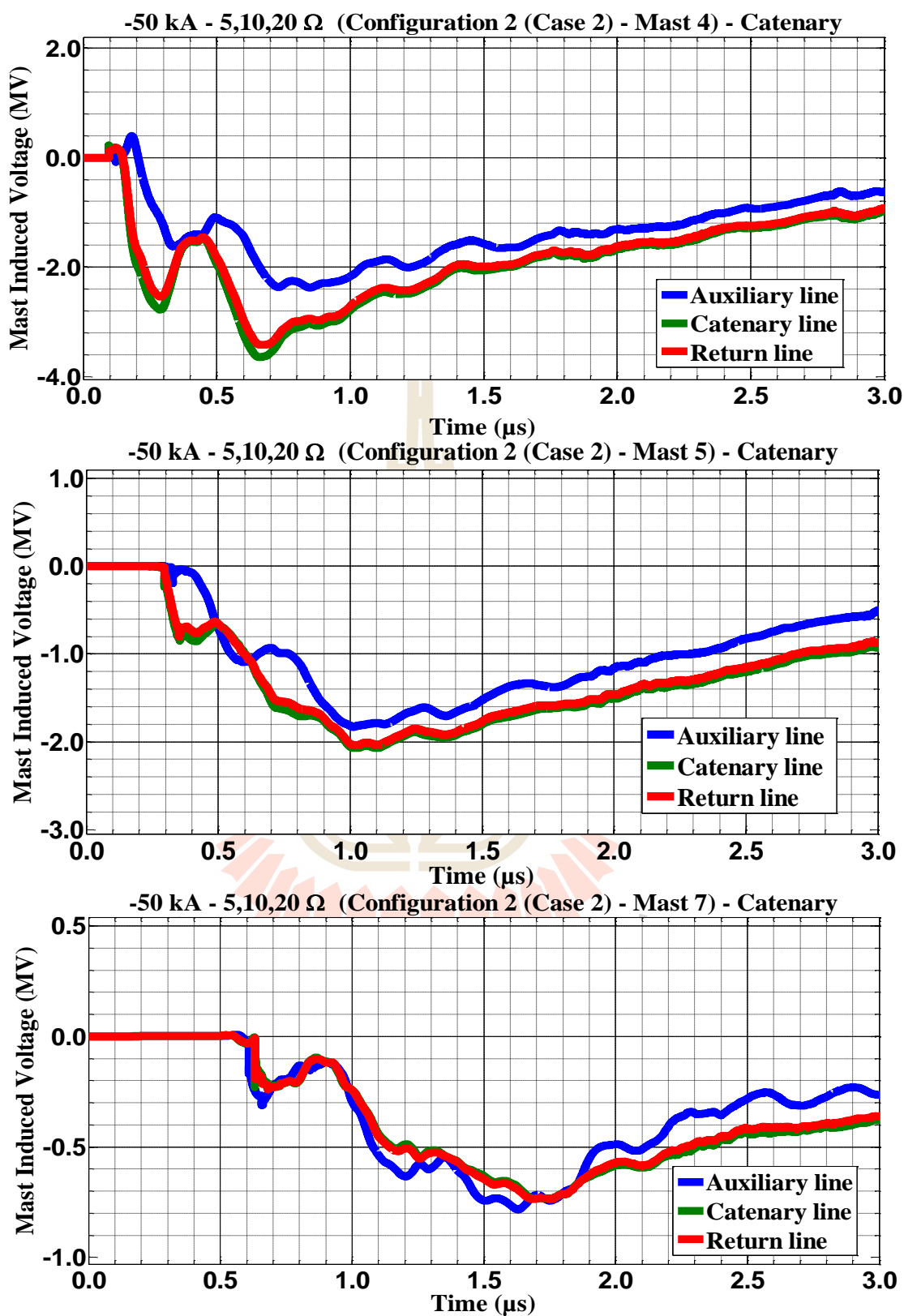
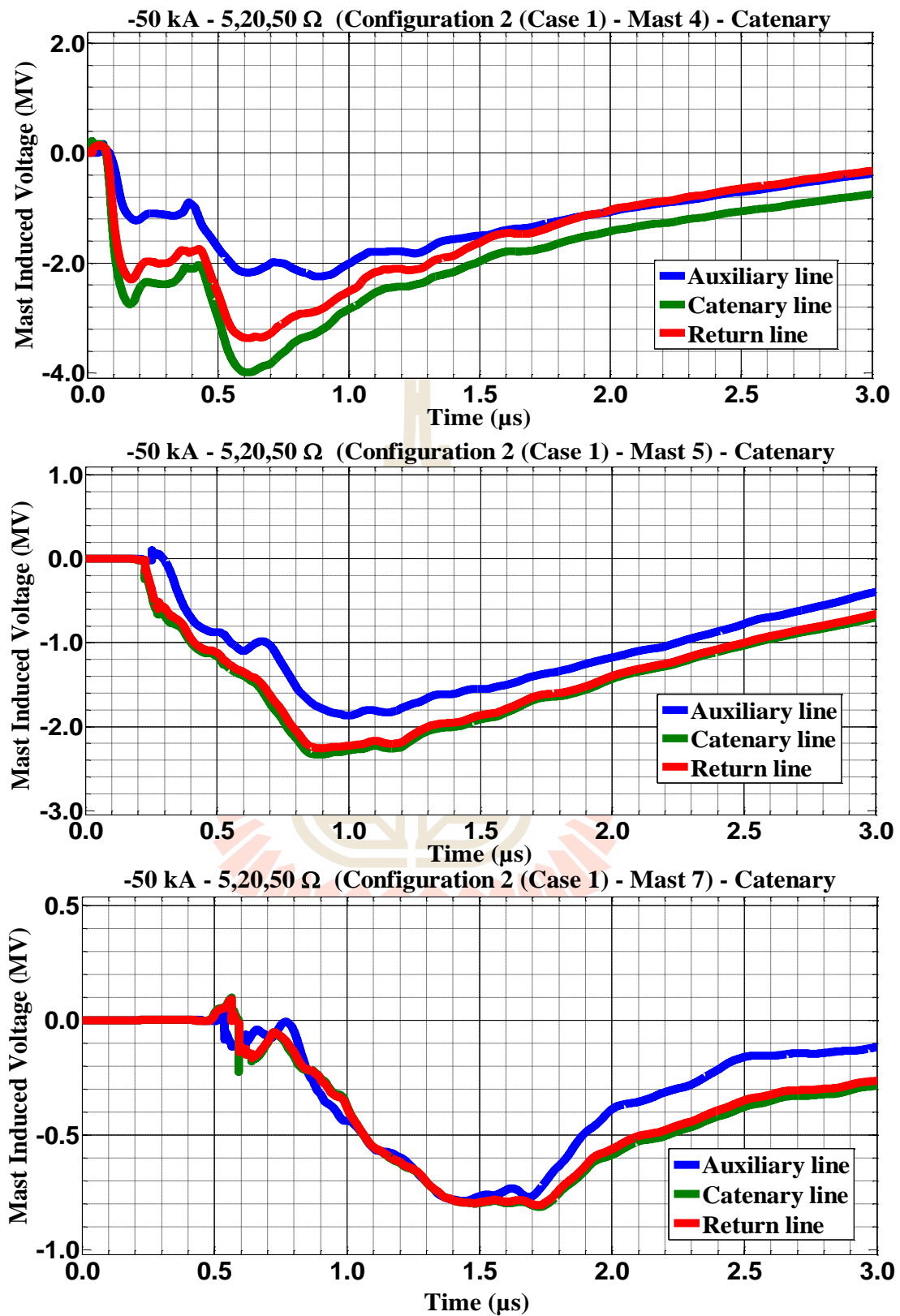


Figure C.184 Mast 4, 5, and 7 with 5,10,20 Ω induced voltage waveform of -50 kA first stroke-(1.0/100 μs), subsequent stroke-(0.2/50 μs) strikes on Mast 4 for Case 1



**Figure C.185** Mast 4, 5, and 7 with 5,10,20 Ω induced voltage waveform of -50 kA first stroke-(1.0/100 μs), subsequent stroke-(0.2/50 μs) strikes on Mast 4 for Case 1



**Figure C.186** Mast 4, 5, and 7 with 5,20,50 Ω induced voltage waveform of -50 kA first stroke-(1.0/100 μs), subsequent stroke-(0.2/50 μs) strikes on Mast 4 for Case 1



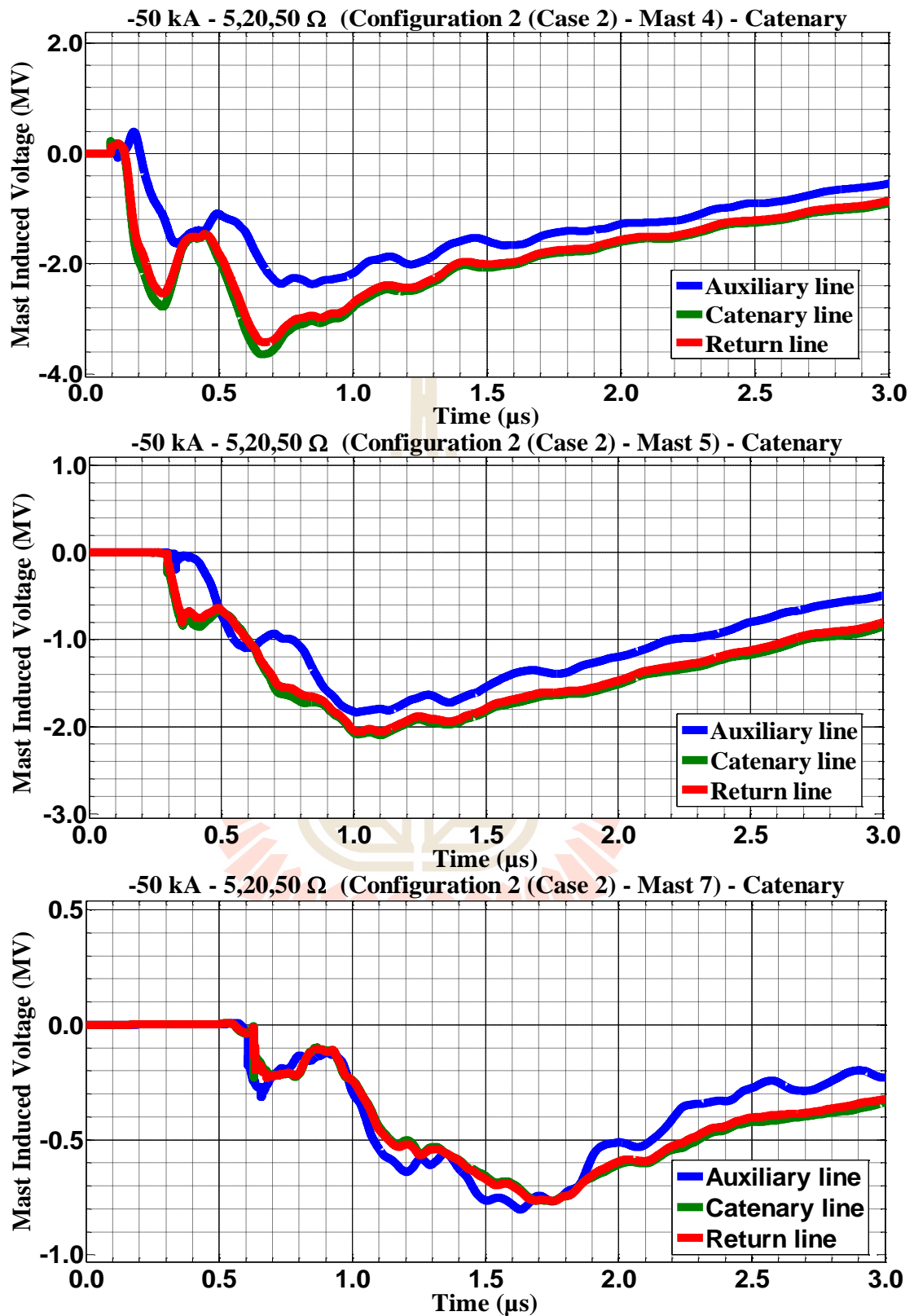


**Figure C.187** Mast 4, 5, and 7 with 5,20,50 Ω induced voltage waveform of -50 kA first stroke-(1.0/100 μs), subsequent stroke-(0.2/50 μs) strikes on Mast 4 for Case 2

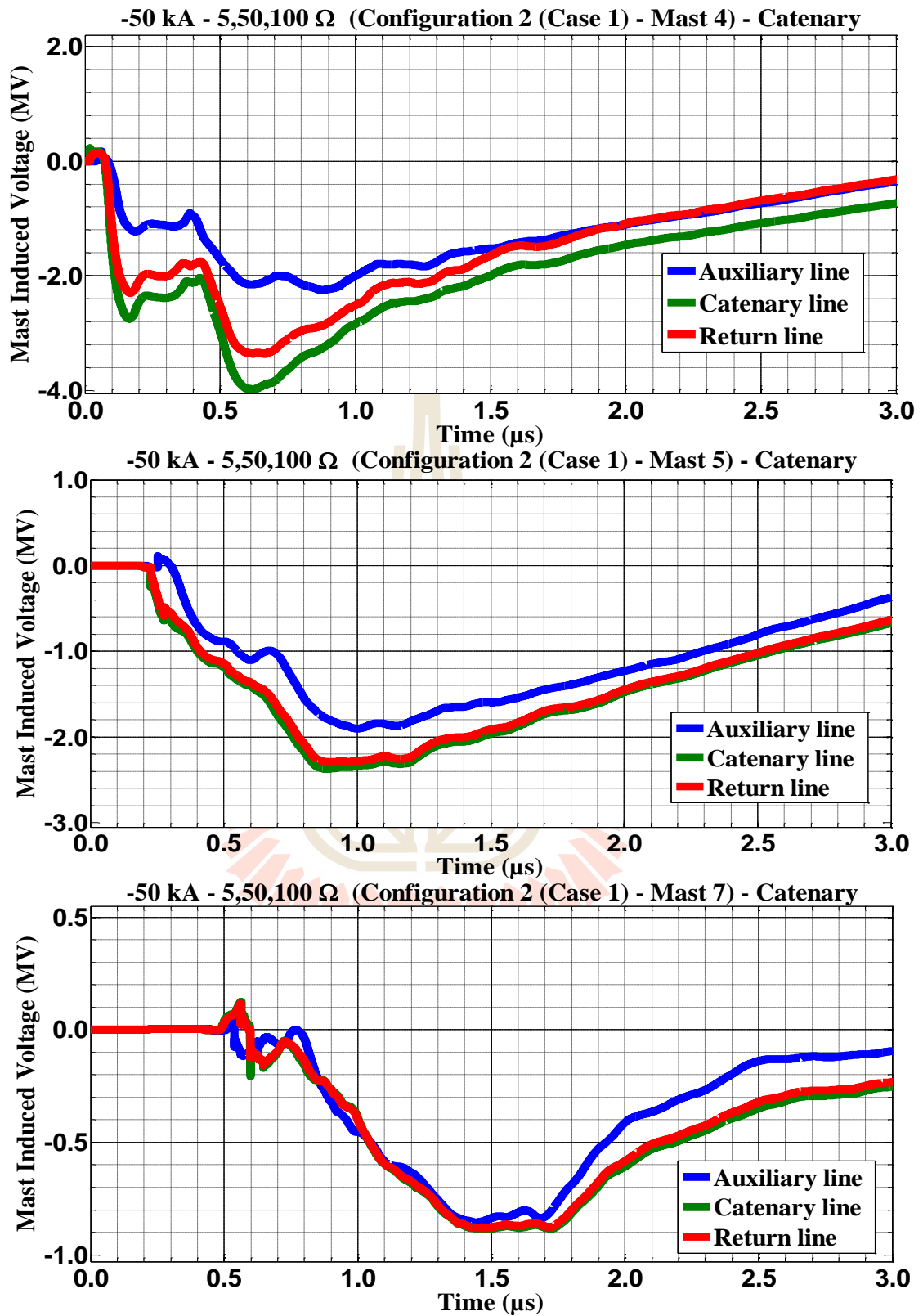
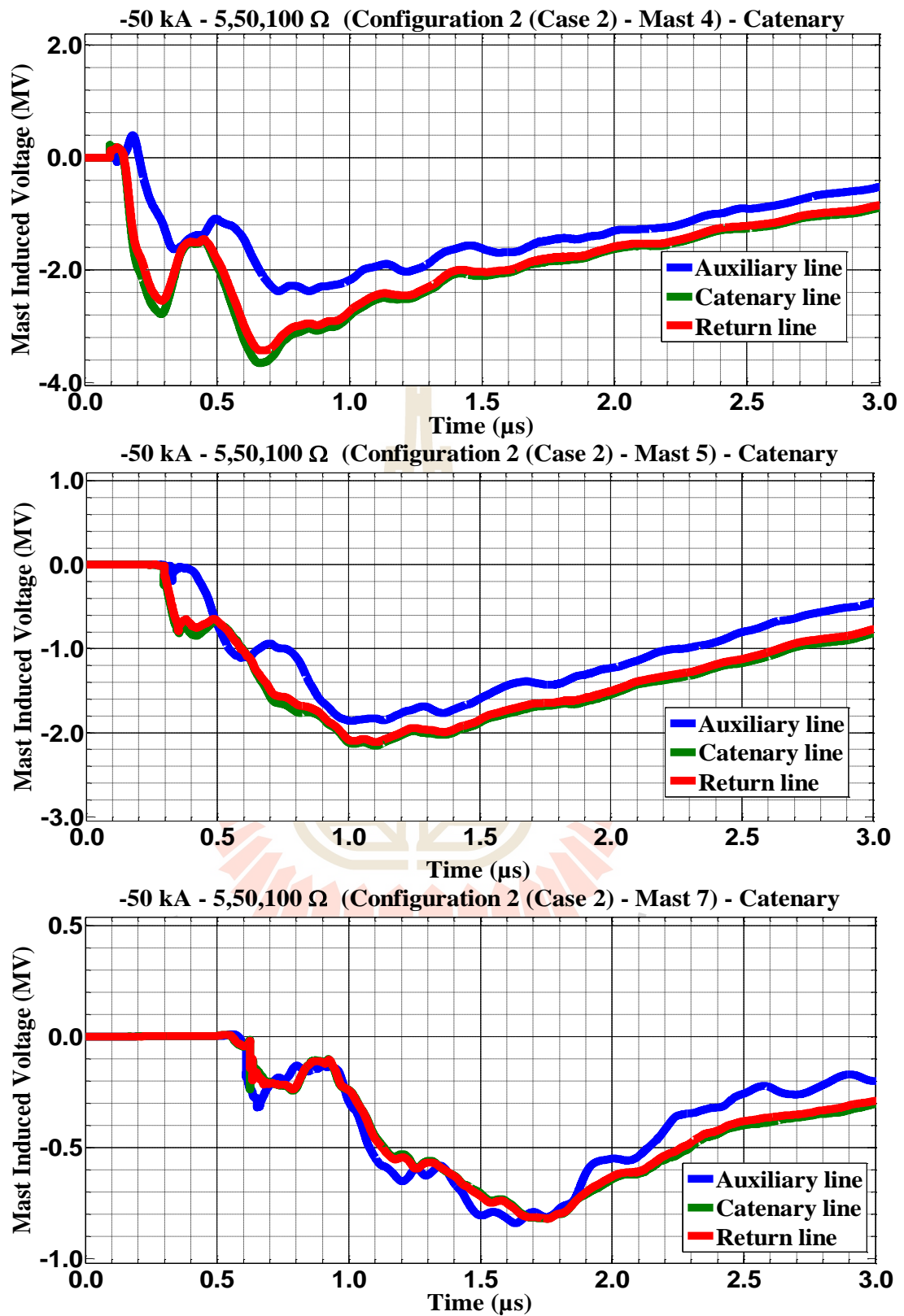
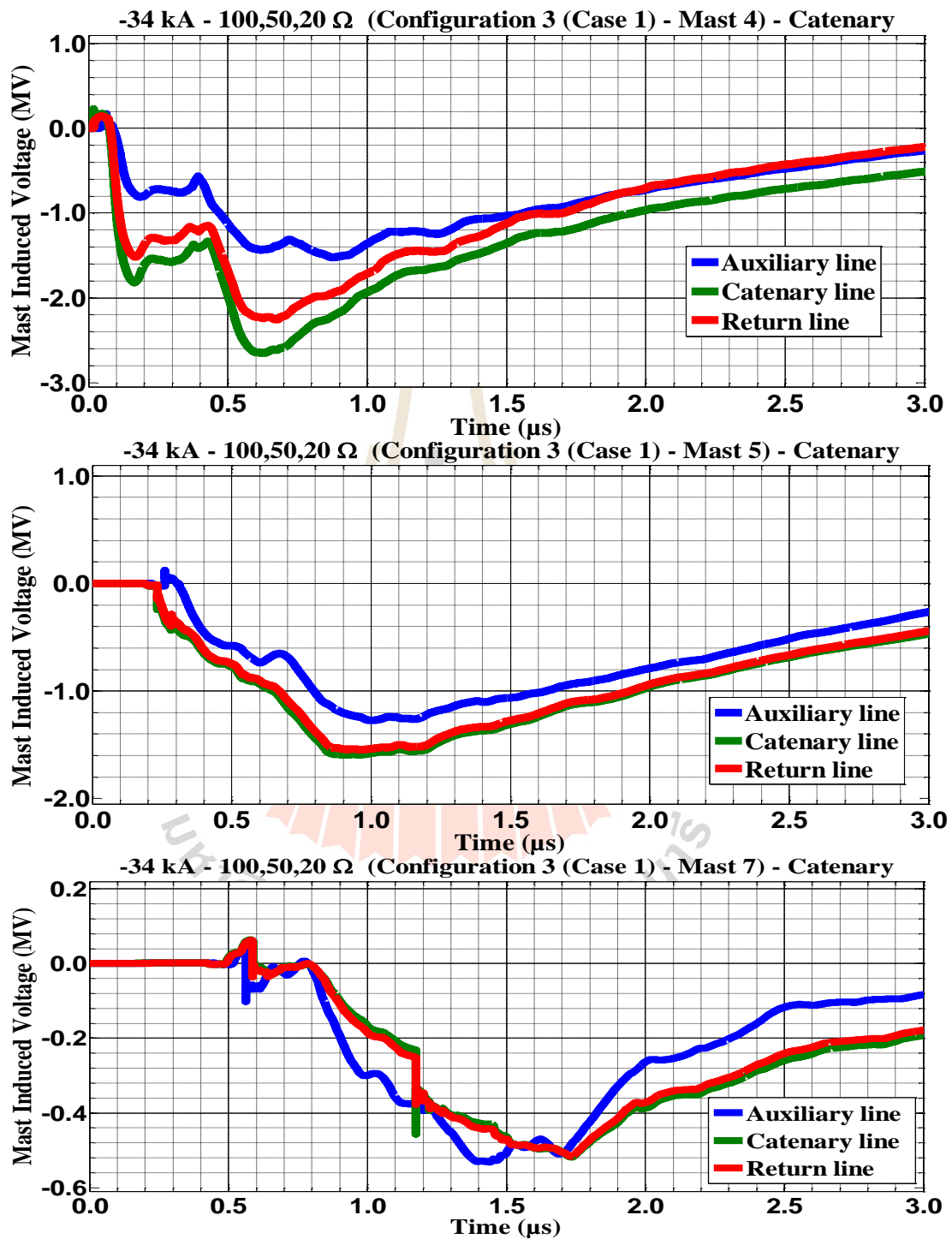


Figure C.188 Mast 4, 5, and 7 with 5,50,100 Ω induced voltage waveform of -50 kA first stroke-(1.0/100 μs), subsequent stroke-(0.2/50 μs) strikes on Mast 4 for Case 1



**Figure C.189** Mast 4, 5, and 7 with 5,50,100 Ω induced voltage waveform of -50 kA first stroke-(1.0/100 μs), subsequent stroke-(0.2/50 μs) strikes on Mast 4 for Case 2

**C.10 The consequences when the catenary struck by negative multiple lightning strokes for Configuration 3 in Case 1 and 2.**



**Figure C.190** Mast 4, 5, and 7 with 100,50,20  $\Omega$  induced voltage waveform of -34 kA first stroke-(1.0/100  $\mu\text{s}$ ), subsequent stroke-(0.2/50  $\mu\text{s}$ ) strikes on Mast 4 for Case 1

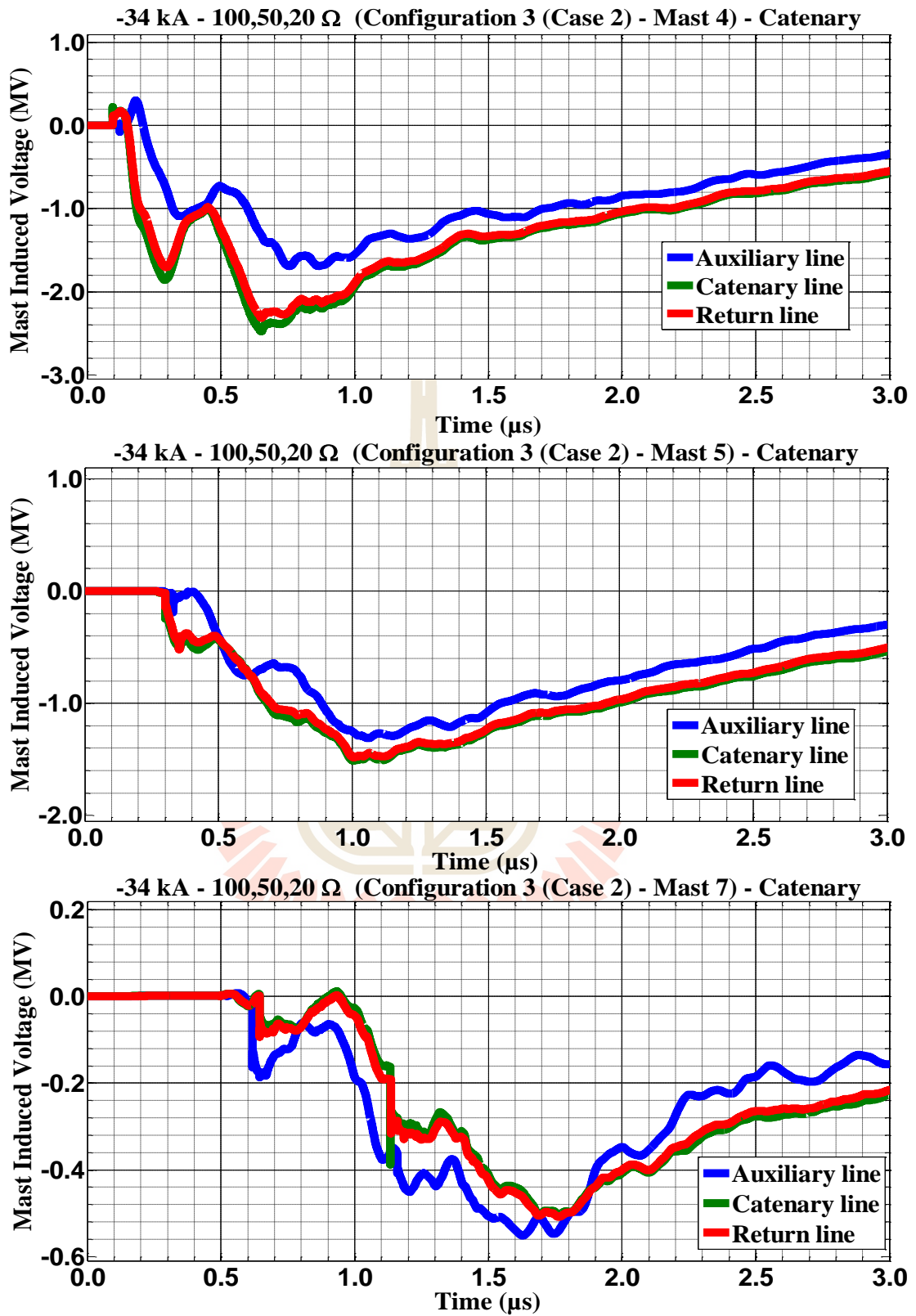


**Figure C.191** Mast 4, 5, and 7 with 100,50,20 Ω induced voltage waveform of -34 kA first stroke-(1.0/100 μs), subsequent stroke-(0.2/50 μs) strikes on Mast 4 for Case 2

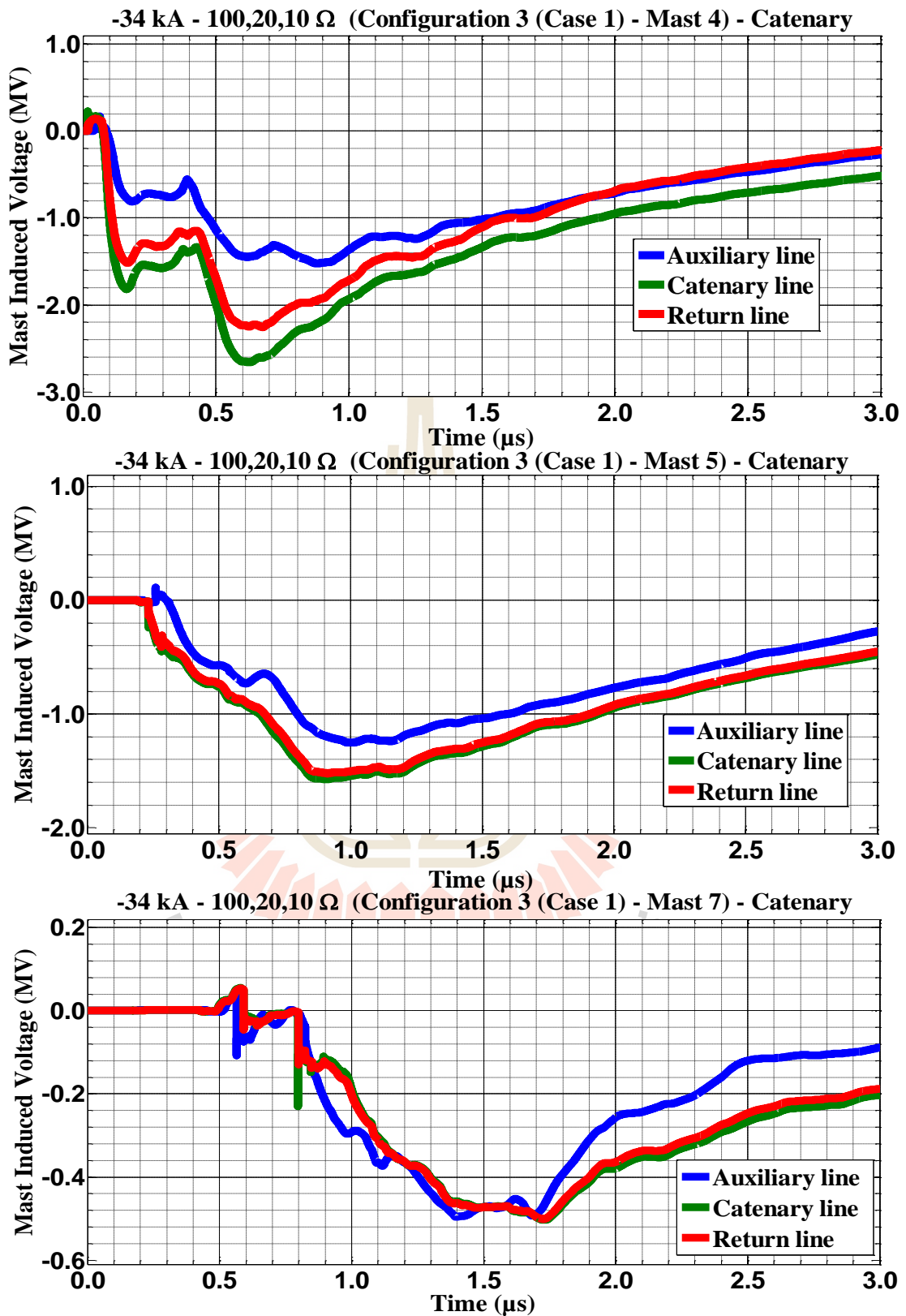


**Figure C.192** Mast 4, 5, and 7 with 100,20,10  $\Omega$  induced voltage waveform of -34 kA first stroke-(1.0/100  $\mu$ s), subsequent stroke-(0.2/50  $\mu$ s) strikes on Mast 4 for Case 1

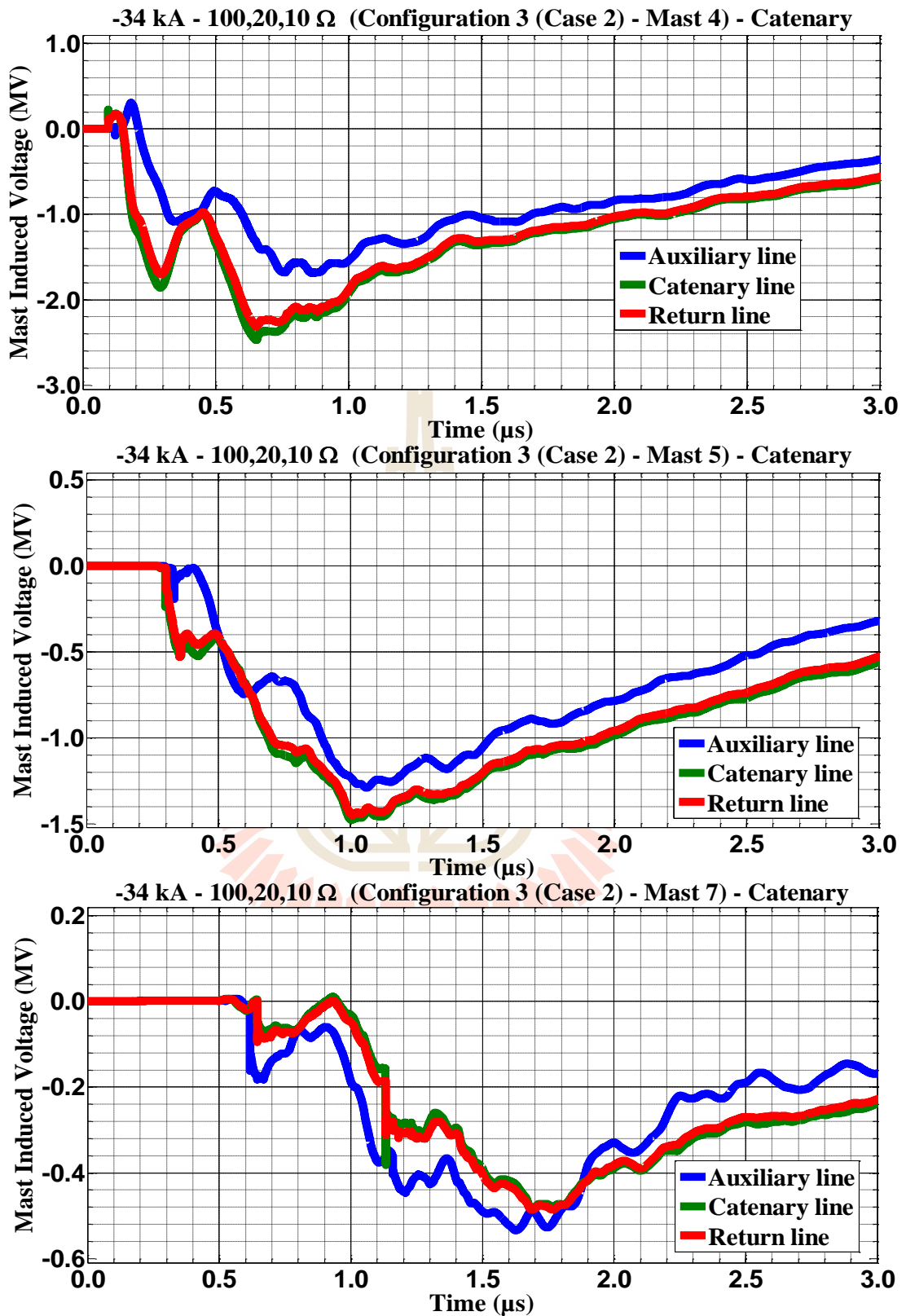


**Figure C.193** Mast 4, 5, and 7 with 100,20,10  $\Omega$  induced voltage waveform of -34 kA first stroke-(1.0/100  $\mu$ s), subsequent stroke-(0.2/50  $\mu$ s) strikes on Mast 4 for Case 2

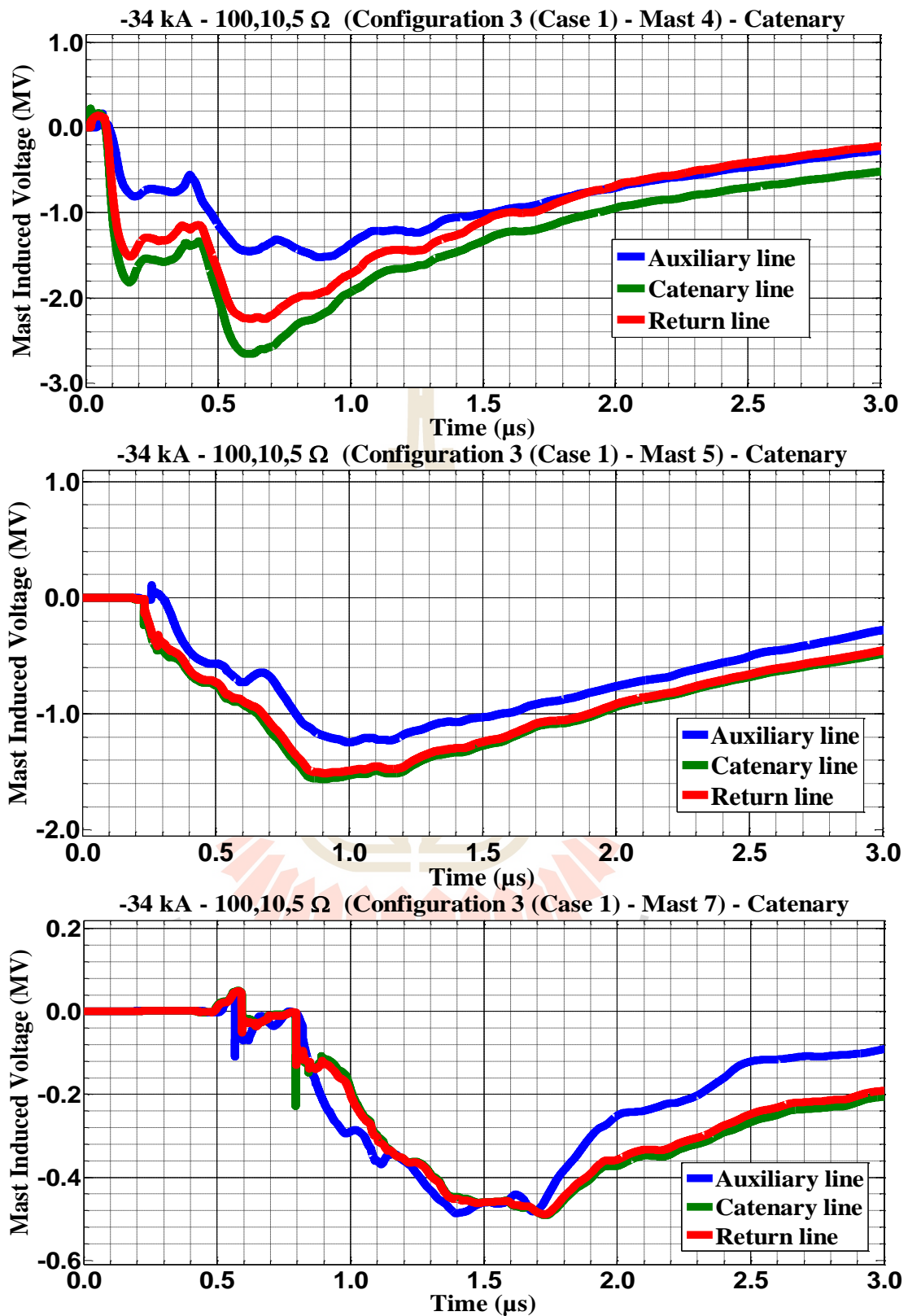


**Figure C.194** Mast 4, 5, and 7 with 100,10,5  $\Omega$  induced voltage waveform of -34 kA first stroke-(1.0/100  $\mu$ s), subsequent stroke-(0.2/50  $\mu$ s) strikes on Mast 4 for Case 1



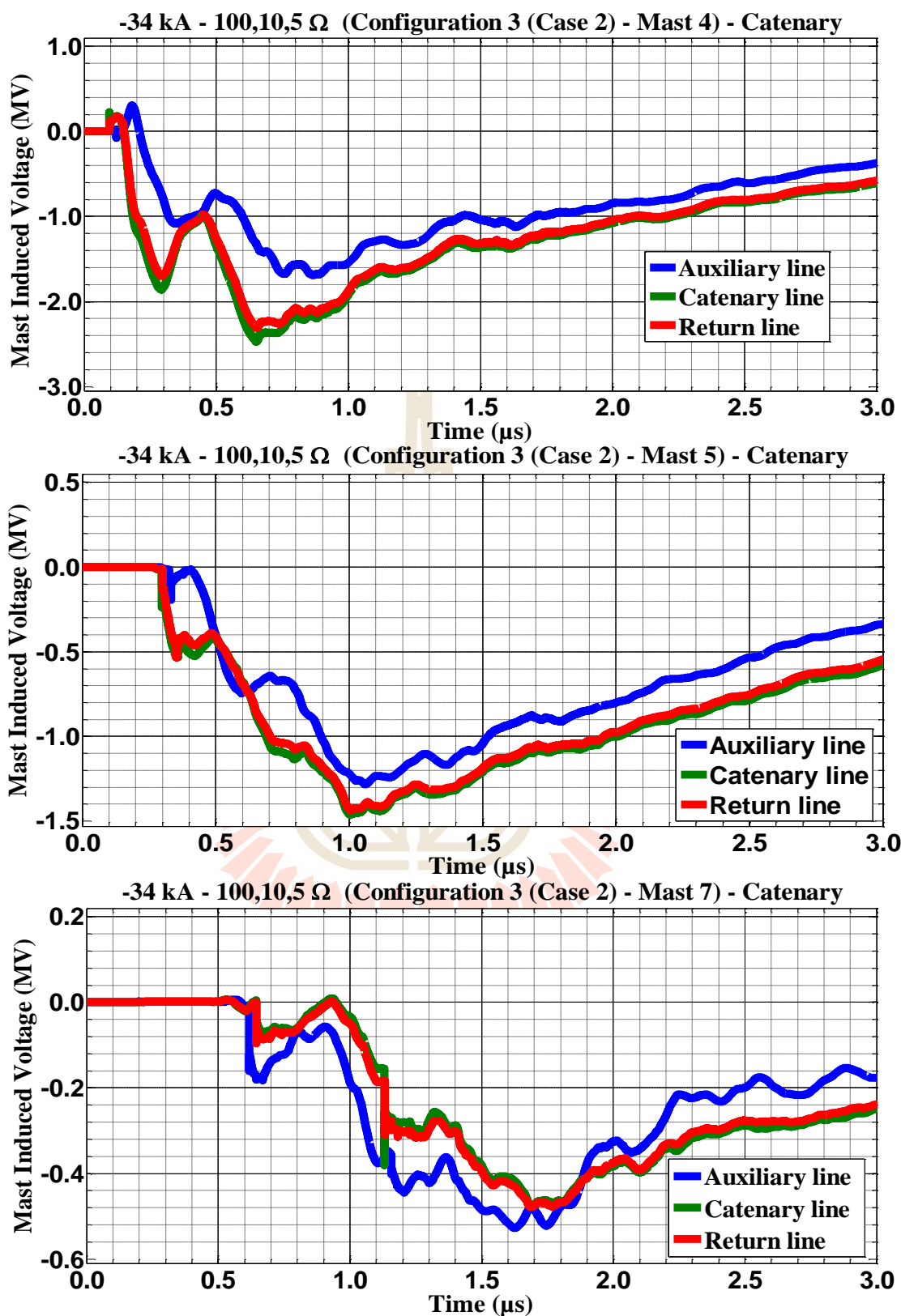


**Figure C.195** Mast 4, 5, and 7 with 100,10,5 Ω induced voltage waveform of -34 kA first stroke-(1.0/100 μs), subsequent stroke-(0.2/50 μs) strikes on Mast 4 for Case 2

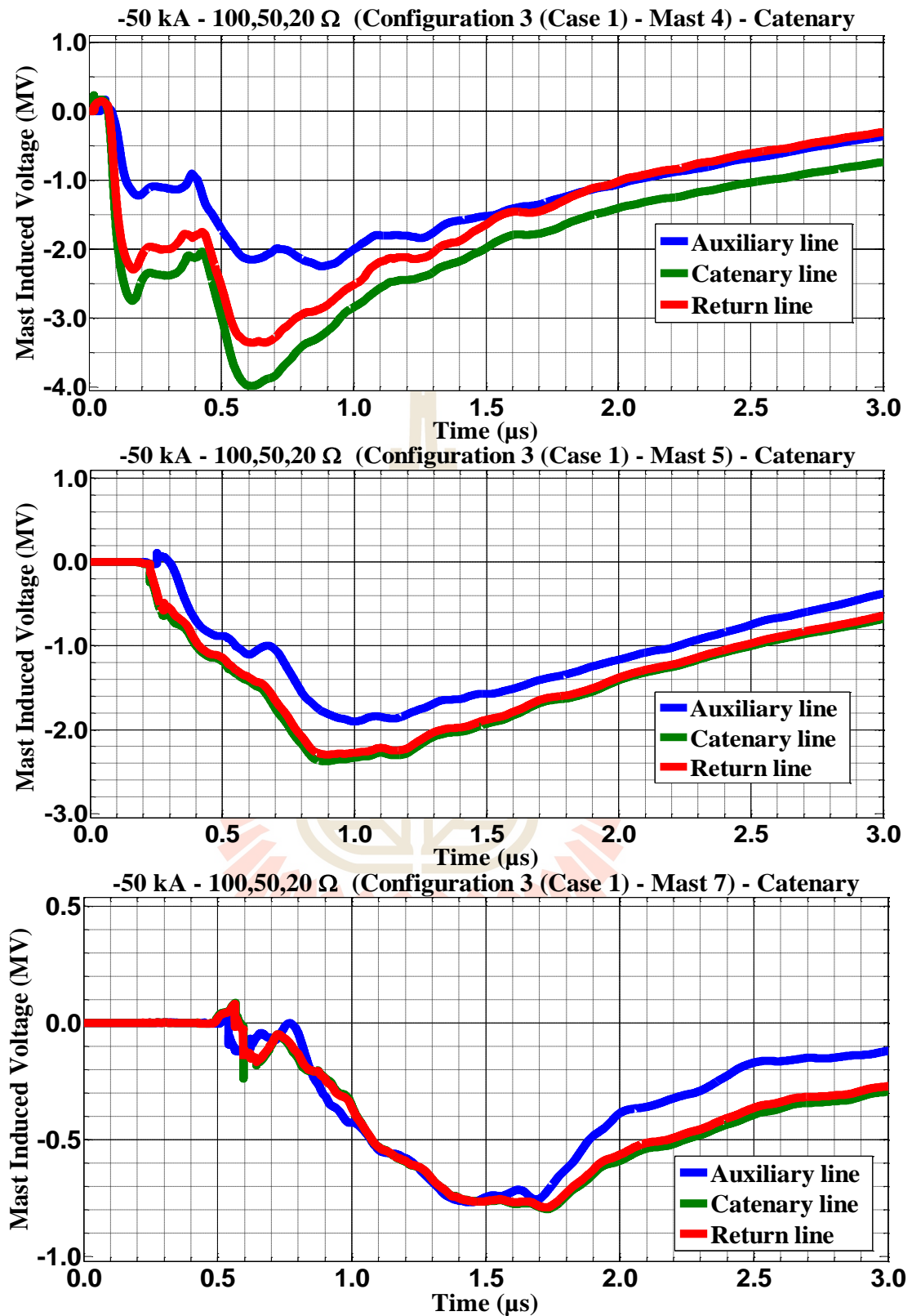


**Figure C.196** Mast 4, 5, and 7 with 100,50,20  $\Omega$  induced voltage waveform of -50 kA first stroke-(1.0/100  $\mu$ s), subsequent stroke-(0.2/50  $\mu$ s) strikes on Mast 4 for Case 1

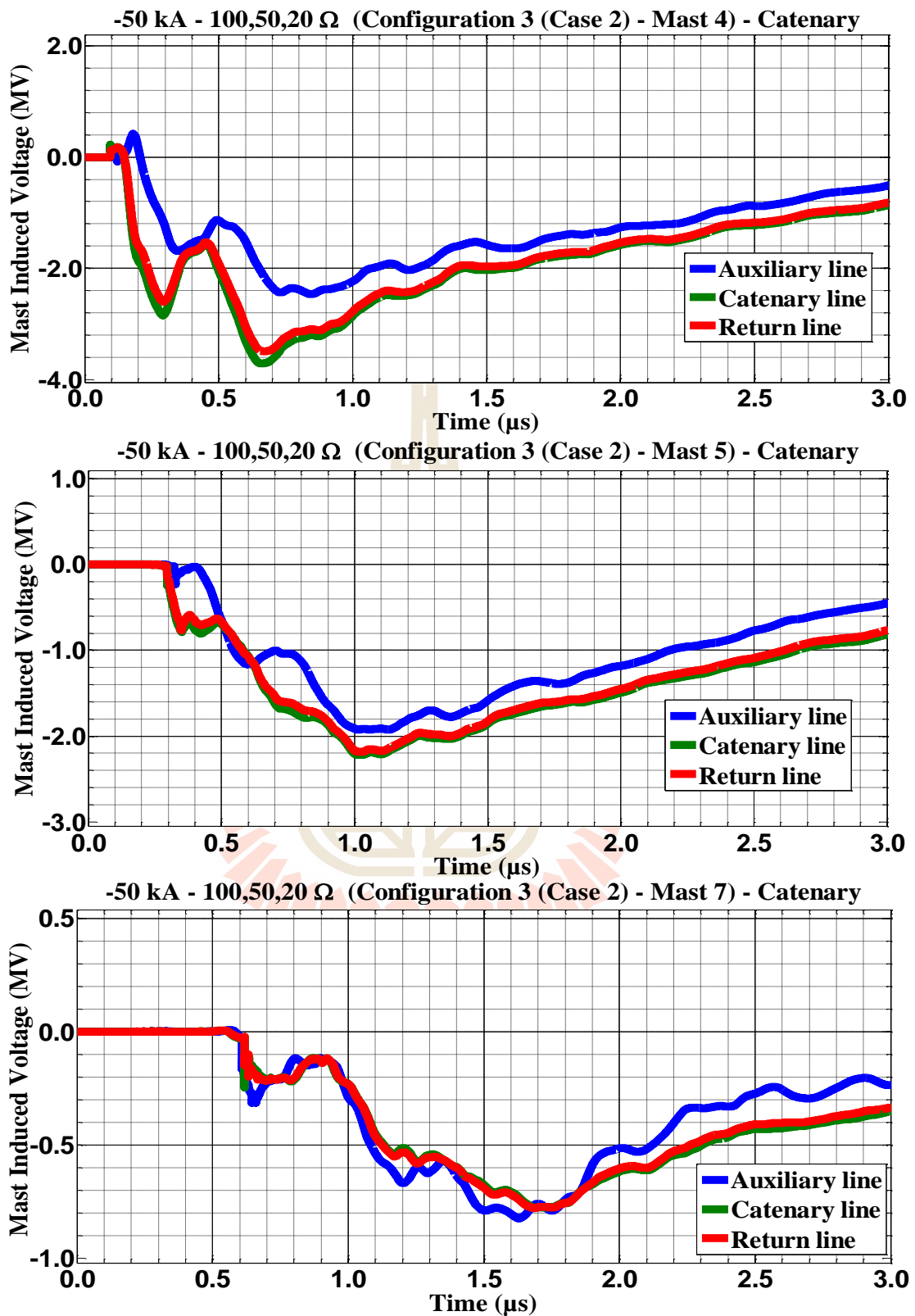


**Figure C.197** Mast 4, 5, and 7 with 100,50,20 Ω induced voltage waveform of -50 kA first stroke-(1.0/100 μs), subsequent stroke-(0.2/50 μs) strikes on Mast 4 for Case 2

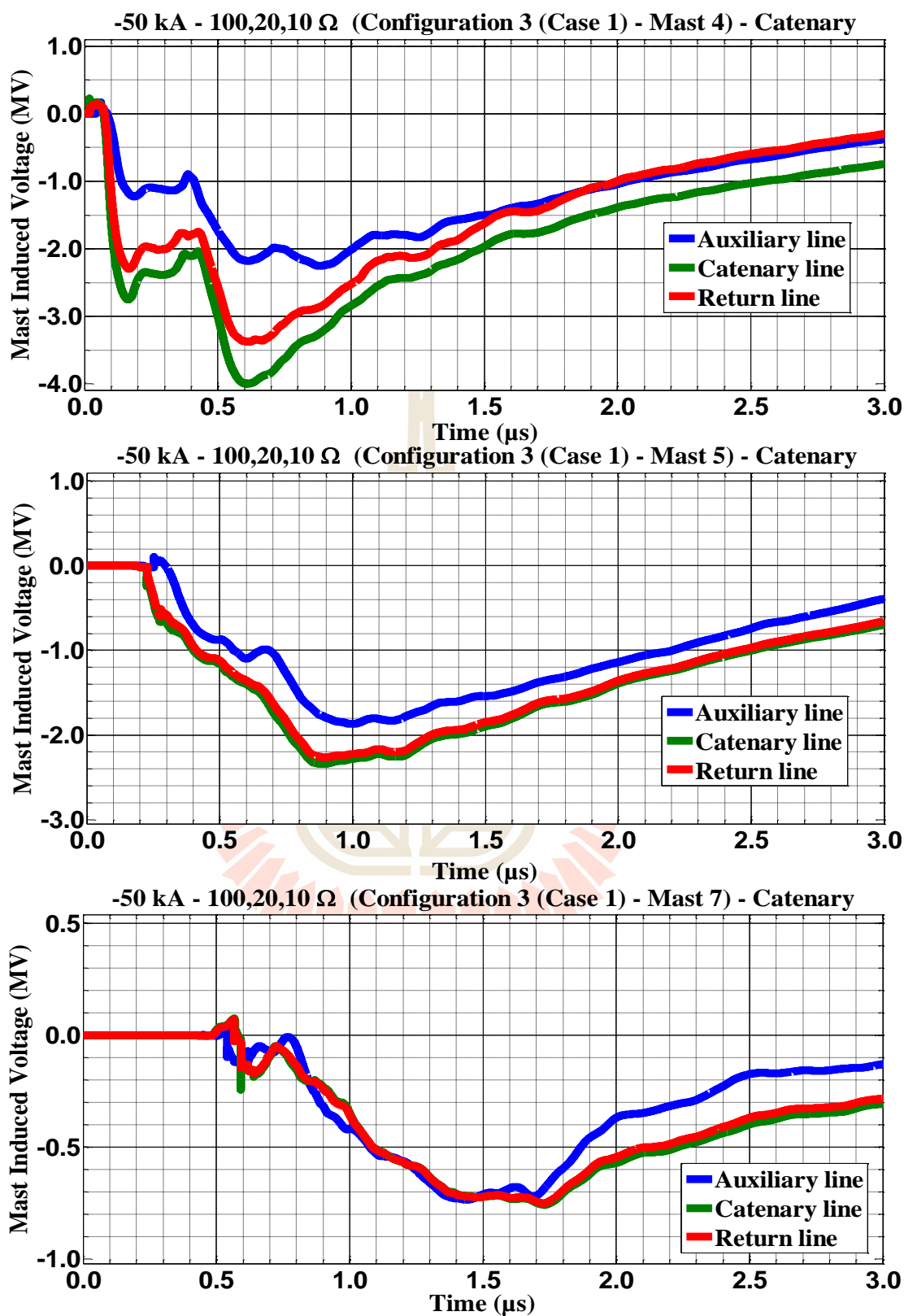
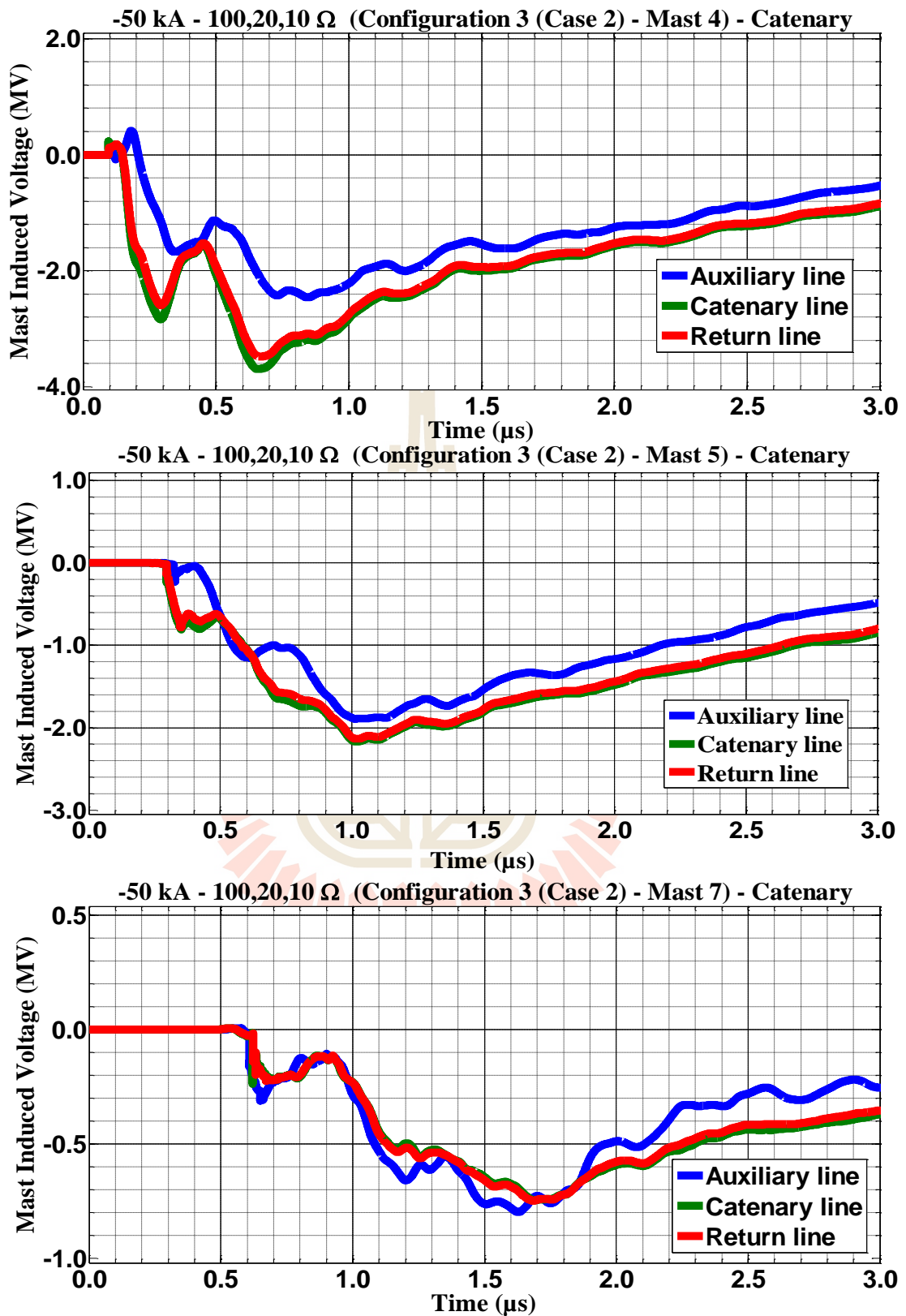


Figure C.198 Mast 4, 5, and 7 with 100,20,10 Ω induced voltage waveform of -50 kA first stroke-(1.0/100 μs), subsequent stroke-(0.2/50 μs) strikes on Mast 4 for Case 1



**Figure C.199** Mast 4, 5, and 7 with 100,20,10 Ω induced voltage waveform of -50 kA first stroke-(1.0/100 μs), subsequent stroke-(0.2/50 μs) strikes on Mast 4 for Case 2

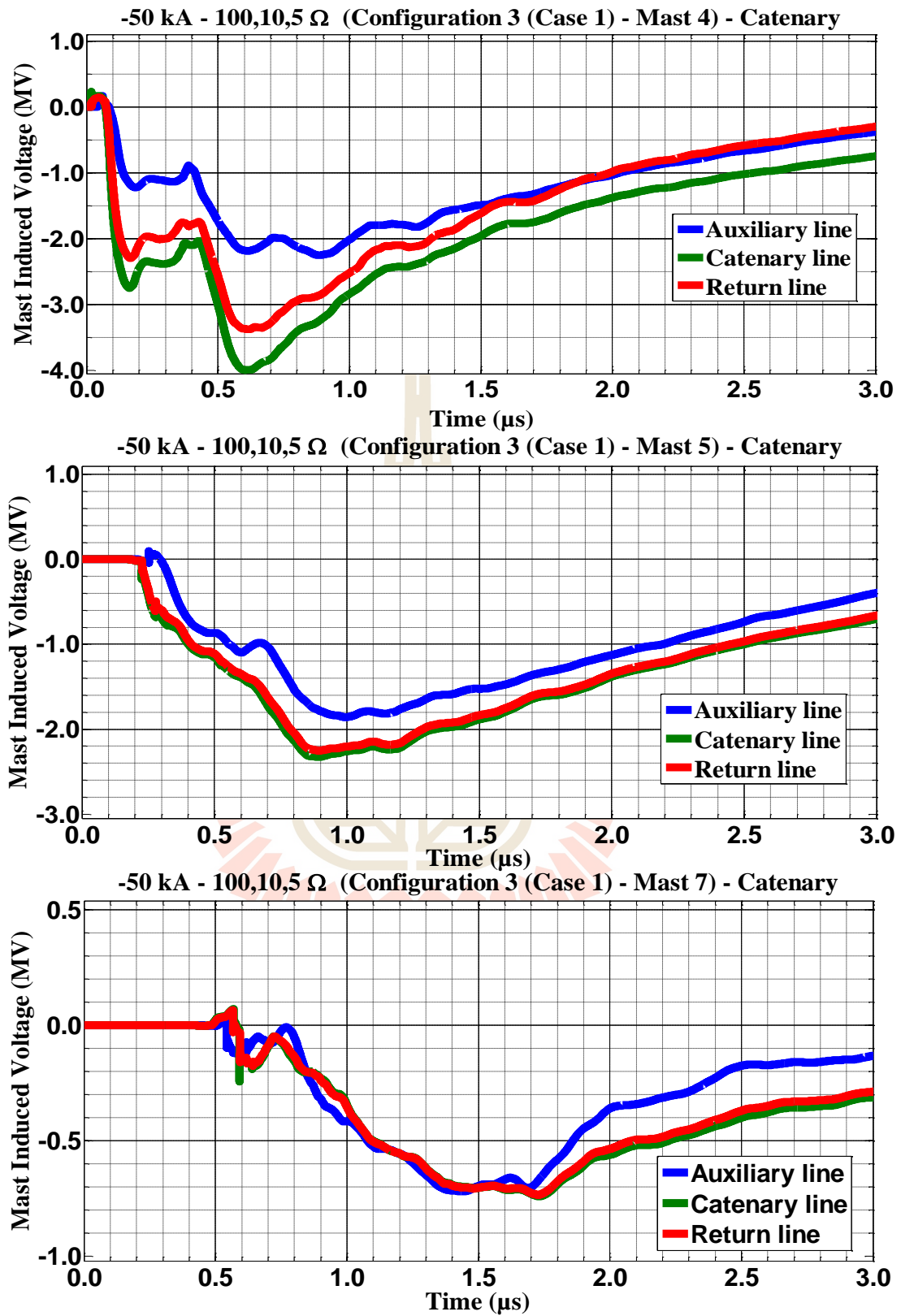


Figure C.200 Mast 4, 5, and 7 with 100,10,5  $\Omega$  induced voltage waveform of -50 kA first stroke-(1.0/100  $\mu\text{s}$ ), subsequent stroke-(0.2/50  $\mu\text{s}$ ) strikes on Mast 4 for Case 1

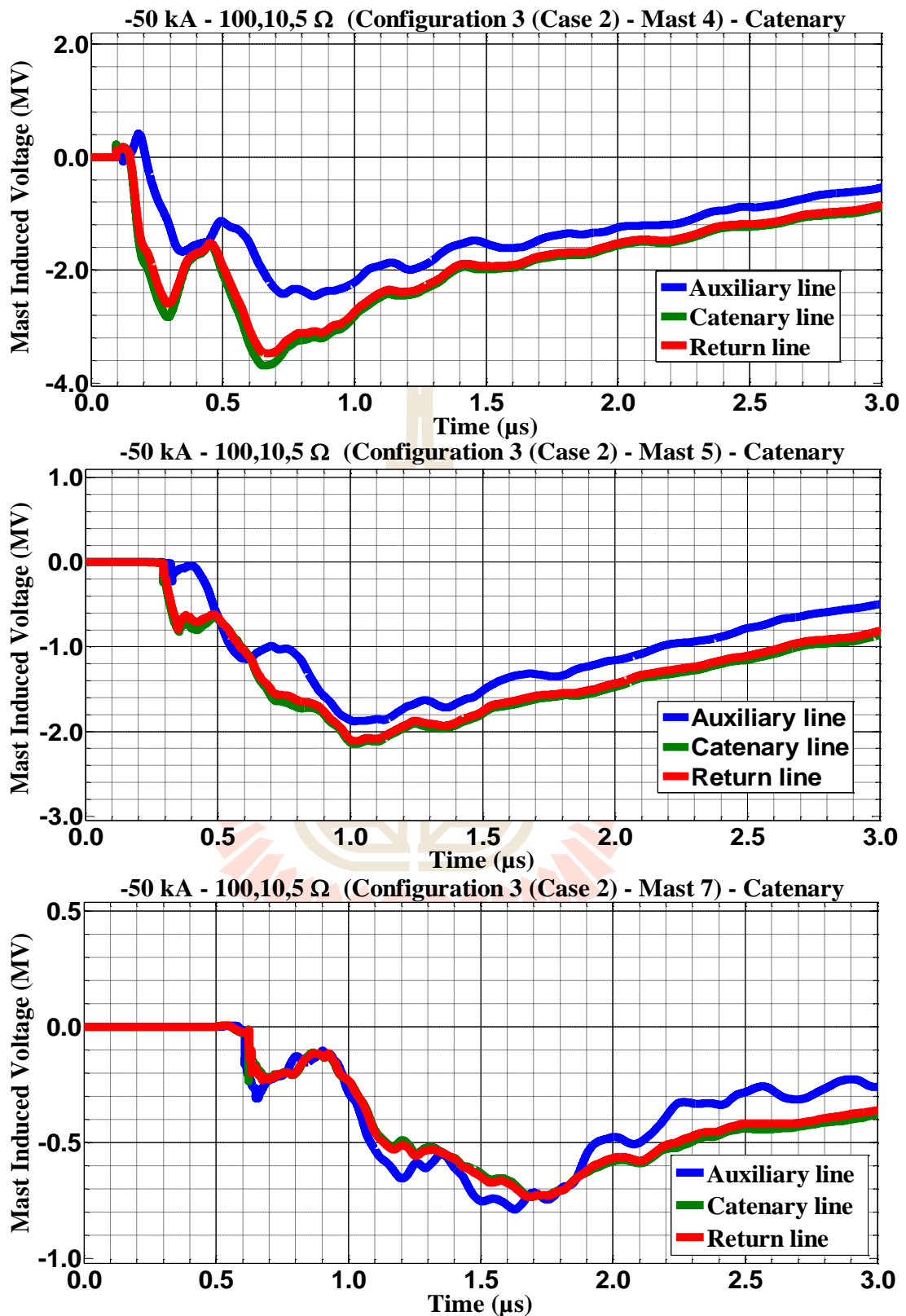
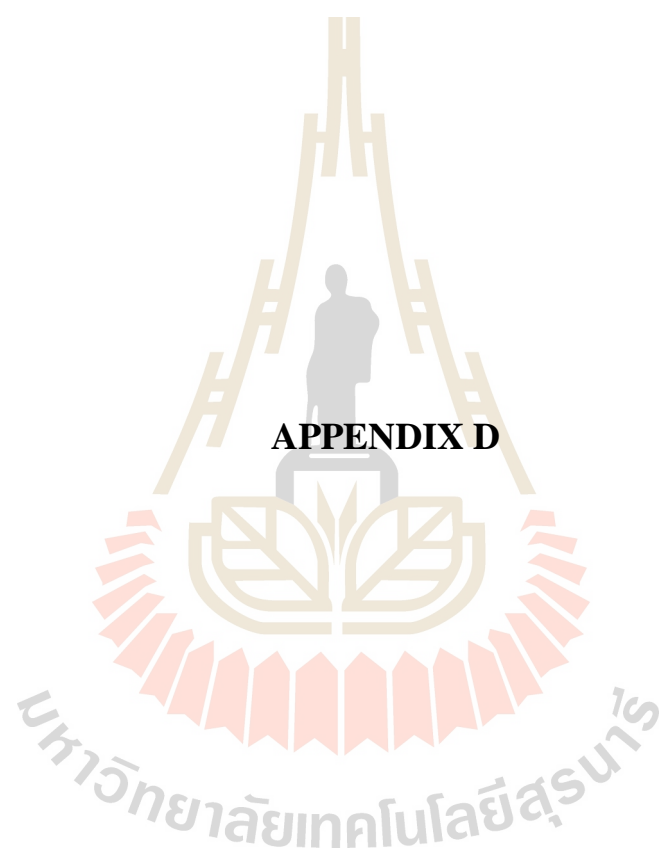


Figure C.201 Mast 4, 5, and 7 with 100,10,5 Ω induced voltage waveform of -50 kA first stroke-(1.0/100 μs), subsequent stroke-(0.2/50 μs) strikes on Mast 4 for Case 2



**APPENDIX D**



## **THE AMPLITUDE VALUES OF INDUCED VOLTAGE IN OVERHEAD LINES**

This appendix shows the analyzed outcomes from APPENDIX C of peak Mast induced voltages across the insulators in the auxiliary, return and Catenary lines as emphasized lines when lightning stroke strike on mast, catenary line, pantograph and auxiliary line of overhead catenary system in Airport Rail Link, Bangkok, Thailand

### **C.1 Simulation Analysis**

Starting from the point of hitting, direct lightning strikes have tendency to lead the charges to flow in the form of two equal current waves in equal directions. By arranging the masts with its ground resistances into three configurations with two cases each, one side from the stroke point was contemplated and perused. The first configuration was based on studying the effect of flashover from the affected mast to nearby masts when their grounding resistances ( $R_f$ ) are similar (same soil profile) when lightning strikes on train's pantograph based on two cases (see Figures 3.8-3.10). The second configuration was done when their grounding resistances ( $R_f$ ) are different but in increasing order (different soil profile). Lastly, the third configuration was done when their grounding resistances are also different but in decreasing order (different soil profile). Table D.1 and D.2 show the arrangement of configuration 2 and 3 respectively. Since the lightning source was set in Train's pantograph at respective positions near to mast 4 (M4), the concern was to check the effect of flashover into the nearby mast (mast 5 or M5) and far end mast (mast 7 or M7) under same and different soil profiles. The amplitude values of Mast induced voltages in the catenary, auxiliary and return lines from APPENDIX C for Case one and two are

reiterated in Tables D.3-D.128 for both cases. The values in Tables D.3-D.128 were obtained after being analyzed the data from the Figures in APPENDIX C. The 1<sup>st</sup> row details configuration, the cases and stroked points. The 2<sup>nd</sup> row shows the position of the affected mast. 3<sup>rd</sup> row illustrate the type of waveforms. The 4<sup>th</sup> row starts from the 2<sup>nd</sup> column gives the magnitude of lightning strokes that have been used. The 1<sup>st</sup> column starts from the 5<sup>th</sup> row shows the ground resistances that have been exploited. The 2<sup>nd</sup> to the 4<sup>th</sup> column and the 5<sup>th</sup> to the 7<sup>th</sup> column start from the 6<sup>th</sup> row indicate the magnitude of mast induced voltages in different lines of an overhead catenary system for 34 kA and 50 kA respectively. For configuration 2 and 3, respective rows for each tables at a time represent the arrangement of grounding resistance as shown in simulation setup in Tables D.1-D.2.

**Table D.1** Simulations setup for Configuration 2 for both Cases

Simulation	First			Second			Third		
Mast	M4	M5	M7	M4	M5	M7	M4	M5	M7
Rf( $\Omega$ )	5	10	20	5	20	50	5	50	100

**Table D.2** Simulations setup for Configuration 3 for both Cases

Simulation	First			Second			Third		
Mast	M4	M5	M7	M4	M5	M7	M4	M5	M7
Rf( $\Omega$ )	100	50	20	100	20	10	100	10	5

**Table D.3** Mast 4 induced voltages in Case 1 with single lightning strokes on the mast for configuration 1

Configuration 1 - Case 1 (Mast)						
Mast 4 (MV)						
Single stroke-(2.0/100 $\mu$ s)						
Rf	- 34 kA			- 50 kA		
( $\Omega$ )	Auxiliary	Return	Catenary	Auxiliary	Return	Catenary
5	1.75	0.650	0.537	2.600	0.980	0.808
10	1.75	0.650	0.537	2.600	0.980	0.808
20	1.75	0.650	0.537	2.600	0.980	0.808
30	1.75	0.650	0.537	2.600	0.980	0.808
40	1.75	0.650	0.537	2.600	0.980	0.808
50	1.75	0.650	0.537	2.600	0.980	0.808
60	1.75	0.650	0.537	2.600	0.980	0.808
70	1.75	0.650	0.537	2.600	0.980	0.808
80	1.75	0.650	0.537	2.600	0.980	0.808
90	1.75	0.650	0.537	2.600	0.980	0.808
100	1.75	0.650	0.537	2.600	0.980	0.808

**Table D.4** Mast 5 induced voltages in Case 1 with single lightning strokes on the mast for configuration 1

Configuration 1 - Case 1 (Mast)						
Mast 5 (MV)						
Single stroke-(2.0/100 $\mu$ s)						
Rf	- 34 kA			- 50 kA		
( $\Omega$ )	Auxiliary	Return	Catenary	Auxiliary	Return	Catenary
5	1.37	0.615	0.497	2.02	0.888	0.714
10	1.37	0.619	0.501	2.02	0.894	0.720
20	1.37	0.623	0.505	2.03	0.900	0.727
30	1.37	0.628	0.510	2.04	0.906	0.733
40	1.38	0.630	0.512	2.04	0.909	0.736
50	1.38	0.632	0.514	2.04	0.913	0.740
60	1.38	0.636	0.518	2.04	0.919	0.746
70	1.38	0.641	0.522	2.05	0.925	0.753
80	1.39	0.645	0.527	2.05	0.931	0.759
90	1.39	0.647	0.529	2.06	0.934	0.763
100	1.39	0.650	0.531	2.06	0.938	0.766

**Table D.5** Mast 7 induced voltages in Case 1 with single lightning strokes on the mast for configuration 1

Configuration 1 - Case 1 (Mast)						
Mast 7 (MV)						
Single stroke-(2.0/100 $\mu$ s)						
Rf	- 34 kA			- 50 kA		
( $\Omega$ )	Auxiliary	Return	Catenary	Auxiliary	Return	Catenary
5	0.560	0.290	0.255	0.834	0.443	0.382
10	0.563	0.299	0.263	0.841	0.455	0.394
20	0.568	0.308	0.272	0.848	0.467	0.406
30	0.574	0.317	0.281	0.856	0.479	0.419
40	0.577	0.321	0.285	0.859	0.485	0.425
50	0.582	0.326	0.290	0.863	0.491	0.432
60	0.587	0.335	0.298	0.870	0.503	0.444
70	0.593	0.344	0.307	0.877	0.515	0.457
80	0.599	0.353	0.316	0.885	0.527	0.469
90	0.601	0.357	0.320	0.888	0.533	0.475
100	0.605	0.362	0.325	0.893	0.540	0.483

**Table D.6** Mast 4 induced voltages in Case 2 with single lightning strokes on the mast for configuration 1

Configuration 1 - Case 2 (Mast)						
Mast 4 (MV)						
Single stroke-(2.0/100 $\mu$ s)						
Rf	- 34 kA			- 50 kA		
( $\Omega$ )	Auxiliary	Return	Catenary	Auxiliary	Return	Catenary
5	1.89	0.908	0.760	2.82	1.4	1.18
10	1.89	0.917	0.760	2.83	1.41	1.19
20	1.90	0.927	0.770	2.84	1.43	1.20
30	1.90	0.937	0.780	2.85	1.44	1.21
40	1.91	0.942	0.790	2.86	1.45	1.23
50	1.91	0.947	0.800	2.86	1.46	1.24
60	1.91	0.956	0.810	2.87	1.47	1.25
70	1.92	0.966	0.820	2.88	1.48	1.26
80	1.93	0.976	0.830	2.89	1.49	1.27
90	1.93	0.981	0.835	2.90	1.51	1.29
100	1.94	0.986	0.840	2.91	1.53	1.31

**Table D.7** Mast 5 induced voltages in Case 2 with single lightning strokes on the mast for configuration 1

Configuration 1 - Case 2 (Mast)						
Mast 5						
Single stroke-(2.0/100 $\mu$ s)						
Rf	- 34 kA			- 50 kA		
( $\Omega$ )	Auxiliary	Return	Catenary	Auxiliary	Return	Catenary
5	1.40	0.703	0.595	2.10	1.06	0.906
10	1.41	0.720	0.613	2.11	1.08	0.932
20	1.42	0.737	0.631	2.13	1.10	0.958
30	1.43	0.754	0.649	2.15	1.12	0.985
40	1.44	0.762	0.658	2.16	1.14	1.012
50	1.45	0.772	0.667	2.17	1.16	1.013
60	1.46	0.789	0.685	2.18	1.18	1.039
70	1.47	0.806	0.703	2.20	1.20	1.066
80	1.48	0.823	0.721	2.22	1.22	1.093
90	1.49	0.831	0.730	2.23	1.24	1.106
100	1.51	0.842	0.740	2.24	1.27	1.12

**Table D.8** Mast 7 induced voltages in Case 2 with single lightning strokes on the mast for configuration 1

Configuration 1 - Case 2 (Mast)						
Mast 7 (MV)						
Single stroke-(2.0/100 $\mu$ s)						
Rf	- 34 kA			- 50 kA		
( $\Omega$ )	Auxiliary	Return	Catenary	Auxiliary	Return	Catenary
5	0.576	0.288	0.244	0.870	0.436	0.368
10	0.585	0.299	0.255	0.882	0.452	0.385
20	0.594	0.310	0.267	0.895	0.469	0.402
30	0.604	0.321	0.278	0.908	0.485	0.419
40	0.612	0.332	0.283	0.914	0.493	0.427
50	0.615	0.333	0.291	0.921	0.502	0.436
60	0.624	0.344	0.302	0.933	0.518	0.453
70	0.634	0.355	0.313	0.946	0.535	0.470
80	0.644	0.366	0.324	0.959	0.551	0.487
90	0.648	0.372	0.329	0.965	0.559	0.495
100	0.654	0.378	0.338	0.973	0.568	0.505

**Table D.9** Mast 4 induced voltages in Case 1 with single lightning strokes on the mast for configuration 2

Configuration 2 - Case 1 (Mast)						
Mast 4						
Single stroke-(2.0/100 $\mu$ s)						
Rf	- 34 kA			- 50 kA		
( $\Omega$ )	Auxiliary	Return	Catenary	Auxiliary	Return	Catenary
5	1.75	0.650	0.537	2.60	0.970	0.800
5	1.75	0.650	0.537	2.60	0.970	0.800
5	1.75	0.650	0.537	2.60	0.970	0.800

**Table D.10** Mast 5 induced voltages in Case 1 with single lightning strokes on the mast for configuration 2

Configuration 2 - Case 1 (Mast)						
Mast 5						
Single stroke-(2.0/100 $\mu$ s)						
Rf	- 34 kA			- 50 kA		
( $\Omega$ )	Auxiliary	Return	Catenary	Auxiliary	Return	Catenary
10	1.37	0.620	0.500	2.02	0.892	0.720
20	1.38	0.600	0.510	2.02	0.900	0.727
50	1.38	0.634	0.517	2.04	0.920	0.746

**Table D.11** Mast 7 induced voltages in Case 1 with single lightning strokes on the mast for configuration 2

Configuration 2 - Case 1 (Mast)						
Mast 7						
Single stroke-(2.0/100 $\mu$ s)						
Rf	- 34 kA			- 50 kA		
( $\Omega$ )	Auxiliary	Return	Catenary	Auxiliary	Return	Catenary
20	0.568	0.307	0.267	0.842	0.460	0.399
50	0.588	0.326	0.287	0.858	0.486	0.428
100	0.600	0.354	0.316	0.884	0.527	0.471

**Table D.12** Mast 4 induced voltages in Case 1 with single lightning strokes on the mast for configuration 3

Configuration 3 - Case 1 (Mast)						
Mast 4						
First stroke-(1.0/100 $\mu$ s), Subsequent stroke-(0.2/50 $\mu$ s)						
Rf	- 34 kA			- 50 kA		
( $\Omega$ )	Auxiliary	Return	Catenary	Auxiliary	Return	Catenary
100	1.75	1.38	0.635	2.59	0.967	0.800
100	1.75	0.650	0.536	2.59	0.972	0.800
100	1.75	0.650	0.537	2.59	0.975	0.800

**Table D.13** Mast 5 induced voltages in Case 1 with single lightning strokes on the mast for configuration 3

Configuration 3 - Case 1 (Mast)						
Mast 5						
Single stroke-(2.0/100 $\mu$ s)						
Rf	- 34 kA			- 50 kA		
( $\Omega$ )	Auxiliary	Return	Catenary	Auxiliary	Return	Catenary
50	1.38	0.635	0.518	2.04	0.920	0.744
20	1.38	0.623	0.506	2.03	0.900	0.726
10	1.37	0.617	0.500	2.02	0.892	0.718

**Table D.14** Mast 7 induced voltages in Case 1 with single lightning strokes on the mast for configuration 3

Configuration 3 - Case 1 (Mast)						
Mast 7						
Single stroke-(2.0/100 $\mu$ s)						
Rf	- 34 kA			- 50 kA		
( $\Omega$ )	Auxiliary	Return	Catenary	Auxiliary	Return	Catenary
20	0.574	0.313	0.273	0.850	0.467	0.407
10	0.566	0.302	0.262	0.840	0.451	0.390
5	0.562	0.300	0.256	0.835	0.444	0.383

**Table D.15** Mast 4 induced voltages in Case 2 with single lightning strokes on the mast for configuration 2

Configuration 2 - Case 2 (Mast)						
Mast 4						
Single stroke-(2.0/100 $\mu$ s)						
Rf	- 34 kA			- 50 kA		
( $\Omega$ )	Auxiliary	Return	Catenary	Auxiliary	Return	Catenary
5	1.89	0.900	0.760	2.82	1.40	1.17
5	1.89	0.900	0.761	2.82	1.39	1.17
5	1.89	0.900	0.761	2.82	1.39	1.17

**Table D.16** Mast 5 induced voltages in Case 2 with single lightning strokes on the mast for configuration 2

Configuration 2 - Case 2 (Mast)						
Mast 5						
Single stroke-(1.0/100 $\mu$ s)						
Rf	- 34 kA			- 50 kA		
( $\Omega$ )	Auxiliary	Return	Catenary	Auxiliary	Return	Catenary
10	1.41	0.710	0.601	2.10	1.07	0.916
20	1.42	0.728	0.620	2.11	1.09	0.934
50	1.43	0.753	0.650	2.14	1.13	0.972

**Table D.17** Mast 7 induced voltages in Case 2 with single lightning strokes on the mast for configuration 2

Configuration 2 - Case 2 (Mast)						
Mast 7						
Single stroke-(2.0/100 $\mu$ s)						
Rf	- 34 kA			- 50 kA		
( $\Omega$ )	Auxiliary	Return	Catenary	Auxiliary	Return	Catenary
20	0.581	0.297	0.253	0.877	0.447	0.381
50	0.595	0.314	0.271	0.889	0.470	0.408
100	0.616	0.345	0.302	0.920	0.512	0.450



**Table D.18** Mast 4 induced voltages in Case 2 with single lightning strokes on the mast for configuration 3

Configuration 3 - Case 2 (Mast)						
Mast 4						
Single stroke-(2.0/100 $\mu$ s)						
Rf	- 34 kA			- 50 kA		
( $\Omega$ )	Auxiliary	Return	Catenary	Auxiliary	Return	Catenary
100	1.94	0.988	0.838	2.91	1.53	1.32
100	1.95	1.00	0.851	2.91	1.53	1.32
100	1.96	1.00	0.853	2.91	1.53	1.32

**Table D.19** Mast 5 induced voltages in Case 2 with single lightning strokes on the mast for configuration 3

Configuration 3 - Case 2 (Mast)						
Mast 5						
Single stroke-(2.0/100 $\mu$ s)						
Rf	- 34 kA			- 50 kA		
( $\Omega$ )	Auxiliary	Return	Catenary	Auxiliary	Return	Catenary
50	1.47	0.806	0.700	2.20	1.21	1.06
20	1.45	0.763	0.656	2.17	1.16	1.00
10	1.44	0.750	0.643	2.15	1.14	0.981

**Table D.20** Mast 7 induced voltages in Case 2 with single lightning strokes on the mast for configuration 3

Configuration 3 - Case 2 (Mast)						
Mast 7						
Single stroke-(2.0/100 $\mu$ s)						
Rf	- 34 kA			- 50 kA		
( $\Omega$ )	Auxiliary	Return	Catenary	Auxiliary	Return	Catenary
20	0.612	0.322	0.276	0.921	0.482	0.415
10	0.600	0.309	0.263	0.901	0.460	0.392
5	0.600	0.303	0.257	0.894	0.451	0.382

**Table D.21** Mast 4 induced voltages in Case 1 with single lightning strokes on the return line for configuration 1

Configuration 1 - Case 1 (Return)						
Mast 4 (MV)						
Single stroke-(2.0/100 $\mu$ s)						
Rf	- 34 kA			- 50 kA		
( $\Omega$ )	Auxiliary	Return	Catenary	Auxiliary	Return	Catenary
5	0.677	1.31	0.850	1.007	1.96	1.26
10	0.677	1.31	0.851	1.008	1.96	1.26
20	0.677	1.31	0.853	1.009	1.96	1.26
30	0.678	1.31	0.854	1.010	1.96	1.26
40	0.678	1.31	0.855	1.011	1.96	1.26
50	0.678	1.31	0.856	1.012	1.96	1.26
60	0.678	1.31	0.857	1.013	1.96	1.26
70	0.679	1.31	0.859	1.014	1.96	1.26
80	0.679	1.31	0.860	1.015	1.96	1.26
90	0.680	1.31	0.862	1.016	1.96	1.26
100	0.680	1.31	0.862	1.017	1.96	1.26

**Table D.22** Mast 5 induced voltages in Case 1 with single lightning strokes on the return line for configuration 1

Configuration 1 - Case 1 (Return)						
Mast 5 (MV)						
Single stroke-(2.0/100 $\mu$ s)						
Rf	- 34 kA			- 50 kA		
( $\Omega$ )	Auxiliary	Return	Catenary	Auxiliary	Return	Catenary
5	0.545	0.543	0.544	0.835	0.834	0.834
10	0.549	0.547	0.548	0.842	0.840	0.840
20	0.553	0.551	0.552	0.849	0.847	0.847
30	0.558	0.556	0.556	0.856	0.853	0.854
40	0.561	0.558	0.559	0.859	0.856	0.857
50	0.562	0.560	0.561	0.863	0.860	0.861
60	0.566	0.564	0.565	0.870	0.866	0.867
70	0.571	0.569	0.569	0.877	0.873	0.874
80	0.575	0.573	0.574	0.884	0.880	0.881
90	0.578	0.575	0.577	0.887	0.884	0.884
100	0.580	0.578	0.579	0.891	0.887	0.888

**Table D.23** Mast 7 induced voltages in Case 1 with single lightning strokes on the return line for configuration 1

Configuration 1 - Case 1 (Return)						
Mast 7 (MV)						
Single stroke-(2.0/100 $\mu$ s)						
Rf	- 34 kA			- 50 kA		
( $\Omega$ )	Auxiliary	Return	Catenary	Auxiliary	Return	Catenary
5	0.217	0.187	0.183	0.330	0.281	0.273
10	0.226	0.200	0.196	0.343	0.300	0.293
20	0.235	0.214	0.212	0.357	0.319	0.314
30	0.246	0.227	0.225	0.371	0.339	0.334
40	0.251	0.233	0.231	0.378	0.348	0.344
50	0.257	0.241	0.239	0.385	0.360	0.356
60	0.266	0.254	0.252	0.398	0.379	0.377
70	0.275	0.268	0.264	0.412	0.399	0.398
80	0.285	0.281	0.278	0.426	0.419	0.419
90	0.292	0.287	0.286	0.432	0.428	0.429
100	0.297	0.295	0.295	0.440	0.440	0.440

**Table D.24** Mast 4 induced voltages in Case 2 with single lightning strokes on the return line for configuration 1

Configuration 1 - Case 2 (Return)						
Mast 4 (MV)						
Single stroke-(2.0/100 $\mu$ s)						
Rf	- 34 kA			- 50 kA		
( $\Omega$ )	Auxiliary	Return	Catenary	Auxiliary	Return	Catenary
5	0.274	0.258	0.235	0.419	0.416	0.420
10	0.275	0.259	0.237	0.422	0.419	0.421
20	0.276	0.260	0.239	0.424	0.421	0.422
30	0.276	0.262	0.243	0.426	0.423	0.423
40	0.277	0.263	0.247	0.428	0.424	0.424
50	0.277	0.264	0.251	0.429	0.425	0.425
60	0.277	0.265	0.255	0.431	0.427	0.426
70	0.278	0.266	0.259	0.433	0.429	0.427
80	0.278	0.267	0.263	0.434	0.430	0.428
90	0.279	0.269	0.265	0.436	0.432	0.429
100	0.279	0.270	0.266	0.438	0.434	0.430

**Table D.25** Mast 5 induced voltages in Case 2 with single lightning strokes on the return line for configuration 1

Configuration 1 - Case 2 (Return)						
Mast 5						
Single stroke-(2.0/100 $\mu$ s)						
Rf	- 34 kA			- 50 kA		
( $\Omega$ )	Auxiliary	Return	Catenary	Auxiliary	Return	Catenary
5	0.241	0.160	0.185	0.355	0.270	0.259
10	0.243	0.172	0.190	0.362	0.282	0.272
20	0.246	0.184	0.194	0.369	0.294	0.285
30	0.248	0.196	0.198	0.376	0.306	0.298
40	0.251	0.202	0.200	0.379	0.313	0.305
50	0.254	0.208	0.203	0.383	0.319	0.312
60	0.257	0.214	0.207	0.390	0.331	0.325
70	0.259	0.220	0.212	0.397	0.343	0.338
80	0.261	0.232	0.216	0.404	0.355	0.351
90	0.263	0.244	0.219	0.407	0.362	0.359
100	0.266	0.255	0.221	0.411	0.368	0.366

**Table D.26** Mast 7 induced voltages in Case 2 with single lightning strokes on the return line for configuration 1

Configuration 1 - Case 2 (Return)						
Mast 7 (MV)						
Single stroke-(2.0/100 $\mu$ s)						
Rf	- 34 kA			- 50 kA		
( $\Omega$ )	Auxiliary	Return	Catenary	Auxiliary	Return	Catenary
5	0.180	0.106	0.176	0.234	0.211	0.211
10	0.181	0.109	0.176	0.235	0.213	0.213
20	0.182	0.112	0.176	0.236	0.215	0.215
30	0.182	0.115	0.176	0.237	0.218	0.218
40	0.183	0.116	0.176	0.238	0.221	0.221
50	0.183	0.118	0.176	0.239	0.222	0.222
60	0.183	0.121	0.176	0.240	0.224	0.224
70	0.184	0.124	0.176	0.241	0.227	0.227
80	0.184	0.127	0.176	0.242	0.230	0.230
90	0.185	0.129	0.176	0.243	0.231	0.231
100	0.185	0.131	0.176	0.245	0.233	0.233

**Table D.27** Mast 4 induced voltages in Case 1 with single lightning strokes on the return line for configuration 2

Configuration 2 - Case 1 (Return)						
Mast 4						
Single stroke-(2.0/100 $\mu$ s)						
Rf	- 34 kA			- 50 kA		
( $\Omega$ )	Auxiliary	Return	Catenary	Auxiliary	Return	Catenary
5	0.677	1.31	0.862	1.01	1.95	1.26
5	0.678	1.31	0.862	1.02	1.95	1.26
5	0.680	1.31	0.862	1.02	1.95	1.26

**Table D.28** Mast 5 induced voltages in Case 1 with single lightning strokes on the return line for configuration 2

Configuration 2 - Case 1 (Return)						
Mast 5						
Single stroke-(2.0/100 $\mu$ s)						
Rf	- 34 kA			- 50 kA		
( $\Omega$ )	Auxiliary	Return	Catenary	Auxiliary	Return	Catenary
10	0.548	0.546	0.547	0.838	0.837	0.838
20	0.552	0.551	0.552	0.846	0.845	0.845
50	0.565	0.563	0.564	0.860	0.860	0.860

**Table D.29** Mast 7 induced voltages in Case 1 with single lightning strokes on the return line for configuration 2

Configuration 2 - Case 1 (Return)						
Mast 7						
Single stroke-(2.0/100 $\mu$ s)						
Rf	- 34 kA			- 50 kA		
( $\Omega$ )	Auxiliary	Return	Catenary	Auxiliary	Return	Catenary
20	0.188	0.188	0.188	0.349	0.310	0.304
50	0.230	0.229	0.229	0.376	0.357	0.353
100	0.287	0.285	0.285	0.424	0.423	0.423

**Table D.30** Mast 4 induced voltages in Case 1 with single lightning strokes on the return line for configuration 3

Configuration 3 - Case 1 (Return)						
Mast 4						
First stroke-(1.0/100 $\mu$ s), Subsequent stroke-(0.2/50 $\mu$ s)						
Rf	- 34 kA			- 50 kA		
( $\Omega$ )	Auxiliary	Return	Catenary	Auxiliary	Return	Catenary
100	0.678	1.31	0.860	1.01	1.95	1.26
100	0.678	1.31	0.860	1.01	1.95	1.26
100	0.678	1.31	0.850	1.01	1.95	1.26

**Table D.31** Mast 5 induced voltages in Case 1 with single lightning strokes on the return line for configuration 3

Configuration 3 - Case 1 (Return)						
Mast 5						
Single stroke-(2.0/100 $\mu$ s)						
Rf	- 34 kA			- 50 kA		
( $\Omega$ )	Auxiliary	Return	Catenary	Auxiliary	Return	Catenary
50	0.567	0.565	0.566	0.863	0.860	0.861
20	0.553	0.552	0.553	0.846	0.846	0.846
10	0.548	0.547	0.547	0.839	0.839	0.839

**Table D.32** Mast 7 induced voltages in Case 1 with single lightning strokes on the return line for configuration 3

Configuration 3 - Case 1 (Return)						
Mast 7						
Single stroke-(2.0/100 $\mu$ s)						
Rf	- 34 kA			- 50 kA		
( $\Omega$ )	Auxiliary	Return	Catenary	Auxiliary	Return	Catenary
20	0.197	0.197	0.197	0.358	0.320	0.314
10	0.175	0.174	0.174	0.339	0.294	0.287
5	0.170	0.170	0.170	0.331	0.282	0.274

**Table D.33** Mast 4 induced voltages in Case 2 with single lightning strokes on the return line for configuration 2

Configuration 2 - Case 2 (Return)						
Mast 4						
Single stroke-(2.0/100 $\mu$ s)						
Rf	- 34 kA			- 50 kA		
( $\Omega$ )	Auxiliary	Return	Catenary	Auxiliary	Return	Catenary
5	0.270	0.257	0.258	0.420	0.420	0.420
5	0.270	0.257	0.258	0.420	0.420	0.420
5	0.270	0.257	0.258	0.424	0.420	0.420

**Table D.34** Mast 5 induced voltages in Case 2 with single lightning strokes on the return line for configuration 2

Configuration 2 - Case 2 (Return)						
Mast 5						
Single stroke-(1.0/100 $\mu$ s)						
Rf	- 34 kA			- 50 kA		
( $\Omega$ )	Auxiliary	Return	Catenary	Auxiliary	Return	Catenary
10	0.250	0.147	0.130	0.357	0.272	0.266
20	0.250	0.151	0.135	0.360	0.288	0.283
50	0.250	0.183	0.178	0.386	0.320	0.320

**Table D.35** Mast 7 induced voltages in Case 2 with single lightning strokes on the return line for configuration 2

Configuration 2 - Case 2 (Return)						
Mast 7						
Single stroke-(2.0/100 $\mu$ s)						
Rf	- 34 kA			- 50 kA		
( $\Omega$ )	Auxiliary	Return	Catenary	Auxiliary	Return	Catenary
20	0.182	0.166	0.110	0.235	0.127	0.205
50	0.182	0.166	0.116	0.235	0.199	0.205
100	0.182	0.166	0.116	0.236	0.200	0.205

**Table D.36** Mast 4 induced voltages in Case 2 with single lightning strokes on the return line for configuration 3

Configuration 3 - Case 2 (Return)						
Mast 4						
Single stroke-(2.0/100 $\mu$ s)						
Rf	- 34 kA			- 50 kA		
( $\Omega$ )	Auxiliary	Return	Catenary	Auxiliary	Return	Catenary
100	0.280	0.270	0.271	0.430	0.436	0.441
100	0.278	0.272	0.274	0.426	0.441	0.446
100	0.277	0.272	0.275	0.425	0.442	0.447

**Table D.37** Mast 5 induced voltages in Case 2 with single lightning strokes on the return line for configuration 3

Configuration 3 - Case 2 (Return)						
Mast 5						
Single stroke-(2.0/100 $\mu$ s)						
Rf	- 34 kA			- 50 kA		
( $\Omega$ )	Auxiliary	Return	Catenary	Auxiliary	Return	Catenary
50	0.267	0.177	0.162	0.387	0.308	0.302
20	0.260	0.163	0.147	0.375	0.291	0.281
10	0.260	0.157	0.140	0.369	0.283	0.271

**Table D.38** Mast 7 induced voltages in Case 2 with single lightning strokes on the return line for configuration 3

Configuration 3 - Case 2 (Return)						
Mast 7						
Single stroke-(2.0/100 $\mu$ s)						
Rf	- 34 kA			- 50 kA		
( $\Omega$ )	Auxiliary	Return	Catenary	Auxiliary	Return	Catenary
20	0.185	0.175	0.115	0.240	0.131	0.200
10	0.185	0.169	0.110	0.239	0.131	0.200
5	0.187	0.110	0.110	0.230	0.122	0.202



**Table D.39** Mast 4 induced voltages in Case 1 with single lightning strokes on the catenary line for configuration 1

Configuration 1 - Case 1 (Catenary)						
Mast 4 (MV)						
Single stroke-(2.0/100 $\mu$ s)						
Rf	- 34 kA			- 50 kA		
( $\Omega$ )	Auxiliary	Return	Catenary	Auxiliary	Return	Catenary
5	0.592	0.873	1.02	0.920	1.33	1.53
10	0.592	0.873	1.02	0.920	1.33	1.53
20	0.592	0.873	1.02	0.920	1.33	1.53
30	0.592	0.873	1.02	0.920	1.33	1.53
40	0.592	0.873	1.02	0.920	1.33	1.53
50	0.592	0.873	1.02	0.920	1.33	1.53
60	0.592	0.873	1.02	0.921	1.34	1.54
70	0.592	0.873	1.02	0.921	1.34	1.54
80	0.592	0.873	1.02	0.921	1.34	1.54
90	0.592	0.873	1.02	0.921	1.34	1.54
100	0.592	0.873	1.02	0.921	1.34	1.54

**Table D.40** Mast 5 induced voltages in Case 1 with single lightning strokes on the catenary line for configuration 1

Configuration 1 - Case 1 (Catenary)						
Mast 5 (MV)						
Single stroke-(2.0/100 $\mu$ s)						
Rf	- 34 kA			- 50 kA		
( $\Omega$ )	Auxiliary	Return	Catenary	Auxiliary	Return	Catenary
5	0.505	0.630	0.650	0.769	0.949	0.978
10	0.507	0.632	0.653	0.774	0.955	0.984
20	0.509	0.634	0.656	0.779	0.961	0.991
30	0.511	0.636	0.660	0.784	0.968	0.997
40	0.513	0.638	0.664	0.786	0.971	1.000
50	0.515	0.641	0.668	0.789	0.974	1.004
60	0.517	0.643	0.672	0.794	0.980	1.011
70	0.519	0.645	0.676	0.799	0.987	1.017
80	0.521	0.648	0.680	0.804	0.993	1.023
90	0.523	0.649	0.683	0.807	0.997	1.026
100	0.525	0.663	0.686	0.810	1.00	1.030

**Table D.41** Mast 7 induced voltages in Case 1 with single lightning strokes on the catenary line for configuration 1

Configuration 1 - Case 1 (Catenary)						
Mast 7 (MV)						
Single stroke-(2.0/100 $\mu$ s)						
Rf	- 34 kA			- 50 kA		
( $\Omega$ )	Auxiliary	Return	Catenary	Auxiliary	Return	Catenary
5	0.225	0.152	0.142	0.329	0.311	0.309
10	0.231	0.163	0.151	0.339	0.323	0.322
20	0.238	0.175	0.160	0.349	0.335	0.334
30	0.245	0.187	0.169	0.359	0.348	0.347
40	0.248	0.192	0.173	0.364	0.354	0.353
50	0.252	0.199	0.178	0.369	0.361	0.360
60	0.258	0.210	0.187	0.379	0.373	0.372
70	0.265	0.222	0.196	0.389	0.386	0.385
80	0.272	0.233	0.205	0.399	0.398	0.397
90	0.276	0.238	0.209	0.404	0.404	0.405
100	0.280	0.246	0.215	0.410	0.412	0.412

**Table D.42** Mast 4 induced voltages in Case 2 with single lightning strokes on the catenary line for configuration 1

Configuration 1 - Case 2 (Catenary)						
Mast 4 (MV)						
Single stroke-(2.0/100 $\mu$ s)						
Rf	- 34 kA			- 50 kA		
( $\Omega$ )	Auxiliary	Return	Catenary	Auxiliary	Return	Catenary
5	0.631	0.863	0.900	0.965	1.331	1.388
10	0.633	0.869	0.910	0.968	1.334	1.393
20	0.636	0.873	0.913	0.972	1.338	1.398
30	0.639	0.876	0.915	0.978	1.347	1.407
40	0.643	0.883	0.922	0.984	1.356	1.418
50	0.647	0.889	0.930	0.991	1.364	1.425
60	0.651	0.891	0.936	0.997	1.368	1.429
70	0.652	0.893	0.941	1.005	1.373	1.434
80	0.653	0.895	0.945	1.011	1.381	1.444
90	0.653	0.907	0.955	1.014	1.389	1.454
100	0.664	0.915	0.961	1.018	1.398	1.463

**Table D.43** Mast 5 induced voltages in Case 2 with single lightning strokes on the catenary line for configuration 1

Configuration 1 - Case 2 (Catenary)						
Mast 5						
Single stroke-(2.0/100 $\mu$ s)						
Rf	- 34 kA			- 50 kA		
( $\Omega$ )	Auxiliary	Return	Catenary	Auxiliary	Return	Catenary
5	0.498	0.568	0.580	0.761	0.860	0.879
10	0.501	0.573	0.587	0.766	0.866	0.885
20	0.505	0.577	0.592	0.771	0.873	0.892
30	0.511	0.586	0.596	0.781	0.886	0.906
40	0.518	0.595	0.612	0.791	0.899	0.919
50	0.525	0.603	0.616	0.801	0.913	0.933
60	0.528	0.607	0.625	0.806	0.919	0.939
70	0.532	0.612	0.629	0.811	0.926	0.946
80	0.538	0.621	0.634	0.821	0.940	0.960
90	0.545	0.630	0.643	0.831	0.954	0.973
100	0.552	0.638	0.652	0.842	0.967	0.987

**Table D.44** Mast 7 induced voltages in Case 2 with single lightning strokes on the catenary line for configuration 1

Configuration 1 - Case 2 (Catenary)						
Mast 7 (MV)						
Single stroke-(2.0/100 $\mu$ s)						
Rf	- 34 kA			- 50 kA		
( $\Omega$ )	Auxiliary	Return	Catenary	Auxiliary	Return	Catenary
5	0.228	0.118	0.100	0.348	0.290	0.290
10	0.230	0.121	0.104	0.351	0.295	0.295
20	0.233	0.124	0.109	0.355	0.298	0.300
30	0.239	0.131	0.114	0.362	0.311	0.309
40	0.244	0.137	0.121	0.369	0.321	0.318
50	0.250	0.144	0.127	0.377	0.331	0.328
60	0.253	0.147	0.131	0.380	0.336	0.332
70	0.256	0.150	0.134	0.384	0.341	0.337
80	0.261	0.157	0.141	0.391	0.351	0.347
90	0.266	0.164	0.148	0.398	0.362	0.357
100	0.272	0.171	0.155	0.406	0.372	0.367

**Table D.45** Mast 4 induced voltages in Case 1 with single lightning strokes on the catenary line for configuration 2

Configuration 2 - Case 1 (Catenary)						
Mast 4						
Single stroke-(2.0/100 $\mu$ s)						
Rf	- 34 kA			- 50 kA		
( $\Omega$ )	Auxiliary	Return	Catenary	Auxiliary	Return	Catenary
5	0.592	0.873	1.02	0.920	1.33	1.53
5	0.591	0.872	1.02	0.912	1.328	1.53
5	0.588	0.871	1.02	0.911	1.324	1.53

**Table D.46** Mast 5 induced voltages in Case 1 with single lightning strokes on the catenary line for configuration 2

Configuration 2 - Case 1 (Catenary)						
Mast 5						
Single stroke-(2.0/100 $\mu$ s)						
Rf	- 34 kA			- 50 kA		
( $\Omega$ )	Auxiliary	Return	Catenary	Auxiliary	Return	Catenary
10	0.503	0.633	0.655	0.773	0.953	0.983
20	0.510	0.640	0.661	0.786	0.962	0.992
50	0.516	0.650	0.674	0.798	0.978	1.011

**Table D.47** Mast 7 induced voltages in Case 1 with single lightning strokes on the catenary line for configuration 2

Configuration 2 - Case 1 (Catenary)						
Mast 7						
Single stroke-(2.0/100 $\mu$ s)						
Rf	- 34 kA			- 50 kA		
( $\Omega$ )	Auxiliary	Return	Catenary	Auxiliary	Return	Catenary
20	0.234	0.166	0.155	0.342	0.327	0.327
50	0.250	0.186	0.176	0.363	0.356	0.355
100	0.250	0.187	0.177	0.395	0.399	0.400

**Table D.48** Mast 4 induced voltages in Case 1 with single lightning strokes on the catenary line for configuration 3

Configuration 3 - Case 1 (Catenary)						
Mast 4						
First stroke-(1.0/100 $\mu$ s), Subsequent stroke-(0.2/50 $\mu$ s)						
Rf	- 34 kA			- 50 kA		
( $\Omega$ )	Auxiliary	Return	Catenary	Auxiliary	Return	Catenary
100	0.588	0.870	1.017	0.910	1.32	1.53
100	0.590	0.872	1.02	0.918	1.32	1.53
100	0.592	0.873	1.02	0.920	1.33	1.53

**Table D.49** Mast 5 induced voltages in Case 1 with single lightning strokes on the catenary line for configuration 3

Configuration 3 - Case 1 (Catenary)						
Mast 5						
Single stroke-(2.0/100 $\mu$ s)						
Rf	- 34 kA			- 50 kA		
( $\Omega$ )	Auxiliary	Return	Catenary	Auxiliary	Return	Catenary
50	0.518	0.650	0.674	0.801	0.980	1.01
20	0.510	0.638	0.660	0.779	0.960	1.00
10	0.507	0.633	0.655	0.773	0.954	0.983

**Table D.50** Mast 7 induced voltages in Case 1 with single lightning strokes on the catenary line for configuration 3

Configuration 3 - Case 1 (Catenary)						
Mast 7						
Single stroke-(2.0/100 $\mu$ s)						
Rf	- 34 kA			- 50 kA		
( $\Omega$ )	Auxiliary	Return	Catenary	Auxiliary	Return	Catenary
20	0.241	0.172	0.162	0.351	0.341	0.339
10	0.231	0.160	0.148	0.337	0.321	0.320
5	0.227	0.154	0.143	0.330	0.313	0.311

**Table D.51** Mast 4 induced voltages in Case 2 with single lightning strokes on the catenary line for configuration 2

Configuration 2 - Case 2 (Catenary)						
Mast 4						
Single stroke-(2.0/100 $\mu$ s)						
Rf	- 34 kA			- 50 kA		
( $\Omega$ )	Auxiliary	Return	Catenary	Auxiliary	Return	Catenary
5	0.665	0.879	0.920	0.965	1.332	1.389
5	0.640	0.870	0.916	0.966	1.332	1.389
5	0.631	0.863	0.900	0.996	1.350	1.410

**Table D.52** Mast 5 induced voltages in Case 2 with single lightning strokes on the catenary line for configuration 2

Configuration 2 - Case 2 (Catenary)						
Mast 5						
Single stroke-(1.0/100 $\mu$ s)						
Rf	- 34 kA			- 50 kA		
( $\Omega$ )	Auxiliary	Return	Catenary	Auxiliary	Return	Catenary
10	0.520	0.581	0.600	0.765	0.868	0.885
20	0.520	0.581	0.593	0.772	0.878	0.895
50	0.520	0.595	0.590	0.804	0.920	0.940

**Table D.53** Mast 7 induced voltages in Case 2 with single lightning strokes on the catenary line for configuration 2

Configuration 2 - Case 2 (Catenary)						
Mast 7						
Single stroke-(2.0/100 $\mu$ s)						
Rf	- 34 kA			- 50 kA		
( $\Omega$ )	Auxiliary	Return	Catenary	Auxiliary	Return	Catenary
20	0.226	0.124	0.107	0.352	0.298	0.295
50	0.238	0.134	0.117	0.360	0.313	0.310
100	0.252	0.151	0.135	0.377	0.342	0.339

**Table D.54** Mast 4 induced voltages in Case 2 with single lightning strokes on the catenary line for configuration 3

Configuration 3 - Case 2 (Catenary)						
Mast 4						
Single stroke-(2.0/100 $\mu$ s)						
Rf	- 34 kA			- 50 kA		
( $\Omega$ )	Auxiliary	Return	Catenary	Auxiliary	Return	Catenary
100	0.675	0.935	0.984	1.016	1.40	1.465
100	0.675	0.933	1.000	1.016	1.39	1.460
100	0.675	0.930	1.000	1.016	1.39	1.470

**Table D.55** Mast 5 induced voltages in Case 2 with single lightning strokes on the catenary line for configuration 3

Configuration 3 - Case 2 (Catenary)						
Mast 5						
Single stroke-(2.0/100 $\mu$ s)						
Rf	- 34 kA			- 50 kA		
( $\Omega$ )	Auxiliary	Return	Catenary	Auxiliary	Return	Catenary
50	0.580	0.620	0.632	0.819	0.936	0.955
20	0.545	0.614	0.626	0.798	0.908	0.925
10	0.517	0.592	0.603	0.788	0.895	0.912

**Table D.56** Mast 7 induced voltages in Case 2 with single lightning strokes on the catenary line for configuration 3

Configuration 3 - Case 2 (Catenary)						
Mast 7						
Single stroke-(2.0/100 $\mu$ s)						
Rf	- 34 kA			- 50 kA		
( $\Omega$ )	Auxiliary	Return	Catenary	Auxiliary	Return	Catenary
20	0.250	0.138	0.120	0.376	0.321	0.317
10	0.237	0.124	0.107	0.365	0.305	0.301
5	0.237	0.124	0.100	0.361	0.298	0.294

**Table D.57** Mast 4 induced voltages in Case 1 with single lightning strokes on the train's pantograph for configuration 1

Configuration 1 - Case 1 (Pantograph)						
Mast 4 (MV)						
Single stroke-(2.0/100 $\mu$ s)						
Rf	- 34 kA			- 50 kA		
( $\Omega$ )	Auxiliary	Return	Catenary	Auxiliary	Return	Catenary
5	0.591	0.871	0.988	0.917	1.35	1.55
10	0.591	0.871	0.988	0.917	1.35	1.55
20	0.591	0.871	0.988	0.917	1.35	1.55
30	0.592	0.871	0.988	0.917	1.35	1.55
40	0.592	0.871	0.988	0.917	1.35	1.55
50	0.593	0.871	0.988	0.917	1.35	1.55
60	0.593	0.871	0.988	0.917	1.35	1.55
70	0.594	0.871	0.988	0.917	1.35	1.55
80	0.595	0.871	0.988	0.917	1.35	1.55
90	0.595	0.871	0.988	0.917	1.35	1.55
100	0.596	0.871	0.988	0.917	1.35	1.55

**Table D.58** Mast 5 induced voltages in Case 1 with single lightning strokes on the train's pantograph for configuration 1

Configuration 1 - Case 1 (Pantograph)						
Mast 5 (MV)						
Single stroke-(2.0/100 $\mu$ s)						
Rf	- 34 kA			- 50 kA		
( $\Omega$ )	Auxiliary	Return	Catenary	Auxiliary	Return	Catenary
5	0.510	0.610	0.629	0.777	0.940	0.970
10	0.511	0.612	0.634	0.779	0.945	0.974
20	0.512	0.615	0.639	0.781	0.955	0.977
30	0.513	0.620	0.645	0.785	0.962	0.985
40	0.514	0.625	0.647	0.790	0.966	0.992
50	0.515	0.630	0.650	0.794	0.970	1.000
60	0.516	0.633	0.653	0.796	0.977	1.007
70	0.517	0.635	0.655	0.799	0.985	1.015
80	0.518	0.640	0.661	0.803	0.992	1.022
90	0.520	0.645	0.667	0.808	0.996	1.026
100	0.521	0.650	0.672	0.812	1.00	1.030

**Table D.59** Mast 7 induced voltages in Case 1 with single lightning strokes on the



train's pantograph for configuration 1

Configuration 1 - Case 1 (Pantograph)						
Mast 7 (MV)						
Single stroke-(2.0/100 $\mu$ s)						
Rf	- 34 kA			- 50 kA		
( $\Omega$ )	Auxiliary	Return	Catenary	Auxiliary	Return	Catenary
5	0.196	0.198	0.212	0.327	0.307	0.304
10	0.205	0.206	0.218	0.332	0.317	0.317
20	0.214	0.214	0.223	0.337	0.327	0.330
30	0.223	0.222	0.226	0.347	0.337	0.343
40	0.227	0.226	0.233	0.357	0.347	0.349
50	0.232	0.231	0.238	0.367	0.357	0.356
60	0.241	0.239	0.244	0.377	0.367	0.369
70	0.250	0.247	0.251	0.387	0.377	0.382
80	0.259	0.255	0.257	0.394	0.387	0.395
90	0.264	0.259	0.260	0.399	0.397	0.401
100	0.268	0.264	0.264	0.407	0.407	0.408

**Table D.60** Mast 4 induced voltages in Case 2 with single lightning strokes on the train's pantograph for configuration 1

Configuration 1 - Case 2 (Pantograph)						
Mast 4 (MV)						
Single stroke-(2.0/100 $\mu$ s)						
Rf	- 34 kA			- 50 kA		
( $\Omega$ )	Auxiliary	Return	Catenary	Auxiliary	Return	Catenary
5	0.610	0.833	0.869	0.934	1.28	1.337
10	0.613	0.838	0.875	0.939	1.28	1.345
20	0.617	0.843	0.881	0.944	1.29	1.353
30	0.621	0.848	0.887	0.950	1.30	1.362
40	0.623	0.850	0.890	0.954	1.30	1.366
50	0.625	0.854	0.893	0.957	1.31	1.370
60	0.628	0.859	0.899	0.962	1.32	1.372
70	0.632	0.864	0.905	0.968	1.33	1.380
80	0.636	0.869	0.911	0.974	1.34	1.388
90	0.639	0.872	0.913	0.977	1.35	1.396
100	0.641	0.875	0.916	0.980	1.35	1.404

**Table D.61** Mast 5 induced voltages in Case 2 with single lightning strokes on the train's pantograph for configuration 1

Configuration 1 - Case 2 (Pantograph)						
Mast 5						
Single stroke-(2.0/100 $\mu$ s)						
Rf	- 34 kA			- 50 kA		
( $\Omega$ )	Auxiliary	Return	Catenary	Auxiliary	Return	Catenary
5	0.486	0.550	0.563	0.740	0.839	0.855
10	0.492	0.558	0.571	0.750	0.851	0.868
20	0.499	0.567	0.580	0.760	0.863	0.881
30	0.505	0.575	0.589	0.770	0.876	0.894
40	0.508	0.579	0.593	0.775	0.884	0.900
50	0.512	0.584	0.598	0.780	0.889	0.907
60	0.514	0.592	0.606	0.790	0.901	0.920
70	0.521	0.601	0.615	0.800	0.914	0.933
80	0.527	0.610	0.624	0.810	0.926	0.946
90	0.534	0.614	0.628	0.815	0.935	0.955
100	0.539	0.619	0.633	0.821	0.941	0.960

**Table D.62** Mast 7 induced voltages in Case 2 with single lightning strokes on the train's pantograph for configuration 1

Configuration 1 - Case 2 (Pantograph)						
Mast 7 (MV)						
Single stroke-(2.0/100 $\mu$ s)						
Rf	- 34 kA			- 50 kA		
( $\Omega$ )	Auxiliary	Return	Catenary	Auxiliary	Return	Catenary
5	0.096	0.113	0.218	0.340	0.281	0.277
10	0.117	0.119	0.218	0.347	0.290	0.286
20	0.138	0.126	0.219	0.354	0.300	0.296
30	0.159	0.132	0.219	0.361	0.310	0.306
40	0.169	0.135	0.220	0.364	0.315	0.310
50	0.180	0.139	0.220	0.368	0.320	0.316
60	0.201	0.145	0.221	0.375	0.329	0.325
70	0.222	0.151	0.221	0.382	0.339	0.335
80	0.243	0.158	0.222	0.389	0.349	0.345
90	0.253	0.161	0.222	0.392	0.359	0.350
100	0.264	0.165	0.223	0.397	0.360	0.355

**Table D.63** Mast 4 induced voltages in Case 1 with single lightning strokes on the train's pantograph for configuration 2

Configuration 2 - Case 1 (Pantograph)						
Mast 4						
Single stroke-(2.0/100 $\mu$ s)						
Rf	- 34 kA			- 50 kA		
( $\Omega$ )	Auxiliary	Return	Catenary	Auxiliary	Return	Catenary
5	0.592	0.860	0.988	0.917	1.35	1.55
5	0.592	0.869	0.988	0.917	1.35	1.55
5	0.595	0.870	0.988	0.917	1.35	1.55

**Table D.64** Mast 5 induced voltages in Case 1 with single lightning strokes on the train's pantograph for configuration 2

Configuration 2 - Case 1 (Pantograph)						
Mast 5						
Single stroke-(2.0/100 $\mu$ s)						
Rf	- 34 kA			- 50 kA		
( $\Omega$ )	Auxiliary	Return	Catenary	Auxiliary	Return	Catenary
10	0.509	0.613	0.633	0.779	0.946	0.976
20	0.510	0.618	0.639	0.780	0.955	0.985
50	0.511	0.633	0.655	0.796	0.975	1.008

**Table D.65** Mast 7 induced voltages in Case 1 with single lightning strokes on the train's pantograph for configuration 2

Configuration 2 - Case 1 (Pantograph)						
Mast 7						
Single stroke-(2.0/100 $\mu$ s)						
Rf	- 34 kA			- 50 kA		
( $\Omega$ )	Auxiliary	Return	Catenary	Auxiliary	Return	Catenary
20	0.220	0.209	0.207	0.340	0.323	0.321
50	0.240	0.227	0.227	0.362	0.351	0.349
100	0.260	0.255	0.254	0.395	0.391	0.391

**Table D.66** Mast 4 induced voltages in Case 1 with single lightning strokes on the train's pantograph for configuration 3

Configuration 3 - Case 1 (Pantograph)						
Mast 4						
First stroke-(1.0/100 $\mu$ s), Subsequent stroke-(0.2/50 $\mu$ s)						
Rf	- 34 kA			- 50 kA		
( $\Omega$ )	Auxiliary	Return	Catenary	Auxiliary	Return	Catenary
100	0.591	0.870	0.987	0.915	1.35	1.55
100	0.591	0.871	0.989	0.917	1.35	1.55
100	0.592	0.872	0.989	0.917	1.35	1.55

**Table D.67** Mast 5 induced voltages in Case 1 with single lightning strokes on the train's pantograph for configuration 3

Configuration 3 - Case 1 (Pantograph)						
Mast 5						
Single stroke-(2.0/100 $\mu$ s)						
Rf	- 34 kA			- 50 kA		
( $\Omega$ )	Auxiliary	Return	Catenary	Auxiliary	Return	Catenary
50	0.522	0.633	0.654	0.800	0.976	1.008
20	0.514	0.629	0.649	0.786	0.955	0.986
10	0.513	0.626	0.647	0.780	0.947	0.976

**Table D.68** Mast 7 induced voltages in Case 1 with single lightning strokes on the train's pantograph for configuration 3

Configuration 3 - Case 1 (Pantograph)						
Mast 7						
Single stroke-(2.0/100 $\mu$ s)						
Rf	- 34 kA			- 50 kA		
( $\Omega$ )	Auxiliary	Return	Catenary	Auxiliary	Return	Catenary
20	0.228	0.217	0.215	0.353	0.338	0.335
10	0.216	0.205	0.202	0.337	0.318	0.315
5	0.212	0.199	0.197	0.330	0.309	0.307

**Table D.69** Mast 4 induced voltages in Case 2 with single lightning strokes on the train's pantograph for configuration 2

Configuration 2 - Case 2 (Pantograph)						
Mast 4						
Single stroke-(2.0/100 $\mu$ s)						
Rf	- 34 kA			- 50 kA		
( $\Omega$ )	Auxiliary	Return	Catenary	Auxiliary	Return	Catenary
5	0.610	0.833	0.869	0.934	1.28	1.34
5	0.610	0.833	0.869	0.935	1.28	1.34
5	0.610	0.834	0.870	0.936	1.28	1.34

**Table D.70** Mast 5 induced voltages in Case 2 with single lightning strokes on the train's pantograph for configuration 2

Configuration 2 - Case 2 (Pantograph)						
Mast 5						
Single stroke-(2.0/100 $\mu$ s)						
Rf	- 34 kA			- 50 kA		
( $\Omega$ )	Auxiliary	Return	Catenary	Auxiliary	Return	Catenary
10	0.490	0.554	0.567	0.744	0.845	0.860
20	0.494	0.561	0.574	0.752	0.855	0.871
50	0.508	0.578	0.590	0.770	0.880	0.896

**Table D.71** Mast 7 induced voltages in Case 2 with single lightning strokes on the train's pantograph for configuration 2

Configuration 2 - Case 2 (Pantograph)						
Mast 7						
Single stroke-(2.0/100 $\mu$ s)						
Rf	- 34 kA			- 50 kA		
( $\Omega$ )	Auxiliary	Return	Catenary	Auxiliary	Return	Catenary
20	0.221	0.118	0.101	0.344	0.289	0.285
50	0.228	0.128	0.112	0.354	0.305	0.301
100	0.242	0.145	0.130	0.370	0.331	0.327

**Table D.72** Mast 4 induced voltages in Case 2 with single lightning strokes on the train's pantograph for configuration 3

Configuration 3 - Case 2 (Pantograph)						
Mast 4						
Single stroke-(2.0/100 $\mu$ s)						
Rf	- 34 kA			- 50 kA		
( $\Omega$ )	Auxiliary	Return	Catenary	Auxiliary	Return	Catenary
100	0.640	0.876	0.920	0.980	1.34	1.40
100	0.640	0.878	0.921	0.978	1.34	1.41
100	0.640	0.880	0.922	0.977	1.34	1.41

**Table D.73** Mast 5 induced voltages in Case 2 with single lightning strokes on the train's pantograph for configuration 3

Configuration 3 - Case 2 (Pantograph)						
Mast 5						
Single stroke-(2.0/100 $\mu$ s)						
Rf	- 34 kA			- 50 kA		
( $\Omega$ )	Auxiliary	Return	Catenary	Auxiliary	Return	Catenary
50	0.522	0.597	0.610	0.796	0.908	0.928
20	0.507	0.578	0.590	0.775	0.880	0.900
10	0.500	0.570	0.582	0.766	0.869	0.887

**Table D.74** Mast 7 induced voltages in Case 2 with single lightning strokes on the train's pantograph for configuration 3

Configuration 3 - Case 2 (Pantograph)						
Mast 7						
Single stroke-(2.0/100 $\mu$ s)						
Rf	- 34 kA			- 50 kA		
( $\Omega$ )	Auxiliary	Return	Catenary	Auxiliary	Return	Catenary
20	0.240	0.132	0.115	0.368	0.314	0.310
10	0.231	0.123	0.106	0.357	0.296	0.292
5	0.228	0.120	0.102	0.352	0.289	0.285

**Table D.75** Mast 4 induced voltages in Case 1 with multiple lightning strokes on the mast for configuration 1

Configuration 1 - Case 1 (Mast)						
Mast 4						
First stroke-(1.0/100 $\mu$ s), Subsequent stroke-(0.2/50 $\mu$ s)						
Rf	- 34 kA			- 50 kA		
( $\Omega$ )	Auxiliary	Return	Catenary	Auxiliary	Return	Catenary
5	4.50	1.65	1.40	6.60	2.50	2.19
10	4.50	1.65	1.40	6.60	2.51	2.2
20	4.50	1.65	1.40	6.60	2.51	2.2
30	4.50	1.65	1.40	6.60	2.51	2.2
40	4.50	1.65	1.40	6.60	2.51	2.2
50	4.50	1.65	1.40	6.60	2.51	2.2
60	4.50	1.65	1.40	6.60	2.51	2.2
70	4.50	1.65	1.40	6.60	2.51	2.2
80	4.50	1.65	1.40	6.60	2.51	2.2
90	4.50	1.65	1.40	6.60	2.51	2.2
100	4.50	1.65	1.40	6.60	2.51	2.2

**Table D.76** Mast 5 induced voltages in Case 1 with multiple lightning strokes on the mast for configuration 1

Configuration 1 - Case 1 (Mast)						
Mast 5						
First stroke-(1.0/100 $\mu$ s), Subsequent stroke-(0.2/50 $\mu$ s)						
Rf	- 34 kA			- 50 kA		
( $\Omega$ )	Auxiliary	Return	Catenary	Auxiliary	Return	Catenary
5	3.31	1.53	1.26	4.89	2.30	1.91
10	3.31	1.54	1.26	4.89	2.31	1.92
20	3.31	1.55	1.27	4.89	2.33	1.94
30	3.32	1.55	1.27	4.90	2.34	1.95
40	3.32	1.55	1.28	4.90	2.36	1.97
50	3.32	1.56	1.29	4.90	2.37	1.98
60	3.32	1.57	1.30	4.91	2.38	2.00
70	3.32	1.57	1.30	4.91	2.40	2.01
80	3.32	1.58	1.31	4.91	2.40	2.02
90	3.32	1.59	1.32	4.92	2.41	2.03
100	3.33	1.59	1.33	4.92	2.41	2.04

**Table D.77** Mast 7 induced voltages in Case 1 with multiple lightning strokes on the mast for configuration 1

Configuration 1 - Case 1 (Mast)						
Mast 7						
First stroke-(1.0/100 $\mu$ s), Subsequent stroke-(0.2/50 $\mu$ s)						
Rf	- 34 kA			- 50 kA		
( $\Omega$ )	Auxiliary	Return	Catenary	Auxiliary	Return	Catenary
5	1.24	0.60	0.50	1.83	0.90	0.77
10	1.24	0.61	0.51	1.84	0.92	0.78
20	1.24	0.62	0.53	1.85	0.94	0.81
30	1.24	0.70	0.61	1.86	0.97	0.83
40	1.25	0.71	0.63	1.87	0.99	0.86
50	1.27	0.73	0.64	1.88	1.01	0.88
60	1.28	0.73	0.64	1.90	1.03	0.90
70	1.29	0.73	0.64	1.90	1.05	0.92
80	1.30	0.73	0.64	1.92	1.07	0.93
90	1.31	0.73	0.64	1.93	1.08	0.95
100	1.31	0.73	0.64	1.95	1.10	0.97

**Table D.78** Mast 4 induced voltages in Case 2 with multiple lightning strokes on the mast for configuration 1

Configuration 1 - Case 2 (Mast)						
Mast 4						
First stroke-(1.0/100 $\mu$ s), Subsequent stroke-(0.2/50 $\mu$ s)						
Rf	- 34 kA			- 50 kA		
( $\Omega$ )	Auxiliary	Return	Catenary	Auxiliary	Return	Catenary
5	4.78	2.41	2.06	7.08	3.61	3.09
10	4.79	2.43	2.08	7.10	3.64	3.13
20	4.82	2.46	2.12	7.14	3.70	3.18
30	4.84	2.50	2.15	7.17	3.74	3.24
40	4.86	2.52	2.17	7.20	3.78	3.28
50	4.87	2.55	2.20	7.22	3.82	3.31
60	4.89	2.57	2.22	7.24	3.85	3.32
70	4.90	2.58	2.24	7.26	3.85	3.36
80	4.91	2.60	2.26	7.27	3.88	3.40
90	4.92	2.62	2.27	7.29	3.90	3.42
100	4.93	2.63	2.29	7.31	3.93	3.45



**Table D.79** Mast 5 induced voltages in Case 2 with multiple lightning strokes on the mast for configuration 1

Configuration 1 - Case 2 (Mast)						
Mast 5						
First stroke-(1.0/100 $\mu$ s), Subsequent stroke-(0.2/50 $\mu$ s)						
Rf	- 34 kA			- 50 kA		
( $\Omega$ )	Auxiliary	Return	Catenary	Auxiliary	Return	Catenary
5	3.55	1.81	1.55	5.26	2.71	2.31
10	3.56	1.83	1.56	5.28	2.74	2.35
20	3.59	1.88	1.61	5.33	2.81	2.43
30	3.63	1.92	1.65	5.37	2.87	2.48
40	3.65	1.96	1.69	5.41	2.92	2.53
50	3.67	1.99	1.73	5.45	2.98	2.60
60	3.69	2.02	1.75	5.48	3.04	2.67
70	3.71	2.04	1.78	5.51	3.09	2.71
80	3.73	2.07	1.81	5.52	3.13	2.76
90	3.74	2.09	1.83	5.54	3.16	2.80
100	3.76	2.12	1.86	5.56	3.20	2.83

**Table D.80** Mast 7 induced voltages in Case 2 with multiple lightning strokes on the mast for configuration 1

Configuration 1 - Case 2 (Mast)						
Mast 7						
First stroke-(1.0/100 $\mu$ s), Subsequent stroke-(0.2/50 $\mu$ s)						
Rf	- 34 kA			- 50 kA		
( $\Omega$ )	Auxiliary	Return	Catenary	Auxiliary	Return	Catenary
5	1.33	0.65	0.55	1.97	0.97	0.82
10	1.33	0.67	0.57	1.98	0.99	0.84
20	1.34	0.69	0.59	2.00	1.03	0.88
30	1.36	0.72	0.62	2.03	1.15	1.02
40	1.38	0.75	0.65	2.04	1.19	1.06
50	1.40	0.77	0.67	2.06	1.22	1.08
60	1.42	0.79	0.69	2.09	1.25	1.11
70	1.44	0.82	0.72	2.12	1.28	1.15
80	1.46	0.84	0.74	2.15	1.31	1.17
90	1.47	0.86	0.76	2.17	1.33	1.20
100	1.49	0.88	0.78	2.20	1.36	1.23

**Table D.81** Mast 4 induced voltages in Case 1 with multiple lightning strokes on the mast for configuration 2

Configuration 2 - Case 1 (Mast)						
Mast 4						
First stroke-(1.0/100 $\mu$ s), Subsequent stroke-(0.2/50 $\mu$ s)						
Rf	- 34 kA			- 50 kA		
( $\Omega$ )	Auxiliary	Return	Catenary	Auxiliary	Return	Catenary
5	4.47	1.64	1.40	6.60	2.50	2.19
5	4.46	1.63	1.40	6.58	2.50	2.19
5	4.44	1.63	1.40	6.55	2.50	2.20

**Table D.82** Mast 5 induced voltages in Case 1 with multiple lightning strokes on the mast for configuration 2

Configuration 2 - Case 1 (Mast)						
Mast 5						
First stroke-(1.0/100 $\mu$ s), Subsequent stroke-(0.2/50 $\mu$ s)						
Rf	- 34 kA			- 50 kA		
( $\Omega$ )	Auxiliary	Return	Catenary	Auxiliary	Return	Catenary
10	3.31	1.54	1.26	4.89	2.31	1.92
20	3.32	1.54	1.26	4.89	2.33	1.94
50	3.33	1.56	1.29	4.90	2.37	1.98

**Table D.83** Mast 7 induced voltages in Case 1 with multiple lightning strokes on the mast for configuration 2

Configuration 2 - Case 1 (Mast)						
Mast 7						
First stroke-(1.0/100 $\mu$ s), Subsequent stroke-(0.2/50 $\mu$ s)						
Rf	- 34 kA			- 50 kA		
( $\Omega$ )	Auxiliary	Return	Catenary	Auxiliary	Return	Catenary
20	1.23	0.62	0.53	1.85	0.93	0.80
50	1.25	0.71	0.63	1.87	0.98	0.85
100	1.29	0.71	0.63	1.91	1.06	0.92

**Table D.84** Mast 7 induced voltages in Case 1 with multiple lightning strokes on the mast for configuration 3

Configuration 3 - Case 1 (Mast)						
Mast 4						
First stroke-(1.0/100 $\mu$ s), Subsequent stroke-(0.2/50 $\mu$ s)						
Rf	- 34 kA			- 50 kA		
( $\Omega$ )	Auxiliary	Return	Catenary	Auxiliary	Return	Catenary
100	4.44	1.63	1.40	6.55	2.51	2.20
100	4.46	1.63	1.40	6.58	2.51	2.19
100	4.47	1.64	1.40	6.60	2.51	2.19

**Table D.85** Mast 5 induced voltages in Case 1 with multiple lightning strokes on the mast for configuration 3

Configuration 3 - Case 1 (Mast)						
Mast 5						
First stroke-(1.0/100 $\mu$ s), Subsequent stroke-(0.2/50 $\mu$ s)						
Rf	- 34 kA			- 50 kA		
( $\Omega$ )	Auxiliary	Return	Catenary	Auxiliary	Return	Catenary
50	3.32	1.56	1.29	4.91	2.37	1.98
20	3.31	1.55	1.27	4.90	2.33	1.94
10	3.30	1.54	1.26	4.89	2.31	1.92

**Table D.86** Mast 7 induced voltages in Case 1 with multiple lightning strokes on the mast for configuration 3

Configuration 3 - Case 1 (Mast)						
Mast 7						
First stroke-(1.0/100 $\mu$ s), Subsequent stroke-(0.2/50 $\mu$ s)						
Rf	- 34 kA			- 50 kA		
( $\Omega$ )	Auxiliary	Return	Catenary	Auxiliary	Return	Catenary
20	1.24	0.69	0.61	1.86	0.97	0.83
10	1.24	0.61	0.52	1.84	0.93	0.79
5	1.24	0.60	0.51	1.83	0.91	0.77

**Table D.87** Mast 4 induced voltages in Case 2 with multiple lightning strokes on the mast for configuration 2

Configuration 2 - Case 2 (Mast)						
Mast 4						
First stroke-(1.0/100 $\mu$ s), Subsequent stroke-(0.2/50 $\mu$ s)						
Rf	- 34 kA			- 50 kA		
( $\Omega$ )	Auxiliary	Return	Catenary	Auxiliary	Return	Catenary
5	4.78	2.41	2.06	7.08	3.61	3.10
5	4.77	2.42	2.06	7.07	3.62	3.10
5	4.76	2.42	2.07	7.06	3.63	3.12

**Table D.88** Mast 5 induced voltages in Case 2 with multiple lightning strokes on the mast for configuration 2

Configuration 2 - Case 2 (Mast)						
Mast 5						
First stroke-(1.0/100 $\mu$ s), Subsequent stroke-(0.2/50 $\mu$ s)						
Rf	- 34 kA			- 50 kA		
( $\Omega$ )	Auxiliary	Return	Catenary	Auxiliary	Return	Catenary
10	3.55	1.82	1.55	5.27	2.73	2.33
20	3.57	1.85	1.58	5.29	2.77	2.38
50	3.60	1.91	1.65	5.34	2.88	2.50

**Table D.89** Mast 7 induced voltages in Case 2 with multiple lightning strokes on the mast for configuration 2

Configuration 2 - Case 2 (Mast)						
Mast 7						
First stroke-(1.0/100 $\mu$ s), Subsequent stroke-(0.2/50 $\mu$ s)						
Rf	- 34 kA			- 50 kA		
( $\Omega$ )	Auxiliary	Return	Catenary	Auxiliary	Return	Catenary
20	1.34	0.68	0.58	1.98	1.00	0.85
50	1.35	0.72	0.62	2.01	1.13	1.00
100	1.40	0.80	0.70	2.07	1.23	1.10

**Table D.90** Mast 4 induced voltages in Case 2 with multiple lightning strokes on the mast for configuration 3

Configuration 3 - Case 2 (Mast)						
Mast 4						
First stroke-(1.0/100 $\mu$ s), Subsequent stroke-(0.2/50 $\mu$ s)						
Rf	- 34 kA			- 50 kA		
( $\Omega$ )	Auxiliary	Return	Catenary	Auxiliary	Return	Catenary
100	4.93	2.61	2.27	7.30	3.90	3.41
100	4.93	2.60	2.25	7.30	3.87	3.39
100	4.93	2.59	2.24	7.30	3.85	3.36

**Table D.91** Mast 5 induced voltages in Case 2 with multiple lightning strokes on the mast for configuration 3

Configuration 3 - Case 2 (Mast)						
Mast 5						
First stroke-(1.0/100 $\mu$ s), Subsequent stroke-(0.2/50 $\mu$ s)						
Rf	- 34 kA			- 50 kA		
( $\Omega$ )	Auxiliary	Return	Catenary	Auxiliary	Return	Catenary
50	3.71	2.02	1.76	5.49	3.05	2.67
20	3.66	1.95	1.68	5.41	2.93	2.54
10	3.64	1.92	1.64	5.39	2.88	2.49

**Table D.92** Mast 7 induced voltages in Case 2 with multiple lightning strokes on the mast for configuration 3

Configuration 3 - Case 2 (Mast)						
Mast 7						
First stroke-(1.0/100 $\mu$ s), Subsequent stroke-(0.2/50 $\mu$ s)						
Rf	- 34 kA			- 50 kA		
( $\Omega$ )	Auxiliary	Return	Catenary	Auxiliary	Return	Catenary
20	1.39	0.75	0.65	2.05	1.19	1.05
10	1.36	0.70	0.60	2.02	1.03	0.88
5	1.35	0.68	0.58	2.01	1.01	0.86

**Table D.93** Mast 4 induced voltages in Case 1 with multiple lightning strokes on the return line for configuration 1

Configuration 1 - Case 1 (Return)						
Mast 4						
First stroke-(1.0/100 $\mu$ s), Subsequent stroke-(0.2/50 $\mu$ s)						
Rf	- 34 kA			- 50 kA		
( $\Omega$ )	Auxiliary	Return	Catenary	Auxiliary	Return	Catenary
5	1.68	3.24	2.15	2.58	4.93	3.37
10	1.68	3.24	2.15	2.58	4.93	3.37
20	1.68	3.24	2.15	2.58	4.93	3.37
30	1.68	3.24	2.15	2.58	4.93	3.37
40	1.68	3.25	2.16	2.58	4.94	3.37
50	1.68	3.25	2.16	2.58	4.94	3.37
60	1.68	3.25	2.16	2.58	4.94	3.37
70	1.68	3.25	2.16	2.58	4.94	3.37
80	1.68	3.26	2.17	2.58	4.96	3.37
90	1.68	3.26	2.17	2.58	4.96	3.37
100	1.68	3.26	2.17	2.58	4.96	3.37

**Table D.94** Mast 5 induced voltages in Case 1 with multiple lightning strokes on the return line for configuration 1

Configuration 1 - Case 1 (Return)						
Mast 5						
First stroke-(1.0/100 $\mu$ s), Subsequent stroke-(0.2/50 $\mu$ s)						
Rf	- 34 kA			- 50 kA		
( $\Omega$ )	Auxiliary	Return	Catenary	Auxiliary	Return	Catenary
5	1.39	1.33	1.33	2.13	2.05	2.06
10	1.40	1.34	1.34	2.14	2.06	2.07
20	1.40	1.35	1.35	2.15	2.07	2.08
30	1.41	1.36	1.36	2.16	2.08	2.10
40	1.41	1.36	1.36	2.16	2.10	2.12
50	1.42	1.37	1.37	2.17	2.12	2.13
60	1.42	1.37	1.37	2.17	2.13	2.14
70	1.43	1.38	1.38	2.18	2.14	2.15
80	1.43	1.39	1.39	2.19	2.15	2.16
90	1.44	1.40	1.40	2.20	2.16	2.18
100	1.44	1.41	1.41	2.21	2.18	2.19

**Table D.95** Mast 7 induced voltages in Case 1 with multiple lightning strokes on the return line for configuration 1

Configuration 1 - Case 1 (Return)						
Mast 7						
First stroke-(1.0/100 $\mu$ s), Subsequent stroke-(0.2/50 $\mu$ s)						
Rf	- 34 kA			- 50 kA		
( $\Omega$ )	Auxiliary	Return	Catenary	Auxiliary	Return	Catenary
5	0.49	0.42	0.42	0.73	0.62	0.61
10	0.50	0.45	0.45	0.74	0.63	<b>0.62</b>
20	0.51	0.47	0.47	0.76	0.66	0.65
30	0.53	0.49	0.49	0.78	0.69	0.68
40	0.55	0.51	0.51	0.81	0.73	0.72
50	0.57	0.53	0.53	0.84	0.76	0.75
60	0.58	0.55	0.55	0.86	0.78	0.77
70	0.59	0.57	0.57	0.88	0.82	0.81
80	0.61	0.59	0.60	0.90	0.84	0.83
90	0.63	0.62	0.63	0.93	0.88	0.87
100	0.64	0.64	0.65	0.95	0.90	0.89

**Table D.96** Mast 4 induced voltages in Case 2 with multiple lightning strokes on the return line for configuration 1

Configuration 1 - Case 2 (Return)						
Mast 4						
First stroke-(1.0/100 $\mu$ s), Subsequent stroke-(0.2/50 $\mu$ s)						
Rf	- 34 kA			- 50 kA		
( $\Omega$ )	Auxiliary	Return	Catenary	Auxiliary	Return	Catenary
5	0.91	0.86	0.86	1.42	1.29	1.29
10	0.91	0.86	0.86	1.42	1.29	1.29
20	0.91	0.86	0.86	1.42	1.29	1.29
30	0.91	0.86	0.86	1.42	1.30	0.30
40	0.91	0.86	0.86	1.42	1.30	0.30
50	0.91	0.87	0.87	1.42	1.30	0.30
60	0.91	0.87	0.87	1.42	1.31	0.31
70	0.91	0.87	0.87	1.42	1.31	0.31
80	0.91	0.87	0.87	1.42	1.31	0.31
90	0.91	0.88	0.88	1.42	1.32	1.32
100	0.91	0.88	0.88	1.42	1.32	1.32

**Table D.97** Mast 5 induced voltages in Case 2 with multiple lightning strokes on the return line for configuration 1

Configuration 1 - Case 2 (Return)						
Mast 5						
First stroke-(1.0/100 $\mu$ s), Subsequent stroke-(0.2/50 $\mu$ s)						
Rf	- 34 kA			- 50 kA		
( $\Omega$ )	Auxiliary	Return	Catenary	Auxiliary	Return	Catenary
5	0.80	0.67	0.65	1.18	1.01	1.00
10	0.81	0.68	0.66	1.19	1.02	1.01
20	0.81	0.69	0.67	1.19	1.04	1.03
30	0.82	0.70	0.68	1.20	1.06	1.05
40	0.82	0.71	0.69	1.21	1.08	1.07
50	0.83	0.73	0.70	1.22	1.09	1.08
60	0.83	0.74	0.72	1.22	1.10	1.09
70	0.83	0.75	0.75	1.23	1.11	1.10
80	0.84	0.76	0.76	1.24	1.13	1.12
90	0.84	0.77	0.77	1.25	1.14	1.13
100	0.85	0.78	0.78	1.26	1.16	1.15

**Table D.98** Mast 7 induced voltages in Case 2 with multiple lightning strokes on the return line for configuration 1

Configuration 1 - Case 2 (Return)						
Mast 7						
First stroke-(1.0/100 $\mu$ s), Subsequent stroke-(0.2/50 $\mu$ s)						
Rf	- 34 kA			- 50 kA		
( $\Omega$ )	Auxiliary	Return	Catenary	Auxiliary	Return	Catenary
5	0.42	0.32	0.34	0.63	0.47	0.45
10	0.42	0.33	0.35	0.64	0.48	0.46
20	0.42	0.34	0.37	0.65	0.50	0.48
30	0.42	0.36	0.38	0.66	0.53	0.52
40	0.42	0.38	0.40	0.67	0.56	0.55
50	0.42	0.39	0.41	0.69	0.59	0.59
60	0.42	0.41	0.43	0.70	0.61	0.62
70	0.42	0.42	0.44	0.71	0.63	0.64
80	0.42	0.43	0.45	0.72	0.64	0.66
90	0.42	0.44	0.47	0.73	0.67	0.69
100	0.42	0.46	0.48	0.74	0.70	0.72



**Table D.99** Mast 4 induced voltages in Case 1 with multiple lightning strokes on the return line for configuration 2

Configuration 2 - Case 1 (Return)						
Mast 4						
First stroke-(1.0/100 $\mu$ s), Subsequent stroke-(0.2/50 $\mu$ s)						
Rf	- 34 kA			- 50 kA		
( $\Omega$ )	Auxiliary	Return	Catenary	Auxiliary	Return	Catenary
5	1.68	3.24	2.15	2.58	4.94	3.36
5	1.68	3.25	2.15	2.58	4.94	3.36
5	1.68	3.25	2.16	2.58	4.94	3.36

**Table D.100** Mast 5 induced voltages in Case 1 with multiple lightning strokes on the return line for configuration 2

Configuration 2 - Case 1 (Return)						
Mast 5						
First stroke-(1.0/100 $\mu$ s), Subsequent stroke-(0.2/50 $\mu$ s)						
Rf	- 34 kA			- 50 kA		
( $\Omega$ )	Auxiliary	Return	Catenary	Auxiliary	Return	Catenary
10	1.40	1.34	1.34	2.13	2.06	2.06
20	1.40	1.35	1.35	2.14	2.09	2.09
50	1.42	1.38	1.39	2.17	2.13	2.13

**Table D.101** Mast 7 induced voltages in Case 1 with multiple lightning strokes on the return line for configuration 2

Configuration 2 - Case 1 (Return)						
Mast 7						
First stroke-(1.0/100 $\mu$ s), Subsequent stroke-(0.2/50 $\mu$ s)						
Rf	- 34 kA			- 50 kA		
( $\Omega$ )	Auxiliary	Return	Catenary	Auxiliary	Return	Catenary
20	0.57	0.46	0.45	0.77	0.67	0.66
50	0.57	0.53	0.53	0.84	0.75	0.75
100	0.62	0.62	0.62	0.93	0.86	0.86

**Table D.102** Mast 4 induced voltages in Case 1 with multiple lightning strokes on the return line for configuration 3

Configuration 3 - Case 1 (Return)						
Mast 4						
First stroke-(1.0/100 $\mu$ s), Subsequent stroke-(0.2/50 $\mu$ s)						
Rf	- 34 kA			- 50 kA		
( $\Omega$ )	Auxiliary	Return	Catenary	Auxiliary	Return	Catenary
100	1.68	3.26	2.16	2.58	4.96	3.37
100	1.68	3.25	2.16	2.58	4.95	3.36
100	1.68	3.25	2.15	2.58	4.95	3.36

**Table D.103** Mast 5 induced voltages in Case 1 with multiple lightning strokes on the return line for configuration 3

Configuration 3 - Case 1 (Return)						
Mast 5						
First stroke-(1.0/100 $\mu$ s), Subsequent stroke-(0.2/50 $\mu$ s)						
Rf	- 34 kA			- 50 kA		
( $\Omega$ )	Auxiliary	Return	Catenary	Auxiliary	Return	Catenary
50	1.42	1.38	1.38	2.18	2.14	2.15
20	1.41	1.35	1.35	2.16	2.10	2.11
10	0.40	1.34	1.34	2.15	2.07	2.08

**Table D.104** Mast 7 induced voltages in Case 1 with multiple lightning strokes on the return line for configuration 3

Configuration 3 - Case 1 (Return)						
Mast 7						
First stroke-(1.0/100 $\mu$ s), Subsequent stroke-(0.2/50 $\mu$ s)						
Rf	- 34 kA			- 50 kA		
( $\Omega$ )	Auxiliary	Return	Catenary	Auxiliary	Return	Catenary
20	0.53	0.48	0.47	0.81	0.74	0.72
10	0.50	0.44	0.43	0.75	0.66	0.65
5	0.49	0.42	0.41	0.73	0.63	0.62

**Table D.105** Mast 4 induced voltages in Case 2 with multiple lightning strokes on the return line for configuration 2

Configuration 2 - Case 2 (Return)						
Mast 4						
First stroke-(1.0/100 $\mu$ s), Subsequent stroke-(0.2/50 $\mu$ s)						
Rf	- 34 kA			- 50 kA		
( $\Omega$ )	Auxiliary	Return	Catenary	Auxiliary	Return	Catenary
5	0.91	0.86	0.85	1.41	1.29	1.28
5	0.91	0.86	0.85	1.41	1.29	1.28
5	0.91	0.86	0.85	1.41	1.29	1.28

**Table D.106** Mast 5 induced voltages in Case 2 with multiple lightning strokes on the return line for configuration 2

Configuration 2 - Case 2 (Return)						
Mast 5						
First stroke-(1.0/100 $\mu$ s), Subsequent stroke-(0.2/50 $\mu$ s)						
Rf	- 34 kA			- 50 kA		
( $\Omega$ )	Auxiliary	Return	Catenary	Auxiliary	Return	Catenary
10	0.80	0.67	0.65	1.18	1.02	1.00
20	0.80	0.67	0.66	1.18	1.03	1.01
50	0.80	0.69	0.68	1.19	1.06	1.05

**Table D.107** Mast 7 induced voltages in Case 2 with multiple lightning strokes on the return line for configuration 2

Configuration 2 - Case 2 (Return)						
Mast 7						
First stroke-(1.0/100 $\mu$ s), Subsequent stroke-(0.2/50 $\mu$ s)						
Rf	- 34 kA			- 50 kA		
( $\Omega$ )	Auxiliary	Return	Catenary	Auxiliary	Return	Catenary
20	0.52	0.33	0.35	0.75	0.46	0.50
50	0.53	0.36	0.38	0.76	0.51	0.54
100	0.55	0.39	0.41	0.80	0.55	0.59

**Table D.108** Mast 4 induced voltages in Case 2 with multiple lightning strokes on the return line for configuration 3

Configuration 3 - Case 2 (Return)						
Mast 4						
First stroke-(1.0/100 $\mu$ s), Subsequent stroke-(0.2/50 $\mu$ s)						
Rf	- 34 kA			- 50 kA		
( $\Omega$ )	Auxiliary	Return	Catenary	Auxiliary	Return	Catenary
100	0.96	0.92	0.91	1.45	1.34	1.35
100	0.96	0.92	0.91	1.47	1.36	1.36
100	0.96	0.92	0.91	1.47	1.36	1.36

**Table D.109** Mast 5 induced voltages in Case 2 with multiple lightning strokes on the return line for configuration 3

Configuration 3 - Case 2 (Return)						
Mast 5						
First stroke-(1.0/100 $\mu$ s), Subsequent stroke-(0.2/50 $\mu$ s)						
Rf	- 34 kA			- 50 kA		
( $\Omega$ )	Auxiliary	Return	Catenary	Auxiliary	Return	Catenary
50	0.84	0.72	0.74	1.25	1.12	1.10
20	0.83	0.71	0.69	1.23	1.07	1.06
10	0.83	0.70	0.68	1.22	1.06	1.04

**Table D.110** Mast 7 induced voltages in Case 2 with multiple lightning strokes on the return line for configuration 3

Configuration 3 - Case 2 (Return)						
Mast 7						
First stroke-(1.0/100 $\mu$ s), Subsequent stroke-(0.2/50 $\mu$ s)						
Rf	- 34 kA			- 50 kA		
( $\Omega$ )	Auxiliary	Return	Catenary	Auxiliary	Return	Catenary
20	0.53	0.33	0.35	0.76	0.46	0.49
10	0.52	0.32	0.34	0.75	0.45	0.47
5	0.51	0.31	0.33	0.74	0.44	0.46

**Table D.111** Mast 4 induced voltages in Case 1 with multiple lightning strokes on the catenary line for configuration 1

Configuration 1 - Case 1 (Catenary)						
Mast 4						
First stroke-(1.0/100 $\mu$ s), Subsequent stroke-(0.2/50 $\mu$ s)						
Rf	- 34 kA			- 50 kA		
( $\Omega$ )	Auxiliary	Return	Catenary	Auxiliary	Return	Catenary
5	1.52	2.25	2.65	2.25	3.37	3.98
10	1.52	2.25	2.65	2.25	3.37	3.98
20	1.52	2.25	2.65	2.25	3.37	3.98
30	1.52	2.25	2.65	2.25	3.37	3.98
40	1.52	2.25	2.65	2.25	3.37	3.98
50	1.52	2.26	2.65	2.25	3.37	3.98
60	1.52	2.26	2.65	2.25	3.37	3.98
70	1.52	2.26	2.65	2.25	3.37	3.98
80	1.52	2.26	2.65	2.25	3.37	3.98
90	1.52	2.26	2.65	2.25	3.37	3.98
100	1.52	2.26	2.65	2.25	3.37	3.98

**Table D.112** Mast 5 induced voltages in Case 1 with multiple lightning strokes on the catenary line for configuration 1

Configuration 1 - Case 1 (Catenary)						
Mast 5						
First stroke-(1.0/100 $\mu$ s), Subsequent stroke-(0.2/50 $\mu$ s)						
Rf	- 34 kA			- 50 kA		
( $\Omega$ )	Auxiliary	Return	Catenary	Auxiliary	Return	Catenary
5	1.23	1.50	1.55	1.85	2.24	2.32
10	1.24	1.51	1.56	1.86	2.25	2.33
20	1.25	1.52	1.57	1.87	2.27	2.34
30	1.26	1.53	1.58	1.88	2.27	2.35
40	1.27	1.53	1.59	1.89	2.29	2.37
50	1.27	1.54	1.59	1.90	2.30	2.38
60	1.27	1.55	1.60	1.91	2.31	2.39
70	1.28	1.56	1.61	1.92	2.32	2.40
80	1.29	1.58	1.62	1.93	2.32	2.40
90	1.29	1.58	1.62	1.93	2.33	2.41
100	1.30	1.58	1.63	1.94	2.34	2.42

**Table D.113** Mast 7 induced voltages in Case 1 with multiple lightning strokes on the catenary line for configuration 1

Configuration 1 - Case 1 (Catenary)						
Mast 7						
First stroke-(1.0/100 $\mu$ s), Subsequent stroke-(0.2/50 $\mu$ s)						
Rf	- 34 kA			- 50 kA		
( $\Omega$ )	Auxiliary	Return	Catenary	Auxiliary	Return	Catenary
5	0.49	0.49	0.49	0.71	0.73	0.74
10	0.49	0.50	0.50	0.73	0.74	0.75
20	0.52	0.50	0.50	0.75	0.77	0.78
30	0.53	0.52	0.52	0.77	0.79	0.80
40	0.55	0.53	0.53	0.79	0.81	0.82
50	0.56	0.55	0.54	0.81	0.83	0.84
60	0.57	0.55	0.56	0.83	0.85	0.86
70	0.58	0.56	0.58	0.84	0.86	0.87
80	0.59	0.57	0.58	0.86	0.88	0.89
90	0.60	0.58	0.59	0.87	0.90	0.90
100	0.61	0.60	0.60	0.89	0.91	0.92

**Table D.114** Mast 4 induced voltages in Case 2 with multiple lightning strokes on the catenary line for configuration 1

Configuration 1 - Case 2 (Catenary)						
Mast 4						
First stroke-(1.0/100 $\mu$ s), Subsequent stroke-(0.2/50 $\mu$ s)						
Rf	- 34 kA			- 50 kA		
( $\Omega$ )	Auxiliary	Return	Catenary	Auxiliary	Return	Catenary
5	1.62	2.29	2.45	2.37	3.42	3.65
10	1.63	2.30	2.45	2.38	3.43	3.65
20	1.64	2.30	2.46	2.40	3.44	3.66
30	1.65	2.30	2.46	2.41	3.45	3.67
40	1.66	2.30	2.46	2.42	3.46	3.68
50	1.67	2.31	2.47	2.43	3.47	3.69
60	1.69	2.32	2.47	2.44	3.48	3.70
70	1.69	2.32	2.48	2.45	3.49	3.71
80	1.70	2.32	2.48	2.46	3.49	3.72
90	1.71	2.32	2.48	2.46	3.50	3.72
100	1.71	2.32	2.48	2.47	3.50	3.72

**Table D.115** Mast 5 induced voltages in Case 2 with multiple lightning strokes on the catenary line for configuration 1

Configuration 1 - Case 2 (Catenary)						
Mast 5						
First stroke-(1.0/100 $\mu$ s), Subsequent stroke-(0.2/50 $\mu$ s)						
Rf	- 34 kA			- 50 kA		
( $\Omega$ )	Auxiliary	Return	Catenary	Auxiliary	Return	Catenary
5	1.23	1.38	1.41	1.82	2.03	2.06
10	1.24	1.39	1.42	1.83	2.05	2.08
20	1.25	1.41	1.44	1.85	2.08	2.11
30	1.25	1.42	1.44	1.87	2.10	2.14
40	1.29	1.45	1.48	1.88	2.13	2.17
50	1.29	1.46	1.49	1.90	2.15	2.19
60	1.30	1.47	1.50	1.92	2.17	2.22
70	1.31	1.49	1.52	1.93	2.19	2.24
80	1.32	1.50	1.53	1.95	2.21	2.25
90	1.34	1.52	1.55	1.96	2.23	2.27
100	1.35	1.53	1.57	1.98	2.25	2.29

**Table D.116** Mast 7 induced voltages in Case 2 with multiple lightning strokes on the catenary line for configuration 1

Configuration 1 - Case 2 (Catenary)						
Mast 7						
First stroke-(1.0/100 $\mu$ s), Subsequent stroke-(0.2/50 $\mu$ s)						
Rf	- 34 kA			- 50 kA		
( $\Omega$ )	Auxiliary	Return	Catenary	Auxiliary	Return	Catenary
5	0.52	0.47	0.47	0.78	0.72	0.72
10	0.52	0.47	0.47	0.78	0.72	0.72
20	0.53	0.49	0.48	0.79	0.75	0.75
30	0.54	0.50	0.49	0.81	0.76	0.76
40	0.55	0.51	0.51	0.82	0.78	0.78
50	0.56	0.52	0.52	0.83	0.80	0.80
60	0.57	0.53	0.53	0.85	0.81	0.81
70	0.58	0.54	0.54	0.86	0.83	0.83
80	0.59	0.55	0.55	0.87	0.84	0.84
90	0.60	0.56	0.56	0.88	0.86	0.86
100	0.61	0.57	0.57	0.89	0.87	0.87

**Table D.117** Mast 4 induced voltages in Case 1 with multiple lightning strokes on the catenary line for configuration 2

Configuration 2 - Case 1 (Catenary)						
Mast 4						
First stroke-(1.0/100 $\mu$ s), Subsequent stroke-(0.2/50 $\mu$ s)						
Rf	- 34 kA			- 50 kA		
( $\Omega$ )	Auxiliary	Return	Catenary	Auxiliary	Return	Catenary
5	1.52	2.25	2.65	2.25	3.37	4.00
5	1.52	2.25	2.65	2.25	3.37	4.00
5	1.52	2.25	2.65	2.25	3.37	4.00

**Table D.118** Mast 5 induced voltages in Case 1 with multiple lightning strokes on the catenary line for configuration 2

Configuration 2 - Case 1 (Catenary)						
Mast 5						
First stroke-(1.0/100 $\mu$ s), Subsequent stroke-(0.2/50 $\mu$ s)						
Rf	- 34 kA			- 50 kA		
( $\Omega$ )	Auxiliary	Return	Catenary	Auxiliary	Return	Catenary
10	1.24	1.51	1.56	1.86	2.25	2.32
20	1.25	1.52	1.57	1.87	2.26	2.34
50	1.27	1.54	1.59	1.90	2.29	2.37

**Table D.119** Mast 7 induced voltages in Case 1 with multiple lightning strokes on the catenary line for configuration 2

Configuration 2 - Case 1 (Catenary)						
Mast 7						
First stroke-(1.0/100 $\mu$ s), Subsequent stroke-(0.2/50 $\mu$ s)						
Rf	- 34 kA			- 50 kA		
( $\Omega$ )	Auxiliary	Return	Catenary	Auxiliary	Return	Catenary
20	0.50	0.51	0.51	0.74	0.76	0.77
50	0.55	0.53	0.53	0.79	0.81	0.81
100	0.59	0.57	0.57	0.86	0.88	0.89



**Table D.120** Mast 4 induced voltages in Case 1 with multiple lightning strokes on the catenary line for configuration 3

Configuration 3 - Case 1 (Catenary)						
Mast 4						
First stroke-(1.0/100 $\mu$ s), Subsequent stroke-(0.2/50 $\mu$ s)						
Rf	- 34 kA			- 50 kA		
( $\Omega$ )	Auxiliary	Return	Catenary	Auxiliary	Return	Catenary
100	1.52	2.26	2.66	2.25	3.36	4.00
100	1.52	2.25	2.66	2.25	3.37	4.00
100	1.52	2.25	2.66	2.25	3.38	4.00

**Table D.121** Mast 5 induced voltages in Case 1 with multiple lightning strokes on the catenary line for configuration 3

Configuration 3 - Case 1 (Catenary)						
Mast 5						
First stroke-(1.0/100 $\mu$ s), Subsequent stroke-(0.2/50 $\mu$ s)						
Rf	- 34 kA			- 50 kA		
( $\Omega$ )	Auxiliary	Return	Catenary	Auxiliary	Return	Catenary
50	1.27	1.54	1.60	1.90	2.30	2.38
20	1.25	1.52	1.57	1.87	2.27	2.34
10	1.24	1.51	1.56	1.86	2.26	2.33

**Table D.122** Mast 7 induced voltages in Case 1 with multiple lightning strokes on the catenary line for configuration 3

Configuration 3 - Case 1 (Catenary)						
Mast 7						
First stroke-(1.0/100 $\mu$ s), Subsequent stroke-(0.2/50 $\mu$ s)						
Rf	- 34 kA			- 50 kA		
( $\Omega$ )	Auxiliary	Return	Catenary	Auxiliary	Return	Catenary
20	0.53	0.52	0.52	0.77	0.79	0.80
10	0.50	0.50	0.50	0.73	0.75	0.76
5	0.49	0.49	0.49	0.72	0.73	0.74

**Table D.123** Mast 4 induced voltages in Case 2 with multiple lightning strokes on the catenary line for configuration 2

Configuration 2 - Case 2 (Catenary)						
Mast 4						
First stroke-(1.0/100 $\mu$ s), Subsequent stroke-(0.2/50 $\mu$ s)						
Rf	- 34 kA			- 50 kA		
( $\Omega$ )	Auxiliary	Return	Catenary	Auxiliary	Return	Catenary
5	1.62	2.29	2.45	2.37	3.42	3.64
5	1.63	2.29	2.45	2.37	3.42	3.65
5	1.64	2.29	2.45	2.38	3.43	3.65

**Table D.124** Mast 5 induced voltages in Case 2 with multiple lightning strokes on the catenary line for configuration 2

Configuration 2 - Case 2 (Catenary)						
Mast 5						
First stroke-(1.0/100 $\mu$ s), Subsequent stroke-(0.2/50 $\mu$ s)						
Rf	- 34 kA			- 50 kA		
( $\Omega$ )	Auxiliary	Return	Catenary	Auxiliary	Return	Catenary
10	1.23	1.39	1.41	1.83	2.04	2.07
20	1.24	1.39	1.42	1.84	2.06	2.10
50	1.26	1.43	1.46	1.86	2.11	2.16

**Table D.125** Mast 7 induced voltages in Case 2 with multiple lightning strokes on the catenary line for configuration 2

Configuration 2 - Case 2 (Catenary)						
Mast 7						
First stroke-(1.0/100 $\mu$ s), Subsequent stroke-(0.2/50 $\mu$ s)						
Rf	- 34 kA			- 50 kA		
( $\Omega$ )	Auxiliary	Return	Catenary	Auxiliary	Return	Catenary
20	0.52	0.48	0.48	0.74	0.74	0.78
50	0.54	0.50	0.50	0.80	0.77	0.76
100	0.57	0.54	0.54	0.84	0.82	0.82

**Table D.126** Mast 4 induced voltages in Case 2 with multiple lightning strokes on the catenary line for configuration 3

Configuration 3 - Case 2 (Catenary)						
Mast 4						
First stroke-(1.0/100 $\mu$ s), Subsequent stroke-(0.2/50 $\mu$ s)						
Rf	- 34 kA			- 50 kA		
( $\Omega$ )	Auxiliary	Return	Catenary	Auxiliary	Return	Catenary
100	1.69	2.32	2.48	2.47	3.50	3.71
100	1.69	2.32	2.47	2.46	3.48	3.70
100	1.69	2.32	2.47	2.46	3.47	3.69

**Table D.127** Mast 5 induced voltages in Case 2 with multiple lightning strokes on the catenary line for configuration 3

Configuration 3 - Case 2 (Catenary)						
Mast 5						
First stroke-(1.0/100 $\mu$ s), Subsequent stroke-(0.2/50 $\mu$ s)						
Rf	- 34 kA			- 50 kA		
( $\Omega$ )	Auxiliary	Return	Catenary	Auxiliary	Return	Catenary
50	1.31	1.48	1.51	1.93	2.19	2.22
20	1.29	1.44	1.48	1.89	2.14	2.17
10	1.28	1.43	1.46	1.88	2.11	2.15

**Table D.128** Mast 7 induced voltages in Case 2 with multiple lightning strokes on the catenary line for configuration 3

Configuration 3 - Case 2 (Catenary)						
Mast 7						
First stroke-(1.0/100 $\mu$ s), Subsequent stroke-(0.2/50 $\mu$ s)						
Rf	- 34 kA			- 50 kA		
( $\Omega$ )	Auxiliary	Return	Catenary	Auxiliary	Return	Catenary
20	0.55	0.51	0.50	0.82	0.78	0.78
10	0.54	0.49	0.48	0.80	0.75	0.75
5	0.53	0.48	0.48	0.73	0.74	0.79

## BIOGRAPHY



Kelvin Melckzedek Minja was born on Saturday, 03 June 1989 in Tanga region, Tanzania. He completed his Bachelor degree in Electrical Engineering in January 2015 from Dar es Salaam Institute of Technology. He later continued a master's degree in Electrical Engineering since March 2016 at the School of Electrical Engineering, Institute of Engineering, Suranaree University of Technology, Nakhon Ratchasima, Thailand. His area of interest in research include transient over voltages in power system. Additionally, he is now likely focusing on smart modern public transportation due to the revolution going on the power-system domain.

มหาวิทยาลัยเทคโนโลยีสุรนารี